

Lecture Notes in Electrical Engineering 645

Shengzhao Long  
Balbir S. Dhillon *Editors*

# Man-Machine- Environment System Engineering

Proceedings of the 20th International  
Conference on MMESE



 Springer

# Lecture Notes in Electrical Engineering

## Volume 645

### Series Editors

Leopoldo Angrisani, Department of Electrical and Information Technologies Engineering, University of Napoli Federico II, Naples, Italy

Marco Arteaga, Departament de Control y Robótica, Universidad Nacional Autónoma de México, Coyoacán, Mexico

Bijaya Ketan Panigrahi, Electrical Engineering, Indian Institute of Technology Delhi, New Delhi, Delhi, India  
Samarjit Chakraborty, Fakultät für Elektrotechnik und Informationstechnik, TU München, Munich, Germany

Jiming Chen, Zhejiang University, Hangzhou, Zhejiang, China

Shanben Chen, Materials Science and Engineering, Shanghai Jiao Tong University, Shanghai, China

Tan Kay Chen, Department of Electrical and Computer Engineering, National University of Singapore, Singapore, Singapore

Rüdiger Dillmann, Humanoids and Intelligent Systems Laboratory, Karlsruhe Institute for Technology, Karlsruhe, Germany

Haibin Duan, Beijing University of Aeronautics and Astronautics, Beijing, China

Gianluigi Ferrari, Università di Parma, Parma, Italy

Manuel Ferre, Centre for Automation and Robotics CAR (UPM-CSIC), Universidad Politécnica de Madrid, Madrid, Spain

Sandra Hirche, Department of Electrical Engineering and Information Science, Technische Universität München, Munich, Germany

Faryar Jabbari, Department of Mechanical and Aerospace Engineering, University of California, Irvine, CA, USA

Limin Jia, State Key Laboratory of Rail Traffic Control and Safety, Beijing Jiaotong University, Beijing, China

Janusz Kacprzyk, Systems Research Institute, Polish Academy of Sciences, Warsaw, Poland

Alaa Khamis, German University in Egypt El Tagamoa El Khames, New Cairo City, Egypt

Torsten Kroeger, Stanford University, Stanford, CA, USA

Qilian Liang, Department of Electrical Engineering, University of Texas at Arlington, Arlington, TX, USA

Ferran Martín, Departament d'Enginyeria Electrònica, Universitat Autònoma de Barcelona, Bellaterra, Barcelona, Spain

Tan Cher Ming, College of Engineering, Nanyang Technological University, Singapore, Singapore

Wolfgang Minker, Institute of Information Technology, University of Ulm, Ulm, Germany

Pradeep Misra, Department of Electrical Engineering, Wright State University, Dayton, OH, USA

Sebastian Möller, Quality and Usability Laboratory, TU Berlin, Berlin, Germany

Subhas Mukhopadhyay, School of Engineering & Advanced Technology, Massey University, Palmerston North, Manawatu-Wanganui, New Zealand

Cun-Zheng Ning, Electrical Engineering, Arizona State University, Tempe, AZ, USA

Toyoaki Nishida, Graduate School of Informatics, Kyoto University, Kyoto, Japan

Federica Pascucci, Dipartimento di Ingegneria, Università degli Studi "Roma Tre", Rome, Italy

Yong Qin, State Key Laboratory of Rail Traffic Control and Safety, Beijing Jiaotong University, Beijing, China

Gan Woon Seng, School of Electrical & Electronic Engineering, Nanyang Technological University, Singapore, Singapore

Joachim Speidel, Institute of Telecommunications, Universität Stuttgart, Stuttgart, Germany

Germano Veiga, Campus da FEUP, INESC Porto, Porto, Portugal

Haitao Wu, Academy of Opto-electronics, Chinese Academy of Sciences, Beijing, China

Junjie James Zhang, Charlotte, NC, USA

The book series *Lecture Notes in Electrical Engineering* (LNEE) publishes the latest developments in Electrical Engineering - quickly, informally and in high quality. While original research reported in proceedings and monographs has traditionally formed the core of LNEE, we also encourage authors to submit books devoted to supporting student education and professional training in the various fields and applications areas of electrical engineering. The series cover classical and emerging topics concerning:

- Communication Engineering, Information Theory and Networks
- Electronics Engineering and Microelectronics
- Signal, Image and Speech Processing
- Wireless and Mobile Communication
- Circuits and Systems
- Energy Systems, Power Electronics and Electrical Machines
- Electro-optical Engineering
- Instrumentation Engineering
- Avionics Engineering
- Control Systems
- Internet-of-Things and Cybersecurity
- Biomedical Devices, MEMS and NEMS

For general information about this book series, comments or suggestions, please contact [leontina.dicecco@springer.com](mailto:leontina.dicecco@springer.com).

To submit a proposal or request further information, please contact the Publishing Editor in your country:

#### **China**

Jasmine Dou, Associate Editor ([jasmine.dou@springer.com](mailto:jasmine.dou@springer.com))

#### **India, Japan, Rest of Asia**

Swati Meherishi, Executive Editor ([Swati.Meherishi@springer.com](mailto:Swati.Meherishi@springer.com))

#### **Southeast Asia, Australia, New Zealand**

Ramesh Nath Premnath, Editor ([ramesh.premnath@springernature.com](mailto:ramesh.premnath@springernature.com))

#### **USA, Canada:**

Michael Luby, Senior Editor ([michael.luby@springer.com](mailto:michael.luby@springer.com))

#### **All other Countries:**

Leontina Di Cecco, Senior Editor ([leontina.dicecco@springer.com](mailto:leontina.dicecco@springer.com))

**\*\* Indexing: The books of this series are submitted to ISI Proceedings, EI-Compendex, SCOPUS, MetaPress, Web of Science and Springerlink \*\***

More information about this series at <http://www.springer.com/series/7818>

Shengzhao Long · Balbir S. Dhillon  
Editors

# Man-Machine-Environment System Engineering

Proceedings of the 20th International  
Conference on MMESE



 Springer

*Editors*

Shengzhao Long  
Astronaut Research and Training  
Center of China  
Beijing, China

Balbir S. Dhillon  
Department of Mechanical Engineering  
University of Ottawa  
Ottawa, ON, Canada

ISSN 1876-1100

ISSN 1876-1119 (electronic)

Lecture Notes in Electrical Engineering

ISBN 978-981-15-6977-7

ISBN 978-981-15-6978-4 (eBook)

<https://doi.org/10.1007/978-981-15-6978-4>

© The Editor(s) (if applicable) and The Author(s), under exclusive license to Springer Nature Singapore Pte Ltd. 2020

This work is subject to copyright. All rights are solely and exclusively licensed by the Publisher, whether the whole or part of the material is concerned, specifically the rights of translation, reprinting, reuse of illustrations, recitation, broadcasting, reproduction on microfilms or in any other physical way, and transmission or information storage and retrieval, electronic adaptation, computer software, or by similar or dissimilar methodology now known or hereafter developed.

The use of general descriptive names, registered names, trademarks, service marks, etc. in this publication does not imply, even in the absence of a specific statement, that such names are exempt from the relevant protective laws and regulations and therefore free for general use.

The publisher, the authors and the editors are safe to assume that the advice and information in this book are believed to be true and accurate at the date of publication. Neither the publisher nor the authors or the editors give a warranty, expressed or implied, with respect to the material contained herein or for any errors or omissions that may have been made. The publisher remains neutral with regard to jurisdictional claims in published maps and institutional affiliations.

This Springer imprint is published by the registered company Springer Nature Singapore Pte Ltd. The registered company address is: 152 Beach Road, #21-01/04 Gateway East, Singapore 189721, Singapore



Grandness Scientist Xuesen Qian's Sky-high Estimation for the Man-Machine-Environment System Engineering

龙升照同志:

我收到您主编的《人机环境系统工程研究进展(第一卷)》, 翻阅了之后, 感到非常高兴, 1985年秋提出的一个想法, 现在8年之后已编出成书, 500多页的巨卷! 而且研究范围已大大超出原来航天, 内容涉及航空、航天、舰海、兵器、电子、能源、交通、电力、煤炭、冶金、体育、康复、管理……等领域! 你们是在社会主义中国开创了这门重要现代科学技术!

此致

敬礼!

钱学森

1993.10.22



Grandness Scientist Xuesen Qian's Congratulatory Letter to the 20th Anniversary Commemorative Conference of Man-Machine-Environment System Engineering Foundation

龙升照同志：

你的来信已收到。欣悉人-机-环境系统工程创立 20 周年纪念大会暨第五届全国人-机-环境系统工程学术会议即将召开，我向你们表示最热烈的祝贺！

20 年来，你们在人-机-环境系统工程这一新兴科学领域进行了积极的开拓和探索，并取得了非常可喜的成绩，我感到由衷的高兴。

希望你们今后再接再厉，大力推动人-机-环境系统工程理论及应用的蓬勃发展，为中国乃至世界科学技术的进步作出积极贡献！

祝

工作顺利！

钱学森  
2001年6月26日

# **Program and Technical Committee Information**

## **General Chairman**

Professor Shengzhao Long, Astronaut Research and Training Center of China

## **Program Committee Chairman**

Professor Balbir S. Dhillon, University of Ottawa, Canada

## **Technical Committee Chairman**

Professor Enrong Mao, College of Engineering, China Agricultural University, China

## **Program and Technical Committee Members**

Professor Yanping Chen, University of Management and Technology, USA

Professor Hongfeng Gao, University of California, USA

Professor Michael Greenspan, Queen's University, Canada

Professor Birsen Donmez, University of Toronto, Canada

Professor Xiangshi Ren, Kochi University of Technology, Japan

Professor Kinhuat Low, Nanyang Technological University, Singapore

Professor Baiqiao Huang, System Engineering Research Institute of China, State Shipbuilding Corporation, China

Professor Baoqing Xia, Weapon Industrial Hygiene Research Institute, China

Professor Chenming Li, The Quartermaster Research Institute of Engineering and Technology, China

Professor Fang Xie, China North Vehicle Research Institute, China

Professor Guangtao Ma, Shenyang Jianzhu University, China

Professor Haoting Liu, University of Science and Technology Beijing, China

Professor Hongjun Xue, Northwestern Polytechnical University, China

Professor Lijing Wang, Beijing University of Aeronautics and Astronautics, China

Professor Long Ye, Beijing Jiaotong University, China

Senior Engineer, Qichao Zhao, Beijing King Far Technology Co., Ltd., China

Professor Qing Liu, Jिंगgangshan University, China



Professor Weijun Chen, Shanghai Maritime University, China  
Professor Xiaochao Guo, Institute of Aviation Medicine, Air Force, China  
Professor Yongqing Hou, China Academy of Space Technology, China  
Professor Yanqi Wang, Weapon Industrial Hygiene Research Institute, China  
Professor Yinying Huang, Agricultural Bank of China, China  
Professor Yuhong Shen, The Quartermaster Research Institute of Engineering and Technology, China

# Preface

In 1981, under the directing of the great Scientist Xuesen Qian, an integrated frontier science—Man-Machine-Environment System Engineering (MMESE)—came into being in China. Xuesen Qian gave high praise to this emerging science. In the letter to Shengzhao Long, he pointed out, **“You are creating this very important modern science and technology in China!”** in October 22, 1993.

In the congratulation letter to the commemoration meeting of 20th anniversary of establishing the Man-Machine-Environment System Engineering, the great Scientist Xuesen Qian stated, “You have made active development and exploration in this new emerging science of MMESE, and obtained encouraging achievements. I am sincerely pleased and hope you can do even more to make prosper development in the theory and application of MMESE, and **make positive contribution to the progress of science and technology in China, and even in the whole world**” in June 26th, 2001.

October 22, which is the day that the great Scientist Xuesen Qian gave high praise to MMESE, was determined to be Foundation Commemoration Day of MMESE by the second conference of the 5th MMESE Committee on October 22, 2010. On this very special day, the great Scientist Xuesen Qian pointed out in the letter to Shengzhao Long, **“You are creating this very important modern science and technology in China!”**

The 20th International Conference on MMESE will be held in Zhengzhou, China, on October 24–26 of this year; hence, we will dedicate *Man-Machine-Environment System Engineering: Proceedings of the 20th International Conference on MMESE* to our readers.

*Man-Machine-Environment System Engineering: Proceedings of the 20th International Conference on MMESE* is the academic showcases of the 20th International Conference on MMESE joint held by MMESE Committee of China and Beijing KeCui Academe of MMESE in Nanjing, China. The *Man-Machine-Environment System Engineering: Proceedings of the 20th International Conference on MMESE* consisted of 123 more excellent papers selected from more than 500 papers. Due to limitations on space, some excellent papers have been left out, we feel deeply sorry for that. Crudeness in contents and possible incorrectness

are inevitable due to the somewhat pressing editing time and we hope you kindly point them out promptly, and your valuable comments and suggestions are also welcomed.

*Man-Machine-Environment System Engineering: Proceedings of the 20th International Conference on MMESE* will be published by Springer-Verlag, German. Springer-Verlag is also responsible for the related matters on index of the index to EI, so that the world can know the research quality and development trend of MMESE theory and application. Therefore, the publication of *Man-Machine-Environment System Engineering: Proceedings of the 20th International Conference on MMESE* will greatly promote the vigorous development of MMESE in the world and realize the grand object of “**making positive contribution to the progress of science and technology in China, and even in the whole world**” proposed by Xuesen Qian.

We would like to express our sincere thanks to Springer-Verlag, German, for their full support and help during the publishing process.

Beijing, China  
July 2020

Professor Shengzhao Long

# Contents

<b>Research on the Man Character</b>	
<b>Research on the Integrated Situation Analysis of Ship Mariners Team</b> .....	3
Kun Yu	
<b>An Investigation on the Demand of Psychological Data Collection in Military Pilots</b> .....	15
Yang Liao and Huamiao Song	
<b>Chinese Drivers' Preferred Posture for Sedans' Seat Ergonomic Design</b> .....	23
Jiaxun You, Lipeng Qin, Peiwen Zuo, Xuelei Wang, and Chao Zhang	
<b>The Effect of Osteoporosis on Spine Following Osteotomy</b> .....	33
Tianhao Wang, Chenming Li, and Yan Wang	
<b>Study on Human Factor Evaluation of Aviation Maintenance During Flight Test</b> .....	41
Haijing Song, Kai Feng, and Yuqi Zhang	
<b>The Effect of Music Relaxation Training on Relieving the Psychological Fatigue After Simulated Flight</b> .....	49
Yan Zhang, Liu Yang, Yang Liao, Yishuang Zhang, Fei Peng, and Huamiao Song	
<b>Study on the Airworthiness Certification of Human Factor in Flight Test for Civil Aircraft</b> .....	59
Haijing Song, Li Han, and Hongjiao Wu	
<b>Study on Autonomic Nervous Stability Training of Military Pilots</b> .....	67
Yishuang Zhang, Yan Zhang, Fei Peng, Yang Liao, Xueqian Deng, Huamiao Song, Duanqin Xiong, Juan Liu, and Liu Yang	

**Research on Recognizable Physiological Signals of Workers Working at Heights** . . . . . 75  
Guilei Sun, Fangming Pang, Qi Liu, Yun Lin, Luyao Xu, and Yanhua Meng

**A Study on the Construction of Mental Fatigue Model and the Change of Psychological Efficacy** . . . . . 83  
Liu Yang, Yishuang Zhang, Yan Zhang, Yang Liao, Duanqin Xiong, Rong Lin, Jian Du, and Xichen Geng

**Research on Psychological Management Problems of Military Cadets Under the Angle of Group Psychology** . . . . . 93  
Peng Gong, Ye Tao, Huiyong Wang, Kun Cao, and Yuxi Peng

**Research on the Effects of Pilots Psychological Trainings Based on Different Military Application Purposes** . . . . . 101  
Yishuang Zhang, Yan Zhang, Fei Peng, Yang Liao, Huamiao Song, Xueqian Deng, Duanqin Xiong, Juan Liu, and Liu Yang

**Human Factor Analysis on the Effect of Pilot’s Interpretation of Airborne Radar Warning Information** . . . . . 111  
Juan Liu, Shuang Bai, Jiabo Ye, Lin Zhang, Jian Du, Wei Pan, Yubin Zhou, Qiming Cheng, Liu Yang, and Duanqin Xiong

**Qualitative Analysis on the Factors Influencing Pilot Functional Status** . . . . . 119  
Shuang Bai, Juan Liu, Jiabo Ye, Lin Zhang, Jian Du, Wei Pan, Yubin Zhou, Qiming Cheng, Liu Yang, Duanqin Xiong, Peng Du, Ruoyong Wang, Huiling Mu, Ximeng Chen, and Hua Ge

**Study on Sensory Evaluation of Instant Rice by Fuzzy Mathematics Method** . . . . . 127  
Huiling Mu, Peng Du, Longmei Fang, Shuang Bai, Ximeng Chen, Peng Liu, and Ruoyong Wang

**Study on the Workload of 12 h Simulated Flight Continuously Across Day and Night** . . . . . 135  
Feng Wu, Dawei Tian, Hua Ge, Shuang Bai, Andong Zhao, Ruoyong Wang, Yanpeng Zhao, Quan Wang, and Lue Deng

**Study on Nutritional Status and Changing Trend of Air Force Pilots** . . . . . 143  
Peng Du, Huiling Mu, Shuang Bai, Longmei Fang, Ximeng Chen, Hongjiang Jing, Feng Li, Peng Liu, Lili Zhang, and Ruoyong Wang

**Simulation and Verification of a Vestibular Perception Model** . . . . . 149  
Cong Wang, Dalong Guo, Hongbo Jia, Yuliang Li, Fang Su, Yuanjing Zheng, Yao Liu, Chenlong Jia, and Qi Zhang

**Analysis of Man’s Role in Unmanned Operations** . . . . . 157  
 Hongjun Cheng, Huifang Wang, and Yinxi Yang

**An Experimental Study of the Effects of Subliminal Stimulation on Attention Perception** . . . . . 163  
 Juan Liu, Wei Pan, Duanqin Xiong, Rong Lin, Jian Du, Jiabo Ye, Yubin Zhou, Qiming Cheng, Liu Yang, Yishuang Zhang, and Shuang Bai

**3D Head Anthropometry for Head-Related Transfer Function of Chinese Pilots** . . . . . 171  
 Xiaochao Guo, Yu Bai, Qingfeng Liu, Duanqin Xiong, Yanyan Wang, and Jian Du

**The Mental Health and Correlated Factors of Medical Team Members in an Aerospace Medical Unit Before Conducting Non-war Military Operations** . . . . . 179  
 Yang Liao, Yishuang Zhang, Yan Zhang, Xueqian Deng, and Liu Yang

**Research on the Construction of Ship Operator’s Cognitive Behavior Model** . . . . . 187  
 Weiming Fang, Shuqin Zhao, Jun Peng, and Chuan Wang

**Analysis of Human Factor Characteristics of Ship Control System** . . . . . 195  
 Jun Peng, Guangjiang Wu, and Chuan Wang

**Study on Fatigue Detection of Ship Operator Based on Eye Features** . . . . . 203  
 Chuan Wang, Jun Peng, Xiaoxi Han, Shenghang Xu, and Jian Zhang

**Study on Fatigue Detection Method of Ship Operator Based on Face Recognition Technology** . . . . . 211  
 Jian Zhang, Jun Peng, Xiaoxi Han, Shenghang Xu, and Chuan Wang

**Hybrid Model of Eye Movement Behavior Recognition for Virtual Workshop** . . . . . 219  
 Mengyao Dong, Zenggui Gao, and Lilan Liu

**Research on Influence of Organizing and Training Capabilities Towards Officers Positions Capabilities** . . . . . 229  
 Junlong Guo, Zaochen Liu, Jianfeng Li, and Jiwen Sun

**Interaction Effect of Workload and Circadian Rhythm in Air Traffic Controllers’ Fatigue** . . . . . 235  
 Zhenling Chen, Jianping Zhang, Guoliang Zou, Pengxin Ding, Shunqing Li, Yanzhong Gu, and Yiyou Chen

**A PERCLOS Method for Fine Characterization of Behaviour Circadian Rhythm** . . . . . 243  
 Yanzhong Gu, Zhenling Chen, Jianping Zhang, Guoliang Zou, Pengxin Ding, and Weinan Deng

**Research on Fatigue Monitoring of Forklift Driver Driving in an Automobile Enterprise** . . . . . 251  
Zhenjun Du and Xinmin Zhang

**Research on the Machine Character**

**Parameter Optimization Design of a Cable-Driven Bionic Muscle Mechanism Based on Hill Muscle Model for Flexible Upper Limb-Assisted Exoskeleton** . . . . . 263  
Hongrun Lu, Bingshan Hu, Hongliu Yu, Tong Ma, and Xinran Zhang

**Design of Female Office Chairs Based on Ergonomics and Emotional Design** . . . . . 273  
Yi Chen, Canqun He, and Yuqi Lin

**Prototype Design and Performance Experiment of Passive Compliant Mechanism for the Automatic Charging Robot End Effector** . . . . . 281  
Bingshan Hu, Ke Cheng, Weilun Zhang, and Xinran Zhang

**Facilities Design of Fume Protection and Ventilation System in Welding Workshop of an Automotive Enterprise** . . . . . 289  
Chen Ding, Bin Yang, Jianwu Chen, Pei Wang, and Ying Wang

**Study on Optimization Design of Drive Seat Based on Body Comfort** . . . . . 301  
Yu Wang, Yongqin Wang, Xiangcao Niu, and Yi Liu

**Analysis on Armor Protection Requirements of the Top of Self-propelled Antiaircraft Gun** . . . . . 307  
Zhenyou Zhang, Qian Liu, and Pengdong Zhang

**Development of Principle Prototype of Digital Bright Spot Scintillator** . . . . . 313  
Hua Ge, Andong Zhao, Yuefang Dong, Feng Wu, Weiwei Fu, Xi Zhang, and Hao Zhan

**Information Processing System Design for Multi-rotor UAV-Based Earthquake Rescue** . . . . . 321  
Haoting Liu, Ming Lv, Yun Gao, Jiacheng Li, Jinhui Lan, and Wei Gao

**Multiple Missiles Launch Assignment Based on AHP and Genetic Algorithm** . . . . . 331  
Fang Liu and Jinshi Xiao

**Study on Female Caring Office Chair Design Based on Ergonomics** . . . . . 341  
Tianqi Yuan and Xiaohui Tao

**Research on Blackness Classification of Polyester Knitted Printed Black Cloth** . . . . . 351  
 Jingying Xu, Qiubao Zhou, Zimin Jin, and Kun Chen

**Evaluation of Dietary Quality of Aircrew by Military Diet Balance Index** . . . . . 359  
 Huiling Mu, Ruoyong Wang, Shuang Bai, Longmei Fang, Ximeng Chen, Hongjiang Jing, Feng Li, Peng Liu, Lili Zhang, and Peng Du

**Numerical Simulation Research on Design of Displacement Ventilation System in Large Painting Workshop** . . . . . 369  
 Bin Yang, Jianwu Chen, Lindong Liu, Yanqiu Sun, Shulin Zhou, and Weijiang Liu

**Application of Comprehensive Preference and Fuzzy Mathematics Method in Sensory Evaluation of Ready-to-Eat Meatballs** . . . . . 379  
 Ruoyong Wang, Huiling Mu, Peng Du, Ximeng Chen, Peng Liu, and Shuang Bai

**Research on STK-Based 3D Model Transformation and Optimization** . . . . . 387  
 Kunfu Wang, Wanfeng Mao, Wei Feng, Jian Su, Xing Li, and Peng Zhang

**Quality Control of Measuring for Head-Related Transfer Functions of Chinese Pilots** . . . . . 395  
 Xiaochao Guo, Qingfeng Liu, Yanyan Wang, Duanqin Xiong, Yu Bai, and Jian Du

**An Automatic Meter Recognition Method for In-Orbit Application** . . . . . 403  
 Weijie Wu, Haoting Liu, and Jiacheng Li

**Investigation of Image Classification Using HOG, GLCM Features, and SVM Classifier** . . . . . 411  
 Jianyue Ge and Haoting Liu

**Relationship Between Individual Perceptual Feature Demand and Satisfaction in the Small Assistant Robot Modeling Design** . . . . . 419  
 Yankun Yang, Bo Wang, Changhua Jiang, Yujing Cui, Ling Song, and Xiaomeng Ma

**Model Evaluation of South Official Hat Chairs Based on Image Recognition Method** . . . . . 429  
 Hanzhou Qiu and Yun Liu

**Design of College Student Luggage Based on User Experience** . . . . . 439  
 Xiao Han, Ting Dong, Dongli Wang, and Xin Chen



**The Usability of Advance Intersection Lane Control Signs at Intersections** . . . . . 449  
Leibing An, Jun Ma, and Dan Zhao

**Explore the Comfortable Seat Armrest Height During the Upper Limb Motor Imagery Training** . . . . . 459  
Lu Liu, Xueying Sun, Hechen Zhang, and Feng He

**A Generation Method and Verification of Virtual Dataset** . . . . . 469  
Pengxin Ding, Qingyang Shen, Tianguo Huang, and Minghui Wang

**Study on the Influence Factors of Garment Pattern Design Based on Quantification Theory** . . . . . 477  
Zhaowei Su, Yuhui Wei, and Long Sun

**Design of Feed Mechanism Based on Computer Cooperative Human-Computer Interaction Design Concept** . . . . . 485  
Zijing Wang

**Research on the Environment Character**

**Study on Life Prediction Method of MOSFET Thermal Environment Experiments Based on Extended Kalman Filter** . . . . . 495  
Ke Li, Yuxiang Zhang, Shimin Song, Zhijian Zhao, and Lijing Wang

**Research and Application of Multi-node Wireless Skin Temperature Measurement System** . . . . . 505  
Chenming Li and Yuhong Shen

**Research on Calculation Method of Aircraft Skin Temperature Based on Parameter Sensitivity Analysis** . . . . . 513  
Yi Cao

**Research on Adaptive Anti-interference of Fire Control Radar Network** . . . . . 523  
Jiang Luo, Yanyan Ding, Boqi Wang, and Wei Yu

**Study of Fire Control Radar Technology Countering Electronic Attack** . . . . . 531  
Wei Yu, Xiaolong Liang, Yan Sun, Jiang Luo, and Shilei Xin

**Experimental Study on Color Optimization of Fighter Cockpit Interior Decoration** . . . . . 539  
Jian Du, Xiaochao Guo, Duanqin Xiong, Yanyan Wang, Wei Pan, Shuang Bai, Liu Yang, and Juan Liu

**The Construction of Marine Combat Flight Environment Based on 4D Simulation Technology** . . . . . 555  
Yishuang Zhang, Yan Zhang, Fei Peng, Yang Liao, Huamiao Song, Xueqian Deng, Duanqin Xiong, Juan Liu, and Liu Yang

**Spacecraft Multifunctional Micro-vibration Environment Laboratory** . . . . . 561  
 Yao Wu, Tingfei Yan, Guiqian Fang, Xinming Li, Jungang Zhang, Lei Wang, and Bo Wei

**Study on the Paving Density of Lunar Soil Simulant in the Indoor Ground Test of Lunar Rover** . . . . . 571  
 Yanjing Yang, Shichao Fan, and Shuhong Xiang

**Numerical Study of Thermal Comfort for Door Area in Civil Aircraft Cabin** . . . . . 579  
 Quan Peng, Chengyun Wu, Yudi Liu, Xuhan Zhang, and Huayuan Liu

**Research on the Uniform Air Supply Technology of the Static Pressure Chamber in a Spray Room** . . . . . 589  
 Jianwu Chen, Yuan Bai, Bin Yang, Lindong Liu, Ye Tian, Yanqiu Sun, and Weijiang Liu

**Research on the Man-Machine Relationship**

**Research on the Effect of Elasticity Distribution of Five-Zone Spring Mattress on Human Supine Position Spine Form** . . . . . 599  
 Huaiqiu Zhu, Tianyi Hu, Yuding Zhu, and Ronghui Yuan

**Attentional Allocation with Low-Limb Assisted Exoskeleton During Sit-to-Stand, Stand-to-Sit, and Walking** . . . . . 609  
 Jing Qiu, Lanlan Xu, and Jinlei Wang

**The Influence of Mattress Material on Sleeping Comfort of Different Age** . . . . . 619  
 Jianjun Hou and Yuchun Zhang

**Study on Anthropomorphism in Human-Computer Interaction Design** . . . . . 629  
 Weizhen Xiao and Canqun He

**Study on the Influence of Touch Screen Button Size on Operation Performance** . . . . . 637  
 Bei Zhang, Ning Li, and Yingwei Zhou

**Research on Man-Car Relationship in 5G Era** . . . . . 645  
 Ting Tang and Qiang Zhang

**Optimal Design of Man-Machine Interface for Integrated Situation Display of Vehicle-Mounted Command and Control Equipment** . . . . . 655  
 Mingjie Wan, Jinkuang Zhang, Jianjun Gao, Zaochen Liu, Xuewei Liu, and Xiaolong Chang

**Research on Respiratory Signals for Visual Fatigue Caused by 3D Display** . . . . . 663  
Guilei Sun

**Man-Machine System Design for Rest-Office Seats** . . . . . 673  
Jiawei Tang, Canqun He, Yuhong Wei, and Chenfei Cao

**Concept Plan and Simulation of On-Orbit Assembly Process Based on Human–Robot Collaboration for Erectable Truss Structure** . . . . . 683  
Xinyue Zhu, Changhuan Wang, Meng Chen, Shiqi Li, and Junfeng Wang

**Experimental Study on Dynamic and Static Work of Shoulder-Mounted Portable Equipment Operators** . . . . . 693  
Zhaofeng Luo, Meng Kang, Peng Zhang, Han Zhang, Huashan Li, Fan Zhou, and Kun Qu

**Research on the Comfort of Human Upper Back in Different Seat Back Angles** . . . . . 701  
Ligang Luo, Tianyi Hu, and Tinghua Wu

**An Organic Design for Human–Computer Interaction** . . . . . 707  
Hongjun Zhang and Baiqiao Huang

**Human–Machine Interface Optimization Design Based on Ecological Interface Design (EID) Theory** . . . . . 715  
Guangjiang Wu, Yiqian Wu, Xi Lu, Shenghang Xu, and Chuan Wang

**Human–Computer Interaction Analysis and Prediction for Task Operating System Based on GOMS Model** . . . . . 725  
Fang Xie, Yaofeng He, Sijuan Zheng, Liang Ling, and Zhiyou Fan

**Research on Visual Perception and Modern Inheritance and Innovation of Models of Traditional Sleeping Beds in Eastern Fujian** . . . . . 733  
Hanzhou Qiu and Yun Liu

**Research on User Interface Perception Usability Evaluation of B2C Retailers in Large Appliances** . . . . . 745  
Xiaofang Yuan, Meng Zhang, Linhui Sun, and Qin Tian

**Research on the Man-Environment Relationship**

**Analysis of Human Heat Stress Response in High Temperature Environment** . . . . . 757  
Yuhong Shen and Chenming Li

**Study on Attention Characteristics of Small-Arms Shooting at Moving and Looming Targets** . . . . . 765  
Xiang Gao, Haoyuan Li, Zhengbu Liu, Xin Wang, and Yang Li

**The Survey of Hand Grinding Operation Work-Related Musculoskeletal Disorders** ..... 771  
 Zidai Xia, Yanqiu Sun, Jianwu Chen, Pei Wang, and Jie Xie

**Study on Pilots’ Color Requirements for See-Through Displays in Desert Flight** ..... 779  
 Duanqin Xiong, Tao Jiang, Liu Yang, Yanyan Wang, Xiaochao Guo, Jian Du, Yu Bai, Fang Su, Wen Dong, Rong Lin, and Juan Liu

**Analysis of the Diffusion of Cough Particles in Non-full Load Cabin** ..... 789  
 Xianlin Shi and Xuhan Zhang

**Study on the Diffusion of Gaseous Pollutants from Passenger Cough in Aircraft Cabin** ..... 797  
 Xianlin Shi and Xuhan Zhang

**The Empirical Research of the Emotional Experience Ambulatory Assessment of Built Environment by Wearable Interactive Technologies** ..... 805  
 Liang Zhang, Xiangning Li, Lingxuan Cheng, Yuan Kang, Yu Zhang, and Qi Guo

**Study on the Effect of 12-h Flight Simulated on Visual Function** ..... 815  
 Dawei Tian, Feng Wu, Haibo Sheng, Yange Zhang, Qin Yao, Bin Ma, Bin Li, Fengfeng Mo, and Lue Deng

**Research on the Machine-Environment Relationship**

**Evaluation and Analysis of Intelligent Early Warning System in Crowded Places** ..... 825  
 Qiquan Wang, Meiming Liu, Haibo Xu, Yanhua Meng, Ping Chen, Yu Zhu, and Xi Sun

**Application of RULA to Research the Ergonomics Risk of Hand-Held Grinding Operation** ..... 833  
 Yanqiu Sun, Zhenlong Lu, Jianwu Chen, Bin Yang, Weijiang Liu, and Zidai Xia

**Analysis of the Fighter Pilots Acceleration Tolerance Selection Method and Results** ..... 841  
 Rong Lin, Baohui Li, Yan Xu, Lihui Zhang, Hong Wang, Xiaoyang Wei, Yifeng Li, Jinghui Yang, Xichen Geng, Liu Yang, Juan Liu, Duanqin Xiong, and Zhao Jin

**Study on the Impact and Countermeasure of Plateau Alpine Region on Shooting of a Type of Light Weapons** ..... 847  
 He Wu, Xiang Gao, Zhengbu Liu, Yanyan Ding, Haoyuan Li, and Xin Wang

**Research on the Overall Performance of Man-Machine-Environment System**

**Study on the Organic Integration of High Intensity Interval Training Regime and Physical Fitness Training of Special Operation Forces** . . . . . 857  
 Chunlai Wang

**Study on Training of 400-m Armed Island-Landing Obstacles** . . . . . 867  
 Min Chen, Huifang Wang, Zhengbu Liu, Xiang Gao, Xin Wang, and Ming Kong

**Application of Virtual Reality Technology in Man-Machine Interactive Equipment Virtual Maintenance System** . . . . . 875  
 Mingjie Wan, Xiaolong Chang, Yuhui Li, Zaochen Liu, and Shiyong Ma

**Research on Technical Method of Cognitive Behavior Training During the Maritime Flight and Its Effect Evaluation** . . . . . 881  
 Yan Zhang, Yishuang Zhang, Yang Liao, Fei Peng, and Liu Yang

**Industrial Robot Training Platform Based on Virtual Reality and Mixed Reality Technology** . . . . . 891  
 Zhe Chen, Zhuohang Cao, Peili Ma, and Lijun Xu

**An Oversea Flight Preadaptive Training System-Based 4D Scene** . . . . . 899  
 Liu Yang, Yan Zhang, Yishuang Zhang, Duanqin Xiong, Yang Liao, Juan Liu, Xueqian Deng, and Hua Guo

**Analysis on Countermeasure of Troops Delicacy Management in the Process of the Newly-Typed Army Construction** . . . . . 909  
 Zaochen Liu, Peng Gong, Xiaoping Wang, Yujin Wang, and Dongdong Cui

**A Method for Evaluating the Level of Shooting that Attenuates the Effect of Small Arms on Accuracy** . . . . . 917  
 Xin Wang, Haoyuan Li, Xiang Gao, Min Chen, Ming Kong, and He Wu

**On the Re-understanding and Prospect of Warfighting Experiment** . . . . . 925  
 Boqi Wang, Jiang Luo, Wei Yu, and Hongjun Cheng

**Research on the Method of Aviation Maintenance Work Based on Hall’s Three-Dimensional Structure** . . . . . 931  
 Bing Zhao and Haiming Li

**The Use of Unmanned Aerial Vehicle in Military Operations** . . . . . 939  
 Huifang Wang, Hongjun Cheng, and Heyuan Hao

**The Construction Method and Research of Military Online Courses** . . . . . 947  
 Hai Chang, Shuai Mu, and Rui jie Wang

**Effectiveness Evaluation of VTS Measures on Pilot Candidates Selection** . . . . . 953  
 Yu Bai, Qingfeng Liu, Huifeng Ren, Xiaochao Guo, Duanqin Xiong, Yan Zhang, Guowei Shi, and Yanyan Wang

**Research on Internet of Things in Space Flight Training Simulation** . . . . . 961  
 Shang Huan, Suqin Wang, and Shaoli Xie

**Study on Optimization Design for Man–Machine Combination of a Self-propelled Anti-aircraft Gun Vehicle (SODMMCS PAGV)**. . . . . 973  
 Jiwen Sun, Heyuan Hao, Jinxin Li, Junlong Guo, Tao Li, JianFeng Li, Ke Zhang, and Pengdong Zhang

**Research on the Designing of Guiding System of Tiexi Workers’ Village in Shenyang Under Industrial Culture** . . . . . 981  
 Zize Guo, Yang Liu, Guojing Wu, Zhaoding Kun, and Liyi Han

**Assessment on the Availability of Domestic MMORPG Games Official Web Site Based on Eye Movement** . . . . . 993  
 Xiaofang Yuan, Yuan Yuan, Linhui Sun, and Lv yuan Sun

**Reliability Modeling and Analysis of Teleoperation System with Path-Dependence Effect Considered** . . . . . 1003  
 Shanshan Zhang, Xiaopeng Li, Wei Zhang, Wenming Zhou, Sha Qin, Lu Chen, and Yi Xiao

**Framework of Performance Shaping Factors for Human Reliability Analysis of Digitized Nuclear Power Plants** . . . . . 1013  
 Li Zhang, Jianqiao Liu, and Yanhua Zou

**Preliminary Establishment of Emotion-Inducing Library of Chinese Folk Music and Embodying Effect in Emotion Inducing** . . . . . 1021  
 Bo Wang, Hong Yuan, Huijiong Yan, Changhua Jiang, and Shaowen Ding

**Design and Research on Guide Blind Device Based on User Experience** . . . . . 1029  
 Jiani Zhang, Xinyu Shi, Xinqin Jin, Fengfeng Li, and Xin Chen

**Theory and Application Research**

**Analysis of Differences Between ISO and China Ergonomics Standards** . . . . . 1039  
 Zhenlong Lu and Yanqiu Sun

**Analysis on Core Capabilities and Key Technologies of Future Air Defense Anti-missile Operations** . . . . . 1047  
 Jinxin Li, Zhenguo Mei, Qian Shen, and Tao Li

**Research on the System Architecture of Scientific Data Management** . . . . . 1055  
Rui Man, Guomin Zhou, and Jingchao Fan

**Military Applications of Artificial Intelligence** . . . . . 1067  
Liang Du, Guangdong Li, Hai Chang, and Heyuan Hao

**Multi-dimensional Safety of Intelligent and Connected Vehicles for Future Traffic Scenarios** . . . . . 1073  
Quan Yuan and Junwei Zhao

## About the Editors

**Professor Shengzhao Long** is the founder of the Man-Machine-Environment System Engineering (MMESE), the chairman of the Man-Machine-Environment System Engineering (MMESE) Committee of China, the chairman of the Beijing KeCui Academy of Man-Machine-Environment System Engineering (MMESE), and the former director of Ergonomics Laboratory of Astronaut Research and Training Center of China. In October 1992, he is honored by the National Government Specific Allowance.

He graduated from the Shanghai Science and Technology University in 1965, China and in 1981, directing under famous Scientist Xuesen Qian, founded MMESE theory. In 1982, he proposed and developed human fuzzy control model using fuzzy mathematics. From August 1986 to August 1987, he conducted research in Man-Machine System as a visiting scholar at Tufts University, Massachusetts, USA. In 1993, he organized Man-Machine-Environment System Engineering (MMESE) Committee of China, published “Foundation of theory and application of Man-Machine-Environment System Engineering”(2004) and “Man-Machine-Environment System Engineering”(1987), and edited “Proceedings of the 1st—19th Conference on Man-Machine-Environment System Engineering”(1993–2019). e-mail: [shzhlong@sina.com](mailto:shzhlong@sina.com)

**Dr. Balbir S. Dhillon** is a professor of Engineering Management in the Department of Mechanical Engineering at the University of Ottawa, Canada. He has served as a chairman/director of Mechanical Engineering Department/ Engineering Management Program for over 10 years at the same institution. He has published over 345 (i.e., 201 journals + 144 conference proceedings) articles on reliability, safety, engineering management, etc. He is or has been on the editorial boards of nine international scientific journals. In addition, he has written 34 books on various aspects of reliability, design, safety, quality, and engineering management published by Wiley (1981), Van Nostrand (1982), Butterworth (1983), Marcel Dekker (1984), Pergamon (1986), etc. His books are being used in over 85 countries, and many of them are translated into languages such as German, Russian,



and Chinese. He has served as the general chairman of two international conferences on reliability and quality control held in Los Angeles and Paris in 1987.

He has served as a consultant to various organizations and bodies and has many years of experience in the industrial sector. At the University of Ottawa, he has been teaching reliability, quality, engineering management, design, and related areas for over 29 years, and he has also lectured in over 50 countries, including keynote addresses at various international scientific conferences held in North America, Europe, Asia, and Africa. In March 2004, he was a distinguished speaker at the Conference/Workshop on Surgical Errors (sponsored by White House Health and Safety Committee and Pentagon), held at the Capitol Hill (One Constitution Avenue, Washington, D.C.).

He attended the University of Wales where he received a BS in electrical and electronic engineering and an MS in mechanical engineering. He received a Ph.D. in industrial engineering from the University of Windsor. e-mail: [dhillon@genie.uottawa.ca](mailto:dhillon@genie.uottawa.ca)

# **Research on the Man Character**

# Research on the Integrated Situation Analysis of Ship Mariners Team



Kun Yu

**Abstract** The situation of mariners team has an important influence on the ship operation. The decrease of the integrated situation of ship mariners team will affect the safety and efficiency of ship operation. The integrated situation analysis model of ship mariners team is researched in this paper, established based on hierarchical architecture, indexes, weight, data, and mapping relation. According to the composition of SHEL model, the architecture of situation analysis for mariners team is established, covering liveware and software of ship mariners team. The architecture validation method is constructed to test the completeness and the redundancy, and to test the necessity, identification, and feasibility of mariners team indexes in architecture construction. The analysis indexes of integrated situation analysis for mariners team is established, which can provide specific feedback on the situation information of mariner individual, mariners team, management, culture, and other aspects. The research results are significance for the analysis and understanding of situation of ship mariners team.

**Keywords** Ship mariners team · Situation · SHEL model · Analysis indexes

## 1 Introduction

The ship is a complex integration of command, operation and monitoring, navigation, management, and other functions. Moreover, the working environment in ship is different from that on land in terms of swing, jolt, and closure. In ship system, the ship mariners team is the most positive factor, but also the most unstable and difficult to control influence factor. Mistakes or unsafe behaviors of the mariners team usually lead to ship accidents [1]. The statistics and analysis of ship accidents' causes show that human causes accounted for an important proportion. In 2009, a domestic shipping company made a statistical analysis of ship accidents from 2003 to 2008, shown that 86% of the accidents involved human causes, and 95% were

---

K. Yu (✉)

China Ship Development and Design Center, 430064 Wuhan, China  
e-mail: [kunyu2013@163.com](mailto:kunyu2013@163.com)

© The Editor(s) (if applicable) and The Author(s), under exclusive license to Springer Nature Singapore Pte Ltd. 2021

S. Long and B. S. Dhillon (eds.), *Man-Machine-Environment System Engineering*, Lecture Notes in Electrical Engineering 645, [https://doi.org/10.1007/978-981-15-6978-4\\_1](https://doi.org/10.1007/978-981-15-6978-4_1)

caused by human causes [2]. The actual situation proves that more attention should be paid to the mariners team in ship. In recent years, management, organization, and cooperative relationship of ship mariners team have been researched to maximize team performance [3]. Typical important research projects include the ship SRDs system set up by British ministry defense and the MARs project plan, sorting out and integrating various issues involved in ship, and taking human research as an important link in ship system design, to improve the priority of human factors in ship projects [4]. Research and analysis of ship mariners team identifies the integrated situation and existing problems and defects. Scientific and reliable integrated situation analysis results can effectively assist to make reasonable decisions for ship mariners team and can provide reliable basis data to improve and optimize the ship mariners team.

## 2 Situation Analysis Model for Ship Mariners Team

The integrated situation model of ship mariners team includes five basic elements: hierarchical architecture, indexes, weight, data, and mapping relation. The mathematical model is expressed in (1).

$$S = f(H, I, W, D) \quad (1)$$

In which,  $H$  is the hierarchical architecture of integrated situation,  $I$  is the indexes system in architecture construction of ship mariners team,  $W$  is the weight of indexes,  $D$  is the analysis data, and  $f$  is the mapping relationship of  $H, I, W, D$  of integrated situation model for ship mariners team.

## 3 Architecture of Situation Analysis for Mariners Team

### 3.1 Architecture Based on SHEL Model

The SHEL model is proposed to summarize the research scope of human factor problems in complex systems. The name is composed of the first letter of four words: Hardware, Software, Environment and Liveware [5]. In SHEL model, “liveware” refers to the mariners team members, including the captain, deputy chief officer, helmsman, bell operator, etc., who conduct command, management, and specific equipment operation; “software” refers to organization management, specification, culture, value, etc. Therefore, Fig. 1 shows the architecture construction of situation analysis for ship mariners team based on SHEL model. Research results on the relationship between psychosomatic diseases and psychological stress of ship mariners team members show that the incidence of psychological diseases of team members is as high as 49.9% [6]. Therefore, it should be to ensure the mariner’s mental health

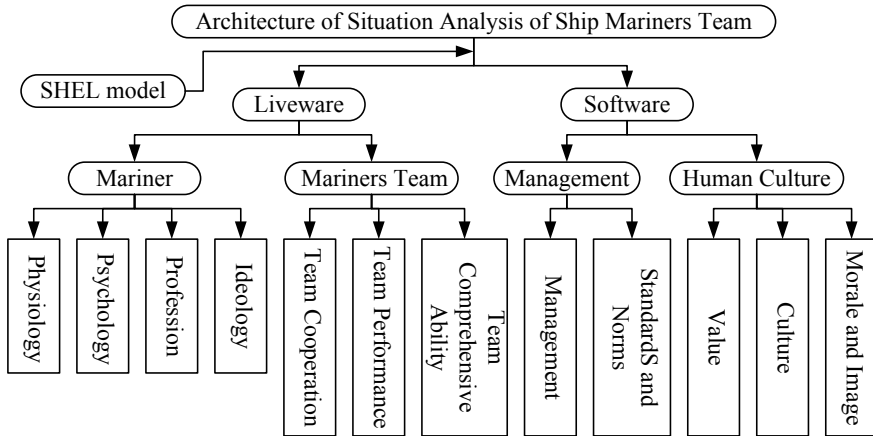


Fig. 1 Architecture construction of situation analysis based on SHEL model

by evaluating cognitive ability, perceptual ability, emotional state, and others. The advantage of the team is that it can respond to tasks quickly and collaboratively, pool wisdom of members through the exchange of information, knowledge and experience [7]. Team capability refers to the ability of the team to allocate, organize, and coordinate resources and achieve the goals, which involves the basic profession ability, information ability, planning and execution ability, resource coordination and allocation ability, etc. [8]. Team performance refers to the team’s task execution efficiency, team task goal consistency, and result quality.

In which, organizational management is the leadership and management of the team, mainly including organizational management, resource management, consulting, and training system. Organizational culture, morale, image, and value idea belong to the humanities software: Organizational culture is all the team members formed in work and life of the tradition, habit and atmosphere, reflected in the team, care about each other, mutual respect, love, team identification and willing to work in team, team reputation, attract and acceptance to the individual, and the team together for the whole goals and tasks, etc. The value concept is the value idea that the team follows personally, behavior way, establish correct, outstanding team value concept, can enhance cohesive force, enhance the team’s professional ethics, make up the shortage of material incentive, and enhance team’s job satisfaction. Organizational image is the overall impression and evaluation of an organization. The morale of the organization reflects the mental state of the whole organization in carrying out tasks, which is reflected by the concerted efforts of the team.

### 3.2 Validation Method

The validation method mainly used to test the advantages and disadvantages of the architecture construction of situation analysis for ship mariners team. For the analysis of architecture construction, the completeness test is mainly to check whether the architecture construction covering the factors that need to be analyzed and whether there are any omissions or not considered. The redundancy test means to check whether the content of the analysis factors of the architecture construction is duplicated. The test of completeness and redundancy is to seek the balance between completeness and simplicity. Set up its analysis factors set  $T' = \{t'_1, t'_2, \dots, t'_m\}$ ; set up the integrated indexes system to analysis factors set  $T = \{t_1, t_2, \dots, t_n\}$ . The completeness coefficient  $A$  of architecture construction is shown in (2). In which, correspondence model  $f$  is correspondence model. When the corresponding relationship between analysis factors and indexes,  $C(t_i, t'_j) = 1$ ; when there is no correspondence,  $C(t_i, t'_j) = 0$ .

$$A = \frac{1}{m} f(T \rightarrow T'), f(T \rightarrow T') = \sum_{j=1}^m \sum_{i=1}^n C(t_i, t'_j) \quad (2)$$

In the practical integrated analysis, the completeness coefficient of architecture construction needs to meet  $A \geq 1$ , to demonstrate that the integrated analysis architecture covers the factors that need to be analyzed.

The redundancy test of the integrated architecture construction is carried out by using the statistical method of repeatability between analysis factors. Establish the corresponding overlap matrix  $R$  of the analysis factors. When elements  $t_i$  is completely related to  $t_j$ ,  $r_{ij} = 1.0$ ; when there is no overlap between  $t_i$  and  $t_j$ ,  $r_{ij} = 0$ . The redundancy coefficient  $C$  of architecture construction is shown in (3). In principle, require  $C < n\rho$ ,  $\rho$  is the test coefficient. When the  $C$  is closer to 0, the redundancy of architecture construction is lower.

$$C = \sum_{i=1}^n C_i, C_i = \frac{1}{n-1} \left( \sum_{j=1}^n r_{ij} - 1.0 \right) \quad (3)$$

The necessity, identification, and feasibility of mariners team in architecture construction need to be tested. There are  $n$  analysis indexes and  $p$  evaluators participate in evaluation. Five grades  $k = 1, 2, 3, 4, 5$  represent the indexes necessity. Necessity degree is to test the purpose and necessity of indexes, and to verify the necessity degree from concentration degree and dispersion degree [9]. Combined with the concentration degree and dispersion degree, the necessity degree coefficient  $V_i$  of the  $i$ th analysis index is shown in (4).  $F_i$  is the concentration of evaluators' comments on necessity of the  $i$ th analysis index. The smaller the  $\delta_i$ , the more concentrated the judgment.

$$V_i = \delta_i / F, F_i = \frac{1}{p} \sum_{k=1}^5 E_k P_{ik}, \delta_i = \left( \frac{1}{p-1} \sum_{k=1}^5 P_{ik} (E_k - F_i)^2 \right)^{1/2} \quad (4)$$

Identification refers to the ability of indexes to distinguish certain features and values of the analyzed object. A high degree of identification means that the analysis index has a good effect on the description of the analysis object, while a low degree of identification will make it impossible to judge the advantages and disadvantages. The identification coefficient  $B_i$  of the  $i$ th index is shown in (5). The  $b_k$  is the necessary degree of grade  $k$  of the  $i$ th index. It requires  $B_i \geq 3$ , which indicates that the index has high identification.

$$B_i = \frac{1}{p} \sum_{k=1}^5 b_k P_{ik} \quad (5)$$

Feasibility is based on whether the analysis data can be correctly obtained, some indexes that cannot obtain accurate data, or the acquisition cost of analysis data is significantly greater. Value analysis method is used to judge and compare the relationship between input and output effects to determine the feasibility of the analysis indexes. The feasibility coefficient  $U_i$  of the  $i$ th index is shown in (6). The  $T_i$  is input value of the  $i$ th index,  $S_i$  is revenue value of the  $i$ th index.

$$U_i = \frac{\sum_{j=1}^p S_j P_{ij}}{\sum_{j=1}^p T_j P_{ij}} \quad (6)$$

In principle, it requires  $U_i > 1.0$ , which indicates that the  $i$ th analysis index is feasible. When  $U_i \geq 1.25$ , it indicates that the  $i$ th analysis index has higher feasibility.

#### 4 Analysis Indexes of Situation Analysis for Mariners Team

The situation analysis indexes system is the premise and basis of effective integrated analysis. There are many indexes and a complex hierarchical structure. It is impossible to obtain integrated and reasonable result. Integrated analysis requires accurate aggregation of multi-level, multi-indexes, and group analysis opinions, and the weight distribution of analysis. The method is proposed to calculate the comprehensive clustering coefficient of the integrated evaluation value. The integrated analysis result  $\sigma_i^k$  is shown in (7). The  $\eta_j$  is the clustering weight of index.

$$\sigma_i^k = \sum_{j=1}^m f_j^k(x_{ij}) \eta_j \quad (7)$$

The initial situation analysis indexes system is established based on the architecture. The psychological traits as an example include team perception ability, thinking ability, language ability, self-discipline, and so on. Psychological traits contain 15 initial analysis indexes: perception (1), memory (2), thinking ability (3), language skills (4), self-discipline (5), hostility (6), relationships (7), emotional stability (8), terrorism (9), focus (10), the self-confidence (11), job satisfaction (12), nervous state (13), self-harm and self-abuse (14), and symptoms of psychosis (15). Qualitative method is adopted to test the necessity, identification, and feasibility. The initial situation analysis indexes of the psychological traits contain 15 initial analysis indicators. The necessity, identification, and feasibility of initial situation analysis indexes of the psychological traits were evaluated by ten evaluators. Table 1 shows the necessary and identification appraisal value of initial indexes for psychological traits. Table 2 shows the input and income appraisal value of initial indexes for psychological traits.

According to the above formula and data, the concentration vector of the staff opinion of indexes necessity  $F$ , dispersion vector  $\delta$ , necessary degree coefficient vector  $V$  are as follows:

$$F = [4.0, 3.8, 3.6, 4.0, 4.2, 1.8, 4.0, 3.8, 1.9, 4.0, 4.1, 4.2, 4.0, 1.6, 4.2]$$

$$\delta = [0.67, 1.03, 0.69, 0.82, 0.92, 0.79, 0.47, 1.03, 0.73, 0.47, 0.74, 0.79, 0.67, 0.84, 0.63]$$

$$V = [0.17, 0.27, 0.19, 0.20, 0.22, 0.44, 0.12, 0.27, 0.39, 0.12, 0.18, 0.19, 0.17, 0.53, 0.15]$$

Set boundary value of  $F_i$  is 2, the limit  $V_i \leq 0.63 / 2 = 0.315$ .  $V_6 = 0.43 > 0.315$ ,  $V_9 = 0.39 > 0.315$ ,  $V_{14} = 0.53 > 0.315$ .

The identification coefficient vector  $B$ :

**Table 1** Necessary and identification appraisal value of initial indexes for psychological traits

	1	2	3	4	5	6	7	8	9	10
1	(4,4)	(5,5)	(4,3)	(3,4)	(4,4)	(4,5)	(4,3)	(3,5)	(4,5)	(5,5)
2	(5,5)	(3,5)	(3,4)	(3,3)	(5,3)	(4,4)	(5,5)	(2,5)	(4,4)	(4,4)
3	(4,3)	(4,4)	(4,3)	(3,4)	(3,4)	(5,3)	(3,3)	(3,2)	(4,3)	(3,5)
...	...	...	...	...	...	...	...	...	...	...
15	(5,3)	(3,4)	(5,5)	(4,5)	(4,4)	(5,3)	(4,3)	(4,3)	(4,3)	(4,5)

**Table 2** Input and income appraisal value of initial indexes for psychological traits

	1	2	3	4	5	6	7	8	9	10
1	(3,5)	(3,3)	(2,4)	(4,5)	(3,5)	(2,3)	(1,3)	(4,4)	(4,5)	(3,4)
2	(2,4)	(3,4)	(4,4)	(5,5)	(3,4)	(2,4)	(1,2)	(3,4)	(3,4)	(3,5)
3	(2,3)	(3,3)	(2,2)	(4,4)	(2,4)	(1,2)	(2,2)	(3,4)	(3,3)	(3,4)
...	...	...	...	...	...	...	...	...	...	...
15	(2,4)	(4,4)	(3,5)	(2,4)	(4,4)	(2,4)	(3,4)	(5,4)	(3,4)	(4,4)



$$B = [4.3, 4.2, 3.4, 3.5, 4.0, 3.7, 3.6, 3.2, 3.5, 4.3, 3.8, 3.6, 3.5, 4.1, 3.8]$$

The feasibility coefficient vector  $U$ :

$$U = [1.41, 1.38, 1.24, 1.16, 1.29, 1.38, 1.27, 1.44, 1.33, 1.52, 1.71, 1.4, 1.31, 1.37, 1.28]$$

The elements in  $U$  are all greater than 1, and most of them are greater than 1.25. The statistical benefits are basically greater than the statistical costs, indicating that the indexes are highly feasible and the data can be obtained correctly. In  $V, V_6, V_9, V_{14} > 0.315$ , hostile psychology and terrorist activities are rare among the psychological characteristics. The necessary degree coefficients of hostility (6), terrorism (9), and self-harm and self-abuse (14) of mariners team are excluded. Finally, the determined analysis indexes of psychological traits for mariners team are shown in Table 3.

## 5 Conclusion

The integrated situation analysis model of ship mariners team is researched in this paper. First, the established integrated situation model of ship mariners team has a systematic structure, which can comprehensively cover the situation analysis elements and guide the integrated situation analysis. Second, architecture of situation analysis for mariners team is constructed based on SHEL model, which can comprehensively cover the four aspects of mariner: individual, mariners team, management and human culture, and describe the relationship between mariners, team members, and the working environment of team members. Third, the architecture validation method can be used to systematically test the completeness and the redundancy of architecture of situation analysis, and to test the necessity, identification, and feasibility of mariners team indexes in architecture construction. Fourth, the analysis indexes of integrated situation analysis for mariners team can provide specific feedback on the situation information of mariner individual, mariners team, management, culture, and other aspects.

**Table 3** Layout verification indexes for nuclear power control room

Mariners	Physical traits	Psychological traits	Professional ability	Ideological quality
Indexes	<ol style="list-style-type: none"> <li>1. Heart function index</li> <li>2. The vital capacity</li> <li>3. The vision</li> <li>4. Listening</li> <li>5. Body strength index</li> <li>6. Athletic ability index</li> <li>7. Physical ability index</li> <li>8. Symmetrical body shape</li> <li>9. Flexibility of body movement</li> <li>10. Physical agility and coordination</li> <li>11. Metabolic status of the body</li> <li>12. The body's ability to regulate physiology</li> <li>13. Fatigue tolerance</li> <li>14. Your body's ability to adapt to the environment</li> </ol>	<ol style="list-style-type: none"> <li>1. Perception</li> <li>2. Memory</li> <li>3. Thinking ability</li> <li>4. Language skills</li> <li>5. Self-discipline</li> <li>6. Relationships</li> <li>7. Emotional stability</li> <li>8. Focus</li> <li>9. The self-confidence</li> <li>10. Job satisfaction</li> <li>11. Nervous state</li> <li>12. Symptoms of psychosis</li> </ol>	<ol style="list-style-type: none"> <li>1. Professional theoretical knowledge</li> <li>2. Professional skills and specialties</li> <li>3. Work experience</li> <li>4. Learning experiences</li> <li>5. Job familiarity</li> </ol>	<ol style="list-style-type: none"> <li>1. Ideological cultivation</li> <li>2. Ideological awareness</li> <li>3. Work style</li> <li>4. Sense of responsibility</li> <li>5. Occupational safety awareness</li> <li>6. Dedication to the position</li> </ol>

(continued)

**Table 3** (continued)

Mariners team	Team comprehensive ability	Team cooperation	Team performance
Indexes	<ol style="list-style-type: none"> <li>1. Basic professional and technical ability of team</li> <li>2. Ability to plan and achieve team goals</li> <li>3. Basic profession ability of team</li> <li>4. Ability of team organization and coordination</li> <li>5. Team interpersonal coordination skills</li> <li>6. Communication and coordination skills of team</li> <li>7. Ability to coordinate the goals of the whole team</li> <li>8. Ability to coordinate differences among team members</li> <li>9. Human resource allocation and control ability</li> <li>10. Ability to allocate and control team financial resources</li> <li>11. Allocation and control of team skills and resources</li> <li>12. Team organization and leadership skills</li> <li>13. Team task management</li> <li>14. Team command execution ability</li> <li>15. Team emergency response capability</li> <li>16. Team problems solving ability</li> </ol>	<ol style="list-style-type: none"> <li>1. Responsibility distribution of team members is reasonable</li> <li>2. Reasonable workload distribution of team members</li> <li>3. Definition of team's role objectives</li> <li>4. Mutual familiarity and understanding between members</li> <li>5. Team respect and friendship</li> <li>6. Team members are interdependent in their work</li> <li>7. Information, knowledge and experience sharing among team members</li> <li>8. Information and knowledge exchange between team members</li> <li>9. Mutual trust and support among team members</li> <li>10. Complementary specialities among team members</li> <li>11. Complementary personalities among team members</li> <li>12. Harmonious interpersonal relationship of the whole team</li> </ol>	<ol style="list-style-type: none"> <li>1. Consistency of team objectives</li> <li>2. Team task execution efficiency</li> <li>3. Ability to solve problems quickly</li> <li>4. Team is motivated to perform tasks</li> <li>5. Proficiency in performing tasks as a team</li> <li>6. Security of team performance</li> <li>7. Standardized team execution procedures</li> <li>8. Fewer execution errors</li> <li>9. Team spirit</li> <li>10. Satisfaction of team task results</li> <li>11. Teamwork sense of mission and responsibility</li> </ol> <p>Job satisfaction of team members</p>

(continued)

Table 3 (continued)

Soft culture	Organizational Management	Standardizing system	Value concept	Organizational culture	Organizational morale and image
Indexes	<ol style="list-style-type: none"> <li>1. Organizational management mechanism</li> <li>2. Team resource management</li> <li>3. Information resource management</li> <li>4. Material resources management</li> <li>5. Authority of leadership</li> <li>6. Leadership affinity</li> <li>7. Team spirit motivation</li> <li>8. Emotional stimulation of team members</li> <li>9. Job training mechanism</li> <li>10. Work consultation mechanism</li> </ol>	<ol style="list-style-type: none"> <li>1. Complete normative system</li> <li>2. Complete operational task procedures</li> <li>3. Standard of team conduct is complete</li> <li>4. Standardization of work process</li> <li>5. Standardization of work output</li> <li>6. Well-regulated leadership</li> <li>7. Team succession procedures are complete</li> <li>8. Troubleshooting rules</li> <li>9. Rules for inter-team supervision</li> <li>10. Rules and regulations are suitable for seafarers to learn</li> </ol>	<ol style="list-style-type: none"> <li>1. Team life values</li> <li>2. Professional values</li> <li>3. Social ideological values</li> <li>4. Identify with the concept of hard work</li> <li>5. Identify with the concept of career dedication</li> <li>6. Value recognition of social system</li> <li>7. Recognize the value of real life</li> </ol>	<ol style="list-style-type: none"> <li>1. Organizational work philosophy</li> <li>2. Organize work mission</li> <li>3. Organizational dedication</li> <li>4. Organizational integrity</li> <li>5. Harmonious organization</li> <li>6. Organizational affinity</li> <li>7. Organizational ethics</li> <li>8. Competitive culture</li> <li>9. Executive culture</li> <li>10. Service culture</li> </ol>	<ol style="list-style-type: none"> <li>1. Organizational identity</li> <li>2. Organization and action</li> <li>3. Organizational cohesion</li> <li>4. Organize mental strength</li> <li>5. Team features</li> <li>6. Act confident</li> <li>7. Work etiquette</li> <li>8. Organization of social responsibility image</li> </ol>

## References

1. Mullai A, Paulsson U (2011) A grounded theory model for analysis of marine accidents. *Accid Anal Prev* 43:1590–1603
2. Tianxue Y (2019) On giving play to the initiative of seafarers under the new circumstances of ship management. *China Maritime* 2019(8):31–33
3. Xi YT, Chen WJ, Fang QG, Hu SP (2010) HFACS model based data mining of human factors-a marine study. China, IEEE International conference on industrial engineering and engineering management. Macao, pp 1499–1504
4. Ranasinghe S, Osmond JP (2005) The structure of human factors requirements in warship SRDs. RINA, Royal institution of naval architects international conference-human factors in ship design, safety and operation. London, United kingdom 83–90
5. Hawkins FN (1995) Human factors in flight. Avebury aviation, Hants, pp 18–24
6. Yanhong S (2017) To explore the influence of psychological factors on ship safety. *Navigation* 3:74–75
7. Ying S (2011) Human factors. Tsinghua University Press, Beijing, pp 179–184
8. Ning L, Hua L (2010) Study on comprehensive evaluation method of team capability based on DEA. In: 2010 International conference on machine learning and cybernetics. Qingdao, China, vol 4, pp 1987–1992
9. Jun Y, Yuanyuan L (2008) Screening method of indicator system based on rough set theory. The 3rd International conference on product innovation management. Wuhan, China, pp 1308–1311

# An Investigation on the Demand of Psychological Data Collection in Military Pilots



Yang Liao and Huamiao Song

**Abstract** To investigate the demand of psychological data collection in military pilots, questionnaire investigation was implemented and included demographic data and rank of psychological indicators. Four kinds of psychological indicators, such as personality trait, cognitive ability, emotional state, motivation, were ranked among 1–4 in four different application scenarios. The demands of psychological data collection were different among different application scenarios. Personality trait was the most important indicators in psychological selection and psychological appraisal. Emotion state was the most important indicators in mental training and mental health service. Cognitive ability was played an important role in all the four application scenarios. These results suggest that psychological data collection should be specific for the particular application scenarios and then the collected data would maximize its reference value.

**Keywords** Psychological data · Demand of collection · Psychological selection · Mental training · Psychological appraisal · Mental health service

## 1 Introduction

With a high-performance fighter aircraft equipped the air force, the mechanical equipments were more complex and manoeuvrability of aircraft was increasing, excellent cognitive ability and steady psychological quality became essential to pilot. To ensure the pilots' ability fulfil the needs, psychologist should construct an efficient psychological indicator system for evaluation. Based on multidimensional data, we can then clarified how to select a suitable person to be pilot cadet and learned ways to assessment train effectiveness [1]. Additionally, with increased training time and

---

Y. Liao · H. Song (✉)  
Air Force Medical Center, Fourth Military Medical University, Beijing 100142, China  
e-mail: [shmiao@163.com](mailto:shmiao@163.com)

intensity, military pilots faced multiple stressors. Mental issues and psychiatric disorders among military pilots have become growing challenges; accurate and sufficient data are necessary for quantized psychological appraisal and mental health service.

Psychological data are multidimensional, such as personality and mental health scale data, cognitive data, electrophysiological data, neuroimaging data and biochemical data et al. [2–4]. Without screen out appropriate indicators, the collection and analysis of psychological data among military pilot would be difficult and useless. Indeed, base on specific needs of different application scenarios, identify which indicators are important and select particular psychological indicators for evaluation seemed to be the appropriate solution.

In the current study, questionnaire investigation was implemented which includes demographic data and rank of psychological indicators. The importance of four kinds of psychological indicators (personality trait, cognitive ability, emotional state and motivation) was ranked among 1–4 in four different application scenarios (psychological selection, mental training, psychological appraisal and mental health service). The results would clarify which psychological data would be useful for the particular application scenarios and then the collected data would maximize its reference value.

## 2 Method

### 2.1 Participants

The systematic sampling methods were used. 57 participants, who were engaged in psychosocial service for military pilots, were recruited among different branches of air force. Three unfinished questionnaires were excluded, 54 questionnaires were effective and the effective rate was 94.74%. The duration of psychological service among the participants ranged from 1 to 18 years, average at  $3.83 \pm 3.96$  years.

### 2.2 Tools

Self-made scale was used to investigate the demand of psychological data collection among military pilots. Four main application scenarios were selected, such as psychological selection, mental training, psychological appraisal and mental health service. Based on the result of competency research of military pilot, the psychological indicators were classified into four kinds in general, for instance, personality trait, emotion state, cognitive ability and motivation. Participants required to rank the importance of the four kinds of psychological indicators among 1–4 in each application scenarios.

**Table 1** Comparison of importance ranks of four kinds of psychological indicators in psychological selection

	Personality trait		Emotion state		Cognitive ability		Motivation	
	<i>N</i>	Pct (%)	<i>N</i>	Pct (%)	<i>N</i>	Pct (%)	<i>N</i>	Pct (%)
Rank 1	27	50.0	4	7.4	12	22.2	11	20.4
Rank 2	16	29.6	8	14.8	21	38.9	9	16.7
Rank 3	9	16.7	21	38.9	12	22.2	12	22.2
Rank 4	2	3.7	21	38.9	9	16.7	22	40.7
Mean rank	67.5		140.5		99.5		126.5	

### 2.3 Statistics

Ranks were analysed with Kruskal–Wallis test by SPSS 20.0 version, and the significant levels are  $P < 0.05$ .

## 3 Results

### 3.1 The Importance Ranks in Psychological Selection

As shown in Table 1, the importance rank of four kinds of psychological indicators in psychological selection arranged from high to low as: personality trait, cognitive ability, motivation, emotion state. Kruskal–Wallis test shown that  $H = 45.86$ ,  $P < 0.01$ , which indicated that there was significant difference between these ranks. Pairwise comparison shown that the mean rank of personality trait was significant higher than the mean rank of emotion state ( $P < 0.01$ , adjusted), cognitive ability ( $P < 0.05$ , adjusted) and motivation ( $P < 0.01$ , adjusted). The mean rank of cognitive ability was significant higher than the mean rank of emotion state ( $P < 0.01$ , adjusted). There was no significant difference between other indicators in pairwise comparison.

### 3.2 The Importance Ranks in Mental Training

As shown in Table 2, the importance rank of four kinds of psychological indicators in mental training arranged from high to low as: emotion state, cognitive ability, personality trait, motivation. Kruskal–Wallis test shown that  $H = 35.92$ ,  $P < 0.01$ , which indicated that there was significant difference between these ranks. Pairwise comparison shown that the mean rank of emotion state was significant higher than



**Table 2** Comparison of importance ranks of four kinds of psychological indicators in mental training

	Personality trait		Emotion state		Cognitive ability		Motivation	
	<i>N</i>	Pct (%)	<i>N</i>	Pct (%)	<i>N</i>	Pct (%)	<i>N</i>	Pct (%)
Rank 1	11	20.4	25	46.3	12	22.2	6	11.1
Rank 2	8	14.8	17	31.5	20	37.0	9	16.7
Rank 3	13	24.1	7	13.0	16	29.6	18	33.3
Rank 4	22	40.7	5	9.3	6	11.1	21	38.9
Mean rank	127.5		73.5		97.5		135.5	

the mean rank of personality trait ( $P < 0.01$ , adjusted) and motivation ( $P < 0.01$ , adjusted). The mean rank of cognitive ability was significant higher than the mean rank of motivation ( $P < 0.01$ , adjusted). There was no significant difference between other indicators in pairwise comparison.

### 3.3 The Importance Ranks in Psychological Appraisal

As shown in Table 3, the importance rank of four kinds of psychological indicators in psychological appraisal arranged from high to low as: personality trait, cognitive ability, emotion state, motivation. Kruskal–Wallis test shown that  $H = 44.48$ ,  $P < 0.01$ , which indicated that there was significant difference between these ranks. Pairwise comparison shown that the mean rank of personality trait was significant higher than the mean rank of emotion state ( $P < 0.01$ , adjusted), cognitive ability ( $P < 0.01$ , adjusted) and motivation ( $P < 0.01$ , adjusted). There was no significant difference between other indicators in pairwise comparison.

**Table 3** Comparison of importance ranks of four kinds of psychological indicators in psychological appraisal

	Personality trait		Emotion state		Cognitive ability		Motivation	
	<i>N</i>	Pct (%)	<i>N</i>	Pct (%)	<i>N</i>	Pct (%)	<i>N</i>	Pct (%)
Rank 1	34	63.0	4	7.4	7	13.0	9	16.7
Rank 2	7	13.0	14	25.9	24	44.4	9	16.7
Rank 3	9	16.7	21	38.9	14	25.9	10	18.5
Rank 4	4	7.4	15	27.8	9	16.7	26	48.1
Mean rank	64.5		128.5		106.5		134.5	

**Table 4** Comparison of importance ranks of four kinds of psychological indicators in mental health service

	Personality trait		Emotion state		Cognitive ability		Motivation	
	<i>N</i>	Pct (%)	<i>N</i>	Pct (%)	<i>N</i>	Pct (%)	<i>N</i>	Pct (%)
Rank 1	15	27.8	24	44.4	11	20.4	4	7.4
Rank 2	10	18.5	14	25.9	22	40.7	9	16.7
Rank 3	15	27.8	13	24.1	16	29.6	10	18.5
Rank 4	14	25.9	3	5.6	5	9.3	31	57.4
Mean rank	110		76.90		97.05		150.06	

### 3.4 The Importance Ranks in Mental Health Service

As shown in Table 4, the importance rank of four kinds of psychological indicators in mental health service arranged from high to low as: emotion state, cognitive ability, personality trait, motivation. Kruskal–Wallis test shown that  $H = 42.16, P < 0.01$ , which indicated that there was significant difference between these ranks. Pairwise comparison shown that the mean rank of emotion state was significant higher than the mean rank of personality trait ( $P < 0.05$ , adjusted) and motivation ( $P < 0.01$ , adjusted). The mean rank of cognitive ability was significant higher than the mean rank of motivation ( $P < 0.01$ , adjusted). There was no significant difference between other indicators in pairwise comparison.

## 4 Discussion

Select suitable candidates into training could reduce the grounding rate of pilot cadet and save training costs. According to the result in the current study, assessment of personality trait is the primary goal of psychological selection, which could help to screen out candidates with mental disorder tendency. Based on personality trait data form scale, projective test or interview, abnormal individual could be recognized. Apart from screen out standards, inclusion criteria are also necessary for selection. Competency, especially cognitive competence, is another focus. According to the previous studies of pilot selection, assessment of cognitive ability is an important part of pilot psychological selection [5]. The cognitive ability tests always include single items, such as memory task, spatial cognition task, motor control. Additionally, multitasking tests are indispensable now, and to assess situation awareness under dynamic environments are more close to actual flight activity.

On account of the result of the current study, assessment of pilots' emotion state is of great importance during mental training. Quantified data about emotional arousal or emotional stability could help to learn pilots' emotion state and its influence on

behaviour in facing stressors during flight. This assumption was supported by the previous studies about pilots' emotion [6]. Military flight as a high intensity and stress occupation, pilot needs to keep clam when incidents happen during flight training or combat. Overstrain or fear-induced to pilots would cause negative effect to flight safety and combat effectiveness [7]. Thus, the evaluation of emotion state plays a key role during pilots' mental training. Moreover, the assessment of the cognitive ability is necessary in mental training scenarios. Cognitive ability is not only part of content of mental training, but also an important indicator to evaluate training effect [8]. Previous cognitive training study carried out by US Air Force had found that transcranial direct current stimulation could improve pilots' cognitive ability, which shown that assessment of cognitive ability is an inseparable part of pilots' mental training [9].

Psychological appraisal is key part to assess whether a pilot is suitable to continue his flight occupation. The result of current study indicated that assessment of personality trait is a chief part in psychological appraisal [10]. To evaluate the integrity of personality would help to decide whether a pilot should be grounded. Pilot with personality disorder could cause disasters to flight safety affairs. Several recent investigations afterwards flight accidents of civil aviation had found that involved pilot always had abnormality in personality, which could highlight the importance of personality assessment in psychological appraisal of pilot [11].

According to the result of current study, emotion state data is most needed in mental health service scenarios. Abnormality in emotion is a high incidence symptom in most of the mental disorders. Data about emotion state could help doctor to learn the recovery progress and adjust the dosage of medicine. Besides, cognitive and personality data are also needful in mental health service. Based on cognitive data, doctors could assess whether pilots' performance had been damaged. Personality data could provide information about personality integrity. All these data would help doctors to evaluate treatment progress when offer mental health service to pilots.

## 5 Conclusion

The demands of psychological data collection were different among different application scenarios. Personality trait was the most important indicators in psychological selection and psychological appraisal. Emotion state was the most important indicators in mental training and mental health service. Cognitive ability was played an important role in all the four application scenarios. These results suggest that psychological data collection should be specific for particular application scenarios and then the collected data would maximize its reference value.

**Compliance with Ethical Standards** The study was approved by the Logistics Department for the Civilian Ethics Committee of Air Force Medical Center.

All subjects who participated in the experiment were provided with and signed an informed consent form.

All relevant ethical safeguards have been met with regard to subject protection.

## References

1. Carretta TR (2011) Pilot candidate selection method. *Aviat Psychol Appl Hum Factors* 1:3–8
2. Lennoxbuchthal M, Buchthal F, Rosenfalck P (2010) Correlation of electroencephalographic findings with crash rate of military jet pilots. *Epilepsia* 1:366–372
3. Bartram D, Dale HCA (2011) The Eysenck Personality Inventory as a selection test for military pilots. *J Occup Organ Psychol* 55:287–296
4. Meško M, Karpljuk D, Štok ZM et al (2013) Motor abilities and psychological characteristics of Slovene military pilots. *Int J Aviat Psychol* 23:306–318
5. Carretta TR (2010) Predictive validity of the air force officer qualifying test for non-rated officer specialties. *Mil Psychol* 22:450–464
6. Vine J, Uiga L, Lavric A et al (2015) Individual reactions to stress predict performance during a critical aviation incident. *Anxiety Stress Coping* 28:467–477
7. Catino M, Patriotta G (2013) Learning from errors: cognition, emotions and safety culture in the Italian air force. *Organ Stud* 34:437–467
8. Fornette P, Bardel H, Lefrançois C et al (2012) Cognitive-adaptation training for improving performance and stress management of air force pilots. *Int J Aviat Psychol* 22:203–223
9. Choe J, Coffman A, Bergstedt T et al (2016) Transcranial direct current stimulation modulates neuronal activity and learning in pilot training. *Front Hum Neurosci* 10:34
10. Callister JD, King RE, Retzlaff PD et al (1999) Revised NEO personality inventory profiles of male and female US Air Force pilots. *Mil Med* 164:885–890
11. Kelly D, Efthymiou M (2019) An analysis of human factors in fifty controlled flight into terrain aviation accidents from 2007 to 2017. *J Saf Res* 69:155–165

# Chinese Drivers' Preferred Posture for Sedans' Seat Ergonomic Design



Jiaxun You, Lipeng Qin, Peiwen Zuo, Xuelei Wang, and Chao Zhang

**Abstract** This study collected data concerning preferred driving postures for sedans of Chinese driving population, aiming for investigating the relationships between drivers' joint angles and their gender, region and anthropometry, and also finding observed optimum driving postures for Chinese drivers. Nine joint angles were measured in preferred postures to more completely describe driving postures, as were the perceptual response, with 1861 subjects. A subset of preferred joint angle range was identified through a filtering mechanism that ensured desired levels of perceptual response. It is found that gender and region both have a significant effect on all angles except torso angle. Stature, weight and sitting acromion height all have effects on different joint angles. The recommended range of 9 joint angles of preferred driving postures is obtained, and the analysis on differences between this study and the previous studies, and on reasons for those differences was conducted.

**Keywords** Sedan seat comfort · Preferred driving postures · Sedan · Perceptual response

## 1 Introduction

Specifying comfortable driving postures is essential for ergonomic design and evaluation of a driver workspace. Traditionally, vehicle designers use SAE's two-dimensional accommodation tools to design the cockpit. The anthropometric characteristics of Chinese adults are different from Europeans', not only in stature but also in segment portion based on the survey conducted by Rebiffé et al. [1].

The factors affecting preferred driving postures were stated in previous studies. Park et al. [2] and Hanson et al. [3] both investigated the effects from gender, and they drew contradictory conclusions. Hanson et al. [3] and Kyung and Nussbaum et al. [4] both discussed stature's influence on the driving postures and came to reverse results.

---

J. You · L. Qin (✉) · P. Zuo · X. Wang · C. Zhang  
China Automotive Technology and Research Center Co., Ltd., 300300 Tianjin, China  
e-mail: [qinlipeng@catarc.ac.cn](mailto:qinlipeng@catarc.ac.cn)

© The Editor(s) (if applicable) and The Author(s), under exclusive license to Springer Nature Singapore Pte Ltd. 2021

S. Long and B. S. Dhillon (eds.), *Man-Machine-Environment System Engineering*, Lecture Notes in Electrical Engineering 645, [https://doi.org/10.1007/978-981-15-6978-4\\_3](https://doi.org/10.1007/978-981-15-6978-4_3)

**Table 1** Observed information and measured anthropometric data of subjects

Anthropometric measurements	Overall	Gender		Region	
		Male	Female	North	South
	Mean (SD)				
STA (mm)	167.02(7.74)	170.40(6.24)	159.66(5.15)	168.28(7.58)	165.55(7.69)
WEI (kg)	71.92(14.76)	76.47(13.92)	62.04(11.31)	75.27(15.29)	68.02(13.09)
SST (mm)	90.90(4.23)	92.64(3.47)	87.11(3.12)	91.64(4.34)	90.05(3.94)
TRH (mm)	82.22(4.75)	83.87(4.21)	78.62(3.76)	82.17(4.59)	82.27(4.94)
SAH (mm)	60.66(3.57)	61.97(3.17)	57.80(2.56)	61.78(3.40)	59.35(3.30)
ATO (mm)	31.07(2.12)	31.91(1.83)	29.25(1.50)	31.20(2.16)	30.92(2.07)

The objective of this study is to investigate the relationships between preferred driving postures and gender, age, region, target sedan and anthropometric measurements, and to identify the key factors affecting the postures, as well as to specify the recommended ranges of male and female drivers through perceptual response filtering, which will facilitate ergonomic design and evaluation of a driver workspace and sedan seat.

## 2 Experiment Methods

### 2.1 Participants

One thousand and eight hundred and sixty-one subjects are selected from 6 cities of China which were divided into 2 regions: north and south, as the anthropometric measurement data of drivers varies between the two regions. The subjects include 1287 males and 574 females, which is in accordance with the gender proportion of overall drivers in China. The subjects, whose age ranges from 25 year to 60 year, are all passenger sedan drivers and have driving experience for more than 1 year.

The anthropometric measurements include: stature (STA), weight (WEI), sitting height (SST), trochanter height (TRH), sitting acromion height (SAH), acromion to olecranon length (ATO), as shown in Table 1.

### 2.2 Experiments

Previous studies used different experiment methods to collect the preferred driving postures. Electromyography by Hose et al. [5] and goniometer by Porter and Gyi [6] were used to gather data; however, more studies used cameras to record the driving posture. 3-D scanner is adopted in this study, as Fig. 1a shows.

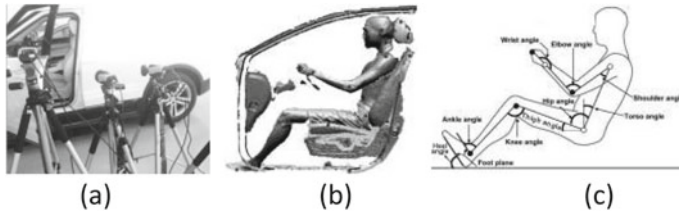


**Fig. 1** **a** Scanning rig for sitting posture, **b** point cloud and landmarks of sitting posture, **c** joint angle definitions. All angles shown are positive. •, joint centers defined by a surface landmark. ○, joint centers determined by spatial relationships between landmarks

Each participant was involved in three sedans, which were selected according to the scores of China Automotive Consumer Research and Testing Center (CCRT for short) in 2018. The three sedans are numbered as S1, S2 and S3.

Each participant entered every sedan driver workspace after landmarks were fixed on the joint points, as shown in Fig. 1b. They were guided to put their hands on wheel's sides laterally, leave foot on rest pedal and right foot on the acceleration pedal with position in the 1/3 travel, and adjust seat to the best position they feel. Participants' postures are recorded by the cameras after all these procedures.

Perceived comfort was measured with a rating scale ranging from 1 to 10 in Table 2, after the participants stayed on seats for 20 min. The filtering based on the subjective evaluation excluded the participants who rated 1–4.

The joint angles are calculated based on the scanned files as Fig. 1b shows. Nine joint angles were discussed in this study, as shown in Table 3 and Fig. 1c.

### 3 Data Analysis—Results and Discussion

Whether the postural data is distinct in gender (male/female), region (north/south) and target sedan (S1/S2/S3) was explored using repeated measures ANOVA. The Bonferroni correction was adopted to make multiple comparisons among different factors to investigate the simple main effect of one factor in different levels of another factor if interaction effect exists between the two factors. Effects were considered as “significant” when  $p < 0.05$ .

The stepwise regression model was used to explore the relationships between the postural data and the age and anthropometric measurements of the participants. Define the entry and removal of using probability of  $F$  as 0.05 and 0.1, respectively.

Finally, the 95% reference range of joint angles was calculated as the recommended ranges. The calculation equation is shown as follows:

$$95\% \text{ reference range} = \mu \pm 1.96 s \tag{1}$$

where  $\mu$  is sample mean value and  $s$  is sample standard deviation.

**Table 2** Subjective evaluation method

1	2	3	4	5	6	7	8	9	10
Unacceptable		Extreme uncomfortable		Marginal	Acceptable	Ordinary	Comfortable	Very comfortable	Extreme comfortable



**Table 3** Joint angle names and definition

No.	A1	A2	A3	A4	A5	A6	A7	A8	A9
Joint angle	Torso angle	Hip angle	Knee angle	Ankle angle	Shoulder angle	Elbow angle	Wrist angle	Heel angle	Thigh angle

### 3.1 Effects on Postural Angles from Gender, Region and Target Sedan

As shown in Table 4, gender has effects on almost joint angles, except torso angle A1, knee angle A3 in S3 sedan and ankle angle in S2 and S3 sedans. Region makes impact on knee angle A3, ankle angle A4 in S1 and S3 sedans, shoulder angle A5, elbow angle A6, wrist angle A7 with male subjects. Target sedan has significant effects on nearly all the postural angles, which indicates that a different seat design contributes postural angles, even for same type of vehicles.

**Table 4** ANOVA results for the effects on joint angles from gender, region and sedan

Postural angles	Significance							
	Gender		Region		Target sedan			
A1	0.392		0.275		<0.001			
A2	<0.001		0.423		<0.001			
A3	S1	<0.001	<0.001		<0.001			
	S2	<0.001						
	S3	0.054						
A4	S1	0.003	S1	0.022	0.069			
	S2	0.500	S2	0.354				
	S3	0.528	S3	0.010				
A5	<0.001		<0.001			S1 versus S2	S1 versus S3	S2 versus S3
					North	<0.001	<0.001	0.058
					South	0.379	0.416	1.000
A6	<0.001		<0.001		North	<0.001	<0.001	<0.001
					South	<0.001	0.605	<0.001
A7	North	<0.001	Male	<0.001	<0.001			
	South	0.002	Female	0.184				
A8	<0.001		0.108		<0.001			
A9	<0.001		>0.05			S1 versus S2	S1 versus S3	S2 versus S3
					North	<0.001	0.240	<0.001
					South	<0.001	0.261	<0.001

### 3.2 *Effects on Postural Angles from Anthropometric Measurement and Age*

Just as the above description states, target sedan is making an impact to all postural angles from A1 to A9 generally; therefore, it is necessary to discuss the effect on angles from anthropometric measurement and age based on each target sedan.

In the next, the standardized regression coefficients were obtained through another regression process after standardization process on data, which is shown as the following, to compare the contribution of each factor's effect to postural angles.

$$\tilde{x}_i = (x_i - \bar{x}_i)/s_{x_i} \quad (2)$$

$$\tilde{y}_i = (y_i - \bar{y}_i)/s_{y_i} \quad (3)$$

where  $x_i$  is each of anthropometric measurements and age and  $y_i$  is each postural angle.

The absolute values of standardized regression coefficients were obtained and drew a radar map with all three target sedans' coefficients for each postural angle, shown in Fig. 2.

The common influential factors for all three sedans are WEI, which makes a negative effect on torso angle A1. As for hip angle A2, the main factor to make an effect is STA, whose increase causes descending of the hip angle, which is consistent with the research of Park's. In the case of knee angle A3, what affects it most is TRH. Knee angle (A3) shows a reducing tendency as the TRH increases. There is little consistency for the affecting factor on ankle angle for three target sedans. For shoulder angle A5, it is the WEI that has the biggest effect positively while it affects torso angle A1 negatively. Elbow angle (A6) is affected mainly by SAH positively. SAH is also the main factor affects wrist angle (A7) most, but negatively. No single one factor was found to have a main effect on heel angle (A8) as the main influential factor for three sedans. It is obvious that thigh angle (A9) is affected by STA most, and that taller drivers have bigger thigh angle. Based on the above analysis, it might be inferred that Chinese drivers with a bigger body size and stature are inclined to have a more upright and a tighter sitting posture. That obvious effects on the driving posture have been stated clearly in previous studies; however, the different and interesting findings come up with by the research.

Significant effects are found existing on almost all 9 angles except torso angle (A1) from gender. The previous studies have also explored the same question and have drawn different and even contradictory conclusions. Hanson et al. [3] found no significant difference existing between male and female subjects. Park et al. [2] maintained that a significant difference exists in elbow, shoulder and foot-calf angles, but not in torso angle. Porter and Gyi [6] and Kyung and Nussbaum [4] also found the difference between male and female, which is consistent with this current study.

It is found in this study, shown in Fig. 3, that female's hip (A2), knee (A3), wrist (A7) and heel angles (A8) are bigger than male's, and are smaller in ankle, shoulder,

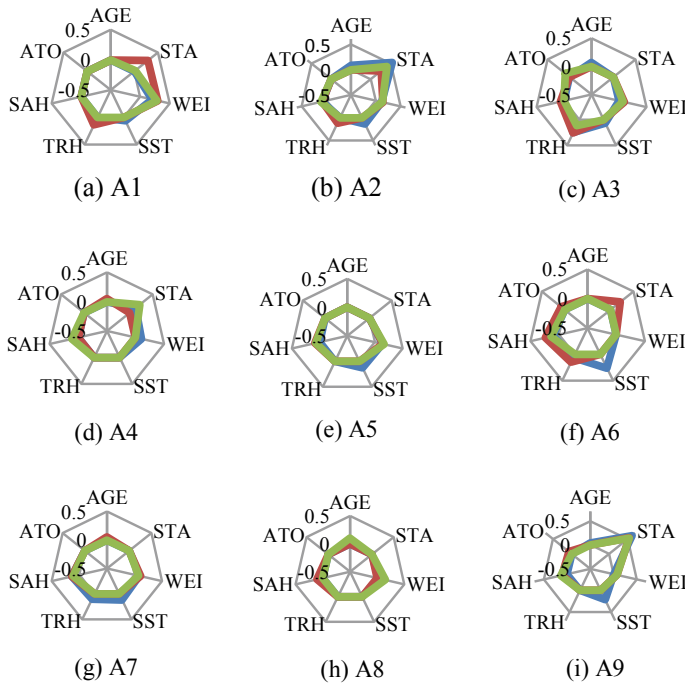


**Fig. 2** Radar maps with all three target sedans’ coefficients for each postural angle (blue, red and green are S1, S2 and S3 sedan, respectively)

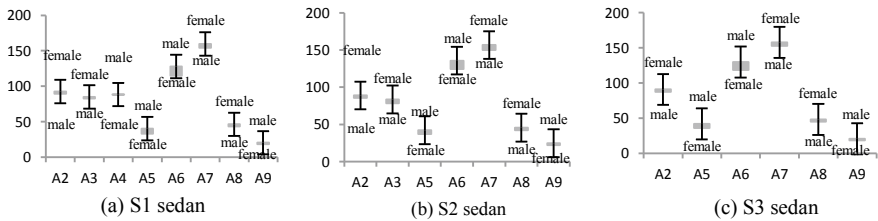


**Fig. 3** Difference of joint angles between male and female

elbow and thigh angles. It indicates that the female tends to adopt more forward and upright posture than the male in order to reach and operate acceleration and brake pedals.

That knee angle (A3), shoulder angle (A5) and elbow angle (A6) of drivers in north areas are bigger than the ones of drivers in south areas are found in this study. South drivers’ wrist angle (A7) is in turn bigger than north drivers’ which tells that north drivers incline to take a more open posture than the south, as Fig. 4 shows.

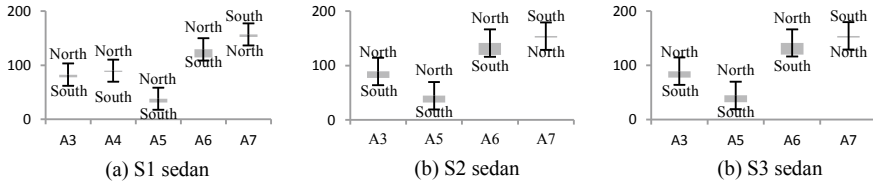


Fig. 4 Difference of joint angles between north and south region

### 3.3 Recommended Joint Angles for Sedan

The 95% reference range of preferred postural angles for sedan is calculated and contrasted to the previous studies which rarely involved driving postures based on Chinese population anthropometric characteristics, as Fig. 5 shows.

Drivers' seated postures were defined and measured in this study using 9 joint angles, whereas a relatively limited set of joint angles has been included in previous studies, ranging from two (Dupuis [7]) to 10 (Hanson et al. [3]). The current study adopted torso angle, heel angle and thigh angle, which has not been used in previous studies, to define the preferred driving postures.

Some differences can be found between the current study and previous ones, which are mainly caused by the following facts: First, an inherent difference in anthropometric measurements and driving habits exists between the Chinese population and

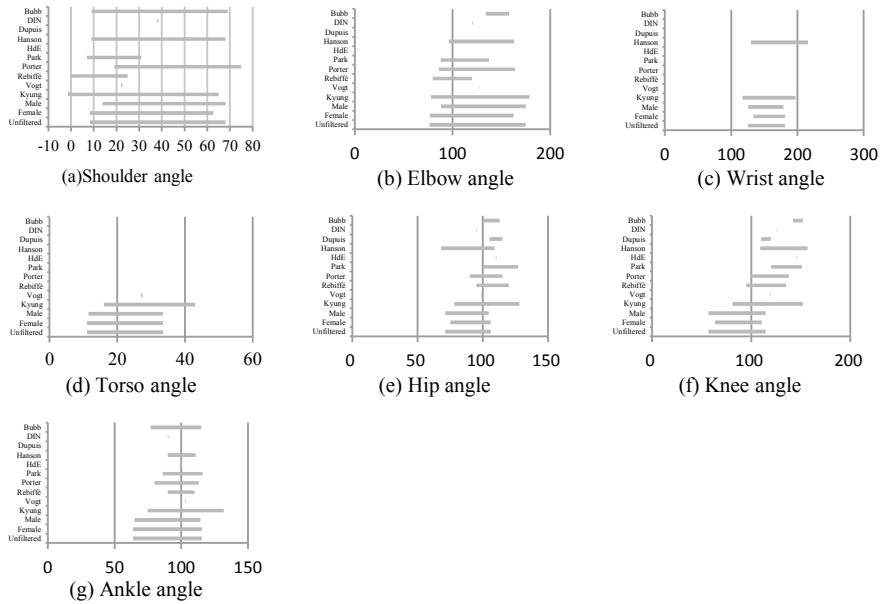


Fig. 5 Comparison of recommended joint angles among current study and previous ones [8–11]

the European and American ones. Secondly, it plays a key role in results that whether a subjective evaluation method was adopted to filter real preferred and comfortable postures. Thirdly, different sedans were selected to collect data and even seating bucks were used in previous studies.

## 4 Conclusion

This study collected 9 driving joint angles of Chinese drivers through scanning measurement and filtered the real preferred and comfortable postural data by perceptual evaluation. The key factors influencing driving postural angles, including sedan type, areas, ages and anthropometric measurements, are identified using ANOVA and stepwise regression analysis methods, which is expected to facilitate to use DHMs or HPMs in seat comfort and driver workspace design.

Finally, the recommended ranges of driving joint angles for both male and female are compared with those in previous studies.

The study was approved by the Logistics Department for Civilian Ethics Committee of China Automotive Technology and Research Center Co., Ltd. All subjects who participated in the experiment were provided with and signed an informed consent form. All relevant ethical safeguards have been met with regard to subject protection.

## References

1. Rebillé R, Guillien J, Pasquet P (1982) Enquête anthropométrique sur les conducteurs français. Laboratoire de physiologie et de biomécanique de l'association Peugeot-Renault
2. Park SJ, Kim H-K, Kim C-B, Kwon KS, Lee J-W (1999) Preferred driving posture and driver's physical dimension. In: human Factors and Ergonomics Society. In: 43rd annual meeting. Proceedings, human factors and ergonomics society, Santa Monica, Calif, vol 1, pp 742–746
3. Hanson L, Sperling L, Akselsson R (2009) Preferred car driving posture using 3-D information. *Int J Vehicle Des* 42(1/2):154–169
4. Kyung G, Nussbaum MA (2009) Specifying comfortable driving postures for ergonomic design and evaluation of the driver workspace using digital human models. *Ergonomics* 52(8):939–953
5. Hosea TM, Hsieh C-C, Wong MA, Delatizky J, Simon SR (1986) Myoelectric analysis of the paraspinal musculature in relation to automobile driving. *Spine* 11(2):928–936
6. Porter JM, Gyi DE (1998) Exploring the optimum posture for driver comfort. *Int J Vehicle Des* 19(3):255–266
7. Dupuis H (1983) Knowledge on assessing sitting postures while driving a vehicle. Auftragsstudie für das Bundesamt für Wehrtechnik und Beschaffung, Bericht Nr.21. Koblenz. Germany: Bundesamt für Wehrtechnik und Beschaffung
8. Bubb P (1992) Microergonomics in car development. VDI-Bericht 968. Düsseldorf: VDI-Verlag
9. HdE (1989) Handbook of micro ergonomics. Hanser-Verlag, Koblenz, Germany
10. Vogt C, Mergl C, Bubb H (2005) Interior layout design of passenger vehicles with RAMSIS. *Human Factors Ergonom Manuf* 15(2):197–212
11. DIN (1981) Körperumrißschablonen [Body contour templates]: DIN 33408. Beuth-Verlag, Deutsches Institut für Normung e.V

# The Effect of Osteoporosis on Spine Following Osteotomy



Tianhao Wang, Chenming Li, and Yan Wang

**Abstract** *Objective* To analyse the effect of osteoporosis on spine following osteotomy. *Methods* The basic finite element model was constructed by CT scanning images of a male volunteer of 34 years old who underwent spinal osteotomy and long-segment fixation. Material parameters were set according to previous studies to simulate normal bone mass osteoporosis. Loads were acted to the upper endplate of the top vertebrae of model to simulate axial compression, flexion, extension and lateral bending. *Results* The peak stress on osteotomy site was reduced in mild osteoporosis model compared with normal bone mass. Under axial compression, screws and rods suffered higher pressure level in osteoporosis. When conducting flexion and lateral bending conditions, it was found that the peak stress on screws was greater than normal bone mass, while the peak stress on rods was less. Severe osteoporosis made the stress concentration more obviously. *Conclusions* The distribution patterns of stress on the models were similar under different degrees of osteoporosis. However, osteoporosis can be regarded as one of risks of fracture and instrumentation failure.

**Keywords** Osteoporosis · Spine · Osteotomy · Internal fixation · Finite element analysis

## 1 Introduction

Osteoporosis is one of the common diseases of the elderly and even middle-aged people [1]. It is accepted that osteoporosis is caused by the hormonal imbalances, leading to the decline of bone mass and quality, which is most common in the elderly. In order to maintain reliable spinal instrumentation and to achieve solid fusion, rod screw system is used most commonly [2, 3]. In clinical, in addition to fractures,

---

T. Wang · Y. Wang (✉)

Department of Orthopaedics, The First Medical Centre, Chinese PLA General Hospital, 100853 Beijing, China  
e-mail: [yanwang\\_301@126.com](mailto:yanwang_301@126.com)

C. Li

The Quartermaster Research Institute of Engineering and Technology, 100010 Beijing, China

© The Editor(s) (if applicable) and The Author(s), under exclusive license to Springer 33  
Nature Singapore Pte Ltd. 2021

S. Long and B. S. Dhillon (eds.), *Man-Machine-Environment System Engineering*, Lecture Notes in Electrical Engineering 645,  
[https://doi.org/10.1007/978-981-15-6978-4\\_4](https://doi.org/10.1007/978-981-15-6978-4_4)

loosening and pullout of screws were also observed in patients with osteoporosis following osteotomy and fixation of the spine, so revision surgery was needed [4]. In this study, FE models of osteotomized and fixed spine of different degrees of osteoporosis were established and the biomechanical responses were analysed.

## **2 Methods**

### ***2.1 Basic Finite Element Model of Spine***

The DICOM data postoperative CT scanning images of spine of a 34-year-old male patient with kyphosis were used to reconstruct three-dimensional point cloud data. Then, the geometric models of spine were established and meshed by hexahedral unit. The model of screw was meshed by ICEM-CFD. The model of rod was established as a 5.5-mm diameter cylinder. The model of osteotomized and fixed spine is shown in Fig. 1.

### ***2.2 Parameters of Vertebral Material***

The material properties of basic FE model were set according to previous studies [5–7]. According to previous study [8], osteoporosis only affects elastic modulus of vertebral endplate, but has no obvious effect on other material parameters. The thickness of cortical bone in the lower thoracolumbar vertebrae did not change significantly [9]. The elastic modulus under different degrees of osteoporosis is listed in Table 1 [8, 10].

### ***2.3 Validation***

We selected segments of L2-S1 of the intact model for simulation to validate the FE model. 10 Nm was applied at the upper surface of L2 to simulate extension, flexion and bending [11, 12]. The results of simulation were compared with reference models. The differences between the results were less than 10%. Therefore, this model was reliable to reflect actual biomechanical responses of postoperative spine.



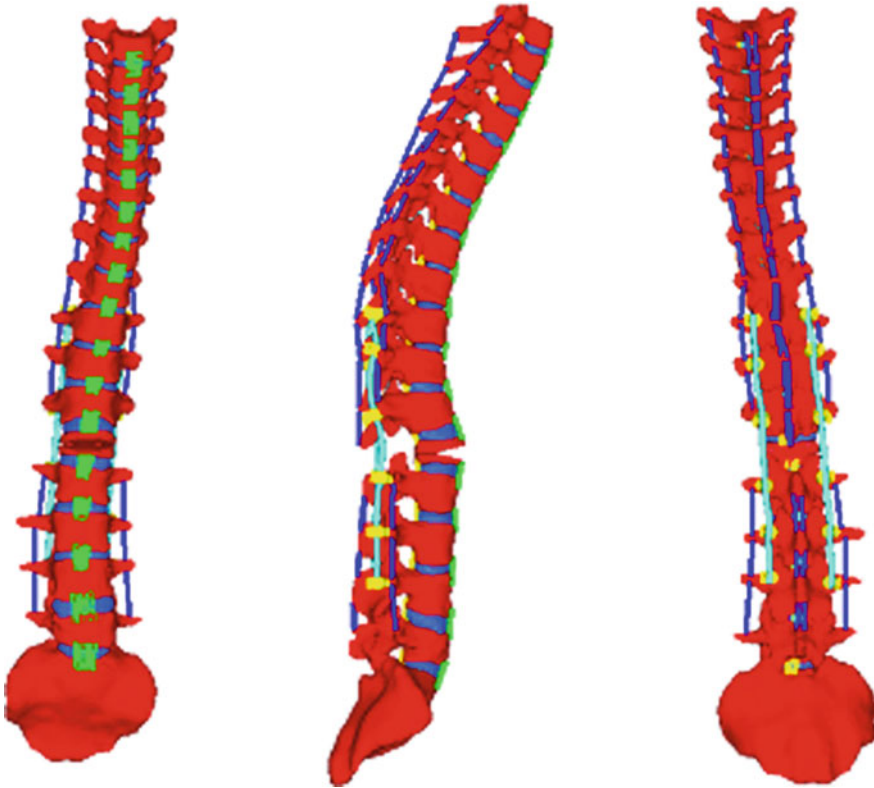


**Fig. 1** Basic FE model of osteotomized and fixed spine

**Table 1** Elastic modulus under different degrees of osteoporosis

	Normal (MPa)	Mild osteoporosis (MPa)	Sever osteoporosis (MPa)
Cortical bone	1200	8040	5030
Cancellous bone	100	34	16.5
Endplate	1000	670	420

### 2.4 Loading Conditions

To simulate the condition of axial compression, a load of 300 N was applied to the upper surface of the most proximal vertebra of the model, T1 [5]. In order to simulate various conditions, including flexion–extension and lateral bending, a 1 Nm amount was acted from different directions to T1 upper endplate [5].

### 3 Results

Under the axial compression load, the stress level of osteoporosis model and normal bone model is the highest (Fig. 2). The simulation results showed that the level of peak stress of normal bone mass model was higher than that of osteoporotic model, but lower than that of the screw and rod. With the increase of osteoporosis, the stress level of screw and rod increased.

Under flexion loading, the peak of screw stress appeared on the screw in all models including osteoporosis and normal (Fig. 3). The results showed that the stress level of the vertebrae and screws was, respectively, 2.03% and 4.39% in the mild and severe osteoporosis model, and it was, respectively, 0.95% and 1.90% lower than that in the normal bone mass model. Furthermore, the peak stress on rods noticed an increase following the increased severity of osteoporosis.

Interestingly, under extension load, the stress level at the screw is the highest in osteoporosis model, but not the highest in model of normal bone mass (Fig. 4). With the severity of osteoporosis increasing, the vertebrae stress of mild osteoporosis model decreased from 47.11 to 29.78 MPa, and decreased to 24.79 MPa in severe osteoporosis model. The same results were observed. The screw stress of osteoporosis model was 39.49 and 47.51 MPa, which was higher than that of normal bone model (35.38 MPa).

The vertebrae of osteoporosis model and normal bone model showed the highest stress level under lateral bending (Fig. 5). By comparing the models, it is noticed that the stress level of vertebrae and screws in mild osteoporosis model decreased, the stress level of rods increased from 41.88 to 47.72 MPa, and the stress level of vertebrae and screws in severe osteoporosis model increased from 48.12 to 48.12 MPa. With the increase of osteoporosis, the stress level of the proximal vertebral body decreased.

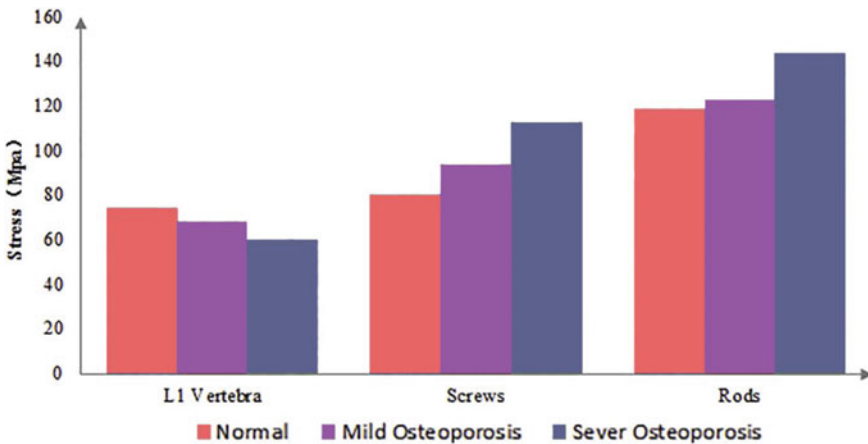


Fig. 2 Peak stress of models under axial compression

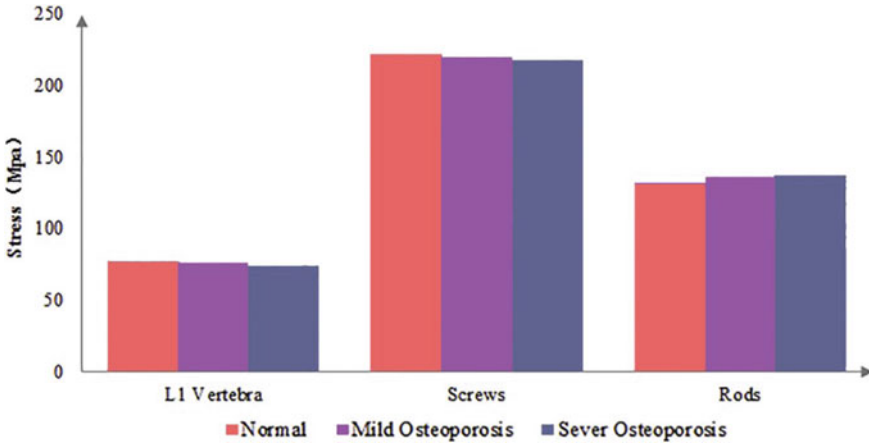


Fig. 3 Peak stress of models under flexion

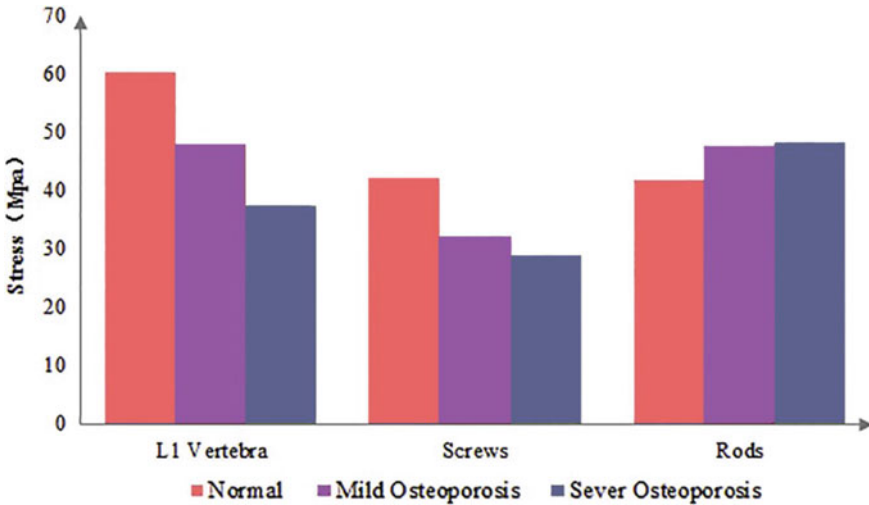


Fig. 4 Peak stress of models under extension

## 4 Conclusions

By using three-dimensional finite element method, this study simulated the effect of osteoporosis on spine which underwent osteotomy and long-segment instrumentation. The bone mass does not obviously affect stress distribution pattern of vertebra and internal fixations. The parts of strength concentration in osteoporosis model are same with model of normal bone mass. Under various conditions, the peak stress of vertebrae and internal fixation in osteoporosis model was lower and higher than that

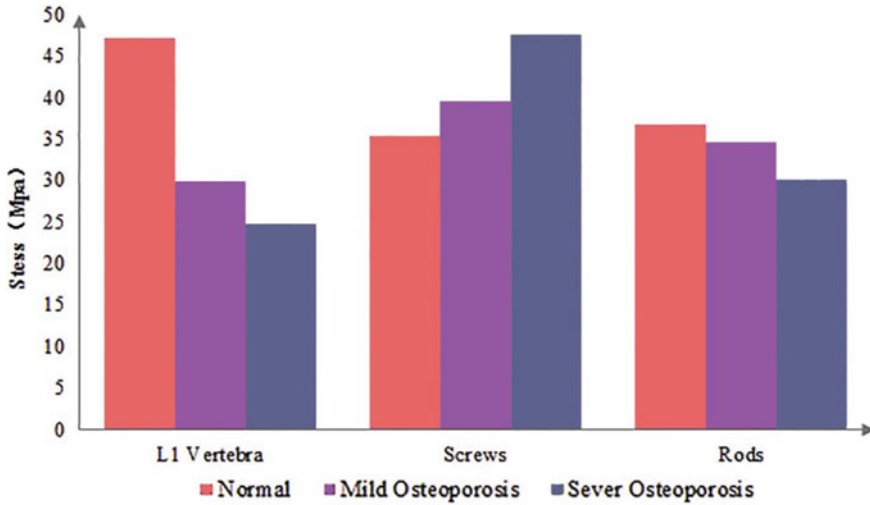


Fig. 5 Peak stress of models under lateral bending

in model of normal bone mass, respectively. As a result, the risk of internal fixation failure may increase.

## References

1. Herkowitz HN, Kurz LT (1991) Degenerative lumbar spondylolisthesis with spinal stenosis. A prospective study comparing decompression with decompression and intertransverse process arthrodesis. *J Bone Joint Surg Am* 73:802–808
2. Pritchett JW, Bortel DT (1993) Degenerative symptomatic lumbar scoliosis. *Spine (Phila Pa 1976)* 18:700–703
3. Bridwell KH, Berven S, Edwards C, Glassman S, Hamill C, Schwab F (2007) The problems and limitations of applying evidence-based medicine to primary surgical treatment of adult spinal deformity. *Spine (Phila Pa 1976)* 32:S135–139
4. Jimbo S, Kobayashi T, Aono K, Atsuta Y, Matsuno T (2012) Epidemiology of degenerative lumbar scoliosis: a community-based cohort study. *Spine (Phila Pa 1976)* 37:1763–1770
5. Wang T, Cai Z, Zhao Y, Zheng G, Wang W et al (2019) Development of a three-dimensional finite element model of thoracolumbar kyphotic deformity following vertebral column decancellation. *Appl Bionics Biomech* 2019:5109285
6. Gzik M, Wolanski W, Tejszerska D (2008) Experimental determination of cervical spine mechanical properties. *Acta Bioeng Biomech* 10:49–54
7. Yoganandan N, Kumaresan S, Pintar FA (2001) Biomechanics of the cervical spine Part 2. Cervical spine soft tissue responses and biomechanical modeling. *Clin Biomech (Bristol, Avon)* 16:1–27
8. Polikeit A, Nolte LP, Ferguson SJ (2003) The effect of cement augmentation on the load transfer in an osteoporotic functional spinal unit: finite-element analysis. *Spine (Phila Pa 1976)* 28:991–996

9. Ritzel H, Amling M, Pösl M, Hahn M, Delling G (1997) The thickness of human vertebral cortical bone and its changes in aging and osteoporosis: a histomorphometric analysis of the complete spinal column from thirty-seven autopsy specimens. *J Bone Miner Res* 12:89–95
10. Mizrahi J, Silva MJ, Keaveny TM, Edwards WT, Hayes WC (1993) Finite-element stress analysis of the normal and osteoporotic lumbar vertebral body. *Spine (Phila Pa 1976)* 18(14):2088–2096
11. Shirazi-Adl SA, Shrivastava SC, Ahmed AM (1984) Stress analysis of the lumbar disc-body unit in compression. A three-dimensional nonlinear finite element study. *Spine (Phila Pa 1976)* 9:120–134
12. Yamamoto I, Panjabi MM, Crisco T, Oxland T (1989) Three-dimensional movements of the whole lumbar spine and lumbosacral joint. *Spine (Phila Pa 1976)* 14:1256–1260

# Study on Human Factor Evaluation of Aviation Maintenance During Flight Test



Haijing Song, Kai Feng, and Yuqi Zhang

**Abstract** Human error is one of the main factors leading to flight accidents. Previous human factor analysis in aviation maintenance mainly focused on qualitative evaluation with subjective results. Combined with the actual maintenance work during flight test, the paper proposed a comprehensive evaluation method including modified analytical hierarchy process, expert evaluation and grey relational analysis, fully considering the inevitable fuzziness and subjectivity of human factors. Then, the influence degrees of human factors on aviation maintenance were analyzed and recognized quantitatively for the specific accidents based on the huge data during flight test, and the corresponding risk management tips and other prophylactic measures were raised. Finally, this model was applied in one real test aircraft, and the results proved the validity of this study.

**Keywords** Human factor · Aircraft maintenance · Flight test · Grey relational analysis · Influence factors · Risk management

## 1 Introduction

As we all know, aircraft maintenance is an important means to ensure the inherent reliability of aircraft. However, with the highly integrated aircraft system equipment, aviation safety is under great pressure. According to the statistics of the United States Boeing Company, 70% of global civil aviation jet plane accidents were caused by human factors. It can clearly be seen that in aviation accidents, human factor is the main cause of aircraft maintenance failure [1, 2]. For the flight test aircraft, the maintenance object of aircraft maintenance is advanced with new system equipment, and the maintenance effect relies on the knowledge and work experience of aircraft maintenance technicians. It is especially important to evaluate how to deal with human factor during aircraft maintenance. This article studies how to objectively and scientifically analyze and identify the most important human error causes and

---

H. Song (✉) · K. Feng · Y. Zhang  
Chinese Flight Test Establishment, Xi'an 710089, China  
e-mail: [shjaj@163.com](mailto:shjaj@163.com)

© The Editor(s) (if applicable) and The Author(s), under exclusive license to Springer Nature Singapore Pte Ltd. 2021

S. Long and B. S. Dhillon (eds.), *Man-Machine-Environment System Engineering*, Lecture Notes in Electrical Engineering 645, [https://doi.org/10.1007/978-981-15-6978-4\\_5](https://doi.org/10.1007/978-981-15-6978-4_5)

influencing factors in accidents in order to take measures in advance and prevent accidents effectively. By summarizing a large number of previous troubleshooting examples of similar aircraft in the flight test phase, the human–equipment–environment and other influencing factors in aircraft maintenance errors were quantified and sorted, and the main set of influencing factors for human errors was found, so that countermeasures can be taken according to the degree of relevance of influencing factors to reduce and control the occurrence of human errors.

## 2 Comprehensive Evaluation Method for Human Factors of Aircraft Maintenance

This article proposes a comprehensive evaluation system of human factors that integrates improved expert scoring, three-scale analysis, and grey relational analysis. The evaluation system was validated, and the effectiveness of this method was proved.

### 2.1 Determine the Human Error Influence Factor Set

Traditional human factors analysis often invites experienced aircraft maintenance technicians, relying on their rich experience and intuitive feelings, to evaluate it with some vague concepts and comprehensive judgments in practice [3, 4]. Therefore, the actual work often lacks a certain degree of scientificity, comprehensiveness and standardization. This article introduces expert consensus and expert self-confidence to improve the expert scoring method to build a multi-level set of human error influence factors, including the following steps:

1. Establishing coordination group. The coordination group shall consist of 5 persons, including 1 researcher, 2 senior engineers and 2 engineers. The main tasks include designing theme, identifying expert consultants, redacting consultation forms, organizing consulting work and processing statistical data.
2. Identifying expert consultants. Experts who are willing to participate and have rich practical experience and certain expertise in human factor analysis should be selected. This method stipulates that the selected maintenance experts should have aircraft maintenance experience (more than 5 years), and the number of experts should be 10–30 people.
3. The first round of expert consultation. Based on the preliminary set of human error influence factors  $U_k$ , the consensus of experts was introduced to formulate the first round of expert consultation form. Each expert was required to judge the importance of each influencing factor. The 5-point Likert scale was used to classify the degree of influence [5]. The expert consensus here is defined as: no less than  $2/3$  of the expert judgment results are better than “important” (The responding notes  $P_{33}$ ) [6].

4. The second round of expert consultation. Experts are required to give the confidence level when judging the importance of human error factors, with the Group Confidence Ranking (GCR). A 5-point scale is used to divide the confidence level, including “very low,” “low,” “normal,” “high” and “very high.” The data show that [7], when the average confidence level (GCR) of the expert group is not less than 3, the consultation result is closer to the “real” situation of subjective judgment. After two rounds of screening, the human error influence factors system for aviation maintenance was determined, as shown in Fig. 1.

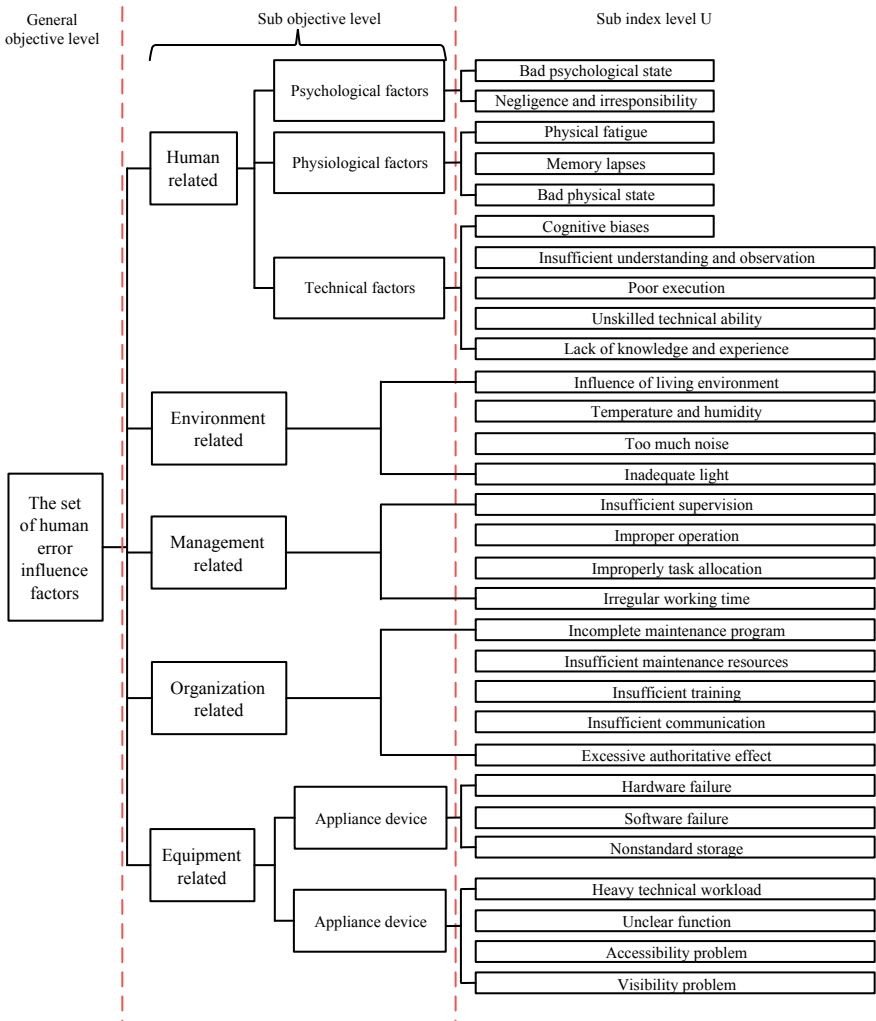


Fig. 1 Human error influence factors system for aviation maintenance



## 2.2 Determine Weight Coefficient of Influence Factor

In order to determine the probability of accidents caused by various factors and their impact on the severity of the accident, this article introduces the “three-scale” principle to improve the AHP analysis [8, 9], reduce the number in pairwise comparisons of indicators and meet the requirements of consistency. It includes the following four steps:

1. Establishing the judgment matrix  $C$  (obtained by experts)

$$C_{ij} = \begin{cases} 1 & \text{Indicator } i \text{ is more severe than indicator } j \\ 0 & \text{Indicator } i \text{ is same severe as indicator } j \\ -1 & \text{Indicator } i \text{ is less severe than indicator } j \end{cases} \quad \forall i, j \quad (1)$$

2. Calculating the optimal transfer matrix based on the judgment matrix  $D$

$$d_{ij} = \frac{1}{m} \sum_{k=1}^m (c_{ik} - c_{jk}) \quad \forall i, j \quad m \text{ is the order of } C \quad (2)$$

3. Determining the consistency matrix  $Q$

$$q_{ij} = \exp(d_{ij}) \quad \forall i, j \quad (3)$$

4. Finding the maximum eigenvalue corresponding to the characteristic vector of  $Q$ , The unitized characteristic vector is the relative weight of each index  $a_i$ .

In actual evaluation, in order to give a more accurate and objective judgment matrix, at least  $d(d > 1)$  experts can be hired to compare and judge the same influencing factors at the same time, and determine the impact level  $S_p$  of each factor on the severity of the accident, causing the probability of an accident  $S_s$ , and then perform a gray correlation calculation to “synthesize” a better result.

## 2.3 Ranking Influencing Factors Based on Grey Relational Analysis

Grey relational analysis calculation is proposed in this article as the following three steps [10, 11]:

1. Building the raw data matrix  $R$

According to the analysis of human error causes in various types of aircraft during flight test, the corresponding influencing factors were classified into human factors  $u(1)$ , equipment  $u(2)$ , management organization  $u(3)$ , environment  $u(4)$  and other first-level indicator layers together form the raw data matrix  $R$ .

## 2. Normalization of raw data matrix $R$

In order to eliminate the impact of the dimension,  $R$  is normalized to obtain the matrix  $RI$ . According to the characteristics of human error influencing factors, they are all “positive indicators” (the larger the value, the better).

## 3. Calculating the grey correlation degree

Based on  $RI$ , the optimal mother sequence  $Y_0 = (y_0(j)) (j = 1, 2, 3, 4, 5)$  according to the optimal normalized evaluation index of  $V$ . At this time was obtained,  $y_0$  is the reference sequence and the  $y_i (i = 1, 2, 3, \dots, m)$  is comparison sequence. The correlation coefficient  $\varphi_i(j)$  of  $y_0$  and  $y_i$  is calculated as follows:

$$\varphi_i(j) = \frac{\min_i \min_j |y_0(j) - y_i(j)| + \rho \max_i \max_j |y_0(j) - y_i(j)|}{|y_0(j) - y_i(j)| + \rho \max_i \max_j |y_0(j) - y_i(j)|} \quad (4)$$

where  $\rho$  is the distinguishing coefficient,  $\rho \in [0, 1]$ , often taken 0.5. Correlation degree  $G_i$  can be calculated from correlation coefficient  $\varphi_i(j)$ ,

$$G_i = \frac{1}{5} \sum_{j=1}^5 \delta_j \varphi_i(j) \quad (5)$$

Among them,  $\delta_j$  represents the weight coefficient, which means the impact severity and probability by each factor on the accident.

## 3 Example Application

This article uses a certain type of aircraft appearing fire alarm in the third engine. The main instrument indications were disordered, the throttle was not operated, the crew extinguished and stop the engine, and the aircraft had to early return to the ground. After investigation, the causes of human error this time were as follows:

1. The aircraft maintenance technicians incorrectly disconnected the tee valve pipe connection of thrust reverser and forgot to recover.
2. Aircraft maintenance technicians misunderstood the maintenance work instructions during execution.
3. The aircraft maintenance technicians were overconfident and did not conduct inquiries, exchanges, or reports.
4. On the day, six members of aircraft maintenance technicians did the third engine troubleshooting. The squadron leader did not organize the division of labor.
5. Due to the tight requirements of the flight nodes, the troubleshooting staff did work with a lot of time pressure and work tension, which induced human error.
6. High-temperature operation at the airport, the physical and mental working conditions of the aircraft maintenance technicians were affected by environment.

7. The aircraft preparations work at noon in summer. The sunlight was too strong, which also induced aircraft maintenance error.
8. The aircraft maintenance technicians did not sign as required after performance, and the inspector did not correct it, so there was opportunity to review the work and remedy the mistake.
9. In accordance with the relevant requirements of the maintenance work documents, the implementer must be signed after completing the work.

From the above analysis, the main reasons for the accident are problems with the management organization, such as insufficient planning supervision, flawed maintenance data and failure to work according to procedures. Based on the model in Fig. 1 and analyzing the results of the accident investigation, the structure of the factors affecting human error in this accident can be obtained, as shown in Fig. 2.

In response to the accident analysis, 25 aircraft maintenance experts were invited to discuss and confirm the factors affecting the human error accident, and the expert scoring results by formula (3) were analyzed, so that we get the statistical results. And then, we combined with the actual historical data of human errors from four flight aircrafts, the original data matrix  $R$  is obtained by statistics, and it is standardized to  $RI$ :

$$R = \begin{bmatrix} 10 & 7 & 5 & 4 \\ 6 & 4 & 3 & 7 \\ 2 & 3 & 4 & 6 \\ 5 & 5 & 2 & 3 \end{bmatrix} \quad RI = \begin{bmatrix} 1 & 1 & 1 & 0.25 \\ 0.5 & 0.25 & 0.333 & 1 \\ 0 & 0 & 0.667 & 0.75 \\ 0.375 & 0.5 & 0 & 0 \end{bmatrix}$$

Since the optimal normalization index of the decision objects  $V$  is 1, determine the optimal mother sequence  $Y_0 = \{1, 1, 1, 1, 1\}$ , according to  $RI$  and  $Y_0$ , and use

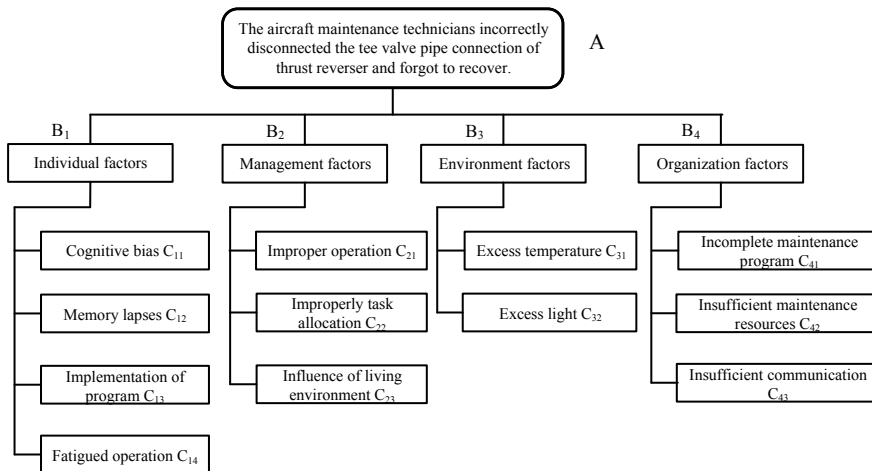


Fig. 2 Hierarchy framework for influence factors in example analysis

**Table 1** Weight coefficient for evaluation indexes during aviation maintenance safety analysis

First-level index	$S_p$	$S_s$	Second-level index	$S_p$	$S_s$	$G_i$	Level
Individual factor	0.3563	0.3141	$C_{11}$	0.2345	0.2197	0.7065	$G_i \geq 0.7$
			$C_{12}$	0.2455	0.3101	0.587	$G_i \geq 0.4$
			$C_{13}$	0.2500	0.2489	0.8176	$G_i \geq 0.8$
			$C_{14}$	0.2700	0.2233	0.7443	$G_i \geq 0.7$
Management factor	0.3310	0.2874	$C_{21}$	0.3698	0.4120	0.7182	$G_i \geq 0.7$
			$C_{22}$	0.2900	0.2005	0.6175	$G_i \geq 0.6$
			$C_{23}$	0.4412	0.3975	0.8275	$G_i \geq 0.8$
environmental factor	0.1007	0.1980	$C_{31}$	0.5642	0.5435	0.6727	$G_i \geq 0.6$
			$C_{32}$	0.4358	0.4565	0.4539	$G_i \geq 0.4$
Organizational factor	0.2120	0.2105	$C_{41}$	0.3055	0.3608	0.7273	$G_i \geq 0.7$
			$C_{42}$	0.2678	0.3577	0.8075	$G_i \geq 0.8$
			$C_{43}$	0.4267	0.2815	0.8253	$G_i \geq 0.8$

Notes  $S_p$  is accident probability weight;  $S_s$  is severity impact weight;  $G_i$  is gray correlation degree

the Formula (4) to calculate the gray correlation coefficient. Bring the correlation coefficient into the Formula (5) to get the corresponding gray correlation degree. The calculation results are listed in Table 1.

According to the calculation results, it can be seen that the insufficient supervision of the plan, communication, plan implementation and inadequate maintenance data are highly correlated and are serious influencing factors, followed by operational fatigue, incomplete maintenance procedures and inappropriate operations. The expert team carried out a risk analysis for this type of accident prevention and proposed four types of risk avoidance tips and measures:

1. The work should fully consider the maintenance ergonomics, such as technical workload, environment and so on. The corresponding emergency plan should be programed in advance;
2. Implementing full supervision and inspection to prevent lax management and unclear duties of the monitoring staff;
3. Improving the accuracy and clarity of maintenance manuals description and make comments and discussion in places where ambiguities are likely to occur;
4. Strengthening the communication between aircraft maintenance members, the training of team spirit and overcoming personal cognitive preferences.

## 4 Conclusions

1. Combined with the actual aircraft maintenance of the flight test phase, the expert consensus and self-confidence were introduced. After two rounds of index screening, the scientificity of the construction results was obviously enhanced;
2. Considering the ambiguity of human factors concept and the differences in expert recognition, the three-scale and gray correlation algorithms are integrated to realize the quantification of the qualitative evaluation, and the persuasive classification indicates the reason of human errors more efficiency.
3. The human factors are classified into four categories based on the ranking set of correlation degree. The main influencing factors of human error are identified, and the risk warning and avoidance management measures have been applied to multiple models during the test flight maintenance work, the effect was good.
4. The results of application show that the comprehensive evaluation method of human error influencing factors proposed in this paper, combined with improved expert scoring method, three-scale analysis and gray correlation calculation, has improved the accuracy and operability of human factor influence analysis to a certain extent. This method can be further extended to other complex systems.

## References

1. Boeing Commercial Airplane Group (2002) Statistical summary of worldwide operations for commercial jet aircraft accidents 1991–2001. Boeing Corporation
2. Li X, Guo J, Zhou C (2005) Study on human factor accidents analysis system for aviation maintenance. *Aviat Maintenance Eng* 2005(5):23–42
3. Faber MH, Stewart MG (2003) Risk assessment for civil engineering facilities: critical overview and discussion. *Reliab Eng Syst Saf* 80:173–184
4. Xiao J, Douglas D (1997) A Delphi evaluation of the factors influencing length of stay in Australian hospitals. *Int J Health Plann Manage* 12(3):207–218
5. Ritva K, Risto T (2004) Expert assessment of physical ergonomics at video-display unit workstations: repeatability, validity and responsiveness to changes. *Environ Health* 77:437–442
6. Wong WG (1999) Grey evaluation method of concrete pavement comprehensive condition. *J Transp Eng* 25(6):27–31
7. Zhang J (2000) Fuzzy analytical hierarchy process. *Fuzzy Syst Math* 14(2):80–88
8. Rousseau RJ, Trauwaert E, Kaufman L (1997) Fuzzy clustering with high contrast. *Comput Appl Math* 64(2):81–90
9. Usanmaz O (2011) Training of the maintenance personnel to prevent failures in aircraft systems. *Eng Fail Anal* 18(7):1683–1688
10. Chen CB, Klien CM (1997) A simple approach to ranking a group of aggregated fuzzy utilities. *IEEE Trans Syst Man Cybern* 27(1):26–35
11. Deng J (1987) *The basic theory and methods of grey system*. Press of Huazhong University of Science and Technology, Wuhan

# The Effect of Music Relaxation Training on Relieving the Psychological Fatigue After Simulated Flight



Yan Zhang, Liu Yang, Yang Liao, Yishuang Zhang, Fei Peng, and Huamiao Song

**Abstract** *Objective:* To explore the effect of music relaxation training on relieving the psychological fatigue after simulated flight. *Methods:* The experiment object was divided into the music relaxation group and deep breath relaxation group. After completing the simulated flight mission, electroencephalogram (EEG), the heart rate variability (HRV), and mental state indexes were collected before and after relaxation training. *Results:* After training, compared with those in the deep breath relaxation group, there were much more indexes of EEG, HRV, and mental state in the music relaxation group which were improved significantly and thoroughly. *Conclusion:* Music relaxation training can more effectively relieve the psychological fatigue after simulated flight.

**Keywords** Music relaxation · Psychological training · Simulated flight · UAV operator

## 1 Introduction

Fatigue can reduce the ability and efficiency of flight work and seriously threaten flight safety. It has become a common sense of the aviation community at home and abroad [1, 2]. As a new force in modern warfare, the unmanned aerial vehicles (UAV) will enable its operators to experience flight without undergoing incident physical challenges and the risk of injury. The characteristics of this position make UAV operators will often need to work long hours and maintain high vigilance and attention, which will cause a high incidence of psychological fatigue. Psychological fatigue is mainly a sense of uneasy fatigue caused by intense brain work. It lays particular stress on mental and emotional performance and emphasizes more on central fatigue [3]. The inherent characteristics of music make it possible to be used to affect people's emotions and cause various physiological reactions, significantly promoting the homeostasis of the human body, reducing tension and anxiety,

---

Y. Zhang · L. Yang · Y. Liao · Y. Zhang · F. Peng · H. Song (✉)  
Air Force Medical Center, Fourth Military Medical University, Beijing 100142, China  
e-mail: [ksspsy@126.com](mailto:ksspsy@126.com)

© The Editor(s) (if applicable) and The Author(s), under exclusive license to Springer Nature Singapore Pte Ltd. 2021

S. Long and B. S. Dhillon (eds.), *Man-Machine-Environment System Engineering*, Lecture Notes in Electrical Engineering 645, [https://doi.org/10.1007/978-981-15-6978-4\\_6](https://doi.org/10.1007/978-981-15-6978-4_6)

and promoting relaxation. Therefore, this research aimed at the characteristics of psychological fatigue and adopted music relaxation training methods to evaluate the effectiveness for mitigating psychological fatigue after simulated flight, so as to conduct a preliminary research on the appropriate psychological training method of the UAV operators.

## **2 Object and Method**

### **2.1 Object**

14 volunteers are taken as the experiment object, including 5 female and 8 male. All these people have right-handedness, and they are aged 19–40. All experimental subjects have no history of cardiovascular disease, have not taken any medications recently, and had no complaints. The day before the experiment everyone had an adequate sleep, did not drink any tea, coffee, or any other beverage, food, or medication that stimulated the central nervous system, and did not exercise vigorously before the experiment.

### **2.2 Method**

#### **2.2.1 Psychological Fatigue Model**

The flight fatigue model was constructed by simulating the flight operation task. The task contents include single task (single-axis operation), triple task (pitch–yaw–tilt operation), and quadruple task (additional mental arithmetic and pitch–yaw–tilt operation). The duration lasted for 2 h.

#### **2.2.2 Training Method**

The smart music relaxation system (including the tablet and somatosensory music cushion) was used as the training tool. The device played the standard relaxation training instructions through a tablet computer and was complemented by environmental sound effects and background music on the object at the same time. At the same time, the low-frequency signal from 16 to 150 Hz in the music was converted into vibrations through physical energy conversion and transmitted through the somatosensory music cushion on the targeted object.

### 2.2.3 Collection Index

1. EEG index: The present study used the neuroflight cognitive assessment and training analysis system developed by Beijing Yiran Sunshine Technology Co., Ltd. The EEG indexes being collected include alpha ( $\alpha$ ), beta ( $\beta$ ), and theta ( $\theta$ ).
2. HRV index: The present study adopted the physiological coherence and autonomous balancing system developed Beijing Haofeng Co., Ltd. The time-domain indexes being collected include successive heartbeat interval standard deviation (SDNN), standard deviation of adjacent successive heartbeat interphase difference value (SDSD), mean square root of adjacent successive heartbeat interphase difference (RMS-SD), the proportion of the difference value of adjacent successive heartbeat interphase difference greater than 50 ms (PNN 50). The frequency domain indexes include: general frequency spectrum (TF), extreme-low-frequency power (VLF), low-frequency power (LF), high-frequency power (HF), ratio between the low-frequency power and high-frequency power (LF/HF), corrected low-frequency power (LFnorm) and corrected high-frequency power (HFnorm).
3. Psychological status index: The present study adopted “mental status scale” [4], including fatigue feeling, excitability (irritability), and calmness (relaxation status). A higher score represents a higher level of measured psychological index, in which fatigue feeling component is from “Profile of Mood States (POMS) Scale” [5], excitability and calmness (relaxation status) component scale is from “BFS (Befindlichkeitsskalen) mood scale” [6].

### 2.2.4 Experiment Process

The single factor (training method) and two levels (music relaxation, deep breath relaxation) were conducted with the repeated measurement and design within the subjects. The experiment objects were divided into the music relaxation group (MG) and deep breath relaxation group (DG). After the simulated flight missions, all objects were collected of the HRV, EEG, and psychological status indexes. Afterward, the MG performed the 30-min music relaxation training, and the above physiological and psychological indexes were collected once again. The DG was collected of the same indexes after 30 min of deep breath relaxation training. In order to eliminate the sequence error, the two training methods were conducted with the Latin party design to make the sequence balanced. In other words, each subject was randomly divided into two sequential groups, and each sequential group conducted experiments of two training methods in different sequences.

### 2.2.5 Statics Analysis

The present study adopted the SPSS19.0 statistical software for data processing. The experimental results were represented by ( $\bar{x} \pm s$ ), and the index comparison adopted



**Table 1** Comparison of EEG indexes ( $\bar{x} \pm s$ )

	Music relaxation group (MG)		Deep breath relaxation group (DG)	
	Before training	After training	Before training	After training
$\alpha$	28.04 $\pm$ 2.04	32.20 $\pm$ 2.90**	27.85 $\pm$ 0.96	28.62 $\pm$ 1.54
$\beta$	27.36 $\pm$ 1.1	23.01 $\pm$ 2.84**	26.88 $\pm$ 0.80	26.19 $\pm$ 1.17
$\theta$	9.99 $\pm$ 0.46	8.37 $\pm$ 0.88**	10.31 $\pm$ 1.03	9.60 $\pm$ 0.75

Note Comparison before and after training: \* $p < 0.05$ , \*\* $p < 0.01$

the pairing  $t$  inspection. Taking  $p < 0.05$  as the difference is considered statistically significant.

### 3 Result

#### 3.1 Comparison of EEG Index Results

In the MG, after training, compared with before training, the  $\alpha$  index increased significantly, and the  $\beta$  and  $\theta$  index decreased significantly ( $p < 0.01$ ). The index was no statistically significant change in the DG ( $p > 0.05$ ) (Table 1).

#### 3.2 Comparison of HRV Time-Domain Index Results

After training, compared with before training, all indexes of the MG significantly increased ( $p < 0.01$ ,  $p < 0.05$ ). The SDD of the DG after training was significantly higher than that before training, and the difference was statistically significant ( $p < 0.05$ ). The other indexes had no statistically significant change ( $p > 0.05$ ) (Table 2).

**Table 2** Comparison of HRV time-domain indexes ( $\bar{x} \pm s$ )

	Music relaxation group (MG)		Deep breath relaxation group (DG)	
	Before training	After training	Before training	After training
SDNN	78.71 $\pm$ 24.91	123.74 $\pm$ 49.23**	82.39 $\pm$ 23.76	118.38 $\pm$ 68.24
RMS-SD	65.52 $\pm$ 27.90	128.93 $\pm$ 69.28**	62.82 $\pm$ 20.34	120.28 $\pm$ 102.91
SDD	46.45 $\pm$ 19.84	102.08 $\pm$ 64.18**	42.66 $\pm$ 16.62	101.41 $\pm$ 105.01*
PNN50	29.80 $\pm$ 16.93	45.81 $\pm$ 13.70*	32.38 $\pm$ 16.14	33.89 $\pm$ 15.57

Note Comparison before and after training: \* $p < 0.05$ , \*\* $p < 0.01$

**Table 3** Comparison of HRV frequency domain indexes ( $\bar{x} \pm s$ )

	Music relaxation group (MG)		Deep breath relaxation group (DG)	
	Before training	After training	Before training	After training
TP	667.47 ± 370.50	1401.58 ± 1022.31*	765.95 ± 523.45	1269.14 ± 1033.30
VLF	218.72 ± 158.57	441.08 ± 384.96	268.56 ± 242.61	424.34 ± 373.32
LF	381.06 ± 203.61	708.73 ± 529.15*	431.60 ± 270.52	700.84 ± 590.19
HF	67.05 ± 44.91	251.76 ± 242.02**	65.80 ± 53.97	143.96 ± 120.78*
LF/HF	6.47 ± 3.04	3.41 ± 2.05**	7.26 ± 2.18	5.50 ± 2.76
LFnorm	85.06 ± 4.63	74.58 ± 7.05**	87.01 ± 3.74	82.78 ± 5.41*
HFnorm	14.94 ± 4.63	25.42 ± 7.05**	12.99 ± 3.74	17.22 ± 5.41*

Note Comparison before and after training: \* $p < 0.05$ , \*\* $p < 0.01$

### 3.3 Comparison of HRV Frequency Domain Index Results

In the MG, after training, compared with before training, the TP, LF, HF, and HFnorm were significantly increased ( $p < 0.01$ ,  $p < 0.05$ ), and the LF/HF, LFnorm were significantly decreased ( $p < 0.01$ ). By making a comparison of the situation before and after training of the DG, the HF and HFnorm were significantly increased ( $p < 0.05$ ), the LFnorm was significantly decreased ( $p < 0.05$ ), and the other indexes variation had no significant significance ( $p > 0.05$ ) (Table 3).

### 3.4 Comparison of Psychological Status Index Results

After training, compared with before training, the calmness of the MG was significantly increased ( $p < 0.05$ ), and the fatigue and excitability of the MG were significantly reduced ( $p < 0.01$ ,  $p < 0.05$ ). Compared with before and after training, the calmness of DG increased significantly ( $p < 0.05$ ), and other indexes had no statistically significant changes ( $p > 0.05$ ) (Table 4).

**Table 4** Comparison of psychological status indexes ( $\bar{x} \pm s$ )

	Music relaxation group (MG)		Deep breath relaxation group (DG)	
	Before training	After training	Before training	After training
Fatigue	14.00 ± 7.26	7.07 ± 2.30**	13.37 ± 6.66	9.57 ± 3.80
Calmness	13.79 ± 5.95	18.64 ± 4.52*	12.64 ± 4.52	16.79 ± 3.91*
Excitability	9.21 ± 4.53	5.86 ± 0.95*	10.50 ± 5.20	7.71 ± 2.73

Note Comparison before and after training: \* $p < 0.05$ , \*\* $p < 0.01$

## 4 Discussion

The music relaxation training is a systematic intervention process. On the one hand, through the regular rhythm change, it affects the cerebral cortex, so as to improve emotion and relieve tension. On the other hand, through the physical effect of music, the vibration generated by the music will have resonance with the human body, enabling the human body to secrete a kind of physiological activator to regulate blood flow and central nervous [7, 8]. In particular, it integrates the emerging somatosensory vibration audio technology, which can transfer the 16–150 Hz low-frequency signal with the consistent inherent frequency of human body and the deepest and most comfortable feeling into vibration through physical energy conversion, thus activating brain pivot in a short time, so that people will obtain high-quality mind and body relaxation and pleasure. Therefore, music relaxation training has good psychological regulation effect [9, 10]. The research has verified that the college students with exercise fatigue can shorten the reaction time, improve the calculation ability, reduce the subjective fatigue feeling through music relaxation. Moreover, the regulation and control of relaxation music can promote the recovery of the short-term mental fatigue [11–13].

The UAV operators usually work in shifts, and they will probably work for the whole night, or/and for a long time. Although they might experience several hours of low-level activities, they are required to be self-discipline and maintain vigilant. Their works are interspersed with very nervous and pressured activities in the meanwhile, namely, they usually have to perform several tasks at the same time. There is a lot of information exceeding one channel to be noticed and disposed [14]. The simulated flight task adopted to construct the psychological fatigue model is similar to the working scene of the UAV operator. In other words, in the entire simulated flight task, the long-period single-shaft pitching, deflection, and inclined tracking operations were accompanied by the rather difficult triaxial comprehensive tracking operation and additional calculation combined multiple task operation alternatively.

HRV refers to the phenomenon that the instantaneous heart rate fluctuates continuously between successive heartbeats. Through analyzing the changes of the successive heartbeat cycles, the relevant information on the control of the heart rhythm can be obtained, so as to distinguish the respective activities of the sympathetic nerve and the parasympathetic nerve. It can better reflect the activity of autonomic nerve functions than traditional physiological indexes such as breathing and heart rate [15, 16]. The results show that the changes of each time-domain indexes of the MG before and after training have significant change, in which SDNN reflects the overall condition of the autonomic nerve function, SDSD mirrors the sympathetic nerve value, both RMS-SD and PNN 50 show the pneumogastric nerve tension, indicating that the overall level of the automatic nerve function of the MG increases after training, and the function of the pneumogastric nerve is relatively superior. However, the DG only had the significant increased SDSD, showing that the sympathetic nerve is relevantly dominant, prompting that the body status of the MG is more relaxed than the DG.

In terms of frequency domain index, TF represents the overall variability of frequency, VLF mainly reflects the functional level of the sympathetic nerve, LF mainly mirrors the dual influence of sympathetic nerve and pneumogastric nerve, HF reflects the functional level of pneumogastric nerve, and LF/HF reflects the balancing between sympathetic nerve and pneumogastric nerve [17, 18]. The correction units LFnorm and HFnorm indicate the proportion of each power component in the TP minus the VLF component and emphasize more the relationship between sympathetic and parasympathetic nerve functions [19]. The result shows that, except for VLF, all other indexes of the MG have significant changes before and after training in the MG. As to the DG, only HF and HFnorm increased significantly, and LFnorm decreased significantly, and the amplitude of change was smaller than that in the MG, indicating that the music relaxation training can better enhance the activity of the pneumogastric nerve, balance functions of the sympathetic nerve and pneumogastric nerve, thereby improving the level of autonomic nervous regulation.

EEG is the aggregate performance of spontaneous and rhythmic electrophysiological activities of neurons in the skin of the head, and it can directly reflect the activities of the cerebral nervous system. Different EEG signal characteristics can reflect different psychological, physical, and mental states of humans [20, 21]. When the cerebral cortex is awake and quiet,  $\alpha$  wave is more active. When the brain is in a state of excitement, alertness, and tension,  $\beta$  wave activity is more intense. When the brain is in a low-wake state, the individual is in a fatigue state, or the cerebral nervous system is in a suppressed state, the  $\theta$  wave is more obvious [22, 23]. The experimental results show that before and after training, the  $\alpha$  wave index of the MG is significantly increased, and the  $\beta$  wave and  $\theta$  wave index are significantly reduced. By making a comparison before and after self-training, the EEG indexes of the DG have no significant changes. It prompts that the brain activity of the MG is more calm, quiet, and relaxed than that of the DG after music relaxation training, and the fatigue level is decreased significantly. On the other hand, the psychological status index result shows that various indexes of the MG have significant changes after training. The DG only has significant rise in the calmness index, indicating that the initiative feeling of fatigue and excitability of the MG is significantly lower than that of the DG.

## 5 Conclusion

The present study preliminary explores the effects of music relaxation training methods on psychological training after performing simulated flight missions. From the perspective of the results, compared with the traditional deep breath relaxation training, music relaxation training has significant psychological and physical changes, which can more effectively alleviate psychological fatigue. In addition, it has the characteristics of high acceptability, unrestricted venue, easy promotion, and so on. It will lay a sound foundation for further establishing the psychological training system for UAV operators in the future.

**Compliance with Ethical Standards** The study was approved by the Logistics Department for the Civilian Ethics Committee of Air Force Medical Center.

All subjects who participated in the experiment were provided with and signed an informed consent form.

All relevant ethical safeguards have been met with regard to subject protection.

## References

1. Yong C, Qiri W (2012) Comprehensive assessment of military flying fatigue and strategy of its rapid elimination. *J Navy Med* 33(3):152–155
2. Ling L, Yan Z (2015) Current status and future direction of mental fatigue research in civil aviation pilots. *Space Med Med Eng* 28(1):74–78
3. Jie W, Cong W, Bao-gang L et al (2011) Evaluation on effectiveness of mental fatigue countermeasure in simulated long haul flight. *Chin J Aerosp Med* 22(4):254–258
4. Zhi W, Rui D, Wei Z (2010) Effects of different feedback forms in biofeedback and music relaxation training on physiological responses and psychological variable. *China Sport Sci* 30(4):34–42
5. Berger BG, Motl RW (2000) Exercise and mood: a selective review and synthesis of research employing the profile of mood states. *J Appl Sport Psychol* 12(1):69–92
6. Abele BA, Brehm W (1986) Zur konzeptualisierung und messung von befindlichkeit. Die entwicklung der “befindlichkeitskalen” (BFS). *Diagnostica* 32(3):209–228
7. Fachner J, Gold C, Erkkilä J (2013) Music therapy modulates fronto-temporal activity in rest-EEG in depressed clients. *Brain Topogr* 26:338–354
8. Zhou K, Li X, Li J et al (2015) A clinical randomized controlled trial of music therapy and progressive muscle relaxation training in female breast cancer patients after radical mastectomy: results on depression, anxiety and length of hospital stay. *Eur J Oncol Nurs* 19:54–59
9. Lee D, Henderson A, Shum D (2004) The effect of music on preprocedure anxiety in Hong Kong Chinese day patients. *J Clin Nurs* 13(3):7
10. Evans D (2010) The effectiveness of music as an intervention for hospital patients: a systematic review. *J Adv Nurs* 37(1):8–18
11. Jing X (2008) Evaluation on the effects of relaxing music on the recovery from aerobic exercise-induced fatigue. *J Sports Med Phys Fitness* 48(1):102
12. Xiao-Guang C, Liang XU, Ying LI (2003) The study of negative oxygen ionplus musical adjustment to remove fatigue in s ports. *J Pingyuan Univ* 20(2)
13. Sihua L, Liwei Z (2015) Light music conduces to releasing short-term mental fatigue of college students. *Chin J Sports Med* 34(6)
14. Thomas RC (2013) Predictive validity of pilot selection instruments for remotely piloted aircraft training outcome. *Aviat Space Environ Med* 84(1):47–53
15. Malik M, Hnatkova K, Huikuri HV, Lombardi F, Schmidt G et al (2019) Crosstalk proposal: heart rate variability is a valid measure of cardiac autonomic responsiveness. *J Physiol* 597(10):2595–2598
16. Forte G, Favieri F, Casagrande M (2019) Heart rate variability and cognitive function: a systematic review. *Front Neurosci* 13(9):710
17. Patricia H, Claire S, Phyllis S et al (2014) Heart rate variability measurement and clinical depression in acute coronary syndrome patients: narrative review of recent literature. *Neuropsychiatr Dis Treat* 1335–1347
18. Uchida C, Waki H, Minakawa Y et al (2018) Evaluation of autonomic nervous system function using heart rate variability analysis during transient heart rate reduction caused by acupuncture. *Med Acupunct* 30(2):89–95

19. Liu Y, Huamiao S, Yishuang Z et al (2015) Effect of floating feedback training capsule in defending psychological stress on military flight personnel. *Med J Air Force* 1:5–8
20. Asif A, Majid M, Anwar SM (2019) Human stress classification using EEG signals in response to music tracks. *Comput Biol Med* 182–196
21. Jebelli H, Hwang S, Lee SH (2018) Eeg-based workers' stress recognition at construction sites. *Autom Constr* 93:315–324
22. Michael AJ, Krishnaswamy S, Mohamed J (2005) An open label study of the use of EEG biofeedback using beta training to reduce anxiety for patients with cardiac events. *Neuropsychiatr Dis Treat* 1(4):357–363
23. Formaggio E, Storti SF, Pastena L et al (2019) How expertise changes cortical sources of EEG rhythms and functional connectivity in divers under simulated deep-sea conditions. *IEEE Trans Neural Syst Rehabil Eng* 27(3):450–456

# Study on the Airworthiness Certification of Human Factor in Flight Test for Civil Aircraft



Haijing Song, Li Han, and Hongjiao Wu

**Abstract** With the development of system reliability for aircraft, human error is becoming one of the main factors that leading to flight accidents, which has been a key and difficult challenge for the design and airworthiness authorized departments. This paper analyzes the airworthiness certification process based on CCAR 25, including the selection of regulations relevant to human factor based on SHELL model and T.E.S.T matrix, the means of compliance verification for experimental aircraft based on MOC5 and MOC6; the compliance test program is determined, and a data analysis example based on fuzzy evaluation method is shown. The thought for airworthiness certification of human factor and verification method proposed in this paper has been applied preliminarily in ARJ21-700, and it can provide the technical support for the design and airworthiness certification of human factor for other civil aircraft such as C919.

**Keywords** Human factor · Airworthiness certification · Compliance test · Flight test method · Fuzzy evaluation method

## 1 Introduction

Boeing's survey shows that 10% of air accidents involve aircraft system failures, and 70–80% of flight accidents are related to human errors [1]; human factor gradually becomes the key to aviation safety and draws the design and airworthiness certification departments' attention [2, 3]. At present, human factor has been treated as an independent system for certification, and the relevant regulations are being revised abroad [4, 5]. But domestic research on human-oriented airworthiness certification is still at the very beginning. Thus, civil human factor is becoming the focus in aviation efficiency evaluation and airworthiness certification.

So how to verify whether the human factor meets the requirements of the relevant airworthiness? This paper analyzes the specific requirements of the relevant

---

H. Song (✉) · L. Han · H. Wu  
Chinese Flight Test Establishment, General Technology Institute, 710089 Xi'an, China  
e-mail: [shjaj@163.com](mailto:shjaj@163.com)

provisions of CCAR 25 on human factor based on the “SHELL model”, determines the authorization basis of human factor based on the analysis of regulation suitability (25.1302 and 25.1523), and proposes the evaluation thought based on “T.E.S.T matrix.” Furthermore, the compliance verification method (MOC5 and MOC6) which is suitable for the application in flight test phase is put forward. Combining with the flight test of ARJ21-700, this paper gives examples of data analysis, which can provide technical support for the follow-up aircraft design and airworthiness certification of C919, MA700, and other civil aircraft products.

## **2 Human Factor Airworthiness Certification Regulation**

### ***2.1 The Regulation Selection and Adaptability Analysis Related to Human Factor Based on SHELL Model***

According to the SHELL model [6–8] in the ICAO Safety Management Manual, the model mainly includes software, environment, hardware, Livewire, and their respective functional interfaces and interrelationships. Based on the specific elements of the SHELL model, the regulations in 25 serial related to human factor are as follows:

General performance rules, controllability and maneuverability, design and structure, accessibility measures, control system, pilot tiredness device operability, pilot view, etc.

The analysis of the adaptability of the regulations shows that they are based on specific system validation and are not specific to the validation of human factor, and most of them are generally broad and difficult to verify.

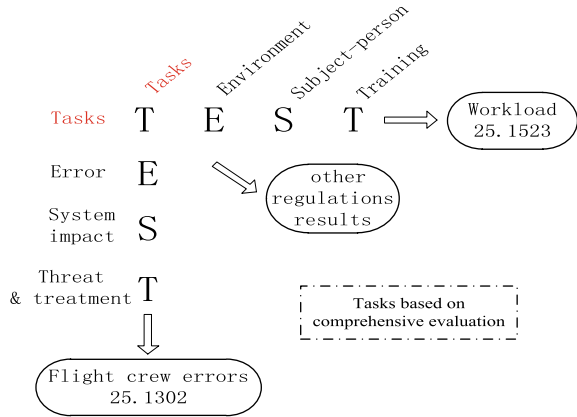
### ***2.2 Identification of Human Factor Certification Regulations Based on the “T.E.S.T Matrix”***

According to the analysis above, we can see that there are two regulations which require the validation of human factor and special test flight, namely the minimum flight crew regulation which considers the workload and the system safety regulation for reducing human error, so this article determines them as the basis for the airworthiness assessment of human factor. Considering the real work in flight test, the author and the French Academy of Aeronautics and Astronautics Professor Frederic Dehais proposed “T.E.S.T” matrix model based on the task analysis as the guiding ideology of airworthiness certification of civil aircraft human factor, shown in Fig. 1.

In the above T.E.S.T matrix model, the row and column coordinates can be expressed as T.E.S.T, but the meaning is different. The specific column coordinates



**Fig. 1** Thought of T.E.S.T matrix



T.E.S.T mean: T: flight mission; E: human error; S: system conflict; and T: the threat of flight safety.

And the specific row coordinates “T.E.S.T” mean:

T: flight mission; E: flight environment; S: the subject is the pilot; and T: flight training.

Among them, the column coordinate indicates that the pilot will make mistakes under the specific flight mission which must be considered in the airworthiness validation process of human factor, and the interaction between man and machine also must be considered, while the row coordinate indicates that four factors must be considered in the airworthiness of human factor.

Therefore, the column coordinates represent the pilot error, and the corresponding regulation is term 25.1302; then, the row coordinate considers the pilot workload, and the corresponding is airworthiness regulation 25.1523.

### 2.3 Certification Method for Human Factor in Flight Test

This paper analyzes the specific contents of 25.1523 and 25.1302, and provides the evaluation module, the specific engineering verification method, and the technical means used. The concrete frame of the validation method of human factor in flight test phase is shown as follows (see Fig. 2).

From the figure, we can see in this paper the regulation verification is divided into five modules before the airworthiness certification of human factor, and then we provide the verification method for engineering application stage, determine the technical means for achieving the result and data processing methods, and finally achieve the verification results.

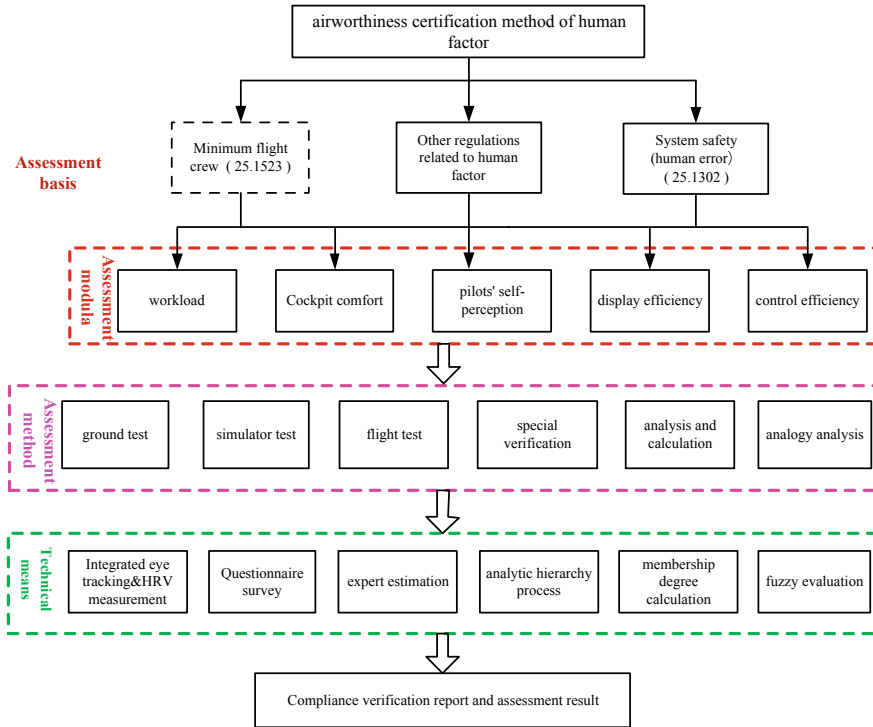


Fig. 2 Method framework for airworthiness certification of human factor during flight test phase

### 3 Human Factor Airworthiness Certification Method in Flight Test

#### 3.1 Matrix Design of Flight Test Verification

Based on the minimum crew workload verification subjects, the special flight test verification subjects for human factors in the cockpit comprehensively consider the systems and equipments which must be used by the crew to complete relevant tasks and related to crew procedures, as well as the urgency, frequency, and duration of crew’s operation to determine the flight test scenario.

The verification subjects of human factors in the cockpit include special flight tests and combined flight tests. Special flight tests include 16 subjects such as manual flight, departure of standard instruments, and precise approach, while combined flight tests mainly use the compliance verification results of over 30 articles related to human factors (except 25.1523 and 25.1302) sorted out in the first part of the paper to analyze the impacts on man-machine interface, workload, and pilot situational awareness.

### 3.2 Scenario Design of Flight Test Verification

Three cameras which are installed on the left and right side of the rear end of the cockpit top panel and above the cockpit door are used to record the captain's hand perspective, copilot's hand perspective, and front panoramic perspective, respectively, in the process of validation test. Human physiological data acquisition device is equipped to collect the pilot's heart rate data. Eye movement tracker is equipped to record the pilot's eye movements during a flight test.

### 3.3 Data Acquisition of Flight Test Verification

The verification data of special test flight mainly includes airborne equipment data, physiological and psychological data of pilots, flight comments of pilots in special test flight subjects, assessment table of Bedford aircrew workload, NASA-TLX rating table, and other relevant data.

The verification data of combined test flight mainly consists of two aspects. On the one hand, it includes the human-machine interface, workload, and situational awareness issues reflected in the validation of human factor articles. On the other hand, the assessment of daily subjects on each system and data of special verification are also required, including: a comprehensive daily use review based on cockpit interface; man-machine interface verification based on normal flight operation procedures; man-machine interface verification combined with typical flight test subjects; special verification of man-machine interface based on cockpit display security; and special test verification based on dynamic task scenario design.

## 4 An Example for Flight Test Data Analysis

Taking quantifying the qualitative evaluation for ARJ21-700 aircraft cockpit man-machine interface as an example, the evaluation system forms are as follows:

Comment level:  $V = \{v_1, v_2, v_3, v_4, v_5\} = \{\text{excellent, good, medium, bad, awful}\}$ , and the specific adjustment level and the comment meaning are in Table 1.

Evaluation index set:  $U = \{u_1, u_2, u_3, u_4, u_5\} = \{\text{workload, comfort, pilots' self-perception, display efficiency, control efficiency}\}$ .

Fuzzy weight vector set:  $= \{0.27, 0.3, 0.2, 0.1, 0.13\}$ .

Evaluation matrix:

**Table 1** Specific adjustment level and meaning of cockpit interface

Level	V	Score	Comment meaning
Excellent	$v_1$	90–100	Very satisfied, achieve satisfactory performance and no additional compensation is required
Good	$v_2$	70–90	With negligible defects, achieve satisfactory performance without additional compensation from pilot or maintainer
Medium	$v_3$	50–70	With moderately unsatisfied defects, achieve satisfactory performance with moderate compensation from pilot and maintainer
Bad	$v_4$	30–50	With intensely unsatisfied defects, achieve satisfactory performance with intense compensation from pilot and maintainer
Awful	$v_5$	0–30	With defects, some necessary operation cannot be achieved

$$R = \begin{bmatrix} r_{11} & r_{12} & r_{13} & r_{14} & r_{15} \\ r_{21} & r_{22} & r_{23} & r_{24} & r_{25} \\ r_{31} & r_{32} & r_{33} & r_{34} & r_{35} \\ r_{41} & r_{42} & r_{43} & r_{44} & r_{45} \\ r_{51} & r_{52} & r_{53} & r_{54} & r_{55} \end{bmatrix} = \begin{bmatrix} 0.45 & 0.45 & 0.15 & 0.05 & 0.05 \\ 0.2 & 0.45 & 0.125 & 0.125 & 0.125 \\ 0 & 0.35 & 0.35 & 0.2 & 0.1 \\ 0.1 & 0.45 & 0.3 & 0.1 & 0.05 \\ 0 & 0.05 & 0.4 & 0.4 & 0.4 \end{bmatrix}$$

Qualitative analysis:  $B = A \cdot R = (0.1915 \ 0.3375 \ 0.23 \ 0.153 \ 0.088)$ ;

The comment level corresponding to 0.3375 membership rating is good, so ARJ21-700 cockpit man-machine interface level can be set as good. And the evaluation value is  $W = B \cdot V^T = 3.3915$  through quantitative analysis, so the cockpit man-machine interface overall evaluation value is 3.3915.

The cockpit interface assessment example is part of the data processing in the process of human factor verification. In the practical operation, the subordinate indexes of each evaluation index are evaluated firstly and the weights are given. The display effectiveness indexes, such as the display device layout, colour and comfort, were given weights for data processing [9, 10]. The evaluation is integrated from the lowest level indicators to the next level; in the process, the low-score indexes are fed back, and then the problems are found.

Through analyzing the results, we can see that the workload and the spatial layout both get high scores; that is, the pilots and maintenance personnel are satisfied; and the display interface has the glare, the manipulation position gets a low score, and the performance is poor, which means there are moderate defects which catch the crew and maintainers' more attention. The evaluation results have been confirmed with the ARJ21-700 aircraft test crew and design department to verify the objective authenticity of the evaluation results. And, it can provide the basis for the follow-up design changes, improve the man-machine interface problems, and finally improve the interface efficiency for the finalized aircraft.

## 5 Conclusion

This paper puts forward the “SHELL model” and “TEST matrix” to airworthiness certification of human factor in the flight test phase, and determine the basis of airworthiness certification of human factor, considering the fuzziness of the definition of man-machine interface and the subjectivities in experts’ knowledge propose compliance verification method based on combined MOC5 and MOC6 which is practicality, and propose the flight test data processing method based on that integrated expert estimation, analytic hierarchy process, and fuzzy evaluation, realize the quantitative evaluation of man-machine interface, and the problems of cockpit interface can be explained more persuasively. In short, the study in this paper provides the method of airworthiness certification and comprehensive assessment of cockpit man-machine interface for civil aircraft and can provide the technical support for airworthiness certification of human factor for other civil aircraft such as C919 and MA700 as well as fills the blank of the engineering application of human factor airworthiness certification and the evaluation of interface effectiveness in the flight test phase, and provides the basis for the design changes of man-machine interface efficiency indexes for various aircraft.

## References

1. Human Factors—Harmonization Working Group (2004) Flight Crew Error/Flight Crew Performance Considerations in the Flight Deck Certification Process, Human Factors—HWG Final Report
2. Federal Aviation Administration (1996) The Interfaces between Flight crews and Modern Flight Deck Systems, FAA Report
3. Don Harris (2011) Human Performance on the Flight Deck, Ashgate
4. ICAO DOC9859 (2009) Safety Management Manual
5. MIL-STD-1472F (1999) Human engineering
6. MIL-HDBK-759C (1995) Human engineering design guidelines
7. Osborne J, Collins S, Ratcliffe M et al (2003) What ideas-about-science school be taught in school science? A delphi study of the expert community. *J Res Sci Teach* 40(7):692–720
8. Rowe J (2012) Analysis of installed systems and equipment for use by flight crews. Australian Civil Aviation Authority
9. AC25 1302 (2013) installed systems and equipment for use by flight crews. Federal Aviation Administration
10. Guo Y (2002) The theory and method of comprehensive evaluation. Science Press, Beijing, pp 41–46

# Study on Autonomic Nervous Stability Training of Military Pilots



Yishuang Zhang, Yan Zhang, Fei Peng, Yang Liao, Xueqian Deng, Huamiao Song, Duanqin Xiong, Juan Liu, and Liu Yang

**Abstract** *Objective*—to study the methods and procedures of autonomic nervous stability training for military pilots, then provide effective training program recommendations for all the training departments to organize and carry out autonomic nervous stability training for pilots. *Methods*—a total of 101 military pilots were studied, based on the three-step method, a three-stage autonomic nervous stability training was conducted for pilots by the physiological coherence and autonomic balance system (SPCS), the data of “0.1 Hz index” before and after each stage of training were collected and marked in chronological order as  $R_{1/2/3/4/5/6}$ . Then analyze and evaluate the training effect. *Results*—there was a significant difference in the 0.1 Hz index before and after the pilot training, the post-training data  $R_{2/4/6}$ , and the pre-training data  $R_{3/5}$  were significantly higher than  $R_1$ ;  $R_{3/5}$  is significantly lower than  $R_{2/4/6}$ ; there was no significant difference between  $R_2$ ,  $R_4$  and  $R_6$ , or between  $R_3$  and  $R_5$ . *Conclusion*—the three-stage pilot autonomic nervous stability training scheme, both in and without the system have remarkable effects. And the two trainings can be combined with each other.

**Keywords** Autonomic nervous stability · Training · 0.1 Hz index · Military pilots

## 1 Introduction

Military pilots often face with multiple physical and psychological challenges due to the particularity of their profession. On the one hand, the overload caused by high intensity and long-time training mission, as well as various environmental factors like high altitude hypoxia, acceleration, noise, radiation and others; for another, the higher requirements for the combat training of pilots results by the constantly improving fighter performance [1], all above making them suffer more psychological stress. According to the Yerkes–Dodson Law, work stress and work performance show an inverted u-curve, either too high or too low stress levels are detrimental to

---

Y. Zhang · Y. Zhang · F. Peng · Y. Liao · X. Deng · H. Song · D. Xiong · J. Liu · L. Yang (✉)  
Air Force Medical Center, Fourth Military Medical University, 100142 Beijing, China  
e-mail: [yangliuhenry@aliyun.com](mailto:yangliuhenry@aliyun.com)

© The Editor(s) (if applicable) and The Author(s), under exclusive license to Springer Nature Singapore Pte Ltd. 2021

S. Long and B. S. Dhillon (eds.), *Man-Machine-Environment System Engineering*, Lecture Notes in Electrical Engineering 645, [https://doi.org/10.1007/978-981-15-6978-4\\_8](https://doi.org/10.1007/978-981-15-6978-4_8)

optimal performance. Therefore, it is of great significance to study how to reduce the stress level of pilots through psychological training to improve their operational psychological effectiveness.

Autonomic nerve stability training refers to enhancing autonomic nerve regulation ability through active training, so that one can maintain a stable and coordinated state. Previous studies have shown that the enhancement of autonomic nervous stability may strengthen individual functions of cardiovascular, endocrine and gastrointestinal tract, meanwhile relieve anxiety, depression and other emotional problems [2], to maintain psychosomatic health and help individuals maintain the best work performance [3]. Previous studies by Yang Liu et al. have proved that the autonomic nervous stability training can effectively regulate the balance of autonomic nervous function of military pilots and maintain their excellent flight combat effectiveness, but the practical applicability of the training methods and training procedures involved remains to be further studied and improved [4]. This paper will further explore the autonomic nervous stability training methods and procedures for pilots.

## **2 Objects and Methods**

### **2.1 Objects**

The study involved 101 military pilots recently trained in aviation medical identification. The general condition of the subject: all male; average age  $33.70 \pm 9.34$  years (range 22–57 years); average flight time  $2670.87 \pm 2069.93$  h (range 120–1110 h).

### **2.2 Methods**

#### **2.2.1 Autonomic Nervous Stability Training Equipment**

The tool for training and data collection is self-generate physiological coherence system (SPCS) developed by Beijing Haofeng Technology Company. The system records the indicators of heart rate variability (HRV) by means of the ear-wearing information collector. In addition, the changes in HRV indicators during training will be fed back through SPCS, so that the subjects can feel the changes in autonomic nerve activities and learn to adjust them consciously.

#### **2.2.2 Three Steps for Autonomic Nervous Stability Training**

Step 1: Focus on the heart. Imagine the heart as a command center, issuing commands to the brain and other organs of the body. Step 2: Breathe evenly through the heart,

keep focusing on the heart, breathe out—imagine draining excess air from the heart, breathe in—imagine oxygen filling the heart, and your mind getting clearer, pay attention to the rhythm between exhale and inhale, and keep breathing evenly and deeply; Step 3: Keep in good condition as in the first two steps, to experience positive emotions and the joy of good feelings with heart.

### 2.2.3 Training Steps

Each subject was required to complete three stages of autonomic nervous stability training, and relevant data indicators were collected before and after training. Specific implementation steps are as follows:

(The first stage)

1. Inform the subjects of the training principle, guide them to watch the video teaching of “three steps for autonomic nervous stability training” in SPCS, and learn the training method;
2. The subjects were equipped with ear-wearing information collector, sit down and relax, with their arms lying naturally on both sides of the body, trying to keep a clear mind, without considering anything, and keep natural breathing. The state of the subjects before training was detected for 3 min in the state assessment interface, and the result was recorded as  $R_1$ ;
3. Enter the training center then guide the subjects to carry out the three times trainings for easy–medium–difficult by the training module of “Bodhi tree”;
4. Return to the state assessment interface and conduct the subjects’ state test again for 3 min according to the method just learned. The result is recorded as  $R_2$ ;

(The second stage)

5. On day 2, repeat the 2–4 process, during the pre-training state assessment, the subjects were prompted to recall the training methods learned on day 1, and the result was recorded as  $R_3$ . The state assessment result after training in this stage is recorded as  $R_4$ ;

(The third stage)

6. On day 3, repeat the 5 process, the state assessment result before training in this stage was recorded as  $R_5$ , and which after training was recorded as  $R_6$ .

### 2.2.4 Collecting Indicators

Total power (TP): The total power spectrum is a frequency-domain indicator of HRV automatically collected by the system, which reflects the overall functional level and running state of the autonomic nervous system. In the data collection of this experiment, the power spectrum in frequency domain is divided into 64 data points to maximize the accuracy of frequency resolution. Number the 64 data points in order and indicate as  $PWR_n$  ( $n = 1, 2, \dots, 64$ ), then,



$$TP = \sum_{n=1}^{64} PWR_n \quad (1)$$

0.1 Hz index (R): refers to the ratio of power around 0.1 Hz to the total power, reflecting the stable state of autonomic nerves. In this study,

$$R = \sum_{n=6}^8 PWR_n / TP \quad (2)$$

### 2.3 Statistical Processing

Preprocess data With EXCLE preprocessing data, and calculating the participants  $R$  with EXCLE value, then use PASW 18 statistical software for data analysis. Measurement data was expressed as  $\bar{x} \pm s$ , Friedman test and Wilcoxon test were used for results comparison, while  $p < 0.05$  was considered statistically significant.

## 3 Results

### 3.1 Overall Effect of Autonomic Stability Training

The 0.1 Hz index of subjects before and after training was tested by Friedman, and the results are shown in Table 1, which showed that there was a statistically significant difference in the 0.1 Hz index before and after training ( $p < 0.01$ ).

**Table 1** Friedman test results of 0.1 Hz index before and after the three-stage training ( $\bar{x} \pm s$ )

	0.1 Hz index	$\chi^2$ value	$p$ value
Before the first training stage ( $R_1$ )	0.2074 $\pm$ 0.1166	105.55	0.00
After the first training stage ( $R_2$ )	0.4689 $\pm$ 0.2278		
Before the second training stage ( $R_3$ )	0.3960 $\pm$ 0.2367		
After the second training stage ( $R_4$ )	0.4976 $\pm$ 0.2453		
Before the third training stage ( $R_5$ )	0.4213 $\pm$ 0.2316		
After the third training stage ( $R_6$ )	0.4756 $\pm$ 0.2485		

**Table 2** Results of Wilcoxon test in different stages (Z value)

	Before the first training stage ( $R_1$ )	After the first training stage ( $R_2$ )	After the second training stage ( $R_4$ )
Before the first training stage ( $R_1$ )	–		
After the first training stage ( $R_2$ )	** –7.881 <sup>a</sup>	–	
After the second training stage ( $R_4$ )	** –7.673 <sup>a</sup>	–0.556 <sup>a</sup>	–
After the third training stage ( $R_6$ )	** –6.839 <sup>a</sup>	–0.203 <sup>a</sup>	–1.055 <sup>b</sup>

Note \* $p < 0.05$ , \*\* $p < 0.01$ , <sup>a</sup>based on negative ranks, <sup>b</sup>based on positive ranks

### 3.2 Staged Effect of Autonomic Nervous Stability Training

In order to further analyze the source of the difference and study the training effect of each stage of autonomic nervous stability training, the nonparametric signed rank difference test (Wilcoxon test) was performed on the baseline index before training ( $R_1$ ) and the index after three-stage training ( $R_{2/4/6}$ ). The results are shown in Table 2. Results of  $R_{2/4/6}$  were significantly higher than  $R_1$ , while there was no significant difference between  $R_2$ ,  $R_4$  and  $R_6$ .

### 3.3 Effect of Autonomic Nervous Stability Training Based on Recalls

The collecting indicators before the second stage of training ( $R_3$ ) and the third stage of training ( $R_5$ ) were all 0.1 Hz index when the subjects conducted without SPCS training by means of recall. To study the actual effect of training based on recalls, the 0.1 Hz index collected before and after the three-stage training was compared (by Wilcoxon test), and the results are shown in Table 3. The results of  $R_{3/5}$  were significantly higher than  $R_1$ , and  $R_{3/5}$  was significantly lower than  $R_{2/4/6}$ , while there was no significant difference between  $R_3$  and  $R_5$ .

## 4 Discussion

In recent years, psychological training has been regarded as the key to improve the psychological performance of military personnel in combat, which is being taken seriously by the armed forces of developed countries such as Britain and the

**Table 3** Wilcoxon test results of 0.1 Hz index before and after three-stage training (Z value)

	Before the first training stage ( $R_1$ )	After the first training stage ( $R_2$ )	Before the second training stage ( $R_3$ )	After the second training stage ( $R_4$ )	Before the third training stage ( $R_5$ )
Before the first training stage ( $R_1$ )	–				
After the first training stage ( $R_2$ )	**–7.881 <sup>a</sup>	–			
Before the second training stage ( $R_3$ )	**–6.500 <sup>a</sup>	**–2.959 <sup>b</sup>	–		
After the second training stage ( $R_4$ )	**–7.673 <sup>a</sup>	–0.556 <sup>a</sup>	**–3.722 <sup>a</sup>	–	
Before the third training stage ( $R_5$ )	**–7.219 <sup>a</sup>	*–2.053 <sup>b</sup>	–1.076 <sup>a</sup>	**–2.673 <sup>b</sup>	–
After the third training stage ( $R_6$ )	**–6.839 <sup>a</sup>	–0.203 <sup>a</sup>	**–2.846 <sup>a</sup>	–1.055 <sup>b</sup>	*2.346 <sup>a</sup>

Note \* $p < 0.05$ , \*\* $p < 0.01$ , <sup>a</sup>based on negative ranks, <sup>b</sup>based on positive ranks

USA. Aerospace medicine is also focusing on how to improve the combat psychological effectiveness of pilots through psychological training. In our army, how to combat psychological stress and optimize military performance through psychological training has also become a research hotspot. So it is of great military significance to study and popularize the method of autonomic nervous stability training, which is suitable for all training departments.

The level of autonomic nervous stability is an effective indicator to evaluate the degree of individual stress, the training method of which has been widely concerned at home and abroad. Available techniques include breathing training, cooling water training [5], aerobic exercise [6], floating relaxation feedback training [7], relaxation training [8], etc. Among them, the self-balancing three-step method proposed by the American Heart Math institute is a simple and effective way of training, which help improve the pilot psychological coherence state, the sympathetic and parasympathetic nerve activity to achieve a balance in this state. In other words, the pilots' autonomic nervous function will be "mobilized" to the appropriate height, entering the best psychological energy area (excited but not tense), and the pilots should achieve the best performance in flight operation [4]. The studies have shown that when the body is in the state of autonomic nervous coherence, the heart rate is close

to the sinusoidal waveform, and the HRV power spectrum will change significantly, adjusting to the resonance frequency of the pressure-sensitive feedback loop (about 0.1 Hz) [9], which is shown in this paper as an exponential increase of 0.1 Hz.

The effect of pilot autonomic stability training also depends on the training program design. In this study, based on the full investigation of the pilot selection training procedure, taking into account the location, time and equipment configuration of the pilot training, and referring to other physiological indicators training standards, the period of completing the medical identification is set as the training period, and the training program is designed into three stages. It can be seen from the research results that, (1) after the end of the first stage of training, the 0.1 Hz index of subjects were significantly increased, indicating that the autonomic nervous stability was significantly enhanced and the training method was effective; (2) the autonomic nervous stability level after the second and third stages of training was similar to that after the first stage (no statistical differences), and 0.1 Hz index after three stages of training were much higher than before, improve rate  $(R_{2/4/6}-R_1)/R_1 * 100\%$  have reached more than 110%, indicating that in the three-stage training, the autonomic nervous stability training method based on the guidance of the software is easy to master and has a good effect. The subjects may master the basic methods in just one stage of training; (3) the autonomic nerve stability level of the subjects before the training in the second and third stages was similar and significantly higher than the baseline level. The improvement rate of the training results in the two stages  $(R_{3/5}-R_1)/R_1 * 100\%$  both reached more than 90%, reflecting that after the study of the first stage of training, the subjects could still achieve a good-enough training effect by only memory, without the help of software guidance. However, due to the forgetting effect, relying on memory can only achieve part of the training effect. Software exercises should be used as often as possible to make the training permanent.

In conclusion, it is considered to set the pilot autonomic nervous stability training mode as the combination of in-software training and without-software training. The training process is divided into at least three stages: the first stage is the “learning stage”, and the second and third stages are the “consolidation stage.” All the training stages should be completed with the help of equipment and application system, the interval of each training stage shall not be less than one day, but not more than three days. And the pilots are recommended to extend the consolidation stage according to his own training conditions. During the extended practice days, they can also choose without-software training method.

**Compliance with Ethical Standards** The study was approved by the Logistics Department for Civilian Ethics Committee of Air Force Medical Center, PLA.

All subjects who participated in the experiment were provided with and signed an informed consent form.

All relevant ethical safeguards have been met with regard to subject protection.

## References

1. Tomczak, Andrzej (2015) Coordination motor skills of military pilots subjected to survival training. *J Strength Cond Res* 29(9):2460–2464
2. Shin KA, Shin KS, Hong SB (2015) Heart rate recovery and chronotropic incompetence in patients with prehypertension. *Minerva Med* 106(2):87–94
3. Garet M, Tournaire N, Roche F et al (2004) Individual interdependence between nocturnal ans activity and performance in swimmers. *Med Sci Sports Exerc* 36(12):2112–2118
4. Liu Y, Yishuang Z, Wen D et al (2017) Effect of autonomic nervous stability training on military flight personnel. *J Prevent Med Chinese People's Liberation Army* 35, 200(12):42–45
5. Rathus JH, Miller AL (2015) DBT skills manual for adolescents. Guilford, New York, pp 140–142
6. de Sá JCF, Costa EC, Silva ED, Tamburús NY, Azevedo GD (2015) Aerobic exercise improves cardiac autonomic modulation in women with polycystic ovary syndrome. *Int J Cardiol Heart Vasc* 202(5):356–361
7. Liu Y, Huamiao S, Yishuang Z et al (2015) Effect of floating feedback training capsule in defending psychological stress on military flight personnel. *Med J Air Force* 1:5–8
8. Guoqin Y, Huamiao S, Zhenzhen W et al (2017) A research about the influence of military pilot psychological energy storage training to major military operations. *Med J Air Force* 01:22–25
9. Miyata M, Sano Y, Suzuki K, Yamazaki T, Hata T (2002) Evaluation of respiratory modulation on the pulse wave amplitude in low-birth-weight neonate. *Biol Sci Space* 16(3):215–216

# Research on Recognizable Physiological Signals of Workers Working at Heights



Guilei Sun, Fangming Pang, Qi Liu, Yun Lin, Luyao Xu, and Yanhua Meng

**Abstract** In order to reduce the accident rate of workers working at heights, state identification is very important for the workers. VR technology was used to simulate operations and environment at heights, and man-machine-ring synchronization platform was used to collect six kinds of physiological signal data in the scenes, which are working on the ground, 4 m high, and 8 m high. SPSS was used to analyze the data. The results show that operators at different heights have a significant effect on the time domain of the skin electrical signal, but do not have a significant correlation with the time domain of other physiological signals. A formula,  $IEDA = 0.0284H^2 + 0.7377H + C$  ( $C$  is the correction constant), was given for personal test. Then, EDA can be used as a judgment basis for workers at heights, and it can be used as a manager's monitoring for workers' states at heights, thereby reducing the occurrence of high-altitude operating accidents.

**Keywords** Working at heights · Physiological signals · Virtual reality (VR) · Electrodermal activity (EDA) · Quadratic polynomial correlation

## 1 Introduction

Work at heights is a very high-risk operation activity. Among all types of accidents, height fall accident has the highest incidence and the greatest risk [1]. Every year, the proportion of high falling is about 50% of all types of accidents. At present, the management of high-place workers mainly depends on training and wearing personal protective equipment, while the recognition of human physiological state is currently in the development stage of wearable body area network products. Since 2013, the health monitoring system of wearable sensors has gradually developed

---

G. Sun · F. Pang · Q. Liu · Y. Lin · L. Xu · Y. Meng (✉)  
Department of Safety Engineering, China University of Labor Relations, 100048 Beijing, China  
e-mail: [mengyh2008@126.com](mailto:mengyh2008@126.com)

G. Sun  
e-mail: [sunguilei@culr.edu.cn](mailto:sunguilei@culr.edu.cn)

in the biomedical field, which will integrate heart rate and respiratory rate to judge the physiological state of human body [2]. Singh et al. [3] collect skin resistance signal and pulse wave signal to classify the pressure level of drivers through wearable sensors. Kavsaoglu et al. [4] use pulse wave signal to classify and predict the hemoglobin level of human body through machine learning. Li et al. [5] used the method of support vector machine (SVM) to classify the pulse wave signals and determine whether the human body is in the state of sinus bradycardia. Lee et al. [6] used the EMG signal, pulse signal, and inertial sensor signal collected by wearable sensors to classify the driver's emotional state. Egger et al. [7] studied people's emotions through pulse wave signals. Wu et al. [8] studied the injury and influencing factors of repetitive ipsilateral lifting on the erector spine muscle by EMG detection. Hu et al. [9] used the measured EEG signals to carry out driving simulation experiments to get the safest driving state.

At present, physiological signals have not been used for detection at China and abroad. In view of the high risk and accident rate of work at height, the research is based on virtual reality. At the same time, six physiological indexes of the subjects were collected by using the human-machine-environment synchronous platform to analyze the correlation with the high-place work, in order to identify the high-place work. Through physiological signal recognition, using wireless detection technology to detect real time the working status of operators is of great significance to prevent falling accidents.

## 2 Experimental Design

### 2.1 Experiment Scheme

Vizable software was used to set up three groups of test scenes: "ground", "work at 4 m high from the ground", and "work at 8 m high from the ground". "Painting work" was set as the type of operation. Six kinds of data, including electrocardiograph (ECG), electromyogram (EMG), photoplethysmographic (PPG), respire (RESP), electrodermal activity (EDA), and skin temperature (SKT), were intercepted in the virtual reality experiment in three experimental scenarios by using the human-machine-environment synchronous platform. The questionnaire survey and physiological signal analysis were analyzed by SPSS.

### 2.2 Subjects

According to the questionnaire, the ratio of male and female was set as 8:2. And in the VR experiments, 30 subjects, healthy, were selected. All of the subjects attending

**Fig. 1** Experimental scene

a. a subject enters the work site

b. a subject is operating

the experiments were voluntary and had no other emotional impact. The experiment was shown in Fig. 1.

### 3 Data Statistics and Analysis

#### 3.1 Questionnaire Analysis

##### 3.1.1 Analysis of Questionnaire Before Experiment

An electronic questionnaire was designed and distributed to the workers on site to fill in. A total of 239 questionnaires were received, including 228 valid ones. According to the questionnaire, 78.9% of the workers were male, mainly aged 20–35 years old. The data shows that 60.6% of the workers have been engaged in work at heights, and the proportion of the workers who have had dangerous conditions is as high as 55%, of which more than half suffer from the risk of falling from height. The statistical data is shown in Fig. 2.

For work at heights, it is of fundamental significance for management to find the physiological signals that change obviously when the construction workers are in danger.

##### 3.1.2 Subjective Questionnaire Survey After the Experiment

Using psychological ruler, as shown in Fig. 3, 30 subjects were surveyed and analyzed for risk perception at different heights. The results were described statistically with the ruler length as the standard by subjective measurement. The average ruler length at a height of 4 m was 3.9875 cm long; the average length at the scene of 8 m high



**Fig. 2** Proportion of construction accident types

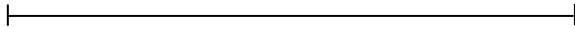
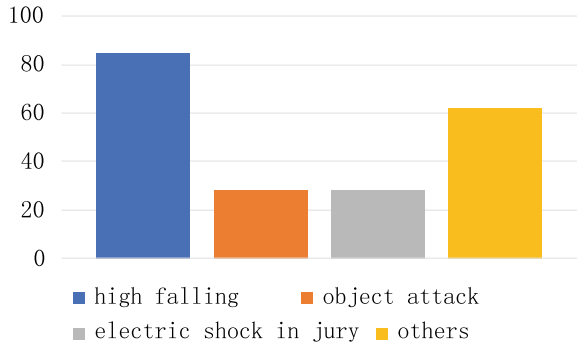


**Fig. 3** Risk-subjective measurement scale

was 5.9375 cm, whereas on the ground value, it was 0. Correlation analysis was only performed on paired samples with a height of 4 and 8 m, and the correlation coefficient was 0.907, which shows a very strong correlation. The data was tested for normality, and the test results were shown in Table 1. The data shows a normal distribution. Therefore, the data was subjected to a paired sample *t*-test. The results were shown in Table 2.

Table 2 shows that at different heights, the subjective feelings of the subjects also showed statistical significance at a statistical level of 0.05, indicating that the difference in height affects the subjective feelings. It can be seen from Fig. 4 that the higher the distance from the ground, the more obvious the subjective feeling of the

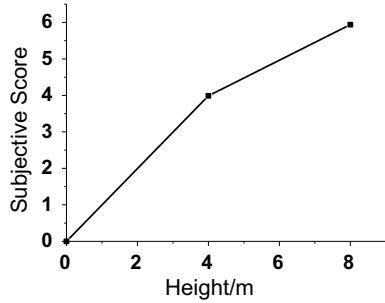
**Table 1** Tests of normality

Height (m)	Shapiro–Wilk	
	Statistic	Sig.
4	0.914	0.381
8	0.962	0.832

**Table 2** Paired sample *t*-test for questionnaire

Comparison	Paired differences				<i>t</i>	Sig. (two-tailed)	
	Mean	Std. deviation	Std. error mean	95% confidence interval of the difference			
				Lower			Upper
8 m versus 4 m	1.95000	1.02678	0.36302	1.09159	2.80841	5.372	0.001

**Fig. 4** Subjective scoring of risk



operator, but the increase from the ground to 4 m high is greater than the increase from 4 m high to 8 m high. It indicates that as the distance from the ground increases, this growth rate gradually slows down.

### 3.2 Physiological Signal Analysis

In order to conduct a more objective analysis of the subjects, wireless test method for physiological signals was used to extract six types of physiological signals of 30 subjects at work. Preliminary analysis revealed that two person’s data was abnormal. One of them had abnormal data collection, and the others’ data was more than twice of standard deviation ( $|Z| > 2$ ). After removing the abnormal data, Pearson’s correlation analysis was performed on the mean of all data. The results are shown in Table 3.

From the correlation analysis, among the six physiological signals, only the EDA time-domain mean and SKT showed statistical significance at the test level of 0.05.

**Table 3** Correlation analysis of time-domain mean of physiological signals

Comparison		0 m versus 4 m	0 m versus 8 m	4 m versus 8 m
EDA	Pearson’s correlation	0.64	0.594	0.898
	Sig. (two-tailed)	0	0	0
EMG	Pearson’s correlation	0.204	0.192	0.419
	Sig. (two-tailed)	0.279	0.311	0.021
PPG	Pearson’s correlation	0.059	-0.251	0.026
	Sig. (two-tailed)	0.756	0.181	0.892
SKT	Pearson’s correlation	0.497	0.732	0.882
	Sig. (two-tailed)	0.005	0	0
RESP	Pearson’s correlation	0.29	-0.014	0.539
	Sig. (two-tailed)	0.12	0.842	0.002
ECG	Pearson’s correlation	0.33	0.282	0.137
	Sig. (two-tailed)	0.075	0.13	0.47

If physiological signals are used as the methods for measuring the status of workers, then based on statistical significance, the three correlations need to be further studied. However, from the data itself, the correlation of physiological signals between 4 m high and ground should be greater than 8 m high and ground as the group of subjects was the same. EDA meets the requirements, while SKT has the opposite. Therefore, the height recognition of work at heights cannot be calibrated using the time-domain value of SKT. Further analysis was performed on the EDA time-domain average value (synthesized from the average value of tonic data, phase data, and SC signal to indicate the skin electrical signal), and Shapiro–Wilk was used to perform normality test. The results are shown in Table 4, which shows that the data conform to the normal distribution.

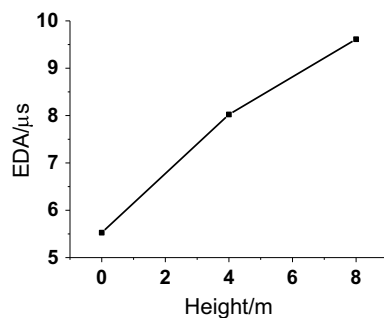
Figure 5 shows the relationship between the mean of the EDA time-domain parameters and the height. It shows that the increase in EDA in the figure gradually decreases as the height is same, which is consistent with the trend of subjective scores. And it also illustrates the effectiveness of using EDA to analyze operators at heights. A binomial fit of the data is given,

$$\text{Mean} = -0.0284H^2 + 0.7377H + 5.5264, R^2 = 1 \tag{1}$$

**Table 4** Paired sample *t*-test

Comparison	Paired differences					<i>t</i>	Sig. (two-tailed)
	Mean	Std. deviation	Std. error mean	95% confidence interval of the difference			
				Lower	Upper		
0 m versus 4 m	2.49679	3.06997	0.58017	1.30638	3.68720	4.304	0.000
0 m versus 8 m	4.08536	3.49368	0.66024	2.73065	5.44006	6.188	0.000
4 m versus 8 m	1.58857	1.86642	0.35272	0.86485	2.31229	4.504	0.000

**Fig. 5** Correlation between mean and height in EDA time domain



The relationship between the EDA mean and height is parabolic. In order to calculate for each subject's data, the personal basic state constant  $C$  is introduced to modify the parameters, that is, the value of the constant  $C$  is obtained after measuring the value of the individual when on the ground. Then, Formula (1) is modified as:

$$\text{IEDA} = -0.0284H^2 + 0.7377H + C \quad (2)$$

This formula can be used to calculate the data of each worker to measure whether the worker has entered the working state at heights and further estimate to the position of the worker.

## 4 Conclusions

1. In the time-domain analysis of physiological signals for subjects at different heights to the ground, the mean value of EDA shows significant differences at different heights; therefore, EDA signal can be used as a physiological signal for identifying the persons who works at heights.
2. When working at heights, the mean of EDA of individual and work position height have the relationship of quadratic nonlinearity:  $\text{IEDA} = 0.0284H^2 + 0.7377H + C$  ( $C$  is a correction constant), and the increase of IEDA decreases with the increase in height.
3. There is no significant correlation between the time domains of the five physiological parameters, EMG, PPG, SKT, RESP, and ECG, and the height for workers at heights.

**Acknowledgements** This work is supported by General project of China University of Labor Relations (20XYJS020).

**Compliance with Ethical Standards** The study was approved by the Logistics Department for Civilian Ethics Committee of China University of Labor Relations.

All subjects who participated in the experiment were provided with and signed an informed consent form.

All relevant ethical safeguards have been met with regard to subject protection.

## References

1. Li XD, Chen Q (2012) Main types and prevention measures on construction production safety accidents in China. *China Civ Eng J* 45(S2):245–248
2. Banaee H, Ahmed MU, Loutfi A (2013) A framework for automatic text generation of trends in physiological time series data. In: 2013 IEEE international conference on systems, man, and cybernetics, IEEE, pp 3876–3881

3. Singh RR, Conjeti S, Banerjee R (2013) A comparative evaluation of neural network classifiers for stress level analysis of automotive drivers using physiological signals. *Biomed Signal Process Control* 8(6):740–754
4. Kavsaoğlu AR, Polat K, Hariharan M (2015) Non-invasive prediction of hemoglobin level using machine learning techniques with the PPG signal's characteristics features. *Appl Soft Comput* 37:983–991
5. Li F, Yang L, Shi H, Liu C (2017) Differences in photoplethysmography morphological features and feature time series between two opposite emotions: Happiness and sadness. *Artery Res* 18:7–13
6. Lee BG, Chong TW, Lee BL, Park HJ, Kim YN, Kim B (2017) Wearable mobile-based emotional response-monitoring system for drivers. *IEEE Trans Human-Mach Syst* 47(5):636–649
7. Egger M, Ley M, Hanke S (2019) Emotion recognition from physiological signal analysis: a review. *Electro Notes in Theor Comput Sci* 343(4):35–55
8. Wu H, Pan JG, Fu JW, Liang GC, Qi W, Wu D (2017) Effects of repetitive transcranial magnetic stimulation with different frequencies on swallowing function and surface electromyography of stroke patients with swallowing dysfunction. *Chongqing Med J* 46(32):4564–4566
9. Hu JF, Wang TT (2018) Riving fatigue detection and analysis based on fuzzy entropy of EEG signal. *Chinese J Safety Sci* 28(04):13–18

# A Study on the Construction of Mental Fatigue Model and the Change of Psychological Efficacy



Liu Yang, Yishuang Zhang, Yan Zhang, Yang Liao, Duanqin Xiong, Rong Lin, Jian Du, and Xichen Geng

**Abstract** *Objective* The mental fatigue model was constructed to explore the dynamic characteristics of psychological efficacy such as emotion, cognition and simulated flight mission (SFM) performance. *Methods* A total of 37 healthy male subjects were recruited in this study. The mental fatigue model was constructed by using 40 h sleep deprivation. The body emotion state, alertness, risk decision-making and SPF performance were collected at 15 time points, respectively. The dynamic changes were studied by psychophysiological interaction and correlation analysis. *Result* Compared with the baseline, the subjects' (1) fatigue, drowsiness and negative emotion increased significantly; (2) attention decreased, risk decision-making was impaired; (3) SFM performance decreased; (4) SFM performance decreased the earliest, followed by emotion, attention and risk decision-making; (5) there was a positive correlation between anger and the performance impairment of SFM. *Conclusion* The model of mental fatigue was successfully constructed, and the dynamic changes of various behavioral indicators and their correlation were analyzed in detail, which provided a reliable basis for the follow-up study.

**Keywords** Mental fatigue · Psychological efficacy · Emotion · Attention · Risk decision-making · Simulated flight mission

## 1 Introduction

With the acceleration of the modernization of the Chinese army, a large number of high-performance fighters have gradually become the main equipment. The high performance improves the reliability and automation of the aircraft, and the pilot's control load is greatly reduced. However, due to the increase of information equipment and the change of display mode, pilots need to process a lot of information data timely and accurately. All of these make the pilot's cognitive load extremely heavy, which is easy to lead to mental fatigue. When the pilots suffer from mental

---

L. Yang · Y. Zhang · Y. Zhang · Y. Liao · D. Xiong · R. Lin · J. Du · X. Geng (✉)  
Air Force Medical Center, Fourth Military Medical University, 100142 Beijing, China  
e-mail: [gxc365@126.com](mailto:gxc365@126.com)

© The Editor(s) (if applicable) and The Author(s), under exclusive license to Springer Nature Singapore Pte Ltd. 2021

S. Long and B. S. Dhillon (eds.), *Man-Machine-Environment System Engineering*, Lecture Notes in Electrical Engineering 645, [https://doi.org/10.1007/978-981-15-6978-4\\_10](https://doi.org/10.1007/978-981-15-6978-4_10)

fatigue, they will become slow in response, lose situational awareness and weaken in emotional regulation, which will lead to the decline of flight ability and serious accidents. According to a survey in the USA, 93% of pilots have experienced flight fatigue. 10–54% of all combat casualties are caused by fatigue, so mental fatigue in flight is a common and important aviation hygiene support issue. In this background, it has become an important research direction in modern military medicine to study the negative effects of mental fatigue on human body and the countermeasures to ensure the operational effectiveness of military personnel.

It is one of the key issues to effectively induce mental fatigue and build a reliable model in the laboratory. At present, sleep deprivation (SD) is often used to build mental fatigue model. According to the degree of sleep deprivation, it can be divided into total sleep deprivation (TSD) and partial sleep deprivation (PSD). TSD refers to complete no sleep for at least 24 consecutive hours, and PSD refers to the daily sleep amount less than 50% of the normal sleep amount. In the study in military personnel, it is found that SD can seriously damage the combat effectiveness of military personnel and the whole team, especially the impact on important positions such as fighter pilots, which require a higher level of sustained attention and more stringent error tolerance [1]. It can be seen that SD is not only a reliable means to induce mental fatigue in the laboratory, but also a reality of military personnel in the battlefield environment, which has good scientific and application value. Therefore, in this paper, we use the method of TSD to build a mental fatigue model and study the dynamic changes of mental functions.

## **2 Subjects and Methods**

### **2.1 Subjects**

The subjects were 37 volunteers, all of whom were young healthy men from universities in Beijing, aged 21–25 (average  $23.1 \pm 1.9$ ) years old.

### **2.2 Methods**

#### **2.2.1 Experimental Design**

The experiment was designed with self-control and repeated measurement. All subjects were deprived of sleep for 40 h, and the whole experiment was completed within two months.

**Table 1** Experimental data collection schedule

Serial number	Day	Time	Collection project	Experiment point of time (h)
01	D1	08:00	Enrollment registration	
02		09:00	<input type="checkbox"/> SFM	1
03		10:00	<input type="checkbox"/> PVT <input type="checkbox"/> GDT <input type="checkbox"/> Scale	2
04		15:00	<input type="checkbox"/> SFM	7
05		16:00	<input type="checkbox"/> PVT <input type="checkbox"/> GDT <input type="checkbox"/> Scale	8
06		20:00	<input type="checkbox"/> SFM	12
07		23:00	<input type="checkbox"/> PVT <input type="checkbox"/> GDT <input type="checkbox"/> Scale	15
08	D2	02:00	<input type="checkbox"/> Scale	18
09		04:00	<input type="checkbox"/> PVT <input type="checkbox"/> GDT <input type="checkbox"/> Scale	20
10		06:00	<input type="checkbox"/> Scale	22
11		08:00	<input type="checkbox"/> SFM	24
12		09:00	<input type="checkbox"/> PVT <input type="checkbox"/> GDT <input type="checkbox"/> Scale	25
13		15:00	<input type="checkbox"/> SFM	31
14		16:00	<input type="checkbox"/> PVT <input type="checkbox"/> GDT <input type="checkbox"/> Scale	32
15		20:00	<input type="checkbox"/> SFM	36
16		21:00	<input type="checkbox"/> PVT <input type="checkbox"/> GDT <input type="checkbox"/> Scale	37

**2.2.2 Experimental Process and Schedule**

Take 08:00 on the day of experiment (D1) as the starting point, and its acquisition time point is transformed into TSD time point, as shown in Table 1.

**2.3 Data Statistics**

During the whole experiment, there was no loss of samples. SPSS statistics 20.0 software package (IBM Corporation) was used for the statistical analysis of all data. Repeated measurement, Spearman correlation and other statistical methods were used to analyze data results. Bonferroni method was used for multiple comparisons to correct P value, and all significance  $\alpha$  value was set as 0.05.



## 3 Results

### 3.1 *Results of Physical and Emotional Status Assessment Questionnaire*

See Table 2 for the results of each index

### 3.2 *PVT Results*

See Table 3 for the results

### 3.3 *GDT Results*

See Table 4 for the results of each index

### 3.4 *SFM Performance Results*

See Table 5 for the results

### 3.5 *Correlation Between Scale and SFM Performance*

As shown in Fig. 1, through correlation analysis, we found that there was a significant negative correlation between angry state (37 h) and SFM performance (36 h) after sleep deprivation ( $r = -0.285$ ,  $P < 0.05$ ). The results showed that the higher the anger state, the worse the SFM performance (Fig. 1).

## 4 Discussion

Different studies have shown that SD has a great difference in the impact on the body's subjective feelings, but most of the results still show that TSD will lead to the deterioration of the body's subjective feelings, such as decreased physical strength, increased fatigue and drowsiness disorder [2, 3]. Our research results also show that with the progress of SD, the subjective body feelings such as pressure, fatigue and drowsiness are constantly increasing, among which the time point of drowsiness

**Table 2** Results of physical and emotional assessment questionnaire ( $n = 37, \bar{x} \pm s$ )

Index	TSD experiment point of time										
	Baseline	8 h	15 h	18 h	20 h	22 h	25 h	32 h	37 h		
Stress	3.15 ± 1.31	3.34 ± 1.5	3.6 ± 1.68	4.26 ± 1.48**	4.97 ± 1.48**	4.88 ± 1.78**	5.32 ± 1.98**	4.97 ± 1.74**	5.12 ± 2.01**		
Fatigue	3.18 ± 0.23	3.53 ± 0.26	4.09 ± 0.26	5.44 ± 0.25**	6.03 ± 0.24**	5.64 ± 0.31**	6.18 ± 0.32**	5.88 ± 0.29**	6.14 ± 0.32**		
Drowsiness	2.15 ± 0.14	2.42 ± 0.15	2.79 ± 0.17**	4.12 ± 0.19**	4.56 ± 0.19**	4.18 ± 0.23**	4.68 ± 0.23**	4.35 ± 0.22**	4.29 ± 0.24**		
Tension	1.72 ± 0.21	0.97 ± 0.13	1.43 ± 0.19	2.24 ± 0.22**	2.96 ± 0.27**	3.24 ± 0.34**	4.06 ± 0.37**	3.73 ± 0.36**	4.03 ± 0.42**		
Anger	0.5 ± 0.28	0.22 ± 0.1	1.06 ± 0.35	1.76 ± 0.42	2.06 ± 0.48**	2.7 ± 0.64**	3 ± 0.63**	3.06 ± 0.66**	3.09 ± 0.77		
Fatigue	3.18 ± 0.24	3.53 ± 0.26	4.09 ± 0.26	5.44 ± 0.25**	6.03 ± 0.24**	5.65 ± 0.31**	6.18 ± 0.32**	5.88 ± 0.29**	6.15 ± 0.32**		
Depression	0.94 ± 0.25	0.75 ± 0.17	1.38 ± 0.3	2.46 ± 0.4**	3.36 ± 0.42**	3.49 ± 0.53**	3.91 ± 0.57**	3.37 ± 0.6**	3.61 ± 0.64**		
Energy	13.42 ± 0.76	11.21 ± 0.94	8.94 ± 0.78**	5.55 ± 0.75**	2.97 ± 0.55**	3.97 ± 0.62**	3.58 ± 0.56**	4.18 ± 0.6**	5 ± 0.62**		
Confusion	2.06 ± 0.28	1.41 ± 0.27	1.91 ± 0.22	2.94 ± 0.32	4.12 ± 0.45**	3.97 ± 0.51**	4.18 ± 0.48**	4.49 ± 0.61**	4.09 ± 0.56**		
Self-esteem	9.34 ± 0.46	8.06 ± 0.55**	7.16 ± 0.54**	4.7 ± 0.53**	3.91 ± 0.46**	4.15 ± 0.45**	4.27 ± 0.42**	3.88 ± 0.42**	4.67 ± 0.54**		

Note \* $P < 0.05$ ; \*\* $P < 0.01$

**Table 3** Reaction time results of PVT ( $n = 37, \bar{x} \pm s$ )

Index	TSD experiment point of time						
	Baseline	8 h	15 h	20 h	25 h	32 h	37 h
Reaction time	327.27 ± 4.53	307.84 ± 12.61	324.8 ± 10.11	352.13 ± 5.98**	359.49 ± 6.29**	352.46 ± 5.75**	353.6 ± 6.63**

Note \* $P < 0.05$ ; \*\* $P < 0.01$

**Table 4** GDT indicator results ( $n = 37, \bar{x} \pm s$ )

Index	TSD experiment point of time							
	Baseline	8 h	15 h	20 h	25 h	32 h	37 h	
Risk choice times	15.87 ± 0.97	25.64 ± 1.03	36.47 ± 1.06	47.42 ± 1.11	56.57 ± 0.98	68.05 ± 1.18*	78.78 ± 1.1**	
Safety choice times	12.14 ± 0.97	12.36 ± 1.03	11.58 ± 1.06	10.58 ± 1.11	11.43 ± 0.98	9.95 ± 1.18*	9.92 ± 1.1**	
Net score	6.27 ± 1.94	6.72 ± 2.06	5.19 ± 2.12	3.17 ± 2.21	4.86 ± 1.96	1.89 ± 2.36*	0.43 ± 2.21**	

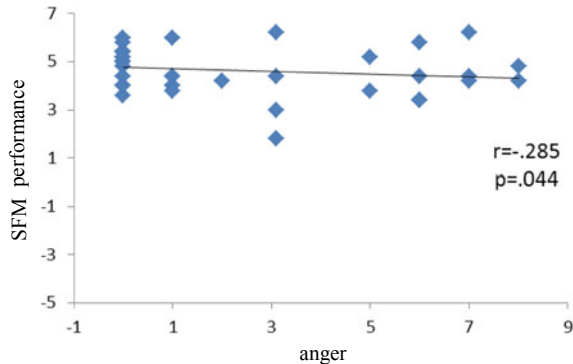
*Note* \* $P < 0.05$ ; \*\* $P < 0.01$

**Table 5** SFM performance results ( $n = 37, \bar{x} \pm s$ )

Serial number	TSD experiment point of time					
	Baseline	7 h	12 h	24 h	31 h	36 h
1-21	5.76 ± 0.25	5.64 ± 0.24	3.98 ± 0.25**	/	/	4.42 ± 0.23**
21-37	5.59 ± 0.22	/	/	3.5 ± 0.3**	3.86 ± 0.27**	4.88 ± 0.18*

Note \* $P < 0.05$ ; \*\* $P < 0.01$

**Fig. 1** Correlation between anger state and SFM performance



rising is the earliest (15 h), and the pressure and fatigue appear later (18 h), which is also consistent with the previous research findings.

Research shows that emotion is easily affected by SD, and significant changes in emotion may occur before affecting work performance [4]. In our study, POMS was also used to evaluate the emotional changes of the subjects. The results showed that in the early stage of TSD (18 h), negative emotions such as anger, depression and tension increased significantly, while positive emotions such as energy and self-esteem decreased significantly. Moreover, positive emotion changes occurred earlier than negative emotions; especially, self-related emotions (such as self-confidence and self-control) decreased significantly at the beginning of the experiment (8 h). This is also consistent with Lieberman’s research on the emotional changes of soldiers after SD. This study also found that POMS had similar changes in depression, confusion, fatigue, anger and energy after SD [5].

It is believed that the decline of cognitive performance after SD is only due to the decrease of general arousal and alertness, that is to say, sleep loss affects almost all cognitive abilities by reducing alertness and alertness [6]. Alertness is continuous attention, the ability of an individual to pay attention to the same stimulus for a long time [7]. PVT is a measure of mental reaction speed, which can accurately reflect the individual’s attention persistence ability with ms time resolution. It has become a gold standard to evaluate the impact of sleep loss on alertness, and also an effective detection method of flight fatigue. In our study, the results showed that TSD had a significant effect on PVT, and its response time increased significantly at 20 h, and all subsequent time points were higher than the baseline value. This shows that

alertness of cognitive function has been significantly impaired, which is consistent with the previous conclusions [8].

SD can cause a wide range of effects on cognitive function, but for complex cognitive abilities such as decision-making, it seems to be relatively small and inconsistent [9]. In this study, we used a computerized GDT program to test the subjects and found that with the prolongation of SD duration, there were significant changes in the net score, risk choice times and safety choice times at the 32 h. The risk choice times were significantly higher than the baseline, while the net score and safety choice times were significantly lower than the baseline, which was consistent with the previous studies. It shows that long-term SD makes the subjects prefer to take risks in decision-making and give up safe and reliable choices. Finally, the decreases in the net score of GDT suggested that the risk decision-making is significantly impaired. In our study, the subjects' response time of PVT increased significantly at 20 h, while the three indicators of GDT changed at 32 h, which was significantly later than the former. It also suggests that attention impairment caused by SD is not the whole reason for the reduction of risk decision-making, which may play a greater role in the trade-off of risk-benefit ratio and the modification of decision-making strategies.

In terms of military flight, it is a common technical means to evaluate the real occupation load and mental fatigue by SFM [10]. The SFM used in this study has very good fidelity and actual validity. The results showed that compared with the baseline, the performance of SFM in the 12 h of SD began to decline significantly and continued to decline with the extension of time. It recovered at the end of the experiment, but it did not reach the baseline level. It suggested that SD might cause damage to the subjects' ability to perform complex tasks, which can reflect the change of real professional ability. We also found that the decline time point of SFM performance in SD was 12 h, much earlier than PVT (20 h) and GDT (32 h). This also showed that using simulated real occupational tasks can reflect the changes of mental fatigue more timely and accurately, and it is more suitable to evaluate and predict the changes of occupational-related abilities after mental fatigue than other simple cognitive tasks. We also found that there had been a significant correlation between the subjects' physical emotional feelings and cognitive task performance in SD. For example, anger was negatively correlated with SFM performance, indicating that there was an interaction between the subjective feelings and cognitive ability in SD.

In this paper, we build a mental fatigue model and use a variety of techniques to analyze the dynamic changes of various behavioral indicators in detail, as well as the correlation between them, so as to provide a comprehensive perspective for a better understanding of the impact of mental fatigue on the body.

**Compliance with Ethical Standards** The study was approved by the Logistics Department for Civilian Ethics Committee of Former Army General Hospital. All subjects who participated in the experiment were provided with and signed an informed consent form. All relevant ethical safeguards have been met with regard to subject protection.

## References

1. Wesensten NJ, Balkin TJ (2013) The challenge of sleep management in military operations. *US Army Med Dep J* 4(4–13):109
2. Fallone G, Acebo C, Arnedt JT et al (2001) Effects of acute sleep restriction on behavior, sustained attention, and response inhibition in children. *Percept Mot Skills* 93(1):213–229
3. Skein M, Duffield R, Edge J et al (2011) Intermittent-sprint performance and muscle glycogen after 30 h of sleep deprivation. *Med Sci Sport Exer* 43(7):1301–1311
4. Dinges DF, Pack F, Williams K et al (1997) Cumulative sleepiness, mood disturbance, and psychomotor vigilance performance decrements during a week of sleep restricted to 4–5 hours per night. *Sleep* 20(4):267
5. Lieberman HR, Niro P, Tharion WJ et al (2006) Cognition during sustained operations: comparison of a laboratory simulation to field studies. *Aviat Space Envir Md* 77(9):929–935
6. Killgore WDS (2010) Effects of sleep deprivation on cognition. *Prog Brain Res* 185(1):105–129
7. Thorne DR, Johnson DE, Redmond DP et al (2005) The walter reed palm-held psychomotor vigilance test. *Behav Res Methods* 37(1):111
8. de Bruin EJ, Dewaldkaufmann JF, Oort FJ et al (2015) Differential effects of online insomnia treatment on executive functions in adolescents. *Sleep Med* 16(4):510–520
9. Diekelmann S, Born J, Diekelmann S, Born J (2010) The memory function of sleep. *Nat Rev Neurosci* 11(2):114–126
10. Russo MB, Kendall AP, Johnson DE et al (2005) Visual perception, psychomotor performance, and complex motor performance during an overnight air refueling simulated flight. *Aviat Space Envir Md* 76(7):92–103

# Research on Psychological Management Problems of Military Cadets Under the Angle of Group Psychology



Peng Gong, Ye Tao, Huiyong Wang, Kun Cao, and Yuxi Peng

**Abstract** Under the information zed condition, the outcome of a war will depend on competition of human talents to larger degree. Military academy is the foundation, base and cradle in which our army cultivates human talents. Compared to other general objects, military cadets can show more group psychological characteristics in practical psychological management. From the angle of group psychology, the essay analyzes the three characteristics of group psychology for military cadets and sums up the four types of psychological management for the current military cadets, and finally, combined with management reality of military academy, the essay puts forward the three countermeasures—that is, firstly, we should grasp internally psychological regularity and reinforce the scientific nature of psychological management; secondly, we should enhance personal charm and improve effectiveness of psychological management; thirdly, we should create better psychological atmosphere and intensify permeability of psychological management.

**Keywords** Group psychology · Military cadets · Psychological management

Military academies are the base and cradle of human talents, with constant deepening of economic globalization, profound transformation of social living patterns and frequent improvement of military reform they must have much greater innovation on military cadet's management. The most important core factor is human management in management; as long as we innovate human management pattern, we can basically promote management level for controllers and further develop management efficiency. In them, psychological management is the basis by which good management is conducted to human. From the angle of psychology, compared to management concerning the students from local colleges and universities and other general objects, military cadets can show more group psychological characteristics in practical management. Thus, as long as we really analyze their group psychological characteristics, we can conduct pertinent psychological management, practicably

---

P. Gong (✉) · Y. Tao · H. Wang · K. Cao · Y. Peng  
Artillery and Air Defense Forces Academy (Zhengzhou Campus), Zhengzhou 450052, China  
e-mail: [2495625853@qq.com](mailto:2495625853@qq.com)

© The Editor(s) (if applicable) and The Author(s), under exclusive license to Springer Nature Singapore Pte Ltd. 2021

S. Long and B. S. Dhillon (eds.), *Man-Machine-Environment System Engineering*, Lecture Notes in Electrical Engineering 645, [https://doi.org/10.1007/978-981-15-6978-4\\_11](https://doi.org/10.1007/978-981-15-6978-4_11)



improve management level of controller and further promote cultivating quality of human talents [1].

## **1 Characteristics of Group Psychology for Military Cadets**

Group psychology of military cadets is the psychological process and characteristics which are produced and can influence separately personal feeling, thoughts and behavior when military cadets with different backgrounds and different personalities work together for a common goal. French scholar, Gustave Le Bon, described the group psychology, “no matter who constitute the special group and no matter how different they are in the living ways, professions, personality or intelligence, this is a fact that they have formed a special group, group life makes them acquire the group psychology in which their feelings, thoughts and behaviors are greatly different from those when they are alone. If the group is not formed some ideas and feelings can’t be produced at all or can’t be converted into action.” At present, the characteristics of group psychology for military cadets include the following three points.

### ***1.1 Fading Individual Consciousness***

Gustave Le Bon said, “Unconscious phenomenon plays a completely overwhelming role not only in the lives of the organic body but also in the intelligent activities.” After the cadets from different places assemble together, the feelings about “overwhelming with numerical strength” are inevitably emerging because the number of cadets is increasing. Some intention constrained in their minds can be put into effect by instinct, after all the idea that “the law can’t be enforced when everyone is an offender” is always embodied in individual mind of the whole group. Thus, their self-consciousness is gradually fading, and group psychology will be in the leading position; some incredible phenomena seem to appear. For example, after arriving at the academy, some cadets who performed very well in the field forces loosen their requirements and violate regulations and rules, even rush into risk. What is more, these phenomena may not exist only in individuals; they can be scaled up by invisible effect and directly influence individual consciousness [2].

### ***1.2 Weak Logic Reasoning***

Gustave Le Bon still stressed, “Group is usually in the expecting state for attracting attention, so they are easily subject to hint, the initial hint can quickly enter into the human brains of the group by the process of mutual transmission.” After the individuals are integrated into the group, they are extremely subject to intimation

and emotional impact from surrounding situation and suggestion from others, their self-logic reasoning may be weakened, on general issues they have been softheads, some phenomenon on “swimming with the stream” is relatively apparent in their mind. For instance, when postgraduate group has got a hint that “the major work for postgraduates is to write essays and they must never mind other matters.” Then the hint quickly has been personal idea and is rapidly transmitted to other cadets. The idea makes most of cadets not to focus on improvement of military quality but to attach importance to professional knowledge [3]. From the angle of logic reasoning, the idea is untenable: after all postgraduates will serve field forces after graduation, if they only have professional knowledge without better military quality, it is impossible for them to perform their missions. The simple truth cannot be understood for the whole group, or it is ignored or excluded by instinct.

### ***1.3 Extremalization of Group Feeling***

Gustave Le Bon thought, “the group only know simple and extreme feeling; they either fully accept all kinds of advice, ideas and believes offered to them or completely reject them; thus, these advice, ideas and believes are considered as absolute truth or fallacy.” Under the real background of military management, it is much more difficult for the cadet group to arrive at the level of irrationally accepting education. They are often moved by simple but extreme feeling; in the meantime, it is more difficult for them to accept complicated ideas and thoughts. So, it is not much difficult to understand some problems in political work for military cadets. When a careful-thinking speech with logical rigor is put in front of him, he can really read and benefit from it. However, when the speech was delivered by the administrator in public, he may be dozing and cannot concentrate on the speech; finally, copying the notes is only the last resort; however, when a high-spirited administrator with distinct attitude delivers the speech, it is much easier to arouse their feelings regardless of illogic of the contents and the leak of the thinking ways. This will show that if the feeling is not expressed very well the terrible result will be emerging.

## **2 Psychological Management Types for Military Cadets**

The book named *Psychology of Modern Management* thoughts, “psychological management is a kind of detailed methods which integrated the related contents of many subjects such as psychology, education, politics and management to manage human. It regards human as the objects, researches their psychological characteristics, grasps their psychological laws, purposefully arouses human subjective initiative with intent depending on a variety of media, and makes human keep a good psychological state to realize common aims.” From the present management situation of military cadets, psychological management mainly includes the following four types.

### ***2.1 Unconsciously-Typed Psychological Management (Surface Management)***

Unconsciously-typed psychological management mainly embodies in administrative management. That is, administrators themselves are not aware of conducting psychological management; however, they can interact with subordinates by way of all kinds of media in management process and influence their psychological state. These media may be tangible such as issuing instructions, distributing papers and laying down plan, and they may also be intangible such as personal charm of administrators, level of thoughts, working style; anyway, they may play a certain psychological influence on subordinates. From certain sense, unconscious psychological management is an appendage in administrative management.

### ***2.2 Empirically-Typed Psychological Management (Junior-Level Management)***

Empirically-typed psychological management is that administrators themselves are aware of the importance of psychological management and also understand the expected result psychological management requires, but they cannot effectively conduct psychological management scientifically because of lack of theoretical guidance and knowledge accumulation; they can only analyze and summarize gains or losses in practice according to their past experience; based on these conditions, they improve and enrich their management patterns.

### ***2.3 Actively-Typed Psychological Management (Middle-Level Management)***

Actively-typed psychological management is that under the guidance of scientific theory, administrators follow the laws of psychological activities, precisely grasp psychological state of subordinates; based on the principle of classified guidance, they manage subordinates from person to person in accordance with their aptitude, fully arouse their enthusiasm and subjective initiative and inspire their inner potential. The types of management emphasize less obedience but mostly can inspire self-awareness and innovation of military cadets, and these can make them accept education and guidance from administrators in a pleasant way and fully develop their intelligence.

## **2.4 *Culturally-Typed Psychological Management (Senior-Level Management)***

Culturally-typed psychological management is that based on actively-typed psychological management, administrators borrow and abstract all kinds of brilliant culture essence, create uniquely special culture of the working units, develop the functions of soul casting from advanced culture, lead and cultivate outlook on life and the world of military cadets and finally form common value pursuits of the cadet group in accordance with historical heritage, brilliant tradition and the characteristics of the cadets.

## **3 Countermeasures by Which Psychological Management of Military Cadets Is Strengthened**

Grassroots cadres are the direct implementers of psychological management to military cadets. They must intensify their psychological self-management ability; particularly, they should study the related theory on psychology, grasp general process and laws of their psychological activities, hold the inner requirement of psychological management and transform from unconsciously-typed and empirically-typed psychological managements to actively-typed and culturally-typed ones.

### **3.1 *Grasping the Inner Psychological Regularity, Improving Scientificity of Psychological Management***

Firstly, we should hold the pulse of the questions. We must really analyze the formation and development of group psychology and find out the best opportunity to conduct psychological management. After the cadets who have different personalities from different places are put into a group, individual awareness may be weakening and group psychological awareness apparently begin to emerge, however, group psychology can't be formed at one stroke, it need experience a process step by step. Implementing psychological management can achieve the best result just before military cadets adapt the surrounding situation and group psychology isn't yet formed, otherwise more efforts will be further made. So, just after the cadet's admission, they should be intensified in the following aspects including educational management, strict disciplines and requirements; their awareness of discipline, safety, law and regulation should be really reinforced so as to build a good fundament of thoughts for regularized construction of military cadets [4]. Secondly, we should find specific ways. When conducting psychological managements to the cadets, we must consider the factors of group psychology and cannot analyze the psychological state of the cadets only from an individual's perspective; otherwise, some seemingly

good remedy for questions cannot achieve ideal effect. For example, if we want to make the cadets abide by all regulations and rules purposefully, we may adopt the pattern on “one forum for everyone,” and we separate the cadets from the group and take the opportunity to get rid of some worse group psychological idea that “law can’t be enforced when everyone is an offender” or “overwhelming with numerical strength.” Finally, from the bottom of our hearts, we agree with and abide by psychological management consciously.

### ***3.2 Reinforcing Personal Charm and Progressing Effectiveness of Psychological Management***

“The key to psychological management is to make subordinates sense the respectable personality, good character and substantial ability of administrators through their words and deeds, not only through their wonderful speech. That many excellent administrators have lofty image in the minds of the masses lies not in their ranks, but in their personal charm. The power is huge and makes people respect and miss them for a long time.” So, management cadres in grassroots units must enhance personal cultivation and influence the group of the cadets through teaching by their example as well as verbal instruction under the stronger personal charm. Thus, their ideas will be agreed and influenced mutually; in the meantime, some worse thoughts can be stopped to spread in the group. One is to firm ideals and beliefs. Grassroots management cadres should enhance study on political theory, firmly build communism beliefs, forge steely will by way of firm belief and take the opportunity to show special personal charm. Two is to improve humanistic literacy. There is an old saying, “wisdom in hold, elegance in mold.” Management cadres must read a lot of good books and are diligent in thinking and researching. As long as they continuously absorb all sorts of cultural knowledge and promote the depth and breadth in thinking level they can reinforce personal cultivation. Three is to reinforce working style cultivation. As administrators, they must consider regulations, rules and doctrines as management criterion, leave no loopholes for subordinates to exploit and not turn a blind eye to the mistakes of the subordinates; they influence the group of the cadets and further improve effectiveness of psychological management by an excellent working style [5].

### 3.3 *Creating Better Psychological Atmosphere and Intensifying the Permeability of Psychological Management*

Just like some scholars pointing out, “psychological atmosphere is a kind of comprehensive psychological state. It derives and develops from interaction among administrators, subordinates and managing environments, it is composed of common attitude, dominantly emotional state of most people in the group. The atmosphere is a kind of psychological background to show human working state. It influences human psychological health and working emotion.” Creating better psychological atmosphere is the best way to inspire the warmth of the group, accept ideas and thoughts of administrators and consciously put into practice. There are a variety of ways to create better psychological atmosphere, combined with some psychological characteristics like extremalization of group feeling several advice that grassroots cadres accept political education is put forward [6].

Firstly, emotion should be involved. When educators give their lessons, they should be flexible and cannot only read the prepared speech word by word, but also read wonderfully with a silver voice and deep feeling and win the cadets’ acknowledgment through emotional influence. Secondly, language should be concise. When talking to subordinates, administrators try their best to avoid detailed explanation and deep analysis to the ideas and directly express their ideas using simple but imaginable language; only in this way, can the emotion of the group be inspired. Thirdly, the ideas should be repeated. From the angle of psychology, frequent repeating can produce a kind of special power to human brains; “in the long run, frequently repeating can enter into unconsciously deep area in our mind, just here our behavioral motivation is formed.” Thus, when conducting political education, administrators must repeatedly talk if possible; only when the ideas are rooted in human brains, can they be changed into instinctive habits.

**Compliance with Ethical Standards** The study was approved by the Logistics Department for Civilian Ethics Committee of Artillery and Air Defense Forces Academy (Zhengzhou Campus).

All subjects who participated in the experiment were provided with and signed an informed consent form.

All relevant ethical safeguards have been met with regard to subject protection.

## References

1. Le Bon G [France] (2015) *The crowd: a study of the popular mind*. Keli Feng (translating) Central Compiling & Translating Press, Beijing
2. Bai Z, Chen Y (1997) *Psychology of modern management*. Qingdao Press, Qingdao
3. Fu K (1999) On psychological management. *J Jiangsu Inst Educ* (4):43–45
4. Yu G (2006) *On social psychology*, 499. Beijing Normal University Press, Beijing

5. Wu X, Lin L (2012) On psychology in the military. China Light Industry Press, Beijing, pp 145–165
6. Hu L (2009) On social stability in contemporary China. Hongqi Press, Beijing

# Research on the Effects of Pilots Psychological Trainings Based on Different Military Application Purposes



Yishuang Zhang, Yan Zhang, Fei Peng, Yang Liao, Huamiao Song, Xueqian Deng, Duanqin Xiong, Juan Liu, and Liu Yang

**Abstract** *Objective* To explore the effects of pilot psychological trainings based on different military application purposes, in order to provide evidence for carrying out all-round psychological training in the future. *Methods* A total of 101 military pilots were trained in three-stage autonomic nervous stability training, and their HRV indexes before and after were compared, then compared these indexes data to the stress protection training to study the different effects. *Results* 1. After autonomic nervous stability training, the overall level of autonomic neurological function increased, and the balance of sympathetic and parasympathetic functions significantly enhanced; 2. HRV power spectrum adjusted to low frequency; 3. Stress level of pilots after flight mission is higher than their daily lives; 4. After the stress protection training, the stress level of pilots decreased obviously and they were in the state of relaxation, while after autonomic nervous stability training, the stress level of pilots was mobilized to a more suitable working state. *Conclusion* The psychological training of pilots based on different military application purposes has gained prominent and targeted effects.

**Keywords** Autonomic nervous stability · Stress protection · Training · Heart rate variability

## 1 Introduction

Military psychological training, which is considered to be an important means to improve the military's ability to complete combat tasks, to enhance the combat effectiveness and recover quickly, has been concerned since the birth of the army. In recent year, some developed countries pay attention to the psychological training to improve the military operation efficiency of soldiers [1]. Military pilots as special operation soldiers who always in special situations. The effect of psychological training will

---

Y. Zhang · Y. Zhang · F. Peng · Y. Liao · H. Song · X. Deng · D. Xiong · J. Liu · L. Yang (✉)  
Air Force Medical Center, Fourth Military Medical University, Beijing 100142, China  
e-mail: [yangliuhenry@aliyun.com](mailto:yangliuhenry@aliyun.com)



directly affect the function of the role, which is related to flight safety and combat effectiveness.

At present, the researches on the purpose of military pilots' psychological training show that hot spots mainly focus on: (1) pre-adaptation of the special environment; (2) counteract and reduce stress response; (3) improve the psychological efficiency of combat. Because of the different purposes, the selections of training effect evaluation indexes are also different. Generally, most of them take the ways such as psychological scale, physiological index, subjective evaluation, Yoshihara et al. [2]. Among them, heart rate variability (HRV), which can reflect the level of autonomic nerve function, is a recognized and objective evaluation index. The research shows that autonomic nerve function is connected to psychological stress and work performance [3, 4]. In research of Yang L., Song H. and Zhang Y., the differences of key indicators in HRV before and after psychological training were observed [5, 6], and the actual effect such as the stress protection training on pilots after flying was verified, which provide effective methods and data supports to pilots psychological training [7]. This article will observe the effect of autonomic nervous stability training based on HRV, then comparing to the previous research data to study the different effects of pilots' psychological training on two different purposes, in order to provide all-round psychological training reference scheme for the future combat training in high-tech war.

## 2 Objects and Methods

The study was divided into two training groups: autonomic nervous stability training and stress protection training after flight. The experimental scheme of stress protection training after flight has been introduced in detail in the previous literature [7]. This part only reported the content about autonomic nervous stability training.

### 2.1 Objects

A total of 101 male pilots who were taking part in aviation medical identification training were researched. The general condition of the subject is as follows: average age  $33.70 \pm 9.34$  years (range 22–57 years) and average flight time  $2670.87 \pm 2069.93$  h (range 120–1110 h). Equilibrium test results show that it is balanced with the work stress protection group in age, education background, flight time, training experience, training level, etc. ( $p > 0.05$ ).

## **2.2 Methods**

### **2.2.1 Experimental Equipment**

The tool for training and data collection is self-generate physiological coherence system (SPCS). The system records the indicators of heart rate variability (HRV) by means of the ear-wearing information collector. In addition, the changes in HRV indicators during training will be fed back through SPCS, so that the subjects can feel the changes in autonomic nerve activities and learn to adjust them consciously.

### **2.2.2 Training Method**

The three-stage autonomic nervous stability training was carried out with the help of SPCS. The details are as follows:

(The first stage) 1. Guide the subjects to learn “three steps for autonomic nervous stability training.” Step 1: Focus on the heart. Imagine the heart as a command center, issuing commands to the brain and other organs of the body. Step 2: Breathe evenly through the heart, keep focusing on the heart, breathe out—imagine draining excess air from the heart, breathe in—imagine oxygen filling the heart, and your mind getting clearer, pay attention to the rhythm between exhale and inhale, and keep breathing evenly and deeply. Step 3: Keep in good condition as in the first two steps, to experience positive emotions and the joy of good feelings with heart.

2. The subjects were equipped with ear-wearing information collector, sit down and relax, with their arms lying naturally on both sides of the body, trying to keep a clear mind, without considering anything, and keep natural breathing. Using the “state assessment” module for 3 min, the system will automatically collect the HRV indicators of the subjects as the baseline data;

3. Enter the training center and then guide the subjects to carry out the three times trainings for easy–medium–difficult by the training module of “bodhi tree”.

4. Return to the “state assessment” module and instruct the subjects to recall and use the training method in the assessment, and then, tell them how well they’ve done.

(The second stage) 5. On day 2, repeat 2–4 processes, and during the pre-training state assessment, the subjects were prompted to recall the training methods learned on day 1.

(The third stage) 6. On day 3, repeat the fifth process. The HRV indexes after training in this stage were collected as training effect data.

### 2.2.3 Research Design

The effect of autonomic nervous stability training was analyzed by self-comparison before and after, and then compared training results with the data in the previous research ‘Empirical study of psychological stress protection training for the flight over sea,’ to study the differences of psychological training effects under two different purposes.

### 2.2.4 Collecting Indicators

The following indicators will be collected:

*Time domain indexes* Standard deviation of NN intervals (SDNN): affect the general condition of autonomic nerve function; standard deviation of successive difference between adjacent NN intervals (SDSD): reflect the activity of sympathetic nerve; root mean square of successive difference between adjacent NN intervals (RMS-SD): reflect the activity of parasympathetic nerve; proportion of NN50 in total NN intervals (PNN50): also reflect the activity of parasympathetic nerve.

*Frequency domain indexes* Total power (TP): reflect the overall level of neurological function; very low frequency (VLF): reflect the level of para-sympathetic nerve; low frequency (LF): reflect the dual effects of sympathetic and parasympathetic nerves; high frequency (HF): reflect the level of parasympathetic function; LF to HF ratio (LF/HF): reflect the balance of sympathetic and parasympathetic functions; normalized LF (LFnorm) and normalized HF (HFnorm): reflect the coordinated state of mental energy.

## 2.3 Statistical Processing

Use PASW 18 statistical software for data analysis. Measurement data was expressed as  $\bar{x} \pm s$ . Wilcoxon test was used for self-comparison. The independent two-sample test (Mann Whitney test) was used to compare with the training data of stress protection training after flight. The difference was statistically significant when  $p < 0.05$ .

**Table 1** Change of HRV time domain indexes before and after autonomic nervous stability training on 101 pilots ( $\bar{x} \pm s$ )

Indexes	Pre-training	Post-training	Z value	p value
SDNN (ms)	73.62 ± 40.90	82.41 ± 47.91	-1.682 <sup>a</sup>	0.093
RMS-SD (ms)	69.10 ± 50.89	63.44 ± 67.27	-1.980 <sup>b</sup>	0.048
SDSD (ms)	55.10 ± 45.54	48.93 ± 60.01	-1.980 <sup>b</sup>	0.048
PNN50 (%)	19.24 ± 15.06	18.22 ± 14.08	-0.801 <sup>b</sup>	0.423

Note <sup>a</sup>Based on negative ranks, <sup>b</sup>Based on positive ranks

### 3 Results

#### 3.1 The Change of HRV Time Domain Indexes Before and After Autonomic Nervous Stability Training

From Table 1, after autonomic nervous stability training, the data of RMS-SD and SDSD decreased significantly ( $p < 0.05$ ), with no significant difference seen in other indexes.

#### 3.2 The Change of HRV Frequency Domain Indexes Before and After Autonomic Nervous Stability Training

In frequency domain indexes, except the index HF was no significant different, TP, LF, LF/HF, LFnorm indexes significantly increased ( $p < 0.01$ ), and HFnorm, VLF indexes significantly decreased ( $p < 0.01, p < 0.05$ ). The above results are shown in Table 2.

**Table 2** Change of HRV frequency domain indexes before and after autonomic nervous stability training on 101 pilots ( $\bar{x} \pm s$ )

Indexes	Pre-training	Post-training	Z value	p value
TP (ms <sup>2</sup> )	626.47 ± 916.93	922.73 ± 1146.45	-3.538 <sup>a</sup>	0.000
VLF (ms <sup>2</sup> )	198.06 ± 375.94	141.91 ± 207.92	-2.078 <sup>b</sup>	0.038
LF (ms <sup>2</sup> )	328.73 ± 442.41	679.12 ± 851.16	-5.229 <sup>a</sup>	0.000
HF (ms <sup>2</sup> )	99.68 ± 167.41	101.70 ± 239.93	-0.842 <sup>b</sup>	0.400
LF/HF	5.97 ± 4.55	20.00 ± 21.63	-6.215 <sup>a</sup>	0.000
LFnorm	78.58 ± 13.72	88.01 ± 12.15	-4.924 <sup>a</sup>	0.000
HFnorm	21.42 ± 13.72	11.99 ± 12.15	-4.924 <sup>b</sup>	0.000

Note <sup>a</sup>Based on negative ranks, <sup>b</sup>Based on positive ranks

### 3.3 Comparison of Psychological Training Effects Based on Different Training Purposes

From Table 3, before the psychological training, the data of SDNN, RMS-SD, SDDSD and HF in autonomic nervous stability training group were higher than stress protection training group ( $p < 0.05$ ). After the training, the difference of SDNN between the two groups was more significant ( $p < 0.01$ ). TP, LF, LF/HF, LFnorm indexes of autonomic nervous stability training group were higher, while HFnorm indexes of autonomic nervous stability training group were lower than stress protection training group ( $p < 0.01$ ).

## 4 Discussions

The most fundamental goal of China's military flight psychological training is to improve the psychological function of flight personnel to ensure their normal actions in high-tech warfare through training; therefore, their operational capabilities can be maximized. In modern air combat, pilots stay in the air longer, fly intensity harder, and the pilots would psychologically feel more shocking and destructiveness. This requires the pilot not only to have the better stress recover ability, but also to have the ability which can keep a good working condition under great pressure and timely to make correct operational judgment. Stress protection training after flight and autonomic nervous stability training are the training means to achieve the two goals, respectively.

HRV refers to small differences between the interval of successive heartbeats which can appraise the indices of sympathetic and parasympathetic activity. HRV refers to the continually modified phenomenon in the RR interphase of successive heartbeat (instantaneous heart rate), which can reflect the comprehensive regulation of the sympathetic nerve and parasympathetic nerves of the heart in actual time. When individuals are stimulated by stressors, parasympathetic nerve activity is weakened, the sympathetic nerve activity is relatively enhanced, that will lead to some cardiovascular response such as rapid heartbeat and elevated blood pressure, while the individual would have conversely response when he is in relaxation. Therefore, the change of HRV index can reflect individual stress level. The preliminary research results showed that after the stress protection training, pilots' stress level has decreased significantly which was achieved the corresponding training objectives [7].

Autonomic nervous stability training aims to regulate and control the sympathetic and parasympathetic functions in a psychological coherence state through certain methods. The research shows that when someone's body is in a state of autonomic nerve coherence, his heart rate will close to the sinusoidal waveform, and the sympathetic & parasympathetic nerve activity achieves a balance that the autonomic nerve function of pilot was mobilization to the right height into the best mental energy area

**Table 3** Comparison of HRV indexes before and after psychological trainings based on different military application purposes ( $\bar{x} \pm s$ )

Indexes	Pre-training				Post-training			
	Autonomic nervous stability	Protection training group after operation	Z value	p value	Autonomic nervous stability	Protection training group after operation	Z value	p value
SDNN (ms)	73.62 ± 40.90	52.65 ± 27.07	-3.073	0.002	82.41 ± 47.91	58.32 ± 31.01	-3.897	0.000
RMS-SD (ms)	69.10 ± 50.89	48.22 ± 30.35	-2.424	0.015	63.44 ± 67.27	57.98 ± 37.68	-0.233	0.816
SDSD (ms)	55.10 ± 45.54	32.84 ± 27.18	-3.046	0.002	48.93 ± 60.01	41.11 ± 34.80	-0.572	0.568
PNN50 (%)	19.24 ± 15.06	20.55 ± 15.68	-0.256	0.798	18.22 ± 14.08	23.96 ± 17.10	-1.802	0.072
TP (ms <sup>2</sup> )	626.47 ± 916.93	373.17 ± 418.94	-1.381	0.167	922.73 ± 1146.45	603.34 ± 1008.48	-4.002	0.000
VLF (ms <sup>2</sup> )	198.06 ± 375.94	133.51 ± 137.87	-1.075	0.282	141.91 ± 207.92	183.77 ± 392.77	-1.432	0.152
LF (ms <sup>2</sup> )	328.73 ± 442.41	196.59 ± 249.60	-1.555	0.120	679.12 ± 851.16	309.85 ± 558.99	-5.223	0.000
HF (ms <sup>2</sup> )	99.68 ± 167.41	43.07 ± 100.83	-2.785	0.005	101.70 ± 239.93	109.71 ± 241.32	-0.352	0.725
LF/HF	5.97 ± 4.55	19.67 ± 81.71	-1.610	0.107	20.00 ± 21.63	4.12 ± 3.99	-6.174	0.000
LFnorm	78.58 ± 13.72	83.45 ± 9.35	-1.610	0.107	88.01 ± 12.15	70.92 ± 16.25	-6.174	0.000
HFnorm	21.42 ± 13.72	16.55 ± 9.35	-1.610	0.107	11.99 ± 12.15	29.08 ± 16.25	-6.174	0.000

(exciting but not nervous), and flight operations can achieve the best performance [8]. In this study, the indexes of TP, LF, HF and LFnorm were significantly increased, while HFnorm was significantly decreased, which reflects the pilot overall level of neurological function was increased, the balance of sympathetic and parasympathetic functions and the coordinated state of mental energy were significantly enhanced. According to previous research, when someone reached the physiological coherence state, HRV power spectrum would change significantly, adjusting to the resonance frequency (about 0.1 Hz) of the feedback loop of baroreceptors [9]. This is consistent with the results that the very low frequency (bands 0.003–0.04 Hz) and high frequency (bands 0.15–0.4 Hz) significantly decreased and the low frequency power (bands 0.04–0.15 Hz) significantly increased in the study. In the later research, we will further discuss the changing situation of frequency power near 0.1 Hz band.

The before–after comparison of the two types training results clearly shows that psychological state differences of pilots after different psychological training. When the pilot just finished the flight, he was in a higher stress state with significantly lower indicators of overall level of neurological function (SDNN, HF) and of activity of parasympathetic/sympathetic nerve (RMS-SD, SDDSD). After the stress protection training, the pilots' high-frequency power (HF) increased significantly and the pilot was in rest state; after the autonomic nervous stability training, pilots' frequency domain indexes concentrated on the low frequency (LF), whereas the high frequency (HF) is significantly lower than the stress protection training level. That reminds us the pilot's stress level is mobilized to a certain height. Combined with the results of its overall level of neurological function rising faster, we can analyze that the pilot might in a better operating state, which is also consistent with the Yerkes–Dodson law, which means that the operating stress and operating performance were inverted u-shaped curve—too high or too low stress level will go against to the best operating performance.

In conclusion, the psychological training of pilots based on different military application purposes has gained prominent and targeted effects. Among them, stress protection training which can help pilots to relax quickly is suitable for pilots who have just finished their mission, while autonomic nervous stability training is suitable for pilots on mission, which should be helpful for them to maintain the best working condition, and help pilots to play the best operation level. It will plan to further standardization study these methods and eventually form mature training subjects and evaluation standards in the future, in order to guide and evaluation pilots' psychological training under the new combat training mode better.

### **Compliance with Ethical Standards**

The study was approved by the Logistics Department for Civilian Ethics Committee of Air Force Medical Center, Fourth Military Medical University.

All subjects who participated in the experiment were provided with and signed an informed consent form.

All relevant ethical safeguards have been met with regard to subject protection.

## References

1. Taylor MK, Sausen KP, Potterat EG, Mujica-Parodi LR, Reis JP, Markham AE et al (2007) Stressful military training: endocrine reactivity, performance, and psychological impact. *Aviat Space Environ Med* 78(12):1143–1149
2. Yoshihara K, Hiramoto T, Oka T, Kubo C, Sudo N (2014) Effect of 12 weeks of yoga training on the somatization, psychological symptoms, and stress-related biomarkers of healthy women. *BioPsychoSocial Med* 8(1):1
3. Goessl VC, Curtiss JE, Hofmann SG (2017) The effect of heart rate variability biofeedback training on stress and anxiety: a meta-analysis. *Psychol Med* 47(15):2578–2586
4. Cheshier NJ (2014) The generalization of videogame-based heart rate variability biofeedback training and physiological arousal to psychological stressors. *Dissertations & Theses—Gradworks*
5. Yang L, Song H, Zhang Y et al (2015) Effect of floating feedback training capsule in defending psychological stress on military flight personnel. *Med J Air Force* 31(1):5–8
6. Yang L, Song H, Zhang Y et al (2015) Effect of psychological stress defense training on military flight personnel. *Chin J Behav Med Sci* 24(5):464–467
7. Zhang Y, Wang H, Fu H, Zhang Y, Song H, Peng F, Bai H, Liu J, Liao Y, Yang L (2018) Empirical study of psychological stress protection training for the flight over sea. *Chin J Aerosp Med* 29(3–4):181–187
8. Yang L, Zhang Y, Dong W, Shao F, Bai H, Peng F et al. (2017) Effect of autonomic nervous stability training on military flight personnel. *J Prev Med Chin Peop Lib Army* 35(12):42–45
9. Miyata M, Sano Y, Suzuki K et al (2002) Evaluation of respiratory modulation on the pulse wave amplitude in low-birth-weight neonate. *Biol Sci Space* 16(3):215–216



# Human Factor Analysis on the Effect of Pilot's Interpretation of Airborne Radar Warning Information



Juan Liu, Shuang Bai, Jiabo Ye, Lin Zhang, Jian Du, Wei Pan, Yubin Zhou, Qiming Cheng, Liu Yang, and Duanqin Xiong

**Abstract** *Objective*—This paper summarizes and sorts out existing deficiencies of the human–computer interaction interface design of the current mainstream aircraft airborne radar warning system, and further puts forward the principle of optimization design, in order to shorten pilot's reaction time in “dangerous target identification” and “dangerous target locking and disposal.” *Methods*—The methods of literature analysis, questionnaire survey and expert interview were used to complete the human factor analysis. A total of 40 pilots were recruited to participate in this study, and each pilot completed one-on-one interview according to the established outline, then finished a questionnaire survey. The interview lasted for 60 min. *Results*—This study completed the analysis of the existing deficiencies of the current mainstream aircraft airborne radar warning system, putting the emphasis on the human–computer interface design. On this basis, this study further puts forward the design principles from four aspects. *Conclusions*—The designers need to give priority to the problems that the information presentation mode takes up too much cognitive resource of the pilots, which may cause pilots to miss information, or fail to obtain information in time, and fail to operate effectively.

**Keywords** Human factor analysis · Warning · Human–machine interface · Threat perception · Visual coding · Visual search

## 1 Introduction

Pilots need to obtain and maintain the global awareness of the air situation timely during flight. The most important task for pilots is to find out the threat in time, determine the direction of the threat source and evaluate its threat level. Therefore, threat perception is an important psychological ability for pilots. On the one hand, the level of threat perception ability depends on the pilot's innate cognitive ability and motion perception ability. On the other hand, it largely depends on the warnings

---

J. Liu (✉) · S. Bai · J. Ye · L. Zhang · J. Du · W. Pan · Y. Zhou · Q. Cheng · L. Yang · D. Xiong  
Air Force Medical Center of FMMU, Beijing 100142, China  
e-mail: 13910259429@139.com

© The Editor(s) (if applicable) and The Author(s), under exclusive license to Springer 111  
Nature Singapore Pte Ltd. 2021

S. Long and B. S. Dhillon (eds.), *Man-Machine-Environment System Engineering*, Lecture Notes in Electrical Engineering 645,  
[https://doi.org/10.1007/978-981-15-6978-4\\_13](https://doi.org/10.1007/978-981-15-6978-4_13)

of the alert system on the airborne radar. The on-board radar measures and analyzes the radar signals reflected by the carrier to prompt the pilot the direction, type and working status of the threat in a concise and easy-to-read manner. Therefore, the design of the human-machine interface of the airborne radar warning system is very important. It is very necessary to conduct human factors investigation and analysis on the human-machine interface of Chinese current mainstream aircraft airborne radar warning system, so as to find out the problems existing in the actual use of pilots.

## 2 Materials and Methods

### 2.1 Research Objectives

Research objectives: The radar screen presents a large amount of information and updates extremely fast, having a high timeliness. Therefore, pilots take a lot of effort to read the information and often worry about some important information missing. This research aims to analyze and sort out the existing problems in the human-machine interface design of the current mainstream aircraft airborne radar warning system, then propose optimization design principles to shorten the time for pilots to complete “dangerous target identification” and “target locking” during the mission.

### 2.2 Research Method

The methods of human factor analysis, including literature review, questionnaire survey and expert interview, were used.

### 2.3 Research Participants

A total of 40 male pilots were recruited to participate in the interview. The driving grade and age distribution of the participants are provided in Table 1.

**Table 1** Characterization of participants

Driving grade	Number	Average age (years)
Aircraft commander	20	47.90 ± 4.96
Co-pilot	20	34.80 ± 4.49

## 2.4 Contents of Human Factors Investigation

The interview content includes the following five aspects, and the summary is listed in Table 2.

- Question 1 When the radar catches the dangerous target, can the pilot detect it in time? What kind of warnings does the radar system give? Can the pilot identify the target quickly and accurately? How do pilots prioritize when selecting targets? Do pilots select priority target depending on their own judgment or through the automatic warnings of the radar system? When the radar detects multiple targets, how are the multiple targets arranged on the Head Up Display (HUD)? How does the radar system inform the pilot when it automatically selects priority targets?
- Question 2 What manual operation steps do pilots need to take to complete "Dangerous Target Lockout"? What signs will appear on the radar screen after the target is locked? Under what circumstances is the "locking action" performed automatically by the radar system, and under what circumstances is it manually operated by the pilot?
- Question 3 When the target is locked, when does the pilot determine to take action? What steps are required to complete the operation? What kind of prompt messages will be displayed on the radar screen during this process?
- Question 4 In the target recognition phase and target lock phase, what kind of information does the radar system give? What is the effect of prompt information? Do you have any advice or suggestions on the content and presentation mode of the existing prompt messages?
- Question 5 Studies have shown that somatosensory cues can shorten the pilot's response time and improve the accuracy rate. What is the feasibility of improving the human-machine interface of the radar warning system

**Table 2** Summary of interview content

No.	Interview question	Content outline
1	Question 1	Understanding the basic characteristics of the existing radar warning man-machine interface
2	Question 2	In the process of locking the dangerous target understanding the content and mode of the human-computer interaction of the radar warning system
3	Question 3	In the process of handling the dangerous target, understanding the content and mode of the human-computer interaction of the radar warning system
4	Question 4	Understanding the suggestions of the pilots on the improvement of the current interface
5	Question 5	Proposing the optimization scheme of adding body sense cues in radar warning human-computer interaction, ask for the opinions of pilots

based on this research results? What are the merits and disadvantages? The vibration intensity of the cabin itself is very strong, if there is more vibration cue under the seat, will the vibration cue be effective? Where the vibration sensor should be placed to be more easily detected by pilots?

### **3 Analysis of Human Factor and Optimization Design Principle**

#### ***3.1 Human Factor Analysis of Radar Interface Information Processing***

##### **3.1.1 Problem of Mismatch Between Task Demand and Cognitive Ability**

Some studies confirm that the cognitive load from visual and auditory channels has exceeded the psychological and physiological limits of pilots. This phenomenon may lead to mental overloading and human error increasing, which may lead to efficiency decreasing and safety reduction of man-machine system [1]. When pilots encounter flight special situations in the air, the current traditional human-computer interaction mode mainly composed of visual and auditory channels can hardly meet the needs of information exchange between pilots and airplanes.

James Reason, a psychologist at University of Manchester, believes that human error is related to the response of human information processing system to various human-computer factors. The possible phenomenon is that the demand of the system does not match the ability of human beings. The external influencing factors that have a great influence on human errors include three categories: unfamiliar scenarios, excessive workload and ongoing tasks disturbed. Workload is the most important environmental factor which includes physical load and cognitive load. Pilots need to pay more attention to cognitive load. Generally, the bottleneck of cognitive resources (attention, memory, judgment, analysis ability, etc.) can cause the increase of cognitive load [2]. In a certain period of time, there is a limit to the number of characters the pilot can read and the speed of eye tracking. If the limit is exceeded, it will lead to wrong operation.

##### **3.1.2 Problem of Limitations of Vision**

The physiological and psychological load of pilots is increasing due to the increase of flight altitude, speed, cruise time, and the highly intelligent aircraft display and operation system. Ergonomic design is becoming one of the main problems affecting flight safety. Therefore, human-machine interface design is very important. As we

all know, vision is an important channel for human to obtain information. About 80–90% of information comes from vision channel. During the flight, the pilots' central nervous system and visual organs are always in a state of intense attention: constantly collecting and analyzing information, making judgments, giving instructions, etc. Therefore, when designing the cockpit interface, we should go deep into the characteristics of visual cognition of pilots. In flight activities, besides monitoring the changes of the external environment, the pilot also needs to know the situation of his own aircraft and the threat to himself. Because most of the working condition parameters and external input parameters of the aircraft are transmitted to the pilot by display instrument, the pilot needs to scan the dashboard at all times and process the provided information, and then control the aircraft. The pilot has limited time to scan the instrument panel, and they cannot always scan the information. Time limit and search difficulty of scanning the dashboard will increase the pressure of pilots, which will affect the physiology and psychology health of pilots.

Airborne radar warning system mainly brings two kinds of visual limitations: keyhole effect and position sense disappearing.

(1) Keyhole effect

The information displayed by the airborne radar warning system is distributed on several different screens, mainly on the head-up display and a small part on the down-view display. The pilot's line of sight needs to switch between different screens, which make it possible that they cannot grasp the overall situation. The meaning of keyhole effect is that when people view information through the display, if the information needs to be displayed across pages, viewing a computer screen is like viewing an object from the keyhole. Because most of the information is hidden from the pilot's view, they will be forced to memorize a lot of information. More concretely, the pilot must remember what information is in the computer system, and they also need to think about where and how to find those information. These cognitive processes greatly increase pilot's cognitive load and reduces the efficiency of information processing.

(2) Position sense disappearing

The disappearance of the sense of position will lead to pilot's inability to obtain effective information from the radar screen. The pilot is easily lost in the messy information due to the excessive information. The pilot will not be able to continuously and skillfully understand the logical relationship of the information provided by the radar display screen. So the pilot is usually unable to judge the change of the current situation in time and does not know what to do next. This will lead to a decrease in pilot capacity. The disappearance of position sense will cause more cognitive resources to be occupied.

## **3.2 *Design Principle of Radar Display Interface Based on Visual Search***

### **3.2.1 The Highlight Way of Visual Coding**

The meaning of visual coding is to code information with visual stimuli such as color, number, letter and figure. Visual coding is divided into single-dimension and multi-dimension visual coding. Single-dimension visual coding is to encode information with one kind of visual stimulus; correspondingly, multi-dimension visual coding is to combine two or more kinds of visual attributes. With the development of science and technology, complex man-machine system appears constantly. Under these circumstances, the visual display interfaces of single element have gradually decreased, and the multiple visual display interfaces have gradually increased. In the multi-visual display interfaces, the visual information is not only displayed through a variety of elements, but also with integrated information of various sources, which will help the observer make a judgment on the overall state of the system. Multi-graphics visual display is a kind of visual display which takes graphics as the display mode and integrates multiple graphics elements. In the process of pilot's operation, it is difficult for the operator to obtain comprehensive information from multiple interfaces at the same time. Some researches on visual search have proved that brightness, flicker, color and other display methods can significantly reduce visual search time. Flicker is the best mode among the three prompt methods of color, brightness and flicker [3].

### **3.2.2 Graphic Display and Recognition**

Under the condition of multi-interface and multi-task, the observer needs to allocate attention well. For the display and recognition of graphics, in order to improve the detection rate of visual search, we must pay attention to the following ergonomic design principles: ① Triangle is the most ideal target shape coding in interface design; square and circle are only suitable for target shape coding when necessary. And the correct recognition rate of triangle is the highest regardless of task weight; ② Green and red are most suitable for target color coding no matter what the task weight is; blue is only suitable for target color coding with high task weight when necessary, and blue is not suitable for target color coding with low task weight; ③ human's recognition ability of targets at different positions is affected by the influence of task weight. In the human-computer interaction interface, the task weight should be fully considered in the arrangement of the target position. Task weight means the importance of a task.

### 3.2.3 Digital Display and Recognition

Previous studies have suggested that the length of digital presentation time has a great influence on the accuracy of the operator's judgment. When the information needs to be presented to the observer through the computer screen, in order to ensure the accuracy, the screen time change of digital information should be controlled within 1500–2000 ms. According to this standard of screen display time, the display of digital parameter information is designed, which is helpful for the operator to observe and complete the relevant operation correctly.

### 3.2.4 Text Display and Recognition

Location coding is related to the field of vision and attention allocation strategy. When it is in the center, the recognition efficiency is higher than when the text information is on the edge; and when the text information is on the left, the recognition efficiency is higher than when it is on the right. The recognition efficiency of Chinese information is better than that of English information. The features of native language should be taken into account in the practical application of display interface. In cognitive science, the theory of feature integration holds that the processing of characters by visual system is a bottom-up process from extracting local features to obtaining overall features [4]. Chinese and English belong to two different symbol systems, respectively. English words are linear strings arranged from left to right, which is not easy to form the integrity of perception; Chinese characters are square characters, which are concentrated in one square, matching the focus width of the central fovea of retina, and easy to form the integrity of perception. Human processing of information can be divided into automatic processing and control processing. When people are familiar with information in a certain field, they often use automatic processing. Automatic processing does not need a lot of attention, so automatic processing speed is faster. Therefore, when the presentation time of Chinese characters is the same as that of English characters, the recognition accuracy of Chinese characters is higher and the response time is shorter.

## 4 Discussion and Conclusion

The radar screen has a large amount of information and a fast update speed, and most of the radar information is currently displayed through the visual channel. There are few auditory cues of pure tone signals. The current way of presenting radar information leads to laborious interpretation by pilots. There are concerns about information missing and not being able to obtain in a timely manner for pilots' effective manipulation. The pilots invited to the interview made it clear that the human-machine interface of the radar warning system was ought to be optimized urgently. If there is information omission, it will lead to serious consequences and

even directly to threat safety, which will cause greater psychological pressure on the pilots. The optimization of the radar warning human-machine interface will greatly enhance the pilots' cognitive efficiency.

The ergonomic design of the cockpit information display system is an important foundation in determining whether the aircraft can perform their task efficiently. This article analyzes the deficiencies of the human-machine interface design in the current mainstream aircraft airborne radar warning system and proposes optimized design principles based on visual search. In the next step, it is urgent to take the mission demand as the practical guidance of scientific research, and to carry out exploratory research on pilots' threat perception improvement. Finally, this article proposes a multi-channel interaction technology that integrates vision, hearing and tactile perception in order to provide theoretical basis and technical support for the design of the radar warning system. This intelligent radar warning system is expected to reduce pilots' cognitive load and accelerate pilots' response speed.

### **Compliance with Ethical Standards**

The study was approved by the Logistics Department for Civilian Ethics Committee of Air Force Medical Center of Fourth Military Medical University. All subjects who participated in the experiment were provided with and signed an informed consent form. All relevant ethical safeguards have been met with regard to subject protection.

### **References**

1. Schriver AT, Morrow DG, Wickens CD, Talleur DA (2008) Expertise differences in attentional strategies related to pilot decision making. *J Hum Factors Ergon Soc* 50(6):864–878
2. Marieke HA, Van DO, Judith KS (2014) Differences in physical workload between military helicopter pilots and cabin crew. *Int Arch Occup Environ Health* 87(4):381–386
3. Wang Q, Sun M, Liu H, Pan Y, Wang L, Ge L (2018) The applicability of eye-controlled highlighting to the field of visual searching. *Aust J Psychol* 70(3)
4. Pooja, Renu D (2016) Video text extraction and recognition: a survey. In: *IEEE International Conference on Wireless Communications Signal Processing and Networking (WISPNET-2016)*. IEEE



# Qualitative Analysis on the Factors Influencing Pilot Functional Status



Shuang Bai, Juan Liu, Jiabo Ye, Lin Zhang, Jian Du, Wei Pan, Yubin Zhou, Qiming Cheng, Liu Yang, Duanqin Xiong, Peng Du, Ruoyong Wang, Huiling Mu, Ximeng Chen, and Hua Ge

**Abstract** *Objective*—When the pilot’s function status is low, he can’t complete the task effectively, which may cause the whole system to malfunction or even cause serious accidents. So, in order to provide scientific basis for maintaining and improving pilot functional state, this paper studies the concept, connotation and influencing factors of pilot’s functional state. *Methods*—Qualitative research methods were used, including literature analysis, questionnaire survey and expert interview. And 30 pilots were recruited to an in-depth interview. *Results*—There are three main factors that affect pilots’ functional status: special flying environment, physiological factors and psychological factors. Among these three factors, the perception ability, information processing ability, comprehensive cognitive ability and social psychological state of psychological factors are particularly important for flight function. *Conclusions*—The pilot’s functional state directly affects flight safety. It is necessary to pay attention to the factors that may affect flight functional state, and to monitor the characterization of functional state regularly. Therefore, corresponding preventive measures can be formulated to reduce the potential risk of threat to flight safety.

**Keywords** Qualitative analysis · Pilot · Pilot functional status · Psychological factors

## 1 Introduction

The pilot’s functional state refers to the integration of physiological function and cognitive ability required to complete the flight mission. It can be regarded as the unity of pilots’ physiological state, psychological state and working state. It focuses

---

S. Bai · J. Liu (✉) · J. Ye · L. Zhang · J. Du · W. Pan · Y. Zhou · Q. Cheng · L. Yang · D. Xiong · P. Du · R. Wang · H. Mu · X. Chen · H. Ge  
Air Force Medical Center of FMMU, 100142 Beijing, China  
e-mail: [13910259429@139.com](mailto:13910259429@139.com)

S. Bai  
e-mail: [b17s@163.com](mailto:b17s@163.com)

© The Editor(s) (if applicable) and The Author(s), under exclusive license to Springer Nature Singapore Pte Ltd. 2021

S. Long and B. S. Dhillon (eds.), *Man-Machine-Environment System Engineering*, Lecture Notes in Electrical Engineering 645, [https://doi.org/10.1007/978-981-15-6978-4\\_14](https://doi.org/10.1007/978-981-15-6978-4_14)

on the maintenance of workability. The high level of functional status means that the pilot can work continuously and efficiently and keep appropriate vigilance during the whole process of work. In flight, the pilot's functional state will be affected by many factors. When the pilot flying in the air focuses on one or more tasks for a long time, the risk of neglecting some important information will increase. In addition, as the flight gets longer, the pilot is increasingly prone to inattention and slow response, which will further lead to sharp decline in cognitive ability, including a decline in operational skills, decision making, analytical and judgment abilities, fracture ability and monitoring ability [1]. These are the signs of a low function state. The pilot's functional state is closely related to flight safety. According to the statistics of flight accidents from the Federal Aviation Administration (FAA) and the National Aeronautics and Space Administration (NASA), 52,000 of the 261,000 flight accident reports submitted to NASA by 2010 were caused by the poor functional status of pilots, accounting for 21% of the total. The analysis of flight accidents in the past 20 years shows that with the progress of aviation technology, the proportion of accidents caused by mechanical factors in all accidents is decreasing. And the opposite of that is the proportion of accidents caused by human factors in all accidents is increasing year by year, reaching about 80% [2]. Therefore, it is helpful to reduce the risk of flight safety by studying pilot function status in depth and mastering its changing rule accurately. The purpose of this study is to explore the factors that influence the functional status, especially by integrating analysis of the views of experienced pilots, so as to provide references for maintaining and improving the functional status of pilots.

## **2 Materials and Methods**

### ***2.1 Research Objectives***

This paper expounds the concept and connotation of pilot functional state and puts forward the operational definition of pilot functional state. On this basis, this paper summarizes the main factors affecting the functional state of pilots from the aspects of physiological factors, psychological factors and flight environment factors, and focuses on the study of the psychological influencing factors. This study provides an entry point for the monitoring and maintenance of pilot functions, which will further guarantee flight safety.

### ***2.2 Research Method***

The methods of qualitative analysis, literature review, questionnaire survey, and expert interview were used.

**Table 1** Characterization of participants

Type of airplane	Number	Average age (years)
Fighter pilot	15	42.10 ± 5.03
Transport pilot	15	46.78 ± 3.19

**Table 2** Summary of interview content

No.	Interview question	Content outline
1	Question 1	From the perspective of senior pilots, what are the connotations and concepts of pilot functional status
2	Question 2	Understanding the experience of senior pilots on different levels of functional status and their judgment criterials
3	Question 3	Collecting the factors that senior pilots think can affect the functional status, and which factor can be improved by training

### 2.3 Research Participants

A total of 30 senior pilots were interviewed, and their general information is shown in Table 1.

### 2.4 Contents of Investigation

The subjects were interviewed in a semi-structured way. Before the formal interview, the researchers made an interview outline based on literature review and previous research. The interview summary is listed in Table 2. The main content of the interview includes three questions: (1) What do you think of the pilot function state includes and what are the main points of its definition? (2) Please describe in detail when you have better functional status? When do you have poor functional status? And what are your subjective and objective criteria for functional status? (3) What factors do you think can affect pilot function status? And which of these factors can be improved by pilot training?

## 3 Main Factors Affecting Pilot's Functional Status

### 3.1 Physiological Factor

Healthy physiological state is the first condition to achieve a high level of functional state. To be able to successfully complete the mission, the pilot needs the body's

various systems to work together, especially the eyes, ears, vestibular, skeletal muscle system, central nervous system, cardiovascular system, etc. The health of every organ in the body may directly affect the function of various systems, such as the eyes, which affect visual and cognitive functions, and finally affect the completion quality of the flight task. The maintenance of good physiological status needs to meet certain standards in nutrition, sleep, comfort, health and other aspects; otherwise, it will lead to the rapid decline of the ability of pilots to complete tasks. In addition, the skeletal muscle system is the physiological basis of the pilot's body movement and various control actions. The flying environment has put forward clear requirements for the pilot's body shape, range and intensity of joint motion. Human body measurements and skeletal muscle condition of the pilot must be mastered, which is the basis of cockpit layout design and aircraft pilot equipment size design.

## **3.2 Psychological Factor**

### **3.2.1 Cognitive Ability**

#### 1. Perceptual ability

Perceptual ability is an important condition for pilots to complete flight tasks. The sensory and perceptual system is the basic structure for human body to receive external stimulation and produce sensation. The input of various senses (vision, hearing, balance sense, tactile sense, proprioception, etc.) is the basis for pilots to complete aircraft control tasks timely, accurately, safely and effectively. When flying in the air, environmental stimuli such as low air pressure, hypoxia, acceleration overload, vibration and high noise have a great impact on human perception ability, which interferes with the functions of various sensory channels. As a result, pilots are prone to spatial disorientation, visual degradation and motor dysfunction.

#### 2. Information processing capacity

With the development of aircraft manufacturing technology, aircraft system design has been highly informationized and automated, which makes the pilot gradually become a monitor and operator of a complex system. That is to say, the pilot needs to quickly make accurate situation analysis and make timely decisions when they are overloaded with information. Massive multi-channel information input, multi-task parallel processing, complex decision-making environment and time pressure bring great challenges to the cognitive ability of pilots [3, 4]. The pilot's ability of information processing, such as vision, hearing, spatial cognition, continuous attention and attention distribution, and accurate response operation, is the key ability needed to complete the mission.

### 3. Comprehensive cognitive ability

Through the analysis of pilots' work tasks, the Royal Air Force (RAF) puts forward five kinds of flight abilities: attention capacity, logical thinking ability, thinking speed, reasoning ability and spatial orientation ability. From these five aspects, a complete set of pilot selection and assessment system has been developed. The system has been used in all air force pilot selection in the UK since 1997. A survey of a large number of flight instructors conducted in Russia determined that the most important abilities of pilots were: wide attention span, fast attention transfer, high stability of attention, fast and long memory, high spatial and temporal capacity, fast reaction speed, wide range and high perceptual accuracy. In the field of civil aviation, Deutsche Lufthansa summarized the essential skills of a pilot as follows: language expression, mathematical thinking and reasoning, memory, perception, attention, spatial positioning and psychological movement. In cooperation with the Psychological Department of the German Aerospace Center, Lufthansa has jointly developed a psychological selection system for pilots. According to the theory of psychology and the content of flight training, Chinese scholars divide flight ability into two aspects: general ability and special ability. These abilities can be subdivided into: (1) good spatial orientation ability; (2) good attention; (3) sensitive perception and observation ability; (4) quick thinking ability; (5) fast and accurate memory; (6) flexible adaptability; (7) fast and accurate action response ability; (8) strong creativity; (9) high emotion control ability; (10) good organization and management ability.

#### 3.2.2 Social Psychological State

Social psychological state not only affects the cognitive ability, but also has an important impact on the decision-making stability of pilots.

##### 1. The influence of emotion on cognition and decision

In recent years, researchers pay more and more attention to the influence of emotion on human cognitive process, especially the influence of emotion on decision making. Among them, the phenomenon that anxiety affects decision making has become a research hotspot in the field of decision making because of its outstanding universality and practical significance. Anxiety is the most common negative emotional state of modern people. When people are faced with uncertain situations, they subjectively feel anxious, nervous and troubled. Meanwhile, the autonomic nervous system is activated to deal with potential threats. Anxiety has a profound impact on human decision making and behaviors—the most prominent performance is that the improvement of anxiety level makes decision makers tend to avoid risks and make conservative choices.

## 2. The influence of personality on decision making

Personality is a person's stable attitude to the real world and the habitual way of behaviors based on his attitude. It is an outstanding aspect of human's psychological outlook, and its structure is multi-level, usually including the realistic attitude characteristics of personality, the will characteristics of personality, the emotional characteristics of personality and the rational characteristics of personality. For example, carefulness, dogmatism, firmness and decisiveness, arbitrariness and calmness, which are embodied in personality differences, will bring different effects to decision making. Generally speaking, positive personality traits are conducive to decision-making optimization, while negative personality traits greatly hinder the best decision making.

## 3. The influence of team compatibility on team performance

Team conflict has a very important impact on team performance. Team conflict can be divided into relationship conflict and task conflict. Relationship conflict always plays a negative role, which arouses hatred and hostility among members, leading to the degradation of decision quality. Task conflict has both positive and negative effects: On the one hand, task conflict can increase the exchange of information, stimulate new ideas and improve the quality of decision making; on the other hand, with the strengthening of task conflict, the harmonious relationship of the team will be destroyed, which may cause relationship conflict, and then have a negative impact on the quality of decision making. Therefore, to explore the impact of team compatibility on team decision-making performance, we should focus on task conflict. It should be explored in depth how to play a positive role of task conflict in decision-making quality and how to minimize its possible negative effects.

### ***3.3 Influence of Flight Environment on Function State***

When flying in the air, pilots need to suffer from low air pressure, lack of oxygen, acceleration overload, vibration and high noise, and sometimes fatigue and sleep deprivation, or sometimes have to fly in the dark with limited vision. These environmental factors have a huge negative impact on the functional status of pilots, which will damage their cognitive function and operational ability of pilots. According to the research of the US Army Research Institute, fatigue and sleep deprivation can lead to the decline of soldiers' work performance; acceleration overload can sometimes lead to "black vision" in pilots, and short-term "black vision" can lead to the decline of visual sensitivity and tracking ability, messy mind, amnesia, nausea, vertigo (dizziness or sense of rotation) and disorientation. The brain tissue of pilots suffering from acceleration overload for a long time may be permanently damaged, and their vision, memory, cognitive function may correspondingly decline. In addition to acceleration overload, low air pressure and hypoxia can also cause pilots' headache, dizziness,

panic, and shortness of breath, nausea, vomiting and other symptoms, which have a negative impact on the cognitive function of pilots. The negative influence of extreme flight environment on pilot's functional state is an important bottleneck to limit pilot's operational ability. At present, the principle of reducing the negative impact of flight environment to the pilot's functional state is not completely clear. In the future, it is necessary to deeply study the law of the pilot's cognitive decision-making ability from the perspective of brain operation mechanism and analyze the changes of brain in the flight environment, so as to maintain the pilot's air functional state. On the other hand, it is necessary to establish an effective, reliable and sensitive pilot functional state monitoring technology [5], in order to grasp the changes of pilot's functional state during the mission, and effectively discover the signs of accidents to ensure flight safety.

#### 4 Discussion and Conclusion

This study synthesizes the views of all invited interviewed pilots. The functional status of pilots is affected by many factors, among which the most important safety factor is the pilot. The pilot is the most active factor in the aviation man-machine system [6], and the pilot is also the most vulnerable factor in the system. The working ability of the pilot is limited by the physiological limit and the consciousness limit, and is also easily affected by the environmental or equipment factors. In short, pilot functional state has a great impact on flight safety. Pilot functional state is affected by many factors, including workload and pilot internal state. Workload mainly includes the task requirements and environmental requirements of human-aircraft system for pilots; the internal state is affected by comprehensive factors, such as cognitive ability, psychological load, physiological state, working environment, personality traits, psychological sensitivity and work experience. In addition to routine physical examinations, pilots also need to check their functional status before performing major missions. Flight surgeons should not only pay attention to the physical conditions of pilots, but also evaluate their functional state. By judging the physiological and psychological conditions of the pilot, it can be inferred whether the pilot is fit to perform a certain task, so as to make a comprehensive judgment. The comprehensive evaluation of the pilot's function state before flight is helpful to improve the scientificity of the flight control decision. The internal state of pilots is an important factor that affects their functional state. And the internal state is not static, so it requires close attention and regular monitoring by flight surgeons. According to its characteristics, pilot functional state may have the following six manifestations: (1) a quiet state of active preparation; (2) a state of nervous and emotional stress; (3) a state of comfort and relaxation; (4) an overly emotional state of tension; (5) a state of depression after a long monotonous flight; (6) a state of fatigue or over fatigue. The over fatigue state is the extreme of the development and change of the pilot's functional state, and it is also an important subject of aviation health protection. Although it cannot be absolutely considered that fatigue will certainly lead to

the decline of flight performance, but in the fatigue state, the consumption of energy resources of pilots can further reduce their physiological and psychological reserves, weaken their anti hypoxia and acceleration capacity. In such cases, if an accident or emergency occurs, improper handling and flight accidents are likely to occur.

**Compliance with Ethical Standards** The study was approved by the Logistics Department for Civilian Ethics Committee of Air Force Medical Center of Fourth Military Medical University. All subjects who participated in the experiment were provided with and signed an informed consent form. All relevant ethical safeguards have been met with regard to subject protection.

## References

1. Anthony W (2003) Fatigue assessment and performance protection. In: Hockey G, Gaillard A, Burov O (eds) *Operator functional state: the assessment and prediction of human performance degradation in complex tasks*. IOS Press, Amsterdam, pp 24–35
2. Hockey GR (2003) *Operator functional state: the assessment and prediction of human performance degradation in complex tasks*. IOS Press, US, pp 8–23
3. Benitez DM, Valiente ADC, Lanzi P (2018) A novel global operational concept in cockpits under peak workload situations. *Saf Sci* 102:38–50
4. Yang K, Feng C, Bai J (2018) Comprehensive assessment of pilot mental workload in various levels. *J Harbin Institut Technol* 25(2):59–72
5. Yang XM, Yuan JY, Yuan JS, Mao HN (2010) An improved WM method based on PSO for electric load forecasting. *Expert Syst Appl* 37(12):8036–8041
6. Feng C, Wan YX, Yang K, Zhuang D, Wu X (2018) A comprehensive prediction and evaluation method of pilot workload. *Technol Health Care Off J Eur Soc Eng Med* 26(1):1–14



# Study on Sensory Evaluation of Instant Rice by Fuzzy Mathematics Method



Huiling Mu, Peng Du, Longmei Fang, Shuang Bai, Ximeng Chen, Peng Liu, and Ruoyong Wang

**Abstract** *Objective:* To study the sensory quality of six kinds of instant rice by fuzzy mathematics method. *Methods:* Adopted the method of fuzzy mathematics with color, status, smell, texture and taste as evaluation factors and carried out fuzzy mathematics judgment of the sensory quality of six kinds of instant rice: rice, five grains rice, coix seed rice, mung bean rice, highland barley rice and black rice. *Results:* The fuzzy comprehensive sensory evaluation scores of six kinds of instant rice from high to low were black rice, coix seed rice, five grains rice, mung bean rice, highland barley rice and rice. *Conclusions:* The fuzzy mathematics method can reflect the sensory quality of military instant rice objectively, which provided a reference method for the comprehensive sensory quality evaluation of military food.

**Keywords** Instant rice · Sensory evaluation · Fuzzy mathematics method

## 1 Introduction

Instant rice is a kind of staple instant food that can be industrialized and mass produced. The color, texture, taste and other sensory quality of instant rice are basically the same as the fresh rice [1]. It can be eaten directly or after simple heating. Because it is easy to eat and carry and can meet people's traditional eating habits and nutritional needs, it brings us a lot of convenience in our life. Military instant rice is a part of long duration flight food, which is a kind of food developed for pilots to eat on airplanes in order to carry out long-distance flight missions [2]. It belongs to military food, and its shelf life usually needs to be more than 2 years or even longer, which also puts forward higher requirements for the acceptability of sensory quality of military food.

At present, fuzzy mathematics method had been widely used in food sensory evaluation [3–11]. However, it had not been reported in the comprehensive sensory evaluation of military food. Therefore, comprehensive fuzzy mathematics evaluation

---

H. Mu · P. Du · L. Fang · S. Bai · X. Chen · P. Liu · R. Wang (✉)  
Air Force Medical Center, 100142 Beijing, China  
e-mail: [mhl2001@126.com](mailto:mhl2001@126.com)

© The Editor(s) (if applicable) and The Author(s), under exclusive license to Springer Nature Singapore Pte Ltd. 2021

S. Long and B. S. Dhillon (eds.), *Man-Machine-Environment System Engineering*, Lecture Notes in Electrical Engineering 645, [https://doi.org/10.1007/978-981-15-6978-4\\_15](https://doi.org/10.1007/978-981-15-6978-4_15)

**Table 1** Main raw materials proportion of six kinds of military instant rice

Sample code	Product	The main raw materials proportion
S <sub>1</sub>	Rice	100% rice
S <sub>2</sub>	Five grain rice	60% rice, 20% corn, 10% millet, 5% glutinous rice, 5% wheat
S <sub>3</sub>	Highland barley rice	60% brown rice, 20% corn, 10% millet, 10% highland barley
S <sub>4</sub>	Mung bean rice	80% rice, 10% mung bean, 10% millet
S <sub>5</sub>	Black rice	75% rice, 15% black rice, 10% millet
S <sub>6</sub>	Coix seed rice	85% rice, 10% coix seed, 5% yam

of six kinds of military instant rice was carried out, which selected color, status, smell, texture and taste as the evaluation factors of sensory quality of military instant rice in this study, in order to evaluate the sensory quality of military instant rice objectively and fairly, and provide a reference method for the comprehensive sensory quality evaluation of military instant rice.

## 2 Materials and Methods

### 2.1 Preparation of Military Instant Rice

Military instant rice was made of rice as the main raw material, with or without all kinds of edible raw grains such as millet, corn, highland barley and so on. It was processed by raw grain processing, flour mixing, molding, maturing, cooling, packaging and other processes. It can be eaten after being soaked in hot water (above 90 °C) for 10 min.

Six kinds of military instant rice were rice, five grain rice, coix seed rice, mung bean rice, highland barley rice and black rice, respectively. The main raw materials proportion of the products was shown in Table 1.

### 2.2 Sensory Evaluation

Forty-five male fighter pilots with an average age of (34.2 ± 6.9) years were selected for sensory evaluation of six kinds of military instant rice samples. According to personal preferences, they evaluated the color, status, smell, texture and taste of the instant rice by the nine-point system and the sensory evaluation criterion of military instant rice (Table 2). The nine-point system included nine levels: extremely like (nine points), very like (eight points), like (seven points), a little like (six points),

**Table 2** Sensory evaluation criterion of military instant rice

Indicator	Criterion	Preference	Score
Color (15%)	The color of rice should be bright and luster	like–extremely like	7–9
	The color of rice is normal and slightly glossy	less like–a little like	4–6
	The color of rice is abnormal and lusterless	extremely dislike–not like	1–3
Status (15%)	The structure of rice is compact, and the integrity of rice grains is good	like–extremely like	7–9
	Most of the structure of rice is compact and complete	less like–a little like	4–6
	Rice burst	extremely dislike–not like	1–3
Smell (20%)	With the unique aroma of rice, which is strong	like–extremely like	7–9
	With the unique aroma of rice, which is fragrant	less like–a little like	4–6
	With the unique aroma of rice, which is not obvious	extremely dislike–not like	1–3
Texture (25%)	The rice is chewy, moderate in hardness, not sticky	like–extremely like	7–9
	The rice is a little bit chewy, feels a little hard or soft and basically does not stick to teeth	less like–a little like	4–6
	The rice feels dross, very hard or soft, sticky	extremely dislike–not like	1–3
Taste (25%)	Strong fragrance and sweet taste when chewing	like–extremely like	7–9
	Light fragrance and sweet taste when chewing	less like–a little like	4–6
	No fragrance and sweetness when chewing	extremely dislike–not like	1–3

general (five points), less like (four points), not like (seven points), very dislike (eight points) and extremely dislike (one point); the more you like, the higher the score is.

Before sensory evaluation, the evaluators should be trained to understand the meaning and scoring standards of various sensory evaluation indexes. Each evaluation should be recorded by each evaluation personnel independently, without contact and communication with each other, and each sample evaluation should be rinsed with water.

### 2.3 Establishment of Fuzzy Mathematical Model

1. Determined the factor set. The color, status, smell, texture and taste were selected as evaluation factors,  $U_1, U_2, U_3, U_4$  and  $U_5$  represented color, status, smell, texture and taste, respectively. The factor set  $U = \{U_1, U_2, U_3, U_4, U_5\}$ .
2. Determined the comment set  $V = \{V_1, V_2, V_3, V_4, V_5, V_6, V_7, V_8, V_9\}$ , where  $V_1$  meant extremely like (nine points),  $V_2$  meant very like (eight points),  $V_3$  meant like (seven points),  $V_4$  meant a little like (six points),  $V_5$  meant general (five points),  $V_6$  meant less like (four points),  $V_7$  meant not like (three points),  $V_8$  meant very dislike (two points) and  $V_9$  meant extremely dislike (one point).
3. Determined the weight set  $W = \{W_1, W_2, W_3, W_4, W_5\}$ . This experiment was based on sensory evaluation criteria of military instant rice (Table 2): color 15%, status 15%, smell 20%, texture 25% and taste 25% as the distribution basis of weight coefficients. The weight coefficients of color, status, smell, texture and taste were 0.15, 0.15, 0.20, 0.25 and 0.25, respectively, and the total was 1, the weight set  $W = \{0.15, 0.15, 0.20, 0.25, 0.25\}$ .
4. Determined fuzzy relation comprehensive evaluation set. The comprehensive evaluation set of fuzzy relation is  $Y = W \cdot R$ , where  $Y$  is the comprehensive evaluation set,  $W$  is the weight set, and  $R$  is the fuzzy evaluation matrix.

## 3 Results and Analysis

### 3.1 Sensory Evaluation Results

According to the sensory evaluation methods and criteria, six kinds of military instant rice were evaluated. The results were shown in Table 3.

### 3.2 Establishment of Fuzzy Comprehensive Evaluation Set

Divide the data in Table 3 by the total number of evaluators (45) to get six fuzzy evaluation matrices:

$$R_1 = (r_{ij})_{5 \times 9} = \begin{pmatrix} 14/45 & 1/5 & 13/45 & 1/15 & 4/45 & 1/45 & 1/45 & 0 & 0 \\ 2/5 & 1/9 & 11/45 & 4/45 & 1/9 & 1/45 & 1/45 & 0 & 0 \\ 4/15 & 7/45 & 13/45 & 1/9 & 2/15 & 1/45 & 1/45 & 0 & 0 \\ 2/9 & 14/45 & 11/45 & 2/45 & 4/45 & 1/15 & 1/45 & 0 & 0 \\ 8/45 & 17/45 & 2/9 & 1/15 & 4/45 & 2/45 & 1/45 & 0 & 0 \end{pmatrix}$$

**Table 3** Sensory evaluation results of six kinds of military instant rice ( $n = 45$ )

Sample code	Indicator	Score								
		9	8	7	6	5	4	3	2	1
S <sub>1</sub>	Color ( $U_1$ )	14	9	13	3	4	1	1	0	0
	Status ( $U_2$ )	18	5	11	4	5	1	1	0	0
	Smell ( $U_3$ )	12	7	13	5	6	1	1	0	0
	Texture ( $U_4$ )	10	14	11	2	4	3	1	0	0
	Taste ( $U_5$ )	8	17	10	3	4	2	1	0	0
S <sub>2</sub>	Color ( $U_1$ )	12	18	5	8	2	0	0	0	0
	Status ( $U_2$ )	16	11	11	3	4	0	0	0	0
	Smell ( $U_3$ )	10	14	12	6	3	0	0	0	0
	Texture ( $U_4$ )	8	16	11	7	3	0	0	0	0
	Taste ( $U_5$ )	8	17	12	5	3	0	0	0	0
S <sub>3</sub>	Color ( $U_1$ )	12	11	6	13	3	0	0	0	0
	Status ( $U_2$ )	14	12	8	6	5	0	0	0	0
	Smell ( $U_3$ )	9	14	8	11	3	0	0	0	0
	Texture ( $U_4$ )	10	13	10	5	7	0	0	0	0
	Taste ( $U_5$ )	7	14	14	5	5	0	0	0	0
S <sub>4</sub>	Color ( $U_1$ )	12	12	10	5	6	0	0	0	0
	Status ( $U_2$ )	14	13	6	5	7	0	0	0	0
	Smell ( $U_3$ )	8	18	9	8	2	0	0	0	0
	Texture ( $U_4$ )	6	13	20	3	3	0	0	0	0
	Taste ( $U_5$ )	6	17	11	8	3	0	0	0	0
S <sub>5</sub>	Color ( $U_1$ )	22	9	10	2	2	0	0	0	0
	Status ( $U_2$ )	20	9	9	3	4	0	0	0	0
	Smell ( $U_3$ )	17	13	6	7	2	0	0	0	0
	Texture ( $U_4$ )	15	12	13	2	3	0	0	0	0
	Taste ( $U_5$ )	13	15	11	3	3	0	0	0	0
S <sub>6</sub>	Color ( $U_1$ )	14	17	8	4	2	0	0	0	0
	Status ( $U_2$ )	14	15	9	3	4	0	0	0	0
	Smell ( $U_3$ )	14	13	6	9	3	0	0	0	0
	Texture ( $U_4$ )	10	14	13	5	3	0	0	0	0
	Taste ( $U_5$ )	10	15	14	3	3	0	0	0	0

$$R_2 = (r_{ij})_{5 \times 9} = \begin{vmatrix} 4/15 & 2/5 & 1/9 & 8/45 & 2/45 & 0 & 0 & 0 & 0 \\ 16/45 & 11/45 & 11/45 & 1/15 & 4/45 & 0 & 0 & 0 & 0 \\ 2/9 & 14/45 & 4/15 & 2/15 & 1/15 & 0 & 0 & 0 & 0 \\ 8/45 & 16/45 & 11/45 & 7/45 & 1/15 & 0 & 0 & 0 & 0 \\ 8/45 & 17/45 & 4/15 & 1/9 & 1/15 & 0 & 0 & 0 & 0 \end{vmatrix}$$

$$R_3 = (r_{ij})_{5 \times 9} = \begin{vmatrix} 4/15 & 11/45 & 2/15 & 13/45 & 1/15 & 0 & 0 & 0 & 0 \\ 14/45 & 4/15 & 8/45 & 2/15 & 1/9 & 0 & 0 & 0 & 0 \\ 1/5 & 14/45 & 8/45 & 11/45 & 1/15 & 0 & 0 & 0 & 0 \\ 2/9 & 13/45 & 2/9 & 1/9 & 7/45 & 0 & 0 & 0 & 0 \\ 7/45 & 14/45 & 14/45 & 1/9 & 1/9 & 0 & 0 & 0 & 0 \end{vmatrix}$$

$$R_4 = (r_{ij})_{5 \times 9} = \begin{vmatrix} 4/15 & 4/15 & 2/9 & 1/9 & 2/15 & 0 & 0 & 0 & 0 \\ 14/45 & 13/45 & 2/15 & 1/9 & 7/45 & 0 & 0 & 0 & 0 \\ 8/45 & 2/5 & 1/5 & 8/45 & 2/45 & 0 & 0 & 0 & 0 \\ 2/15 & 13/45 & 4/9 & 1/15 & 1/15 & 0 & 0 & 0 & 0 \\ 2/15 & 17/45 & 11/45 & 8/45 & 1/15 & 0 & 0 & 0 & 0 \end{vmatrix}$$

$$R_5 = (r_{ij})_{5 \times 9} = \begin{vmatrix} 22/45 & 1/5 & 2/9 & 2/45 & 2/45 & 0 & 0 & 0 & 0 \\ 4/9 & 1/5 & 1/5 & 1/15 & 4/45 & 0 & 0 & 0 & 0 \\ 17/45 & 13/45 & 2/15 & 7/45 & 2/45 & 0 & 0 & 0 & 0 \\ 1/3 & 4/15 & 13/45 & 2/45 & 1/15 & 0 & 0 & 0 & 0 \\ 13/45 & 1/3 & 11/45 & 1/15 & 1/15 & 0 & 0 & 0 & 0 \end{vmatrix}$$

$$R_6 = (r_{ij})_{5 \times 9} = \begin{vmatrix} 14/45 & 17/45 & 8/45 & 4/45 & 2/45 & 0 & 0 & 0 & 0 \\ 14/45 & 1/3 & 1/5 & 1/15 & 4/45 & 0 & 0 & 0 & 0 \\ 14/45 & 13/45 & 2/15 & 1/5 & 1/15 & 0 & 0 & 0 & 0 \\ 2/9 & 14/45 & 13/45 & 1/9 & 1/15 & 0 & 0 & 0 & 0 \\ 2/9 & 1/3 & 14/45 & 1/15 & 1/15 & 0 & 0 & 0 & 0 \end{vmatrix}$$

$r_{ij}$  indicates the degree of subordination from the evaluation indexes of military instant rice to the evaluation results of the indexes.

The comprehensive membership degree of samples was calculated by using matrix multiplication [9–11]. The result vector of the comprehensive sensory quality evaluation of military instant rice was as follows:

$$Y_1 = W \cdot R_1 = \{0.15, 0.15, 0.20, 0.25, 0.25\} \begin{vmatrix} 14/45 & 1/5 & 13/45 & 1/15 & 4/45 & 1/45 & 1/45 & 0 & 0 \\ 2/5 & 1/9 & 11/45 & 4/45 & 1/9 & 1/45 & 1/45 & 0 & 0 \\ 4/15 & 7/45 & 13/45 & 1/9 & 2/15 & 1/45 & 1/45 & 0 & 0 \\ 2/9 & 14/45 & 11/45 & 2/45 & 4/45 & 1/15 & 1/45 & 0 & 0 \\ 8/45 & 17/45 & 2/9 & 1/15 & 4/45 & 2/45 & 1/45 & 0 & 0 \end{vmatrix}$$

Among them,  $y_{11} = 0.15 \times 14/45 + 0.15 \times 2/5 + 0.20 \times 4/15 + 0.25 \times 2/9 + 0.25 \times 8/45 = 0.260$ ,  $y_{12} = 0.15 \times 1/5 + 0.15 \times 1/9 + 0.20 \times 7/45 + 0.25 \times 14/45 + 0.25 \times 17/45 = 0.250$ .

Similarly,  $y_{13} = 0.254$ ,  $y_{14} = 0.073$ ,  $y_{15} = 0.101$ ,  $y_{16} = 0.039$ ,  $y_{17} = 0.022$ ,  $y_{18} = 0$ ,  $y_{19} = 0$ . Therefore,  $Y_1 = \{0.260, 0.250, 0.254, 0.073, 0.101, 0.039, 0.022, 0, 0\}$ .

Similarly,

$$\begin{aligned}
 Y_2 &= \{0.227, 0.342, 0.234, 0.130, 0.067, 0, 0, 0, 0\} \\
 Y_3 &= \{0.221, 0.289, 0.216, 0.168, 0.107, 0, 0, 0, 0\} \\
 Y_4 &= \{0.189, 0.330, 0.266, 0.130, 0.086, 0, 0, 0, 0\} \\
 Y_5 &= \{0.371, 0.268, 0.223, 0.076, 0.062, 0, 0, 0, 0\} \\
 Y_6 &= \{0.267, 0.326, 0.233, 0.108, 0.067, 0, 0, 0, 0\}
 \end{aligned}$$

The comprehensive scores of each sample were calculated according to the comprehensive score formula 1:

$$H_i = \sum_{j=1}^n jY_i \tag{1}$$

$H_1 = 9 \times 0.260 + 8 \times 0.250 + 7 \times 0.260 + 6 \times 0.089 + 5 \times 0.068 + 4 \times 0.016 + 3 \times 0 + 2 \times 0 + 1 \times 0 = 7.29$ . Similarly,  $H_2 = 7.53, H_3 = 7.35, H_4 = 7.41, H_5 = 7.81, H_6 = 7.62$ . Therefore, the sensory quality of six kinds of military instant rice from high to low was  $S_5 > S_6 > S_2 > S_4 > S_3 > S_1$ . Sensory evaluation results showed that the sensory quality of black rice samples was the best, and the sensory quality of rice samples was the worst. The comprehensive scores of black rice, coix seed rice and five grains rice are between 7 and 8, close to 8, which indicates that the three kinds of rice preferred to very like between like and very like. The comprehensive scores of mung bean rice, highland barley rice and rice were between 7 and 8, close to 7, which indicates that the three kinds of rice preferred to like between like and very like.

## 4 Conclusions

At present, the sensory evaluation of military food in our army is using the nine-point system. This evaluation method can fully reflect the personal preferences, but there is subjectivity. The individual differences of the evaluation personnel will significantly affect the evaluation results. Therefore, in this study, the sensory quality of six kinds of instant rice was evaluated by fuzzy mathematics sensory evaluation method with color, status, smell, texture and taste as evaluation factors. The results showed that the fuzzy comprehensive sensory evaluation scores of six kinds of instant rice from high to low were black rice, coix seed rice, five grains rice, mung bean rice, highland barley rice and rice. Fuzzy mathematics method overcame the influence of subjective factors, can reflect the sensory quality of military instant rice objectively and accurately and provided a reference method for the comprehensive sensory quality evaluation of military food.

**Compliance with Ethical Standards** The study was approved by the Logistics Department for Civilian Ethics Committee of Air Force Medical Center. All subjects who participated in the experiment were provided with and signed an informed consent form. All relevant ethical safeguards have been met with regard to subject protection.

## References

1. Liu QS, Zhu JL (2016) Study on the processing technology of convenient rice. *Food Eng* 1:59–61
2. Gao LX, Guo JS, Guo CJ (2008) *Military nutrition and food science*. Military Medical Science Press, Beijing, p 464
3. Hu X, Xia YB (2011) An improved sensory comprehensive evaluation method for chopped hot pepper based on fuzzy mathematics. *Food Sci* 32(1):95–98
4. Pan ZM, Zou WZ, Zhang XF et al (2014) Study on evaluation of sensory fuzzy mathematics of soybean dietary fiber biscuit for breakfast. *Guangxi Sci* 21(3):300–305
5. Zolfaghari ZS, Mohebbi M, Najariyan M (2014) Application of fuzzy linear regression method for sensory evaluation of fried donut. *Appl Soft Comput J* 22:417–423
6. Fu L, Zhang Y, Gong H et al (2017) Formular optimization of starch in crystal shrimps based on the fuzzy mathematics evaluation. *Sci Technol Food Indus* 38(11):209–218
7. Chen SM (2016) Improvement of the recipe of the okara walnut cake by fuzzy mathematic sensory evaluation. *Cereals Oils* 29(7):66–69
8. Zhao ZX, Sun Y, Guan LN et al (2019) Study on the process optimization of sprouting brown rice based on fuzzy synthetical evaluation. *Grain Process* 44(3):28–38
9. Xiong DG, Xian XF (2003) Improvement of fuzzy comprehensive evaluation method. *J Chongqing Univ* 26(6):93–95
10. Zhu W, Fu XZ, Guan TQ et al (2007) Sensory analysis on pinckled potherb mustard quality by fuzzy comprehensive evaluation. *Food Sci* 28(11):176–178
11. He XY, Ni XG, Li LH et al (2009) Preparation and sensory evaluation of pepper wine. *Liquor-making Sci Technol* 11:101–103



# Study on the Workload of 12 h Simulated Flight Continuously Across Day and Night



Feng Wu, Dawei Tian, Hua Ge, Shuang Bai, Andong Zhao, Ruoyong Wang, Yanpeng Zhao, Quan Wang, and Lue Deng

**Abstract** *Objective:* To investigate the workload of 12 h simulated long-haul flight continuously across day and night. *Methods:* Six healthy male young volunteers, aged from 19 to 21 years, were trained in simulated flight and skilled in operating flight simulation software before the experiment. Subjects began the simulated flight every day at 20:00 and lasted for 12 h that ended at 8:00. Subjects flew for three consecutive days and slept at least 6 h during the day. Workload evaluation indicators were tested before and after simulated flights on the first, second, and third days, respectively. Reaction time (RT), motion time (MT), critical flicker fusion frequency (CFF), Stanford Sleepiness Scale (SSS), and rating of perceived exertion scale (RPE) were measured. *Results:* RT increased after simulated flights on the second and third days, but there was no significant difference between before and after flights. MT increased after the first and second days of simulated flight, but the difference was statistically significant only after the first day of flight. There was no significant difference in CFF between before and after three consecutive days of simulated flight. SSS and RPE scores were significantly increased after 12 h simulated flight for three consecutive days. *Conclusions:* 12 h simulated long-haul flight continuously across day and night could aggravate the flight workload and heavy fatigue.

**Keywords** Simulated flight · Long-haul flight · Fatigue · Workload

## 1 Introduction

The physical and mental loads of military pilots are different with the different time schedule of flight mission and the interval of repeating flight mission. Generally speaking, the longer the duration of flight, the more obvious the impact on the physical and mental functions of the pilots is. Flying at night or across the day and sudden emergencies has a greater impact on the physical and mental functions of pilots than flights in daytime and routine missions. Long-haul continuous flight or cross time

---

F. Wu · D. Tian · H. Ge · S. Bai · A. Zhao · R. Wang · Y. Zhao · Q. Wang · L. Deng (✉)  
Air Force Medical Center, Fourth Military Medical University, 100142 Beijing, China  
e-mail: [denglue@sina.com](mailto:denglue@sina.com)

© The Editor(s) (if applicable) and The Author(s), under exclusive license to Springer Nature Singapore Pte Ltd. 2021

S. Long and B. S. Dhillon (eds.), *Man-Machine-Environment System Engineering*, Lecture Notes in Electrical Engineering 645, [https://doi.org/10.1007/978-981-15-6978-4\\_16](https://doi.org/10.1007/978-981-15-6978-4_16)

zone flight will disturb the normal work and rest rules of pilots, resulting in sleep rhythm disorder, and the adverse effects on mental status and cognitive performance of pilots are more obvious. The research on the prevention and control measures of long-haul flight fatigue has become a hot issue in aviation medicine research [1, 2]. In this paper, from the perspective of workload, the effects of 12 h simulated flight continuously across the day and night on body and mind were studied, the characteristics of psychological and physiological changes of long-haul pilots were discussed, and effective long-haul flight support measures were developed to improve combat capability of military pilots.

## **2 Methods**

### **2.1 Subjects**

Six healthy young male volunteers, aged from 19 to 21 years, with height of  $(171 \pm 1.7)$  cm and weight of  $(68.7 \pm 7.1)$  kg, were all right-handed, had no hobbies such as smoking and drinking, no habits such as drinking strong tea and coffee, life rules, no self-reported sleep disorders, and no medication history and history of neurology and psychiatry.

### **2.2 Methods and Steps**

Subjects were trained in simulated flight before the experiment and skilled in operating flight simulation software (Lock On Flaming Cliffs 3). Subjects were allowed to work and rest normally 1 week before the experiment, and smoke, alcohol, tea, coffee, and other drinks were prohibited. Subjects are prohibited from using central excitatory or inhibitory drugs to avoid strenuous exercise. Subjects began the simulated flight every day at 20:00 and lasted for 12 h that ended at 8:00. Subjects flew for three consecutive days and slept at least 6 h during the day. Workload evaluation indicators were tested before and after simulated flights on the first, second, and third days, respectively.

### **2.3 Parameters and Equipments**

#### **1. Reaction Time (RT), Motion Time (MT)**

Reaction time and motion time tester (BEIDA JADE BIRD BD-II-513) was used. The stimulation mode was simultaneous presentation of sound and light stimulation,

and the number of experiments was 10. The measurements were repeated three times before and after 12 h flight, and the average values were obtained.

## 2. Critical Flicker Fusion Frequency (CFF)

Window flicker meter (BEIDA JADE BIRD BD-II-118) was used. Red spot was selected, light intensity was 1/2, bright black ratio was 1: 1, and the background light intensity was 1/16. According to the order of “raise, cut,” recording a total of two frequency values takes the arithmetic mean as one result. Repeat measurements three times before and after flight to get the average value.

## 3. Stanford Sleepiness Scale (SSS) and Rating of Perceived Exertion Scale (RPE)

SSS is divided into seven grades, from “awake and alert” for 1 score to “almost fall to sleep” for 7 scores. RPE is used to evaluate fatigue autonomously according to 0–10 points, 0 points are no fatigue, 1–4 points are relatively light fatigue, 5 points are a little heavy fatigue, 6–9 points are heavy fatigue, and 10 points are very heavy fatigue.

## 2.4 Statistical Analysis

SPSS18.0 statistical software was used for paired sample T-test analysis, with  $P < 0.05$  as the difference was statistically significant.

## 3 Results

As shown in Fig. 1, RT increased after simulated flights on the second and third days, but there was no significant difference between before and after flights. MT increased after the first and second days of simulated flight, but the difference was statistically significant only after the first day of flight ( $P < 0.05$ ).

There was no significant difference in CFF between before and after three consecutive days of simulated flight ( $P > 0.05$ ), as shown in Fig. 2.

As shown in Fig. 3, SSS and RPE scores were significantly increased after 12 h simulated flight for three consecutive days ( $P < 0.01$  or  $P < 0.05$ ).

## 4 Discussion

Military pilots who perform long-haul flight tasks are prone to flight fatigue, which seriously affects performance and even causes flight safety problems. Continuous long-haul flight across the day and night will cause disturbance of circadian sleep

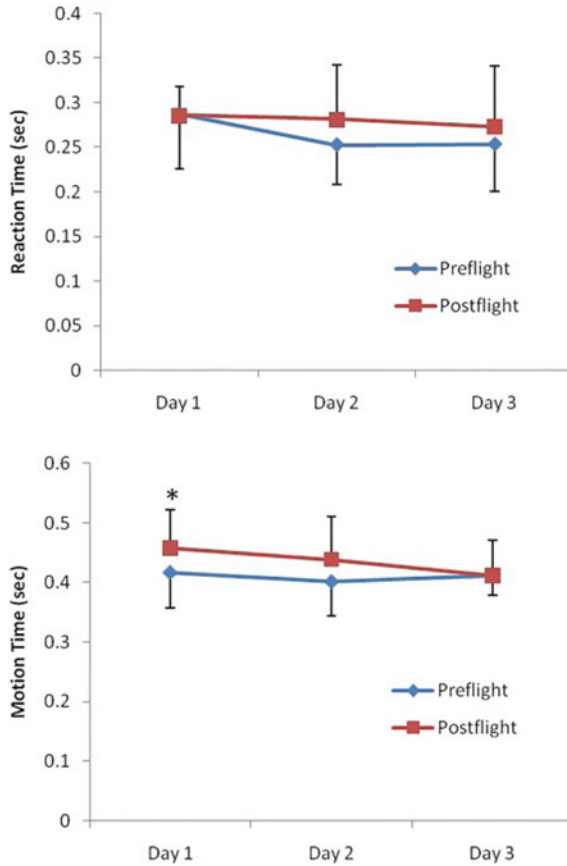


**Fig. 1** Reaction time and motion time of subjects during 12 h simulated flight for three consecutive days (Note \* $P < 0.05$ , \*\* $P < 0.01$  compared with preflight)

rhythm, increase fatigue and sleepiness, and decrease cognitive ability [3]. Workload evaluation is an important research tool to improve work efficiency, prevent fatigue, and maintain the physical and mental health of pilots.

CFF and reaction time and motion time measurement are commonly used physiological and psychological indicators of fatigue. In the results of this study, although only the first 12 h of simulated flight motion time increased significantly, but the reaction time and motion time also increased after the second 12 h simulated flight. CFF changed before and after three consecutive days of simulated flight, but there was no significant difference. This indicates that the simulated flight workload increases and fatigue occurs in 12 h across the day and night, but because the subjects may produce adaptability for three consecutive days of simulated flight, the indicator difference is not significant. In addition, the subjects slept at least 6 h during the day after the end of each day's flight in the experiment, which alleviated sleep deprivation and adjusted

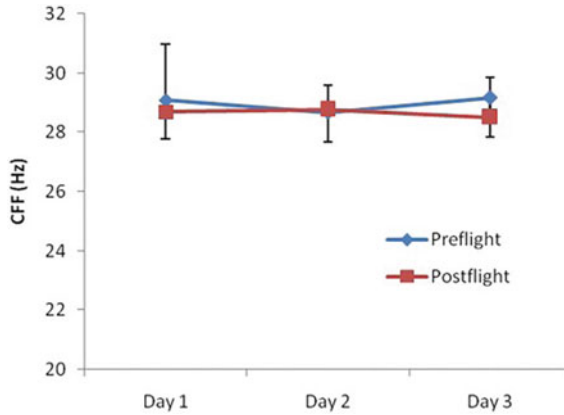


**Fig. 2** CFF of subjects during 12 h simulated flight for three consecutive days (Note  $*P < 0.05$ ,  $**P < 0.01$  compared with preflight)

the sleep rhythm during the day and night flights. This may also be the reason why there is no significant difference in RT and MT and CFF between before and after three consecutive days of simulated flight. Studies have shown that sleep less than 6 h before the task 24 h will lead to impaired operational ability and increased error rate [4]. Dawson and McCulloch suggested that 6 h sleep was obtained 24 h before the task could be used as a threshold for assessing increased fatigue risk [5]. Six-hour sleep can be used as an important reference to improve the sleep rhythm disorders of long-haul flight in the future.

Since people have a certain perception of workload, subjective evaluation of workload can be judged by subjective scale. In this study, 12 h of simulated flight across the day and night caused a significant increase in subjective fatigue and sleepiness. The evaluation of simulated long-haul flight workload is of great significance to flight training and formulation of aviation health support measures [6]. This study only preliminarily explores the evaluation indicators of long-haul flight workload. In the subsequent experiments, we should continue to improve the evaluation method to provide the basis for the development of long-haul flight support measures.

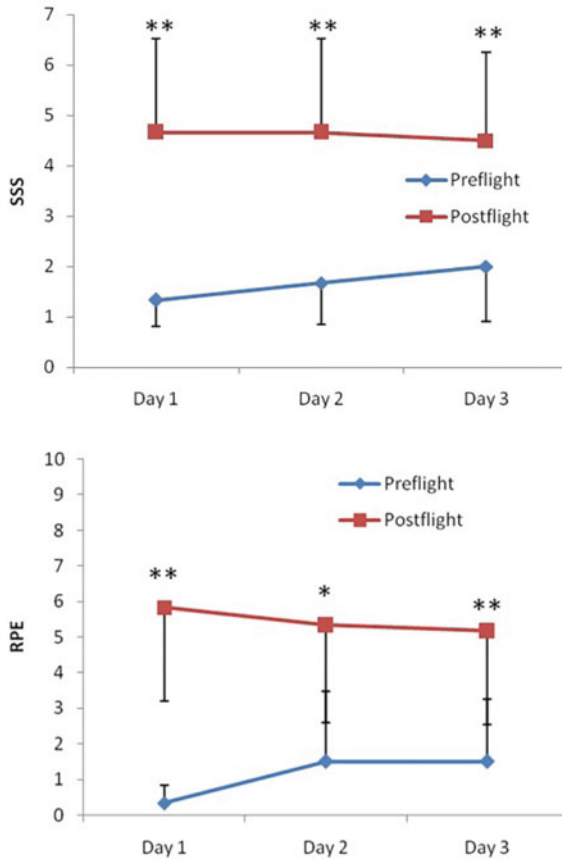


**Fig. 3** SSS and RPE of subjects during 12 h simulated flight for three consecutive days (Note \* $P < 0.05$ , \*\* $P < 0.01$  compared with preflight)

**Acknowledgements** This work is supported by the Military Medical Research Foundation, China, No. AKJ15J002. Feng Wu and Dawei Tian contributed equally to this work.

**Compliance with Ethical Standards** The study was approved by the Logistics Department for Civilian Ethics Committee of Air Force Medical Center.

All subjects who participated in the experiment were provided with and signed an informed consent form.

All relevant ethical safeguards have been met with regard to subject protection.

## References

1. Armentrout JJ, Holland DA, O'Toole KJ et al (2006) Fatigue and related human factors in the near crash of a large military aircraft. *Aviat Space Environ Med* 77(9):963–970
2. Caldwell JA, Mallis MM, Caldwell JL et al (2009) Fatigue countermeasures in aviation. *Aviat Space Environ Med* 80(1):29–59
3. Zhan H, Jiao ZG, Zhang QJ (2013) Advances on the workload of long-range flight and medical support measures. *Chin J Aerospace Med* 24(1):68–74
4. Thomas MJ, Ferguson SA (2010) Prior sleep, prior wake, and crew performance during normal flight operations. *Aviat Space Environ Med* 81(7):665–670
5. Dawson D, McCulloch K (2005) Managing fatigue: it's about sleep. *Sleep Med Rev* 9(5):365–380
6. Zhang QJ, Zhan H (2014) Evaluation system of simulated long haul flight performance and its application prospect. *Chin J Aerospace Med* 25(2):129–132

# Study on Nutritional Status and Changing Trend of Air Force Pilots



Peng Du, Huiling Mu, Shuang Bai, Longmei Fang, Ximeng Chen, Hongjiang Jing, Feng Li, Peng Liu, Lili Zhang, and Ruoyong Wang

**Abstract** *Objective* To understand the nutritional status of air force pilots and explore its changing trend, so as to provide scientific basis for guiding reasonable nutrition and improving operational performance of the air force pilots. *Methods* 125–147 male pilots were included in the study. The energy intake was estimated by weighing method. The energy consumption was assessed by life observation method. The body mass index (BMI) was calculated by height and weight. Serum total cholesterol (TC) and triglyceride (TG) were determined by double reagent enzyme method. The results were compared with that of nutrition survey for air force pilots in 1997 and 2007. *Results* The average daily energy intake and consumption was 3375.2 kcal and 3091.5 kcal, respectively. Protein, fat, and carbohydrate provided 17.4%, 43.9%, and 38.7% of the daily energy intake, respectively. The incidence of underweight, overweight, and obesity was 4.8%, 16.8%, and 4.0%, while the prevalence of hypertriglyceridemia and hypercholesterolemia was 31.2% and 36.1%, respectively. The nutritional status of air force pilots changed a lot compared with that of 1997. However, the situation seemed to be improved compared with that of 2007. *Conclusions* The dietary pattern of air force pilots was not reasonable and the incidence of overweight, obesity, and dyslipidemia was high. Nutritional intervention and guidance should be strengthened.

**Keywords** Pilots · Nutritional status · Nutrition evaluation · BMI

## 1 Introduction

The incidence of overweight and obesity in air force pilots is increasing as well as the incidence of chronic non-infectious diseases closely related to nutritional status in recent years, posing a serious threat on the health of the pilots [1, 2]. Therefore, this study investigated the nutritional status of the air force pilots and compared the results with those of 1997 and 2007, exploring the development trend, so as to

---

P. Du · H. Mu · S. Bai · L. Fang · X. Chen · H. Jing · F. Li · P. Liu · L. Zhang · R. Wang (✉)  
Air Force Medical Center of FMMU, 100142 Beijing, China  
e-mail: [dupengaf@163.com](mailto:dupengaf@163.com)

© The Editor(s) (if applicable) and The Author(s), under exclusive license to Springer Nature Singapore Pte Ltd. 2021

S. Long and B. S. Dhillon (eds.), *Man-Machine-Environment System Engineering*, Lecture Notes in Electrical Engineering 645, [https://doi.org/10.1007/978-981-15-6978-4\\_17](https://doi.org/10.1007/978-981-15-6978-4_17)



provide scientific basis for guiding reasonable nutrition and physical fitness of air force pilots.

## 2 Subjects and Methods

### 2.1 Subjects

125–147 male air force pilots were included, with an average age of  $(36.9 \pm 6.3)$  years, an average height of  $(174.4 \pm 4.7)$  cm, and an average weight of  $(74.8 \pm 8.5)$  kg.

### 2.2 Methods

#### 2.2.1 Energy Indexes

Energy intake was estimated by weighing method for 3 consecutive days, including one flight day. The energy intake and the energy supply ratio of the three major nutrients were calculated. The data of the food composition used was from “2018 China food composition tables-standard edition (6th Edition)” [3]. Life observation method was used for the energy consumption survey. 12 pilots with representative height and weight were selected as the survey subjects, and their 24-h activities were recorded for 3 consecutive days. The daily energy consumption of each person was calculated according to the energy consumption rate of various activities.

#### 2.2.2 BMI

The height and weight of the pilots was measured. BMI was calculated according to Eq. (1). According to the criteria of “Evaluation of nutritional status for air force pilots,” the normal range of BMI was 20–26. If the BMI was lower than 20, it was underweight. If  $\text{BMI} \geq 26$ , it was overweight. If  $\text{BMI} \geq 28$ , it was obesity.

$$\text{BMI} = \frac{\text{Weight}(\text{kg})}{\text{Height}^2(\text{m}^2)} \quad (1)$$

### 2.2.3 Serum Lipid

Serum TG and TC were detected by Roche C501 automatic biochemical analyzer. TC and TG were evaluated by the criteria of “Guidelines for prevention and treatment of dyslipidemia in Chinese adults (2016 Revision)” [4].

## 2.3 Statistical Analysis

SPSS 18.0 was used for statistical analysis. The data were compared between the two groups by t test and  $\chi^2$  test, with  $p < 0.05$  as the statistically significant.

## 3 Results and Analysis

### 3.1 Energy Indexes

The results were shown in Tables 1 and 2. The average daily energy consumption of air force pilots was 3375.2 kcal, which decreased compared with that of 1997 and 2007 survey. The average daily energy consumption was 3091.5 kcal, which was lower than that of 1997, but higher than that of 2007. The difference of 2018 between energy intake and energy consumption was close to that in 1997, but significantly lower than that of 2007. Compared with 1997 and 2007, the ratio of energy provided by protein was on the rise. The ratio of energy provided by fat was higher than that of 1997 but lower than that of 2007. The ratio of energy provided by carbohydrate was lower than that of 1997 but higher than that of 2007.

**Table 1** Average daily energy intakes and expenditures for air force pilots (kcal)

Year	Energy intake ( $\bar{x} \pm s$ )	Energy expenditure ( $\bar{x} \pm s$ )	Difference value
2018	3375.2 $\pm$ 347.5	3091.5 $\pm$ 283.5	283.7
2007	3 412.6 $\pm$ 363.7	2 995.1 $\pm$ 237.6	417.5
1997	3908.2 $\pm$ 298.5	3633.5 $\pm$ 185.1	274.7

**Table 2** Energy supply ratios of protein, fat and carbohydrate for air force pilots (%)

Year	Protein	Fat	Carbohydrate
2018	17.4	43.9	38.7
2007	16.4	45.7	37.9
1997	15.6	36.3	48.1

**Table 3** Evaluation of BMI for air force pilots

Year	N	Underweight	Normal	Overweight	Obesity
2018	125	6(4.8%)**	93(74.4%)	21(16.8%)**	5(4.0%)*
2007	212	4(1.9%)##	164(77.4%)	32(15.1%)##	12(5.7%)##
1997	163	42(25.8%)	112(68.7%)	8(4.9%)	1(0.6%)

The results of 2018 compared with the results of 1997, \* $p < 0.05$ , \*\* $p < 0.01$ . The results of 2007 compared with the results of 1997, # $p < 0.05$ , ## $p < 0.01$

### 3.2 BMI

The results were shown in Table 3. Six of the 125 pilots were underweight, accounting for 4.8% of the total. Ninety-three pilots were in normal weight, accounting for 74.4% of the total. Both of them were significantly lower than that of 1997 ( $p < 0.01$ ). Twenty-one pilots were overweight, accounting for 16.8% of the total, which was significantly higher than that of 1997 ( $p < 0.01$ ). Five pilots were obese, which was higher than that of 1997 ( $p < 0.05$ ). Compared with the results of 1997, the trend of 2007 was the same as that of 2018. There was no significant difference between the survey results of 2018 and 2007 ( $p > 0.05$ ).

### 3.3 Serum Lipid

The results were shown in Table 4. The prevalence of hypertriglyceridemia was 31.2%, which was significantly lower than that of 2007 ( $p < 0.01$ ). The average serum TG level also decreased compared with that of 2007. The prevalence of hypercholesterolemia was 36.1%, which was significantly higher than that of 2007 ( $p < 0.01$ ). The average serum TC level increased compared with that of 2007.

**Table 4** Analysis of serum lipid for air force pilots

Year	Total number	Hypertriglyceridemia			Hypercholesterolemia		
		N	Ratio (%)	$\bar{x} \pm s$ (mmol/L)	N	Ratio (%)	$\bar{x} \pm s$ (mmol/L)
2018	147	46	31.3**	$1.65 \pm 1.03$	53	36.1**	$4.95 \pm 0.92$
2007	186	89	47.8	$2.07 \pm 0.97$	33	17.7	$4.60 \pm 0.86$
1997 <sup>a</sup>	–	–	–	–	–	–	–

<sup>a</sup>The data of 1997 was missing. Compared with the results of 2007, \* $p < 0.05$ , \*\* $p < 0.01$

## 4 Conclusions

The nutritional status of the air force pilots was closely related to physical fitness, which was directly related to the health status and the operational performance of the air force pilots. Several large-scale nutrition surveys had been carried out in recent years. This study summarized some results of the latest nutrition survey in 2018 and compared them with those in 1997 and 2007. All the indexes listed in this paper were determined by the same method, which ensured the scientificity and comparability of the research.

The results showed that in the past 20 years, the energy intake of pilots has been decreasing year by year and the energy consumption was also significantly lower in 2018 than that of 1997 but a little bit higher than that of 2007. The difference between energy intake and energy consumption in 2018 was also significantly lower than that of 2007. In recent years, the air force pilots gradually realized the importance of reasonable nutrition and balanced diet. The exercise and training intensity was also strengthened in recent years. That maybe the reason for the change of energy intake and consumption. However, the dietary pattern of the air force pilots deviated a lot from the recommended standard. It was recommended that the energy provided by protein, fat, and carbohydrate should be 12%–15%, 20%–30%, and 55%–65%, respectively while the actual distribution ratio was 17.4%, 43.9%, and 38.7%, showing a “high protein, high fat, and low carbohydrate” pattern. The air force pilots took in too much fat while the carbohydrate was not enough. The unbalanced dietary pattern may be one of the important reasons for the high incidence of overweight, obesity, and nutrition-related chronic diseases [5]. It was suggested that pilots should adjust their dietary pattern, increase their effective exercise thus building up their health.

BMI was a combination of height and weight used to determine whether the human body was overweight or not. In 2003, the Cooperative Meta-Analysis Group of China obesity task force suggested that the normal range of BMI for chinese adults should be 18.5–23.9. If  $BMI \geq 24$ , it is overweight. If  $BMI \geq 28$ , it is obesity [6]. Considering the strong figure of the pilots, the normal BMI range of the pilots was defined as 20.0–26.0. According to the standard, the overweight proportion of the pilots was on the rise in the past 20 years, but the rising speed had slowed down significantly in the past 10 years, and the proportion of obesity also slightly decreased compared with that of 2007, suggesting that the pilots gradually realize the harm of overweight and obesity and start weight control. However, the effect and measures need to be further strengthened.

The incidence rate of dyslipidemia in air force pilots was high. The incidence of hypertriglyceridemia and hypercholesterolemia was 36.1% and 31.2%, respectively. The incidence of hypertriglyceridemia was lower than that of 2007. However, the incidence of hypercholesterolemia increased significantly, which was almost 2 times of that of 2007. The mechanism for it was not clear and needed further study. In addition, the incidence of hypertriglyceridemia and hypercholesterolemia in chinese general population was 18.9% and 28.9%, respectively [7]. It can be seen that not only

the incidence of dyslipidemia for air force pilots was high, but also the composition of lipidemia spectrum was quite different from that of the general population, which was consistent with the investigation results of Zhang et al. [8]. In addition to dietary factors, it may also be related to special aviation environment such as hypoxia, acceleration, radiation, and psychological stress Savransky et al. [9].

In conclusion, the nutritional status of pilots has changed greatly in the past 20 years. Although the energy intake showed a downward trend, the energy consumption was also declining, and the dietary pattern has changed from carbohydrate based to fat based, which may be an important reason for the increase of the incidence of overweight, obesity, and dyslipidemia. But generally speaking, the nutritional status was better than that of 2007, suggesting that with the improvement of living standards and the development of nutrition science, the pilots gradually realized the importance of reasonable nutrition and has started to improve it. The nutritional status of the pilots was related to the maintenance of the operational performance of the pilots [10], which should highly emphasized and corresponding measures should be taken, such as dietary pattern adjustment, sports strengthening, to actively prevent and control the occurrence and development of overweight, obesity, and the chronic non-infectious diseases related to nutritional status of the air force pilots.

**Compliance with Ethical Standards** The study was approved by the Logistics Department for Civilian Ethics Committee of Air force Medical Center of FMMU. All subjects who participated in the experiment were provided with and signed an informed consent form. All relevant ethical safeguards have been met with regard to subject protection.

## References

1. Chen Q, Wei AM, Shen X (2017) Dietary survey and nutritional status evaluation of 775 Air force pilots. *Med J Air Force* 33(04):231–233
2. Liu TB, Wang SS, Zi Chen et al (2016) Prevalence of Dyslipidemia among Pilots in China: a Meta-analysis. *Military Med J South China* 30(10):649–653
3. Yang YX (2018) 2018 China food composition tables-standard, 6th edn. Peking University Medical Press, Beijing
4. Zhu JR, Gao RL, Zhao SP (2016) Guidelines for the prevention and treatment of dyslipidemia in Chinese adults (2016 Revision). *Chinese Circ J* 31(10):937–953
5. Dong L, Quan SZ, Ma HY et al (2012) Analysis of risk factors of dyslipidemia in military pilots. *Mil Med Sci* 36(9):683–686
6. Cooperative Meta-analysis Group of China Obesity Task Force (2002) Predictive values of body mass index and waist circumference to risk factors of related diseases in Chinese adult population. *Chin J Epidemiol* 23(1):5–10
7. Chang JL, Wang Y (2013) Comprehensive report on the monitoring of nutrition and health status of Chinese residents in 2010–2013. Peking University Medical Press, Beijing
8. Zhang JY, Gao YX (2007) Analysis on the types of lipid abnormality in fighter pilots. *J Prev Med Chin Peopl Liber Army* 25(2):98–100
9. Li J, Savransky V, Nanayakkara A, Li J et al (2007) Hyperlipidemia and lipid peroxidation are dependent on the severity of chronic intermittent hypoxia. *J Appl Phys* 102(2):513
10. Yang JS, Lan F, Cang J et al (2019) Disease spectrum of hospitalized Air force pilots. *Med J Air Force* 35(6):470–473

# Simulation and Verification of a Vestibular Perception Model



Cong Wang, Dalong Guo, Hongbo Jia, Yuliang Li, Fang Su, Yuanjing Zheng,  
Yao Liu, Chenlong Jia, and Qi Zhang

**Abstract** *Objective* To develop a vestibular perception model for human space orientation and to verify the effectiveness of the model through simulation experiments. *Methods* Based on the theory of the multisensory modeling for human space orientation, a MATLAB/Simulink based vestibular perception model including otoliths, semicircular canals and their interactions was developed. By inputting the motion stimuli including linear acceleration and angular velocity into the model, simulation experiments of Coriolis effect and somatogravic illusion were performed. *Results* The model outputs of linear acceleration, angular velocity, Euler angle and gravity were in good agreement with the results of relevant research or analysis. The perception model could simulate human vestibular perception function and predictive responses on vestibular flight illusion accurately. *Conclusions* It proves that the perception model presented in this paper has a high credibility. It would contribute to the study on flight orientation and flight illusion.

**Keywords** Perception model · Vestibular model · Space orientation · Flight illusion

## 1 Introduction

The spatial orientation in flight refers to the perceptual process of pilots for the position, motion or attitude of airplanes in the earth-fixed coordinate system [1]. It develops based on the integration of the visual, vestibular and proprioceptive information the pilot received by the basic sensory systems [2].

Visual information is the most important sensory information in flight [3, 4]. The vestibular organs, including otolith and semicircular canal, can feel gravity as well

---

C. Wang · D. Guo · H. Jia · Y. Li · F. Su · Y. Zheng · Y. Liu · C. Jia  
Air Force Medical Center, Air Force Military Medical University, PLA, 100142 Beijing, China

Q. Zhang (✉)  
6th Medical Center, General Hospital of Chinese PLA, 100142 Beijing, China  
e-mail: [48767625@qq.com](mailto:48767625@qq.com)

© The Editor(s) (if applicable) and The Author(s), under exclusive license to Springer Nature Singapore Pte Ltd. 2021

S. Long and B. S. Dhillon (eds.), *Man-Machine-Environment System Engineering*, Lecture Notes in Electrical Engineering 645,  
[https://doi.org/10.1007/978-981-15-6978-4\\_18](https://doi.org/10.1007/978-981-15-6978-4_18)

as the linear acceleration and angular acceleration motion of human body in three-dimensional space [5]. The proprioception refers to the kinesthesia of muscles, tendons, joint capsules and the touch–pressure sensation of body surface skin. It generally does not play a supporting role in spatial orientation.

For decades, some scholars have developed different perception models [6, 7] of spatial orientation with cybernetics and estimation theory based on vestibular physiology study, such as observer model [8], Kalman filtering model [9]. These models can be used to predict spatial orientation perception of human body according to the known dynamic and motion sensory information.

In this paper, based on the modeling theory of observer model, the MATLAB/Simulink software was used to develop a spatial orientation perception model of human body with the multisensory channel. The prediction effect of the model was verified by vestibular function and flight illusion simulation tests.

## 2 Vestibular Perception Model

### 2.1 Otolith Model

Otolith includes utricle and saccule, mutually perpendicular to each other. They are responsible for feeling the linear acceleration motion and gravity at the horizontal plane and sagittal plane, respectively. The function threshold of otolith is between 0.001 and 0.05 g [1]. Its response characteristics can be expressed by the following transfer function [10].

$$H(s)_{\text{oto}} = \frac{K_{\text{oto}}(1 + T_1s)}{(1 + T_2s)(1 + T_3s)} \quad (1)$$

The input of the transfer function is the specific force, or the vector sum of the linear acceleration and the gravitational acceleration of the human body. The output is the specific force perceived by the otolith where  $K_{\text{oto}}$  is the model coefficient with a value of 0.4.  $T_1$ ,  $T_2$  and  $T_3$  are the time constants with the values of 10, 5 and 0.016, respectively.

### 2.2 Semicircular Canal Model

The semicircular canal consists of three pipelines with an orthogonal arrangement. The appropriate stimulus of the semicircular canal is the angular acceleration. Usually, the angular velocity is taken as the input and output of the transfer function of semicircular canal [11]. The average value of function thresholds of semicircular canal is  $0.5^\circ/\text{s}^2$  [1]. Its transfer function can be expressed as:

$$H(s)_{scc} = \frac{K_{scc}s^2}{(1 + T_1s)(1 + T_2s)} \tag{2}$$

where  $K_{scc}$  is the coefficient of the model with a value of 1.  $T_1$  and  $T_2$  are the long and short time constants with the values of 80 and 5.73, respectively.

### 2.3 Vestibular Perception Model

The sensory information of angular acceleration or linear acceleration is detected by the semicircular canal or otolith, respectively. The two kinds of sensation are integrated into spatial orientation perception of human body in central vestibular system.

On the basis of the theory of observer model, the vestibular perception model is built, and its schematic diagram [8] is shown in Fig. 1. In the vestibular perception model, the inputs are linear acceleration  $a$  and angular velocity  $\omega$  as well as the outputs are linear acceleration  $a_{est}$ , angular velocity  $\omega_{est}$ , gravity  $g_{est}$  and attitude angle  $Angle_{est}$ , perceived by human body. The above variables are three-dimensional vectors in the coordinate system of the human head, and the subscript  $est$  represents the estimated value of the motion sensation by the internal model of the central nervous system.  $f$  is the specific force,  $f = a - g$ .  $g(\omega)$  refers to the gravity direction update by angular motion in the coordinate system of the human head, and the formula is  $dg/dt = g \times \omega$ .  $H(S)_{oto}$  and  $H(S)_{scc}$  are the transfer functions of otolith and semicircular canal, respectively. Furthermore,  $H(S)_{oto\_est}$  and  $H(S)_{scc\_est}$  are the transfer functions of their internal models, respectively.  $GIF\_Err$  module is used to

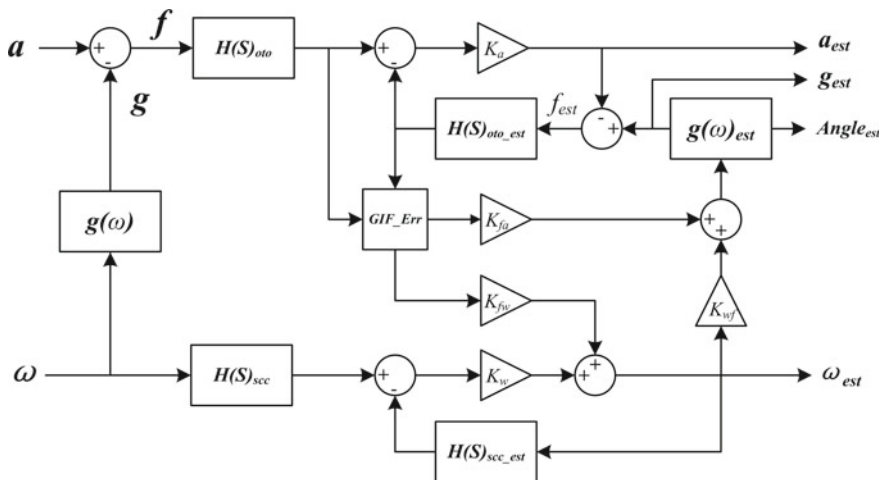


Fig. 1 Diagram of the vestibular perception model



correct the vertical direction of subjective gravity in the internal model by calculating the rotation error between the vector vestibular estimated value and the central estimated value of specific force.  $K_a$ ,  $K_{fa}$ ,  $K_w$ ,  $K_{fw}$  and  $K_{wf}$  are the parameters of feedback loops in the internal model.

### 3 Simulation Test Results

Based on the above principle of vestibular perception model, the MATLAB/Simulink software was used to develop the vestibular perception simulation model of spatial orientation. The numerical solution algorithm of 4–5-order Runge–Kutta method with a variable step size was used. And the time step of simulation was 0.01 s.

#### 3.1 Vestibular Coriolis Effect Simulation Test

The test conditions are set as follows. Under an initial state in the vertical direction, the human body counterclockwise rotated for 120 s with a  $57.3^\circ/\text{s}$  angular velocity. At the 70th seconds, the head rolled around the X-axis with a speed of  $60^\circ/\text{s}$ . After 0.5 s, the head swung  $30^\circ$  to the right and then kept about 50 s. During the test process, the angular velocity motion curves of the head in three axial directions are shown in the upper image of Fig. 2. The lower image of Fig. 2 shows the prediction results of angular velocities around three axes for the vestibular Coriolis effect by model.

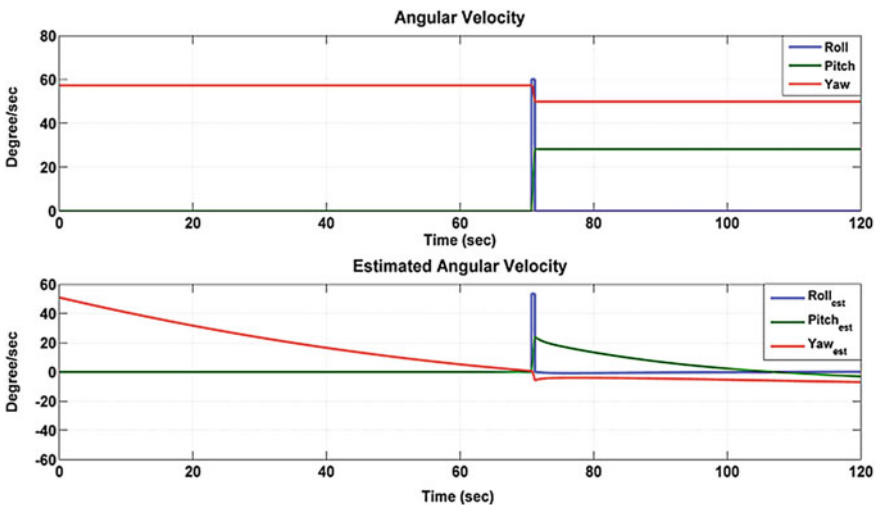


Fig. 2 Model predictions on angular velocity for Coriolis effect

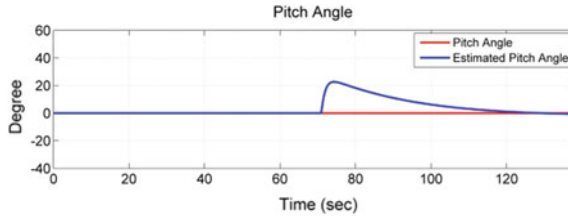


Fig. 3 Model predictions on pitch angle for Coriolis effect

Obviously, before the 70th second, the angular velocity around Z-axis  $\omega_{z\_est}$  gradually decreased from 57.3°/s to nearly 0. At the 70th second, the head swung around X-axis, as well as the anterior semicircular canal and the horizontal semicircular canal, was stimulated by angular motion at the same time. And, there would generate a cross-couple, that is, Coriolis force. It acted on the posterior semicircular canal, thus making human body generate a rotation sensation around the third axis (Y-axis).  $\omega_{y\_est}$  gradually decayed to 0 after rapidly reaching a maximum of about 27.5°/s.

The prediction results of pitching angle perception by model are shown in Fig. 3. At the 70th second, the head swung toward the right, there would generate a bending down sensation around Y-axis. Moreover, this sensation would gradually decrease to disappearance within 50 s.

### 3.2 Somatogravic Illusion Simulation Test

According to the mechanism of Somatogravic illusion, the test conditions are set as follows. The airplane is accelerated to 1G linear acceleration along the X-axis at the horizontal plane with a linear acceleration growth rate of 0.5 G/s. Holding for 20 s, the acceleration decreased to 0 with a linear acceleration growth rate of -0.5G/s. Then, after 15 s, the acceleration increased to 3G linear velocity along X-axis with a linear acceleration growth rate of 1.5 G/s. Holding for 20 s, the acceleration decreased to 0 with a linear acceleration growth rate of -1.5 G/s. The upper image of Fig. 4 displays the inertial acceleration curves along three axial directions of model input. The simulated inertial accelerations are equal to the actual linear acceleration in size but opposite to the actual linear acceleration in direction. Furthermore, the sensory perception of pilot on the inertial acceleration predicted by model is shown in the lower image. It can be seen that the pilot would take the direction of resultant force of inertia force  $a_x$  and gravity  $g$  as the vertical direction of gravity. Therefore, as the airplane accelerates along the X-axis, the pilot generates a misperception of rotation of gravity direction around Y-axis, thus feeling a pitching motion with a tilt angle of  $\theta$ .

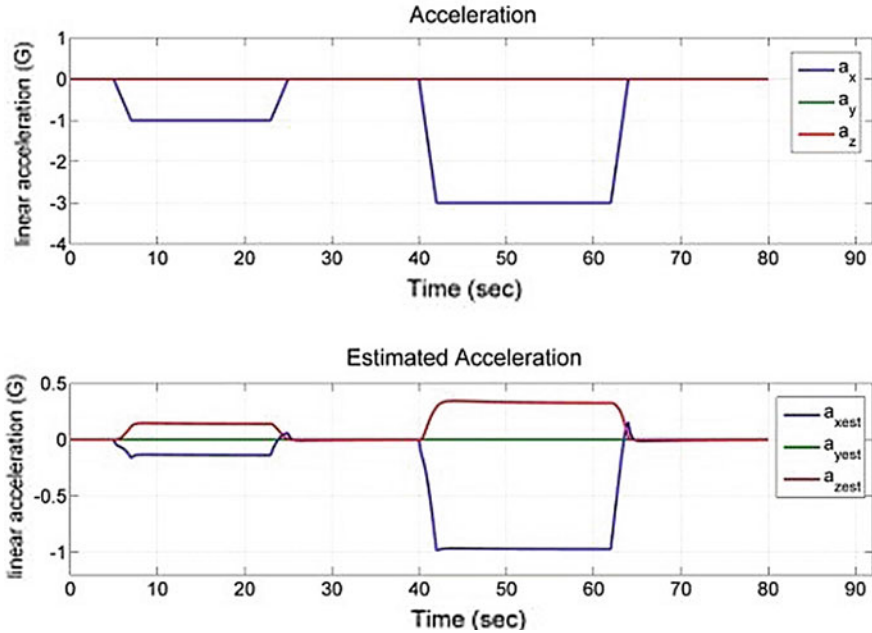


Fig. 4 Model predictions on inertial acceleration for Somatogravic illusion

$$\theta = \arctan\left(\frac{a_x}{g}\right) \quad (3)$$

In addition, the sensory perception of pilot on the tilt angle relative to the vertical direction of gravity predicted by model is shown in Fig. 5. During the periods of 1G and 3G constant acceleration, the tilt angle sensations predicted by model are  $45^\circ$  and  $72^\circ$ , respectively, consistent with the theoretical calculation results of Formula (3).

## 4 Discussion

Compared with the single sensory organ model, the vestibular model can simulate the spatial orientation perception function of human body more completely and accurately. The results of Coriolis effect simulation test are basically consistent with those of Coriolis effect vector test or calculation of Newman [11]. This verifies the accuracy of prediction results by the model. The results of Somatogravic illusion simulation successfully predicted the tilt perception of human body in the linear acceleration process, as well as the predicted tilt angle was consistent with that of the theoretical analysis. It is proved that the model can simulate the physiological

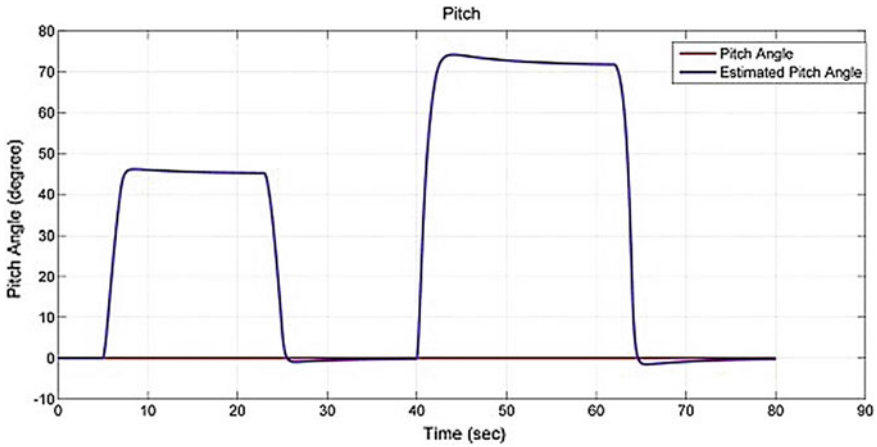


Fig. 5 Model predictions on pitch angles for Somatogravic illusion

characteristics of otolith system, that is, with a difficulty in distinguishing between the inertia force of acceleration and gravity.

The model developed in this paper is a spatially oriented perception model based on the vestibular sensory information. It can predict some vestibular function test results and vestibular flight illusion well. However, the visual information plays a very important role in the formation of spatial orientation perception of pilots in the actual flight. In the following work, it is needed to increase the visual organ model and visual–vestibular interaction model so as to expand the simulation efficiency of the model as well as the scope of research and application.

## 5 Conclusions

In this paper, the MATLAB/Simulink software was used to develop a vestibular perception model for human space orientation based on the theory of observer model. The results of simulation tests show that the model can simulate the vestibular perception function of human body more accurately, and it can predict the vestibular flight illusion such as Somatogravic illusion, etc. The model proposed in this paper can be used to study the spatial orientation in flight and flight illusion analysis.

## References

1. Yu LS, Chen TS, Yu G, et al (2013) Vestibular function examination technique. Xi'an: The fourth military medical university press, pp 531–533

2. Miao DM, Liu XF (2010) Aerospace psychology. Xi'an:the fourth military medical university press, p 32
3. Previc FH, Ercoline WR (2004)Space disorientation in aviation. Virginia: American Institute of Aeronautics and Astronautics, pp 37–38
4. Markus L, Frank B, Van der Berg AV (1999) Perception of self-motion from visual flow. *Trends in Cogn Sci* 3(9):329–336
5. Allerton D (2009) Principles of flight simulation. John Wiley and Sons Ltd Publication, UK, pp 98–299
6. Wei C, Jiangang C (2014) Research on space flight training simulation technology based on human perception theory. *Space Med Med Eng* 27(3):223–229
7. Angelaki DE, Cullen KE (2008) Vestibular system:the many facets of a multimodal sense. *Annu Rev Neurosci* 31:125–150
8. Merfeld DM, Young LR, Oman CM et al (1993) A multidimensional model of the effects of gravity on the spatial orientation of the monkey. *J Neurophysiol* 3:141–161
9. Borah J, Young LR, Curry RE (1988) Optimal estimator model for human spatial orientation. representation of three-dimensional space in the vestibular, oculomotor, and visual system. *Ann New York Acad Sci* 545:51–73
10. Telban RJ, Cardullo FM (2005) Motion cueing algorithm development:human-centered linear and nonlinear approaches:NASA/CR-2005-213747 [R]. USA:NASA Langley Research Center, pp 23–43
11. Newman MC (2009) A multisensory observer model for human spatial orientation perception. MSc thesis, 2009, Department of Aeronautics and Astronautics, MIT, Boston

# Analysis of Man's Role in Unmanned Operations



Hongjun Cheng, Huifang Wang, and Yinxi Yang

**Abstract** Unmanned operations have changed the patterns of war, which also enlightens people to understand some recognized war ethics in a new sight of view. Man is both of the designer and beneficiary of unmanned operations. However, faced with abuse of force, the risk of weapons out of control, weakening morals, to some extent, man is also the victim of unmanned operations. Man is the designer of unmanned operation methods. Therefore, man should keep unmanned equipment under good control and avoid the abuse of unmanned equipment, making full use of advantages of unmanned operations. In this thesis, a deep analysis is made on the four roles of man in unmanned operations.

**Keywords** Unmanned operations · Role · Analysis

With the rapid development and wide application of modern technology, in which information technology is the core, weaponry and equipment are becoming informationized, intelligent, and unmanned. The intelligent unmanned operation in battlefield is beginning to emerge and showing vitality. The changes in the form of war and the style of operations are, in a sense, the result of long-term efforts of man and an important manifestation of the development of human civilization. The emergence of unmanned operations has led to a re-understanding of some recognized war ethics. It is worth of deep reflection and research what role man plays in unmanned warfare.

## 1 Man Is the Designer of Unmanned Operations

To conduct unmanned operations, the first and foremost factor is whether various types of applicable unmanned weapons and equipment can be developed and produced [1]. Since the 1980s, under the joint promotion of high-tech groups such

---

H. Cheng · H. Wang (✉) · Y. Yang  
Army Academy of Artillery and Air Defense, 450052 Zhengzhou, China  
e-mail: [peony1001@126.com](mailto:peony1001@126.com)

as new material technology, new energy technology, information technology, and automation technology, the military of countries around the world have increased the research and development of unmanned weapon systems and made great progress. Some unmanned aircraft, self-homing warheads, unmanned submarines, and unmanned vehicles have been successfully developed, and some have even begun to enter actual combat. Man-machine combined operations, drone swarm operations, and other operation methods have been successively put into practices.

### ***1.1 Man Is the Designer of Unmanned Equipment***

The cruel nature of the battlefield environment of modern warfare, the danger of operations, and the huge cost of war have become increasingly prominent, forcing people to seek ways to keep combatants away from the battlefield and to decrease casualties. Due to its advantages, the emergence and development of unmanned weapon systems have become a logical necessity.

It is the US military that earliest applied unmanned technology to military purposes [2]. On the Vietnam battlefield in the 1960s, the US military often used night-vision robots for guard in case of a surprise attack by the Vietnamese army. After the Gulf War, with the development of sensor and computing processor technologies, the performance of unmanned systems has become more and more powerful. In 1995, unmanned systems and Global Positioning System (GPS) were combined, and the development of unmanned systems really ushered in a magical moment. Pentagon policymakers are increasingly realizing the superiority of unmanned systems in the military. In 2004, the US military had 150 robots on the Iraqi battlefield, and a year later, this number increased to 2400. By the end of 2008, nearly 50 types and 12,000 robots had carried out various military tasks on the Iraqi battlefield. At present, unmanned weapon systems are everywhere from the air to the ground, from land to sea. They are widely used to replace or assist man in tasks such as reconnaissance, defense, alert, demining, bait, relay, and transportation.

### ***1.2 Man Is the Designer of Unmanned Operation Method***

Unmanned operation method is the study of ways to use unmanned weapon systems to achieve combat objectives. It is both of a new combat theory and an inheritance and development of traditional operation methods. In the future unmanned operations, it requires man planning and organization and the adoption of strategic, tactical, and operational methods to find how to combine man and unmanned combat equipment best, how to maximize the effectiveness of unmanned combat equipment, and how to achieve superiority over the enemy.

Specifically, it is necessary to combine the characteristics of unmanned combat forces, pay attention to giving play to their advantages, organize reasonably the

combat forces, determine the timing of operations, select strike opportunities and targets, use innovative operation methods and styles, design various specific actions, and to be able to use strategies and tactics flexibly in changing moments of offensive and defensive operations, based on objective conditions of operation objectives, strengths, operation time and space, and battlefield environment, so as to achieve operational purposes. For example, the swarm tactics proposed by the US military is a new type of operation developed on the basis of its swarm concept. The main method is to use a large number of low-cost drones to carry out saturated attacks on combat targets and strive to achieve greater combat effectiveness at small cost.

## **2 Man Is the Beneficiary of Unmanned Operations**

The USA has deployed a large number of unmanned combat systems in the battlefields of Iraq and Afghanistan, which has produced significant combat effectiveness. These combat practices have demonstrated to the world the great military value of unmanned systems. In some sense, men are the beneficiaries of unmanned operations.

### ***2.1 Get Rid of Physical Restraints***

For manned operation platforms, physical limits are an important consideration, which is always the prerequisite and basis which influence the choice of operation patterns and methods. The widespread use of unmanned equipment has freed combatants from a large amount of intense, tense, and dangerous physical labor, and to some extent, freed them from simple and boring mental labor, which allows them spending more time engaging in more important, more complex battlefield control, strategic thinking, and tactical confrontation [3]. In an unmanned battlefield, the physical and psychological qualities of soldiers are still important, but these qualities are mainly used in the field of intelligent confrontation. Unlike in previous wars, soldiers need to have comprehensive physical fitness, skills, and intelligence.

### ***2.2 Reduce Own Casualties***

With the development of society, countries can bear less and less casualties in wars. Casualties in wars will bring tremendous political pressure, and the psychological trauma and incidental compensation caused by wars are also difficult to estimate. Therefore, the zero-casualty war has become an ideal for military experts and commanders. In previous wars, siege and taking up positions require a lot of manpower and material resources, at the cost of big soldier casualties. The military experts and commanders pursued the principle of operations with the primary goal of



eliminating the living force of the enemy, which manifested the cruelty of war. The unmanned operation system can effectively reduce the direct involvement of combatants in high-risk battles. Due to the unmanned platforms, combatants have become system operators, being freed from the front-line battlefield. The stress and injuries caused by high-intensity and precise fire–electricity confrontation to be impacted on combatants would also be reduced.

### **3 Man Is the Victim of Unmanned Operations**

#### ***3.1 Man Is Faced with Abuse of Force***

Huge casualties of soldier have always been an important factor that stops the occurrence of war. Due to the extensive use of unmanned systems, in the future unmanned battlefields, casualties will mainly be the loss of intelligent machines that have no life and can be quickly produced in large numbers. The cost of war will be greatly reduced, and it is possible to achieve zero casualty for our combatants. The political and diplomatic risks of war will be significantly reduced. It may lower the threshold of war decision making due to less war concerns and stimulate the arbitrariness of military powers in the use of force. As a result, the outbreak of war or conflict is much easier and more frequent, leading to the use of force from being the last choice to being the preferred means [4]. In May 2013, when explaining the US military armed drone policy, then-President Obama stated that the use of conventional military means to enter other countries to fight terrorists would be considered a territorial invasion, which actually implied that if drones were used, there would be no problem. Unmanned operation technology will lower the threshold for use of violent forces, just as explosives invented by Nobel. It will only lead to opposite effects to reduce bloodshed and innocent casualties through the development of new weapons.

#### ***3.2 Man Is Faced with the Risk of Weapons Out of Control***

The higher intelligent the weapon is, the larger and more complex the internal control software and hardware will be, and the probability of malfunctions will increase accordingly. In a complex battlefield environment, intelligent unmanned operation systems are very likely to have identification errors, degraded communications, or even to be counterattacked by enemy magnetic jamming or cyberattack. In military applications, the intelligent weapons will even bring hidden dangers, such as indiscriminate killings and system out of control. Data show that a U.S. Air Force drone suddenly fired missiles at an important facility on the ground, and the cause of the accident was a malfunction of the aircraft's fire control system. If the unmanned operation system is given the power of life and death and completely replace man to

conduct operations, and the robot proxy war is implemented, as the British physicist Hawking said, autonomous robots will hurt man like that man accidentally steps on one ant [5].

### ***3.3 Man Is Faced with Weakening Morals***

Many studies by psychologists have shown that being out of the scene makes it easier for people to commit atrocities such as murder and abuse. The operator of the unmanned system is far behind, spatially separated from the unmanned operation platform, which makes the operator stay away from danger and other emotions and therefore does not cause his emotions to get out of control, so as to easily take action as planned. However, the long-range killing without physical contact not only makes combatants faced with almost no life danger, but also makes them have no direct perception of the battlefield. Their sense of cruelty of war will be decreased, and the psychological and moral obstacles during the killing will also be weakened. This would further weaken the binding force of man on war, resulting in unlimited attacks and killings. An Air Force lieutenant colonel who commanded the Predator drone said, "When you command them to control a drone, you often can't help but say, 'Kill this, don't kill that'" [6].

## **4 Man Is the Controller of Unmanned Operations**

Whether artificial intelligence and unmanned operations will bring threats or development is up to man how to use them. As the main body of the war loop, man must firmly grasp the open-fire right of future intelligent wars.

### ***4.1 Man Is the Monitor of Unmanned Equipment***

Before the advent of intelligent weapons, if people wanted to effectively control conventional weapons and equipment, they could only directly contact them through their limbs. The giants of conventional artillery, tanks, and warships cannot be independent from the direct control of human limbs. However, in the unmanned battlefield, man implants programs in the machine, which "clone" human thoughts, and equipment is given "ears and eyes" and "brains," People can control equipment through information without relying on the mechanical movement of human limbs to control. Unmanned operation systems with different functions and various forms will either autonomously complete tasks assigned to them by man, or be controlled by personnel outside the battlefield. In this way, the weapons confronting enemy on

the battlefield and the combatants can achieve relative separation in space, and the “machine army” becomes a loyal subordinate to perform various operation missions.

#### ***4.2 Man Is the Main Control Platform of Unmanned System***

At present, various types of unmanned operation platforms are mainly under the control of personnel in the back of battlefield, performing tasks in a semi-autonomous mode individually or in small numbers. However, with the large-scale adoption of unmanned operation forces, this model will be difficult to cope with the complex and changing battlefield, and it is easy to miss fighting opportunities and will restrict the effectiveness of operations. Highly intelligent unmanned operation system with high autonomy will be an inevitable choice of historical development. However, no matter how intelligent the unmanned weapon system is, man must always have the methods to control it and retain the right to plug off its power in the end, in case of unauthorized actions and attacking friendly forces because of errors in the procedure. Now, when the US military develops an autonomous weapon system, in order to prevent accidental engagement due to its failure, it is required that the system should be designed to allow commanders or operators to exercise judgment of appropriate levels before it comes into effect, and to activate or deactivate some system functions when necessary.

### **5 Conclusion**

In the future, unmanned operation systems will largely replace man combat forces to undertake various combat tasks, but man will not be bystanders and outsiders of unmanned operations. On the contrary, unmanned operations will still be “man-oriented.”

### **References**

1. Zeng H et al (2001) Waiting for destruction? High-tech war and man. Guangdong Education Press, Guangdong, p 12
2. Liu J et al (2008) Analysis on the application trend of unmanned weapons and equipment of foreign forces. *Natl Defense Sci Technol* 2:20–22
3. Guo S (2011) Unmanned war. National Defense University Press, Beijing
4. Zhang Y (2008) Intelligent unmanned operation system. University of National Defense Technology Press, Changsha
5. Pang H (2004) Intelligent warfare. National Defense University Press, Beijing
6. Shen S et al (2018) Understanding of intelligent operations. *Liberation Army Daily*, 7th edition

# An Experimental Study of the Effects of Subliminal Stimulation on Attention Perception



Juan Liu, Wei Pan, Duanqin Xiong, Rong Lin, Jian Du, Jiabo Ye, Yubin Zhou, Qiming Cheng, Liu Yang, Yishuang Zhang, and Shuang Bai

**Abstract** *Objective:* To investigate the effect of task difficulty and dual channel subliminal stimulation on people's attention perception. *Methods:* 24 college students were recruited to participate in the experiment. The experimental program was compiled by E-Prime software on the basis of the paradigm of attention span. The experimental task was to determine the number of red pentagram stars presented on the computer screen quickly and accurately. Two factors mixed design was used in this experiment. Task difficulty and subliminal stimulation are the two independent variables, each of which contains three levels. When the number of pentagram stars to be judged was 5–9, it was of low difficulty; correspondingly, 10–14 was of medium task difficulty, and 15–19 was of high task difficulty. The three levels of subliminal stimulation are as follows: “no subliminal stimulus”, which can be regarded as a control group, “auditory subliminal stimulus” and “audiovisual subliminal stimulus”. In order to avoid the effect of experimental sequence, the order of subjects participating in the experiment was balanced in advance according to the independent variable of the type of subliminal stimulation. *Results:* The main effect of task difficulty on perception was significant ( $p < 0.001$ ); the main effect of subliminal stimulation on perception was not significant ( $p > 0.05$ ); the interaction between task difficulty and subliminal stimulation was not significant ( $p > 0.05$ ). *Conclusions:* With the increase of task difficulty, the error of perceptual judgment increases, that is, the accuracy decreases. Subliminal stimulation designed in this paper has no obvious effect on perceptual judgment, but from the mean of the absolute value of perceptual error, it can be seen that judgment bias in the comprehensive intervention group of “audiovisual subliminal stimulation” has a downward trend, which shows that subliminal stimulation can improve the accuracy of attention cognition to a very small extent. The research direction of this experiment is worth further exploration. In future experiments, it is necessary to personalize the intensity and duration of subliminal stimulation according to the definition of sensory threshold, so as to enhance its effect.

---

J. Liu (✉) · W. Pan · D. Xiong · R. Lin · J. Du · J. Ye · Y. Zhou · Q. Cheng · L. Yang · Y. Zhang · S. Bai

Air Force Medical Centre of FMMU, 100142 Beijing, China  
e-mail: [13910259429@139.com](mailto:13910259429@139.com)

© The Editor(s) (if applicable) and The Author(s), under exclusive license to Springer Nature Singapore Pte Ltd. 2021

S. Long and B. S. Dhillon (eds.), *Man-Machine-Environment System Engineering*, Lecture Notes in Electrical Engineering 645, [https://doi.org/10.1007/978-981-15-6978-4\\_20](https://doi.org/10.1007/978-981-15-6978-4_20)

**Keywords** Subliminal stimulation · Audiovisual, · Attention span · Perceptual enhancement

## 1 Introduction

Perception is the key feeling to keep information input between human and surroundings, which is the source of all human experience. In daily life, when people perceive a thing, they need to firstly feel effective stimulation through visual, auditory, olfactory and other sensory channels, and then everyone's brain starts to interpret these sensory inputs to explain and reconstruct the whole feeling. Complete perception cannot be produced before these sensory inputs become meaningful information coding. To form complete and correct perception is the premise of people's complex psychological processes such as judgment, memory, thinking and imagination [1]. Therefore, how to speed up the perception speed and improve the accuracy is a problem that cognitive psychology needs to explore. In order to provide a breakthrough point for the research of perceptual enhancement technology, this study applies the experiment paradigm of attention span and introduces subliminal stimulation as intervention materials to investigate the effect of audiovisual subliminal stimulation on perceptual judgment [2]. Subliminal perception has a "subtle" effect on human cognition and behaviour. Compared with the conscious stimulus, the unconscious stimulus has a greater influence on some psychological features, such as emotions [3]. Therefore, it is of great practical significance to study the effect of subliminal perception on cognition.

## 2 Materials and Methods

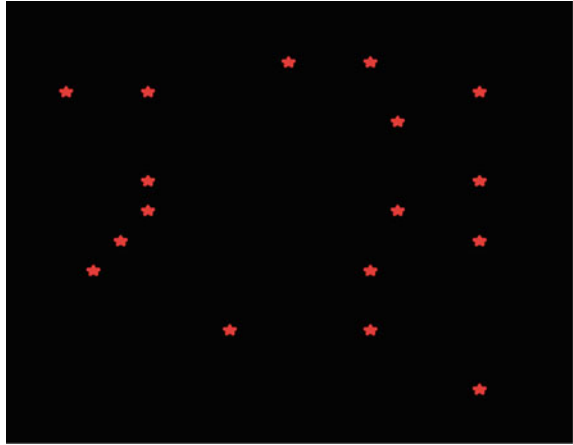
### 2.1 Research Participants

Twenty-four college students were recruited to participate in the experiment, half male and half female. The corrected visual acuity of all subjects was above 1.0, and their hearing was normal. All the subjects did not participate in the similar experiment and were tested separately during the experiment.

### 2.2 Experimental Materials

All the visual stimuli in the experiment were displayed on a 17 inch LCD, and the responses of the subjects were collected by a standard keyboard. The experimental program was written by E-Prime software. Different numbers of red pentagram stars are the experimental materials for perceptual judgment in this experiment, which

**Fig. 1** Schematic diagram of visual stimulation effect



will be quickly displayed on the computer screen. The number of red pentagram stars presented per screen varies from 5 to 19, and the specific number is randomly assigned by the experimental program. The schematic diagram of visual stimulation effect is shown in Fig. 1.

### 2.3 *Experimental Design*

This experiment uses two factors mixed design, containing two independent variables, namely task difficulty and types of subliminal stimulation. Task difficulty is divided into three types, which are represented by the number of red pentagram stars. When the number of pentagram stars to be judged was five to nine, it was of low difficulty; correspondingly, 10–14 was of medium task difficulty, and 15–19 was of high task difficulty. There are three levels of subliminal stimulation: “no subliminal stimulus”, which can be regarded as a control group, “auditory subliminal stimulus” and “audiovisual subliminal stimulus”. In the “auditory subliminal stimulus” group, the subjects will be presented with auditory stimulation below the threshold level through earphones during the experiment, the content of which is the sound files of red pentagram actual number, half male voice and half female voice. In the “audiovisual subliminal stimulus” group, the subjects will be presented with visual and auditory stimuli below the threshold level at the same time. The content and presentation mode of subliminal auditory stimuli are the same as “auditory subliminal stimulus” group. The content of subliminal visual stimuli is the actual number of red pentagrams, which will be presented in a fixed position in the centre of the screen through the 17 inch LCD. The presentation time of subliminal visual stimulation is about 5 ms. In order to avoid the effect of experimental sequence, the order of subjects participating in the experiment was balanced in advance according to the independent variable of the type of subliminal stimulation.

## 2.4 Experimental Process

Set the computer screen background colour to black and the target colour to red. When the experiment began, the red pentagram stars were distributed on the screen continuously, and the presentation locations and specific quantities were randomly assigned by the experiment program. The number of red pentagram stars presented each time was 5–19, and each quantity repeated six times according to the random principle, presenting 1200 ms each time. The subjects were asked to enter the corresponding number through the keypad as soon as possible. After inputting the number, the subjects needed to press enter to start the next trial. The computer automatically recorded the participants' input value and response time. The subjects wore earphones during the whole process of the experiment, through which the light music "spring" above the hearing threshold and the auditory subliminal stimulation were simultaneously played. Everyone had four practice opportunities before the formal experiment. Each experiment included 270 trials, and the subjects rested for 1–2 min every 90 trials to ensure sufficient energy. The whole experiment lasted about 23 min.

## 3 Results

The results of perceptual judgment under different levels of subliminal stimulation and task difficulty were recorded. Table 1 listed the perceptual judgment error, and Table 2 listed the absolute values of perceptual judgment error. The calculation formula of perceptual judgment error determined in this experiment was as follows:

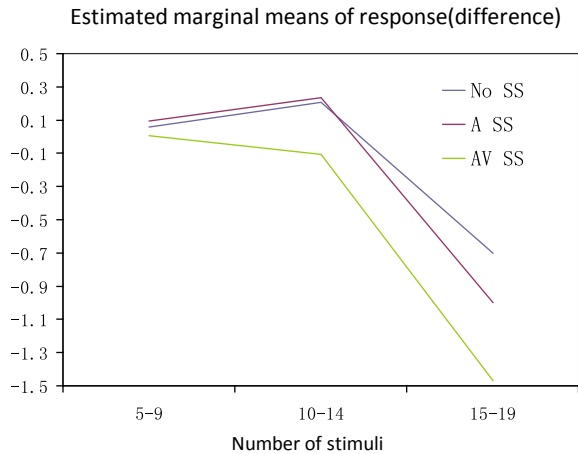
**Table 1** Descriptive statistics of perceptual judgment error ( $N = 24$ )

Type of SS	Low difficulty (5–9)		Medium difficulty (10–14)		High difficulty (15–19)	
	Mean	SD	Mean	SD	Mean	SD
No SS	0.0597	0.1192	0.2083	0.8186	-0.7000	2.0584
A SS	0.0931	0.1981	0.2333	1.0473	-0.9972	2.7377
AV SS	0.0058	0.1520	-0.1058	0.5196	-1.4696	0.9887

**Table 2** Descriptive statistics of absolute value of perceptual judgment error ( $N = 24$ )

Type of SS	Low difficulty (5–9)		Medium difficulty (10–14)		High difficulty (15–19)	
	Mean	SD	Mean	SD	Mean	SD
No SS	0.1536	0.1696	1.1000	0.5718	2.4778	0.8772
A SS	0.2014	0.2197	1.0417	0.8140	2.7056	1.6126
AV SS	0.1458	0.1203	0.9377	0.3893	2.2290	0.7214

**Fig. 2** Perceptual judgment errors under different conditions



perceptual judgment error = the number entered by the subjects—the actual number of red pentagrams displayed on the screen.

For the dependent variable of perceptual judgment error, the results of ANOVA showed that: the main effect of task difficulty was significant ( $p < 0.001$ ); the main effect of subliminal stimuli was not significant ( $p > 0.05$ ); the interaction between task difficulty and subliminal stimuli was not significant ( $p > 0.05$ ). The perceptual judgment errors of the subjects are shown in Fig. 2.

For the dependent variable of absolute value of perceptual judgment error, the results of ANOVA showed that: the main effect of task difficulty was significant ( $p < 0.001$ ); the main effect of subliminal stimuli was not significant ( $p > 0.05$ ); the interaction between task difficulty and subliminal stimuli was not significant ( $p > 0.05$ ). The absolute value of perceptual judgment errors of the subjects is shown in Fig. 3.

## 4 Discussion and Conclusion

In recent years, awareness has become one of the most challenging research fields in the life sciences. Accordingly, subliminal perception is an important psychological issue recently. In this paper, the effects of task difficulty and subliminal stimulation on perceptual judgment were studied. The experiment shows that task difficulty has a significant impact on perceptual judgment. With the increase of task difficulty, the error of perception of attention span increases, that is, the accuracy decreases. Subliminal perception is a kind of unconscious psychological process. People cannot consciously detect the existence of subliminal stimulus, but can affect people’s psychological process. At present, the basic consensus in academia is that subliminal stimulation can trigger low-level cognition processing [4, 5]. In Western countries,



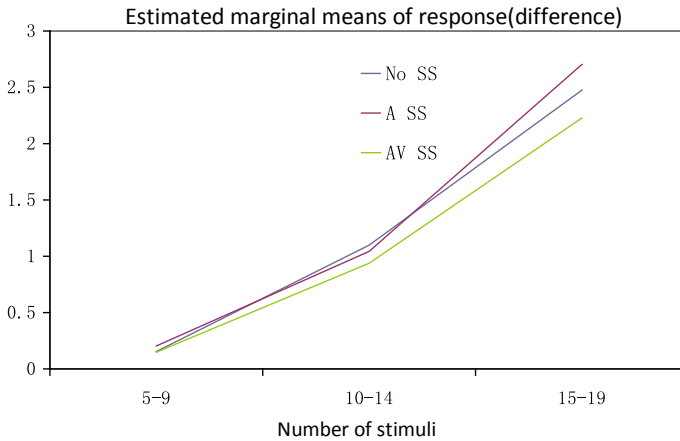


**Fig. 3** Absolute value of judgment errors under different conditions

subliminal stimulation has been widely used in advertising, political campaigns and other fields, in order to “unconsciously” change the attitude and behaviours of the target audience [6]. In this paper, the experimental paradigm of attention span was used to study the effect of subliminal stimulation on perceptual judgment. The results showed that there was no significant effect of subliminal stimulation on perceptual judgment. The reason may be that the intensity or duration of subliminal stimulation was not enough. It should be noted that from the mean value in Table 2, it can be seen that compared with the control group, the absolute value of the judgment error of the number of red pentagram stars in the comprehensive intervention group of “audiovisual subliminal stimulation” has a downward trend. This trend reminds that subliminal stimulation has a certain role to improve the accuracy of attention perceptual to a very small extent. The research direction of this experiment is worth further exploration. In future experiments, it is necessary to personalize the intensity and duration of subliminal stimulation according to the definition of sensory threshold [7, 8], so as to enhance its effect.

**Compliance with Ethical Standards** The study was approved by the Logistics Department for Civilian Ethics Committee of Air Force Medical Center of Fourth Military Medical University. All subjects who participated in the experiment were provided with and signed an informed consent form. All relevant ethical safeguards have been met with regard to subject protection.

## References

1. Hubbard TL (2019) Momentum-like effects and the dynamics of perception, cognition, and action. *Attention Percep Psychophys* 3
2. Greenwood PM, Parasuraman R (2004) The scaling of spatial attention in visual search and its modification in healthy aging. *Percep Psychophys* 66(1):3–22

3. Merikle PM, Smilek D, Eastwood JD (2001) Perception without awareness: perspectives from cognitive psychology. *Cognition* 79:115–134
4. Dreber A, Fudenberg D, Rand DG (2014) Who cooperates in repeated games: the role of altruism, inequity aversion, and demographics. *J Econ Behav Organ* 98:41–55
5. Fada P, Xiaogang W, Li Z, Yuhong O (2017) Inhibition of return is modulated by negative stimuli: evidence from subliminal perception. *Front Psychol* 8:1012–1015
6. Erdelyi M (2004) Subliminal perception and its cognates: theory, indeterminacy and time. *Consc Cognit* 13(1):73–91
7. Klauer KC, Greenwald AG (2000) Measurement error in subliminal perception experiments. *26(4):1461*
8. Schwartz M, Rem M (2010) Does the averaged evoked response encode subliminal perception? *Psychophysiology* 12(4):390–394

# 3D Head Anthropometry for Head-Related Transfer Function of Chinese Pilots



Xiaochao Guo, Yu Bai, Qingfeng Liu, Duanqin Xiong, Yanyan Wang,  
and Jian Du

**Abstract** The 3D head anthropometry of 69 Chinese male pilots was tested in order to build China Air Force head-related transfer function (HRTF) database, i.e. CHNAF HRTF Database in abbreviation. There were totally 93 anthropometric landmarks defined according to principles of physical acoustic reflection and refraction. All the landmarks were measured in sitting with  $(x, y, z)$  coordinate system to get 2D dimensions in GB/T 5703/ISO 7250-1 and GJB 4856 and 3D descriptions of the head with polar coordinate transformation in  $(r, \phi, \theta)$ . The test results of the 3D descriptors showed the 3D positions of anatomical mediators between the outer acoustic signal and pilots' auditory spatial localization, in which there were 50 landmarks about ears or auricle, 33 landmarks about skull, eyes, face and noses and 10 about neck and shoulders. Therefore, the CHNAF HRTF Database could provide about 150 items of anthropometric measurements for HRTF and its personalization especially with focus on the role of ears.

**Keywords** Head · Ear · Auricle · Pinna · Anthropometry · Landmark · Head-related transfer function (HRTF) · Pilots · 3D audio · Ergonomics · Human factors · CHNAF HRTF database · Anatomy

## 1 Introduction

The head-related transfer function (HRTF) is the kernel of 3D audio displays in virtual reality. The HRTFs depended mainly on the anthropometric parameters with sound reflecting, refracting, dispersing or shadowing in the unique style of the listener [1], and the HRTF personalization could be done by HRTF database matching [2] on the hypothesis of the same anthropometric parameters producing the same HRTF given by Zotkin et al. [3] with works of Katz [4, 5]. It is a key to measure head parameters of anthropometry sufficient for HRTF with limited cost. For examples, there were 27 items of anthropometric parameters for 45 subjects in CIPIC HRTF Database

---

X. Guo · Y. Bai · Q. Liu (✉) · D. Xiong · Y. Wang · J. Du  
Air Force Medical Center of FMMU, 100142 Beijing, China  
e-mail: [littleponds@163.com](mailto:littleponds@163.com)

© The Editor(s) (if applicable) and The Author(s), under exclusive license to Springer 171  
Nature Singapore Pte Ltd. 2021

S. Long and B. S. Dhillon (eds.), *Man-Machine-Environment  
System Engineering*, Lecture Notes in Electrical Engineering 645,  
[https://doi.org/10.1007/978-981-15-6978-4\\_21](https://doi.org/10.1007/978-981-15-6978-4_21)

[6]. In China, only four anthropometric parameters were measured by Professor Xie et al. with 52 university subjects [7] while there were 67 anthropometric parameters reported with CHNAF HRTF Database [8, 9].

Human body measurements were defined by landmarks in anthropometry [10]. The adequate head parameters could be attained when the landmarks were correctly identified and measured in 3D coordinates as presented in this paper.

## 2 Method

### 2.1 Landmarks of 3D Head Anthropometry for CHNAF HRTF Database

There were totally 93 anthropometric landmarks or mark points defined in accordance with GJB 4856 [11, 12] or derived from CIPIC HRTF Database [6] and anatomical book [13] as showed in Fig. 1 and Table 1 in view of principles of physical acoustic reflection and refraction. The landmarks were coded as E1–E25 for right ear and E26–E50 for left ear in present paper with opposition relationship of E1–E26, E2–E27 and so on. The sequence guided the test process.

### 2.2 3D Probe in $(x, y, z)$ Coordinates for the Landmarks and Presentation with Polar Coordinates

All the 93 landmarks were tested in sitting by ROMER absolute arm, in which the  $(x, y, z)$  coordinate system was set with the origin  $(0, 0, 0)$  at midpoint of bitragion on the Frankfurt plane, i.e. the *ohr augen ebene* (OAE) in anthropometry. The  $(x, y, z)$  values of the landmarks could be turned into polar coordinates, in which the vectors from the origin to the landmarks described 3D head structures by the distance ( $r$ ) in mm, the elevation angle ( $\phi$ ) and Azimuth angle ( $\theta$ ) in degree.

### 2.3 The Pilots as Participants

There were 69 Chinese male pilots participating in HRTF data collection who aged  $33.89 \pm 3.17$ y with flight experiences in  $1913.92 \pm 932.29$  h totally.

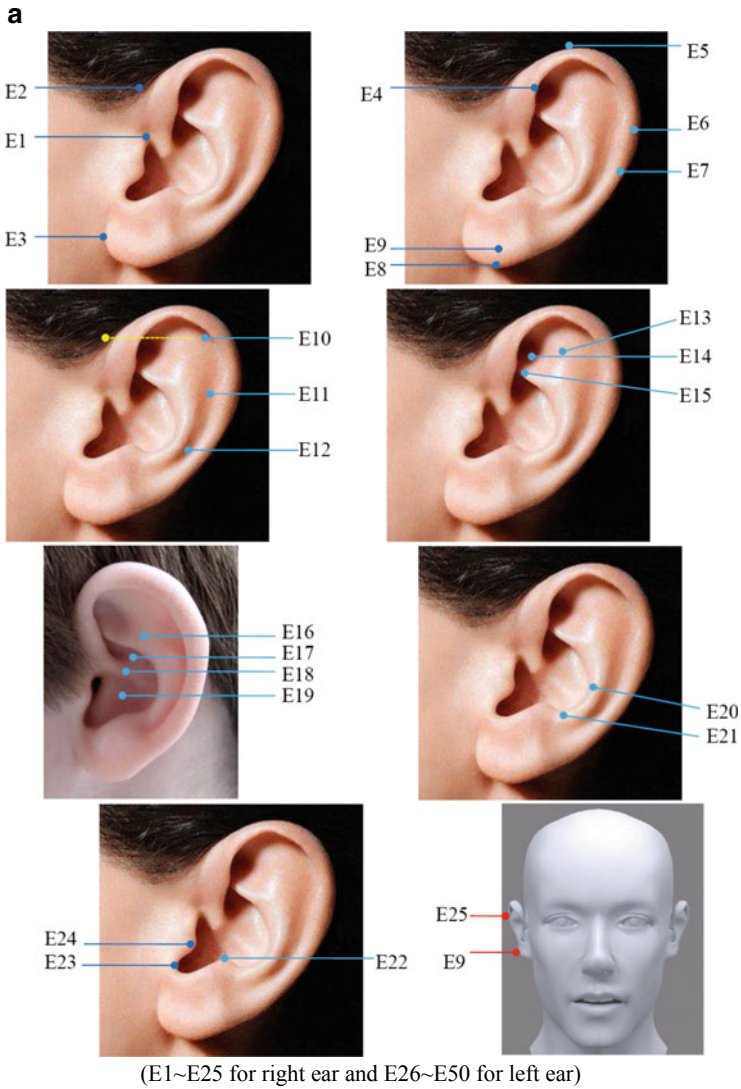
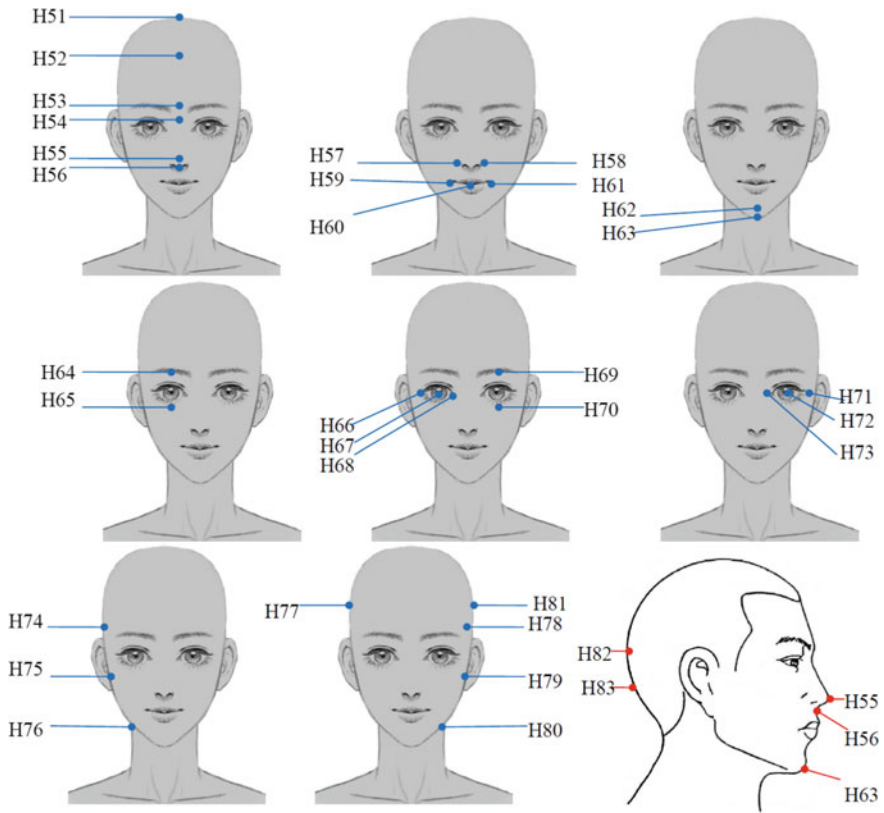


**Fig. 1** a Ninety-three landmarks of 3D head anthropometry on human body—ears. b Ninety-three landmarks of 3D head anthropometry on human body—head. c Ninety-three landmarks of 3D head anthropometry on human body—neck and shoulders

### 3 Results

The results of 3D head anthropometry were in Table 1 as an example of single pilot with polar coordinates. The results of 2D dimensions or anthropometric parameters were seen in reference [8].

**b**



(All pictures were from Internet dotted by the authors)

**c**



**Fig. 1** (continued)

## 4 Discussions

### 4.1 Focus on the Role of the Ears for 3D Audio Localization

The human ears are very important listening devices in daily life to auditory spatial localization. The pinna shape could influence on HRTF [14], and the more numbers of anthropometric parameters entered into HRTF, the better of HRTF personalization

**Table 1** Ninety-three landmarks of 3D head anthropometry for CHNAF HRTF database

Name of landmark		Code	Position in ( $r, \phi, \theta$ )			Code	Position in ( $r, \phi, \theta$ )		
			$r$	$\phi$	$\theta$		$r$	$\phi$	$\theta$
Ears	Tragion	E1	80.18	0.69	88.20	E26	80.18	-0.69	268.20
	Otobasion superius	E2	85.69	12.79	87.09	E27	87.41	13.22	266.96
	Otobasion inferius	E3	78.11	-21.21	82.27	E28	78.92	-19.77	275.63
	Helix anterior	E4	92.34	10.12	91.62	E29	96.31	9.17	264.04
	Supra-auricular point	E5	99.45	12.80	97.69	E30	99.09	11.70	258.73
	Retroaurale	E6	96.74	4.62	105.34	E31	97.65	3.04	249.89
	Helix median	E7	90.39	-5.66	105.81	E32	95.00	0.53	252.99
	Infero-auricular point	E8	83.03	-23.72	88.53	E33	86.21	-23.49	269.68
	Lobule lateral	E9	83.41	-19.08	89.33	E34	86.62	-16.12	269.58
	Scapha fossa superius	E10	92.30	9.46	101.18	E35	92.71	5.20	253.94
	Scapha fossa median	E11	89.83	-0.02	103.86	E36	92.81	-3.90	255.39
	Scapha fossa inferius	E12	90.25	-7.28	101.63	E37	91.72	-10.43	259.27
	Crura of antihelix superius	E13	86.94	9.20	95.22	E38	92.35	6.20	258.42
	Triangular fossa	E14	81.14	7.98	93.98	E39	86.02	6.68	263.04
	Crura of antihelix inferius	E15	82.02	4.23	93.40	E40	83.65	3.54	266.02
	Crura of antihelix apex	E16	86.64	3.43	97.39	E41	91.29	2.18	261.78
	Crmba of auricular concha	E17	74.48	-0.14	98.47	E42	76.56	0.88	261.22
	Crus of helix median	E18	75.07	-4.07	96.13	E43	78.47	-4.23	263.84
	Cavity of auricular concha	E19	69.86	-8.81	96.32	E44	70.51	-9.20	266.40
	Antihelix median	E20	90.66	-5.77	99.48	E45	95.12	-6.15	260.74
	Antihelix inferius	E21	86.94	-8.67	97.93	E46	88.35	-10.87	263.55
	Antihelix superius	E22	79.86	-8.75	91.41	E47	84.88	-9.18	267.52

(continued)

**Table 1** (continued)

Name of landmark		Code	Position in ( $r, \phi, \theta$ )			Code	Position in ( $r, \phi, \theta$ )			
			$r$	$\phi$	$\theta$		$r$	$\phi$	$\theta$	
Head	Intertragic notch	E23	76.79	-13.40	83.81	E48	82.54	-12.48	275.11	
	Tragus posterior	E24	77.83	-7.70	87.14	E49	84.25	-6.49	272.84	
	Auricle lateral	E25	90.77	-8.74	99.80	E50	104.74	6.90	259.10	
	Vertex	H51	132.01	85.24	213.59					
	Trichion	H52	129.25	47.45	355.58					
	Glabella	H53	112.00	19.68	357.57					
	Sellion	H54	106.48	11.45	357.66					
	Pronasale	H55	128.68	-7.90	358.18					
	Subnasale	H56	116.66	-14.24	357.88					
	Alare	H57	116.25	-10.75	7.02	H58	116.54	-11.44	347.79	
	Cheil-angle point	H59	115.18	-29.43	10.62	H61	114.09	-28.81	341.41	
	Stomion	H60	125.06	-26.65	357.66					
	Pogonion	H62	135.06	-38.47	356.43					
	Gnathion	H63	133.45	-47.09	356.54					
	Supraorbital point	H64	112.31	18.32	15.59	H69	110.81	16.00	339.19	
	Orbitale	H65	100.10	-0.88	16.54	H70	101.65	-1.10	338.55	
	Ectocanthion	H66	97.00	6.78	30.51	H71	99.87	6.08	327.14	
	Eye protuberance	H67	103.32	5.76	18.16	H72	105.58	7.30	339.96	
	Entocanthion	H68	97.58	7.04	8.45	H73	99.31	6.86	349.61	
	Frontotemporale	H74	101.14	23.80	42.53	H78	105.09	25.29	311.30	
	Zygion	H75	104.28	-8.83	33.46	H79	107.21	-7.32	323.16	
	Gonion	H76	105.55	-44.20	44.17	H80	97.10	-42.78	291.52	
	Euryon	H77	89.35	30.88	80.81	H81	99.71	27.19	272.21	
	Opisthocranium	H82	74.69	22.56	194.87					
	Inion	H83	65.24	9.64	195.75					
	Neck	Larynx point	B84	137.55	-65.36	351.04				
		Fossa jugularis	B85	194.76	-79.72	323.54				
		Neck lateral	B86	157.16	-67.88	109.53	B91	153.40	-59.71	252.99
		Lateral neck root point	B87	172.71	-61.25	109.63	B92	172.59	-55.22	252.37
Acromial point		B88	273.70	-46.44	90.64	B93	289.80	-39.08	265.13	
Larynx dorsal point		B89	129.98	-61.60	191.90					
Cervicale		B90	158.28	-58.90	189.07					



were by HRTF database matching [9], so it is necessary to measure the pilot's ears in much details for CHNAF HRTF Database.

There were 50 items such as E1–E25 for right ear and E26–E50 for left ear with polar coordinates listed in Table 1, and more than 18 additional items of 2D anthropometric parameters about the pilot's ears derived from the measured values of the landmarks in  $(x, y, z)$  coordinates, which could be used to build HRTF.

## ***4.2 Describing 3D Head Structures with Polar Coordinates***

The descriptions of adult headforms were popular in  $(x, y, z)$  coordinates such as GB/T 23461 to give the 3D positions of the landmarks measured and some 2D dimensions about the subtypes of the headforms [15]. In these cases, the origin  $(0, 0, 0)$  was set at the vertex coded as H51 in present paper, and the layered descriptions of the headforms were made by 2D popular coordinates built in the planes paralleling the Frankfurt plane with the origin of the popular coordinates' own. This method might be suitable to technological design such as helmet, mask and so on to ensure harmony between pilots' head shape and personal products [16], but it is difficult to show directly the relationship of the pilots' head to the outer acoustic signal/target reported with  $(r, \phi, \theta)$  data in practical flight tasks.

## ***4.3 To Explore the Valid Representation of 3D Head***

Personalization of HRTF is essential to the better 3D audio displays. Good 3D head representation will require the fittest features to be identified. Its potential is to find more better representation of head-related structural characteristic from the pool of 3D head anthropometry in CHNAF HRTF Database because of about 150 items of anthropometric measurements more than that in CIPIC database.

## **5 Conclusions**

Measuring is the most direct method to obtain user's head-related transfer function (HRTF), and HRTF personalization for incomer is also relied on the capacity of HRTF database in existence. In the development of China Air Force head-related transfer function (HRTF) database, i.e. CHNAF HRTF Database, there were totally 93 landmarks defined according to principles of physical acoustic reflection and refraction for 3D head anthropometry of Chinese male pilots. All the landmarks were measured in sitting with  $(x, y, z)$  coordinate system and transformed into polar coordinates of  $(r, \phi, \theta)$  which were the distance ( $r$ ) in mm, the elevation angle ( $\phi$ ) and azimuth angle ( $\theta$ ) in degree. The vectors from the origin to the landmarks gave the

3D positions of anatomical mediators between the outer acoustic signal and pilots' auditory spatial localization and described 3D head structures. The partial results of 69 pilots were reported here. Some influences and applications were discussed.

**Acknowledgements** The work was supported by the Defense Industrial Technology Development Program No. JCKY2018000B001 with pre-research program No. 51326050203.

The authors are thankful to Mr Kang Zhang for his contribution to data transformation from  $(x, y, z)$  to  $(r, \phi, \theta)$ .

### Compliance with Ethical Standards

The study was approved by the Academic Ethics Committee of Air Force Medical Center of FMMU. All subjects were provided with and signed an informed consent form. All relevant ethical safeguards have been met with regard to subject protection.

## References

1. Wenzel E, Arruda M, Kistler D (1994) *J Acoust Soc Am* 94:111–123
2. Moller H, Sorensen M, Hammershoi D (2003) *J AES* 43:300–321
3. Zotkin D, Hwang J, Duraiswami R et al (2003) IEEEWASPAA. New Paltz, New York, USA
4. Katz BFG (2001) *Acoust Soc Am* 110:2440–2448
5. Katz BFG (2001) *Acoust Soc Am* 110:2449–2455
6. Algazi VR, Duda RO, Thompson DM et al (2001) The CIPIC HRTF database. In: Proceedings of 2001 IEEE workshop on applications of signal processing to audio and electroacoustics. Mohonk Mountain House, New Paltz, NY, 21–24 Oct 2001, pp 99–102
7. Xie B, Zhong X, Rao D et al (2007) Head-related transfer function database and its analyses. *Sci China, Ser G* 50(3):267–280
8. Guo X, Xiong D, Wang Y, et al (2016). Head related transfer function database of Chinese male pilots. In: Long S, Dhillon BS (eds) *Man-machine-environment system engineering, Lecture Notes in Electrical Engineering*, vol 406, pp 3–11
9. Lu D, Zeng X, Guo X et al (2019) Personalization of head-related transfer function based on sparse principle component analysis and sparse representation of 3D anthropometric parameters. *Acoust Aust* <https://doi.org/10.1007/s40857-019-00169-y>
10. GB/T 5703-2010/ISO 7250-1 (2008) Basic human body measurements for technological design. China Standard Press, Beijing
11. GJB 4856-2003 (2003) Human dimensions of Chinese male pilot population. Military standard Publishing House of the General Armament Department, Beijing
12. Guo X, Zhang L, Xiong D, et al (2015) Selection of basic measurements on head segment of male pilots for 3-D anthropometry. In Long S, Dhillon BS (ed) *Proceedings of the 15th international conference on man-machine-environment system engineering, lecture notes in electrical engineering*, vol 356, pp 29–38
13. Wang Q (ed) (2010) *Practical anatomy of the otolaryngology–head & neck surgery*. People's Medical Publishing House, Beijing, p 2010
14. Xu X, Zhong X (2014) Influence of pinna shape on head-related transfer function. *Tech Acoust* 33(S2):304–306
15. GB/T 23461-2009 (2009) 3D dimensions of male adult headforms. China Standard Press, Beijing
16. Li J, Hong Z, Xu Y et al (2014) Research on the characteristics and classification of pilots' head. *Space Med & Med Eng* 27(6):430–433

# The Mental Health and Correlated Factors of Medical Team Members in an Aerospace Medical Unit Before Conducting Non-war Military Operations



Yang Liao, Yishuang Zhang, Yan Zhang, Xueqian Deng, and Liu Yang

**Abstract** To investigate the mental health and correlated factors of medical team members in an aerospace medical unit before fight COVID-19 pneumonia, which would provide quantitative data to help keeping mental health. Cluster sampling method was used and 193 medical team members were engaged. Eysenck personality questionnaire, symptom checklist-90 and self-made scale were used to evaluate the medical team members' personality, mental health level, personal protection and risk of infection. The levels of personal protection and risk of infection may have an influence on medical team members' mental health. Medical team members with low personal protection may more likely to be obsessive-compulsive ( $t = 3.20$ ,  $P < 0.01$ ), anxiety ( $t = 2.00$ ,  $P < 0.05$ ). Medical team members with high risk of infection may have multiple types of mental problems. Medical team members with higher introversion, higher psychoticism and neuroticism characteristics were more likely to be in low level of mental health. These results could help us to find out the target population of mental protection before military operations other than war.

**Keywords** Medical team members · Eysenck personality questionnaire · Symptom checklist-90 · Mental health

## 1 Introduction

With the increased demand of quick response ability to aerospace medical unit, the organization of aviation medical team is needed. Except battlefield medical treatment during war, aviation medical team would also play an important role in military operations other than war, such as medical assistance after the disaster and control of major epidemic diseases. In fact, the military medical team always is the premier emergency rescue force deployed to the frontline [1, 2]. Due to the strike of disasters and unpredictable security risk, stress reaction would happen to medical team members, which may in turn induce negative emotion such as anxiety, depression

---

Y. Liao · Y. Zhang · Y. Zhang · X. Deng · L. Yang (✉)

Air Force Medical Center, Fourth Military Medical University, 100142 Beijing, China  
e-mail: [yangliuhenry@aliyun.com](mailto:yangliuhenry@aliyun.com)

© The Editor(s) (if applicable) and The Author(s), under exclusive license to Springer Nature Singapore Pte Ltd. 2021

S. Long and B. S. Dhillon (eds.), *Man-Machine-Environment System Engineering*, Lecture Notes in Electrical Engineering 645, [https://doi.org/10.1007/978-981-15-6978-4\\_22](https://doi.org/10.1007/978-981-15-6978-4_22)

and fear. To some extent, the continuous stress event may induce serious psychological problems and mental diseases among medical team members during performing military operations other than war [3]. In order to sustain medical team members' working performance in a normal level, mental health service during the mission period is of great importance. Additionally, psychological screening before mission is indispensable. Using psychological scales, to investigate the mental health levels and influence factors among medical team members could help to identify the person with overstress reactions. The target of mental health service would emerge and the direction of mental protection would then show. These quantitative data could help to maintain medical team members' mental health and normal performance.

In the current study, Eysenck personality questionnaire, symptom checklist-90 (SCL-90) and self-made scale were used to evaluate the medical team members' personality, mental health level, personal protection and risk of infection, which may provide reference data for mental protection.

## 2 Method

### 2.1 Participants

The cluster sampling methods were used. 193 medical team members in an aerospace medical unit who prepared for fighting COVID-19 pneumonia were engaged. All questionnaires were completed, no sample was excluded. There were 31 males and 162 females. The average age was at  $34.66 \pm 3.6.88$  years.

### 2.2 Tools

Eysenck personality questionnaire (EPQ) was developed by a British psychologist named Eysenck in 1975 [4]. The questionnaire was based on personality type theory, included four dimensions as introversion-extroversion, psychoticism, neuroticism and validity. There were 88 items, participants required to rank whether the symptom described in each item was occurred on him. The version of the questionnaire used in the current study was adult version, which had been confirmed to have high reliability and validity in previous study by other researchers. Symptom checklist-90 was developed by L. R. Derogatis in 1975 and included 90 items [5]. There were nine factors, such as somatization (SOM), obsessive-compulsive (OBS), inter-personal sensitivity (INT), depression (DEP), anxiety (ANX), hostility (HOS), phobic anxiety (PHOB), paranoid ideation (PAR) and psychoticism (PSY). Participants required to rank the level of their symptoms in the lasted week from 1 to 5 point. 1 refers to none, 2 refers to mild, 3 refers to medium, 4 refers to mild severity and 5 refers to great severity. The global severity index (GSI)  $\geq 160$ , positive symptom total (PST)

**Table 1** Comparison of personality between participants with high and low level of personal protection

	Introversion-extroversion	Psychoticism	Neuroticism
Low personal protection	48.76 ± 10.94	38.00 ± 5.45	44.42 ± 11.74
High personal protection	56.07 ± 10.26	37.17 ± 6.26	37.35 ± 10.97

≥ 43 or any of the nine factors ≥ 2, and then the participant’s result is positive, which mean his mental health level is low. Previous study had indicated SCL-90 got a high reliability and validity [6]. Additionally, self-made scale was used to evaluate the medical team members’ personal protection and risk of infection.

### 2.3 Statistics

Data were analysed with independent sample t-test and Pearson correlation coefficient by SPSS 20.0 version, the significant levels is  $P < 0.05$ .

## 3 Results

### 3.1 The Personality and Mental Health Difference Between Participants with High and Low Level of Personal Protection

As shown in Table 1, compared with medical team members with high personal protection, medical team members with low personal protection were more introversion ( $t = -3.06, P < 0.01$ ) and neuroticism ( $t = 2.77, P < 0.01$ ).

As shown in Table 2, medical team members with low personal protection had higher score than medical team members with high personal protection in obsessive-compulsive ( $t = 3.20, P < 0.01$ ), anxiety ( $t = 2.00, P < 0.05$ ).

### 3.2 The Personality and Mental Health Difference Between Participants with High and Low Risk of Infection

As shown in Table 3, compared with medical team members with low risk of infection, medical team members with high risk of infection were more introversion ( $t = -2.69, P < 0.01$ ) and higher neuroticism ( $t = 2.93, P < 0.01$ ).

**Table 2** Comparison of mental health between participants with high and low level of personal protection

	Low personal protection	High personal protection
SOM	1.18 ± 0.19	1.13 ± 0.30
OBS	1.51 ± 0.49	1.23 ± 0.37
INT	1.25 ± 0.35	1.15 ± 0.33
DEP	1.26 ± 0.41	1.13 ± 0.34
ANX	1.30 ± 0.33	1.15 ± 0.32
HOS	1.18 ± 0.26	1.12 ± 0.30
PHOB	1.16 ± 0.36	1.15 ± 0.29
PAR	1.11 ± 0.30	1.07 ± 0.21
PSY	1.10 ± 0.22	1.08 ± 0.22
GSI	112.24 ± 26.44	102.56 ± 25.20
PST	15.76 ± 13.41	9.51 ± 16.11

**Table 3** Comparison of personality between participants with high and low level of risk of infection

	Introversion-extroversion	Psychoticism	Neuroticism
High risk of infection	53.90 ± 10.13	37.33 ± 6.50	39.32 ± 12.21
Low risk of infection	58.46 ± 9.52	36.95 ± 5.23	34.63 ± 7.80

As shown in Table 4, medical team members with high risk of infection had higher score than medical team members with low risk of infection in somatization ( $t = 2.96$ ,  $P < 0.01$ ), obsessive-compulsive ( $t = 3.10$ ,  $P < 0.01$ ), inter-personal sensitivity ( $t = 3.30$ ,  $P < 0.01$ ), depression ( $t = 3.18$ ,  $P < 0.01$ ), anxiety ( $t = 2.91$ ,  $P < 0.01$ ), phobic anxiety ( $t = 2.39$ ,  $P < 0.05$ ), paranoid ideation ( $t = 2.61$ ,  $P < 0.01$ ), psychoticism ( $t = 2.54$ ,  $P < 0.05$ ), global severity index ( $t = 3.18$ ,  $P < 0.01$ ), positive symptom total ( $t = 3.28$ ,  $P < 0.01$ ).

**Table 4** Comparison of mental health between participants with high and low level of risk of infection

	High risk of infection	Low risk of infection
SOM	1.16 ± 0.32	1.06 ± 0.12
OBS	1.31 ± 0.45	1.14 ± 0.24
INT	1.21 ± 0.39	1.07 ± 0.15
DEP	1.18 ± 0.38	1.05 ± 0.11
ANX	1.20 ± 0.36	1.08 ± 0.15
HOS	1.14 ± 0.34	1.07 ± 0.17
PHOB	1.18 ± 0.33	1.08 ± 0.20
PAR	1.09 ± 0.26	1.02 ± 0.08
PSY	1.10 ± 0.24	1.03 ± 0.11
GSI	106.36 ± 28.53	96.46 ± 10.82
PST	12.05 ± 18.08	5.36 ± 7.79

**Table 5** Correlation with personality and mental health level among medical team members in an aerospace medical unit

	Introversion-extroversion	Psychoticism	Neuroticism
SOM	-0.24	0.30	0.56
OBS	-0.38	0.32	0.69
INT	-0.34	0.38	0.69
DEP	-0.37	0.39	0.71
ANX	-0.36	0.38	0.72
HOS	-0.33	0.38	0.64
PHOB	-0.27	0.39	0.65
PAR	-0.24	0.38	0.64
PSY	-0.25	0.37	0.60
GSI	-0.36	0.39	0.73
PST	-0.33	0.40	0.74

### ***3.3 The Relationship Between Personality and Mental Health Level Among Medical Team Members in an Aerospace Medical Unit***

The score of introversion-extroversion dimension of medical team members' personality had significant correlations with their scores in the nine factors in SCL-90, global severity index and positive symptom total ( $P < 0.01$ ), the correlation coefficients were between  $-0.24$  and  $-0.38$ . The score of psychoticism dimension of medical team members' personality had significant correlations with their scores in the nine factors in SCL-90, global severity index and positive symptom total ( $P < 0.01$ ), the correlation coefficients were between  $0.30$  and  $0.40$ . The score of neuroticism dimension of medical team members' personality had significant correlations with their scores in the nine factors in SCL-90, global severity index and positive symptom total ( $P < 0.01$ ), the correlation coefficients were between  $0.56$  and  $0.74$ , as shown in Table 5.

## **4 Discussion**

In the current study, we found that medical team members with low self-protection were relatively in a low level of mental health, and they were more likely to be obsessive and anxiety. The level of self-protection reflects one's ability in medical protection against pneumonia in the current study, which could be look as a protective factor for sustaining mental health level. The result indicated that the training of protection strategies before mission in of great importance, it may increase the self-protection ability among medical team members in the aerospace medical unit. And it may play a role in decrease the occurrence rate of obsessive and anxiety problems.

Result from the previous study had shown similar evidence. Fan et al. found that medical staff who had been trained with emergency rescue course were more likely to handle with multiple stressors in a right way, which could indicate the positive effect of targeted training related to mission on sustaining mental health [7].

The result of the current study indicated that the risk of infection was an important influence factor for mental health among medical team members who were prepared to carry out a military operation other than war. Previous study about rescuers after earthquake has shown similar evidence. Zhang et al. found that rescuers in epicentre area had higher scores than those rescuers in peripheral areas in nine factors and global severity index in SCL-90 [8]. Rescuers in epicentre area faced more stressors, such as aftershock, sever damage environment, insufficient logistics support and so on, which may damage mental health.

The score in all the nine factors, global severity index and positive symptom total were all significant correlated with any of the three dimensions in EPQ, which indicated that personality could be used as an important predictor for mental health. Based on data of personality, we may seek out the target groups for mental protection before mission. The high correlation between personality and mental health had also been found in the previous study in a different population, Wei et al. found that the introversion-extroversion score was positive correlated to any of the nine factors in SCL-90 [9]. According to the evidence of the current study, the correlation coefficient between neuroticism and factor scores of SCL-90 was the highest among the three dimensions of EPQ, which indicated that emotional stability was effective predictors for mental health. Thus based on the data of neuroticism in EPQ, we could screen out the individual with low emotional stability and diminished the risk of mental health problems during mission.

## 5 Conclusion

Medical team members with low self-protection and high risk of infection may have multiple types of mental problems. Medical team members with higher introversion, higher psychoticism and neuroticism characteristics were more likely to be low levels of mental health. These results could help us to find out the target population of mental protection before military operations other than war. Due to the limitation of cross-section study, the predictor found in the current study still needs to be verified in further longitudinal tracking study.

**Compliance with Ethical Standards** The study was approved by the Logistics Department for Civilian Ethics Committee of Air Force Medical Centre.

All subjects who participated in the experiment were provided with and signed an informed consent form.

All relevant ethical safeguards have been met with regard to subject protection.



## References

1. Yang J, Li N (2011) Investigation of psychologically healthy of doctor and nurse in the earthquake relief work. *Med J West* 23(12):2464–2465
2. Xie M, Wang XS, Wang GL et al (2011) Investigation of the influence of earthquake disaster on the mental health of emergency rescue medical staff of PLA. *Med Pharm J Chin People's Liberation Army* 23(6):55–57
3. Wang JL (2010) Investigation on mental health of medical professionals joining the relief action in earthquake-stricken Wenchuan. *J Nurs Sci* 25(6):65–66
4. Hemert DA, Vijver FJ, Poortinga YH et al (2003) Structural and functional equivalence of the eysenck personality questionnaire within and between countries. *Pers Ind Differ* 33(8):1229–1249
5. Holi MM, Sammallahti PR, Aalberg V (1998) A Finnish validation study of the SCL-90. *Acta Psychiatr Scand* 97(1):42–46
6. Feng ZZ, Hu F, Liu YB et al (2016) Establishment of norm of symptom check list 90 (2016 Edition) for Chinese military personnel. *J Third Mil Med Univ* 38(20): 2210–2214
7. Fan XB, Dong HJ, Wang YL et al (2012) Analysis and suggestions on mental health of emergency rescue medical staff in disaster events. *Disaster Med Rescue: electronic version* 1(3):167–168
8. Zhang B, Song KX, Yang X et al (2009) Relationship between rescuing time or zone and mental status of succors after earthquake. *Chin J Clin Healthc* 12(5):462–464
9. Wei SL, Wang YP, Wang Y et al (2019) Correlation analysis among personality characteristics, coping style and mental health of Armed Police Force recruits. *Med J National Defending Forces in Northwest China* 40(1):57–61

# Research on the Construction of Ship Operator's Cognitive Behavior Model



Weiming Fang, Shuqin Zhao, Jun Peng, and Chuan Wang

**Abstract** The establishment of the cognitive model is beneficial to the identification of the operator's cognitive error model and its cognitive stages and causes, so as to provide the corresponding basis for the design of the ship's human-machine interface and the training of the operator. This paper studies the construction of a cognitive behavior model for ship operators, and results show that the behavior of ship control system operators is mainly manifested as cognitive behavior, including monitor/discover, state evaluation, response plan, response execution. The three main feedbacks (state evaluation, response plan, response execution) in the cognitive model can be seen as a series of cognitive cycles, each providing information for the next stage.

**Keywords** Ship · Operator · Cognitive behavior model

## 1 Introduction

In the complex society-technology system, human error has become one of the main causes of accidents [1]. The construction of the cognitive model is conducive to identify the operator's cognitive error mode and the cognitive stage and root of the occurrence so as to provide the corresponding basis for designing the ship human-machine interface and training the operator. However, all existing individual cognitive error models are based on assumptions and experience, and they cannot enough understand the operator's complex cognitive process, nor reflect the characteristics of the operator's cognitive behavior in the ship control system.

---

W. Fang · S. Zhao  
China Ship Development and Design Center, 430061 Wuhan, China

J. Peng  
Naval Equipment Department, 100089 Beijing, China

C. Wang (✉)  
Naval Medical Center of PLA, 200433 Shanghai, China  
e-mail: [hg04381@163.com](mailto:hg04381@163.com)

## 2 Overview of Cognitive Behavior Model

Rasmussen [2] combined and integrated the human information processing stage with human practical skills and knowledge proficiency into a model as shown in Fig. 1.

He divided human organizational form of knowledge into a skill level, a rule level, and a knowledge level. At the skill level, it is highly controlled by the skillful practice and experience, the individual's perceived information, motor nerves, and muscle action are processed automatically, and the operator performs his familiar state. His state features are very consistent with the preset action sequence storing memory, and human's attention resource is hardly consumed. At the rule level, a large number of automatic behavior modes are integrated into a new behavior mode by using the existing rules as well as being limited and influenced by the rules. After target determination, it is required to keep the original action or perform another action. Therefore, it is necessary to make choices at key points according to the rules, and such behaviors need intention control. At the knowledge level, such information processing mode occurs when the operator faces a novel situation or has no experience of the situation. Therefore, the operator must rely on information processing for reasoning, calculation, etc., but due to the inherent limitation of the human information processing system, the knowledge-based reasoning may lead to misinterpretation and other errors, while the deductive reasoning needs to strengthen cognitive efforts, thus, the time to find the solution to the problem is prolonged.

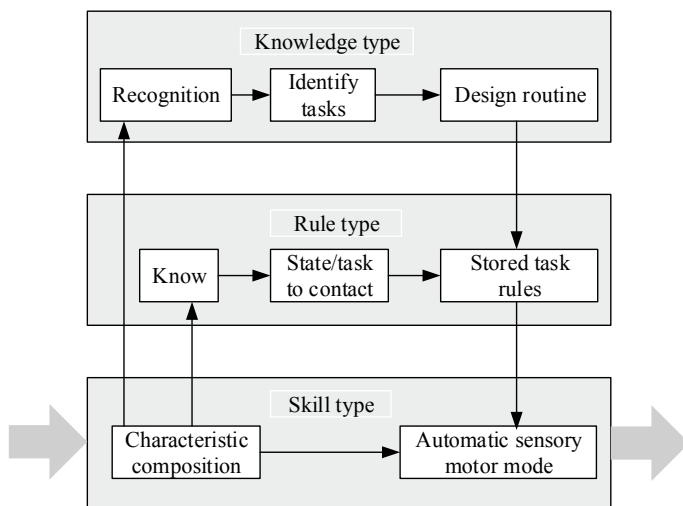


**Fig. 1** Rasmussen's three levels of error model

### 3 Ship Main Control Room Operator's Cognitive Behavior Model

Human operation response behaviors are performed in specific scenarios. Due to the development of technology and the improvement of automation, the operator's main task in the complex system of ships is cognitive tasks which mainly include (1) monitoring and detection, (2) state evaluation, (3) response plan and (4) response execution [3, 4], as shown in Fig. 2.

The control room operator monitors and controls the system with the human-machine interface. When the system state is abnormal, the system will alarm and shows the abnormality in the display through sensors. The operator can get the system state information from the human-machine interface through the display system, and evaluate the current system state on this basis. Then, the operator can determine the abnormal state according to the evaluation and diagnosis results, select the operation program and route, and execute and control the response task at last. All kinds of cognitive and behavior errors may occur in every stage above.

With the development of cognitive engineering, it is recognized that the human cognitive process does not handle continuously by stages, for example, when dealing with complex events, the human decision-making and interpretation are carried out simultaneously. Therefore, the human cognitive process can be described by cognitive domain [5], namely, the operator's cognitive domain can be divided into four parts which are monitoring and detection, state evaluation, response plan and "response execution". However, the operator needs to assist the first kind of tasks by executing and the second kind of tasks while executing the first kind of tasks (the main cognitive

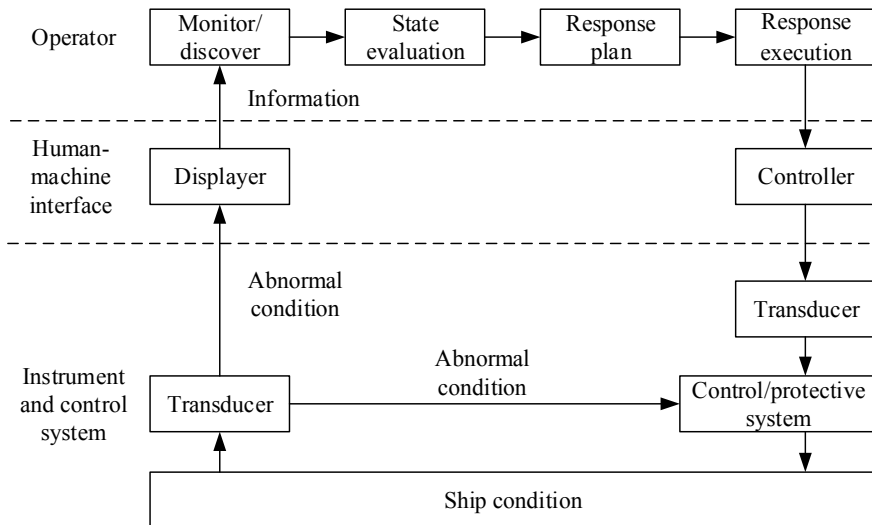


Fig. 2 Ship operator's operation processes

behaviors). The second kind of tasks generally refers to interface management tasks, i.e., screen configuration, navigation, screen adjustment, query, and shortcut, etc. Therefore, integrating the cognitive models of the first kind of tasks and the second kind of tasks can describe the ship's main control room operator's main cognitive behaviors, as shown in Fig. 3.

However, the above-sequential cognitive process does not describe the dynamic and real-time features of human cognition, and each of the four cognitive stages can be embedded with the cognitive functions of monitoring/detection, state assessment, response plan, response execution, etc., such as an IDAC embedded in the IDAC (information processing, decision-making and execution) model [6], as shown in Fig. 4. It is true, in fact. Although it is the high automated behavior in the monitoring stage, it is also necessary to identify the collected information and decide how to

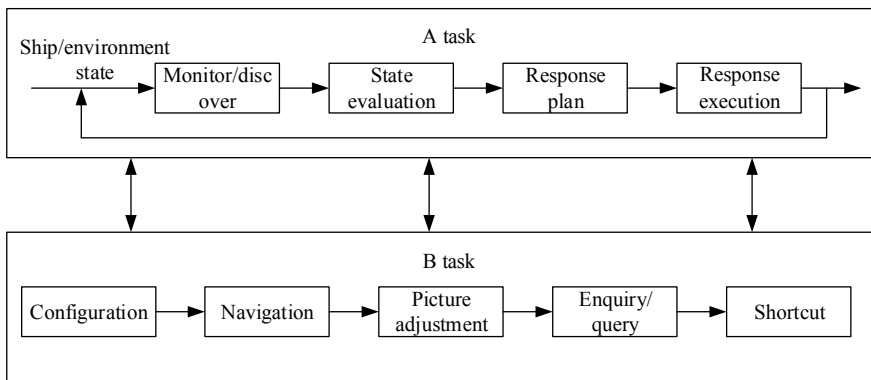


Fig. 3 Cognitive behavior model of ship main control room operator

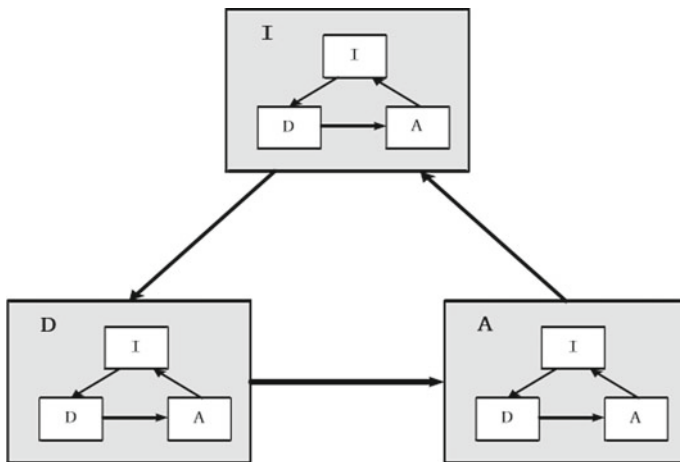


Fig. 4 Cognitive functions IDA is embedded in IDAC model

deal with this information, such as by screening, retention and reorganization, in the monitoring stage. In addition, it is necessary to constantly monitor, explain and select procedures and steps in the state evaluation stage. Therefore, the human cognitive mechanism is very complex. In order to clarify the cognitive process, it is necessary to analyze the specific task and cognitive function requirements in detail and expand the human cognitive behavior model, which is conducive to the in-depth understanding of the cognitive mechanism. Therefore, based on Rasmussen's three-level error model (i.e., skill-level model, rule-level model, and knowledge-level model), this paper expands the sequential cognitive behavior model (monitoring/detection, state evaluation, response plan, and response execution) so as to better understand the human cognitive process and cognitive types, which is conducive to accident management and operator training.

## **4 Expanded Operator's Cognitive Behavior Model**

To better understand the human cognitive process and cognitive skill, identify the possible error source and error form and improve the quality of ship accident management and operator training, the operator's cognitive behavior model in the ship control system is expanded based on Rasmussen's three-level error model and the expanded cognitive behavior model is established which comprises of main cognitive behaviors, interface management behaviors, and a cognitive function model. Apparently, many interface management tasks have to be executed in the ship control system to assist the completion of the main task. In addition, same as the IDAC model, the main cognitive behaviors can encapsulate a cognitive behavior model which is similar to the simple cognitive function model proposed by Hollnagel [7]. Therefore, the contents which are expanded in all stages of the main task are introduced as follows.

### ***4.1 Monitoring/Detection***

The expanded monitoring/detection stage comprises three sub-elements, which are monitoring, detection and information integration [8]. Monitoring/detection refers to the behavior of obtaining information from a complex dynamic working environment. Monitoring is to check the ship state data to determine whether the system is operating normally. Monitoring takes an active way to obtain the ship state data, while detection takes a passive way to obtain the ship state data, such as alarming through the control room. Thus, in terms of the detection behavior, the operator does not actively look for the obvious indicator/indication light. When the operator has found that there is an abnormal condition, he will obtain the ship data in a more active way, actively find out the specific parameter value or indication mark, and evaluate the higher-level ship process, state or function through information integration. The cognitive behaviors

of information integration include information retrieval, information understanding, information filtering (i.e., internal filtering), association and grouping, and further reasoning based on the above process to differentiate priorities and draw conclusions [9]. The cognitive behaviors of the whole process above can be respectively divided into the information integration processes of skill-based type, rule-based type and knowledge-based type according to different cognitive ability needs.

## ***4.2 State Evaluation***

When the ship is in an abnormal state, the operator will construct a proper and logical explanation according to the state parameters of the ship so as to evaluate the ship state as the basis for the decisions of the subsequent response plan and response implementation. This series of processes is called state evaluation and involves two related models which are the state model and the mental model [10]. The state model is the operator's understanding of the specific state, and when new information is collected, the state model will be updated frequently. The mental model is constructed through formal education, specific training and operator experience, and stored in the brain. The state evaluation process is to develop a state model to describe the current ship state. If an event (such as an alarm) is very simple and the operator does not need any reasoning for the identification of the ship state, it is considered as the state evaluation of skill-based type. If an abnormal event belongs to the so-called problem, the operator is required to explain the causes and influences of the problem to construct a state model, and the constructed state model matches the operator's mental model (i.e., similarity matching), then the process is called as the state evaluation of rule-based type. Similarly, for the unfamiliar state mode, if the operator is required to evaluate and predict the possible ship state, then analyze the more abstract logical relationship between the structure and function of the problem space, carry out deep reasoning, gradually form a state model and verify it, and finally determine the ship state, then the process is called as the state evaluation of knowledge-based type.

## ***4.3 Response Plan***

The response plan refers to the decision-making process of making the action policy, method or plan to solve the abnormal event. After state evaluation, the action to be performed shall be planned. Under abnormal conditions, in order to identify the appropriate method to achieve the target, the operator shall identify the alternative methods, strategies and plans, evaluate them, and select the optimal or feasible response plan. If none of them is appropriate, a new response plan needs to be reconstructed. If the response plan is simple enough to respond to human behavior without or with little human cognitive effort, it is the response plan of skill-based type, such as

the response to an alarm. When an alarm occurs, the behavior directly corresponds to an action, such as the response to an emergency standard, and the standard is directly followed without selecting a route. Similarly, for a given ship state, if there is an effective standard (such as EOP) applicable to the handling of the given ship state, then the process is the response plan of rule-based type. On the contrary, if there is no corresponding standard, procedure or rule to handle, or the existing standards have proven incomplete or invalid, the operator shall reconstruct a new response plan and evaluate the feasibility and effectiveness of the plan, then the process is the response plan of knowledge-based type.

#### ***4.4 Response Execution***

Response execution is to execute the action or behavior sequence defined in the response plan. The process can be very simple, such as that the operator operates by pressing a control button or a virtual icon. However, it is worth mentioning that the simple process also includes a complete cognitive function process (such as I-D-A), such as finding the icon information on the screen (monitoring/detection), identifying the icon to be found (interpretation and evaluation), determining the execution mode (pressing or rotating?) or the sequence of steps and executing pressing operation, etc., and perhaps determining whether it is done (via information feedback). In addition, for different tasks of the ship, the response execution may also need different levels of team communication and cooperation, which requires mutual cooperation and assignment and arrangement of tasks. For those unconventional and complex control behaviors, especially when the response plan has no regular mode for guidance, the priorities of behaviors need to be changed or established according to the ship state by cooperation and coordination among multiple personnel in multiple locations, and it is defined as the response execution of knowledge-based type.

### **5 Conclusion**

This paper researches the construction of the ship operator's cognitive behavior model. The research result shows that the ship operator's behaviors in the ship control system mainly include the cognitive behaviors, including monitoring/detection, state evaluation, response plan and response execution. The three main feedbacks (submodels of state evaluation, response plan, and response execution) in the cognitive model can be seen as a series of cognitive cycles, each provides information for the next stage.



## References

1. Study on human-machine interface design of nuclear power plant control room. In: 19th International conference on man-machine-environment system engineering, Shanghai, P.R. China (2019)
2. Rasmussen J (1986) Information processing and human machine interaction: an approach to cognitive engineering. Amsterdam:North-Holland
3. Thompson CM, Cooper SE, Bley DC et al (1997) The application of ATHEANA: a technique for human error analysis. In: IEEE sixth annual human factors meeting, Orlando, Florida, pp 13–17
4. Lee SJ, Kim MC, Seong PH (2008) An analytical approach to quantitative effect estimation of operation advisory system based on human cognitive process using the Bayesian belief network. *Reliab Eng Syst Safety* 93(4):567–577
5. Shorrck S, Kirwan B (2002) Development and application of a human error identification tool for air traffic control. *Appl Ergon* 33(4):319–336
6. Chang YHJ (1999) Cognitive modeling and dynamic probabilistic simulation of operating crew response to complex system accident (ADS-IDACrew). University of Maryland, Maryland
7. Hollnagel E (1998) Cognitive reliability and error analysis method. Elsevier Science Ltd., Oxford (UK)
8. Randall JM, Isabelle ES, Julius JP (1992) Training cognitive skills for severe accident management. Human factors and power plants. In: Conference record for 1992 IEEE fifth conference, Monterey, CA
9. Chang YHJ, Mosleh A (2007) Cognitive modeling and dynamic probabilistic simulation of operating crew response to complex system accidents—part 4. IDAC causal model of operator problem-solving response. *Reliab Eng Syst Safety* 92(8):1061–1075
10. John MO, James CG, Joel K (2002) Advanced information systems design: technical basis and human factors review guidance. U.S. NRC, Washington, DC

# Analysis of Human Factor Characteristics of Ship Control System



Jun Peng, Guangjiang Wu, and Chuan Wang

**Abstract** With the development of computer and information technology, the level of human-machine interface automation of ship control system is improved continuously. Based on the definition of human factor error and human factor concept, this paper analyzes the typical human factor characteristics in the digitized ship control system through on-site observation and operator interview, which are mainly manifested in the changes of the operator's role and function, task load, cognitive factors and experience ability, operation team structure and size, the level of team communication and cooperation, operating procedure, information display and control based on VDU, alarm screen, etc.

**Keywords** Ship · Control system · Human factor error · Human factor characteristics

## 1 Introduction

In the complex society-technology system, human error has become one of the main causes of accidents [1]. Statistical data of accidents at home and abroad show that the contribution rate of human error to accidents has reached about 85%. How to prevent human error and minimize its consequence has become an important problem to be solved at home and abroad. With the development of computer and information technology and the continuous improvement of the automation level of the human-computer interface of the ship control system, the role of the operator of the main control room of the ship is gradually changing from the traditional operator to the supervisor and manager. The operator's main tasks are characterized by cognitive

---

J. Peng · G. Wu  
Naval Equipment Department, 100089 Beijing, China

C. Wang (✉)  
Naval Medical Center of PLA, 200433 Shanghai, China  
e-mail: [hg04381@163.com](mailto:hg04381@163.com)

tasks, such as monitoring, detection, state evaluation, response plan, and decision-making. The traditional human reliability analysis methods, such as THERP [2], HCR [3], and SLIM [4], mainly focus on the quantitative evaluation of the observed errors rather than the qualitative analysis of the operator's cognitive behavior. According to Jung et al. [5], the HRA method without detailed cognitive error analysis may underestimate the probability of human errors and may ignore their severe consequences on the system or environment. In order to overcome the above limitations, some new cognitive behavior models and cognitive error analysis methods based on cognitive psychology have been developed at present, such as HRMS [6], CREAM [7], IDA [8] and IDAC method [9]. Although the above models and methods explain human cognitive behaviors in detail, after partially digitizing the traditional main control room, the operator's context changes, and the operator's role and function in the system and the human–computer interaction mode are changed; therefore, the operator's psychological cognitive process and behavior characteristics are affected.

## 2 Concept of Human Error

Different people have different definitions of human error. Rigby [10] believed that when human behavior acting on the system does not or does not fully meet the requirements of the system, it is called human error. The definition is strictly based on the requirements of the system to define but does not take into account of limitations of human themselves and human cognitive errors. Therefore, the definition is biased. Swain and Guttman [2] believed that human error is any human action beyond the acceptable limit of the system. Swain defined human error as any human behavior or omission that may cause unexpected events [10]. According to Swain's definition, human has been regarded as an integral part of the technical system. Leplat believed that "when the human behavior exceeds the acceptable limit of the system, then the behavior is human error" [11]. In the same way, the above definitions are the same as Rigby's definition for human error, which also defined from the perspective of engineering application and according to the performance limit of the system. Reason believed that human error is the result that the planned psychological and physical behavior sequence fails to achieve the expected result after execution, and this failure cannot be attributed to the interference of random trigger factors [12]. Reason believed that human is an information processing component of the technology system. The definition defines from the perspective of psychology. Although the definition tries to define human error from the perspective of human and includes human cognitive errors as much as possible, it still fails to take into account human limitations. Swain's definition of human error [10]. A human error exists in the work system all the time. It has the characteristics of causing the work system to be in an unexpected or wrong state. Its generation causes the system requirements to be in a state of not being satisfied or not being fully satisfied. The individual is a component of the work system and interacts with other components in the work. All components in the work system rely on and affect each other. The definition defines human

error from the limitation of the technology system and the limitation of human, but it does not involve all human errors, either. According to the above definitions, we can know that human error is diversely defined, and people have different definitions from different perspectives. However defined, human error generally has the following three basic properties:

1. Same as the hardware and software of the system, manual operation is an organized body that also has failure rate and tolerance.
2. Human error includes the implicit error (cognitive error) and explicit error (behavior error). The implicit error is one of the causes of the explicit error, and it is also an indispensable part of human error analysis, such as error prediction and error cause analysis.
3. Compared with normal human behavior, human error is a derogatory term and is generally caused by various adverse contexts. Human error needs to be determined according to the consequences of human behavior.

For a long time, the term “human error” has been used to describe the situation which causes the unexpected consequence as well as part or all of the causes of events caused by human behavior (this can be found in the so-called root cause analysis, but in the field of human behavior, the root cause is actually a fiction, because it can always be traced back and analyzed endlessly). Indeed, “human error” can be used to represent the cause of the event (for explaining the cause of the accident) and the specific classification of the behavior (for the classification in the cognitive field). However, it is necessary to define each part clearly to avoid confusion and be conducive to the development of research at the same time.

This paper comprehensively defines human error from theory and engineering application and takes into account of the limitations of the technology system and human, as follows: Human error is caused together by the combined action of several individual’s internal factors and external situation factors and leads to human cognitive failure and behavioral failure which make human unable to accurately, appropriately, fully and acceptably complete the task specified in the performance standard range. In short, human error is human cognitive error and behavior error, and human cognitive function and behavior response fails to meet the correct and expected standards. Human error mainly has the following characteristics.

1. Repeatability of human error. Human error often occurs repeatedly under different conditions or even in the same condition. One of the root causes is the mismatch between human ability and external requirements. Human error cannot be eliminated completely, but it can be avoided as much as possible by effective means; however, once the failure cause of the common component or equipment is found, it can often be overcome by modifying the design.
2. Potential of human-induced failure. One of the causes of the Three Mile Island accident is the potential failure of the valve caused by the maintenance personnel. A large number of facts show that once such potential error is combined with an excitation condition, it will lead to an inevitable disaster.

3. Human error behavior is often driven by context. Any activity of human in the system is inseparable from the context at that time. The joint effect of hardware failure, false display signal, pressing time pressure, etc., will greatly induce human unsafe behavior. This emphasis on the role of context is the research focus of human error behavior.
4. The inherent variability of human behavior. The inherent variability of human behavior is a characteristic of human, namely a person cannot repeat a task in the exact same way (accuracy, precision, etc.) without using external force. Too big fluctuation will cause random fluctuation of performance, which is enough to cause failure. This variability is also an important reason for people's wrong behavior.
5. Repairability of human error. Human error can lead to system failure or fault. However, many situations indicate that under the condition with good feedback devices or redundancy of personnel, the human may find out and correct the previous error. In addition, the abnormality of the system can often be alleviated or overcome due to human participation so that the system can return to the normal working condition or safety state.
6. Human's ability to learn. People can improve their work performance through continuous learning, which is impossible for the machine. During task execution, adapting to the environment and learning are the important behavioral characteristics of human, but the effect of learning is affected by many factors, such as motivation and attitude.

### 3 Concept of Human Factor

Human factors refer to (a) the research of human abilities and limitations in the design of tools, machinery, systems, tasks, work, and environment; (b) the application of the above knowledge in the design; and (c) the use of human factor methodology in the design to achieve the goals of safety, effectiveness, and satisfaction [13]. Dhillon B. S. believed that human factors are the science related to the research of human characteristics, which includes all biomedical and psychological considerations, as well as life support, personnel selection and training, training equipment, work performance support, performance measurement, and evaluation, etc. From the above definition, the human factor is a broader concept that can refer to discipline and involve various research fields. However, from the perspective of human error, there is no detailed discussion on the definition of the human factor.

So far, although human error and human factors are both researched independently, the relationship between them is usually ignored by researchers. At the same time, the distinction between their definitions is not very clear, and the term of human factor has not been precisely defined yet at home and abroad. The reasons are as follows: On the one hand, it is not very significant to make a clear distinction between human error and human factor, and they have been used without distinction in many industrial accident reports; and on the other hand, it may be difficult

to make a clear distinction between them due to the fact that their essential differences and relations are not clear up to now. However, in order to improve the way of accident reports and as needed by development, it is necessary to distinguish human error and human factor. Based on the nuclear power organization, this paper defines human factor as various types of human factors in the organization, which potentially affect people's cognitive behavior, including individual human factors (such as individual knowledge, experience, ability, pressure, attitude, and motivation), team human factors (such as team communication, cooperation, supervision, and management) and organizational human factors (such as organizational policy, organizational structure, organizational culture, and organizational procedures).

#### **4 Human Factor Characteristics of Ship Control System**

It is a very complex system for the operator to observe and operate in the ship control room. In the traditional simulation control room, the operator has to walk around to read information from the instruments on the large control panel, operate buttons, and adjust knobs. Although the system and equipment in the advanced control room based on the transformation and upgrading of digital technology are improved in reliability and can be corrected and compensated under the influences of various types of disturbances, there is no fixed value drift, and some functions (such as fault tolerance, self-detection, and automatic calibration) are not improved. In terms of human performance, new human-system interfaces such as computerized procedure system, advanced alarm system, and graphical information display system have provided positive effects on team performance, such as reducing the operator's workload and reducing human errors (such as with the computer-based system, the shift supervisor can directly read the state information of the ship control console and does not need to ask the board operator for some parameter values of the ship control console as much as before); with the advanced alarm system and graphical information display system, the instrument operators can obtain more abundant state information of the ship control console than before, and they can more widely monitor the (process) state of the ship control console; the team members use multiple independent information sources and independent opinions, and the crew members share the information of the ship control console. Therefore, the possibility of detecting and correcting errors is improved in the process of state evaluation to reduce the possibility of errors of intention and improve the reliability of the team. However, the change of context factors (such as the information display based on VDU, the process control based on mouse and touch screen, the computerized procedure system, the added task characteristics of interface management tasks, the system complexity brought by the decision-making support system, the changes of team structure and communication and cooperation level) may also bring adverse effects on the operator's performance, such as the emergence of new types of human errors (such as pattern confusion, data input errors and loss of situation awareness) and new human error distribution (such as the increase of executive errors).

**Table 1** Human factor characteristics of ship control system

Number	Human factor characteristics
1	Manipulator role and function
2	Manipulator task load
3	Manipulator cognitive factors and experience ability
4	Operation team structure and scale
5	The level of communication and cooperation of team
6	Computerized operating procedure
7	Information display and control based on VDU
8	Alarm screen

After interviewing the operator of the ship control room, the human factor characteristics in the ship control system are analyzed and summarized as follows, as shown in Table 1.

1. Operator's role and function. The operator's role in the digitized ship control system is different from that in the traditional analog control system. In the traditional control room, generally, the operator's role is to monitor and operate the system, while in the digitized main control room, the operator's role changes from a manual controller to a monitor and a decision-maker, the operator's task includes more cognitive work, and the operator executes the task through a series of cognitive behaviors. Besides, in the traditional simulation control system, the shift supervisor has absolute authority and responsibility, while in the digitized control system, the shared state information and procedure information (computer-based digital procedure) of the ship control console are convenient for the exchange and cooperation of the team, which relatively weakens the authority and responsibility of the shift supervisor and changes the operator's role and function.
2. Operator's task load. The information display based on the computer is different from that on the panel of the traditional simulator. The information displayed in the traditional simulation system is clear at a glance, while the digitized control system displays the information as a whole on the large screen and based on the computer workstation. In case of emergency, the operator not only needs to complete the main task (monitoring, state evaluation, response plan, and response execution), but also needs to execute the secondary task (i.e., interface management task), such as screen configuration, navigation, and query, in order to obtain more information. When the operators are required to obtain the information about the state of the whole ship control console from the screen of a small range, they need to navigate repeatedly because the limited visual window of the visual display units (VDUs) will bring the so-called keyhole effect. Especially in an emergency, the operator's task load will be increased by a large number of displayed data, heavy interface management work, and the condition of executing multiple programs at the same time.

3. Operator's cognitive factors and experience ability. The higher the degree of automation is, the more complex the system will be. The original manual control system is completed by the automation system, which changes the operator from an operator to a monitor and a diagnosis person. Therefore, it shall understand how the ship control console works, then higher requirements are put forward on the ability and experience of personnel, and people's cognitive load is increased.
4. Operation team structure and size. In the traditional simulation control system, generally, the operator walks around the corresponding panel of the main control room to get information, and it is difficult to share the information of the ship control console. The digitized ship control system is based on the overall information display of the large screen of the computer, and the operation team shares the information of the ship control console, which changes the team structure and size.
5. Team communication and cooperation level. The sharing of the information, such as the parameter information of the ship control console (temperature, pressure, water level, etc.), alarm information, computerized procedures, and computerized operation support system, changes the team structure and information exchange mode and increases the communication and cooperation among operators and between the operators and on-call personnel.
6. Computerized operation procedures. The traditional simulation adopts paper procedures, while the digitized ship control system adopts the computer-based procedures. The complexity of the procedure structure increases the risks of program skip or error; for example, the state-oriented procedure (SOP) includes the main program and an operation sheet, and the main program and the digitized operation sheet are separated. When executing the main program, the operation sheet is often called to complete a specific operation, which increases the number and level of program calls. In addition, program skip or the use of the wrong operation sheet or program is easy to occur when the program is changed frequently.
7. VDU-based information display and control. Unlike the indicator on the traditional control panel, the computer-based information display is not limited to the physical space. Any amount of information can be displayed through scrolling, partial window overlapping and the hierarchical configuration of the screen. However, the same information may have different positions on different screens. Therefore, a large amount of information is displayed in the same window, which increases the difficulty for the operator to locate, search, and identify. In addition, the soft control of the digitized ship control system is more complex than the hard control of the traditional control system, and the pop-up dialog box of the soft control will cover some important information of the screen, which will increase the operator's cognitive load and prolong the execution time.
8. Alarm screen. Compared with the traditional simulation control system, the alarm display in the digitized ship control system is not intuitive. The computer-based alarm is displayed on the display screen. When the operator needs to know whether an alarm appears in an emergency, he may need to find the required alarm through a series of behaviors such as filtering, querying, and information



classification. Therefore, the operator has to spend more time to search and confirm the alarm, which delays the operation of other tasks.

## 5 Conclusion

Based on the definition of human factor error and human factor concept, this paper analyzes the typical human factor characteristics in the digitized ship control system through on-site observation and operator interview, which are mainly manifested in the changes of the operator's role and function, task load, cognitive factors and experience ability, operation team structure and size, the level of team communication and cooperation, operating procedure, information display and control based on VDU and alarm screen.

## References

1. Study on human-machine interface design of nuclear power plant control room. In: 19th international conference on man-machine-environment system engineering, Shanghai, P.R. China (2019)
2. Swain AD, Guttman HE (1983) A handbook of human reliability analysis with emphasis on nuclear power plant applications. USNRC, USA, Washington DC
3. Hannaman GW, Spurgin AJ, Lukic YD (1984) Human cognitive reliability model for PRA analysis. Electric Power Research Institute, Nuclear Utility Service Corp, Palo Alto, California
4. Embrey DE (1986) SLIM-MAUD: a computer-based technique for human reliability assessment. *Int J Qual Reliab Manage* 3(1):5-12
5. Jung W, Kim J, Ha J et al (1999) Comparative evaluation of three cognitive error analysis methods through an application to accident management Tasks in NPPs. *J Korean Nuclear Soci* 31(6):8-22
6. Kirwan B (1997) The development of a nuclear chemical plant human reliability management approach: HRMS and JHEDI. *Reliab Eng Syst Saf* 56(2):107-133
7. Hollnagel E (1998) Cognitive reliability and error analysis method. Elsevier Science Ltd. Oxford(UK)
8. Shen S-H, Smidts C, Mosleh A (1997) A methodology for collection and analysis of human error data based on a cognitive model: IDA. *Nuclear Eng Design* 172(1-2):157-186
9. Chang YHJ (1999) Cognitive modeling and dynamic probabilistic simulation of operating crew response to complex system accident (ADS-IDACrew). University of Maryland, Maryland
10. Sträter O (2000) Evaluation of human reliability on the basis of operational experience. Köln, Germany: GRS
11. Marie-odile B (1999) A case study of a human error in a dynamic environment. *Interact Comput* 11(5):525-534
12. Reason J (1990) human Error. Cambridge University Press, New York
13. Day MC, Joyce SJ (1993) Computer system design. *Adv Comput* 36(2):333-430

# Study on Fatigue Detection of Ship Operator Based on Eye Features



Chuan Wang, Jun Peng, Xiaoxi Han, Shenghang Xu, and Jian Zhang

**Abstract** Aiming at the problem of human error caused by the fatigue driving, domestic and foreign scholars have done a lot of research on driving behavior model, traffic safety risk, curve track distribution features, curve speed characteristics and road infrastructure, etc., but few have done much research on driver behavior. In this paper, combined with Haar-related feature templates, the face of the ship operator is identified and detected. The face-related data is measured by the geometric method to locate the human eye, and the eye state of the operator is located and detected by the PERCLOS algorithm. The results show that real-time detection and early warning of fatigue state are of great significance to reduce the human error caused by ship operators.

**Keywords** Fatigue detection · Eye feature · PERCLOS algorithm

## 1 Introduction

In the complex social-technical system, human error has become one of the main causes of accidents [1]. Computer technology, artificial intelligence technology, and sensor technology have experienced continuous development and reform. In order to protect the physical and mental health of drivers, scholars at home and abroad have begun to study the application of on-board sensors in obtaining a driver's driving behavior information and physiological information for the determination of driver state [2–4]. Improving the work efficiency of operators is of great significance to preventing and controlling ship accidents due to human factors caused by fatigue operation [5].

---

C. Wang · J. Zhang (✉)  
Naval Medical Center of PLA, 200433 Shanghai, China  
e-mail: [hg04381@163.com](mailto:hg04381@163.com)

J. Peng · X. Han · S. Xu  
Naval Equipment Department, 100089 Beijing, China

This paper presents an operator fatigue detecting method based on human eye features, that is, recognizing and detecting the face of ship operators in combination with Haar-related feature templates; applying the geometric method to measure human face-related data and locate human eyes; applying PERCLOS algorithm to locate and detect the operator's eye state.

## 2 Haar Features

### 2.1 Haar Feature Templates

At present, the commonly used features can be divided into three categories: edge feature, point feature (center feature), and linear feature.

$(s, t)$  condition means: The edge length of a rectangular feature in the  $X$ -direction must be divided by the natural number,  $s$ , with no remainder; and its edge length in the  $Y$ -direction must be divided by the natural number,  $t$ , with no remainder. If the dimensions of the detection window are  $w \times w$ , the minimum dimensions of the rectangular feature of the feature template are  $s \times t$  and the maximum dimensions are  $([w/s] \times s, [w/t] \times t)$ . As it can be seen from the constraint  $(s, t)$ , the dimensions of the detection window determine the dimensions of the rectangular feature of the feature template and possess rectangular features of different dimensions. When calculating facial features, a rectangle of certain dimensions passes through the detection window in the form of a moving window, that is, each different position is a brand new feature.

As can be seen from the above algorithm: As long as any parameter among the structure, dimensions, and position of a rectangular feature changes, it becomes a brand new face feature. The number of features of each feature template can be calculated by the formula.

$$X = [m/s], Y = [m/t]$$

$$\text{feature Number} = X \cdot Y \cdot \left( m + 1 - s \frac{X + 1}{2} \right) \cdot \left( m + 1 - t \frac{Y + 1}{2} \right)$$

Where  $w \times w$  is the dimensions of the detection window;  $s \times t$  is the dimensions of the feature template;  $X$  and  $Y$  refer to the integral-multiple proportional relation between the width and height of the detection window and those of the feature template and they are a number of features of the feature template in the detection window. With respect to an edge feature template of dimension  $(1, 3)$ , internal matching shall be performed in a detection window with width and height of 27 pixels. As calculated according to the formula, the feature template can generate a total of 44,226 features in the detection window [6]. Calculate the number of features generated by other feature templates and accumulate the number of features of all feature templates for the total number of features generated in the detection window of such dimensions.

**Table 1** Facial feature data

Face height	Face width	Eye center spacing	Eye width	Eye height	Eye distance from chin	Eye distance from forehead
15.29	10.88	7.16	3.51	1.07	10.43	5.24
17.62	12.62	8.19	4.82	1.17	10.51	6.11
18.53	12.44	7.58	4.71	1.12	11.80	7.85
20.41	14.97	9.22	5.32	2.47	12.64	6.32
24.33	13.62	8.64	5.00	2.09	12.57	7.54
19.21	13.81	8.40	4.56	1.36	12.43	5.59
18.85	14.25	8.62	4.97	1.65	11.96	6.06
23.94	15.46	9.77	5.43	2.50	11.25	6.48
18.78	15.27	9.68	5.39	2.50	11.21	6.57
17.20	12.73	7.63	4.68	1.00	12.48	5.60

### 2.2 Locating of Eyes by Geometric Method

According to the actual measurement of human faces, the results are shown in Table 1.

From the above table, the limited eye features are obtained:

1.  $1 \leq \frac{\text{Eye Width}}{\text{Eye Height}} \leq 4.5$
2.  $\frac{1}{20} \text{ Face Width} \leq \text{Eye Width} \leq \frac{1}{3} \text{ Face Width}$
3.  $\frac{\text{Eye Center Height}}{\text{Face Height}} \leq \frac{5}{9}$
4. Area Difference between Two Eyes  $\leq$  Reduced Eye Area
5. Forehead Length  $= \frac{1}{4} \text{ Face Length}$

### 2.3 Rough Locating of Left and Right Eyes by Geometric Method

Firstly, the geometric feature relation between face and eyes is obtained by collecting and analyzing samples. The formula for calculating the distance between eyes is as follows:

$$D = \sqrt{(x1 - x2)^2 + (y1 - y2)^2}$$

Where  $D$  represents the distance between two eyes;  $(X1, Y1)$  and  $(X2, Y2)$  represent the position coordinates of the center points of the left eye and the right eye in the image. The formula is used to confirm the range of distance between two eyes and ensure the distance between the face image and the sample to be collected. In the actual experiment, the threshold value of  $D$  can be set to 50; the upper left corner of the face image can be taken as the origin; and width and height of the face image can

be set as width and height. Then, the calculation formula of eyes relative to the area of the face image is as follows:

$$|AB| = |CD| = \frac{7}{24} \text{height}$$

$$|AH| = |ED| = \frac{1}{6} \text{width} - \frac{1}{4}D$$

### 3 PERCLOS Algorithm

Studies have shown that fatigue is related to factors such as blinking, a glimpse of the eyebrows, rapid eye movement, eye gaze, and pupil diameter. The percentage of eyelid-closure time per unit time is the percentage of total time. This method uses an operator's eye information to evaluate fatigue and extracts information required by PERCLOS (percentage of eyelid closure) from the operator's eye locating information obtained to realize fatigue test for operators. These data can truly reflect fatigue and realize fatigue test for operators.

### 4 Principle of PERCLOS Algorithm

The principle of PERCLOS algorithm is to calculate the proportion of an operator's eyelid-closure time at a specific time.

According to the degree of eyelid closure, PERCLOS has three standards.

EM: If the eyelid area covering the pupils is above 50%, the eyes are considered to be in a semi-closure state, and the proportion of eyelid-closure time in a given time shall be calculated.

P70: If the eye area covering the pupils is above 70%, the eyes are considered to be slightly closed, and the proportion of eyelid-closure time in a given time shall be calculated and the eyelid-closure times counted within a specific period.

P80: If the eye area covering the pupils is above 80%, the eyes are considered to be in a complete-closure state and the proportion of eyelid-closure times within a specific period of time shall be calculated.

### 5 Operator Fatigue Detection

In this paper, the percentage of eyelid closure (PERCLOS) is calculated to determine whether an operator is in a fatigue state.

Since there is no time scale in a continuous image sequence, but the number of image frames read per second is fixed, the PERCLOS value can be calculated according to the number of frames instead of the time scale. It is defined as:

$$f_p = \frac{n_c}{N_t} \times 100\%$$

Where  $n_c$  is the total number of eyelid-closure frames in a specific time and  $N_t$  is the total number of frames in a specific time. The PERCLOS value is calculated by calculating the ratio of eyelid-closure frames to the total number of frames in a specific time. When the PERCLOS value of an operator is higher than the normal value, the operator can be judged to be in the fatigue state according to the eye state.

## 6 Experiment and Result Analysis

### 6.1 Experiment platform

The test adopts Visual Studio 2013 software, Win7 System: Intel(R)Core(TM)i7-6700HQ, CPUs(3.40 GHz), 32 GB Memory.

### 6.2 Data Used in Training

In order to overcome a certain influence of illumination and enhance the human eye images used as data for network robustness training, images containing different illumination intensities must be collected.

### 6.3 Experiment Results and Analysis

After training for the eye state recognition model, in order to test the performance of the network model, three pieces of video data (the total numbers of frames of the videos are 982, 1327 and 1231, respectively) were collected, and the corresponding accuracy rates of eyelid-opening and eyelid-closure state detection were 96.87%, 95.21%, and 95.64%, respectively.

Four pieces of  $320 \times 240$  video frames were collected for the real-time test to measure the eye area obtained (including detection and positioning), eye state recognition and the total time: Video 1: 23.38, 7.00, 41.00 ms; Video 2: 23.51, 7.03, 41.86 ms; Video 3: 24.33, 7.05, 42.31 ms; Video 4: 24.47, 7.08, 41.55 ms. As can be seen, this method has good real-time performance and meets the actual requirements.

**Table 2** Fatigue state test results

Test serial number	$f_p$ (threshold 0.3)	Fatigue judging
1	0.3095	Fatigue
2	0.2715	Normal
3	0.1675	Normal
4	0.2250	Normal

The PERCLOS value of an operator in a fatigue state is higher than that in a normal state. Through multiple groups of experiments and analyses, the threshold value of each parameter is set to conduct fatigue detection for 4 groups of experimental subjects in the simulated ship operating environment, with 1 person in each group as the experimental subject. The experimental subjects of the 4 groups are all actual ship operators (the experimental subjects are all male, and the 4 groups of experimental subjects cover different age groups and different operating posts). The results are as shown in Table 2.

## 7 Conclusion

There are still many limitations in the current fatigue detecting mechanism in the world, and there is no clear classification standard for the fatigue level of operators. For ship operators, their long working time, bad working environment, and heavy and complicated operating tasks easily lead to fatigue driving problems and then cause human errors. If the fatigue state of operators can be detected in real time and early warning can be timely given in the ship operating process, it is of great practical significance to reducing ship accidents, casualties and property losses.

**Compliance with Ethical Standards** The study was approved by the Logistics Department for the Civilian Ethics Committee of Naval Medical Center of PLA.

All subjects who participated in the experiment were provided with and signed an informed consent form.

All relevant ethical safeguards have been met with regard to subject protection.

## References

1. Study on human-machine interface design of nuclear power plant control room. In: 19th international conference on man-machine-environment system engineering, Shanghai, P.R. China (2019)
2. Chen Z (2017) Research and application of feature selection and extraction. Heilongjiang Education Press (7)
3. Wang W (2012) Study on real-time face detection algorithm based on video. Shandong University (11)

4. Cao Y (2009) Research and implementation of face detection based on Adaboost algorithm. Tianjin Normal University
5. Chen J (2009) Research on 3D model control method based on face detection. Southeast University
6. Liu X (2011) Research on face detection technology based on video image sequence. Southeast University (3)



# Study on Fatigue Detection Method of Ship Operator Based on Face Recognition Technology



Jian Zhang, Jun Peng, Xiaoxi Han, Shenghang Xu, and Chuan Wang

**Abstract** Aiming at the problem of human error caused by the fatigue operation of ship operators, this paper proposes a method for fatigue detection of ship operators. The AdaBoost algorithm is used to detect the face of the ship operator, locate and analyze the eyes and mouth in the detected face area, and judge the fatigue state by information fusion in the decision-making stage. The results show that the method can accurately detect the state of eyes and mouth and effectively detect whether the ship operator is in the state of fatigue operation.

**Keywords** Fatigue detection · Face recognition · AdaBoost algorithm · Information fusion

## 1 Introduction

In the complex social-technical system, human error has become one of the main causes of accidents [1]. Most of the accidents are caused by fatigue operation, so it is of considerable significance to develop a system to monitor whether the ship operator is in the fatigue state.

At present, the methods for detecting fatigue operation are mainly divided into the following three types:

1. Physiological signal method: it analyzes the fatigue state with the help of physiological indicators of medical instruments and equipment [2].
2. Use the sensor to monitor the running state parameters of the vehicle to judge whether it is running normally and analyze whether the operator is fatigue.

---

J. Zhang · C. Wang (✉)  
Naval Medical Center of PLA, 200433 Shanghai, China  
e-mail: [hg04381@163.com](mailto:hg04381@163.com)

J. Peng · X. Han · S. Xu  
Naval Equipment Department, 100089 Beijing, China

3. According to the operator's response features, use the image detection and segmentation algorithm to find the mouth, eyes and other organs [3, 4], recognize the response features of human fatigue state according to the mouth and eyes [5, 6], and judge whether the operator is fatigue for operation through these response features.

This paper proposes an operator fatigue detection algorithm based on human facial features. It adopts the AdaBoost cascade classifier to detect the face, then locates the human eyes and mouth the basis of the extracted face image, and then detects the operator's state by the information fusion of the opening and closing of eyes and mouth to accurately determine whether the operator is fatigue for operation.

## 2 Overall Scheme Design of Fatigue Detection System

The fatigue operation detection system is mainly composed of an image acquisition module, a face recognition module, a feature location, status analysis module, and an information fusion module. The system flow is shown in Fig. 1.

## 3 Face Recognition

When the AdaBoost algorithm is used for detection, different weak classifiers are obtained at first, and then they are linearly combined into strong classifiers. At last, the final cascaded classifiers are constructed by cascading. The algorithm mainly includes the following essential parts:

1. Use Haar features to describe the common attributes of the face;
2. A feature named as the integral image is established to acquire several different image rectangle features quickly;
3. Use the AdaBoost algorithm for training;
4. Establish a hierarchical classifier.

## 4 Detection of Eyes and Mouth State

### 4.1 Detection of Eyes State

While locating the eyes area, it can judge the condition of the human eyes and realize the effect of replacing measurement with detection. The flow of distinguishing the situation of eyes opening and closing is shown in Fig. 2.

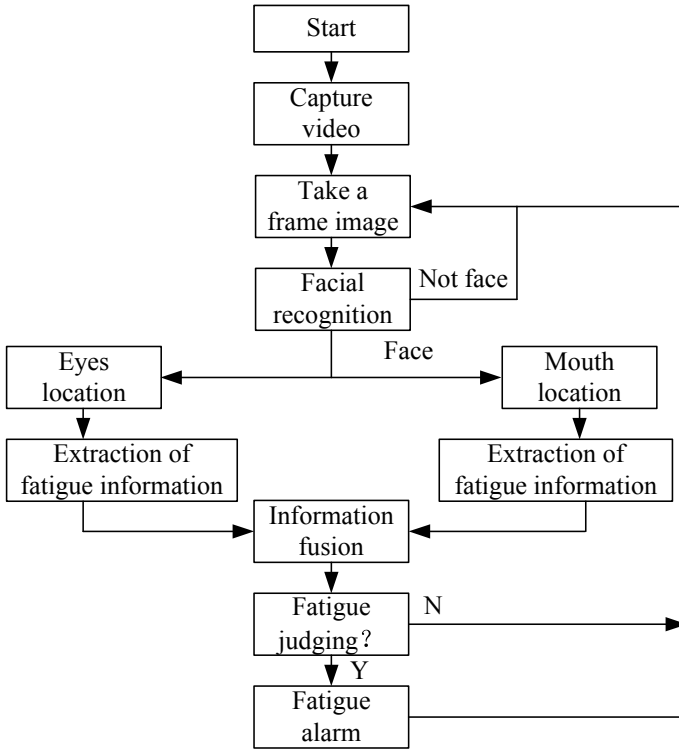


Fig. 1 Structure diagram of fatigue detection system

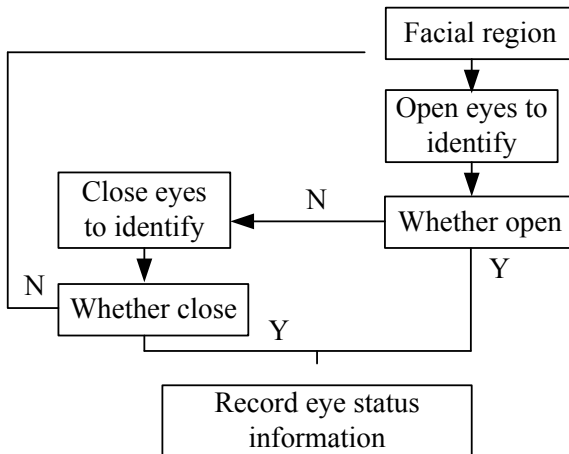


Fig. 2 Classification map of eye location and state

The detection of human eyes state is based on the image of each frame in the video. The fatigue state of human eyes is a state within a period. Therefore, the PERCLOS (Percentage of Eyelid Closure over the Pupil over Time, PERCLOS) method is used for determination [7]. The eyes are open when the opening degree of the eyes is greater than 20%, and closed when less than or equal to 20%. In the actual situation, we can judge whether the eyes are closed or not according to the image. The PERCLOS calculation is based according to formula (1):

$$\text{PERCLOS} = \frac{N_{\text{close}}}{N_{\text{sum}}} \quad (1)$$

$N_{\text{close}}$  is the total number of frames of closed eyes per unit time, and  $N_{\text{sum}}$  is the total number of frames per unit time. When PERCLOS is higher than 20%, the operator is judged to be in the fatigue state during the detection cycle.

## 4.2 Detection of Mouth State

There are many kinds of mouth states, and wherein, yawning is the feature of a fatigue state, so the operator can be judged as fatigue as long as the yawning mouth state is distinguished from other states. The opening degree  $O$  is calculated by the geometric shape of the mouth, the position of the mouth is marked with a rectangular frame, and the opening degree of the mouth is calculated by the ratio of the height  $H$  to the width  $W$  of the mouth:

$$O = \frac{H}{W} \quad (2)$$

Different  $O$  values represent that the mouth is in different open states. When the mouth is fully open, the  $O$  value is about 0.8. This value is taken as the threshold value to judge whether the operator yawns to determine whether he is fatigue.

## 5 Judgement of Fatigue State

Two kinds of information are fused to reduce the error, and wherein, the mouth feature (yawning) is better than the eye feature (PERCLOS). In addition, yawning lasts as long as about 5 s, which is longer than blinking in the fatigue state, so yawning is less affected by the outside. Once yawning for a long time, the operator can be judged to be in the fatigue state.

According to the PERCLOS standard used to detect the eyes state, the following two types can be divided: Awake state (PERCLOS parameter value <20%) and



Fig. 3 AdaBoost algorithm face recognition detection results

fatigue state (PECRCLOS parameter value  $\geq 20\%$ ). According to whether the operator yawns, the mouth opening sizes can be divided into two types: fatigue state (yawn) and awake state (not yawn). This paper combines the above two standards to determine whether the operator is in the fatigue state.

## 6 Result of Fatigue Test and Analysis

### 6.1 Face Recognition

The OpenCV open-source library is used to train a large number of pictures so as to get the face classifier and realize the detection and location of the face, and the results are shown in Fig. 3.

### 6.2 Fatigue Test

The test results of eyes state are shown in Table 1. The accuracy of judging fatigue by eyes state is 80.83%, which proves that the method of detecting fatigue by eyes state is feasible. At the same time, it can be seen from the results of false detection that there is still a problem if detecting fatigue only from the eyes state.

The test results of the mouth state are listed in Table 2. Sometimes the system misjudges the operator as yawning when the operator is speaking, but when yawning, because the operator's mouth opening degree is too small, it also leads to detection errors.

Table 1 Eye condition test results

State	Test QTY	Error QTY	Accuracy (%)
Normal	600	589	98.2
Fatigue	600	579	96.5

**Table 2** Mouth condition test results

State	Test QTY	Error QTY	Accuracy (%)
Normal	600	592	98.7
Fatigue	600	583	97.2

**Table 3** Combined eye and mouth features

State	Test QTY	Error QTY	Accuracy (%)
Normal	600	594	99.0
Fatigue	600	593	98.8

The combination of eyes and mouth features is listed in Table 3. When the information fusion judgment criteria proposed in this paper are used for fatigue detection, it can be seen that the accuracy of fatigue detection is significantly improved at this time, and good results are obtained.

## 7 Conclusion

This paper is based on the face recognition algorithm of the AdaBoost cascade classifier to detect human eyes and mouth, reduce the search range, and improve the speed. With the operator's eyes and mouth features extracted from the analysis, we can accurately detect fatigue. The test results show that in different environments, the method proposed in this paper can basically detect the fatigue operation in each stage; however, the detection time of the method used in this paper is long, and the detection efficiency is low. How to improve the detection efficiency will be the focus of the next stage.

## References

1. Study on human-machine interface design of nuclear power plant control room. In: 19th international conference on man-machine-environment system engineering, Shanghai, P.R. China (2019)
2. Li R, Cai B, Liu L etc (2016) Driver's eye state recognition based on model. *J Instrum* 37(1):184–191
3. Zou X, Wang S, Zhao W etc (2017) Fatigue driving detection based on state recognition of eyes and mouth. *J Jilin Univ* 35(2):204–211
4. Zhang C, Liu H, Lei B etc (2011) An image segmentation method based on rough set and FCM. *J Jiangxi Univ Sci Technol* 32(1):60–65
5. Li M, Fu M, Cao D etc (2013) Improved Adaboost face detection algorithm based on skin color detection. *Comput Eng* 38(19):147–150

6. Wang Junling, Peng Wen (2017) Face recognition algorithm based on Daubechies wavelet. J Jiangxi Univ Sci Technol 38(3):81-85
7. Kanghua Wu (2018) Design of driving fatigue detection system based on PERCLOS. Zhejiang Univ, Hangzhou

# Hybrid Model of Eye Movement Behavior Recognition for Virtual Workshop



Mengyao Dong, Zenggui Gao, and Lilan Liu

**Abstract** *Purpose* This paper is oriented to the virtual workshop scenario, discusses the creation of a feasible eye movement recognition model and provides new ideas for eye movement recognition and eye movement interaction in the virtual workshop. *Method* Obtain user's eye movement data through eye tracker in real time, create blink behavior recognition model and gaze/saccade behavior recognition model based on convolutional neural network (CNN) and bidirectional long short-term memory network (Bi-LSTM). A data set was created by collecting eye movement data of three subjects for comparative experiments to verify the performance of the proposed model. *Results* The experimental results showed that the recognition accuracy, Kappa coefficient, F1 score and running time of the proposed model had certain advantages over other models. *Conclusion* The created hybrid model of eye movement recognition for virtual workshops has high reliability and effectiveness, which will create a foundation for future research on building eye movement interaction systems.

**Keywords** Virtual workshop · Eye movement interaction · Eye movement behavior recognition · Convolutional neural network · Bidirectional long short-term memory network

## 1 Introduction

As various computer functions become increasingly powerful and the diversity of interactive systems becomes very wide, man-machine interaction becomes more frequent and complex. However, traditional interaction modes, such as keyboard and mouse interaction, are limited by shortcomings including their weak adaptability, lack of nature and insufficient input bandwidth. In addition, the "user-centered" design concept shows that man-machine interaction technology is moving toward the goal of

---

M. Dong · Z. Gao (✉) · L. Liu  
Shanghai Key Laboratory of Intelligent Manufacturing and Robotics, Shanghai University,  
Shanghai, China  
e-mail: [gaozg@shu.edu.cn](mailto:gaozg@shu.edu.cn)

© The Editor(s) (if applicable) and The Author(s), under exclusive license to Springer Nature Singapore Pte Ltd. 2021  
S. Long and B. S. Dhillon (eds.), *Man-Machine-Environment System Engineering*, Lecture Notes in Electrical Engineering 645,  
[https://doi.org/10.1007/978-981-15-6978-4\\_27](https://doi.org/10.1007/978-981-15-6978-4_27)



people-oriented, natural and efficient development. Since eyes are important organs for human beings to obtain information, eye movement is closely related to human emotional state, target of concern and intention of tasks [1]. Therefore, eye movement can be used as not only a channel for receiving information, but also an input channel for man-machine interaction, and has the characteristics of bidirectional input and output. When eye movement is used as an interactive input channel, it is needed to recognize eye movement behaviors and issue corresponding operating instructions according to the eye movement behaviors recognized. Therefore, whether the eye movement behavior can be accurately recognized as an important factor affecting the performance of the eye movement interaction system.

In recent years, the powerful representation learning capacity of in-depth learning has injected great vitality into studies of behavior recognition. It adjusts its parameters through the training of data sets to get the optimal model. The convolutional neural network (CNN) in in-depth learning is used to automatically extract features from original data, learn static features of the data and explore local features of data to achieve the aim of enhancing features and reducing parameters for model calculation. Bidirectional long short-term memory network (Bi-LSTM) has a good time-series processing ability. It grabs the sequential and antitone feature relations in data from local feature information in two directions, so as to enrich the feature representation of data [2, 3].

## 2 Eye Movement Behavior Recognition for Virtual Workshop

### 2.1 Real-Time Data Acquisition of Eye Tracker

In this paper, Tobii Glasses 2 Eye Tracker with 50 Hz sampling is used to collect the user's eye movement data in real time and the eye movement data is extracted from the recording unit of eye tracker in real time through API.

The recording unit of eye tracker consists of four API interfaces: POST API, REST API, Livestream API and Discovery API. Through calling API, the corresponding interface function is created to communicate the script with the recording unit, so as to complete information interaction. The procedure of real-time acquisition of eye movement data is as shown in Fig. 1, and the specific steps are as follows [4]:

1. Initialization: Firstly, start the recording unit of the eye tracker, initialize the API and then call Discovery API to discover the recording unit through the network, so as to create connection;
2. Transmission equipment parameters: After connecting with the recording unit, submit all relevant parameters of the eye tracker equipment to the recording unit. In this paper, the equipment parameters transmission is to initialize default value and wait for the response of the recording unit;

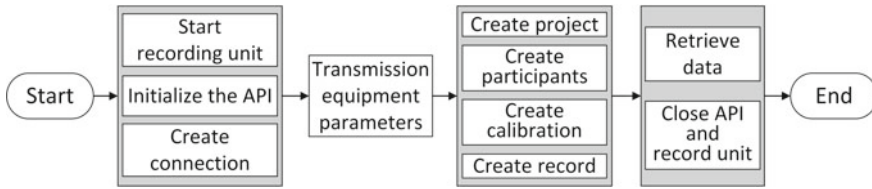


**Fig. 1** Flow chart of real-time eye movement data acquisition

3. Subscription of eye movement data: Retrieve the information of the recording unit through calling REST API, follow the steps of creating project, creating participants and creating calibration and create record to subscribe relevant eye movement data;
4. Eye movement data reception: After subscription is completed, the eye movement data returned by the recording unit will be acquired in real time. Finally, it can be ended only by closing API and the recording unit.

After the above steps are completed, the user can wear the eye tracker and run the script to extract eye tracker data in real time.

## 2.2 Eye Movement Behavior Recognition Model

Accurate recognition of eye movement behaviors is the most important part of the model created in this paper and the premise of man-machine interaction for eye movement. In this paper, with respect to three kinds of eye movement behaviors, namely blink, gaze and saccade, a hybrid model of eye movement behavior recognition for virtual workshop is established to recognize the eye movement data acquired in real time. The procedure of eye movement behavior recognition for virtual workshop is as shown in Fig. 2.

1. Eye tracker acquires user’s behaviors in real time;
2. Unity acquires eye movement data in real time with API of eye tracker;

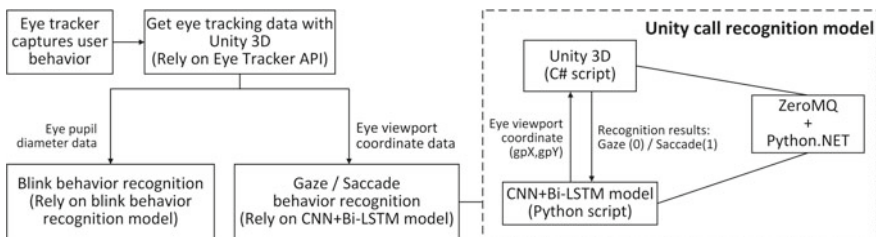


**Fig. 2** Flowchart of realizing eye movement recognition in virtual workshop

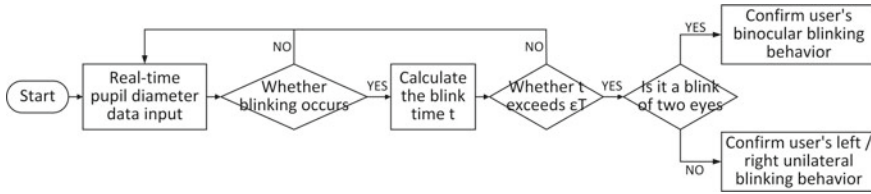


Fig. 3 Blink behavior recognition model

- 3. Eye movement behavior recognition: Blink behaviors are recognized by blink behavior recognition model, while gaze/saccade behaviors are recognized by CNN and Bi-LSTM models.

Unity call recognition model as shown in Fig. 2 mainly uses two tools, ZeroMQ and Python.NET, to realize inter-process communication between Unity and Python [5], so that Python can obtain real-time eye movement data acquired by Unity, calculate with the model and transmit the recognition results to Unity, while Python.NET is mainly to call Python scripts in C# simply and quickly to make the model work.

### 2.2.1 Blink Behavior Recognition Model

A normal person blinks more than 10 times per minute, and each blink takes 0.3–0.4 s, with an interval between blinks of 2.8–4 s. Therefore, interaction can be achieved through deliberately pausing blinks for a long time [1]. The blink behavior recognition model created in this paper is as shown in Fig. 3. According to the pupil diameter data generated by the eye tracker in real time, the threshold value  $\epsilon_T$  of the total blinking time is set up to judge conscious blinks.

### 2.2.2 Gaze/Saccade Behavior Recognition Model

The overall framework of CNN and Bi-LSTM models is based on a convolutional neural network of Marie E. Bellet et al.—U'n'Eye [6]. It conducts feature extraction for the eye movement data acquired because of its characteristics of universality and self-actuated feature extraction, extracts time-series features of data sequence in a deeper level with Bi-LSTM due to the time characteristics of eye movement data and finally conducts feature classification with the classifier. The network architecture of CNN and Bi-LSTM models is as shown in Fig. 4.

The input dimension of the model is  $N \times T \times 2$ , where  $N$  is the batch size;  $T$  is the number of time points; and 2 is the dimension of eye movement velocity calculated by the first-order difference of eye movement point coordinates.

CNN in the model mainly consists of 6 convolutional layers with kernel size 5 and 3 pooling layers. In order to accelerate convergence and avoid overfitting, each convolution layer is followed by a linear rectification activation function layer (ReLU)

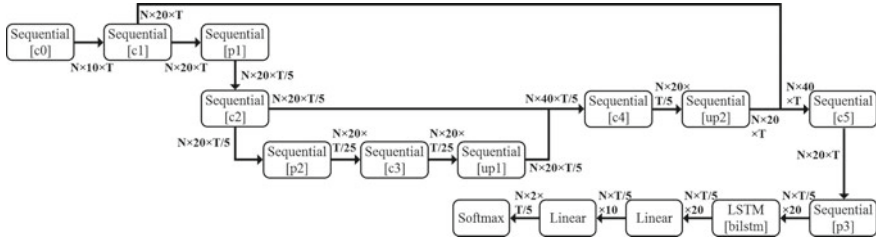


Fig. 4 CNN and Bi-LSTM models

and a BatchNorm layer. It captures the features of context information with Bi-LSTM and acquires eye movement timing information through building two LSTM layers in different directions. At the same time, the input layers of the two LSTM layers are the same [7]. Bi-LSTM is connected to the last pooling layer of CNN, and conduct time-series coding on the eye movement sequential features learned by CNN to obtain time-series feature vectors, and finally connected to the Softmax classification layer for feature classification.

The output dimension of the model is  $N \times 2 \times T/5$ , where 2 is the number of classes, that is, gaze and saccade. The Softmax classifier adopted outputs prediction probability for each eye movement class at each time point, where  $k$  represents the number of classes;  $x_i$  is the layer corresponding to class  $i$ . Therefore, when giving the eye movement velocity  $x$  and weight  $w$ , the output  $Y$  of the model represents the sample-by-sample conditional probability of each class, and the final prediction represents the class maximizing the conditional probability [6]:

$$\text{Softmax}(x_i) = \frac{e^{x_i}}{\sum_{j=1}^k e^{x_j}} \tag{1}$$

$$Y_k = p(k = 1|x, w) \tag{2}$$

$$\hat{k} = \text{argmax}_k p(k = 1|x, w) \tag{3}$$

### 3 Contrast Experiment

The eye movement data of three subjects were collected when they operated the virtual workshop application software to create the data sets. The recording time for Subject A is 00:14:08; the recording time for Subject B is 00:14:34; and the recording time for Subject C is 00:14:32. The original data includes saccade, gaze, blink and other eye movements. By preprocessing the original data, after removing the invalid data, Data Sets A, B and C contain 45, 52 and 65 8-second eye movement

track segments, respectively. The labels created for the data of gaze and saccade eye movement behaviors are 0 and 1. The data sets are randomly divided into training sets and test sets according to the proportion of 9:1.

In order to verify the effect of CNN and Bi-LSTM models on gaze/saccade behavior recognition, experiments were conducted on three test sets to compare the recognition performance of the proposed model with that of CNN, I-HMM and EM models.

Accuracy, kappa coefficient and F1 score are adopted as indexes to evaluate model performance. The accuracy is based on the confusion matrix, where TP is the number of true positives; FP is the number of false positives; FN is the number of false negatives; TN is the number of true negatives. Kappa coefficient is used for consistency test and measurement of classification accuracy. Its calculation is based on confusion matrix. F1 score is an index used to measure the accuracy of binary classification model and can be regarded as the harmonic mean of model accuracy rate and recall rate.

$$\text{Accuracy} = \frac{\text{TP} + \text{TN}}{\text{TP} + \text{FP} + \text{TN} + \text{FN}} \times 100\% \tag{4}$$

$$\kappa = \frac{p_0 - p_e}{1 - p_e} \tag{5}$$

$$F_1 = 2 \times \frac{\text{TP}}{2 * \text{TP} + \text{FN} + \text{FP}} \tag{6}$$

The recognition accuracy of each model is as shown in Fig. 5. In terms of the accuracy of gaze and saccade behavior recognition, the proposed model achieves

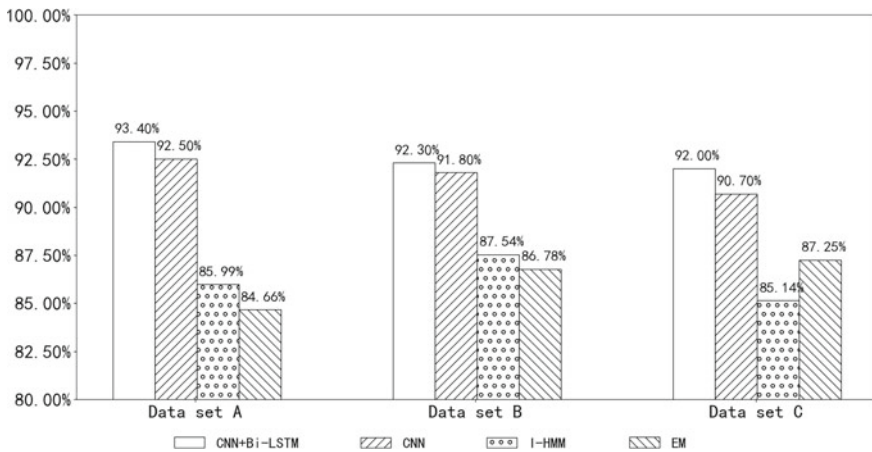


Fig. 5 CNN + Bi-LSTM, CNN, I-HMM and EM recognition accuracy comparison chart

**Table 1** Performance comparison between CNN + Bi-LSTM and other models

Data set	Performance	Models			
		CNN + Bi-LSTM	CNN	I-HMM	EM
A	Kappa coefficient	<b>0.812</b>	0.747	0.646	0.623
	F1 score	<b>0.871</b>	0.756	0.822	0.810
	Running time-consuming/s	0.0359	0.0263	0.2593	0.2025
B	Kappa coefficient	<b>0.726</b>	0.718	0.638	0.620
	F1 score	0.736	0.717	<b>0.817</b>	0.808
	Running time-consuming/s	0.0478	0.0399	0.4149	0.3142
C	Kappa coefficient	<b>0.817</b>	0.790	0.609	0.687
	F1 score	<b>0.842</b>	0.807	0.803	0.833
	Running time-consuming/s	0.0508	0.0383	0.4937	0.4109

Bold represents the best performances for each data set

the highest recognition accuracy in all three data sets, with an average recognition accuracy of 92.57%. Compared with I-HMM and EM models, its accuracy can be improved by 8% on average; compared with CNN model, its accuracy is also improved. The performance index results of Kappa coefficient, F1 score and running time-consuming for each model are as listed in Table 1, and the bold-type figures in the table represent the highest value of each index in each data set. The proposed model obtains the highest Kappa coefficient value in three data sets and the highest F1 score value in two data sets. Compared with CNN, both indexes increase; its Kappa coefficient is significantly higher than that in I-HMM and EM models; and its F1 score also reaches the level of good. In terms of running time-consuming, the running time-consuming of the proposed model is similar to that of CNN, but greatly shorter than that of I-HMM and EM models.

## 4 Discussion

According to the formulas related to blink recognition in Reference [1], a blink recognition model is created in this paper and the legal values of two eyes are determined by pupil diameter data to judge the conscious blink, together with the time threshold. With respect to gaze and saccade behaviors, Reference [1] distinguishes the gaze and saccade points with eye movement velocity according to the velocity threshold algorithm. Generally, CNN is often used in image processing. For example, the video-based CNN eye movement recognition method proposed in Reference [8] can recognize gazing behavior in eight directions. It conducts network training through establishing data sets with eye movement images. Data collection is a preprocessing of selecting useful images from eye movement videos captured and cutting them and transforming them into gray-scale images. In this paper, CNN and Bi-LSTM

models are created to distinguish eye movement behaviors through eye movement velocity features, obtain eye movement velocity data through first-order difference of obtained eye movement coordinate points as input of CNN and automatically extract eye movement velocity features. After obtaining data with eye tracker and distinguishing the data according to behaviors with supporting software of the eye tracker, we can directly get the data with behavior labels and create data sets as long as we remove the invalid data. Compared with Reference [8], the data preprocessing in this paper is more simple and convenient and can recognize two kinds of eye movement behaviors, namely gaze and saccade, with eye movement velocity features. However, the recognition effect of gazing direction needs to be further discussed.

According to the analysis of the contrast experiment results, the model based on neural network has obvious advantages in feature extraction and accurate and rapid behavior recognition. With respect to CNN model in Reference [6], this paper adds Bi-LSTM to extract the time features of data, which improves the accuracy of eye movement behavior recognition and classification performance of the model. Therefore, CNN and Bi-LSTM models are of great potential application possibility to rapid and accurate recognition of user's gaze and saccade eye movement behaviors.

In view of the small sample size of the contrast test and no special requirements for the subjects in operating the virtual workshop application program, the performance of the proposed recognition model needs to be further improved.

## 5 Conclusion

With respect to user's eye movement behaviors in virtual workshop scenes, this paper achieves rapid and accurate eye movement behavior recognition through real-time collection and transmission of eye movement data, according to the blink behavior recognition model and the gaze/saccade behavior recognition model based on CNN and Bi-LSTM, and compares its accuracy, Kappa coefficient, F1 score and running time-consuming with CNN, I-HMM and EM models to verify the feasibility of CNN and Bi-LSTM models. Finally, it is concluded that the hybrid model of eye movement behavior recognition for virtual workshop proposed in this paper can realize effective recognition of user's eye movement behaviors in a short running time, which meets the needs of rapid and accurate recognition and lays a foundation for relevant studies of eye movement interaction for virtual workshop.

**Acknowledgements** The work is supported by Shanghai Municipal Commission of Economy and Informatization of China (No. 2018-GYHLW-02009).

### Compliance with Ethical Standards

The study was approved by the Logistics Department for Civilian Ethics Committee of Shanghai University.

All subjects who participated in the experiment were provided with and signed an informed consent form.

All relevant ethical safeguards have been met with regard to subject protection.

## References

1. Wang S, Wang Q, Chen H et al (2018) Research and application of eye movement interaction based on eye movement recognition. MATEC web of conferences 246
2. Zheng Z, Li L, Jing C (2018) Deeply hierarchical bi-directional LSTM for sentiment classification. *Comput Sci* 045(008):213–217,252
3. Xiao-ying WU, Rui LI, Sheng-xi WU (2020) Action recognition algorithm based on CNN and bidirectional LSTM. *Comput Eng Des* 41(02):361–366
4. Xin L (2019) Research on intelligent human-computer interaction technology and application based on eye movement. Nanjing University
5. Pai YS, Dingler T, Kunze K (2019) Assessing hands-free interactions for VR using eye gaze and electromyography. *Virtual Reality* 23:119–131
6. Bellet Marie E, Bellet Joachim, Nienborg Hendrikje et al (2019) Human-level saccade detection performance using deep neural networks. *J Neurophysiol* 121:646–661
7. Tian-yi LUO, Da-yun LIU, Xiu-zheng LI et al (2019) Research on lip-reading recognition based on CNN and Bi-LSTM. *Software Guide* 18(10):36–39
8. Bing C, Chao Z, Xiaojuan D et al (2018) Convolutional neural network implementation for eye movement recognition based on video. In: *Proceedings—2018 33rd youth academic annual conference of chinese association of automation, YAC2018*, pp 179–184



# Research on Influence of Organizing and Training Capabilities Towards Officers Positions Capabilities



Junlong Guo, Zaochen Liu, Jianfeng Li, and Jiwen Sun

**Abstract** Practical teaching is the main path to cultivate and improve combat capabilities of growing cadre cadets Li (The new phase in new century research on military academy transformation construction and talents cultivation (Part 1), 2005 [1]). As the main evaluation, contents of practical teaching organizing and training capabilities include writing teaching schemes, drawing up working plans, giving lessons and conducting training. Organizing and training capabilities have a fundamental and promoting role on the formation of organizing and commanding capabilities; they also have a guiding and facilitating role on management and political work; and they take on an elevating role on coordinating, controlling and adapting to changing circumstance. By intensifying their qualities, cultivating good personality, establishing a sense of responsibility and grasping the soldiers' thoughts the grassroots officers must improve their organizing and training capabilities, and at the same time, promote their first-position capabilities Zhou (A study on the basic standard of growing officers cultivation, 2005 [2]).

**Keywords** Practical teaching · Organizing and training capabilities · Commanding officers · Positions

During position training of growing cadre cadets, practical teaching percentage is up to 60%; the basic position courses and the main evaluating contents of practical teaching in professional position courses operating skills and organizing and training capabilities directly influence their cultivation of the first-position capability.

---

J. Guo · Z. Liu · J. Li · J. Sun (✉)

Army Academy of Artillery and Air Defense, Zhengzhou Campus, 450052 Zhengzhou, China  
e-mail: [269596825@qq.com](mailto:269596825@qq.com)

© The Editor(s) (if applicable) and The Author(s), under exclusive license to Springer Nature Singapore Pte Ltd. 2021

S. Long and B. S. Dhillon (eds.), *Man-Machine-Environment System Engineering*, Lecture Notes in Electrical Engineering 645, [https://doi.org/10.1007/978-981-15-6978-4\\_28](https://doi.org/10.1007/978-981-15-6978-4_28)

# **1 Contents that Organizing and Training Capabilities Contain**

Organizing and training capabilities refer to the following ones such as writing teaching schemes, drawing up working plans, giving lessons and conducting training, in which weapons and equipment operation is considered as the main contents.

## ***1.1 Writing Teaching Schemes***

Teaching schemes are the products in which trainers combine teaching contents with detailed practice; it is the personalized lecture notes that trainers create according to lecturing style and units training practical situation.

From the nature of the training contents and training stages, teaching schemes can be classified into different types such as common subjects, specialized technology or operating skills, specialized tactics and combined tactics. From the angle of the training contents coverage or application time span, they can be classified into the following types such as the whole process of the subjects, special topics and teaching periods. From the angle of the application form, they can be classified into the following types such as narrative contents, explanatory contents, reading contents, discussing contents and demonstrating contents. From the angle of compiling form and adoptable pattern, they can be classified into the following types such as written description, formats and map lettering [3].

## ***1.2 Drawing up Working Plans***

### **1.2.1 Basis for Drawing up Military Training Plans**

Drawing up military training plans must be based on military training syllabus; they should be drawn up in accordance with the real situation such as forces (units) operation tasks, training levels, support capabilities, weapons and equipment conditions and geographically environmental characteristics.

### **1.2.2 The Form of Military Training Plans**

According to the contents of training plans, the tabular text plans fill the related contents with different items of the form one by one. Written description plans are compiled in the light of the narrative pattern, the layout of the whole training work is clearly differentiated and stated one by one. According to the training process and

the organic linkage among different subjects, network lettering plans are made into network operational map [4].

### **1.2.3 The Contents of Military Training Plans**

Forces (units) training majors include gunners, radar operators, testers, scouts, plotters, diesel engine operators, weathermen, telephone operators, wireless operators, cook, technicians and drivers.

Training subjects reflect the main training contents annually, embody the basic training procedures annually and reveal the intrinsic connection among different subjects. Annual training subjects for units generally are composed of common training, individual training, squad (group, section, station, platoon) training, battery (battalion) training and army group (brigade, regiment) training, etc.

Annual index of training contents must complete the training contents required according to the requirements of military training syllabus. The training plans need mark different training stages, the detailed training contents, the index and measures in accordance with task need and the real forces (units) situation.

## ***1.3 Giving Lessons in the Classroom***

### **1.3.1 Preparing Lessons**

Preparing lessons must be based on the requirement of cultivation schemes [5] and courses standard, trainers need to investigate and research teaching objects, familiarize textbooks and teaching contents, make course designs very well.

### **1.3.2 Trial Lessons**

Combined with the teaching sites and equipment, trial lessons should be conducted according to the real teaching procedures and requirements.

### **1.3.3 Teaching Implementation**

In the actual operations, trainers should clearly describe its purpose, contents and requirements and demonstrate those when explaining the contents, in the meantime point out possible barriers and preventive measures. The whole working procedures should be from simple, individual and separate way to complicated, integrated and joint way.

## ***1.4 Implementing Training***

### **1.4.1 Teaching Demonstration and Practicing**

Teaching demonstration and practicing are the demonstration of the teaching methods and training methods. Generally combining with the actual objects, equipment and models the trainers or the demonstrators teach their operating essentials and demonstrate the training methods through the whole flow and steps [6].

### **1.4.2 Conducting Exercise**

Before exercise trainers should make clear training contents, methods, steps and requirements to the soldiers, distinguish training sites and equipment, etc. Exercise should abide by the following sequences: imitating, reinforcing and applying. The methods can be followed in accordance with decompositions, steps, stages, integrations, evaluation and competitions.

### **1.4.3 Checking and Evaluating**

Checking is divided into general test and selective test. According to training grouping, general test should be organized and conducted by battery units or trainers who are in charge of professional training or may be organized and conducted by professional departments in brigade or regiment level. Selective test should be organized by professional departments in battalion or brigade (regiment) level generally after professionally individual training is over.

## **2 Influence of Organizing and Training Capabilities Towards Officers Position Capabilities**

### ***2.1 It Plays a Fundamental and Promoting Role on the Formation of Organizing and Command Capabilities***

That one can organize and conduct training means that he or she can prepare for plan very well ahead of time, can coordinate and control in the training process and can summarize and evaluate in the terminal stage. In the meantime, scientific training methods are also scientific organizing ones and are the forming fundament to

organizing and commanding capabilities of junior commanding officers; they have imperceptible promoting role on the formation of their organizing and command capability.

## ***2.2 It Plays a Leading and Catalytic Role on Management and Political Work***

By organizing and training junior, commanding officers strengthen constraints and guidance to soldiers, achieve ideal management effect relying on training and further improve the formation of their management and education capabilities. In the training process, they conduct organizing and training by acting as commanders in rotation, experience the capability demand in different positions, practice and promote management capabilities. Through a series of activities such as propaganda, competition and evaluation, they arouse training enthusiasm of soldiers and improve the pertinence and timeliness of political work.

## ***2.3 It Plays Progressive Role on Such Capabilities as Coordination, Control and Adapting to the Changing Circumstance***

Through a series of activities such as preparing training sites and equipment, designing training background and holding joint teaching conferences, all capabilities of trainers such as organizing and planning, communicating skills, coordination and control, temporary adaptability, finding and solving problems can be correspondently practised and improved with the four working practice of organizing and training capabilities.

# **3 Methods by Which Improving Organizing and Training Capabilities for Officers**

## ***3.1 Intensifying Personal Quality***

Firstly, grassroots officers should build a right outlook on life. When remaking objective world, they should work hard to remake subjective world and try to make their thoughts conform to development law and keep up with the times. Secondly, they should study modern military knowledge with advanced science and technology. They should focus on researching their professional work, familiarize the

performance of equipment, organizing technological training and cultivate excellent working style. Thirdly, they should reinforce accumulation about scientific and cultural knowledge. They should attach importance to studying and accumulating cultural knowledge, lead soldiers to make great progress and adapt the demand for future war.

### ***3.2 Cultivating Good Character***

Firstly, they should teach trainees by personal example as well as verbal instructions. They should lead soldiers through good military and political quality, educate soldiers by explaining profound theory in a simple way, influence soldiers by their own experience. Secondly, they should build their own image by exemplary action. Officers should set a good example for soldiers, keep “follow-me” enthusiasm and “watch-me” standard at any time. Thirdly, they should influence soldiers through strict fighting style. They should be strict with themselves and set a good example for soldiers by selfless work and hard-working spirit.

### ***3.3 Building a Sense of Responsibility***

Firstly, grassroots officers should improve political awareness and regard political qualification as the prime requirements, attach importance to studying political theory, develop political work and others by their positions and responsibilities. Secondly, they should reinforce their self-cultivation, focus on developing good military tradition and guide their own words and deeds by morality, set a good example for soldiers. Thirdly, they should intensify their responsibilities and awareness by law; they should make education, managements, training and security further standardized and institutionalized and bring soldiers to perform all tasks legally.

## **References**

1. Li C (2005) The new phase in New Century research on military academy transformation construction and talents cultivation (Part 1), vol 231, Haichao Press, Beijing, pp 1–11
2. Zhou Q (2005) A study on the basic standard of growing officers cultivation, vol 12. Haichao Press, Beijing, pp 4–9
3. Cai J (2009) On units military training methods, vol 146. Xian Army Academy, Xian, pp 5–21
4. Wu W (1992) On military training methods of AA gun units for army air defense force. Tactical teaching & researching section of Zhengzhou Anti-aircraft Artillery Academy
5. Zhang J (2012) An effective study on military position education, vol 50. Military Science Press, Beijing, pp 17–21
6. Meng F (2009) On army units military training, vol 100. Military Science Press, Beijing, pp 10–14

# Interaction Effect of Workload and Circadian Rhythm in Air Traffic Controllers' Fatigue



Zhenling Chen, Jianping Zhang, Guoliang Zou, Pengxin Ding, Shunqing Li, Yanzhong Gu, and Yiyou Chen

**Abstract** *Objective* To investigate interaction effect of workload and circadian rhythm in air traffic controllers' fatigue. *Methods* At one busy international airport, air traffic controllers for the terminal area were recruited in this study. The volunteers were asked to fill out the questionnaire of the Stanford Sleepiness Scale about their fatigue feelings before, in the middle, and after their work. The questionnaire survey followed up with four-period groups including morning, afternoon, the first half of the night, and the second half of the night. The statistical results of the questionnaires showed that the fatigue levels of air traffic controllers increased very significantly during work periods; the levels were also influenced by circadian rhythm. The covariance analysis results showed that there was a very significant interaction effect of workload and circadian rhythm. *Conclusions* There existed a very significant interaction effect of workload and circadian rhythm in air traffic controllers' fatigue. These results require more objective data to verify and will prompt to consider the effect in the assignment of workload and human resource for fatigue management.

**Keyword** Fatigue · Air traffic controller · Workload · Circadian rhythm

---

Z. Chen · J. Zhang (✉) · P. Ding · S. Li · Y. Gu · Y. Chen  
The Second Research Institute of Civil Aviation Administration of  
China, 610041 Chengdu, China  
e-mail: [zhangjp@caacsri.com](mailto:zhangjp@caacsri.com)

Z. Chen  
Civil Aviation Medicine Center, Civil Aviation Administration of China (Civil Aviation Hospital),  
100123 Beijing, China

G. Zou  
Air Traffic Management Regulation Office, Civil Aviation Administration of China, 10071  
Beijing, China

P. Ding  
College of Computer Science, Sichuan University, 610056 Chengdu, China

Y. Chen  
Civil Aviation Flight, University of China, 618307 Guanghan, China

# 1 Introduction

The fatigue of air traffic controllers (ATCO) seriously threatens aviation safety. In March and April 2011, the incidences of ATCO sleeping on duty occurred continuously four times in the USA [1]. In July 2014, ATCO at Tianhe Airport, Wuhan slept on duty [2]. In Oct. 2017, a serious runway incursion incidence of two passenger aircrafts occurred at the Tongren Fenghuang Airport. According to the incidence investigation report, the partial ability of the air traffic controller was disturbed by fatigue risk causing his performance to decrease [3]. The International Civil Aviation Organization (ICAO) convened a symposium on fatigue management on the theme of “evolution from the cockpit to the air traffic control unit” in 2016 [4]. The fatigue management of ATCO became a research hotspot in recent years [5, 6]. Based on the summary of previous related works, the four scientific principles for fatigue management were put forward in the document of ICAO including circadian rhythm effects and workload influence [7]. In recent years, the workloads of ATCO continued increasing along with the rapid growth of air traffic. Meanwhile ATCOs’ work on 24/7 schedules under the pressure of circadian rhythm. It is necessary to understand whether there is interaction effect between workload and circadian rhythm in ATCOs’ fatigue in order to manage fatigue effectively. In this paper, we investigated the fatigue of air traffic controllers working for the terminal area at one international airport with the Stanford Sleepiness Scale. The statistical analysis of questionnaires showed that there was an interaction effect in ATCOs’ fatigue. The results will prompt to consider the interaction effect when arranging workload and human resource for fatigue management.

## 2 Experiment

### 2.1 Questionnaire Survey

The study was carried out at one busy international airport where the number of takeoff and landing flights was over 1000 a day during our survey period. Volunteers of air traffic controllers who worked for the terminal area at the airport were recruited in this study. On the premise to limit disturbance to the bare minimum possible to ATCOs’ work, we selected the Stanford Sleepiness Scale as the fatigue questionnaire which was simple, only having 7 options, easy to understand, reliable, and valid [8, 9]. The volunteers were required to fill out the questionnaire just before, in the middle, and just after they were on duty. We surveyed the volunteers working on the four periods separately including 8:00–12:00, 12:00–18:00, 18:00–24:00, and 0:00–8:00 described as morning (I), afternoon (II), the first half of the night (III), the second half of the night (IV). The volunteers were male, aged from 23 to 35, on average 28.4. The survey was carried out from Aug. 26 to 30, 2019. 205 person-times took part in the experiment, and 600 completed questionnaires were collected.



## 2.2 Statistical Analysis

The collected questionnaires were input into excel table and analyzed with statistical analysis. The repeated measures analysis of variance, multiple comparison analysis, and covariance analysis were employed to analyze the questionnaires.

## 3 Results and Discussion

Air traffic controllers for the terminal area at an airport are responsible for commanding departure and arrival flights. Therefore, the workloads of ATCO for the terminal area are able to be estimated based on the number of departure and arrival flights. The airport selected in this study is one busy international airport with a throughput of over 1000 flights per day based on two runways. The departure and arrival flight rate distribution per day are shown in Fig. 1 during the study period. The number of flights was not uniformly distributed among 24 h a day. The total flight rate was only about 22.6% from 0:00 to 8:00 in the second half of the night (IV) for 8 h, average rate (AR) 2.8% per hour. The total flight rate was about 20.2% from 8:00 to 12:00 in the morning (I) for 4 h, AR 5.0% per hour. The total flight rate was about 29.3% from 12:00 to 18:00 in the afternoon (II) for 6 h, AR 4.7% per hour. The total flight rate was about 27.9% from 18:00 to 24:00 in the first half of the night (III) for 6 h, AR 4.6% per hour. These data indicated the workload level of ATCO in the four periods.

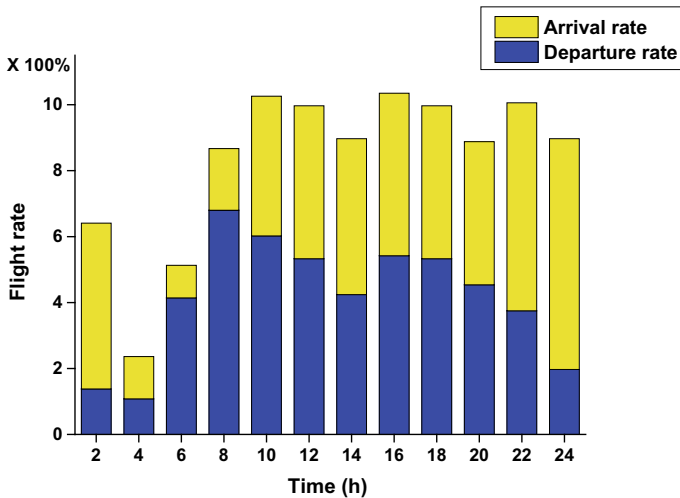
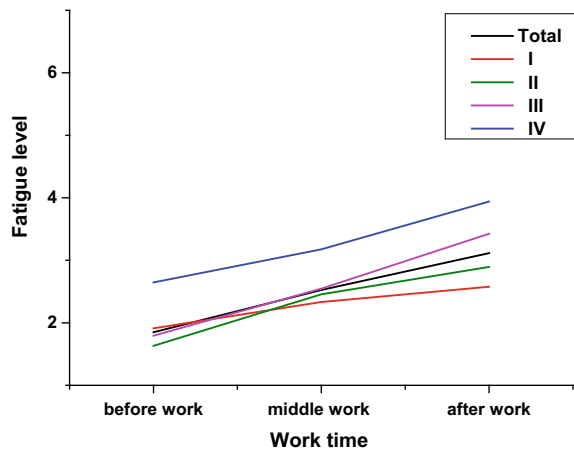


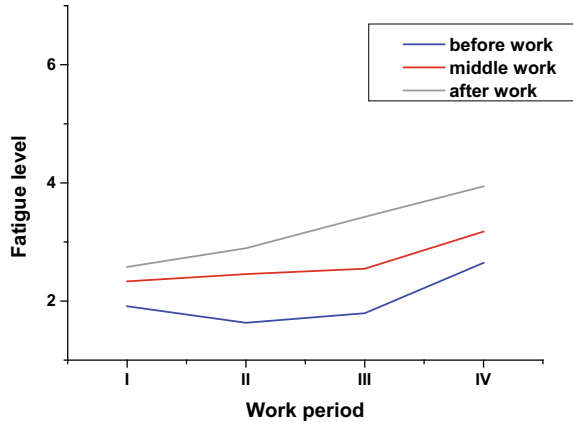
Fig. 1 Distribution of takeoff and landing flight rate per day

We investigated the influence of workload to ATCOs' fatigue. The three questionnaires including a volunteer before, middle, and after work regarded as a whole set of questionnaires for one person-time. Box-plot analysis was employed to examine abnormal values, and 8-set data were rejected. 192 person-times and their 576 questionnaires were input into the following analysis. Firstly, we analyzed the workload influence to fatigue levels (Fig. 2). The variance analysis was employed to treat the repeated measure data of before, middle, and after work. The result showed that the influence of workload to ATC fatigue was very significant ( $P < 0.001$ , Fig. 2 black line). Multiple comparison analysis of the repeated measure data discovered that the fatigue levels in the middle work (mean 2.53) and after work (mean 3.11) were very significant increase compared with that before work (mean 1.85), respectively ( $P < 0.001$ ,  $P < 0.001$ ), and the fatigue level after work (mean 3.11) increased very significantly compared with that in the middle of work (mean 2.53) ( $P < 0.001$ ). These results declared that the ATCOs' duty-work resulted in their fatigue level rapid increasing, and the fatigue level kept to increase rapidly along with work time extension as workload accumulation. We further investigated the influence of the different workloads in the four periods. The workloads in IV period were lighter than that in other three periods as above analysis. However, the fatigue level after work (IV mean 3.94) in IV period (Fig. 2 blue line) was very significant higher than that in other three periods (I mean 2.58, II mean 2.89, and III mean 3.42, in Fig. 2 the red, green, and purple lines). And even the fatigue level before work (IV mean 2.65) in IV period was higher than that after work in I period. Although the workloads were almost equal in I, II, and III periods, the growth levels of fatigue for the three periods were not equal, and the most rapid increment occurred in the III period. These results indicated that the workload was not the unique factor which leads to ATCOs' fatigue level increasing, the period for work in a day circle as circadian rhythm factor was another important reason necessary to consider seriously.

**Fig. 2** Fatigue levels of ATC changing along with before, middle, and after work



**Fig. 3** Fatigue levels of ATC changing along with work period



The circadian rhythm influence and the interaction effect between circadian rhythm and workload to ATCOs' fatigue were investigated. In order to provide the 24 h continuous air traffic service for the international airport, several kinds of work shifts coexisted on the schedules for ATCO for the terminal area. We selected the ATCO group working in the morning (I), afternoon (II), the first half of the night (III), and the second half of the night (IV) for the circadian rhythm study. The person-times distribution in the four periods were 45 (I), 57 (II), 73 (III), 17 (IV). The variance analysis of independent measurement for questionnaires before work in four periods discovered that ATCOs' fatigue level in IV period (Fig. 3 blue line) was very significantly high compared with that in I period ( $P < 0.002$ ), II period ( $P < 0.001$ ), and in III period ( $P < 0.001$ ). There was no significant difference of fatigue level appeared among I, II, and III periods. These analysis results of ATCOs' fatigue level data before work indicated that the ATCOs' volunteers' fatigue level fluctuated smoothly from 8:00 to 18:00 in the daytime and significantly increased up in the second half of the night. This changing curve coincided with cortisol production of a kind of general circadian rhythm which kept a stable level during day time and changed significantly decreased at night, while melatonin (another circadian rhythm related secrete) began to increase secretion and lead to people sleepy [10, 11]. The variance analysis of independent measurement employed to the questionnaires in the middle of work in four periods (Fig. 3 orange line). The results were similar to that before work. The fatigue level in IV period was significantly higher compared with that in other three periods, concretely very significantly high with that in I period ( $P < 0.001$ ), in II period ( $P < 0.003$ ), and in III period ( $P < 0.009$ ). And there was no significant difference among I, II, and III periods. Then, the variance analysis of independent measurement employed to the questionnaires after work in four periods (Fig. 3 gray line). The results showed different to those before and in the middle of work. The fatigue levels in III and IV periods were very significantly higher compared with that in I and II periods. Concretely, the fatigue level in IV period was very significant high compared with that in I period ( $P < 0.001$ ) and II period ( $P$

< 0.001), and no significance with that in III period ( $P < 0.086$ ); the fatigue level in III period was very significant high compared with that in I period ( $P < 0.001$ ) and II period ( $P < 0.007$ ); the fatigue level in II period was no significance with that in I period ( $P < 0.059$ ). The sharp increase of the fatigue level in III period after work strongly suggested that there was very possibly an interaction effect between circadian rhythm and workload. Furthermore, the multiple factors covariance analysis employed to the questionnaires. The result showed that the interaction effect of workload and circadian rhythm was very significant ( $P < 0.001$ ).

## 4 Conclusion

Many evidences have made clear that either workload or circadian rhythm is able to result in ATCOs' fatigue [5, 7]. However, workload and circadian rhythm were usually regarded as independent factors [12, 13]. To our knowledge, we investigated and preliminarily demonstrated the interaction effect of workload and circadian rhythm in ATCOs' fatigue with the questionnaire survey. Moreover, the interaction effect requires more objective data to verify and deeply understand the interaction mode of workload and circadian rhythm.

In conclusion, ATCOs' fatigue seriously menaces the aviation safety. Either workload or circadian rhythm leads to ATCOs' fatigue. In air traffic control work conditions, the two factors often appeared simultaneously. It is necessary to learn the relationship of workload and circadian rhythm in ATCOs' fatigue in order to manage fatigue effectively. In this study, we preliminarily demonstrated the interaction effect of workload and circadian rhythm in ATCOs' fatigue with subjective questionnaire survey. The effect requires objective data to verify and further explore the interaction mode of workload and circadian rhythm. The results will help to arrange workload and human resource for fatigue management more efficiently.

**Acknowledgements** We acknowledge the financial support of the Sichuan Science and Technology Program, under Grant 2019YFG0390, Safety Foundation of Civil Aviation Administration of China, and the Joint Funds of the National Natural Science Foundation of China (No. U1333132).

**Compliance with Ethical Standards** The study was approved by the Logistics Department for the Civilian Ethics Committee of the Second Institute of Civil Aviation Administration of China. All subjects who participated in the experiment were provided with and signed an informed consent form. All relevant ethical safeguards have been met with regard to subject protection.

## References

1. Levin A (2011) Four more air controllers suspected of sleeping on the job, government says. USA Today, April 11. Retrieved from <http://travel.usatoday.com/flights/story/2011/04/FAA-Four-more-air-controllers-suspectedof-sleeping-on-the-job/46087082/1>

2. Southcentral Regional Administration of Civil Aviation Administration of China (2014) Report the investigation report on the air traffic controller sleeping on duty causing CEA MU2528 go around, Plain code telegram form the Southcentral Regional Administration [2014]1289
3. Southwest Regional Administration of Civil Aviation Administration of China (2017) Report on the investigation and handing of the runway incursion incidence at the Tongren Fenghuang airport in Oct. 10, Plain code telegram form the Southwest Regional Administration [2017]2096
4. ICAO FMA symposium (2016) <https://www.icao.int/Meetings/fmas/Pages/default.aspx>
5. Nalley MA, Gawron VJ (2015) The effect of fatigue on air traffic controllers. *Inter J Aviat Psychol* 25:14–47
6. Chen Z, Xu X, Zhang J et al (2016) Application of LC-MS-based global metabolomics profiling methods to human mental fatigue. *Anal Chem* 88:11293–11296
7. International Civil Aviation Organization (2016) Doc 9966 (2nd edn), Manual for the oversight of fatigue management approaches
8. Arora V, Dunphy C, Chang VY et al (2006) The effects of on-duty napping on intern sleep time and fatigue. *Ann Intern Med* 144:792–798
9. Hoddes E, Zarcone V, Smythe H et al (1973) Quantification of sleepiness: a new approach. *Psychophysiology* 10:431–436
10. Den R, Toda M, Nagasawa S et al (2007) Circadian rhythm of human salivary chromogranin A. *Biomed Res* 28:57–60
11. Carrier J, Monk TH (2000) Circadian rhythms of performance: new trends. *Chronobiol Inter* 17:719–732
12. Grech MR, Neal A, Yeo G et al (2009) An examination of the relationship between workload and fatigue within and across consecutive days of work: Is the relationship static or dynamic? *J Occup Heal Psychol* 14:231–242
13. May JF, Baldwin CL (2009) Driver fatigue: the importance of identifying causal factors of fatigue when considering detection and countermeasure technologies. 12:218–224

# A PERCLOS Method for Fine Characterization of Behaviour Circadian Rhythm



Yanzhong Gu, Zhenling Chen, Jianping Zhang, Guoliang Zou, Pengxin Ding, and Weinan Deng

**Abstract** *Objective* To establish a measurement method of the percentage of eyelid closure over the pupil over time (PERCLOS) to finely characterize behaviour circadian rhythm. *Methods* A computer program was designed based on multitask convolutional neural network for the treatment of videos to get PERCLOS quantitative values. 7 volunteers were recruited in this research. The volunteers were asked to face the personal computers and play a simple game for 5 min, doing the test 4 times a day that was just after getting up in the morning, at noon, in the evening and just before going to bed. Their videos were recorded and treated with the computer program to obtain PERCLOS results. The results showed that the PERCLOS values of 6 young persons increased from morning to night in accordance with the circadian rhythm of youth, while an elder female volunteer showed a different circadian rhythm from that of the youth. *Conclusions* The PERCLOS method for characterization of behaviour circadian rhythm was successfully developed, which would serve as effective tool for circadian rhythm related studies.

---

Y. Gu · Z. Chen · J. Zhang (✉) · P. Ding · W. Deng  
The Second Research Institute of Civil Aviation Administration of China, 610041  
Chengdu, China  
e-mail: [zhangjp@caacsri.com](mailto:zhangjp@caacsri.com)

Z. Chen  
e-mail: [chenzhenling@caacsri.com](mailto:chenzhenling@caacsri.com)

Y. Gu · W. Deng  
Civil Aviation Flight, University of China, 618307 Guanghan, China

Z. Chen  
Civil Aviation Medicine Center, Civil Aviation Administration of China (Civil Aviation Hospital),  
100123 Beijing, China

G. Zou  
Air Traffic Management Regulation Office, Civil Aviation Administration of China, 10071  
Beijing, China

P. Ding  
College of Computer Science, Sichuan University, 610056 Chengdu, China

© The Editor(s) (if applicable) and The Author(s), under exclusive license to Springer Nature Singapore Pte Ltd. 2021

S. Long and B. S. Dhillon (eds.), *Man-Machine-Environment System Engineering*, Lecture Notes in Electrical Engineering 645,  
[https://doi.org/10.1007/978-981-15-6978-4\\_30](https://doi.org/10.1007/978-981-15-6978-4_30)

**Keywords** Percentage of eyelid closure over the pupil over time · Circadian rhythm · Multitask convolutional neural network

## 1 Introduction

Circadian rhythm exists in human body and influences people's life and production. The discovery of the molecular mechanism for circadian rhythm in organisms won the Nobel Prize in 2017 [1]. Circadian rhythm molecular mechanism controls body's nervous systems and influences body behaviours, further affecting people's life and production, such as to keep health, to work at sunrise and sleep at sunset and to lead to fatigue and further decreasing productivity, threatening production safety. The circadian rhythms of individuals are regulated by endogenous (e.g., circadian pace-maker, peripheral oscillators, clock genes) and exogenous factors (e.g., light, feeding, age, social behaviour, work and schedules) and are different from each other [2, 3]. Therefore, it is necessary to establish simple and objective methods to learn individual behaviour circadian rhythm more precisely and accurately in order to arrange individual life more efficiently, keep health and ensure production safety. There are several methods available to assess circadian rhythm including measurement of core body temperature and melatonin, cortisol production, questionnaires, actigraphy. The methods for measurement of temperature, melatonin and cortisol production require rigid detection conditions to avoid disturbances. The questionnaires are subjective and classify only rough three kinds. The actigraphy is susceptible to masking and artefacts [4]. In this paper, we established a behavioural method to finely characterize circadian rhythm through measurement of volunteers' eye behaviours by combining convolutional neural network and the percentage of eyelid closure over the pupil over time (PERCLOS). The method was applied to 7 volunteers. The results showed that 6 young volunteers' PERCLOS values increased from morning to night in accordance with the circadian rhythm of youth. The method is easy to operate and objective. There is reason to believe that the established method will expand to use and help individuals to learn their behavioural circadian rhythm and arrange their life more efficiently.

## 2 Experiment

### 2.1 *Establishment of the Convolutional Neural Network Model*

The Keras was applied to construct the neural network model on the platform of IntelCore i7, NVIDIA GTX 1080Ti GPU and the operating system of Ubuntu 16.04. The convolutional neural network (CNN) model was written in Python programming language. The model consisted of three convolutional layers, three maximum pooling

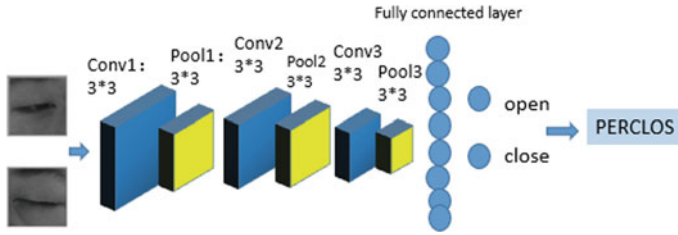


**Fig. 1** Structure of the convolutional neural network model for PERCLOS detection

layers, one fully connected layer and a sigmoid classifier (Fig. 1). The Zhejiang University (ZJU) public data (index P70) was set as the training data. The input image was a  $26 * 34$  greyscale image. After a convolution layer,  $26 * 34 * 32$  feature maps were output. After a maximum pooling layer,  $13 * 17 * 32$  feature maps were output. After the second convolution layer,  $13 * 17 * 64$  feature maps were output. After the second maximum pooling layer,  $6 * 8 * 64$  feature maps were output. After the third convolutional layers,  $6 * 8 * 128$  feature maps were output. After the third maximum pooling layer,  $3 * 4 * 128$  feature maps were obtained. Then, the feature maps dimension was transformed into one-dimensional vector with inputting a fully connected layer, of which the length was 512, and finally, through sigmoid classifier classification, results were output with the category of open or close status.

## 2.2 Data Collection and Treatment

7 healthy volunteers were recruited in this research: one was a female at the age of 51 and the other 6 volunteers were aged from 25 to 30, 3 male. During the experiment, the volunteers were on their holidays and woke up naturally without drinking coffee or tea. Each volunteer was asked to play a simple game on a personal computer with a camera to get his/her videos for 5 min on the test. The speed of collecting videos was 24 images every second. The volunteers were required to do the test 4 times a day that was just after getting up in the morning (I), at noon (II), in the evening (III) and just before going to bed (IV).

The collected videos were treated with the CNN model according to the process as shown in Fig. 2. Briefly, the video was inputted into multitask convolutional neural network (MTCNN) to detect the face and locate the eyes. Then the image was converted into greyscale image by greyscale processing. The greyscale image was processed with the combination of convolutional layer and pooling layer \* 3, and the feature maps dimension was transformed into one-dimensional vector with inputting a fully connected layer. Finally, the classification results of open or close status were output through sigmoid classifier as the PERCLOS value and recorded as 0 for open or 1 for close. The PERCLOS values were calculated out as an average percentage of close status every minute.



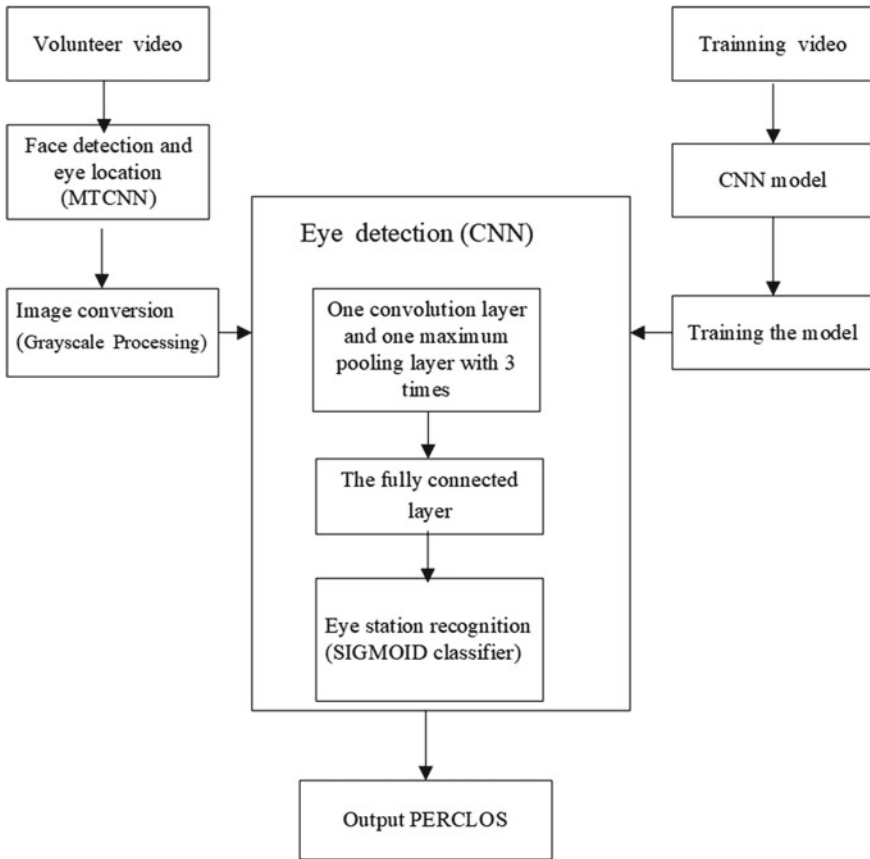


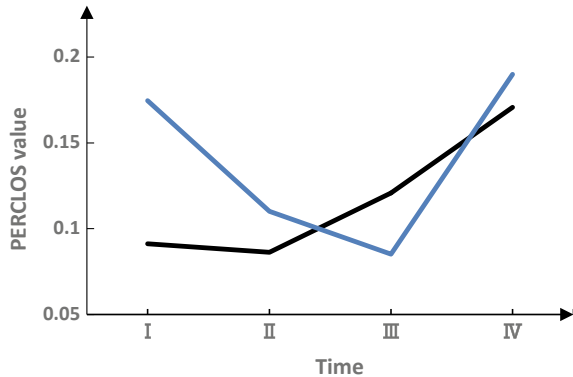
Fig. 2 Process of volunteer video treatment for PERCLOS

The PERCLOS data were treated with variance analysis, repeated measurement and multiple comparisons.

### 3 Result Discussion and Conclusion

In the recent years, the application of convolutional neural network algorithm to PERCLOS detection became prevalent because of its good performance and easy to get related resources [5]. In this study, we established a CNN model for PERCLOS detection. In order to increase the CNN model performance, we employed the ZJU public database to train and optimize the parameters of the model. There were two kinds of images in the ZJU database including 7000 eye open images and 1984 eye close images. 5770 eye open images applied to training, the other 1230 to test. And

**Fig. 3** Curve of PERCLOS values



1574 eye close images applied to training, the other 410 to test. After the training, the validation accuracy rate of the model reached about 99.96%, which was a satisfactory result in eye detection for PERCLOS values.

For face detection and eye location, we compared MTCNN algorithm and Haar-like algorithm. Results showed that the Haar-like algorithm was tended to false recognition that nares recognized as eyes. However, we found that MTCNN algorithm overcame the difficulty easily in accordance with other researchers [6].

The PERCLOS detection results for volunteers in 4 certain times (including I, II, III, IV time) shown in Fig. 3. We noted that volunteers were tending to shake their heads at the onset of tests. Therefore, we intercepted videos from 2 to 5 min for statistical analysis. In considering the influence of age, we separated the 7 volunteers into two group as young group (aged from 25 to 30, black curve in Fig. 3) and elder group (blue curve in Fig. 3). The results of young group showed that the average PERCLOS values were 0.091 (I), 0.086 (II), 0.121 (III), 0.172 (IV) for 4 times, and their standard deviations were 0.018 (I), 0.016 (II), 0.024 (III), 0.032 (IV), separately. The PERCLOS data of young group were analysed with 1-factor repeated measures analysis of variance, multiple comparison analysis and pairwise T-test. The results showed that: circadian rhythm effect was very significant ( $P, 0.001$ ); the PERCLOS value of IV time was significantly different from that of I ( $P, 0.007$ ), II ( $P, 0.016$ ) and III ( $P: 0.016$ ); while the average PERCLOS value of I time was not significantly different from that of II ( $P, 0.672$ ) and that of III ( $P, 0.330$ ), the average PERCLOS value of II time was not significantly different from that of III ( $P, 0.350$ ). The curve of PERCLOS was stable at the onset part from I to III, appearing no significant difference among the three times and increased sharply at the IV time, appearing significant difference from I to III time. These results illustrated that people keep energetic in the daytime from morning to evening (from I to III) and fell to sleepy at night (at IV). The curve of PERCLOS was similar to cortisol production of youth which kept a stable level during daytime and changed significantly decreased at night, while melatonin (another circadian rhythm-related secrete) began to increase

secretion and lead to people sleepy [7, 8]. In order to investigate the effectivity, we recruited an elder female volunteer for the test. Her PERCLOS curve (blue curve in Fig. 3) was very different from that of young persons (black curve in Fig. 3). In the morning and at noon, she showed sleepier than youth, and her energetic time was in the evening. These results indicated that our PERCLOS method was able to distinguish the different circadian rhythm effectively and to finely characterize individual circadian rhythm.

Circadian rhythm is very important for children growing, people health and production. Several methods have established for learning individual circadian rhythm, but these methods are complex and difficultly available. PERCLOS has been applied as an index to detect driver fatigue since the recommend of the office of motor carriers, Federal highway administration, the USA in 1998 [9]. To a certain extent, there are some relationships between circadian rhythm and fatigue. The circadian rhythm is regarded as one of the important reasons to lead to fatigue [10]. To our knowledge, we, for the first time, tried to employ PERCLOS as an index to characterize circadian rhythm. We established a simple and easy to operate method to measure the PERCLOS value. The measurement results of volunteers showed that the method was successfully detecting PERCLOS values, and the change of PERCLOS values was consistent with circadian rhythm.

In conclusion, circadian rhythm is very important for child growing, health keeping, and efficient and safe working. It is necessary to learn individual circadian rhythm for arranging his/her life more efficiently. In this paper, we were inspired by fatigue detection to have established a PERCLOS method for fine characterization of the individual circadian rhythm. The method was simple and easy to operate. We believe that this method will expand to use and help individuals to learn their behavioural circadian rhythm and arrange their life more efficiently.

**Acknowledgements** We acknowledge the financial support of the Sichuan Science and Technology Program, under grant 2019YFG0390, Safety Foundation of Civil Aviation Administration of China and the Joint Funds of the National Natural Science Foundation of China (No. U1333132).

### **Compliance with Ethical Standards**

The study was approved by the Logistics Department for the Civilian Ethics Committee of the Second Institute of Civil Aviation Administration of China. All subjects who participated in the experiment were provided with and signed an informed consent form. All relevant ethical safeguards have been met with regard to subject protection.

## **References**

1. Ledford H, Callaway E (2017) Circadian clocks scoop Nobel prize. *Nature* 55:18
2. Gau SS, Shang CY, Merikangas KR et al (2007) Association between morningness-eveningness and behavioral/emotional problems among adolescents. *J Biol Rhythms* 22:268–274
3. Escobar C, Salgado R, Rodriguez K et al (2011) Scheduled meals and scheduled palatable snacks synchronize circadian rhythms: consequences for ingestive behavior. *Physiol Behav* 104:555–561

4. Hofstra WA, Weerd AW (2008) How to assess circadian rhythm in humans: a review of literature. *Epilepsy Behav* 13:438–444
5. Ngxande M, Tapamo J-R, Bruke M (2017) Driver drowsiness detection using behavioural measures and machine learning techniques: a review of state-of-art techniques. 2017 Pattern recognition association of south Africa and robotics and mechatronics (PRASA-RobMech), 156–160. <https://doi.org/10.1109/robomech.2017.8261140>
6. Ergun H, Sert M (2016) Fusing deep convolutional networks for largescale visual concept classification. In 2016 IEEE second international conference on multimedia big data (BigMM). IEEE, pp 210–213
7. Den R, Toda M, Nagasawa S et al (2007) Circadian rhythm of human salivary chromogranin A. *Biomed Res* 28:57–60
8. Carrier J, Monk TH (2000) Circadian rhythms of performance: new trends. *Chronobiol Inter* 17:719–732
9. Dinges D, Grace R (1998) PERCLOS: a valid psychophysiological measure of alertness as assessed by psychomotor vigilance. Tech Rep No FHWA-MCRT-98–006
10. May JF, Baldwin CL (2009) Driver fatigue: the importance of identifying causal factors of fatigue when considering detection and countermeasure technologies. *Transport Res Part F* 12:218–224

# Research on Fatigue Monitoring of Forklift Driver Driving in an Automobile Enterprise



Zhenjun Du and Xinmin Zhang

**Abstract** In order to monitor the driving fatigue of forklift drivers in automobile enterprises and improve the driving operations of forklift drivers, a third-class forklift driver in the automobile assembly shop of a certain company was used as the research object to conduct a driving fatigue monitoring study. The subjective monitoring uses the questionnaire of basic conditions of forklift drivers and the questionnaire of subjective feelings of forklift drivers' operating fatigue to determine the causes of fatigue, symptoms and changes in symptoms of forklift drivers. Objective monitoring uses an EEG signal analysis method to monitor and record the EEG signals of the forklift driver during each working period, and use EEGLAB to analyze the driver's  $\delta$  wave spectrum chart. Taking the unloading driver as an example, the driving fatigue time and fatigue degree are analyzed and judged from two perspectives: subjective and objective. The results show that the driving fatigue of the forklift driver is obvious, and it is difficult to recover effectively. The forklift driver is in a state of severe fatigue while driving.

**Keywords** Forklift driver · Driving operation · Fatigue state · Subjective and objective monitoring

## 1 Introduction

The timeliness of workshop logistics of modern automobile companies is extremely high [1, 2]. In order to ensure the timeliness of logistics, in most automobile companies at this stage, workshop logistics is mainly completed by forklifts. Forklift driving is a special operation with long operation time, high intensity and great difficulty. Prolonged high-load operation may cause fatigue of the forklift driver and severely reduce the production efficiency of the enterprise. Therefore, an in-depth analysis of the daily operation of forklift drivers, an ergonomics-based research method for

---

Z. Du (✉) · X. Zhang

School of Mechanical Engineering, Shenyang University of Technology, Shenyang, China  
e-mail: [2580870149@qq.com](mailto:2580870149@qq.com)

monitoring fatigue of forklift drivers, and carrying out targeted improvement activities have become urgent problems to improve the efficiency of forklift drivers' operations, the logistics efficiency of enterprise workshops and the comfortable operation of drivers.

At home and abroad, some in-depth studies have been conducted on work fatigue. Francisco and others performed muscle load analysis on two operators from two different automotive clutch disk production lines [3]. Philippa Gander studied the relationship between sleep and fatigue of nursing staff by regression analysis [4]. Joseph investigated the risk of musculoskeletal diseases of the upper and lower limbs with a modified nordic musculoskeletal disease questionnaire [5]. Charlotte and others proposed a scientific method on the concept of fatigue and the physiological and behavioral indicators that support the emergence of individual and team fatigue management systems through the study of the fatigue status of divers [6]. Riedy studied the potential relationship between bio-mathematical models of fatigue and working schedules and performance [7]. Kubo and others have determined through observational studies that working time control (WTC) can affect objectively measured employee fatigue and sleep [8]. Rannou used experimental means to build a mathematical model to explore the relationship between muscle fatigue and time of intense exercise [9].

Liu and others improved the fatigue of firefighters training by improving the athlete training state monitoring scale [10]. Xu studied the muscle fatigue characteristics of drilling workers in confined spaces during operation, measured the electromyography of workers in confined spaces through simulation experiments and guided the median electromyographic frequency as an evaluation index [11]. Based on EEG signals, Jin proposed a real-time driving fatigue monitoring algorithm based on the spatial distance of characteristic rhythm wave samples [12]. Wang proposed a driving fatigue detection method based on deep apology learning [13]. Liu studied the work fatigue improvement strategies of civil aviation control personnel under the shift system [14]. Wu discussed the feasibility of restoring fatigue from the perspective of music theory [15].

Although there have been more in-depth researches on work fatigue at home and abroad, most of the researches mainly monitor or evaluate unilaterally from the perspective of subjective evaluation or objective measurement. Therefore, based on domestic and foreign research, this paper analyzes and judges the causes of fatigue and specific manifestations of fatigue by compiling a basic information questionnaire and a subjective self-assessment scale for fatigue using a wireless EEG system to objectively and continuously monitor the EEG of the forklift driver's driving operation signals and extract and analyze typical bands to determine the fatigue time and fatigue level of driving operations to determine whether the driver is in a fatigue state.



a. Unloading operation



b. Empty equipment operation



c. Production line distribution operation

**Fig. 1** Workshop logistics operation situation

## 2 Research Object

As shown in Fig. 1, the company's workshop logistics mainly relies on forklifts at the logistics department for material transportation, stacking and storage. The forklift driver first unloads the goods and then transports the empty appliances to the truck; the unloaded goods are transported by the forklift to the designated storage area for storage; when the production line needs materials, the forklift is distributed to each station on the production line.

Based on this, the company's assembly shop forklift drivers are divided into three categories: unloading drivers, production line distribution drivers and returning equipment drivers. The main working hours of all drivers are 6:00–7:00. Among them: 6:00–8:00, 15:00–17:00, the amount of tasks is small, the labor intensity is small, the work is idle; within 8:00–15:00, the arrival is concentrated, and the driver has a large amount of tasks.

## 3 Subjective Measurement of Forklift Driver Driving Fatigue

### 3.1 Questionnaire Design

This article issues basic information questionnaires and self-assessment scales for fatigue symptoms. Of the study population, 45 subjects completed and returned the questionnaire for each type, and 40 were valid questionnaires. Among them, 15 were for unloading drivers, 14 were for distribution line drivers, and 11 were for returning appliances.

**Table 1** Fatigue symptom checklist self-assessment project

1. Sleepiness	2. Restlessness	3. Discomfort	4. Soreness	5. Ambiguity
Sleepy	Feeling anxious	Headache	Weak arms	Eyes cannot open
Want to lie down	Moody	Head weight	Lumbago	Eyes are tired
Yawn	Feel calm	Feeling bad	Hand or finger pain	Eye pain
No motivation	Grumpy	Dazed	Leg weakness	Dry eyes
Weak body	Confusion	Dizziness	Shoulder pain	Blurred vision

The basic situation questionnaire can be divided into four parts: the basic situation of the driver, working hours, sleep conditions and driver’s fatigue knowledge. The fatigue symptoms self-assessment scale items and groups are shown in Table 1. Each of the symptom factors has five assessment levels, ranging from “not at all” to “very obvious.” Scores can be calculated from low to high.

### 3.2 Processing of Survey Data

1. Statistics of basic survey data. The results of the basic situation questionnaire, the basic information of the forklift driver and the factors that lead to its subjective driving fatigue are basically determined after the summary. The cause of subjective driving fatigue mainly lies in two aspects of driving method and workshop environment: long-term driving, frequent turning to observe road conditions, forklift pickup difficulties, vehicle vibration, poor road conditions, lack of sleep and avoid pedestrian factors.
2. Statistics of self-assessment scale survey data. As can be seen from Fig. 2, firstly, the forklift driver in the unloading area has a very obvious peak and trough period.

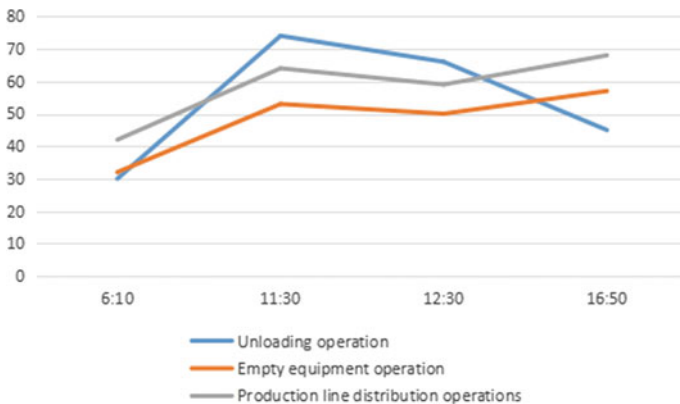


**Fig. 2** Fatigue scale total score map



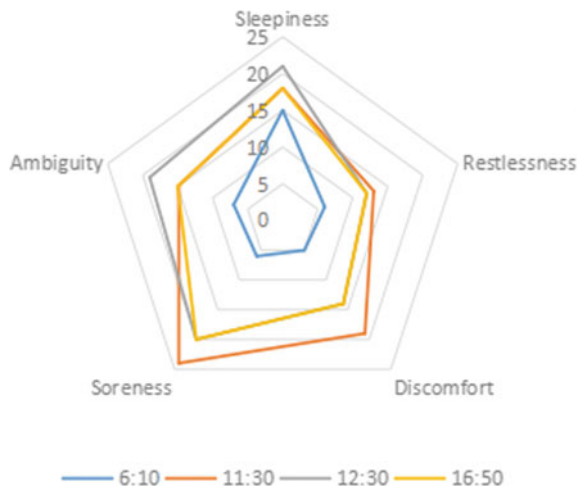
**Table 2** Subjective self-assessment results of three types of forklift drivers

Driver category	Self-assessment results
Unloading driver	Obvious sleepiness and soreness
Production line distribution driver	Obvious sleepiness and soreness
Empty equipment driver	Obvious restlessness and discomfort

The load distribution is significantly higher, indicating that there are problems with the forklift driver’s shifting system and task allocation. Secondly, although the drivers of the three types of forklifts passed their lunch break, they were never able to return to normal conditions. These results suggest that workers may have insufficient lunch breaks. In addition, the line chart also reflects that the overall score of the fatigue scale is increasing during each working period, which indicates that the forklift driver will have a certain degree of fatigue symptoms during working hours.

Table 2 provides the subjective self-assessment results of the three types of forklift drivers. By summarizing and analyzing the five fatigue symptoms of the subjective fatigue self-assessment scale for three different types of work, we can get the change of each index in the fatigue scale. Taking the unloading operation as an example, it can be seen from Fig. 3 analysis that the main factors of fatigue of the forklift driver during unloading are drowsiness, fatigue and ambiguity, which are more obvious in the second and third stages. After lunch break, it still shows that the driver is suffering fatigue accumulation cannot be alleviated due to time driving, uneven workload distribution and insufficient rest time.

**Fig. 3** Unloading driver fatigue feeling map



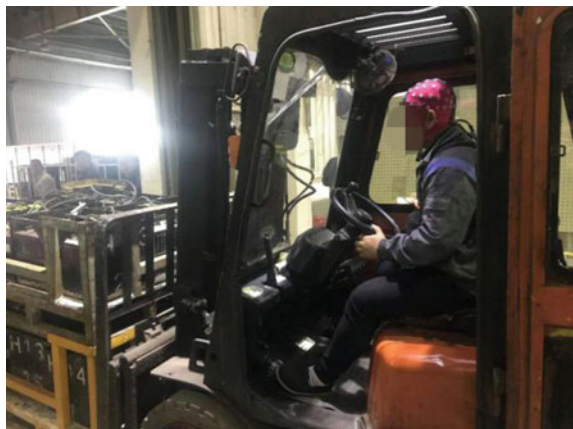
## 4 Fatigue Analysis of Forklift Driver Driving Operation Based on EEG

This paper adopts the ultra-portable Eegosports 64-channel wireless EEG system as a device for collecting EEG signals. In order to ensure the validity of the measurement results, the test subject should be mentally normal, has adequate sleep and has a clean head. When capturing EEG signals, the operator wears a measuring instrument for the measured object and checks whether the positions of the electrodes on the EEG cap are consistent with the positions indicated on the computer screen. Set the EEG acquisition parameter settings and inject EEG paste for the test object. Wait for a few seconds after the injection and observe and test whether the electrode hole is in good contact with the scalp. After the injection is complete, check that it is securely worn before starting the test. Figure 4 shows the process of EEG experiment.

After collecting the data, use the EEGLab toolbox in MATLAB to process the collected EEG data. This article collects the EEG data of the unloading driver, the returning equipment driver and the production line distribution driver during different working hours in the morning and afternoon. The data collection time is 5 min before the start of work in the morning and the end of work in the afternoon, and 8 and 10 a.m., 2 and 4 p.m. Take the unloading driver as an example to analyze the  $\delta$  wave of the forklift driver by brain wave analysis to determine the overall brain load, fatigue level and specific fatigue time. Figure 5 shows that the comparison of the  $\delta$  delta wave spectrum of the driver of the unloading forklift at various time periods in the morning.

From the data in Fig. 6, it can be seen that in the morning work, the high-frequency part of the driver's  $\delta$ -wave brain waves is distributed in the right forehead region of the brain, and the rest is distributed in the left occipital region, and the brain wave energy accumulation is stable without major changes. It means that although the forklift driver's mental load is more serious than that of other positions during the morning work, the mental load does not further deepen, which means that the fatigue

**Fig. 4** EEG signal acquisition experiment



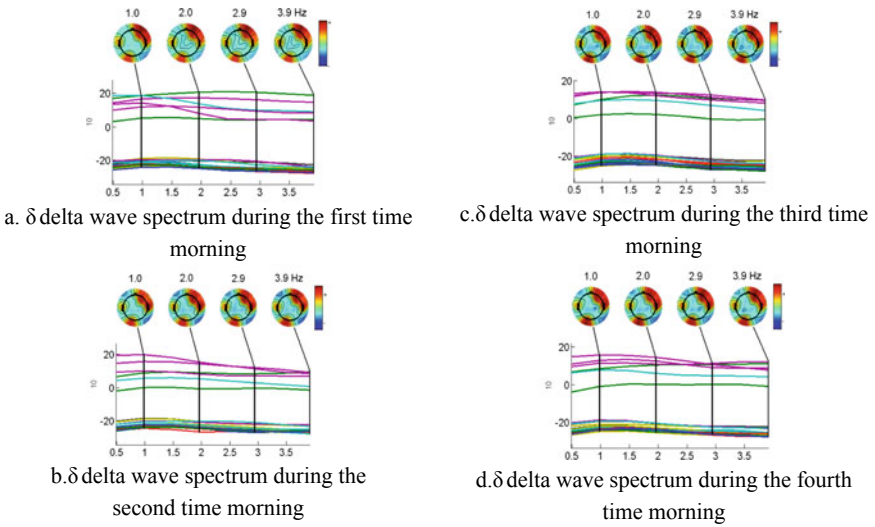


**Fig. 5** Comparison of the  $\delta$  delta wave spectrum of the driver of the unloading forklift in the morning

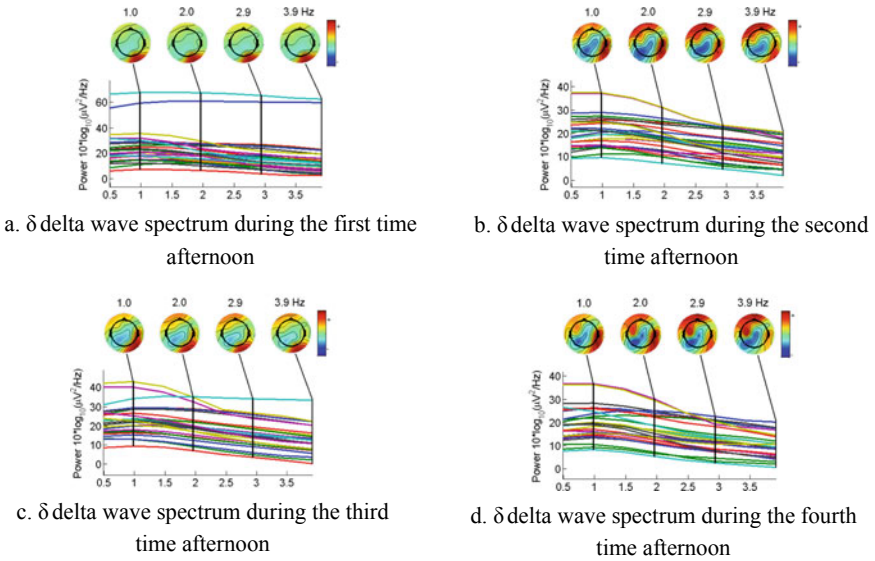


**Fig. 6** Comparison of the  $\delta$  delta wave spectrum of the driver of the unloading forklift in the afternoon

has not continued to increase and always stays at the state of the morning work. Figure 7 shows the comparison of the  $\delta$  delta wave spectrum of the driver of the unloading forklift at various time periods in the afternoon.

It can be seen in Fig. 6a, b that with the passage of time, the area of the high-frequency part of the  $\delta$  wave of the driver during the afternoon work has increased and has significantly increased in the right central region and left forehead region of the brain. This shows that the increasing mental load in these two parts also means that the fatigue level is increasing, and the fatigue level has increased significantly. However, it can be found in Fig. 6b, c and d that during the measurement before the end of the afternoon work, the EEG aggregation level has decreased. It can be considered that the situation of going to work has relieved the driver's mental load, but its overall fatigue. The degree is still high.

## 5 Conclusion

This paper discusses the work fatigue monitoring of forklift drivers during driving operations. Taking the forklift driver of three kinds of work in the automobile assembly shop of an enterprise as the research object, the subjective evaluation scale of forklift driver's operating fatigue was compiled, and the results of the survey of the basic situation of driving operation were used to determine the cause and fatigue of the fatigue from the subjective perspective specific performance. For the objective monitoring of the forklift driver's driving operations, the driver's working hours were segmented, and the EEG signals of the forklift driver's driving operations were collected during each period. The objective analysis of the forklift driver's EEG changes during each time period determined the driver's specific fatigue time and specific fatigue changes. In this paper, the result of subjective and objective monitoring indicates that the forklift driver had severe fatigue during driving.

### 5.1 *Compliance with Ethical Standards*

The study was approved by the Logistics Department for Civilian Ethics Committee of School of Mechanical Engineering, Shenyang University of Technology.

All subjects who participated in the experiment were provided with and signed an informed consent form.

All relevant ethical safeguards have been met with regard to subject protection.

## References

1. Chang J, Wang L, Mo Y et al (2017) Study on AHP-based logistics performance evaluation index system of automobile assembly workshops. *Logistics Technol.* <https://doi.org/10.3969/j.issn.1005-152x.2017.04.032>
2. Zheng J (2018) Layout optimization of logistics buffer zone in certain Sedan assembly workshop. *Logistics Technol.* <https://doi.org/10.3969/j.issn.1005-152x.2018.06.026>
3. Francisco LN, Gert-Ake H, Helen CN (2018) Biomechanical exposure of industrial workers— influence of automation process. *Int J Industrial Ergon.* <https://doi.org/10.1016/j.ergon.2018.04.002>
4. Philippa G, Karyn OK, Edgar S et al (2019) Fatigue and nurses work patterns: an online questionnaire survey. *Int J Nursing Stud.* <https://doi.org/10.1016/j.ijnurstu.2019.06.011>
5. Joseph C, Walters AUC, Lawrence WL et al (2018) An ergonomic evaluation of pannists. *Int J Occup Safety Ergon.* <https://doi.org/10.1080/10803548.2018.1522856>
6. Charlotte CG, Stephanie C, Philippe R et al (2019) Framework and metrics for online fatigue monitoring within submarine teams working in 24/7 environments. *IFAC PapersOnLine.* <https://doi.org/10.1016/j.ifacol.2019.12.104>
7. Riedy SM, Dawson D, Vila B (2019) U.S. police rosters: fatigue and public complaints. *Sleep.* <https://doi.org/10.1093/sleep/zsy231>
8. Kubo T, Takahashi M, Xinxin L et al (2016) Fatigue and sleep among employees with prospective increase in work time control: a 1-year observational study with objective assessment. *J Occup Environ Med.* <https://doi.org/10.1097/jom.0000000000000858>
9. Rannou F, Nybo L, Andersen JE et al (2019) Monitoring muscle fatigue progression during dynamic exercise. *Med Sci Sports Exercise.* <https://doi.org/10.1249/mss.0000000000001921>
10. Liu F, Shao Z (2019) Research on application of monitor scale on exercise-induced fatigue of firefighters. *J Safety Sci Technol.* <https://doi.org/10.11731/j.issn.1673-193x.2019.05.025>
11. Xv S, Jin L, Xv M (2019) Study on muscle fatigue characteristics of drilled workers in confined space. *China Safety Sci J.* <https://doi.org/10.16265/j.cnki.issn1003-3033.2019.03.0133>. Slifka MK, Whitton JL (2000) Clinical implications of dysregulated cytokine production. *J Mol Med.* <https://doi.org/10.1007/s001090000086>
12. Jin C, Zeng W (2015) Fatigue monitor algorithm research based on EEG. *Sci Technol Eng.* <https://doi.org/10.3969/j.issn.1671-1815.2015.34.041>
13. Fei W, Wu S, Liu S (2019) Driver fatigue detection through deep transfer learning in an electroencephalogram-based system. *J Electronics Inf Technol.* <https://doi.org/10.11999/jeit180900>
14. Liu Q (2015) Analysis of countermeasures to prevent fatigue of control personnel under the shift system. *China Manage Informationization.* <https://doi.org/10.3969/j.issn.1673-0194.2015.06.071>
15. Wu M (2019) Feasibility analysis of application of music adjustment method in driving fatigue recovery. *Electronic World.* <https://doi.org/10.19353/j.cnki.dzsj.2019.07.055>

# **Research on the Machine Character**

# Parameter Optimization Design of a Cable-Driven Bionic Muscle Mechanism Based on Hill Muscle Model for Flexible Upper Limb-Assisted Exoskeleton



Hongrun Lu, Bingshan Hu, Hongliu Yu, Tong Ma, and Xinran Zhang

**Abstract** In this paper, a cable-driven bionic muscle is designed for the flexible upper limb-assisted exoskeleton. And, it simulates the characteristic of muscle output force from the perspective of mechanism design. The structure of the designed exoskeleton and the designed bionic muscle are introduced. Then, the dynamics model of elbow joint is established based on the Hill muscle model and musculoskeletal model. Finally, by optimizing the key parameters, the force-displacement curve of the mechanism is approximately consistent with that of human muscle. That means, in the stable state, the stiffness of the bionic muscle is similar to that of the human body. It helps the flexible upper limb-assisted exoskeleton improve its bionic performance.

**Keywords** Exoskeleton · Cable-driven · Bionic muscle · Hill muscle model

## 1 Introduction

People with upper limb dysfunction are seriously affected by insufficient muscle strength of upper limb, and upper limb-assisted exoskeleton can effectively help them.

In recent years, due to its safety and flexibility, the flexible upper limb-assisted exoskeleton has been widely concerned by researchers. At present, the actuating mechanism of flexible upper limb-assisted exoskeleton can be divided into pneumatics, shape memory alloy and cable. The power to weight ratio of pneumatic drive is high, but the performances are not ideal in control stability and response speed [1, 2]. Shape memory alloy drive realizes lightweight noiseless drive, but its drive bandwidth and efficiency are low [3]. There are more flexible upper limb exoskeletons which are driven by Bowden cable now. The early study on cable drive made the flexible exoskeleton have the characteristics of human arm movement from the

---

H. Lu · B. Hu (✉) · H. Yu · T. Ma · X. Zhang

Institute of Rehabilitation Engineering and Technology, University of Shanghai for Science and Technology, Shanghai, China

e-mail: [hubingshan@usst.edu.cn](mailto:hubingshan@usst.edu.cn)

© The Editor(s) (if applicable) and The Author(s), under exclusive license to Springer Nature Singapore Pte Ltd. 2021

S. Long and B. S. Dhillon (eds.), *Man-Machine-Environment System Engineering*, Lecture Notes in Electrical Engineering 645, [https://doi.org/10.1007/978-981-15-6978-4\\_32](https://doi.org/10.1007/978-981-15-6978-4_32)

263

perspective of degree of freedom [4, 5]. Li Ning et al. analyzed the characteristics of the starting and stopping point and force transmission path of human upper limb muscles and arranged the bionic muscles accordingly [6].

Medical research has shown that making full use of the residual muscle strength of patients can be beneficial to the muscle strength training and rehabilitation of patients [7]. It requires that the characteristics of the assisted exoskeleton output force are consistent with the characteristics of human muscle force.

In this paper, a cable-driven bionic muscle is designed for the flexible upper limb-assisted exoskeleton. And it simulates the characteristic of muscle output force from the perspective of mechanism design.

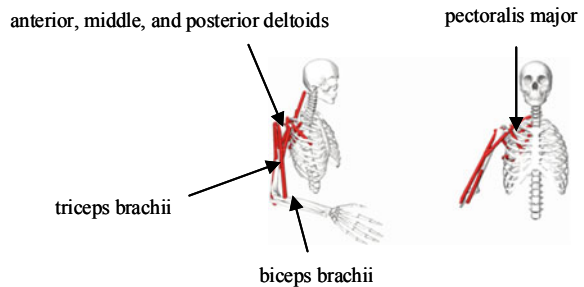
## 2 Mechanism Design of Flexible Upper Limb-Assisted Exoskeleton

As shown in Fig. 1, the major muscles which assisted include anterior deltoids, middle deltoids, posterior deltoids, biceps brachii, triceps brachii and clavicular part of pectoralis major muscle. Kevlar cable is used in this paper, which is suppler than Bowden cable.

As shown in Fig. 2a, the designed flexible upper limb-assisted exoskeleton is composed of elastic base clothing, actuator control box, bionic muscles, anchor joints and inertial sensors. The elastic base clothing is made of elastic soft fabric and can be worn close to the body. The position of anchor joints is set according to the starting and ending points of muscle distribution as shown in Fig. 1. As shown in Fig. 2b, the actuator control box mainly includes the cable-driven bionic muscle, the central controller, the motor drive controller, the bus communication card and the lithium battery.

The structure diagram of the cable-driven bionic muscle is shown in Fig. 3. The cable-driven bionic muscle is driven by the motor with reduction gear box, and then the cable rod is driven to rotate and pull the cable, so that the rotation is converted into linear motion. The cable is deflected through three pulleys in the bionic muscle

**Fig. 1** Main primary motor muscles of shoulder and elbow joints of upper limb





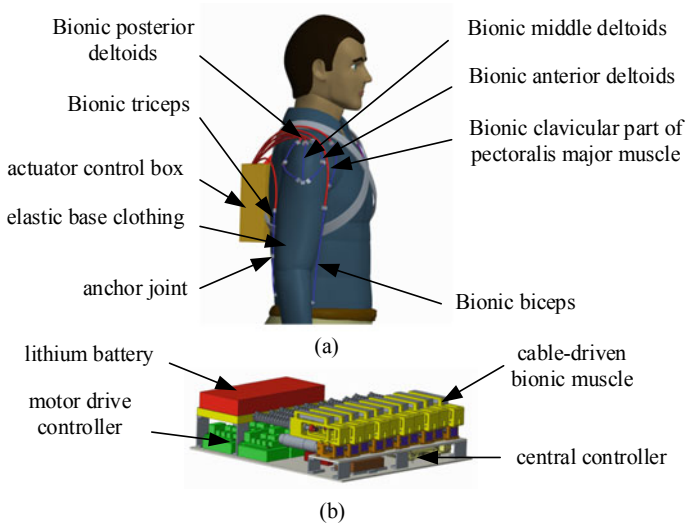
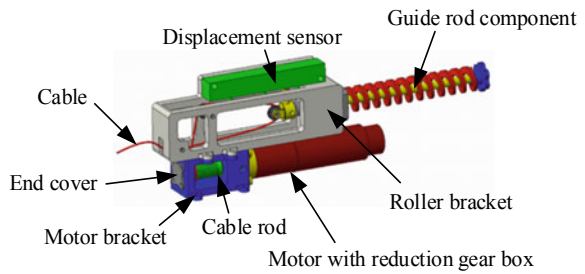


**Fig. 2** Structure of flexible upper limb-assisted exoskeleton

**Fig. 3** The cable-driven bionic muscle



structure. The guide rod component includes springs, guide rods and linear bearings. The displacement sensor is used to measure the deformation of the spring.

The section diagram and force analysis diagram of the cable-driven bionic muscle are shown in Fig. 4. Set  $A, B, C$  at three rollers center, respectively.  $b$  is the initial vertical distance between  $A$  and  $B$ .  $c$  is the vertical distance between the horizontal

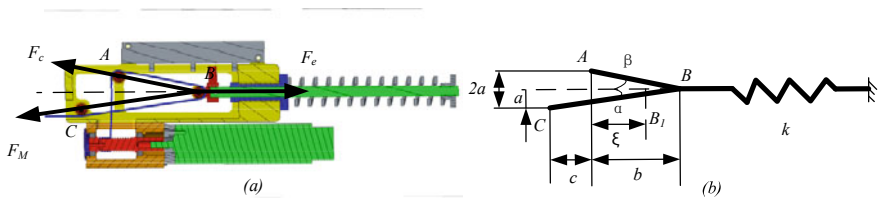


**Fig. 4** The section diagram (a) and force analysis diagram (b) of the cable-driven bionic muscle

distance between  $A$  and  $C$ . The horizontal distance between  $A$  and  $B$  is  $a$ .  $\alpha$  is the angle between the line  $BC$  and the perpendicular line.  $\beta$  is the angle between the line  $AB$  and the perpendicular line.  $\xi$  is the vertical distance between  $AB$  after spring compression.  $k$  is the elastic coefficient.  $F_M$  is the output force.  $F_c$  is the cable tension.  $F_e$  is the spring force.

$$F_e = F_c \cdot (\cos \alpha + \cos \beta) \quad (2.1)$$

The cable tension  $F_c$  can be converted into the following formula:

$$F_c = \frac{k(b - \xi)\sqrt{(a^2 + \xi^2)[a^2 + (\xi + c)^2]}}{\xi(\sqrt{a^2 + (\xi + c)^2} + \sqrt{a^2 + \xi^2}) + c \cdot \sqrt{a^2 + \xi^2}} \quad (2.2)$$

Setting the change in cable caused by spring deformation as  $l$ , then  $l$  conforms to the following formula:

$$l = \sqrt{a^2 + b^2} + \sqrt{a^2 + (b + c)^2} - \sqrt{a^2 + \xi^2} - \sqrt{a^2 + (\xi + c)^2} \quad (2.3)$$

As the cable moves, the end load of the force  $FM$  changes and then the corresponding cable tension  $F_c$  changes, thus making the spring compression. If the relationship between  $l$  and  $F_c$  is consistent with the relationship between  $F_M$  and  $l_m$ , then the cable displacement of muscle contraction is equal to  $l$ . Setting the stiffness of the bionic muscle be  $K_m$ , then

$$K_m = \delta F / \delta l = (\delta F / \delta \xi)(\delta l / \delta \xi)^{-1} \quad (2.4)$$

### 3 Musculoskeletal Dynamics Model

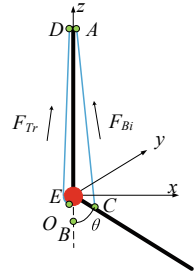
Taking elbow joint movement as an example, musculoskeletal model and Hill muscle model of related muscle were established to be analyzed.

#### 3.1 Musculoskeletal Model of Elbow Joint

The Musculoskeletal model of the elbow joint is shown in Fig. 5. The  $F_{Bi}$  is biceps contraction force,  $F_{Tr}$  is triceps contraction force, and the red center  $O$  is the rotation center. In addition, the bone radius is added at the starting and ending points to ensure that the initial moment arm of the muscle is not 0.

For the contraction movement of the biceps, set the muscle starting point  $A(x_1, y_1, z_1)$ , the initial muscle ending point  $B(x_2, y_2, z_2)$  and the position of point  $B$  after

**Fig. 5** Musculoskeletal model of the elbow joint



rotation point  $C(x_3, y_3, z_3)$ . The transformation formulas are:

$$\vec{OC} = R\vec{OB}, \quad R = \begin{bmatrix} \cos \theta & 0 & -\sin \theta \\ 0 & 1 & 0 \\ \sin \theta & 0 & \cos \theta \end{bmatrix} \tag{3.1}$$

$\vec{OC}$  is the directed vector from the origin  $O$  to the point  $C$ .  $\vec{OB}$  is the directed vector from  $O$  to  $B$ .  $R$  is the transformation matrix. Then, the muscle length after the rotation of the biceps joint  $l_{mBi}$  is:

$$l_{mBi} = \sqrt{(x_3 - x_1^2 + y_3 - y_1)^2 + (z_3 - z_1)^2} \tag{3.2}$$

For the contraction movement of triceps brachii, namely rotation of theta from  $\pi/2$  to 0, the calculation formula of the rotated muscle length  $l_{mTr}$  is:

$$l_{mTr} = l_0 - \theta \cdot l_{armTr} \tag{3.3}$$

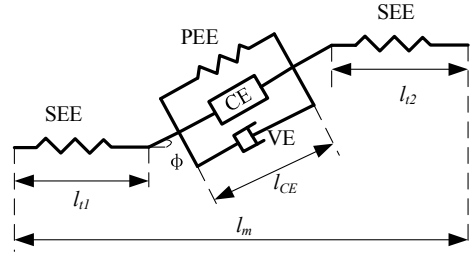
### 3.2 Hill Muscle Model

Hill muscle model is a muscle model which is widely used, and Zajac et al. improved the Hill muscle model on this basis, achieving better results [8]. Martin et al. added viscous elements to this model [9]. As shown in Fig. 6, the main contents of the muscle model include series elastic element (SEE), parallel elastic element (PEE), contractile element(CE), viscous element (VE) and feather angle  $\varphi$ .  $l_m$  is the muscle length,  $l_{CE}$  is the muscle fiber length, and  $l_{t1}$  and  $l_{t2}$  are the tendon length at both ends, respectively. Feather angle is extremely small in the biceps and triceps and is generally negligible [10].

The calculation formula of muscle force  $F_M$  is as follows:

$$F_M = F_{CE} + F_{PE} + F_{VE} \tag{3.4}$$

**Fig. 6** Main contents of the muscle model



The main muscle fiber power  $F_{CE}$  is:

$$F_{CE} = a \cdot f_l \cdot f_v \cdot F_0 \tag{3.5}$$

where  $a$  is the normalized muscle activation.  $f_l$  is the influence factor of muscle fiber length [11].  $f_v$  is the influence factor of muscle fiber contraction rate [12, 13].  $F_0$  is the maximum isometric contractile muscle force.

$$f_l = 1 - ((L_m - 1)/0.5)^2 \tag{3.6}$$

$$f_v = 0.1433/(0.1074 + e^{-1.409 \cdot \sinh(3.2V+1.6)}) \tag{3.7}$$

$$V = v/(0.5 \cdot v_0 \cdot (a + 1)) \tag{3.8}$$

where  $L_m$  is the normalized muscle fiber length,  $v$  is muscle contraction velocity and  $v_0$  is the maximum contraction velocity [14].

The calculation formula of muscle fiber dynamic  $F_{PE}$  is as follows [15]:

$$F_{PE} = 1.3 \cdot \arctan 0.1 \cdot (L_m - 0.22)^{10} \cdot F_0 \tag{3.9}$$

The calculation formula of viscous damping force  $F_{VE}$  is as follows [16]:

$$F_{VE} = D \cdot V \cdot F_0 \tag{3.10}$$

where  $D$  is the damping coefficient.

## 4 Parameter Optimization Design Based on Musculoskeletal Model

In order to verify the rationality of the structure, the biceps brachii is taken as an example to carry out simulation and determine the corresponding parameters of the

**Table 1** Biceps model parameters

Parameters	Value	Unit
$(x_1, y_1, z_1)$	(0.012, 0, 0.300)	m
$(x_2, y_2, z_2)$	(0.012, 0, -0.050)	m
$l_{opt}$	0.308	m
$F_0$	568	N
$D$	1	Ns/m

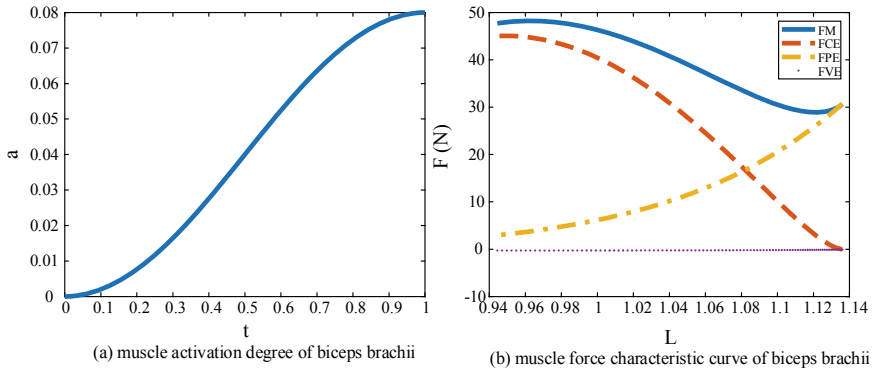


**Fig. 7** Simulation data of biceps brachii

bionic muscle. The setting of parameters was comprehensively referred to Chinese adult body size (GB/T 10000-1988) and other literatures [10, 15]. The biceps model parameters are shown in Table 1.

It is assumed that the elbow joint flexes 90° within 1 s. Set the muscle activation degree of biceps brachii as shown in Fig. 7a. According to the muscle model formula in Sect. 3, the muscle force characteristic curve of biceps obtained by simulation is shown in Fig. 7b, whose abscissa is the normalized muscle length.

In order to reduce the uncertainty of the curve, the value of  $c$  can be set to a fixed value, which is set to 26 mm. L9 (3<sup>4</sup>) orthogonal test table (a kind of three-factor with three-level test scheme) is used to quickly get a good combination of  $k$ ,  $a$  and  $b$ . The bionic muscle optimization program obtained by simulation is shown in Fig. 8a. After fine-tuning test, bionic muscle tuning program is obtained, and the value of  $(k, a, b)$  is (1.6, 10, 80), as shown in Fig. 8b. It can be seen from Fig. 8 that the output force characteristics of the designed cable-driven bionic muscle are approximately in line with the bicep contraction force characteristics.

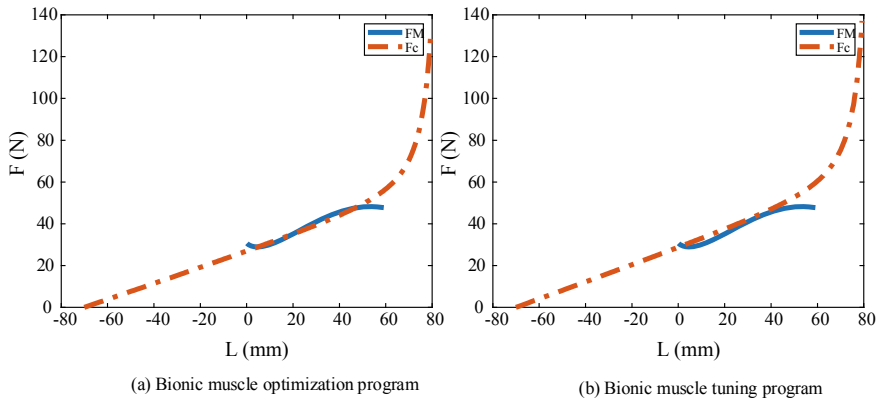


**Fig. 8** Results of bionic muscle simulation

## 5 Results and Conclusions

In this paper, a cable-driven bionic muscle is designed for the flexible upper limb-assisted exoskeleton. The purpose of parameter optimization design is that to make the force–displacement characteristics of the rope-drive biomimetic muscle approximate to that of human muscle. The theoretical model of cable-driven biomimetic muscle was derived, and the elbow dynamics model was established based on the human Hill muscle model and musculoskeletal model. Finally, taking the biceps as an example, parameters  $k$ ,  $a$  and  $b$  were determined for the rope-driven biomimetic muscle mechanism through the simulation test. The value of  $(k, a, b)$  is  $(1.6, 10, 80)$ .

The nonlinear stiffness of muscles is realized by means of springs and rollers. The stiffness of the bionic muscle is similar to that of the human body. It helps the flexible upper limb-assisted exoskeleton improve its bionic performance.

## References

1. Wang B, Aw KC, Biglari-Abhari M, McDaid A (2016) Design and fabrication of a fiber-reinforced pneumatic bending actuator. In: 2016 IEEE International Conference on Advanced Intelligent Mechatronics (AIM), vol 16, pp 83–88
2. Belforte G, Eula G, Ivanov A, Raparelli T, Sirolli S (2018) Presentation of textile pneumatic muscle prototypes applied in an upper limb active suit experimental model. *J Textile Inst* 109(6):757–766
3. Villoslada A, Flores A, Copaci D, Blanco D, Moreno L (2015) High-displacement flexible shape memory alloy actuator for soft wearable robots. *Robot Autonomous Syst* 73:91–101
4. Mustafa SK, Agrawal SK (2011) On the force-closure analysis of n-DOF cable-driven open chains based on reciprocal screw theory. *IEEE Trans Robot* 28(1):22–31
5. Mao Y, Agrawal SK (2012) Design of a cable-driven arm exoskeleton (CAREX) for neural rehabilitation. *IEEE Trans Robot* 28(4):922–931

6. Li N, Yu P, Yang T, Zhao L, Liu Z et al (2017) Bio-inspired wearable soft upper-limb exoskeleton robot for stroke survivors. In: 2017 IEEE International Conference on Robotics and Biomimetics (ROBIO), vol 17, pp 2693–2698
7. Xiloyannis M, Cappello L, Dinh B K, Antuvan CW, Masia L (2017) Design and preliminary testing of a soft exosuit for assisting elbow movements and hand grasping. In: *Converging clinical and engineering research on neurorehabilitation II*. Springer, Cham, vol 17, pp 557–561
8. Zajac FE (1989) Muscle and tendon: properties, models, scaling, and application to biomechanics and motor control. *Critical Rev Biomed Eng* 17(4):359–411
9. Martin A, Martin L, Morlon B (1994) Theoretical and experimental behaviour of the muscle viscosity coefficient during maximal concentric actions. *Eur J Appl Physiol Occup Physiol* 69(6):539–544
10. Holzbaur KR, Murray WM, Delp SL (2005) A model of the upper extremity for simulating musculoskeletal surgery and analyzing neuromuscular control. *Ann Biomed Eng* 33(6):829–840
11. Buchanan TS, Lloyd DG, Manal K, Besier TF (2004) Neuromusculoskeletal modeling: estimation of muscle forces and joint moments and movements from measurements of neural command. *J Appl Biomech* 20(4):367–395
12. Vilimek M (2007) Musculotendon forces derived by different muscle models. *Acta Bioeng Biomech* 9(2):41–47
13. Rosen J, Fuchs MB, Arcan M (1999) Performances of Hill-type and neural network muscle models—toward a myosignal-based exoskeleton. *Comput Biomed Res* 32(5):415–439
14. Thelen DG (2003) Adjustment of muscle mechanics model parameters to simulate dynamic contractions in older adults. *J Biomech Eng* 125(1):70–77
15. Pennestri E, Stefanelli R, Valentini PP, Vita L (2007) Virtual musculo-skeletal model for the biomechanical analysis of the upper limb. *J Biomech* 40(6):1350–1361
16. Shao Q, Bassett DN, Manal K, Buchanan TS (2009) An EMG-driven model to estimate muscle forces and joint moments in stroke patients. *Comput Biol Med* 39(12):1083–1088

# Design of Female Office Chairs Based on Ergonomics and Emotional Design



Yi Chen, Canqun He, and Yuqi Lin

**Abstract** With the development of urbanization and information technology, the efficiency and comfort of the office environment have become the two major concerns of the office market and users. This article analyzes the psychological characteristics and emotional needs of young women, studies the user's sitting posture, determines the structure and size of the chair based on ergonomics, improves the chair structure adjustment form, and approaches the aesthetic requirements of young women through design methods such as symbolic metaphors on the appearance. The design of female office chairs based on ergonomics and emotional design is conducive to improving people's work efficiency and work comfort, thereby enhancing users' happiness in life.

**Keywords** Ergonomics · Office chair · Body size · Emotional design

## 1 Introduction

With the development of typewriters and computers, the office community in the office building has been on the rise. Prolonged work at desk has caused more and more young people to suffer from low back muscle damage and lumbar disk herniation. An uncomfortable office chair will directly affect the user's work efficiency and health [1]. It is urgent to optimize the existing chair to improve the quality and efficiency of work based on sitting habits and contemporary living concepts of modern office employees to improve the user experience and meet their deeper physiological and psychological needs, which must be resolved in the ergonomically optimized design of modern office chairs.

---

Y. Chen · C. He (✉) · Y. Lin  
College of Mechanical and Electrical Engineering, Hohai University, Changzhou 213022, China  
e-mail: [hecq@163.com](mailto:hecq@163.com)

© The Editor(s) (if applicable) and The Author(s), under exclusive license to Springer Nature Singapore Pte Ltd. 2021  
S. Long and B. S. Dhillon (eds.), *Man-Machine-Environment System Engineering*, Lecture Notes in Electrical Engineering 645, [https://doi.org/10.1007/978-981-15-6978-4\\_33](https://doi.org/10.1007/978-981-15-6978-4_33)



## 2 Analysis of User Demands

In Maslow's Hierarchical Demand Theory, human needs are divided into five categories [2]. In the analysis of user demands, the article extends the user-level requirements for the office chair product.

- Sit-down needs: The chair quality meets national standards.
- Comfort needs: The chair conforms to ergonomics and satisfies the change of sitting posture of human body. The structure has certain adjustability.
- Emotion needs: The shape is beautiful and aesthetically pleasing. It gives a positive psychological hint that people can rely on for safety.
- Value needs: It has distinctive features and is symbolic of identity. It can represent a certain social status.

Considering that the office chair users in this article are young female officers who are 20–40 years old, the chair in this article is guided by lightweight design “comfortable, practical, and stylish” in terms of structure and appearance.

## 3 Ergonomic Analysis in Chair Design

### 3.1 Analysis of Sitting Behavior of Office Crowd

Most office workers face the computer, place their hands on the desk, and stare at daily tasks shown on the computer screen. Grandjean [3] has studied the proportion of time spent in different sitting positions in the office, and the result showed that the sitting time of “sitting in the middle of the chair” and “table supporting arm” accounts for a large proportion of time.

In this case, prolonged desk work may cause soreness in the cervical spine, arms, waist, and hips, so the back support is particularly important [4]. It can enable the chair to provide support for people's waists at all times and reduce waist fatigue in this sitting position.

Due to less demand for headrests and armrests in this sitting position and the demand of lightweight design, this article focuses on designing waist and shoulder rests that fit the body but no headrests and armrests. Only the chair height can be adjusted.

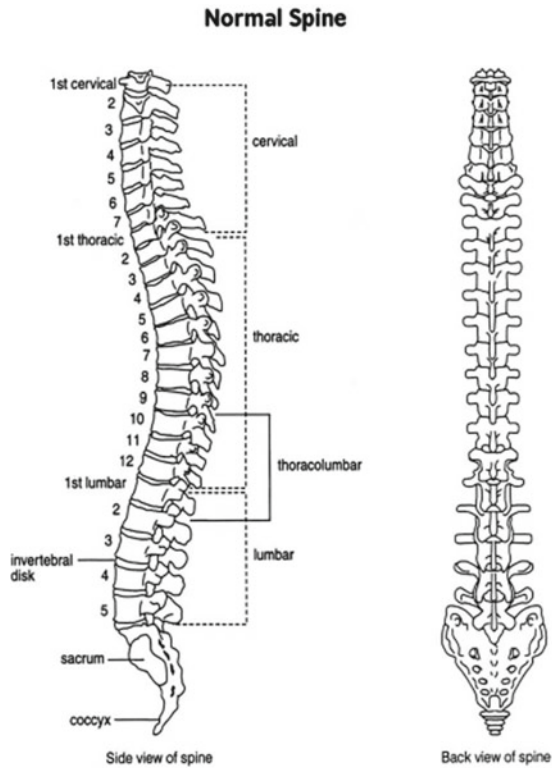
### 3.2 Theory of Sitting Physiological Structure

In a sitting position, the human body is mainly supported by the spine, pelvis, legs, and pedals [5]. Less disk pressure and proper spinal flexion are the keys to a comfortable sitting position.

In the sitting position, the seat body pressure is mainly distributed on the hips, and the greatest pressure is generated in the ischium part [6]. In order to reduce the pressure on the lower hip, the chair surface should generally be designed as a cushion. The backrest body pressure is mainly distributed in the scapula and lumbar vertebrae. These two support positions are often referred to as “waist back” and “shoulder back.”

Taking into account the “two-point support” effect at these two places, in general, a “waist rest” is set between the 3–4th section of lumbar and a “shoulder rest” is set between the 5–6th section of the thoracic. Among them, “waist back” is more important than “shoulder back” [7]. At the same time, the chair back should fit the curve of the human body’s waist and back as much as possible. Through the elasticity and plasticity of the material, it supports the waists of different users and satisfies the comfort of using as many people as possible as shown Fig. 1.

**Fig. 1** Human spine normal view

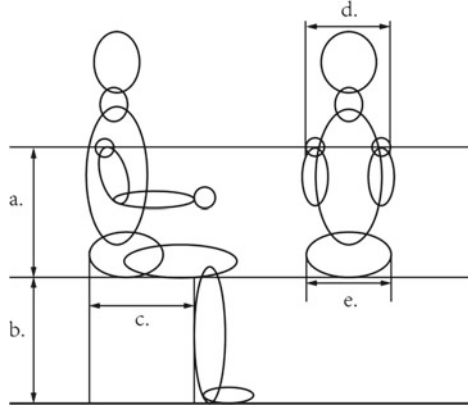


### 3.3 Setting Chair Size Based on Human Body Size

The size of each part of the chair should meet the standard of ergonomics, and at the same time, it must have certain adjustability. For the parameters of the chair, the specific values can be determined according to the size of the Chinese adult body (GB 10000-88.1989). Based on this parameter, it is adjusted according to the special requirements of the female population as shown Table 1.

The target group of the office chair designed in this article is young female office workers, and chairs are general industrial products; therefore, these products belong to the category III product size design, which needs to be based on the 50th percentile applicable to women to meet the generality. Secondly, it is necessary to determine the correction amount, including the functional correction amount and the psychological correction amount [8]. In the design of office chair products, considering the female's

**Table 1** Size of the Chinese adult body (GB 10000-88.1989)



26~35years old							
Percentile	1	5	10	50	90	95	99
a	506	520	528	556	587	596	610
b	334	345	353	383	399	405	417
c	390	403	409	434	463	470	485
d	347	363	371	396	426	435	455
e	295	311	318	345	372	381	398

dressing habits indoors, it is necessary to increase the appropriate dressing correction amount on the body size.

The amount of psychological correction is to increase the minimum functional size of the product in order to meet people's psychological needs. In product functional dimensions, the general formula for optimal functional dimensions is as follows:

$$h = p_0 + x + y \quad (1)$$

$h$  is the optimal functional size,  $p_0$  is the percentile of body size,  $x$  is the functional correction amount, and  $y$  is the psychological correction amount. The detailed dimensions of the chair design are as follows.

- Chair back height: Due to the sitting posture of the feet on the floor when sitting at the desk, the characteristics of women's dress, select the calf plus foot height  $p_{50} = 383$  mm,  $x \approx 10$  mm,  $y \approx 4$ , finally determined 397 mm as the initial chair height.
- Chair width: Select hip width  $p_{50} = 345$  mm,  $x \approx 50$  mm,  $y \approx 25$  mm, and about 420 mm as the initial frame chair width to facilitate the later addition of materials and modeling design.
- Chair depth: To prevent the thigh from being stressed in a forward leaning posture, this article selects a chair depth of  $p_{50} = 433$  mm,  $x \approx -50$  mm,  $y \approx -3\sim 7$  mm. The chair depth dimension is about 380–390 mm.
- Chair inclination angle  $\alpha$ : Set a certain chair inclination angle at the same time, which is about  $4^\circ$  backward; while the back of the chair satisfies the shape of the back curve, the square is tilted back about  $3\sim 5^\circ$  in the square phase. Plastic and elastic materials ensure that the user's waist and back are stretched during a break.

## 4 Emotional Design and Scheme of the Chair

Based on the requirements of emotional design, this article fully considers the user's behavioral level of experience in the design of female office chairs [9]. In the case of no armrest design, convex structures are added on both sides to enhance the user's psychological security while ensuring stability.

Secondly, the overall shape of the back refers to the design of the Coca-Cola bottle. The metaphorical design is reminiscent of the graceful figure of the girl, highlighting the curvy beauty of the woman (Figs. 2 and 3).

## 5 Conclusion

With the increase of the office crowd and the accompanying office diseases, the demand for a good and comfortable office environment, especially a comfortable office chair, has become more urgent. Aiming at the user group of ordinary



Fig. 2 Chair size view

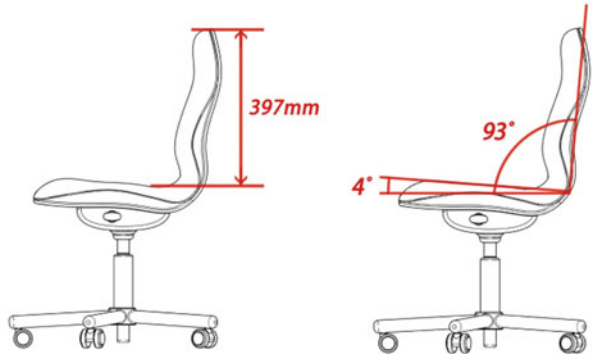


Fig. 3 Chair design renderings



young female employees, this article designed a “comfortable, practical, and stylish” office chair through user demand analysis and ergonomics. It has certain guiding significance and reference value for modern office chair design improvement and innovation.

**Acknowledgements** This study is financially supported by National Undergraduate Training Program for Innovation and Entrepreneurship (2019102941052).

## References

1. Liu Y, Guan X (2019) Evaluation of ergonomic design of office seats based on market research. *Furniture Interior Decoration* (01):28–29
2. Wang J (2019) Maslow needs a reinterpretation of the hierarchy theory. *Chin J Social Sci* 2019-11-04 (007)
3. Tian L (2018) Design and research of desk and chair based on ergonomics. Henan University of Science and Technology
4. Xu J, Zhang H, Cui T (2013) Design and innovation of office chair based on sitting posture. *Packaging Eng* 34(08):52–56
5. Zhang L, Shi X, Li J, Wang F (2014) Review on ergonomic design of seats. *Mech Des* 31(06):97–101
6. Liu L (2014) Analysis and application of humanized office chair design. Xi'an University of Technology, Xi'an, pp 20–22
7. Yang W, Zhang F (2017) Research on comfort design of office seat based on ergonomics. *Packaging Eng* 38(12):187–191
8. Ding Y (2011) *Ergonomics*, 4th edn. Beijing Institute of Technology, China
9. Norman D (2015) *Emotional design*. CITIC Publishing Group, Beijing

# Prototype Design and Performance Experiment of Passive Compliant Mechanism for the Automatic Charging Robot End Effector



Bingshan Hu, Ke Cheng, Weilun Zhang, and Xinran Zhang

**Abstract** Aiming at the demand of charging automation of electric vehicles, a charging robot end passive compliant mechanism based on Stewart parallel mechanism is designed based on the analysis of the requirements of electric vehicle charging plug and socket docking in this paper. The position and attitude deviation adaptability of the compliant mechanism under various deviation conditions are simulated, and a test platform is built by using a robot arm, and the docking experiments are carried out. The research results show that the passive compliant mechanism can meet the demands of reliable docking and has an inserting force less than 100 N in the case of large deviation.

**Keywords** Electric vehicles · Charging robot · Passive compliant mechanism

## 1 Introduction

Electric vehicles have been promoted and popularized due to the characteristics of energy saving and low emission [1]. After the popularization of automatic driving in the future, the automation of electric vehicle charging will be an inevitable development trend.

Under Volkswagen's v-charge program, electric cars can park themselves on inductive charging piles, but its charging efficiency is low (about 20%) [2]. VOLTERIO's NRG-X Charging Systems use wired charging, and an additional vehicle unit will be needed on the electric vehicle [3]. Other researchers have used robotic arms to insert the plug into car sockets [4, 5]. Considering the pose error and visual recognition error at the end of the manipulator, the traditional passive compliant mechanism is difficult to meet the demand of reliable plug-in of electric vehicle charging plug [6, 7]. If the compliance control strategy based on force feedback is adopted, the cost will rise sharply [8, 9].

---

B. Hu (✉) · K. Cheng · W. Zhang · X. Zhang  
Institute of Rehabilitation Engineering and Technology, University of Shanghai  
for Science and Technology, Shanghai, China  
e-mail: [hubingshan@usst.edu.cn](mailto:hubingshan@usst.edu.cn)

In this paper, based on the analysis of the requirements on the docking performance of electric vehicle charging plug and socket, a passive end-compliant mechanism of charging robot based on Stewart parallel mechanism is designed. Simulation analysis is carried out on the plugging and pulling ability of the mechanism under various deviation conditions, and the test platform is built for experiment.

## 2 Preliminary Design of Automatic Charging Robot

Theoretically, the charging robot should have six degrees of freedom to make up for the deviation between the charging plug and the charging port of the electric car. The base of charging robot is setted as the coordinate origin to establish the charging robot coordinate system  $O-xyz$ , and the charging socket of electric vehicle is setted as the coordinate origin to establish the socket coordinate system  $O_1-x_1y_1z_1$  (Fig. 1).

It is assumed that the charging socket is behind the side of the electric vehicle. After the observation and statistics of the relative position and pose data of different vehicle types and different drivers after parking, the design index of charging robot was obtained and shown in Table 1.

**Fig. 1** Definition of related coordinate system of charging robot



**Table 1** Design index of charging robot

Number	Parameters	Design index
1	$x$	0–600 mm
2	$y$	0–770 mm
3	$z$	0–400 mm
4	$\alpha$	$\pm 10^\circ$
5	$\beta$	$\pm 2.3^\circ$
6	$\gamma$	0–35°



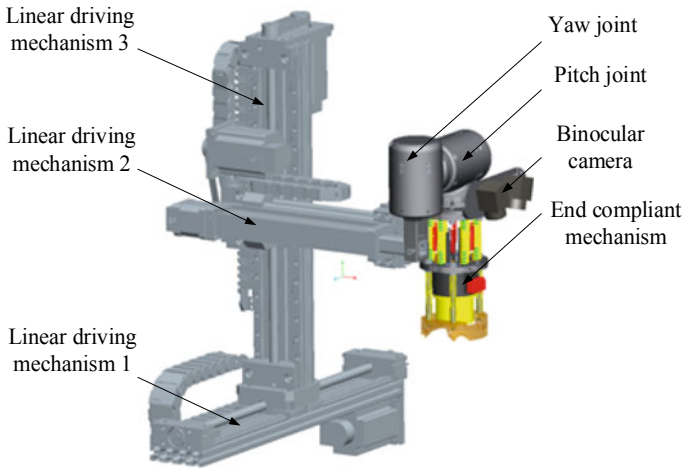


**Fig. 2** Charging robot model and mechanism configuration

In this table,  $x$  is the distance perpendicular to the ground from the charging socket to the origin of the charging robot coordinate system.  $y$  is the distance perpendicular to the car head from the charging socket to the origin of the charging robot coordinate system.  $z$  is the distance along the direction of the car head between the charging socket and the origin of the charging robot coordinate system.  $\alpha$  is the yaw angle of the docking face of the charging socket.  $\beta$  is the roll angle of the docking face of the charging socket.  $\gamma$  is the pitch angle of the docking face of the charging socket. Figure 2 is charging robot model and mechanism configuration.

### 3 Compliant Mechanism Design

When designing the first five active degrees of freedom of the charging robot, its terminal pose accuracy should be designed according to the requirements of  $\pm 5^\circ$  and  $\pm 3$  mm, and the insertion force should be designed according to 100 N. Therefore, the compliant mechanism should be able to achieve reliable fitting of the docking face of plug and socket under the condition of attitude deviation  $\pm 5^\circ$  (roll, pitch and yaw), position deviation  $\pm 3$  mm ( $x$ -,  $y$ - and  $z$ -axes) and insertion force of 100 N. The weight of the compliant mechanism is not more than 1 kg.

In the preliminary design, the compliant mechanism adopts the Stewart parallel mechanism configuration. Stewart parallel mechanism is a 6-SPS parallel mechanism, with a ball pair at both ends of each branch chain and a moving pair in the middle. The terminal motion is characterized by six degrees of freedom, including triaxial translation and triaxial rotation. In the compliant mechanism for the charging robot, the translation pair in the middle of the branch chain is replaced by a spring

rod. The axial deformation of the spring rod is used to simulate the linear motion of the branch chain of the Stewart parallel mechanism. The tangential deformation of the spring rod can enhance the tangential compliance of the compliant mechanism, so as to realize the six-dimensional motion of the moving platform of the compliant mechanism.

The metal rubber material is often used as the elastic element in the existing compliant mechanism. In the design of the principle prototype, the linear spring is used as the elastic element for easy manufacturing. The compliant mechanism includes a moving platform and a static platform, between which a number of compression springs and tension springs are arranged. The compression spring is arranged axially along the guide rod mounted on the static platform. The guide rods are arranged along the circumference between the moving platform and the stationary platform. The compression spring is in a precompression state. As shown in Fig. 3, four tension springs are also installed between the moving platform and the static platform. The tension spring is in a pretension state. The compression spring and tension spring cooperate to make the moving platform in a state of tension to maintain the plug position. When the plug is exposed to the contact force/torque of the socket, the compression spring and tension spring are deformed, so that the plug has six degrees of freedom of movement to adapt to the position and attitude deviation.

The floating guidance devices are arranged above the moving platform. It consists of guide block, compression spring of moving platform and compression spring guide rod of moving platform. The guide block is specially designed according to the shape of the electric car charging socket. During the insertion process, under the action of the charging robot's insertion force, the compression spring of the moving platform compresses along the guide rod. The guide block also gradually moves backward toward the direction of the static platform. Due to the guiding effect of the guide block's cone face, if the plug is further close to the socket along the socket axis, it can be guaranteed that the plug can be inserted into the socket reliably when the

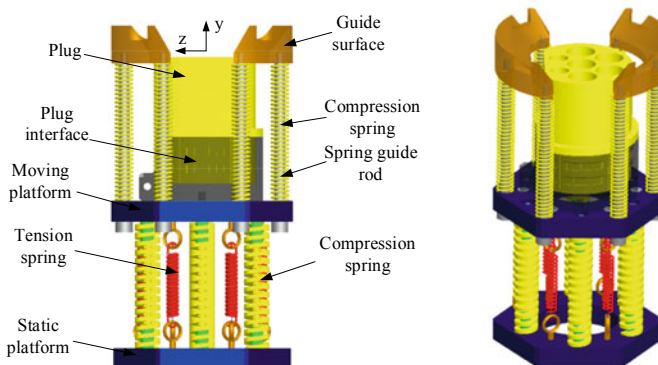


**Fig. 3** Schematic diagram of the end-compliant mechanism prototype

deviation of the charging plug and socket position is within  $\pm 5^\circ$  (roll, pitch and yaw) and  $\pm 3$  mm ( $x$ ,  $y$  and  $z$ ).

### 4 Simulation and Experimental Verification

The model of compliant mechanism and socket is established in ADAMS, and then, the working condition of compliant mechanism is simulated under the deviation condition. Before the simulation starts, the pose deviation between the plug and the socket is artificially set and the plug moves in a straight line along the axial direction of the socket. Simulation shows that the maximum position deviation adaptability of  $x$ -axis is  $\pm 5$  mm and that of  $z$ -axis is  $\pm 9$  mm when only position deviation exists. In this case, the plug and socket can be reliably connected. The reason why  $x$ -axis position error adaptability is weaker than  $z$ -axis position error adaptability is that in order to avoid the interference of socket cover and accessories on the socket, there is a gap on the guide block as shown in Fig. 3, which makes the guide block's guiding ability in  $x$ -axis direction weaker than  $z$ -axis.

In terms of attitude adaptability, when only attitude deviation exists, the maximum attitude deviation adaptability around the  $x$ -axis is  $\pm 7^\circ$ , and the maximum attitude deviation adaptability around the  $z$ -axis is  $\pm 6^\circ$ . The reason why the attitude error adaptability about the  $x$ -axis is stronger than that about the  $z$ -axis is the same as above. The maximum attitude deviation adaptability around the  $y$ -axis is  $\pm 10^\circ$ . In the case of composite pose deviation (attitude deviation about  $z$ -axis is  $5^\circ$ , and transverse deviation of  $Z$ -axis is 3 mm), the simulation shows that the plug can be reliably inserted into the socket (Fig. 4).

In order to verify the performance of end-compliant mechanism under different working conditions and test the maximum insertion force in the process of insertion and extraction, a performance testing platform was built by using a robot arm. The platform layout is shown in Fig. 5, including UR5 robot arm, end-compliant mechanism, six-dimensional force/torque sensor, simulated socket, etc. The compliant

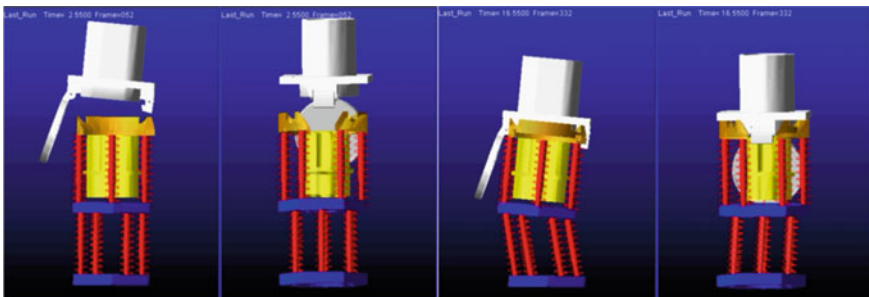
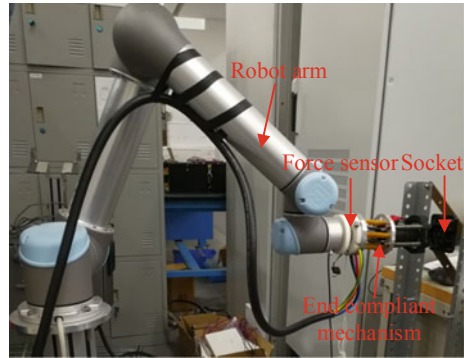
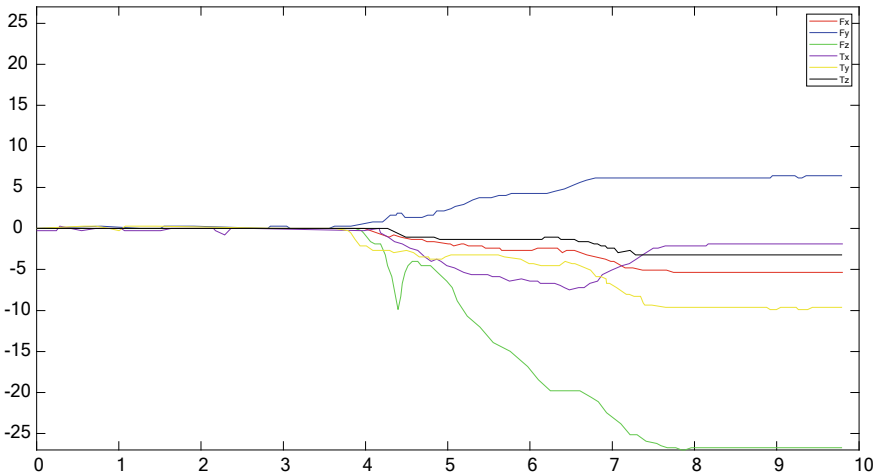


Fig. 4 Simulation schematic diagram in the case of composite pose deviation (attitude deviation about  $z$ -axis is  $5^\circ$ , transverse deviation of  $z$ -axis is 3 mm)

**Fig. 5** Testing platform for end-compliant mechanism



mechanism is installed at the end of the robot arm, and the deviation working condition between the plug and socket is established by the arm. Then, the arm approximates the simulated socket and plugs with linear motion and records whether the plug-in the end-compliant mechanism is successfully inserted into the socket. Repeat the above steps to find out the ultimate deviation working condition of the end-compliant mechanism and record the insertion force. Through experiments, it is found that the plug can be inserted reliably under various deviation conditions in the simulation experiment, which verifies the correctness of the above simulation results. The maximum normal insertion force occurs in the case of compound deviation (attitude deviation about z-axis is  $5^\circ$ , transverse deviation of z-axis is 3 mm), reaching 97.9 N, which meets the requirements of national standard. Figure 6 shows the forces/torques measured by the six-dimensional force sensor at this time.



**Fig. 6** Inserting force under compound deviation

## 5 Conclusion

Based on the analysis of the requirements of the docking performance index of electric vehicle charging plug and socket, a charging robot terminal passive compliant mechanism based on Stewart parallel mechanism is designed, and its plug-in ability under various deviation conditions is verified by simulation and experiments in this paper. The results show that the maximum position deviation adaptability of the compliant mechanism in the  $x$ -axis direction is  $\pm 5$  mm, and the maximum position deviation adaptability of the  $z$ -axis is  $\pm 9$  mm when only position deviation exists. When only attitude deviation exists, the maximum attitude deviation adaptability is  $\pm 7^\circ$  around the  $x$ -axis and  $\pm 6^\circ$  around the  $z$ -axis. Under the condition of compound deviation (attitude deviation about  $z$ -axis  $5^\circ$  and transverse deviation of  $z$ -axis 3 mm), the passive end-compliant mechanism can also realize reliable inserting and the maximum inserting force is less than 100 N.

## References

1. Bunsen T, Cazzola P, Gorner M, Paoli L, Scheffer S, Schuitmaker R, Teter J et al (2018) Global EV Outlook 2018: towards cross-modal electrification. In: International Energy Agency
2. Schwesinger U, Bürki M, Timpner J, Siegwart R et al (2016) Automated valet parking and charging for e-mobility: results of the V-charge project. In 2016 IEEE Intelligent Vehicles Symposium. <https://doi.org/10.1109/ivs.2016.7535380>
3. NRG-X—Automatic Charging for E-Mobility. <http://www.nrg-x.com/impressum.html>. Accessed on 6 Mar 2017
4. <https://www.volkswagenag.com/en.html>. Accessed on 6 Mar 2017
5. Miseikis J, Rütthe M, Walzel B, Hirz M, Brunner H (2017) 3D vision guided robotic charging station for electric and plug-in hybrid vehicles. In: ArXiv abs/1703.05381
6. Whitney DE (1982) Quasi-static assembly of compliantly supported rigid parts. *J Dyn Syst Meas Control* 104:65–77
7. Haskiya W, Maycock K, Knight JAG (1998) A passive compliant wrist for chamferless peg-in-hole assembly operation from vertical and horizontal directions. *Proc Inst Mech Eng Part B: J Eng Manuf* 212(6):473–478
8. Kramberger A, Gams A, Nemeč B, Chrysostomou D, Madsen O, Ude A (2017) Generalization of orientation trajectories and force-torque profiles for robotic assembly. *Robot Autonomous Syst* 98:333–346
9. Hyeonjun P, Jaeheung P, Dong-Hyuk L, Jae-Han P, Moon-Hong B, Ji-Hun B (2017) Compliance-based robotic peg-in-hole assembly without force feedback. In: *IEEE Transactions on Industrial Electronics*, pp 1-1. <https://doi.org/10.1109/tie.2017.2682002>

# Facilities Design of Fume Protection and Ventilation System in Welding Workshop of an Automotive Enterprise



Chen Ding, Bin Yang, Jianwu Chen, Pei Wang, and Ying Wang

**Abstract** The welding fume in the welding workshop has an important impact on the occupational health of the workers in the workshop. Scientific and reasonable design of the ventilation system in the welding workshop can effectively reduce the concentration of the welding fume and ensure the occupational health of the workers. This paper uses the method of controlling wind velocity to design the ventilation system of workshop. The results show that the system can effectively control the welding fume, and the concentration is less than  $4 \text{ mg/m}^3$ .

**Keywords** Welding workshop · Ventilation system · Facilities design · Exhaust hood

## 1 Background

Welding is the main process in the automotive manufacturing industry. Welding technology is used in the manufacture of automobile body, frame, engine, compartment and transmission [1]. The welding process is also used to complete most of the work during vehicle repairs. Wu Qi and others have tested the welding fume in a workshop of an automobile factory. The test results show that the over-standard points of spot welding fume concentration in welding procedure of the workshop account for 60% of the total inspection points [2].

Welding is an important technology widely used in industrial fields. According to statistics, the annual consumption of metal welding materials worldwide is about 1 million tons, of which about 0.5% of metal welding materials are converted into

---

C. Ding · P. Wang

Capital University of Economics and Business, Beijing 100070, China

B. Yang (✉) · J. Chen

China Academy of Safety Science and Technology, Beijing 100029, China

e-mail: [ybustb@163.com](mailto:ybustb@163.com)

Y. Wang

CRRC Changchun Railway Vehicles Co. Ltd., Jilin 130062, China

© The Editor(s) (if applicable) and The Author(s), under exclusive license to Springer Nature Singapore Pte Ltd. 2021

S. Long and B. S. Dhillon (eds.), *Man-Machine-Environment System Engineering*, Lecture Notes in Electrical Engineering 645, [https://doi.org/10.1007/978-981-15-6978-4\\_35](https://doi.org/10.1007/978-981-15-6978-4_35)

welding fumes [3]. The welding automation level is less than 30% in China. Most of the welding is still completed by manual argon arc welding [4]. Scientific research shows that there are lots of inhalable substances in welding fumes (such as manganese oxide, hexavalent chromium) [5]. Inhalation of these fumes and gases has a great effect on lung function and causes acute as well as chronic diseases like lung cancer, metal fume fever [6], which seriously affects the occupational health of workers. Relevant data show that injuries to workers cannot be underestimated.

Negative pressure ventilation system is a ventilation method which can effectively reduce the concentration of harmful substances in welding workshop, but the annual operation cost is increased by about 180% [7]. Flynn et al. [8] pointed that when the position of welding point changes, the smoke absorption performance of local exhaust hood will be reduced. Li [9] found that after the partial ventilation and dust removal facilities were set up, because of the process limitations.

Thus, it is necessary to design the fume protective ventilation system in the welding workshop to improve the working environment and protect the workers' health.

This paper takes frame-welding workshop of an automobile manufacturing enterprise in Suzhou as an example to analyze.

## 2 Basic Conditions of Welding Workshop

The basic conditions of the workshop are as follows: The dimensions of the frame-welding workshop are 100 m × 24 m, the area is 2400 m<sup>2</sup>, and the width of the safe passage in the middle is 2 m. An air outlet is provided at the top every 10 m.

### 2.1 Existing Layout of Welding Work in Workshop

Welding and grinding are mainly carried out in the workshop. There are two welding production lines in the workshop, with seven welding stations per production line. The welding area is shown on one side of the workshop, and the welding platform is 1 m × 1 m, as shown in Fig. 1.

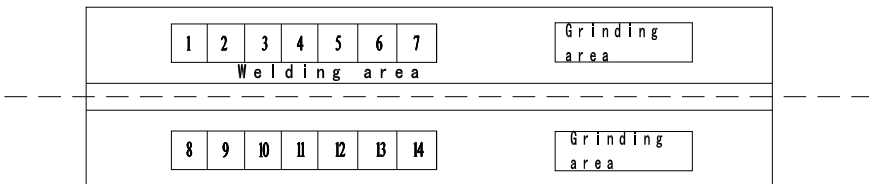


Fig. 1 Layout of welding workshops

**Table 1** Dust concentration at each station (mg/m<sup>3</sup>)

Location determination	Dust concentration (mg/m <sup>3</sup> )	Location determination	Dust concentration (mg/m <sup>3</sup> )
1	8.38	8	5.43
2	7.46	9	9.72
3	13.64	10	12.33
4	12.35	11	11.47
5	6.42	12	7.46
6	10.74	13	8.73
7	12.76	14	13.12

### 2.2 Existing Ventilation in the Workshop

Workshop ventilation mainly relies on natural ventilation. It is found that the allowable dust concentration of welding fume in the air of each station is not up to the national standard for 4 mg/m<sup>3</sup> [10]. Detection result is shown in Table 1.

## 3 Design of Ventilation System in Welding Workshop

In this design, local ventilation mode is mainly considered. Flynn et al. have shown that local exhaust ventilation is an effective control method for welding fume [8]. It not only saves cost and energy for enterprises, but also achieves adequate ventilation effect with minimum ventilation volume.

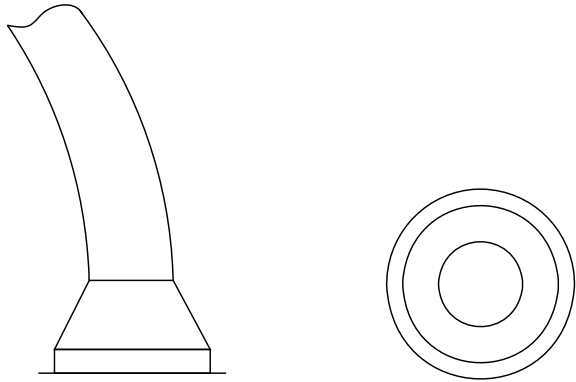
Local ventilation mainly controls pollutants through the local exhaust hood. Pollutants can be directly trapped at the site where they are emitted to ensure that the concentration of dust in the royal household does not exceed the standards [11].

### 3.1 Determination of Exhaust Hood

The external suction hood can be designed because of the small area of dust produced during electric welding and the limitation of layout conditions. The outer suction hood generates a certain air flow through the suction effect of the hood, which makes the dust enter the exhaust hood along with the air flow at the source point a certain distance from the suction nozzle. A properly designed external suction hood can achieve optimal control with less air volume [12].

According to relevant national standards GB/T16758-2008, the classification and technical specification of exhaust hood. (In China) and basic conditions of workshop, Because the welding fumes mainly float upwards, the welding joints are not fixed



**Fig. 2** Local exhaust hood

when welding, if design a fixed exhaust hood to reduce the ventilation effect, the exhaust hood is designed as a locally aspirated exhaust hood that can be partially moved at each station. The welding operator can manually adjust the air exhaust hood cover to the proper position above the welding joint according to the change of welding joint.

### 3.1.1 Dimensional Design of Air Exhaust Hood

Considering the influence of the transverse air flow in the workshop, because it is a local movable exhaust hood, the hood opening of the exhaust hood is designed as a circular umbrella hood of  $0.5\text{ m} \times 0.5\text{ m}$ , the expansion angle  $\alpha$  of the umbrella cover select  $60^\circ$  [13], The exhaust hood is flexible coupling connected by soft connecting pipe. The shape of exhaust hood is shown in Fig. 2. Relevant data show that if the exhaust hood is added with flange edge, the ventilation efficiency will be significantly improved, so a flange edge of 60 mm is added to the exhaust hood [14].

### 3.1.2 Position of Exhaust Hood Cover

On the premise of not affecting the operation, the local exhaust hood shall be surrounded or close to the source of harmful substances as far as possible, which is convenient for catching and control [15]. The distance  $h$  from the hood to the working face shall be less than or equal to  $0.3 A$  (the long side size of the hood) [16], so the distance  $h$  from the hood to the welding workplace is designed as 0.5–0.7 m.

### 3.1.3 Calculation of Exhaust Volume of Exhaust Hood

According to the method of wind speed control, the exhaust velocity formula [13]:

$$\frac{v_0}{v_x} = 0.75 \left[ \frac{10x^2 + F}{F} \right] \quad (1)$$

where  $V_0$  is average velocity of suction port, m/s;  $V_x$  is suction speed of control point, m/s;  $x$  is distance from control point to suction port, m;  $F$  is area of suction port,  $m^2$ .

Taking the average velocity of the suction port of the local exhaust hood as 8 m/s, the control wind speed at the welding point is about 0.7 m/s. Because the particle size of the welding fume is quiet small, the wind speed can absorb the welding fume.

Exhaust volume formula [13]:

$$L = KPHv_x \quad (2)$$

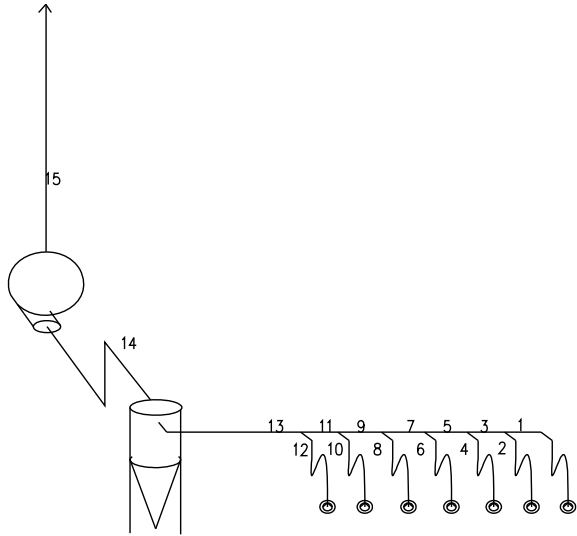
where  $P$  is perimeter of open face of exhaust hood and the  $K$  means safety factor, which usually takes 1.4. The result shows that the exhaust air quantity  $Q$  of the system is  $1.08 \text{ m}^3/\text{s}$  ( $H$  to 0.7 m), i.e.,  $3888 \text{ m}^3/\text{h}$ .

### 3.2 Piping Arrangement

According to relevant national regulations [17], the pipeline layout shall be as straight as possible without bending; it shall be arranged vertically or obliquely as far as possible, and the included angle with the horizontal plane shall be more than  $45^\circ$  when it is arranged obliquely. The commonly used air duct materials of ventilation system are divided into metal materials and non-metal materials. The metal materials include ordinary steel sheet, galvanized steel sheet and stainless steel sheet. Galvanized steel plate can prevent rust due to its galvanized surface, so, among them, galvanized steel air duct is the most widely used [18]. Galvanized steel plate has a certain anti-corrosion performance, which is suitable for ventilation and air conditioning systems with high air humidity or indoor humidity.

Due to the high hardness of particles and the high wind speed, the wear of dust on the pipe wall in the welding workshop is large, and under the same cross-sectional area, the circular air pipe is more material saving and has strong resistance to wind. Therefore, the round, 3-mm-thick galvanized steel plate is selected as the air duct, and the standard air duct diameter is selected according to the (GB50243-2016) code of acceptance for construction quality of ventilation and air conditioning works (In China). Piping arrangement is shown in Fig. 3. Layout of pipes avoids excessive bending and reduces wind resistance during air exhaust [13].

**Fig. 3** Piping arrangement



## 4 Hydraulic Calculation of Air Duct

### 4.1 Length and Air Volume of Each Pipe Section

Pipe section 1 is:  $L_1 = 6$  m, pipe sections 2, 4, 6, 8, 10, 12 is:  $L_2 = L_4 = L_6 = L_8 = L_{10} = L_{12} = 2.5$  m, pipe sections 3, 5, 7, 9, 11 is:  $L_3 = L_5 = L_7 = L_9 = L_{11} = 6$  m, pipe section 13 is:  $L_{13} = 5$  m,  $L_{14} = 6$  m, and pipe section 15 is:  $L_{15} = 6$  m.

The system selects 1-3-5-7-9-11-13-dust collector-14-fan-15 as the most disadvantageous loop. According to (GB50243-2016) code of acceptance for construction quality of ventilation and air conditioning works (In China), when conveying gas containing steel dust, the minimum wind speed in the duct is 13 m/s in vertical duct and 15 m/s in horizontal duct. Considering the air leakage of air duct and dust collector, the calculated air flow  $Q$  for pipe sections 14 and 15 is [13]:

$$Q_{14,15} = 3888 \times 7 \times 1.05 = 28576.8 \text{ m}^3/\text{h}$$

To pipe section 1, based on  $Q_1 = 3888 \text{ m}^3/\text{h}$ ,  $v_1 = 15 \text{ m/s}$ , find the corresponding diameter  $D$  and the friction resistance  $R_m$  per unit length:  $D_1 = 280 \text{ mm}$ ,  $R_{m1} = 12 \text{ Pa/m}$ .

Similarly, the pipe diameters and specific frictional resistance of sections. 3, 5, 7, 9, 11, 13, 14, 15, 2, 4, 6, 8, 10, 12 can be calculated; the result is shown in Table 2.

**Table 2** Parameters of each pipe section

Pipe section number	Air volume (m <sup>3</sup> /h)	Length (m)	Pipe diameter (mm)	Current speed (m/s)	Specific frictional resistance (Pa/m)	Friction (Pa)
1	3888	6	280	15	12	72
3	7776	4	400	15	7	28
5	11,664	4	500	15	5.9	23.6
7	15,552	4	550	15	4.8	19.2
9	19,440	4	670	15	3.9	15.6
11	23,328	4	700	15	3.5	14
13	27,216	5	800	15	3.2	16
14	28,576.8	6	850	13	2.2	13.2
15	28,576.8	6	850	13	2.2	13.2
2	3888	3	280	15	12	36
4	3888	3	280	15	12	36
6	3888	3	280	15	12	36
8	3888	3	280	15	12	36
10	3888	3	280	15	12	36
12	3888	3	280	15	12	36

### 4.2 The Local Resistance in Each Pipe Section

Each pipe section’s exhaust hood, elbow, DC tee pipe, variable diameter pipe, local resistance factor  $\zeta$  and local resistance’s calculation formula are on the basis of industrial ventilation [13]. Pipe sections 1–12 all have 90° elbow ( $R/D = 1.5$ ) 1,  $\zeta = 0.18$ .

1. Pipe section 1. Exhaust hood,  $\alpha = 60^\circ$ ,  $\zeta = 0.09$ ;  $\Sigma\zeta = 0.27$ .
2. Pipe section 2. Exhaust hood,  $\alpha = 60^\circ$ ,  $\zeta = 0.09$ ; DC tee 2–3,  $\zeta = -0.31$ ;  $\Sigma\zeta = -0.04$ .
3. Pipe section 3. DC tee 3–5,  $\zeta = 0.11$ .
4. Pipe section 4. Exhaust hood,  $\alpha = 60^\circ$ ,  $\zeta = 0.09$ ; DC tee 4–5,  $\zeta = 0.71$ ;  $\Sigma\zeta = 0.98$ .
5. Pipe section 5. DC tee 5–7,  $\zeta = -0.01$ .
6. Pipe section 6. Exhaust hood,  $\alpha = 60^\circ$ ,  $\zeta = 0.09$ ; DC tee 6–7,  $\zeta = 1.02$ ,  $\Sigma\zeta = 1.29$ .
7. Pipe section 7. DC tee 7–9,  $\zeta = -0.78$ .
8. Pipe section 8. Exhaust hood,  $\alpha = 60^\circ$ ,  $\zeta = 0.09$ ; DC tee 8–9,  $\zeta = 2.84$ ,  $\Sigma\zeta = 3.11$ .
9. Pipe section 9. DC tee pipe (Pipe Sections 9–11),  $\zeta = -0.82$ .

10. Pipe section 10. Exhaust hood,  $\alpha = 60^\circ$ ,  $\zeta = 0.09$ ; DC tee 10–11,  $\zeta = 3.12$ ,  $\Sigma\zeta = 3.39$ .
11. Pipe section 11. DC tee 11–13,  $\zeta = -0.95$ .
12. Pipe section 12. Exhaust hood,  $\alpha = 60^\circ$ ,  $\zeta = 0.09$ ; DC tee 12–13,  $\zeta = 12.4$ ,  $\Sigma\zeta = 12.7$
13. Pipe section 13. Dust collector outlet variable diameter pipe (diverging pipe): The size of bag filter LHF-380C's inlet is 524 mm  $\times$  974 mm, and the length of the variable diameter pipe is 200 mm,
14.  $\tan\alpha = \frac{1}{2} \frac{(974 - 800)}{200} = 0.435$

Diverging pipe's angle  $\alpha = 23.5^\circ$ , check from the book,  $\zeta = 0.626$ , 90° elbow ( $R/D = 1.5$ ) 1,  $\zeta = 0.18$ ,  $\Sigma\zeta = 0.806$ .

15. Pipe section 14. Dust collector outlet variable diameter pipe (Reductive pipe): The size of bag filter's outlet is 524 mm  $\times$  974 mm, the length of the variable diameter pipe is 200 mm,  $\tan\alpha = 0.31$ , reductive pipe's angle  $\alpha = 17.2^\circ < 45^\circ$ , check from the book,  $\zeta = 0.1$ , 90° elbow ( $R/D = 1.5$ ) 2,  $\zeta = 0.36$ .

Diverging pipe of fan inlet: First, a fan is approximately selected. The inlet diameter of the fan  $D_f = 900$  mm and the length of the variable diameter pipe are 100 mm,  $\tan\alpha = 0.25$ , diverging pipe's angle  $\alpha = 14^\circ$ , check from the book,  $\zeta = 0.379$ ,  $\Sigma\zeta = 0.839$ .

16. Pipe section 15. Reductive pipe of fan outlet: The size of fan outlet is 570 mm  $\times$  810 mm, and the length of reducer is 100 mm,  $\tan\alpha = 0.2$ , reductive pipe's angle  $\alpha = 11.3^\circ$ , check from the book,  $\zeta = 0.61$ . Calculating friction resistance along pipe sections  $P_m$ :

$$P_m = R_m l \quad (3)$$

$R_m$  means specific frictional resistance, Pa/m.  $l$  is the length of pipe, m. And local resistance is  $Z$ :

$$Z = \zeta \frac{v^2 \rho}{2} \quad (4)$$

$\rho$  is air density, which usually takes 1.29 kg/m<sup>3</sup>. Calculation results are shown in Table 3.

**Table 3** Local resistance of each pipe section

Pipe section number	Local resistance factor $\zeta$	Local resistance (Pa)	Total resistance of pipeline (Pa)
1	0.27	36.45	108.45
3	0.11	14.85	42.85
5	-0.01	-1.35	22.25
7	-0.78	-105.3	-86.1
9	-0.82	-110.7	-95.1
11	-0.95	-128.25	-114.25
13	0.806	108.81	124.81
14	0.839	84.9068	98.1068
15	0.61	61.732	74.932
2	-0.04	-5.4	30.6
4	0.98	132.3	168.3
6	1.29	174.15	210.15
8	3.11	419.85	455.85
10	3.39	457.65	493.65
12	12.67	1710.45	1746.45
Bag filter			1000

### 4.3 Select Fan

Considering the error of air leakage and resistance calculation of fan, in order to operate the system effectively, the air flow and pressure of selected fan should be calculated as follows [13]:

1. Fan air volume:

$$L_f = K_L \cdot L$$

$K_L$  is the additional coefficient of air flow. The dust removal system  $K_L = 1.1-1.15$ , takes  $K_L = 1.1$ . Reach that the air flow of fan  $L_f = 31,434.5 \text{ m}^3/\text{h}$ .

2. Fan air pressure:

$$P_f = K_P \cdot \Delta P$$

$K_P$  is the additional coefficient of wind pressure. The dust removal system  $K_P = 1.15-1.2$ , which takes  $K_P = 1.15$ . Reach that the wind pressure of the fan  $P_f = 5498.1 \text{ Pa}$ . Therefore, type 9-19-16D centrifugal fan is selected for the fan, with

**Table 4** Dust concentration at each station ( $\text{mg}/\text{m}^3$ )

Location determination	Dust concentration ( $\text{mg}/\text{m}^3$ )	Location determination	Dust concentration ( $\text{mg}/\text{m}^3$ )
1	0.92	8	0.59
2	0.82	9	1.07
3	1.5	10	1.36
4	1.36	11	1.26
5	0.71	12	0.82
6	1.18	13	0.96
7	1.4	14	1.44

air flow  $L_f = 33,762 \text{ m}^3/\text{h}$ , air pressure  $P_f = 6180 \text{ Pa}$ , fan's speed  $n = 960 \text{ r}/\text{min}$ , equipped with Y315L1-6 motor, power  $N = 110 \text{ w}$ .

## 5 Dust Removal Effect of Ventilation System

According to formula Dennis-klemm [19], the dust removal efficiency of the system is estimated to be 89.6%. The results of welding fume concentration at each station are shown in Table 4.

## 6 Conclusion

This paper draws the following conclusions through the design of ventilation system in welding workshop.

1. The use of locally movable umbrella-shaped air exhaust hood can adjust the position of air exhaust hood to the welding spot at any time according to the different welding work position, which solves the problem that the welding fume cannot be effectively absorbed when the welding joint is not fixed.
2. Galvanized steel sheet is used as piping material and can be used for a longer period of time under the circumstance of welding fume. The arrangement of pipes has less bending, less resistance, less material consumption and better wind resistance for circular ducts with the same cross-sectional area, and lower maintenance and replacement costs.
3. By hydraulic calculation of air duct, under the condition that there are seven workstations in one production line of the workshop, only one system can fulfill the ventilation requirements of the workshop, which not only controls the spread of welding fume, but also meets the requirements of energy saving and emission reduction.

The above design optimization can reduce the concentration of welding fume to below  $4 \text{ mg/m}^3$ , which shows that the design method is reliable and effective, and can provide reference for the design of ventilation system in welding workshop.

**Acknowledgements** This work was supported by the National key R&D Program of China (2016YFC0801700), the basic research funding of China Academy of Safety Science and Technology (2019JBKY11 and 2019JBKY04) and the Graduation design (Scientific Research) project of “practical training plan” for cross training of high-level talents in Beijing institutions of higher learning in 2019 (No.1600, 2019).

## References

1. Ouyang X (2016) Application of welding process in automotive manufacturing and quality control. *Modern SOE Res* 22:117
2. Huang J, Shen A, Zhang Z (2015) Hazards of occupational exposure to welding fume and related control measures. *Occup Health Emergency Rescue* 33(1):22–25, 33
3. Popović O, Prokić-Cvetković R, Burzić M, Lukić U, Beljić B (2014) Fume and gas emission during arc welding: Hazards and recommendation. *Renew Sustain Energy Rev* 37(3):509–516
4. Cao Y (2019) Current situation of welding production and development of welding technology in China. *Sci Technol Inf* 17(11):73–74
5. Xu F (2008) Research on forming fume influenced by process parameters in GMA Welding. Tianjin University
6. Antonini J, Lewis A, Roberts J, Whaley D (2003) Pulmonary effects of welding fumes: review of worker and experimental animal studies. *Am J Ind Med* 43:350–360
7. Xie L, Cao H, Ding L, Zhang Y, Zhou Z (2013) Ventilation system retrof it design of welding workshop. *Constr Des Project* 4:92–93
8. Flynn MR, Susi P (2012) Local exhaust ventilation for the control of welding fumes in the construction industry—a literature review. *Ann Occup Hygiene* 56(7):764–776
9. Li X, Yin H, Shan B (2011) Evaluation on ventilation system in welding workshop. *Chin J Public Health Manage* 27(3):278–279
10. GBZ 2.1-2007 Occupational exposure limits for hazardous agents in the Workplace-Part1: Chemical hazardous agents (In China)
11. Cui T (2016) Research on control technology of welding fume in multi-span large space factory building. Anhui University of Science & Technology
12. Li H (2018) Research on diffusion value and comprehensive control measures of welding fume in an electro-welding plant. Capital University of Economics and Business
13. Sun Y, Shen H (2010) Industrial ventilation (4th). China Architecture & Building Press, Beijing
14. Wang H, Wang X (1998) Design optimization of local air-exhaust hoods. *HV & AC* 5:11–15
15. Zhao R (2005) Design requirements for common local exhaust hood. *Labor Protection* 11:84–85
16. Sun Y (1997) Concise ventilation design manual. China Architecture & Building Press, Beijing
17. GB 50019-2015. Design code for heating ventilation and air conditioning of industrial buildings (In China)
18. Liu H (2013) Design of ventilation system in chemical plant. *China Constr Metal Struct* 4:129–130
19. Teaching plan of air pollution control. <http://www.docin.com/app/p?id=343597635>. p 9. Last visit: 2020.2.17



# Study on Optimization Design of Drive Seat Based on Body Comfort



Yu Wang, Yongqin Wang, Xiangcao Niu, and Yi Liu

**Abstract** The research work of this paper is about the design of driver seat in the research of armored vehicles. In the design process, the seat function, vehicle space and riding comfort are mainly considered based on man-machine-environment system of armored vehicles. The working state of the driver is simulated by applying the seat model and the human body model. In order to design the shape of seat cushion and seat back, the human body model is used to simulate the driving posture. Then, the stiffness of the damping shock absorber is simulated and analyzed. By optimizing the stiffness and damping of damping shock absorber, the driving comfort is further improved, and the working efficiency of driver is enhanced. The comfort of driver is improved by optimal design.

**Keywords** Seat · Comfort · Damping shock absorber · Stiffness

## 1 Introduction

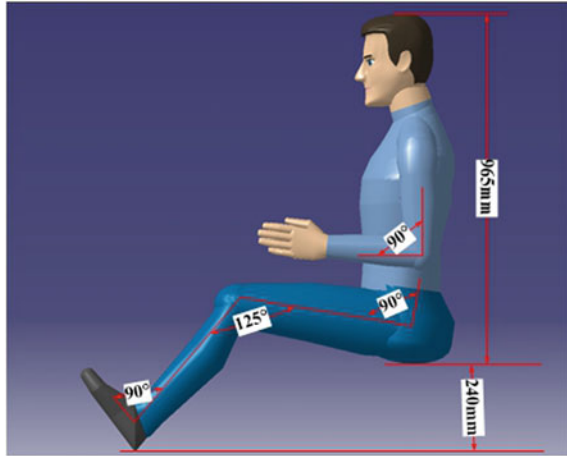
The seat of tracked armored vehicle mainly provides reliable support for the driver. The seat is an important component of tracked armored vehicle. Its design is directly related to the comfort performance of the driver, while the comfort of the seat directly affect the continuous operation time of the driver [1–3]. The seat not only requires to be satisfied with the shape, but also needs human factors, such as comfortable sitting posture, light operation position, reasonable body pressure distribution, etc. At present, the driver often feels that the vehicle vibration is strong, and the seat is uncomfortable which brings security risks to driving. In order to improve the riding comfort of the driver seat, it is significant to improve the performance of the seat.

---

Y. Wang (✉) · Y. Wang · X. Niu · Y. Liu  
JiangLu Mechanical & Electrical Group Co., Ltd, Hunan 411100, China  
e-mail: [wyuone@163.com](mailto:wyuone@163.com)

© The Editor(s) (if applicable) and The Author(s), under exclusive license to Springer 301  
Nature Singapore Pte Ltd. 2021  
S. Long and B. S. Dhillon (eds.), *Man-Machine-Environment  
System Engineering*, Lecture Notes in Electrical Engineering 645,  
[https://doi.org/10.1007/978-981-15-6978-4\\_36](https://doi.org/10.1007/978-981-15-6978-4_36)

**Fig. 1** Seat model of the 95th percentile



## 2 Ergonomic Design of Seat

The comfort of the driver is directly related to the seat, which directly affects the continuous operation time of the driver. The driver not only needs to be satisfied with the shape, but also pays more attention to the human factors, sitting posture, operating posture and body pressure distribution.

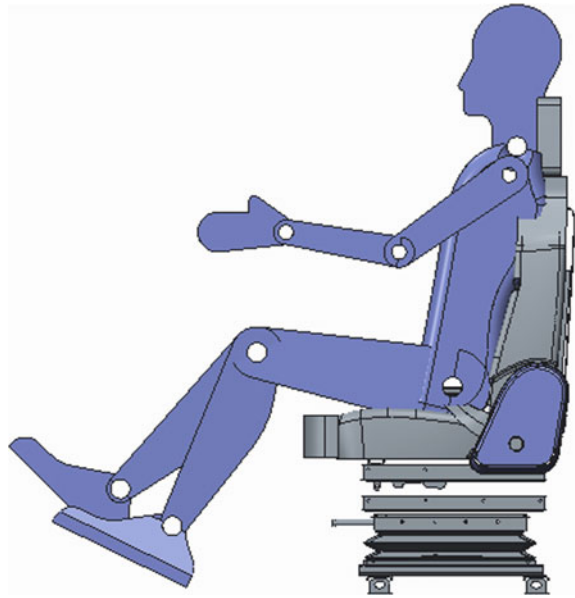
### 2.1 *Sitting Position*

Seat design should consider the perspective of ergonomics. The height and position of different people need different requirements. In this paper, the driver seat is designed for the 95th percentile. The height of the driver is 1785 mm, and the sitting height is 965 mm. According to the ergonomics, the angle between trunk and thigh is 90–100°. The angle of knee is 125°, the angle of elbow is 80–120°, and the angle of ankle is 90–100°. In the 95th percentile, the driver leans back with his eyes at the angle of about 100° between the torso and the thigh. The distance from the front to the heels is 240 mm. The angle between trunk and thigh is about 90° and the distance between sitting face and heel is 240 mm, as shown in Fig. 1.

### 2.2 *Driver Seat Design*

The driver seat is composed of backrest, cushion, backrest angle adjuster, vibration damping device and so on. The seat with the function of lifting up and down, front

**Fig. 2** Simulation model of driving posture



and rear adjustment can satisfy the needs of different drivers in cockpit driving and closed cabin driving.

Seat cushion and backrest bear most of the weight of human body, which plays a very important role in satisfying the comfort and safety protection of passengers. The excellent seat cushion and backrest should provide comfortable driving feel for drivers, so as to effectively reduce the fatigue of drivers caused by long-distance driving [4–7].

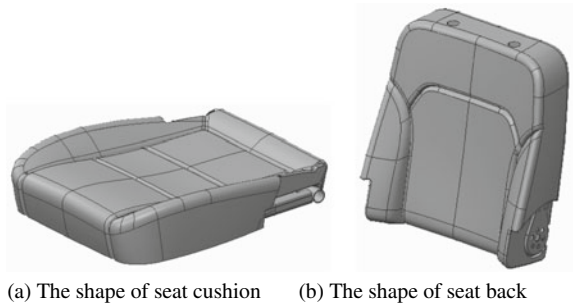
Firstly, the human body model is used to simulate the riding posture, as shown in Fig. 2. The length and width of seat cushion and seat back are designed by the analysis of human–machine effect.

According to the principle of ergonomics, the human pelvis profiling design is adopted. The cushion is designed to be low in the middle and high in both sides, so as to improve the fit between the cushion and the human body. The front angle of the cushion is inclined upward  $5^\circ$  with the vertical direction, as shown in Fig. 3a. The backrest angle is designed to be low in the middle and high in both sides, so as to improve the fit between the backrest and the human body. The top angle of the backrest leans backward  $5^\circ$  with the vertical direction, as shown in Fig. 3b.

### **2.3 Design of Adjustment of Seat**

According to the requirement of the vehicle, the human body model is used to simulate the driving posture of the driver in cockpit driving (see Fig. 4a) and closed

**Fig. 3** Shape of seat cushion and seat back



cabin driving (see Fig. 4b). The space size between the driver and steering control, electric control shift device, brake control device, accelerator pedal is checked and adjusted, so as to ensure that the adaptability, maneuverability and maintenance can be satisfied by the design of seat. Finally, the adjusted value of upper and down is identified as 250 mm, and the adjusted value of front and back is identified as 160 mm, which can ensure observing and driving conveniently.

### 3 Design and Analysis of Damping Shock Absorber

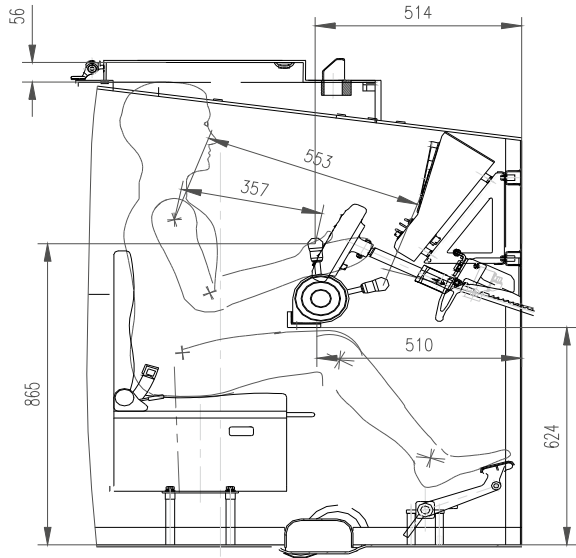
In order to reduce the discomfort to the driver, the damping shock absorber is designed to absorb the energy from bumpy road to reduce vibration [7].

The Adams software is used to establish the simulation model. *X*-direction points to the rear of the seat, *Y*-direction points to the upper part of the seat, and *Z*-direction points to the left part of the seat.

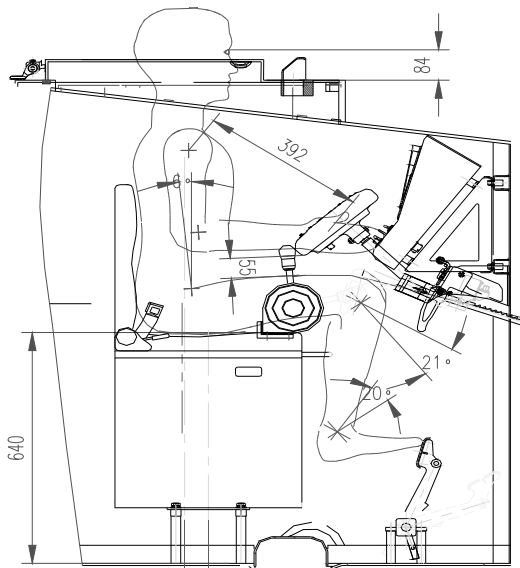
The bearing capacity and buffering effect of static load should be considered in the design of main stiffness. According to the working weight and displacement constraints, the static deflection is set as 5 mm, the ultimate impact acceleration is set as 230 g for the initial condition. By simulation, the initial value of the static stiffness of the driver seat is identified as 100 N/mm, and the static load displacement is identified as 6.8 mm. The curve of vibration attenuation and curve of vibration attenuation of seat are obtained by the preliminary simulation, as shown in Fig. 5.

Further calculation is simulated in the stiffness range of 100–500 N/mm. The result shows that the compression stroke decreases with the increase of the stiffness, but the rate of change decreases at the stiffness of 480 n/mm. The result is best at the stiffness of 380 n/mm. Further optimization of the damping is applied, and the damping setting of 2.5 n/(s/mm) can reduce the vibration amplitude further. Then, the attenuation coefficient is 35 g, and the attenuation rate is 0.15. The cushion ratio of the seat is 0.076 by test. The result of test is better than the calculated value, mainly because the friction of the seat, and the cushion is useful. By optimizing the stiffness and damping of damping shock absorber, the riding comfort is further improved, and the working efficiency of driver is enhanced.

**Fig. 4** Simulation of driving state



(a) Simulation of cockpit driving



(b) Simulation of closed cabin driving

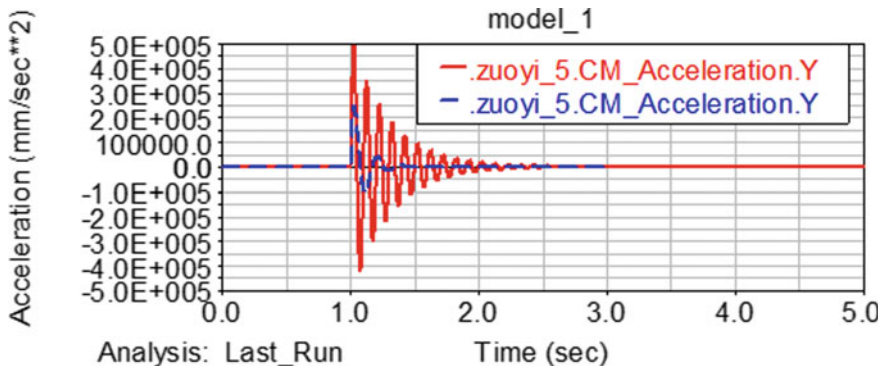


Fig. 5 Initial curve of vibration attenuation of seat

## 4 Conclusion

The driver seat of tracked armored vehicle mainly provides reliable support for the driver and is an important component of tracked armored vehicle. The research of this paper is based on the design of driver seat in the actual development of armored vehicles. In the design process, based on man–equipment–environment system of armored vehicles, the functions of seats, the space of the vehicle and the riding comfort are mainly considered. The working state of the driver is simulated by considering the seat model and the human body model. The shape of seat cushion and seat back and the damping shock absorber are analyzed and simulated, which improves the comfort of the driver and working efficiency.

## References

1. Koli M (2008) A conceptual framework proposed to formalize the scientific investigation of automobile seat comfort. *Appl Ergon* 39(1):15–27
2. Zemp R, Taylor WR, Lorenzetti S (2016) Seat pan and backrest pressure distribution while sitting in office chairs. *Appl Ergon* 53:1–9
3. Meng X, Li X (2004) *Interactive technology principles and applications*. Tsinghua University Press, Beijing
4. Li J, Xu B (2017) Optimization design of seat shape surface based on body pressure distribution. *Autom Eng* 39(1):1457–1463
5. Li J, Xu B, Lian J et al (2014) Seat comfort characterization by body-seat interface pressure distribution. *Mech Sci Technol Aerospace Eng* 33(9):1298–1303
6. Liu Y, Zhang XF, Ma Y (2014) Experiments and evaluation of body pressure distribution on wheelchair cushion. *Appl Mech Mater* 529:317–320
7. Kilincso U, Wanger A, Vink P et al (2016) Application of ideal pressure distribution in development process of automobile seats. *Work* 54(4):895–904

# Analysis on Armor Protection Requirements of the Top of Self-propelled Antiaircraft Gun



Zhenyou Zhang, Qian Liu, and Pengdong Zhang

**Abstract** According to the mission of self-propelled antiaircraft guns in future air defense operations and the all-directional three-dimensional threats they may face, the protection requirements of the top of self-propelled antiaircraft guns and the standards for level of protection should be met are proposed. On the basis of the existing protective technology of armor equipment, this paper points out the application direction of installing optical and electromagnetic transparent protective components by the use of bullet-proof glass, transparent ceramics armor and wave-transmitting composite materials. According to the characteristics that the operational employment of self-propelled antiaircraft gun requires high maneuverability, this paper analyzes the shortcomings of the current active protection means, points out the development direction and technical countermeasures of the soft killing protection system, which can be used as reference to the development of equipment technology of self-propelled antiaircraft guns.

**Keywords** Self-propelled antiaircraft gun · Armor protection · Protection standard

## 1 Introduction

With the development of air strike and anti-air strike technology, from the air to the ground, from the long range to the short range, from ordinary to precision guidance, the self-propelled antiaircraft gun has been confronting all-directional three-dimensional threats. The anti-radiation missile, anti-tank missile and other air strike ammunition as well as intelligent top attack ammunition launched outside the air defense fire killing zone have become the main threats to self-propelled antiaircraft guns. The air strike ammunition has the capability of top attack and pop-up attack, which brings a new threat to the top equipment of the self-propelled antiaircraft gun. Therefore, the design of the self-propelled antiaircraft gun should break away from

---

Z. Zhang (✉) · Q. Liu · P. Zhang  
Artillery and Air Defense Forces Academy (Zhengzhou Campus), Zhengzhou 450052, China  
e-mail: [meizg\\_zz@sina.com](mailto:meizg_zz@sina.com)

the traditional pattern of attaching importance to the protection of the arc area ahead and improve the protection capability of the top part.

## **2 Protection Requirements of the Top of Self-propelled Antiaircraft Guns**

### ***2.1 Structural Features of the Top of Self-propelled Antiaircraft Guns***

#### **2.1.1 The Obvious Target Features Make It Easy to Be Identified**

For the guidance, terminal guidance, terminal sensitivity and intelligent overhead attack ammunition, the target feature extraction is of crucial importance, and the target detection, identification and locking are the preconditions for the attack on self-propelled antiaircraft guns. The search radar antenna and tracking radar antenna at the top of self-propelled antiaircraft gun have obvious electromagnetic wave feature; the engine compartment cover, exhaust louver and gun automaton have distinct infrared feature; and external physical feature of turret, gun tube, missile launcher and stabilized tracking platform are apparent. Compared with tanks, infantry fighting vehicles and other equipment, the top of self-propelled antiaircraft gun has obvious target feature, making them easier to be accurately located and attacked.

#### **2.1.2 The Weak Protection Makes It Easy to Be Damaged**

As the first gun–missile hybrid weapon equipped troops in the world, all six Russian “Tunguska” were destroyed at the very beginning of the battle due to weak protection of the top part in the First Chechnya War [1]. The chassis and turret of the self-propelled antiaircraft gun are welded with armored steel, which has a certain protection capability. However, the equipment exposed at the top has relatively thin protective armor and even in the state of no protection. For instance, there is an obvious “shot trap” at the joint position of the stabilized tracking servo platform installed in front of the turret and the turret, which is easy to be damaged and sometimes plays the role of collecting shrapnel and caving objects. No protective measures were taken for gun automaton, missile launcher, optical observation device (window), etc. The radome of the search radar and tracking radar only has functions of rain and dust prevention, and the ballistic protection capability is very limited. In recent years, self-propelled antiaircraft guns newly developed abroad have enhanced protection design for the top part. For instance, the tracking radar of the Italian “Draco” self-propelled antiaircraft gun can be retractable in the armored protective cabin behind the turret, which improves the protection capability against shrapnel [2].



## **2.2 Protection Standard of the Top of Self-propelled Antiaircraft Guns**

The protection system must be able to adapt to the changing threat forms. Based on the past operational experiences and mission assessments, many countries have set ballistic protection and mine protection standards for military vehicles, such as NATO STANG4569 “Ballistic Protection Standards for the Crew and Light Protective Vehicles”, the American NIJ, the German DIN standards and the protection standards of standard ballistic of European Standards Committee. The ballistic protection of foreign light tactical vehicles is generally level 3 of NATO standard agreement and can be raised to level 4 or above after installing additional armor. The general requirement for the ballistic protection of armored combat vehicles is that the vehicle should reach NATO standard level 4 and the front part of the hull should reach level 5. In addition, it must be able to defend against attacks from anti-tank mines (class 3a/3b), improvised explosive devices and RPG series rocket shells [3]. With the development of the air strike ammunition precision, explosive power as well as integration of reconnaissance and strike, the need of self-propelled antiaircraft gun against light strike is increasingly urgent. For instance, the “Korkut” 35 mm self-propelled antiaircraft gun shaped in Turkey in 2015, the hull around of which can defend the 14.5 mm armor-piercing incendiary fired from 200 m away, and 155 mm grenade fragments exploded from 30 m away, reaching the level 4 of NATO standard agreement. The ballistic protection capability with additional armor can reach above level 5. The bottom armor is able to resist the explosion of an anti-tank mine with a 6 kg charge, reaching level 2 of NATO standard agreement [4]. With overall consideration of the operational tasks and operational environment of the self-propelled antiaircraft guns, the ballistic protection standard for the top of self-propelled antiaircraft guns should reach level 2 or above of NATO standard agreement and level 3 or above after installing additional armor.

## **3 Protection Countermeasures for the Top of Self-propelled Antiaircraft Guns**

With the increasing types of threats that self-propelled antiaircraft guns faced and the increasing effectiveness of anti-armor weapons, the traditional passive protection methods such as increasing armor thickness and draping reactive armor are not enough to cope with various threats in air defense operations. Therefore, adopting innovative methods to solve such problems as weak local protection of self-propelled antiaircraft guns and low information level of smoke interference and other soft killing protection systems, without affecting the maneuver capability, significantly increasing the mass, operation complexity and cost-effectiveness, is the development direction to effectively improve the battlefield survival of self-propelled antiaircraft guns.

### ***3.1 Installing Transparent Armor Protective Components with New Materials***

#### **3.1.1 Installing the Bullet-Proof Glass Protector**

The bullet-proof glass has been extensively popularized and applied in the field such as windshield and weapon shield of ground vehicles. In the field of self-propelled anti-aircraft gun protection, in addition to the application of observation window protection for the driver, gunner, vehicle commander and other crew, the bullet-proof glass also can be applied to the protector for driver who drives when the cabin is in open state, protective shield for gunners of battery command vehicles and missile rack protectors.

#### **3.1.2 Installing the Transparent Ceramic Protective Plate**

The damage rate of optical components in viewing and sighting equipment has become a serious problem in modern warfare. According to the statistics of Chechen War, about 40% of the tanks attacked by RPG series rockets had been suffered some degree of damage to their sighting devices. The tracking telescope with visible light, laser, low-level light triad and other equipment of the self-propelled anti-aircraft gun are installed with protective glass devices in order to prevent the optical instrument from erosion of dust or mildew and mechanical bruising. The common materials for protective glass include crown glass, monocrystalline silicon, monocrystalline germanium, etc., which have problems as weak capability of shell proof and multiple strikes resistance. However, it has been proved that the transparent ceramics are able to provide stronger shell-proof ability with lighter weight. For example, the Stryker armored vehicle has been installed an additional transparent ceramic deck above the hatch cover of vehicle commander cabin, enhancing the protection capability when the crew leader commands out of the hatch.

#### **3.1.3 Installing the Radar Antenna Protector**

Due to the development of modern air strike operation style, the radar antenna of the self-propelled anti-aircraft gun mounted outside the turret has been seriously threatened by various air strike ammunitions. In particular, all kinds of explosive fragments and explosion shock on the battlefield can easily damage the antenna and affect the combat employment of self-propelled anti-aircraft guns. At present, aramid fiber is the most commonly used reinforcing materials for radar radome. Under the condition of the same surface density, the impact resistance ability of resin/aramid fiber composite material is 2–3 times as that of the resin/glass fiber composite material and about 5 times as that of the steel [5]. The ultra-high molecular weight polyethylene

(UHMWPE) is the lightest among the developed high-performance fibers with excellent shell-proof performance and very low permittivity and dielectric loss, making it an ideal material for the shell-proof radome. Research shows that the sandwich structure shell-proof radome with UHMWPE as shell-proof material is able to defend against fragmentation shock caused by the explosion of an anti-radiation missile 15 m away, and the average transmissivity in the S-band reaches 98.6% [6].

### ***3.2 Actively Developing the Active Soft-Kill Protection System***

Due to the influence of operational requirements such as maneuverability, relying solely on increasing armor thickness or developing hard killing protection system to improve the protection capability of self-propelled antiaircraft gun is greatly limited, so the active soft killing protection system has become main development direction of protection system of the self-propelled antiaircraft gun. A laser alarm device is installed at the top of the turret of the Japanese type 87 self-propelled antiaircraft gun. When the self-propelled antiaircraft gun is irradiated by the enemy's laser, the device can immediately send out the sound and light alarm and start the smoke bomb launcher to fire smoke bomb. The Russian "Shtora-1" active soft killing protection system can make the hit probability of "Hellfire" and other missiles drop to 1/5~1/4 of the original, hit probability of "HOT" missile fall to 1/3 of the original. The self-propelled antiaircraft gun has no special active protection system. Although it is equipped with TV, infrared, radar and other target detection devices, it is still weak in detecting the high speed and small target such as incoming ammunition, in particular, and it does not have the warning function for anti-radiation missile and laser-guided bomb. The self-propelled antiaircraft gun is equipped with smoke bomb firing and hot smoke screen releasing devices; however, smoke screen bomb has a single function, with weak multi-spectrum or full-spectrum jamming capability, and the firing time of smoke screen is fully controlled by the crew, which result in low degree of informatization and automation. Therefore, effective measures for improving protection capability of the self-propelled antiaircraft gun shall be as follows: the laser, infrared alarm, photoelectric interference and other auxiliary protection system are supposed to be adding self-propelled antiaircraft gun; making use of multi-spectrum smoke bomb; ensuring the integrated management computer of the self-propelled antiaircraft gun conducting integrated control to realize informatization and automation of alarm and interference.

## **4 Conclusion**

At present, the development trend of armored vehicle protection technology is to strive for the establishment of an "integrated protection system", which enable armored vehicles to achieve: not to be found, not to be captured, not to be hit,

not to be penetrated, not to be destroyed. For self-propelled antiaircraft guns, their firepower flexibility has obvious advantages compared with tanks, making them can “hard damage” air strike ammunition, nonetheless, the passive armor and active protection are still the basic protection against various threats, and the protection of the self-propelled antiaircraft gun should be developed in a three-dimensional and all-round direction.

**Compliance with Ethical Standards** The study was approved by the Logistics Department for Civilian Ethics Committee of Artillery and Air Defense Forces Academy (Zhengzhou Campus).

All subjects who participated in the experiment were provided with and signed an informed consent form.

All relevant ethical safeguards have been met with regard to subject protection.

## References

1. Song X (2015) Review on the development of Russian “Tunguska” antiaircraft cartridge-gun firearm system[J]. *Modern Weapons* 6:28–33
2. Zhang L, Ling Y (2013) Alternative vulcan. *Modern Weapons* (6):43–48
3. Li Bulian (2010) Pondering on the development of light tanks and heavy armored vehicles. *Foreign Tanks* 1:22–31
4. Xiong J (2017) The Turkish “Korkut” 35 mm self-propelled antiaircraft gun[J]. *Weapon Knowl* 2:50–52
5. Guan Z (2016) Research on the application of new aramid fiber composite material in manufacturing millimeter-wave radome. *New Technol New Process* 11:57–60
6. Chen X, Zhu X, Zhang L (2010) Research on sandwich structure design and performance of radar shell-proof radome. *J Eng* 10:12–30

# Development of Principle Prototype of Digital Bright Spot Scintillator



Hua Ge, Andong Zhao, Yuefang Dong, Feng Wu, Weiwei Fu, Xi Zhang, and Hao Zhan

**Abstract** *Objective*—to establish a digital bright spot flicker detection technology and make a principle prototype. *Methods*—the hardware part of the principle prototype of the digital bright spot scintillator includes the shell, eye mask, bright spot scintillation module, monitoring and imaging module and the host computer. The software system is embedded in the host computer, including the user information management module, parameter setting module, CFF measurement module, test data management module and system maintenance module. *Results*—the principle prototype is convenient for individual and group evaluation. The reliability of the detection results is improved by tracking the pupil of the tested personnel through the monitoring camera and eye movement tracking module, drawing the critical flash fusion frequency curve and real-time display. The detection results of 15 subjects show that the principle prototype is accurate, reliable and repeatable. *Conclusions*—the digital bright spot scintillator principle prototype has the advantages of high degree of automation, simple operation, accurate and good repeatability.

**Keywords** Digital bright spot scintillator · Principle prototype · Critical flash fusion frequency

---

H. Ge · A. Zhao · F. Wu (✉) · H. Zhan

Aeromedical Support and Flight Safety Research Office, Air Force Medical Center, Fourth Military Medical University, Beijing 100142, China  
e-mail: [wufeng879@126.com](mailto:wufeng879@126.com)

Y. Dong · W. Fu

Suzhou Institute of Biomedical Engineering and Technology, Chinese Academy of Science, Suzhou 215163, China

X. Zhang

General Hospital of PLA, Beijing 100853, China

© The Editor(s) (if applicable) and The Author(s), under exclusive license to Springer Nature Singapore Pte Ltd. 2021

S. Long and B. S. Dhillon (eds.), *Man-Machine-Environment System Engineering*, Lecture Notes in Electrical Engineering 645, [https://doi.org/10.1007/978-981-15-6978-4\\_38](https://doi.org/10.1007/978-981-15-6978-4_38)

## 1 Introduction

When the flash frequency reaches a certain number of times, due to the effect of the visual afterimage, the human body will not feel the flash and view it as continuous light, which is flash fusion. The lowest frequency is called critical flick fusion frequency (CFF) [1]. Because the detection of CFF is convenient and the result is stable, it has been widely used in the evaluation of sleep deficiency and rhythm disorder, cognitive work fatigue and the central effect of drugs [2–4]. At present, many brands of bright spot scintillation instruments have been used in research work. Most of such classic scintillator adopts the way of detection results reported by the subjects and the results recorded by the main test personnel with paper and pen, which has the disadvantages of low automation and strong subjectivity [5]. In this study, based on the analysis of the performance characteristics and shortcomings of the classical bright spot scintillation meter, combined with the development of computer and optical detection technology, the digital bright spot flicker detection technology is established and the principle prototype is made. The aim of this study is to provide scientific technical means for quickly and effectively monitoring the fatigue state of workers in special environment, so as to effectively maintain their physical and mental health.

## 2 Functional Requirements

The principle prototype of digital bright spot scintillator (hereinafter referred to as the principle prototype) adopts the technical form of computer-controlled optical detection and processing related information and has the function of critical flash fusion frequency detection. In the detection process, video surveillance, critical flash fusion frequency curve drawing and display are carried out to realize automatic recording and analysis of data.

## 3 System Design

The principle prototype is composed of critical flash fusion frequency measurement, computer control analysis and the peripheral structure of input and output. The composition and layout are shown in Fig. 1. The flash fusion frequency measurement subsystem includes five light sources, background light sources and monitoring cameras. The computer control and analysis subsystem includes signal control, data processing and data storage analysis. Peripheral mechanical structure subsystem includes control input, subject feedback input and display output.

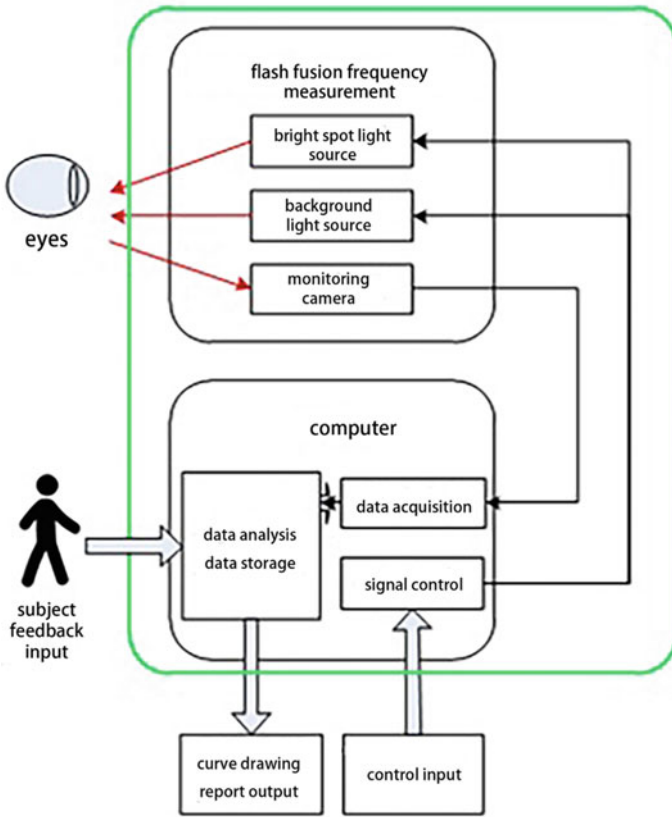


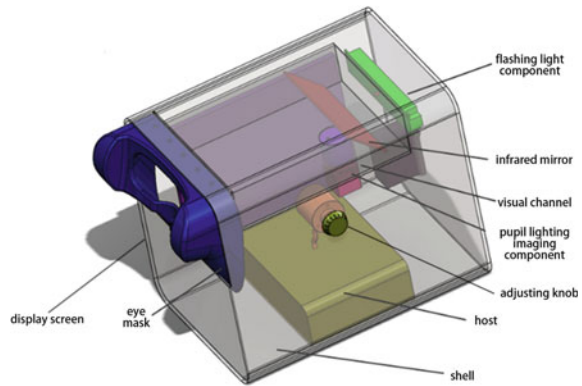
Fig. 1 Schematic diagram of the composition and layout of the principle prototype

## 4 Development Result

### 4.1 Hardware System

The digital bright spot scintillator is composed of eye mask, visual channel, host, display screen, pupil lighting imaging module, flashing light component, infrared mirror, adjusting knob and so on, and the overall structure is shown in Fig. 2. The luminous surface of the bright spot flicker assembly is at a certain distance from the human eye, and the pupil lighting imaging module is perpendicular to the visual channel; the light emitted by the bright spot can enter the pupil through the infrared reflector, and the change of the pupil after being stimulated by the bright spot will be monitored by the pupil imaging assembly in real time and the results will be displayed on the display screen; the rotating adjustment knob can adjust the flicker frequency and color of the bright spot.

**Fig. 2** Schematic diagram of principle prototype



## 4.2 Software System

The principle prototype of digital bright spot scintillator mainly includes user information management module, parameter setting module, CFF measurement module, data management module and system maintenance module. Its functional structure is shown in Fig. 3.

Figure 4 shows the login interface. The administrator logs in the application software by entering the user name and password. After logging in successfully, the operator enters the main interface of the digital bright spot scintillator software, as shown in Fig. 5. The main interface includes detection, data management, subject management, user management, system settings, logout and other modules. The detection module mainly carries out CFF testing, and the data management mainly realizes the functions of querying, deleting, importing/exporting and viewing reports of CFF data. The subject management mainly realizes the operation of adding, deleting, modifying and querying the basic information of the subjects. The user management realizes the addition, deletion, modification and query operation of the basic information of the administrator/maintenance personnel, and the system setting mainly realizes the printer and other settings. The logout module realizes the exit of the system.

## 5 Experimental Test and Analysis

### 5.1 Subjects

Fifteen healthy volunteers, with an average age ( $31.20 \pm 5.03$ ) years old, had no internal and external eye diseases and reported no sleep disorders.



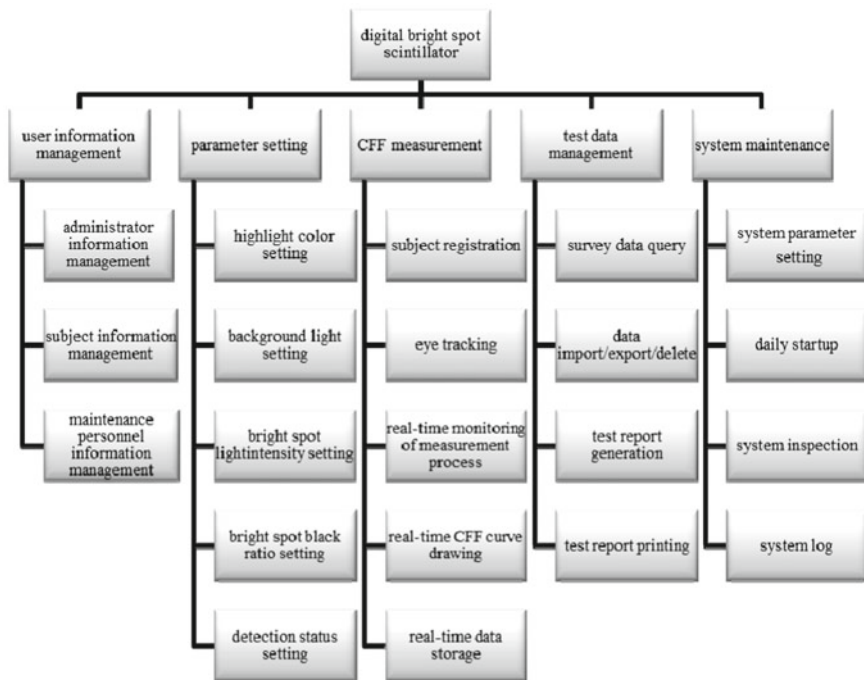


Fig. 3 Software functional structure diagram

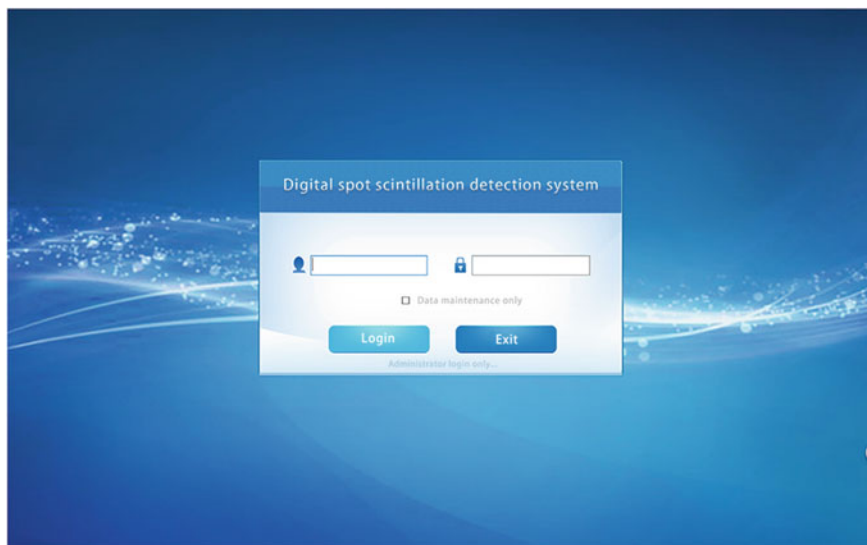


Fig. 4 Login interface



**Fig. 5** Main interface

## **5.2 Testing Method**

The principle prototype and Beida Bluebird BD-II-118 bright spot scintillator (hereinafter referred to as BD-II-118) were used to test and compare the CFF value, and the accuracy of the prototype was initially verified. At the same time, the subjects were measured repeatedly for 3 days to observe the stability of the measured data. BD-II-118 was tested in the form of subjective report, recording two reported values (frequency increasing and decreasing once respectively) as its frequency value. The measurement order of different bright spot colors of each subject was randomly arranged by computer.

## **5.3 Statistic Analysis**

SPSS18.0 was used for statistical analysis, and the measurement data were expressed in  $(\bar{x} \pm s)$ . Paired t-test was used to compare the accuracy of the equipment, and repeated measurement analysis of variance was used to compare the stability.

## **5.4 Result Analysis**

Table 1 shows the detection results of the principle prototype and BD-II-118 bright

**Table 1** Comparison of detection results between principle prototype and BD-II-118 bright spot scintillator

Bright spot color	Instrument	CFF value	<i>t</i> value	<i>P</i> value
Red	Principle prototype	25.62 ± 2.93	0.467	0.647
	BD-II-118	25.15 ± ± 4.48		
Yellow	Principle prototype	31.14 ± 3.40	0.065	0.949
	BD-II-118	31.10 ± 3.05		
Green	Principle prototype	28.20 ± 2.69	0.792	0.442
	BD-II-118	28.57 ± 2.44		
Blue	Principle prototype	31.36 ± 3.79	1.344	0.200
	BD-II-118	32.10 ± 2.78		
White	Principle prototype	32.07 ± 3.03	0.833	0.419
	BD-II-118	32.65 ± 2.67		

**Table 2** Stability detection results of principle prototype

Bright spot color	CFF value			<i>F</i> value	<i>P</i> value
	I	II	III		
Red	25.62 ± 2.93	25.82 ± 2.99	26.26 ± 3.22	1.465	0.250
Yellow	31.14 ± 3.40	30.94 ± 3.04	31.47 ± 2.98	1.678	0.225
Green	28.20 ± 2.69	28.61 ± 3.03	28.83 ± 3.26	0.722	0.490
Blue	31.36 ± 3.79	32.54 ± 3.48	31.69 ± 2.69	2.615	0.092
White	32.07 ± 3.03	32.34 ± 2.96	32.76 ± 3.58	0.438	0.655

spot scintillator: There is no significant difference in CFF values of each bright spot color tested on the two devices, and the five bright spot colors have good consistency. It is suggested that the detection validity of the principle prototype is good. Table 2 shows the stability results of the principle prototype: There is no significant difference in the results of three repeated measurements of each bright spot color, the measurement results are stable. It is suggested that the principle prototype is reliable.

## 6 Conclusion

The principle prototype of digital bright spot scintillator adopts computer-controlled optical detection and processing related information technology and has the function of critical flash fusion frequency detection. Video surveillance, drawing and display of critical flash fusion frequency curve are carried out to realize automatic recording and analysis of data in the detection process. The preliminary experimental results show that, compared with the subjective report bright spot scintillator, the detection results of the five bright spot colors of the principle prototype are accurate, reliable

and reproducible. The next step of this study is to expand the sample size for reliability and validity test of principle prototype. It is hoped that the equipment can be used as an objective means to evaluate pilots' flight fatigue and improve flight safety. It can also be used to evaluate the fatigue status of operators in special environment, maintain their physical and mental health, and improve the technical ability and level of health support.

### **Compliance with Ethical Standards**

The study was approved by the Logistics Department for Civilian Ethics Committee of Air Force Medical Center.

All subjects who participated in the experiment were provided with and signed an informed consent form.

All relevant ethical safeguards have been met with regard to subject protection.

### **References**

1. Zhan H (2014) Application of critical flash fusion frequency and eye movement response detection in central fatigue assessment of different tasks. *Chin J Aerospace Med* 25(1):62–68
2. Qin XL (2006) Application research of CFF in the evaluation of fencers' function. *J Sports Sci* 27(5):77–79
3. Sq GE, Wu GC, Xu XH (2005) The effect of flight fatigue on visual fusion of civil aviation pilots of different ages. *Chin J Aerospace Med* 16(3):180–183
4. Jin HB, Zhu GL (2018) Effectiveness of eye movement index detection and control fatigue. *Sci Technol Eng* 18(19):136–140
5. Li XJ, Hu WD, Geng Y (2010) Design and pilot experimental applicability analysis of objective digitron critical fusion frequency test apparatus. *Chin Med Equipment J* 31(6):1–4

# Information Processing System Design for Multi-rotor UAV-Based Earthquake Rescue



Haoting Liu, Ming Lv, Yun Gao, Jiacheng Li, Jinhui Lan, and Wei Gao

**Abstract** A design method of an information processing system for the multi-rotor unmanned aerial vehicle (UAV)-based earthquake rescue application is proposed. As a kind of new rescue measurement in the third medical center of the People's Liberation Army (PLA) general hospital, this system is designed for the UAV of calamity rescue team. Four key functions are developed: the environment perception-based image enhancement, the homography matrix estimation-based image mosaicing, the imaging earthquake damage degree (EDD) evaluation, and the rescue plan recommendation. The blind image quality evaluation metrics are utilized to percept the changes of imaging environment. The homography matrix is employed to carry out the image mosaicing. Lots of image texture features are computed to assess the imaging EDD. The rescue plan is recommended by the backpropagation neural network (BPNN) with the considerations of EDD and other factors such as the population size or the weather condition. The practical tests have verified the effectiveness of the proposed system and method.

**Keywords** Earthquake rescue · UAV · Image processing · Rescue plan

## 1 Introduction

In recent years, the earthquake rescue technique in China has met its great development opportunity with the fast economy advancement [1]. Many new materials, new sensors, and new data processing methods are utilized to assist the earthquake rescue.

---

H. Liu (✉) · J. Li · J. Lan

School of Automation and Electrical Engineering, Beijing Engineering Research Center of Industrial Spectrum Imaging, University of Science and Technology, Beijing 100083, China  
e-mail: [liuhaoting@ustb.edu.cn](mailto:liuhaoting@ustb.edu.cn)

M. Lv · Y. Gao

The Third Medical Center of PLA General Hospital, Beijing 100039, China

W. Gao

Beijing University of Pharmaceutical Staff and Workers, Beijing 100079, China

© The Editor(s) (if applicable) and The Author(s), under exclusive license to Springer Nature Singapore Pte Ltd. 2021

S. Long and B. S. Dhillon (eds.), *Man-Machine-Environment System Engineering*, Lecture Notes in Electrical Engineering 645, [https://doi.org/10.1007/978-981-15-6978-4\\_39](https://doi.org/10.1007/978-981-15-6978-4_39)

First, the portable and miniaturized equipment can be used to replace the old and low-technique-integration ones. Second, the new equipment can take advantage of all kinds of new measurements including the air-based, the land-based, and even the space-based techniques to accomplish the rescue task. Third, the applications of new rescue equipment begin to cover the whole lifetime of the rescue mission. Clearly, the advanced equipment cannot leave the support of information processing system. The powerful information analysis techniques still play one of the most important roles in the equipment development regarding the earthquake rescue.

The third medical center of the People's Liberation Army (PLA) general hospital is the leading power in the research field of earthquake medical rescue in China. The famous China's International Search and Rescue Team (CISRT) affiliates to it. Recently, the third medical center of PLA general hospital is concentrating on the development of new-type earthquake rescue equipment. Since 2013, a kind of rescue hospital in vehicle was developed there. The vehicle hospital can work like a tertiary referral center when it arrives in the calamity region. Another progress is that a special BeiDou satellite communication system is applied in the rescue task. Figure 1 shows the corresponding equipment. In Fig. 1, (a) is the photograph of the fleet of vehicle hospital; (b) is the photograph of the communication command vehicle; and (c) is the photograph of ground terminal of satellite communication system.

In this paper, a kind of six-rotor unmanned aerial vehicle (UAV) and its information processing system is developed for the third medical center of PLA general hospital. A series of image-based algorithms is developed: First, an imaging environment perception-based image enhancement algorithm is designed. The blind image quality evaluation metrics [2] are used to percept the imaging environment changes; and the multiple scale retinex (MSR) method is used to improve the imaging quality. Second, the homography matrix-based image mosaicing method is considered. Third, the imaging earthquake damage degree (EDD) evaluation metrics [3] are developed to analyze the ground target damage level. Many image texture features [4] and the backpropagation neural network (BPNN) [5] are used to assess the EDD metric for the general ground target. Fourth, a recommendation method of the rescue plan is designed. The BPNN is used again to estimate the optimal rescue plan.



**Fig. 1** Equipment illustrations of earthquake medical rescue which are developed in the third medical center of PLA general hospital

## 2 The UAV and Its Information Processing System

A kind of commercial UAV system is employed in this paper. This UAV has six rotors which can improve its hovering stability in air. It can realize the basic information collection functions, including the image capture, the image transmission, and the image play, etc., almost in real time. Currently, this UAV system uses the battery to provide power. Table 1 shows the basic technique parameters of that UAV system. This UAV can reach more than 50 m height from the ground; and its largest flight distance is about 2000 m. It can be taken by one person to the disaster area easily. From Table 1, a commercial sport camera is utilized in that system. Because the size of sport camera is small, its imaging quality such as the image contrast or the imaging detail is limited. To improve its output effect, it is needed to improve the image quality for that system by the corresponding image processing methods.

Figure 2 shows the function design of the proposed information processing system. Currently, the main functions of this system include: the image enhancement for the outdoor imaging data, the aerial image mosaicking, the imaging EDD estimation, and the rescue plan recommendation. The image enhancement processing is necessary because of UAV's fast flight speed and its multiple attitude tuning. The aerial image mosaicking is needed because the user wants to watch the image with big view in many situations. The imaging EDD estimation metrics are defined to assess the damage level of the important ground target. The corresponding computational results are the effective supplements to the traditional earthquake evaluation indexes, such as the magnitude or the intensity. Then the rescue plan can be recommended by the

**Table 1** Basic technique parameters of a kind of commercial UAV system

Item	Parameter
Takeoff weight	4.7–8.2 kg
UAV weight	3.3 kg
Hovering time	18 min (the takeoff weight is 6.8 kg)
Maximum power	3000 W
Working temperature	–10–40 °C

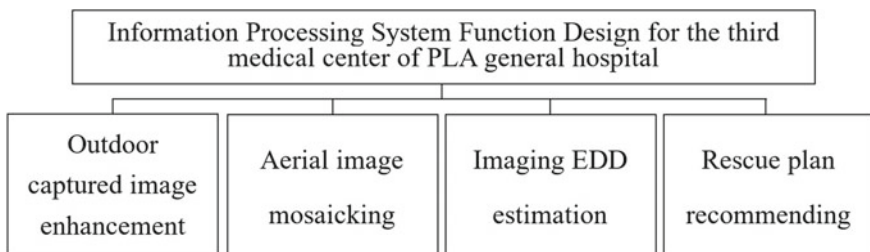


**Fig. 2** Information processing system design of the third medical center of PLA general hospital

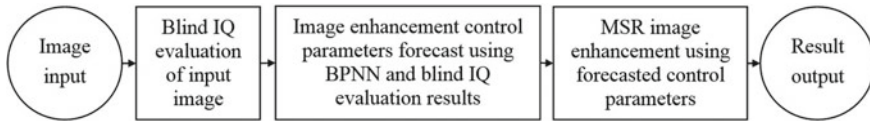


**Fig. 3** Computational flowchart of environment perception-based image enhancement

integrated consideration of the imaging EDD and other factors such as the population size, or the population density.

### 3 The Key Algorithms

#### 3.1 The Image Enhancement with Environment Perception

In this paper, a blind image quality (IQ) evaluation metrics are utilized to percept the environment light change firstly; and then the BPNN is considered to improve the robustness of image enhancement algorithm. Figure 3 shows the computational flowchart of the proposed method. In Fig. 3, first the blind IQ evaluation metrics are computed, and they include the image brightness degree, the image region contrast degree, and the image edge blur degree. Then the BPNN is employed to estimate the optimal control parameters of the enhancement algorithm by the IQ evaluation metrics above. After that the MSR is utilized to perform the enhancement computation. The inputs of BPNN are the blind IQ evaluation metrics; its outputs are the control parameters of MSR.

#### 3.2 The Image Mosaicing Method

The image mosaicing is necessary because the user needs to watch the imaging scene with big view in many cases. Figure 4 shows the computational flowchart of that algorithm. First, the point features are calculated from the captured image pairs. The scale-invariant feature transform (SIFT) points are computed in this paper; and then the random sample consensus (RANSAC) method is utilized to find the matching points between the image pairs. After that the least squares technique is employed to

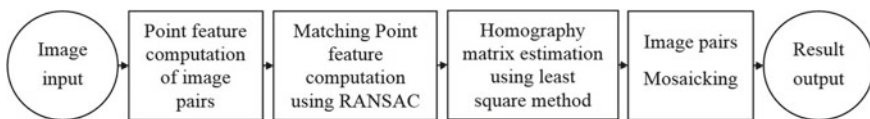


**Fig. 4** Computational flowchart of the homography matrix-based image mosaicing



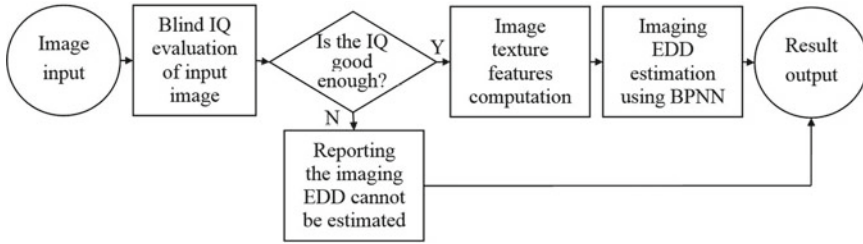


Fig. 5 Computational flowchart of the imaging EDD of the general ground target

estimate the homography matrix. Finally, the image with big view can be generated by using the mapping relationship above. To improve the computation precision further, the Levenberg–Marquardt method can be utilized.

### 3.3 The Imaging EDD Estimations

The imaging EDD metric uses the image texture features to assess the earthquake damage degree. The graylevel cooccurrence matrix (GLCM) features, the Tamura features, and the Gabor wavelet features are computed to analyze this EDD above. The GLCM features, such as the angular second-moment index, the contrast index, and the inverse difference moment index, etc., are computed. The Tamura features include the coarseness and the contrast metrics. And the Gabor wavelet features with 30 filters are also considered. Some typical ground targets such as the building, the road, the mountain, the riverway, and the vegetation can be evaluated. Figure 5 shows the computational flowchart of imaging EDD of the general ground target. First, the blind IQ evaluation metrics in Sect. 4.1 are computed. Then, if the IQ is good enough, the corresponding image texture features will be computed. Finally, the BPNN is used to assess that EDD. The supervising data of BPNN comes from the opinion of earthquake rescue expert.

### 3.4 The Rescue Plan Recommendation

The rescue plan is a kind of predefined and definitized program which can explain and guide the earthquake rescue steps in details for the CISRT when the sudden earthquake happens. It always covers the specific manpower, material resources, and financial resources for the calamity rescue. Table 2 shows the specific definitions and explanations of these factors in this paper. The BPNN is utilized again to perform the rescue plan recommendation task. Its inputs include the population size, the population density, the vulnerable population ratio, the population quality, the reported casualty, the temperature, the relative humidity, the wind speed, the weather, the

**Table 2** Evaluation factors of rescue plan and their explanations

No.	Factor name	Explanation
1	Population size	This factor is divided into five degrees (person): $\leq 50 \times 10^4$ ; $50 \times 10^4 - 100 \times 10^4$ ; $100 \times 10^4 - 300 \times 10^4$ ; $300 \times 10^4 - 1000 \times 10^4$ ; $^3 1000 \times 10^4$
2	Population density	This factor is divided into five degrees (person per square kilometer): $\leq 50$ ; $50-300$ ; $300-500$ ; $500-1000$ ; $^3 1000$
3	Vulnerable population ratio	This factor is divided into five degrees: $\leq 5\%$ ; $5-10\%$ ; $10-30\%$ ; $30-50\%$ ; $350\%$ .
4	Population quality	This factor is divided into five degrees (crime rate): $^3 1000/10^5$ ; $500/10^5 - 1000/10^5$ ; $300/10^5 - 500/10^5$ ; $150/10^5 - 300/10^5$ ; $0-150/10^5$
5	Reported casualty	This factor is divided into five degrees (the death number (person) or the serious injury number (person)): (0, 3] or (0, 10]; (3, 10] or (10, 50]; (10, 30] or (50, 100]; (30, 100] or (100, 500]; $> 100$ or $> 500$
6	Temperature	This factor is divided into five degrees ( $^{\circ}\text{C}$ ): $\leq 0$ ; $0-23$ ; $23-33$ ; $33-40$ ; and $340$
7	Relative humidity	This factor is divided into five degrees (%RH): $\leq 20\%$ ; $20-40\%$ ; $40-50\%$ ; $50-70\%$ ; $370\%$
8	Wind speed	This factor is divided into five degrees (m/s): $\leq 0.2$ ; $0.2-7.9$ ; $7.9-13.8$ ; $13.8-24.4$ ; $324.4$
9	Weather condition	This factor is divided into five degrees: sunny day; light rain, or light snow, or light fog; middle rain, or middle snow, or middle fog; large rain, or large snow, or large fog; heavy rain, or heavy snow, or heavy fog
10	Epidemic situation	This factor is divided into five degrees: level 1 to level 5, the large the level is the severe the situation is
11	Earthquake intensity	This factor is divided into five degrees: $\leq 3.0$ ; $3.0-4.5$ ; $4.5-6.0$ ; $6.0-8.0$ ; $38.0$
12	EDD metric	This factor is divided into five degrees: level 1 to level 5, the large the level is the severe the situation is

epidemic situation, the earthquake intensity, and the corresponding EDD metrics. And its output is the rescue emergency degree. Then each rescue emergency degree can be equivalent to a professional rescue plan. The training of BPNN is accomplished by the opinion of the earthquake medical rescue expert.

## 4 Experiment Results and Discussions

To test the validity of the proposed algorithms, a series of drills are designed. The proposed software system is written by C and MATLAB in our PC (2.4 GHz CPU and

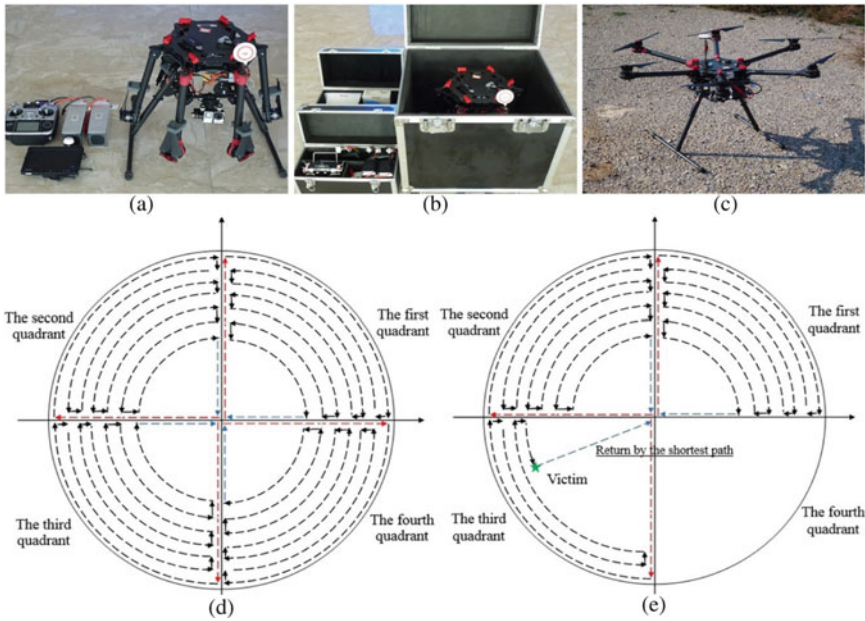
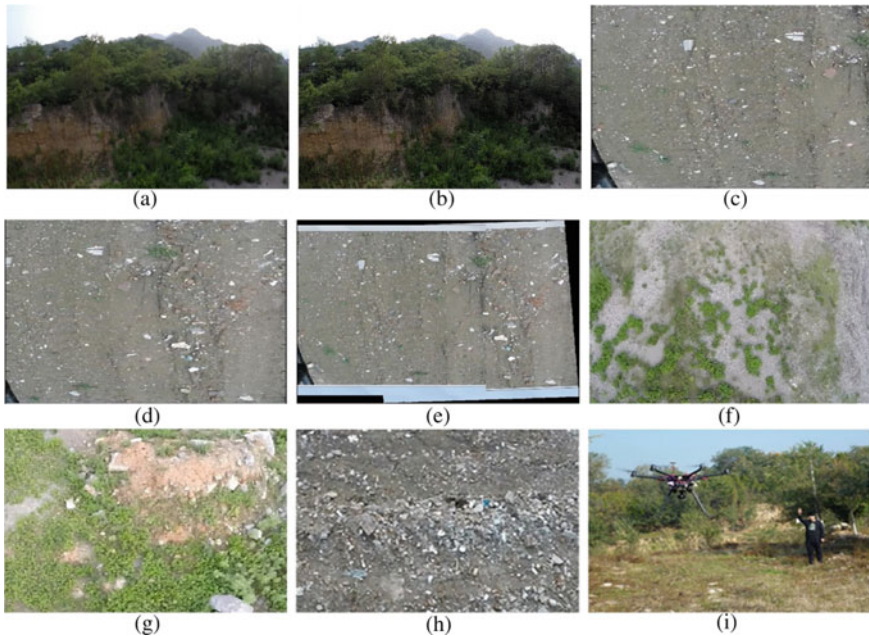


Fig. 6 Preparation state and the searching plan of the proposed system

3 GB RAM). It is supposed an earthquake-caused landslide happens in autumn, north-east of China. The rescue team receives the order to search the victim and performs the medical rescue task. Figure 6 shows the preparation state and the searching plan of the proposed system. In Fig. 6, (a) and (b) are the UAV hardware system; (c) is the photograph that the UAV is preparing to flight; (d) and (e) are the flight route designs of the victim searching task. The searching region is divided into four quadrants. During each flight, the UAV will traverse only one quadrant. And each flight will cost the UAV one battery. From (e), once the victim is found, the UAV will record the geographic coordinates of victim and return to the starting point immediately. Then the rescue team can go to the recorded position to perform the medical rescue.

Figure 7 shows the application results of proposed methods: (a) shows an original image which is influenced by the blaze; (b) is the environment perception-based enhancement result of (a); (c) and (d) are the image pairs which are captured from the video; (e) is the mosaicing results of (c) and (d); images (f), (g), and (h) are the image data which are used for the EDD evaluation; (i) is the victim searching photograph. From Fig. 7, it can be seen that the proposed image processing methods can improve the imaging quality, build the image with a big view, and realize the victim searching task correctly. Table 3 shows the imaging EDD evaluation results of the general ground targets. The image data in Fig. 7 (f) to (h) are used. From Table 3, it can be seen that the ground vegetation, the slope, and the building are all destroyed by the natural calamity; and the imaging EDD can give some objective evaluations of them.



**Fig. 7** Computation results of proposed image processing algorithm

**Table 3** Imaging EDD estimation results of Fig. 10 (f), (g), and (h)

Image Name	Imaging EDD	Descriptions
Figure 10 (f)	4	The ground vegetation which was washed by heavy rain
Figure 10 (g)	2	The slope which was eroded by the landslide
Figure 10 (h)	5	The building which was destroyed by the landslide

After the information analysis of natural calamity, the rescue plan can be deduced automatically. Table 4 shows the examples of related factor of rescue mission. Clearly, they are also the input parameters of the BPNN. Table 5 shows the examples of the recommended rescue plan. From Table 5, it can be seen the rescue plan includes the specific details of the rescue equipment and the rescue medicine resource. Thus, this plan has a practical performability for the rescue team. Other rescue plan can also be estimated if the inputs of BPNN are different. The differences among these rescue plans lie in the different amounts or types of rescue resources, such as the vehicle or the medical drag. In this test experiment, only few people acts as the victims and the natural environment is not rigorous seriously; thus, the practical needs of rescue equipment and resources are small.

**Table 4** Input parameters of BPNN for rescue plan recommendation

Population size (person)	Population density (person/square kilometer)	Vulnerable population ratio	Population quality (crime rate)
≈6500	12	27.6%	53/105
Reported casualty (person)	Temperature (°C)	Relative humidity (%RH)	Wind speed (m/s)
7	21	83.3%	9.3
Weather	Epidemic situation	Earthquake intensity	EDD metrics
Light rain	1 (no epidemic)	2	2

**Table 5** Recommended rescue plan

The recommended rescue plan
(1) The ordinary medical rescue drugs should include the ordinary first-aid medicine, the hemostatics, the whole blood, the blood components, the dextran, and the stupeficient, etc.
(2) The emergency medical equipment should include the surgical instrument box, the portable ventilator, the electrocardiogram monitor, the water and poison examination kit, etc.
(3) The medical supplies should include one ambulance, three stretchers, three first-aid kits, the emergency plaster, the medical paper, the bandage, the neck support, the limbs brace, the medical oxygen, and the intravenous infusion needle, etc.
(4) The emergency engineering equipment should include two big wreckers, three small wreckers, three emergency vehicles, two cranes, and two mobilities, etc.

## 5 Conclusion

A kind of ground information processing system is proposed for the multi-rotor UAV-based earthquake rescue. Four key computation functions of information processing system are developed: the environment perception-based image enhancement, the homograph matrix estimation-based image mosaicing, the imaging earthquake damage degree evaluation, and the rescue plan recommendation. The related image processing algorithms are developed for this system. The practical test experiment has shown the validity and effectiveness of the proposed system and methods.

**Acknowledgements** This work was supported by the National Natural Science Foundation of China under Grant No. 61975011, and the Fundamental Research Fund for the China Central Universities of USTB under grant No. FRF-BD-19-002A.

## References

1. Lu Y, Xu J (2014) The progress of emergency response and rescue in China: a comparative analysis of Wenchuan and Lushan earthquakes. *Nat Hazards* 74:421–444
2. Liu H, Lu H, Zhang Y (2017) Image enhancement for outdoor long-range surveillance using IQ-learning multiscale Retinex. *IET Image Process* 11:786–795
3. Chen J, Liu H, Zheng J et al (2016) Damage degree evaluation of earthquake area using UAV aerial image. *Int J Aerosp Eng* 2016:2052603–1–2052603-10
4. Liu P, Liu H, Jin J et al (2015) Water wave visualization simulation using feedback of image texture analysis. *Multimed Tools Appl* 74:8379–8400
5. Wang W, Yu B (2009) Text categorization based on combination of modified back propagation neural network and latent semantic analysis. *Neural Comput Appl* 18:875–881

# Multiple Missiles Launch Assignment Based on AHP and Genetic Algorithm



Fang Liu and Jinshi Xiao

**Abstract** A kind of launch assignment method of the multiple missiles which uses the analytic hierarchy process (AHP) method and the genetic algorithm (GA) is proposed for the navy ship. In this model, the missiles include both the surface combat missile and the electromagnetic compaction missile. When implementing the simulation, first, the three threaten factors are modelled. They are the anti-ballistic missile threaten factor, the radar threaten factor, and the weather threaten source. Second, a GA model is constructed to solve the mission assignment problem of multiple missiles. The corresponding threaten factors are used to build the optimal function of GA. Third, the AHP model is considered to estimate the weight of the optimal function. Many simulation results have verified the correctness of proposed method.

**Keywords** Multiple missile · Threaten source · Genetic algorithm · Launch assignment · Navy ship

## 1 Introduction

The modern warship has the ability to launch multiple missiles simultaneously when it faces any threatens. In general, the equipped missiles can include the surface combat missile and the electromagnetic compaction missile, etc. And the equipment amounts of these missiles are also large. When launching the missile, some threaten factors should be considered, such as the radar, the weather, and even the performance of missile itself. Thus, how to assign the missiles reasonably under the consideration of these threaten factors should be researched. Clearly, the issue about launching different missiles to different targets is a typical multi-mission assignment problem [1] from the mathematical modelling point of view.

---

F. Liu (✉) · J. Xiao

College of Weaponry Engineering, Naval University of Engineering, Wuhan, China

e-mail: [jzbliufang@163.com](mailto:jzbliufang@163.com)

© The Editor(s) (if applicable) and The Author(s), under exclusive license to Springer Nature Singapore Pte Ltd. 2021

S. Long and B. S. Dhillon (eds.), *Man-Machine-Environment System Engineering*, Lecture Notes in Electrical Engineering 645, [https://doi.org/10.1007/978-981-15-6978-4\\_40](https://doi.org/10.1007/978-981-15-6978-4_40)

331

Many research works have been done to solve the multiple mission assignment problem. For example, in [2], an embedding algorithm was proposed to solve the offloading issue of networks. The road traffic allocation scheme could be solved well in this research. In [3], a hierarchical coloured Petri net model of the fleet maintenance was proposed. The effects of multiple cannibalisation policies were modelled. In [4], an iterative strategy for the task assignment and path planning of multiple unmanned aerial vehicles were proposed. Currently, the research of the multiple missiles launch assignment is still rare; however, with the fast development of modern science and technology, the age of missile battle has come. As a result, it is necessary to build a mathematical model for the multiple missiles mission assignment.

In this paper, to solve the multi-mission assignment problem to some extent, both the analytic hierarchy process (AHP) [5] and the genetic algorithm (GA) [6] are considered. First, three threaten factors are modelled. They include the anti-ballistic missile threaten factor, the radar threaten factor, and the weather threaten source (the wind and the rain). Second, the GA is used to solve the multiple mission assignment problem. A kind of optimal function is constructed according to the threaten factor above. And the coding method of the GA's chromosome is also designed. Both the flight distance factor and the propellant residual factor are also considered. Third, the AHP is employed to estimate the weights of the optimal function of GA.

## 2 The Multiple Missiles Launch Assignment Using GA

### 2.1 The Design of Optimal Function

The definition of the GA optimal function is shown by Eqs. (1), (2), and (3). First, the Eq. (1) means the optimal cost function. Six factors such as the distance factor, the propellant residual factor, the radar factor, the missile threaten factor, the wind factor, and the rain factor are all considered. The electromagnetic compaction missile can decrease the threaten degree of the radar factor, the missile threaten factor, and even the weather threaten factor to some extent. The larger the amount of the electromagnetic compaction missile is, the smaller the corresponding threaten factors would be. Second, Eq. (2) indicates the optimal revenue function. The revenue of target point comes from the combat value of that target itself. And the larger the amount of the battle combat missile is, the better the combat effect would be. Third, Eq. (3) is the final target of the optimal function.

$$C = \sum_{k=1}^K [\delta_D P_D + \delta_P P_P + (1 - t \times \gamma)(\delta_R P_R + \delta_M P_M + \delta_{W\_W} P_{W\_W} + \delta_{W\_R} P_{W\_R})] \quad (1)$$



**Table 1** Definitions of the flight distance and the propellant residual

Flight distance		Propellant residual	
Degree	Relative remaining distance	Degree	Relative propellant residual
1	<0.3	1	>0.8
2	[0.3, 0.8]	2	[0.3, 0.8]
3	>0.8	3	<0.3

$$R = \sum_{k=1}^K [1 - (1 - \alpha)^r] \times R(k) \tag{2}$$

$$T = \max(w_1 \times R - w_2 \times C) \tag{3}$$

where  $K$  is the maximum amount of the battle target;  $\delta_D, \delta_P, \delta_R, \delta_M, \delta_{W_W}$ , and  $\delta_{W_R}$  are the weights of the distance factor, the propellant residual factor, the radar factor, the missile threaten factor, the wind factor, and the rain factor, respectively;  $P_D, P_P, P_R, P_M, P_{W_W}$ , and  $P_{W_R}$  are the corresponding costs of the factors above;  $R(k)$  is the revenue of the  $k$ -th battle target;  $t$  and  $r$  are the amount of the electromagnetic compaction missile and the surface combat missile;  $\gamma$  is the parameter which can represent the threaten decreasing level of the whole combat system;  $\alpha$  is the parameter which can indicate the success rate of missile combat;  $w_1$  and  $w_2$  are the weights of the revenue function  $R$  and the cost function  $C$ .

The threaten factors illustrated in Eq. (1) are defined in this paper. The definitions of the flight distance and the propellant residual are presented in Table 1. In Table 1, for the sake of simpleness, the relative remaining flight distance and the relative propellant residual are utilized. These data can be estimated by the flight time and the telemetry data. The radar can detect the approaching missiles, identify their types, and forecast their placements. In this paper, it is supposed that the antenna can scan 360° in the battlefield; thus, the radar threaten source can be defined by (4). In general, the flight scope of the anti-ballistic missile can look like a waist drum; thus, its threaten degree can be defined in (5). The threaten degree of the weather factor is shown in Table 2. Here, the weather factor is considered by both the rain factor and the wind factor. The values of these factors are defined by their practical intensity.

**Table 2** Definition of the weather threaten factor

Wind		Rain	
Degree	Value (m/s)	Degree	Level
1	<13.8	1	Small rain
2	[13.8, 24.4]	2	Middle rain
3	>24.4	3	Heavy rain

$$P_R = \begin{cases} 0 & d_R > d_{R\_max} \\ \frac{1}{d_r} & d_R \leq d_{R\_max} \end{cases} \tag{4}$$

$$P_M = \begin{cases} 0 & d_M > d_{M\_max} \\ \frac{1}{d_M} & d_{M\_min} \leq d_M \leq d_{M\_max} \\ 1 & d_M < d_{M\_min} \end{cases} \tag{5}$$

where  $d_R$  is the distance between missile and radar;  $d_{R\_max}$  is the maximum detection distance;  $d_M$  is the distance between the missile and the anti-ballistic missile;  $d_{M\_min}$  and  $d_{M\_max}$  are the minimum and the maximum shoot down distances.

### 2.2 The Chromosome Coding Method of GA

The GA is a kind of evolutionary algorithm which imitates the biological reproduction processing. The computation step of GA includes the selection operation, the crossover operation and the mutation operation. The selection operation needs to use the fitness function to implement the optimal evolution. In this paper, the target function in Eq. (3) is employed as the fitness function. Figure 1 shows the designing method of the chromosome of the GA. Without loss of generality, let us consider the mission assignment problem of two groups. In Fig. 1, the chromosome is divided into two same groups. In the first group, the former two codes indicate the amount of the surface combat missile and the electromagnetic compaction missile. The left codes mean whether the missile group will attack that target point (Fig. 2).

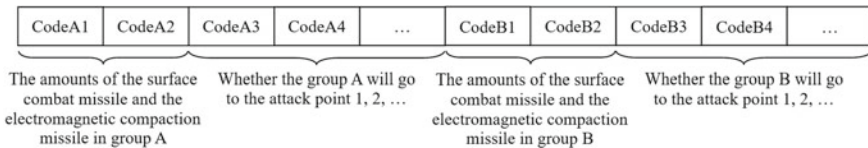


Fig. 1 Sketch map of the chromosome coding method of GA

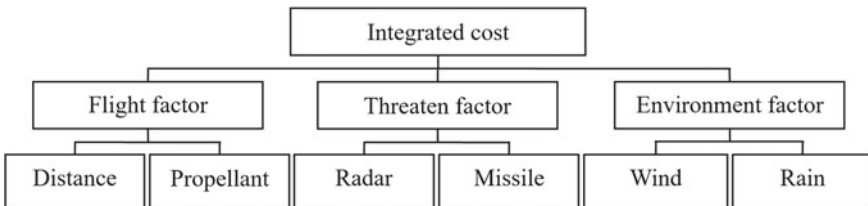


Fig. 2 Hierarchy structure of proposed AHP model

### 3 The Weight Computation Using AHP

The AHP is utilized to determine the weights of the threaten factors above. The AHP is a kind of operation method which can get the ranking estimation for its investigated factors. Figure 1 shows the basic structure of AHP model regarding the multiple missiles launch assignment problem. In Fig. 1, the decision hierarchy is the final cost. The middle hierarchy includes the flight factor, the threaten factor, and the environment factor. The factor hierarchy defines six factors which are same to the factors presented in Eq. (1). When carrying out the AHP computation, the classic 1–9 evaluation criterion is utilized. The navy experts are asked to give the evaluation scores for the AHP model.

### 4 The Experiments and Discussions

#### 4.1 The Results of Launch Assignment

A series of simulation experiments are performed to test the validity of proposed algorithm. All the simulation experiments are accomplished by the C code in our PC (4.0 GB RAM, 1.70 GHz Intel (R) Core (TM) i3-4005U CPU). Figure 3 presents the 2D sketch map of the multiple missiles launch assignment simulation. In Fig. 3,

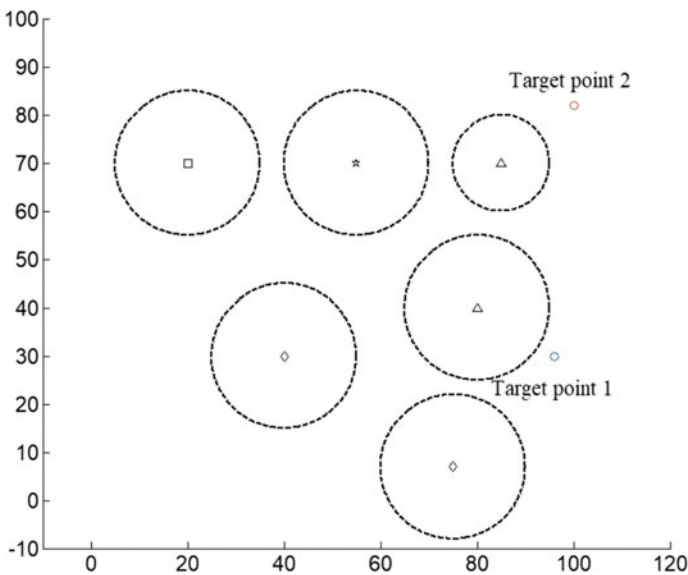


Fig. 3 2D sketch map of multiple missiles launch assignment simulation

**Table 3** Definition of the weather threaten factor

Group A			Group B		
The amount of surface combat missile	The amount of electromagnetic compaction missile	The attack point	The amount of surface combat missile	The amount of electromagnetic compaction missile	The attack point
8	1	1	7	2	2

the warship is set in the coordinate (0, 0), and two target points are also marked in that map. The square, the triangle, the diamond, and the five-pointed star represent the centres of the missile, the radar, the wind, and the rain, respectively. Clearly, in this simulation, we only consider the mission assignment issue of two groups of the warship missile. The corresponding control parameters of our proposed algorithm are:  $K = 2, t = 3, r = 15, \gamma = 0.1, \alpha = 0.5, R(1) = 1.0, R(2) = 1.3, w_1 = 1.0, w_2 = 0.75$ . And the maximum iteration times of the GA is set by 100.

Table 3 presents the assignment results of Fig. 3. From Table 3, it can be seen that the mission assignment of the multiple missiles can be realized by the proposed method well. For example, regarding the attack point 1, the amount of surface combat missile and the amount of electromagnetic compaction missile are 8 and 1, respectively. The practical flight path of the missile group is the line between the warship and the target point. Because the electromagnetic compaction missile can decrease the exterior threaten degree for the surface combat missile, 3 electromagnetic compaction missiles are distributed to the target points after the computation. Obviously, the simulation result considers the flight factor, the threaten factor, and the environment factor. Currently, the average simulation time is about 20 s.

### 4.2 The Results of AHP Modelling

The AHP is used to estimate the weights of the cost function in Eq. (1). Comparing with the traditional artificial experience-based weight setting method, the application of AHP is more objective. Table 4 shows the judgemental matrix results of the AHP criteria hierarchy (the middle hierarchy); Table 5 presents the judgemental matrix results of the AHP alternative hierarchy (the factor hierarchy), and Table 6 illustrates the estimated importance weights of AHP. The comparison of the importance between

**Table 4** Judgemental matrix results of the AHP criteria hierarchy

	Threaten factor	UAV factor	Environment factor
Threaten factor	1	8	8
UAV factor	1/8	1	1
Environment factor	1/8	1	1

**Table 5** Judgemental matrix results of the AHP alternative hierarchy

	Radar	Missile		Distance	Propellant		Wind	Rain
Radar	1	1/8	Distance	1	1/6	Wind	1	5
Missile	8	1	Propellant	6	1	Rain	1/5	1

**Table 6** Final estimated importance weights of AHP model

Name	Radar	Missile	Distance	Propellant	Wind	Rain
Value	0.0889	0.7111	0.0143	0.0857	0.0833	0.0167

any two factors comes from the subjective evaluation of the sea battle experts. From these results, it can be seen that—first, the most importance factor which influences the mission seriously is the anti-ballistic missile factor whose weight is 0.7111. Second, the most un-important factor is the flight distance factor whose weight is 0.0143; and the final importance ranking of these factors is: the missile factor, the radar factor, the propellant factor, the wind factor, the rain factor, and the distance factor.

### 4.3 Discussions

The modern naval battle needs the combat system to be intelligent, fast, and efficient. With the fast development of weapon technology, more and more new type weapons are equipped to the warship; thus, how to use them properly should be researched carefully. In this paper, the launch assignment of multiple missiles is studied. Different from the traditional operation method which only launches one missile to implement the combat mission, multiple missiles which have different combat functions are considered simultaneously here. Clearly, this is the development trend of the naval battle in the future. For example, the surface combat missile is used to destroy the enemy’s warship, while the electromagnetic compaction missile can be employed to suppress and decrease the threaten degree of other exterior factors. Thus, the integrated combat effect can be achieved by the mission assignment.

The GA is considered to carry out the multiple missiles assignment in this paper. The GA belongs to a kind of stochastic computational method which can solve the optimal computational problem well. The GA almost has no application limitations for the mathematical problem itself, and it can solve all kinds of optimal problems, such as the linear function and the nonlinear function, as well as the continuous function and the discrete function. The GA also has a good performance on conquering the local optimization problem. Its convergence speed and its computational speed are

also fast. Clearly, some other methods can also be used here, such as the greedy algorithm, the Munkres algorithm, and the artificial network-based method [7]. However, after the consideration of both the computational complexity and the computational accuracy, only the GA is utilized in this paper.

The proposed method at least has three advantages. First, the design of the optimal issue for the multiple missiles combat is reasonable. Six factors are considered when constructing the optimal function of GA. Second, the computation speed of proposed algorithm is comparable fast. The response speed will determine the victory of the war; thus, the analysis speed of the intelligent algorithm cannot be too long. Third, the scalability of proposed method is also good. Many new factors can be added to improve its computational effect, and some improved GAs [8] can also be employed. Clearly, the proposed method also has some drawbacks. For example, the stochastic interference factor should be considered in the future. The situations in the combat field vary from minute to minute; thus, the stochastic changes should be considered in this model.

## 5 Conclusion

A multiple missile launch assignment method is proposed. Two kinds of missile are considered here, i.e. the surface combat missile and the electromagnetic compaction missile. When implementing the optimal computation, first, three threaten sources, i.e. the anti-ballistic missile threaten factor, the radar threaten factor, and the weather threaten source, are modelled. Second, the GA is used to estimate the optimal solution of the mission assignment. Third, to improve the objective computational effect, the AHP is used to compute the weights of the optimal weights of the GA. In the future, other evolution algorithms can be tested for this multiple missiles launch assignment problem.

## References

1. Stanton NA, Harvey C, Alison CK (2019) Systems theoretic accident model and process (STAMP) applied to a royal navy hawk jet missile simulation exercise. *Safety Sci* 113:461–471
2. Baron B, Spathis P, Rivano H et al (2016) Offloading massive data onto passenger vehicles: topology simplification and traffic assignment. *IEEE ACM T Network* 24:3248–3261
3. Sheng J, Prescoat D (2017) A hierarchical coloured Petri net model of fleet maintenance with cannibalisation. *Reliab Eng Syst Safe* 168:290–305
4. Yao W, Qi N, Wan N, Liu Y (2019) An iterative strategy for task assignment and path planning of distributed multiple unmanned aerial vehicles. *Aerosp Sci Technol* 86:455–464
5. Gnanavelbabu A, Arunagiri P (2018) Ranking of MUDA using AHP and fuzzy AHP algorithm 5:13406–13412
6. Karaman S, Shima T, Frazzoli E (2012) A process algebra genetic algorithm. *IEEE T Evolut Comput* 16:489–503

7. Koprulu I, Kim Y, Shroff NS (2019) Battle of opinions over evolving social networks. *IEEE ACM T Network* 27:532–545
8. Su Y, Guo N, Zhang X (2020) A non-revisiting genetic algorithm based on a novel binary space partition tree. *Inform Sci* 512:661–674

# Study on Female Caring Office Chair Design Based on Ergonomics



Tianqi Yuan and Xiaohui Tao

**Abstract** This article studies the design of office chairs for professional sedentary women. First, it investigated the hidden health hazards of women caused by sedentary, analyzed the man–machine system of office chairs, and summarized the relationship between seats and hidden health hazards. In addition to the common low back and cervical diseases caused by improper sitting posture, female reproductive system diseases and anorectal diseases are also related to sedentary. This article combines the ergonomics theory to propose design criteria in the design of women’s seats, which aims to improve the health problems of women’s sedentary from the perspective of the seat, to give women health care from both physical and psychological dimensions. On the basis of existing chairs, an office chair design plan for women’s care is proposed.

**Keywords** Women’s physical health · Office chair · Ergonomics · Sedentary

## 1 Preface

According to the 2017 White Paper on the Health Status of Working Women in China, which was conducted in major first-tier cities in China, only 5% of the total number of women surveyed were truly healthy, 20% were confirmed to have a disease, and 75% were in a sub-health state [1]. Gastrointestinal diseases, cervical spondylosis, and other diseases often plague women, and sub-health states such as decreased memory and poor sleep have become common problems among working women. In addition, women’s physiological characteristics are different from men’s. Women face many different physical health problems than men after long periods of sedentary. For female employees, sedentary office work can cause gynecological inflammation and other diseases. One of the reasons is that the office chair does not deal with the man–machine relationship well. The existing office chair design focuses on universality

---

T. Yuan (✉) · X. Tao

College of Mechanical and Electrical Engineering, Hohai University, Changzhou 213001, China  
e-mail: [1361909258@qq.com](mailto:1361909258@qq.com)



and often ignores the actual needs of the professional female group. Therefore, the design of office chairs needs to dig deeper into the needs of women, fully consider the potential risk of disease, and optimize the working status.

## **2 Women's Health and Office Chair Man–Machine System**

### ***2.1 Sedentary Effects on Female Reproductive System***

Studies have shown that more than 70% of working women have different types of gynecological diseases, and in recent years, the proportion is still on the rise and younger [2]. Long-term sedentation of professional women can easily lead to pelvic congestion, causing blood circulation in the annex and the cervix to be blocked. The anatomical structure of the pelvic cavity prevents venous return, which leads to diseases such as pelvic inflammatory disease. In addition, due to the difference of physical structure, women are more likely than men to suffer from a urinary tract infection. The vulva is in a humid and hot state for a long time, which will accelerate the growth and reproduction of bacteria around the urinary system, thereby accelerating the disease.

In addition, studies have found that sedentary behavior increases the likelihood of ovarian cancer. Ovarian cancer is the seventh most common cancer in women and the leading cause of mortality among gynecological malignancies. The aetiology of ovarian cancer is relatively unknown, but it has been suggested that physical inactivity as reflected by prolonged sitting can reduce insulin sensitivity, leading to a growth-promotional environment that facilitates neoplasia [3].

### ***2.2 Sedentary Causes Anorectal Disease***

Sedentary not only affects the female reproductive system, leading to an increased prevalence of gynecological diseases, but also causes anorectal diseases. According to a census, the prevalence of hemorrhoids in adults is 59%, that is, 6 out of 10 people suffer from hemorrhoids. The population with a high prevalence has a significant feature-long sedentary habits. As the human body is in the same fixed posture for a long time, it affects the blood circulation and makes the anorectal venous blood return poorly. In addition, the portal vein system has no venous valves to help the blood return. Over time, it will easily cause hemorrhoidal vein congestion and varicose veins to become hemorrhoids [4].

### **3 Design Principles of Man–Machine System of Office Chair**

#### ***3.1 Thermal Comfort and Breathability***

In view of the above health hazards that are prone to sedentary women, we have made some considerations. One of the important causes of sedentary female gynecological diseases is the damp and sultry seat cushion. This problem is particularly prominent in summer, so it is necessary to study the thermal comfort and breathability of the office chair seat surface. We have summarized three factors that influence the thermal comfort and breathability of the office chair seat surface: the material, thickness, and shape of the cushion. Therefore, how to design an office chair with higher caring for women needs to start from these three aspects.

Cushion material is divided into seat surface material and seat surface filling material. Common seat surface filling material is foam material, its kind is various, usually use hardness 70, density 30, 24 foam sponge. The size and gap of the sponge are all factors that affect the breathability of the cushion. Therefore, we choose a sponge with a larger gap as the filling material.

The thickness of seat surface should be in the range of 10–15 cm. The seat surface of the mesh and cloth is thinner. Through investigation and analysis, users tend to choose office chairs with thin seats, so choosing single mesh office chairs has gradually become a design trend.

According to the survey, when the skin temperature reaches 34°C, the human body will begin to sweat and regulate the physiological heat balance through sweating. As a result, the humidity of the contact surface will increase, creating conditions for bacterial reproduction. From the perspective of the shape of the cushion, we can create the space between the key part of the human body and the cushion to reduce unnecessary contact, thereby reducing pressure and achieving the purpose of heat dissipation and ventilation.

#### ***3.2 Reasonable Distribution of Body Pressure***

The pressure distribution of sitting position is the main factor to evaluate the comfort of the seat [5]; it refers to the pressure distribution of the human body on the seat surface when sitting [6]. Seated pressure distribution can be divided into seat pressure distribution and back pressure distribution. For the hip (Fig. 1), the pressure on the ischial tuberosity is the largest and gradually decreases outward in order, reaching the lowest value at the front of the seat and the thigh [6]. Among them, the provision of lumbar support is indispensable, and its specific position should be 20 cm away from the seat cushion. Therefore, the lower backrest that plays a reasonable supporting

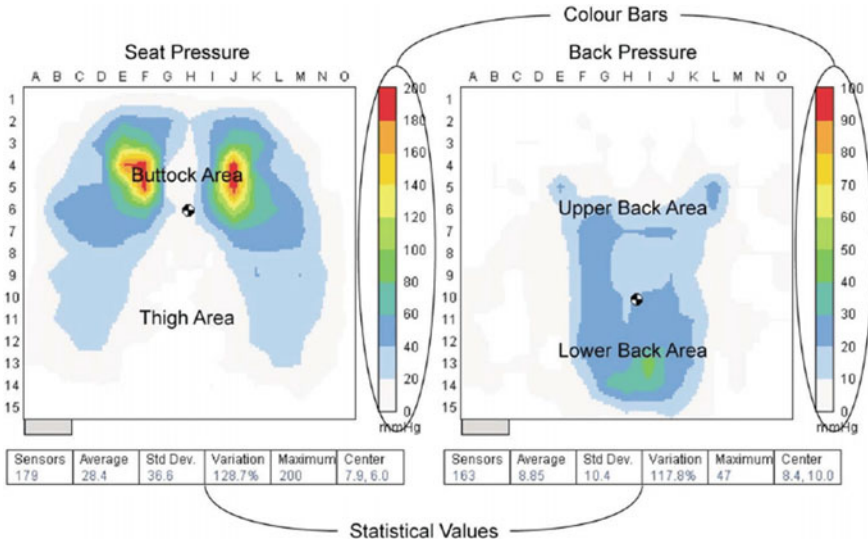


Fig. 1 Reasonable distribution of body pressure

role has always been the focus of consideration in the design of office chairs. In addition, due to individual differences, the backrest of the seat should be adjustable in multiple dimensions, such as up and down or back and forth.

Women are usually lighter than men, so we will use “feminine care” as the starting point for design and follow the seated body pressure distribution of women for the research and design of office chair.

### 3.3 Keep Users in a Healthy Posture

The normal behavior of a person using an office chair can be broken down into: standing, holding on to the armrest in preparation for sitting, relying on the back of the chair, stabilize the limbs, adjust the sitting posture, support the armrests to stand, and stand as shown in Fig. 2 [7]. It can be seen that during the use of the office chair, the bottom surfaces of the thigh, buttocks, and back are the most contacted parts. Support not only affects the user’s use status and work efficiency, but also targets female workers’ physical condition and temperament.

Cervical and lumbar spine activities are most frequent in daily life [6]. Figure 3 shows the curvature of the spine in different behavioral states. It can be seen from the figure that when the seat is in a sitting position, the angle of the lumbar spine is closest to the angle in the natural state when the waist is supported.

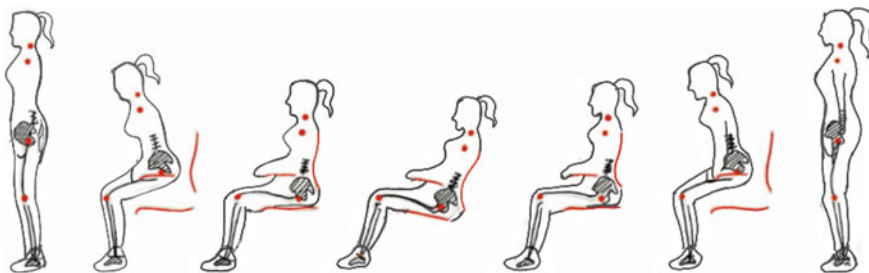


Fig. 2 Process of using office chair

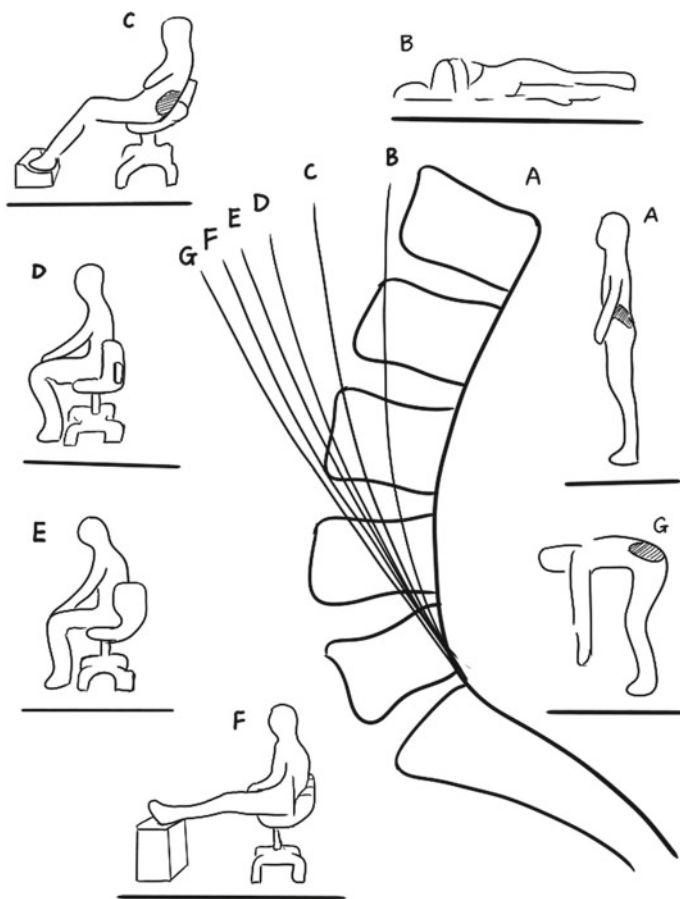


Fig. 3 Lumbar spine angles in various positions

### ***3.4 Meet the Emotional Needs of Female Groups***

A survey of World Health Organization shows that women have a higher incidence of abnormal psychology than men. In the female population, professional women are more likely to develop mental illness than non-professional women [8]. Compared with men, women are richer and more delicate in their emotional needs, and the emotions conveyed by products are often easier to perceive and accept. Office chair and user contact for a long time, but it often pays more attention to the function, only by paying more attention to the female emotion in the research can we grasp the needs of women and reflect the humanistic care of the design.

The shape of product should be soft, elegant, and rhythmic, with soft transitions and curved lines, which can make female users feel safe, and they are not susceptible to sharp collision injuries when moving it. At the same time, the curve on the product shape is also the intentional projection of the female body curve. The tenderness, intimacy, and roundness are character of women, which make people associate with the seat user. The colors of women's product are usually relatively bright, which generate positive psychological cues. Women's ability to perceive color is relatively higher than men's, and the impact of color on women is also stronger. Therefore, women's products are more colorful than men's.

## **4 Analysis of Design Scheme**

### ***4.1 Design of Cushion***

From the perspective of biological anatomy, about 75% of the weight of the upper body on the hard seat surface is transmitted through the spine to the ischial tuberosity which is 25 cm below the apex of the bone. Two contact points are formed on the contact surface of the seat, and they bear most of the weight of the hips and above. In an ideal state, the pressure on the human body is largest at the ischial tuberosity and decreases in order until it approaches the edge of the thigh in contact with the seat [9].

Taking into account the different needs when sitting in the office for a long time, the cushion is designed as A and B two-sided, and the A and B surface can be flipped and switched as needed; among them, the "A" surface is approximately horizontal. In order to reduce the body pressure at this position and avoid compression on the thigh roots, the seat surface near the edge of the thigh is a waterfall shape. "A" surface meets the basic needs of office chairs.

Surface "B" adds a hole in the middle of the seat on the basis of Face A. The role of Face B is to provide a healthier sitting experience for women with gynecological or anorectal infections. In an ideal state, most of the body compressive stress is concentrated at the ischial tuberosity. The middle area of ischial bulge requires relatively little stress, while anus and genital area need better ventilation and less compression



Fig. 4 Design dimensions and final scheme

for better blood circulation. So, we set a cavity with a radius of about 100 mm in the middle of the “B” surface to achieve the effect of ventilation and decompression of the anus and genitals, and to a certain extent, reduce the possibility of gynecological diseases and anorectal diseases.

### 4.2 Design of Pedal

Considering that the legs need to be supported parallel to the body when lying down and resting, the design scheme combines the support of the legs with the function of relaxing the muscles of legs. The pedal is designed to be two-sided, and one side is cushioned to provide rest. The other side is a massage module (Fig. 4), which relaxes the leg muscles, relieves muscle stiffness after sedentary, avoids varicose veins in the lower limbs, and also exercise the abdomen and other parts during active massage. The pedal can be adjusted by telescopic adjustment. Its length range from 660 to 800 mm, and the width is 98 mm. The material of the pedal is silicone, which is not easy to damage the skin of the legs and easy to clean.

### 4.3 Detailed Design

Human waist curve is slightly forward, and in this scheme, the back of the chair is an irregular S-shaped curve that conforms to the physiological characteristics of the back. There is a backrest with a height of 220 mm between the 4th to 5th lumbar vertebra. It can be adjusted back and forth or up and down through the control device. Two-dimensional adjustment provides a more comfortable experience. The neckrest is designed as a movable neckrest that can be adjusted in height and angle to accommodate people of different heights and different postures.

Neckrest is an important part of office chairs, the neckrest designed by us can be adjusted in height and angle to accommodate people of different heights and different postures, and it is 300 mm long and 104 mm wide.

Common office chairs need to meet the needs of both rest and work; the backrest inclination angle is small during work and large during rest. The inclination angle is too large or too small to provide reasonable support. Among them, the most suitable angle for work is  $95^{\circ}$ – $105^{\circ}$ , and the rest is  $105^{\circ}$ – $110^{\circ}$ . In order to meet the needs of work and rest at the same time, this plan chooses a wide range of backrest adjustment angle:  $90^{\circ}$ – $135^{\circ}$ .

Taking into account the factors such as women's chills and prone to stomachaches, this design scheme comes with a heating accessory—Nanshubao, which aims to warm the body of women. Its shape can be changed at will, and it can be tied to the waist, abdomen, neck, etc., to apply heat or provide additional support.

Health hazards from frequent sedentary are difficult to completely avoid. This design scheme reminds the user to exercise by timing the vibration device placed on the back of the seat to, then relieve the tense muscle. The vibration time can be set according to specific conditions.

#### ***4.4 Semantic Design and Color Schemes***

In order to make the seat more in line with the female image, the back of the seat is designed with a multi-dimensional curve (Fig. 4), while the shoulder curve provides more reasonable support for the shoulders, and with the looming support frame on the back, the overall seat back looks like a butterfly with wings spread, showing the characteristics of women, achieved a unified function and beauty.

In terms of color matching, the back of the chair, the cushion, and the neckrest adopt soft colors with moderate brightness and low purity, which shapes the psychological peace through soft visual feelings. The legs of the chair are covered with a gray plastic metal frame, which is both stable and resistant to dirt.

### **5 Conclusions**

This article has conducted in-depth research and discussion on women's health risks, and explored the design points of women's seats from multiple dimensions, and designs a female office chair whose main function is to reduce the harmful effects of sedentary working on female reproductive system and anorectal system, so as to increase the care for women. This article provides a new way of thinking for seat design, but no product can help people completely avoid health risks. Therefore, the exploration of seat design should be continuously developed.

## References

1. Jufang S (2019) Research on the influencing factors of occupational women's health status. *Econ Res Guide* 390(04):147–149
2. Xiaopu S (2013) Discussion on gynecological health care of modern professional women. *China Foreign Med Treatment* 032(027):144–145
3. Zhang M, Xie X, Lee AH, Binns CW (2004) Sedentary behaviours and epithelial ovarian cancer risk. *Cancer Causes Control* 15(1):83–89
4. Jitang W (2010) Discussion on the pathogenesis and clinical treatment of hemorrhoids. *Jilin Med J* 31(5):4754
5. Lingling H, Zuoxin L, Jilei Z (2015) Discussion on the stress of the soft tissue of the buttocks in sitting position. *Furniture* (3):50–53
6. Jian G (2015) Research on the application of ergonomics in the design and innovation of office chair. *China Packaging Industry*
7. Huimin Z. Research on interactive healthy chair design for Sedentary Group. *Hubei University of Technology, Hubei*
8. Chenghong L (2005) Mental health status of working women. *Social Sci Guangxi* 000(012):183–185
9. Ming X, Qunsheng X (1997) Index of body pressure distribution. *Chin Mech Eng* (01):65–68 + 124



# Research on Blackness Classification of Polyester Knitted Printed Black Cloth



Jingying Xu, Qiubao Zhou, Zimin Jin, and Kun Chen

**Abstract** This paper analyzes and simplifies the commonly used color index Lab, combines the reflectivity integration curve, and divides the fabric blackness into two categories according to the degree of color. The concepts of achromatic blackness and chromatic blackness are proposed to create a classification method. The achromatic blackness classification is considered to be  $a \leq 1$ ,  $b \leq 1$ , and  $L \leq 22$  which is divided into 5 levels for evaluation, with 5 as the highest and 1 as the lowest. The chromatic blackness classification is evaluated by the method of integrating the reflectance curve of the test sample and the standard sample. The method of number of level–number of segment is divided into 6 levels, of which 6 is the highest, 1 is the lowest, and each level is divided into 3 segments, which are represented by I, II, and III, with I being the highest and III being the lowest. These two categories can more intuitively reflect the user’s blackness classification requirements for black fabrics.

**Keywords** Blackness characterization · Blackness evaluation · Polyester knitted fabric · Color index · Reflectance curve

## 1 Introduction

Black textile fabrics are highly favored by the public, but because black fabrics have not been quantified, in the business process, buyers and sellers have different understandings of the blackness requirements of black fabrics, and they have mistaken navy blue for black. Therefore, it is of great significance to explore a reasonable blackness grading method. Polyester knitted fabrics are widely used and have good ductility and elasticity, and it has good warmth and comfort, rich organizational structure changes, and unique varieties and appearances [2]. In market, the demand for polyester knitted

---

J. Xu (✉) · Q. Zhou · Z. Jin · K. Chen  
College of Textile Science and Engineering, Zhejiang Sci-Tech University, 310018 Hangzhou,  
China  
e-mail: [a785436476@163.com](mailto:a785436476@163.com)

black fabrics is increasing day by day, so this paper takes polyester knitted fabrics as a representative, performs printing proofing, and constructs a classification method to measure the blackness of the fabric.

Chie Muraki Asano and others proposed an objective evaluation method of human impression based on logical discriminant analysis from the perspective of Kansei project, which played a certain role in visual inspection [3]. Eda Tetsuya et al. studied the effect of surround brightness on perceived blackness, and discussed the impact of the environment on visual inspectors in the process of evaluating blackness [1]. Lan Tao et al. studied the degree of blackness preference and perception of different races and proposed a cultural impact on color preference [6]. Renzo Shamey et al. used the experimental black data set to evaluate the performance of various color difference formulas, and the model based on CIECAM02 showed the best performance [4]. Through colorimetric analysis of black-coated fabrics, R. Jafari et al. found that brightness plays a very important role in blackness preference, but it does not affect the results alone and evaluates the effectiveness of some suggested blackness indicators [5]. Xie Wanzi used mathematical modeling to obtain two new color depth formulas in the objective evaluation formula of color depth based on theoretical design. Then, he designed six color depth formulas based on colorimetric theory [7].

## 2 Collection of Polyester Knit Printed Black Cloth

There are two types of sample collection methods for polyester knitted printed black fabrics. One is the 17 special polyester low-elastic knitted black fabrics provided by the manufacturer. As shown in Table 1, the numbers are #1- #17 and record their Lab color indicators. The other type is based on computer color measurement and color matching technology, through the established basic dyestuff database, 77 different kinds of dye combinations with different concentrations given by the computer, according to printing paste → automatic scraping → drying in the oven → 195 °C curing for 3 min → reduction washing for 10 min → water washing → drying → cooling and balancing process to print, in order to obtain 77 pieces of polyester low-elastic knitted black fabrics with ordinary printing process. Their Lab spatial distribution is shown in Fig. 1. Among these 77 cloths, select 8 black cloths with large differences in color index and visual difference. As shown in Table 2, they are numbered #A- #H and record their Lab color indexes. All samples were studied using a black tube as a standard.

**Table 1** Polyester low stretch knitted black cloth with special blackening printing process

	<i>L</i>	<i>a</i>	<i>b</i>	DE*
#1	17.19	0.92	0.18	16.22
#2	13.64	0.48	0.61	12.67
#3	10.8	0.85	-0.13	9.84
#4	9.75	0.55	-0.79	8.81
#5	11.65	0.55	-0.87	10.71
#6	12.85	0.23	0	11.86
#7	12.4	0.59	0.31	11.42
#8	15.11	0.38	-0.16	14.12
#9	13.09	0.54	-0.98	12.15
#10	20.41	0.69	-0.23	19.43
#11	13.05	0.23	-0.61	12.09
#12	14.81	0.39	-0.96	13.86
#13	11.74	0.25	-0.65	10.78
#14	14.67	0.66	-0.65	13.71
#15	9.46	0.59	-0.19	8.01
#16	12.07	0.72	-0.49	10.6
#17	2.1	0.21	0.12	0.78

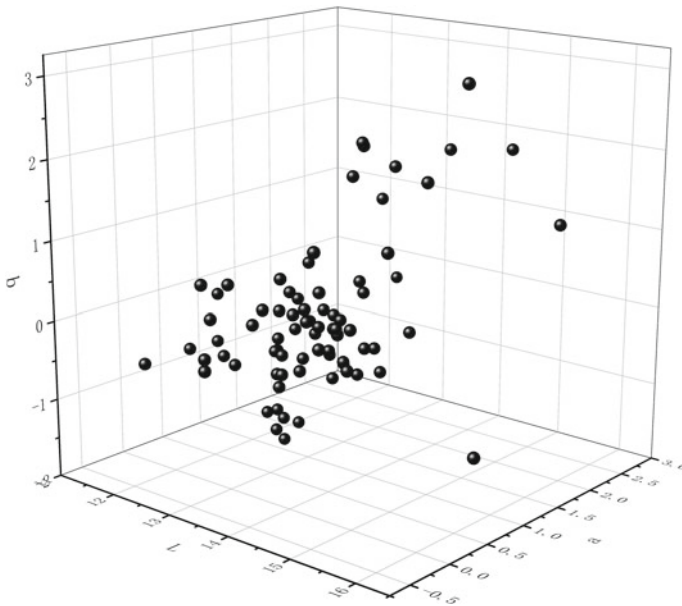


**Fig. 1** Lab space distribution of printed black cloth

**Table 2** Polyester low-elastic knitted black cloth with ordinary technology

	$L$	$a$	$b$	DE*
#A	12.92	2.33	-0.05	12.12
#B	13.49	1.23	1.67	12.64
#C	13.26	1.83	1.2	12.43
#D	14.12	2.06	1.9	13.38
#E	13.83	1.53	1.77	13.02
#F	13.47	1.34	0.3	12.53
#G	12.86	1.13	0.5	11.91
#H	15.58	2.34	1.09	14.77

### 3 Research on the Classification Method of Fabric Blackness

At present, the research on the blackness grading method of textiles is not perfect, and more discussion is made on the blackness in thermodynamics. French scientist Ringelman divided the smoke blackness from 0 (full white) to 5 (full black), a total of six levels, and it is an indicator used to reflect the concentration of smoke and dust emitted by the boiler. A similar grading method can also be established for textiles, which are classified according to the degree of color and divided into achromatic blackness and chromatic blackness.

#### 3.1 Achromatic Blackness Classification

Achromatic blackness refers to blacks with low chroma values and almost 0 in ideal. Since  $a$  and  $b$  are in a certain range, lightness  $L$  is the main factor affecting DE\*. Fig. 2 shows the linear relationship between  $L$  and DE. It is positively correlated; that is, the lower the brightness, the smaller the color difference, and the better the blackness, so if  $a$  and  $b$  are close to 0, they can be regarded as achromatic blackness. The manufacturer provided in this experiment provides seventeen polyester low-elastic silk knitted black cloths with special blackening printing process, and their color index Lab range is  $a \leq 1, b \leq 1, L \leq 22$ , which are all visually black. Sample 10 is close to the critical point. At this time, their blackness is only related to lightness, so in this experiment, the achromatic blackness can be divided into 5 levels according to the lightness  $L$ , as shown in Table 3. Among them, 5 is the highest and 1 is the lowest. According to the method of achromatic blackness classification, the results of #1- #17 are shown in Table 4. Among them, #17 is level 5 with the best blackness, and #1 and #10 are level 1 with the worst blackness.

**Fig. 2** Linear relationship between  $L^*$  and  $DE^*$

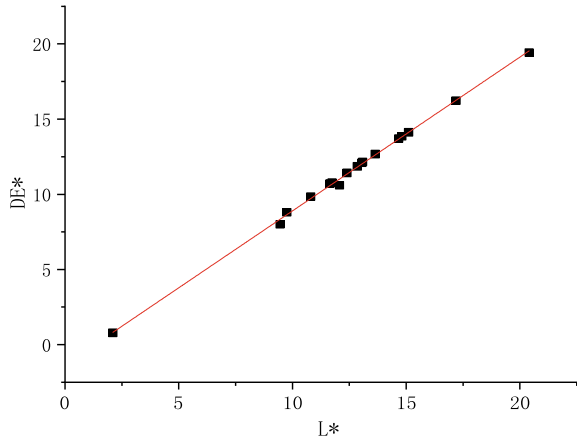


**Table 3** Achromatic blackness classification

Level	$L$ range
Level 5	$L \leq 8$
Level 4	$8 < L \leq 10$
Level 3	$10 < L \leq 13$
Level 2	$13 < L \leq 17$
Level 1	$17 < L \leq 22$

**Table 4** #1-#17 Achromatic blackness classification results

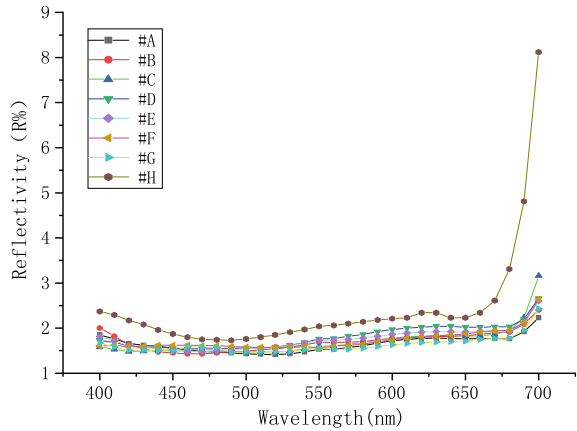
Number	#1	#2	#3	#4	#5	#6	#7	#8	#9	#10	#11	#12	#13	#14	#15	#16	#17
Level	1	2	3	4	3	3	3	2	2	1	2	2	3	2	4	3	5

### 3.2 Chromatic Blackness Classification

When  $a$  and  $b$  exceed a certain range, the hue of the black cloth is changed, resulting in red shift or blue shift, but in the visual category, it is still black. For the gradation method with chroma and blackness, it is difficult to achieve grading according to the hue range. Therefore, considering the reflectivity curve, when the average reflectance of black cloths of different tones is the same, it is used to judge the black of the color sample and the standard sample. The degree of coincidence cannot fully reflect the chroma situation, so the point and line processing methods are generalized to the surface, and the reflectance curve of #A- #H is drawn, as shown in Fig. 3.

Calculate the integrated value of the reflectance curve of the test sample and the standard sample, divide the wavelength range of 400–700 nm into 6 sections every 50 nm, and construct a  $k$  value expression,  $k = k_0 + \sum k_x$  ( $x$  is a positive integer less than 7), where  $k_0$  represents the integral ratio of the reflectance curve of the test

**Fig. 3** Reflectivity curve of #A–#H



sample to the standard sample at the entire visible light wavelength of 400–700 nm,  $k_x = S_x/S_{max}$ ,  $S_x$  represents the integration value of the sample in any of the 6 sections, and  $S_{max}$  is the maximum integral value of the standard sample in this 6 sections. In this experiment, the integrated value of the standard sample at 400–700 nm is 48.8, and the value of  $S_{max}$  is 20.7. The  $k$ ,  $k_0$ , and  $k_x$  values of samples #A- #H are shown in Table 5.

First, use  $k_0$  and  $k_x$  values to create rating levels, and the representation method is described as number of level. As shown in Table 6, using  $k_0$  as the classification result, there are a total of levels, with 6 being the highest. Among them, level 1 is the lowest, and each level is divided into 3 segments. As shown in Table 7, the  $k_x$  is used as the segmentation result, which is recorded as I, II, and III, where segment I represents the highest and segment III represents the lowest. According to the gradation method of chromatic blackness, the evaluation results of #A- #H are shown in Table 8. In Fig. 8, the number of #G is 4-I. It means that the number of level of #G is 4, and the number of segment of #G is I.

**Table 5**  $k$ ,  $k_0$ , and  $k_x$  values of samples #A–#H

	$k_0$	$k_1$	$k_2$	$k_3$	$k_4$	$k_5$	$k_6$	$k$
#A	10.04	4.05	3.6	3.5	3.89	4.28	4.47	33.83
#B	10.4	3.97	3.52	3.82	4.15	4.38	4.79	35.03
#C	10.3	3.67	3.6	3.64	4.05	4.42	5.02	34.7
#D	11.04	3.93	3.75	3.93	4.48	4.9	5.16	37.19
#E	10.71	3.93	3.65	3.91	4.31	4.62	4.94	36.07
#F	10.53	3.9	3.9	3.82	3.99	4.41	4.94	35.49
#G	9.9	3.73	3.72	3.62	3.77	4.08	4.52	33.34
#H	14.16	5.16	4.29	4.58	5.15	5.51	8.86	47.71

**Table 6** Level of chromatic blackness

Level	$k_0$
Level 6	$k_0 \leq 6$
Level 5	$6 < k_0 \leq 8$
Level 4	$8 < k_0 \leq 10$
Level 3	$10 < k_0 \leq 12$
Level 2	$12 < k_0 \leq 14$
Level 1	$14 < k_0 \leq 16$

**Table 7** Segmentation of chromatic blackness

Segment	$k_x$
I	$k_x \leq 5$
II	$5 < k_x \leq 8$
III	$8 < k_x \leq 11$

**Table 8** #A–#H chromatic blackness classification results

Number	#A	#B	#C	#D	#E	#F	#G	#H
Number of level–number of segment	3-I	3-I	3-II	3-II	3-I	3-I	4-I	1-III

## 4 Conclusion

Achromatic blackness classification divides the brightness  $L$  and divides  $L \leq 22$  into 5 levels, of which 5 is the highest and 1 is the lowest. The chromatic blackness classification uses the method of number of level–number of segment, which is divided into 6 levels, of which 6 is the highest, 1 is the lowest, and each level is divided into 3 segments, which are expressed by I, II, and III. I is the highest segment, and the III is the lowest segment. In summary, the concepts of achromatic blackness grading and chromatic blackness grading are proposed, and a grading method is created accordingly, which helps guide the production of black textiles and evaluate the blackness levels of textiles.

## References

1. Asano CM, Hirakawa S, Asano A (2004) Exploration of image features for describing visual impressions of black fabrics. In: International conference on knowledge-based and intelligent information and engineering systems. Springer, Heidelberg, pp 756–763
2. Cheng L (2017) New knitted fabrics and their dyeing and finishing. Tianjin Textile Sci Technol (3):40–44

3. Eda T, Koike Y, Matsushima S et al (2010) Influence of blackness on visual impression of color images. *Kansei Eng Int J* 10(1):49–58
4. Haslup JRC, Shamey R, Hinks D (2013) The effect of hue on the perception of blackness using Munsell samples. *Color Res Appl* 38(6):423–428
5. Jafari R, Amirshahi SH, Ravandi SAH (2016) Colorimetric analysis of black coated fabrics. *J Coat Technol Res* 13(5):871–882
6. Tao L, Westland S, Cheung V (2012) Blackness: preference and perception (value and chroma). In: *Conference on colour in graphics, imaging, and vision*. Society for imaging science and technology, issue 1, pp 253–258
7. Xie W (2019) Design an objective evaluation formula for color depth based on theory. Zhongyuan Institute of Technology



# Evaluation of Dietary Quality of Aircrew by Military Diet Balance Index



Huiling Mu, Ruoyong Wang, Shuang Bai, Longmei Fang, Ximeng Chen, Hongjiang Jing, Feng Li, Peng Liu, Lili Zhang, and Peng Du

**Abstract** *Objective*—To evaluate the dietary quality of aircrew by using military diet balance index (DBI) and provide basis for their dietary guidance and nutritional intervention. *Methods*—Dietary survey was carried out by weighing method. The dietary quality of aircrew was evaluated by using military DBI. *Results*—The intakes of red meat and egg met the standard, the intake of vegetable oil was over the standard, the intakes of other kind of food did not meet the standard. The intakes of calcium, iodine, vitamin A, vitamin B<sub>1</sub> and vitamin B<sub>2</sub> did not meet the standard. The energy supply ratio of protein, fat and carbohydrate was 16%, 46% and 38%, respectively, showing a “high protein, high fat and low carbohydrate” pattern. The food quantitative results were basically consistent with the military DBI scores, showing a slight nutritional imbalance. *Conclusions*—The dietary pattern of the investigated aircrew was unreasonable; part of the food and nutrients intake was insufficient; the military DBI score showed that the dietary pattern was slightly unbalanced. The dietary pattern should be further adjusted.

**Keywords** Aircrew · Diet balance index · Dietary survey · Dietary quality

## 1 Introduction

Flight is a special kind of work which is strenuous and complicated, completed by aircrew under the influence of comprehensive stress factors such as low oxygen, low pressure, noise, vibration, acceleration, radiation and constantly changing climate environment [1]. The aircrew is in a special aviation operating environment, under comprehensive effect of various environmental factors. The body is in a state of high physiological and psychological stress, which puts forward special nutrition requirements of the aircrew. Reasonable nutrition and balanced diet are the important basis to ensure the health of aircrew and also the prerequisite to complete complex flight tasks.

---

H. Mu · R. Wang · S. Bai · L. Fang · X. Chen · H. Jing · F. Li · P. Liu · L. Zhang · P. Du (✉)  
Air Force Medical Center, Beijing 100142, China  
e-mail: mhl2001@126.com

© The Editor(s) (if applicable) and The Author(s), under exclusive license to Springer Nature Singapore Pte Ltd. 2021  
S. Long and B. S. Dhillon (eds.), *Man-Machine-Environment System Engineering*, Lecture Notes in Electrical Engineering 645,  
[https://doi.org/10.1007/978-981-15-6978-4\\_43](https://doi.org/10.1007/978-981-15-6978-4_43)

The diet balance index (DBI) was established according to the dietary guidelines and dietary pagoda for Chinese residents [2–4]. It is applicable to the dietary evaluation of all healthy people except infants under 2 years old. For people with special nutritional needs, the evaluation criteria should be adjusted appropriately according to the needs [4]. The military DBI [5] was established by referring to the dietary balance index of Chinese residents 2007 (DBI-07) [3] and the dietary guidelines for Chinese residents (2016) [6], combined with the characteristics of the recommended amount of food for military. In this study, the military DBI was used to evaluate the dietary quality of aircrew, so as to provide basis for the dietary guidance and nutritional intervention of aircrew.

## **2 Subjects and Methods**

### **2.1 Subjects**

Thirty-three healthy male aircrews were included in this study. The average age was  $(36.9 \pm 6.3)$  years old, the average height was  $(174.4 \pm 4.7)$  cm, and the average weight was  $(74.8 \pm 8.5)$  kg.

### **2.2 Dietary Survey**

Dietary survey was carried out by weighing method for three consecutive days. The intake of energy and nutrients was calculated according to the Chinese food composition [7].

### **2.3 Dietary Quality Evaluation**

According to the evaluation method of military DBI, the DBI index score of the investigated aircrew was calculated, and then, the high bound score (HBS), the low bound score (LBS), the diet quality distance (DQD) and the total score (TS) were calculated; these four indexes can reflect the dietary quality.

**Table 1** Daily food intakes of aircrew

Variety of food	Intakes (g/per capita per day)	Standard (g/per capita per day)	Rate (%)
Cereal	357.8	500	71.6
Red meat	208.6	200	104.3
Poultry meat	37.2	140	26.6
Egg	103.7	100	103.7
Fish shrimp	133.2	240	55.5
Milk	116.9	300	39.0
Soybean	49.7	80	62.1
Addible sugar	12.1	30	24.2
Plant oil	96.2	70	137.4
Vegetable	613.9	750	81.9
Fruit	379.9	300	126.6
Edible fungi	20.9	15	52.3

### 3 Results and Analysis

#### 3.1 Results of Food Intakes

The daily food intakes of aircrew were shown in Table 1. It was regulated that the intake of nutrients met the standard if its value is within  $\pm 10\%$  of the standard. According to the survey, only the intake of red meat and egg met the standard, the intake of vegetable oil was over the standard by 126.6%, the intakes of other kind of food did not meet the standard. The intakes of cereal, soybean and vegetable were insufficient, reaching 71.6%, 62.1% and 81.9% of the standard, respectively; the intakes of fish, shrimp and edible fungi were obviously insufficient, only reaching 55.5% and 52.3% of the standard, respectively; the intakes of milk and poultry meat were seriously insufficient, only reaching 39.0% and 26.6% of the standard, respectively.

#### 3.2 Intake of Energy and Nutrients

The energy and nutrient intakes were shown in Table 2. It was regulated that the intake of nutrients met the standard if its value is within  $\pm 10\%$  of the standard. The survey showed that the intakes of calcium, iodine, vitamin A, vitamin B<sub>1</sub> and vitamin B<sub>2</sub> did not meet the standard and the intakes of sodium, iron and vitamin E were over the standard by 230%, energy and other nutrients met the standard. The intakes of protein, fat and carbohydrate were 125.1 g, 160.1 g and 292.5 g, respectively, and the energy supply ratio was 16%, 46% and 38%, respectively. Compared with

**Table 2** Daily dietary intake of energy and nutrients of aircrew

Energy and nutrients	Intake	Standard	Rate (%)
Energy (MJ)	13.1	13.0–15.1	100.7–86.8
Protein (g)	125.1	120	104.3
Sodium (mg)	8085.9	3400	237.8
Potassium (mg)	3327.5	3000	110.9
Magnesium (mg)	466.1	410	113.7
Calcium (mg)	706.9	800	88.4
Phosphorus (mg)	1606.2	1000	160.6
Iron (mg)	35.1	15	233.7
Zinc (mg)	18.0	20	90.1
Selenium ( $\mu\text{g}$ )	95.8	60	159.7
Iodine ( $\mu\text{g}$ )	121.0	150	80.7
Vitamin A ( $\mu\text{gRE}$ )	1155.3	1500	77.0
Vitamin E (mg)	112.4	30	374.6
Vitamin B <sub>1</sub> (mg)	1.4	3	47.0
Vitamin B <sub>2</sub> (mg)	1.8	3	59.0
Vitamin C (mg)	216.6	150	144.4
Nicotinic acid (mg)	28.3	20	141.7

the recommended ratio of 12%–15%, 20%–30%, 55%–65%, the energy supply ratio was obviously unbalanced, showing a “high protein, high fat and low carbohydrate” pattern.

### 3.3 DBI Score

According to the military DBI, the DBI index scores of the investigated aircrew were calculated, as shown in Table 3. The HBS, LBS, DQD and TS were 10, –15, 25, –5, respectively. The survey lacked water consumption data, so it was ignored in the assessment. The military DBI scores showed that there was a slight nutritional imbalance in the investigated aircrew.

In this study, the quantitative results of food in the aircrew were basically consistent with the military DBI scores. For example, the intakes of cereal and vegetable did not meet the standard, and the DBI scores were –8 and –2, respectively; the intake of milk did not meet the standard, and the DBI score was –4; the intake of soybean did not meet the standard, and the DBI score was –2; the intake of fish and shrimp did not meet the standard, and the DBI score was –1; the intakes of vegetable oil and salt were over the standard, and the DBI scores were 2 and 4, respectively.

**Table 3** Military DBI

Components	Subgroup	Intake range by energy intake level				Score range	Actual intake (g)	Score
		10.9 ~ 12.6 MJ	12.6 ~ 14.6 MJ	14.6 ~ 16.7 MJ	16.7 ~ 18.8 MJ			
Cereal*	Cereal	<210 g = -12 460 ~ 540 g = 0 >790 g = 12	<290 g = -12 540 ~ 620 g = 0 >870 g = 12	<370 g = -12 620 ~ 700 g = 0 >950 g = 12	<450 g = -12 700 ~ 780 g = 0 >1030 g = 12	-12 ~ 12	357.8	-8
		Vegetable and fruit	Vegetable	Vegetable	Vegetable	-6 ~ 0	613.9	-2
Vegetable and fruit	Fruit	≥200 g = 0 100 ~ 199 g = -2 2	≥250 g = 0 125 ~ 249 g = -2 2	≥300 g = 0 150 ~ 299 g = -2 2	≥350 g = 0 175 ~ 349 g = -2 2	-6 ~ 0	379.9	0
		Milk and dairy products, Soybean and soybean products	Dairy	Dairy	Dairy	-6 ~ 0	116.9	-4
Soybean	Soybean	≥80 g = 0, 40 ~ 79 g = -2, 1 ~ 39 g = -4, 0 g = -6	≥250 g = 0 125 ~ 249 g = -2 2	≥300 g = 0 150 ~ 299 g = -2 2	≥350 g = 0 175 ~ 349 g = -2 2	-6 ~ 0	49.7	-2

(continued)

Table 3 (continued)

Components	Subgroup	Intake range by energy intake level					Score range	Actual intake (g)	Score
		10.9 ~ 12.6 MJ	12.6 ~ 14.6 MJ	14.6 ~ 16.7 MJ	16.7 ~ 18.8 MJ				
Animal food	Red meat and products, Poultry and products	>240 g = 4	>280 g = 4	>320 g = 4	>340 g = 4		-4 ~ 4	245.8	2
		120 ~ 240 g = 2	140 ~ 280 g = 2	160 ~ 320 g = 2	170 ~ 340 g = 2				
		60 ~ 120 g = 0	70 ~ 140 g = 0	80 ~ 80 g = -2	85 ~ 170 g = 0				
		1 ~ 60 g = -2	35 ~ 70 g = -2	0 g = -4	42.5 ~ 85 g = -2				
		0 g = -4	0 g = -4		0 g = -4				
Animal food	Fish and shrimp	<30 g = -4	<80 g = -4	<130 g = -4	<180 g = -4		-4 ~ 0	133.2	-1
		30 ~ 49 g = -3	80 ~ 99 g = -3	130 ~ 149 g = -	180 ~ 199 g = -				
		50 ~ 69 g = -2	100 ~ 119 g = -	3	3				
		70 ~ 89 g = -1	2	150 ~ 169 g = -	200 ~ 219 g = -				
		≥ 90 g = 0	120 ~ 139 g = -	2	2				
			1	170 ~ 189 g = -	220 ~ 239 g = -				
		≥ 140 g = 0	1	≥ 190 g = 0	≥ 240 g = 0				
Egg		0 g = -4, 1 ~ 69 g = -2, 70 ~ 100 g = 0, 101 ~ 130 g = 2, >130 g = 4				-4 ~ 4	103.7	2	

(continued)

**Table 3** (continued)

Components	Subgroup	Intake range by energy intake level			Score range	Actual intake (g)	Score
		10.9 ~ 12.6 MJ	12.6 ~ 14.6 MJ	14.6 ~ 16.7 MJ			
Condiments and alcoholic beverage	Cooking oil	≤50 g = 0, 50 ~ 100 g = 2, >100 g = 4		≤70 g = 0, 70 ~ 140 g = 2, >140 g = 4	0 ~ 4	96.2	2
	Salt	<6 g = 0, 6 ~ 12 g = 2, >12 g = 4			0 ~ 4	14.9	4
	Alcoholic beverage	Male: ≤ 25 g = 0, 26 ~ 50 g = 1, 51 ~ 75 g = 2, 76 ~ 100 g = 3, >100 g = 4 [25 g alcohol = 750 ml beer or 250 ml wine or 75 g liquor (< 38°) or 50 g liquor (> 38°)] Female: ≤ 15 g = 0, 15 ~ 30 g = 1, 31 ~ 45 g = 2, 46 ~ 60 g = 3, >60 g = 4 [(15 g alcohol = 450 ml beer or 150 ml wine or 50 g liquor(38°) or 30 g liquor(> 38°)]			0 ~ 4	0	0
Diet variety	Rice and products	For consumption of greater than 25 g of foods (soybean is 5 g), otherwise score is -1			-1, 0	>25	0

(continued)

Table 3 (continued)

Components	Subgroup	Intake range by energy intake level				Score range	Actual intake (g)	Score
		10.9 ~ 12.6 MJ	12.6 ~ 14.6 MJ	14.6 ~ 16.7 MJ	16.7 ~ 18.8 MJ			
	Wheat and products					>25	0	
	Corn, coarse grains and roots and products					>25	0	
	Dark colored vegetables					>25	0	
	Light colored vegetables					>25	0	
	Fruit					>25	0	
	Soybean and products					>25	0	
	Milk and dairy products					>25	0	
	Red meat and products					>25	0	
	Poultry and products					>25	0	
	Egg					>25	0	
	Fish and shellfish					>25	0	

\*Cereal includes rice, wheat, dried legumes (exclude soybean) and tubers. Intake amount means fresh amount. Score increased (decreased) 2 with 50 g intake increased (decreased) from 0 to maximal (minimal) score



## 4 Conclusions

The dietary pattern of the investigated aircrew was unreasonable, and part of the food and nutrients intake was insufficient. The results of the food diversity analysis of the aircrew in this survey showed that although there were many kinds of food that the aircrew ate, only the intakes of red meat and egg met the standard; the intake of vegetable oil was over the standard; the intakes of other kind of food did not meet the standard. The energy supply ratio of protein, fat and carbohydrate was 16%, 46% and 38%, respectively, showing a “high protein, high fat and low carbohydrate” pattern. The food quantitative results were basically consistent with the military DBI scores, showing a slight nutritional imbalance. The dietary pattern of the aircrew should be further adjusted, and the nutritional health education should be strengthened to promote reasonable nutritional behavior.

**Compliance with Ethical Standards** The study was approved by the Logistics Department for Civilian Ethics Committee of Air Force Medical Center. All subjects who participated in the experiment were provided with and signed an informed consent form. All relevant ethical safeguards have been met with regard to subject protection.

## References

1. Gao LX, Guo JS, Guo CJ (2008) Military nutrition and food science. Military Medical Science Press, Beijing, p 337
2. He YN, Zhai FY, Ge KY (2005) Approaching Chinese diet balance index. *J Hygiene Res* 34(2):208–211
3. He YN, Zhai FY, Yang XG, Ge KY (2009) The Chinese diet balance index revised. *Acta Nutrimenta Sinica* 31(6):532–536
4. He YN, Fang YH, Xia J (2018) Update of the Chinese diet balance index: DBI<sub>16</sub>. *Acta Nutrimenta Sinica* 40(6):526–530
5. Gao WN, Pu LL, Yao ZX et al (2016) Investigation and evaluation of dietary nutrition status of special forces. *People’s Military Surgeon* 59(11):1131–1134
6. Chinese Nutrition Society (2016) Dietary guidelines for Chinese residents. People’s Health Press, Beijing
7. Yang YX (2018) 2018 China food composition tables-standard, 6th edn. Peking University Medical Press, Beijing

# Numerical Simulation Research on Design of Displacement Ventilation System in Large Painting Workshop



Bin Yang, Jianwu Chen, Lindong Liu, Yanqiu Sun, Shulin Zhou, and Weijiang Liu

**Abstract** This article takes the paint spraying operation of the paint shop of a shipyard as the research object and uses ANSYS FLUENT numerical simulation software to apply displacement ventilation to the paint shop under different conditions of the size of the supply and exhaust vents and the location of the supply and exhaust vents. The airflow organization and the diffusion law of toxic substances were studied numerically. It is concluded that when replacement ventilation is used in the painting workshop, the length and width of the air supply and exhaust vents should be larger than the length and width of the work piece to be sprayed at the same time as long as the air supply and exhaust volume are the same. The supply and exhaust air arrangement method of the lower apply and lower exhaust is used to achieve the best ventilation and detoxification effect. It can effectively discharge toxic substances into the workshop and reduce the exposure of paint spraying workers to toxic substances.

**Keywords** Large painting workshop · Displacement ventilation · Numerical simulation · Ventilation protection technology

## 1 Introduction

With the rapid development of high-end railway, automobile, and offshore equipment manufacturing in China, painting operations as an indispensable process has also increased significantly [1]. The toxic substances generated during the coating operation are mainly composed of two parts: One is the suspended paint mist and paint powder, and the other is the exhaust gas generated by the paint, which mainly contains benzene, toluene, xylene, butyl acetate, and other toxic substances [2, 3].

---

B. Yang · J. Chen (✉) · Y. Sun · S. Zhou · W. Liu  
China Academy of Safety Science and Technology, Beijing 100029, China  
e-mail: [cjw3000@126.com](mailto:cjw3000@126.com)

L. Liu  
University of Science and Technology, No. 30 Xueyuan Road, Haidian District, Beijing 100083, China

However, the spraying operation in the painting workshop generally has a concentration of toxic substances such as toluene that exceeds the standard, which has a great impact on the health of spraying workers [4]. A reasonable and effective ventilation system is an effective way to discharge toxic substances in the painting workshop and reduce the concentration of toxic substances such as toluene. Displacement ventilation technology is a common ventilation method in large painting workshops [5].

## **2 Methods**

### ***2.1 Analysis of On-Site Investigation of Painting Workshop***

In this study, a field survey of a sub-painting shop of a shipyard was conducted. It can be seen that the toxic substances generated during the coating operation cannot be effectively discharged from the workshop, due to the large space of the painting shop, the painting operation position is not fixed, and the existing unreasonable design of ventilation system [6]. In order to improve the current situation of excessive concentrations of toxic substances such as toluene during the coating operation in the painting workshop, a reasonable and effective air flow organization was designed for the ventilation system of the painting workshop. By comparing and researching various ventilation methods, the section coating was obtained. The workshop should adopt displacement ventilation [7].

### ***2.2 Numerical Simulation Research Method of Displacement Ventilation***

#### **2.2.1 Establishment of Geometric Model of Displacement Ventilation in Painting Workshop**

Taking the painting workshop as an example, the geometric model of the painting workshop was established according to the field situation, and studying the air distribution and toluene diffusion in the workshop by using computational fluid numerical simulation [8].

When the replacement ventilation method is used in the painting workshop, due to the large building size of the workshop, excessive ventilation times will inevitably lead to the huge supply and exhaust system and waste of operating costs. According to the relevant design manual of spraying operation ventilation [9], it can be known that the number of air changes during spraying is controlled at about 6 times/h. At the same time, in order to make the painting workshop a slight negative pressure, the air supply volume of the workshop is determined by 90% of the exhaust air volume.

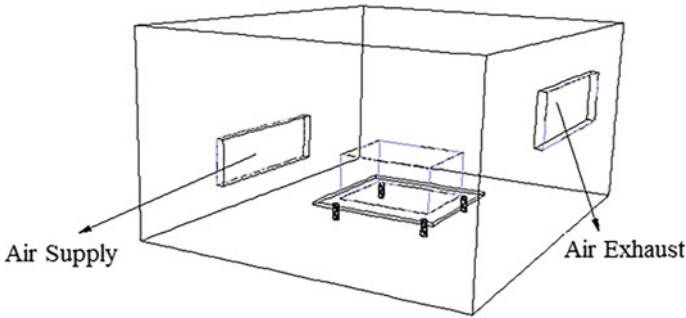


**Fig. 1** Geometric model of painting shop

Painting workshop size is 25 m in length  $\times$  20 m in width  $\times$  12 m in height [10], and the workshop volume is 6000 m<sup>3</sup>. The effective volume in the workshop is the workshop volume minus the bracket and work piece occupation in the workshop volume (about 500 m<sup>3</sup>), and the number of air changes in the workshop is 6 times/h, the hourly air change in the workshop must reach 33,000 m<sup>3</sup>. If the air supply volume of the painting workshop is not less than 33,000 m<sup>3</sup>/h, the air exhaust volume is 36,000 m<sup>3</sup>/h. When the paint shop adopts displacement ventilation, its geometric model is as shown in Fig. 1.

**2.2.2 Setting of Numerical Simulation Solving Parameters**

(1) Numerical Simulation Study on the Size of Air Supply and Exhaust Vents

When using displacement ventilation system, the air supply and exhaust vents in the workshop are simplified as square supply and exhaust vents, according to the size of the painting workshop and the workpiece to be sprayed. Under the condition of certain air supply and exhaust air volume, simulation study on the effects of different sizes of air supply and exhaust outlets on air distribution and poison diffusion in workshop [11, 12].

- ① Length and width of air supply and exhaust: 15 m  $\times$  1 m;
- ② Length and width of air supply and exhaust: 12 m  $\times$  2 m;
- ③ Length and width of air supply and exhaust: 10 m  $\times$  3 m.

The sides of the workpiece are set as the divergent source of toluene. The divergent state is the divergent source [13]. The boundary conditions are shown in Table 1.

(2) Numerical Simulation Study of Different Air Vent Positions

Based on the determination that the size of the replacement ventilation air supply and exhaust outlet is 10 m long  $\times$  3 m wide, the distribution of air flow in the workshop is simulated when three different arrangements of air supply and exhaust outlet are arranged.

**Table 1** Parameter setting of boundary conditions and solve

Boundary conditions	Define
Solver	Segregated
Viscous model	k-epsilon
Species model	Species transport
Reactions volumetric	Off
mixture-template	C <sub>7</sub> H <sub>8</sub> -Air mixture template
Inlet boundary type	Velocity inlet
Outlet boundary type	Velocity inlet
Inlet velocity magnitude (m/s)	① Air supply: 0.6; air exhaust: 0.67 ② Air supply: 0.4; air exhaust: 0.45 ③ Air supply: 0.35; air exhaust: 0.4
Hydraulic diameter (m)	① 2.18; ② 2.76; ③ 3.09
Turbulence intensity (%)	① 3.85; ② 3.94; ③ 3.95
Species mass fractions	C <sub>7</sub> H <sub>8</sub> 0.0001658

The geometric models of displacement ventilation with three different positions of air supply and exhaust vents are shown in Fig. 2.

The divergent surface source of toluene is set on the side of the workpiece to be sprayed, and the boundary conditions are shown in Table 2.

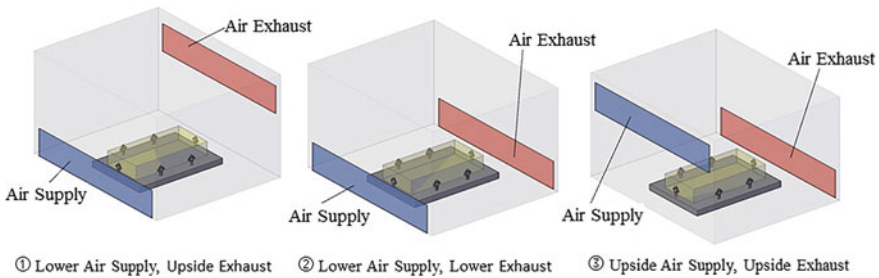


**Fig. 2** Layout of different air supply and exhaust vents in the painting workshop

**Table 2** Parameter setting of boundary conditions

Boundary conditions	Define
Inlet boundary type	Velocity inlet
Inlet velocity magnitude (m/s)	③ Air supply: 0.35; air exhaust: 0.4
Hydraulic diameter (m)	3.09
Turbulence intensity (%)	3.95

### 3 Result

#### 3.1 Analysis of Numerical Simulation Research Results on the Size of Air Supply and Exhaust Vents

The velocity vector diagram and velocity cloud diagram of the flow field in the centre section of the painting workshop are obtained through simulation as shown in Fig. 3. The mass fraction of toluene and the mass fraction of toluene in the breathing zone of spray painters are shown in Fig. 4.

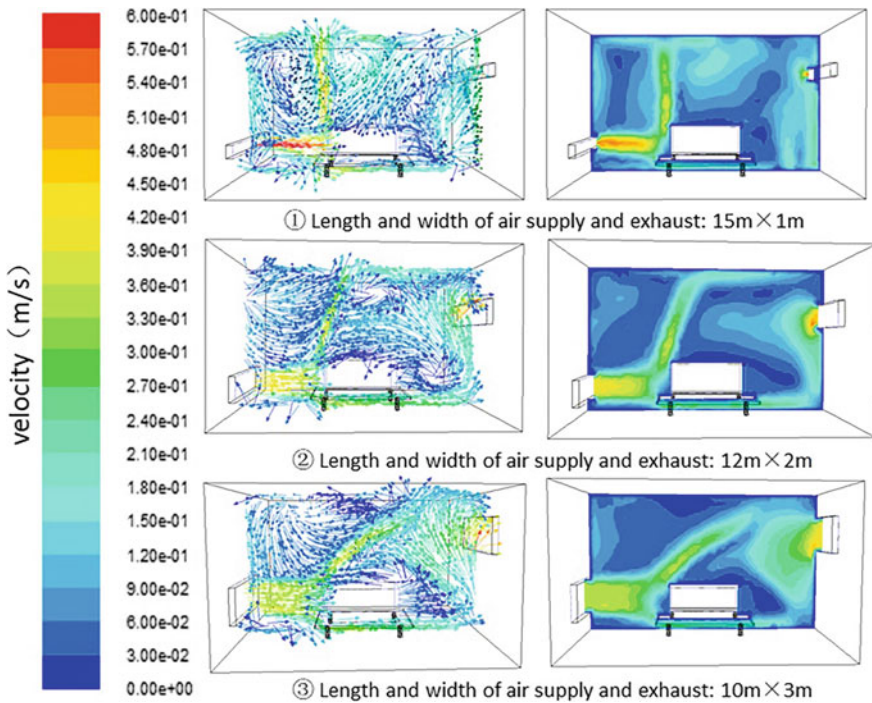


Fig. 3 Airflow organization in the workshop when the air supply and exhaust of different sizes

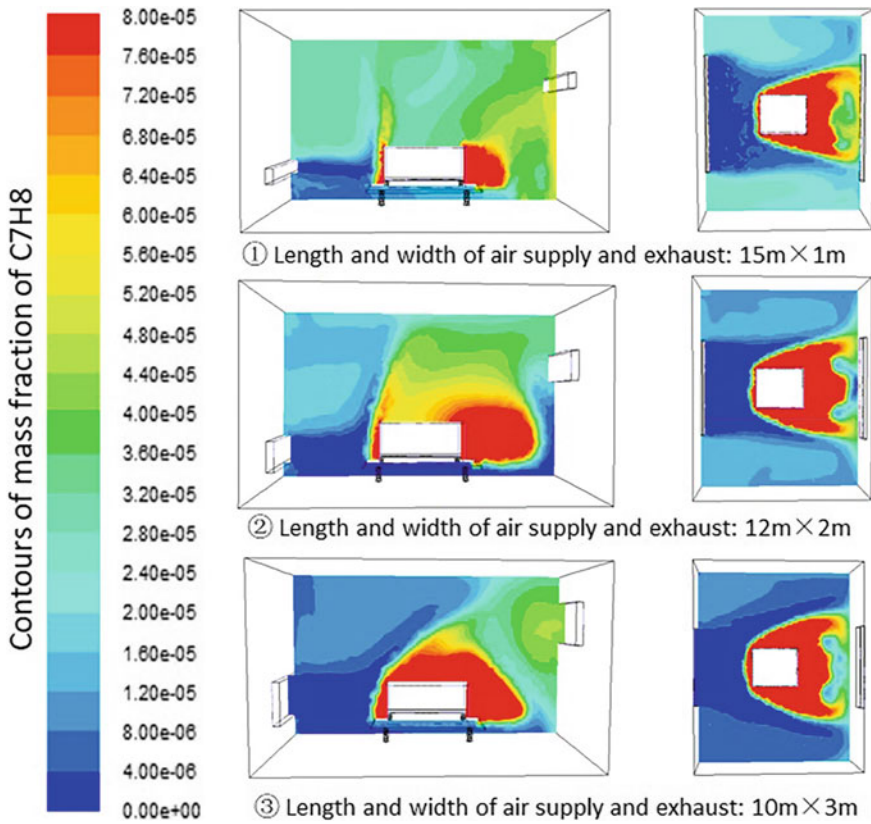


Fig. 4 Contours of mass fraction of C<sub>7</sub>H<sub>8</sub> when the air supply and exhaust of different sizes

It can be seen from the above figure that as the width of the air supply and exhaust vents increases, the mass fraction of toluene gradually decreases. When the size of the air supply and exhaust vents is 10 m long × 3 m wide, the control effect of toxic substances is the best.

### 3.2 Analysis of Numerical Simulation Research Results of Different Air Vent Positions

The simulation results are shown in Figs. 5 and 6.

As can be seen from the above figure, when the positions of the air supply and exhaust vents are located below, the airflow organization in the workshop has the best effect and the toxic substance discharge effect is the best.

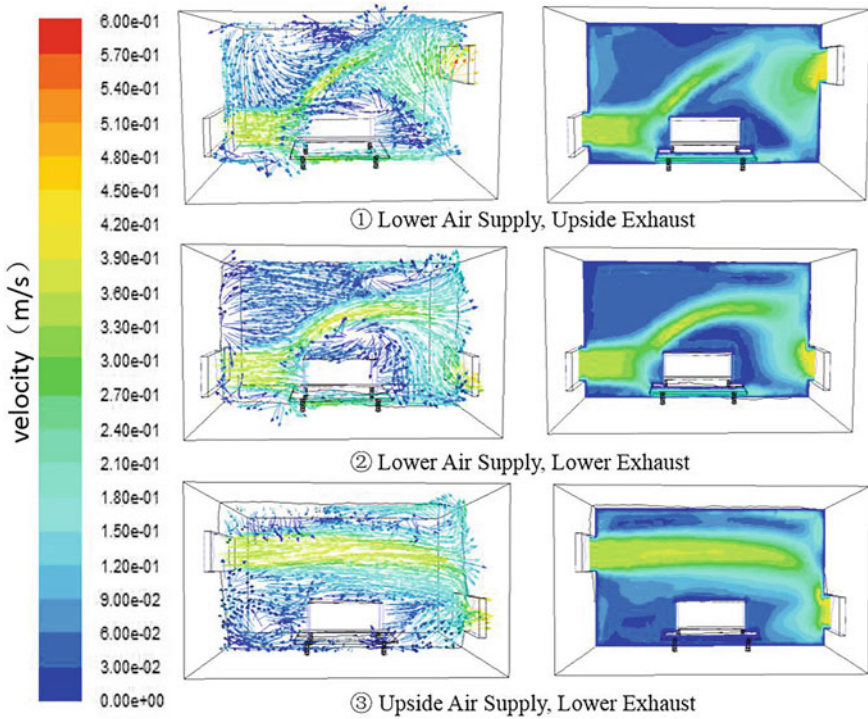
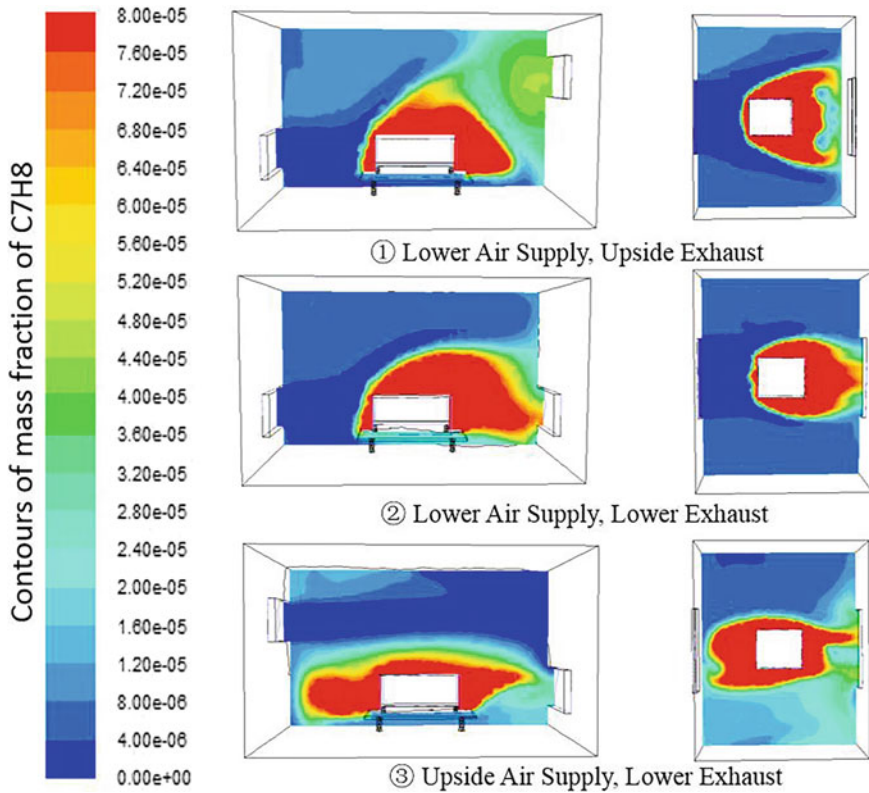


Fig. 5 Airflow organization in the workshop when layout of different air supply and exhaust

## 4 Conclusions

When large-scale coating workshops use displacement ventilation, the length and width of the supply and exhaust vents should be larger than the length and width of the work piece to be sprayed at the same time, so that the supply air flow can be completely cover toxic substances from spraying operations. When the arrangement of the air supply vents and the air exhaust vents is arranged in the form of the air supply and exhaust vents for the lower and lower rows, the air flow in the workshop can be effectively organized, and the toxic substances are discharged from the workshop.





**Fig. 6** Contours of mass fraction of  $C_7H_8$  when layout of different air supply and exhaust

**Acknowledgements** This work was funded by the National key R&D Program of China (2016YFC0801700) and the basic research funding of China Academy of Safety Science and Technology (2019JBKY11 and 2019JBKY04).

## References

1. Li X, Su S, Ya X et al (2013) Analysis of occupational hazard risks and protective measures in shipbuilding industry. *China Work Safety Sci Technol* 9(3):87–93
2. Yang W (2012) Identification and analysis of occupational hazards in shipyards. *China Work Safety Sci Technol* 8(6):178–182
3. Yang B, Hu P, Chen J et al (2019) Research on numerical simulation of push-pull ventilation system exhaust effect in a painting workshop of a shipyard in Tianjin. *Occup Health* 8(15):2020–2024
4. Li X, Song X et al (2016) Occupational hygiene site survey in a paint shop of a shipyard. *Chin J Industrial Med* 29(6):440–441
5. Hu W, Liu C, Zhao X et al (2012) Ventilation status and plan analysis of island shipyard. *China Water Transp* 12(1):225–226

6. Chen J, Yang B, Liang S et al (2018) Study on the performances of supply air for uniform air supply square hood by numerical simulation. *Man-Machine-Environ Syst Eng* 456:449–455
7. Chen J, Liu C et al (2005) A new method for controlling paint fog in tall space painting operation environment. *HVAC* 10:111–113
8. Dong Y, Qu S, Wang H et al (2003) CFD simulation of air conditioning airflow in tall and large buildings. *J Hebei Inst Arch Sci Technol* 3:23–27
9. Zhang D, Wang C (2010) Dust removal engineering design manual. Chemical Industry Press, Beijing, pp 129–150
10. Chen J, Jiang Z, Yang B et al (2012) Numerical simulation of spatial distribution of dust concentration in broken chamber. *J China Coal Soc* 37(11):1865–1870
11. Wang F (2004) Computational fluid dynamics analysis. Tsinghua University Press, Beijing, pp 205–206
12. Hang Z, Wang J, Lan X et al (2004) Fluent fluid engineering simulation calculation example and application. Beijing Institute of Technology Press, Beijing, pp 260–271
13. Tang Jiapeng (2016) ANSYS FLUENT super study manual. People Post Press, Beijing, pp 395–404

# Application of Comprehensive Preference and Fuzzy Mathematics Method in Sensory Evaluation of Ready-to-Eat Meatballs



Ruoyong Wang, Huiling Mu, Peng Du, Ximeng Chen, Peng Liu, and Shuang Bai

**Abstract** *Objective*—This paper verifies a sensory evaluation method that adds fuzzy mathematical evaluation on the basis of preference evaluation. *Methods*—Four kinds of ready-to-eat meatballs with different flavors were used as sensory evaluation objects. Based on the preference evaluation, fuzzy mathematics was added to evaluate the sensory quality of meatballs. *Results*—The results showed that among the four kinds of ready-to-eat meatballs, cumin meatballs, beef meatballs, onion meatballs and spicy meatballs ranked in order of popularity. *Conclusions*—On the basis of preference evaluation, fuzzy mathematical method can be added to improve the objectivity of food sensory evaluation.

**Keywords** Fuzzy mathematics method · Sensory evaluation · Ready-to-eat meatballs

## 1 Introduction

In order to judge the palatability of military food, scholars have proposed many methods. The evaluation method specified by the current Chinese military standards is the Preference Method: Tasters score samples (9-point scale) according to their preferences and use the arithmetic average of the score to determine the palatability of the samples. From a statistical point of view, the score given by the taster is a discrete variable, and the discrete variable is often used for analysis after being transformed into a continuous variable. The act of calculating the arithmetic mean is equivalent to upgrading the low-level statistics and does not meet the statistical norms. The fuzzy

---

R. Wang (✉) · H. Mu · P. Du · X. Chen · P. Liu · S. Bai (✉)  
Air Force Medical Center of FMMU, Beijing 100142, China  
e-mail: [wryafmcfmmu@163.com](mailto:wryafmcfmmu@163.com)

S. Bai  
e-mail: [b17s@163.com](mailto:b17s@163.com)

mathematical method can abstract scores and establish a more ideal evaluation mode through membership degree and membership function theory. The biggest advantage of the fuzzy mathematical method is that it can mathematically complex and unclear factors, but it also has disadvantages such as computational complexity [3, 6]. This article attempts to comprehensively and objectively evaluate ready-to-eat meatballs by comprehensively using the above two methods.

## **2 Materials and Methods**

### ***2.1 Main Raw and Auxiliary Materials***

Chicken, beef, surimi, onion, cumin, edible modified starch, edible salt, edible spice, compound seasoning, water. Raw materials are made by cooking and seasoning.

### ***2.2 Groups Participating in Taste Evaluation and the Method***

90 male volunteers participated in the evaluation of instant meatballs with an average age of  $33.03 \pm 4.20$  years. 90 evaluation forms were issued, 90 were recovered and 81 were valid. The design of the evaluation form is based on the requirements of the military food evaluation method (JXUB 6-96) issued by the military supplies Department of the General Logistics Department of the Chinese PLA. Divide the Color, Shape, Smell, Texture, Taste, Convenience into 9 levels and write a questionnaire (1—dislike extremely, 2—dislike very much, 3—dislike moderately, 4—dislike slightly, 5—neither like nor dislike, 6—like slightly, 7—like moderately, 8—like very much, 9—like extremely) were set according to personal preference (Do not like it). After evaluating the samples, collect the evaluation table and make a statistical analysis. The evaluators shall not smoke or drink coffee within 60 min before the evaluation and analysis and shall not drink spicy or other stimulating food within 12 h. Before and after tasting each sample, they should rinse with water and evaluate the next sample every 8 min.

### ***2.3 The Establishment of Fuzzy Mathematical Model***

Taking color, shape, smell, texture, taste and convenience as the factor set, adopting the 9-point system, the more you like, the higher the score. According to the evaluation results of liking degree, nine single factor evaluation matrixes are established and analyzed by fuzzy mathematics evaluation method. 9—extremely like, 8—very

like, 7—like, 6—a little like, 5—general, 4—less like, 3—not like, 2—very dislike and 1—extremely dislike.

### 2.3.1 Determine the Evaluation Field

The evaluation domain refers to a set of indicators that can best reflect the quality of the food, which is  $U = \{U_1, u_2, U_3 \dots U_N\}$ ;  $U$  is the corresponding evaluation index. In this paper, the color, shape, smell, texture, taste and convenience of meatballs are selected as sensory evaluation indexes. Therefore,  $U_1$  can be used to represent color,  $U_2$  to represent shape,  $U_3$  to represent smell,  $U_4$  to represent texture,  $U_5$  to represent the taste and  $U_6$  to represent convenience. An evaluation domain  $U = \{U_1, U_2, U_3, U_4, U_5, U_6\}$  on meatballs is obtained. Sensory quality index set:  $U = [\text{color} < U_1 >, \text{shape} < U_2 >, \text{smell} < U_3 >, \text{texture} < U_4 >, \text{taste} < U_5 >, \text{convenience} < U_6 >]$ .

### 2.3.2 Determine the Comment Field

The evaluation field is the collection of feedback information of the participants in the evaluation indexes. The evaluation can be expressed in words, or in specific values or grades, as follows:  $V = \{V_1, V_2, V_3 \dots V_n\}$ ,  $v$  represents the corresponding rating or score. According to the quality rating standard stipulated in jxub6-96 “military food evaluation method,” an evaluation field of ready-to-eat meatballs is obtained:  $V = \{v_9, v_8, v_7, v_6, v_5, v_4, v_3, v_2, v_1\}$ .

### 2.3.3 Determine the Weight Vector and the Weight Assignment

According to the weight of each index of meatballs, the weight vector related to ready-to-eat meatballs is 20 points for color, 15 points for shape, 20 points for smell, 20 points for texture, 15 points for taste, 20 points for convenience, a total of 100 points, and the weight set is written as a fuzzy vector  $X (0.10, 0.15, 0.20, 0.20, 0.15, 0.20)$ .

## 3 Results and Analysis

### 3.1 Determine the Fuzzy Evaluation Matrix

The evaluators' evaluation results of six different kinds of meatballs are shown in Table 2.

### 3.2 Fuzzy Judgment Matrix

Divide the data in Table 1 by the total number of reviewers and get six fuzzy evaluation matrices (Table 2).

**Table 1** Sensory evaluation standard of ready-to-eat meatballs

Items	Scoring criteria	Preference	Scores
Color	Gray white, uniform and consistent color	Like ~ like extremely	7 ~ 9
	Gray white, uneven color	Less like ~ a little like	4 ~ 6
	Browning or yellowing, abnormal	Dislike extremely ~ dislike moderately	1 ~ 3
Shape	Moderate size, even, smooth surface, round	Like ~ like extremely	7 ~ 9
	Slightly different size, smooth and round surface	Less like ~ a little like	4 ~ 6
	Uneven size, potholes on the surface, not round	Dislike extremely ~ dislike moderately	1 ~ 3
Smell	With the flavor of meatballs	Like ~ like extremely	7 ~ 9
	It is light and fragrant	Less like ~ a little like	4 ~ 6
	Bad taste, even abnormal taste	Dislike extremely ~ dislike moderately	1 ~ 3
Texture	The section is full of even and small pores, with good chewing elasticity	Like ~ like extremely	7 ~ 9
	There are some larger pores on the section, and the chewing elasticity is general	Less like ~ a little like	4 ~ 6
	There are large pores on the cutting surface, and the chewing is inelastic	Dislike extremely ~ dislike moderately	1 ~ 3
Taste	It has the fresh taste of pork	Like ~ like extremely	7 ~ 9
	The taste is normal. The taste is not strong enough. It is average	Less like ~ a little like	4 ~ 6
	The smell of meat is heavy	Dislike extremely ~ dislike moderately	1 ~ 3
Convenience	The package is easy to tear and easy to eat with regular edges	Like ~ like extremely	7 ~ 9
	The package is easy to tear, and the edge is regular. It can only be eaten with proper force	Less like ~ a little like	4 ~ 6
	The package is difficult to tear, and the edge is irregular. It needs to be repeatedly squeezed to eat	Dislike extremely ~ dislike moderately	1 ~ 3

**Table 2** Evaluators' evaluation results of six different kinds of meatballs

Products	Items	Scores								
		9	8	7	6	5	4	3	2	1
Scallion rice meatballs <i>n</i> = 79	Color (U1)	10	26	21	12	8	1	1	0	0
	Shape (U2)	16	20	19	14	9	0	1	0	0
	Smell (U3)	9	16	27	16	9	1	1	0	0
	Texture (U4)	12	21	19	14	8	4	1	0	0
	Taste (U5)	10	24	21	12	8	2	2	0	0
	Convenience (U6)	17	25	22	4	7	1	1	0	0
Cumin rice meatballs <i>n</i> = 81	Color (U1)	19	20	19	12	9	2	0	0	0
	Shape (U2)	20	19	23	8	9	2	0	0	0
	Smell (U3)	15	21	23	13	8	1	0	0	0
	Texture (U4)	19	21	21	8	8	4	0	0	0
	Taste (U5)	17	20	25	10	5	4	0	0	0
	Convenience (U6)	20	25	20	3	9	1	0	0	0
Beef meatballs <i>n</i> = 80	Color (U1)	14	28	13	17	8	0	0	0	0
	Shape (U2)	20	21	17	11	10	1	0	0	0
	Smell (U3)	12	22	27	8	8	1	2	0	0
	Texture (U4)	15	24	20	11	8	2	0	0	0
	Taste (U5)	15	17	26	10	9	2	0	0	0
	Convenience (U6)	21	26	19	6	6	1	0	0	0
Spicy rice meat meatballs <i>n</i> = 80	Color (U1)	10	26	22	12	9	1	0	0	0
	Shape (U2)	15	23	19	11	11	1	0	0	0
	Smell (U3)	9	16	28	15	8	4	0	0	0
	Texture (U4)	11	17	29	11	8	3	1	0	0
	Taste (U5)	9	14	27	18	9	2	1	0	0
	Convenience (U6)	18	25	19	6	9	1	0	0	0

$R_1 = (r_{ij})_{6 \times 9} =$	0.160	0.369	0.261	0.128	0.071	0.007	0.005	0	0
	0.253	0.281	0.234	0.148	0.079	0	0.005	0	0
	0.148	0.234	0.346	0.176	0.082	0.007	0.005	0	0
	0.196	0.304	0.241	0.152	0.072	0.029	0.005	0	0
	0.162	0.346	0.265	0.130	0.072	0.014	0.011	0	0
	0.267	0.349	0.269	0.042	0.061	0.007	0.005	0	0
$R_2 = (r_{ij})_{6 \times 9} =$	0.290	0.272	0.226	0.122	0.076	0.014	0	0	0
	0.303	0.256	0.271	0.081	0.076	0.013	0	0	0
	0.230	0.287	0.275	0.133	0.068	0.007	0	0	0

(continued)

(continued)

	0.290	0.285	0.249	0.081	0.068	0.027	0	0	0
	0.260	0.272	0.297	0.102	0.042	0.027	0	0	0
	0.307	0.341	0.239	0.031	0.077	0.007	0	0	0
$R_3 = (r_{ij})_{6 \times 9} =$	0.216	0.384	0.156	0.175	0.069	0	0	0	0
	0.307	0.286	0.203	0.112	0.085	0.007	0	0	0
	0.189	0.308	0.331	0.084	0.070	0.007	0.011	0	0
	0.232	0.330	0.241	0.114	0.069	0.014	0	0	0
	0.239	0.240	0.322	0.106	0.080	0.014	0	0	0
	0.315	0.347	0.222	0.060	0.050	0.007	0	0	0
$R_4 = (r_{ij})_{6 \times 9} =$	0.157	0.363	0.269	0.126	0.079	0.007	0	0	0
	0.234	0.319	0.231	0.114	0.095	0.007	0	0	0
	0.147	0.232	0.356	0.163	0.073	0.029	0	0	0
	0.177	0.243	0.363	0.118	0.072	0.021	0.005	0	0
	0.148	0.205	0.346	0.198	0.082	0.015	0.005	0	0
	0.279	0.345	0.229	0.062	0.078	0.007	0	0	0

$r_{ij}$  indicates the degree of subordination of each evaluation index of meatball to the evaluation result of this index.

### 3.3 Calculate the Comprehensive Membership

According to the standard mathematical model principle of fuzzy comprehensive evaluation, the evaluation result vector  $Y = X \cdot R$  is obtained by taking the large and taking the small algorithm. This method will bring errors to the evaluation result, which can be avoided by replacing the large and taking the small algorithm with the ordinary matrix multiplication and calculating the comprehensive score according to the comprehensive scoring formula [1, 2, 4, 5]. The comprehensive membership degree of the sample pairs of all types calculated by matrix multiplication is  $Y = X \cdot R = (b_1, b_2, b_3 \dots)$ . The result vector of comprehensive evaluation of sensory quality of ready-to-eat meatballs is as follows:  $Y = X \cdot R = (0.10, 0.15, 0.20, 0.20, 0.15, 0.20)$ .

$Y = X \cdot R = (0.10, 0.15, 0.20, 0.20, 0.15, 0.20)$	0.160	0.369	0.261	0.128	0.071	0.007	0.005	0	0
	0.253	0.281	0.234	0.148	0.079	0	0.005	0	0
	0.148	0.234	0.346	0.176	0.082	0.007	0.005	0	0
	0.196	0.304	0.241	0.152	0.072	0.029	0.005	0	0

where  $y_{11} = 0.10 \times 0.160 + 0.15 \times 0.253 + 0.20 \times 0.148 + 0.20 \times 196 + 0.15 \times 0.162 + 0.20 \times 0.267 = 0.279$ ,  $y_{12} = 0.10 \times 0.369 + 0.15 \times 0.281 + 0.20 \times 0.243 + 0.20 \times 304 + 0.15 \times 0.346 + 0.20 \times 0.349 = 0.289$ . Similarly,  $y_{13} =$



0.260,  $y_{14} = 0.089$ ,  $y_{15} = 0.068$ ,  $y_{16} = 0.016$ ,  $y_{17} = 0$ ,  $y_{18} = 0$ ,  $y_{19} = 0$ . That is,  $Y_1 = \{0.279 \ 0.289 \ 0.260 \ 0.089 \ 0.068 \ 0.016 \ 0 \ 0 \ 0\}$ .

The same can be:

$Y_1 =$	{	0.279	0.289	0.260	0.089	0.068	0.016	0	0	0	}
$Y_2 =$	{	0.251	0.314	0.253	0.102	0.069	0.009	0.002	0	0	}
$Y_3 =$	{	0.200	0.309	0.272	0.128	0.073	0.012	0.006	0	0	}
$Y_4 =$	{	0.194	0.279	0.303	0.128	0.079	0.015	0.002	0	0	}

### 3.4 The Comprehensive Score

According to the comprehensive scoring formula:

$$H = \sum_{j=1}^n j b$$

The comprehensive score of each sample is calculated:  $H_1 = 9 \times 0.279 + 8 \times 0.289 + 7 \times 0.260 + 6 \times 0.089 + 5 \times 0.068 + 4 \times 0.016 + 3 \times 0 + 2 \times 0 + 1 \times 0 = 7.38$ . Similarly,  $H_2 = 7.58$ ,  $H_3 = 7.54$ ,  $H_4 = 7.33$ ,  $H_5 = 7.07$ ,  $H_6 = 7.03$ . The comprehensive score of no. 1 ready-to-eat meatball is between 7 and 8 and 7, indicating that the meatball is between like and very like. The comprehensive score of no. 2 meatball is between 7 and 8, indicating that the meatball is between like and like very much. The comprehensive score of no. 3 meatball is between 7 and 8, indicating that the meatball is between like and like very much. The comprehensive score of no. 4 meatball is between 7 and 8 and 7, indicating that the meatball is between like and very like. The comprehensive score of no. 5 meatball is between 7 and 8, and the comprehensive score of no. 6 meatball is between 7 and 8 and 7, indicating that the meatball is between like and very like.

## 4 Discussion

Sensory analysis of food is a scientific method, which means to analyze the food characteristics obtained by subjects, relying on vision, smell, taste and hearing. It is based on modern experimental science, sociology, physiology, psychology and statistics. Using the method of food sensory evaluation, researchers can solve the complex physiological feeling problems which cannot be solved by the usual physical and chemical analysis and provide the basis for the production management and quality control of products. The comprehensive evaluation method of fuzzy mathematics can abstract the relationship between various factors that affect the sensory

quality of food and establish an ideal evaluation model through the membership degree and membership function theory of fuzzy mathematics. The quality of meatballs is complex. Only by combining the three indexes of nutrition, hygiene and sensory quality can the quality of Meatballs be judged completely. This study not only fully absorbed the personal preference evaluation, but also used the method of fuzzy mathematics to evaluate the sensory characteristics of related products. It is of great significance to purchase military food, improve its acceptability and effectively guarantee military operations. The research object of this paper is instant meatball, which is its outstanding characteristic. Therefore, this paper takes convenience as an important index and gives convenience a higher weight. The emphasis on convenience reflects even the military use of meatballs. Szaesniak et al. showed that only the maximum similarity between texture parameters and sensory evaluation indicators can ensure that the experimental error and subjective error are within the acceptable range. In this study, if the electronic sensory evaluation equipment is added to obtain objective, quantitative parameters, the evaluation error caused by human factors and the irrationality of standard algorithm in the sensory evaluation process will be avoided which is also the direction of military food research in the next step.

**Compliance with Ethical Standards** The study was approved by the Logistics Department for Civilian Ethics Committee of Air Force Medical Center of Fourth Military Medical University. All subjects who participated in the ex-parliament were provided with and signed an informed consent form. All relevant ethical safeguards have been met with regard to subject protection.

## References

1. Fengqin Z, Shuzhen Z, Heyuan Z (1998) Fuzzy evaluation method of food sensous quality. *J Shenyang Agric Univ* 04:63–65
2. Lawless HY, Heymann H (2010) Sensory evaluation of food: principles and practices. Springer Science & Business Media, New York
3. Shengkun J, Yong L (2011) Fuzzy comprehensive evaluation applied in food sensory evaluation. *Meat Res* 25(01):64–67
4. Yongyi W, Chaomin L (2013) Study on preference assessment of vinegar. *China Condiment* 38(11):7–9
5. Yuhong X, Geng Z (2009) Application of fuzzy comprehensive evaluation in oil sensory analysis. *China Oil Fats* 34(08):72–74
6. Yuzhen L, Huaiqiu X (2016) Application of fuzzy mathematical evaluation method in food sensory evaluation. *China Brewing* 35(05):16–19

# Research on STK-Based 3D Model Transformation and Optimization



Kunfu Wang, Wanfeng Mao, Wei Feng, Jian Su, Xing Li, and Peng Zhang

**Abstract** It is necessary to establish a 3D model with vivid effects in order to improve human–computer interaction (HCI) efficiency in the field of operation simulation. Based on the particularity of the 3D model format in the Satellite Tool Kit (STK)/VO module, this paper analyzes the data structure of the STK 3D model, describes how to directly acquire the model in MDL format, and analyzes its shortcomings and deficiencies. Taking the common 3D modeling software 3DMax as an example, this paper focuses on the description of how to transform 3D models in different formats into MDL models and subsequently forms a model solution for STK software to achieve high complexity, streamlined structure data, and vivid lighting effects during mission simulation, including the model transformation process, geometry data optimization of the model, and optimization solutions in model transformation. Practice has proven that the proposed method offers effective optimization and more vivid effects and can greatly improve the efficiency and effectiveness of HCI.

**Keywords** 3DMax · 3D model · MDL model · STK · Model optimization · Human–computer interaction (HCI)

## 1 Introduction

Man-Machine-Environment System Engineering is a science that uses system science theory and system engineering methods to correctly handle the relationships between the three major elements of humans, computers and environment and deeply study the optimal combination of human–computer–environment systems [1]. Human–computer interaction (HCI) is an essential part of human–computer–environment

---

K. Wang (✉) · W. Mao · W. Feng · J. Su · X. Li · P. Zhang  
System Engineering Research Institute of China State Shipbuilding Corporation,  
100094 Beijing, China  
e-mail: [wangkunfu1166@163.com](mailto:wangkunfu1166@163.com)

© The Editor(s) (if applicable) and The Author(s), under exclusive license to Springer Nature Singapore Pte Ltd. 2021  
S. Long and B. S. Dhillon (eds.), *Man-Machine-Environment System Engineering*, Lecture Notes in Electrical Engineering 645,  
[https://doi.org/10.1007/978-981-15-6978-4\\_46](https://doi.org/10.1007/978-981-15-6978-4_46)

system engineering. Therefore, optimizing and improving the 3D model are important ways to improve HCI. With high-tech development, computer simulation technology has been rapidly promoted worldwide. Satellite Tool Kit (STK), the world's leading satellite simulation software produced by the AGI company (US) [2], has been expanded from providing full-cycle simulation support in the field of aerospace to the simulation analysis of electronic warfare operation in all areas, land, sea, and air [3], including radar, sensors, jammers, and communication equipment. It also provides a high-precision visualization simulation module which offers high-fidelity visualization support.

As one of the most important functional modules in STK, the visualization module (STK/VO) enables users to accurately observe the whole process of mission execution during mission simulation [4]. MDE is a 3D model editing tool provided by the VO module. The easiest way to build a 3D model is to directly obtain the model in MDL format, that is, modify the existing model file. The editing may be completed by using a standard text editor [4]. All 3D model files are standard ASCII files with the extension name \*.mdl.

However, the 3D model generated by this \*.mdl ASCII code editing mode has the following deficiencies:

1. Difficulty in making complex 3D models such as vehicles, equipment, and characters, and low production efficiency;
2. Difficulty in calibrating the mapping coordinates of heterogeneous models to the 3D geometry data;
3. Difficulty in achieving a balance between the data optimization of simulation 3D models, the accurate performance of its own structure, and the true indication of details; this is because STK simulation software needs to perform real-time calculations on the data which requires streamlined 3D model data;
4. Relatively dull lighting effects, making the \*.mdl model deficient for the development of simulation software with high fidelity and immersion, and the pursuit of HCI.

Therefore, for the above problems with the STK simulation model, such common 3D modeling software as Maya, Rhino, 3DMax, Softimage, LightWave, and even AutoCAD may be used to achieve production transformation and subsequently improve production efficiency and lighting effects [5]. 3DMax, which is very versatile, rich in plug-ins, easy to learn, and has a large number of application staff, is taken as an example in this paper to describe how to produce and transform in order to achieve a model in \*.mdl format.

## 2 STK 3D Model Analysis

The created new 3D model file must conform to the standards and formats defined by STK. A file in \*.mdl format has a hierarchical structure, including body with certain parameters and component formed through Refer [6].

The geometry data of a solid model contains the solid material parameters, solid texture types, model and texture coordinates, and vertex description of topological surfaces.

An object is composed of several basic model element components (Component) [7], and its composition is mainly formed by Refer syntax commands which can form multiple combination levels.

After mastering the construction syntax of the \*.mdl model, the transformations of objects can add joint control parameters to modify model components and make adjustments such as position movement, size scaling, and direction rotation [8].

### 3 MDL Model Transformation Process and Optimization

There is a large number of 3D models in MDL format on the Web site and software of STK, which basically cover land, sea, air, and space object models such as typical air, land, misc, missiles, sea, and space. Each category contains some common physical models, such as the Fengyun (FY) satellite model and Long March series rocket model. New models are also released on the official Web site of STK for users to adopt to meet their simulation needs. In addition, STK-related technical forums also provide models for users to download. However, some domestic rocket models found in the model library are not sufficient to meet the needs of STK 3D mission simulation.

#### 3.1 Model Transformation Process

It is often necessary to transform general 3D models to \*.mdl models in specific applications. STK is equipped with the special transformation tool LwCovert.exe, which is mainly used to transform 3D models in \*.lwo format into \*.mdl format (Fig. 1).

An \*.lwo model is the standard format of LightWave 3D production software. The transformation software DeepExploration may be used to transform 3D models in other formats (\* 0.3ds, \*.dae, and \*.obj) into \*.lwo format.

The transformation process is shown below (Fig. 2).

#### 3.2 Model Geometry Data Optimization

STK software is mainly based on simulation calculations and requires streamlined data. Due to large amount of data in a 3D model, it is necessary to weigh and control the accuracy of the model and the effect of the details. The software advantages of 3DMax can be utilized to make high-precision models with baked textures and

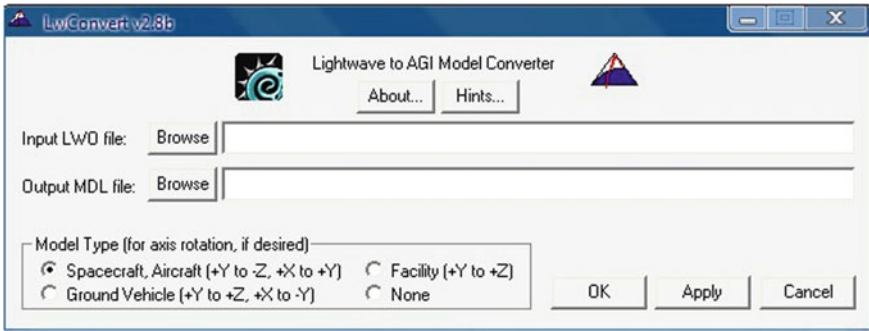


Fig. 1 Model transformation software LwConvert.exe

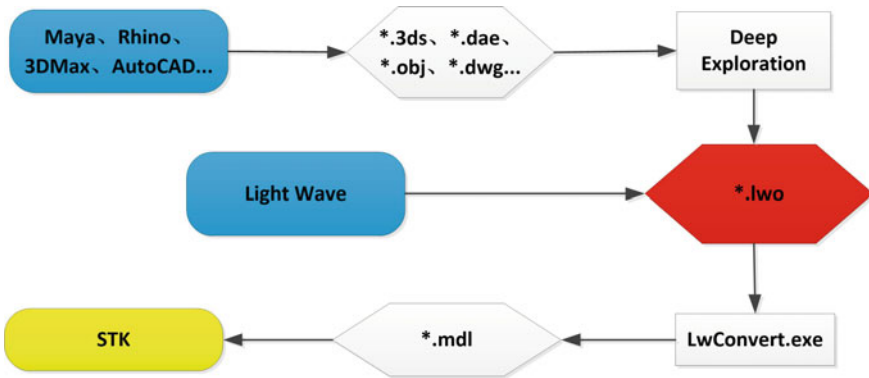


Fig. 2 Model transform process

reprint streamlined models with sufficient details and a reduced amount of model data (Fig. 3).

Meanwhile, the skylight or rendering plug-in in 3DSMax may be used to simulate natural lighting effects, and details may be subsequently added via image processing software to obtain a 3D model with vivid effects, optimized data, and rich details,

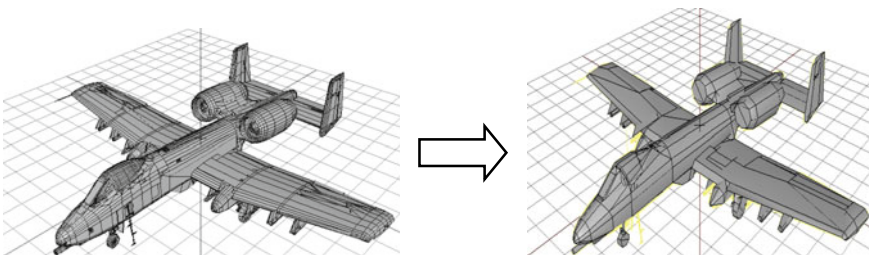


Fig. 3 Model refinement optimization

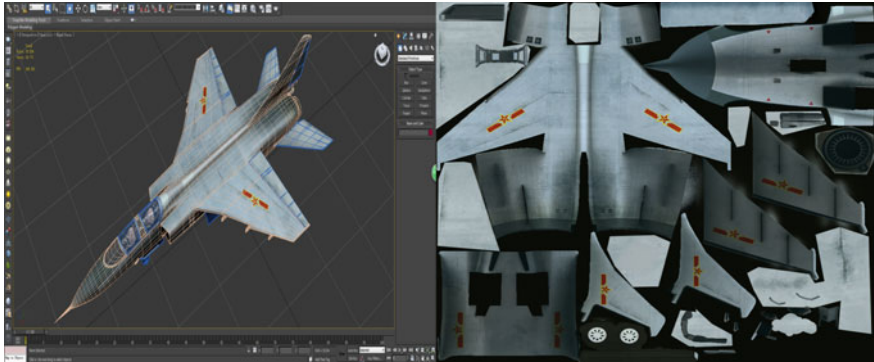


Fig. 4 Model texture instance

laying the foundation for the model in \*.mdl format. Therefore, the data optimization of the model is mainly used in combination with control of the number of model faces and performance of texture details (Fig. 4).

### 3.3 Optimization Solutions in Model Transformation

- Necessity of model collapse

Many problems including disordered model data, UV mismatch, and coordinate axis displacement may occur after a 3D model is produced by 3DSMax software and transformed into \*.mdl format. This reason is that the Max model after multiple modification commands is usually recorded in the modifier stack and is not compatible during transformation. Therefore, the model must be set to XForm and collapse before being exported as \*.3DS or other formats.

- Smoothing group setting for surface models

Multiple different smoothing groups are required in some complex surface models, and these are separated as different elements in the 3DSMax model; in other words, models in different smoothing groups cannot share vertices. This can avoid the display error of lighting information in the same model in \*.mdl format.

- Component-level control relationship

The setting of multiple levels of link relationships in the \*.mdl model is also important and tedious. For example, controlling the movement of the vehicle transporter to the specified position, missile exit, nozzle orientation adjustment, and other control actions requires driving different component levels separately and forming a certain hierarchical link relationship for each component. In 3DSMax, the group command

may be used to conveniently implement this function. The group name and each object element form the layer in the \*.mdl statement. The components are used to form the link-nesting relationships between layers.

- Coordinate adjustment of models and components

In 3DsMax, the world coordinate system is used as the basis for constructing the three-dimensional space of the model, in which the X- and Y-axes represent the two-dimensional plane, and the Z-axis represents the height dimension. However, in an \*.mdl model running in an STK simulation, the space trajectory is based on the body coordinate system. The X-axis is forward along the longitudinal axis of the model, and rotation around the X-axis is Roll. The Y-axis is perpendicular to the X-axis in the symmetry plane of the model, and movement around the Y-axis is Yaw. The Z-axis and the other two axes form a right-handed coordinate system, and movement around the Z-axis is a Pitch. Therefore, before exporting a 3DsMax model, the orientation setting of its coordinate axis should be noted to set the corresponding transformation in the transformation tool LwCovert.exe.

In addition, during the production of a 3DsMax model, position points requiring joint control may be moved to the corresponding control points through adjust pivot under hierarchy. The joint control points of the non-collapsible group may move during transformation into an \*.mdl model. In this case, the translate command may be used to correct the situation after transformation (Fig. 5).

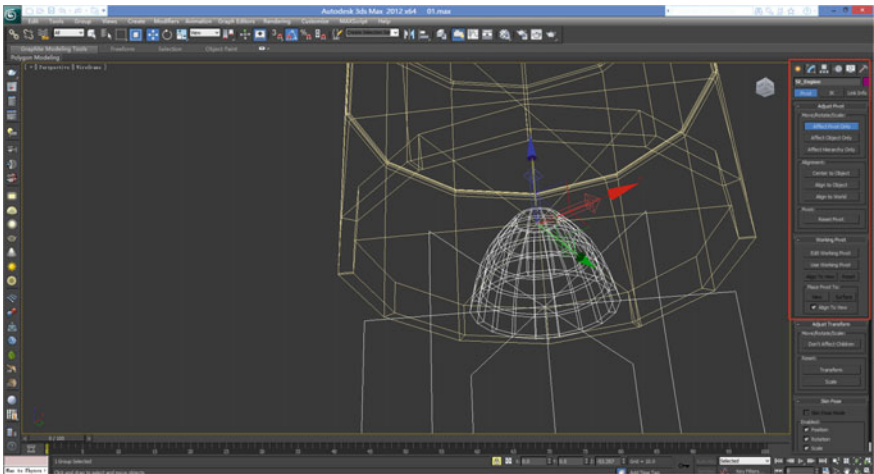


Fig. 5 Correction through translate command



- Setting of dynamic model tail flame

Joint control may be used to scale up and down some 3D models in STK, such as the tail flames of nozzles in missiles, aircraft, and rockets, and to simulate dynamic effects. However, the jet stream effect is not expressed. In this case, a multi-channel transparent hybrid mapping method of the texture may be used to achieve a dynamic jet effect by superimposing the multi-channel texture and dynamic control over the texture, including such commands as displacement and scaling. The transparent channel texture can be made into a two-sided continuous pattern by the image processing software Photoshop, with the seamless looping of dynamic effects during simulation driving (Fig. 6).

Some of the above solutions can be used to initially complete the transformation of most 3DsMax models into \*.mdl format and improve effect performance. Similarly, such related parameters as related materials and textures may be adjusted in DeepExploration during transformation to achieve more ideal effects.

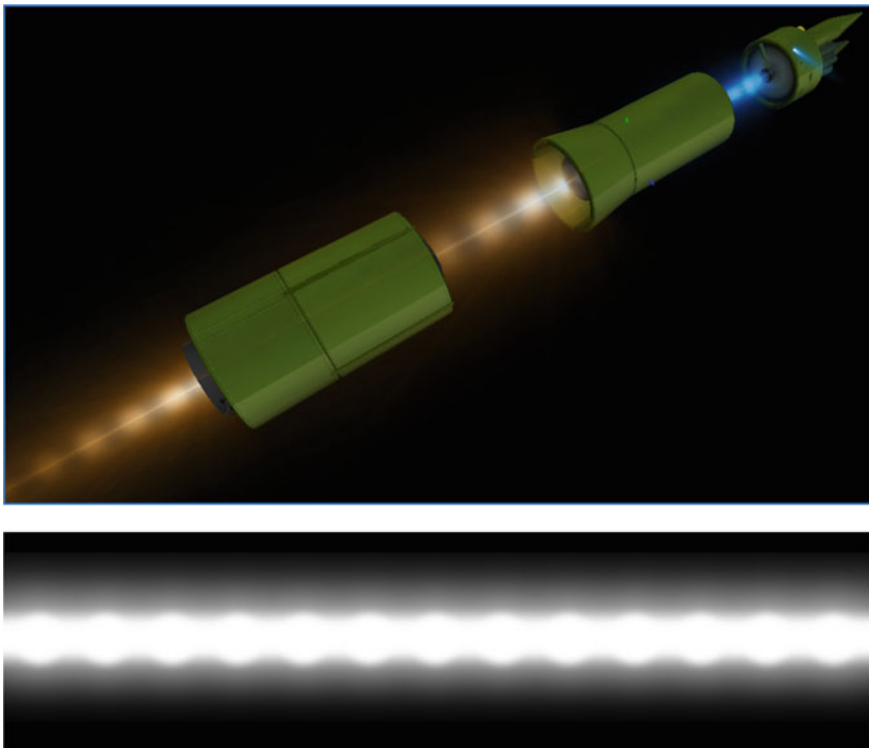


Fig. 6 Dynamic effect of tail flame

## 4 Conclusions

In one scenario, it is necessary to load a rocket fairing into a satellite model for demonstration. In this case, instead of creating a new model, one only needs to incorporate the existing satellite model file code into the rocket model file and adjust some of the offset rotation parameters of the components in the satellite model, to achieve model merging. The MDL model accompanied by STK is modified with the NumSides parameter value of cylinder. The display effects are further improved: The parameter values of the invisible part on the reverse side of the model are changed, solving the problem of some parts of the model being invisible on the reverse side. An action is assigned to the model: Steps are added to the satellite model in the STK model library in accordance with the action to expand the joint activity process in the component. Setting of special effects: the “Pointing” parameter is set in the model component to simulate the real-time effects of radar tracking targets. This application example proves that this method of model transformation and optimization is feasible, and the HCI effects are improved significantly.

With the wide application of simulation technology, the demand for the production of 3D models has also increased. A model in \*.mdl format is more complicated than 3D models on other software platforms such as visual display, virtual simulation, and simulation training with regard to process and solution. According to the exploration of these projects, the channels for making simulation models are broadened, the simulation display effects are improved, and the efficiency of HCI is effectively improved. It is believed that with the development of software technology, integrated and comprehensive applications will better solve these problems, such as file format upgrades, simulated skylight systems, and real-time reflection of lights, which will promote the software to a higher level and make it more convenient and effective.

## References

1. Shengzhao L (1993) Man-machine-environment system engineering theory and its significance in productivity development. Progress in man-machine-environment system engineering research, vol 01. Beijing Science and Technology Press, Beijing, pp 2–13
2. Gao J, Luo LJ, Format analysis and making of 3D model in STK software, Jiu Quan, Gan su 732750
3. Yao Y, Nian F, Zhang J (2013) PEI research on building and optimization methods for 3D STK models. J Spacecraft TT & C Technol 32(2):156–161
4. Fuchun NIAN, Jinbiao ZHOU, Jianwei HE (2012) Research on building and optimizing methods of STK 3D scenario. J Syst Simul 24(1):197–201
5. Du Z (2015) Application development based on STK Software Package. Software 36(4):102–106
6. Li Y, Jin G, Zhong X (2013) Modeling and simulation of visible light scattering properties of spatial object using STK. Chin J Space Sci 33(2):188–193
7. Jiang H, Ren H, Wu Z, Gao M (2014) STK-based modeling and simulation of communications link for reconnaissance platform and satellite. Comput Simul 31(11):51–55
8. Liu F, Liu C, Liu W, Liang D (2014) Space target sequence image simulation based on STK/matlab. Infrared Laser Eng 43(9):3157–3161

# Quality Control of Measuring for Head-Related Transfer Functions of Chinese Pilots



Xiaochao Guo, Qingfeng Liu, Yanyan Wang, Duanqin Xiong, Yu Bai, and Jian Du

**Abstract** A specified procedure was conducted for measuring HRTF database. The experimenters were trained to reduce the tester errors. Pilot as participator was sat in  $(x, y, z)$  coordinates with the origin at midpoint of bitracion on his Frankfurt plane same as polar coordinates of  $(r, \phi, \theta)$ , keeping his posture to reduce the testee errors during each block of the experiment. The test–retest checks were arranged at  $(\phi, 0^\circ)$ ,  $(\phi, 180^\circ)$  and  $(\phi, 360^\circ)$  for data quality control. Other strategies were done such as the division of the experiment into 13 blocks and schedules of rest by turns to reduce human errors from fatigue. Three testers were trained with dummy head MK2B, and 63 male pilots were measured in hemi-anechoic room to build CHNAF HRTF database. The results were found that the tester error was about 0.29 dB of ILD and  $-0.75^\circ$  azimuth deviation, the 2.0 dB of ILD was acceptable alarm threshold for binaural spatial symmetry because of pilots posture change, and the data quality of the CHNAF HRTF database was well validated.

**Keywords** Quality control · Measuring · Measurement · Data quality · Human error · Head-related transfer function (HRTF) · Head-related impulse response (HRIR) · Interaural level difference (ILD) · Spatial symmetry · Pilots · 3D audio · Ergonomics · Human factors · CHNAF HRTF database

## 1 Introduction

The head-related transfer function (HRTF) is the key to 3D audio displays. There are four popular methods to get HRTF that were experimental measurement method, mathematical modeling method, database matching method and subjective selection method [1]. The best way is acoustics measuring to get HRTF [2] since the measuring could obtain high accuracy of HRTF and make better HRTF database matching for personalization. But the standardized procedure is absent of the experimental measurement method [3]. It is found that the measurement errors were spectral

---

X. Guo · Q. Liu · Y. Wang (✉) · D. Xiong · Y. Bai · J. Du  
Air Force Medical Center of FMMU, 100142 Beijing, China  
e-mail: [wyytv@sohu.com](mailto:wyytv@sohu.com)

© The Editor(s) (if applicable) and The Author(s), under exclusive license to Springer Nature Singapore Pte Ltd. 2021  
S. Long and B. S. Dhillon (eds.), *Man-Machine-Environment System Engineering*, Lecture Notes in Electrical Engineering 645,  
[https://doi.org/10.1007/978-981-15-6978-4\\_47](https://doi.org/10.1007/978-981-15-6978-4_47)

magnitude variations up to 12.5 dB for frequency bands below 6 kHz and up to 23.0 dB above that as well as large spectral left/right asymmetries for high-frequency content with a Neumann KU-100 dummy head [4], and the errors could blur HRTF auditory localization and timbre perception [3] to make comparable localization performances between only 4 of 12 HRTF databases [5].

In development of CHNAF HRTF database [6], quality control was carried out to reduce human errors from both of the experimenter and the human subjects as presented in this paper.

## 2 Method

### 2.1 Training the Experimenters to Reduce the Tester Errors

All the experimenters should do exercises in a pre-test training to reduce the tester errors because who were responsible for sound source positioning in azimuth ( $\theta$ ) within same elevation ( $\phi$ ) manually during one turn of test and putting DPA 4060-BM microphones correctly into bi-ears of pilots [6].

The pre-test training was worked on standard dummy head MK2B in hemi-anechoic room with three experimenters coded as E1, E2 and E3. Training tasks were to position the sound source at  $(0^\circ, 0^\circ)$  repeatedly in  $+/-$  direction more than 30 times and adjust the sound source position within  $(0^\circ, \pm 10^\circ)$  by  $1^\circ$  azimuth angle.

The head-related impulse responses (HRIRs) of MK2B dummy head were measured in order to examine the tester errors with posture changes of human subjects. HRIRs are time-domain transforms of HRTFs, which can be captured using specialized configurations of loudspeakers and microphones.

### 2.2 Keeping Posture of Pilots to Reduce the Testee Errors

Pilots were positioned in  $(x, y, z)$  coordinates with the origin  $(0, 0, 0)$  at midpoint of bitrigrion on the Frankfurt plane in sitting, which the coordinates were identical to the polar coordinates of  $(r, \phi, \theta)$  [7] as well as that of a human HRTF measurement redirector [8] in free field of hemi-anechoic room.

The main tasks of pilots were keeping his posture not to move during one turn of test after positioning and checking by the experimenters. The test–retest checks were arranged at  $(\phi, 0^\circ)$ ,  $(\phi, 180^\circ)$  and  $(\phi, 360^\circ)$  to control the testee errors from head moving, because the asymmetries between the ears should be minimal on midsagittal plane in theory. If the interaural level difference (ILD) of binaural signals was more than alarm threshold such as 2.0 dB on test–retest checks, the pilot would be adjusted back to his correct posture whether having a rest or not.

Whole experiment was divided into 13 blocks by elevations ( $\phi$ ) (see Table 1) for

**Table 1** Training performances of sound source positioning at ( $0^\circ, 0^\circ$ )

The experimenters	<i>N</i>	Mean	Std. Dev.	95% confidence interval
E1	60	0.27	0.11	0.24–0.30
E2	30	0.26	0.12	0.22–0.31
E3	90	0.29	0.06	0.28–0.30
Total	180	0.28	0.09	0.27–0.29

single pilot, so the full time of the measuring experiment was also separated into each block necessarily. Two pilots were selected by similar stature before test and then took turn each other between blocks and kept measuring in Latin square for elevation adjustment in order to reduce fatigue effects.

### 2.3 *Validate the Data Quality of CHNAF HRTF Database*

The binaural HRIRs of 63 male pilots in CHNAF HRTF database were analyzed especially on ILD of binaural recording with SPSS.

## 3 Results

The training results of three experimenters are in Table 1 and Fig. 1. The results of human error reduction for pilots are as shown in Table 2 and Fig. 2 by contrast with standard dummy head MK2B.

## 4 Discussions

### 4.1 *The Tester Errors After Pre-test Training*

Binaural technology is important for 3D audio in which binaural signals are collected and recorded near the external ear orifices and the incumbent cues for 3D audio spatial localization [9]. The cues of auditory spatial localization include interaural time difference (ITD), interaural level difference (ILD) and interaural phase difference (IPD). The ITD and ILD are theoretically zero when the sound source is position at  $(\phi, 0^\circ)$ ,  $(\phi, 180^\circ)$  or  $(\phi, 360^\circ)$  toward the subject because the distances are equal between the sound source and the ears of the subject. So, the ILD could be used to judge the posture of pilots with or without movement and the human errors from experimenter(s) with dummy head MK2B as subject.

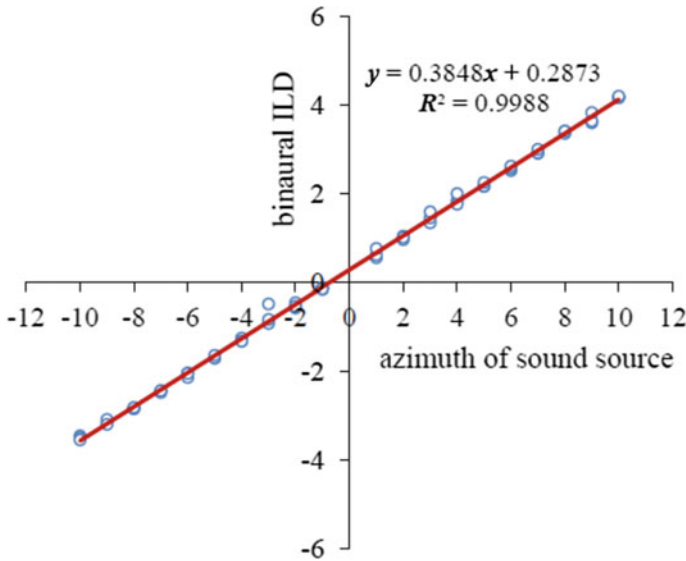


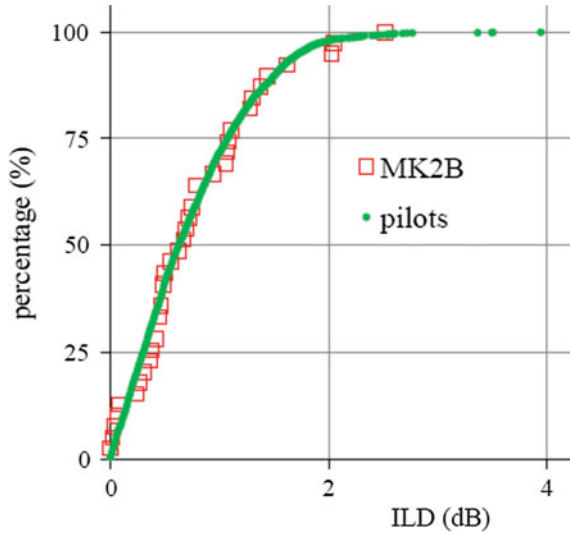
**Fig. 1** Human errors from the testers

**Table 2** ILD data of pilots at test–retest positions in CHNAF HRTF database

Elevation $\phi$	Left ear			Right ear		
	$(\phi, 0^\circ)$	$(\phi, 180^\circ)$	$(\phi, 360^\circ)$	$(\phi, 0^\circ)$	$(\phi, 180^\circ)$	$(\phi, 360^\circ)$
80°	-18.19	-18.26	-18.19	-17.75	-17.78	-17.77
70°	-18.08	-18.27	-18.24	-17.86	-17.93	-17.93
60°	-18.17	-18.29	-18.52	-17.91	-17.83	-18.10
50°	-18.29	-18.54	-18.38	-18.03	-17.99	-18.05
40°	-18.10	-18.59	-18.31	-18.16	-18.17	-18.21
30°	-18.24	-18.60	-18.28	-17.89	-18.25	-18.00
20°	-17.84	-18.86	-17.82	-17.57	-18.45	-17.58
10°	-17.63	-18.96	-17.65	-17.48	-18.41	-17.40
0°	-17.30	-18.62	-17.31	-16.92	-17.94	-16.96
-10°	-17.27	-18.44	-17.19	-16.84	-17.82	-17.01
-20°	-17.33	-18.19	-17.54	-17.12	-17.67	-17.16
-30°	-17.50	-17.89	-17.67	-17.06	-17.54	-17.29
-40°	-17.70	-17.88	-17.99	-17.30	-17.40	-17.41

For the purpose of data quality control, all three experimenters were trained in pre-test program. The results are found in Table 1 that their performances were not different significantly in statistics after training of sound source positioning at (0°,

**Fig. 2** Human errors from the testees



0°), and the human errors were about 0.29 dB of ILD and  $-0.75^\circ$  azimuth deviation made by the testers (see Fig. 1). It suggested that the training was valid.

#### 4.2 Acceptable ILD of 2.0 dB as Alarm Threshold

The HRIR data were binaural recoded with dummy head MK2B as subject. The results are shown in Fig. 2. All the ILDs were in range of 0–2.52 dB with the 95% of 2.05 dB when the sound source was at  $(\phi, 0^\circ)$ ,  $(\phi, 180^\circ)$  or  $(\phi, 360^\circ)$  toward the subject like somewhat pilots without head moving or posture change.

#### 4.3 ILD Data of the Test–Retest Checks

There were 63 male pilots measured for HRIRs of CHNAF HRTF database. The ILDs of all pilots were in range of 0–3.95 dB with 97.96% of that less than 2.0 dB when the sound source was at  $(\phi, 0^\circ)$ ,  $(\phi, 180^\circ)$  or  $(\phi, 360^\circ)$  toward the pilots.

The difference was not found between the means of the pilots and the dummy head MK2B ( $F(1,2491) = 0.001, P = 0.98$ ). It indicated that both of the sound source positioning by the experimenters and keeping posture by pilots had been well done at starts for each block of elevation adjustment even reset on  $(\phi, 180^\circ)$  after pause.

The other interesting results were also found by farther analyses. Firstly, the ILD did exist in Table 2 (Left ear—18.06 dB vs. Right ear—17.69 dB;  $F(1,62) = 60.65, P < 0.001$ ), which might be related to the spatial symmetry of head with binaural

microphones because of mild motion. Secondly, the HRIR levels were seemed in two groups with different elevation sound sources, in which the binaural HRIRs were bigger for the sound sources below the Frankfurt plane in sitting than that above the plane as shown in Fig. 3 (main effect for elevations  $F(12,744) = 12.64, P < 0.001$ ; pair contrast between groups  $P < 0.05 - 0.001$ ). Thirdly, the binaural HRIRs were smaller for the sound sources dorsal than that ventral ( $F(2,124) = 22.91, P < 0.001$ ) because of pinna obstructing as well as the ILDs ( $F(2,124) = 5.40, P < 0.01$ ). Finally, the interaction effect was found between the test–retest checks and the elevations as shown in Fig. 4.

**Fig. 3** Binaural HRIR levels in elevations

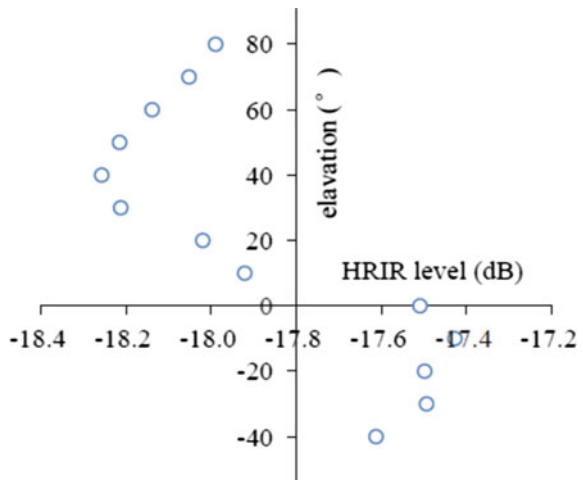
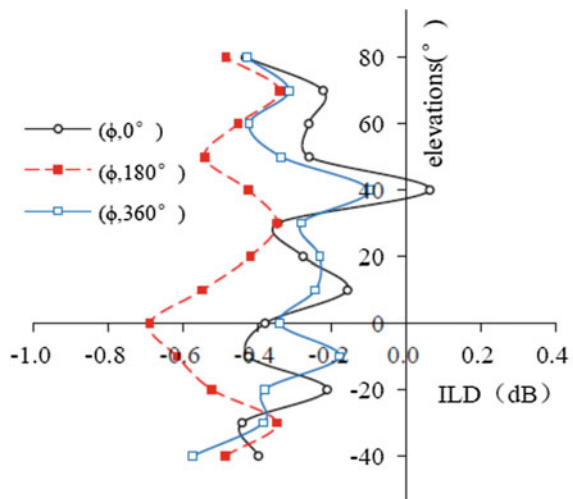


**Fig. 4** ILDs in test–retest checks





#### 4.4 Other Helpful Strategies for Data Quality

The completion of the HRTF measuring experiment was carried out by 13 blocks with an additional 3D head anthropometry [7] for single pilot. The bigger blocks spent times less than 30 min for most of the pilots in the present paper. This would shorten the time to keep posture of pilots and reduce their possible fatigue.

The relax schedule was administered at every interval for one pilot about 10–30 min, while another pilot was participating in experiment on duty. And so did the experimenters to release the stress of works.

It is reported that there was no significant difference between the CHNAF HRTF database and the CIPIC database for personalization of HRTF database matching in spectral distortion (SD), but the CHNAF HRTF database matching error in the full bandwidth was smaller than that of the CIPIC database because of the richer physiological parameters [10].

## 5 Conclusions

A specified method and procedure were proposed and conducted for HRTF measuring experiment of China Air Force head-related transfer function (HRTF) database, i.e., CHNAF HRTF database. A pre-test training was carried out for all the experimenters to reduce the tester errors in operations of 3D sound sources positioning, microphones putting into bi-ears of pilots and posture correcting with interaural level difference (ILD) of head-related impulse responses (HRIRs). Pilot was sat in  $(x, y, z)$  coordinates with the origin  $(0, 0, 0)$  at midpoint of bitracion on his Frankfurt plane in which the coordinates were identical to the polar coordinates of  $(r, \phi, \theta)$ , keeping his posture to reduce the testee errors during each block in the experiment. The test–retest checks were arranged at  $(\phi, 0^\circ)$ ,  $(\phi, 180^\circ)$  and  $(\phi, 360^\circ)$  for data quality control. Other strategies were done such as the division of the measuring into 13 blocks, and schedules of rest by turns to reduce human errors from fatigue effects. All 3 testers were trained with MK2B dummy head, and 63 male pilots were measured for head-related impulse responses (HRIRs) in hemi-anechoic room with binaural recording. The results were found that the tester error was about 0.29 dB of ILD and  $-0.75^\circ$  azimuth deviation, the 2.0 dB of ILD was acceptable alarm threshold for binaural spatial symmetry because of pilots posture change, and the data quality of the CHNAF HRTF database was well validated in contrast with the CIPIC database for personalization of HRTF database matching in spectral distortion (SD). The results also found that the ILDs of all pilots were in range of 0 to  $-3.95$  dB with 97.96% of that less than 2.0 dB when the sound source was at  $(\phi, 0^\circ)$ ,  $(\phi, 180^\circ)$  or  $(\phi, 360^\circ)$  toward the pilots, and the difference did not exist between the means of the pilots and the dummy head MK2B which indicated that both of the sound source positioning by the experimenters and keeping posture by pilots had been well done to ensure the better data quality of the CHNAF HRTF database. Some influences were discussed.

**Acknowledgements** The work was supported by Defense Industrial Technology Development Program No. JCKY2018000B001 with pre-research program No. 51326050203.

The authors are thankful to Mr. Dongdong Lu for his contribution to data extraction from binaural HRIRs.

**Compliance with Ethical Standards** The study was approved by the Academic Ethics Committee of Air Force Medical Center of FMMU. All subjects were provided with and signed an informed consent form. All relevant ethical safeguards have been met with regard to subject protection.

## References

1. Yang L, Jiao H (2019) The key technology research of head-related transfer function acquisition and development. *Softw Guide* 18(1):34–39
2. CHEN XP (2018) HRTF Implementation modelling in binaural synthesis. *Audio Eng* 42(5):36–41
3. Zhong X, Xu X (2018) Influence of different measuring procedures of head-related transfer functions on auditory perception. *Acta Acustica* 43(1):83–90
4. Andreopoulou A, Begault DR, Katz BFG (2015) Inter-laboratory round robin HRTF measurement comparison. *IEEE J Selected Topics Signal Process* 9(5):895–906
5. Barumerli R, Geronazzo M, Avanzini F (2018) Round robin comparison of inter-laboratory HRTF measurements—assessment with an auditory model for elevation. In: 2018 IEEE 4th VR workshop on sonic interactions for virtual environments (SIVE), Reutlingen, Germany, 18 Mar 2018
6. Guo X, Xiong D, Wang Y et al (2016). Head related transfer function database of Chinese male pilots. In: Long S, Dhillon BS (eds) *Man-machine-environment system engineering. Lecture Notes in Electrical Engineering* 406, pp 3–11
7. Guo X, Bai Y, Liu Q et al (2020) 3D head anthropometry for head related transfer functions of Chinese pilots. In: Long S, Dhillon BS (eds) *Man-machine-environment system engineering. Lecture Notes in Electrical Engineering* XXX. pp XX–XX (in press)
8. Guo X, Shi G, Wang C et al (2014) A human HRTF measurement redirector. China patent ZL 2013 2 0782 113.2. In: CN203675323U, State Intellectual Property Office of the P.R.C., 25 June 2014
9. CHEN XP (2018) AES monograph-binaural technology: binaural encoding and decoding in binaural technology. *Audio Eng* 42(4):31–37
10. Lu D, Zeng X, Guo X et al (2019) Personalization of head-related transfer function based on sparse principle component analysis and sparse representation of 3D anthropometric parameters. *Acoust Aust*. <https://doi.org/10.1007/s40857-019-00169-y>

# An Automatic Meter Recognition Method for In-Orbit Application



Wei jie Wu, Haoting Liu, and Jiacheng Li

**Abstract** With the development of machine vision technology, more and more vision-based recognition methods have appeared. However, the artificial meter readings are still widespread in the astronautic application. Astronauts' works are complex, and the meter readings reduce their efficiencies. To solve this problem, in this paper, we propose a method that can automatically recognize the meter readings. The automatic recognition method includes the following three major components: (1) the digit extraction, (2) the digit segmentation, and (3) the digit recognition. The experiment results show that the digits of the meter can be successfully recognized. The automatic readings can reduce astronauts' works and make them more convenient while working. This new automatic recognition system has great promise for the practical application.

**Keywords** Astronaut · Image recognition · Meter reading · Digit recognition · KNN

## 1 Introduction

At present, many meters used for the measurement do not have a special communication interface in astronautic application, which makes it impossible to read them automatically. Reading the meters still requires artificial operation. However, the astronauts themselves have a high degree of work intensity and complicated operations [1]. Reading meters will increase the workload of astronauts and make them unable to concentrate on their missions. Machine vision can solve these problems, recognize the meters automatically, and give feedback results to the astronauts. This will make them work more easily.

---

W. Wu · H. Liu (✉) · J. Li

Beijing Engineering Research Center of Industrial Spectrum Imaging, School of Automation and Electrical Engineering, University of Science and Technology Beijing, 100083 Beijing, China  
e-mail: [liuhaoting@ustb.edu.cn](mailto:liuhaoting@ustb.edu.cn)

W. Wu

e-mail: [wuweijieh@163.com](mailto:wuweijieh@163.com)

© The Editor(s) (if applicable) and The Author(s), under exclusive license to Springer Nature Singapore Pte Ltd. 2021

S. Long and B. S. Dhillon (eds.), *Man-Machine-Environment System Engineering*, Lecture Notes in Electrical Engineering 645, [https://doi.org/10.1007/978-981-15-6978-4\\_48](https://doi.org/10.1007/978-981-15-6978-4_48)

## 2 Digit Extraction Algorithm

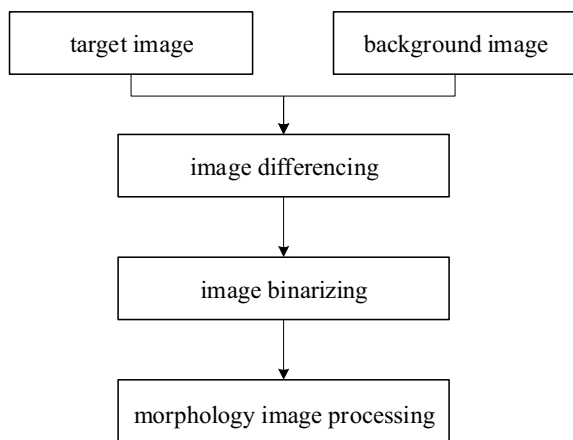
Digit extraction refers to detecting the position of a digit in the image and extracting images of a digit.

### 2.1 Background Subtraction Method

Since the camera position is fixed and the position of the meter will hardly be changed, the background area of the meter will not change in the picture. The frame subtraction method can be used to subtract two images. After the subtraction, the areas that have not changed in the image will be close to zero, while the areas that have changed will still retain a certain gray value. Therefore, this method can be used to exclude background interference terms and extract digital areas. The background subtraction method is a pixel-based target detection method, which extracts target areas by performing a difference operation on similar frames in an image sequence. The method is simple to implement and has high real-time performance [2].

The proposed main steps are shown in Fig. 1. First, we construct a background model image to describe the background information. Then, we use the target image and the background model to obtain the subtraction image, and then binarize it to get the target image. In this image, if the value of a pixel is larger than or equal to a certain threshold, the pixel is considered to belong to the certain target; otherwise, the pixel is considered to belong to the background area if the value of the pixel is less than this threshold. However, this method is also easy to cause “holes” and “ghosting.” To solve that problem, we need a further mathematical morphology image processing to reduce the impact [3].

**Fig. 1** Computational flowchart of background subtraction



Let us suppose the target image sequences are  $f_1, f_2, \dots, f_n$ , the image is  $f_k(x, y)$ , and its background image is  $f_m(x, y)$ . Their subtraction image  $D_k(x, y)$  is computed by Eq. 1.

$$D_k(x, y) = |f_k(x, y) - f_m(x, y)| \tag{1}$$

In Eq. 1,  $(x, y)$  represents the spatial coordinates of the pixels in the image. The subtraction image  $D_k(x, y)$  is compared with a threshold  $T$  to determine whether each pixel in the image is a target pixel or a background pixel. And then, we can extract the target  $R_k(x, y)$ . The threshold  $T$  can be given or determined by an adaptive method shown in Eq. 2. Figure 2 shows the corresponding result of background subtraction.

$$R_k(x, y) = \begin{cases} 1 & \text{target } D_k(x, y) > T \\ 0 & \text{background } D_k(x, y) \leq T \end{cases} \tag{2}$$

In order to accurately recognize the characters, we need the further processes of the image and binarize the image to maximize the required information. We use the Otsu algorithm which can automatically determine the threshold to binarize the image [4] in this paper. Its basic principle is: The grayscale range of the image is  $[0, 255]$ , the gray value of the point  $(x, y)$  is expressed as  $I(x, y)$ , and the probability of the point of gray level  $x$  is  $P(x)$ . Then, the Otsu method can find the gray value  $m$  shown in Eq. 1 that reaches the maximum value. Figure 3 presents the result of binary processing. As we can see from Fig. 3, the information of the image that we need is

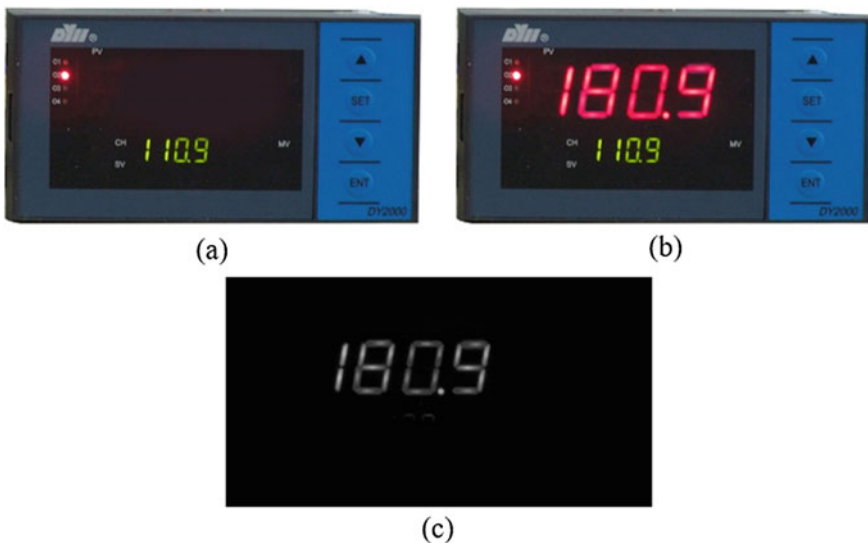


**Fig. 2** Computational result of background subtraction method. Image **a** is the background image, **b** is the target image, and **c** is the subtraction image



**Fig. 3** Original subtraction image and the image after binarization using the Otsu method

enhanced after the binarization. But it still has noise which needs to be removed.

$$Y_m = \frac{\left[ \sum_{x=0}^{255} xp(x) \times \sum_{x=0}^m p(x) - \sum_{x=0}^m xp(x) \right]^2}{\sum_{x=0}^m p(x) \times (1 - \sum_{x=0}^m p(x))} \quad (3)$$

where  $m$  is the gray threshold.

## 2.2 Mathematical Morphology

The mathematical morphology operation can be regarded as the correspondence between the shape of the figure in the image and the probe with a certain shape and state in the morphology. It can use the “probe” to scan the image to get the graphic structure of the image. The detection results are extracted and applied to the analysis and the processing of the image. The application of mathematical morphology to image analysis processing, regardless of the element, can be removed while maintaining the image structure and morphology to enable the maximum degree of data reduction, so that it is simple and clear. The mathematical morphology operation of the image can be divided into the following two parts: the corrosion computation and the dilation computation.

- The corrosion computation

When the structural element  $S$  moves on a given target image  $X$ , the  $S[x]$  has the following three possible states relative to  $X$ :

1.  $S[x] \subseteq X$ ,  $S[x]$  has the largest correlation with  $X$ .
2.  $S[x] \subseteq X^C$ ,  $S[x]$  is not related to  $X$ .
3. Neither  $S[x] \cap X$  nor  $S[x] \cap X^C$  is empty.

In point 1,  $S[x]$  has the biggest correlation with  $X$ , so all the structural elements in image point  $X$  are the maximum correlation point set  $S[x]$  of the image. We call it  $S$  corrodes  $X$ , and it is denoted as  $X \ominus S$ . The way is defined as Eq. 4. The corrosion of the image can eliminate the information about the boundary points of the target image. By selecting the appropriate structural element to remove objects smaller than

**Fig. 4** Result after the corrosion and expansion operation



the structural element, the edge of the contour of the object will be reduced by one or more pixels. The eliminated objects are also different in size. The application of the corrosion algorithm can reduce more useless background information and improve the calculation speed.

$$X \ominus S = \{x | S[x] \subseteq X\} \tag{4}$$

- The dilation computation

The dilation of images is regarded as the dual operation of the erosion operation. The dilation operation is to expand each point  $x$  in the image  $X$ , and it is denoted as  $X \oplus S$ , which is defined by a set method as Eq. 5. This algorithm is essentially equivalent to moving the structural element on the original image. The pixels are added according to the structural elements at positions that do not contain information in the image to make the image larger. It is equivalent to merge the structural elements with the original image. The dilation operation can make background information to be close to the edges of the image, or two small parts are connected together. Therefore, after the image processing, the expansion operation can be used to fill and repair the image holes, which is used to reduce the target caused by the corrosion. After the corrosion and expansion operation on the image, the image is obtained as shown in Fig. 4. At the same time, this study uses a connected domain-based digit segmentation method. The expanded digits can form a connected domain and avoid the fragmentation.

$$X \oplus S = \{x | S[x] \neq \Phi\} \tag{5}$$

### 2.3 Digit Segmentation Method

The digit segmentation generally includes the connected domain-based numeric character segmentation and the projection methods. This study uses the digit segmentation method based on the connected domains [5]. We suppose  $f(x, y)$  is the pixel value

**Fig. 5** Digit segmentation results



of the  $x$ th and  $y$ th columns in the image array, an  $m \times n$  image has  $m$  rows and  $n$  columns, and  $f(m-1, n-1)$  represents the pixel value in the lower right corner of the image. We can traverse the image and find all the connected domains based on the neighborhood connectivity criteria. Each separated area in the image can be detected in this way. After finding all connected domains, the filtering is performed according to the area of the connected domain, the shape of the reading, and the aspect ratio. Then, we can exclude areas that do not meet the criteria. Then, we can directly locate and divide each digit. The specific processes are: We calculate the area of the connected domain; the area of the connected domain  $A$  is the number of points with a pixel value of 255; that is, the number of pixels contained in the boundary of the area is shown in Eq. 6. If the area of the connected domain is greater than 500 and less than 5000, the aspect ratio of the connected domain is bigger than 1.5 and less than 2.5, and it will be extracted. If the above conditions are not met, it will be discarded. We can get each digit by filtering out the connected domains that meet the requirements. The digit segmentation results are shown in Fig. 5.

$$A = \sum_{x=0}^{m-1} \sum_{y=0}^{n-1} f(x, y) \quad (6)$$

### 3 Digit Recognition Algorithm

After the digital area is successfully extracted, we need to recognize the digits. The most commonly used digit recognition algorithms are the template matching, the artificial neural network-based, etc. The neural networks are also often used for the digits' recognition in recent years. This paper adopts the K-nearest neighbor (KNN) algorithm. The KNN is a classic classification algorithm, which is mature in application and has high recognition accuracy [6].

The KNN algorithm was originally proposed by Cover and Hart in 1968. The basic idea of the algorithm is: According to the traditional vector space model, the image is formalized into a weighted feature vector in the feature space,  $D = D(T_1, W_1, T_2, W_2, \dots, T_n, W_n)$ . For the image to be detected, we can calculate the



similarity between it and each image in the training sample set, find the  $K$  most similar images, and determine the category to which the test image belongs according to the weighted distance sum. The algorithm recognition steps are as follows:

1. A set is generated for the images to be detected.
2. The similarity between the images to be detected and the images in the training set are calculated. The calculation equation is shown in Eq. 7, where  $d_i$  is the feature vector of the images to be detected,  $d_j$  is the center vector of the  $j$  class,  $M$  is the dimension of the feature vector, and  $W_k$  is the  $k$  dimension of the vector.

$$\text{Sim}(d_i, d_j) = \frac{\sum_{i=1}^M W_{ik} \times W_{jk}}{\sqrt{\sum_{k=1}^M W_{ik}^2} \sqrt{\sum_{k=1}^M W_{jk}^2}} \tag{7}$$

3. The weight of each class in the  $K$ -nearest neighbors of the images to be detected in turn is computed. The calculation equation is presented in Eq. 8, where  $x$  is the feature vector of the image to be detected,  $\text{Sim}(x, d_i)$  is the similarity calculation equation, and  $b$  is a threshold.

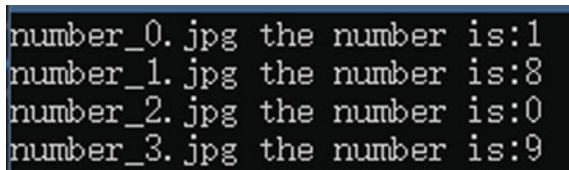
$$P(X, C_j) = \begin{cases} 1 & \sum_{d \in \text{KNN}} \text{Sim}(x, d_i) y(d_i, C_j) - b \geq 0 \\ 0 & \text{else} \end{cases} \tag{8}$$

4. The images are classified by comparing the weights. Train the KNN model to recognize the images.

## 4 The Experiments

A simulation experiment is performed to test the algorithm. The program is written by C++ on VS 2017. First, we extract the difference image and preprocess the image. Then, we train the KNN model. The training of the KNN model is implemented by an online database. There are totally 10 characters from 0 to 9, and each character has 120 pictures. And then use the KNN model to recognize the images. Figure 6 shows out the simulation result.

Fig. 6 Recognition results



## 5 Conclusion

In this paper, we present a method to recognize the digits on meter. According to the digits displayed on meter, we use the background subtraction method to extract the digital region; then, we use the method of the minimum connected domain to segment each digit; finally, we use the KNN to recognize the digits. This study can accurately recognize the meter reading automatically, which can be used for further research experiments in the astronautic application.

**Acknowledgements** This work was supported by the National Natural Science Foundation of China under Grant No. 61975011 and the Fundamental Research Fund for the China Central Universities of USTB under Grant No. FRF-BD-19-002A.

## References

1. Xue-wen C, Yu-qing L, Xiu-qing Z, Ming A, Bo-he Z, Jin-kun W et al (2011) Research of space operation simulation based on virtual reality. *J Syst Simul* 23(03):516–521
2. Spagnolo P, Orazio TD, Leo M, Distanto A (2006) Moving object segmentation by background subtraction and temporal analysis. *Image Vision Comput* 24(5):411–423
3. Zhijia Z, Yuan L (2009) Research on the pre-processing method of automatic reading water meter system. In: 2009 international conference on artificial intelligence and computational intelligence, Shanghai, pp 549–553
4. Xiangyun Y, Mohamed C, Ching YS (2001) Stroke-model-based character extraction from gray-level document images. *IEEE T Image Process* 10(8):1152–1161
5. Jianjun Z, Heng Y, Xiaoguang G, Sheng W (2010) The edge detection of river model based on self-adaptive Canny algorithm and connected domain segmentation. In: 2010 8th world congress on intelligent control and automation, Jinan, pp 1333–1336
6. Gu-yuan L, Shih-chiang L, Jane YH, Wan-rong J (2010) Applying power meters for appliance recognition on the electric panel. In: 2010 5th IEEE conference on industrial electronics and applications, Taichung, pp 2254–2259

# Investigation of Image Classification Using HOG, GLCM Features, and SVM Classifier



Jianyue Ge and Haoting Liu

**Abstract** Recently, in order to solve the problem of image classification, some image features and classifiers play more and more important role in the related research field. This article investigates an image classification method by the histogram of oriented gradient (HOG) features, the gray-level co-occurrence matrix (GLCM) features, and the support vector machine (SVM) classifier. By obtaining the HOG and the GLCM features of image, the combination of them is inputted into the SVM for the training and the test. The experiment results have manifested the effectiveness of the proposed method. The use of the combination of HOG features and GLCM features in image classification is far superior to the use of them alone.

**Keywords** HOG · Gray-level co-occurrence matrix · SVM · Image classification

## 1 Introduction

With the rapid development of science and technology, the research trend of artificial intelligence is constantly rising. More and more people are investigating in the field of machine learning and deep learning. As the direct carrier of information transmission, people have paid more attention to the image classification. Including the subjective image quality evaluation, the machine learning quality evaluation of the SVM + SVR system formed by the BRISQUE [1] algorithm, and the deep learning quality evaluation model of CNN IQA [2], people's passion for image research burst out constantly. Image classification is one of the contents in the field of image quality evaluation. The results of image classification often have a great impact on the subsequent image computation. This paper proposes an image classification method using the histogram of oriented gradient (HOG) features, the gray-level co-occurrence matrix (GLCM) features, and the support vector machine (SVM) classifier. By extracting the HOG features and the GLCM features, the SVM is used to perform the prediction.

---

J. Ge · H. Liu (✉)

Beijing Engineering Research Center of Industrial Spectrum Imaging, School of Automation and Electrical Engineering, University of Science and Technology Beijing, 100083 Beijing, China  
e-mail: [2488238078@qq.com](mailto:2488238078@qq.com)

© The Editor(s) (if applicable) and The Author(s), under exclusive license to Springer 411  
Nature Singapore Pte Ltd. 2021

S. Long and B. S. Dhillon (eds.), *Man-Machine-Environment System Engineering*, Lecture Notes in Electrical Engineering 645,  
[https://doi.org/10.1007/978-981-15-6978-4\\_49](https://doi.org/10.1007/978-981-15-6978-4_49)

## 2 Algorithm Flow

There are about 300 pictures in this experiment, which are divided into four types: car, cat, flower, and fish. The pictures above are divided into a test set and a training set according to a certain proportion. The test set contains 50 pictures of car, 35 pictures of cat, 35 pictures of flower, and 60 pictures of fish. The test set sample is shown in Fig. 1.

The algorithm flowchart is shown in Fig. 2, and the computation steps are illustrated as follows.

- Step 1: The system batches the pictures into the certain size for the following experiment computation.
- Step 2: This system reads the picture information, extracts the HOG features and the GLCM features of the picture, and then merges the two features above.

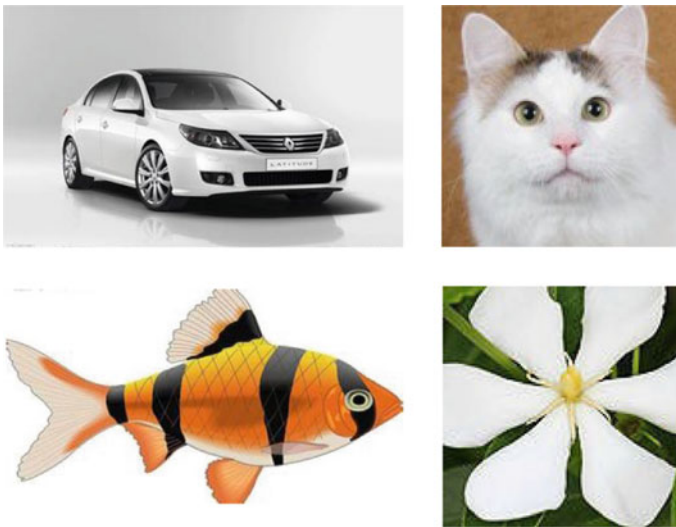


Fig. 1 Samples of test set

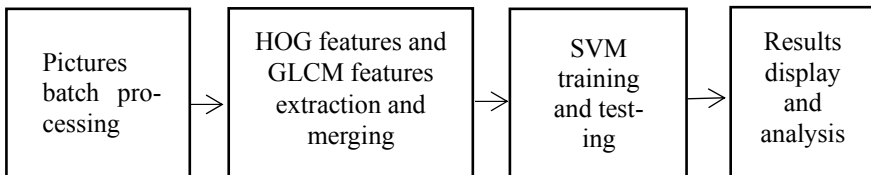


Fig. 2 Algorithm computation flowchart

Step 3: The system inputs the feature vectors into the SVM and adopts a one-to-one solution to train and test the SVM.

Step 4: This system displays the classification results and analyzes the results.

## 2.1 HOG Feature Extraction

The HOG feature is a kind of directional histogram feature. It is a typical image feature that is widely used in various fields of image research. The general acquisition of HOG features roughly goes through the following steps [3].

Step 1: The algorithm converts the original image into a grayscale image. The Eq. (1) shows the process of converting a color image into a grayscale image:

$$\text{Gray} = 0.3 * R + 0.59 * G + 0.11 * B \quad (1)$$

where  $R$ ,  $G$ , and  $B$  represent the color components of the corresponding position of the image;

Step 2: The Gamma correction method [4] is used for image normalization. In the case of uneven image illumination, Gamma correction can be used to increase or decrease the overall brightness of the image. In practice, Gamma standardization can be performed in two different ways, i.e., the square root and the logarithmic method. In general, the square root method is usually used, and its formula is as follows:

$$Y(x, y) = I(x, y)^{1/2} \quad (2)$$

where  $I(x, y)$  represents the brightness of the corresponding position of the image;

Step 3: The algorithm calculates the gradient of each pixel of image separately;

Step 4: The algorithm divides the image into cell units and counts the gradient direction of each cell unit;

Step 5: The algorithm combines several cell units into blocks and then connects the gradient directions of all blocks in the series to obtain the HOG features (Fig. 3).



**Fig. 3** Example of HOG features. The original picture is shown in left and the picture of HOG features is presented in right

### 2.2 GLCM Feature Extraction

The GLCM [5] is an image recognition technology with strong robustness and adaptability which can effectively realize the classification and retrieval of images. The GLCM actually refers to the probability that a gray-level point leaves a certain position  $d(Dx, Dy)$  and therefore reaches a  $j$  gray level. Equation (3) shows its definition method. In this paper, in order to obtain the GLCM at different angles, four directions are computed: 0, 45, 90, and 135. The corresponding features, including the contrast, the inverse gap, the entropy, and the autocorrelation, are all calculated. And then, the average and the variance of them are computed as the final extracted features.

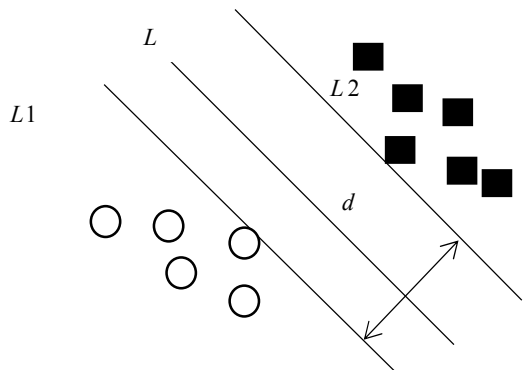
$$Pd(i, j) \quad (i, j = 0, 1, 2, 3, \dots, L - 1) \tag{3}$$

where  $L$  represents the gray level of the image pixel;  $i, j$  are used for the gray level of pixel;  $d$  mainly refers to the direction and distance between two different pixels.

### 2.3 Svm

The SVM is a typical binary classifier. It is widely used in the field of machine learning. As shown in Fig. 4, the hollow circles and black squares, respectively, represent two types of linearly separable training samples. The symbol  $L$  is a classification line that separates the two classes without errors. The symbols  $L1$  and  $L2$  are the straight lines that pass through the nearest point in the two types of samples to the classification line. And they are also parallel to  $L$ . The interval  $d$  between  $L1$  and  $L2$  is called the classification interval. The optimal classification line can maximize the classification interval  $d$ . If the above situation is extended to a high-dimensional space, the optimal classification line is called the optimal classification surface. The kernel function-based SVM maps linearly inseparable problems from

Fig. 4 SVM algorithm sketch map



the low-dimensional space to high-dimensional space through kernel mapping. Similarly, the optimal classification surface in high-dimensional space can also be found to solve the classification problem.

Although the SVM is just a typical binary classifier, it can also achieve the effect of multi-classification. There are usually three types of schemes for implementing the SVM: the remaining schemes, the one-to-one scheme, and the directed acyclic graph scheme. We use a one-to-one solution in this paper. It is assumed that there are a total of  $K$  categories in the sample; for a one-to-one solution, you need to train a classifier for any two of the categories; thus, it is needed to train a number of classifiers  $K(K - 1)/2$  for each category. Although the number of classifiers is larger, the total time spent in the training phase is much less than the other methods.

### 3 The Experiment Results

This experiment mainly uses MATLAB programming to process 300 pictures and extracts the HOG features and the GLCM features. We also use the SVM algorithm to classify and obtain the classification results. And then, we calculate them in the form of a confusion matrix [6]. The accuracy and the recall of various image classifications are used to judge the performance of our proposed method. There are 180 pictures in the test set, which are divided into four types of pictures, including 50 pictures of car, 35 pictures of cat, 35 pictures of flower, and 60 pictures of fish. The classification results are shown in Table 1.

It can be seen from Table 1 that the fish-type picture classification can get the best result, and the flower type classification result is poor. After the data processing, the accuracy and the recall rate are also obtained. The results are shown in Table 2. According to Table 2, it can be obtained that the average correct rate of the

**Table 1** Test set classification results

	Car	Cat	Flower	Fish
Car	46	0	0	4
Cat	0	32	1	2
Flower	0	4	30	1
Fish	0	0	1	59

**Table 2** Accuracy and the recall rate of test set

	Car	Cat	Flower	Fish
Accuracy	0.9200	0.9143	0.8571	0.9833
Recall rate	1	0.8889	0.9375	0.8939

classification result of the test set is about 91.87%, and the classification effect is relatively satisfactory.

In order to reflect the rationality of the combination of the HOG features and the GLCM features, the classification experiments using only the HOG features or the GLCM feature are done, respectively, in this paper. The respective classification results are shown as follows.

From these Tables 3, 4, 5 and 6, it can be obtained that the average correct rate of the classification result of the test set only using the HOG feature is about 88.61%, and the average correct rate of the classification result of the test set only using the GLCM feature is about 83.06%. However, the average correct rate of the classification result of the test set using both the HOG feature and the GLCM feature is about 91.87%. Clearly, the use of the combination of HOG features and GLCM features in image classification is far superior to the use of them alone.

**Table 3** Test set classification results only using the HOG feature

	Car	Cat	Flower	Fish
Car	44	0	0	6
Cat	0	31	0	4
Flower	0	3	29	3
Fish	1	0	2	57

**Table 4** Accuracy and the recall rate of test set only using the HOG feature

	Car	Cat	Flower	Fish
Accuracy	0.8800	0.8857	0.8286	0.9500
Recall rate	0.9778	0.9118	0.9354	0.8142

**Table 5** Test set classification results only using the GLCM feature

	Car	Cat	Flower	Fish
Car	46	0	0	4
Cat	2	26	4	3
Flower	1	7	26	1
Fish	4	1	0	55

**Table 6** Accuracy and the recall rate of test set only using the GLCM feature

	Car	Cat	Flower	Fish
Accuracy	0.9200	0.7428	0.7428	0.9167
Recall rate	0.8679	0.7647	0.8667	0.8730



## 4 Conclusion

This paper analyzes a SVM image classification method based on the combination of the HOG features and the GLCM feature. We also conduct the experimental analysis of the corresponding algorithms. The classification results of this method are reasonable.

**Acknowledgements** This work was supported by the Fund of State Key Laboratory of Intense Pulsed Radiation Simulation and Effect under Grant No. SKLIPR1713, the National Natural Science Foundation of China under Grant No. 61975011, and the Fundamental Research Fund for the China Central Universities of USTB under grant No. FRF-BD-19-002A.

## References

1. Mittal A, Moorthy AK, Bovik AC (2012) No-reference image quality assessment in the spatial domain. *IEEE Trans Image Process* 21:4695–4708
2. Kang L, Ye P, Li Y, Doermann D (2014) Convolutional neural networks for no-reference image quality assessment. In: *Proceedings of the 2014 IEEE conference on computer vision and pattern recognition*, pp 1733–1744
3. Zhijun Fu (2020) Design and implementation of face recognition system based on hog image features. *Automat Technol Appl* 39:117–120
4. Hui Z (2018) Improved color data acquisition scheme for fast gamma correction. *J Nanjing Institut Technol* 16:34–38
5. Chaoyang W (2019) Classification and processing of remote sensing images based on gray level co-occurrence matrix. *Comput Knowl Technol* 15:167–168
6. Wang Yao Xu, Chang SF (2019) Analysis of two image classification methods based on SVM algorithm for feature extraction. *Comput Inf Technol* 27:18–20

# Relationship Between Individual Perceptual Feature Demand and Satisfaction in the Small Assistant Robot Modeling Design



Yankun Yang, Bo Wang, Changhua Jiang, Yujing Cui, Ling Song, and Xiaomeng Ma

**Abstract** Quantifying the human emotional experience for product modeling design has been a research hotspot. Focusing on the personalized design of small assistant robots, the relationship between individual's perceived feature needs and satisfaction is studied. Five experiments were designed, including perceptual image vocabulary selection, image mood board eye movement experiment, satisfaction survey, perceptual imagery feature demand survey, and experiment on scoring the conformity of modeling samples on different perceptual imagery vocabularies. Forty subjects participated in the experiment. The results show that due to the diversity of individual needs and the different degrees of perceived features, the satisfaction with the same product modeling design is different. In addition, based on the Kano model, a quantitative relationship between perceived features and overall satisfaction was found. This study provides new ideas for further research on the needs of different people for external modeling and the quantitative relationship between feature needs and satisfaction.

**Keywords** Small assistant robot modeling · Kano model · Kansei engineering · Perceptual feature demand · Satisfaction

## 1 Introduction

There are many varieties of small assistant robots, ranging from personal applications to military applications. The traditional small assistant robot modeling design is mainly based on the designer's aesthetic consciousness. Donald Norman [1] pointed out that people's emotional experience with products is related to the level of brain activity. By quantifying the level of human emotional experience, the model design can be quantified.

---

Y. Yang (✉) · B. Wang · C. Jiang · Y. Cui · L. Song · X. Ma  
China Astronaut Research and Training Center, 100094 Beijing, China  
e-mail: [15313261462@163.com](mailto:15313261462@163.com)

Bi [2] drew an image scale diagram containing shape, color, and material and converted the perceptual image of the elderly user group into design elements. Based on the matching data of industrial robot appearance modeling and user preferences and emotional needs, Wang and Xiao [3] studied the mapping relationship between typical perceptual image vocabulary and industrial robot key modeling features. Li [4] used factor analysis and K-means cluster analysis to select perceptual vocabulary that conforms to the image of the product and then used gray correlation analysis to obtain the priority of modeling elements. Yao [5] carried out research on the modeling features and perceptual image demand of automobile headlights based on morphological analysis and Kano model and obtained the mapping relationship between the modeling features of automobile headlights and the user perceptual image demand level. Zhao [6] used eye tracker data acquisition and genetic algorithm to optimize the design of the car's front face and gave a behavior data-driven modeling design method.

However, the existing modeling research methods have the following problems: (1) lacks in-depth research on the difference of individual perceptual needs; (2) lacks quantitative research on the relationship between the degree of modeling perceptual feature and satisfaction. Satisfaction is the sense of pleasure after the demand is satisfied, and it is the relative relationship between the customer's expectation of the product or service in advance and the actual experience obtained after actually using the product or service. The higher the actual perception of the product than the expectation, the more satisfied, and otherwise the less satisfied.

Under the trend of personalized consumption, studying the needs of different individuals for external modeling will be the new direction of modeling research. Therefore, using the perceptual image vocabulary (PIV) research method and Kano model, this study is aimed at the modeling design of small assistant robots, collecting eye movement fixation times and fixation time and exploring different individual modeling needs. In addition, the quantitative relationship between modeling needs and satisfaction is also studied.

## 2 Methods

### 2.1 Subjects

The experiment was conducted in the Usability Laboratory of the Astronaut Center. We recruited a total of 40 participants, half male and female, aged between 24 and 40 years old, with normal or corrected vision. The academic qualifications of the subjects are all undergraduate and above, and they are familiar with smart products. All subjects have not been exposed to similar experiments. After the test, the subjects can get corresponding remuneration.

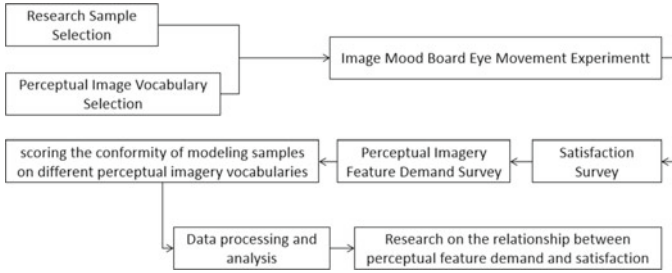


Fig. 1 Experiment flow

## 2.2 Experiment Process

The experiment is carried out as shown in Fig. 1.

The specific process is as follows:

### 2.2.1 Selection of Samples

In order to eliminate the impact of functional differences on follow-up research, the scope of the robot is constrained: fixed, with voice and display interaction, the outer contour is not more than 15 cm × 12 cm × 30 cm, and it is used in private life or workplace. Twelve small assistant robots were selected as the research samples (Fig. 2).

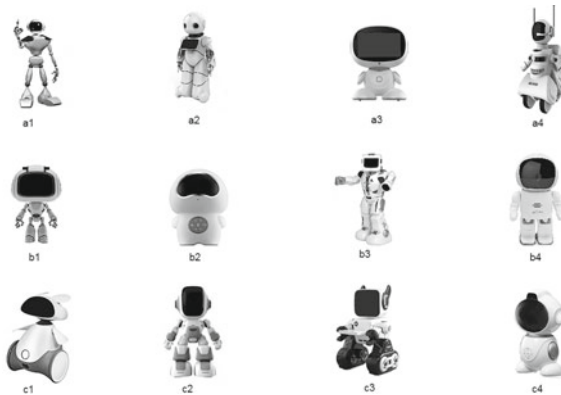


Fig. 2 Samples for this study

### 2.2.2 Collection of Perceptual Image Words

From related literature, 48 pairs of perceptual image word pairs were collected. Then, 40 subjects were invited to select the pairs of perceptual imagery vocabulary that they thought were suitable for describing the models of the small assistant robot and screened with 80% as the critical ratio. Finally, 12 pairs of perceptual imagery vocabulary were selected, including: (1) Smart versus Stiff; (2) Alienated versus Affinity; (3) Bored versus Interest; (4) Coordinated versus Awkward; (5) Cheap versus High-end; (6) Conservative versus Avant-garde; (7) Wisdom versus Clumsy; (8) Lively versus Stable; (9) Serious versus Cute; (10) Individualized versus Popular; (11) Cumbersome versus Concise; and (12) Untrustworthy versus Trustworthy.

### 2.2.3 Eye Movement Experiment

In this experiment, the research sample was used as the mood board materials, which can ensure that the subjects understand the meaning of the perceptual imagery vocabulary in the small assistant robot’s modeling range, and was more familiar with the research sample. The subjects were asked to express each material encoding that matched the perceptual imagery vocabulary, and at the same time, we collect their eye movement data.

We screened and counted the data to obtain 25 sets of valid data. The results showed that the subjective and objective experimental data had the same results (as in Example 1, shown in Fig. 3); for the same perceptual imagery vocabulary, the matching models selected by different subjects may be different (as shown in Fig. 4).

**Example 1** For the perceptual imagery vocabulary “smart,” the subject 33 subjective feedback matching modeling and eye-tracking results were both “a1” (a1 is the modeling code).

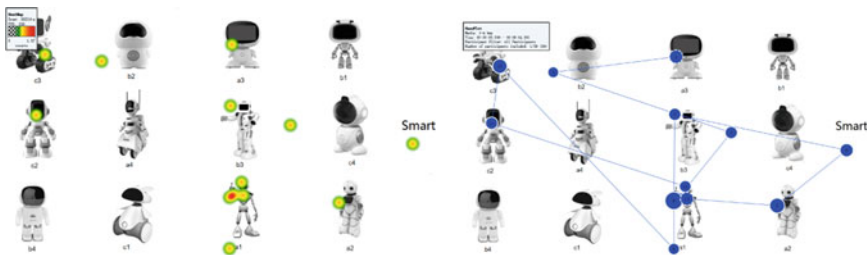
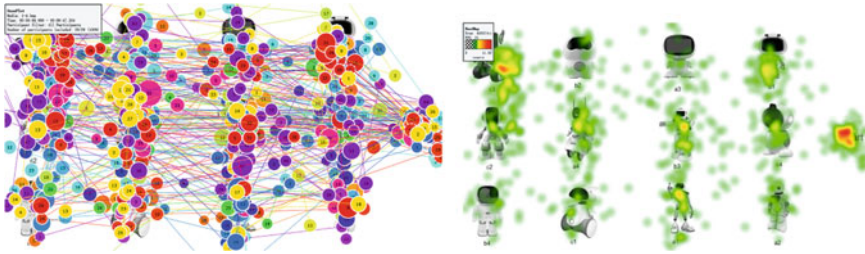


Fig. 3 Eye movement test results of subject 33



**Fig. 4** Eye-tracking data

**2.2.4 Modeling Satisfaction Survey**

Twelve encoded material pictures are arranged randomly. The subjects scored the satisfaction of the research samples. There are 21 grades; the higher the score is, the higher the satisfaction is.

**2.2.5 Perceptual Imagery Feature Demand Survey**

The subjects ranked the importance of perceptual image vocabulary and answered the positive and negative questions related to perceptual image vocabulary. According to Kano evaluation standard (Table 1), the subjects’ perceptual images were classified, and the perceptual features that had no effect on satisfaction results were screened out according to the definition of non-difference attributes (whether or not the features had no effect on satisfaction).

**Table 1** Kano evaluation standard

User’s attitude toward perceptual features		If the product does not have feature				
		Like	It should be so	Indifferent	Accept reluctantly	Dislike
If the product have feature	Like	Q	A	A	A	O
	It should be so	R	I	I	I	M
	Indifferent	R	I	I	I	M
	Accept reluctantly	R	I	I	I	M
	dislike	R	R	R	R	Q

### 2.2.6 The Conformity of the Modeling Samples on Different Perceptual Imagery Vocabularies

Twelve modeling samples and 12 pairs of perceptual image vocabularies appeared randomly. The subjects evaluated the conformity of modeling samples on different perceptual image vocabularies. Scores range from  $-3$  to  $+3$ , corresponding to two pairs of perceptual image words.

## 3 Results

Take the data of subject 33 as an example to analyze the quantitative results.

Perceptual imagery feature demand investigation experiment completed the attribute classification of perceptual imagery vocabulary, and the importance of each perceptual feature was assigned according to the ranking results of the importance.

Satisfaction is related to the availability of perceptual feature. The importance of each perceptual feature is different, and the impact on satisfaction is different. Therefore, to calculate the relationship between multiple features and satisfaction, it is necessary to convert the degree of possession of each perceptual feature into the same impact dimension. Satisfaction score was obtained from satisfaction survey. According to the perceptual imagery feature demand survey and the scoring experiment of the degree of perceptual imagery features, the importance and initial degree of perceptual features were obtained, respectively. The degree of perceptual feature is equal to the importance of perceptual feature multiplied by the degree of initial perceptual feature. Based on the Kano evaluation criteria, perceptual image vocabulary can be classified into three attributes related to satisfaction. Charisma attributes, expected attributes, required attributes, and the results were shown in Table 2. Attribute is a multi-dimensional variable, including different perceptual image features. The conformity of the attributes contains the degree of conformity of all perceptual intent features belonging to this attribute. Table 3 shows subject 33 evaluated the conformity of modeling samples on different attributes.

Suppose  $y = F(x_a, x_o, x_m)$ ,  $y$  is the calculated degree of satisfaction,  $x_a$  is the degree of conformity with the charm attribute,  $x_o$  is the degree of conformity with the expected attribute, and  $x_m$  is the degree of conformity with the required attribute. Curve fitting is carried out in MATLAB. Among the 25 sets of effective data in the experiment, each group is an independent satisfaction data because of the differences in personality, experience, aesthetic etc, the coefficient of the formula can be different in the formula of predicted satisfaction. If there are coefficients that make the formula true, it shows that the relationship between the degree of satisfaction and the multiple perceptual features can be calculated by this research method.

Taking subject 33 as an example, the formula for calculating satisfaction is:

$$y = 0.6869x_a + 0.1731x_o - 0.216x_m + 0.6494 \quad (1)$$

**Table 2** Perceptual imagery vocabulary survey results of subject 33

Perceptual feature	Attributes	Importance ranking	Importance of perceptual feature
Individuality	M	4	9/78
Smart	A	6	7/78
Interest	I	7	6/78
Trustworthy	I	12	1/78
High end	O	1	12/78
Affinity	I	10	3/78
Avant-garde	M	2	11/78
Cute	A	5	8/78
Concise	O	3	10/78
Wise	I	9	4/78
Stable	I	11	2/78
Coordinated	I	8	5/78

**Table 3** Conformity of each attribute and satisfaction value score of modeling

Modeling coding	Conformity of charm attributes ( $x_a$ )	Conformity of conformity attributes ( $x_o$ )	Conformity of required attributes ( $x_m$ )	Satisfaction ( $Y$ )
a1	21/78	6/78	60/78	15/21
a2	- 30/78	- 54/78	- 40/78	4/21
a3	9/78	- 4/78	29/78	18/21
a4	7/78	4/78	31/78	11/21
b1	- 30/78	- 34/78	- 40/78	13/21
b2	31/78	30/78	29/78	19/21
b3	- 30/78	- 8/78	- 22/78	7/21
b4	- 15/78	- 2/78	- 2/78	10/21
c1	31/78	32/78	29/78	17/21
c2	15/78	- 18/78	20/78	13/21
c3	22/78	14/78	13/78	17/21
c4	0	- 2/78	- 9/78	18/21

$R^2 = 0.6521$ ,  $F_{\text{Inspection value}} = 4.9977 > 1$ ,  $p$  (associated with significance probability) =  $0.0246 < 0.05$ , the formula holds. The satisfaction graph is as follows (Fig. 5).



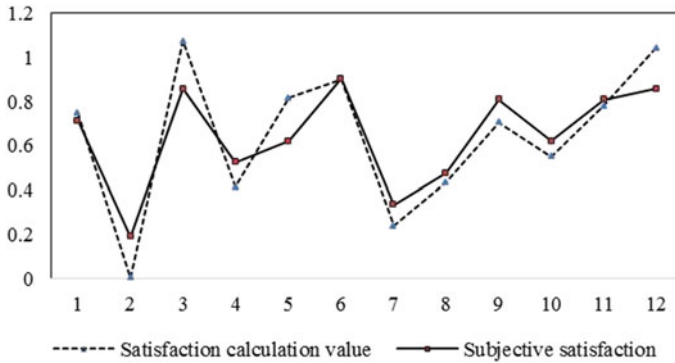


**Fig. 5** Satisfaction fitting curve of subject 33

## 4 Conclusions

It was verified that individuals have different perceptual needs for product modeling; for the same product modeling, individuals had different levels of perceptual feature and different satisfaction levels. Based on the Kano model, the individual's modeling feature needs were classified, and on this basis, it was found that the relationship between the perceptual feature needs and overall satisfaction can be expressed by. This study reveals the differences in individual's perceptual needs for external modeling and provides new ideas for further research on the quantitative relationship between perceptual feature and satisfaction, which has practical application significance for modeling design. The disadvantage is that this study can collect multi-source data, such as EEG, to further study its mechanism.

**Acknowledgements** This study was supported by the project SYFD160091812 and 61400040103.

**Compliance with Ethical Standards** The study was approved by the Logistics Department for Civilian Ethics Committee of China Astronaut Research and Training Center.

All subjects who participated in the experiment were provided with and signed an informed consent form.

All relevant ethical safeguards have been met with regard to subject protection.

## References

1. Norman Donald A (2005) Emotional design: why we love (or hate) everyday things. Basic Books, New York
2. Bi Y (2018) Modeling design of elderly accompanying robot based on perceptual engineering. *Packag Eng* 39(2):160–165
3. Wang X, Xiao W (2016). Research on modeling design of industrial robot based on perceptual image. *Mech Des* 33(08):117–120
4. Li L (2020) Research status and trend of modeling optimization design for product perceptual images. *Packag Eng* 41(2):65–79

5. Yao X, Yu X (2020) Research on the mapping characteristics of automobile headlights and user image under context semantics. *Packag Eng* 41(2):154–160
6. Zhao L (2012) Car front face modeling optimization design based on perceptual engineering. Northeastern University

# Model Evaluation of South Official Hat Chairs Based on Image Recognition Method



Hanzhou Qiu and Yun Liu

**Abstract** Furniture is the art of modeling. The beautiful modeling of a piece of furniture is the first condition for people to have a feeling of love and then be willing to buy or collect. When people observe the furniture, they scan and gaze at the parts of the elements quickly, process the information of “feature binding” in the human brain at the same time, and then make an overall evaluation of the furniture model. The detailed information of the conscious eye movement process can be obtained through the eye movement tracking experience. Based on this paper, an eye tracking experiment hot spot image is proposed, which uses digital image recognition processing method to extract relevant data for processing, analysis, and evaluation. The hot spot image can transform eye tracking data into two-dimensional color image, and image the number of fixation points, fixation duration, percentage of total time, scanning path and other data into color, transparency, and so on. Visual parameters are superimposed on the eye movement experimental stimulus material as the background, which is represented by “green yellow red” color mapping. The color features are extracted by “hue saturation brightness (HSV)” model, and the discriminant function model of shape evaluation is constructed to realize the aesthetic evaluation of the traditional furniture models of south official hat chairs.

**Keywords** Pattern recognition · Eye tracking · Furniture model · Overall evaluation · South official hat chairs

---

H. Qiu (✉)  
Ningde Normal University, Fujian 352100, China  
e-mail: [80706779@qq.com](mailto:80706779@qq.com)

Y. Liu  
Fuzhou University, Fujian 350108, China

## 1 Overall Perception of Furniture Model Based on Eye Tracking

In February 2018, Zhejiang University and Alibaba established a joint laboratory of intelligence, design, experience, and aesthetics. The IDEA Lab is committed to promoting the research and industrial application of human–computer natural interaction from three dimensions of design intelligence, experience computing, and perception enhancement. In the vision of the IDEA Lab, there is a new dimension in the field of design, which is AI [1]. If using the front camera of the mobile phone for eye movement analysis, it can break through the small sample data research in the laboratory research and invite the real user authorization, so as to analyze the big data of eye movement in the real use situation and construct an emotion calculation model with visual elements for optimization and expression, and then guide the designer to research users, find problems, and make clear the design needs, and then think about its function and content, etc., and then carry out user test, which is also a design loop in design practice [2]. The design of making the robot “understand emotion and aesthetics” is to turn the research related to human performance into a computable formula algorithm and then verify with data. For example, the color, angle, and geometric relationship distribution of graphic design can all affect human’s overall perception. In the same way, the preference evaluation of furniture model can also be obtained by extraction and analysis of big data.

## 2 Construction of Data Index System of Eye Movement Hot Spot Image Processing

Define the hot spot image as a 2D function and then transform it into a matrix for operation [3]. The color is sensed by the three basic characteristic variables of hue ( $H$ ), saturation ( $S$ ), and value ( $V$ ) [4]. Its components are relatively independent and independent of display equipment, and therefore, it is very suitable for color image processing. Thus, the RGB mode of the hot spot image is transformed into the HSV color model for color feature extraction. Because the eye movement hot spot image adopts the unified saturation and value, the two components are not distinguishable, and therefore, only the hue value is taken as the color feature, and the hue is generally described by the angle, its  $H \in [0, 360]$ , and the average value  $H$  of hue is taken as the index [5].

$$H = \frac{1}{N} \sum_{m=0}^N H_m \quad (1)$$

In formula (1):  $N$  is the total number of pixels in the hot spot image, and  $H_m$  is the hue value corresponding to the  $m$ th pixel (Table 1).

**Table 1** Statistical indicators based on grayscale histogram

Index name	Interpretation	Calculation formula
Gray mean value	Reflect the average gray level of the image	$\mu = \sum_{i=0}^{L-1} i P(i)$
Gray variance	Reflect the discrete distribution of image gray value	$\sigma^2 = \sum_{i=0}^{L-1} (i - \mu)^2 P(i)$
Skewness	Reflect the asymmetry degree of gray histogram distribution of image	$\mu_S = \frac{1}{\sigma^3} \sum_{i=0}^{L-1} (i - \mu)^3 P(i)$
Kurtosis	It reflects the gray distribution of the image when it is close to the mean value	$\mu_K = \frac{1}{\sigma^4} \sum_{i=0}^{L-1} (i - \mu)^4 P(i) - 3$
Energy	Reflect the uniformity of histogram gray distribution	$\mu_N = \sum_{i=0}^{L-1} P(i)^2$

### 3 Discriminant Function Model and Rule of Furniture Model Evaluation

#### 3.1 Linear Function Model Based on Fisher Discriminant

In essence, the evaluation of traditional folk furniture model can be classified as the problem of sample classification. The common method is to show a group of pictures of the furniture to be evaluated. Through observation or measurement, the furniture models can be divided into several evaluation levels, such as “like”, “OK”, and “dislike”. In practical application, the research samples are divided into two categories, which is also known as binary classification problem [6].

Fisher discriminance [7] is the most suitable method for binary discriminant analysis, which basically has no requirement for sample data and is a method with high accuracy and widely used in practice. In terms of coordinates, it uses the method of projection to reduce the d-dimensional features to only one dimension, that is, to project the samples of multi-dimensional space on a straight line in a certain direction so as to minimize the differences of similar samples [8].

Such as the training sample set  $X: X = \{X_1, X_2, \dots, X_n\}$ ; each sample is d-dimensional, set one group of samples (category w1) from the whole as  $X_1 = \{x_1^1, x_2^1, \dots, x_{n_1}^1\}$ , set the second group of samples (category w2) as  $X_2 = \{x_1^2, x_2^2, \dots, x_{n_2}^2\}$ , and set the samples after projection as  $y_i = w^T x_i, i = 1, 2, \dots, n$ .

At first, the mean vector of each sample of the original multi-dimensional sample space is calculated as:

$$m_i = \frac{1}{n_i} \sum_{x_j \in X_i}^{i=1,2} x_j \tag{2}$$

In formula (3),  $n_i$  is the number of samples.

The dispersion matrix among samples in each group can be defined as:

$$S_i = \sum_{x_j \in X_i}^{i=1,2} (x_j - m_i)(x_j - m_i)^T \tag{3}$$

The overall dispersion matrix in the group is

$$S_w = S_1 + S_2 \tag{4}$$

the values of (3) and (4) shall be as small as possible during discriminance:

The inter-group dispersion matrix is:

$$S_b = (m_1 - m_2)(m_1 - m_2)^T \tag{5}$$

the value shall be as high as possible during discriminance;

After projection, multiple dimensions are transformed to be 1D space, and the mean of the two categories is:

$$\tilde{m}_i = \frac{1}{n_i} \sum_{y_j \in y_i}^{i=1,2} y_j = \frac{1}{n_i} \sum_{x_j \in x_i}^{i=1,2} w^T x_j = w^T m_i \tag{6}$$

While the intra-group dispersion matrix is transformed to be one value:

$$\tilde{s}_i = \sum_{y_j \in y_i}^{i=1,2} (y_j - \tilde{m}_i)^2 \tag{7}$$

The overall intra-group dispersion matrix is:

$$\tilde{S}_w = \tilde{S}_1 + \tilde{S}_2 \tag{8}$$

The inter-group dispersion matrix is:

$$\tilde{S}_b = (\tilde{m}_1 - \tilde{m}_2)^2 \tag{9}$$

After calculation on the basis of the principle of minimizing the intra-group variance and maximizing the inter-group variance, the following Fisher's criterion function can be obtained:

$$\max J_F(\omega) = \frac{\tilde{S}_b}{\tilde{S}_w} \quad J_F(\omega) = \frac{|m_1 - m_2|^2}{S_1^2 + S_2^2} = \max . \tag{10}$$

The biggest solution of  $J_F(\omega)$  is the best vector and Fisher’s linear discriminant.

### 3.2 Sample Classification and Characteristic Index of Furniture Models

One group of furniture models of the same category are divided into two categories: i.e.,  $G_1$  very like, and  $G_2$  dislike. By further compare the furniture models of the two categories, the discriminative method of which the modeling aesthetics is more suitable for the user is concluded and it can be used for the prediction and analysis of the modeling aesthetics of other similar or newly designed furniture. Thus, based on Fisher’s linear discriminant principle and criterion, the following definitions are given:

Definition 1: suppose a set includes  $n$  furniture samples,  $A = \{A_1, A_2, A_3 \dots A_n\}$ , taking the statistical data of color features and gray histogram features of the eye movement hot spot image of furniture models as indicators, and the feature set is  $X = \{X_1, X_2, \dots, X_6\}$  wherein:  $X_1$  is gray mean ( $\mu$ );  $X_2$  is gray variance ( $\sigma^2$ );  $X_3$  is skewness ( $\mu_S$ );  $X_4$  is kurtosis ( $\mu_K$ );  $X_5$  is energy ( $\mu_N$ );  $X_6$  is hue mean ( $\overline{H}$ ). The values above constitute a feature matrix of 6 rows and  $n$  columns.

$$\begin{bmatrix} X_{11} & X_{21} & X_{31} & \cdots & X_{n1} \\ X_{12} & X_{22} & X_{32} & \cdots & X_{n2} \\ X_{13} & X_{23} & X_{33} & \cdots & X_{n3} \\ X_{14} & X_{24} & X_{34} & \cdots & X_{n4} \\ X_{15} & X_{25} & \cdots & \cdots & X_{n5} \\ X_{16} & \cdots & \cdots & \cdots & X_{n6} \end{bmatrix}$$

For the furniture  $j$  with the modeling  $A_j \in A$  in a category, its feature value is  $\{X_{j1}, X_{j2}, X_{j3}, X_{j4}, X_{j5}, X_{j6}\}$ , It can constitute a 6D feature vector,

$$X_j = (x_1, x_2, x_3, x_4, x_5, x_6)^T \tag{11}$$

According to the 6 feature values, for the evaluation of the furniture model  $A_j$ , it can be judged to belong to category  $G_1$  or category  $G_2$ .

Definition 2 construct the linear discriminant function facing furniture model, its form is

$$u(x) = a^T x = a_1x_1 + a_2x_2 + a_3x_3 + \cdots + a_6x_6 \tag{12}$$

In formula (12):  $u(x)$  is the discriminant value,  $x_1, x_2, \dots, x_6$  are the 6 feature values based on the hot spot image of the furniture models of a category,  $a_1, a_2, \dots, a_6$  are discriminant coefficients and the weights of the discriminant feature values. The

following decision-making rule is used for the binary classification judgment of the furniture models:

$$u(x) = \begin{cases} < 0 & S \text{ belongs to } G_1 \\ > 0 & S \text{ belongs to } G_2 \\ = 0 & \text{belongs to any category above or rejects classification} \end{cases} \quad (13)$$

## 4 Design of Experimental Method for the Evaluation of Traditional Folk Furniture Models in Eastern Fujian

### 4.1 Selection of Training Samples and Related Eye Movement Hot Spot Images

It is confirmed that the furniture models of each category can be classified as very like ( $G_1$ ) and dislike ( $G_2$ ).

Eye movement experiment is carried out with the subjective scale for the purpose of visual aesthetics. The mean value and median value of preference of all samples of each group are used as the reference; the samples with the highest and lowest scores in each group are selected as training samples; and the eye movement hot spot images of these samples are extracted for feature analysis.

### 4.2 Feature Data Extraction of Eye Movement Hot Spot Images of Training Samples

Based on MATLAB software [9], take a group of samples as the example to extract the features of digital graphic processing of the eye movement hot spot images of the two training samples with the highest and lowest scores of preference. The two training samples both have eye movement hot spot images of 15 subjects, which are generated by eye movement instrument, and the process is as follows:

1. Subtract with the generated eye movement hot spot image and its original image without hot spot to remove the background of the training materials [10] and carry out quantization and coding to color information and extract the hue value;
2. Process the pure hot spot color image of which the background is removed into a gray image and then further transforms it into a gray histogram;
3. Extract the feature indexes of the eye movement hot spot images of 15 subjects and then make the statistical table according to the scores of preference from high to low.



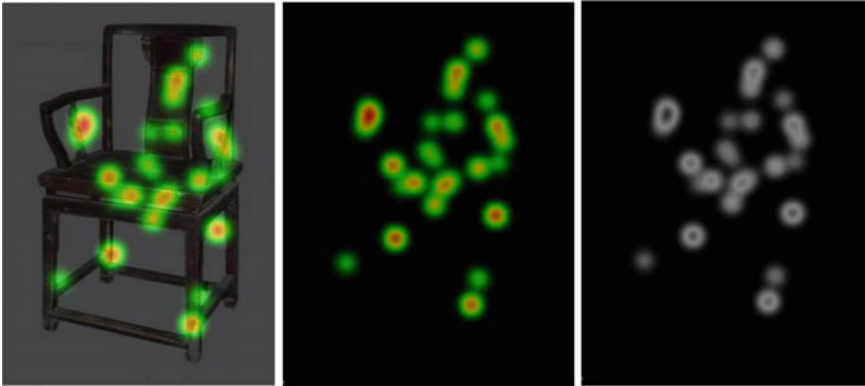


Fig. 1 Hot spot peeling and gray effect of training sample No. 1

## 5 Establishment and Verification of Discriminant Function Models for the Evaluation of Traditional South Official Hat Chairs in Eastern Fujian

### 5.1 Selection and Feature Extraction of Eye Movement Hot Spot Image

The experiment result shows that the mean value of preference of all samples is 0.47 and the median is 0.43. The highest and lowest scores are 1.00 (original sample 6) and 0.13 (original sample 5), respectively, which are of typical significance. They are selected as training samples and numbered No.1 and No.2, respectively. Background removal and gray processing are carried out to all subjects' eye movement hot spot images about these two pieces of furniture, and the processing effect is shown in Fig. 1.

After processing the 15 subjects' eye movement hot spot images, the statistical value of the feature index is shown in Table 2.

### 5.2 Establishment and Test of Discriminant Function Model

(1) Establishment of the discriminant function model

In the R software environment, call the function `discriminant.fisher()` to write [11], and input Table 2 as the training sample. The obtained discriminant equation is as follows:

$$u(x) = 0.6188x_1 - 0.0037x_2 + 0.3895x_3 - 0.0118x_4 - 12.6449x_5 - 0.2055x_6$$

**Table 2** Analysis results of training sample No. 1

Subjects	$X_1 = \mu$	$X_2 = \sigma^2$	$X_3 = \mu_S$	$X_4 = \mu_K$	$X_5 = \mu_N$	$X_6 = H$
1	1.9644	69.3177	11.4361	145.2446	0.9284	4.2064
2	3.5503	179.4820	6.4695	45.3709	0.8587	8.6251
3	3.1027	153.6397	8.0989	79.3796	0.8743	7.5593
4	2.7971	119.8173	7.9331	70.5355	0.8817	7.2676
5	3.2902	186.7135	7.4103	62.9334	0.8875	6.8390
6	3.2882	148.2194	6.8577	51.8819	0.8510	9.2948
7	4.0515	203.6368	6.2889	48.0101	0.8190	11.4977
8	4.2516	219.9634	5.7513	35.6603	0.8043	12.2386
9	2.7984	111.2022	8.0369	73.7647	0.8638	8.4157
10	2.4817	104.0897	8.8596	87.6951	0.9072	5.5102
11	4.3621	245.9518	5.5940	32.7950	0.8254	11.0471
12	3.3764	155.8286	6.7426	50.0881	0.8444	9.7430
13	2.8831	105.9707	7.5537	66.2359	0.8461	9.7067
14	3.6050	163.6870	6.6256	49.3398	0.8159	11.4926
15	3.8575	218.9424	6.4405	47.7556	0.8595	8.5999

It is the discriminant of category II of the models of south official hat chairs. Take 0 as the dividing point to carry out the eye tracking test for the user and substitute the feature values of his hot spot image into the discriminant equation. If the score is greater than 0, it indicates that the user does not like the chair, and if the score is less than 0, it indicates that the user likes the chair.

(2) Test of the discriminant function model

Select the models of south official hat chairs as the samples to test the above function models, and process the tested hot spot image and extract the feature values according to the above process. Compare the results with those of SD scale (-2 ~ 2). The T-test results of the independent samples show that  $P = 0.079$ , and there is no significant difference in the results.

## 6 Conclusion

The traditional folk furniture in eastern Fujian has rich and beautiful modeling, ingenious structure, elegant and popular decorative theme and exquisite and restrained expression which condenses the aesthetic emotion and rich philosophy of the local people. The inheritance of design of these design ideas is the contemporary expression of regional culture. According to today's life and consumption style, it shall not only absorb its classic modeling form, but also pay attention to the understanding,

expression, and sublimation of the regional cultural symbols, and use more accurate and richer design forms to awaken people's memory and sense of identity of the traditional culture, so that the traditional ideas and modern design and life can complement each other.

**Acknowledgements** This work is supported by the study on the protection planning and cultural heritage of ancient villages in eastern Fujian and study on the regional landscape characteristics of Ningde City, No. (15XGL027), No. (2016Z16).

**Compliance with Ethical Standards** The study was approved by the Logistics Department for the Civilian Ethics Committee of Ningde Normal University.

All subjects who participated in the experiment were provided with and signed an informed consent form.

All relevant ethical safeguards have been met with regard to subject protection.

## References

1. Guanfu Museum (2018) Robot "Berenson" [EB/OL]. [https://www.sohu.com/a/223173584\\_](https://www.sohu.com/a/223173584_). 19 Feb 2018
2. International design and Research Institute of Zhejiang University. Zhejiang University Alibaba idea lab established [EB/OL]. <https://www.idi.zju.edu.cn/?P=2943>. 10 Feb 2018
3. Andrienko G, Andrienko N, Burch M, Weiskopf D (2012) Visual analytics methodology for eye movement studies. *IEEE Trans Visual Comput Graphics* 18(12):2889–2898
4. Hyoense J, Radach R, Deubel H (2003) The mind's eye: cognitive and applied aspects of eye movement research. Elsevier Science BV, Amsterdam, Netherlands, pp 13–15
5. Djamasbi S, Siegel M, Tullis T, Dai R (2010) Efficiency, trust, and visual appeal: usability testing through eye tracking. In: Proceedings of the forty-third annual Hawaii international conference on system sciences (HICCS). Computer Society Press, pp 1–10.
6. Keping W (2015) Digital image processing (matlab version). Mechanical Industry Press, Beijing, pp 62–72
7. Tao Z (2014) MATLAB image processing programming and application. Mechanical Industry Press, Beijing, pp 142–159
8. Shan Wu (2009) Emotional research on furniture form elements. *Beijing Forestry University* 10:65
9. Wang EM-y, Lin H-y (2009) A comment on the Ming dynasty chair from modern ergonomics thinking. Beijing, China
10. Nan J (2015) Research on Chinese modern furniture from the perspective of design principle inheritance. Jiangnan University
11. Xihui L (2000) Research on Chinese folk furniture. Jiangnan University

# Design of College Student Luggage Based on User Experience



Xiao Han, Ting Dong, Dongli Wang, and Xin Chen

**Abstract** It aims to redesign the college student luggage by surveying local college students' luggage usage habits and introducing the method of user experience trip in service design. The study used questionnaire, external observation, participatory observation and indirect observation methods. Use the customer journal map to visualize the user needs and experience process. Identify typical user roles, and summarize design opportunities. Clarify the characteristics and needs of college students in the process of using luggage, and propose a more usable luggage design plan to meeting the habits of college students. In the process of researching user needs, while meeting the basic requirements for product usability, we should pay more attention to the user's emotional needs in the process of using the product. Design product functions from the perspective of users' psychological feelings and behaviors as much as possible to make product services more suitable for user needs.

**Keywords** User experience map · Service design · College student · Luggage

## 1 Introduction

As a large group with frequent cross-regional exchanges, the demand for luggage products by college students is increasing [1]. In recent years, the user groups and user scenarios of luggage have been subdivided. But college students, as an important user group of luggage products, have not received enough attention. At present, the solutions proposed by domestic and foreign product manufacturers to the traditional luggage pain point research institutes are highly homogenized and cannot be well applied to the current status of domestic college students' travel [4]. For this reason, it is necessary to research the characteristics of the college students and find their unique needs in the process of using the product in order to achieve a better using experience.

---

X. Han (✉) · T. Dong · D. Wang · X. Chen  
Jiangsu University, Zhenjiang 212000, China  
e-mail: [501386528@qq.com](mailto:501386528@qq.com)

© The Editor(s) (if applicable) and The Author(s), under exclusive license to Springer Nature Singapore Pte Ltd. 2021

S. Long and B. S. Dhillon (eds.), *Man-Machine-Environment System Engineering*, Lecture Notes in Electrical Engineering 645, [https://doi.org/10.1007/978-981-15-6978-4\\_52](https://doi.org/10.1007/978-981-15-6978-4_52)

## 2 User Experience Design and Customer Journal Map

User experience was proposed by interaction design expert Donald Norman, which refers to the purely subjective experience established by users in the process of using the product. In the context of technology development and consumption upgrade, the form of technological innovation is changing. User experience is more concerned by designers and consumers, that is, how products or services connect with users and play a role, and how people “contact” and “use” products [3]. The service experience is composed of service contacts, presented by service contacts [8]. User experience design methods can help designers better grasp the commonality of specific users on the experience level, bringing better user experience and stronger user stickiness to products.

Service design emphasizes the design of service experience for different service contacts of the target user. Sort out the user touchpoints during product use, using the UX journey method [9]. The user journey map used in this way is a form of visualizing flowcharts to show the user needs and experiences in the service process. The most important thing is the user’s behaviors and psychological feelings during the process [7]. The corresponding touch points, emotions, and pain points are integrated to identify pain points and find opportunities for product design.

### 2.1 User Analysis and Role Building of College Students

A questionnaire survey for students of Jiangsu University was used to investigate the use of luggage among college students. In March 2019, 206 questionnaires were issued through the online questionnaire. Statistics and analysis of the questionnaire data can draw some conclusions.

- The luggage size of the respondents is mainly 24–28 inches, and the price is less than 550 yuan. They have higher requirements on the durability and aesthetics of the products. In terms of storage, most people said that they would classify and place the items, and the bulge of luggage pull rod in the interior and the storage of shoes often bothered them.
- In terms of use, majority of respondents said that they had encountered the situation that the luggage was inconvenient to carry when traveling, and when the luggage was not in the sight range, they would worry about financial safety, with an average score of 4.87 in the 7-level Likert scale. When they need to pick up things from the suitcase, inconvenient opening and closing the suitcase and worrying about being seen by others are their main concerns.
- Cross-analysis of suitcase usage habits based on user gender can also see the difference: Female users have more suitcases than men. They prefer to use personalized identification stickers to improve suitcase recognition; men’s luggage is generally slightly larger than women’s, and they are more inclined to identify the suitcase by its shape. In the use of shelves when traveling by high-speed rail, female

respondents are often troubled by the weight of the luggage, while men are often troubled that the size of the luggage is too large to be placed on the shelves. Among college students participating in the questionnaire, women have higher concerns about financial security and personal privacy than men (Fig. 1).

The method of establishing user roles can reduce the risk of designers relying on subjective speculations to provide a basis for understanding the real needs of users, better serving different types of users [2]. Analyzing the survey results can cluster users, identify typical users of college students' luggage, and determine user roles. After a preliminary investigation, it can be seen that college students often use backpacks and handbags when traveling with luggage. Electronic products are used more frequently. In the school dormitory environment, the luggage also plays a storage function (Fig. 2).

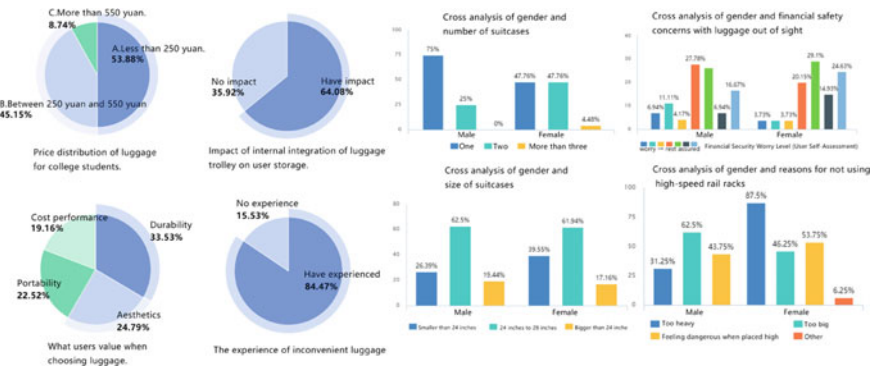


Fig. 1 Data analysis of some questionnaires

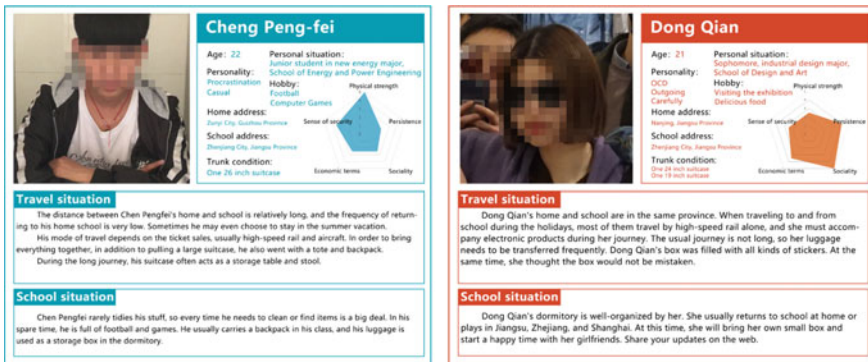


Fig. 2 Typical user portrait of college student luggage

## 2.2 Construction of University Students' Luggage Customer Journey Maps and Pain Points and Opportunities

The customers' journey map covers the user journey stages, requirement, behavior, emotion, pain point, and opportunity point. By integrating these elements in the journey map, designer can clearly see the corresponding relationship between the elements and it is easy to find out the design opportunity points in the product use process. The behavior of users in the context of returning home and school is mainly divided into three stages: packing up, using and moving, and dormitory storage (Fig. 3).

According to the user journey map, we can conclude that for Chen Pengfei, the problem of sorting, moving, and accessing luggage is the main reason for depression. For Dong Qian, the handling of the suitcase and the financial security in a

### Customer journal map

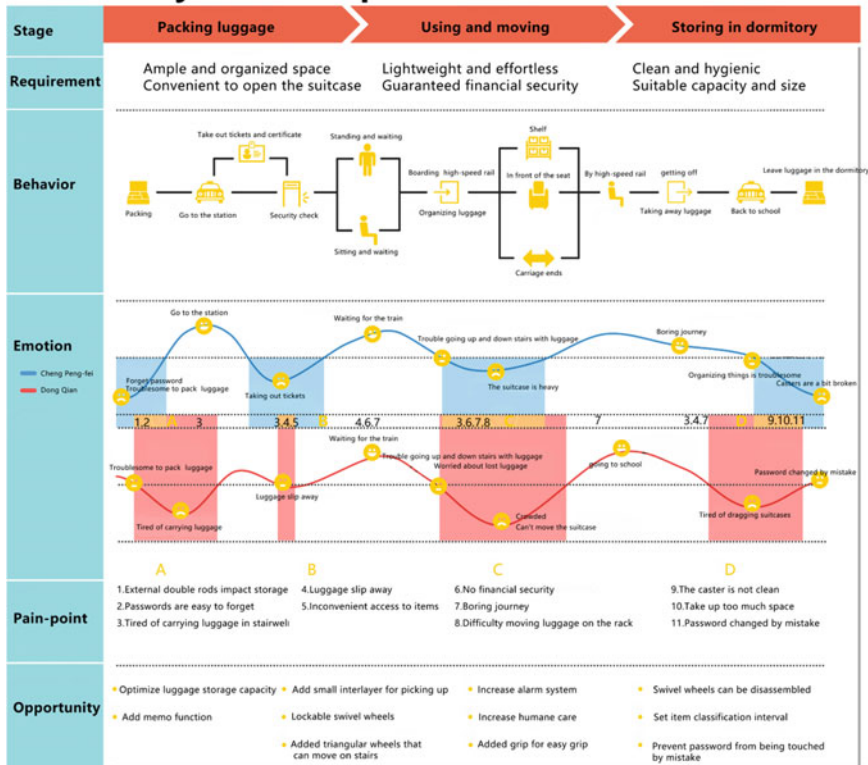


Fig. 3 Customer journal map for typical user

crowded environment will greatly reduce her experience. We can find design opportunities from customer journal map and consider design improvements in terms of luggage storage, storage, handling, alarming, and improving the compatibility of the dormitory environment.

### 2.3 In-Depth Research

Focus on user pain points and product design opportunities to conduct in-depth research on users and luggage products on the market.

#### 1. In terms of storage items

In the previous questionnaire survey, most users indicated that items would be classified and stored. In order to understand the classification habits of users, we used thinking aloud to observe the classification and storage process of eight typical users in the context of returning home and school. Thinking aloud is widely used in the study of the thinking process of specific groups of people, and it can reflect the thinking process of the user in a specific working state [10]. After certain training and habitual thinking methods, users can choose their own types of luggage and place travel items in accordance with their storage habits. At the same time, investigators record the thinking process and count the types and placement of objects after completion position (Fig. 4).

#### 2. In terms of using and moving

Through the full-participation observation method, take the high-speed rail to Shanghai and from Zhenjiang to learn about the user’s experience during the trip. According to the previous questionnaire survey, we learned that users have high

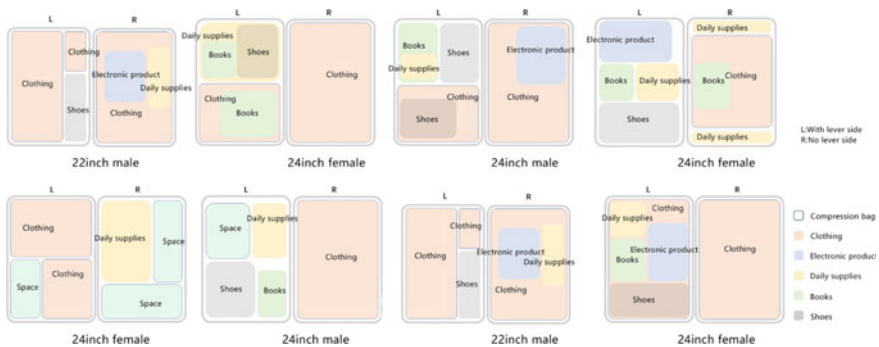


Fig. 4 Luggage item storage classification chart by thinking aloud





**Fig. 5** Visualization of damage observations

requirements for the durability of the luggage, and the damage to the luggage mainly comes from the handling process. Choose to indirectly observe the damage signs of the luggage to trace and understand the possible sources of injury during the transportation process [5] (Fig. 5).

### 3 Product Improvement Innovation

The innovative design of the luggage described in the article is targeted at the group of college students who shuttle between home and school frequently. The shape of it meets the taste of young people. The product is more convenient to handle and use, adding intelligent functions. Product innovation design is based on user experience.

#### 3.1 Design Concept

The product concept is based on the research results and design innovation. Using structural design knowledge and brainstorming methods in combination with existing luggage design concepts, mainly by raising the crests, filling the emotional troughs and optimizing the critical moments of contact with customers User experience.

According to the collation results after the storage by the think-aloud observation, no particularly obvious commonality in storage habits was found. Therefore, more consideration is given to the planning of the internal space to make the internal space of the luggage more regular.

In terms of accessing items, most of the interviewees said that they need to temporarily access items such as certificates and ticket manuals during the trip. Considering the situation of the external tie rod, there will be a small amount of flat space for the tie rod and the luggage. So that designers set a small mezzanine between

the two levers to facilitate the user's access to ticket. The opening and closing position of the luggage is shifted away from the side of the tie rod. This way of opening the luggage allows the luggage to be used in a smaller space, which meets the needs of the user in schools with high traffic or limited space. Open and closed suitcase needs in the dormitory scenario.

The inconvenience of the luggage in moving is mainly reflected in two aspects: weight and poor placement. The weight mainly comes from the difficulty of reducing the weight of the items stored by the user. Combined with previous research, the price of luggage purchased by college students is mainly concentrated below 550 yuan, which is a mid-to-low-end positioning on the market. So, designers could not add the self-driving and auto-following design. In order to optimize the man-machine relationship of the suitcases moving up and down from the high-speed rail racks, designers utilize the mezzanine bottom space of the external pull rod to increase the handle. Designers flatten the top of the luggage by using soft handles and recessing around the top, in order to optimize the luggage experience as a storage table and seat during the user's journey.

From the collected damage traces of the luggage, we learned that the most severely damaged portion of the luggage is the universal wheel. The damage mainly comes from bumps during dragging and shocks similar to violent consignment, and it is mainly caused by bumps and scratches which concentrated on the four corners of the box away from the rod. Designers avoid this kind of shock by locking and retracting the caster; at the same time, the shrinkable universal wheel is beneficial to meet the cleaning requirements of storage in the dormitory environment.

Although the concept of a luggage design with its own power supply and intelligent services has emerged, such designs can easily reduce the durability of the luggage and are more difficult to implement in the market positioning that users generally choose. We are considering designing a functional accessory for the luggage, which can be installed on the top of the luggage to provide electrical power for the user's electronic equipment, as well as provide the luggage positioning alarm function.

According to the situation of college students returning from home to school, they have strong independence and are usually a person traveling. They are prone to loneliness during the journey due to the change in the social circle accompanying the change of location. It can meet the hidden needs of users through the modeling semantics of "companion" and certain functional services, and pass the emotional care of products to users [6] (Fig. 6).

### ***3.2 Product Design Presentation***

Based on the above design concept, on the basis of the original luggage structure model, the three-dimensional modeling software *Rhino* and *Creo* were used to model the structure of the product, and the material and model were given in combination with the renderer *KeyShot* to derive the product rendering.

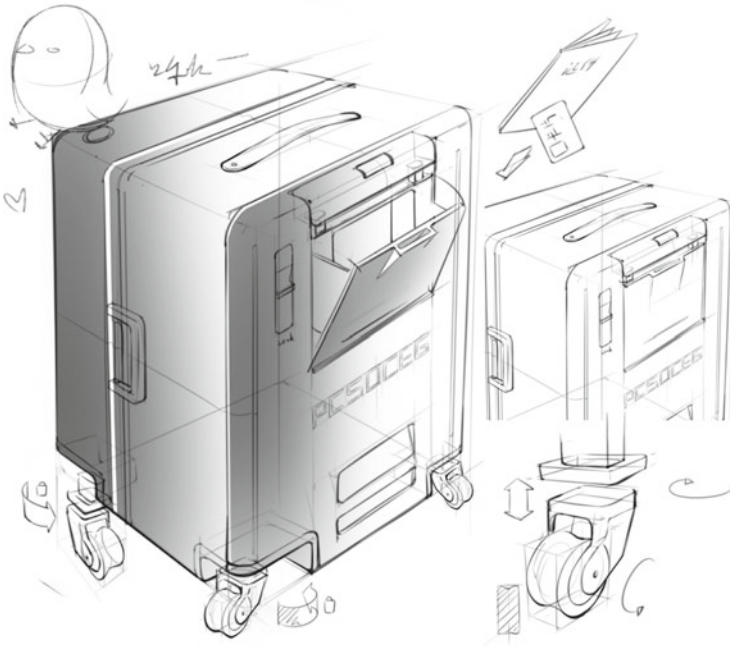


**Fig. 6** Product concept sketch

The main design point of the product is to optimize the product storage space and the picking and carrying function by asymmetric opening, external tie rods, and the use of external tie rods to set the pickup sandwich, and use the method of locking and retracting the universal wheel to enhance luggage. The durability of the box, combined with smart accessories, provides users with location alarms and travel care (Fig. 7).

## 4 Summary

User experience is a new category in the field of product design in recent years. Based on the user experience journey method, designers can understand users more comprehensively and intuitively. They are able to propose product designs centered on the user. This article studies the questionnaire method and interview method, and observation conducts user surveys to identify typical users. Combined with the customer journey map method, the user's behaviors, emotions, and requirements are analyzed, the pain points of the user in the process of using the product are sorted out, and the product design opportunities are explored. From the user's perspective,

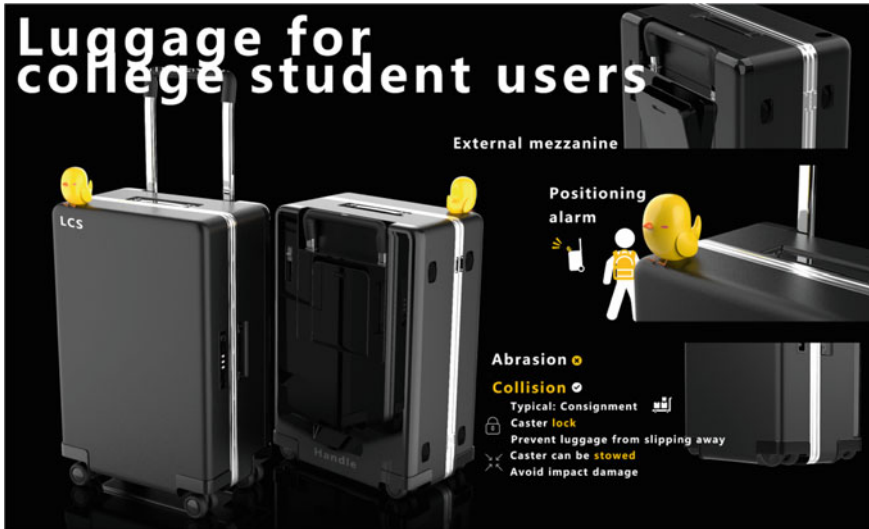


Fig. 7 Product illustration

the luggage design scheme for college students is proposed, which provides a reference for the future user’s more segmented luggage product design, which has good practical significance.

**Acknowledgements** Funded projects. 2019 Zhenjiang Key R&D Program (Social Development) “Research on VR, AR and 3D Printing Technology Application for Jiao Shan Inscriptions”.

**Compliance with Ethical Standards** The study was approved by the Logistics Department for Civilian Ethics Committee of Jiangsu University.

All subjects who participated in the experiment were provided with and signed an informed consent form.

All relevant ethical safeguards have been met with regard to subject protection.

## References

1. Chen X-c, Li H (2017) An analysis of tourism demand characteristics and market status of college students. Ability and Wisdom 2017(16):36
2. Dai L-n (2016) (2016) Design Research. Publishing House of Electronic Industry, Beijing, p 8
3. Garrett JJ (2019) The elements of user experience: user-centered design foe the web and beyond. Beijing: Mechanical industry press, p 8
4. Guo P-c, Wang Y, Yang F (2019) Design and study of multifunctional luggage for “north drifting” tenants. Ind Des 10:45–46
5. Hu F (2010) Explore the customer’s need: user research methods and applications. Beijing, China Architecture & Building Press, p 8
6. Lan Y-q, Pai L (2019) Research on emotionalization of interactive products based on user experience. Packag Eng 40(12):23–28

7. Li S-d, Ding Z-c (2018) *An introduction to service design*. Tsinghua University Press, Beijing
8. Wang X (2019) Design makes intangible services perceived. *Art Res* 05:70–71
9. Wang Y-m, Hu W-f, Tang J, Liang Q (2016) Travel postcard service design based on user experience trip. *Packag Eng* 37(22):158–163
10. Zhai M, Mou X (2017) The application of thinking aloud method in the listening and speaking teaching of college English. Atlantis Press, Paris, pp 272–274

# The Usability of Advance Intersection Lane Control Signs at Intersections



Leibing An, Jun Ma, and Dan Zhao

**Abstract** *Objectives* To examine what and how factors affect the usability of Advance Intersection Lane Control (AILC) signs. *Method* The naturalistic driving test method and the eye tracker system were used to collect data of drivers using AILC signs and arrow markings. A binary logistic regression model was established to identify contributing factors of the usability of signs. *Results* The usability of signs is positively correlated with the need of lane change, the number of lanes, and the number of vehicles lined up in front, while negatively correlated with the lateral distance between driver and sign and the use of arrow markings. The eye movement data of drivers using AILC signs are significantly different from those of using arrow markings by t-test: Drivers spend a shorter time in using signs, which means that the efficiency of signs is higher than that of markings. However, the utilization rate of signs is lower. *Conclusions* AILC signs convey information efficiently but are ignored frequently for the improper position. It is suggested that we can improve the self-explaining properties of roads or change the form of signs to upgrade guide services provided by the road environment.

**Keywords** Usability of traffic sign · Naturalistic driving · Advance intersection lane control sign · Situation awareness

## 1 Introduction

Drivers face three stages of decision-making when approaching an intersection: driving route choice, lane choice, and driving operation. First, drivers make choices among the different routes depending on the destination. Then, they decide to choose a specific lane to go straight or make a turn. Finally, drivers take appropriate operation based on the traffic condition. Among them, if lane choice is not smooth, it may impact on route choice and lead to driving errors [1].

---

L. An · J. Ma (✉) · D. Zhao  
People's Public Security University of China, Beijing 100038, China  
e-mail: [majun1963@163.com](mailto:majun1963@163.com)

Lane choice problems are related to factors such as lane configuration and traffic facilities. In the wake of increasing measures such as setting multiple left-turn lanes to reconstruct intersection to solve heavy traffic jams, roads lost regularity, consistency and became unpredictable [2]. It is related to the concept of “self-explaining road” which means drivers would develop expectations of the road without additional explanation for the fixed pattern [3]. And the expectations are based on the schemata and good situation awareness drivers developed in their brain when they encounter a relatively certain and easy situation, which may lead to correct driving behaviors [4, 5]. However, because of the uncertainty and irregularity of current road environments, drivers can no longer form predictions about the road, because the complicated situation could not help them to develop clear schema in their brain [6]. Drivers must rely on traffic signs and other facilities, which inform drivers to take actions that are necessary for the situation ahead [7]. This prior knowledge is essential for safe driving, especially on roads lacking self-explanation. The road environment, especially road sign, is increasingly important in the study of the driver–vehicle–environment system [8].

Advance intersection lane control (AILC) signs are the most commonly used signs on urban roads in China. These signs are usually cantilevered and indicate the configuration of all lanes ahead [9]. In the past, most studies focused on the visibility of signs including text, color, and other characteristics [10–12], while usability is a broader concept involving form and other characteristics of signs affecting driver’s psychology. Drivers always ignore traffic signs which are located improperly and make good visibility of signs meaningless [13].

Usability is a significant concept in ergonomics. The definition given by the IEEE (1990) is as follows: Usability is the convenience for users to learn the operation of a system or component, prepare inputs, and interpret outputs [14]. According to ISO 9241, usability includes effectiveness, efficiency, and satisfaction [15]. Traffic signs provide drivers with guide services. From the perspective of usability, the effectiveness of signs focuses on results, which means they should effectively guide drivers to accomplish driving tasks; efficiency emphasizes that the process of acquiring sign information takes a short time.

Based on a long-term investigation, this study put forward the following hypotheses: a. The effectiveness of the AILC sign is weak, and the utilization rate of it is low. b. The effectiveness of AILC signs is correlated with the number of lanes, the use of arrow markings, etc. In the case of multiple lanes (especially more than four), drivers in the fast lane rarely use AILC signs but use arrow markings. c. Although drivers often use arrow markings, the efficiency of arrow markings is lower than that of AILC signs. Arrow markings are not an ideal alternative to AILC signs.

## 2 Data Collection

### 2.1 Naturalistic Driving Test

The naturalistic driving test and eye tracker system were employed with ErgoLAB multimodal data synchronization cloud platform to collect relevant parameters of using facilities during driving. A total of 12 drivers with normal vision were recruited, and all of them had a driving age of more than one year. They were unfamiliar with the experimental route. No mobile navigation equipment was allowed during driving. Eye movement data of drivers were recorded at a frequency of 30 times per minute, and the road condition was recorded synchronously (Fig. 1). There were two personnel monitoring data in the test vehicle to ensure that the equipment was running normally and recording the driving events. After driving, drivers completed a questionnaire to collect basic information such as age and gender. Then drivers watched the driving replay to recall the psychological activities while driving and were asked some questions about the process.

The test required drivers to follow the given route, with a total length of 15.9 km, passing seven arterial roads, three sub-trunk roads, and two branch ways. Drivers needed to turn left five times, go straight through intersection 24 times, and turn right once; and the route contained 28 signalized intersections and two unsignalized intersections. There were 14 intersections with AILC signs and 16 without AILC signs. The distribution of AILC signs was as shown in Table 1.

The eye tracker equipment was greatly affected by the sunlight, and the missing and abnormal values of eye movement data were removed. After processing, the eye movement data of seven drivers (including 102 records of using facilities) were valid samples. We also collected environment information and behavior of drivers.

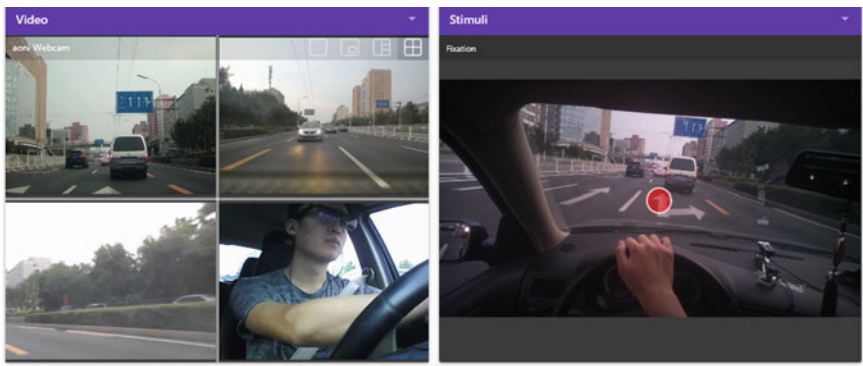


Fig. 1 Experimental scenes and eye movement process of drivers showed in ErgoLAB platform



**Table 1** Information about the installation of AILC signs on test intersections

Number of lanes	Number of intersections	Sign setting rate (%)	Number of lanes	Number of intersections	Sign setting rate (%)
2	6	0.00	5	5	80.00
3	7	14.29	6	3	66.67
4	9	88.89	More than 6	0	0.00

**Table 2** Parameter index of eye movement characteristics

Eye movement characteristics	Indicator meaning
AOI total saccade duration	Sum of duration of each entry in the area of interest
AOI average saccade duration	Average time per visit to this area of interest
AOI saccade count	Visits to this area of interest
AOI total fixation duration	Total duration of fixation at the area of interest
AOI average fixation duration	Average time of fixation at the area of interest
AOI fixation count	Number of fixations on the area of interest

## 2.2 Eye Movement Characteristics Data

On the platform interface, AILC signs and arrow markings were delineated as areas of interest (AOI) where eye movement data were collected, including saccade and fixation. The meaning of each index is shown in Table 2. The main difference between saccade and fixation is that the former is the search for information without cognitive processing, but the latter completes the information processing. The data are sorted as follows: (a) If the saccade time at AOI of the sign is not 0 and the driver chooses lane correctly (the forced lane change is not included), the sign is considered to be effective; otherwise it is ineffective. (b) If the fixation time on signs is not 0 and the lane choice is correct, use both the saccade and fixation to evaluate the efficiency of the sign.

## 3 Usability Analyses of AILC Signs

### 3.1 Extraction of Factors Influencing Sign Usability

Lane choice behavior of drivers is affected by factors such as the availability of facilities and traffic conditions. In this study, the effectiveness of the AILC sign was the dependent variable, 13 other variables were extracted to perform correlation analysis, and uncorrelated variables were eliminated. The results show the usability of AILC signs is correlated with five factors. The variables are shown in Table 3.

**Table 3** Model variables and their explanations

Variable	Symbolic	Meaning
Effectiveness of sign	$Y$	If the eye movement data indicate that the driver has seen the sign and chooses the correct lane, then $Y = 1$ , otherwise $Y = 0$
Need of lane change	$X_1$	Whether the driver needs to change lanes before driving to the sign, “Yes” is 1 and “No” is 0
Number of lanes	$X_2$	The number of lanes on the road (not at the intersection) before the driver approaches the sign, an integer from 2 to 5
Number of vehicles lined up in front	$X_3$	The number of vehicles lined up in the lane which driver is in before the driver approaches the sign
Use of arrow markings	$X_4$	If the eye movement data indicate that the driver has seen the arrow marking, the value is 1; otherwise it is 0
Lateral distance between driver and sign	$X_5$	We use the position of vehicle on the road cross section (integer from 1 to 5) to represent the distance, and when the vehicle is in the near-side lane, the value is 1

### 3.2 Model Building and Interpretation

Binary logistic regression was used to analyze the usability of AILC signs, and the estimation results are shown in Table 4. As can be seen, every independent variable has a significant impact ( $p < 0.05$ ), and the overall goodness of fit of the model is 40.5%,  $X^2(5) = 30.855$ ,  $p < 0.001$ , indicating the model reveals the impact of influencing factors for dependent variable well. The prediction accuracy of the model is 85.1%. Analysis of coefficients is as follows:

**Table 4** Analysis of factors affecting the usability of AILC signs

	Coefficients ( $\hat{\beta}$ )	Standard error	$p$ -value	Odds ratio	95% confidence interval	
					Lower-bound	Upper-bound
$X_1$	1.443	0.680	0.034	4.235	1.118	16.043
$X_2$	1.402	0.468	0.003	4.064	1.624	10.166
$X_3$	0.140	0.070	0.044	1.151	1.004	1.319
$X_4$	-1.295	0.628	0.039	0.274	0.080	0.937
$X_5$	-1.286	0.540	0.017	0.276	0.096	0.796
Constant	-3.369	1.325	0.011	0.034		

1. The coefficients of  $X_1$ ,  $X_2$ , and  $X_3$  are positive. Take  $X_1$  as an example. The results indicate that the need to change lanes greatly increases the estimated probability of sign effectiveness. The odds ratio of sign effectiveness between lane change required and lane change not required is 4.235. Similarly, each additional lane on the road and each additional car in the queue ahead multiply the odds by three times and 15.1%, respectively. Drivers are more likely to use signs in a complicated environment.
2. The coefficients of  $X_4$  and  $X_5$  are negative. The odds ratio of sign effectiveness between using markings and not using markings is 0.274, and we could infer that the markings could be used as an alternative to AILC signs to a certain extent. Each additional lane between driver and sign diminished the odds by 72.4%; maybe it is the driving vision that restricts the effectiveness of signs, because using AILC signs needs longer gaze distance and drivers have to look askance at signs.

### 3.3 Analysis of Sign Use Efficiency

From the results above, it can be known that the effectiveness of AILC signs is negatively correlated with the usage of arrow markings, and the effectiveness of AILC signs is lower than that of arrow markings. Therefore, we studied the difference between the two in efficiency to improve the usability of AILC signs.

#### 3.3.1 Description of Eye Movement Data

Eye movement data at intersections were calculated where both AILC signs and arrow markings existed (Table 5). Generally, a conclusion could be drawn that when drivers use AILC signs, saccade and fixation time are shorter.

#### 3.3.2 Difference of Eye Movement Data Between Signs and Markings

In order to further clarify the difference between signs and markings in efficiency, t-test was performed, as shown in Table 6. Take AOI total saccade duration (s) as an example; Levene's test results show the two sets of data have unequal variances ( $F = 5.428$ ,  $p < 0.05$ ). Then the t-test results show the mean value difference is statistically significant ( $t(28.4) = 2.694$ ,  $p < 0.05$ ).

Similarly, results indicate that the average saccade duration, total fixation duration, and average fixation duration of drivers using AILC signs are significantly different from arrow markings separately ( $t(24.3) = 3.282$ ,  $p < 0.05$ ;  $t(29.4) = 2.704$ ,  $p < 0.05$ ;  $t(42) = 2.439$ ,  $p < 0.05$ ).

**Table 5** Eye movement data of drivers using AILC signs and arrow markings

		Sample size	Minimum value	Max value	Average value	Standard deviation
AOI total saccade duration (s)	AILC signs	21	0.033	0.700	0.283	0.1850
	Arrow markings	23	0.060	2.400	0.584	0.5007
AOI average saccade duration (s)	AILC signs	21	0.033	0.273	0.159	0.0673
	Arrow markings	23	0.060	1.200	0.374	0.3059
AOI saccade count	AILC signs	21	1.000	3.000	1.760	0.8310
	Arrow markings	23	1.000	3.000	1.650	0.8320
AOI total fixation duration (s)	AILC signs	21	0.060	0.840	0.270	0.1848
	Arrow markings	23	0.060	2.160	0.551	0.4605
AOI average fixation duration (s)	AILC signs	21	0.060	0.260	0.149	0.0523
	Arrow markings	23	0.060	1.180	0.271	0.2228
AOI fixation count	AILC signs	21	1.000	5.000	1.810	0.9810
	Arrow markings	23	1.000	5.000	2.170	1.3020

As for AOI saccade count, Levene’s test results show the variances of two sets of data are homogeneous. Then the t-test results show there is no significant difference between drivers using AILC signs and arrow markings in saccade count. As well, there is no significant difference between the two in fixation count.

It can be known that the saccade time and the fixation time of drivers using AILC signs are shorter than arrow markings, which indicates that the searching time and the cognition time are shorter when drivers use AILC signs.

## 4 Conclusions and Discussion

The results involve three aspects. First, determine whether drivers use AILC signs and choose the correct lane through eye movement data and behavior data. If drivers heed the AILC sign and choose the correct lane, the sign is effective. Results show the effectiveness of the sign is poor (44.9%) and the usability is not good.

**Table 6** Difference test between AILC signs and arrow markings in efficiency

	Homogeneity test for variance		Mean t-test						
	<i>F</i>		<i>t</i>	df	<i>p</i> -value, two-tailed	Standard error	95% confidence interval		
		Sig					Lower-bound	Upper-bound	
AOI total saccade duration (s)	Equal variance	5.428	0.003	2.601	42.0	0.013	0.1160	0.0675	0.5356
	Heteroscedasticity			2.694	28.4	0.012	0.1120	0.0724	0.5307
AOI average saccade duration (s)	Equal variance	14.391	0.000	3.146	42.0	0.003	0.0683	0.0770	0.3525
	Heteroscedasticity			3.282	24.3	0.003	0.0654	0.0798	0.3497
AOI saccade count	Equal variance	0.011	0.916	-0.437	42.0	0.664	0.2510	-0.6160	0.3970
	Heteroscedasticity			-0.437	41.7	0.664	0.2510	-0.6160	0.3970
AOI total fixation duration (s)	Equal variance	6.426	0.015	2.615	42.0	0.012	0.1077	0.0643	0.4990
	Heteroscedasticity			2.704	29.4	0.011	0.1041	0.0688	0.4945
AOI average fixation duration (s)	Equal variance	3.722	0.060	2.439	42.0	0.019	0.0499	0.0210	0.2223
	Heteroscedasticity			2.543	24.6	0.018	0.0478	0.0231	0.2202
AOI fixation count	Equal variance	3.541	0.067	1.041	42.0	0.304	0.3500	-0.3420	1.0710
	Heteroscedasticity			1.054	40.6	0.298	0.3460	-0.3340	1.0630

Then, binary logistic regression was used to establish a model predicting the effectiveness of AILC signs, which indicates the effectiveness of AILC signs is positively correlated with the need of lane change, the number of lanes, and the number of vehicles lined up in front, while negatively correlated with the lateral distance between driver and sign and the use of arrow markings. As the number of lanes increases, drivers should be more likely to use signs. However, when a vehicle is in the fast lane of a multilane road, the effectiveness of AILC signs is worse, indicating that the form of AILC signs makes the distance between driver and sign longer and drivers have to look askance at them. It also shows for roadside signs, the time for a driver to detect them depends on the position of vehicle on the road cross section and the lateral offset of signs [16]. From a security perspective, drivers should not move their eyes more than ten degrees away from the road ahead [17]. Then, when drivers miss AILC signs, they depend on arrow marking.

The t-test was used to explore the difference between AILC signs and arrow markings in efficiency. Results indicate that drivers are more efficient in keeping sights on signs and using them. The reason may be as follows: On the one hand, the observation of arrow markings is a continuous process. Drivers notice arrow marking first and then keep track of it to know the whole arrow. The attention is more direct to use signs, which is also mentioned by Costa [18]. On the other hand, when drivers miss AILC signs in a complicated situation, they can only make up for the poor situation awareness by detecting arrow markings. In a complicated environment, using arrow markings is even more inefficient.

In summary, it is proposed to change the AILC sign to arrows for each lane on separate signs and set them over the lane separately to improve the usability of signs. Or we could improve the self-explaining properties of roads instead of setting AILC signs to upgrade the quality of guide services provided by road environment. However, this test is limited by the small number of samples and limited indicators. The solution needs further research to be verified.

**Acknowledgements** The authors are thankful to the technical support for ErgoLAB multimodal data synchronization cloud platform provided by Kingfar International Inc.

**Funding** This paper was supported by the Fundamental Research Funds for the Central Universities (2019JKF226).

**Compliance with Ethical Standards** The study was approved by the Logistics Department for Civilian Ethics Committee of People's Public Security University of China.

All subjects who participated in the experiment were provided with and signed an informed consent form.

All relevant ethical safeguards have been met with regard to subject protection.

## References

1. Xu L, Liu Z (2018) Improved method of intersection lane guidance system based on lane choice. *J East China Jiaotong Univ* 35(1):14–19
2. Yang Y, Ma J et al (2018) The self-explainability of demand-oriented road improvement. In: Wang Y-h (ed) *Connected and autonomous vehicles and transportation safety: proceedings of international conference on transportation and development*, pp 305–313
3. Jan T, Kuiken M et al (2012) *Designing safe road systems*. APL, England
4. Chowdhury I (2014) A user-centered approach to road design: blending distributed situation awareness with self-explaining roads
5. Weller G, Schlag B et al (2008) Behaviourally relevant road categorisation: a step towards self-explaining rural roads. *Accid Anal Prev* 40:1581–1588
6. Stelling-Konczak A, Aarts L, Duivenvoorden K (2011) Supporting drivers in forming correct expectations about transitions between rural road categories. *Accid Anal Prev* 43(1):101–111
7. Koyunku M, Amado S (2008) Effects of stimulus type, duration and location on priming of road signs: implications for driving. *Transp Res Part F* 11:108–125
8. Cacciabue PC, Carsten O, Tango F (2010) AE special issue on “driver modelling in automotive systems.” *Appl Ergon* 41(2):177–178
9. Obeidat MS, Rys MJ, Rys A, Du J (2016) Evaluation of overhead guide sign sheeting materials to increase visibility and safety for drivers. *Appl Ergon* 56:136–143
10. Jin Z (2017) *Recognition of sign based on multi-feature fusion*. Xi’an: Chang’an University Dissertation for a Master’s Degree.
11. Ke C, Wu M et al (2018) Research on legibility of speed limit-traffic signs with different color schemes. *Chin J Ergon* 24(6):6–10
12. Lu J, Xu T (2018) Visibility of LED active luminous traffic signs. *China J Highway Transp* 31(4):147–155
13. Martens MH, Fox MRJ (2007) Do familiarity and expectations change perception? Drivers’ glances and response to changes. *Transp Res Part F Traffic Psychol Behav* 10(6):0–492
14. IEEE (1990) *Glossary of data management terminology*
15. Yao X, Zhao X et al (2019) An approach for evaluating the effectiveness of traffic guide signs at intersections. *Accid Anal Prev* 129:7–20
16. Pietrucha M, Donnell E et al (2003) *Sign visibility*. United States Sign Council
17. Department for Transport, UK Government (1982) *Traffic sign manual*. TSO, London
18. Costa M, Simone A et al (2014) Looking behavior for vertical road signs. *Transp Res* 23:147–155

# Explore the Comfortable Seat Armrest Height During the Upper Limb Motor Imagery Training



Lu Liu, Xueying Sun, Hechen Zhang, and Feng He

**Abstract** In the upper limb motor imagery (MI) rehabilitation training, patients need to naturally place their upper arm on the seat armrest for minimum 40 min. The armrest height affects comfort and has become an important factor influencing the training. In order to find the comfortable height, 19 healthy participants were invited to this study. Localized postural discomfort (LPD) body map and comfort/discomfort questionnaire were used as subjective evaluation indicators. Heart rate variability (HRV) and electroencephalogram (EEG) signals were recorded as objective measures. Participants were asked to train tasks at different armrest heights (83 cm, 86 cm, 89 cm, and 92 cm) in a same chair. The results indicated that when the height is 89 cm, the participant's overall comfort is the best, especially in the quality of EEG signals. In conclusion, the height of arm placement during the MI training may affect the user's comfort experience. An appropriate height may obtain high-quality EEG signals, which is helpful to the rehabilitation training.

**Keywords** MI-BCI · Comfort · Rehabilitation chair · Seat armrest height

## 1 Introduction

Ergonomically sized products which improve work efficiency and reduce error rates can provide users with a comfortable experience. In the motor imagery (MI) rehabilitation training, patients need to perform the motor imagery of upper limbs or lower limbs based on the MI system [1]. Especially during upper limb rehabilitation training, patients need to naturally place their upper arms on the seat armrests for minimum 40 min. The height of the armrest has become an important factor in

---

L. Liu · H. Zhang (✉) · F. He  
Tianjin University, Tianjin 300354, China  
e-mail: [hechen\\_zhang@tju.edu.cn](mailto:hechen_zhang@tju.edu.cn)

X. Sun  
Shanghai Maritime University, Shanghai 201306, China



the training. It will affect the user experience and even cause poor quality of the electroencephalogram (EEG) signals and affect the rehabilitation effectiveness.

A comfortable upper limb position can reduce stress on the human body. Wells et al.'s research has showed that using elbow supports with the armrest can minimize muscle load on the upper limbs [2]. Studies by Aaras et al. also demonstrated that arm support can reduce spinal load [3]. Meanwhile, in the medical field, the main approaches to improve adverse outcomes (such as extended hospital stay, fatality, incorrect treatment) still mainly due to industrial design and human factors [4]. Focusing on human–computer interaction (HCI), Raffaele et al. studied that if the upper limbs are supported by armrests during laparoscopic surgery, the accuracy of laparoscopic surgery can be improved [5].

Many physicians are overly focused on the effects of medicaments on the treatment of patients while neglecting the user experience of the medical device. As a result, many medical devices still maintain poor design and are not improved [2]. Jie Zhou et al. conducted an ergonomic study regarding the position of the brake pedals and armrests in hospital beds. Their research showed that improper position of the brake pedal can cause injuries to the lumbar spine of medical staff and bring a poor experience for patients [6].

As motor imagery brain computer interface (MI-BCI) is researched more deeply and applied more widely, its user group is also constantly expanding and may even develop into a new interaction mode. Although the current research has some support for the function and reliability of MI-BCI, the basic research of ergonomics for related devices is seldom [7].

The objective of this study is to find the optimal seat armrest height to optimize the user experience, improve the quality of EEG signals during MI training, and increase the purity of EEG signals.

## 2 Experiment

### 2.1 Experiment Plan

In order to explore the comfort of MI training at different seat armrest heights, an experiment was designed. Participants need to complete two parts of an MI task at four armrest heights of 83 cm, 86 cm, 89 cm, and 92 cm, respectively.

The first part is a pilot test, and the data was not collected. During the test, participants were trained and instructed on MI tasks. Through such process, they can identify the experimental purpose, process and specific MI tasks. In this way, we ensure that they can meet the task requirements and proficient in imaginary actions.

The second part is the formal experiment, and the data were recorded. Participants were asked to perform MI tasks at four different seat armrest heights, respectively. Each height was randomly set to avoid the impact of fatigue at the later stage on the experimental results. The specific process is as follows: The computer is used to

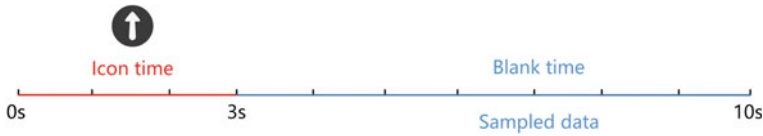


**Fig. 1** Required time to complete one unit of imagery using stimuli

display the video stimulus material. The participant watched it and interacted with action imagery at the same time. The stimulus material is some directional icons that appears randomly for 3 s and then enters a 7-s blank. These 10 s are a set of action imagery, like shown in Fig. 1.

Participant was asked to start imagining when he saw a directional icon until the next one appeared. Each piece of data contains the participant’s action label and the length of actual sampled data (7 s). After each height test, the participant needed to scan QR code with their mobile phone to complete three subjective questionnaires regarding comfort/discomfort and emotional effects.

Before the experiment, the participant needs 20 mins to wear the devices, including EEG cap with the conductive paste (no damage), heart rate and skin conductance recorder. In the experiment, the first part takes 3 min. The second part takes 6 min, including 3 min for the formal experiment and 3 min for the questionnaires. Each height-experiment consists of the two parts. It takes about 56 min for one participant to complete the entire content.

## 2.2 Equipments and Materials

The experiment setup is shown in Fig. 2. Each participant should wear: (1) An EEG acquisition equipment (Brand: NeuroSky) with a sampling frequency of 1024 Hz. The matched EEG cap with 64 active electrodes uses 10–20 system for data collection. (2) Heart rate recorder (Brand: Ergolab) is used to measure participants’ heart rate variability (HRV) during the experiment. (3) An ordinary computer is placed directly in front of the participant to play the stimuli.

The materials for this experiment are as follows: (1) Questionnaires include the comfort/discomfort questionnaire, local postural discomfort (LPD, 19 questions). (2) A self-made height-adjustable armrest bracket was used in the experiment instead of the armrests of the original seat to adjust different height. (3) The stimulus materials are arrow icons in four directions: up, down, left, and right (Table 1).

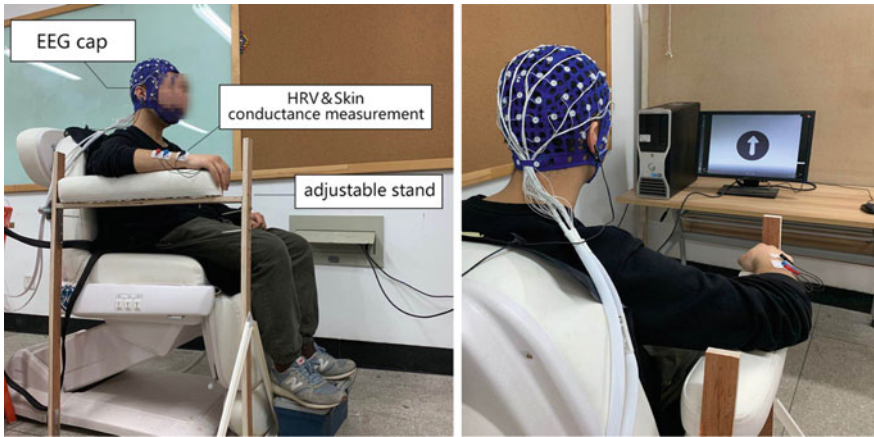


**Fig. 2** Experiment setup

**Table 1** Imagination actions corresponding to four arrow icons

↑	↓	←	→
Tongue against palate	Calf pacing	Grab the ball with your left hand	Grab the ball with your right hand

### 2.3 Participants

A total of 19 healthy participants (11 men and 8 women, right-handed) were recruited into this experiment. Their basic information is shown in Table 2.

## 3 Results

All collected subjective data was preprocessed, where MinMaxScaler [8] was used to normalize all data to the span from 0 to 1. The student t-test was used to determine the statistical difference between the two sets of data.

**Table 2** Basic information of the participants

Quantity (n)	Age (years)	Height (cm)	Weight (kg)
19	24.4 ± 3.35	171.8 ± 7.2	66.4 ± 13.1

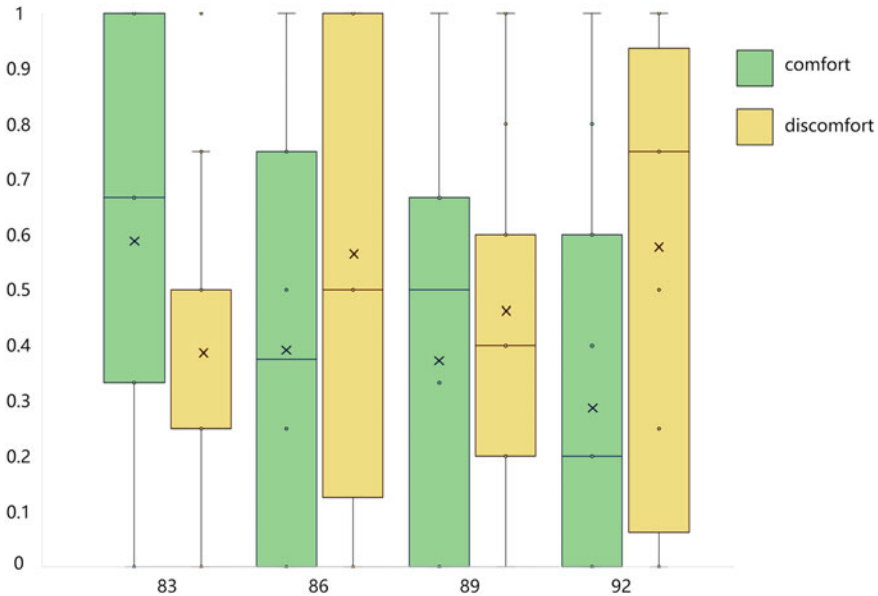


Fig. 3 Comfort/discomfort regarding the four height-settings (0: min, 1: max)

### 3.1 The Results of Comfort/Discomfort Questionnaire

The normalized results of the comfort/discomfort questionnaire for the four different heights are shown in Fig. 3. Green represents the level of comfort, and yellow represents discomfort. It can be observed that when the height is 83 cm (mean = 0.63, STD = 0.31), the comfort is significantly better than 92 cm (mean = 0.29, STD = 0.58). In the other two options, 86 cm (mean = 0.39, STD = 0.56) and 89 cm (mean = 0.38, STD = 0.35) are slightly different, but those differences are not statistically significant ( $P = 0.90$ ). Regarding discomfort, the means and STDs of the four height-settings are  $0.39 \pm 0.26$  (83 cm),  $0.56 \pm 0.39$  (86 cm),  $0.46 \pm 0.29$  (89 cm), and  $0.59 \pm 0.38$  (92 cm). There is no significant difference between the four heights ( $P > 0.05$ ).

### 3.2 The Result of LPD Body Map

Figure 4 shows the result of LPD body map. The study found that the participants only have significant differences under Q (left hand), S (neck), X (right shoulder), G (right back), and P (right hip). There are no significant differences in the remaining parts ( $P > 0.05$ ). Regarding Q (left hand), 86 cm is slightly better than 89 cm, but it has no statistical significance ( $P = 0.82$ ), followed by 83 cm. The worst is 92 cm. Only

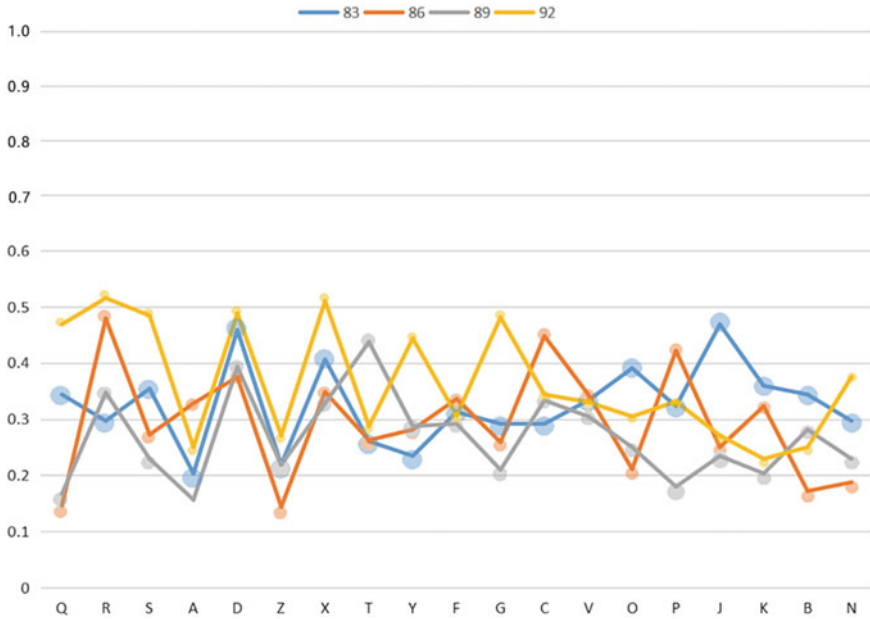


**Fig. 4** Normalized scores of LPD on four height-settings (vertical axis: discomfort, 0 = minimal level, 1 = maximal level, horizontal axis definitions can be found in [9], except W = head)

in X (right shoulder), the maximum score is 86 cm. The rest (S, G, P) scores were best at 89 cm. Overall, when the height was 89 cm (average = 0.27, STD = 0.08), the comfort level was better than 83 cm ( $P = 0.02$ , average 0.33, STD = 0.07) and 92 cm ( $P = 0.02$ , average = 0.37, STD = 0.10). Although they are slightly different from 86 cm (mean = 0.29, STD = 0.10), these are not statistically significant ( $P = 0.56$ ).

### 3.3 HRV Index

The four different heights have different effects on the HRV characteristics of the participants (as shown in Table 3), which can be observed by the differences in the Standard Deviation of the Normal, Normal (R-R) intervals (SDNN), and Proportion of NN50 divided by the total number of normal to normal (R-R) intervals (PNN50) and HF% (HF/(VLF + LF + HF), HF is a high frequency band of 0.15–0.4 Hz. LF is a low frequency band of 0.04–0.15 Hz. VLF is a very low frequency band of 0.003–0.4 Hz). The results show that regarding SDNN, the score was slightly higher than the other three, when the height was 89 cm. The lowest score was at 86 cm, which was not statistically significant ( $P = 0.17$ ). Regarding HF%, the score of the height 89 cm was the lowest. But it was not statistically significant ( $P = 0.24$ ,  $P =$

**Table 3** Mean values of features of HRV regarding four different armrest heights

	SDNN (ms)	PNN50 (%)	HF (%)
83	104.24	24.102	44.31
86	86.99	20.26	46.64
89	126.78	21.75	42.45
92	107.13	23.53	45.66

0.42). Regarding PNN50, the score of the height 83 cm was the highest. But it was still not statistically significant ( $P = 0.43$ ).

### 3.4 EEG Signals Quality

The result of EEG signal quality of 19 participants at four heights is shown in Table 4, and the calculation method can be found in the discussion. The results show that

**Table 4** EEG signal quality of all participants at four different armrest heights

$mv^2$	'83'	'86'	'89'	'92'	min
1	3.68135E-12	3.68454E-12	5.84601E-12	5.72648E-12	83
2	1.55881E-12	1.58247E-12	1.35106E-12	1.74098E-12	89
3	1.09798E-13	5.23184E-13	7.89148E-13	1.19259E-13	83
4	2.82898E-11	1.45584E-11	4.12511E-11	2.02345E-11	86
5	7.04773E-14	8.69623E-14	2.09302E-13	7.59660E-14	83
6	3.88568E-14	2.51990E-14	3.20746E-14	2.82311E-14	86
7	7.37252E-15	1.12622E-14	6.78513E-15	8.47270E-15	89
8	4.71921E-14	6.22805E-14	8.11677E-14	5.27851E-14	83
9	2.35743E-12	1.47878E-12	1.75612E-12	1.37172E-12	92
10	1.71719E-12	1.22319E-12	1.02688E-12	5.70432E-12	89
11	1.00540E-11	5.33061E-12	3.98196E-12	7.92126E-12	89
12	4.16228E-12	3.39644E-12	3.06452E-12	3.16454E-12	89
13	1.36791E-15	5.26427E-15	9.80703E-16	1.75997E-15	89
14	4.99751E-14	4.05605E-14	3.13627E-14	9.03451E-14	89
15	5.47580E-13	2.65747E-13	2.09809E-13	3.48865E-13	89
16	1.66043E-15	1.43792E-15	3.21619E-15	2.06138E-15	86
17	6.62606E-14	7.30896E-14	6.32695E-14	6.96338E-14	89
18	2.55539E-13	1.64701E-13	3.73881E-13	1.9982E-13	86
19	1.31461E-13	1.70819E-13	1.14673E-13	1.03785E-13	92

different participant showed different seat armrest comfort heights. Nine of the 19 participants were preferred armrest height at 89 cm, while only two were at 92 cm.

## 4 Discussions

Vink and Hallbeck defined comfort as ‘a pleasant state or a feeling of relaxation of human beings in their environment’ and discomfort as ‘an unpleasant state of the human body in their physical environment’ [10]. The research in this article still follows this conclusion.

From the results of the LPD body map, it can be concluded that when using the 89 cm height, the participant’s discomfort in different parts of the body was lower than other subjects, which is mainly due to changes in the participant’s mood. Previous studies have shown that HRV can be used as an objective measure of assessing emotional response [11], because the features of HRV are significantly correlated with happiness and sadness [12]. The research by Ryuya et al. proves that HF% can be used as a better tool to evaluate comfort [13]. In this experiment, the larger values of SDNN and HF% indicated that 89 cm as the user’s first choice for the height can bring a more comfortable experience and trigger user’s positive emotions, while significantly improving the collected EEG signal quality.

In addition to recording and analysing the subjective and objective data, the influence of different heights on EEG signals is also been focused in this study. Because the EEG signal has the features of random signals of non-stationary, non-linear, non-Gaussian processes, we cannot apply a specific model to extract the EEG signal. However, after the unremitting efforts of many researchers, we can know that the frequency domain of EEG signals is in the range of 0–50 Hz [14]. Most of the EEG studies focused on five frequency bands such as  $\alpha$ ,  $\beta$ ,  $\mu$ ,  $\theta$ , and  $\delta$  [15]. In this study, we use wavelet packet [16] to decompose the 64-channel EEG signal into five sub-bands and then get a reconstructed signal matrix  $N$ . A formula was defined to calculate the distance between the original signal matrix  $R$ , and reconstruct signal matrix  $N$ . It’s used to judge the quality of the collected signal. The formula is as follows:

$$\frac{1}{64N} \sum_{j=1}^{64} \left( \sum_{i=0}^{N-1} (R_{ij} - N_{ij})^2 \right)$$

Through this method to analyse the EEG signal collected from the same subject at four different heights, it can be known that the smaller the difference the less noise was mixed in the collected data, which implied the less for this subject’s influence due to external changes. From the result in Table 4, we collected that half of the participants have the minimum value of mean square of the EEG signal noise at the height of 89 cm.

## 5 Limitations

There are some limitations to this study. Firstly, all participants were young, and most of them were students. In fact, stroke patients are currently users during BCI rehabilitation treatment, so the participants in this study may have some deviations in their understanding of comfort. Secondly, in the results of comfort/discomfort questionnaire, the comfort scores in descending order are 83 cm, 86 cm, 89 cm, and 92 cm. This is inconsistent with the results presented by other data, which may be due to the subject's bias in understanding the concepts of comfort and discomfort.

## 6 Conclusion

This study found that the 89 cm seat armrest height is the best choice for user comfort and EEG signal quality in motor imagery training. With this height, it can be obtained comfortable posture and minimal discomfort. In order to more effectively collect EEG data with better quality and improve the treatment effect, more attention should be paid to similar configurations in this MI-BCI training.

**Compliance with Ethical Standards** The study was approved by the Logistics Department for Civilian Ethics Committee of Tianjin University.

All subjects who participated in the experiment were provided with and signed an informed consent form.

All relevant ethical safeguards have been met with regard to subject protection.

## References

1. Christoph G, Millán José del R, Donatella M, Junichi U, Soekadar SR, Vivek P et al (2018) Brain-computer interfaces for stroke rehabilitation: summary of the 2016 BCI meeting in ASILOMAR. *Brain-Comput Interfaces*, 1–17
2. Wells R, Lee IH, Bao S (1997) Investigations of the optimal upper limb support conditions for mouse use. In: Marconi research conference, Berkeley, UCSF
3. Aaras A, Fostervold KI, Thoresen M, Larsen S (1995) Postural load at VDU work: a comparison between different workplace designs. In Kumashiro M (ed) *The paths to productive aging*. Taylor & Francis, Philadelphia, pp 151–156
4. Acharya C, Thimbleby HW, Oladimeji P (2010) Human computer interaction and medical devices. In: British Computer Society conference on human-COMPUTER interaction. DBLP
5. Galleano R, Carter F, Brown S, Frank T, Cuschieri A (2006) Can armrests improve comfort and task performance in laparoscopic surgery? *Ann Surg* 243(3):329–333
6. Zhou J, Wiggermann N (2017) Ergonomic evaluation of brake pedal and push handle locations on hospital beds. *Appl Ergon* 60:305–312
7. Ekandem JI, Davis TA, Alvarez I, James MT, Gilbert JE (2012) Evaluating the ergonomics of BCI devices for research and experimentation. *Ergonomics* 55(5):592–598
8. Scikit-learn. MinMaxScaler [Internet] (2019) Available from: <https://scikit-learn.org/stable/modules/generated/sklearn.preprocessing.MinMaxScaler.html>



9. Vink P, Hallbeck S.(2012). Editorial: comfort and discomfort studies demonstrate the need for a new model. *Appl Ergon* 43(2):271–276
10. Vink P, Looze MPD (2008) Crucial elements of designing for comfort. *Product Experience*
11. Valenza G, Citi L, Lanatá A, Scilingo EP, Barbieri R (2014) Revealing real-time emotional responses: a personalized assessment based on heartbeat dynamics. *Sci Rep*, 4
12. Lane RD, Mcrae K, Reiman EM, Chen K, Ahern GL, Thayer JF (2009) Neural correlates of heart rate variability during emotion. *NeuroImage* 44(1):213–222
13. Yanagihashi R, Ohira M, Kimura T, Fujiwara T (1997) Physiological and psychological assessment of sound. *Int J Biometeorol* 40(3):157–161
14. Doyle J, Ornstein R, Galin D (1974) Lateral specialization of cognitive mode: ii. EEG frequency analysis. *Psychophysiology* 11(5):567–578
15. Scerbo MW, Freeman FG, Mikulka PJ, Raja P, Di NF, Prinzel ILJ (2001) The efficacy of psychophysiological measures for implementing adaptive technology
16. Ting W, Guo-Zheng Y, Bang-Hua Y, Hong S (2008) EEG feature extraction based on wavelet packet decomposition for brain computer interface. *Measurement* 41(6):618–625

# A Generation Method and Verification of Virtual Dataset



Pengxin Ding, Qingyang Shen, Tianguo Huang, and Minghui Wang

**Abstract** *Target* To construct a method for generating object detection dataset based on the virtual environment. The generated dataset can be used for object detection tasks based on deep learning algorithms. *Methods* The procedural generation method was used to create the city's virtual environment, and also computer graphics were used for rendering and automatic labeling. *Results* We constructed a virtual reality environment and collected 1500 images through the virtual environment, including 1307 images containing valid vehicle and pedestrian information, and trained a deep learning model based on this dataset. *Conclusions* A virtual reality environment is successfully created, and the generated dataset can be used to train deep learning object detection algorithms, and the trained models can also effectively perform object detection in real world.

**Keywords** Virtual reality · Deep learning · Object detection · Dataset

## 1 Introduction

Creating a deep learning dataset is time-consuming and laborious, in order to solve this problem, we propose to use a virtual environment to generate datasets and use them to train and evaluate object detection algorithms. We name the dataset generated by virtual environment a virtual dataset. A virtual dataset is a collection of images and annotations. Through the experiments, we proved that the virtual dataset can be

---

P. Ding · M. Wang (✉)

College of Computer Science, Sichuan University, Chengdu 610056, China  
e-mail: [wangminghui\\_papers@163.com](mailto:wangminghui_papers@163.com)

P. Ding

The Second Research Institute of Civil Aviation Administration of China,  
Chengdu 610041, China

Q. Shen · T. Huang

College of Computer Science,  
Chengdu University of Information Technology, Chengdu 610225, China

© The Editor(s) (if applicable) and The Author(s), under exclusive license to Springer Nature Singapore Pte Ltd. 2021

S. Long and B. S. Dhillon (eds.), *Man-Machine-Environment System Engineering*, Lecture Notes in Electrical Engineering 645,  
[https://doi.org/10.1007/978-981-15-6978-4\\_55](https://doi.org/10.1007/978-981-15-6978-4_55)

used to train object detection algorithms, and models that were trained by virtual dataset can be effectively applied in real-world images.

The synthetic image of the virtual dataset has great advantages over real-world dataset. The first is that it can quickly obtain large batches of data for training neural networks [1], and the second is that it can save a lot of time when labeling datasets and get accurate labeling. In terms of social impact, the use of cameras and other data obtained in the real world requires consideration of personal privacy, laws and regulations. While in virtual datasets, those needs are no longer considered at all.

## 2 City Virtual Environment Content Generation Technology

The virtual environment is used to generate the object detection dataset. The idea is to use computer graphics and virtual simulator to render and label the dataset [2]. Meanwhile, we also use simulated scenes and virtual cameras instead of real scenes and cameras. Using the virtual environment can quickly generate the object detection dataset in a large scale [3], and it is easier to modify the dataset.

In order to quickly obtain the vehicle object detection dataset, we introduced a procedural generation method to create virtual environment of a city.

### 2.1 Virtual Environment Generation Process

First, we determine the scene composition of the virtual environment. A well-simulated city scene should have static scene objects and dynamic scene objects. In a virtual city, static scene objects mainly are road networks, buildings, street signs, and some detail objects. A dynamic scene object consists of pedestrians, vehicles, bicycles, and traffic lights [4]. All categories of objects in the dataset should be included in the virtual environment, but objects in the virtual environment do not necessarily have categories in the dataset. Extra objects can add some complexity to the samples in the dataset, making the virtual dataset closer to the real-world dataset.

The purpose of procedural generation of road network is to accurately describe the geometry and data structure of road networks. Before generating the road networks in virtual city, we need to define the data structure to describe the roads [5]. The road network mainly consists of several roads and intersections, each road consists of several road sections, and a road section is described by two-way points and information describing the road.

Through this road network generation method, urban road networks with certain randomness can be created. The virtual environment of the city can be obtained by assigning corresponding textures to the road model and filling the three-dimensional model of the building along the generated road (Fig. 1).



**Fig. 1** Screenshot of the urban virtual environment rendering

## ***2.2 Synthetic Virtual Environment Datasets***

The virtual dataset for object detection in this paper used a partial synthesis method. Some 3D models in this virtual environment are created by hand [6], and other 3D models are generated using procedural generation methods. In the process of synthesizing the images of the virtual dataset, it is necessary to introduce randomness in terms of color, texture, position, scale, rotation, deformation, and camera angle. The use of a 3D graphics engine can easily control these features and produce real-time, realistic graphics rendering. In recent years, game engines such as Unity3D and Unreal Engine have developed rapidly and also meet the requirements for generating and rendering virtual datasets. By using these engines, we can obtain the images and appropriate labels of virtual dataset easily. For object detection tasks, the labels are bounding boxes and categories. Synthetic datasets are also suitable for machine learning tasks such as image classification, semantic segmentation, and autonomous driving [7].

### **2.2.1 Automatic Labeling Method for Virtual Datasets**

Through procedural generation method, we can create a virtual environment that consists of road networks, vegetation, traffic lights, vehicles, and pedestrians. Adding this virtual environment to Unity3D engine can produce real-time, realistic rendering results [8], which are the images corresponding to traditional datasets captured by cameras. In the process of creating a traditional dataset, after the images are obtained, the images need to be manually labeled. This is because computers cannot directly obtain information such as the category and position of objects in the images from the

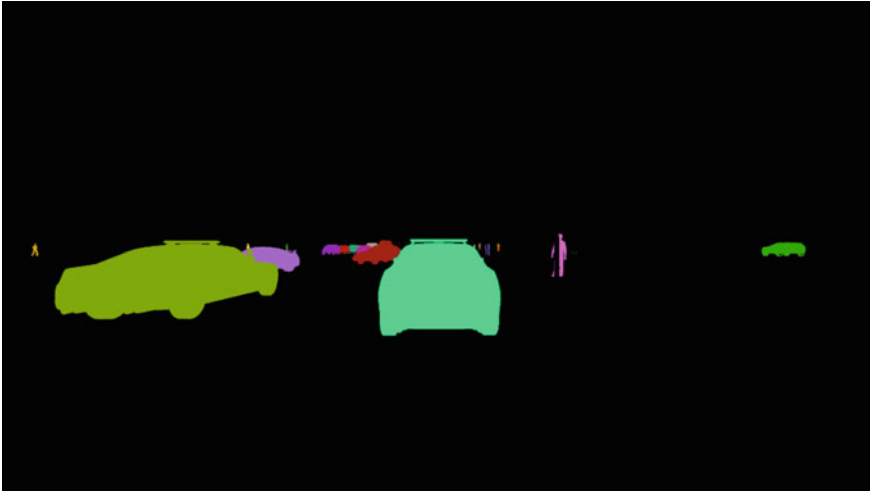


**Fig. 2** Single color rendering of each scene object

real world. But the images rendered by the 3D graphics engine can accurately obtain those information. Therefore, the images in the virtual dataset can be automatically labeled by the computer (Fig. 2).

To manage the rendering colors of all meshes in a virtual scene, we need to track different instances with the same parent object. The manager script is used for storing the category of scene objects, references to all meshes, the RGB color that encoded by instance ID, and the controller for rendering. In this way, when creating a dataset, we can choose whether to render objects of the same category to the same color to create a semantic segment dataset, or to render an instance with different colors to automatically label the object detection dataset.

### 3 Validation of the Dataset

In order to verify the effectiveness of virtual dataset in object detection tasks, we designed the following experiment. First, we use the virtual dataset to train Yolo-v3 algorithm [9] and freeze the model after the model converged. Experiments showed that using the model trained on our dataset can effectively perform object detection tasks on real-world images.

We prepared 12 vehicle models and 15 human models, and then, added these objects of vehicles and pedestrians to the virtual environment in the experiment, and controlled the behavior of AI through the points and behavior trees. In the process of creating the virtual dataset, by changing the lighting angle, light intensity, sky box texture, and the visible distance of the volumetric fog, we created different scenarios such as sunny, cloudy, sunset, and night, and then, used them in these



**Fig. 3** Model performs object detection on real-world pictures (vehicles and pedestrians)

environments. The camera bounded to the vehicle hood captures the rendered images and the instance segmentation images. We take the batch size as 300 and output both the images and the bounding box information when every 300 images were collected.

We collected 1500 images in virtual environment, of which 1307 contained valid vehicle and pedestrian information. Using Yolo-v3 as the object detection algorithm, mAP was 90.78% when IoU was 0.5; mAP was 88.12% when IoU was 0.75, which basically achieved the object detection task for vehicles and pedestrians (Figs. 3 and 4).

Yolo-v3 object detection model trained on the virtual dataset running on real-world pictures is shown in the figures above. The training data of the algorithm is all synthetic data, without the participation of real-world data. It can be seen that the trained model can detect vehicles and pedestrians in the photos and has successfully marked the bounding boxes and categories. This can prove that the object detection dataset generated by the virtual environment can achieve a predetermined effect.

## 4 Results and Conclusions

This article used the procedural generation method to create a virtual environment of a city and then used this virtual environment to quickly create a labeled object detection dataset. Experimental verification shows that the virtual dataset can quickly and effectively generate datasets that are suitable for object detection tasks. The



**Fig. 4** Model performs object detection on real-world pictures (only vehicles)

following work mainly includes two aspects: (1) improve the virtual environment and implement the generation and automatic labeling of more models and scenes and (2) implement automatic screening of images in the virtual dataset to obtain higher-quality datasets.

## References

1. Zhu Y, Urtasun R, Salakhutdinov R (2015) segDeepM: exploiting segmentation and context in deep neural networks for object detection. In: 2015 IEEE conference on computer vision and pattern recognition (CVPR). IEEE
2. Arcuri A, Briand L (2014) A hitchhiker's guide to statistical tests for assessing randomized algorithms in software engineering. *Softw Test Verification and Reliab* 24(3):219–250
3. Torralba A, Fergus R, Freeman WT (2008) 80 million tiny images: a large dataset for nonparametric object and scene recognition. *IEEE Trans Software Eng* 30(11):1958–1970
4. Togelius J, Chamandard AJ, Lanzi PL, Mateas M, Paiva A, Preuss M, Stanley KO () Procedural content generation: goals, challenges and actionable steps
5. Tian J, Qingsong HE, Yan F (2014) Formalization and new algorithm of STROKE generation in road networks. *Geomat Inf Sci Wuhan Univ* 39(5):556–560
6. Li R, Li P, Zhang X et al (2003) Optimization of hierarchical details in virtual environment modeling. *Comput Simul* 20(1):73–75
7. Perez L, Wang J (2017) The effectiveness of data augmentation in image classification using deep learning. arXiv preprint arXiv:1712.04621

8. Andaluz VH, Sánchez JS, Chamba JI et al (2016) Unity3D virtual animation of robots with coupled and uncoupled mechanism. *Augmented Reality, Virtual Reality, and Computer Graphics*
9. Qi CR, Su H, Mo K et al (2017) Pointnet: deep learning on point sets for 3D classification and segmentation. In: *Proceedings of the IEEE conference on computer vision and pattern recognition*, pp 652–660



# Study on the Influence Factors of Garment Pattern Design Based on Quantification Theory



Zhaowei Su, Yuhui Wei, and Long Sun

**Abstract** In order to systematically explore the main factors and its degree of the overall design effect of garment pattern, taking the summer t-shirt as an example, the overall design effect of pattern color (lightness, purity, hue), size, density of arrangement, angle of inclination and fabric color (lightness, purity, hue) was studied with the help of eye tracking technology and quantification theory. The results show that the above factors will affect the overall design effect of clothing pattern to varying degrees. Hue, size and layout density of pattern and fabric hum had a great influence on the overall effect of garment design; pattern lightness and purity have a slight influence on the overall effect of garment design. This conclusion provided theoretical reference and data support for fashion designers to design pattern of garment that is more in line with the aesthetic needs of consumers.

**Keywords** Pattern design · Summer T-shirt · Eye tracking technology · Heat map · Overall effect of garment

## 1 Introduction

Pattern design is one of the key factors that restrict consumers' purchasing decision because of its decorative and beautifying function [1–3]. However, the current research on clothing pattern design mainly focuses on the pattern modeling features,

---

Z. Su (✉)

High Fashion Womenswear Institute, Hangzhou Vocational Technical College, 310018 Hangzhou, China

e-mail: [suzhaowei@126.com](mailto:suzhaowei@126.com)

Z. Su · Y. Wei

College of Textile and Clothing, Anhui Polytechnic University, 241000 Wuhu, China

Y. Wei

Anhui Hong Ai Industrial Co., Ltd, 246500 Anqing, China

L. Sun

School of Psychology, Liaoning Normal University, 116029 Dalian, China

© The Editor(s) (if applicable) and The Author(s), under exclusive license to Springer Nature Singapore Pte Ltd. 2021

S. Long and B. S. Dhillon (eds.), *Man-Machine-Environment System Engineering*, Lecture Notes in Electrical Engineering 645,

[https://doi.org/10.1007/978-981-15-6978-4\\_56](https://doi.org/10.1007/978-981-15-6978-4_56)

cultural connotation, communication path and its modern application [4, 5]. And little research provides feasible evidence of whether pattern design affects the final purchase decision of consumers [3, 5]. The purpose of this study is to systematically analyze the influence of pattern design on the overall effect of clothing and the relationship between pattern design and consumers' purchase decision. Moreover, with the development of eye tracking technology, eye tracker has been widely used quantitative analysis method in human eye activities related to interface assessment, cognitive research, scene research, human-computer interaction and so on [3–5]. Therefore, the influence of pattern color (lightness, purity, hue), size, arrangement density and angle on the overall design effect of clothing pattern and consumers preference was analyzed by using eye tracking technology and statistical analysis in this study.

## 2 Experimental Details

### 2.1 Experimental Design

In order to quantitatively study the main factors of influencing garment pattern design and its' degree, summer T-shirt was used in this study. The specifications of experimental variables and levels are listed in Table 1. Moreover, 24 college students and postgraduates of different grades (12 male and 12 female, aged 18–27 years old, colorless blindness or hypochromia) were recruited according to the accuracy requirement of eye tracker experiment.

### 2.2 Test Methods







In order to quantitative analysis the effects of pattern size, color (lightness, purity, hue), density and angle on the overall design of garment pattern, Tobiii Pro X3-120 eye tracker equipment (Beijing KingFa Technology Co. Ltd.) and data software ErgooLAB33.0 were used in this study.

## 3 Results and Discussion

### 3.1 Analysis of the Influence of Pattern Color

Table 2 showed the measurement results of the influence of pattern color on garment design, T-shirt C<sub>1</sub> (red) and C<sub>5</sub> (black) had higher average fixation time, conversion frequency and fixation number compared to T-shirt with yellow, gray and blue pattern.

**Table 1** Experimental variables and levels

Variables	Levels
Color	 C1    C2    C3    C4    C5
Lightness	 L1    L2    L3    L4
Purity	 P1    P2    P3    P4
Size	 S1    S2    S3    S4
Permutation density	 D1    D2    D3    D4
Angle of inclination	 A1    A2    A3    A4    A5    A6    A7

This indicated that the color and hue of the design significantly affect the overall effect of clothing design. And it founded that the average value of the conversion frequency, the number of fixation points and the hot spot map were changed with difference of the lightness and purity of the color. Compared with the four level of lightness, the mean of fixation time, conversion frequency and number of fixation points of L<sub>4</sub> were higher than the other three levels of lower lightness. And the mean values of P<sub>1</sub> were 1.386 s, 3.569 and 3.159, respectively, which were higher than those of the other three levels of purity. It can be concluded that the higher the purity of the pattern color, the higher the average value of the conversion frequency, the number of fixation points and the hot spot map. This is because the higher the lightness and purity, the easier to be spotted the pattern, and thus is easy to lead consumer attention

**Table 2** Effect of pattern color on garment design

Number	Average fixation time/s	Average saccade count (Ns <sup>-1</sup> )	Average blink count (N)
C <sub>1</sub>	1.126	3.497	5.955
C <sub>2</sub>	0.835	1.334	1.012
C <sub>3</sub>	1.151	3.335	2.169
C <sub>4</sub>	1.163	3.314	3.982
C <sub>5</sub>	2.117	8.993	7.382
L <sub>1</sub>	1.126	3.496	2.995
L <sub>2</sub>	1.736	4.833	3.799
L <sub>3</sub>	2.216	5.828	4.166
L <sub>4</sub>	2.722	6.331	5.334
P <sub>1</sub>	1.386	3.568	3.159
P <sub>2</sub>	1.139	2.331	1.988
P <sub>3</sub>	0.967	1.499	1.342
P <sub>4</sub>	0.908	1.217	1.027

and purchase behavior. In addition, combined with the hot spot chart (Table 6), it found that the location of the pattern and near the collar was the focus of consumer attention.

### 3.2 Analysis of the Influence of pattern's Size

As seen from Table 3, the size of pattern was too big or too small, the fixation time, the number of fixation points, the number of fixation points and the degree of attention decrease in varying degrees. This was because when the pattern was too large (S<sub>1</sub>), the pattern was shown as a face instead of dot, and lead to the fixation time, the number of fixation points, the number of fixation points and the degree of attention decrease. When the size of the pattern was suitable (S<sub>3</sub>), the sense of magnitude was relatively strong, and the pattern was easier to be recognized, and thus, the fixation time was shorter. On the contrary, the pattern was too small (S<sub>4</sub>), it is not easy to

**Table 3** Effect of pattern size on garment design

Number	Average fixation time (s)	Average saccade count (Ns <sup>-1</sup> )	Average blink count (N)
S <sub>1</sub>	1.126	3.503	3.102
S <sub>2</sub>	0.704	1.323	1.497
S <sub>3</sub>	1.975	6.167	5.667
S <sub>4</sub>	1.151	4.494	2.493

**Table 4** Effect of pattern's permutation density on garment design

Number	Average fixation time (s)	Average saccade count ( $Ns^{-1}$ )	Average blink count (N)
D <sub>1</sub>	1.205	2.988	2.331
D <sub>2</sub>	1.338	2.671	1.499
D <sub>3</sub>	2.572	6.393	5.497
D <sub>4</sub>	3.105	7.161	6.995

be captured, and thus, the fixation time was prolonged. Therefore, the size of the pattern should be taken into account when the designer was engaged in the pattern design. In addition, comparing the eye movement data of four levels of pattern sizes, it concluded that the pattern size also had a significant effect on the dispersion degree of attention and the attention of the whole garment (Table 6).

### 3.3 Analysis of the Influence of pattern's Permutation Density

The fixation time decreased with the increase of pattern arrangement density as shown in Table 4. And the conversion frequency and the fixation points increase with the increase of pattern arrangement density. This was because the visual fatigue was gradually enhanced with the increase of density, and, then the number of blink per unit time and version frequency increased. In addition, it was found that the density of pattern arrangement had little influence on the area of consumer's attention (Table 6). In other words, people's observation was both the collar and the center of the garment regardless of the arrangement density.

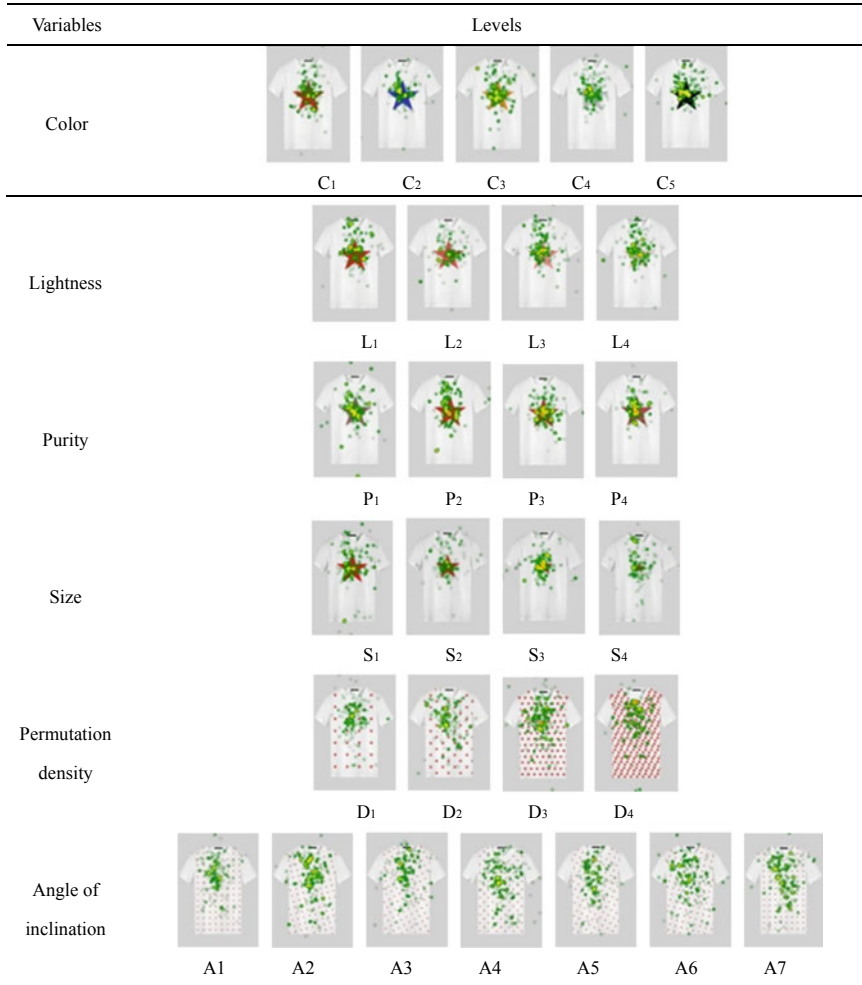
### 3.4 Analysis of the Influence of pattern's Angle

As seen from Table 5, the pattern inclination angle slightly affects the overall effect of garment design, when the clothing pattern was composed of individual patterns arranged in a certain order to form a surface feeling pattern. This is because the angle of single pattern did not bring a big visual impact contrast. Therefore, the differences in the number of fixation times, fixation time, fixation point number and hotspot map were not obvious (as shown in Table 6).

**Table 5** Effect of pattern's angle on garment design

Number	Average fixation time (s)	Average saccade count (Ns <sup>-1</sup> )	Average blink count (N)
A <sub>1</sub>	1.151	2.664	1.162
A <sub>2</sub>	1.181	2.332	1.837
A <sub>3</sub>	1.203	2.067	2.332
A <sub>4</sub>	1.163	2.831	2.161
A <sub>5</sub>	1.102	2.967	1.901
A <sub>6</sub>	1.241	2.498	1.832
A <sub>7</sub>	1.238	2.004	1.167

**Table 6** Hot spot map of different experiments



## 4 Conclusions

The influence of different pattern color (lightness, purity, hue), size, arrangement density and inclination angle on the overall design effect of garment pattern were systematically studied with the help of the TOBII PRO X3-120 eye tracker. Results showed that the overall effect of the pattern was greatly influenced by the size, the hue and the density of pattern, instead of the angle of the pattern. This conclusion provided an effective method that designers obtained clothing pattern with more in line with consumers' aesthetic preferences through reasonable design of pattern color, size and density and then solves the current clothing market supply and demand imbalance.

**Acknowledgements** This research was supported by Teachers Enterprise Experience Engineering School-level Key project of Hangzhou Vocational Technical College Vocational and Technical College (XQ20191002); Zhejiang Province Colleges and Universities Visiting Scholar (visiting Engineer) project; Joint research fund project of the ergonomics association and the JEF (CES-KINGFAR-2019-005); School-level research Foundation of Anhui Polytechnic University (Xjky03201908).

**Compliance with Ethical Standards** The study was approved by the Logistics Department for Civilian Ethics Committee of Hangzhou vocational technical college.

All subjects who participated in the experiment were provided with and signed an informed consent form.

All relevant ethical safeguards have been met with regard to subject protection.

## References

1. Park J, DeLong M, Woods E (2012) Exploring product communication between the designer and the user through eye-tracking technology. *Int J Fash Des Technol Educ* 5(1):67–78
2. Wood JM, Tyrrell RA, Lacherez P et al (2017) Night-time pedestrian conspicuity: effects of clothing on drivers' eye movements. *Ophthal Physiol Opt* 37(2):184–190
3. Yu L, Deng H (2016) Design elements and principles of children sweater based on market research. *Light Text Ind Technol* 45(05):37–39+19
4. Cao Z, Su Z, Wei Y (2019) Application of eye movement tracking technology in the pattern design of sweater for middle-aged and elderly person. *Wool Text J* 47(06):71–74
5. Glaholt MG, Reingold EM (2011) Eye movement monitoring as a process tracing methodology in decision making research. *J Neurosci Psychol Econ* 4(2):125

# Design of Feed Mechanism Based on Computer Cooperative Human–Computer Interaction Design Concept



Zijing Wang

**Abstract** This article constructs a collaborative work model for project design and illustrates it with typical examples. It is pointed out that the concept of human–computer interaction design based on computer collaboration technology determines the quality of project design. By adopting serial or parallel design methods, it not only provides methods and support for the modeling, simulation and implementation of complex project design but also greatly shortens the project development cycle, reduces costs and improves project completion efficiency. The design scheme can also be revised based on the simulation feedback, thereby greatly improving the reliability of the project design. Further research shows that the human–computer interaction design concept and working model based on computer collaboration technology have important application value for timely understanding of design dynamics, obtaining information on staged design results, promoting collaborative communication among designers and sharing design resources.

**Keywords** Computer collaboration · Human computer interaction · Project design · Design pattern

## 1 Introduction

Human–computer interaction and collaborative project design mean that under the condition of computer technology, a group of designers relies on computers (systems) to complete project design tasks together. It mainly involves real-time and non-real-time interaction of design ideas, ideas and sub-project data. Realize serial, parallel and interactive feedback of information between sub-projects. The serial, parallel and mutual integration modes between projects not only provide methods and support for the modeling, simulation and implementation of complex project designs but also greatly shorten the project development cycle, reduce costs and increase project efficiency and reliability.

---

Z. Wang (✉)  
Shandong Normal University, 250358 Jinan, China  
e-mail: [1092857798@qq.com](mailto:1092857798@qq.com)



The engineering design process is a process that reflects the overall technical level and mutual coordination. In the process of human–computer interaction design based on computer collaboration technology, design schemes and parameters of different types and different paths can be collected by a computer system, and matching simulations can be verified. However, the main feature of collaborative design is that the design of distributed sub-projects goes hand in hand. Therefore, it is necessary to rely on an integrated platform of network information, functions, management, processes and operations supported by big data and cloud computing. The platform can provide a full range of specific design task collaborations, fully consider the parallelism in project design and quickly respond to changes in the collaborative design process, making it easy to query, locate and solve problems in order to coordinate the design process management.

The main function of human–computer interaction collaborative engineering design is not only to make different design contents cooperate with each other in the design process, but also to make the design subject and computer system cooperate with each other. The autonomy and innovation of distributed participants will be the same by computer systems. It can make design content such as function, structure, layout, form, ergonomics work together to achieve the same purpose.

In the human–computer interaction design method based on computer collaboration technology, different project tasks can achieve the same project goal. In order to achieve a unified goal, there will be a cooperative mechanism to achieve the common design goal and the common design goal, including communication protocols, communication structures, conflict detection and arbitration [1]. In other words, if the design ideas of any sub-project designer change, its design ideas and design data will be quickly fed back to the entire system. The designers of each sub-project will revise the design plan based on the information feedback. The final design will be verified through modeling and simulation. The collaborative system will feedback the problems in the simulation verification to the distributed designers in time. The designer can further improve the design scheme based on the feedback information.

In project design, how to apply human–computer interaction design method based on computer collaboration technology to accelerate the process of project design has become a hot issue for experts and scholars.

## **2 Construction of Collaborative Project Design Model**

### ***2.1 Computer-Supported Collaborative Design Model***

Model construction is the product of the combination of collaborative design technology and project information. Combined with the main content and characteristics of the project design process and taking into account the cost, cycle, quality and other factors of the project design, different project purposes and types will adopt different

design methods. Therefore, computer-supported project design is also a multi-modal collaborative design.

Generally, projects can be executed as a set of sub-projects, forming a project tree. There is a certain relationship between projects, and the good collaborative relationship between sub-projects determines the efficiency and quality of the project.

Collaborative design mode is a method to ensure the successful completion of the project by coordinating and controlling the important design parameters and design progress of each sub-project. In this design mode, a powerful project management system is needed to complete the project decomposition, sub-project definition, constraint management and project process control of collaborative design.

Generally speaking, computer-supported co-design models have two modes: serial and parallel. The application of serial and parallel modes relying on computer collaboration technology not only provides methods and supports for modeling, simulation and implementation of complex project designs but also greatly shortens the project development cycle, reduces costs and improves the efficiency and reliability of project design completion [2].

## ***2.2 Project Design Mode***

Each sub-project is interrelated, and the modification of one sub-project may lead to forced modification of other sub-projects. Due to the diversity and complexity of the project, there must be a sub-project classification model, which is the key to achieving collaborative project design. There are several typical collaborative design patterns.

### **2.2.1 Serial Mode**

The serial mode is to decompose the entire project into several sub-projects. Each sub-project is independent and interrelated and is designed according to the order of the projects. After the design of one project is completed, the second project design is executed and merged until multiple sub-projects are completed to complete the entire project design. In the serial process, the complete information generated by the previous project is passed to the next project, while the next project design is activated. Then, proceed in the same way, in order of items. This is a typical sequential design pattern.

The general process of the serial mode is as follows: Step 1: Propose the target main project; step 2: Decompose the main project into sub-projects 1 to  $n$ ; step 3: Make design plans and steps for each sub-project and design; complete sub-projects 1, 2, ... and  $n$  design tasks; step 6: Combine design sub-projects; step 7: Complete the entire project design as shown in Fig. 1.

**Fig. 1** Serial pattern

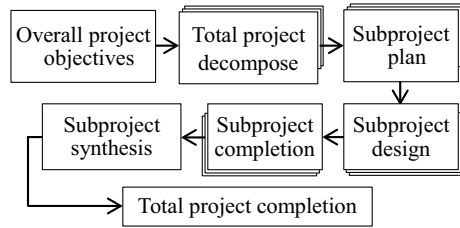
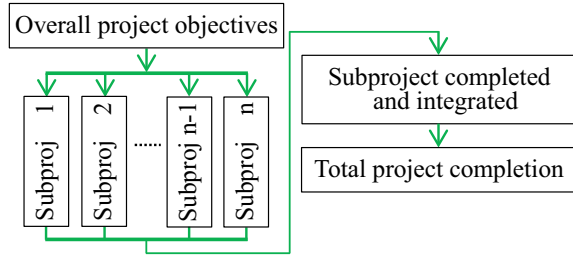


**Fig. 2** Parallel mode



**2.2.2 Parallel Mode**

The parallel mode is to divide the entire project into several sub-projects. All sub-projects are independent and coordinated at the same time. In the synchronous design process, not only are there related relationships such as independence, no related information, resource occupation, but also information exchange and constraints such as mutual synchronization, interlocking and conflict arbitration as shown in Fig. 2.

In the above-mentioned parallel mode, in order to realize the collaborative design of the entire project, it is necessary to establish the parameter relationship between the sub-projects and synchronize the design according to the virtual parameters to manage and control the progress of the sub-projects. All sub-projects are checked after the design is completed and integrated to complete the entire project design smoothly.

**3 Empirical Analysis**

**3.1 Review of Research Status**

This research takes the feeding mechanism of the automated production line as an example for empirical analysis.

With the continuous research on cam mechanism dynamics and vibration, the performance of high-speed cams has been further optimized, and ultra-small and

ultra-large worm cam mechanisms have appeared. The research on the theory of cam mechanism kinematics, cam indexing mechanism, cam mechanism conjugate surface and expert system has reached a high level. Some progress has been made in CAD/CAM, application fields, processing equipment, CAM and supporting parts processing technology. The future research direction is to improve the integrated CAD system of plane cam and cylindrical cam, introduce artificial intelligence CAD system or expert system and strengthen computer simulation research and CAD/CAM integration. This is the integration and penetration of multiple disciplines.

### ***3.2 Collaborative Design of Feeding Mechanism***

The good cooperation between the components of the feeding mechanism determines the good performance and safe operation of the feeder. The movement of the feed mechanism is relatively complicated. Generally, it can only achieve a given movement, so a large movement accuracy error and cumulative error will occur, which will seriously affect the performance of the feed mechanism.

The design path of the feeding mechanism is on-site investigation > data collection > innovative design > scheme demonstration > computer-aided analysis > determine the best design > verification conclusion.

In serial mode, when the previous task is completed, the complete information it generates can be passed to the next task as input to the next task, and the next task is activated at the same time.

Obviously, the collaborative design of the feed mechanism fully shows that the application of the human-computer interaction design method of the computer collaborative technology can improve the motion characteristics, mechanical performance and service life of the existing transmission mechanism system and obtain high calculation accuracy and precise position [3].

In parallel mode, multiple sub-projects are designed using virtual parameters simultaneously. When all sub-projects have been designed, they rely on computer systems for verification and integration. After the verification and integration work is completed, all parameters are generated at the same time to achieve the completion of the overall goal.

### ***3.3 Empirical Analysis***

#### **1. Empirical design**

The feed mechanism studied in this paper consists of a cam, a follower and a frame, also known as a cam mechanism. Generally, a cam is used as a driving part, which rotates, swings or moves back and forth at the same speed [4].

The feed mechanism relies on the direct contact between the convex contour line and the follower, forcing the follower to make intermittent or continuous reciprocating motion (or swing). Therefore, in the design of the cam mechanism, in order to obtain a predetermined movement rule of the follower, as long as an appropriate convex contour line is designed, it can be achieved.

Empirical design method and steps:

1. Analyze and calculate the motion characteristics, mechanical properties and service life of the feed mechanism system to determine the exact position of the feed mechanism.
2. The transmission mechanism should have the characteristics of large stroke, small wear, long service life, good flexibility and so on.
3. Determine the best scheme of economic and practical transmission mechanism, and summarize the overall design method with certain significance.

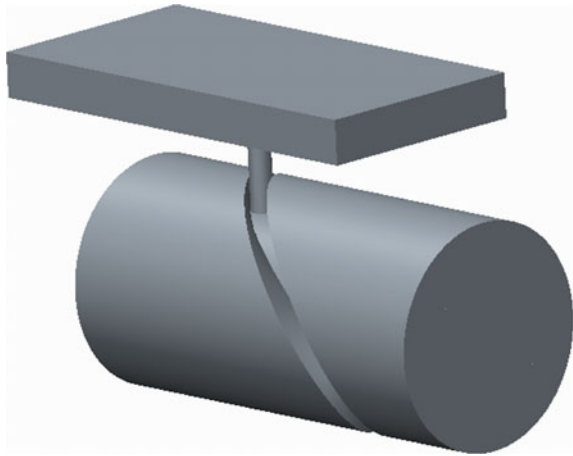
## 2. Simulation modeling

The cam profile determines the change rule of push rod speed, which is the key of design. Therefore, a new PRT part is created in Creo by using MMNs part solid template. Firstly, the main model of the cylindrical indexing cam is established, and then, the driving push rod model and the frame model are established. Finally, the optimal simulation model of the feed mechanism is established according to the motion coordination relationship and combination.

1. Model construction of cylindrical indexing cam: In the feed mechanism, the main model construction method of cylindrical indexing cam is to draw the unfolded section line of the cam, wrap the section line on the cylinder through the envelope command; use the scanning command to build the main body of cylindrical indexing cam, and then, construct the hole, stiffener, chamfer and other detailed features of the cam in turn.

Simulation steps:

- (1) Using the intersection of the projection lines of the RIGHT and TOP planes on the sketching plane as the center of the circle, an extruded surface with a diameter of  $D$  circle is generated. By stretching the axis of 1, the reference plane DTM1 is generated at an angle of  $60^\circ$  with the TOP surface; the reference plane DTM2 is generated perpendicular to DTM1; the FRONT plane is selected as a reference, and the reference plane DTM3 is generated by offset 9. Establish a reference coordinate system, select DTM2 and determine the length of the two horizontal lines, the distance between the right end of the upper right horizontal line and the projection line of DTM1 on the sketch plane and the distance between the two horizontal lines. Furthermore, the developed section line of the cylindrical indexing cam is simulated. Select the model envelope origin, generate the envelope, and generate the cylindrical indexing cam body.
- (2) Create an extruded surface. Select the FRONT plane as the reference and offset 9 to generate the reference plane DTM3. DTM3 and FRONT surfaces

**Fig. 3** Simulation model

were selected as sketching planes to generate extruded surfaces. Select the FRONT surface as the sketching plane and the surface as the extruded surface to create an extruded surface. Select the edges you want to project and the faces you want to project on to create a projection. Select extrude under the Extrude dashboard to create an extruded surface.

- (3) Generate chamfers, fillets and ribs using commands such as extrude, sketch and datum according to the drawing. The final solid model of the cylindrical indexing cam is shown in Fig. 3.
2. Based on the above design data, the follower push rod model is constructed by the same method.
3. Again, build a framework model.
4. According to the motion coordination relationship, the simulation model is synthesized.
5. The simulation model is used to verify the design.

At this point, the optimal simulation model of feeding mechanism is obtained.

## 4 Conclusion

1. The degree of collaborative work determines the quality of the project design. Research shows that the human-computer interaction design string and parallel integration mode based on computer collaborative technology not only provides methods and support for modeling, simulation and implementation of complex project design, but also greatly shortens the project development cycle and reduces costs.

2. Establish the simulation model of the feeding mechanism, and use computer software for simulation analysis to determine the economical and practical optimal feeding mechanism scheme. It is because of the simulation that problems can be found in time and the design plan can be revised.
3. The proposed feed mechanism model improves the mechanical performance and service life of the feed mechanism and obtains higher calculation accuracy and precise position.

## References

1. Peter B (2019) Ten ways to optimize evidence-based policy. *J Comp Eff Res*. <https://doi.org/10.2217/cer-2019-0132>
2. Chen G, Bau HH, Li CH (2019) In-situ TEM liquid cell 3D profile reconstruction and analysis of nanoscale liquid water contact line movements. *Langmuir: ACS J Surf Colloids*. <https://doi.org/10.1021/acs.langmuir.9b01428>.
3. Rueda DR, Cotta C, Fernández-Leiva AJ (2019) Memetic collaborative approaches for finding balanced incomplete block designs. *Comput Oper Res*. <https://doi.org/10.1016/j.cor.2019.104804>
4. Diego R, Darawsheh M, Barrios LA, Sadurní A, García J, Lloyd-Williams P, Teat SJ, Roubeau O, Aguilà D, Aromí G (2019) Designed asymmetric coordination helicates with bis- $\beta$ -diketonate ligands. *Dalton Trans (Cambridge, England: 2003)* 48(45), 16844–16847

# **Research on the Environment Character**



# Study on Life Prediction Method of MOSFET Thermal Environment Experiments Based on Extended Kalman Filter



Ke Li, Yuxiang Zhang, Shimin Song, Zhijian Zhao, and Lijing Wang

**Abstract** The prediction method of the residual service life of power MOSFET is studied in this paper. By analyzing the data collected under the existing thermal overload accelerated aging experiment, after processing the data, the failure threshold was set by using the prediction algorithm based on data drive and model to predict the residual life of power MOSFET. The traditional SVR algorithm requires a lot of parameter selection and only a few parameter convergence. The prediction algorithm model is based on Extended Kalman Filter, the extended Kalman filter is relative to the advantage of support vector machine (SVM) regression is used to predict the variance is small, and can be found in a wide range of required to predict the sample interval and the predicted results are more accurate, the test results verify the feasibility of this method.

**Keywords** Power MOSFET · Accelerated aging · Failure mechanism · Life prediction · Extended Kalman filter

## 1 Introduction

Power electronic devices such as metal-oxide semiconductor field effect transistors (MOSFETs) and insulate-gate bipolar transistor (IGBTs) are important electronic components that are widely used in communications, vehicle control, navigation and radar systems of the spacecraft. Failure of these electronic devices is likely to

---

K. Li (✉) · Y. Zhang · L. Wang

Fundamental Science on Ergonomics and Environment Control Laboratory, School of Aeronautics Science and Engineering & Beijing Advanced Discipline Center for Unmanned Aircraft System, Beihang University, 100191 Beijing, China  
e-mail: [like@buaa.edu.cn](mailto:like@buaa.edu.cn)

S. Song

China Academy of Space Technology, 100094 Beijing, China

Z. Zhao

Naval Aeronautical University, 264000 Yantai, China

© The Editor(s) (if applicable) and The Author(s), under exclusive license to Springer Nature Singapore Pte Ltd. 2021

S. Long and B. S. Dhillon (eds.), *Man-Machine-Environment System Engineering*, Lecture Notes in Electrical Engineering 645, [https://doi.org/10.1007/978-981-15-6978-4\\_58](https://doi.org/10.1007/978-981-15-6978-4_58)

cause overall system failure, so uncontrollable conditions caused by sudden failure of the electronic device must be avoided.

The extended Kalman filter prediction technique proposed for power MOSFETs in this paper is based on the accelerated aging experiment of MOSFET IRF520Npbf. The accelerated aging method is to load a cycle of thermal and electrical power on a 100 V power MOSFET device and verify it through thermal environmental testing. The feature based on the normalized on-resistance is obtained by calculating real-time measurement data of the electrothermal response. Support vector machine (SVM) is one of algorithm method of predictive model. Another one is based on the extended Kalman filter tracking Bayesian framework (the EKF) (Extended Kalman the Filter) [1, 2]. Comparing two method of predict effects is achieved by the presenter, it can be found that the Kalman filter is sufficient for predicting sample data, and prediction is performed at any point after a certain time and the prediction results are relatively accurate.

## 2 Algorithm

### Extended Kalman Filter Principle

In the process of nonlinear relations, the estimated values around the current judgment can be linearized by using the partial differential and measurement functions of the process to calculate the estimator. To this end, some aspects involved in discrete Kalman filtering must be modified.

As shown below:

$$x_k \approx \tilde{x}_k + A(x_{k-1} - \hat{x}_{k-1}) + Ww_{k-1} \quad (1)$$

$$z_k \approx \tilde{z}_k + H(x_k - \tilde{x}_k) + Vv_k \quad (2)$$

$x_k$  is the actual state variable, and  $z_k$  is the measurement variable;

$\tilde{x}_k$  is the approximate state variables, and  $\tilde{z}_k$  is the approximate measured variables;

$\hat{x}_k$  is the state posterior estimate of the step length  $k$ ;

Random variables  $w_k$  and  $v_k$  represent process noise and measurement noise, respectively;

$A$  is the Jacobian matrix of the partial derivative of  $f$  to  $x$ :

$$A_{[i,j]} = \frac{\partial f_{[i]}}{\partial x_{[j]}}(\hat{x}_{k-1}, u_{k-1}, 0) \quad (3)$$

$W$  is the Jacobian matrix of the partial derivative of  $f$  to  $w$ :

$$W_{[i,j]} = \frac{\partial f_{[i]}}{\partial w_{[j]}}(\hat{x}_{k-1}, u_{k-1}, 0) \tag{4}$$

$H$  is the Jacobian matrix of the partial derivative of  $h$  to  $x$ :

$$H_{[i,j]} = \frac{\partial h_{[i]}}{\partial x_{[j]}}(\tilde{x}_k, 0) \tag{5}$$

$V$  is the Jacobian matrix of the partial derivative of  $h$  to  $v$ :

$$V_{[i,j]} = \frac{\partial h_{[i]}}{\partial v_{[j]}}(\tilde{x}_k, 0) \tag{6}$$

Here,  $i$  is the number of functions, and  $j$  is the number of variables. For the sake of simplicity, the time subscripts of Jacobian matrix  $A$ ,  $W$ ,  $H$  and  $V$  are not used, even if they are different at each time step. Define a new symbol for the prediction error:

$$\tilde{e}_{x_k} \equiv x_k - \tilde{x}_k \tag{7}$$

And measuring residuals:

$$\tilde{e}_{z_k} \equiv z_k - \tilde{z}_k \tag{8}$$

Actually,  $x_k$  in Eq. (14) is not available. It is the actual state vector, a value that needs to be tried to estimate. On the other hand,  $z_k$  in Eq. (15) is able to get. It is the actual measured amount for estimating  $x_k$ . Based on Eqs. (16) and (17), the governing equation for error handling can be written as

$$\tilde{e}_{x_k} \approx A(x_{k-1} - \hat{x}_{k-1}) + \varepsilon_k \tag{9}$$

$$\tilde{e}_{z_k} \approx H\tilde{e}_{x_k} + \eta_k \tag{10}$$

$\varepsilon_k$  and  $\eta_k$  represent zero mean and new independent random variable of the covariance matrix  $WQW^T$  and  $VRV^T$ .  $Q$  and  $R$  are the same as expressed by Formulas (3) and (4).

$$\hat{x}_k = \tilde{x}_k + K_k \tilde{e}_{z_k} = \tilde{x}_k + K_k(z_k - \tilde{z}_k) \tag{11}$$

Equation (18) is used to extend the measurement update in the Kalman filter.  $\tilde{x}_k$  and  $\tilde{z}_k$  are from Eqs. (3) and (4). Kalman  $K_k$  is gained by making the appropriate replacement in the measurement error covariance matrix  $R$  ( $K_k = P_k^- H^T (HP_k^- H^T + R)^{-1}$ ).

The complete extended Kalman filter equations are shown below [3]. Attention to that  $\tilde{x}_k$  has been replaced by  $\hat{x}_k^-$ . This is to be consistent with the previous “super subtraction” a priori symbol, and let subscript  $k$  add to the Jacobian matrix  $A$ ,  $W$ ,  $H$  and  $V$ , to reinforce the concept that they are different at different time steps (and therefore must be recalculated at each step).

$$\hat{x}_k^- = f(\hat{x}_{k-1}, u_{k-1}, 0) \quad (12)$$

$$P_k^- = A_k P_{k-1} A_k^T + W_k Q_{k-1} W_k^T \quad (13)$$

Like the basic discrete Kalman filter, the discrete Kalman filter time-update equation pairs from the previous time step  $k - 1$  to the time step  $k$  by now. The state and covariance estimates were predicted.  $f$  in Formula (19) is from  $\tilde{x}_k = f(\hat{x}_{k-1}, u_{k-1}, 0)$ ,  $A_k$  and  $W_k$  are Jacobian matrix of the step size  $k$ ,  $Q_k$  is process noise covariance of the step size  $k$ .

$$K_k = P_k^- H_k^T (H_k P_k^- H_k^T + V_k R_k V_k^T)^{-1} \quad (14)$$

$$\hat{x}_k = \hat{x}_k^- + K_k (z_k - h(\hat{x}_k^-, 0)) \quad (15)$$

$$P_k = (I - K_k H_k) P_k^- \quad (16)$$

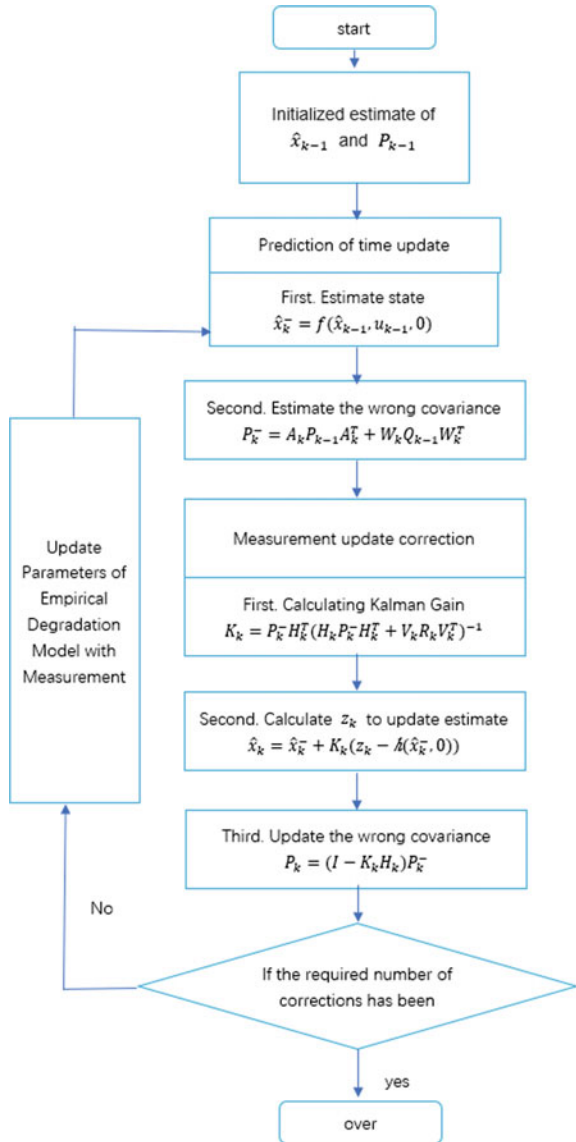
In essence, the discrete Kalman filter modifies the measurement update equation, state estimation and covariance measurement.  $h$  in (15) is from  $\tilde{z}_k = h(\tilde{x}_k, 0)$ ,  $H_k$  and  $V$  are Jacobian matrix of the step size  $k$ , and  $A_k$  is the measured noise covariance of the step size  $k$ .

An important feature of the extended Kalman filter is Jacobian matrix  $H_k$  in the Kalman gain equation  $K_k$ , where the relevant components of the measurement signal can only be accurately propagated or “amplified.” If the measurement  $z_k$  does not pass the one-to-one mapping between States, then the Jacobian matrix  $H_k$  will affect the Kalman gain, so it only amplifies the residuals affecting the state ( $z_k - h(\hat{x}_k^-, 0)$ ).

### 3 Life Prediction Model Based on Algorithm

The life prediction algorithm of the Kalman filter is an algorithm based on the Bayesian estimation framework and based on the degradation model of the power MOSFET. The extended Kalman filter life prediction model used in this paper is shown in Fig. 1.

**Fig. 1** Whole process of life prediction



### 3.1 Empirical Degradation Model

Based on the literature [4–10], it is proposed to observe accelerating the aging process  $\Delta RDS(on)$  of the device [11] and then get the empirical degradation model. The degradation process is used to make a model. Making  $R = \Delta RDS(on)$ , the empirical degradation model for power MOSFET devices based on  $\Delta RDS(on)$  is defined as

follows:

$$R = \alpha(e^{\beta \cdot t} - 1) \quad (17)$$

$t$  is time,  $\alpha$  and  $\beta$  are model parameters that are part of a static or online estimate in the Bayesian tracking framework. The model structure can represent the exponential behavior of different device degradation processes.

### 3.2 Parameter Update of Empirical Degradation Model

In order for the model to fit the data accurately and to predict the life accurately with the model, we need to update the model parameters effectively. So, in this model, state variables  $\alpha$  and  $\beta$  will change with extended Kalman measurement variety in the updated. The parameter update formula is as follows:

$$\alpha_{\text{new}} = \alpha_{\text{old}} + (e^{-\beta_{\text{old}} z_k} - 1) z_k \quad (18)$$

$$\beta_{\text{new}} = \beta_{\text{old}} + (e^{-\beta_{\text{old}} z_k}) z_k \quad (19)$$

Such an update can effectively ensure that the prediction model can effectively converge even if the pre-input parameter deviation is large. The disadvantage is that it acts as an increasing function, the training samples will diverge when there are many training samples, and the number of training samples needs to be controlled.

## 4 Experimental System

This experiment uses an accelerated aging test, which is also called accelerated life testing. For some electronic components and systems with an expected life of thousands of hours, it is not feasible to wait for the device to fail under normal operation in order to calculate the failure time of these components or systems. Therefore, accelerated life testing is required to complete the prediction of component reliability.

The whole idea is to use the trend term of the power MOSFET degradation parameter change to perform degradation modeling and life prediction, and the random term is used as noise rejection. In this paper, the wavelet analysis method is used to decompose the variation of power MOSFET degradation parameters, and the results are analyzed by stationary time series to determine the decomposition dimension and trend term results.

## 5 Remaining Life Prediction Results

The processed sampled data of one of the experimental components is selected for prediction. For the time-ordered samples obtained after processing, the samples are divided into two segments according to the characteristics of the algorithm, and the previous segment is selected for training, and the latter segment is used for prediction. The total sample distinguishes the number of training samples and predicted samples as the distinguishing point parameters, performs mathematical processing to find the distinguishing point parameters that converge the predicted results to the predicted samples and observe the predicted results. In order to ensure the consistency of the two types of algorithms and the practicability of the prediction itself, the interval parameter interval is set at [100, 180].

### 5.1 Prediction Results Based on Support Vector Machine Regression SVR

After debugging, it was found that the training samples were best at around 154. The best 154 samples were chosen to compare the data with the extended Kalman filter. As shown in Fig. 2, although the better results are obtained, the support vector machine regression is extremely sensitive to the selection of the point parameters. It is necessary to accurately select the point parameters to make it converge, and in most cases, the prediction trend is divergent.

**Fig. 2** Prediction effect chart with distinguishing point parameter 154

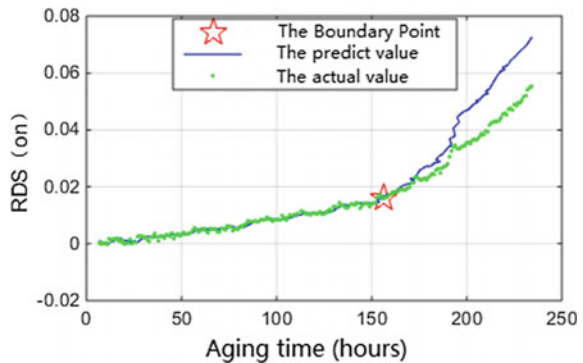
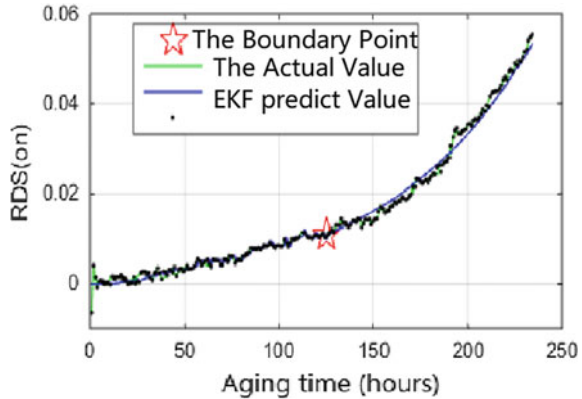


**Fig. 3** Prediction effect chart with distinguishing point parameter 130



## 5.2 Prediction Results Based on Extended Kalman Filter EKF

This paper selects a set of data from all data for forecasting and evaluation. The remaining life prediction begins with a sample of 130. The training samples and the predicted samples are separated by a red five-pointed star. Figure 3 shows the prediction results using extended Kalman filtering. Initialization  $\alpha = 2.7 \times 10^{-3}$ ,  $\beta = 8.55 \times 10^{-5}$  obtained from the former 100 samples by the least square method.

## 6 Conclusions

As can be seen from the results of the two algorithms, the variance of the extended Kalman filtering EKF prediction results is much smaller than the variance of the support vector machine regression analysis results prediction results. Moreover, it can be seen from Fig. 3 that the SVR distinguishing point parameter corresponding to the prediction result variance is much higher than the EKF with the difference of the parameter of the distinguishing point, and it can be said that the SVR algorithm is more unstable. As summarized below, the advantage of EKF over SVR is that it has good convergence and a wide range of results are relatively stable. The disadvantage of EKF is that it relies too much on the degradation model and the parameter update of its model, which limits its application and cannot be used to solve the problem caused by non-RDS (on) rise.

**Acknowledgements** The authors are supported by the Chinese National Natural Science Foundation (No. 61773039).



## References

1. Luo R (2013) Analysis of phm technology for spacecraft. *Spacecraft Engineering*
2. Bing L, Sun Z, Xinwei J (2003) A study of integrated vehicle and ground health management technology for spacecrafts. *Aerospace Control* 21(2):56–61
3. Xin MA (2008) Knowledge acquisition methods for expert systems based on machine learning. *J Beijing Univ Chem Technol* 35(5):89–93
4. Celaya JR, Saxena A, Saha S et al (2011) Prognostics of power MOSFET. 47(10):160–163
5. Sonnenfeld G, Goebel K, Celaya JR (2009) An agile accelerated aging, characterization and scenario simulation system for gate controlled power transistors. *Autotestcon. IEEE*, pp 208–215
6. Saha B, Celaya JR, Wysocki PF et al (2013) Towards prognostics for electronics components. In: *Aerospace conference. IEEE*, pp 1–7
7. Saha S, Celaya JR, Vashchenko V et al (2011) Accelerated aging with electrical overstress and prognostics for power MOSFETs. *Energytech. IEEE*, pp 1–6
8. Razaqpur AG (1987) Discussion: stresses in bi-metal thermostats. *J Appl Mech* 54(2):479
9. (Suhir E (1986) *ASME J Appl Mech* 53:657–660)
9. Li K, Liu W, Wang J et al (2014) Multi-parameter decoupling and slope tracking control strategy of a large-scale high altitude environment simulation test cabin. *Chin J Aeronaut* 27(6):1390–1400.
10. Luo R (2013) Analysis of phm technology for spacecraft. *Spacecr Eng*
10. Li K, Liu W, Wang J, Huang Y (2013) An intelligent control method for a large multi-parameter environmental simulation cabin. *Chin J Aeronaut* 26(6):1360–1369
11. Celaya JR, Saxena A, Kulkarni CS et al (2012) Prognostics approach for power MOSFET under thermal-stress aging. In: *Reliability and maintainability symposium*, pp 1–6

# Research and Application of Multi-node Wireless Skin Temperature Measurement System



Chenming Li and Yuhong Shen

**Abstract** Skin temperature measurement has always been an important method for evaluating the warm-keeping clothing in winter. In order to realize synchronous real-time and accurate measurement of skin temperature, multi-person and multi-node wireless skin temperature measurement system is designed. Based on LoRa wireless transmission network, this research designed communication protocol and low power consumption circuit and developed a multi-person and multi-node wireless skin temperature measurement system. Twenty-four subjects were selected by this system in alpine regions for field tests on two kinds of warm-keeping clothing. The test results show that the skin temperature measurement system has the characteristics of long transmission distance, high measurement accuracy and simple operation and can meet the requirements of warm-keeping clothing test under extreme conditions.

**Keywords** Skin temperature · LoRa · Low power consumption

## 1 Introduction

Skin is the interface between human body and environment for energy exchange.

As an important parameter of human physiology, skin (body surface) temperature plays an important role in calculating human energy loss and analyzing body temperature regulation. Multi-person and multi-node skin temperature measurement has always been an important method for evaluating the warm-keeping clothing in winter. The measurement of human skin temperature in daily life is mainly based on single person and single point measurement. This method cannot reflect the temperature distribution characteristics of different body segments of the human body nor can it realize multi-person comparative test.

---

C. Li (✉) · Y. Shen

The Quartermaster Research Institute of Engineering and Technology, 100010 Beijing, China  
e-mail: [lichenming82@163.com](mailto:lichenming82@163.com)

Wireless sensor network technology has been widely used in industrial temperature and humidity measurement and control. ZigBee, WiFi, FPGA and other technologies provide various solutions for industrial temperature measurement [1, 2]. Compared with industrial wireless temperature measurement technology, human skin measurement requires higher measurement accuracy, transmission mode, transmission distance, sensor structure, etc.

LoRa based on spread spectrum technology is an ultra-long distance and low power data transmission technology below 1 GHz. Compared with the mesh network structure of ZigBee technology, LoRa adopts the star network structure with the lowest delay and simplest. Compared with the high frequency band (2.4 GHz) communication of Bluetooth, WiFi and other communication technologies, LoRa has stronger low frequency band communication penetration capability, the communication distance can even reach 15 km, and the receiving current is only 10 mA, thus realizing low power consumption long-distance wireless transmission.

This paper developed a multi-person and multi-node wireless skin temperature measurement system based on LoRa transmission technology and carried outfield application tests in the field, which solves the problems of limited transmission distance, low measurement accuracy and inconvenient operation in skin temperature measurement of group personnel.

## 2 System Composition

The LoRa-based multi-person wireless skin temperature measurement system is mainly composed of terminal nodes, LoRa gateways, network servers and client terminals, as shown in Fig. 1.

The terminal node comprises a skin temperature measurement node and an ambient temperature measurement node. Each node consists of a temperature sensor and a LoRa terminal module, which mainly completes the measurement, uploading and timing receiving of temperature measurement downlink instructions on human surface and external ambient temperature data. Among them, Murata high-precision NTC temperature chip is selected for temperature sensor, SX1278 is selected for radio frequency module in LoRa terminal module, and STM32F103 module is selected for microcontroller (MCU) module.

LoRa gateway follows LoRaWAN protocol and is equipped with Ethernet, WIFI and 4G modules. It can freely choose the communication mode between gateway and network server according to the actual situation of different test sites. The number of gateways can be freely adjusted according to the number of nodes and transmission distance. The network server converges and analyzes skin temperature data and ambient temperature data. The client terminal uses the form of Web interface to interact with the user, feeds back the test analysis results to the user and accepts the user's instructions at the same time.

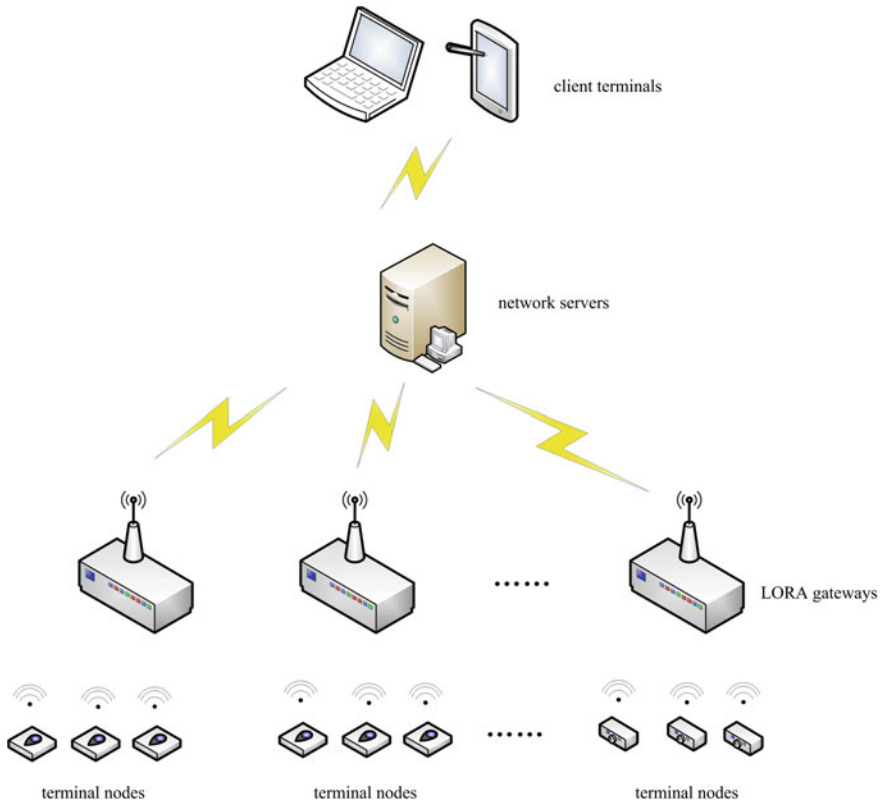


Fig. 1 System composition

### 3 Key Technologies

The multi-node wireless skin temperature measurement system mainly monitors skin temperature and ambient temperature by wearing. The skin temperature fluctuation range is small, and the change frequency is low. Therefore, personalized design and private communication protocol are adopted. At the same time, due to the influence of human body structure, low power consumption design is adopted to reduce the volume of terminal nodes [3].

#### 3.1 Communication Protocol Design

The communication module of the system selects SX1278 radio frequency processor with excellent remote communication capability. SX1278 realizes the physical layer wireless data transceiver function and specifies the data frame format, but SX1278

itself cannot ensure whether the communication data is valid. Therefore, it is necessary to design the upper layer communication protocol to ensure effective data communication. For this reason, DATA frame and Acknowledger (ACK) frame are designed. A DATA frame includes six fields: frame type, frame sequence number, destination address, source address, payload and FCS. The ACK frame acknowledges whether the data is accepted. After the terminal node sends the data, if no acknowledgement frame is received within a given time, the data is retransmitted, and the ACK frame includes the frame type, destination address and FCS.

The communication network undertakes the remote dual-phase transmission of measurement data and control information. The terminal node operates under the timing control of a microcontroller (MCU). The transmitted information includes measurement data and ACK data. The MCU controls the sensor to supply power and collect measurement information by setting timing self-wake-up. Control SX1278 to enter the waiting state, write relevant information into the buffer, and enter the data transmission state after detecting that the channel is idle. The server accepts information in two states: One is to accept ACK data, and the other is to receive control information. SX1278 uses CAD channel detection to ensure the safe reception of data. By setting SX1278 parameters, SX1278 is regularly awakened into CAD channel detection mode. If the preamble is not detected within the specified time, it is transferred to the waiting mode. Once the preamble is detected, the data receiving mode is entered after receiving the preamble and successfully associating the preamble, and the data receiving is completed.

### ***3.2 Low Power Design***

In order to reduce power consumption, the system design adopts the design concept of low power consumption. The hardware platform is based on two processors with low power consumption modes. MCU adopts STM32F103 series products. Its core is a Cortex-M3 architecture microprocessor, which supports three low power operation modes of sleep, stop and wait. It is an ideal MCU for low power system design. SX1278 adopts spread spectrum modulation communication, channel activity detection (CAD) and adaptive data rate (ADR) technologies. It has the characteristics of strong anti-interference capability, high receiving sensitivity, low operating current, adjustable transmission power and long-distance transmission. It supports three low power consumption operation modes of sleep, CAD and waiting. In addition to considering hardware design, it is more important to realize software control when monitoring the low power consumption of the terminal. Software control is considered from two aspects: One is to control the power supply mode of the sensor (execution) component, and only when sensing information is collected regularly can the sensor component be powered; the second is to be awakened regularly to collect, send and receive perceived information. In most cases, the monitoring terminal is in a low power consumption state such as waiting and sleeping, thus greatly reducing the average working current.

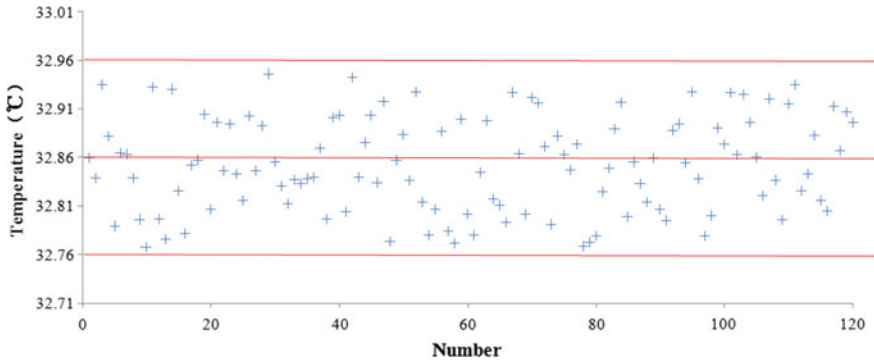


**Fig. 2** Accuracy test result

## 4 Application Testing

### 4.1 Accuracy Test

According to the national measurement standard “JJF1183-2007 Temperature Transmitter Calibration Specification,” the accuracy of 120 skin temperature measurement terminals was tested in the 32.86 °C constant temperature air domain close to the human skin temperature, and the test results are shown in Fig. 2.

As can be seen from Fig. 2, the measurement results for 120 skin temperature measurement terminals are  $(32.85 \pm 0.04)$  °C, and the maximum deviation of a single point is 0.09 °C. Therefore, the multi-node skin temperature measurement system has high measurement accuracy.

### 4.2 Field Application Test

The multi-node skin temperature measurement system is applied to test the warm-keeping performance of winter clothing.

#### 1. Subjects

Twenty-four healthy young men aged 18–24, 12 from the south and 12 from the north, who lived in the test site for one year, were selected. The subjects were randomly divided into two groups with 12 people in each group.

#### 2. Tested Clothing

The tested clothing includes two kinds of matching A and B. Each matching includes underwear, cold-proof vest, velvet clothing, cotton-padded clothing, coat, cold-proof coat, head-mounted velvet hat, hand-mounted cotton gloves, foot-mounted winter

socks and cold-proof shoes. The overall warm-keeping of clothing matching A is 6.58 clo and that of clothing matching B is 6.42 clo. In the first test, the first group of subjects wore matching A, and the second group of subjects wore matching B. In the second test, the two groups of subjects exchanged clothing matching types.

### 3. Test Indicators

Five terminal nodes were distributed on the body surface of each subject, which were placed on the chest, arm, thigh, calf and toe, respectively. The toe temperature was not involved in the calculation as a monitoring index to prevent foot frostbite, and the skin temperature of the other four points was weighted for evaluation [4, 5].

### 4. Test Results

Each test period is 2 h. During the test, the subjects wear different clothes and keep a sit-in posture. The average values of chest, arm, thigh, calf and weighted skin temperatures of 24 subjects with the same clothing matching tested twice were calculated, and the numerical changes are shown in Figs. 3, 4, 5, 6 and 7.

Fig. 3 Temperature curve of chest

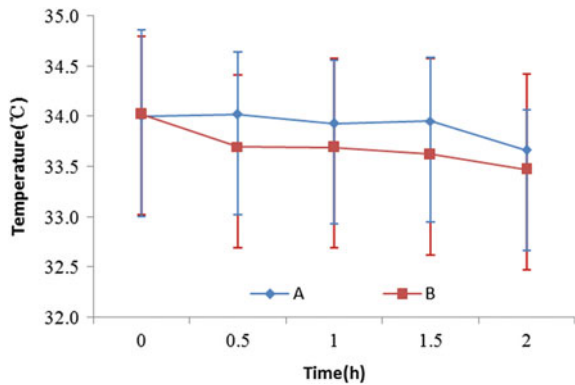
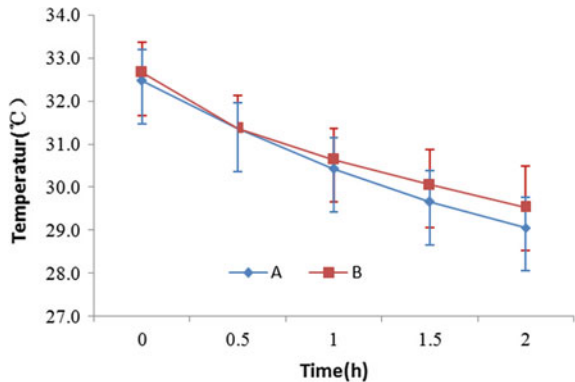
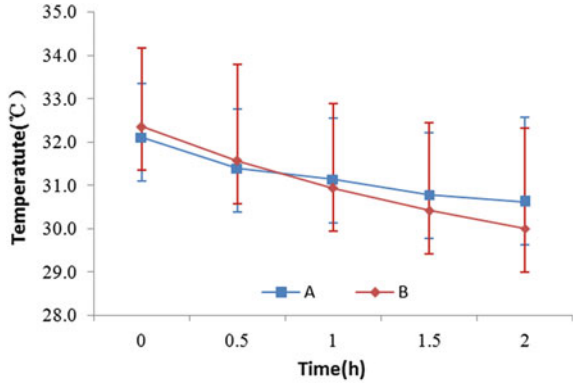


Fig. 4 Temperature curve of arm



**Fig. 5** Temperature curve of leg



**Fig. 6** Temperature curve of calf

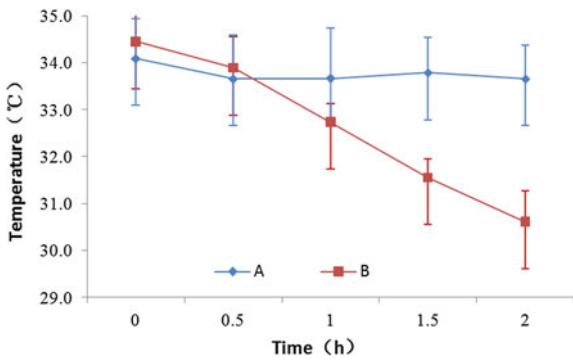
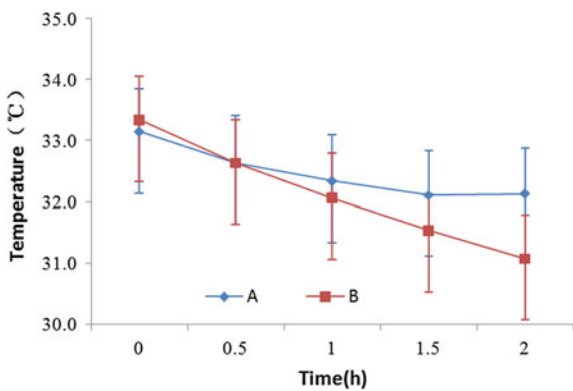


**Fig. 7** Weighted temperature curve



As can be seen from Figs. 3, 4, 5, 6 and 7, at the beginning of the test, the average skin temperature of each part of the subject is not much different, and the test is carried out at any time. Due to the difference in the warm-keeping effect of clothing, the skin temperature difference of each part gradually increases when wearing different



matching. As can be seen from Fig. 7, the average skin temperature of the subjects wearing matching A is 32.47 °C and that of the subjects wearing matching B is 32.12 °C, which is consistent with the overall warm-keeping of the two matching previously measured. The calf temperature measured by the multi-node wireless skin temperature measurement system is quite different when the subjects wear different clothing matching. This is mainly because the warm-keeping layer material of cotton-padded trousers in matching B clothing has poor compression resistance. The subjects use sitting posture to test, resulting in greater stress on the knees and calves of cotton trousers, smaller air layer in cotton trousers, lower warm-keeping effect and lower and faster temperature of calves.

## 5 Conclusion

Based on LoRa wireless transmission network, this paper developed a multi-person and multi-node wireless skin temperature measurement system through communication protocol design and low power consumption design and applied the system to the field test of warm-keeping clothing. The field test results show that the multi-person and multi-node wireless skin temperature measurement system has the characteristics of long transmission distance, high measurement accuracy and simple operation and can meet the requirements of clothing warm-keeping test under extreme conditions.

## References

1. Zhao Q, Xu G, Hao L (2019) Design of wireless multi-parameter environment monitoring node based on LoRa. *Electron Meas Technol* 2019(3):119–122
2. Thoithoi S, Kodur KC, ARIF W (2016) Quaternion based wireless AHRS data transfer using nRF24L01 and HC-05. In: 2016 international conference on microelectronics, computing and communications (MicroCom). *IEEE Conferences*, 2016(7), pp 1–6
3. Liu N (2009) Research on wireless ad hoc network MAC protocol based on LoRa. Xidian University
4. Su J, Cui P, Wang F (2012) Specifications of heat insulation materials for cold protective clothing under different temperatures. *J Donghua Univ (Nat Sci)* 2012(4):175–180
5. Shen Y, Meng C (2009) Study on thermal insulation of winter clothing. *China Pers Prot Equip* 2009(1):16–19

# Research on Calculation Method of Aircraft Skin Temperature Based on Parameter Sensitivity Analysis



Yi Cao

**Abstract** From the perspective of heat transfer, according to factors that affect skin temperature of civil aircraft, combined with the sensitivity analysis method, this paper proposes a method for calculating the skin temperature of an aircraft without inputting the wind speed outside aircraft. The accuracy of this method is verified by the recovery temperature method, and the wind speed outside aircraft is expanded to explain the applicable scope of this method. The results show that when the wind speed outside aircraft is less than 110 m/s, the maximum deviation between the calculated results of this method and the recovery temperature method is 1.9%, and the calculated results are credible. The method is particularly suitable for ground stop and climb condition that the wind speed outside aircraft is less than 110 m/s and difficult to obtain.

**Keywords** Skin temperature of civil aircraft · Parameter sensitivity analysis · Recovery temperature

## 1 Introduction

The composite materialization for large civil aircraft structures has become an inevitable tendency, especially for widebody aircraft that will use composite materials on a large scale. Because the properties of composite materials are particularly sensitive to temperature, aircraft thermal analysis has become one of the most critical parts of large aircraft design and airworthiness certification. In the calculation of civil aircraft temperature field, the skin temperature value is the necessary parameter to set area boundary.

In engineering calculations, the aircraft skin temperature usually uses the recovery temperature value [1], which is the engineering experience value considering the aerodynamic heating of aircraft skin by the wind outside aircraft [2]. The calculation of recovery temperature involves the wind speed outside aircraft, which is usually

---

Y. Cao (✉)

Shanghai Aircraft Design and Research Institute, 201210 Shanghai, China  
e-mail: [caoyi1@comac.cc](mailto:caoyi1@comac.cc)

unavailable for ground stop and climb condition, so the assumed wind speed outside aircraft is generally used for calculation. The assumed wind speed outside aircraft will directly affect the skin temperature of aircraft, thereby affecting the accuracy of the calculated results of the aircraft cabin area temperature field.

From the perspective of heat transfer, according to factors that affect skin temperature of civil aircraft, combined with the sensitivity analysis method, this paper proposes a method for calculating the skin temperature of an aircraft which does not need to input the wind speed outside aircraft during the calculation. The accuracy of this method is verified by the recovery temperature method commonly used in engineering, and the wind speed outside aircraft is expanded to explain the applicable scope of this method.

## 2 Theoretical Analysis of Heat Transfer for Aircraft Skin

Aircraft skin temperature is the result of multiple factors, including external factors, internal factors and thermal characteristics of the skin materials. External factors include convection heat transfer between external environment and skin, solar radiation, ground radiation and sky radiation. Internal factors include convection heat transfer between cabin environment and skin and radiation heat transfer between cabin equipment and skin. The internal and external thermal environment influences each other through aircraft skin. The coupling effect of these heat transfers determines the temperature of aircraft skin [3].

In order to simplify the heat transfer process, the external convective heat transfer coefficient  $h_{out}$  is used to represent the convective and radiative heat transfer intensity outside the cabin, and the internal convection heat transfer coefficient  $h_{in}$  is used to represent the convection and radiative heat transfer intensity in the cabin. When the heat transfer of aircraft skin reaches a steady state, the process can be expressed by the following equation:

$$q = h_{in} \times (T_{in} - T_{w\_in}) \quad (1)$$

$$q = 1/R \times (T_{w\_in} - T_{w\_out}) \quad (2)$$

$$q = h_{out} \times (T_{w\_out} - T_{amb}) \quad (3)$$

where  $q$  is heat flux,  $h_{in}$  is internal heat transfer coefficient,  $T_{in}$  is cabin temperature,  $T_{w\_in}$  is inner skin temperature,  $R$  is skin thermal resistance,  $T_{w\_out}$  is outer skin temperature,  $h_{out}$  is external heat transfer coefficient, and  $T_{amb}$  is ambient temperature.

Therefore, the outer skin temperature of the aircraft is related to environment temperature, cabin temperature, external heat transfer coefficient, internal heat transfer coefficient and skin thermal resistance, which is  $T_{w\_out} = f(T_{amb}, T_{in}, h_{out},$

$h_{in}, R$ ). The following is the sensitivity analysis of each factor to determine the key factor affecting  $T_{w\_out}$ .

### 3 Sensitivity Analysis of Influencing Factors

Sensitivity analysis is a method for analyzing system stability, and this paper uses single factor analysis method. There is a system whose system characteristic  $P$  is mainly determined by  $n$  factors  $a = \{a_1, a_2, \dots, a_n\}$ , which is  $P = f(a_1, a_2, \dots, a_n)$ . In a certain reference state  $a^* = \{a_1^*, a_2^*, \dots, a_n^*\}$ , the system characteristic is  $P^*$ . Make each factor changes within its own possible range and analyze the tendency and extent of deviation of system characteristic  $P$  from the reference state  $P^*$  caused by the changes of these factors, so as to determine the sensitive factors affecting the system characteristics  $P$  [4].

The values of the factors affecting the outer skin temperature  $T_{w\_out}$  are not fixed, but vary within a certain range. Based on engineering experience, the values of each factor are shown in Table 1.

For various working conditions in Table 1, the outer skin temperature value of aircraft is calculated according to Formulas (1)–(3). After fitting, the relationship between  $T_{w\_out}$  and each factor is as follows:

$$T_{w\_out} = 0.99 \times T_{amb} + 2.635 \tag{4}$$

$$T_{w\_out} = 0.0093 \times T_{in} + 214.9 \tag{5}$$

**Table 1** Value list of each factor

No.	$T_{amb}$ (K)	$T_{in}$ (K)	$h_{out}$ (W/(m <sup>2</sup> K))	$h_{in}$ (W/(m <sup>2</sup> K))	$R$ ((m <sup>2</sup> K)/W)
1	217	218	50	1	0.001
2	218	233	75	2.5	0.005
3	233	253	100	5	0.01
4	253	273	125	7.5	0.05
5	273	283	150	10	0.1
6	283	293	175	12.5	0.5
7	288	295	200	15	1
8	293	297	225	17.5	5
9	298	298	250	20	10
10	303	300	275	22.5	15
11	308	303	300	25	20
12	313	313	325	27.5	25
13	328	328	350	30	50

$$T_{w\_out} = 42.25 \times h_{out}^{-0.8537} + 214.9 \tag{6}$$

$$T_{w\_out} = -0.496 \times h_{in}^{-0.481} + 217.9 \tag{7}$$

$$T_{w\_out} = 10.53 \times R^{-0.0693} + 208.3 \tag{8}$$

Based on the Formulas (4)–(8), obtain the sensitivity coefficient within the range of each factor. The sensitivity curves of each factor are shown in Figs. 1, 2, 3, 4 and 5.

In engineering, according to the size of sensitivity coefficient, each factor is divided into: sensitive factor, relatively sensitive factor and insensitive factor. Factors

**Fig. 1** Sensitivity curve of  $T_{amb}$

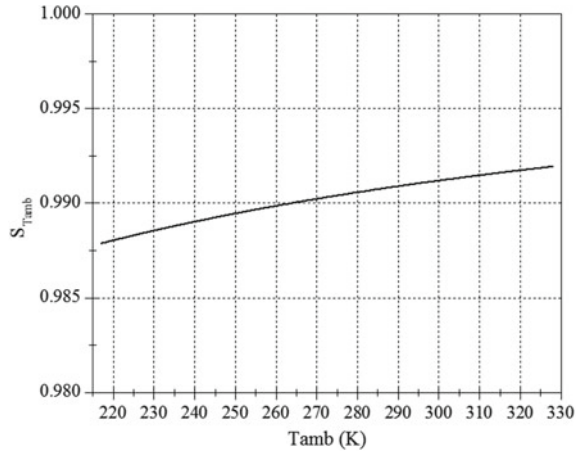


**Fig. 2** Sensitivity curve of  $T_{in}$

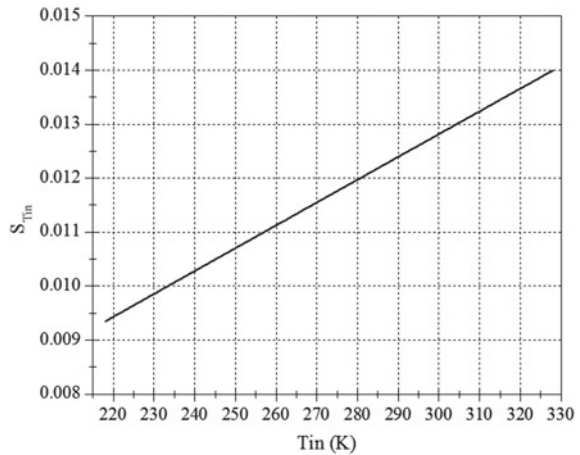


**Fig. 3** Sensitivity curve of  $h_{out}$

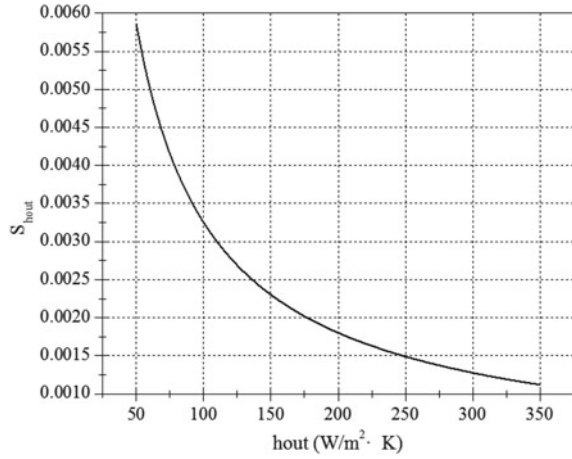
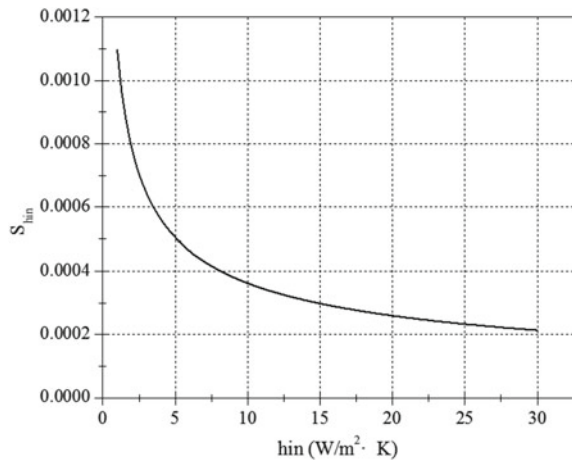


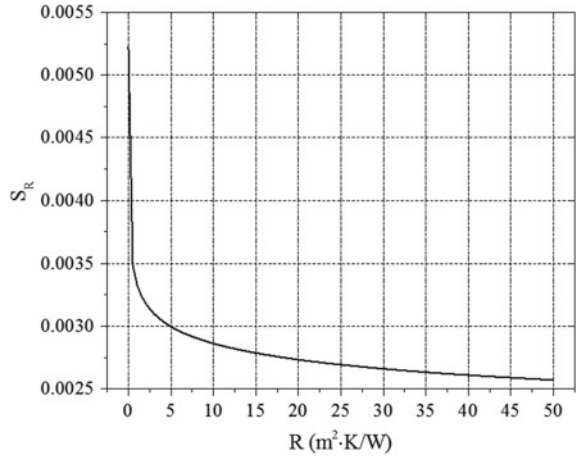
**Fig. 4** Sensitivity curve of  $h_{in}$



with the sensitivity coefficient greater than 0.2 are defined as sensitive factors, between 0.04 and 0.2 are defined as relatively sensitive factors, less than 0.04 are defined as insensitive factors [5]. From Figs. 1, 2, 3, 4 and 5, it can be seen that within the scope of engineering experience, only  $T_{amb}$  is the sensitive factor, while the other factors are the insensitive factors.

Therefore, Formula (4) is the aircraft skin temperature calculation formula proposed from the perspective of heat transfer.

Fig. 5 Sensitivity curve of  $R$

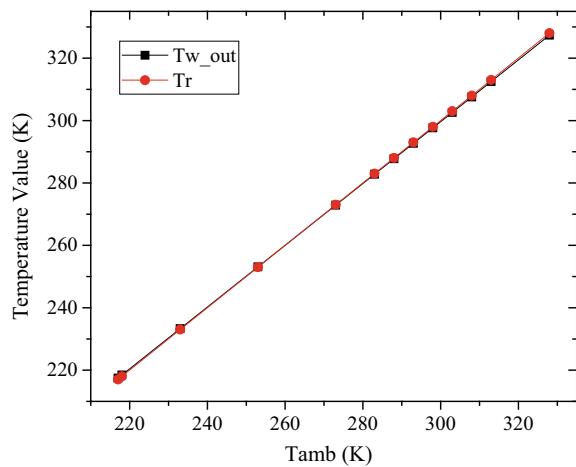


### 4 Verification of Calculation Method and Description of Applicable Scope

At present, the recovery temperature is usually used as the aircraft skin temperature for Mach number between 0 and 2 [6]. In the following, the accuracy and applicable scope of the skin temperature calculation method proposed in this paper are explained by comparison.

The ambient temperature  $T_{amb}$  takes the conditions in Table 1. According to the description in literature [6], the wind speed outside aircraft in the calculation of recovery temperature is 6.5 m/s. The comparison of aircraft skin temperature proposed in this paper and recovery temperature is shown in Fig. 6. As can be seen

Fig. 6 Comparison of aircraft skin temperature values between two methods



from the figure, for this condition, the calculation method proposed in this paper is in good agreement with the value calculated by the recovery temperature method, with a maximum difference of about 0.1%.

Following are the conditions of different ambient temperatures in Table 1, expanding the wind speed outside aircraft from 1 to 300 m/s in the calculation of recovery temperature, to study the applicability of the aircraft skin temperature calculation method proposed in this paper. It can be known from calculation that for the same environment temperature and the same wind speed outside aircraft, the ratio of the difference between the proposed calculation method and the recovery temperature method and the recovery temperature value is basically constant, as shown in Fig. 7. The proportional average value corresponding to each wind speed outside aircraft is selected as an index to measure the deviation degree of the two calculation methods under the corresponding wind speed. Figure 8 shows the ratio of the difference between the two methods and the recovery temperature value under different external wind speeds. As can be seen from the figure, when the outside wind speed is less than 110 m/s, the maximum deviation between the calculation results of this method and the recovery temperature method is 1.9%, with good data consistency. Therefore, the method proposed in this paper for calculating the skin temperature of an aircraft without inputting the wind speed outside aircraft is particularly suitable for ground stop and climb condition that the wind speed outside aircraft is less than 110 m/s and difficult to obtain.

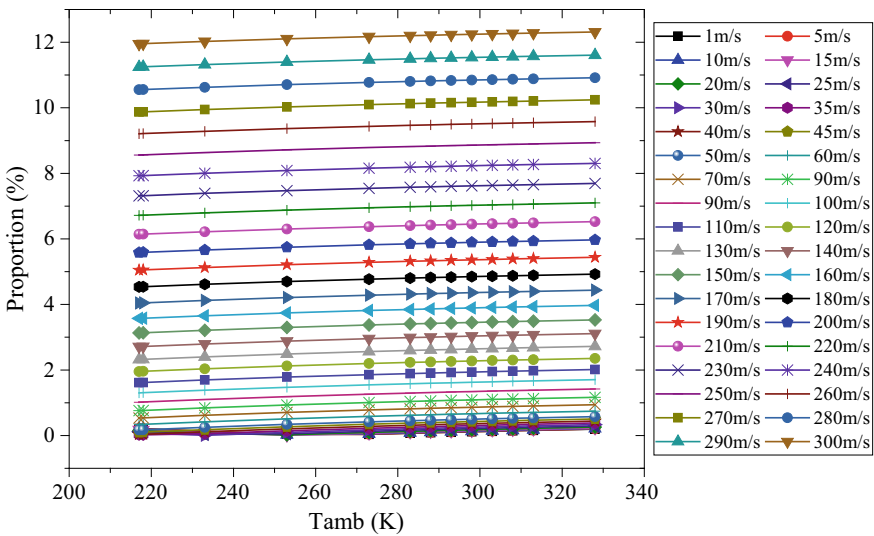
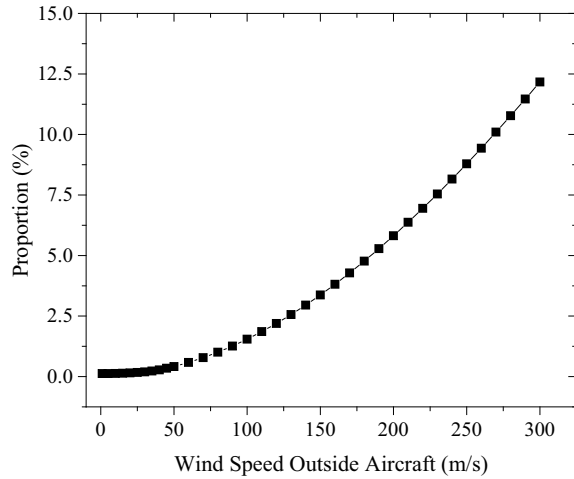


Fig. 7 Different percentage of results calculated by the two methods



**Fig. 8** Different percentage of results calculated by the two methods under different wind speeds



## 5 Conclusion

From the perspective of heat transfer, according to the factors that affect skin temperature of civil aircraft, combined with the sensitivity analysis method, this paper proposes a method for calculating the skin temperature of an aircraft. The accuracy of this method is verified by the recovery temperature method commonly used in engineering, and the wind speed outside aircraft is expanded to explain the applicable scope of this method. The results show that when the wind speed outside aircraft is 6.5 m/s in the calculation of recovery temperature, the maximum difference between the value calculated by this method and the recovery temperature value is about 0.1%, and the calculation result of this method is basically accurate. By the calculation and analysis of expanding the wind speed outside aircraft conditions, when the outside wind speed is less than 110 m/s, the maximum deviation between the calculation results of this method and the recovery temperature method is 1.9%, with good data consistency. Therefore, this method is particularly suitable for ground stop and climb condition that the wind speed outside aircraft is less than 110 m/s and difficult to obtain, so as to provide a simple and accurate calculation method for the aircraft skin temperature.

## References

1. Wu LL (2018) Study on surface temperature field and its similarity of aircraft. Harbin Institute of Technology, Harbin, pp 2–5
2. Wang J (1981) The mathematical model of aircraft cabin temperature. J Beijing Inst Aeronaut Astronaut 2:45–60

3. Fu Y, Chang HJ, Wu YQ et al (2014) Dynamic temperature predicted model for airplane platform based on measured data. *Acta Aeronaut Astronaut Sin* 35(9):2472–2480
4. Zhang G, Zhu WS (1993) Parameter sensitivity analysis and optimizing for test programs. *Rock Soil Mech* 14(1):51–58
5. Wei LX, Sun C, Zhao J et al (2014) Sensitivity analysis of influencing factors on heat transfer coefficient calculation. *Sci Technol Eng* 14(20):294–297
6. Aircraft Design Manual Total editorial board (1999) *Aircraft Design Manual volume 15: Life support and environmental control system design*. Aviation Industry Press, Beijing, pp 3–18

# Research on Adaptive Anti-interference of Fire Control Radar Network



Jiang Luo, Yanyan Ding, Boqi Wang, and Wei Yu

**Abstract** According to the battlefield situation, the real-time accurate operation control is an important prerequisite for giving full play to the operational effectiveness of weapons and equipment. In the face of increasingly complex battlefield environments and real-time changing air situations, it is urgent for army to make research on the accurate control of air defense radars in the best state and full use of the overall operational effectiveness of radar networks under different reconnaissance mission situations. This article takes full advantage of radar anti-interference capability, aims to develop a radar working status control method that fits the radar combat mission, and is suitable for precise use and provides auxiliary decision support for air defense group commanders.

**Keywords** Fire control radar · Networking · Adaptive · Anti-interference

## 1 Introduction

Radar networking is an effective measure against the “four anti-antibodies” and plays a pivotal role in modern warfare. Fire control radar is an important equipment for controlling the weapon system to shoot at the target, and its anti-interference capability is particularly important for the air defense forces to carry out combat tasks. Therefore, research on the dynamic coordination management of the anti-interference means of the fire control radar in the network can effectively improve the air defense fire control radar to complete the air combat mission.

---

J. Luo (✉) · Y. Ding · B. Wang · W. Yu  
Air Defense Forces Academy, 450052 Zhengzhou, China  
e-mail: [luojiang.2010@163.com](mailto:luojiang.2010@163.com)

© The Editor(s) (if applicable) and The Author(s), under exclusive license to Springer Nature Singapore Pte Ltd. 2021  
S. Long and B. S. Dhillon (eds.), *Man-Machine-Environment System Engineering*, Lecture Notes in Electrical Engineering 645,  
[https://doi.org/10.1007/978-981-15-6978-4\\_61](https://doi.org/10.1007/978-981-15-6978-4_61) 523

## 2 Analysis of Radar Anti-interference Resources

Radar anti-interference resources can be divided into controllable resources and uncontrollable resources. Controllable resources refer to its own anti-interference technical means, and uncontrollable resources refer to the anti-interference system of radar when it is designed and manufactured.

### 2.1 *Anti-interference Technology of Fire Control Radar (Controllable Resources)*

Anti-interference factor evaluation model for technical measures—Table 1 shows the 11 types of anti-interference measures nowadays widely used by fire control radar and their contribution to the anti-interference capabilities of fire control radar [1].

In practical applications, after various technical measures are taken, the radar's anti-interference capability is close to the sum of their respective anti-interference capabilities [2]. Therefore, the anti-interference factor evaluation model of technical measures can be established as follows:

$$JK = \sum_{j=1}^{11} \omega_j \cdot \mu_j$$

Among them, the value of  $\omega_j$  is 0 or 1. The radar adopts this system, it can take 1, otherwise take 0;  $\mu_j$  is the contribution degree of the  $j$ -th working system relative to radar anti-interference capability of fire control radar.

### 2.2 *Anti-interference System of Fire Control Radar (Uncontrollable Resources)*

In the anti-interference capability model, some basic factors such as the anti-interference factor of the working system and the anti-interference factor of technical measures are qualitatively described factors, and their quantification can be processed by expert evaluation methods. At present, the common working system of fire control radar and its contribution to radar anti-interference capability are shown in Table 2.

The anti-interference factor evaluation model of the working system established after analysis that is

$$TK = \sum_{i=1}^7 \omega_i \cdot \mu_i$$

**Table 1** Contribution degree of technical measures against interference

Technical measures	Frequency agility	Sidelobe suppression	Constant false alarm	Dicke-fix	MTD	Pulse compression	Variable repetition frequency	Variable polarization	Differential circuit	Frequency diversity	Variable cone sweep frequency
Contribution degree	6	2	4	2	4	4	2	3	2	2	3

**Table 2** Contribution degree of working system to anti-interference capability

Working system	Full coherence	Single pulse	Continuous wave	Cone scan	TV	Infrared	Laser
Contribution degree	6	7	4	1	3	4	5

Among them, the value of  $\omega_j$  is 0 or 1. The radar adopts this system, it can take 1, otherwise take 0;  $\mu_j$  is the contribution degree of the  $i$ -th working system relative to radar anti-interference capability of fire control radar.

### 3 Model Building

Coordinating the use of radar anti-interference measures should be based on the principle of exerting the strongest anti-interference capabilities of radar network. That is, for different types of interference, the radars belonging to the network should be able to take the most suitable anti-interference measures in a short time to ensure the stability of the targets found by the radar network. The essence of anti-interference operation control also belongs to the objective optimization problem of multiple constraints. Therefore, based on the formulation of anti-interference operation constraints, it is necessary to build an anti-interference-oriented working status control model.

#### 3.1 Optional Anti-interference Measures Constraints

In actual use, once the radar chooses one of the anti-interference measures of the same type of control resources, other anti-interference measures will not be available. From the perspective of constraints, the optional anti-interference measure constraint is similar to the optional detection resource constraint, that is, the choice of anti-interference measures can only be made in the anti-interference measures that the radar has, and the selection of the same type of resources is also unique.

Define the optional set of radar anti-interference measures as  $S_{AJ}$ , the anti-interference measures that the  $k$ -th radar has can be expressed as

$$(S_{AJ})_k = \begin{bmatrix} s_{11} & s_{12} & \dots & s_{1m} \\ s_{21} & s_{22} & \dots & s_{2m} \\ \vdots & \vdots & \vdots & \vdots \\ s_{n1} & s_{n2} & \dots & s_{nm} \end{bmatrix}_{n \times m}$$

Therefore, the selection of the  $k$ -th radar anti-interference measures can only be performed in  $(S_{AJ})_k$ . Moreover, the selection of the same type of anti-interference measures needs to meet non-repeatable, that is,

$$s_{i1} + s_{i2} + \dots + s_{ij} + \dots + s_{im} \leq 1$$

### 3.2 Interference Suppression Capability Constraints

Different anti-interference measures have different abilities to suppress interference. For different types and intensity of interference, anti-interference measures with strong ability to suppress interference should be selected first. The ability to suppress interference is mainly reflected in two aspects: the improvement factor of anti-interference measures and the processing loss. The improvement factor indicates the reduction effect of anti-interference measures on interference, and the processing loss indicates the reduction effect of anti-interference measures on normal detection of radar. Therefore, the larger the improvement factor and the smaller the processing loss, the stronger is the ability to suppress interference.

Let  $I_j$  be the improvement factor and  $L_j$  be the processing loss, then the interference suppression capability of the anti-interference measure can be expressed as

$$C_{AJ} = I_j - L_j$$

The larger the improvement factor, the smaller is the processing loss, thus the larger  $c_{AJ}$ , the stronger is the interference suppression ability of the anti-interference measures. In order to ensure the suppression effect of interference, anti-interference measures with larger  $c_{AJ}$  should be selected first. Therefore, the interference suppression capability constraint can be expressed as

$$c_{AJ} = \max(I_j - L_j)$$

### 3.3 Auxiliary Decision-Making Model of Anti-interference Operation Control

Radar network anti-interference capability model is

$$(AJC)_{\text{net}} = \sum_{i=1}^n \sum_{j=1}^m \omega_{ij} \chi_{ij}$$

In the formula:

- $\omega_{ij}$  The entropy weight of the  $j$ -th index in the  $i$ -th layer;
- $\chi_{ij}$  The evaluation value of the  $j$ -th index in the  $i$ -th layer.

The goal of radar anti-interference operation control is to ensure that the radar network has the best anti-interference effect under different types and intensity of interference conditions. Therefore, the objective function of radar anti-interference operation control can be constructed as

$$T_{AJC} = \max(AJC)_{net}$$

In summary, the auxiliary decision-making model of radar anti-interference operation control is as follows:

$$T_{AJC} = \max(AJC)_{net}$$

$$\text{s.t.} = \begin{cases} s_{i1} = s_{i2} + \dots + s_{ij} + \dots + s_{im} \leq 1 \\ 0^\circ < A_i \leq 360^\circ \\ c_{AJ} = \max(I_j - L_j) \\ \sum_{i=1}^n \sum_{j=1}^m \omega_{ij} = 1 \end{cases}$$

## 4 Simulation Experiment and Result Analysis

The specific problem studied in this article is to seek the adjustment scheme of the radar’s working status in the network to maximize the anti-interference efficiency of the radar network under real-time air situation. Therefore, genetic algorithms are selected from many optimization algorithms to solve the problem [3].

### 4.1 Simulation Conditions

Assume that a unit took air combat mission, and each of the radars A, B, and C is deployed. The radar operating systems are full coherence, single pulse, and photoelectric integration, and the numbers, respectively, are 1, 2, and 3.

The controllable working status resources of the three radars are described in Table 3.



**Table 3** Controllable working status resources of three radars

Type	Name	Type	Name
Transmission signal control mode	Pulse compression	Signal processing control style	Sidelobe suppression
	Variable repetition frequency		Dicke-fix
	Frequency agility		Differential circuit
	Variable cone sweep frequency		MTD

## 4.2 Result Analysis

At the beginning of the initial group generation, this article directly incorporates the uniqueness of the same type of working status into the coding strategy, which effectively ensures the purity of the search space. In addition, in order to avoid the occurrence of illegal individuals, the crossover and mutation operations in genetic operations have been improved accordingly. The crossover and operation nodes have been limited to make the algorithm more targeted and effectively and to avoid a large number of invalid solutions. To a large extent, the algorithm optimization time is saved [4].

The optimal individuals generated by the algorithm are mapped to the radar working status enabling programs in the network, and a visual auxiliary decision-making program for radar working status regulation is further generated, which can be used as a reference for air reconnaissance commanders of air defense group.

In order to clearly show the experimental results and further explain the results, the generated control programs are listed, as described in Table 4.

This article assumes that the radar position has been deployed and the radar network’s working status during anti-interference air combat is dynamically adjusted. As can be seen:

1. After adopting corresponding anti-interference measures, the power of each radar station can be effectively connected, which can form a more closely covered air combat effect.
2. In this case, the maximum detection range of the air defense fire control radar in service is about 50 km. From the average running time of the algorithm, it can be known that within the time of generating the radar working status enabling programs, assuming the air attack weapon flight speed is Ma2.0, its straight flight distance is about 1.8 km, which is less than 3.6% of the radar’s maximum detection range; assuming Ma1.0, its straight flight distance is close to 1 km, which is less than 2% of the radar’s maximum detection range. Therefore, the algorithm in this article can meet the real-time requirements of the working status control of the radar network in wartime.

**Table 4** Auxiliary decision-making programs for radar network working status control

Program No.	Radar model	Radar working system	Transmission signal control mode	Signal processing control style
Program No. 1	A	Full coherence	Pulse compression	Sidelobe suppression
	B	Single pulse	Variable repetition frequency	MTD
	C	Photoelectric integration	Variable cone sweep frequency	Differential circuit
Program No. 2	A	Full coherence	Frequency agility	MTD
	B	Single pulse	Variable repetition frequency	Dicke-fix
	C	Photoelectric integration	Variable cone sweep frequency	Sidelobe suppression
Program No. 3	A	Full coherence	Variable repetition frequency	MTD
	B	Single pulse	Pulse compression	Sidelobe suppression
	C	Photoelectric integration	Frequency agility	Dicke-fix

## References

1. Xingwang Y, Junming P, Lei L et al (2006) Evaluation of air defense fire control radar network and anti-interference effectiveness. *Fire Control Radar Technol*
2. Wanjie J (2016) Research on anti-interference measures in radar networking system. *Digital Technol Appl*
3. Ruige W (2013) Research on the method of radar networking based on genetic algorithm. *China Radar*
4. Leiming LD, Peng C, etc (2014) Radar management and control problems based on genetic algorithm. *Firepower and Command Control*

# Study of Fire Control Radar Technology Countering Electronic Attack



Wei Yu, Xiaolong Liang, Yan Sun, Jiang Luo, and Shilei Xin

**Abstract** Providing artillery or missile with firing data, the Fire Control Radar (FCR) is often the key target of hostile electronic attack. Therefore, in order to better counter electronic attack, it has to promote its capabilities in detecting, intercepting and tracking enemy targets, controlling firepower and ensuring its own safety in such six technological aspects as adopting such technologies as phased array radar, broadened spectrum, complex signal processing, photoelectricity combination, bait laying and multi-radar networking, which is of considerable significance in the overall design of Fire Control Radar (FCR) anti-jamming.

**Keywords** Fire control radar · Electronic attack · Technology · Countermeasure

## 1 Introduction

Electronic warfare (EW) is understood as electronic attack, electronic protection and electronic warfare support, of which the electronic attack refers to such offensive actions against hostile personnel, assets or devices to reduce, weaken or destroy enemy combat power by means of electromagnetic-energy or directed energy weapon [1]. Electronic attack against radar may be conducted by way of compression jamming or deception jamming to reduce or offset the radar's combat effectiveness, or by means of anti-radiation weapon to destroy the radar [2]. The Fire Control Radar (FCR) is important air defense equipment to provide anti-aircraft guns or missiles with firing data by detecting, identifying, intercepting and tracking aerial targets and

---

W. Yu (✉) · X. Liang · J. Luo · S. Xin  
Zhengzhou Campus, PLA Army Academy of Ground and Air Defense Artillery, 450052  
Zhengzhou, China  
e-mail: [yuwei\\_19800701@163.com](mailto:yuwei_19800701@163.com)

Y. Sun  
Zhengzhou Power Supply Company, State Grid Henan Electric Power Company, 450052  
Zhengzhou, China

is therefore the prioritized prey in the EW conditions. It is of great significance to analyze the possible influences of electronic attack upon FCR so as to improve the latter's capabilities of anti-jamming and survival.

## **2 Possible Influences of Electronic Attack Upon FCR**

### ***2.1 Capabilities Against Passive Suppression Jamming***

Electronic attack makes it difficult to conduct distant range air situation broadcast, close range target indication and air situation exchanges. Without target indication, the FCR has to depend on itself to search for hostile targets, which will take longer time and make it more difficult and hence more liable to electronic attacks. Besides, the FCR's detecting power, range and efficiency may be reduced due to noise interference. Nowadays, the techniques and technology to cast decoys have been rapidly developed, thus leaving FCR operators unable or difficult to judge genuine targets from quantities of decoys.

### ***2.2 Difficulty in Intercepting Aerial Targets***

Exposed to strong noise interference, the FCR receiver will become saturated and display no target echo waves. Then the FCR is hard to intercept aerial targets. In other words, electronic attack will delay the opportunity for FCR to track targets or even make it unable to track targets at all.

### ***2.3 Reduction of Tracking Capability***

While tracking targets, the FCR may lose stability of angular speed, thus resulting in greater error, if it is under cross-interference or blinking jamming; the FCR's automatic range-tracking system may also mistakenly track the disturbances other than genuine targets and the chain reactions that follow may lead to target loss in bearing, leaving the FCR repeat the proceedings of detecting, intercepting and tracking again and again.

## ***2.4 Reduction in Destructive Capability***

The FCR's increased measuring error due to jamming brings about greater error of firing data, therefore seriously reducing the weapon system's killing probability. Deceptive jamming may even mislead the weapon system to fire at the empty air space. The FCR under jamming that is strong enough may grow blind and fail to compute firing data, leaving the entire weapon system in paralysis.

## ***2.5 Vulnerability to Safety Threat***

Electronic jamming on the FCR results in temporary disabled functionality of detecting, intercepting and tracking, in contrast, the greatest threat in the battle space comes from anti-radiation weapons which pose immediate threat to the FCR and its operators. The anti-radiation weapon often adopted today is anti-radiation missile featured by long striking range, high speed and good accuracy.

# **3 Technological Countermeasures FCR May Adopt**

## ***3.1 Phased Array Radar Technology***

There has been more and more new type FCR adopting reasonably priced phased array radar technology with the rapid development of modern technology. The minor lobe level of phased array radar antenna may reach  $-40$  or  $-50$  dB or even lower if compared with that of the traditional parabolic antenna,  $-20$  to  $-30$  dB. The hostile protective jammer, because of the lower minor lobe level, has to increase its transmitting power to ensure sufficient equivalent jamming power. If having detected anti-radiation missile coming, the phased array radar antenna shall produce adaptive nulls in that direction and effectively reduce the range of being detected and tracked. There are two types of phased array radar: passive phased array and active phased array, with the latter more and more adopted by FCRs.

## ***3.2 Broadened Spectrum Technology***

### **3.2.1 Frequency Hopping (FH)**

Frequency hopping (FH) means that the frequency changes randomly in a wide range so that the radar may be working on the frequency that is not jammed. Faster and more random changes of frequency in a wider range contribute to better anti-jamming

capabilities. It is adaptive frequency hopping (ADFH) other than traditional manual or electronic frequency hopping that is widely adopted in modern FCR, enabling radar to conduct spectral analysis on jamming signals, identify the frequency point with least jamming and change the carrier frequency of transmission signal to it.

### **3.2.2 Broadened Frequency Band**

Traditional radars work on S, C and X wave band. More wave bands occupied by one radar or radar network mean better anti-jamming capabilities. The wave band of FCR tends to be broadened toward high frequency of millimeter wave band, which is characterized by narrow wave beam, high angular resolution, wide frequency band, good concealment, strong anti-jamming, small size and lightweight [3]. Compared with IR or laser devices, it travels with better penetrability through smoke, dust, rain or fog. Besides, the width of millimeter wave radar pulse and wave beam is narrow, and the radar's resolution cell is smaller than interrupted distributions in size, which greatly reduces the jamming into the radar receiver, enhances the radar's signal to interference ratio (SIR) and well controls the adverse influences by meteorological conditions of clouds, rain, snow and fog. With the development of millimeter wave devices, the frequency in millimeter wave band has been broadened from 35 to 94 GHz to 140 GHz.

## **3.3 Complex Signal Processing Technology**

### **3.3.1 Moving Target Detection**

It requires greater than 50 dB of moving target improvement factor to improve the target detecting capability under strong background interference, which is impossible for traditional moving target indication technology to realize completely. According to the relevant radar theory, poor stability of radar's high-frequency system produces some near-even stray component with clutter echoes, preventing the improvement factor from reaching its maximum. The FCR usually adopts moving target detecting technology and phase-coherent power amplifying transmitter instead of traditional phase-locking coherent single-stage oscillators, remarkably enhancing the stability of high frequency of the entire system. With the rapid development of digital signal processing, FCRs may adopt even more complicated signal processors to realize adaptive moving target detection, respond to the varied features of clutter echo's power level, spectral shape and width or Doppler frequency shift, to realize theoretically optimal filtering and signal detection in the cluttering background.

### **3.3.2 Pulse Compression Technology**

Pulse compression means that the radar transmitter sends wide pulse signals which vary regularly and the radar receiver compresses the echoes into narrow pulse signals. Wide pulse transmission with high power ensures sufficient detecting range; narrow pulse echoes produced by pulse compression technology ensure good range resolution, which well addresses the contradiction of long detection range and high range resolution. FCR usually adopts linear, nonlinear frequency modulation and phase-coded pulse compression of various pulse widths and applies narrow pulse in close range tracking and wide pulse in long-range detecting, hence to address the contradiction between tracking distance and detecting power and reduce the likelihood of being detected.

### **3.3.3 Multidimensional Signal Processing Technology**

Multidimensional signal processing technology allows radar to fetch target information out of interference noise as per the differences of target echoes and interference noise in time, Azimuth, polarity, amplitude, Doppler frequency, reflection coefficient as well as statistical data. It is a tendency of technological development of FCR to adopt multifunctional, programmable and adaptive multidimensional signal processing technology so as to address the problem of high-resolution and high-accuracy orientation and location of multiple targets and enhance the anti-jamming capabilities.

## **3.4 Photoelectricity Combination Technology**

It has been a widely used and important supplementary means as well as an anti-jamming measure to adopt photoelectricity combination technology and equip FCRs with various photoelectrical devices, such as command telescope, laser range finder, IR tracking system and TV tracking system, which are immune to active or passive microwave interference and are capable of angle and range measurement either independently or together with the FCR. There is more than one duty type as is listed in Table 1 that follows. The FCR usually adopts the duty type with IR tracking, TV tracking and laser range detecting combined, which is characterized by all-weather, high measurement accuracy, better anti-jamming and visual and overall target information provision. It is worth noting that the laser range finder's continuous working time of is only a few minutes due to heat dissipation or other design issues and may only serve as the temporary replacement of the FCR's range detecting function.

**Table 1** FCR's duty types in common use

S. No.	Angle measurement	Range measurement	Remarks
1	Radar	Radar	Basic duty type
2	TV	Radar	Applicable in good visibility
3	IR	Radar	Applicable in poor visibility, complementary to TV
4	Command telescope	Radar	Applicable to sudden targets in vision coverage area
5	Joystick	Radar	Applicable when radar, TV and IR jammed, with operator controlling antenna manually
6	TV	Laser	High accuracy but limited continuous working time
7	IR	Laser	Applicable in poor visibility with limited continuous working time



### **3.5 Bait Laying**

Due to its inherent limitation, the anti-radiation missile is poor in sorting multiple sources of radiation within its resolving angle and is impossible to differentiate when radar signals are of identical frequency, pulse width and pulse repetition rate [4], which allows one or more sources of radiation as baits laid in the peripheral regions of the radar, leaving the anti-radiation missile diverge from the real radar. High value radars including FCRs ought to have baits round them to improve battle space survivability.

### **3.6 Multi-radar Networking**

Modern air defense operation is featured by the confrontation between systems. An FCR, as a node, cannot perform its maximal combat effectiveness unless connected into an air defense network from which it receives air situation broadcast, target indication and distribution and combat orders, intercepts and tracks targets according to superior instruction and distribution, or reports local air situation. FCRs may as well form a network, either to receive target information from adjacent nodes for target guiding or firing data computation, or to share local tracking information with adjacent units in the fire control network [5]. Networked FCRs may work complementarily and share information precisely and maintain the air defense firepower threat. As long as there is one FCR working normally, all others in the network may still share the captured target's information. In addition, an FCR located by hostile anti-radiation missiles may keep radio silence and work out firing data with the information shared by other FCRs in the network, which makes it difficult for enemy to detect the FCR and increases its survivability and the entire network's destroy resistance.

## **4 Conclusion**

In the future battle space, it is fairly desirable that the FCR adopts advanced anti-jamming technologies for survival and better combat effectiveness because technology serves as the foundation and makes it possible to conduct efficient confrontation with tactical approaches and skillful operation. More efforts in developing new anti-jamming technologies should be made for FCR in order to meet the demands of increasingly important electronic warfare.

## References

1. Elsworth AT (2013) *Electronic warfare*. Translated by HU Shengliang, et al. National Defense Industry Press, Beijing, pp 24–26
2. Zhang Y (2006) *Theories of radar electronic warfare*. National Defense Industry Press, Beijing, pp 1–5
3. Yu J, Chen X (2018) *Millimeter-wave and TeraHertz antenna measurement technology*. Science Press, Beijing, pp 4–6
4. Qiu Y, Ji X, Chen X, Liang J (2014) ARM simulation of networked fire control radar decoy interference. *Fire Power Command Control* 39(4):49–53
5. Lyu X, Yu W (2019) Air defense forces fire control radar networking based upon command information system. PLA Press, Beijing, pp 10–13

# Experimental Study on Color Optimization of Fighter Cockpit Interior Decoration



Jian Du, Xiaochao Guo, Duanqin Xiong, Yanyan Wang, Wei Pan, Shuang Bai, Liu Yang, and Juan Liu

**Abstract** *Objective:* To study the preference of fighter pilots for the color of cockpit interior decoration and put forward the spraying color suitable for the whole cockpit and the devices in it, which provides the basis for the color design of cockpit interior decoration. *Methods:* 164 fighter pilots were selected as experimental subjects. Making two series of palettes of dark and light colors as experimental materials, in which, the light color system is an alternative color for the cockpit bulkhead while the dark system is for the main control devices. During the experiment, the subjects were asked to choose the colors that they considered to be suitable for cockpit bulkhead and main control devices from the two series of palettes and then sort these colors and finally choose the color they like in their daily life. *Results:* (1) The palette number C5 (agate grey) has the highest level of preference among the light color system, followed by C3 (misty grey), C4 (monkey grey) and C6 (beige grey). Among the dark color system, the palette number C'8 (medium grey) and C'1 (concrete grey) are the most popular colors, followed by C'5 (cement grey). (2) The subjects' preference for 12 light colors and 12 dark colors was different, which was statistically significant ( $P < 0.001$ ). *Conclusions:* In this study, the color of the bulkhead and the main control equipment of the fighter cockpit are optimized, and it is found that the daily color preference of pilots has no significant effect on their interior color selection of fighter cockpit. The results can be used as an important reference for color design of cockpit interior decoration.

**Keywords** Aircraft cockpit · Interior decoration color · Visual ergonomic · Fighter

## 1 Introduction

The cockpit is the main place for the pilot to perform tasks and exchange information with the aircraft. During flights, pilots are usually vulnerable to different factors such as the environment in the air, the machines and the physical condition [1]. Because of

---

J. Du (✉) · X. Guo · D. Xiong · Y. Wang · W. Pan · S. Bai · L. Yang · J. Liu (✉)  
Air Force Medical Center of FMMU, 100142 Beijing, China  
e-mail: [dj18500375737@163.com](mailto:dj18500375737@163.com)

© The Editor(s) (if applicable) and The Author(s), under exclusive license to Springer Nature Singapore Pte Ltd. 2021  
S. Long and B. S. Dhillon (eds.), *Man-Machine-Environment System Engineering*, Lecture Notes in Electrical Engineering 645,  
[https://doi.org/10.1007/978-981-15-6978-4\\_63](https://doi.org/10.1007/978-981-15-6978-4_63)

the increasing complexity and integration of aircraft, the limitation of cockpit space and the particularity of flight environment, the design of color matching in cockpit affects the pilot's spatial positioning, visual load, operation comfort, psychological feeling, etc. [2, 3]. Good cockpit color and reasonable color matching are an important guarantee for pilots to complete tasks efficiently and comfortably. At the same time, it can give full play to aircraft performance and improve the psychological comfort of pilots [4]. In this paper, the color optimization experiment of fighter cockpit is carried out, and the spraying color suitable for cockpit interior decoration and important control equipment is proposed, which provides the basis for cockpit interior color design.

## 2 Method

### 2.1 Subjects

One hundred and sixty-four male fighter pilots with normal color perception in active service were selected as subject. The average age was 28–35 years old, and the average flight time was  $1205 \pm 443$  h.

### 2.2 Experimental Materials

The experimental materials mainly include the following four kinds:

1. Questionnaire

A professional questionnaire was designed to collect the personal information of the subjects, including their color preferences in daily life and suggestions on the interior color of the cockpit.

2. Test color palette

The color palettes were produced by specialized coating company and sprayed to the desired colors for this research. On the basis of full investigation, contacting professional manufacturers to make one set of dark color experimental palette and one set of light color experimental palette according to the provisions of the national military standard [5], containing 24 kinds of colors: nine shades of dark greys, ten shades of light greys and five camel colors. The light color palette includes ten light grey and two camel colors, and the dark color palette includes ten dark greys and two camel colors. The color palettes were made of metal with size of 10 cm × 19 cm. Every color palette and the color code are shown in Table 1.

**Table 1** Color palette and the corresponding code

Light colors		Dark colors	
Palette number	Color code	Palette number	Color code
C1	FS36595 Window grey	C'1	FS36118 Concretegrey
C2	FS36495 Light grey	C'2	FS36251 Green grey
C3	FS36473 misty grey	C'3	FS36231 Traffic grey
C4	FS36628 monky grey	C'4	FS36293 Iron grey
C5	FS36463 Agate grey	C'5	FS36173 Cement grey
C6	FS36492 Beige grey	C'6	FS36152 Pebble grey
C7	FS36586 Zephyr grey	C'7	FS36270 Mouse grey
C8	FS36559 Sky grey	C'8	FS36176 Medium grey
C9	FS36440 Slate grey	C'9	FS36280 Anthracite grey
C10	FS36622 Basalt grey	C'10	FS36279 Quartz grey
C11	FS37769 Silver grey	C'11	FS37150 Umbra grey
C12	FS37189 Tele grey	C'12	FS33531 Brown

3. National Standard Color Card

Figure 1 shows the scene in which pilot subjects are using the experimental color palette to complete the experiment. Figure 2 shows a set of National Standard



**Fig. 1** Color palettes for experiment



**Fig. 2** National Standard Color Card

Color Card. During the experiment, the pilots were asked to choose their favorite color and fill them into the questionnaire.

#### 4. Multiple light box for experiment

Judge II standard multiple light box (Fig. 3) produced by American X-Rite Limited Company was used for palette selecting test. In particular, the experiment must be carried out under the same light source.

### ***2.3 Experimental Design and Method***

This study adopted the methods of questionnaire and behavioral experiment. The 24 color palettes were divided into two series: the light (C1-C12) and the dark (C'1-C'12).

Every two subjects formed a group and completed a round of experiments in pairs. The classical ranking method in color preference test was adopted, that is to say, the subjects were asked to sort the 12 colors based on their own preference. The subjects ranked their favorite color as 1, and the least favorite color as 12. Sort the middle colors according to this rule and so on.

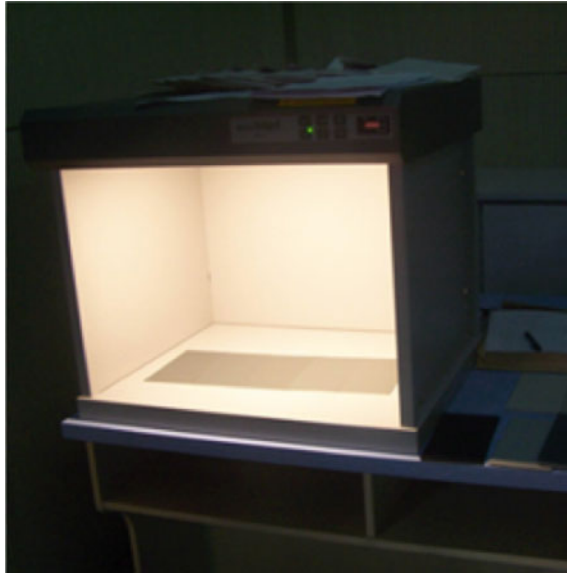


**Fig. 3** Multiple light box

To avoid the influence of order and positions of the palettes, for each color series, two times of sorting and four rounds of experiments were executed. The specific experimental sequence was dark–light–light–dark and, light–dark–dark–light. Before each sorting, the palettes should be shuffled to assure the order was randomized.

## ***2.4 Experimental Data Processing***

SPSS18.0 was used for the statistical analysis of experimental data.

## **3 Results and Analysis**

### ***3.1 Daily Color Preference***

In the experiment of daily color preference, colors of the same color system were combined and recoded, such as dark blue and light blue were uniformly classified as blue. According to their daily preferences, the subjects selected their favorite colors from the National Standard Color Cards containing 83 kinds of colors. The results showed that blue was the most favorite color of the pilot subjects and 94 pilots

**Table 2** Frequency distribution of daily color preference

Color in National standard color card	Approvals of the paratroopers	Percentage (%)
White	2	1.2
Red	17	10.4
Yellow	14	8.5
Gray	9	5.5
Blue	94	57.3
Green	26	15.9
Brown	2	1.2
Total	164	100.0

(57.3%) chose it. Then, the second favorite color was green and 26 pilots chose it (15.9%). And then the third color was red and yellow (10.4 and 8.5%). Relatively, few people like other colors (Table 2).

### 3.2 Results of Light Color System Sorting

Light colors were mainly used for aircraft cabin bulkhead interior. Pilot subjects' ranking results of light colors were as follows. The data of the 12 light colors was further analyzed to choose the best proper colors for fighter aircraft cabin, and the sorting results were C5, C3, C6, C4, C10, C2, C9, C1, C8, C7, C11, C12. Detailed sorting results of light color system were listed in Table 3.

Multiple sample test of nonparametric correlation analysis was taken to further investigate whether the entire pilot subjects in the experiment like the same light color. Statistical results showed significant differences, as shown in Table 4 ( $P < 0.001$ ). It was indicated that among the 12 light colors, the pilots' preferences were not the same.

**Table 3.** 12 Light colors sorting results

	C1	C2	C3	C4	C5	C6	C7	C8	C9	C10	C11	C12
Average grade	6.68	5.59	4.73	5.35	4.31	5.20	8.08	7.09	5.79	5.48	9.70	9.81
Standard deviation	2.2	2.0	3.8	1.9	3.3	2.0	2.8	2.5	4.0	1.8	3.1	3.3
<i>P</i>	0.48	0.58	0.66	0.60	0.70	0.62	0.36	0.45	0.56	0.59	0.21	0.20
<i>Z</i>	-0.06	0.21	0.42	0.26	0.53	0.30	-0.36	-0.13	0.16	0.23	-0.81	-0.85
<i>Z</i> + 0.85	0.79	1.06	1.27	1.11	1.38	1.15	0.49	0.72	1.01	1.08	0.04	0
Ranks	8	6	2	4	1	3	10	9	7	5	11	12



**Table 4** Differences in preference to 12 light colors

Statistical indicator	Friedman test	Kendall's test
<i>N</i>	163	163
<i>df</i>	11	11
Chi-square	491.788	491.788
Asymp. Sig.	0.000	0.000

The data of the 12 light colors sorting was analyzed further to screen out several suitable colors for aircraft. The statistical results showed that C5 is the pilots' favorite color, followed by C3 and C4. The significance level of C5 and C3 is less than 0.01, which are the favorite two colors of pilot subjects. And the pilots have different preferences for these two colors. On the basis of the sorting preference of 12 light colors, the two sample nonparametric tests were carried out between the favorite color C5 and each color of the other 11 colors. The specific results were shown in Table 5.

Similarly, to distinguish how much the pilots liked the chosen color, the two sample nonparametric tests were, respectively, carried out between each color of the other 11 colors and the color of C3 and C4, as shown in Tables 6 and 7.

### 3.3 Results of Dark Color System Sorting

Dark colors were mainly used for the main control devices in aircraft cabin. Pilot subjects' ranking results of dark colors were as follows. The data of the 12 dark colors was further analyzed to choose the best proper colors for the main control devices, and the sorting results were C'8, C'1, C'5, C'6, C'3, C'2, C'4, C'7, C'9, C'10, C'12 and C'11. Detailed sorting results of light color system were listed in Table 8.

Multiple sample test of nonparametric correlation analysis was taken to further investigate whether the entire pilot subjects in the experiment like the same dark color. Statistical results showed significant differences, as shown in Table 9 ( $P < 0.001$ ). It was indicated that among the 12 dark colors, the pilots' preferences were not the same.

The data of the 12 dark colors sorting was analyzed further to screen out several suitable colors for aircraft main control devices. The statistical results showed that C'8 and C'1 were the pilots' favorite colors, followed by C'5. The significance level of C'8 and C'1 is less than 0.01, which are the favorite two colors of pilot subjects. And the pilots have different preferences for these two colors. On the basis of the sorting preference of 12 dark colors, the two sample nonparametric tests were, respectively, carried out between the favorite color C'8, C'1 and each color of the other 11 colors. The specific results were shown in Tables 10 and 11.



**Table 6** Correlation analyses between color C3 and other light colors

Statistical indicator	C1	C2	C3	C4	C5	C6	C7	C8	C9	C10	C11	C12
Z	-4.5	-2.8	/	-1.5	-2.1	-1.9	-6.1	-4.7	-4.0	-2.4	-7.6	-7.7
Asymp. Sig.	0.000	0.005	/	0.136	0.034	0.057	0.000	0.000	0.000	0.017	0.000	0.000

**Table 7** Correlation analyses between color C4 and other light colors

Statistical indicator	C1	C2	C3	C4	C5	C6	C7	C8	C9	C10	C11	C12
Z	-4.9	-3.6	-1.5	/	-3.1	-1.2	-7.4	-5.4	-0.7	-0.7	-9.2	-9.2
Asymp. Sig.	0.000	0.000	0.136	/	0.123	0.232	0.000	0.000	0.490	0.475	0.000	0.000

**Table 8** Twelve dark colors sorting results

	C'1	C'2	C'3	C'4	C'5	C'6	C'7	C'8	C'9	C'10	C'11	C'12
Average grade	3.81	6.21	5.38	6.31	3.92	4.35	6.39	3.63	6.95	10.18	10.53	10.27
Standard deviation	3.6	1.8	1.7	2.0	2.0	2.1	1.9	2.4	1.9	2.0	2.2	2.2
<i>P</i>	0.74	0.53	0.61	0.52	0.73	0.70	0.51	0.76	0.46	0.17	0.13	0.16
<i>Z</i>	0.65	0.08	0.28	0.06	0.62	0.53	0.03	0.71	-0.11	-0.96	-1.13	-1.00
<i>Z</i> + 1.13	1.78	1.21	1.41	1.19	1.75	1.66	1.16	1.84	1.02	0.17	0	0.13
Ranks	2	6	5	7	3	4	8	1	9	10	12	11

**Table 9** Differences in preference to 12 dark colors

Statistical indicator	Friedman test	Kendall's test
<i>N</i>	163	163
<i>df</i>	11	11
Chi-square	942.268	942.268
Asymp. Sig.	0.000	0.000

### 3.4 Correlation Analysis of Daily Color Preference and Sorting

In order to explore whether pilots' daily favorite colors affect their choice of fighter interior colors, the statistical nonparametric test and analysis of multiple independent samples on the ranking of 24 colors and daily favorite colors were carried out. The light color results were shown in Table 12 and dark color in Table 13. The results showed that pilots' daily favorite colors did not affect their sorting results of fighter interior decoration and the main device colors. When the pilot chooses the proper color for the cockpit interior, it depends on their consideration of the work environment, not their own color preferences.

## 4 Conclusions

Based on this experiments study, the following conclusions can be drawn:

1. According to the 164 pilots invited to interview, the 24 colors (12 light colors and 12 deep colors) have different suitability for fighter cockpit interior decoration and main device.
2. The palette number C5 (agate grey) has the highest level of preference among the light color system, followed by C3 (misty grey), C4 (monkey grey) and C6 (Beige grey). Among the dark color system, the palette number C'8 (medium grey) and

**Table 10** Correlation analyses between color C'8 and other light colors

Statistical indicator	C'1	C'2	C'3	C'4	C'5	C'6	C'7	C'8	C'9	C'10	C'11	C'12
Z	-0.1	-7.4	-5.5	-6.7	-2.9	-4.6	-7.1	/	-8.1	-10.2	-9.9	-9.8
Asymp. Sig.	0.917	0.000	0.000	0.000	0.004	0.000	0.000	/	0.000	0.000	0.000	0.000

**Table 11** Correlation analyses between color C'1 and other light colors

Statistical indicator	C'1	C'2	C'3	C'4	C'5	C'6	C'7	C'8	C'9	C'10	C'11	C'12
Z	/	-6.0	-3.6	-5.6	-1.2	-2.9	-0.1	-6.9	-10.0	-9.8	-9.6	-5.7
Asymp. Sig.	/	0.000	0.000	0.000	0.229	0.003	0.017	0.000	0.000	0.000	0.000	0.000

**Table 12** Correlation between daily light color preference and sorting

Statistical index	C1	C2	C3	C4	C5	C6	C7	C8	C9	C10	C11	C12
Chi-square	7.152	9.696	10.263	6.451	7.827	5.347	5.969	7.177	11.622	10.274	14.357	11.292
<i>df</i>	6	6	6	6	6	6	6	6	6	6	6	6
Asymp. Sig.	0.307	0.138	0.114	0.375	0.251	0.500	0.427	0.305	0.071	0.114	0.026	0.080



**Table 13** Correlation between daily dark color preference and sorting

Statistical index	C'1	C'2	C'3	C'4	C'5	C'6	C'7	C'8	C'9	C'10	C'11	C'12
Chi-square	4.819	2.409	5.164	1.585	6.634	1.788	10.001	3.941	3.734	8.860	1.933	10.776
<i>df</i>	6	6	6	6	6	6	6	6	6	6	6	6
Asymp. Sig.	0.567	0.878	0.523	0.954	0.356	0.938	0.125	0.685	0.713	0.182	0.926	0.096

C'1 (Concrete grey) are the most popular colors, followed by C'5 (Cement grey). Camel series colors are not suitable for cockpit interior.

3. The daily color preference of pilots has no significant effect on their interior color selection of fighter cockpit.

**Compliance with Ethical Standards** The study had obtained approval from the Air Force Medical Center of FMMU. All subjects participated in experiment had signed the informed consent. All relevant safety, health and rights had been met in relation to subject protection.

## References

1. Pan LL (2017) Research on the effect of light environment on visual ergonomics in aircraft cabin. Nanjing University of Aeronautics and Astronautics
2. Tan W (2016) Study on the effect of aircraft interior decoration on the pilots' visual ergonomics. College of Civil Aviation
3. Bai X (2017) Color analysis of decoration and living facilities in cockpit of civil aircraft. Internal Combustion Engine & Parts, pp 148–149
4. Zhou Q, Qu Z, Wang C et al (2001) Experimental study on agronomical color matching design of virtual crew cabin layout in manned spacecraft. Space Med Med Eng 14(6):434–438
5. GJB1192-1991. Requirements for internal colors of military aircraft

# The Construction of Marine Combat Flight Environment Based on 4D Simulation Technology



Yishuang Zhang, Yan Zhang, Fei Peng, Yang Liao, Huamiao Song, Xueqian Deng, Duanqin Xiong, Juan Liu, and Liu Yang

**Abstract** Natural scene simulation is an important part of virtual reality technology. When flying on the sea, it is a unique experience with vast expanse, few referential landmarks, low visibility, and “pot bottom illusion”. In order to build a virtual system of marine combat flight environment with strong immersion, based on 4D stereo imaging system, the special texture fusion algorithm is used to simulate the cloud effect through the process of making, coloring, and fusion; the fluid system is used to simulate the sea surface; the method of surface triangle mesh custom polygon is used to simulate the illusion of very low altitude flight by means of deformation modification, etc. Finally, a realistic virtual reality system of marine combat flight environment is realized, which provides a reliable platform for marine flight psychological training.

**Keywords** 4D simulation · Marine combat flight environment · Special texture fusion algorithm · Fluid system · Triangular mesh of curved surface

## 1 Technical Background

Sea flight refers to the flight over the sea area away from the coastline [1]. In recent years, with the change of the international situation and the increase of our military activities in the open sea, our army has paid more and more attention to the training of pilots in sea flight operations [2]. The investigations show that pilots who carry out maritime flight training tasks often face great psychological pressure due to the complex marine environment, few reference points of ground objects and landmarks, prone to delusions, rapid changes in sea conditions and difficulties in navigation [3, 4]. Especially for the pilots who take part in the sea mission for the first time, they are more likely to have stress reactions such as fear and tension due to their lack of understanding of the special environment at sea, which would affect the mental and physical health of the pilots and could also threaten the flight safety if not regulated.

---

Y. Zhang · Y. Zhang · F. Peng · Y. Liao · H. Song · X. Deng · D. Xiong · J. Liu · L. Yang (✉)  
Air Force Medical Center, Fourth Military Medical University, 100142 Beijing, China  
e-mail: [yangliuhenry@aliyun.com](mailto:yangliuhenry@aliyun.com)

The research shows that improving the pre-adaptability of workers to the working environment through certain training methods can alleviate the work stress to a great extent. Therefore, it has become the focus of military training research in various countries that how to conduct pre-adaptation training for sea pilots so that they can be familiar with the sea flight and operational environment as soon as possible.

Virtual reality technology can make use of computer to create a simulation environment, which gives people a sense of immersion in the environment [5]. It has been widely used in military and aerospace fields in recent years for providing pilots with more real air environment experience under safe conditions, reducing the cost of flight training, and improving training safety [6]. The US Army used virtual reality technology to simulate the real battlefield environment to train the air force pilots when they were fighting in Iraq, which greatly reduced the difficulty and casualty rate of the pilots to carry out combat tasks. This kind of training method is also worth using for reference in the sea flight combat training, and how to simulate the real ocean combat training environment and how to provide immersive experience for participants should be one of the technical difficulties. This paper will introduce a method of building virtual marine flight environment based on 4D simulation technology.

## **2 4D Stereo Imaging System**

### ***2.1 Design Principle***

The perception of depth in human visual system is caused by many clues, and binocular parallax, binocular accommodation, convergences are considered as the main stereoscopic cues among them. Four-dimensional simulation products mainly use the perspective difference of human eyes and convergence function to produce four-dimensional effect products. Two pictures overlap on the screen when the product is shown. With the help of special glasses or the radiation semi-cone lens grating in front of the screen, audiences can see the pictures taken from the left perspective through the left eye, the pictures taken from the right perspective through the right eye, and then synthesize the three-dimensional perspective through the convergence function of the two eyes.

### ***2.2 The Realization of 4D Stereo Imaging System***

Based on the principle of stereoscopic imaging system, this system used two projectors to stack two pictures on the screen by off-axis method. Because the effect of stereoscopic image depends on the distance between two projectors and between

them and the projection plane, we set the projection distance as 1/20 of the projection plane distance to ensure a comfortable viewing effect. To ensure that the negative parallax (the projection plane behind the object) does not exceed the eye spacing, the measurement of the parallax angle is defined as follows:

$$\theta = 2 \tan^{-1} \left( \frac{DX}{2D} \right) \tag{1}$$

*DX*: the horizontal interval between the projection points of two eyes; *D*: the distance between the eyes and the projection plane.

### 3 Cloud Simulation

The visibility experience in sea flight mainly depends on the simulation effect of cloud. We use Houdini to simulate the cloud. Houdini supports all nodes to be transformed into OTL, which can be easily controlled and modified. Therefore, the shape of cloud based on Houdini can be controlled at will by adjusting any required parameters. Figure 1 shows the simulation process of cloud effect. The main steps include the following:

1. Use Houdini’s copy and mountain nodes to make some irregular balls in order to simulate irregular clouds of different sizes. The scatter node can control

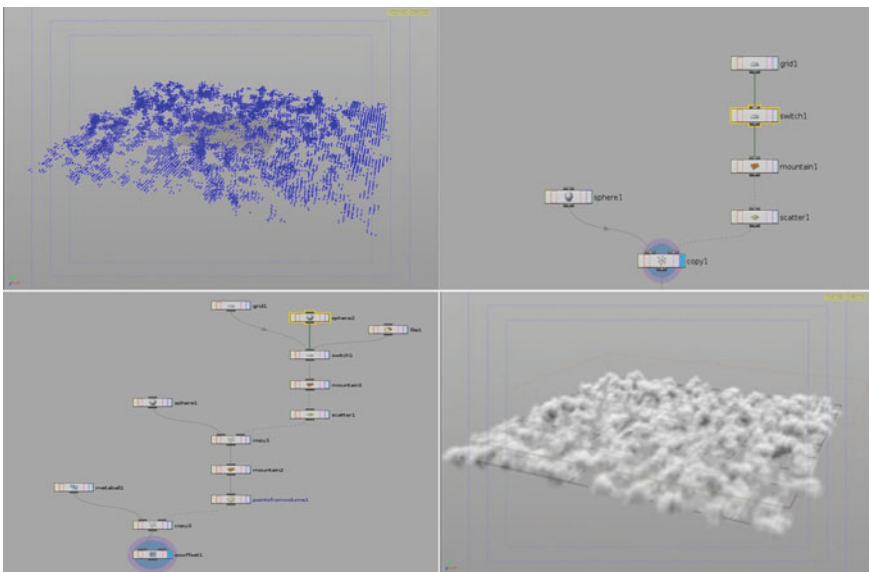


Fig. 1 Cloud simulation process

the number of discrete points, that is, the number of small balls is ultimately controlled;

2. Use the mountain node and the point from volume node to generate many irregular points to determine the general shape of the cloud;
3. Copy many metaballs through the copy node and then generate the cloud through the iso-offset node;
4. Use distance to measure the distance between each point and the point searched, we can get the vector film length of the point. Use this distance to map to the color, take (1-film length) as the output color, if the film length of this point is greater than 1, (1-film length) < 0, the color is black; if the film length of this point is less than 1, (1-film length) > 0, the color tends to red.

## 4 Ocean Simulation

It is an important visual experience when flying in the sea to be vast and open. Use RealFlow, 3ds Max, Photoshop, and other software to simulate the ocean which could be observed when flying at sea. In order to make the pilot really feel the distance between the aircraft and the sea, different methods are used to simulate.

### 4.1 Close Sea Simulation

In order to reflect the effect of wave fluctuation, the real flow particle is used to calculate the sea surface, and the statistical spectrum of “Tessendorf wave” is used to create and adjust the wave crest to simulate the wave. In this way, a highly realistic sea simulation effect can be achieved.

### 4.2 Distant Sea Simulation

For long-distance sea surface, 3ds Max is used for simulation. Firstly, adjust the material type of water to anisotropic and adjust the diffuse, ambient, specular level, glossiness, orientation, and other parameters of the material to simulate the texture of the sea surface. Adjust the wave peaks and troughs of the distant sea surface by adding smoke map in the bump map rollout and adjusting the relevant parameters. In the bump rollout, add noise to simulate the small wave texture in the big wave and add black and white ripple smoke channel in the displacement map to simulate the overall vision. Figure 2 shows the key effects of sea surface and overall visual simulation.

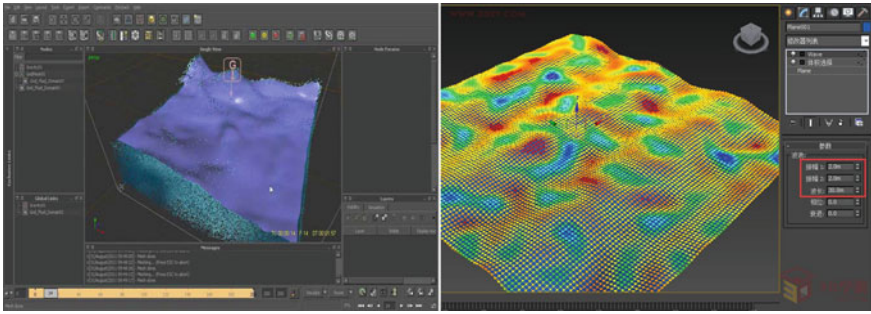


Fig. 2 Effects of sea surface and overall visual simulation

### 4.3 Special Sea Conditions Simulation

When pilots fly at ultra-low altitude, they will have the illusion that the sea antenna is higher than the position of the aircraft. At this time, the ocean is like an endless pot, and the aircraft is flying at the bottom of the pot. This phenomenon could be called as “pot bottom illusion”. In order to simulate this phenomenon, we can use the surface triangle mesh of real wave to customize the polygon, through deformation and displacement, and use a variety of predefined modifiers to simulate the distortion phenomenon of the pilot when flying at low altitude on the sea surface, and more precise in displaying the sense of pressure generated by flying at low altitude on the sea surface. The process is as follows:

1. Import sea sequence frame;
2. Extract the area near the horizon through the color channel;
3. Blur the horizon area to make it look more realistic;
4. Mesh warp special effects are added to the adjusted sea synthesis to distort the sea surface to form the pot bottom phenomenon according to the aircraft animation.

Figure 3 shows the comparison of the sea effects before and after distorted.



Fig. 3 Comparison before and after distorted

## 5 Conclusion

When flying on the sea, it is a common visual experience to have a vast expanse, few referential landmarks, and low visibility, and “pot bottom illusion” is also a unique illusion experience in marine combat flight. In the simulation design, based on the principle of 4D stereo imaging system, the sky, sea, and illusion effects are simulated by various technical means to create a marine combat flight environment with strong immersion, and finally a realistic virtual system of sea combat flight environment is realized. Many flight experts have verified this system and pointed out that the system is very suitable for pilots’ pre-adaptation training before flying at sea.

## References

1. Wen C (2014) Characteristics of sea flight. *Sci Chin* 8S:24
2. Zhang Y, Wang H, Fu H, Zhang Y, Song H, Peng F, Bai H, Liu J, Liao Y, Yang L (2018) Empirical study of psychological stress protection training for the flight over sea. *Chin J Aerosp Med* 29(3–4):181–187
3. Fan J, Zong Y (2001) Investigation on the incidence of illusion of fighter pilots flying at sea. *Flight Surg* 6:233–234
4. Gu S, Zhang Y, Zhang Y, Guo J (2015) A simulator-based maritime flight pilots mental training system. *Ordnance Ind Autom* 11:82–85
5. Shi Y (2019) On the development and application of virtual reality. *Chin Inf* 1:20
6. Ma A (2015) The development and prospect of virtual reality technology. *Digit Ind* 07:107



# Spacecraft Multifunctional Micro-vibration Environment Laboratory



Yao Wu, Tingfei Yan, Guiqian Fang, Xinming Li, Jungang Zhang, Lei Wang,  
and Bo Wei

**Abstract** The problem of orbital micro-vibration has been troubling the development of high-precision spacecraft. Experimental research on on-orbit micro-vibration during the satellite development stage is a very effective method to solve this problem. In order to carry out the ground micro-vibration test of spacecraft with higher accuracy, this paper introduces a micro-vibration laboratory designed in AIT, which has excellent performance of vibration isolation and sound insulation. The background noise index reaches 30 dBA, and the background vibration index reaches  $10^{-5}$  g. At the same time, the laboratory is designed according to the satellite development process, which can be used to conduct all kinds of micro-vibration environmental tests in the satellite development cycle under the same background environment.

**Keywords** Spacecraft · Micro-vibration test · Micro-vibration laboratory · Sound absorption · Vibration isolation

## 1 Introduction

The micro-vibration of the spacecraft in orbit is a kind of vibration accompanying the movement of the moving parts. Different from the general reciprocating vibration that occurs near the equilibrium position, it is a random reciprocating motion that occurs at the movement position. It has the characteristics of small amplitude (typically on the order of micrometers), wide frequency range, nonlinearity, and strong coupling. It changes as the working characteristics of the moving parts change. This kind of vibration caused by the work of moving parts such as the control moment gyro (CMG), solar wing drive mechanism (SADA), and other general micro-vibration sources does not cause structural damage but significantly affects the performance of high-precision payloads [1–3]. On-orbit micro-vibration is an important factor that affects

---

Y. Wu (✉) · T. Yan · G. Fang · X. Li · J. Zhang · L. Wang · B. Wei  
Beijing Institute of Spacecraft Environment Engineering, Beijing, China  
e-mail: [jackyao\\_wu@163.com](mailto:jackyao_wu@163.com)

the key performances of imaging quality and pointing accuracy of high-precision spacecraft such as space telescopes, high-resolution remote sensing satellites, and laser communication satellites [4–6]. It is necessary to analyze the micro-vibration problem at the same time as the satellite development stage [7].

## 2 Ground Micro-vibration Test

Before launching, conducting on-orbit micro-vibration ground evaluation and ground test research are necessary methods to solve this problem. However, each micro-vibration test requires a special test environment, that is, an ultra-low vibration environment, an ultra-low noise environment, and even an ultra-low gas flow environment. This is because the magnitude of micro-vibration is very small, and any minute vibration, noise, or airflow in the surrounding environment may have a great impact on the test results.

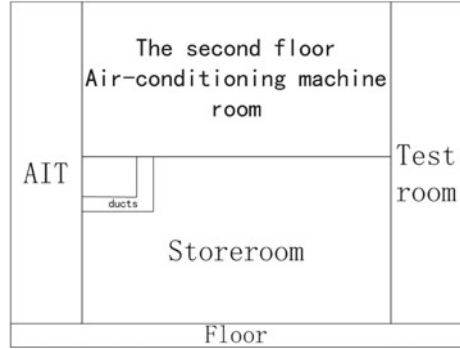
Due to the special requirements of the test environment for the micro-vibration test, the micro-vibration test is best performed in a specially designed micro-vibration test room. At present, most micro-vibration test laboratories only perform a part of the micro-vibration tests in the development stage. The magnitude of the micro-vibration is small, so the background noise will have a great impact on the test results. Since the background noise of each micro-vibration laboratory is different, this will cause different background noises of different single machines of the same satellite to perform micro-vibration tests, which makes it difficult to evaluate the results. Especially for the test of high-precision satellites, the accuracy is higher, so the background noise requirements are higher, so that the test is even difficult to carry out. Therefore, the construction of an ultra-clean laboratory with multi-purpose functions can carry out micro-vibration tests under the same background environment during the product development stage, which will make the research of micro-vibrations of the product more convenient and accurate, and the same background noise will be more conducive to the discovery of problem-solving problem.

## 3 Micro-vibration Laboratory Design

In order to facilitate the implementation of high-precision micro-vibration tests, a multifunctional micro-vibration test laboratory was constructed in this paper.

The laboratory was converted from the original warehouse in the AIT factory. The warehouse is on the first floor and is surrounded by the satellite assembly and test hall (Fig. 1). Therefore, during work hours, other work will generate random vibration and noise in this room. In addition, there is an air-conditioning room directly above the room. The air-conditioning will work continuously day and night. These factors will

**Fig. 1** Original warehouse in the AIT factory



cause continuous vibration and noise interference in the room. Therefore, the original vibration environment in the room is  $10^{-4}$  g, and the noise environment is 55 dB (A). In order to meet the background noise environment required for the micro-vibration test, the room was designed for vibration isolation and acoustic design.

### 3.1 Multistage Vibration Isolation System

Firstly, remove the concrete floor in the middle of the house, dig a deep pit about 2 m downward, and set up a laboratory vibration isolation foundation in the deep pit. The wall and bottom of the vibration-isolating foundation are cast by concrete. Rubber vibration-isolating materials are installed on the outside of the foundation wall to avoid direct contact between the vibration-isolating foundation and the original structure of the house and block the house structure from transmitting vibration signals to the vibration-isolating foundation. The first-stage vibration isolation system was completed (Fig. 2).

Then, two vibration isolation platforms were built at the east and west locations in the vibration isolation foundation. The size of the vibration isolation platforms 1 and 2 was  $8\text{ m} \times 2\text{ m} \times 1\text{ m}$  and  $7\text{ m} \times 2\text{ m} \times 1\text{ m}$  (length  $\times$  Width  $\times$  height).

Each vibration isolation platform is composed of a concrete mass and several spring vibration isolators to form a two-stage vibration isolation system (Fig. 3). The embedded steel plate at the bottom of the concrete mass is linked to the spring isolator and installed on the vibration-isolating foundation. The concrete mass is used to install micro-vibration test equipment.

In order to ensure the installation accuracy of each test equipment, multiple mounting steel plates are embedded in the upper surface of the platform, and ten steel plates are installed on the top of the first vibration isolation platform, and on the top of the second vibration isolation platform two large steel plates and four small steel plates were installed.

**Fig. 2** First-stage vibration isolation system

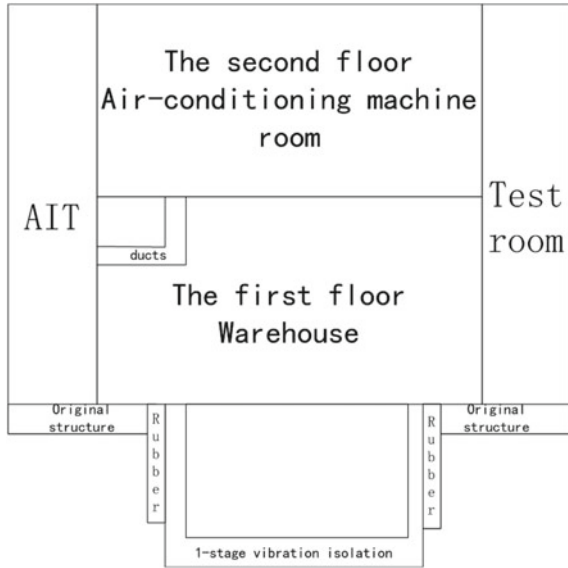
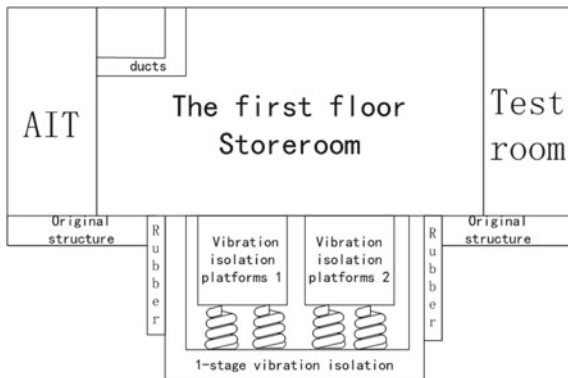


**Fig. 3** Second-stage vibration isolation system



Finally, the two vibration isolation foundations are flexibly connected to the surrounding ground joints. Each vibration isolation platform can be simplified to a mass spring system, and the first-order resonance frequency of the vibration isolation platform is less than 2.5 Hz after construction.

$$f = \sqrt{\frac{K}{M}} \tag{1}$$

*K* The stiffness of the spring.

*M* The weight of the platform.

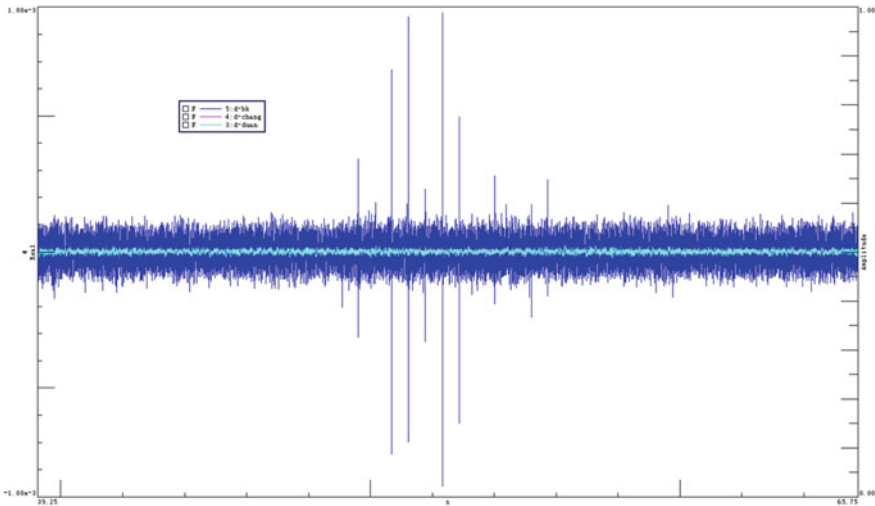


**Fig. 4** Isolation performance of micro-vibration laboratory

Figure 4 shows that when someone walks on the factory floor, it has no effect on the vibration isolation platform. The background noise vibration index on the vibration isolation platform can be better than  $10^{-5}$  g.

Each vibration isolation platform can be simplified to a mass spring system, and the first-order resonance frequency of the vibration isolation platform is less than 2.5 Hz after construction.

### 3.2 Sound Insulation and Absorption System

The noise interference of the micro-vibration laboratory is mainly divided into two parts. One part is the noise transmitted from the surrounding room to the room through the wall. The other part is the noise generated by the work of the test equipment during the micro-vibration test. Noise interference is caused by reflection.

Therefore, the sound insulation design and the sound absorption design were carried out separately.

Since the room above is the room of the air-conditioning unit, the cost of renovation is high and the construction is not convenient. Therefore, a damping layer is applied to the top plate to reduce the floor vibration. The top corner of the room is equipped with ventilation ducts for ventilating the AIT hall, which is very noisy. Therefore, a sound insulation cover is designed for the ventilation duct to reduce the radiated noise from the noise source.

On the wall surface, multilayer sound insulation panels are installed. The sound insulation structure is designed by comprehensively using cavity resonance and structural sound insulation methods. At the outermost side of the sound insulation structure, facing the interior side of the room, install sound-absorbing materials to absorb the sound waves generated by the test product and avoid reflected sound waves from affecting the micro-vibration test. Through sound insulation and sound absorption design, the overall noise reduction of the room is more than 20 dB (A), the background noise is less than 30 dB (A), and the sound absorption rate of the wall is more than 90%, realizing the construction of an ultra-quiet environment (Figs. 5 and 6).

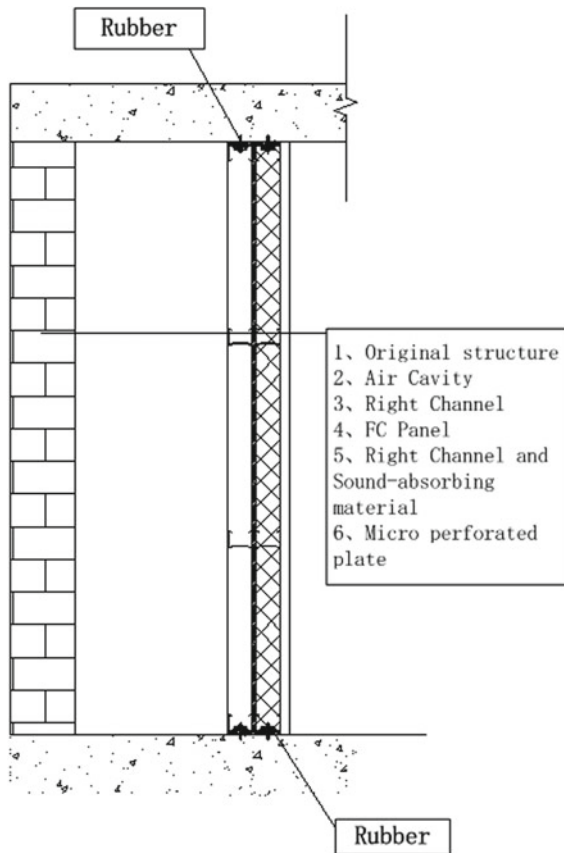


Fig. 5 Multilayer sound insulation panels

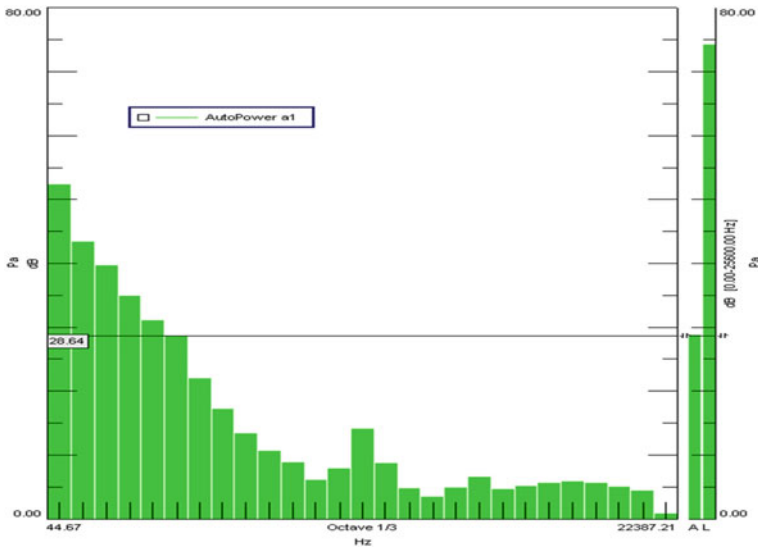


Fig. 6 Background noise of micro-vibration laboratory

### 3.3 Multifunctional Design for Micro-vibration Test

Most of the research on micro-vibration problems comes from three aspects: source, path, and receiver, corresponding to the research of vibration source of micro-vibration, the research of transmission path, and the research of micro-vibration characteristics of sensitive load. Each part corresponds to different types of micro-vibration experiments. It mainly includes micro-vibration disturbance source identification test, satellite system micro-vibration transmission path analysis test, simulation of on-orbit micro-vibration environment test on the ground, sensitive micro-vibration resistance verification test, and so on. In response, the functional design of the micro-vibration laboratory was designed according to the main content of the satellite micro-vibration test and the satellite development process. It mainly includes the following micro-vibration testing equipment:

1. Vacuum disturbance source interference micro-vibration test system
2. Multi-degree-of-freedom interference source simulation system
3. Satellite or payload micro-vibration response test system
4. High-precision optical path simulation system.

The high-precision optical path simulation system is set on the steel plate of No. 1 vibration isolation platform, and the multi-degree-of-freedom interference source simulation system and vacuum disturbance source interference micro-vibration test system are both set on the steel plate of No. 2 vibration isolation platform. In addition,

a steel plate is also installed on the second seismic isolation platform, which is used to carry out satellite or payload micro-vibration response test. The steel plate has threaded holes. The rigid and flexible fixtures required for the micro-vibration test can be directly mounted on this steel plate by bolts.

The function of the disturbance source test system is to identify the disturbance source and quantify the output level of the disturbance source. It is used to identify the micro-vibration disturbance force such as momentum wheel and control torque gyro in a vacuum environment to obtain the micro-vibration output response.

The micro-vibration environmental performance verification system of a payload is very sensitive to micro-vibrations, the main purpose is to create a micro-vibration environment when the payload is working on orbit and then verify the performance of the payload in this environment.

The spacecraft and payload micro-vibration response test system is mainly used to analyze the transmission path of the spacecraft and evaluate the overall micro-vibration response.

## 4 Conclusion

The micro-vibration laboratory established in this paper can perform micro-vibration test analysis under the same background noise during the entire satellite development cycle, such as micro-vibration analysis of interference sources, transmission path analysis, and micro-vibration response analysis. The test data is evaluated at the same background noise level, which is more conducive to product analysis and development. In addition, through the design of vibration reduction and noise reduction, the laboratory has extremely low background noise for micro-vibration testing. The noise environment index of the laboratory is better than 30 dB (A), and the vibration environment index is better than  $10^{-5}$  g. The design method has the function of isolating external vibration and noise interference, and the method can be used for the conventional AIT plant renovation.

## References

1. Bronowicki AJ (2008) Forensic investigation of reaction wheel nutation on isolator. In: 49th AIAA/ASME/ASCE/AHS/ASC structures, structural dynamics, and materials conference, Schaumburg, USA, 7–10 Apr
2. Wu Y, Xie Y, Yan T, Fang G, Jiao A (2018) Micro-vibration testing technology of space station control moment gyroscope. *Equip Environ Eng* 15(8):94–99
3. Wang H, Wang W, Wang X, Zou G, Li G, Fan X (2013) Space camera image degradation induced by satellite micro-vibration. *Acta Photonica Sin* 42(10):1212–1217
4. Chapel J, Stancliffe D, Bevacqua T, Winkler S, Clapp B, Rood T, Gaylor D, Freesland D, Krimchansky A (2015) Guidance, navigation, and control performance for the GOES-R spacecraft. *CEAS Space J* 7(2):87–104



5. Zhang Y, Zhang J, Zhai G, Xu S (2012) High imaging performance of optical payload by vibration isolation system. In: AAIA guidance, navigation, and control conference, Minneapolis, MN, USA
6. Zhang Q, Wang G, Zheng G (2015) Micro-vibration attenuation methods and key techniques for optical remote sensing satellite. *J Astronaut* 36:125–132
7. Fang N, Zu J, Yang W, Zhou H (2014) The design of world view satellite and its demonstrative value. *Spacecr Environ Eng* 31:337–342

# Study on the Paving Density of Lunar Soil Simulant in the Indoor Ground Test of Lunar Rover



Yanjing Yang, Shichao Fan, and Shuhong Xiang

**Abstract** As the basic property of lunar soil simulant, variation of the density will affect the simulant bearing capacity, slope stability, heat exchange property and so on, as well as the mobility of lunar rover. Experiment research reveals that the stacking status has a significant influence on the mechanical property of the lunar soil simulant, and reasonable paving density is critical to the effectiveness of rover mobility experiment on ground. In this paper, the Duncan-Chang–Drucker–Prager model was used for the numerical representation of lunar soil simulant in the finite element model. Based on the analysis of bearing capacity of different lunar soil simulant with different densities, the paving density of lunar soil simulant in the indoor ground test of lunar rover was given.

**Keywords** Lunar rover · Ground test · Lunar soil simulant · Paving density

## 1 Introduction

The lunar gravity is only  $1/6$  g, and since lower gravity field changes the mechanical properties of lunar soil, simulation of the in-situ lunar soil environment on ground remains an important problem during the verification stage of lunar rover.

Considering low gravity environment was difficult to model on ground, numerical method is always an effective tool in terramechanics analysis [1–3], finite element modelling was used to study the mechanical property of lunar soil simulant with different densities here, and proper density of lunar soil simulant was determined to acquire equivalent in site lunar soil property.

In this paper, a nonlinear elastic–plastic constitutive model called DC–DP model was used to model the lunar soil simulant, where the nonlinear elastic modulus of the soil was defined by Duncan-Chang model, and the failure criterion was defined by Drucker–Prager model. The stress varying property of lunar soil simulant can be reflected by this model. The detail of this model can refer to our previous work [4].

---

Y. Yang (✉) · S. Fan · S. Xiang  
Beijing Institute of Spacecraft Environment Engineering, 100094 Beijing, China  
e-mail: [yjpk@163.com](mailto:yjpk@163.com)

© The Editor(s) (if applicable) and The Author(s), under exclusive license to Springer Nature Singapore Pte Ltd. 2021  
S. Long and B. S. Dhillon (eds.), *Man-Machine-Environment System Engineering*, Lecture Notes in Electrical Engineering 645,  
[https://doi.org/10.1007/978-981-15-6978-4\\_66](https://doi.org/10.1007/978-981-15-6978-4_66)

**Table 1** Lunar soil simulant parameters of the DC–DP model

	$c$ (kPa)	$\varphi$ (°)	$P_a$ (kPa)	$\beta$ (°)	$d$ (kPa)	$K$	$n$	$R_f$	$K_{ur}$
( $\rho = 1.46 \text{ g/cm}^3$ )	1.1	39.9	101.3	58.5	2.3	197.9	0.93	0.62	3.0
( $\rho = 1.50 \text{ g/cm}^3$ )	2.3	43.6	101.3	60.8	5.1	239.8	0.92	0.61	3.0
( $\rho = 1.55 \text{ g/cm}^3$ )	2.9	46.1	101.3	62.2	5.5	507.8	0.91	0.75	3.0
( $\rho = 1.65 \text{ g/cm}^3$ )	4.5	52.2	101.3	65.0	7.5	799.5	0.83	0.68	1.2

Using the constitutive parameters calculated via test, the DC–DP model was implemented through UMAT subroutine in ABAQUS. Bearing capacity of lunar soil simulant with different density was analysed to choose a proper simulant paving density during the rover indoor ground test.

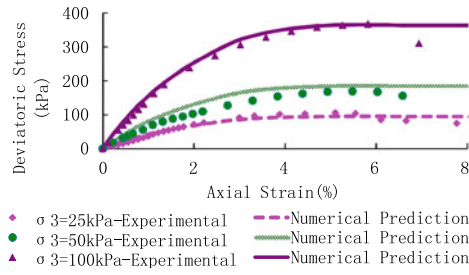
## 2 Model Parameter Determination and Verification

The results of triaxial compression tests were used to estimate four different densities lunar soil simulant material parameters for the proposed model. The material parameters used in the simulation were given in Table 1, where  $c$  is cohesion,  $\varphi$  is angle of internal friction,  $P_a$  is the atmospheric pressure,  $\beta$  is the slope of the linear yield surface in  $p$ - $q$  plane,  $d$  is the material cohesion,  $K$  is the modulus number,  $n$  is the modulus exponent,  $R_f$  is the failure ratio,  $\mu$  is Poisson's ratio which equals to 0.45, and  $K_{ur}$  is the reload modulus number.

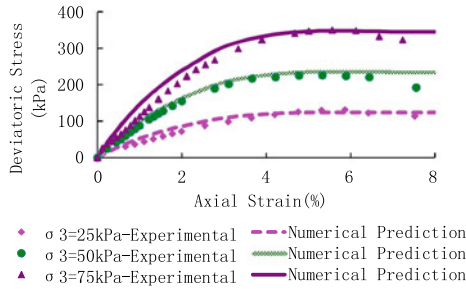
The DC–DP model was implemented into UMAT of ABAQUS [5, 6]. Comparisons of the predicted and measured stress versus strain under three different confining pressures of lunar soil simulant were given in Fig. 1. The modelled and measured data agreed well at low confining pressure and small axial strains.

## 3 Plate Sinkage Test Simulation of Lunar Soil Simulant with Different Densities

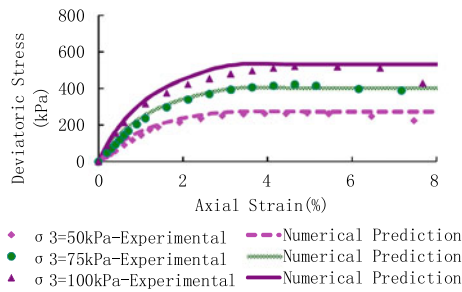
Sinkage characteristics of lunar soil simulant with different densities were analysed in this section. The lunar soil simulant was modelled using a rectangular solid whose sizes were  $120 \times 120 \times 15 \text{ cm}$ ,  $120 \times 120 \times 20 \text{ cm}$ ,  $120 \times 120 \times 30 \text{ cm}$  and  $120 \times 120 \times 50 \text{ cm}$ . A circular plate with a radius of 10 cm was placed on the centre on the top surface of this FE model. Considering the symmetry characteristic of this model, only one quarter of the FE model was built, and element type used in the model was C3D8R. U1, U2 and U3 of the base surface were restricted. A displacement along  $-Z$  was placed on the top surface of this model to simulate the downward sinking process. The plate sinkage test modelled in ABAQUS was shown in the following figure (see Fig. 2).



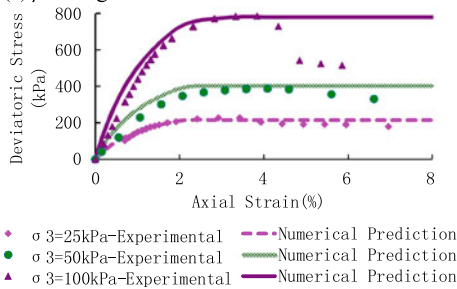
(a)  $\rho=1.46\text{g/cm}^3$



(b)  $\rho=1.50\text{g/cm}^3$



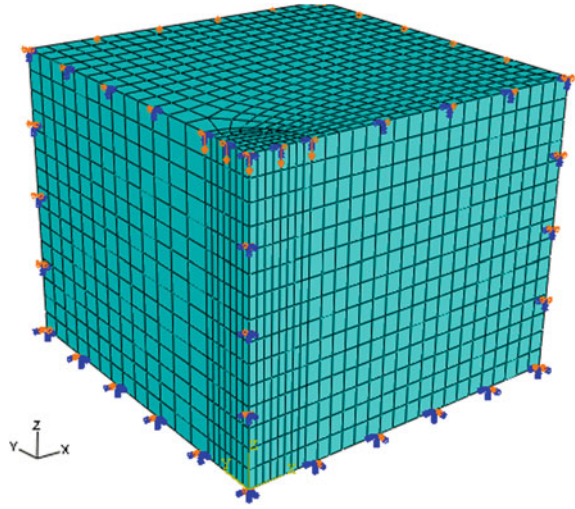
(c)  $\rho=1.55\text{g/cm}^3$



(d)  $\rho=1.65\text{g/cm}^3$

**Fig. 1** Comparison of test results and numerical predictions

**Fig. 2** FEA model of the plate sinkage test (depth = 50 cm)



Sinkage curves of lunar soil simulant of different depths were shown in Figs. 3, 4, 5 and 6. Real lunar soil sinkage curves according to terrain mechanics test results of surveyor mission [7] ( $kc = 1.4 \text{ KN/cm}^{n+1}$ ,  $k\varphi = 820 \text{ KN/cm}^{n+2}$ ,  $n = 1$ ) were also shown in these figures. From these figures, it can be seen that under the same force, the sinkage decreases as the density increases, and under the same force, the sinkage

**Fig. 3** Sinkage curves of lunar soil simulant with different densities (depth = 15 cm)

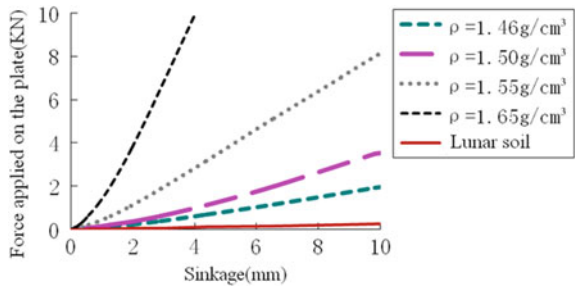


**Fig. 4** Sinkage curves of lunar soil simulant with different densities (depth = 20 cm)

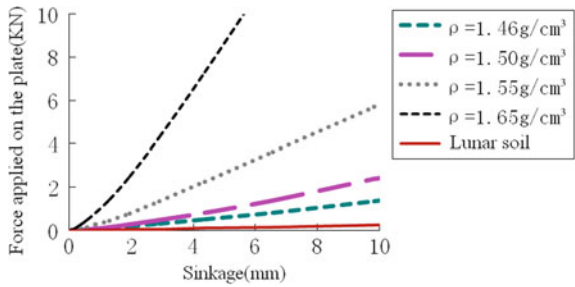


**Fig. 5** Sinkage curves of lunar soil simulant with different densities (depth = 30 cm)

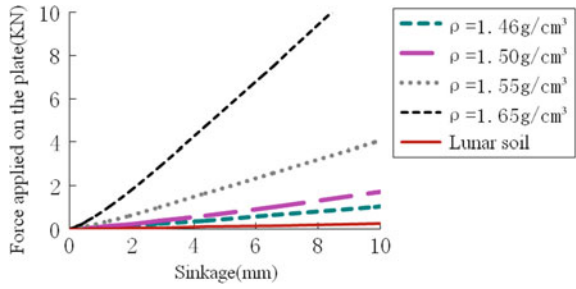
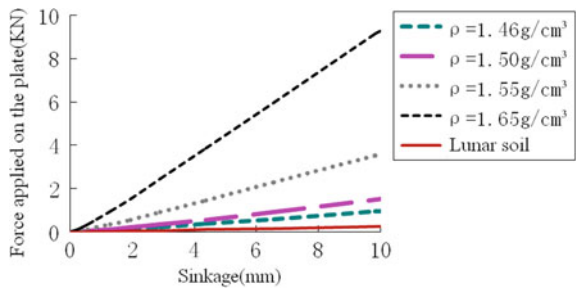


**Fig. 6** Sinkage curves of lunar soil simulant with different densities (depth = 50 cm)



of different density lunar soil simulant was smaller than real lunar soil, which means that these lunar soil simulants with different densities were “stiffer” than the real lunar soil.

According to the relationship between the bearing capacity and density of lunar soil simulant, bearing capacity is consistent with the real lunar soil and can be acquired through adjustment of lunar soil simulant density. Force applied to the plate on lunar soil simulant with different densities and the force on real lunar soil under the same sinkage were shown in Table 2.

The curve fitting results of force applied on the plate versus density were shown in Figs. 7, 8, 9 and 10, and the target density which produces the identical force with the real lunar soil was shown with a dashed line. Target densities at different depths were shown in Table 3.

**Table 2** Force applied to the plate on lunar soil simulant with different densities and the force on real lunar soil under the same sinkage (All forces are measured in KN)

Density (g/cm <sup>3</sup> )	1.46	1.50	1.55	1.65	Force on real lunar soil under same sinkage (KN)
Force (Depth = 15 cm)	1.98	3.56	8.15	27.84	0.26
Force (Depth = 20 cm)	1.40	2.44	5.79	19.81	
Force (Depth = 30 cm)	1.04	1.74	4.04	12.13	
Force (Depth = 50 cm)	0.96	1.52	3.57	9.29	

**Fig. 7** Curve fitting results of force applied on the plate versus lunar soil simulant density (depth = 15 cm)

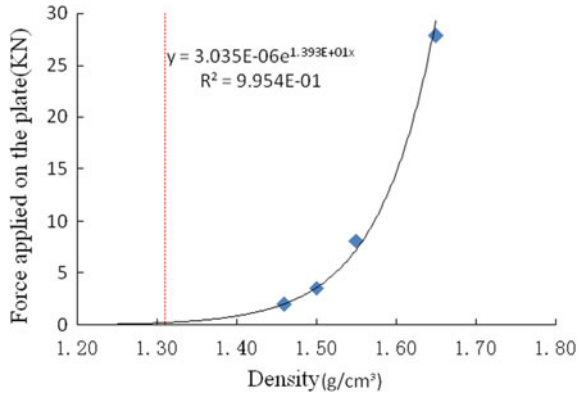


**Fig. 8** Curve fitting results of force applied on the plate versus lunar soil simulant density (depth = 20 cm)

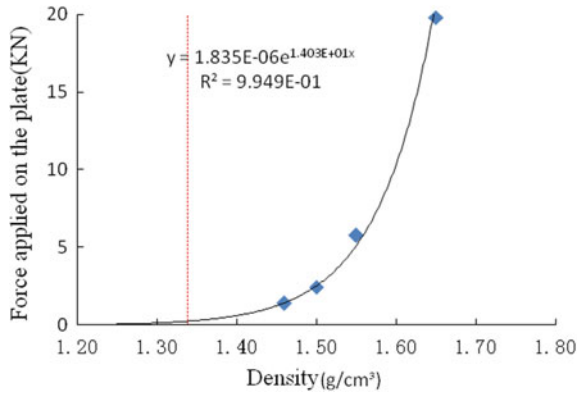


**Fig. 9** Curve fitting results of force applied on the plate versus lunar soil simulant density (depth = 20 cm)

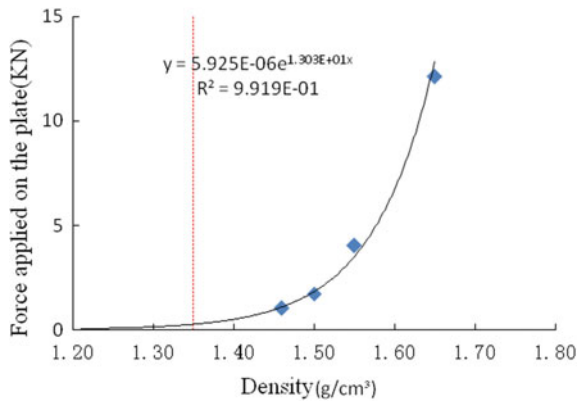


**Fig. 10** Curve fitting results of force applied on the plate versus lunar soil simulant density (depth = 20 cm)

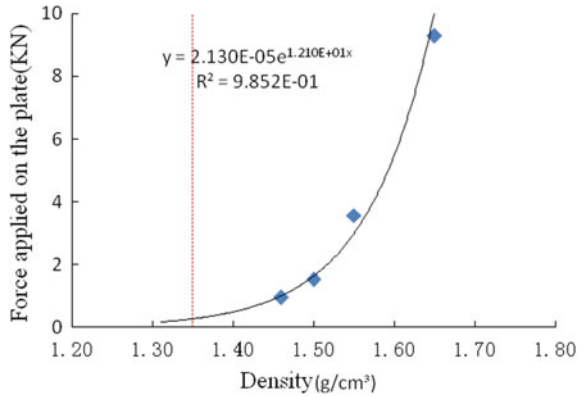


**Table 3** Target densities of lunar soil simulant at different depths

Soil depth (cm)	10	15	20	30	50
Target density (g/cm <sup>3</sup> )	1.29	1.31	1.34	1.35	1.35

## 4 Conclusions

The DC–DP constitutive model was implemented on ABAQUS through UMAT subroutine, and the FE model of lunar soil simulant was built. The plate sinkage test of lunar soil simulant with different densities was simulated, and target paving densities of lunar soil simulant at different depths were recommended according to curve fitting results of forces applied on the plate versus densities.

## References

1. Liu CH, Wong JY, Mang HA (2000) Large strain finite element analysis of sand: model, algorithm and application to numerical simulation of tire-soil interaction. *Comput Struct* 74:253–265
2. Shoop SA (2001) Finite element modelling of tire-terrain interaction. University of Michigan, Michigan
3. Chiroux RC, Foster WA, Johnson CE, Shoop SA, Raper RL (2005) Three-dimensional finite element analysis of soil interaction with a rigid wheel. *Appl Math Comput* 162:707–722
4. Yang YJ, Fan SC, Xiang SH (2014) Proceedings of international conference on noise and vibration engineering, Leuven, Belgium
5. ABAQUS Inc. (2007) ABAQUS analysis user’s manual, Rhode Island
6. ABAQUS Inc. (2007) ABAQUS user subroutines reference manual, Rhode Island
7. Heiken GH, Vaniman D, French BM et al (1991) Lunar sourcebook: a users guide to the moon. Cambridge University Press, Cambridge



# Numerical Study of Thermal Comfort for Door Area in Civil Aircraft Cabin



Quan Peng, Chengyun Wu, Yudi Liu, Xuhan Zhang, and Huayuan Liu

**Abstract** In civil aircraft cabin, the requirement of comfort heating for passengers and crew in door areas is increasing. For the benefit of proper design for supplemental heating systems, a thermal model of door area is developed and the thermal comfort is investigated with CFD method. Human thermal comfort, gray thermal radiation, and Boussinesq hypothesis should be considered in physical modeling. The air distribution including air temperature and air velocity at different height above the floor is presented and analyzed according to ASHRAE 161 standard. The thermal model is validated through flight test, and results show good consistency between CFD solution and flight data.

**Keywords** Civil aircraft · Thermal comfort · Numerical simulation · Door area

## 1 Introduction

Nowadays, more people, including those with impaired health or who are otherwise potentially sensitive to cabin environmental conditions, are traveling by air than ever before. When traveling via short- and medium-haul routes in winter or long-haul routes, passengers and flight attendants adjacent to the doors often complain about coldness in the lower limbs and feet, which is suspected as “leakage of the door.” This is mainly because the door movement area, where the cabin door is connected to the fuselage door frame, is equipped with seals instead of thermal insulation layer. In addition, the thin thermal insulation layer of the cabin door is also the cause of the coldness in the door area.

---

Q. Peng (✉) · C. Wu · Y. Liu · X. Zhang · H. Liu  
Shanghai Aircraft Design and Research Institute, 201210 Shanghai, China  
e-mail: [winnie\\_0805\\_pooh@163.com](mailto:winnie_0805_pooh@163.com)

© The Editor(s) (if applicable) and The Author(s), under exclusive license to Springer Nature Singapore Pte Ltd. 2021  
S. Long and B. S. Dhillon (eds.), *Man-Machine-Environment System Engineering*, Lecture Notes in Electrical Engineering 645,  
[https://doi.org/10.1007/978-981-15-6978-4\\_67](https://doi.org/10.1007/978-981-15-6978-4_67) 579

Airlines and aircraft manufacturers have taken measures to meet the increasing demands for higher comfort level by the flying public, and comfort heating seems to be the most popular one. Comfort heating is realized through supplemental heating systems, mainly in the form of heated floor panels (HFP) or air heaters in ventilation ducts. Comfort heating is widely applied in civil aircrafts by Airbus and Boeing, such as A320, A330, A340, B767, B777, and B787.

Analysis of air distribution in the door area is a must for comfort heating design. Experimental measurements and numerical simulations are the two popular methods used in predicting, designing, and analyzing air distribution in the cabin [1, 2]. The experimental measurements have usually been seen as more reliable although they are more expensive and time-consuming. In fact, most of the numerical simulations use computational fluid dynamics (CFD) can provide effectively detailed information [3].

Studies on air distribution in commercial airliner cabin have been carried out by many researchers [4], but the efforts on simulation of air distribution in door area are extremely limited at this time. In this paper, a thermal model will be developed to investigate air distribution in door area specifically. Distribution of air temperature and air velocity at different height above floor is presented and analyzed according to ASHRAE 161 standard [5]. The thermal model is validated through a flight test, and the flight data is compared with the CFD solution of the flight test condition.

## 2 Thermal Model

### 2.1 Geometrical Model

In general, the computational domain covers two rows of passengers on either side of the cabin door. The geometrical model is bounded by the air that directly contacts the cabin interior and passengers. The components of the model need to be simplified to shorten the computing time, such as seats, passengers, air supply grille. A geometrical model of door area in cabin is shown in Fig. 1.

Accurate solution of numerical model requires high-quality mesh. The grid sizes of the geometrical model of door area are usually set as follows:

1. Global: 30–50 mm
2. Windows, side wall, roof, and floor: 30 mm
3. Air inlet and air outlet: 10 mm.
4. Door: 20 mm.
5. Gap (clearance between the door interior and floor, unequipped with thermal insulation layer): 5 mm.
6. Passengers and seats: 25 mm.
7. Boundary layer: 4 layers with a total thickness of 5 mm and a growth rate of 1.2.

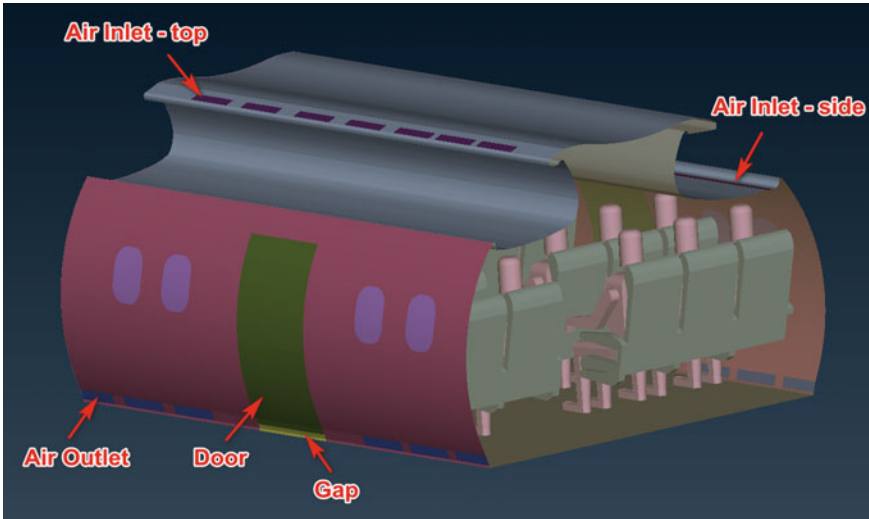


Fig. 1 A geometrical model of door area in cabin

## 2.2 Physical Model

Thermal comfort model, which addresses local thermal sensations of human, is essential for physical modeling of door area in cabin. Developing a thermal comfort model to evaluate thermal comfort asymmetrical environments or transient conditions has been a hotspot of recent study. Cheng et al. [6] coupled two typical thermal comfort models, the simple ISO 14505 standard method and the comprehensive UC Berkeley thermal comfort model (UCB model), to CFD numerical simulation with different process to evaluate thermal environment of a small office, and the results indicated that compared with the UCB model, the ISO 14505 index could be applied with caution as a convenient method to evaluate thermal comfort in non-uniform, overall thermally neutral environments.

Gray thermal radiation and Boussinesq hypothesis should be taken into consideration as well due to the significant temperature difference between the gap of door area and the average operative seating area. In addition, Reynolds-averaged Navier–Stokes equation modeling is recommended for CFD simulation of air distribution in door area.

## 2.3 Analysis of Air Distribution

Aircraft cabin temperature design and operating requirements recorded in ASHRAE 161 standard [5] should be met during the air distribution design for door area, which are listed in Table 1.

**Table 1** Aircraft cabin temperature design and operating requirements (excerpt)

Parameter	Acceptable condition
Temperature spatial variations	Vertical operative temperature variation within a seat (seat centerline): <5 °F (2.8 °C) variation in temperatures measured at 4 in., 24 in., and 43 in. (100 mm, 610 mm, and 1090 mm)
Maximum surface temperature differential for seated occupants	Average temperature of sidewall surface shall be within 10 °F (5.6 °C) of the average operative seating area temperature (the average for 4 in., 24 in., and 43 in. [100 mm, 610 mm, and 1090 mm] from the floor). Temperature of the floor surface measured at the occupant’s feet shall be within 10 °F (5.6 °C) of the average operative seating area temperature (the average for 4 in., 24 in., and 43 in. [100 mm, 610 mm, and 1090 mm] from the floor)
Local airspeed	Seated passengers and crew: <70 ft/min (<0.36 m/s) Draft sensitive bare body areas: <60 ft/min (<0.30 m/s) [<40 ft/min (<0.20 m/s) recommended] Head level with PAO turned on: >200 ft/min (>1.0 m/s) Head level with PAO not installed: >20 ft/min (>0.1 m/s)

By using the thermal model illustrated above, numerical simulation of air distribution for door area in aircraft which is cruising at 35,000 ft in extremely cold weather is conducted. Figure 2 shows the shell temperature of passengers seated in door area. The problem of thermal uncomfot in door area is replicated, since the shell temperatures of passengers adjacent to the doors (3A and 3E) are significantly low in the feet, and the requirement for temperature spatial variations is apparently unmet.

The air temperature distribution at 25 mm, 610 mm, and 1090 mm above floor is detailed in Figs. 3, 4 and 5, respectively. Temperature measured at passenger’s feet adjacent to the door is as low as 14 °C, and the average operative seating area temperature is 24 °C; thus, the requirement for maximum surface temperature differential for seated occupants is unmet. The effect of coldness in door gap area on the section at 610 mm or more above floor is quite limited.

The air velocity distribution at column E is shown in Fig. 6. A uniform velocity distribution is achieved, and the requirement for local airspeed is met.

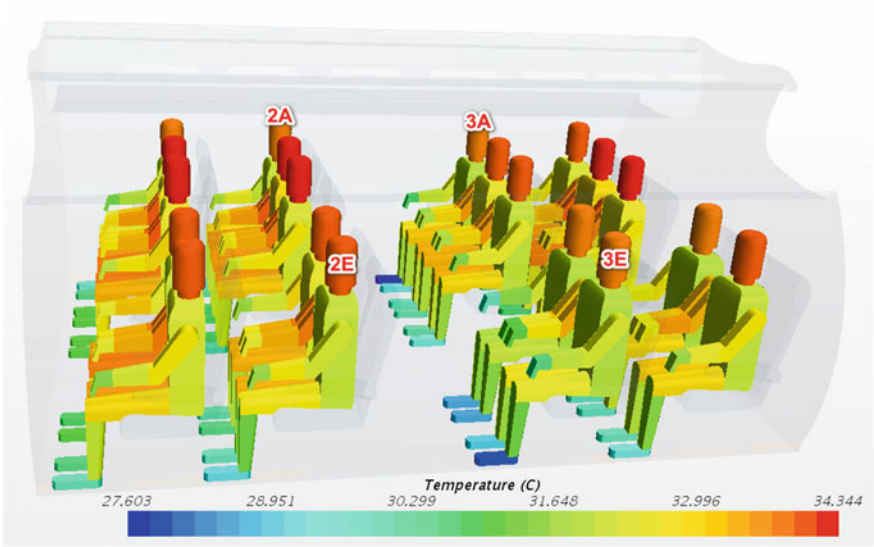


Fig. 2 Shell temperature distribution of passengers seated in door area

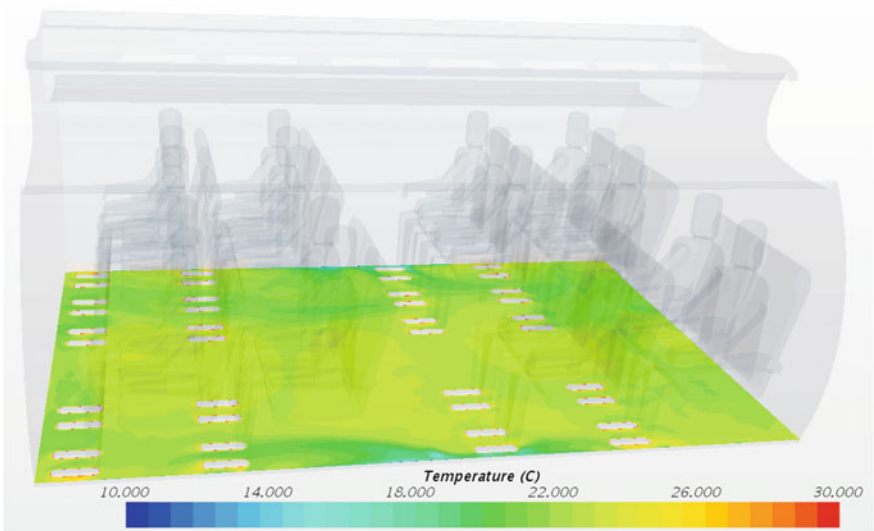


Fig. 3 Air temperature distribution at 25 mm above floor

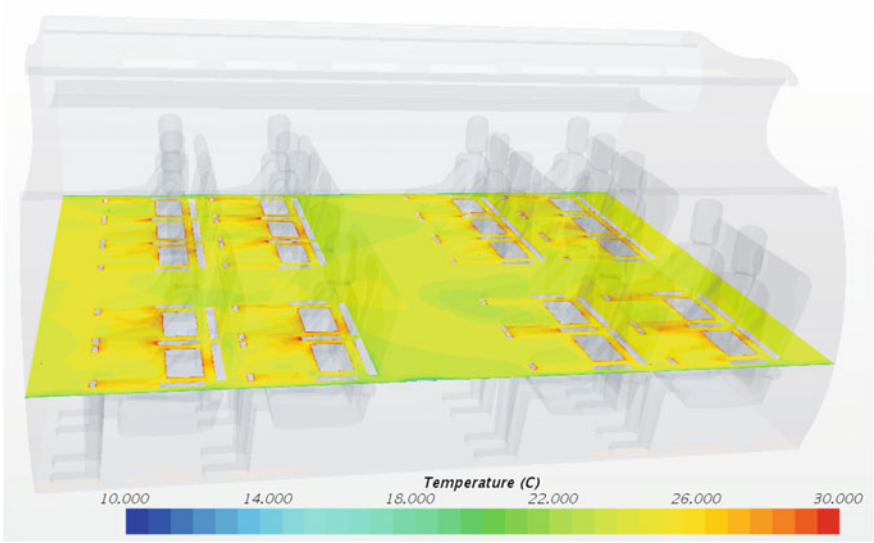


Fig. 4 Air temperature distribution at 610 mm above floor

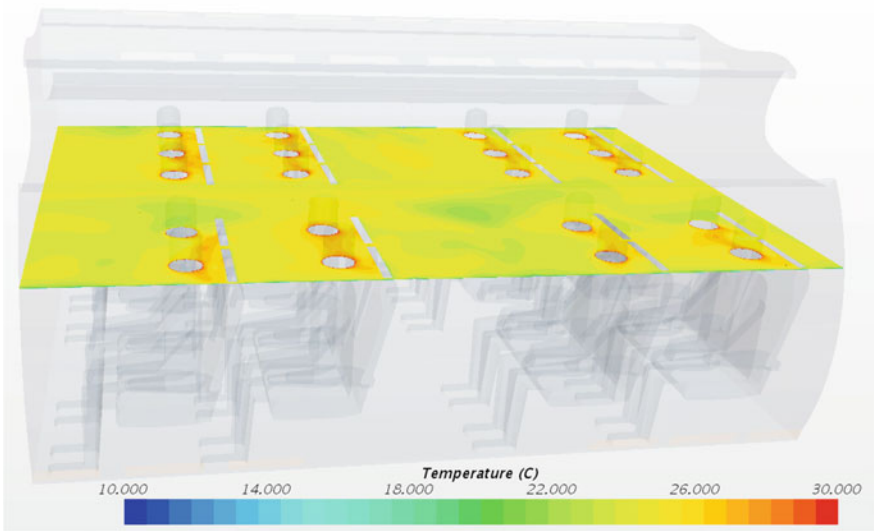
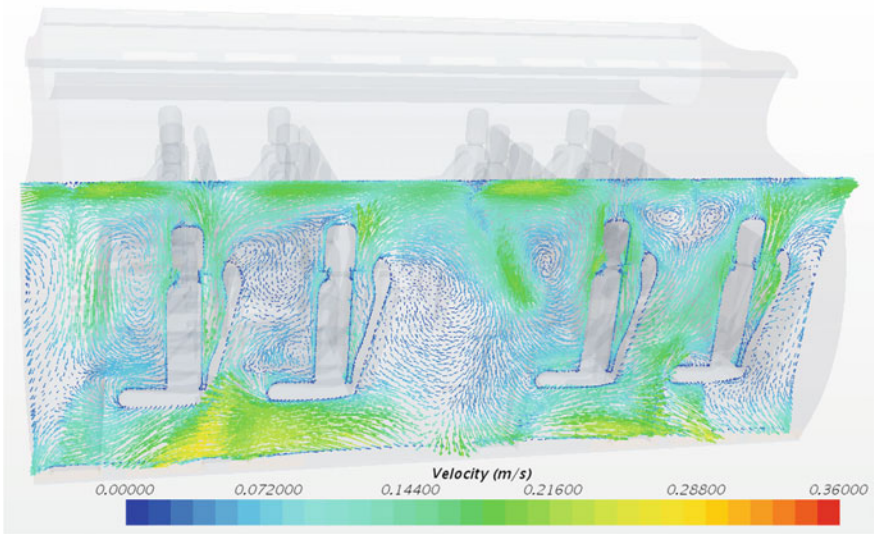


Fig. 5 Air temperature distribution at 1090 mm above floor



**Fig. 6** Air velocity distribution at column E (seat centerline)

### 3 Validation

A flight test is performed on the exact aircraft geometrically modeled in Fig. 1 to validate the thermal modeling of air distribution in cabin door area. Flight data are recorded when the aircraft is cruising at 35,000 ft in hot summer. The measure point layouts in terms of wall temperature and environment temperature are demonstrated in Figs. 7 and 8, respectively.

The description of locations of each measure point is detailed in Table 2, as well as roles they played in the flight test.

The flight data is compared with the CFD solution of the flight test condition, as shown in Table 3. A good consistency is achieved; thus, the thermal model developed in this paper is successfully validated.

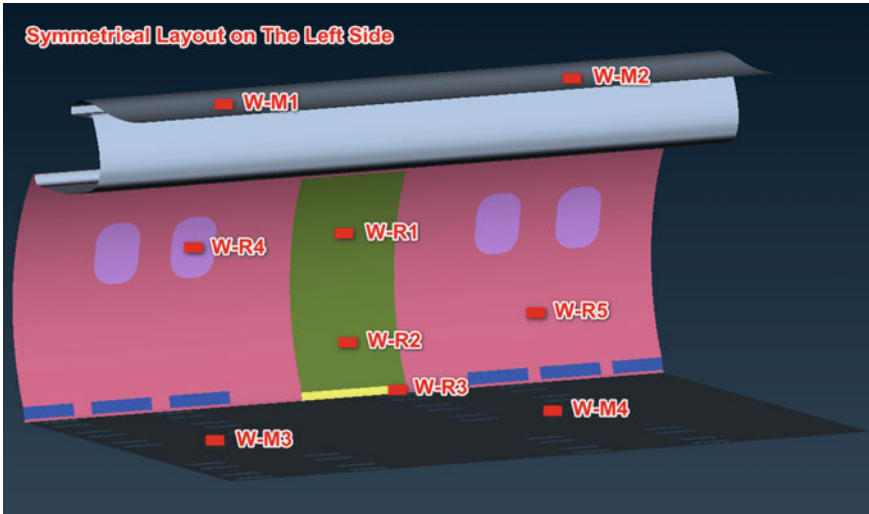


Fig. 7 Layout of measure points for wall temperature

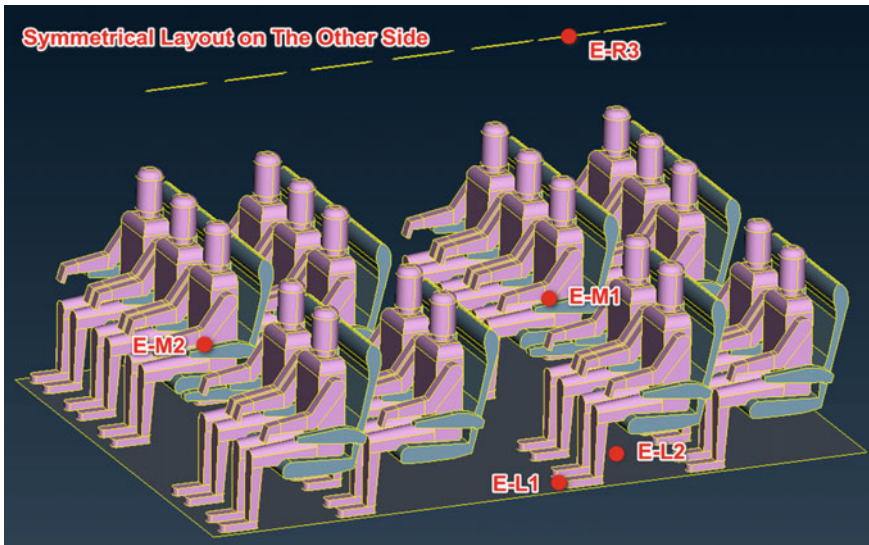


Fig. 8 Layout of measure points for environment temperature



**Table 2** Locations and functions of measure points

Measure point	Location	Function
E-L1, E-R1	Feet of passengers adjacent to doors	Validation
E-L2, E-R2	Lower limbs of passengers adjacent to doors	
E-M1, E-M2	Armrest of seat 3C, 1C	
W-L1, W-R1	Center of upper half of the doors	
W-L2, W-R2	Center of lower half of the doors	
W-L3, W-R3	Gap of the doors	
E-L3, E-R3	Air inlet-top	Boundary condition inputs for CFD
W-L4, W-R4	Center of window	
W-L5, W-R5	Side wall	
W-M1, W-M2	Roof	
W-M3, W-M4	Floor	

**Table 3** Comparison between flight data and CFD solution

Measure point	Flight data (°C)	CFD solution (°C)	Deviation (°C)
E-L1	21.3	24.1	+2.8
E-R1	21.6	20.8	-0.8
E-L2	23.0	25.1	+2.1
E-R2	23.3	24.9	+1.6
E-M1	24.1	25.6	+1.5
E-M2	24.3	26.0	+1.7
W-L1	21.1	23.7	+2.6
W-R1	20.5	24.0	+3.5
W-L2	21.8	23.5	+1.7
W-R2	21.0	23.4	+2.4
W-L3	11.9	8.3	-3.6
W-R3	10.7	7.8	-2.9

## References

1. Liu W (2014) Experimental and numerical study of the air distribution in an airliner cabin. Dissertations & Theses—Gradworks
2. Farag AM (2018) [IEEE 2018 IEEE aerospace conference—big sky, MT, USA (2018.3.3–2018.3.10)] 2018 IEEE aerospace conference—thermal comfort investigation for commercial aircraft cabin by using CFD, pp 1–10
3. Liu W, Mazumdar S, Zhang Z et al (2012) State-of-the-art methods for studying air distributions in commercial airliner cabins. *Build Environ* 47:5–12
4. Liu W, Chen Q (2013) Current studies on air distributions in commercial airliner cabins. *Theor Appl Mech Lett* 3(6):062001

5. American Society of Heating (2011) Refrigerating and Air-Conditioning Engineers, Inc. ASHRAE Handbook, Application. Atlanta, Georgia
6. Cheng Y, Niu J, Gao N (2012) Thermal comfort models: a review and numerical investigation. *Build Environ* 47:13–22

# Research on the Uniform Air Supply Technology of the Static Pressure Chamber in a Spray Room



Jianwu Chen, Yuan Bai, Bin Yang, Lindong Liu, Ye Tian, Yanqiu Sun, and Weijiang Liu

**Abstract** The static pressure chamber has been widely used in the ventilation of a spray room, and the uniform air supply at the bottom of a static pressure chamber is very important for the control of toxic substances; therefore, the internal structure of the static pressure chamber in a spray room is studied in this paper in order to get the uniform air supply. The suitable roof structure of static pressure chamber with uniform air supply in a spray room widely used in wooden furniture manufacturing enterprise is put forward by comparing and analyzing the methods of uniform air supply in duct. The models of static pressure chamber models are established by CAD, and the numerical simulation was carried out by Fluent. The influences of roof structure on the uniform air supply in a static pressure chamber were analyzed based on the results of the simulation. The result shows that the best internal structure of static pressure chamber in the spray room with uniform air supply is that the whole roof is sloping.

**Keywords** Ventilation · Spray room · Static pressure chamber · Simulation · Uniform air supply

## 1 Purpose

A spray room can effectively trap the toxic substances produced by spray painting, reduce the toxic concentration of spray painting environment, and protect the occupational health of workers, so the spray room has been widely used in many fields, such

---

J. Chen · B. Yang · Y. Sun · W. Liu  
China Academy of Safety Science and Technology, 100029 Beijing, China

Y. Bai (✉)  
Xinjiang Uygur Autonomous Region Academy of Safety Science and Technology, 830011  
Urumqi, Xinjiang, China  
e-mail: [baiyuan1215@sina.com](mailto:baiyuan1215@sina.com)

L. Liu · Y. Tian  
University of Science and Technology Beijing, 100083 Beijing, China

as furniture manufacturing [1]. The efficient ventilation system is very important for human health in a spray room [2]. The push–pull ventilation system has been widely used as an efficient ventilation system [3], and a static pressure chamber is often used to achieve uniform air supply at the top of a spray room. Multilayer filter materials are often used in the bottom of the static pressure chamber for the goal of uniform air supply and purifying particles to ensure the quality of spray painting, but the wind resistance lost is high and the effect of equalizing wind needs to be improved. J. Chen et al. researched the performances of supply air for uniform air supply square hood by numerical simulation [4], and X. Wu et al. studied the influence of rectangular elbow on the uniform air supply in an exhaust hood [5]. X. Gao et al. studied and optimized the air-conditioning and air supply system of the spray room [6]. T. Xiao et al. studied the air distribution of uniform air supply in variable cross-sectional duct by CFD simulation [7], and W. Yang et al. analyzed the air supply mechanism of a uniform air supply duct [8]. There is little research on the structure of static pressure chamber in spray room for uniform air supply at present, but an appropriate structure of static pressure chamber can provide the uniformity of air supply and reduce the wind resistance loss. Therefore, this paper studies the structure of static pressure chamber in spray room in order to obtain uniform air supply.

## 2 Research Objects and Methods

### 2.1 Research Objects

Spray room has been widely used in the furniture manufacturing industry, and the vertical push–pull ventilation with uniform air supply on the whole top is mostly adopted [9, 10]. Therefore, the widely used static pressure chamber of spray room in the furniture manufacturing industry was taken as the research object. The size of the spray room is 9 m length  $\times$  7 m width  $\times$  4 m height, and there is a 1 m high static pressure chamber in the upper part of the spray room. The static pressure chamber's structure with uniform air supply in the top of the spray room will be studied in this paper. The top static chamber of the spray room is a cuboid, which can be viewed as a rectangular duct, and the four methods of uniform air supply commonly used in duct are shown in Fig. 1.

Structure (a) and (b) in Fig. 1 can achieve uniform air supply for holes or slots, but the wind speed between hole/slot and hole/slot is difficult to be uniform or even no wind. The uniform air supply on the whole surface of the bottom of the static pressure chamber is needed in the spray room, so structure (a) and structure (b) in Fig. 1 are not suitable for the uniform air supply in the static pressure chamber. Structure (c) and (d) in Fig. 1 can achieve uniform air supply on the whole surface of the bottom of the static pressure chamber, but structure (c) in Fig. 1 needs to set a rectifier device with aperture at the lower part of the static pressure chamber, which is difficult to process, manufacture, and construction. Structure (d) in Fig. 1 can be

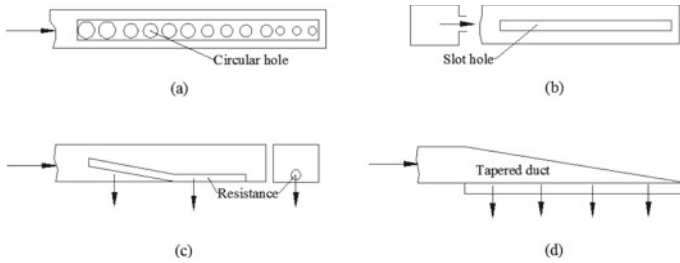


**Fig. 1** Four methods of uniform air supply commonly used in duct

achieved the uniform air supply for the whole bottom surface of the static pressure chamber by improving the roof of the static pressure chamber, and the operation of improving the roof of the static pressure chamber is relatively simple, so structure (d) is the best one for the static pressure chamber with uniform air supply in spray room, which is taken as the basic structure of the static pressure chamber for this research.

### 2.2 Models Establishment

In order to ensure product quality, the efficiency filters should be installed at the bottom of static pressure chamber to filter particulates, which is also helpful for the uniform air supply. In order to study the internal structure of the static pressure chamber with uniform air supply and simplify the numerical simulation analysis, the filter at the bottom of the static pressure chamber is ignored in the model of the static pressure chamber, and the research focuses on the internal structure of the model. The static pressure chamber is located at the top of the spray room, and the size (9 m length  $\times$  7 m width  $\times$  1 m height) of the static pressure chamber commonly used in paint spraying room of furniture manufacturing industry is the basic structure for this research. Based on it, the geometric models of the static pressure chamber with three kinds of roof structures, namely horizontal roof as shown in Fig. 2a, front half horizontal and back half sloping roof as shown in Fig. 2b, and sloping roof as shown in Fig. 2c, are established by CAD, which is used to optimize and determine the roof structure.

The left side of the static pressure chamber in the model is the velocity inlet, and the bottom surface of the static pressure chamber is the pressure outlet, which is shown as Fig. 3. The models are meshed by tetrahedrons with automatic production based on patch-independent algorithm.

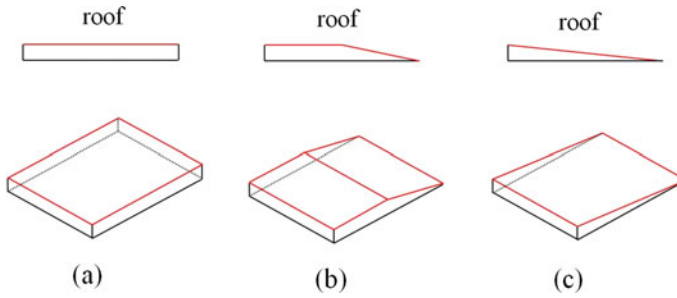


**Fig. 2** Models of static pressure chamber with different roof structures

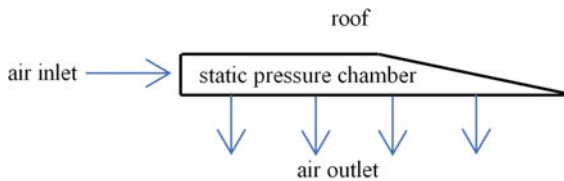


**Fig. 3** Sketch map of air distribution for a static pressure chamber

## 2.3 Calculation Method and Boundary Conditions

### 2.3.1 Calculation Method

In order to simplify the numerical simulation, the filter at the bottom of the static pressure chamber is omitted in the model, and the air in the calculation is assumed to be incompressible. Since the air temperature change is very small, the calculation assumes that the temperature does not change and ignores the heat conduction. The flow was assumed to be a fully developed turbulent flow and the viscosity between fluid molecules was negligible, and only the momentum transfer was considered in this study and heat transfer was ignored. These assumptions coincide with the  $k-\varepsilon$  model, and the standard  $k-\varepsilon$  double-equation model has a reasonable accuracy and has been widely adopted in engineering simulation calculations. The steady incompressible Navier–Stokes equation and the standard  $k-\varepsilon$  double-equation are used in the calculation as the other studies [5, 11, 12].

### 2.3.2 Boundary Conditions and Solution Parameters

The boundary condition of the air outlet, which is the bottom surface of the static pressure model, is set to pressure outflow in the static pressure model. The size of the inlet surface is 9 m length  $\times$  7 m width, so the area of the outlet surface ( $A_{\text{outlet}}$ ) is 63 m<sup>2</sup>. Assume that the velocity of outlet surface ( $v_{\text{outlet}}$ ) is 0.5 m/s commonly used

wind speed in a spray room for the uniform air supply. The boundary condition of the air inlet in the static pressure model is set to velocity inlet. The size of the inlet surface is 7 m width × 1 m height, so the area of the air inlet surface ( $A_{inlet}$ ) is 7 m<sup>2</sup>. According to the law of conservation of air volume, the velocity of inlet surface is 4.5 m/s calculated by Eq. (1).

$$v_{inlet} \times A_{inlet} = v_{outlet} \times A_{outlet} \tag{1}$$

The turbulence intensity ( $I$ ) of the velocity inlet is 3.08% calculated by Eq. (2).

$$I = 0.16Re^{(-1/8)} \tag{2}$$

where Re—Reynolds number, calculated by Eq. (3).

$$Re = \rho \cdot v \cdot d / \eta \tag{3}$$

where

- $\rho$  Gas density, kg/m<sup>3</sup>. The gas density of air is 1.205 kg/m<sup>3</sup> at 20 °C used in this research.
- $v$  Face velocity, m/s. It is 4.5 m/s in this research.
- $d$  Hydraulic diameter, m. It is 1.75 m for the air inlet surface in this research.
- $\eta$  Dynamic viscosity, Pa s. The dynamic viscosity of air is  $1.81 \times 10^{-5}$  Pa s at 20 °C used in this research.

The SIMPLEC algorithm is used in this study as solver, which is a numerical method for solving incompressible flow fields and can be used to solve the Navier–Stokes equation. The boundary conditions and solution parameters used in this paper are shown in Table 1.

**Table 1** Boundary conditions and solution parameters

Boundary conditions and solution parameters	Definition
Inlet boundary type	Velocity inlet
Outlet boundary type	Pressure outlet
Inlet velocity magnitude (m/s)	4.5
Inlet hydraulic diameter (m)	1.75
Inlet turbulence intensity (%)	3.08
Outlet boundary type	Pressure outlet
Solver	Segregated
Viscous model	$k$ -epsilon ( $k$ - $\epsilon$ )
Pressure–velocity coupling	SIMPLEC
Discretization scheme	Second-order upwind
Convergence criterion	$10^{-6}$

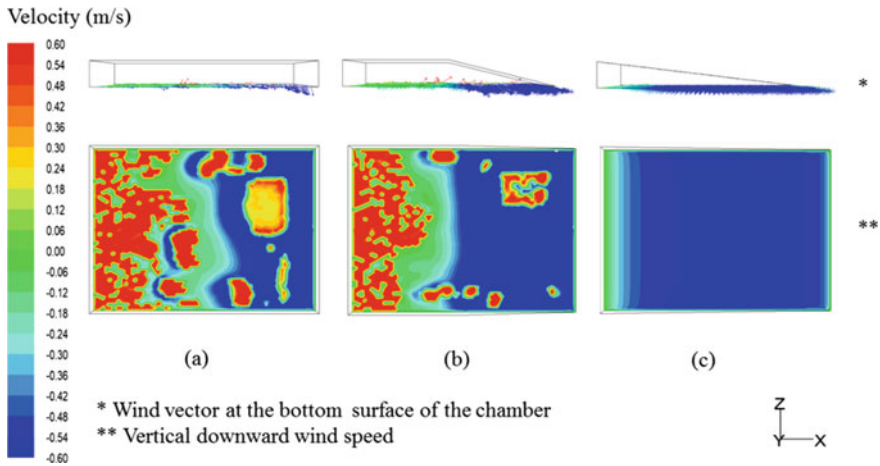


Fig. 4 Wind vector and air distribution for the chamber with different roof structures

### 3 Results

#### 3.1 The Wind Vector and Air Distribution Simulation Results

The wind vector and air distribution simulation results at the bottom surface of the static pressure chamber with different roof structures are shown in Fig. 4.

When the roof of the static pressure chamber is horizontal (as Fig. 4a), there is a large amount of upward wind entering the static pressure chamber at the lower side of the inlet of the chamber. When the back half roof is sloping (as Fig. 4b), the upward airflow decreases, but it still exists. When the whole roof is sloping (as Fig. 4c), there is almost no the upward airflow. It can be seen from Fig. 4 that with the increase of roof inclination, the vertical downward wind speed becomes larger and more uniform, so the whole roof incline is the best structure of the chamber for the uniform air supply.

#### 3.2 The Pressure Distribution Simulation Results

The static and dynamic pressure distribution simulation results at the bottom surface of the static pressure chamber with different roof structures are shown in Fig. 5.

It can be seen from Fig. 5 that with the increase of roof inclination, the dynamic pressure becomes bigger and more uniform, that is why the downward velocity becomes bigger and more uniform.



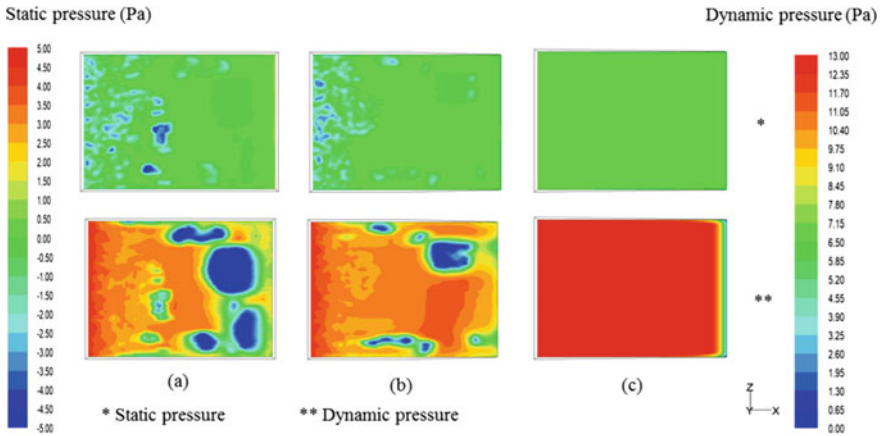


Fig. 5 Pressure distribution for the chamber with different roof structures

As the increase of roof inclination, the upward static pressure is getting smaller and smaller, and this means that more static pressure is converted into dynamic pressure, that is why the dynamic pressure becomes bigger. As the upward negative pressure disappears, the airflow into the static ballast tank is avoided, and the static pressure, dynamic pressure, and airflow are more uniform. The change law of pressure is the same as that of wind speed, and it also explains why the roof is more sloping and the downward wind speed is bigger and more uniform.

### 4 Discussions

The filter at the bottom of the static pressure chamber not only can filter particles, but also has certain resistance. Therefore, it can prevent part of the upward airflow into the static pressure chamber, so the wind speed at the bottom of the chamber is more uniform. It is ignored in this paper in order to study the internal structure of the chamber, but it definitely is used in practice. The optimal structure of the static pressure chamber presented in this paper will have a better performance of air uniform supply with the addition of filter at the bottom.

The optimum structure of static pressure chamber is proposed under the condition of a certain size and a certain wind speed. When the wind speed or the size of static pressure chamber changes, the optimal structure may change. Therefore, it is necessary to study the optimal uniform air supply structure of the static pressure chamber with different sizes and wind speeds in the future, and try to put forward a general rule of eliminating the influence of geometric size and wind speed as in reference [11].

## 5 Conclusions

The sloping roof is helpful to convert the static pressure into dynamic pressure, reduces the pressure loss of the static pressure chamber, and increases the air supply velocity at the bottom surface of the static pressure chamber. When the whole roof is sloping, the air supply at the bottom of the static pressure chamber is the most uniform.

This work was funded by the National Key R&D Program of China (2016YFC0801700) and the basic research funding of China Academy of Safety Science and Technology (2019JBKY04 and 2019JBKY11).

## References

1. Chen J, Zhan J (2016) Hazard protection of spray paint poison in furniture manufacturing enterprises. *Modern Occup Saf* 3:102–105
2. Kim N, Choi WH, Choung SJ et al (2002) Efficient ventilation of VOC spread in a small-scale painting process. *Build Environ* 37(12):1321–1328
3. Chen J (2014) The technology and equipment of hazards protection for spray room in wooden furniture manufacturing enterprises. *Modern Occup Saf* 2:31–33
4. Chen J, Yang B, Liang S et al (2018) Study on the performances of supply air for uniform air supply square hood by numerical simulation. In: Long S, Dhillon B (eds) *Man-machine-environment system engineering*. MMESE 2018. *Lecture Notes in Electrical Engineering*, vol 456. Springer, Singapore
5. Wu X, Liu L, Luo X et al (2018) Study on flow field characteristics of the 90° rectangular elbow in the exhaust hood of a uniform push-pull ventilation device. *Int J Environ Public Health* 15(12):2884–2896
6. Gao X, Li Q (2016) Optimization design and engineering application of air supply system of air conditioning in painting room. *Modern Paint Finish* 19(5):53–55+58
7. Xiao T, Li L, Mei S et al (2016) CFD simulation of air distribution in cross-section duct with air supply. *J Hunan Univ Technol* 30(2):13–20
8. Yang W, Zhang J, Han H (2005) Study on the performances of new model non-adjustment static pressure supply air duct. *J Guangdong Univ Technol* 22(1):110–114
9. Liang S, Chen J, Yang B, Lin M, Liu L, Zhang T (2018) Research on ventilation antivirus technology in a washing board room based on numerical simulation. In: Long S, Dhillon B (eds) *Man-machine-environment system engineering*. MMESE 2017. *Lecture Notes in Electrical Engineering*, vol 456. Springer, Singapore
10. Yang B, Chen J, Liang S, Zhou S, Sun Y, Li Y (2020) Design and application of a ventilation system in a washing board room based on numerical simulation. In: Long S, Dhillon B (eds) *Man-machine-environment system engineering*. MMESE 2019. *Lecture Notes in Electrical Engineering*, vol 576. Springer, Singapore
11. Chen J (2018) Research on the center-line velocity change rule of desktop slot exhaust hood. *Ind Health* 56(4):278–284
12. Chen J, Sun Y, Zhang X, Chen Z, Yang B, Liu W (2020) Study on the upper flange width on grinding worktable and its ergonomics evaluation. In: Long S, Dhillon B (eds) *Man-machine-environment system engineering*. MMESE 2019. *Lecture Notes in Electrical Engineering*, vol 576. Springer, Singapore

# **Research on the Man-Machine Relationship**

# Research on the Effect of Elasticity Distribution of Five-Zone Spring Mattress on Human Supine Position Spine Form



Huaiqiu Zhu, Tianyi Hu, Yuding Zhu, and Ronghui Yuan

**Abstract** Taking zonal spring mattress as the research object, the paper adopted mattress sinking measurement and range method, by evaluation index include the gap of lumbar and back and the sinking ratio of back, studied the effect of elasticity distribution of spring mattress on body lied spine form. The results showed that, the gap of lumbar and back is bigger when the flexibility of hip area of 25 kinds of five-zone spring mattress is bigger and the flexibility of waist area is smaller; the gap of lumbar and back is smaller when the flexibility of hip area and the flexibility of waist area are smaller. When the range of the sinking ratio of back and buttock was 60–100%, the elastic distribution of mattress was good and human spine shape was good. Elasticity distribution of spring mattress was a key factor of effecting body spine form.

**Keywords** Spring mattress · Elastic distribution · Supine position · Spine alignment

## 1 Introduction

One-third of a person's life is spent in bed. Sleep is considered to be the most important of all the ordinary bedroom activities, because it is the key to eliminating fatigue and recovering energy.

The elasticity of each area of the partition spring mattress can be distributed according to the weight of various parts of the body to make the mattress match the body shape of the person as much as possible. According to statistics, only 20% of people have not experienced back pain, and most people's back health problems are caused by prolonged improper posture or movement [1], and incorrect spinal support

---

H. Zhu · T. Hu · R. Yuan  
Zhejiang Light Industrial Products Inspection and Research Institute, 310018 Hangzhou, China

Y. Zhu (✉)  
Zhejiang Agricultural & Forestry University, 310007 Hangzhou, China  
e-mail: 15325665@qq.com

while sitting, working or sleeping often causes or aggravates low back pain. A correct sleeping position should maintain the natural physiological curve of the spine, which is similar to that of an upright position [2]. If this argument is assumed, the human spine will form a straight line while sleeping on the side while maintaining a natural “S” curve of cervical lordosis, thoracic kyphosis, and lumbar lordosis. When sleeping on the back, the thoracic spine and lumbar lordosis are the same as in the upright position, but are slightly smoother due to the longitudinal loss of gravity in the spine.

There have been many researches on the human spine at home and abroad, but there are few studies on the influence of supine posture on the comfort of supine posture in healthy people. Lahm and Lazzo studied 22 subjects with back pain which showed that the stiffness of the sleep system had no significant effect on the subject’s myoelectricity, heart rate, blood pressure, and subjective comfort, but had a greater impact on spinal morphology [3]. Devocht et al. investigated the effects of four mattresses on male subjects using contact surface pressure tests and spinal morphology tests. Studies have shown that the impact of different mattresses on the human body is significantly different, but the results are inconsistent—the mattress with the highest pressure minimizes human spinal deformation [4]. Vincent used intelligent experimental mattresses to study the effects of dynamic supine position spinal support conditions on sleep quality, and discussed the effects of mattress support status on spinal support and sleep quality [5]. Wei Mengmeng et al. measured the supine position spine morphology of three middle-height subjects and explored the effect of changes in the elastic segment of each area of the zonal spring mattress on the spine morphology of the supine position [6]. Yosuke et al. studied the relationship between sleep comfort and sleep posture in 20 subjects on 9 mattresses of different hardness [7].

The human body has a natural curve, and the weight of each part varies greatly. When lying on a mattress of the same hardness, some parts of the human body cannot be fully supported, and the spine will bend. Therefore, this article takes the five-zone spring mattress as the research object and designs the elastic distribution of it, and uses the mattress sink test to measure the effect of the different elastic distribution of the five-zone spring mattress on the human supine position spinal morphology.

## 2 Materials and Methods

### 2.1 Test Subject

The subjects were 12 volunteer students, including 5 men and 7 women, aged 20–30 years. The average weight of these male subjects was 63.5 kg and the average height was 167.6 cm. Female subjects had an average weight of 50.9 kg and an average height of 162.6 cm. The subjects were in good health and were informed of the

experimental process, experimental purpose, and precautions before the experiment. Each subject was uniformly dressed, without a belt, without buttons, and other similar decorations.

## 2.2 Test Method

A spinal morphology sinking measurement system developed by the laboratory was used, and a zonal spring mattress was used as the test object. When the subject lies on a mattress with a benchmark, the spine line can correspond to the straight line formed by the benchmark. At this time, the amount of protrusion of the human body on the mattress before and after the supine position can be measured. Calculate the amount of sinking of each measurement point of the mattress, and draw the spine shape of the human body supine position. By measuring the amount of sinking of the shoulder, back, waist, and buttocks, and the horizontal distance, the waist-back gap is calculated to reflect the spine shape in the supine position of the human body. Waist-back gap [8], that is, the vertical distance from the high point of the waist-back to the low point of the shoulder and hip, as shown in Fig. 1.

In order to quantify the distribution of the amount of mattress sinking when the human body is lying down, by measuring the maximum sinking amount of the back and buttocks, the ratio of the maximum sinking of the back to the buttocks is calculated  $X = b/h$ , where  $b$  is the maximum sinking of the back,  $h$  is the maximum sinking of the buttocks, as shown in Fig. 2.

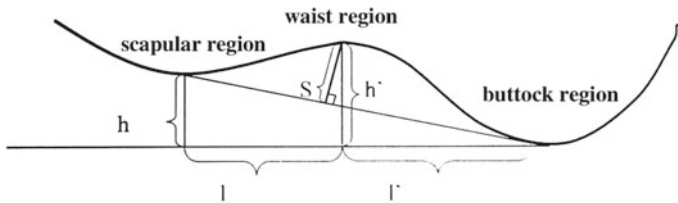


Fig. 1 Waist-back gap schematic diagram

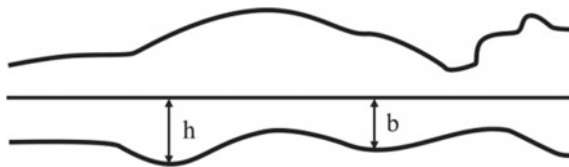


Fig. 2 Maximum sinking of back/buttocks

### 2.3 Test Design

Because the elastic distribution of the five-zone spring mattress is mainly the elastic distribution of the spring layer of the mattress, that is, the elastic distribution of the spring layer, this experiment mainly uses the core layer elasticity (hereinafter referred to as elasticity) of the back, waist, and hip regions that are closely related to spine support as the main factor to design the orthogonal experiment. Taking the elasticity of the back area, the waist area and the hip area as factors take 5 levels for each factor to design orthogonal experiments. The factor levels are shown in Table 1. There are six types of springs ① (1.8 65 6), ② (1.8 65 5), ③ (2.0 65 6), ④ (2.0 65 5), ⑤ (2.2 65 6) and ⑥ (2.2 65 5). The bedding material is a five-zone spring mattress assembled according to the test protocol mattress specifications, which composed of ordinary sponge with a thickness of 3 cm and a density of 20Kg/m<sup>3</sup> and a layer of composite fabric. The type of head and leg springs of the five-zone spring mattress is ④ (2.0 65 5), which due to the large weight of the head and legs, especially the feet, and the small contact area with the mattress while the force increase. Therefore, it is more suitable to choose a spring type with medium hardness. The five types of hardness in the back region, waist region, and buttock region are ① (1.8 65 6) with higher hardness, ② (1.8 65 5) with high hardness, ③ (2.0 65 6) with medium hardness, ⑤ (2.2 65 6) with low hardness, and ⑥ (2.2 65 5) with lower hardness [9]. Because the hardness of the head and leg regions of the 25 test mattresses is the same, only the spring type numbers of the back, waist, and hip regions are used to indicate the type of mattress, such as ①-②-③ type mattresses.

**Table 1** Experimental mattress factor level table

Factor level	A	B	C
	Back elasticity	Waist elasticity	Hip elasticity
1	① (1.8 65 6)	① (1.8 65 6)	① (1.8 65 6)
2	② (1.8 65 5)	② (1.8 65 5)	② (1.8 65 5)
3	③ (2.0 65 6)	③ (2.0 65 6)	③ (2.0 65 6)
4	⑤ (2.2 65 6)	⑤ (2.2 65 6)	⑤ (2.2 65 6)
5	⑥ (2.2 65 5)	⑥ (2.2 65 5)	⑥ (2.2 65 5)

*Note* The horizontal numbers are five kinds of elasticity. The five types of springs represent five kinds of elasticity and the order of ①–⑥ elasticity is from large to small. The size of the back spring module (4 × 15), the size of the waist spring module (3 × 15), and the size of the hip spring module (6 × 15)

### 3 Result and Analysis

#### 3.1 Analysis of Morphological Characteristics of Human Body Supine Position

Spinal support conditions are changed by changes in back elasticity, waist elasticity, and hip elasticity. The measurement of the mattress sinking when the human body is supine can reflect the spine shape of the human body lying on the supine side under different elastic distribution of the spring mattress. Figure 3 shows the human supine position spine curve on 25 mattresses. The statistics of the two evaluation indexes of the waist-back gap and the back-hip sag ratio of 25 five-zone spring mattresses when human body lying on it, as shown in Table 2, are used to reflect the influence of different elastic distributions on the human spine shape.

From the perspective of human bones and muscle structure, the height of the back of the lumbar vertebrae in the supine position is reduced from 40–60 mm in the natural state when standing to about 20–30 mm, which is close to the straight state [10]. In general, the waist-back gap is more comfortable between 20 and 30 mm. If the waist-back gap is too small and the spine is excessively straightened, people will feel tired when lying for a long time; if the waist-back gap is too large, the degree of spine curvature will be too large, and prolonged lying will cause lesions. It can be known from Table 2 that the five-zone spring mattresses with different elastic distributions have a different waist-back gap. Overall, the smaller the elasticity of the mattress, the smaller the waist-back gap; otherwise, the greater the elasticity of

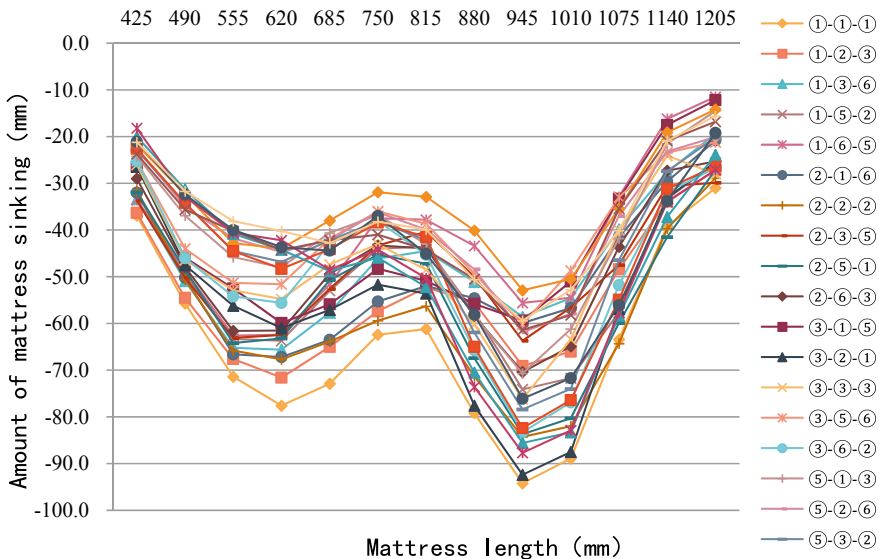


Fig. 3 Human supine spine curve on 25 five-zone spring mattresses



**Table 2** Statistics of spinal morphological characteristics of 25 five-zone spring mattresses

Mattress type	Waist-back gap (mm)		Back-hip sag ratio (%)	
	Mean value	SD ( <i>N</i> = 12)	Mean value	SD ( <i>N</i> = 12)
①-①-①	26.92	6.34	80.3	9.1
②-②-②	23.66	5.28	79.5	15.1
③-③-③	23.53	3.85	75.6	14.7
⑤-⑤-⑤	19.86	1.42	83.5	11.0
⑥-⑥-⑥	19.89	2.87	76.9	10.7
①-②-③	21.75	4.64	99.8	15.3
②-③-⑤	28.47	5.27	109.3	14.9
③-⑤-⑥	24.76	4.73	87.8	12.1
⑤-⑥-①	30.69	4.83	54.4	7.9
⑥-①-②	22.62	3.33	58.9	9.1
①-③-⑥	24.67	4.52	110.8	13.2
②-⑤-①	32.95	4.05	71.9	9.0
③-⑥-②	28.83	4.12	66.9	14.1
⑤-①-③	22.64	4.75	69.5	12.6
⑥-②-⑤	18.91	2.78	81.2	12.2
①-⑤-②	29.42	6.18	86.3	10.5
②-⑥-③	26.05	5.63	90.5	8.9
③-①-⑤	23.47	3.72	94.5	14.8
⑤-②-⑥	18.53	4.61	74.9	11.7
⑥-③-①	23.81	3.79	57.5	10.1
①-⑥-⑤	29.24	4.62	110.1	7.9
②-①-⑥	23.13	5.00	107.3	15.9
③-②-①	26.75	7.86	62.7	8.7
⑤-③-②	25.71	4.96	59.1	12.7
⑥-⑤-③	25.34	3.92	66.8	11.4

the mattress, the greater the waist-back gap. Among the subjects, the waist-back gap of the subjects on the two five-zone spring mattresses of the ②-⑤-① type and ⑤-⑥-① type was greater than 30 mm. The subjects had less than 20 mm of waist-back gap on the four five-zone spring mattresses of the ⑤-②-⑥ type, ⑤-⑤-⑤ type, ⑥-②-⑤ type, ⑥-⑥-⑥ type, and the waist-back gap on the other 19 five-zone spring mattresses is in the range of 20–30 mm. The greater the hip elasticity, the lower the waist elasticity, the larger the waist-back gap; the lower the elasticity of the back and hip regions, the smaller the waist-back gap.

When the elasticity of the back region is greater and the elasticity of the hip region is smaller, that is, the softer the back region and the harder the hip region, the greater the back-hip sag ratio; when the elasticity of the back region is smaller and the

elasticity of the hip region is greater, the smaller the back-hip sag ratio. The back-hip sag ratio of these 25 five-zone spring mattresses is 54.4% minimum and 110.8% maximum. The four types of mattresses ①-③-⑥, ①-⑥-⑤, ②-①-⑥, and ②-③-⑤ are all more than 100%, the elasticity of the back area of which is much greater than that of the hip area, and the back sag is greater than the hip sag. The back-hip sag ratio on the remaining 17 five-zone spring mattresses is in the range of 60–100%. The elasticity of the back region of these five-zone spring mattresses is not much different from the elasticity of the hip region, that is, the same elasticity or slightly larger or smaller.

It can be seen that the spine curves of human supine on different mattresses can be divided into three categories: when the back-to-hip sag ratio is greater than 100%, the human spine curve is inclined to the back, and such supine positions can be called “chest supine positions.” When the back-to-hip sag ratio is less than 60%, the human spine is completely tilted toward the buttocks. Such a supine position can be referred to as a “butt supine position I.” When the back-to-hip sag ratio is in the range of 60–100%, the curve of the supine spine of the human body is similar to the curve of the spine when standing. Such supine position can be called “hip type supine position II” and people could have a better sleep on these elastically distributed mattresses below. As shown in Fig. 4, the results of this study are consistent with the results of Yosuke’s research on the relationship between sleep comfort and sleep posture.

When the human body is in the side-lying position, the human spine appears as a straight line on a mattress with a reasonably elastic distribution, and the human spine appears as a curve on a mattress with an unreasonably elastic distribution. When the elasticity of the back region is greater, the elasticity of the waist region is smaller, that is, the softer the back region and the harder the waist region, the smoother the curve of the human spine. When the elasticity of the back region is smaller and the waist region is larger, the spine line of the human body is more curved. When the elasticity of the back region is the same, the elasticity of the waist region has a greater influence on the human lateral lying spine morphology. The waist area has low elasticity and can play a good role in supporting the spine. If the lumbar region is elastic, the spine cannot be supported well, and the lumbar spine will bend down.

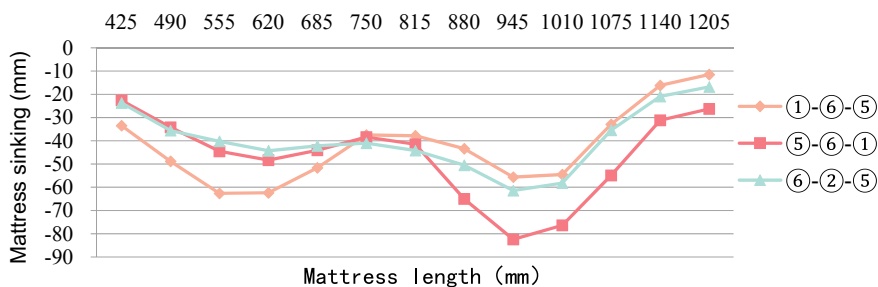


Fig. 4 Three types of supine posture human spine curve

**Table 3** Statistics of the range of factors affecting the spine morphology of the human supine position

Performance indicators	Range	Factors		
		A	B	C
		Back area elasticity	Waist area elasticity	Hip area elasticity
Waist-back gap	R	3.26	4.74	6.03
	Primary and secondary factors	C > B > A		
Back-hip sag ratio	R	2.88	29.20	30.36
	Primary and secondary factors	C > B > A		

### 3.2 Analysis of the Range of Factors Affecting the Spine Morphology of Human Supine Position

In order to examine the degree of influence of back elasticity, waist elasticity, and hip elasticity on various evaluation indicators, a range analysis method was used to calculate the range R of these three factors below, as shown in Table 3.

The larger the range R value, the greater the influence of this factor on the evaluation index value. As can be seen from Table 3, taking the waist-back gap and back-to-hip sag ratio as indicators, the factors affecting the order of primary and secondary are C hip area elasticity > A back area elasticity > B waist area elasticity, and hip area elasticity has the greatest influence.

## 4 Conclusion

To sum up, the evaluation index of waist-back gap, back-hip sag ratio of the supine spine shape, and lateral spinal curve slope can better reflect the spinal support performance of different elastic distribution of zonal spring mattresses. The elastic distribution of the spring mattress is an important factor affecting the spine shape of the human supine position. The greater the hip elasticity, the lower the waist elasticity, the larger the waist-back gap; the lower the elasticity of the back and hip regions, the smaller the waist-back gap. When the elasticity of the back region is greater and the elasticity of the hip region is smaller, that is, the softer the back region and the harder the hip region, the greater the back-hip sag ratio. When the elasticity of the back region is greater, the elasticity of the waist region is smaller, that is, the softer the back region and the harder the waist region, the smoother the curve of the human spine, vice versa. The elasticity of the hip region has the greatest effect on the

waist-back gap and the back-hip sag ratio when supine, and the elasticity of the waist region has the greatest effect on the lateral spine curve. The results of this study can provide reference for the design of zonal spring mattress.

## References

1. Hayne CR (1984) Ergonomics and back pain. *Physiotherapy* 70(1):9–13
2. Adams MA, Hutton WC (1985) The effect of posture on the lumbar spine. *J Bone Joint Surg Br* 67(4):625–629
3. Lahm R, Iaizzo PA (2002) Physiologic responses during rest on a sleep system at varied degrees of firmness in a normal population. *Ergonomics* 45(11):798–815
4. DeVocht JW et al (2006) Biomechanical evaluation of four different mattresses. *Appl Ergon* 31:297–304
5. Verhaert V (2011) Ergonomic analysis of integrated bed measurements: towards smart sleep systems. Catholic University of Louvain
6. Mengmeng W, Liming S (2019) Effect of elastic distribution of mattress core layer on the shape of supine spine. *Furniture* 40(4):98–102
7. Horiba Y, Kamijo M, Inui S et al (2010) Study on relation between sleeping comfort and sleeping posture. In: International conference on Kansei engineering and emotion research
8. Lijuan Z (2010) Research on the optimal design of the core layer of the partitioned pocket spring mattress. Nanjing Forestry University, Nanjing
9. Zhu Y (2013) Study on the effects of geometric and physical characteristics of zonal spring mattress on the spine morphology and comfort of human supine position. Nanjing Forestry University, Nanjing
10. Liming S (2010) *Ergonomics: people furniture interior*. China Forestry Press, Beijing

# Attentional Allocation with Low-Limb Assisted Exoskeleton During Sit-to-Stand, Stand-to-Sit, and Walking



Jing Qiu, Lanlan Xu, and Jinlei Wang

**Abstract** More and more paraplegics and rehabilitation agencies use lower-limb assisted exoskeleton to improve functional walking ability and to increase neuromuscular plasticity. However, users need to allocate their attention to the lower-limb assisted exoskeleton when they wear it. This study aims to analysis how users in the lower-limb assisted exoskeleton allocate their attention in sit-to-stand, stand-to-sit, and walking. Nine participants performed three kinds of tasks (sit-to-stand, stand-to-sit, and walking of four meters) to acquire data of eye movements. The attentional allocation is almost no statistically significant difference between sit-to-stand and stand-to-sit. Walking has statistically significant differences of attentional allocation in many attentional areas. During walking, participants paid more attention to the areas strongly related with manipulation and pay less attention to positions of orienting participants than the other two tasks. Participants select different patterns of eye movements to the specific task context. The results provide effective suggestions for developers and designers who want to integral information of eye movements into control system.

**Keywords** Attentional allocation · Lower-limb assisted exoskeleton · Sit-to-stand · Stand-to-sit · Walking

## 1 Introduction

Eye movements are critical and proactive for humans to gather spatial and egocentric information to plan the motor response, to reorient trunk, to enhance the steering synergy, to initiate body movement of synergy while walking [1–3]. Eye movements can be used to better understand the performance of the operators by identifying links with eye movements. Eye movements such as fixation, saccade, blink, pupil

---

J. Qiu (✉) · L. Xu · J. Wang

University of Electronic Science and Technology of China, Chengdu, China

e-mail: [qiuqing@uestc.edu.cn](mailto:qiuqing@uestc.edu.cn)

diameter are used to probe their attentional focus and trajectory [4], memory accuracy [5], visual search strategies [6, 7], hand–eye coordination [8], and the individual’s actions [4] during operation. However, the literature hardly concerns how users in the lower-limb assisted exoskeleton allocate their attention in activities of daily living.

The robotic exoskeleton in this study is a lower-limb assisted exoskeleton (Fig. 1) that is to assist patients with nervous and muscular diseases to walk and recover. It plays a positive role in gait assistance and rehabilitation for the patients with muscular impairments or neurologic injury and reduces labor costs and therapist effort for them [9]. The paraplegic wearing it can walk like normal people by reducing their net muscle moment to compensate for the added robotic torque [10], which is important to live an independent life for paraplegic patients. Therefore, more and more paraplegics and rehabilitation agencies use the lower-limb assisted exoskeleton to improve functional walking ability and to increase neuromuscular plasticity. The lower-limb assisted exoskeleton should be necessary for paraplegics’ life in the near future. However, it is not easy to control the lower-limb assisted exoskeleton and to keep the human-exoskeleton system balance especially for a novice. Using the lower-limb assisted exoskeleton not only needs the assistance of others such as crutches, but also demands the coordination of other parts of body such as the upper limb, eyes.



**Fig. 1** Participants wearing the lower-limb assisted exoskeleton and the mobile eye tracker

The eye tracking as an important tool is applied to research many human activities that are static [11] or dynamic [12, 13]. Before taking an action, human selectively pays attention to targets and flexibly shift gaze to acquire the passive and active information that serves to allocate resource of working memory and make decision [3, 8]. The aim is to study how users in the lower-limb assisted exoskeleton allocate their attention in activities of daily living and provide effective suggestions for developers and designers who want to integral information of eye movements into control system.

## 2 Method

### 2.1 Participants

We recruited a total of eleven voluntary participants aged 22–34 years with a mean age of 24.44 (SD: 2.81) years. They are all healthy and flexible. All participants in the lower-limb assisted exoskeleton must be able to do actions such as stand-to-sit without eyeglasses. Because if the wearable eye tracker is worn before the participants' eyeglasses, it will slide up and down easily before eyes, which will cause a calibration error. No one used eyeglasses or contact lenses to gain data in the experiment.

Participants did not know the purpose of the study, but they were told that their eye movements were recorded by the wearable eye tracker in doing actions with the lower-limb assisted exoskeleton. Two participants were excluded from the analysis due to the loss of data after buffering of communication in real time. The study was approved by the Sichuan Provincial Rehabilitation Hospital Review Board, and each participant consented before the starting of the study.

### 2.2 Experimental Equipment

Gaza data were acquired with a Tobii Pro Glasses 2 system (Fig. 1), which includes a head unit (a wearable eye tracker) capturing the participants' gaze, a recording unit recording and saving the gaze data to one SD card, a tablet running the controller software and managing the test time. The wearable eye-tracking tool has 4 eye cameras, gaze sampling frequency of 50 Hz, scene camera resolution of  $1920 \times 1080$  pixels.

The lower-limb assisted exoskeleton (Fig. 1) mainly consists of the main controller running control procedure on the back, four-node controllers distributed in hips and knees, two columnar legs of variable length paralleling lateral surfaces of the participants' legs, many plantar sensors fixed in the soles, two adjustable crutches with two control keyboards interacting with the main controller wirelessly to assist the

balance human-exoskeleton system. The interfaces between the lower-limb assisted exoskeleton and the participant's body are: two foot bindings, two bands tied to the front protection pad to constraint the calf, two bands tied to the back protection pad to constraint the thigh, two buckled waist belts limiting the upper body in it.

### **2.3 Procedure**

Prior to the start of the experiment, we asked participants to read and sign consent forms. Then they tried on the lower-limb assisted exoskeleton to adjust the length of leg. We needed to ensure the size of the lower-limb assisted exoskeleton fit each participants' height to complete three kinds of tasks: sit-to-stand, stand-to-sit, walking of four meters. However, if the participant was a novice, he would spend at least half an hour on training before the testing. To collect accurate gaze data, the researcher must choose appropriate nose pad and calibrate each participant individually. Each participant wearing the head unit was asked to focus on the center of the calibration card which was held at a distance from 0.8 m to 1.2 m from the participants' eyes. The head unit was connected to the recording unit placed on the buckled waist belt via a high-definition multimedia interface cable.

The tasks are given to each participant at random. During sit-to-stand, participants wearing the experimental devices sited on cheers and handled the crutches naturally. When they listened to the researcher's order, they would press two keys on the crutches at the same time to stand up and relay on the assistance of crutches to keep human-exoskeleton system balance. Meanwhile, the researcher marked events on the tablet. Likewise, during stand-to-sit participants must stand naturally and keep human-exoskeleton system balance well before sitting down. And then they pressed two keys on the crutches simultaneously to sit down. However, each participant wearing the experimental devices pressed the button on the right crutch for every step and walked 4 m straightly. The events such as one gait cycle in walking were recorded on the controller software. And a researcher followed the participants to ensure their safety throughout the whole experiment.

### **2.4 Data Processing**

Video clips between the logged live events were exported in the Tobii Pro Lab software and then parsed into video frames in MATLAB. The number of video frames was so large that we had to select them combining with video clips. The number of video frames was manually classified by predetermined areas (Fig. 2). The results counted in Excel were analyzed further in SPSS and MATLAB. The main effects of tasks (sit-to-stand, stand-to-sit, walking of four meters) on the collected or computed variables are measured in the one-way repeated measures ANOVAs.



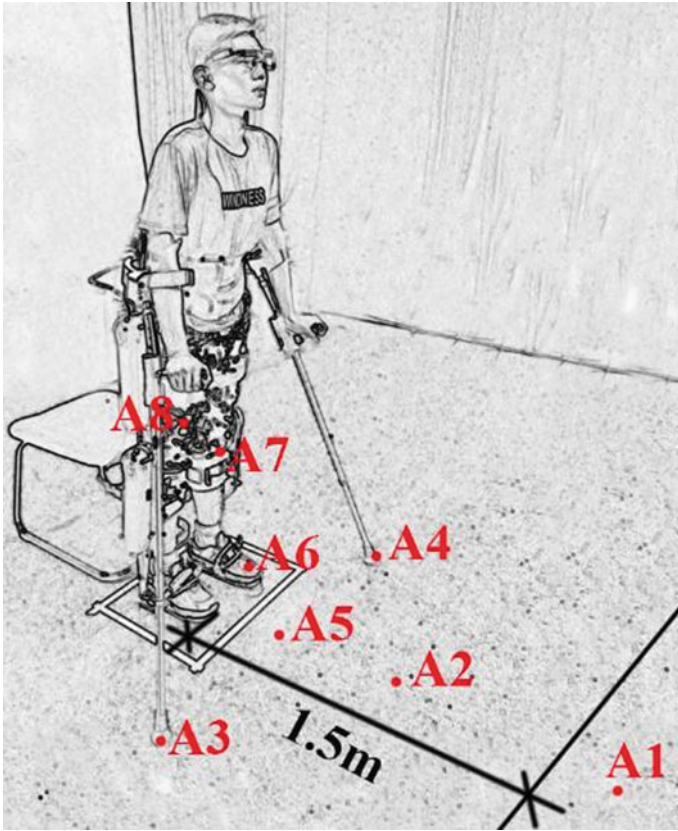


**Fig. 2** Attentional areas: 1.5 m away from the feet (A1), front (A2), the right crutch (A3), the left crutch (A4), the area between two crutches (A5), feet (A6), knee (A7), thigh (A8)

### 3 Results

#### 3.1 Attentional Allocation

The attentional allocation in this study is expressed as the ratio of the number of video frames classified as some area to the total number of the video frames of one task. In Fig. 2, the attentional areas are the distribution of participants' concern in doing tasks. For example, A1, A2 that are relative to the position of feet constantly vary with it and they are weakly linked with operation. And A5 relative to A3, A4 varies with crutches' position in real time and it usually is the instant target for the next step. The participants orient their instant positions by the positions of A6, A7, A8 and prepare to make decision for the next step and to control balance of human-exoskeleton system.

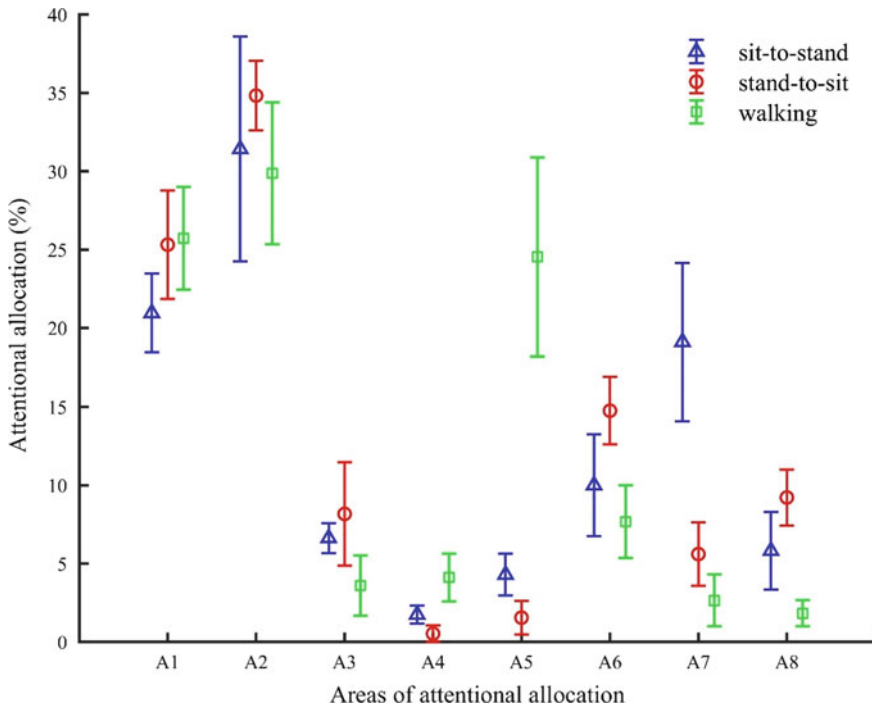


**Fig. 3** Attentional allocation in the eight areas. Means ( $\pm$ SE) in percent for the attentional allocation to the eight attentional areas in tasks

Figure 3 shows the means of attentional allocation with the standard error contour of the collected variables in three tasks. Analysis with one-way repeated measures ANOVAs shows that A5 ( $p = 0.034$ ), A6 ( $p = 0.011$ ), A7 ( $p = 0.009$ ), A8 ( $p < 0.001$ ) have significant differences, while the other attentional areas have no significant difference. The results of pairwise comparisons between three tasks in A5 show that the attentional allocation to A5 during walking is the more than the two other tasks (walking > sit-to-stand,  $p = 0.019$ ; walking > stand-to-sit,  $p = 0.009$ ). Moreover, the results of pairwise comparisons between three tasks in A6 show that the attentional allocation to A6 during stand-to-sit is more than the two other tasks (stand-to-sit > walking,  $p = 0.004$ ). The results of pairwise comparisons between three tasks in A7 also show that the attentional allocation to A7 during sit-to-stand is the more than the two tasks (sit-to-stand > sit-to-stand,  $p = 0.043$ ; walking > walking,  $p = 0.020$ ). Eventually, the results of pairwise comparisons between three tasks in A8 also show that the attentional allocation to A8 during stand-to-sit is the more than the two other tasks (stand-to-sit > walking,  $p = 0.010$ ). The ungiven results of pairwise comparisons between tasks in A5, A6, A7, A8 indicate no significant difference.

## 4 Discussion

From the results of attentional allocation, the only statistically significant difference between stand-to-sit and sit-to-stand of attentional allocation is found in A7, and there might be two reasons: in the initial phase of sit-to-stand participants are easier to see A7 than A6, A8; during sit-to-stand participants mainly orient their instant positions by A7. However, during sit-to-stand participants obviously pay more attention to A4, A5, A7 than during stand-to-sit and pay less attention to A1, A2, A3, A6, A8 than during stand-to-sit. They have more attentional resources to A1, A2 weakly relative to manipulation during stand-to-sit, which indicates that sit-to-stand is more difficult than stand-to sit. The walking has statistically significant differences of attentional allocation in many attentional areas compared to sit-to-stand, stand-to-sit. Participants use top-down steering synergy [14] of human-exoskeleton to complete walking while the use bottom-up control strategy to complete sit-to-stand and stand-to-sit, so they pay the most attentional allocation to the area (A1) weakly related with manipulation and the instant target (A5) for next step [2, 8] among the three tasks. Meanwhile, A6, A7, A8 that are positions of orienting participants' instant positions during walking are given the least attentional allocation in three tasks. To summarize the results of attentional allocation, after participants listened to the researcher's order, they needed to acquire relative information and plan for next step, move crutches and adjust upper body to control the human-exoskeleton balance before pressing control buttons on the crutches. Participants select different patterns of eye movements to specific task context, which is similar to the conclusion from [3].

The results of saccade proportion showed that the largest saccade proportion is found in sit-to-stand and the smallest saccade proportion is found in walking, which proved that participants needed more visual information and took more efforts to complete stand-to-sit, and that the walking is easier than the two other tasks. Furthermore, the results of degree of task difficulty are consistent with feedback from participants after experiments.

## 5 Conclusions

This study aims to analysis how users in the lower-limb assisted exoskeleton allocate their attention in activities of daily living. The results show that attentional allocation is almost no statistically significant difference between sit-to-stand and stand-to-sit except attentional allocation to knee. However, walking has statistically significant differences of attentional allocation in many attentional areas compared to sit-to-stand, stand-to-sit. Moreover, participants paid more attention to the areas (A4, A5) strongly related with manipulation during walking than the other two tasks and pay less attention to positions (A6, A7, A8) of orienting participants than the other two tasks. In conclusion, participants select different patterns of eye movements

to specific task context. The results of saccade proportion and the feedback from participants after experiment showed that degree of task difficulty is: sit-to-stand > stand-to-sit > walking.

There are some limitations related to the current study. First, the ground of laboratory is blue with white and deep blue spots and reflects light highly so that the eye-tracking heat map of areas of interesting could not be obtained. Second, only nine participants are all male and the students of the University of Electronic Science and Technology of China. They also were forced to remove their corrective glasses due to calibration precision in time. Third, the expertise was not considered as one variable that is an import factor of eye movement. Therefore, we suggest that future studies select proper environments, use more participants to acquire data of eye movements, examine the expertise of participants before experiments. Despite these limitations, the results of the current study develop the knowledge of attentional allocation during using exoskeleton and fill the gap in the region. This study also provides useful suggestions for developers and designers who want to integral information of eye movement into control system.

The study was approved by the Logistics Department for the Civilian Ethics Committee of the University of Electronic Science and Technology of China. All subjects who participated in the experiment were provided with and signed an informed consent form. All relevant ethical safeguards have been met with regard to subject protection.

## References

1. Pradeep Ambati VN et al (2013) Constraining eye movement when redirecting walking trajectories alters turning control in healthy young adults. *Exp Brain Res* 226(4):549–556
2. Land MF, Furneaux S (1997) The knowledge base of the oculomotor system. *Philos Trans R Soc Lond* 352(1358):1231–1239
3. Nascimbeni A et al (2015) Gait attentional load at different walking speeds. *Gait Posture* 41(1):304–306
4. Jarodzka H et al (2010) In the eyes of the beholder: How experts and novices interpret dynamic stimuli. *Learn Instr* 20(2):146–154
5. Blavier A, Nyssen AS (2009) How eye movements and expertise can explain memory of visual items of central or marginal interest. *J Vis*
6. Eivazi S et al (2017) Optimal eye movement strategies: a comparison of neurosurgeons gaze patterns when using a surgical microscope. *Acta Neurochir* 159(6):959–966
7. Najar AS, Mitrovic A, Neshatian K (2014) Utilizing eye tracking to improve learning from examples, vol 8514, pp 410–418
8. Jonikaitis D, Deubel H (2011) Independent allocation of attention to eye and hand targets in coordinated eye-hand movements. *Psychol Sci* 22(3):339–347
9. Dollar AM, Herr H (2008) Lower extremity exoskeletons and active orthoses: challenges and state-of-the-art. *IEEE Trans Rob* 24(1):144–158
10. Kao P-C, Lewis CL, Ferris DP (2010) Invariant ankle moment patterns when walking with and without a robotic ankle exoskeleton. *J Biomech* 43(2):203–209
11. Francuz P et al (2018) Eye movement correlates of expertise in visual arts. *Front Human Neurosci* 12:87

12. Bulling A et al (2011) Eye movement analysis for activity recognition using electrooculography. *IEEE Trans Pattern Anal Mach Intell* 33(4):741–753
13. Martell SG, Vickers JN (2004) Gaze characteristics of elite and near-elite athletes in ice hockey defensive tactics. *Hum Mov Sci* 22(6):689–712
14. Ambati VNP et al (2013) Constraining eye movement when redirecting walking trajectories alters turning control in healthy young adults. *Exp Brain Res* 226(4):549–556

# The Influence of Mattress Material on Sleeping Comfort of Different Age



Jianjun Hou and Yuchun Zhang

**Abstract** This paper studied the relationship between the characteristic of mattress materials and sleeping comfort with supine and lateral sleeping of different age groups. The test adopted the pressure distribution system, subjective evaluation and the subjective and objective analysis of correlation on ergonomics methods. The results showed that, as the subjects' age increasing, the subjects' sensitivity of mattress materials increased and had partiality for harder material. The elder subjects had the highest sensitivity on different mattress materials. The young and middle-aged subjects had high evaluation on memory foam, and latex mattress in supine and lateral position. The young-elder subjects had higher evaluation on memory foam, and coir mattress in supine and lateral position. And the elder subjects preferred coir and cotton mattress in supine position and preferred memory foam and coir mattress in lateral position. The subjects lay on back preferred softer material than subjects lay on side.

**Keywords** Material of mattress · Different age groups · Supine and lateral position · Subjective and objective evaluation

## 1 Introduction

With the development of technology and continuous appearance of new materials, the kinds of mattress material on the market are increasing. There are many mattress materials from the traditional cotton, coir, sponge, to modern technology manufacture partition spring, latex, memory foam, as well as the latest trends in the water mattress and air mattress, etc. The diversification of mattress material brings consumers different choices and experience, but what kind of mattress for different age people and how to choose your own mattress become consumers' problems.

In recent years, along with the development of ergonomics, some domestic and foreign researchers studied on the mattress materials. Lee and Park [1] who used

---

J. Hou (✉) · Y. Zhang  
College of Art and Design, Nanjing Institute of Technology, 211167 Jiangsu, China  
e-mail: [178385883@qq.com](mailto:178385883@qq.com)

© The Editor(s) (if applicable) and The Author(s), under exclusive license to Springer Nature Singapore Pte Ltd. 2021  
S. Long and B. S. Dhillon (eds.), *Man-Machine-Environment System Engineering*, Lecture Notes in Electrical Engineering 645,  
[https://doi.org/10.1007/978-981-15-6978-4\\_71](https://doi.org/10.1007/978-981-15-6978-4_71)

electroencephalograph (EEG), electro-oculogram (EOG), electromyogram (EMG) and electrocardiogram (ECG) methods found that the mattress materials not only directly affected the overall softness and flexibility but also made the difference of physical body consumption. Kink [2] researched the different between spring and coir mattresses and found that the subjects' shallow sleep and wakefulness cycle were shorter when used spring mattress. Buckle [3] selected six different mattresses and analyzed the sleeping comfort of the youth and elderly. He found that the elder subjects had more sensitive and easier distinction than youth subjects. Bader [4] studied the influence of mattress hardness on sleeping comfort. They found that hard beds were generally better than soft beds. The researchers come from Sun Yat-Sen University [5] studied the effect of spring mattress, plank bed and foam mattress on subjects' sleeping quality. They found that the subjects used spring mattress which support force was evenly distributed had better sleeping quality than plank bed and foam mattress. In China, the studies of mattress concentrated in 18 to 30 years old healthy subjects and materials of mattress were mostly spring and cotton.

Through the above studies at home and abroad, the researches of mattress materials are still at the beginning stage. The researches lacked of systematicness and had less reference to the users. The elder users who have more sensitive and demanding were ignored in the studies. And the research performance of the elder mattress is almost empty in China.

This paper studied the relationship between the influences of mattress materials on sleeping comfort of different age groups. The test used the ergonomics methods of pressure distribution system, subjective evaluation and the subjective and objective analysis of correlation. This research wants to provide a theoretical basis for different age users to choose the right mattress materials.

## 2 Materials and Methods

### 2.1 Participants

According to World Health Organization criteria for the classification of age (the young less than 44 years old, the middle-age between 45 and 59 years old, the young-elder between 60 and 74 years old, the elder over 75 years old), the information of subjects shown in Table 1.

### 2.2 Experimental Material

This paper selected ① spring, ② cotton, ③ coir, ④ foam, ⑤ latex, ⑥ memory foam, ⑦ waterbed and ⑧ airbed for experimental materials. The information of mattress is shown in Table 2.

**Table 1** Information of subjects

Participant information	Young subject		Middle-age subject			Young-elder subject			Elder subject	
	28	22	52	49	48	62	64	70	85	
Age	28	22	52	49	48	62	64	70	85	
Sex	M	M	F	M	F	M	F	M	F	
Height (cm)	177	172	161	173	163	175	160	175	163	
Weight (kg)	79	87	58	76	57	57	55	72	50	



**Table 2** Information of experimental mattress

Experimental Mattress	Mattress Performance
① Spring Mattress	Thickness of 200 mm
② Cotton Mattress	Thickness of 40 mm
③ Coir Mattress	Thickness of 40 mm coir, compound bedspread <sup>a</sup>
④ Foam Mattress	Thickness of 40 mm, density of 25 kg/m <sup>3</sup> , compound bedspread
⑤ Latex Mattress	Thickness of 40 mm, density of 65 kg/m <sup>3</sup> , compound bedspread
⑥ Memory Mattress	Thickness of 40 mm, compound bedspread
⑦ Waterbed	Thickness of 150 mm, strip structure waterbed, material of PVC
⑧ Airbed	Thickness of 220 mm, honeycomb structure airbed, material of PVC

<sup>a</sup>Compound bedspread: cotton bed sheet + 25 mm polyester cotton + 30 mm foam + non-woven fabrics

### 2.3 Experimental Method

The pressure distribution was measured and recorded using a Tekscan body pressure measurement system (BPMS). Peak pressure and average pressure were calculated based on recorded pressure distribution data. Peak pressure is the maximum pressure on mattress. Average pressure is the mean value of all pressures on mattress.

The pressure-sensing mat placed on the subjects' whole body and experimental mattress. When pressure value was stable, the test recorded for 30 min, each experiment repeated 3 times.

After pressure distribution, the subjects did the subjective evaluation which through subjective status and evaluation of each part, as shown in Table 3.

**Table 3** Standards of subjective evaluation

Part of comfort	Score						
	+3	+2	+1	0	-1	-2	-3
The comfort of back, arm, waist, leg and overall	Very comfort	Comfort	General	Slight pain	Little pain	Pain	Very pain

### 3 Results and Analysis

#### 3.1 Body Pressure Distribution

We dealt with the experiment data, results as shown in Table 4. We put average pressure and average pressure gradient of different age subjects into a chart to compare, as shown in Fig. 1.

When the subjects lying in supine position, the average pressure and peak pressure of young, middle-age and young-elder subjects were lower in airbed, spring and memory foam mattress. The elder subjects' pressure was lower on memory foam, coir mattress and airbed. All subjects' pressure was higher on waterbed and cotton mattress.

When the subjects lying in lateral position, the average pressure and peak pressure of middle-age and the young-elder subjects were lower on airbed, foam and memory foam mattress. The elder subjects' pressure was lower on spring, foam and memory foam mattress, and pressure was higher on coir and cotton.

When the subjects lying in supine or lateral position, the younger subjects' pressure gradient had smaller volatility on mattresses except airbed and waterbed. The pressure gradient of the middle-aged and young-elderly subjects had the same trend, but had greater diversity among different mattresses. The elder subjects' pressure gradient had the greatest diversity among peoples of all ages.

As the pressure gradient value is the measurement of the pressure change in each direction, the value is smaller, the body feels more comfortable. On the contrary, the pressure gradient value is higher, indicating that the difference of mattress is more obvious.

By comparison, it was found that subjects' peak pressure, average pressure, peak pressure gradient, average pressure gradient and contact area when lying in lateral position was greater than supine pressure values.

#### 3.2 Subjective Evaluation

This paper recorded the subjects' subjective evaluation about the body parts comfort with different mattress materials in supine and lateral position, the overall evaluation as shown in Fig. 2.

As shown in Fig. 2, the young and middle-age subjects' overall evaluation was higher on memory foam and latex mattresses. The young-elder subjects preferred the memory foam and coir mattresses. When the elder subjects lying on coir and cotton mattresses, the overall evaluation was higher in supine position, but the arm evaluation was lower in lateral position. It can be found that with increasing age, subjects inclined to the more rigid material.

The younger subjects had higher evaluation on waterbed and airbed, but another age subjects thought them comfortless. When used waterbed and airbed for long

**Table 4** Body pressure distribution of different age subjects

		Material of mattress															
		Supine position					Lateral position										
		①	②	③	④	⑤	⑥	⑦	⑧	①	②	③	④	⑤	⑥	⑦	⑧
Young	I	5.2	18.4	8.6	5.9	6.6	5.0	9.0	3.1	6.5	18.3	9.1	6.9	8.4	7.8	13.5	6.5
	II	1.4	2.7	2.1	1.5	1.6	1.6	1.8	1.2	2.1	3.7	3.5	2.2	2.4	2.1	2.2	1.9
	III	1.16	1.6	1.2	1.46	1.23	1.01	2.46	1.71	2.7	2.68	1.77	2.06	1.61	1.8	1.58	2.15
	IV	0.11	0.17	0.13	0.16	0.11	0.07	0.21	0.15	0.23	0.26	0.15	0.21	0.21	0.28	0.18	0.24
	V	0.38	0.20	0.28	0.34	0.31	0.35	0.46	0.39	0.31	0.16	0.23	0.29	0.24	0.27	0.37	0.33
Middle-age	I	4.8	18.0	8.1	5.0	5.9	5.0	10.2	4.8	8.4	15.5	9.8	5.5	7.3	6.8	9.1	9.0
	II	1.6	2.6	1.8	1.6	1.6	1.5	2.3	1.5	2.3	3.2	2.5	2.1	2.2	2.2	1.9	1.7
	III	2.6	1.16	1.46	1.52	1.27	1.26	3.38	1.55	2.16	1.23	2.5	1.79	1.86	1.55	2.7	1.95
	IV	0.25	0.07	0.11	0.13	0.09	0.06	0.23	0.13	0.15	0.09	0.13	0.18	0.12	0.07	0.24	0.17
	V	0.31	0.20	0.29	0.33	0.31	0.33	0.34	0.40	0.31	0.18	0.23	0.28	0.25	0.26	0.31	0.37
Young-elder	I	6.4	12.8	6.1	6.8	5.1	5.5	13.7	4.8	8.1	17.0	9.5	7.4	6.5	7.0	15.4	7.9
	II	1.7	3.3	2.0	1.8	1.7	1.7	2.4	1.5	2.4	3.8	2.8	2.3	2.6	2.3	2.3	1.9
	III	2.55	0.72	1.93	2.1	1.31	0.76	3.87	1.06	2.36	1.95	2.7	2.1	4.35	1.77	3.6	6.0
	IV	0.26	0.06	0.2	0.2	0.12	0.06	0.29	0.11	0.26	0.21	0.31	0.33	0.39	0.19	0.3	0.41
	V	0.36	0.22	0.29	0.33	0.33	0.35	0.48	0.43	0.31	0.17	0.23	0.29	0.26	0.29	0.37	0.35
Elder	I	4.7	16.3	4.1	6.6	4.5	3.7	12.7	3.7	5.2	16	10.2	7.0	8.3	7.4	11.6	8.6
	II	1.5	2.6	1.4	1.8	1.4	1.2	2.9	1.3	1.7	2.3	2.0	1.9	1.9	1.7	1.8	1.5
	III	1.09	3.35	2.08	1.44	2.4	1.03	6.47	1.05	2.34	1.89	1.25	1.82	3.7	1.53	6.0	7.0
	IV	0.14	0.21	0.16	0.09	0.15	0.09	0.69	0.12	0.18	0.22	0.08	0.11	0.29	0.11	0.77	0.61

(continued)

**Table 4** (continued)

Material of mattress		Material of mattress														
Supine position		Lateral position														
	①	②	③	④	⑤	⑥	⑦	⑧								
V	0.30	0.14	0.22	0.27	0.26	0.27	0.39	0.30	0.28	0.17	0.21	0.23	0.23	0.24	0.33	0.27

*Note 1:* Peak pressure/KPa, *II:* Average pressure/KPa, *III:* Peak pressure gradient/KPa·cm<sup>-1</sup>, *IV:* Average pressure gradient/KPa·cm<sup>-1</sup>, *V:* Contact area/cm<sup>2</sup>. ① Spring, ② Cotton, ③ Coir, ④ Foam, ⑤ Latex, ⑥ Memory Foam, ⑦ Waterbed, ⑧ Airbed

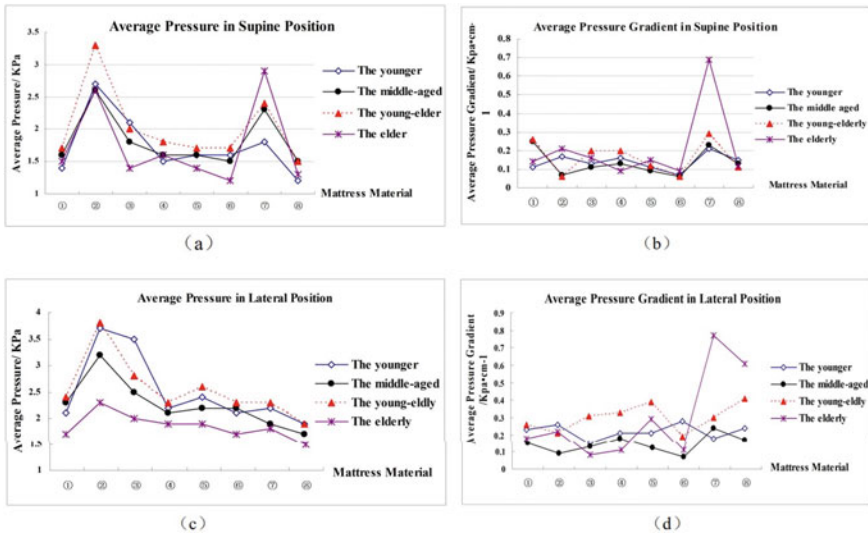


Fig. 1 Average pressure and average gradient of different age subjects

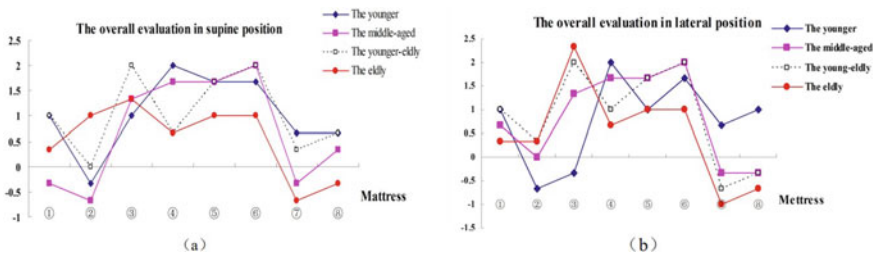


Fig. 2 Overall evaluation of different age subjects

time, the subjects felt turning difficult, poor stability of the mattress, weak points lending up support, and after the test subjects felt exhausted. The spring mattress which is more widely used in life had a general evaluation of all age subjects.

### 3.3 The Correlation of Subjective and Objective

This paper analyzed the correlation of subjective and objective results which used “fuzzy theory,” and the results are shown in Table 5.

When lying in supine position, the young and middle-age subjects’ back comfort had a significant negative correlation with average pressure. The result showed that with the increasing of pressure, the back comfort reduced. When lying in lateral position, the young and elder subjects’ all part comfort had significant negative

**Table 5** Correlativity of subjective and objective results

		Back (arm) comfort	Waist comfort	Leg comfort	Overall comfort
Average pressure	Younger	-0.730* (-0.872**)	-0.440 (-0.826*)	-0.387 (-0.748*)	-0.629 (-0.866**)
	Middle-aged	-0.829* (-0.650)	-0.072 (0.052)	-0.131 (-0.411)	-0.778* (0.048)
	Young-elder	-0.293 (-0.138)	-0.084 (0.301)	-0.185 (-0.285)	-0.586 (0.117)
	elder	-0.202 (0.536)	0.136 (0.418)	-0.289 (0.507)	-0.307 (0.621)
Average pressure gradient	Younger	-0.252 (0.229)	-0.075 (0.187)	-0.428 (0.459)	-0.502 (0.261)
	Middle-aged	0.234 (0.121)	-0.549 (-0.643)	-0.405 (-0.134)	-0.077 (-0.500)
	Young-elder	0.758 (-0.144)	0.266 (-0.404)	0.524 (-0.046)	0.720 (-0.224)
	elder	-0.55 (-0.978**)	-0.21 (-0.965**)	-0.66 (-0.924**)	-0.630 (-0.854**)

Note 1. \* $\alpha = 0.05$ , \*\* $\alpha = 0.01$ : 2. The left number is correlativity in supine position, and the right number is correlativity in lateral position

correlation with average pressure and average pressure gradient. The results showed that the resilience of material had great influence on body pressure.

## 4 Conclusions

All age subjects had different comfort evaluation on a different material mattress. The distribution indicators and subjective comfort evaluation had some relevance, but there also had differences.

Comprehensive subjective and objective test results were found that: The elder subjects had the highest sensitivity on different mattress materials, followed by the young-elder and middle-age subjects, and the young subjects had the lowest sensitivity on each mattress.

The young and middle-age subjects had a consistent evaluation. They had the higher evaluation on memory foam, foam and latex mattress in supine and lateral position.

The young-elder subjects had higher evaluation on memory foam and coir mattress in supine and lateral position. And the elder subjects preferred coir and cotton mattress in supine position and preferred memory foam and coir mattress in lateral position. The people who were accustomed to sleep in lateral position prefers softer mattress.

The younger subjects had higher evaluation on waterbed and airbed, but another age subjects thought them comfortableness. When used waterbed and airbed for long time, the subjects felt turning difficult, poor stability of the mattress, weak points lending up support, and after the test subjects felt exhausted. The spring mattress which is more widely used in life had a general evaluation of all age subjects.

**Acknowledgements** The authors acknowledge the support of the Jiangsu University Philosophy and Social Science Research Fund Projects (2018SJA0386). Youth Fund for Humanities and Social Sciences Research of the Ministry of Education (20YJC760030).

**Compliance with Ethical Standards** The study was approved by the Logistics Department for Civilian Ethics Committee of Nanjing Institute of Technology.

All subjects who participated in the experiment were provided with and signed an informed consent form.

All relevant ethical safeguards have been met with regard to subject protection.

## References

1. Lee H, Park (2006) Quantitative effects of mattress type on sleep quality through polysomnography and skin temperature. *Industrial Ergonomics*
2. Kink HJ, Maxion ELUH. Schlep physiologist Untersuchungen zur Beurteilung verschiedene Maturate. *Int Z angew Physiol* 28:247–262
3. Buckle P, Fernandez A (1998) Mattress evaluation—assessment of contact pressure, comfort and discomfort. *Alperton* 29(1):35–39
4. Bader GG, Engdal S (2000) The influence of bed firmness on sleeping quality. *Appl Ergon* 31(5):487–497
5. Xu M, Xia Q (1997) The indicator of body pressure distribution. *China Mech Eng* 08(01) (in Chinese)
6. Hou J (2011) Partition design of spring mattress. *Furniture* (04)
7. Chen Y, Shen LM (2012) The influences of human design of mattress on sleeping. *Packag Eng* 12:36–40 (in Chinese)

# Study on Anthropomorphism in Human–Computer Interaction Design



Weizhen Xiao and Canqun He

**Abstract** The status of anthropomorphic research is explored, and the anthropomorphized psychological model—the three-factor theory—is expounded in the paper, which reveals that the generation and development of anthropomorphism are influenced by elicited agent knowledge, effectance motivation and sociality motivation. Meanwhile, the human–computer interaction of anthropomorphized model is established from the perspective of emotionalization, combined with Norman’s three-level theory of emotional design and Maslow’s hierarchy of needs. User demands are divided into three types, which are matched with the three factors of anthropomorphic process and the three levels of emotional design. A bridge is built between user anthropomorphic process and designer’s emotional design in the model, and design recommendations are proposed for each level. Finally, how to reach the appropriate degree to cross the uncanny valley and solve the new problem caused by over-dependence on anthropomorphic products are the future prospect of anthropomorphic research in human–computer interaction design.

**Keywords** Anthropomorphism · Human–computer interaction · Emotional design · The uncanny valley

## 1 Introduction

Anthropomorphism refers to giving human characteristics such as characteristics, intentions and psychological conditions to non-human individuals, so that they can be regarded as living and thoughtful people [1], which simply means personifying things. Human beings have an innate tendency of personification, so it has been widely used in literary, film and other artistic creations in the long history of humans. At present, there are abundant researches on anthropomorphism in related fields. For example, Wang et al. [2] studied the changes in consumer attitudes toward the brand and explored the impact of anthropomorphism on the brand image.

---

W. Xiao · C. He (✉)

College of Mechanical and Electrical Engineering, Hohai University, Changzhou 213022, China  
e-mail: [hecq@163.com](mailto:hecq@163.com)

© The Editor(s) (if applicable) and The Author(s), under exclusive license to Springer Nature Singapore Pte Ltd. 2021

S. Long and B. S. Dhillon (eds.), *Man-Machine-Environment System Engineering*, Lecture Notes in Electrical Engineering 645, [https://doi.org/10.1007/978-981-15-6978-4\\_72](https://doi.org/10.1007/978-981-15-6978-4_72)



Although anthropomorphism has appeared frequently in various fields for thousands of years, there are few applications and researches in human–computer interaction and even fewer related researches in China. Yogeewaran et al. [3] found that when the appearance of a robot is highly anthropomorphic, it will be regarded as a threat to human uniqueness, survival security, social resources and job opportunities, thereby creating prejudice.

## 2 The Three-Factor Theory of Anthropomorphism

Anthropomorphization is a process of inductive reasoning on non-human subjects. The basic cognitive operation for such reasoning is the same for anthropomorphism or any other reasoning, including acquiring knowledge, activating or stimulating stored knowledge and applying the activated knowledge to a given goal [4]. Specifically, this process takes a highly accessible knowledge structure as an anchor or inductive reasoning basis and then corrects and applies it to a non-human goal, as shown in Fig. 1.

Epley et al. [5] believe that in this process, anthropomorphism is determined by multiple factors, mainly including cognitive and motivational factors, and motivation can be divided into two kinds. Therefore, they proposed the three-factor theory of anthropomorphism, which includes the elicited agent knowledge, the effectance motivation and the sociality motivation, as shown in Fig. 2.

In anthropomorphism, the general knowledge of human being, that is, the knowledge of self, is known and easily available, which can be used as the basis for inducing

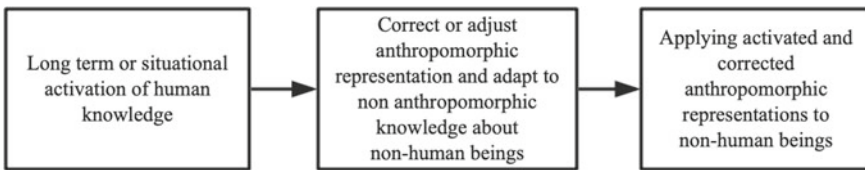


Fig. 1 Anthropomorphic process



Fig. 2 Three-factor theory of anthropomorphism

the characteristics of unknown factors. Human can directly obtain phenomenological experience as human beings, but they cannot directly obtain any phenomenological experience of non-human subjects. Therefore, one of the main determinants of anthropomorphization is the inspiration to the elicited agent knowledge itself.

Anthropomorphism is influenced by human motivations to resolve uncertainty, seek meaning and feel effective. White [6] calls it efficacy motivation, that is, self-knowledge or human's common sense, which can be used as a rich form of expression to obtain a sense of predictability and controllability when reasoning on non-human subjects. Specifically, in anthropomorphism, the effectance motivation refers to the motivation for effective interaction with non-human individuals (or perceived individuals) and the environment, whose function is to enhance the ability of individuals to interpret the current complex stimuli and predict future stimulus behaviors. Attributing human characteristics and motivations to non-human individuals increases the ability to understand their behavior, reduces the uncertainty associated with it and increases confidence in future predictions.

Sociality describes the need and desire to establish social connections with others, and anthropomorphism satisfies this need by establishing a perceived human-like connection with a non-human subject. In other words, in the absence of social connection with others, people create human media from non-human beings through anthropomorphism to meet their motivation for social connection. This need to establish and maintain social contact with others, as well as the distinctiveness of non-human subjects to meet such need, constitutes the sociality motivation of anthropomorphism. Sociality motivation increases the tendency of personalize non-human individuals through two different ways. First, it increases the accessibility criterion of social cues including humanoid features and other features [7], thus increasing the tendency of perceiving humanoid features. Second, it increases the tendency to personalize non-human individuals by increasing the tendency to seek sources of social connections in one's environment actively.

Elicited agent knowledge is the basis for anthropomorphization, and effectance motivation and sociality motivation are the driving forces for anthropomorphization. The three factors above complement each other and are indispensable to constitute a complete anthropomorphic process.

### **3 The Human–Computer Interaction of Anthropomorphized Model**

Design has gradually focused on the user's psychological feelings from the priority of functionality. From the perspective of cognitive psychology, Donald A. Norman proposed the three-level theory of emotional design, which includes instinct level, behavior level and reflection level [8]. In the three-level theory of emotional design, the instinct level is the first level that users directly come into contact with. Users choose products based on human instincts to meet the most basic demands.

The behavior level is based on the user’s experience and feelings, emphasizing the product’s operating efficiency. The reflection level requires users’ personal experience, knowledge reserve, cultural background and other factors to make a comprehensive judgment on the product.

According to Maslow’s hierarchy of needs theory, human needs can be divided into five categories: physiological needs, security needs, social needs, respect needs and self-actualization needs, which are arranged from the low level to the high level like a ladder [9]. Generally speaking, people always produce and give priority to meet the needs of the lower level. When the needs of a certain level are relatively satisfied, they will develop to the higher level, and the pursuit of the higher level’s needs will become the driving force for behavior.

Human has the motivation to promote anthropomorphism, which stems from a variety of needs, and the requirements at various levels overlap with each other, forming the cognitive basis and motivation of anthropomorphism. Meanwhile, the purpose of anthropomorphism is to deepen the cognition of things through “humanizing.” Therefore, anthropomorphism is actually to connect human and non-human objects through emotion, which is part of emotional design.

In summary, the human–computer interaction of anthropomorphized model can be established by combining the three-factor theory of anthropomorphism, three-level theory of emotional design and Maslow’s hierarchy of needs, as shown in Fig. 3.

When users come into contact with anthropomorphic products, basic physiological needs will be generated, which will stimulate the elicited agent knowledge. In the instinct level, designers can design from the aspects of the product’s appearance, materials, colors, texture, voice and tone that are directly related to the user experience channel and attract users to further experience.

When the physiological needs of users are met, security needs will arise, which will affect people’s perception and judgment of the surrounding environment, resulting in effectance motivation, and stimulate the development of behavior level. In practical applications, this can be achieved through the design of anthropomorphic feedback. For example, when a user sends an instruction to an interactive object, the system should reply with text or voice in a human tone to shorten the distance with the

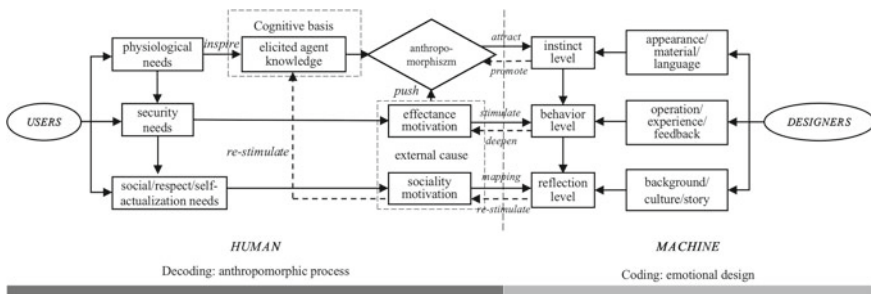


Fig. 3 Human–computer interaction of anthropomorphized model

product. In addition, some feedback can also be anthropomorphic, such as waving and thumbs up.

Social needs, respect needs and self-actualization come from the spiritual level, which have a great impact on people’s communication, sociality and even personality, constituting social motivation and forming a mapping in the reflection level. The background, culture and story behind the product can inspire users to associate and apply more experiences to search for more elicited agent knowledge. For example, by repeating certain feedback actions or inspiring stinger plot introductions, the “character” and “personality” of the product can be enhanced. In addition, we can also integrate brand culture and brand atmosphere into the interactive design.

## **4 Problems and Thinking of Anthropomorphism in Interaction Design**

### **4.1 Concerns About the Uncanny Valley**

The movie of the same name adapted from Disney’s 1994 animated film “Lion King” won a high degree of attention once it was released on July 12, 2019. While receiving applause and cheers, the movie was unexpectedly criticized and questioned. The new version of “Lion King” adopts top-level CG technology, and the picture is extremely realistic, giving people a shocking effect. However, such excellent technology has had an adverse effect. Fans have made fun of the Simba character in the film. This question is worth thinking. Why does such a realistic anthropomorphic character bring a bad viewing experience to the audience?

As early as 1970, Professor Mori of Japan proposed the famous “Uncanny Valley” [10]. According to this theory, the appearance or action of a robot will give a more realistic effect with the increase of the degree of anthropomorphism in a certain range, but it will suddenly drop to a trough after exceeding a certain critical point; robot inside this trough range will give people the discomfort of “zombies,” “corpses,” and “prosthetic limbs.” Only after breaking through this critical point can they get human-like and anthropomorphic feelings again (Fig. 4). This trough range is called the “Uncanny Valley,” which is an unavoidable design obstacle in anthropomorphic design.

Therefore, when we see lifelike lions and hyenas in anthropomorphic behavior, we will have a fear similar to the “Uncanny Valley” effect. Since the valley of terror is an inevitable design obstacle, how to balance this delicate relationship in the design of human–computer interaction?

At the same time, thinking about it from another angle, is there anything useful? The “Uncanny Valley” brings people a kind of fear which causes not only physical discomfort, but also psychological worries about whether they will be replaced. Robots in the future will be more and more intelligent in appearance and behavioral interaction, which will give birth to other human psychological needs and concerns.

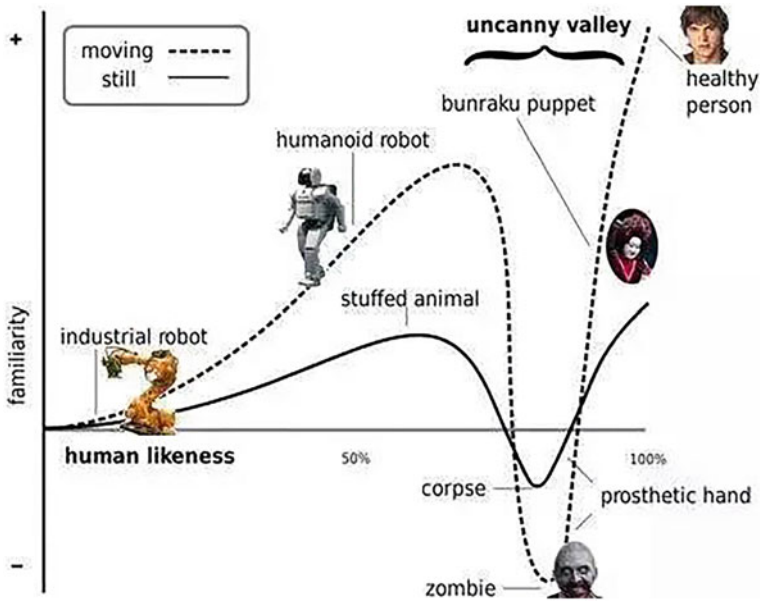


Fig. 4 Curve of the “Uncanny Valley”

Can the “Uncanny Valley” be used to solve the problem of “too anthropomorphic” of robots, and can we design a kind of “clumsy,” lovely and affinity anthropomorphic robot?

## 4.2 Over-Dependence on Anthropomorphic Products

Anthropomorphization is a decoding process with a strong emotional tendency. Users will trigger and invest more emotions in the process of using anthropomorphic products. Compared with general emotional design, it is easier to reach the reflection level. It is good for designers, but if users have been in contact with anthropomorphic products for a long time, their social motivation will gradually strengthen and form a dependency tendency.

An excellent product not only needs to touch the user’s emotion, but also needs to solve problems without bringing other negative effects. While some problems in human–computer interaction can be solved, it may be counterproductive if users develop excessive dependence and escapism from normal society after a long time using, forming bad habits of making friends in real life. Undoubtedly, more and more robots will enter our daily life in the information age. In the face of cold technology products, anthropomorphism will play a greater role and give humans more spiritual

sustenance. Therefore, making anthropomorphism working properly without causing other adverse effects has become an urgent problem to be solved.

## 5 Conclusion

Because of the innate efficacy motivation and social motivation, anthropomorphism is widely used in various fields to meet people’s psychological needs and emotional needs. At present, there are not many researches on the human–computer interaction of anthropomorphism, especially after entering the era of artificial intelligence, the anthropomorphic interaction is not limited to how to make the feedback more humane in some details, but to look at the overall situation, from the aspects of appearance, expression, emotion, interaction mode and so on, to achieve real anthropomorphism, and its carrier will also change from ordinary “machines” to “intelligent robots” with the development of science and technology. Therefore, how to truly meet the needs of users and get rid of the “Uncanny Valley” effect remains to be further studied.

## References

1. Epley N, Waytz A, Cacioppo JT (2007) On seeing human: a three-factor theory of anthropomorphism. *Psychol Rev* 114(4):864–886
2. Wang T, Xie Z, Cui N (2014) have a good chat with the brand: the impact of personified brand communication on consumer brand attitude. *Acta Psychologica Sinica* 46(07):987–999
3. Yogeewaran K, Złotowski J, Livingstone M, Bartneck C, Sumioka H, Ishiguro H (2016) The interactive effects of robot anthropomorphism and robot ability on perceived threat and support for robotics research. *J Hum-Robot Interact* 5:29–47
4. Higgins ET (1996) Knowledge activation: Accessibility, applicability, and salience. In: Higgins ET, Kruglanski AW (eds) *Social psychology: handbook of basic principles*. Guilford Press, New York, pp 133–168
5. Epley N, Waytz A, Akalis S, Cacioppo JT (2008) When we need a human: motivational determinants of anthropomorphism. *Soc Cogn* 26:143–155
6. White RW (1959) Motivation reconsidered: the concept of competence. *Psychol Rev* 66:297–333
7. Gardner WL, Pickett CL, Jefferis V, Knowles M (2005) On the outside looking in: loneliness and social monitoring. *Pers Soc Psychol Bull* 31:1549–1560
8. Norman DA (2003) *Emotional design: why we love(or hate) everyday things*. Basic Books
9. MASLOW (2007) *Motivation and personality*. Renmin University of China Press, Beijing
10. Mori M, Macdorman KF, Kageki N (2012) The Uncanny Valley from the field. *IEEE Robot Autom Mag* 19(2):98–100

# Study on the Influence of Touch Screen Button Size on Operation Performance



Bei Zhang, Ning Li, and Yingwei Zhou

**Abstract** Touch devices are widely used in our lives. The size of the touch screen interface buttons will affect the user's interaction efficiency and accuracy. At present, research on the size of touch screen button is mainly focused on handheld mobile devices and desktop touch devices. Research is still relatively scarce. In order to improve the user's operating efficiency and user's experience, according to the actual needs of the user, this study selects nine types of touch interface buttons sizes for a desktop touch device with a screen tilt angle of  $60^\circ$ , and conducts comparative experimental research, mainly using task performance indicators method of measurement. The experiment results show that the minimum recommended button size for the touch screen interface is 6.25 mm, and the larger the button size, the higher the performance. The research conclusions can be used to support touch screen interface design.

**Keywords** Touch screen · Button · Size

With the development of information technology, as an important input platform and tool, touch screen has been increasingly used in social, personal and work activities [1]. Efficiency is not consistent when performing operational tasks in different interaction modes [2], finger touch and mouse operation have significant differences in the size design of the buttons, so many scholars have researched the size of touch screen buttons.

In the field of mobile handheld devices, parhietal conducted a systematic research on the optimal touch size under thumb operation. The results show that the completion time of the task decreases with the increase of the target size. When the key size is greater than 7.7 mm, there is no significant difference in click operation error rate between the five sizes [3]. Zhang and others found that the button size has a significant impact on the offset and error rate of the click operation [4]. Other scholars researched the minimum center distance of the buttons. The research found that the minimum

---

B. Zhang (✉) · N. Li · Y. Zhou  
China Institute of Marine Technology and Economy, Beijing 100081, China  
e-mail: [zhangbeibj@126.com](mailto:zhangbeibj@126.com)

center distance of the buttons is 3.38 mm and 4.17 mm under the two task scenarios of discrete index finger and discrete thumb [5]. A related study on a 19-inch touch screen shows that if the target width is less than or equal to 0.5 cm, the response error rate is high, which affects the safety and performance of the operation [6].

Combining the above research results, this research is aimed at desktop touch devices with a screen tilt angle of 60°. Based on the current interface display design requirements, the buttons in the interface are used as the object to explore the user's touch of different button sizes in specific application scenarios. The effect of operation performance provides scientific data support for button size design in related interfaces.

## **1 Experimental Method**

### ***1.1 Experimental Device***

The experiment was performed in the laboratory. The experimental materials presented by the computer were used to control the experiment and the test subjects were recorded. The display was a liquid crystal touch screen display (size: 25.8 \* 19.4 cm, resolution: 1600 \* 1200), and the screen inclined angle was 60° (Fig. 1).

### ***1.2 Experimental Variables and Design***

The experimental variable was the size of the button, a total of nine kinds (4 mm, 6 mm, 8 mm, 10 mm, 12 mm, 14 mm, 16 mm, 18 mm, and 20 mm).

The dependent variables were the click accuracy rate and the right click time of the participants.

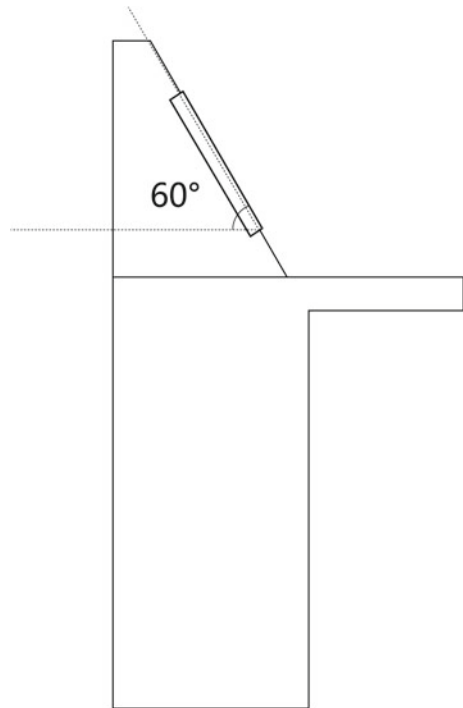
Control variables included lighting, display resolution, button display range, button color and shape, and more.

### ***1.3 Participants***

Twelve male participants were selected in this experiment. All of them had no color blindness or color weakness, and their visual acuity or corrected visual acuity was above 5.0, all were right-handed.



**Fig. 1** Picture of experimental device



#### ***1.4 Experimental Materials and Tasks***

In the experiment, nine kinds of target buttons were randomly displayed in a nine-square grid of 9 cm \* 9 cm in the center of the screen. Each button was marked with a number from 1 to 9, and the digital content appeared randomly in each task. The number font size on each button remained the same, all are 3 mm high. The background color of the entire operation area was dark gray (20.20.20), the background size was full-screen display, the button color was light gray (230.230.230), square, rounded corner radius was 2px, and character color was black (0.0.0).

The task of the participants was to click the corresponding button as quickly as possible, in accordance with the numbers appearing at the top of the screen (Fig. 2).

#### ***1.5 Experiment Process***

After entering the laboratory, the participants first adjusted their sitting position and adjusted the seat height to keep the subjects' eye height at about 105 cm and the line of sight at about 60 cm.

In the experiment, the participants used the right hand for operation.

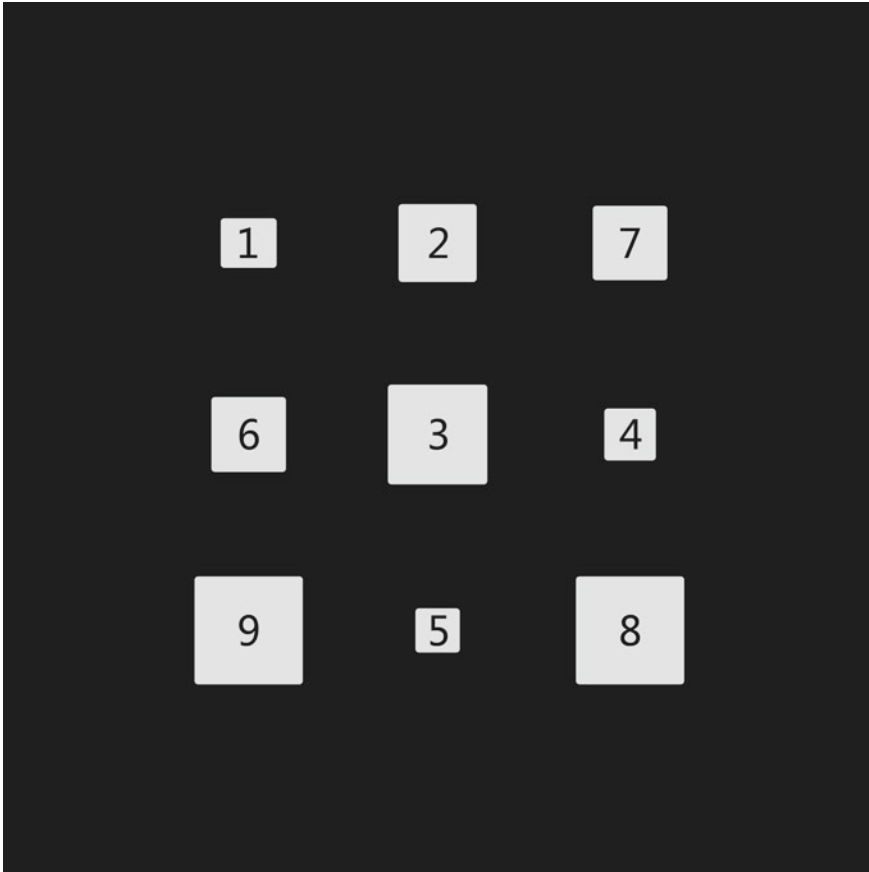


**Fig. 2** Experiment interface

In the middle of the screen, the instructions were presented first, and the participants filled in the information according to the experimental requirements. Then, they started 10 practice experiments. The practice experiments were the same as the formal experimental procedures. They were mainly used to help the participants become familiar with the experimental procedures (Fig. 3).

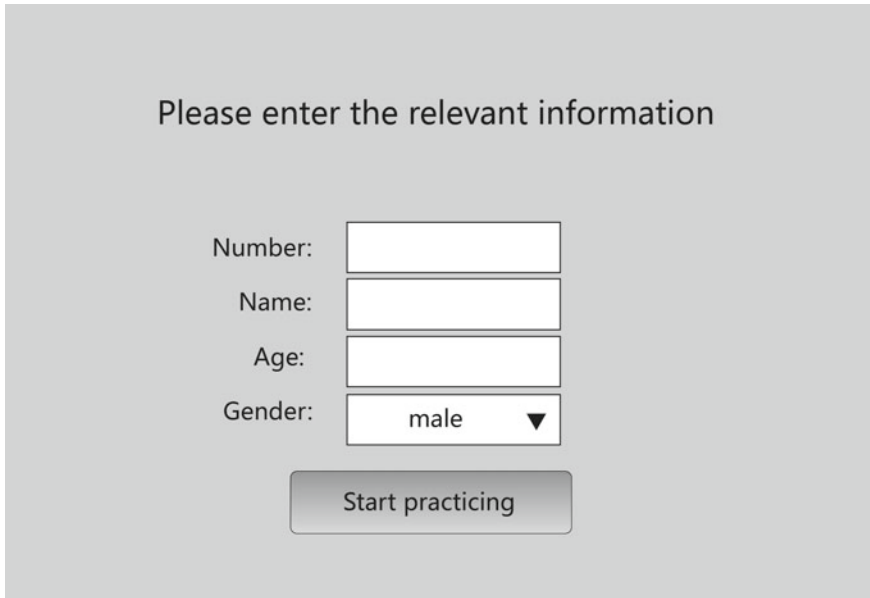
In the formal experiment, participants completed 90 tasks according to the prompts.

Rest for three minutes to adjust eye fatigue.

Continue to complete the remaining 90 missions.

The experiment was over.

In the entire experiment, each participant completed a total of 180 judgments ( $9 * 10 * 2$ ), and the operation time of each task was 10 s. If it was more than 10 s, it was automatically judged as a task failure.



Please enter the relevant information

Number:

Name:

Age:

Gender:

Fig. 3 Experiment first interface

## 2 Experimental Results

### 2.1 Click Response Time for Different Button Sizes

The click response time for different button sizes was analyzed. The experimental results show that there is a negative correlation between the response time and the button size. The larger the button size, the smaller the response time, and the maximum response time is when the button size is 4 mm. Click on the response time to perform a one-way analysis of variance. The results showed that the main effect was significant ( $F = 88.64, p < 0.05$ ). After goodness-of-fit analysis, the difference was gradually reduced after 6.25 mm in size (Fig. 4).

### 2.2 Click Accuracy for Different Button Sizes

The correctness rate of the clicks of different button sizes was analyzed. The experimental results showed that the correctness rate of the nine kinds of button clicks was higher, and the correctness rate was greater than 98%, but the larger the size, the higher the correctness rate (Fig. 5).

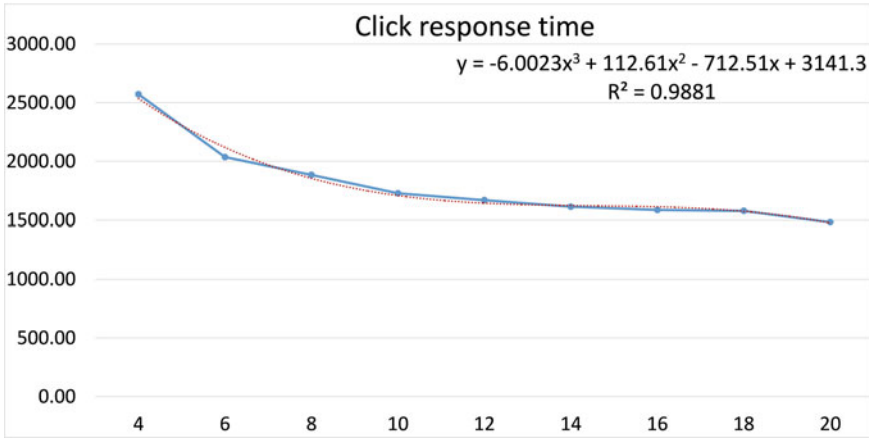


Fig. 4 Click response time for nine sizes of buttons

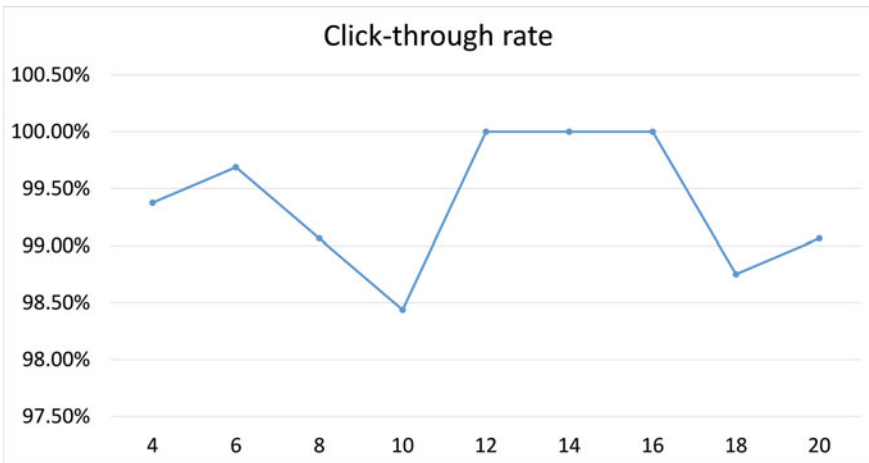


Fig. 5 Click-through rate for nine sizes of buttons

### 3 Discussion

The results of this experiment show that the curve slows down when the button size is above 6.25 mm, indicating that 6.25 mm is a dividing line, and the operating performance is less than 6.25 mm, and the acceptable range is greater than or equal to 6.25 mm, and the larger the size, the higher the efficiency. The higher the trend, that is, the larger the size of the interface button, the larger the operating area, and the higher the operating performance [7].

However, in terms of correctness, the correctness of each size button is higher, which may be due to the relatively small content presented in the interface, the relatively simple experimental tasks, low complexity, and high probability of completion within the time limit of the operation, which is not prone to misuse and operation failure, etc.

## 4 Conclusion

According to the experimental results, when the screen angle is  $60^\circ$ , the recommended minimum size of the touch screen interface button is 6.25 mm. At the same time, it is necessary to consider the buttons that require high performance and safety. According to the interface space and tasks, appropriately increase the size to meet the operation needs.

**Acknowledgements** This study was supported by the projects with No. 41412040304, No. 6141B03020602, and No. 3020105040201.

**Compliance with Ethical Standards** The study was approved by the Logistics Department for Civilian Ethics Committee of China Institute of Marine Technology and Economy.

All subjects who participated in the experiment were provided with and signed an informed consent form.

All relevant ethical safeguards have been met with regard to subject protection.

## References

1. Lv M, Lv Y (2012) Touch screen technology status, development trends and market prospects. *Mach Tool Appl* 03:5–8
2. Alapetite A, Fogh R, Andersen HB et al (2013) A deported view concept for touch interaction. In: The sixth international conference on advances in computer-human interactions. ACHI, pp 22–27
3. Parhi P, Karlson AK, Bederson BB (2006) Target size study for one-handed thumb use on small touchscreen devices. In: Proceedings of the 8th conference on human-computer interaction with mobile devices and services. ACM, New York, USA, pp 203–210
4. Wang W (2011) The influence of the button size and spacing of the touch screen phone keyboard on the operation accuracy. National Taiwan University of Science and Technology Design Institute
5. Wang Q, Ji H, Li D, Li H, Li L (2017) A new soft key design parameter for mobile phonetouch-screen—the shortest central key-to-key distance. *Ergonomics* 023(002):1–5
6. Zhang X, Xue H, Zhang Y (2011) Research on contact motion and interactive interface button design. *Comput Eng Appl* 47(36):83–85
7. Tao D, Yuan J, Shuang L, Xingda Q, Chen X (2016) The effects of button characteristics on the usability of touch screen devices in input tasks. *Ergonomics* 022(005):1–6

# Research on Man–Car Relationship in 5G Era



Ting Tang and Qiang Zhang

**Abstract** *Objective* To study the man–car relationship in the 5G era with the man–computer interaction of future smart cars as the object. *Method* An analysis of the current situation of man–car relations based on the development of automobiles and conduct research on them in the 5G era. Taking the starting point of bringing a better travel experience for users, by building a three-dimensional model of the future smart cars, the man–car relationship in the 5G era will be integrated into the design process of the future smart cars. *Result* (Combining with the changes in user needs and social environment in the 5G era, discuss the relationship between smart cars and people in the future, and form the design trend in the field of smart cars in the future). *Conclusion* With the advent of the 5G era, unmanned driving is gradually realized, users are liberated from the heavy driving tasks, the man and car cooperation will be more harmonious during driving, and the man–car relationship will be closer. The man–car relationship changed from a man adapt to car to a car adapt to man and then a man and car adapt to each other and finally reached harmonious unity. In the future, smart cars are no longer just a means of transportation, but more like a close friend who accompanies you and understands you, bringing you intimate and exclusive travel services.

**Keywords** 5G · Smart cars · Man–car relationship

## 1 Research Background

The birth of the world's first car has a history of more than 100 years. It has played a huge role in social development and human life as the most important means of transportation today. With the rapid development of automobiles, it is no longer just an industrialized and mechanized product, and its role and connotation are constantly being defined. With the integration of artificial intelligence and network information technology with transportation, automobiles have begun to move from traditional

---

T. Tang (✉) · Q. Zhang

Shenyang Aerospace University, 37 Dao Yi South Street, Shenyang, Liaoning, China  
e-mail: [18845646635@163.com](mailto:18845646635@163.com)

© The Editor(s) (if applicable) and The Author(s), under exclusive license to Springer Nature Singapore Pte Ltd. 2021

S. Long and B. S. Dhillon (eds.), *Man-Machine-Environment System Engineering*, Lecture Notes in Electrical Engineering 645,  
[https://doi.org/10.1007/978-981-15-6978-4\\_74](https://doi.org/10.1007/978-981-15-6978-4_74)

645

industrial products to information interaction platforms. For users, the car is not just a mobility tool; it integrates information exchange among man, man and cars, cars and cars and brings users a better travel experience. The car has evolved from a single carrying machine into a multifunctional interactive space.

With the advent of the 5G era, the connected car industry will gain new vitality. The concept of the Internet of Vehicles originates from the Internet of Things; it takes the moving vehicle as the information perception object and uses the new generation of information and communication technology to achieve the network connection between the vehicle and X (i.e., the vehicle and the vehicle, people, roads, and service platforms), improve the overall intelligent driving level of the vehicle, provide users with safe, comfortable, intelligent, and efficient driving experience and transportation services, while improving transportation efficiency and the intelligent level of social transportation services [1].

## 2 Research on Man–Car Relationship

Under the current social model, the vigorous development of Internet technology has profoundly affected all aspects of people's lives. With the continuous change of the social environment, people have higher demand for products. The car as the most important means of transportation for modern people, the ergonomics in the traditional sense cannot fully satisfy the user's diversified and humanized needs for future smart cars.

### 2.1 *Development of Man–Car*

In 1886, the first gasoline engine car was born in Germany. This kind of “self-propelled carts that do not rely on mans” has begun to appear constantly in Europe and even the world, replacing rickshaws and horse-drawn carts as important means of transport for human beings. (In terms of travel, the power of the car changes from being derived from human to relying on itself. This development process has liberated human beings). Humans have begun to adapt to the ease and convenience that this transportation brings to their travels. The relationship between man and cars has changed.

The birth of the car made people feel the impact of the age of industrial mechanization on life. At this time, people only have functional requirements for cars, that is, the “form follows function” advocated by the Bauhaus. At this time, the relationship between the man and the car was a bit stiff and alienated, and there is only the relationship between the need and be needed. With the emergence of assembly line production methods, the cost of automobiles has been reduced, the scale of automobile production has been expanded, and automobile production has developed rapidly. In the early twentieth century, American car companies such as Cadillac and

Lincoln began to design car bodies according to the wishes of customers to serve economically wealthy users. At the same time, some high-end and luxury automobile manufacturing brands in Europe such as Rolls-Royce and Ferrari were exclusively used by the rich. In order to meet the demands of vehicles for different groups of users, armored vehicles, cargo vehicles, racing cars, and other models have appeared one after another, making the types of cars gradually increase and tend to diversify. The practical function of the car at this stage is the basic demand of the user. The personalization, that is, the car can highlight the characteristics of the user's identity more attract the attention of customers. During this time, the car starts to adapt to the demands of man, and the relationship between man and cars is no longer alienated. It tends to "identify," that is, the car can highlight the identity of the user, and users can get psychological satisfaction and fulfillment from the car.

The emergence of user's emotional demands makes designers realize that "form follows not only function but also emotions." Both are indispensable. Automotive design should integrate users' psychological demands (aesthetics, belonging, etc.) in their functions. Seeing a car will produce different psychological characteristics and emotions. The harmonious proportion of the car body can bring more security to the user due to its visual integrity, and the stable morphological feeling can make people feel solid, serene, and relaxed [2]. In today's society, there are many types of cars and prices vary. As long as users with a certain economic foundation will consider buying a car, it is more convenient for them to travel and go wherever they want. There is no need to squeeze the subway to work on weekdays, and you can travel by car with friends or family on the weekends. (You don't have to worry about missing the subway or there is no seat on the bus, owning this car seems you heart to be settled inside). Man and cars began to adapt to each other, and the car to the user brought a sense of security and belonging.

## ***2.2 New Trends in Man–Car Relationships***

After more than a hundred years of continuous improvement and innovation, automobile manufacturing technology has become more and more mature. With the widespread application of computer technology and network technology in the field of vehicle transportation and the continuous development of vehicle-mounted technology, the interior space, man–machine interface, operation and interactive processes of the car are undergoing revolutionary changes [3].

### **2.2.1 Diversity of Driving Modes and Driving Spaces**

At present, the information model inside a car has gradually developed from a single driving and vehicle condition information model to a complex information system including car information, car to car information, car and other information carriers (Car to X) interaction information [4]. In such a complex information interaction





**Fig. 1** Weilai EVE driverless car

system, drivers need to interact with other information in the car in addition to completing tasks such as controlling the car and monitoring road conditions, which can easily distract drivers' attention and affect traffic safety.

With the advent of 5G Internet era, the Internet of vehicles technology will get more rapid development and application, and the unmanned driving technology (automation level: L3–L5) will be applied to future cars. With the improvement of the automation level of intelligent vehicles, users' eyes and hands will be liberated from tedious driving tasks, reducing driving safety risks. Meanwhile, users will lose part of their vehicle control rights, which may be completely controlled by machines in the unmanned driving stage. However, some users enjoy the fun brought by driving, so the trend of smart cars driving way in the future is that unmanned driving cannot completely replace manual driving, both of which coexist, as shown in Fig. 1.

With the change in driving style, the driving space has expanded to other service spaces, namely the "third space," and the layout of the interior of the car has changed dramatically, as shown in Fig. 2. Users can rest, entertain, work, etc., in this space. Cars are evolving from a mechanical vehicle to design objects that include personal, public, and social spaces.

### 2.2.2 Shared Services

The sharing economy will become the dominant consumption model in the twenty-first century [5]. In order to meet the demands of urban traffic pressure and environmental protection, the establishment of Shared Automated Vehicles (SAV) has



**Fig. 2** Internal space layout of Weilai EVE driverless car

become an important content of future urban traffic design and planning [6]. Accenture proposes the concept of “Travel as a Service” for car sharing and services and divides car sharing into multiple models, such as car rental, site-based car sharing, instant use car, and network special car [7]. The emergence of the car sharing mode allows users who cannot afford a car temporarily or do not want to buy a car to use the car anytime, anywhere. At this time, the car is no longer an individual, and the user only has the right to use the car and has no ownership. With the rise of driverless cars in the future, shared car borrowing, car return, autonomous parking, and self-charging experiences will be further enhanced. At the same time, in the future, the user’s private car can also be transformed into a “shared car” to serve those who need it, and they can also make money for the owner to make the car play its biggest role. The emergence of the sharing economy has changed the way users use cars and increased the service value of cars.

### **2.2.3 Personalized**

Personalization and customization have always been user demands and design trends [8]. In the 5G era, the traditional customization model is far from meeting users’ needs for future smart cars’ personalization. Especially in the field of car sharing, users hope that different vehicles used each time can provide exclusive services according to their own needs, which cannot be met by traditional customization models. Biometric technology will be applied to future smart cars. Through the integration of offline biometrics information and online user big data, achieve the acquisition of vehicle to human basic data, make the car is integrated into the user’s life, and man and the car build tacit understanding and trust with each other. For example, the Weimar

EX5 launched by Baidu, Huawei, and Tencent can use face recognition technology to enter a Weimar account that is unique to the user. (According to the user's daily usage data recorded by Weimar account, including navigation route, air-conditioning temperature, etc., from in-car environment setting to travel route planning, it can meet the individual needs of users [9]). Personalized account settings reduce the user's operating costs and use wisdom to provide a personalized experience for each user.

#### **2.2.4 Intelligent Emotional Interaction**

In the 5G era, on the basis of intelligent driving, users also hope that cars have a certain emotional intelligence and intelligence and can "understand and think." In the future era of autonomous driving, smart cars should not only be tools to respond to people's instructions, but should also communicate and collaborate with users [10]. Smart cars improve their IQ through emotion perception, autonomous learning, personalized services, and interactive methods. At the same time, they interact with and learn from users to continuously focus on and digest user demands and feedback to improve their emotional intelligence. With the ability to "understand and think," smart cars can complete difficult tasks, assist users to complete driving tasks more efficiently, and interact with users through multiple interaction modes such as voice, gestures, and eye movements to meet users' needs. As a smart carrier, a smart car not only communicates and interacts with users inside the car, but also interacts with other individuals outside the car, such as pedestrians outside the car, other vehicles, and urban transportation facilities. In the future, the way of communication and interaction between smart cars and surrounding vehicles will no longer rely on the traditional whistle and lights, but pass communicate and interact with vehicles that meet each other through various forms. Honda's 2017 Urban EV concept car, including the front face display of the headlights, can display suggestions, greetings and even emoticons in different languages and interact emotionally with surrounding traffic individuals [11], as shown in Fig. 3. Intelligent and emotional interactions will help form good traffic etiquette in the future, So that everyone can experience the wisdom of travel.

In the future, smart cars will continue to learn and think, and according to the new demands of users, make corresponding upgrades and adjustments to the service system and continue to meet users' internal emotional demands. Let the car change from a machine product to a "friend" with life, wisdom, emotion, resonance, ability to judge, and truly understand users.

### **3 Application of Man–Car Relationship in Design Practice**

Design background: With the popularity of 5G, the speed and scale of data transmission will take a qualitative leap. The development of the Internet of Things and the Internet of Vehicles will definitely bring a new era, and the automobile as a giant



**Fig. 3** 2017 Honda’s concept vehicle Urban EV

of the modern manufacturing industry will also become a major component of the intelligent mobile terminal in the future. What will happen to the future urban form and people’s lives? How will the future smart cars drive? What kind of experience will intelligent transportation bring? Design object: A smart car designed for young people in the smart city of the future. Design process: First, analyze the future smart city road architecture, understand young people’s living, working methods, physiological and psychological demands, and investigate the types of cars that the new generation of young people tends to. Secondly, the overall shape and style of this smart car are determined by combining the new trends of human–car relations in the 5G era. Finally, through continuous improvement and perfection, 3D modeling and rendering are completed, as shown in Fig. 4. Design Result: This smart car is an exclusive car and its size is small and lightweight. It can not only take you to and from the city, but can also understand your “close friend” or accompany your pet, know your demands. It allows you to enjoy your personal space on the road of smart travel without feeling lonely. The overall modeling of the car tends to the upper round lower square, giving a warm and lovely feeling. At the same time, the car uses spherical tires to allow the cockpit to rotate 360° freely, bringing a better experience to driving and making busy life have a little fun. In this design practice, the relationship between man and cars is more intimate, and the emotional demands of man for cars tend to be friendly and accompany, which will also be the trend of smart cars design in the future.

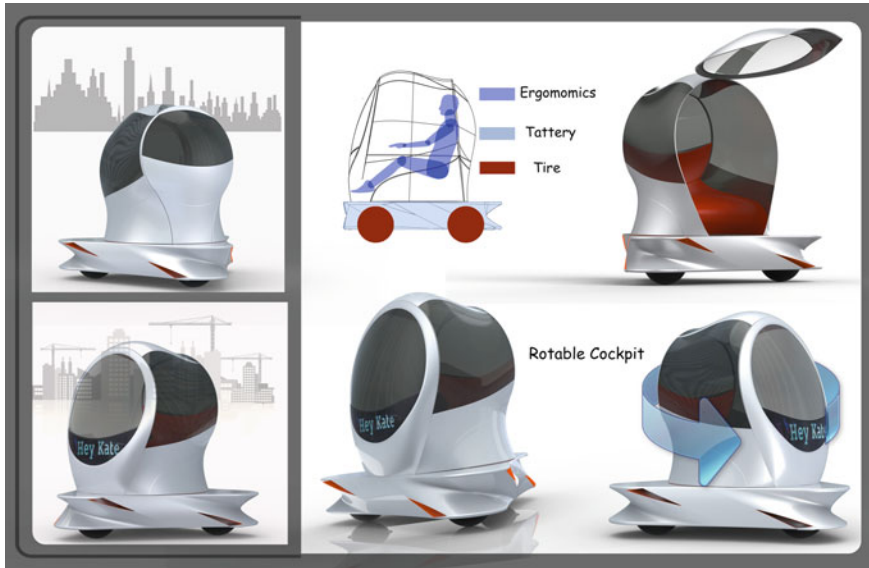


Fig. 4 3D model of smart car

## 4 Conclusion

In the 5G era, the relationship between man and cars in the future is not just to provide simple travel services. Vehicles establish tacit understanding and trust with users through big data. Smart cars are integrated into users' lives, which enhance people's dependence on cars. Man and cars produce more closer relationship and deeper emotional resonance between them. At the same time, smart cars are developing from a mechanical vehicle to design objects that include personal space, public space and social space. Therefore, the new man-car relationship and the "third space" will bring some inspiration to the future smart cars design. Smart cars in the future will play a richer role in smart cities, bringing more smarter travel experiences to people.

## References

1. Jing X (2019) Analysis of internet of vehicles technology and application. *Shanghai Automot* 04:9-12
2. Lu JY, Gao QF, Bai MY (2017) Exploration of the people-car-environment relationship in automobile modeling design. *Design* 11:60-61
3. Tan H, Zhao JH, Wang W (2012) Research on human-computer interface design of automobile. *J Automot Eng* 2(05):315-321
4. Schmidt A, Spiessl W, Kern D (2010) Driving automotive user interface research. *IEEE Pervasive Comput* 1-3:85-88

5. Thebaultspieker J, Terveen L, Hecht B (2017) Toward a geographic understanding of the sharing economy: systemic biases in uber x and task rabbit. *ACM Trans Comput-Hum Interact* 24(3):1–40
6. Bockle MP, Brenden AP, Klingegard M et al (2017) Exploring the impact of an interface for shared automated vehicles on pedestrians' experience. In: *The international ACM conference on automotive user interfaces and interactive vehicular applications* Automotivuei, ACM
7. Accenture (2018) Travel and service: a new ecosystem for the future automotive industry. [https://www.sohu.com/a/256597904\\_468661](https://www.sohu.com/a/256597904_468661). Cited 1 July 2019
8. Tan H, Sun JH, Guan DS, Zhou ML, Qi JP, Zhao Y (2019) Research on the development trend of human-computer interaction in smart cars. *Packag Eng* 40(20):32–42
9. WM Motor, WM ID (2018) Exclusive intelligent internet account. <https://www.wm-motor.com/ex5.html>. Cited 15 April 2019
10. Okamoto S, Sano S (2017) Anthropomorphic AI agent mediated multimodal interactions in vehicles. In: *The international conference*
11. NetCarShow.com (2017) Honda urban EV concept. [https://www.netcarshow.com/honda/2017-urban\\_ev\\_concept/](https://www.netcarshow.com/honda/2017-urban_ev_concept/). Cited 15 April 2019

# Optimal Design of Man–Machine Interface for Integrated Situation Display of Vehicle-Mounted Command and Control Equipment



Mingjie Wan, Jinkuang Zhang, Jianjun Gao, Zaochen Liu, Xuewei Liu, and Xiaolong Chang

**Abstract** *Purpose* is to improve man–machine interaction efficiency and support optimal design of man–machine interface. *Methods* Application of new technology is researched in man–machine interface design of integrated situation based on the theory and researching methods of system engineering. Taking vehicle-mounted command and control equipment of a certain type as the typical case, the integrated situation display man–machine interface is designed and optimized. *Result* After optimization system reaction time is largely shortened, command and control efficiency is greatly improved and users’ demand is perfectly met. *Conclusion* Man–machine interaction efficiency directly affects the combat effectiveness of weapons and equipment. The application of advanced man–machine interaction technology in the integrated situation display of command and control equipment is an effective way to realize the deep integration between commanders and command and control equipment and improve the combat effectiveness.

**Keywords** Command and control equipment · Situation display · Man–machine Interface · Man–machine interaction

## 1 Introduction

The integrated situation display of vehicle-mounted command and control equipment is a kind of integrated digital information set, which takes the form of the graph, text, image, sound, table, military logo and other linkages to reflect the battlefield situation in real time based on graphic interface. It is an important interface and channel to realize bidirectional information interaction between commanders and battlefield, it is a crucial part in the whole design of man–machine interface for command and control equipment, and it is also a basic basis for commanders’ command and decision. Through the command and control equipment, the commanders obtain the

---

M. Wan · J. Zhang · J. Gao · Z. Liu · X. Liu · X. Chang (✉)  
CPLA Army Academy of Artillery and Air Defense, M. Zhengzhou Campus, Zhengzhou 450052, China  
e-mail: [changxiaolon@163.com](mailto:changxiaolon@163.com)

important information such as various combat situation, various operational states of weapon system and battlefield situation evaluation, and make decisions based on these information, and issue various combat instructions through man-machine interface. Obviously, research on the optimal design and application of man-machine interface for integrated situation display of vehicle-mounted control equipment is of great significance toward exercising combat performance of weapons and equipment and improving combat effectiveness.

## **2 The Dynamic Development of Man-Machine Interaction in Integrated Situation Display of Vehicle-Mounted Command and Control Equipment**

### ***2.1 The Present Situation and Deficiencies***

At present, the man-machine interaction technology adopted in the integrated situation display of vehicle-mounted command and control equipment is mostly in the hierarchy of interactive graphical interface. The interactive devices adopted generally are computer display screen, joystick, track ball, etc. The display interface is mostly static/dynamic, 2D graphics/image and other multi-media information. The man-machine interaction stays in the stage of “*centering on the machine*,” which is a kind of “*people adapt to the machine*” interactive mode.

Although considerable progress has been made concerning the research on the man-machine interface of situation display for vehicle-mounted command and control equipment in China, comparing with military transformation need in new era there are still four gaps and deficiencies. Firstly, the integration of situation display interaction means is not high; secondly, there are limitations in the optimal design of situation display interface [1]; thirdly, the interactive operation mode of situation display is not flexible enough; fourthly, the particularity of situation display interaction is not considered comprehensively [2].

### ***2.2 Developing Trend***

In the future, there are four trends in the development of man-machine interaction technology for integrated situation display of vehicle-mounted command and control equipment. Firstly, situation display tends to be more intuitive. With the development of 3D display, holographic projection and other technologies the battlefield situation visualization is realized and the informatization advantage will be transformed into the decision-making advantage, which greatly improves the command efficiency [3].



Secondly, man–machine interaction tends to be more natural. Through the introduction of speech input, touch and control and other multi-channel interaction technologies system operating efficiency is greatly improved. Thirdly, operation design tends to be easier to use. Operation interface and menu are optimized; shortcut menu is designed and warning information is perfected, thus, the professional requirements and training difficulties for the operators will be greatly reduced. Fourthly, the auxiliary decision tends to be more intelligent. Taking big data as support and intelligence processing as the core the system can provide important support for commanders to make correct decisions, implement precise policies and employ troops rationally, which greatly improves the efficiency of command and decision.

### **3 New Man–Machine Interaction Technology for Integrated Situation Display of Vehicle-Mounted Command and Control Equipment**

#### ***3.1 Touch and Control Technology***

In the early 1990s, a new kind of man–machine interaction equipment *touch screen* appeared [4]. The touch screen technology supports single-point touch and multi-point touch, and it provides a newly typed man–machine interaction input mode for people. In vehicle-mounted command and control equipment, the touch screen is applied to conduct integrated situation display. Through the touch screen commanders can intuitively select the location, menu, key control, etc. Thus, the efficiency of man–machine interaction is effectively improved.

#### ***3.2 Speech Recognition Technology***

Speech recognition technology is to convert man speech information into computer-readable input. Under the condition of speech recognition, the language is faster and more effective than the keyboard input, which may reduce system reaction time; it can liberate the users' hands and provides more operation channel. With much higher speech recognition rate, application concerning the important point of equipment interaction will be gradually expanded. Speech recognition technology can be applied to assist text input, data binding, flight information reading, command instruction receiving, etc.

### ***3.3 Multi-channel Man–Machine Interaction Technology***

The multi-channel man–machine interaction technology introduces new interaction channels such as voice, gesture, sight line, etc., which enables users to apply multiple channels to conduct man–machine dialogue in a parallel manner, and improve the flexibility of interaction, make up for the shortcomings of the existing interface. Different from the traditional 2D interaction mode, multi-channel man–machine interaction seeks for new interaction means to make full use of man organs such as ears, mouth, hands and eyes, and make vision, hearing and touching channels for mutual complementation. Thus, this way on man–machine interaction is more similar to the daily communication among people. The interaction timeliness is greatly enhanced and the interaction efficiency is greatly improved.

### ***3.4 3D Situation Display Technology***

Based on the narrow space of vehicle-mounted equipment 3D situation visualization provides commanders with a really and comprehensively virtual natural environment such as topography, landforms, surface features and electromagnetic environments in a particular battlefield area. On this basis, it provides the real representation and description on forces deployment and situation changes of both sides of the enemy and us, so as to provide the commanders with a visual representation of their situation. Thereby, it is very convenient for commanders to make timely decisions according to the battlefield situation [5, 6].

### ***3.5 Big Data Processing Technology***

Big data processing technology combines the advanced technologies such as big data analysis and mining, processing and cloud computing and provides the possibility for the adjustment and control of out of plan. Through specialized knowledge and understanding of objective world from experts combat data is researched and analyzed to form combat model database. When in operation, the integrated situation display system receives battlefield intelligence information such as voice, text, signal, etc., and then uses data mining technology to find meaningful mode from massive databases, convert, and generate corresponding interface display models automatically. At the same time, the continuous intelligence information is frequently updated and integrated, which predicts the development of battlefield situation and provides important reference for commanders' command and decision.

### 4 Empirical Analysis

Taking vehicle-mounted command and control equipment of a certain type as the typical case, the design of man–machine interface for the integrated situation display is optimized.

The man–machine interface for integrated situation display of command console includes two parts: part one is man–machine interface for the integrated situation display; part two is man–machine interface for the command console. Its overall layout is shown in Fig. 1.

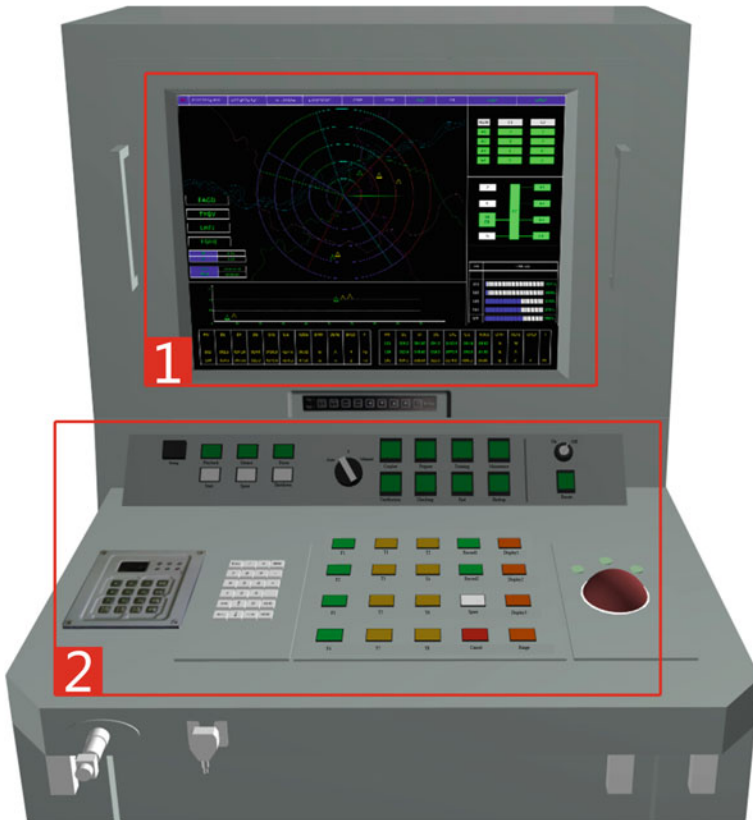


**Fig. 1** System implementation flow. 1—man–machine interface of integrated situation display; 2—man–machine interface of command console

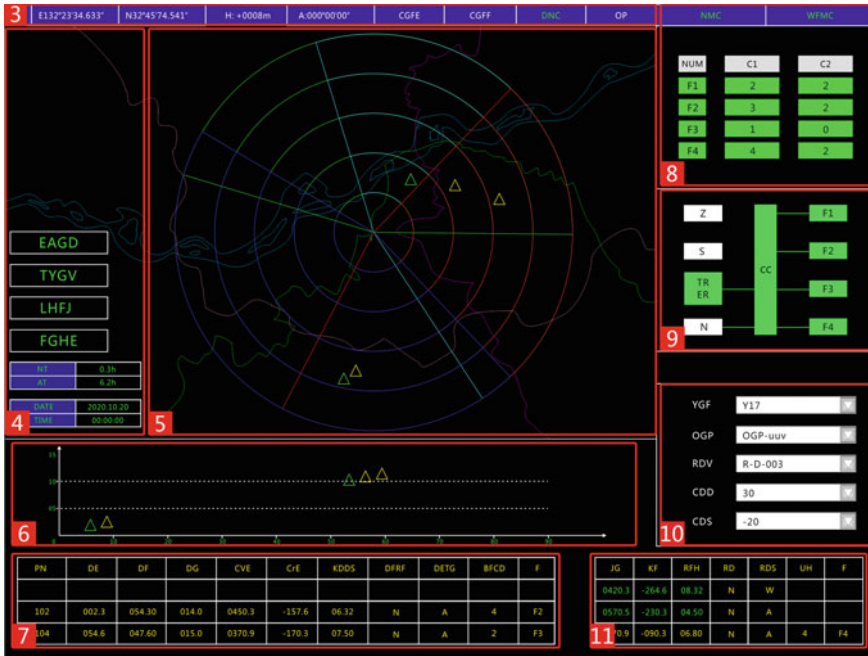


**Fig. 2** Block diagram of equipment three-dimensional modeling. 3—working state display section; 4—weapon unit state display section; 5—air information display section; 6—target flight elements display section; 7—target information display section; 8—ammunition state display section; 9—communication link and equipment status display section; 10—parameter setting display section; 11—flight track list display section

### 4.1 Man–Machine Interface of Integrated Situation Display

Man–machine interaction interface for integrated situation display of command console is composed of nine display sections including air information, working state, ammunition state, weapon units state, communication link and equipment state, target flight elements, parameter settings, target information and track list. Its basic layout is shown in Fig. 2.

### 4.2 Man–Machine Interface of Control Console

The operation panel of command console is divided into 5 sections: operation keyboard 1 section, operation keyboard 2 section, communication equipment operation section, parameter input operation section, cursor operation section, etc. The basic layout is shown in Fig. 3.

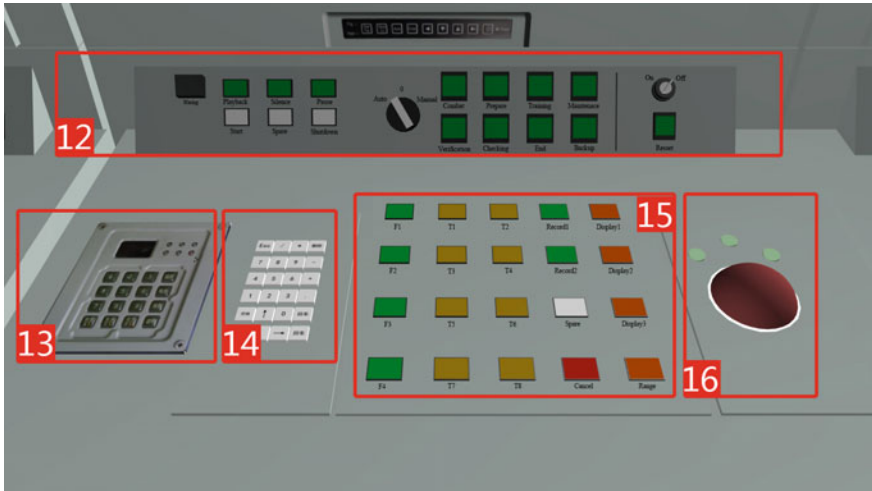


**Fig. 3** Man-machine interface layout of command console. 12—operation keyboard 1 section; 13—communication equipment operation section; 14—parameter input operation section; 15—operation keyboard 2 section; 16—cursor operation section

### 4.3 Analyzing the Result

After optimal design man-machine interface for the integrated situation display of command and control station includes nine sections, which can display the integrated situation, AOR, the distribution of weapon units, the number of current targets, flight direction, distance, altitude, bearing, longitude, latitude, ammunition preparation, recording playback state, ammunition energizing state and mode, users' usage mode, ammunition consumption state, equipment technology state, working state, searching and tracking mode, etc. Compared with the former command console, the three of the integrated situation display sections have been increased and perfected, the 6 of them have been optimized. At the same time, some functions such as speech dialogue and interaction automatically are added to each display section, making man-machine interaction more intuitive, convenient and easy, and the system reaction time has been shortened by 65%.

After optimal design man-machine interface of command console has five sections, which can realize the on/off of the device, selection and switching of working mode and working state, the input and binding of various parameters, weapon units selection, targets selection, Ammunition preparation and state display, switching among various displays, various state changes and displays in combat, work cancellation, stat reset, etc. Compared with the former command and control system, the two of command console sections have been increased and the three of them have been optimized, and the information urgently used and needed by users has increased by 60%. The smooth man-machine interface has greatly improved the working efficiency and met the users' requirements.

## 5 Conclusion

The integrated situation display of modern vehicle-mounted command and control equipment is developing quickly toward intelligence, and the efficiency of man-machine interaction will directly affect the decision-making of commanders. This paper summarizes the present situation and development of man-machine interaction technology of the integrated situation display and studies the related new technology of man-machine interaction. It also analyzes the basic principle, technical characteristics, development status and application prospect of each technology in the integrated situation display, and taking vehicle-mounted command and control equipment as the typical case the paper makes an empirical analysis on optimal design of man-machine interface of the integrated situation display. The result has shown that the application of advanced man-machine interaction technology can greatly improve the man-machine interaction efficiency of the integrated situation display and promote its combat performance. Based on the integrated situation display, the new man-machine interaction technology will take on better developing trends and broad application prospect.

## References

1. Li C, Xu B, Li WH (2014) Multi-channel man-machine interaction model for battlefield. *Fire Control & Command Control* 11:110–114
2. Guo SJ, Zhang HQ, Wang HS (2013) Research on radar structure virtual maintenance system. *Mach Electron J Coll Electron Eng* 6:66–69
3. Xu Y (2015) Development of man-machine interaction technology for ship command & control system. *Ship Electron Eng* 10:5–9
4. Yu LB, Meng FW (2013) New technology of man-machine interaction in weapon and equipment system. *Electron World* 12:164–165
5. Cheng F (2013) Analysis on the development of man-machine interaction technology of submarine command and control system. *Fire Control & Command Control* 5:5–9
6. Fang B, Huan GY, Wu W, Li W (2015) Application of three-dimensional situation display system of space, sky and ground. *Command Inf Sys Technol* 2:76–81

# Research on Respiratory Signals for Visual Fatigue Caused by 3D Display



Guilei Sun

**Abstract** In order to study the relationship between visual fatigue and respiratory characteristic parameters caused by 3D display, 30 subjects were invited to watch 3D videos for 90 min. A questionnaire survey was performed in the initial state and every 15 min after watching the video to obtain the subjective data, and 7 groups of data were collected. The characteristic parameters of breathing were acquired synchronously using breathing sensors. The data was analyzed using SPSS. The results show that subjective fatigue increases with the increase of time spent watching 3D videos, and subjective visual fatigue increases extremely significantly from 45 to 60 min. The mean of power, index of the respiratory frequency domain, and the corresponding standard deviation show a highly significant linear negative correlation with time and the consistency with subjective fatigue score reached 0.970, indicating that the power value is effective for visual fatigue assessment. Therefore, based on the power mean or standard deviation of the breathing signal, the time is used to estimate or evaluate the time of watching 3D display.

**Keywords** Visual fatigue · respiratory signal · Respiratory frequency domain · Power index · Correlation analysis

## 1 Introduction

The development of 3D technology has involved all aspects of life, such as medical, industrial, military, education, entertainment, film, and television. The application of 3D technology also brings a new problem-visual fatigue. Many scholars have carried out related research, such as: Wang [1] studied the effect of visual fatigue on 3D polarized displays based on medical eye symptoms. Yano [2] pointed visual fatigue was induced if the images were moved in depth according to a step pulse function even if images were displayed within the corresponding range of depth of focus. Kooi et al. [3] proposed that crosstalk and blur may be the factors that

---

G. Sun (✉)

Department of Safety Engineering, China University of Labor Relations, Beijing 100048, China  
e-mail: [sunguilei@culr.edu.cn](mailto:sunguilei@culr.edu.cn)

© The Editor(s) (if applicable) and The Author(s), under exclusive license to Springer Nature Singapore Pte Ltd. 2021

S. Long and B. S. Dhillon (eds.), *Man-Machine-Environment System Engineering*, Lecture Notes in Electrical Engineering 645, [https://doi.org/10.1007/978-981-15-6978-4\\_76](https://doi.org/10.1007/978-981-15-6978-4_76)

cause visual fatigue. Matsuura [4] proposed that the influential factors affecting the viewing conditions in 3D stereo vision are interpupillary distance, visual function, and viewers. Alhaag et al. [5] confirmed that 3D display at short distance is more likely to cause visual fatigue than 2D display, but 3D display at a long distance has a lesser effect on visual fatigue.

For the measurement of visual fatigue, the most extensive subjective measurement is a questionnaire. For example, Lambooi [6] gave a visual fatigue questionnaire recognized by most scholars, namely the questionnaire for visual symptoms of Sheedy; Li et al. [7] used EEG and ERP signals to measure 3D visual fatigue and concluded that binocular parallax has effect on 3D visual fatigue. Tam et al. [8] indicated that there is a significant difference in 3D tolerance among individuals, and it is still impossible to distinguish whether it is caused by the stereo or the individual. Park and Mun [9] mentioned that it is also good to use eye movement parameters and physiological signals as 3D visual fatigue evaluation index when measuring visual fatigue. Kim et al. [10] used ECG, GSR, and SKT to measure the degree of fatigue affected by watching 3D video, indicating that skin electrical response (GSR) and skin temperature (SKT) may also be used to assess the extent of 3D visual fatigue. Bruce [11] measured drivers' fatigue by recording heart rate and skin power. Ashrant et al. [12] used physiological indicators such as heart rate, EEG, and infrared temperature to detect the physical fatigue of construction workers. Zhu et al. [13] extracted the cycle, period standard deviation, amplitude, amplitude standard deviation, and frequent yawns of respiratory signals as characteristic parameters for determining driving fatigue. Yu [14] proposed a model for judging the current fatigue level and design and apply it to the mobile terminal (mobile phone application). Xu [15] judged the driver fatigue based on physiological signals EEG and ECG (heart rate signal). Ye [16] used physiological signals to classify driving fatigue and established a driving fatigue evaluation model by collecting and analyzing EMG and ECG. Fu et al. [17] used the wireless measurement equipment of physiological signals to detect the driver's fatigue state, and the prediction results based on the Bayesian model and reached a good agreement with the subjective score results.

In the current research, many scholars use physiological signals to evaluate fatigue, but the evaluation of respiratory signals is mainly for driving fatigue, which is different from visual fatigue caused by 3D display. Therefore, it is necessary to further correlate the respiratory characteristic parameters with 3D visual fatigue.

## 2 Experiment

### 2.1 Subject Selection

Thirty subjects (15 males and 15 females, aged from 19 to 45) were selected. The subjects had naked eye or corrected vision of 5.0. They did not perform strenuous exercise or watch movies and mobile phones for a long time before the test.



## 2.2 Equipment Parameters

LG42LW4500 (resolution  $1920 \times 1080$ , non-flash (i.e., polarized) 3D technology, screen ratio 16:9) was used with the parameters of contrast 95, backlight 100, and brightness 50 (recommended 3D optimal brightness). The measured brightness value in the mode is  $102.12 \text{ cd/m}^2$ , and the photometer is Photo Research PR-680 model in the USA).

## 2.3 Experiment Procedure

1. Fill in the participant information record form and survey questionnaires.
2. Wear physiological signal sensor and setting the viewing distance to 1.5 m.
3. Measure the physiological parameters in the initial state for 5 min in a quiet state.
4. Fill out a questionnaire every 15 min, with a total of 6 times.
5. Keep and back up the test data and export the data.

## 3 Data Analysis

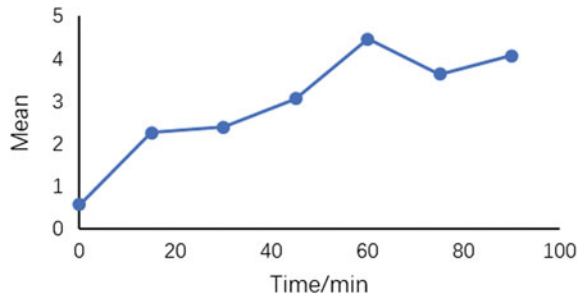
### 3.1 Questionnaire Data Processing and Analysis

Subjective data obtained from subjective questionnaire surveys. The mean statistics of the total subjective fatigue scores are shown in Table 1. The line chart of the changes in scores over time is shown in Fig. 1. At 60 min, due to the limited backup battery, battery replacement and recalibration procedures will be performed, which will make the subjects have 90 s rest time, so 60 min to 75 min, the score may not rise but may be the reason for getting rest. This also shows that during the period of visual fatigue, a short rest period can make people recover to a certain extent.

**Table 1** Statistics of questionnaire score

Time duration/min	Minimum	Maximum	Mean	Std. deviation
0	0.00	3.00	0.57	0.90
15	0.00	10.00	2.27	3.37
30	0.00	7.00	2.40	2.29
45	0.00	8.00	3.07	2.49
60	0.00	10.00	4.47	3.41
75	0.00	8.00	3.64	2.41
90	0.00	8.00	4.07	2.63

**Fig. 1** Polyline for mean of fatigue score



Correlation analysis showed that at a test level of 0.01, the correlation coefficient between the fatigue score of the questionnaire and the time spent watching 3D videos was 0.894, which was extremely strong relationship. The Shapiro–Wilk test method was used to test the fatigue score data for normality. The test results are shown in Table 2.

Table 2 shows that the data for 45 min and after watching the 3D video conform to the normal distribution, and the p-values of the previous data are less than 0.05, which do not conform to the normal distribution. The Wilkerson symbol rank test and the paired t-test were used to compare the different viewing times with those when not watching, and the differences were analyzed. The results are shown in Table 3.

From the pairwise comparison in Table 3, it is known that the *p*-value of the baseline data compared with the data of 30 min, 45 min, 60 min, 75 min, and 90 min are all less than 0.05. It shows that with the increase of time, subjective visual fatigue has shown a significant increase. In addition, the comparison of the data of the adjacent two groups shows that there is significant difference in the comparison between 30–45 min and 45–60 min, which indicates that the subject has a stronger sense of fatigue during this process, especially in the process of 45–60 min, which also has statistically significant at the significance level of 0.01.

**Table 2** Results of normality test for the questionnaire

Time duration/min	Shapiro–Wilk		
	Statistic		Sig
0	0.701		0.000
15	0.686		0.000
30	0.867		0.031
45	0.922		0.205
60	0.886		0.059
75	0.960		0.684
90	0.925		0.231

**Table 3** Pared comparison for fatigue score

Comparison	Test method	<i>p</i> -value
0 versus 15	Wilcoxon signed-rank test	0.058
0 versus 30	Wilcoxon signed-rank test	0.015
0 versus 45	Wilcoxon signed-rank test	0.004
0 versus 60	Wilcoxon signed-rank test	0.002
0 versus 75	Wilcoxon signed-rank test	0.002
0 versus 90	Wilcoxon signed-rank test	0.001
15 versus 30	Wilcoxon signed-rank test	0.796
30 versus 45	Wilcoxon signed-rank test	0.039
45 versus 60	Paired samples t-test	0.001
60 versus 75	Paired samples t-test	0.253
75 versus 90	Paired samples t-test	0.463

### 3.2 RESP Signal Analysis

#### 3.2.1 Time Domain Analysis

Perform time domain analysis on the RESP signal, and analyze the average value of the RESP over a period, that is, the average value of the respiratory frequency.

First, the data was tested for abnormality. Under the criterion of  $z = 3$ , there were no abnormal values. Correlation analysis of respiratory frequency to time showed that the respiratory frequency was significantly negatively correlated with time, with a correlation coefficient of  $-0.784$  and a *p*-value of  $0.037$ .

Descriptive statistics of the mean respiratory frequency showed that the mean value decreased from 24.5 rpm to 19.5714 rpm, but there was no significant change in the entire data and time, as shown in Fig. 2. The normality of each group of data was tested, and all groups were normally distributed. The paired samples t-test was performed on the results. The test results are shown in Table 4. The results show that, under the significance level of 0.05, although the mean value of respiratory frequency is significantly lower than that of the non-watched 3D video when watching 90 min of

**Fig. 2** Mean of RESP value to time

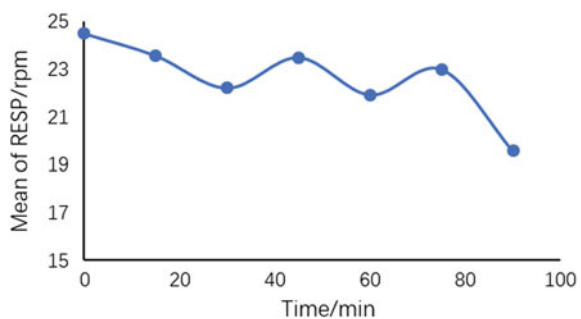


**Table 4** Paired samples t-test results

Comparison	<i>p</i> -value
0 versus 15	0.391
0 versus 30	0.174
0 versus 45	0.576
0 versus 60	0.127
0 versus 75	0.389
0 versus 90	0.078
15 versus 30	0.438
30 versus 45	0.346
45 versus 60	0.403
60 versus 75	0.562
75 versus 90	0.226

3D video, this change has not shown statistical significance. Therefore, visual fatigue under 3D display cannot be accurately measured with the time domain characteristics of respiratory indicators.

### 3.2.2 Frequency Domain Analysis

The frequency domain analysis indicators of the breathing index are power and peak, respectively. The two indexes represent the power of the breathing band and the maximum value of the breathing frequency, that is, breathing power and breathing peak. Descriptive statistics of the two indicators are shown in Table 5.

Correlation analysis between power and peak values and viewing time shows that the average and standard deviation in power are strongly correlated and extremely correlated with time, while all parameters in the peak index are extremely weakly correlated or unrelated. Therefore, only the power value is analyzed.

In the power indicator, it can be seen clearly that the average value and the standard deviation decrease gradually. The power value decreases from  $538.6423\%^{2}$  in the initial state to  $166.24\%^{2}$  in the 90 min.

The data was abnormal at 60 min, which is consistent with subjective measurement data. It shows visual fatigue sharply from 45 to 60 min. And after adjustment, it returns to the normal level at 75 min. Removing the data at 60 min, a curve was drawn for the mean of power and standard deviation as showed in Fig. 3. It shows a general trend of slow decline. This indicator also reflects the decline of the human's breathing power, and the breathing gradually slows down. Combined with the subjective questionnaire, it appears along with visual fatigue caused by 3D video viewing.

After entering the 3D video viewing state, the power mean basically shows an obvious linear distribution. Pearson correlation between power mean and time is  $-0.803$  with sig.(2-tailed) 0.030, while the stand deviation is  $-0.779$  and  $0.039$ , separately.

**Table 5** Paired samples t-test results

Index	Duration/min	Mean	Std	95% confidence interval of the difference	
				Lower	Upper
Power (% <sup>2</sup> )	0	538.6423	471.1533	253.9272	823.3574
	15	296.8508	287.2676	123.256718	470.444821
	30	247.7692	249.6864	96.885269	398.653192
	45	225.02	228.5998	86.878503	363.1615
	60	85.8908	60.96885	49.047659	122.733880
	75	188.9823	181.9452	79.033900	298.930715
	90	166.24	181.1512	56.771437	275.708563
Peak (HZ)	0	0.6214	0.09750	0.5651	0.6777
	15	0.6500	0.08549	0.6006	0.6994
	30	0.6357	0.074495	0.5927	0.6787
	45	0.657 <sup>*</sup>	0.085163	0.6080	0.7063
	60	0.6714	0.091387	0.6187	0.7242
	75	0.6357	0.08419	0.5871	0.6843
	90	0.6214	0.089258	0.5699	0.6730

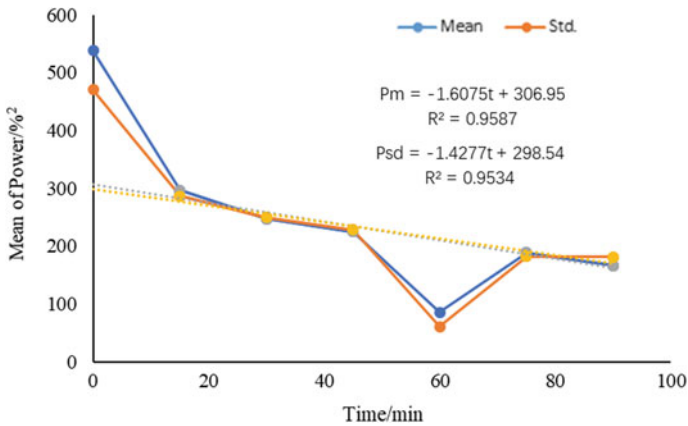


**Fig. 3** Power mean and standard deviation along with time

The trend lines are added separately to find that the relationships between the power mean ( $P_m$ ) for the breathing frequency domain and the time  $t$  for viewing the 3D video is consistent with:

$$P_m = -1.6075t + 306.95, R = 0.9587.$$

**Table 6** Power indicator normally test

Duration/min	Shapiro–Wilk	
	Statistics	Sig
0	0.888	0.092
15	0.859	0.037
30	0.799	0.007
45	0.845	0.024
60	0.919	0.243
75	0.843	0.023
90	0.758	0.002

Relationships between the standard deviation of the power mean ( $P_{sd}$ ) and the time  $t$  for watching 3D video:

$$P_{sd} = -1.4277t + 298.54, R = 0.9534.$$

It can be seen from the fitting degree of the two trend lines that their fitting degrees are both greater than 0.95, which indicates good fitting degree of the regression line to time. Correlation analysis was performed between the mean and standard deviation of power and subjective scores, the correlation coefficients were both  $-0.971$ , and the  $p$ -value was 0. Therefore, visual fatigue can be evaluated using power or standard deviation. And the 3D video viewing time (greater than 15 min) can be estimated based on the power value of the RESP indicator, which provides guidance for the application of future physiological indicators to monitor 3D visual fatigue.

In order to observe the regularity of the data distribution further, a normality test was performed on the power value. The results are shown in Table 6.

Based on the normality test results, under the test level of 0.05, five groups of power indicators do not meet the normal distribution, and two groups of peak indicators do not meet the normal distribution. The initial time is compared with the value of each the remaining time periods, and the paired sample t-test and Wilkerson signed-rank test are used for pairwise analysis, respectively. The results are shown in Table 7. There are significant differences between the viewing time and the initial time, while the  $p$ -value does not show a significant change trend. Among the comparison of neighboring 15 min, there are significant differences between 45 and 60 min and between 60 and 70 min, which is consistent with the questionnaire analysis.

## 4 Conclusions

1. Questionnaire survey showed that subjective visual fatigue increased significantly after watching 3D videos for 30–60 min, especially during the period of 45–60 min, subjective visual fatigue increased significantly.

**Table 7** Pair test of power mean

Comparison	Test method	<i>p</i>
0 versus 15	Wilcoxon signed-rank test	0.039
0 versus 30	Wilcoxon signed-rank test	0.046
0 versus 45	Wilcoxon signed-rank test	0.046
0 versus 60	Pared samples t-test	0.005
0 versus 75	Wilcoxon signed-rank test	0.009
0 versus 90	Wilcoxon signed-rank test	0.016
15 versus 30	Wilcoxon signed-rank test	0.701
30 versus 45	Wilcoxon signed-rank test	0.279
45 versus 60	Wilcoxon signed-rank test	0.009
60 versus 75	Wilcoxon signed-rank test	0.028
75 versus 90	Wilcoxon signed-rank test	0.6

2. The consistency of the power mean and standard deviation in the breathing frequency domain to subjective visual fatigue is 0.971. The power mean and standard deviation shows strong correlation with time, and the correlation coefficient is  $-0.779$  and  $-0.803$ , respectively.
3. After watching the 3D video for 15 min, the relationships between the power mean ( $P_m$ ) and standard deviation ( $P_{sd}$ ) in the breathing frequency domain and time  $t$  meets:  $P_m = -1.6075t + 306.95, R^2 = 0.9587; P_{sd} = -1.4277t + 298.54, R^2 = 0.9534$ .
4. The increase in 3D visual fatigue leads to a decrease in respiratory frequency, but the average respiratory frequency does not reflect the working time of visual fatigue; there is no significant correlation between peak value and visual fatigue.

**Acknowledgements** This work is supported by National Key R&D Program of China (2017YFF0206604) and General Project of China University of Labor Relations (20XYJS020).

**Compliance with Ethical Standards** The study was approved by the Logistics Department for Civilian Ethics Committee of China University of Labor Relations.

All subjects who participated in the experiment were provided with and signed an informed consent form.

All relevant ethical safeguards have been met with regard to subject protection.

## References

1. Wang YJ, Gao XL, Shi HM, Zhang YL, Wang Q, Bai Y (2016) Influence of polarized 3D displayer on visual function. *J Tianjin Med Univ* 22(04):328–331
2. Yano S, Emoto M, Mitsuhashi T (2004) Two factors in visual fatigue caused by stereoscopic HDTV images. *Displays* 25(4):141–150
3. Kooi FL, Toet A (2004) Visual comfort of binocular and 3D displays. *Displays* 25(2–3):99–108
4. Matsuura Y (2019) Aftereffect of stereoscopic viewing on human body II. In: *Stereopsis and hygiene*. Springer, Singapore, pp 89–99

5. Alhaag MH, Ramadan MZ (2017) Using electromyography responses to investigate the effects of the display type, viewing distance, and viewing time on visual fatigue. *Displays* 49:51–58
6. Lambooij M, Fortuin M, Heynderickx I, IJsselsteijn W (2009) Visual discomfort and visual fatigue of stereoscopic displays: a review. *J Imag Sci Technol* 53(3):30201-1
7. Li HCO, Seo J, Kham K, Lee S (2008) Measurement of 3D visual fatigue using event-related potential (ERP): 3D oddball paradigm. In: 2008 3DTV conference: the true vision-capture, transmission and display of 3D video. IEEE, pp 213–216
8. Tam WJ, Speranza F, Yano S, Shimono K, Ono H (2011) Stereoscopic 3D-TV: visual comfort. *IEEE Trans Broadcast* 57(2):335–346
9. Park MC, Mun S (2015) Overview of measurement methods for factors affecting the human visual system in 3D displays. *J Display Technol* 11(11):877–888
10. Kim CJ, Park S, Won MJ, Whang M, Lee EC (2013) Autonomic nervous system responses can reveal visual fatigue induced by 3D displays. *Sensors* 13(10):13054–13062
11. Mehler B (2015) Recording heart rate & electrodermal activity as measures of cognitive load in the driving environment. <https://doi.org/10.13140/RG.2.1.2050.6329>
12. Aryal A, Ghahramani A, Becerik-Gerber B (2017) Monitoring fatigue in construction workers using physiological measurements. *Autom Constr* 82:154–165
13. Yuhong Z, Haiping L, Fusheng Z, Mantian LI, Wei G, Pengfei W (2014) Real-time monitoring system for driver's fatigue states based on respiratory signal. *J Jiangnan Univ (Nat Sci Ed)* 13(01):55–59
14. Yu Q (2018) The design and implementation of the mobile terminal heart rate analysis engine based on photo-plethysmograph imaging technology. Master Thesis of Beijing University of Posts and Telecommunications, Beijing University of Posts and Telecommunications, Beijing
15. Xu S (2012) The study on the discriminating method of driving fatigue based on physiological signal. Master Thesis of Beijing University of Technology, Beijing University of Technology, Beijing
16. Ye CW (2018). Research on automobile driving fatigue based on ECG signal and EMG signal (Doctoral dissertation). Master Thesis of Hefei University of Technology, Hefei University of Technology, Hefei
17. Fu RR, Tian YS, Wang SC, Wang L (2019) The recognition of driver's fatigue based on dynamic Bayesian estimation. *Chin J Biomed Eng* 38(06):759–763



# Man-Machine System Design for Rest-Office Seats



Jiawei Tang, Canqun He, Yuhong Wei, and Chenfei Cao

**Abstract** The modern people's habit of sitting on the seat for a long time and lying on the table for a rest has seriously affected their health. The reasonably designed rest-office seats can provide office workers with healthy work conditions and comfortable rest conditions, helping office workers to reduce diseases such as spondylosis and improve work efficiency. This paper analyzes the existing office seats from the perspective of ergonomics and clarifies the basic functions and potential development possibilities of rest-office seats. The two methods of element shape extraction and user demand analysis were applied to the design and development of rest-office seats. It has a certain guiding significance and reference value for the future office seating style, the development of additional functions and the appearance design of seats. It also improves the user experience.

**Keywords** Ergonomics · Office seats · Healthy sitting position · Rest-office dual use · Optimized design

## 1 Introduction

With the rapid development of technology in modern society, people sit at desks and work longer and longer. According to surveys, modern people have been "sitting" for more than half of their awake time. "Sedentariness" is likely to cause problems such as poor blood circulation, compression of the spine and other problems, which has become the mainstream harmful behavior [1]. Not only that, modern office workers often lie on the desktop to take a break from time to time. Such changes in habits have seriously affected the health of office workers and work efficiency. Therefore, the design of seats that are closely related to rest and work should be based on ergonomics, fully consider the comfort of users when they work and rest, the additional needs of

---

J. Tang · C. He (✉) · Y. Wei · C. Cao  
College of Mechanical and Electrical Engineering, Hohai University, Changzhou 213022, China  
e-mail: [hecq@163.com](mailto:hecq@163.com)

users and alleviate the occupational health problems of workers in the information-based office environment. It further develops the “human-material-environment” system design thinking in ergonomics.

## **2 Ergonomic Analysis of the Existing Seats**

At present, the research of office seats is a popular direction of ergonomics research.

The main research topics include the matching between the size of the office seat components and the size of the human body, the matching between the local adjustment of the office seats and the change in sitting posture and the additional functions of the office seats.

The office seats on the market generally have one or more of the following characteristics: The functional dimensions of the seats conform to the size and curve of the sitting posture, so as to increase the comfort [2]; the seat provides sufficient support and stability; the seat has a high degree of adjustment, especially on the waist support, which can meet the needs of users with different characteristics; the seat is multi-functional, with additional functions to meet the needs of a certain crowd; The cushions and backrests are mostly made of soft materials [3]; the styling lines, texture and color matching are distinctive; the seat is intelligent.

## **3 The Analysis of Man-Machine System Design for Rest-Office Seats**

### **3.1 Sizes**

In the design of a rest-office seat, size is the most basic [4]. The size parameters and structure of the seat must meet the national standard human body size in sitting [5], to meet the sitting comfort, operation comfort, and mobile convenience and so on.

#### **3.1.1 Overall Size of the Seat**

In the case of office seat, a user usually has an upright upper body, with the forearms on the table, legs drooping on the ground, and the seat height can be adjusted to meet the needs of most users [6]. Combined with human body size in sitting, the seat height is designed to be 350–500 mm, adjustable. The main indicator of seat depth is that when the body sits straight on the seat, the feet do not touch the ground [7]. According to the reference values of several common seat surface inclinations, the seat surface inclination of office seats is 5° or less, and the seat surface inclination of sofas is 8°–15° [8]. In order to have both functions of work and rest, according to

the human back electromyography test results, when the seat surface is tilted back about  $23^\circ$ , the muscle activity is the smallest to adapt to different working conditions. Combined with human body size in sitting, the seat width is designed at 480 mm; the seat depth is designed at 350–500 mm, which can be adjusted; the seat inclination is designed at  $3^\circ$ – $20^\circ$ , adjustable. Common seats are 65–75 mm thick. Combined with human body size in sitting, the seat thickness is designed to be 70 mm.

### **3.1.2 Size of Headrest**

User needs to relax for a short time during the work process; the head and neck should be supported accordingly. According to the human body size in sitting, the width of the headrest is 290–330 mm, and the height is the best at 190–200 mm. Therefore, the width of the headrest is designed to be 310 mm, and the height of the headrest is designed to be 195 mm.

### **3.1.3 Size of Backrest and Lumbar Support**

According to the human body size in sitting, the width of the backrest should be slightly larger than the maximum width of shoulder and elbow in sitting position, taking into account actual comfort. Therefore, the width of the backrest is designed to be 480 mm. Depending on different support forms of the backrest [9], the back angle of the office seat should be  $93^\circ$ , and the back angle of the rest seat should be  $127^\circ$ . The height of the backrest can be adjusted from 520 to 640 mm in combination with the human body size in sitting, and the inclination of backrest can be adjusted from  $90^\circ$  to  $140^\circ$ .

The lumbar support is a component that relieves waist fatigue from sitting for a long time. The curve of the lumbar should be as close as possible to the physiological curve of the human body, so as to play an effective supporting role, reduce the pressure of the lumbar spine and reduce the static muscle load [10]. According to the human body size in sitting, the width of the backrest is designed to be 480 mm, the height of the backrest is designed to be 200 mm, and the backrest is about 225 mm from the front edge of the armrest.

### **3.1.4 Size of Armrest**

The distance between the armrests should be slightly wider than the horizontal size of the human body and match the width of the seat back and seat surface, keeping the arm parallel to the keyboard. Combined with human body size in sitting, the width of the armrest is designed to be 50 mm; the height from the seat surface is adjustable from 210 to 270 mm; the distance between the two armrests is adjustable from 380 to 500 mm.

### 3.1.5 Size of Feet

Common seats are made up of five-star feet, consisting of a chassis and casters. In consideration of stability, the diameter of the five-star feet should be compatible with the widest size of the seat, usually 480–600 mm. Therefore, the design is 520 mm.

Based on the above analysis, a rest-office office seat is preliminarily designed. Figure 1 is a schematic view of the back and side views of the rest-office seat.

### 3.2 Patterns

In the design practice, the product form is the appearance and visual experience of the product design, and it is also a result that the designer has completed to achieve product design [11]. The most basic requirement of users for the rest-office seat is safety. On this basis, users want office seats to be elegant and harmonious with the work environment. Through investigation, analysis and screening, the element of Roman columns representing stability and element of shells representing elegant are finally obtained.

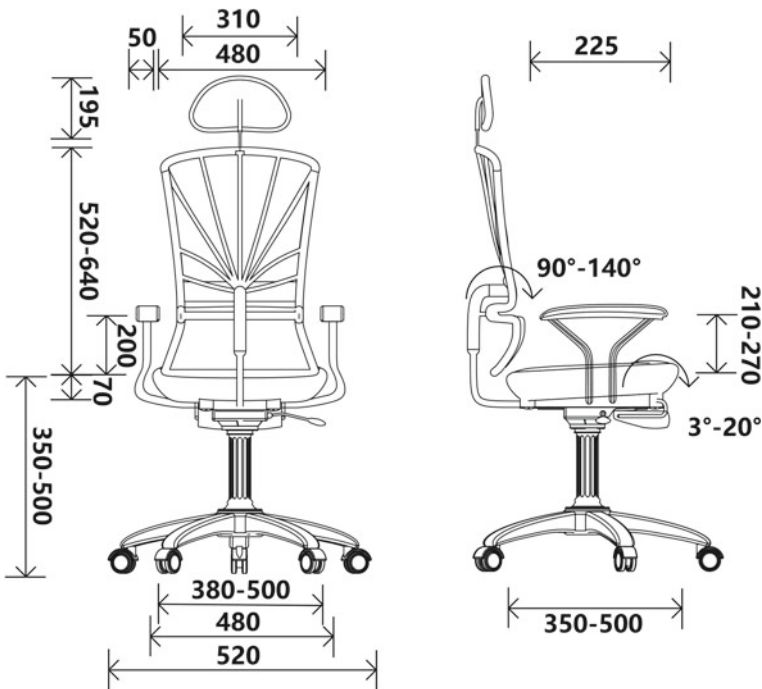


Fig. 1 Rest-office seat

The simplification of element is to gradually refine the element by choosing or changing the secondary structural features while maintaining the main features of the element [12]. The process of extracting the shape of the Roman column is shown in left of Fig. 2. Based on the original shape of the Roman column, the line is simplified to extract the most important stripe features. The selection of the seat bottom supporting pole and armrest supporting pole as the element application objects is based on that they are the main functions of support and related to the inner meaning of the Roman column element. It transforms the characteristics of safety implicitly to users. The design is shown in the right of Fig. 2.

The process of extracting the shell shape is shown in left of Fig. 3. Firstly, the overall texture of the shell is described. Delete the outer contours. Protrude the bumpy lines on the surface of the shell. It maintains the characteristics of the shell and keeps

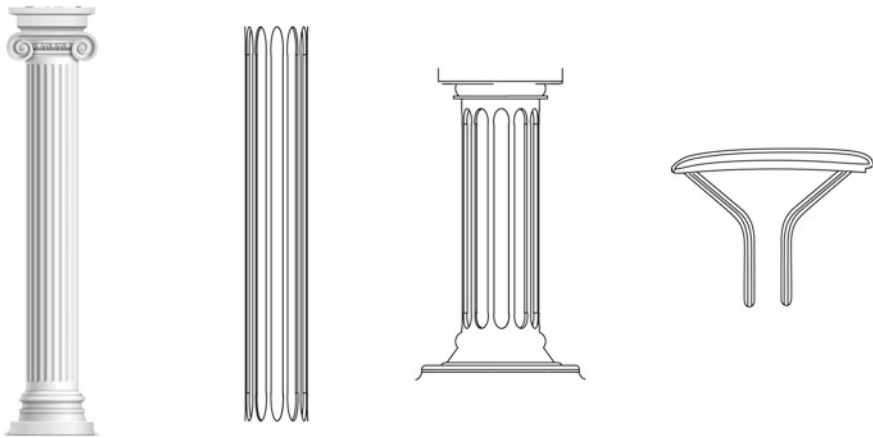


Fig. 2 Extraction process and the application of Roman columns

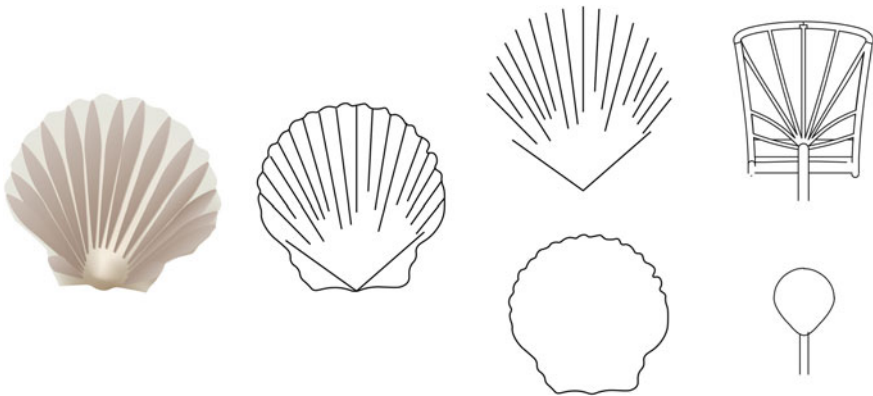


Fig. 3 Extraction process and the application of shells

artistic beauty at the same time. Or delete the inner contour lines to highlight the outer contour of the shell. Choosing the lever handle and the seat back as the design objects is mainly based on the following two points: The lever handle can best reflect the distinctive detail part; the shape of the seat back can best guide the appearance to users. The design is shown in right of Fig. 3.

The shape design of the seat surface not only affects the shape of the entire seat, but also relates to the user experience. The design should consider the principle of uniform pressure distribution on the human body to minimize the pressure on the thighs and concentrate the pressure on the ischial tuberosity [13]. Aiming at the phenomenon of “slipping” (gradual sliding out of the seat) when sitting [14], according to the sit-pressure distribution chart in Fig. 4 [15], the seat surface adopts the W-shaped design as shown in Fig. 5, and the W-shaped design better fits to the human hips. It can disperse force uniformly and relieve the pressure of sitting for a long time.

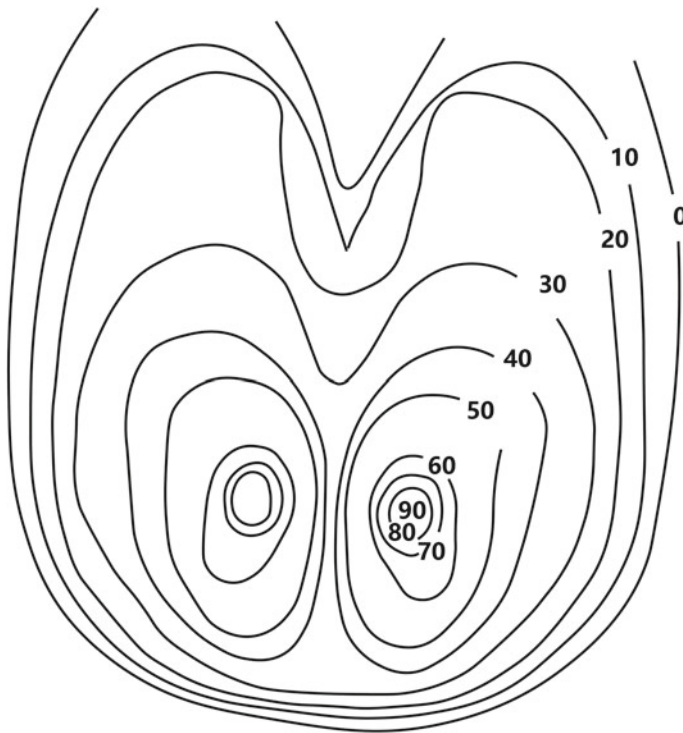
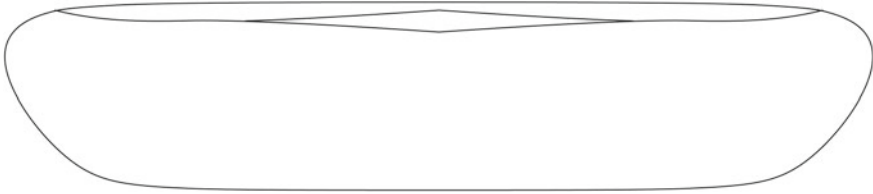


Fig. 4 Sit-pressure distribution chart



**Fig. 5** Improved seat surface design

### **3.3 Features**

Rest-office seats as office supplies should first have practical functions. According to the survey, people are eager to office seat design can break the routine, in terms of functional breakthroughs, should be added some additional features. Therefore, scientific analysis of user behavior and use characteristics of seats is needed to design a rest-office seat that meets the needs of people’s physiological and psychological functions [16].

#### **3.3.1 Automatic Hook, Effective Use of Space**

Office space is limited and the items are cluttered. Clothes are hanging casually on the seat and easily slipping and wrinkled. An automatic hook as shown in Fig. 6 is provided on the backside of the seat, the connection between the headrest and the backrest. It is open when in use. It automatically rebounds and retracts after removing items on the hook. It does not prevent users from passing behind the seat. It makes efficient use of space. This kind of hook has a bearing capacity of about 10 kg and can be used to hang light weight objects such as clothes and briefcases.

#### **3.3.2 Folding Footrest for a Comfortable Rest**

The work area and the rest time are limited. In order to correct harmful sleeping postures, a folding footrest is designed at the bottom of the seat as shown in Fig. 6. It is flexible and scalable, and it does not take up space. Thickened steel pipe and high elastic sponge effectively support legs. Telescopic length and inclination are adjustable. After the leg is increased in support, it is not easy to slide, leg force is reduced, and it gets your blood moving more smoothly.

#### **3.3.3 Smart Automatic Adjustment Lumbar Support**

Because most people use non-adjustable office seats. There are many uncomfortable parts for users. A smart automatic adjustment lumbar support helps maintain accurate

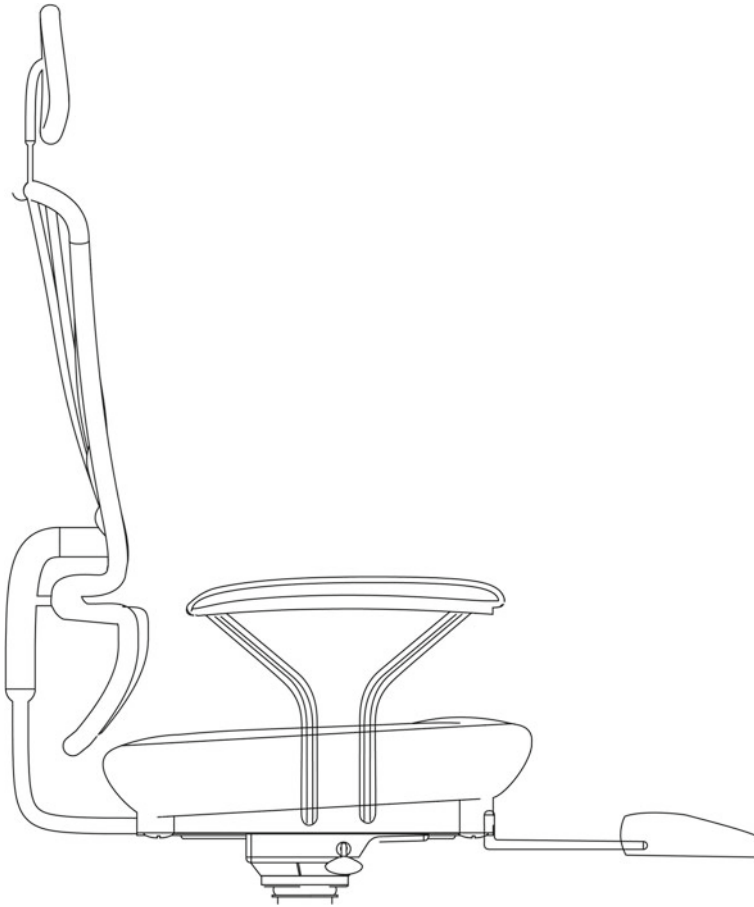


**Fig. 6** Additional functions

body posture and alignment of the spine and neck. However, most users do not know how to use the adjustment function or cannot adjust the product to the most suitable state. In response to the above situation, the seat is designed with a smart lumbar support as shown in Fig. 6. The rear of the smart lumbar support is provided with a spring, which automatically adjusts the lumbar support inclination and elastic output according to different body shapes and body pressures of the user. It maintains close support at any time and reduces the impact of adverse health effects.



## 4 Conclusion

The design of modern rest-office seats should keep “people” in the core and pay more attention to the human-machine interaction factors in the adjustment, functions of the seats to improve the rationality and comfort of the seat. However, the higher the adjustability of the seat is, the worse the stability of the seat is. Therefore, the adjustment designs are designed to use the way of locking adjustment, but the wear caused by frequent adjustments cannot be completely avoided. The paper has certain guiding significance and reference value for future rest methods in the office, development of additional functions and appearance design and provides office staff with more comfortable and healthy work environment.

**Acknowledgements** The study is financially supported by National Innovation Training Program for College Students of Hohai University (2019102941052).

## References

1. Lijun W (2013) Study on the comfort of desk and chair based on physiological and psychological response. Beijing Forestry University, Beijing
2. Wanfu Y, Fuchang Z (2017) Research on comfort design of office seats based on ergonomics. Packaging engineering, China
3. Gang T (2011) Research on the generalization of office chair design. Hunan University, Hunan
4. Jinfeng W, Tiefeng Z, Pengtao S et al (2007) Application of ergonomics in furniture design. Packaging engineering, China
5. National Standard of The People's Republic of China Chinese adult body size. GB 10000-88.1989, China Standard Press, Beijing
6. Jianxiang L, Fuchang Z, Limin S (2005) Ergonomics of sitting posture and seat design. Ergonomics, China
7. Shuqing X, Xinshu J, Yanmei D (1995) Physiology of sitting posture and chair adjustment. Foreign medicine (nursing volume), China
8. Fan Z (2010) Ergonomics design concept and application. Sinohydro Press, Beijing
9. Baoxiang R (2006) Foundation and application of human engineering. Mechanical Industry Press, Beijing
10. Kezhong W (2013) Research and development of sooth multifunctional office chair. Zhejiang University of Technology, Hangzhou
11. Meihong L, Xiu A (2013) How to use form elements to achieve product innovation design. Art and design (Theory), China
12. Canqun H, Jiao L, Xiaomin T, Xianshu L (2016) Research on Wuxi personalized tourism product design based on cultural characteristics. Packaging engineering, China
13. Qiliang Z, Wei Y (2011) Ergonomics analysis in office chair design. J Lanzhou Inst Technol, Lanzhou
14. Gang R, Qinghua M, Wei X, Feng C (2019) Study on static balance parameters of office seats. J Lanzhou Inst Technol Mech Des Manuf, China
15. Yulan D (2000) Ergonomics. Beijing University of Technology Press, Beijing
16. Canqun H, Huijuan Z (2008) Ergonomics research in folding furniture. Decoration, China

# Concept Plan and Simulation of On-Orbit Assembly Process Based on Human–Robot Collaboration for Erectable Truss Structure



Xinyue Zhu, Changhuan Wang, Meng Chen, Shiqi Li, and Junfeng Wang

**Abstract** Considering the future construction of large erectable truss structure in space station, concept design and simulation of on-orbit assembly task are conducted based on human–robot collaboration. The therbligs level tasks of truss structure are decomposed layer-by-layer according to the characteristics of the truss bay. An assembly task model is established based on hierarchical task analysis. The human and robot functional performances associated with the assembly operation in space are compared and analyzed to establish the description of human–robot ability constraints. The comparing allocation principle is adopted to determine the distribution of human and robot collaborative assembly task. DELMIA is used to simulate the assembly process of truss bay and the feasibility of human–robot collaboration is verified.

**Keywords** Erectable truss structure · Human–robot collaboration · On-orbit assembly · Task model · Therbligs · Plan and simulation

## 1 Introduction

On-orbit assembly is considered as an efficient method to construct large structural platform of space station [1]. There are three phases for research and practices of on-orbit assembly according to human–robot collaboration mode.

The first phase is the manual assembly stage of astronauts with assistance. From the 1970s to the early 1990s, Langley Research Center (LRC) conducted a series of research on the astronauts manual assembly with large space structures [2]. NASA carried out the space assembly concept experiment of the erectable truss structure on

---

X. Zhu · S. Li · J. Wang (✉)

School of Mechanical Science and Engineering, Huazhong University of Science and Technology, Wuhan 430074, China

e-mail: [wangjf@hust.edu.cn](mailto:wangjf@hust.edu.cn)

C. Wang · M. Chen

Aerospace System Engineering Shanghai, Shanghai 201108, China

© The Editor(s) (if applicable) and The Author(s), under exclusive license to Springer Nature Singapore Pte Ltd. 2021

S. Long and B. S. Dhillon (eds.), *Man-Machine-Environment System Engineering*, Lecture Notes in Electrical Engineering 645, [https://doi.org/10.1007/978-981-15-6978-4\\_78](https://doi.org/10.1007/978-981-15-6978-4_78)

the space shuttle Atlantis performing the mission STS-61B, which verified the feasibility of on-orbit assembly of large space structures [3]. The second phase is space robot assembly stage. In the early 1990s, LRC developed a remote-controlled robot system for assembling of space truss structure [4]. At the third stage of assembly based on human–robot collaboration, remote-controlled space robots have expanded the opportunities for human and robot to work together in space [5]. Johnson Space Center carried out a simplified extra-vehicular assembly task experiment to evaluate the human–robot team cooperation strategy with different configurations of astronauts and robonauts. Two robonauts and one astronaut participated in the ground experiment of human–robot cooperation truss assembly based on STS-61B flight experiment [6]. On-orbit services at space station based on human–robot collaboration system also were paid more and more attention [7]. Astronauts and robots could work independently and cooperatively so as to achieve their complementary advantages, which can reduce the risk of completing space missions [8].

Aiming at the on-orbit human–robot collaborative assembly of erectable truss structure, hierarchical task analysis (HTA) is adopted to build the task model, and the human–robot characteristics under space environment are analyzed in this paper. The assembly task flow of human–robot collaboration is planned, and the assembly task of erectable truss structure is verified by virtual simulation.

## 2 The Erectable Truss Structure

The erectable truss structure of this paper composes of a several truss bay as shown in Fig. 1a. A truss bay in Fig. 1b includes two pre-assembled components, four electrical struts and four long struts. A pre-assembled component composes of four short struts, four long struts and four nodes.

In the plan of assembly process, it is assumed that the pre-assembled components in the cabin are mounded by long robot of space station and used to connect the adjacent truss elements. The subsequent truss elements will be assembled on the basis of the assembled truss structure. Therefore, the assembly task of truss structure

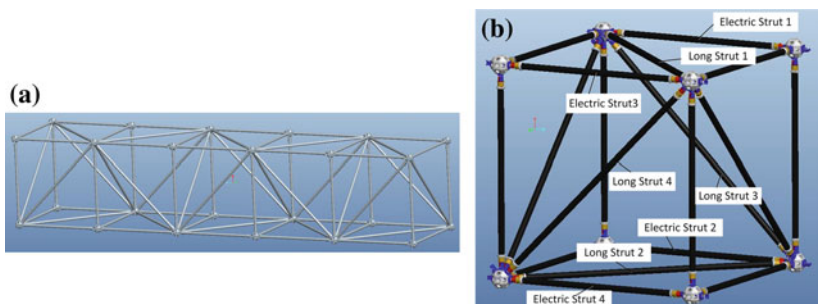


**Fig. 1** Diagram of space truss. **a** Erectable truss and **b** truss bay

in this paper can be regarded as the repeated assembly work of truss element on the unit level. That is, there are eight struts will be assembled repeatedly based on human-robot collaboration.

The assembly scene truss structure mainly includes one astronaut, one 6-DOF robot arm and the truss transportation mechanism (Fig. 2). Considering the smaller movement range and moving difficulty in the space environment, astronaut and robot are fixed at two outsides of truss transportation direction. The transportation mechanism extends outward after assembly of a truss bay.

In this paper, the geometric and process constraints of the truss are clear. Therefore, the assembly sequence of the eight struts can be obtained by the assembly sequence planning method based on the assembly priority constraint relationship and are not detailed here.

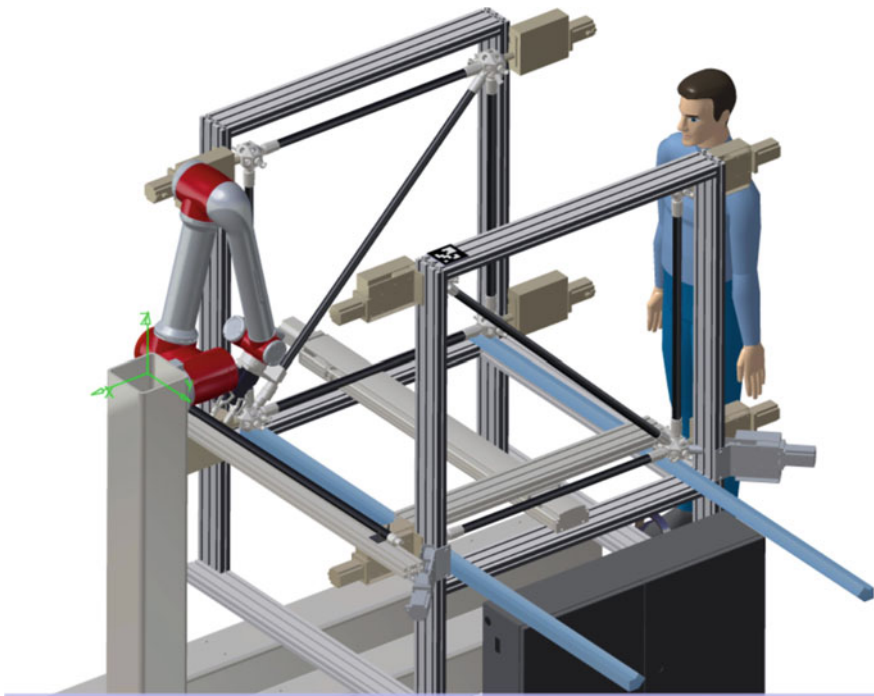


**Fig. 2** Diagram of on-orbit assembly scene

### 3 HTA-Based Assembly Task Model for Truss Struts

#### 3.1 Therbligs of Strut Assembly Tasks

Therblig is defined as the basic action required to complete a task [9]. Through the analysis of therblig, the specific actions and attributes of assembly task are determined, which are the foundation of the modeling and allocation of assembly tasks. The assembly task of truss struts can be regarded as the repeated assembly of a different single strut which includes the similar type of therbligs. In this paper, the assembly process of one strut is taken as an example to describe the analysis process. The basic therbligs needed to complete the assembly of a single strut are reaching, searching, selecting, holding, moving, positioning, assembling and releasing. Based on qualitative and quantitative analysis, the corresponding action attributes of each therblig are determined, as shown in Table 1.

In order to build the overall assembly process of truss structure, four levels architecture is constructed based on task, operation, activity and therblig layer. The highest task level describes the assembly sequence of each truss bay. The three main stages of strut assembly are at operation level. Each stage is then decomposed as several assembly behaviors at activity layer. The lowest level shows the therbligs of each action for assembly behaviors.

**Table 1** Assembly therbligs of truss bay

Behavior	Description of operation	Therbligs	Property
Assembly pre-positioning	Preparatory action for identification	Transport empty (TE)	Reachable range
	Identification	Search (Sh)	/
Choose strut	Select assembly strut	Select (St)	/
Grasp strut	Preparatory action for grasping strut	Transport empty (TE)	Reachable range
	Grasp strut	Grasp (G)	Strut weight
Transport strut	Transport strut to assembly area	Transport loaded (TL)	Reachable range
Position strut	positioning of strut joint and node joint	Position (P)	Precision
Assembly strut	Push down to fit the strut and the node	Assemble (A)	Assembly force
Task complete	Release the strut to complete the task	Release load (RL)	/

### 3.2 Assembly Task Model of Strut Based on HTA

HTA is a method that describes the temporal relationship and the hierarchies between tasks and their subtasks based on structured meta model [10]. On the basis of hierarchical decomposing of truss assembly task, a formal HTA model for assembly task of truss structure is build using goal, task, plan and operation element (Fig. 3). The new parameters of operation element are designed as object and property for strut assembly process. Taken strut 3 as an example, there are seven assembly behaviors which are described as plan 1 to plan 7. For each plan, there are different therbligs, objects and properties in operation elements.

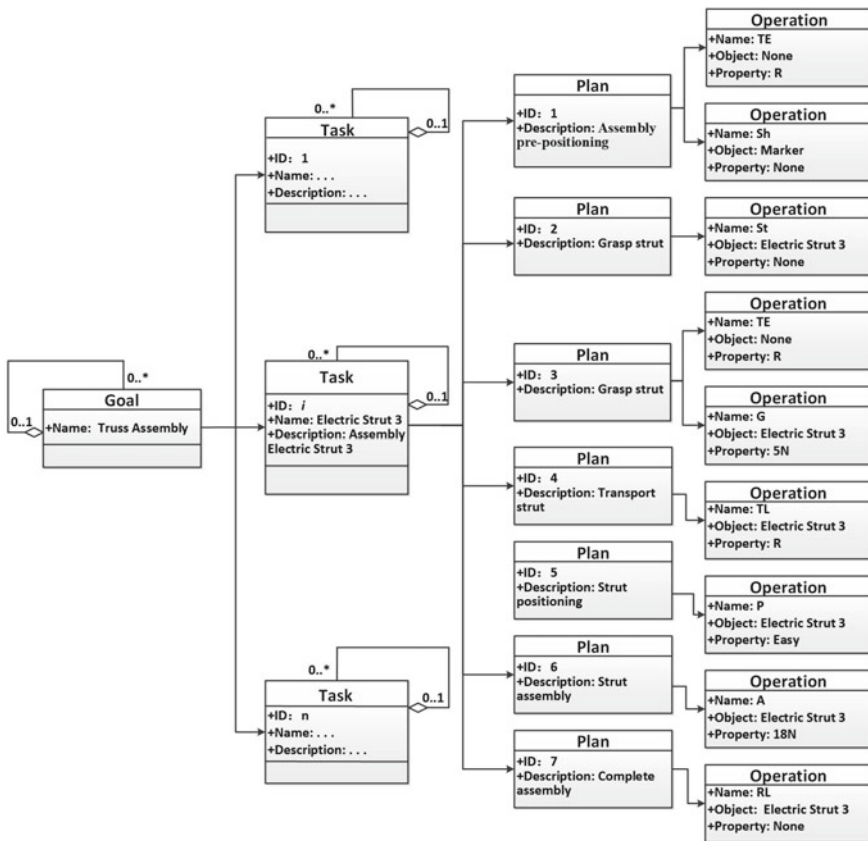


Fig. 3 Assembly task model based on HTA

## 4 Assembly Task Allocation and Simulation

### 4.1 Human–Robot Task Assignment Considering Ability

The working ability of human and robot in space environment must be considered in order to give full play to their advantages and complete space assembly tasks safely, quickly and efficiently.

Under the influence of space environment and spacesuit, the movement ability and operation flexibility of astronauts are reduced. But the hand operation of astronauts is irreplaceable in extra-vehicular activities [11]. The robot arm has the characteristics of high precision, large payload and working radius. From the three aspects [12], i.e., perception, decision-making and execution, the assembly related characteristics of human and robot are summarized in Table 2.

The task allocation principles between human and machine include comparative principle, machine preferential principle, economic principle and dynamic allocation principle [8]. The comparative principle is adopted in this study considering the ability constraints of human–robot and the task allocation flow based on HTA model is shown in Fig. 4.

According to the attribute and object in element of therbligs, four kinds of task for human–robot collaborative work are classified, i.e., H type task executed by human, R type task executed by robot, H/R type task executed by human or robot and H+R type task executed by human–robot cooperation. The main attributes of a therblig are defined differently for assembly operation, e.g., the reachable range is the attribute of TE and TL therblig, the grabbing force is the attribute of G therblig, the accuracy is the attribute of P therblig and the assembly force is the attribute of A therblig.

After the initial assignment of assembly task, H/R tasks are further allocated by judging whether the adjacent therblig is one of the therbligs in an assembly behavior and whether the pre-therblig affects the current one. In order to reduce the complexity and difficulty of operation executed by human or robot independently, we assign higher priority of H+R tasks over H tasks and R tasks. Therefore, H/R tasks may be further assigned as H+R tasks during the task assignment process.

**Table 2** Comparison of human–robot functional characteristics in space

Aspects	Human	Robot
Perception	Perceive overall comprehensive, selective and ambiguous information	Perceive single, precise and quantitative information
Decision-making	Strong comprehensive analysis ability; deal with unexpected events	Large memory; weakness on decision-making; only deal with known issues
Execution	Limited reachable range; small operation force; difficulty of body movement	Wider reachable range; higher accuracy; large operation force and effective load

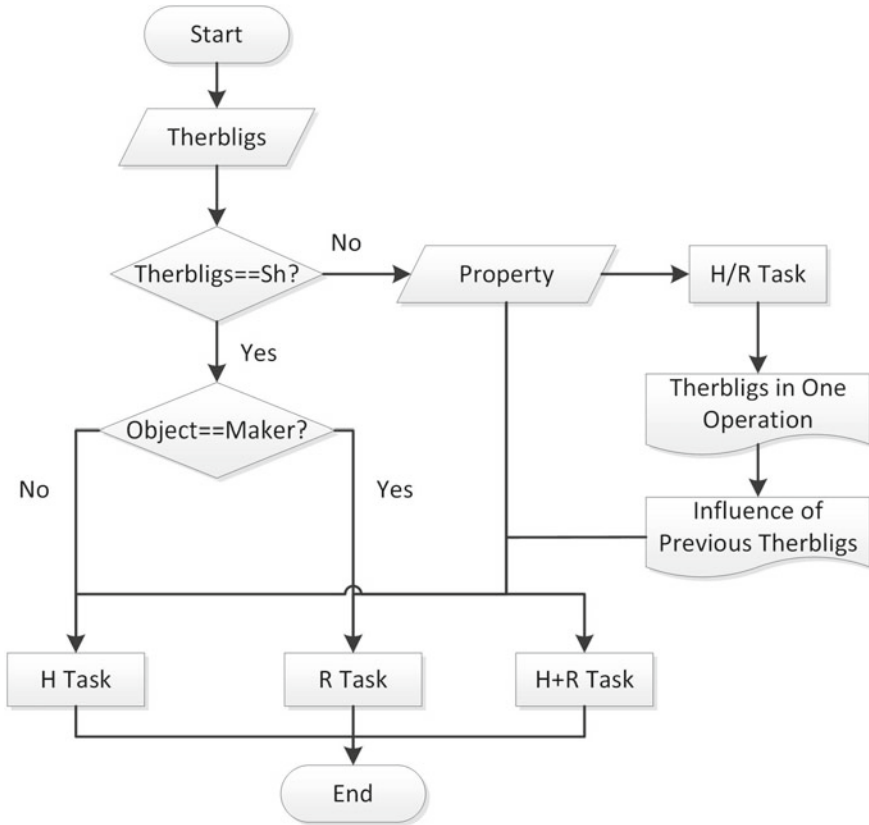


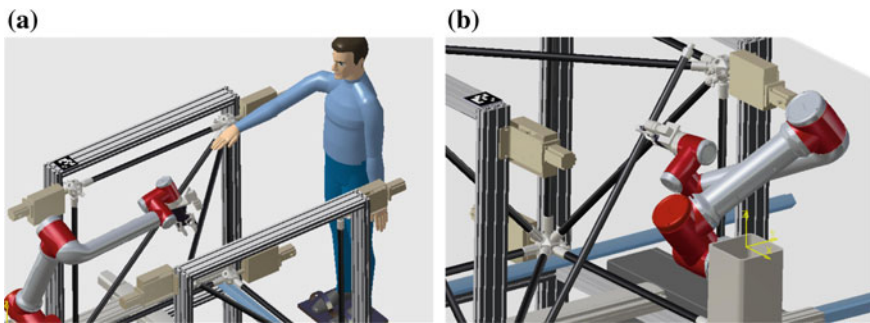
Fig. 4 Human-robot assembly task allocation flow based on ability constraints

According to the above process, the assembly task assignment results of electric strut 3 are shown in Table 3. We take the assembly therblig as an example to explain the task allocation. According to the attribute of assembly therblig, the required assembly force of this strut is within the ability of astronaut and robot. So both human and robot can complete the assembly operation which is classified as H/R task firstly. The assembly therblig in this task has the same object attribute as the pre-therblig position task. In order to keep the continuity of operation, the assembly therblig in this step is assigned as H+R task, which is same as its pre-therblig and executed by human-robot cooperation.



**Table 3** Assembly task allocation of electrical strut 3

Strut	Plan	Therbligs	Property	Correlation
Electric strut 3	Assembly pre-positioning	TE	R task	R task
		Sh	R task	R task
	Choose strut	St	H/R task	H/R task
	Grasp strut	TE	R task	R task
		G	H/R task	R task
	Transport strut	TL	R task	R task
	Position strut	P	H + R task	H + R task
	Assembly strut	A	H/R task	H + R task
Task complete	RL	H/R task	H + R task	

**Fig. 5** Virtual human–robot collaborative assembly simulation. **a** Strut 2 and **b** strut 7

## 4.2 Simulation of Human–Robot Collaborative Assembly Process

DELMIA software is used to simulate the struts assembly process based on the human–robot collaboration. According to the planned assembly sequence of struts, human and robot can independently or collaboratively carry out the assigned assembly tasks, which initially verified the feasibility of the truss assembly task allocation scheme. As an example, the assembly simulation of strut 2 based on human–robot collaboration and the assembly simulation of strut 7 based on robot independent execution are shown in Fig. 5.

## 5 Conclusions and Future Work

Human–robot collaborative assembly of erectable truss structure is needed for future on-orbit service. According to the task characteristics of assembly process, an

assembly task model based on HTA is established. By analyzing the human–robot operation ability in the space environment and adopting comparative assignment principle, the assembly task assignment of the struts between human and robot is completed. The virtual simulation is conducted in DELMIA and the feasibility of assembly task allocation scheme is validated preliminarily. Verifying the scheme rationality of human–robot collaborative truss assembly process based on ground physical experiments is our ongoing work. The operation time of human–robot assembly process will also be studied.

**Acknowledgements** This research is supported by Manned Aerospace Project (040102). The authors thank the reviewers for their helpful suggestions.

## References

1. Bowman LM, Belvin WK, Komendera EE et al (2018) In-space assembly application and technology for NASA's future science observatory and platform missions. In: Space telescopes and instrumentation 2018: optical, infrared, and millimeter wave. International Society for Optics and Photonics
2. Judith JW, Timothy JC, Harold GB (2002). A history of astronaut construction of large space structures at NASA Langley Research Center. In: IEEE aerospace conference proceedings, pp 569–3587
3. Bekey I (1988) Space construction results: the ease/access flight experiment. *Acta Astronaut* 17(9):987–996
4. Ralph W et al (1992) An automated assembly system for large space structure. *Intelligence robotic systems for space exploration*. Kluwer Academic Publishers
5. Sofge D, Bugajska M, Trafton JG et al (2005) Collaborating with humanoid robots in space. *Int J Humanoid Rob* 2(2):181–201
6. Rehnmark F, Currie N, Ambrose RO et al (2004) Human-centric teaming in a multi-agent EVA assembly task. *SAE Trans*, 1105–1113
7. Liangliang H, Jian Y, Meng C et al (2015) Conceptual design of human-robot system for on-orbit service of space station. *Manned Spaceflight* 21(4):322–328
8. Enyong ZHU, Chuanfeng WEI, Zhe LI (2015) Connotation and Key technologies of human-robot collaboration in space. *Spacecraft Eng* 24(03):93–99
9. Oyekan J, Hutabarat W, Turner C et al (2019) Using Therbligs to embed intelligence in work-pieces for digital assistive assembly. *J Ambient Intell Human Comput*. <https://doi.org/10.1007/s12652-019-01294-2>
10. Stanton NA (2006) Hierarchical task analysis: developments, applications, and extensions. *Appl Ergon* 37(1):55–79
11. Wang L, Wang C, Zhou S et al (2012) The demand of EVA work type and movement on astronauts hand operation capability. In: The 12th human-machine-environment system engineering conference. Scientific Research Publishing, China
12. Li H, Zhang B, Huang H (2014) Preliminary concept study on integrated lunar exploration of astronaut and humanoid robot. *Manned Spaceflight* 20(04):301–306

# Experimental Study on Dynamic and Static Work of Shoulder-Mounted Portable Equipment Operators



Zhaofeng Luo, Meng Kang, Peng Zhang, Han Zhang, Huashan Li, Fan Zhou, and Kun Qu

**Abstract** The purpose of this paper is to improve the scientificity of operators' work by analyzing their dynamic and static work performance and how the performance changes through a research on shoulder-mounted equipment operators to measure and compare the operators' work performance at a different time and after a different distance of movement. Based on the Training Achievement Evaluating System, point out the difference of dynamic and static work performance after analyzing the score in a different time. Present the correlations obtained by comparing the performance changes in varied conditions. In this way, find out a method to improve the training of shoulder-mounted portable equipment operators.

**Keywords** Dynamic · Static · Work efficiency

## 1 Significance of Research

The method often used to improve the performance of shoulder-mounted portable equipment operators is to extend their training duration and solidify the operation into habitual practice; however, evidences show it is harmful to operators' health due to erroneous training posture caused by overfatigue. This paper aims to study the influences of training method upon operators' performance and determine reasonable training duration for them, which is of considerable significance as follows.

### 1.1 To Improve Training Scientificity

Quantitative survey of each operator's performance is conducted to unveil the influences on his performance by varied (dynamic/static) training pattern and analyze the availability and practicability of different training methods to improve training

---

Z. Luo (✉) · M. Kang · P. Zhang · H. Zhang · H. Li · F. Zhou · K. Qu  
Air Defence Forces Academy, 450052 Zhengzhou, China  
e-mail: [luoluo2015@qq.com](mailto:luoluo2015@qq.com)

© The Editor(s) (if applicable) and The Author(s), under exclusive license to Springer Nature Singapore Pte Ltd. 2021

S. Long and B. S. Dhillon (eds.), *Man-Machine-Environment System Engineering*, Lecture Notes in Electrical Engineering 645, [https://doi.org/10.1007/978-981-15-6978-4\\_79](https://doi.org/10.1007/978-981-15-6978-4_79)

performance. It is hereby expected to improve the scientificity of training methods [1, 2] by measuring and comparing relevant data.

### ***1.2 To Probe into the Laws of Training Duration***

Analysis of the effectiveness of various work durations is conducted according to the changes of operators' performance with respect to their work duration. Avoid further training if operators are overwrought so as to promote the working efficiency and training validity.

### ***1.3 To Carry Forward Study on Human Factor***

Quest for the noticeable changes of operators' performance caused by variations of training duration and training method in their work [3–5] is conducted to find out similarities and differences so as to carry forward study on human factor based on the analysis of operators' performance in the respective experiment.

## **2 Objects and Methods**

### ***2.1 Objects***

Objects of the experiments are 10 male cadets from an academy. Their average age is 20, average height 173 cm and average weight 64 kg. Conditions of blood pressure and heart rate are fine. All objects have undergone Cattell's 16 Personality Factor test and are psychologically normal.

### ***2.2 Preparations***

Kits: shoulder-mounted portable equipment, 1 set, weighing 13 kg. Experimental instrument: heart rate telemetry watch model ACUMEN TZ-MAX100, 4 pcs; hygrothermograph model CENTER310, 1 pc; Cattell's 16 Personality Factor testing application modified by East China Normal University, 1 set; and stopwatch, 1 pc. Site: 200 m athletic field of good vision and illumination.

### **2.3 Proceedings**

On-the-spot static training stage: Evaluate the operators' performance with the Training Achievement Evaluating System after they have trained for four periods such as 5, 10, 20 and 30 min, respectively. Dynamic training stage: Evaluate the operators' performance for three times with the Training Achievement Evaluating System after their 0 m, 50 m, 100 m and 200 m run, respectively. We wish to better the training method by identifying the possible influences of static and dynamic training pattern upon operators' performance.

## **3 Data Analysis**

### **3.1 Basic Data**

We sorted out the physiological indexes of all operators before training as is shown in Table 1.

### **3.2 Static Performance Analysis**

As operators have completed different rounds of work within unit time, we hereby take the average value of each operator's performance to represent his achievement per unit time as is shown in Table 2.

Seen from Table 2, the training achievement tends to go up as the training duration extends: Compared with that of 5 min, the training achievement of 10 min rises remarkably; compared with that of 10 min, the training achievement of 20 min drops mildly; compared with that of 20 min, the training achievement of 30 min rises slightly. Therefore, the progressive extension of training duration is not witnessed to have generated an evident growth of training achievement.

Now if to take 5 min as a unit time, we may have a close look and more detailed analysis of the 10 and 20 min training, as shown in Table 3.

During the 10 min training, the training achievement appears to rise obviously, and in comparison, the achievement of the first 5 min (5 min-1), 50.660, is superior to that of the single 5 min training, 46.216. However, in the 20 min training, the achievement shows a downward trend: The second 5 min (5 min-2) drops sharply if compared with the first (5 min-1), and the third 5 min (5 min-3) drops a bit compared with the second (5 min-2). It can thus be seen that a continuous training of 10 and 15 min is good for stable achievement, and that a continuous training of 10 min contributes either a rise or a fall of achievement to some extent if compared with a continuous training of 5 min, the reason of which needs further analysis.

**Table 1** Operators' physiological indexes

S. No.	Weight (Kg)	Height (cm)	Eyesight	BP (mmHg)	FVC (ml)	Step test index	Pulse (beats)	SPO <sub>2</sub>	PI	High bar (times)	Push-up (times)	100 m race (ms)
1	65.1	170	4.9	124/77	4192	59	80	98	7.5	14	55	1423
2	67.3	173	4.2	147/81	4416	64	80	98	7	14	40	1480
3	61.9	177	5.1	121/80	4213	86	75	98	5.5	15	53	1453
4	66.7	175	4.9	117/81	4230	58	76	99	2.4	20	60	1413
5	55.7	173	5.1	123/70	4484	78	78	100	2.8	10	100	1330
6	71.7	177	5.0	132/63	3757	56	68	97	7.4	16	50	1329
7	52.9	168	4.5	102/61	3428	68	80	99	4	15	80	1420
8	69.5	173	5.2	124/78	4429	55	96	98	4.7	15	70	1478
9	61.6	173	5.1	105/71	3568	67	80	100	3	8	54	1630
10	71.5	175	5.0	122/80	4891	57	75	100	3.7	10	92	1331

**Table 2** Static training achievement (1)

S. No.	5 min	10 min	20 min	30 min	Average
1	42.750	50.571	56.429	47.633	49.346
2	26.667	48.133	49.457	43.843	42.025
3	43.800	53.684	48.025	40.948	46.614
4	47.750	68.278	60.257	61.246	59.383
5	53.250	56.375	51.550	55.375	54.138
6	47.429	61.214	68.447	64.518	60.402
7	39.750	41.313	46.806	42.590	42.615
8	64.125	56.750	52.935	65.702	59.878
9	50.500	47.455	43.308	53.123	48.597
10	46.143	60.067	63.636	72.712	60.640
Average	<b>46.216</b>	<b>54.384</b>	<b>54.085</b>	<b>54.769</b>	

**Table 3** Static training achievement (2)

S. No.	10 min 5 min-1	10 min 5 min-2	20 min 5 min-1	20 min 5 min-2	20 min 5 min-3	20 min 5 min-4
1	45.571	55.571	59.222	55.333	53.333	58.000
2	41.143	54.250	56.222	43.111	53.000	45.000
3	53.889	53.500	49.300	51.300	42.700	48.800
4	64.125	71.600	71.333	59.333	54.875	54.889
5	66.571	48.444	55.800	46.300	53.800	50.300
6	61.714	60.714	76.100	69.889	72.000	54.556
7	39.000	43.111	49.333	51.125	38.250	48.889
8	59.000	55.000	59.250	53.833	59.250	41.111
9	31.750	56.429	51.000	47.750	48.833	33.111
10	43.833	70.889	71.250	66.429	62.333	56.000
Average	<b>50.660</b>	<b>56.951</b>	<b>59.881</b>	<b>54.440</b>	<b>53.838</b>	<b>49.066</b>

Table 4 shows the average result of operators' training in 30 min, during which the training achievement first rises and then descends, with the climax appearing at 20 min. The achievement of the first 5 min (5 min-1), 48.959, is higher than that of the single 5 min training, 46.216, but lower than that of the continuous training of 10 min, 50.660. Training results of other periods in these 30 min, however, show no noticeable increase than the previous experiments. For instance, it is 53.096 in the third 5 min (5 min-3, from 10 to 15th minutes) but was 53.838 in the third 5 min (5 min-3, from 10 to 15th minutes) of the 20 min training.

**Table 4** Static training achievement (3)

S. No.	30 min 5 min-1	30 min 5 min-2	30 min 5 min-3	30 min 5 min-4	30 min 5 min-5	30 min 5 min-6
1	49.000	37.375	45.000	48.222	49.000	57.125
2	39.250	42.125	42.250	43.889	37.222	57.444
3	30.000	45.000	44.700	43.400	39.200	42.700
4	49.667	57.889	52.400	67.667	70.000	69.000
5	46.000	58.444	57.778	52.556	60.300	56.500
6	70.444	57.778	66.556	59.444	64.700	67.800
7	37.200	43.000	36.100	52.000	44.800	42.455
8	57.333	67.500	57.778	80.500	64.100	65.727
9	37.800	45.000	50.800	68.300	65.700	49.111
10	72.900	73.167	77.600	74.200	67.000	69.556
Average	<b>48.959</b>	<b>52.728</b>	<b>53.096</b>	<b>59.018</b>	<b>56.202</b>	<b>57.742</b>

### 3.3 Dynamic Performance Analysis

Three rounds of operation are evaluated for operators after their 0, 50, 100 and 200 m run, and the results are shown in Table 5:

It is easily seen that the training achievement first descends and then rises as the movement distance increases, which means that the 100 m run before operation adversely affects the operators, but 200 m-plus run poses positive influence, and that there is only a small decrement between the results of 50 and 0 m but a remarkable one between the results of 100 and 50 m.

**Table 5** Dynamic training achievement

S. No.	0 m	50 m	100 m	200 m	Average
1	82.500	72.300	64.300	57.600	66.131
2	78.500	73.000	67.600	57.000	66.910
3	75.500	66.300	68.300	64.600	67.725
4	59.600	81.000	53.600	45.300	56.625
5	62.300	70.300	24.300	50.300	44.689
6	54.300	58.300	65.600	74.600	65.292
7	61.000	68.600	73.300	46.000	57.490
8	55.600	56.300	44.600	74.300	57.233
9	64.000	57.000	32.300	59.500	53.980
10	80.300	61.300	53.000	50.600	59.183
Average	<b>67.360</b>	<b>66.440</b>	<b>54.690</b>	<b>57.980</b>	



### ***3.4 Comparative Analysis Between Static and Dynamic Works***

The operators' achievement of static work is mostly lower than that of dynamic work. The static maximum is 59.881 which appears at the first 5 min of the 10 min continuous work, while the dynamic maximum is 67.360 that appears after 0 m run. The result of 66.440 after 50 m run is still higher than the static maximum, 59.881. The dynamic minimum is 54.690 that appears after 100 m run, but it is in the middle of the list even if compared with the results of static training. Therefore, dynamic training gives better results than static.

That the average achievement after 0 m run, 67.360, outweighs the result of any static work is attributed to this: There are only 3 chances to operate in dynamic work but 6.3 on average even in the shortest, 5 min, round of static work, and so operators psychologically treasure the opportunity and value their achievement in the dynamic training.

That only 2 operators amongst the top 5 operators in static work appear again in the top 5 list of dynamic work indicates that operators perform differently in such varied training patterns as static and dynamic work. According to SPSS analysis [6], static work results are positively correlated with an operator's eyesight, whilst dynamic work results are positively correlated with PI but negatively correlated with SPO<sub>2</sub> and number of push-ups with unit time.

## **4 Conclusions**

The dynamic training is better than static training in effect, no matter seen from training achievement or training duration. Differed methods should be taken for different operators primarily based on their PI value, SPO<sub>2</sub> and number of push-ups with unit time. Additionally, monotonous and repeated training does no good to better performances.

Times of evaluation affect training result. Excessive evaluation gives rise to operators' psychological weariness.

In dynamic training, there is a rebound of training achievement after 200 m run, which suggests a desirable standard or stage of dynamic training.

In static training, the climax appears at 20 min and then the performance drops, which suggests that static training should last no longer than 20 min.

**Compliance with Ethical Standards** The study was approved by the Logistics Department for Civilian Ethics Committee of Air Defence Forces Academy.

All subjects who participated in the experiment were provided with and signed an informed consent form.

All relevant ethical safeguards have been met with regard to subject protection.

## References

1. Pang Z (2000) Man-machine-environment system engineering of air defense forces. Zhengzhou Air Defense Forces Academy, Zhengzhou
2. Wenbin L (2003) Influences of postures and load upon human body balance. *J Beijing Forestry Univ* 1:74–77
3. Wen'an T (2001) An analysis of stability of sporting rifle in standing position. *Sport Sci Technol* 1:32–35
4. Zhaofeng L et al (2017) Research of operating posture of shoulder-mounted equipment. *Man-machine-environment system engineering*, pp 117–124
5. Luo Z ,Pang Z, Kang M (2016) Experimental research of shoulder-mounted portable equipment operator's foot spacing in standing position. In: *Man-machine-environment system engineering—proceedings of the 16th international conference on MMESE*, pp 91–95
6. Shengke C, Rong L (2015) *Easy to master SPSS statistical analysis*. Tsinghua University Press, Beijing

# Research on the Comfort of Human Upper Back in Different Seat Back Angles



Ligang Luo, Tianyi Hu, and Tinghua Wu

**Abstract** This study aimed to investigate the effect of upper seat back in different vertical angles (5°, 10°, 15°, and 20°) on upper back support. The upper seat back was taken as an independent component in experimental facility, so that it could move and rotate in vertical angle relative to seat back of waist. Experimental results showed that comfort sensations in upper back could be perfectly measured by body pressure-measuring parameters and subjective comfort evaluation indicators. Proper leaning of slightly vertical angle upper back support would improve the whole sitting comfort compared with normal chairs.

**Keywords** Ergonomics · Sitting comfort · Upper seat back vertical angles

## 1 Introduction

In modern societies, increasing amounts of time are spent in seat [1]. Lack of upper back support was received much more attention second to the lack of lower back support. To keep a suitable upper back support, the upper seat back should be fit to the body's back plane [2]. The upper back support should be distributed with the teres major, infraspinatus, and serratus posterior around the thoracic vertebra [3].

---

L. Luo · T. Hu (✉) · T. Wu  
Zhejiang Light Industrial Products Inspection and Research Institute, 310018 Hangzhou, China  
e-mail: [15325665@qq.com](mailto:15325665@qq.com)

© The Editor(s) (if applicable) and The Author(s), under exclusive license to Springer 701  
Nature Singapore Pte Ltd. 2021  
S. Long and B. S. Dhillon (eds.), *Man-Machine-Environment System Engineering*, Lecture Notes in Electrical Engineering 645,  
[https://doi.org/10.1007/978-981-15-6978-4\\_80](https://doi.org/10.1007/978-981-15-6978-4_80)

**Table 1** Subjects' information

Item	Average	SD
Body height/cm	167.50	7.06
Seated deep/cm	65.00	9.41
Seated shoulder height/cm	57.25	3.82

## 2 Methods

### 2.1 Study Participants

Six healthy college students were selected in this experiment, including three males and three females. The body size of participants was required to be universally representative. Each part of the human body should stay between the 5th and 95th percent of the human standard library [4]. There is a certain proportional relationship between the sizes of normal human body parts. Therefore, it is reasonable to estimate the structural size of each part based on the normal human body structure relationship and the average standing height as the base. According to the national standard GB 10,000–1988, the height of participants is selected from the 5th percentile, 50th percentile, and 95th percentile [5] (Table 1).

### 2.2 Protocol

The Pressure Distribution: Tekscan pressure distribution measurement system (BPMS, body pressure measure system) is used for pressure distribution measurement. Through the pressure distribution test, the average pressure, maximum pressure, pressure value and pressure distribution matrix were read directly from the contact area of BPMS to estimate the average pressure gradient, the position of hip sciatic joint and the front and rear of total pressure, back pressure point position and the upper and lower total pressure, etc. values.

The subjective comfort indicators: Subjective comfort evaluation semantic difference method was used to quantitatively evaluate comfort, and seven-level gauge was used to reflect the different levels of human feelings and obtain the index values beyond skin comfort, waist and buttock fitness, waist and buttock stress sensation, as shown in Table 2.

**Table 2** Magnitude scale of subjective comfort

Grade	Comfortable sensation	Fitting sensation	Stress sensation
Grade 7	Very comfortable	Very fit	Too much stress
Grade 6	Comfortable	Fit	Great stress
Grade 5	A little comfortable	A little fit	Big stress
Grade 4	Common	Common	Common
Grade 3	A little uncomfortable	A little unfit	A little stress
Grade 2	Not comfortable	Unfit	Little stress
Grade 1	Very uncomfortable	Very unfit	Too little stress

### 3 Results

#### 3.1 *Body pressure distribution of seat back in different vertical angles*

With the increase of upper seat back vertical angle, the contact area to upper seat back varies from larger to smaller with a totally contrary situation to the change in contact area to lower seat back. The contact position of upper seat back with back body changes according to the upper seat back vertical angles (Fig. 1; Table 3).

With the increase of upper seat back vertical angles, the total and average pressure of buttock becomes smaller and then greater while change in total and average pressure of waist is opposite to it. Experiment shows that larger or smaller horizontal angle in upper seat back would cause uncomfortable sensation for back pressure, and hence, body initiatively adjusts back pressure by tightening up latissimus dorsi and making body upright so as to transfer pressure from waist and back to buttocks.

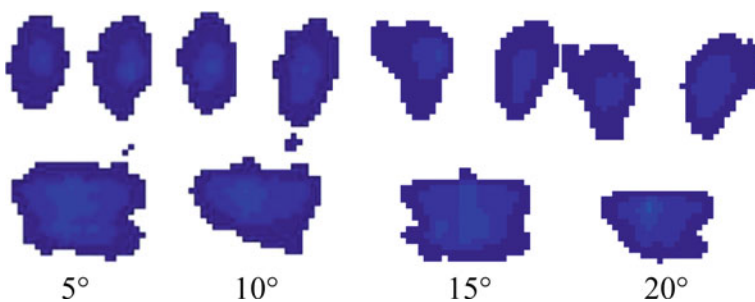


**Fig. 1** Different vertical angle of the back body pressure distribution

**Table 3** Relationship between different vertical angle of seat back and body pressure distribution

Body pressure	Test site	5°		10°		15°		20°	
		Average	SD	Average	SD	Average	SD	Average	SD
Contact area (cm <sup>2</sup> )	Seat	997.7	137.3	979.1	86.2	1019.6	82.2	964.9	73.6
	Lower seat back	273.8	65.0	253.7	39.0	223.0	47.9	233.3	36.2
	Upper seat back	295.0	114.1	349.7	86.1	338.7	85.2	309.2	65.6
Average pressure (kpa)	Seat	2.23	0.36	2.02	0.34	2.12	0.39	2.43	0.42
	Lower seat back	1.88	0.32	2.11	0.33	2.10	0.37	2.01	0.52
	Upper seat back	1.02	0.17	0.97	0.16	0.99	0.24	1.06	0.18
Maximum pressure (kpa)	Seat	12.45	2.05	12.05	2.20	12.56	2.13	15.91	1.35
	Lower seat back	5.11	0.63	6.63	1.04	5.74	0.44	5.28	0.36
	Upper seat back	3.31	3.23	3.31	4.79	3.46	6.04	3.40	3.38
Total pressure (kpa)	Seat	2172.8	551.1	1923.2	378.1	2119.8	523.3	2271.6	414.7
	Lower seat back	509.6	173.5	524.1	145.7	565.6	165.9	466.3	186.8
	Upper seat back	352.3	177.2	298.5	117.3	280.2	156.8	324.3	109.3
Average pressure gradient (kpa/cm)	Seat	0.29	0.04	0.27	0.06	0.29	0.07	0.34	0.08
	Lower seat back	0.36	0.05	0.39	0.05	0.38	0.06	0.38	0.05
	Vertical direction of upper seatback	0.16	0.03	0.15	0.02	0.16	0.03	0.16	0.02
	Horizontal direction of upper seatback	0.23	0.03	0.21	0.05	0.21	0.02	0.24	0.03

With the increase of upper seat back vertical angles, average pressure gradient of back would have a decrease initially but have an increase next, among which horizontal trend of change in average pressure gradient is bigger than vertical trend of it with excessive average pressure gradient causing uncomfortable sensation to people.

### ***3.2 Subjective assessment of seat back in different vertical angles***

When the value of upper seat back vertical angle is grade 2, 10°, over comfortable sensation assessment is best; at the same time, under this condition, overall comfortable sensation assessments of back, waist, and legs are simultaneously best. The best comfortable sensation assessment of buttock is with the value of grade 2, 15° upper seat back vertical angle. With the value of grade 3 to waist, comfortable sensation assessment is a little lower but higher than it with the value of grade 1 and grade 4.

With the increase of upper seat back vertical angles, back support gradually increases and fitting sensation of contact area would go on improving and then lessening. When the value of upper seat back vertical angle is 5°, the position of back support is near to the inside that is the inner edge and the lower angle of the scapula. And when it is 20°, the position of back support is close to the outside that is acromion of scapula with strong sensation of being besieged. The condition of back support position in acromion, and inner edge of scapula would make people uncomfortable for fewer muscles in them.

With the increase of upper seat back vertical angles, back support of waist decreases at first and then increases contrary to the change of fitting sensation of contact area in waist. And when the value of upper seat back vertical angle is 10°, it is the best condition for waist as an indication that appropriate position of upper seat back can improve the comfortable sensation of waist.

With the increase of upper seat back vertical angles, back support of buttock reduces firstly and then increases with opposite situation happening in fitting sensation of contact area in buttock. And when the value of upper seat back vertical angle is 10°, it is the best condition for buttock as an indication that appropriate position of upper seat back can improve the comfortable sensation of buttock.

There is a same trend between sitting posture stability and overall comfortable sensation. When upper seat back horizontal angle is from 10° to 15°, it is the wonderful sitting posture stability.

There is a negative correlation between comfortable sensation of each part and average pressure of upper seat back and the cushion. The values of correlation between average pressure of upper seat back and total comfortable sensation is -0.949 and -0.930 in cushion of it. Experiment shows that consideration should be taken into the influence of pressure in back and buttock to comfortable sensation in the changing process of upper seat back vertical angle.

There is a negative correlation between average pressure gradient of upper seat back, cushion, and the comfortable sensation of each part, which means that when the whole support comes from back, comfortable sensation assessment of each part is bad. The reasonable pressure distribution of back is especially important to comfortable sensation.

## 4 Conclusions

The upper seat back vertical angle affects comfortable sensation to the condition of leaning. Left and right upper seat back vertical angle determines curvature of upper seat back. When the value of included angle is  $0^\circ$ , one upper seat back is flushed with the other with pressure in thoracic vertebra. For fewer muscles and less fat in surface of thoracic vertebra, uncomfortable sensation occurs in back with great pressure. With excessive upper seat back vertical angle, back is surrounded obviously with scapula pressed in two sides. Hence, people also feel uncomfortable. Reasonable fitting of upper seat back can distribute pressure in teres major, infraspinatus, and serratus posterior around the thoracic vertebra. With the analysis of experiment, the value around  $10^\circ$  of upper seat back vertical angle is relatively appropriate choice.

## References

1. Yao CHAO, Liming SHEN, Yang WANG (2018) Study of the pressure distribution and sensitive points on office chair pan on the basis of individual difference. *Furniture* 39(02):93–97
2. Vwegara M, Page A (2002) Relationship between comfort and back posture and mobility in sitting posture. *Appl Ergonom* 33(1):1–8
3. Jianbo J, Liming S, Yang W (2018) Investigation and study of the design features of staff chair seat pan shape. *Furniture* 39(02):98–102
4. Rolf E, Rene H, Kathrin K et al (2007) Effects of using dynamic office chairs on posture and EMG in standardized office tasks. In: Dainoff MJ (eds) *Ergonomics and health aspects, HCII2007, LNCS4566*. Springer, Berlin Heidelberg, pp 34–42
5. Hu T, Shen L (2014) Comfort and supporting ability of waist and haunch by using office chair in forward sitting position. *J Anhui Agric Univ*(1):21–27



# An Organic Design for Human–Computer Interaction



Hongjun Zhang and Baiqiao Huang

**Abstract** The accuracy and efficiency of human–computer interaction are critical to the completion of the set tasks of an engineering system. In traditional human–computer interaction, because software only has solidified logic which does not change with the external conditions, resulting in the failure of operating personnel to perform timely correction in the event of logical errors, an organic human–computer interaction design is proposed which regards software as an autonomous agent capable of perceiving, analyzing and learning. A software architecture with organic characteristics is also put forward to improve the self-adaptability of software by strengthening its perception, learning and optimization abilities, thus providing method guidance for improving the accuracy and coordination of human–computer interaction.

**Keywords** Man-machine-environment system engineering · Human–computer interaction design · Organic · Self-perception · Self-learning · Self-optimization

## 1 Introduction

Man-made engineering systems are established to assist in the task of transforming the world, and hence, humans, engineering systems and the environment constitute a whole man-machine-environment system. Man-machine-environment system engineering is a method for guiding the design of the man-machine-environment system; it is a science that applies system science theories and system engineering methods to correctly handle the relationships between the three elements of human, machine and environment and further study the optimal combination of the man-machine-environment system [1]. Man-machine-environment system engineering was proposed by Long Shengzhao and developed under Qian Xuesen’s recognition and concern, and its research focuses on the characteristics of human, machine and

---

H. Zhang · B. Huang (✉)

System Engineering Research Institute of China State Shipbuilding Corporation, Beijing 100036, China

e-mail: [seafury@buaa.edu.cn](mailto:seafury@buaa.edu.cn)

© The Editor(s) (if applicable) and The Author(s), under exclusive license to Springer Nature Singapore Pte Ltd. 2021

S. Long and B. S. Dhillon (eds.), *Man-Machine-Environment System Engineering*, Lecture Notes in Electrical Engineering 645, [https://doi.org/10.1007/978-981-15-6978-4\\_81](https://doi.org/10.1007/978-981-15-6978-4_81)

environment and the human–machine relationship, human–environment relationship and machine–environment relationship, as well as the overall performance of the man-machine-environment system.

In this world of information explosion, the computer has a special place in the man-made engineering system as it can achieve automated control in combination with information theory and control theory. Nearly, all modern engineering systems involve the computer, which realizes information collection, processing and transmission, as well as decision-making and execution. Therefore, we can conclude that current engineering systems are computer-centered systems. Human–computer interaction (HCI) is of extreme importance in the use of computers to assist in the work, and its efficiency and accuracy will directly affect the use of the system. As such, we chose HCI techniques as the aims of this research.

HCI techniques are technologies that enable human–computer conversation in an effective way through computer input and output devices. HCI techniques include the machine providing humans with abundant relevant information, tips and instructions through the output or display equipment, and humans inputting relevant information into the machine, answering questions and giving tips and instructions through the input equipment. In the course of its development, HCI has undergone three stages: the adaptation of humans to machines, the gradual adaptation of machines to humans and human–machine cooperation design centered on humans [2]. The first stage overemphasized improving mechanical efficiency rather than the adaptive capacity and operating experience of humans and attempted to adapt humans to the operation of machines by strengthening training. The second stage developed after World War II with increasingly sophisticated and complex machines, but it was found that simply emphasizing the adaptation of humans to machines could not guarantee the effectiveness of the “human–machine system,” and only HCI design, which takes the physiological and psychological limitations of humans into account, could help people to better operate machines [3]. In particular, the emergence of graphical user interface (GUI) technology simplified the user learning process and expanded the number of computer users, further bolstering the development of HCI design [4]. In the third stage, the “human-oriented” concept was raised, and importance was attached to the user experience in HCI design [5].

Humans and computers are partners in HCI, and HCI techniques consist of two links: One is the reception, decision-making and operation of the information output from the computer by the human and the other is the reception, decision-making and operation of the human’s input by the computer. Traditional HCI techniques mainly focus on the first link, that is, the cognitive theory of humans from the perspective of operating personnel. A human is an organic object of high intelligence, and human cognition is a kind of comprehensive cognitive ability. As a result, humans can take remedial measures quickly once we realize that an incorrect operation has occurred in the process of HCI, thus minimizing losses. However, for the machine in the second link, its cognition and decision-making are processes based on the logic judgment of code, so the computer will not be capable of correcting errors in the case of incorrect code, and humans can only passively accept the results of system task failures. Therefore, this imbalance between humans with our error correction

ability and computer software with only solidified logic in the interaction process is a natural shortcoming of the current HCI process which sometimes leads to serious consequences. Taking the accidents of the Boeing 737 MAX 8 as an example, this paper analyzes the shortcomings of the existing software architecture and the details of the HCI process model and then puts forward a method for building an adaptability mechanism in software by strengthening its perception, learning and optimization abilities in a bid to improve the adaptability of software to abnormal situations.

## **2 Analysis of the Limitations of Traditional HCI**

### ***2.1 Reflections on the 737 MAX 8***

The Boeing 737 MAX 8 suffered two accidents within five months in 2009, resulting in a global ban on aircraft. The preliminary investigation concluded that due to an added “maneuvering characteristics augmentation system” (MCAS) for automatic anti-stall in the flight control system of the 737 MAX 8 aircraft, which was intended to solve the flight attitude problem caused by the engine replacement, the software would control the aircraft’s nose to automatically lower when the aircraft had too large an angle of attack. The cause of a tragic accident is usually attributable to multiple factors. Therefore, we will not delve into the fact that the Boeing aircraft only had two attack angle sensors, and it only used the data from one of the sensors to trigger the MCAS, causing no channel voting algorithm to be used. A 20-degree difference in data between the two sensors was discovered in the Indonesian Lion Air crash. Meanwhile, we will also not discuss in-depth the procedural issue that the airworthiness certification of the MCAS was evaluated by Boeing itself instead of the FAA. This paper mainly concentrates on the HCI process in the two air crashes. When each crash occurred, the MCAS was mistakenly triggered due to the failure of the attack angle sensor, forcing the aircraft’s nose to be lowered, and the pilot repeatedly tried to pull the aircraft up by manual operation, but failed because of the MCAS. Such accidents speak volumes about the inflexible and obstinate characteristics of software, which can be reflected in three aspects: First, the perception is too simple, so the decision was made only by relying on the data of one sensor. Second, the HCI process lacked cooperation with humans irrespective of its operation intention; for the interaction, the operation of the other, i.e., the operating personnel, should be taken as feedback for making corrections to decisions, which constitutes true cooperation. And third, the HCI process lacked an error correction mechanism, so if a decision was incorrect, it would ultimately remain incorrect.

## 2.2 Analysis of the Shortcomings of Traditional Software Architecture

1. Traditional software architecture is an event-triggered architecture based on the message queue, and as such, it lacks flexibility.  
As shown in Fig. 1, in traditional software system architecture, each module has its own independent perception unit and decision-making unit, and the system manages decision execution actions in a prioritized message queue. Such architecture leads to a dispersed perception that is not conducive to comprehensive decision-making based on external input.
2. Traditional software has a solidified logic without flexibility, so it will always remain incorrect when errors occur.  
The traditional software system has a solidified execution logic, and the software repeats the execution every time according to the established logic, so it cannot adapt but only modify the software code once the external environment changes, for which reason traditional software lacks flexibility and adaptability.
3. Traditional software saves the historical data of system operation, but does not analyze it, so everything will start all over again after the software restarts.

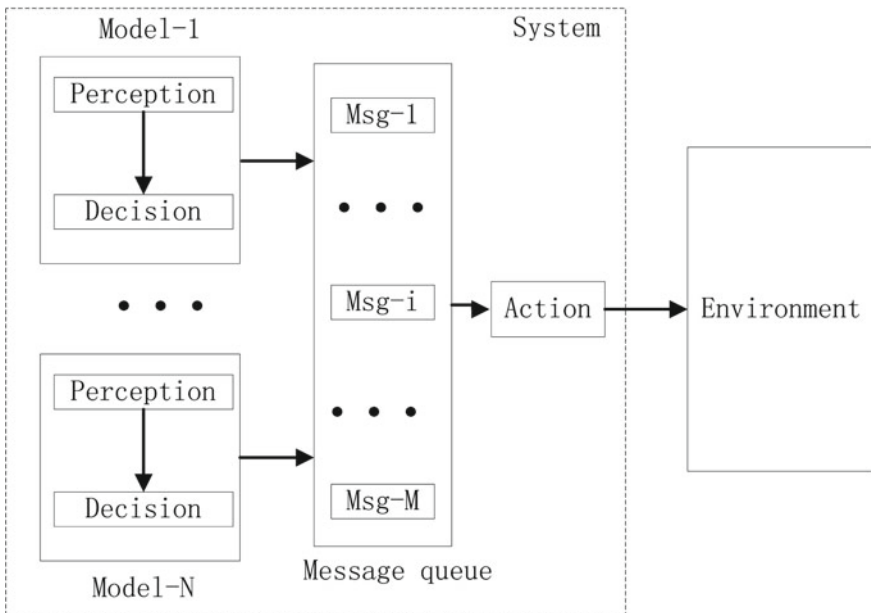


Fig. 1 Traditional software system framework

Traditional software stores a large amount of historical data in the database during use, but the data is not utilized except in data query. Supported by big data and machine learning technology, we can establish an optimized model of software input and output from the stored historical data to guide the operation of the software.

### ***2.3 Analysis of the Decision-Making Model of the HCI Process***

Rasmussen [6] divides the decision-making process of humans in the HCI process into three types, namely skill-based decision-making, rule-based decision-making and knowledge-based decision-making. Because the use of software follows agreed operating processes and specified rules, the decision-making in the HCI process of software mainly follows a rule-based decision-making process, meaning that only when the software encounters unexpected anomalies, will the operating personnel face knowledge-based decision-making, raising the need to make decisions based on the past experience for follow-up processing. Moreover, the human decision-making process is an organic process of dynamic change. Humans have the ability to make decisions in the face of changes and will modify their early decision-making according to temporary new input information. If they realize that their previous decision-making was wrong, humans will adjust their decision-making in time to reduce the impact of incorrect decisions. As such, we believe that the human decision-making process is an organic process that can be adapted flexibly.

At present, the decision-making process of a machine has only one type which is based on rules. Moreover, the decisions are fixed and the machine does not judge whether the decision is appropriate, nor can it adjust the decision dynamically; this is why we say that the decision-making process of machines is an inorganic process.

## **3 Organic HCI Design**

### ***3.1 Organic Characteristics of Software System***

To solve the contradiction between the organic human decision-making process and inorganic software decision-making process in HCI, we chose the strategy of adding an adaptive mechanism to the software. This is a new form of technology developed to improve the ability of engineering systems to cope with complexity [7]. To realize this mechanism, we need to make the following modifications to the software:

1. **Integrated perception.** The perception of the external environment comes from many sources, not just a single one, which is similar to human senses perceiving the outside environment via vision, hearing, smell, touch and taste. We suggest

that the perception data of the software system be integrated for data fusing analysis, and a comprehensive situation cognition model be established for the external input of the software system.

2. Comprehensive decision-making. For some significant decision-making processes, the relevant parameters are fully used for the mutual verification of conditions on the basis of integrated perception, thereby avoiding incorrect decision-making caused by the error of the input conditions when making decisions according to a single condition.
3. Cooperative interaction. In the HCI process, cooperative interaction with human operation can be realized by increasing the understanding of the human operating intentions by sending feedback to the decision-making mechanism of the software system, thus jointly modifying the decision-making of the software.
4. Dynamic adjustment. The software should have a changeable decision model which can adapt to changes in the external environment through dynamic adjustment, thereby further improving its adaptability.

### 3.2 Organic Software System Architecture

Three aspects are mainly considered in human–environment interaction design: influence of environment on human’s physical health, influence of environment on human–machine design and influence of special social environment of naval ships on human’s mental health.

We propose an organic software architecture for realizing the organic characteristics of software described in 3.1, as shown in Fig. 2.

An organic software system framework has the following characteristics compared with the functional construction of humans and traditional software system architecture;

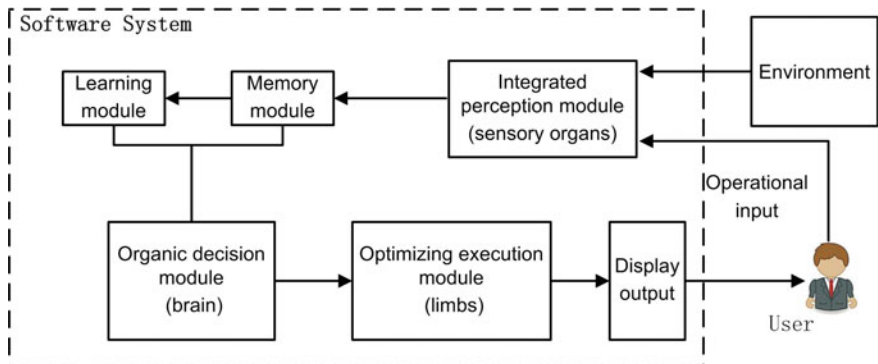


Fig. 2 Organic software system framework

First, the perception, decision-making and execution functions of the software system are managed centrally to form a corresponding integration module.

Second, a learning module can be added so that the results of each execution are fed back from the environment to the learning module. The rule parameters in the system's perception, decision-making and execution modules are updated through the continuous accumulation and analysis of experience data, and the HCI process is continuously optimized, such as modifying the monitoring range of input parameters, modifying the parameters of decision-making conditions and optimizing the parameters of operation control.

Third, comprehensive decision-making and organic decision-making shall be stressed. Comprehensive decision-making means the comprehensive use of relevant parameters for mutual verification between conditions to avoid decision-making based on single conditions, while organic decision-making emphasizes dynamic change in the decision-making process, namely changing decision-making conclusions according to changes in the input parameters and the analysis of intentions fed back from the operation of the user.

Fourth, a self-adaptive display interface shall be realized which can keep a record of common interface configurations according to different user responsibilities, thereby improving HCI efficiency.

### ***3.3 Design Idea for Organic HCI***

As an example, within the framework of organic HCI, we have improved the HCI design for the Boeing 737 MAX 8 crash situation.

First, in terms of integrated perception, the MCAS integrates the perception function into a single module. Data on the angle of attack, speed, altitude, human operation feedback, etc., of the aircraft shall all be collected in the module. Second, in the aspect of comprehensive decision-making, the MCAS cannot judge the status of the aircraft only by the angle of elevation, but through multiple channels such as the elevation angle, the altitude change trend, the speed change trend, and the pilot's operation intention, and other channels, ensuring that it will not to make the incorrect decision to lower the nose. Third, for cooperative interaction, the MCAS obtains the pilot's operation feedback which says that the pilot has repeatedly tried to pull the nose up; now, it can judge that the pilot's operation is contradictory to its own decision-making, so it will dynamically adjust its own decision-making to be in line with that of the pilot. Through the analysis of this example, we can see that such an organic HCI design can greatly improve the accuracy and coordination of HCI.

## 4 Conclusions

By analyzing the Boeing 737 MAX 8 aircraft accidents, this paper highlights the contradiction between the organic and adaptive human decision-making process and the inorganic software decision-making process in the traditional process of human-machine interaction. Based on an analysis of the shortcomings of the traditional software framework and traditional decision-making model of HCI, the organic HCI concept is proposed and the organic characteristics of the software system analyzed. To realize an organic software system, this paper proposes a new software system architecture that can centrally manage the perception, decision-making and execution modules of the software system by analogy with human structure. At the same time, a learning module is added to realize integrated perception, comprehensive decision-making, cooperative interaction and dynamic adjustment in the HCI process. Finally, this paper also explains the advantages of the organic HCI process through the analysis of an example.

## References

1. Long Z (1993) Man-machine-environment system engineering theory and its Significance in productivity development. In: Progress in man-machine-environment system engineering research, vol 01. Beijing: Beijing Science and Technology Press, pp 2–13
2. Wei W, Gong X (2011) HCI develop trend based on user-experience. *J Beijing Univ Aeronaut Astronaut* 37(7):868–871
3. Ding Y, Cheng G (2013) Human factors engineering. Beijing Institute of Technology Press
4. Li S (2009) The fundamental of interaction design. TsingHua University Press
5. Jianming D, Limin F, Peilun R et al. Human-computer interaction: user-centered design and evaluation
6. Rasmussen J (1983) Skills, rules, and knowledge; signals, signs, and symbols, and other distinctions in human performance models. *J IEEE Trans Syst Man Cybern* 13(3):257–266
7. Zhang H, Huang B, Zhang P (2014) A New SoS engineering philosophy-vitality theory. In: 14th annual conference system of systems engineering, pp 19–24, Anchorage, AK, USA



# Human–Machine Interface Optimization Design Based on Ecological Interface Design (EID) Theory



Guangjiang Wu, Yiqian Wu, Xi Lu, Shenghang Xu, and Chuan Wang

**Abstract** With the development and application of digital technology, the human–machine interface of the console has been widely used with the computer as the core of the digital display control interface. The paper analyzes the effect of the application of EID theory in human–machine interface (HMI) in the nuclear power plant based on the actual HMI examples in the nuclear power plant. The analysis shows that EID has important application value in HMI design of the nuclear power plant, and the application of EID theory in the nuclear power plant will better organize the display information and improve operator’s ability to solve problems when encountering unanticipated events.

**Keywords** Nuclear power plant · Control room · Ecological human–machine interface

## 1 Introduction

The human–machine interface of the main control room is the main control medium for the interaction between the operator and the system equipment of the nuclear power plant. The operator completes the operation task of the power plant through the human–machine interface [1–3]. With the rapid development of high-speed processing chip and computer graphics technology, it has become an inevitable trend

---

G. Wu · S. Xu  
Naval Equipment Department, Beijing 100089, China

Y. Wu  
State Key Laboratory of Nuclear Power Safety Monitoring Technology and Equipment, China  
Nuclear Power Engineering Co. Ltd., Shenzhen 518000, China

X. Lu  
Naval Staff Department, Beijing 100089, China

C. Wang (✉)  
Naval Medical Center of PLA, Shanghai 200433, China  
e-mail: [hg04381@163.com](mailto:hg04381@163.com)

© The Editor(s) (if applicable) and The Author(s), under exclusive license to Springer Nature Singapore Pte Ltd. 2021

S. Long and B. S. Dhillon (eds.), *Man-Machine-Environment System Engineering*, Lecture Notes in Electrical Engineering 645, [https://doi.org/10.1007/978-981-15-6978-4\\_82](https://doi.org/10.1007/978-981-15-6978-4_82)

for the new generation of the human–machine interface of the main control room to replace the traditional mechanical interface with the high-definition large-screen computer integrated display equipment and touch control interface. On the one hand, the digital display control technology with the ability of flexible data integration and graphic display provides conditions for optimizing the human–machine interface and human–machine interaction. On the other hand, if the information content, information organization and display mode of the interface are not designed reasonably, it will increase the cognitive load of the operator in the main control room and affect the unit safety.

This paper proposes an idea and a method of human–machine interface design according to the operator’s ecological interface design theory.

## 2 Ecological Interface Design

The ecological interface design is a theoretical system used to design the human–machine interface in the complex social technology system, which is of great significance to knowledge workers. Research shows that it enhances people’s adaptability and improves performance for solving problems. The main idea of ecological interface design [4, 5] is as follows:

1. The interface design shall be user-oriented;
2. The interface design shall comprehensively analyze the working domain of the system (including people, equipment and environment);
3. The interface shall provide enough feedback and appropriate information;
4. The mapping from information to interface shall be consistent and unique and conform to the cognitive model;
5. The interface design shall adopt different levels of abstraction to provide information and support people’s decision-making activities. The configuration diagram is a kind of presentation method that provides information of a high-level abstract level.

## 3 Analysis of Working Domain

For the design of the ecological human–machine interface, the corresponding working domain information must be analyzed. Generally, we use “hierarchical analysis” to analyze the working domain information. The “hierarchical analysis” generally includes the following elements:

1. Hierarchy
2. Tree structure
3. Layered according to different dimensions

In general, we describe a working domain through five different levels, and the levels have a fixed and interrelated relationship. From the abstract to concrete, the five levels are, respectively, functional purpose, abstract function, overall function, physical function, and physical form.

## 4 Application of Ecological Interface

The human–machine interface in the nuclear power plant is the link between the operator and the nuclear power plant system. The operator completes almost all monitoring and operation tasks through the human–machine interface of the main control room. On the one hand, the ecological interface design is based on the human cognitive model and it is user-oriented to put forward the principle and idea of interface graphic design. On the other hand, it uses different abstract levels to provide information to assist in human decision-making activities. The application of the ecological interface design theory in the human–machine interface design of the nuclear power plant can effectively optimize the design, improve the user experience, and reduce the operator’s workload. The following will explain with the screen examples of the nuclear power plant.

### 4.1 *Single Variable Display*

A lot of single variables are displayed in the human–machine interface design of nuclear power plant, such as the water level of water tank, the flow of pipeline, and temperature of pump. For displaying the single variable information, the ecological human–machine interface shall not only display the specific value, but also enable the user to sense the relationship between the number and other related values, such as the example of displaying the water level of water tank as shown in Fig. 1.

It can be seen from the example in Fig. 1 that the screen design before improvement can represent the water level of the water tank through the isolated analog quantity. Although it can meet the user’s basic requirement of monitoring the water level of the water tank, the relationship between the water level of the water tank and the upper and lower limit values as well as the water level change trend cannot be intuitively sensed. The improved ecological human–machine interface adopts the visual bar chart combined with the analog quantity indicator with high accuracy to display the water level of the water tank. At the same time, the upper and lower limit values of the water level of the water tank are clearly identified in the bar chart. The up and down arrows indicate the changing trend of the water level of the water tank. The user can visually observe the relationship between the current water level and the upper and lower limit values. It can be seen from the comparison that the ecological interface not only pays attention to the specific values but also pays more attention to the relationship and change trend between the variable and relevant parameters.

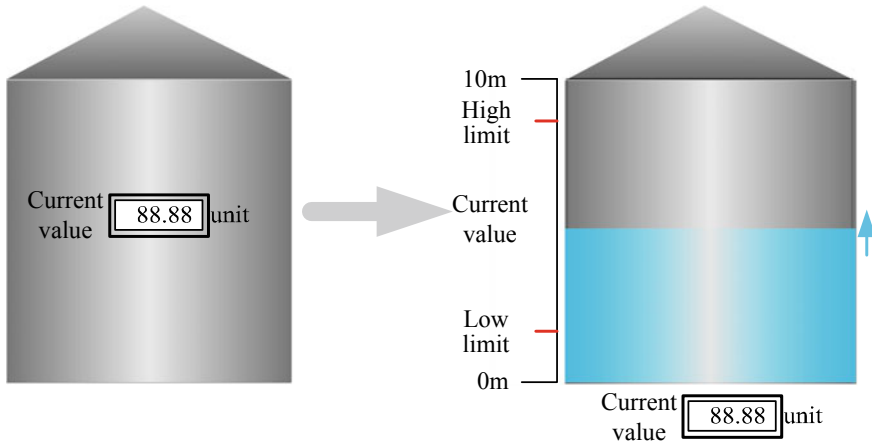


**Fig. 1** Example of single variable display

Through the ecological human–machine interface, the user can intuitively sense the specific condition and development trend of the water level of the water tank, which is conducive to the user’s observation and cognition.

## 4.2 Associated Variable Display

Besides displaying single variables, the nuclear power plant also needs to display multiple associated variables. Because of the intrinsic correlation of these variables, the ecological human–machine interface shall not only present the values of parameters but also present the intrinsic association properties of different parameters.

In the test stage of a nuclear power plant, the pressure deviation among three steam generators exceeds the limit value, which results in safety injection action. Through accident analysis and subsequent reflection, the relevant human–machine interface is optimized based on the design idea of the ecological human–machine interface, and the modification scheme is shown in Fig. 2.

First, reduce the indication of pressure monitoring analog quantity, change the pressure redundant probe into the comprehensive information through calculation, reduce the screen information, and reduce the operator’s visual load. In addition, increase the indication of pressure deviation among the three steam generators. In order to show the deviation intuitively and make the user pay more attention to the deviation and be in line with the user’s cognitive model, we use the bar chart to indicate the pressure value and classify associated pressure bar charts into a group. At the same time, the pressure bar charts are connected through a dynamic line. The safety injection action is caused when the pressure deviation among the three

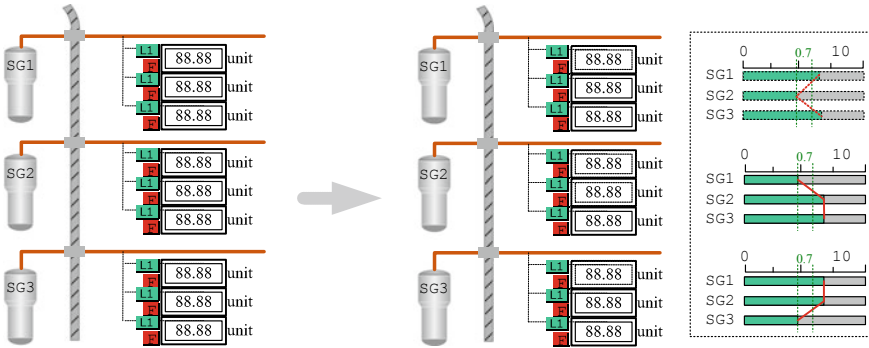


Fig. 2 Example of correlative variable display

steam generators exceeds the limit value. Through accident analysis and subsequent reflection, the relevant human–machine interface is optimized based on the design idea of the ecological human–machine interface, and the modification scheme is shown in the following figure:

When the three steam generators have the same pressure, the dynamic line is vertical. When the three steam generators have different pressure, the dynamic line will change according to the deviation. According to the distortion degree of the dynamic line and the deviation limit reference line, the user can visually observe the pressure deviation of the steam generators, which is convenient for the operator to judge and evaluate the state of the power plant.

There are also many similar correlated parameters in the nuclear power plant, such as the water level of the three pressure regulators, the flow of three loops, the flow of upper flushing, and down discharge. All of these kinds of associated parameters can be designed in the similar way.

### 4.3 Variable Polar Plot Display

Besides the single variable display and associated variable display, there is another situation that the system state is determined together by multiple variables. In this case, the ecological interface is often designed by using a higher level of abstraction to provide information and support people’s decision-making activities, wherein the polar plot is a kind of presentation mode that provides advanced abstract level information.

With normalizing and displaying the data in the polar plot graph, the user could be convenient to find an abnormal situation. The abnormal situation can be expressed by different graphic features as the radial tilt screen shown in the example of Fig. 3.

The radial tilt calculation divides the core into four quadrants. Typical core temperature measuring points are selected and normalized to calculate the radial tilt value.

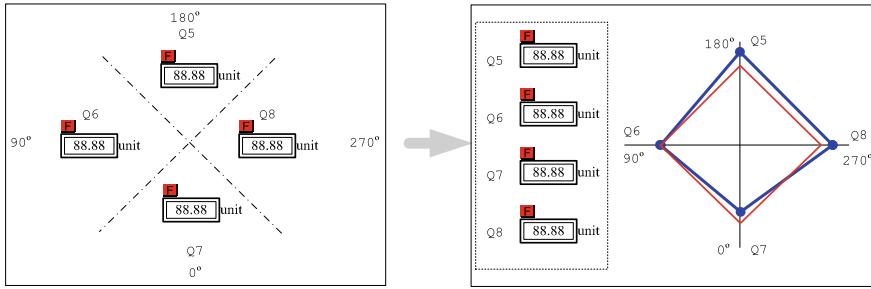


Fig. 3 Example of polar graphic

The normal radial tilt normalized value is “1”, and the radial tilt screen is used for monitoring the radial tilt of the four quadrants of the core. In the original scheme, the radial tilt of the four quadrants is displayed by specific values. After optimization, the radial tilt of the core is displayed by polar coordinates, and the red square background frame is fixed, indicating that the radial tilt of the core is normal. The blue box will change with the change of the radial tilt of the four quadrants. The user can observe the deviation of the blue box from the red box to observe the radial tilt deviation of the core intuitively.

It can be known that the ecological human-machine interface is more intuitive and more in line with human sensing features through the comparison between the former and the latter schemes.

### 4.4 Big Data Display

When a large amount of data shall be displayed, the ecological interface is generally designed and expressed by lines, circles, squares, and other shapes, and the state is expressed by the bending of lines and the change of background color of squares. The advantage of such processing is that the overall normal and abnormal condition of these data can be directly observed, as shown in Fig. 4.

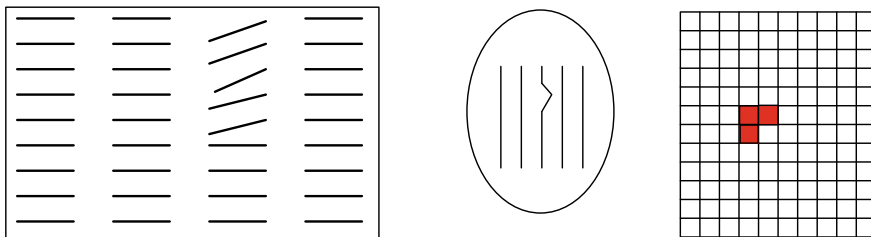


Fig. 4 Example of mass data display

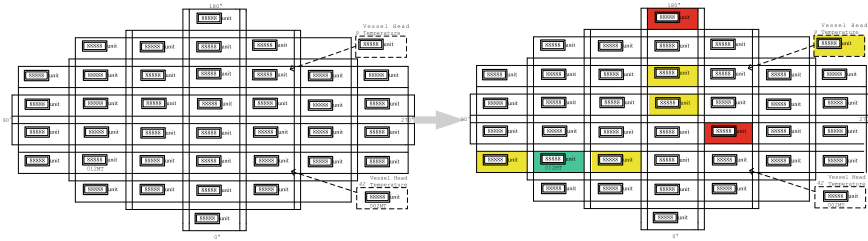


Fig. 5 Example of core temperature monitoring screen

The human–machine interface of the nuclear power plant also has a lot of data that needs to be displayed. In order to make the user see the state of these data intuitively and find abnormalities in time, not only specific values are displayed in the screen, but also the normal and abnormal conditions of relevant parameters are presented through the change of background color according to the idea of ecological interface design, as the example of core temperature monitoring screen shown in Fig. 5.

The monitoring screen of core temperature of nuclear power plant in Fig. 5 continuously monitors the core temperature through 40 sets of core thermocouples, so that the operator can know the change trend of core temperature and core subcooling in real time during and after accidents. For such screen displaying a lot of data, the operator is difficult to obtain the required information in a short time and easy to miss important information. In order to solve the above problems, the screen is optimized according to the ecological interface design idea. On the basis of the original scheme, different background colors representing different temperature ranges are added. No background color represents normal temperature, yellow represents the high temperature needing attention, and red represents over-limit temperature which needs to take corresponding measures immediately. The above optimization increases the intuitiveness of the screen, which is convenient for the operator to observe and quickly find the abnormality.

## 5 Analysis and Application of Working Domain

The safety parameter display screen of the nuclear power plant is used to display the safety-related parameters of the power plant and assist the operator to judge the safety state of the power plant. The traditional safety parameter display screen of the nuclear power plant is shown in Fig. 6.

The analysis of working domain can optimize the above traditional safety parameter display screen into the ecological human–machine interface, and the optimized screen is shown in Fig. 7.

Firstly, six major safety function indicators are arranged at the top of the screen through analyzing the functional purpose of the screen so as to assist the operator to evaluate the overall safety state of the power plant and receive the alarm information

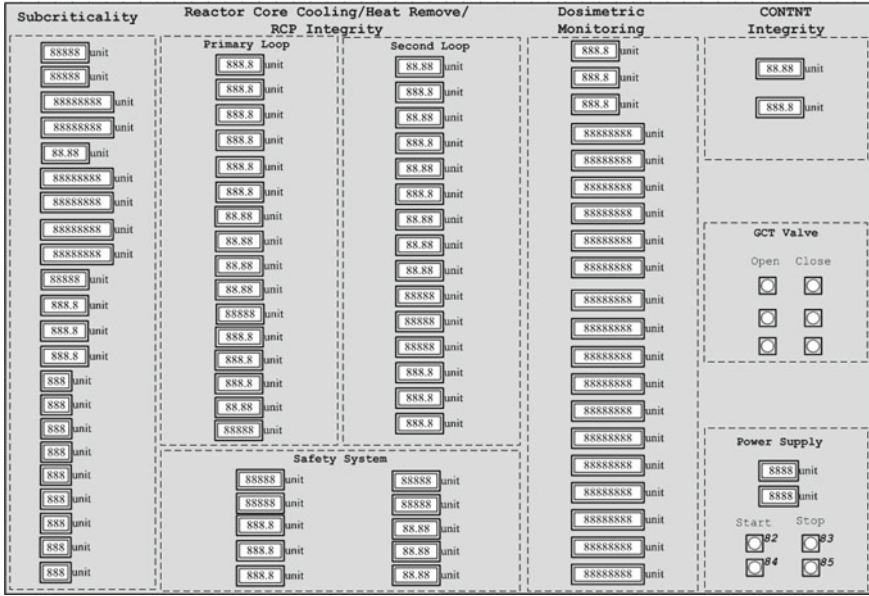


Fig. 6 Example of traditional SPDS display

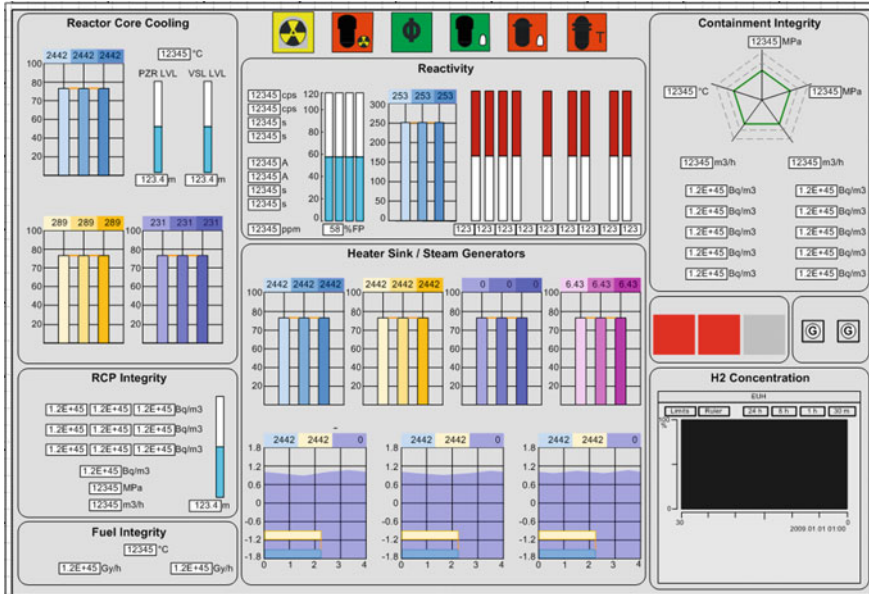


Fig. 7 Example of SPDS display



at the first time; secondly, the polar plot is designed at the top right of the screen to display the integrity of the containment, and the hydrogen concentration is tracked and displayed in real-time through the curve. For the reactor core cooling, the export of heat quantity of one loop and the integrity of one loop, reactivity control, dose monitoring, and other parameters, we group relevant parameters, for example, classifying the cold section temperatures of three loops as a group and displaying them by the bar chart of correlated parameters.

Data are listed mechanically in the traditional safety parameter display screen of the nuclear power plant, which is not convenient for the operator to observe and analyze, nor to remind the operator. However, based on the above analysis of working domain, we design the screen from the perspective of meeting the functional requirements. The data are displayed by means of a bar chart, curve, limit chart, etc. At the same time, the accident situation is alerted to the operator by sound and light alarm. Such design is more conducive to the operator to find and solve the problem in time and also can effectively reduce the operator's observation and analysis load.

## 6 Conclusion

The analysis of the above design examples of the human–machine interface of nuclear power plants proves that the ecological interface design can effectively support the decision-making activities under unexpected events. The idea of ecological interface design has important application value in the human–machine interface design of the main control room as well as a guiding significance for screen design optimization. It is an important direction for the subsequent screen optimization and improvement.

## References

1. National Nuclear Security Administration (2004) HAF 102-2004 Nuclear power plant design safety regulations. National Nuclear Security Administration, Beijing
2. Nuclear Industry Standardization Institute (2002) EJ/T 1143-2002 Nuclear power plant control room design function analysis and distribution. China Standard Press, Beijing
3. Study on Human–Machine Interface Design of Nuclear Power Plant Control Room
4. Room (2019) 19th international conference on human-machine-environment system engineering, Shanghai, P.R. China
5. Burns CM, Hajdukiewicz JR (2002) Ecological interface design. CRC Press LLC

# Human–Computer Interaction Analysis and Prediction for Task Operating System Based on GOMS Model



Fang Xie, Yaofeng He, Sijuan Zheng, Liang Ling, and Zhiyou Fan

**Abstract** *Objective*—In view of the current application status for special vehicles, along with increasing functions of task operating system interface, the operation mode and interactive information are becoming more and more complex. In order to achieve the purpose of optimizing the display-control interface scheme, a human–computer interaction analysis method facing to task operating system is proposed. *Methods*—Combined with the actual special vehicle tasks, quantitative analysis and prediction of human–computer interaction process of task operating system interface are performed using the principle of GOMS model. In addition, the verification experiment is also carried out based on the task simulation platform system of special vehicle. *Results*—The validity of the proposed quantitative analysis method based on GOMS model is proved by the results analysis of the verification experiment. At the same time, it is concluded that there exists a linear relationship between the task completion time and subjective workload in the current test task. *Conclusions*—The analysis results can be used in the ergonomics evaluation for task operating system interface and provide reference for the future interface design and optimization.

**Keywords** Human–computer interaction · GOMS model · Control system · Quantitative analysis

## 1 Introduction

The human–machine interface of the task operating system is the interface and channel between the operator and the system to realize information interaction and energy interaction, which plays a key role in the overall combat effectiveness of the weapon system. At present, with the development of computer technology and

---

F. Xie · S. Zheng · L. Ling · Z. Fan (✉)  
NO. 51 Box 969, Beijing, China  
e-mail: [ZhiyouFan001@163.com](mailto:ZhiyouFan001@163.com)

Y. He  
NO. 3 Huaishuling, Changxindian, Fengtai District, Beijing, China  
e-mail: [lei\\_he2010@126.com](mailto:lei_he2010@126.com)

© The Editor(s) (if applicable) and The Author(s), under exclusive license to Springer Nature Singapore Pte Ltd. 2021  
S. Long and B. S. Dhillon (eds.), *Man-Machine-Environment System Engineering*, Lecture Notes in Electrical Engineering 645,  
[https://doi.org/10.1007/978-981-15-6978-4\\_83](https://doi.org/10.1007/978-981-15-6978-4_83)

725

communication technology [1], the vehicle weapon system is developing toward high speed, high mobility, long range, autonomous operation and high precision, so as to meet the demanding operational functional requirements; however, at the same time, the human-machine interface which adapts to the requirements of combat function is becoming more and more complicated, and the human-machine relationship contained in it is also undergoing profound changes.

The onboard display and control terminal of the special vehicle are an onboard computer with integrated display and control features using for human-computer interaction. With the in-depth application and comprehensive integration of automation, information and intelligent technologies in special vehicles, the task type of special vehicle crew is also gradually changing to the advanced perception and management functions such as multi-dimensional battlefield information collection and monitoring, comprehensive planning, judgment and decision-making, as well as multi-occupant collaborative operation [2]. During this process, the design of human-computer interface interaction operational process, intelligent information processing method, and the rationality and adaptability of multi-channel (visual, auditory, tactile) information flow intensity design will directly affect the workload, attention distribution mode and situation awareness ability of the combatant which will lead to the change of the operational performance of the combatant, and then affect the whole operational effectiveness and personnel safety.

Relevant studies show that at present, there are fewer accidents caused by vehicle performance and working environment, but the proportion of unsafe events resulting from occupant characteristics has not decreased obviously. Statistics show that about 70% of accidents in the field of special equipment are caused by human factors, and the main reason lies in cognitive behavior errors in the process of crew information processing. Therefore, it is of great significance to carry out ergonomic evaluation in the early stage of human-machine interface development of new special vehicle system.

In order to better meet the requirements in various battlefield situations, the ergonomics tests are conducted based on the multi-occupant simulation platform and real special vehicles; besides, the possible risk points in the design of human-computer interface display mode and interactive operational process under the current technical state have been identified and diagnosed, as well as the optimization and improvement suggestions are put forward from the view of ergonomics.

## 2 GOMS Theoretical Analysis Method

GOMS model is a modeling technology used to analyze the complexity of users in interactive systems, which can be used to predict the operation time required by an experienced operator to perform a specific task under a certain interface. It refines a task in multiple levels and describes the behavior of operators according to four elements: goal, operator, method and selection rules [3]. The GOMS model framework is shown in Fig. 1.

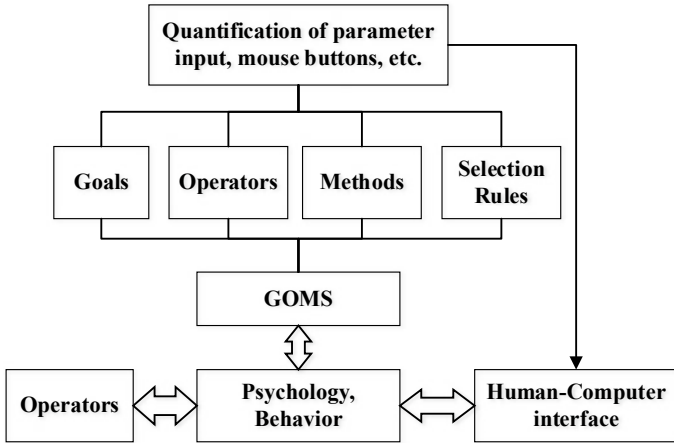


Fig. 1 GOMS modeling framework

Keystroke-level model (KLM) is a common method in GOMS model. According to KLM, task execution includes four different types of body movement operations: K (keystroke), P (pointing), H (homing) and D (drawing). In addition, there are also a mental preparation operation m (mental preparation) and a system response R (response). The total task execution time can be represented by the sum of the individual execution times of these six different operations. Specifically:

- (1) K represents key operation time, including keyboard, mouse or another button operation. Each time of press a key, a key operation is recorded. Although it takes different times to press different keys, however, when a large amount of content is input, the key press time can be converted to an average approximate value.
- (2) P represents the pointing operation time, including the pointing operation time of positioning controllers such as mouse and trackball, which can be calculated by Fitts law, or the reference value obtained in the literature can be used as a rough estimate.
- (3) H represents the switching time of the operator between different devices. For example, when the operator moves the mouse pointer to the target area, the hand will move from the mouse to the keyboard, and then enter the text. The transfer operation during this period is H.
- (4) D represents the time of drawing line segment with mouse, which is related to the number and length of line segment. D operation was defined at the beginning of the theory. In today's human-computer interaction system, there are also some studies that use KLM to predict time without considering D.
- (5) M refers to the psychological preparation of the operator before performing the physical movement operation. In fact, the psychological preparation time of operators before different operations various, but for the sake of simplifying the calculation requirements, M is used in a unified way.

**Table 1** Heuristic rules for placing the M operations

<p>Rule 0: initial insertion of candidate <b>M</b>          Insert <b>M</b> before all keystrokes <b>K</b>; insert <b>M</b> before all points <b>P</b> used to select the command; do not insert <b>M</b> before <b>P</b> used to select command parameters</p>
<p>Rule 1: deletion of expected <b>M</b>          If the operation following an <b>M</b> is fully anticipated in the operation before <b>M</b>, then delete the <b>M</b> (e.g., <b>PMK</b> → <b>PK</b>)</p>
<p>Rule 2: deletion of <b>M</b> in cognitive unit          If a string of <b>MK</b> belongs to the same cognitive unit (e.g., the name of a command), delete all <b>M</b>'s but the first</p>
<p>Rule 3: deletion of <b>M</b> before continuous terminator          If <b>K</b> is the extra separator after a cognitive unit (e.g., the command terminator immediately after the parameter terminator), delete the previous <b>M</b></p>
<p>Rule 4: deletion of <b>M</b> as command terminator          If <b>K</b> is the separator followed by a constant string (e.g., the name of a command), the previous <b>M</b> will be deleted; if <b>K</b> is the separator of a command parameter, the previous <b>M</b> will be retained</p>

- (6) R represents the response time of the system after the operation is completed. This typical value needs to be defined by the analyst according to the actual system performance and task characteristics. It should be noted that if R is followed by a mental preparation m, and M takes longer than R, then r should be deleted in calculation. Or, although the system needs a certain response time R, it does not affect subsequent operations during this period, and the R should also be deleted.

In the analysis of GOMS, the actions of key K, direction P and homing H are relatively clear. When the operators will stop doing unconscious psychological activities, that is, the location of psychological preparation time m, can refer to the following rules [4], as shown in Table 1.

Based on Table 1, the parameters of the general KLM are optimized. Combined with the part of experiment test of touch interaction mode of special vehicle simulation platform in the current technical state, quantitative analysis is carried out on the typical time and operation type for standard average skill subjects. See Table 2 for details [5].

### 3 GOMS Analysis of Typical Tasks

#### 3.1 GOMS Analysis of Direct Fire Task

The mission flow of direct fire mainly includes turn on the control panel equipment low voltage, turn on the high voltage of the equipment, turn on the device, open the turntable and other 16 operation steps, as shown in Fig. 2.

**Table 2** Quantitative analysis of operation execution time for special vehicle simulation platform

Operation type	Operation description or illustration	Time (s)
K_S (keystroking_Software)	The time required to tap a key on the software interface	
	Average skilled operators	0.20
	Enter random letters	0.50
	Input complex symbols	0.75
K_H (keystroking_Hardware)	Time required to touch a key on the hardware control of the control panel	
	Average skilled operators	0.30
U (Understanding)	The average speed of reading is about 300 words per minute, and the number of words understood num	$T = \text{num} * 60 / 300$
H (Homing)	Reset the handle from the keyboard, mouse and other devices	0.40
D (Drawing)	nD is the number of line segments, and lD is the total length of line segments	$0.8nD + 0.16lD$
M (Mentally preparing)	Time for psychological preparation for physical exercise operation	1.35
W (Watching)	The search time $T$ is a linear function of the number of items $N$ when the target exists	$T = Ap + bN/2$

According to the GOMS model, through the quantitative model of operation execution time of special vehicle simulation platform, the above-mentioned operation steps of direct fire task are decomposed, and the total operation time is 127 s.

### 3.2 GOMS Analysis of Command Planning Task

The task flow of command planning task is divided into four steps: task decomposition, path planning, perception planning and strike planning. According to the GOMS model, through the quantitative model of operation execution time of special vehicle simulation platform, the operation steps of command planning task are decomposed, and the total operation time is 178.05 s.

### 3.3 Verification Analysis of GOMS Method Based on Measured Data

Based on the special vehicle simulation platform, the verification experiment is performed according to the operational processes of command planning and direct fire. The operators' completion time of different tasks is recorded and used for

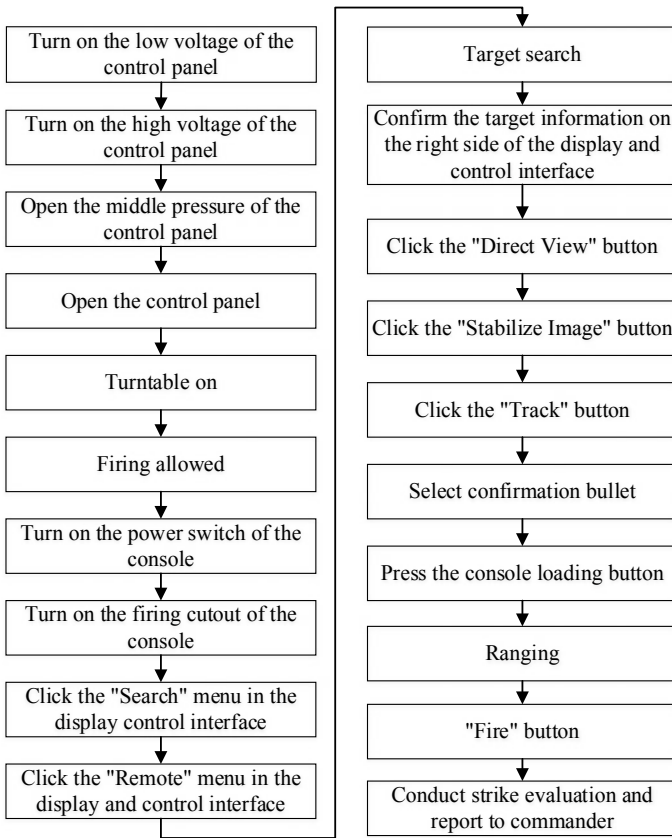


**Fig. 2** Flowchart of direct fire task

verifying the GOMS method. The GOMS theoretical prediction time of command planning and direct fire tasks are shown in Table 3.

The results of correlation analysis between theoretical and practical performances of GOMS model are shown in Table 4.

According to the correlation analysis between the completion time of experimental operation task and the completion time predicted by GOMS theory, there

**Table 3** Comparison of theoretical operation performance and practical operation performance for multi-station

Task type	Completion time of experiment operation (s)	GOMS theoretical prediction time (s)
Command planning	245	178.05
Direct fire	136	127.0

**Table 4** Correlation analysis between theoretical and practical operation performances for multi-station

		Completion time of experiment operation	GOMS theoretical prediction time
Completion time of experiment operation	Pearson correlation	1	0.983*
	Significance (double tail)		0.017
	Number of cases	4	4
GOMS theoretical prediction time	Pearson correlation	0.983*	1
	Significance (double tail)	0.017	
	Number of cases	4	4

\*At 0.05 level (double tail), the correlation was significant

is a significant high correlation between the completion time of experimental operation task and the completion time of actual measurement task ( $r = 0.983$ ,  $P = 0.017$ ). In addition, the trend of the theoretical prediction is consistent with that of the experimental measurement, which verifies the effectiveness of the GOMS theoretical analysis method used in this study.

## 4 Results and Conclusions

The quick, convenient, intuitive and concise operation interface provides an efficient method and platform for the commander's command. However, how to qualitatively and quantitatively describe which operations are simple or difficult is the key to human-computer interface evaluation and optimization design. The GOMS model provides a method for quantitative analysis of interface task operation time. However, the application scope of GOMS model is limited, and the results obtained by using this model are also the results under ideal conditions, so this method cannot be used for unpredictable factors [6, 7]. In this study, we used the GOMS model to analyze the human-computer interaction process of command planning, vertical strike, laser irradiation and direct fire tasks under multi-station tasks, propose a quantitative analysis method based on GOMS, calculate the theoretical prediction task completion time and complete the experimental verification through the task simulation platform system of special vehicle. The theory and experimental method proposed in this study can be used to guide the quantitative evaluation and analysis of human-computer interface and can compare the changes of operation time before and after the improvement of human-computer interface design, which provides a reference for the design, modification and improvement of the interface of airborne command and control system, and is of great significance to the interface optimization.



## References

1. Kieras DE (1996) A guide to GOMS model usability evaluation using NGOMSL. University of Michigan, Ann Arbor
2. Card S, Moran T, Newell A (1983) The psychology of human-computer interaction. Erlbaum, New Jersey
3. Kieras DE, Meyer DE (1994) The EPIC architecture for modeling human information-processing: a brief introduction. University of Michigan, Ann Arbor
4. Kieras DE (2004) EPIC architecture principles of operation. University of Michigan, Ann Arbor
5. Wang C (2013) Research on user interfaces of handheld devices' operation systems based on GOMS model-according to the iOS call interface. Wuhan Textile University, Wu-Han, pp 9–32
6. Hu J (2005) Research and application of human-computer interface design and evaluation technology. Shandong University, Jinan, pp 41–60
7. Kieras DE, Meyer DE (1997) An overview of the EPIC architecture for cognition and performance with application to human-computer interaction. *Human-Comput Interact* (12):391–438

# Research on Visual Perception and Modern Inheritance and Innovation of Models of Traditional Sleeping Beds in Eastern Fujian



Hanzhou Qiu and Yun Liu

**Abstract** Based on the theory of eye movement experiment and subjective evaluation psychology, this paper studies the visual perception of traditional sleeping bed models in eastern Fujian and proposes a visual aesthetic method of traditional folk furniture modelling based on eye movement tracking technology. Based on the subjective intention evaluation, the representative samples are selected, and then the typical samples with the highest and lowest preference are extracted with eye movement hot spot map, and the interest is taken as the basis. Based on the area and eye movement tracking data, according to the principle of “point, line, face and body” modelling elements, the typical samples are divided into AOI, the eye movement variable data of visual attention and visual search are extracted for further analysis, and the integrity characteristics of visual aesthetics and the intensity laws of modelling elements are obtained, and finally, the index system of typical samples is constructed.

**Keywords** Eastern Fujian · Traditional furniture · Sleeping bed

## 1 Summary of Visual Perception of Models of Traditional Furniture

Perception refers to the direct reflection of objective things in the human brain. The objective things transmit stimulus to the brain in the form of images through the human visual system and control the movement of human eyes through the visual cortex area of the brain to express interest in images. This process is called as visual perception [1]. Different persons will measure and judge the visual stimulus according to their own visual experience, cultural literacy, etc., and then output their

---

H. Qiu (✉)  
Ningde Normal University, Fujian 352100, China  
e-mail: [80706779@qq.com](mailto:80706779@qq.com)

Y. Liu  
Fuzhou University, Fujian 350108, China

© The Editor(s) (if applicable) and The Author(s), under exclusive license to Springer Nature Singapore Pte Ltd. 2021

S. Long and B. S. Dhillon (eds.), *Man-Machine-Environment System Engineering*, Lecture Notes in Electrical Engineering 645, [https://doi.org/10.1007/978-981-15-6978-4\\_84](https://doi.org/10.1007/978-981-15-6978-4_84)

cognition of the objects that generate the stimulus, which is visual aesthetics [2]; for example, when people see a piece of furniture through the visual organ, they can quickly perceive its appearance characteristics, proportion, scale, etc., and then get the conclusion that the furniture is beautiful or not beautiful or they like or dislike it by understanding its overall texture sense and spatiality. The visual aesthetic sense is the higher level of emotion of human beings, and the aesthetic sense is a unique higher level of information processing mode of human beings, accompanied by extremely complex aesthetic value judgement and aesthetic experience (aesthetic sense) [3]. The aesthetic experience obtained by the consumer from product design will affect their perception and purchase of the product [4], and therefore, the beauty of the furniture model is the core of design. However, people's aesthetic ability and taste change correspondingly with the changes of the social history and regional environment. The furniture models in different times and different regions have their own characteristics, which is a comprehensive reflection of local people's aesthetic consciousness and ability of the corresponding times [5]. The folk furniture in each region has formed a distinctive model aesthetic feeling in the long historical development, as well as many points worthy of our exploration and reference.

## **2 Result and Analysis of Visual Perception Experiment of Traditional Sleeping Beds in Eastern Fujian**

### ***2.1 Analysis of Shapes and Features of Traditional Sleeping Beds in Eastern Fujian***

The sleeping beds in eastern Fujian are generally divided into Jiazi beds and Babu beds, which are extremely exquisitely made. They integrate wood carving art, japaning art, poetry, calligraphy and painting into a whole. The sleeping beds in eastern Fujian are typically characterized by flat feet, partition-type bed gates, interior cabinets and drawers, unique pattern covers, Tiaoyan, Guangai, etc. The sleeping beds can be divided into the Guangai type and flat-top type. The sleeping beds of flat-top type are divided into the Tiaoyan type, Bingpanyan type and Wuyan type. The sleeping beds of Guangai type are often made by combining with the Tiaoyan with five pattern plates transversely arranged. The solid pattern plate type of the imitated bamboo frame of the Wuyan flat-top type is also the unique shape of eastern Fujian. The overall shape of the sleeping bed is very large, which seems to be a single "body", but in fact it can be abstracted as a comprehensive structure of points, lines, surfaces, bodies and spaces [6].

## 2.2 Model Elements and Shape Differences

The large-volume sleeping beds are enclosed by surfaces which are the important model elements of the sleeping beds in eastern Fujian. The typical three-section bed gates and the bed tops with diversified patterns with the characteristics of eastern Fujian are divided into diversified large, medium and small surfaces. Chuangmei, Chuangban, Chuangting, flat feet, Yaban, etc., are all surface-shaped pattern plates of different sizes and shapes [7]. The boundary lines of different shapes, such as square, round, Weijiao square, oval, Ruyi shape, Malus spectabilis shape and even double frame, window lattice combination, etc., are formed by segmenting or drawing outlines of these surfaces to make the large surfaces comprising of small surfaces be vivid and rich. In the research of eye movement experiment, the front of the sleeping bed can be considered as a large surface of which the areas of interest (AOI) [8] are divided as (1) Chuangmei, (2) Chuangbang, (3) bed gates, (4) base, (5) Tiaoyan and (6) Guangai.

## 3 Experiment Analysis of Visual Perception of Models of Traditional Sleeping Beds in Eastern Fujian

Different senses of layering are formed by the combination of different surfaces of the sleeping beds, and thus, it is more appropriate of changing the traditional feeling as the sense of layering in the four variables of visual perception. In addition, the volume of the sleeping beds is large, and the duration for presenting the picture is set as 15 s.

### 3.1 Subjective Intention Evaluation

The subjective evaluation table corresponds to the subjects' "visual perception of models" and "preference", as shown in Table 1.

The subjects have certain commonness in the visual perception of the models of the sleeping beds in eastern Fujian: the 10 sleeping beds have good stability and high decoration degree with certain differences in the sense of proportion and sense of layering. According to the binary variable correlation analysis of all items of "the visual perception of model" and "preference", when  $P = 0.01$ , the Pearson correlation coefficient between the sense of proportion and preference is 0.867, and therefore, it is believed that there is a strong positive correlation between the sense of proportion and preference of the sleeping beds in eastern Fujian. When  $P = 0.05$ , the Pearson correlation coefficient between the sense of layering and preference is 0.751, and therefore, it is believed that there is also a certain positive correlation between the stability and preference of the sleeping beds in eastern Fujian. At the same time, the

**Table 1** Correlation analysis of visual perception and preference of Eastern Fujian beds

		Stability	Sense of level	Decoration degree	Sense of proportion	Preference
Stability	Pearson Relevance	1	0.025	-0.716*	0.506	0.313
	Saliency		0.944	0.020	0.136	0.379
	<i>N</i>		10	10	10	10
Sense of level	Pearson Relevance		1	0.079	0.639*	0.751*
	Saliency			0.828	0.047	0.012
	<i>N</i>			10	10	10
Decoration degree	Pearson Relevance			1	-0.271	-0.194
	Saliency				0.448	0.592
	<i>N</i>				10	10
Sense of proportion	Pearson Relevance				1	0.867**
	Saliency					0.001
	<i>N</i>					10
Preference	Pearson Relevance					1
	Saliency					
	<i>N</i>					

Pearson correlation coefficient between the decoration degree and the stability is -0.716, indicating that there is negative correlation between the decoration degree and stability.

### 3.2 Eye Movement Tracking Analysis

#### 1. Eye movement tracking hot spot image

The combined hot spot image of 10 individual samples is obtained by the eye movement tracking experiment. In the hot spot images of 10 individual samples, the hot spot images of the sample 8 with the highest preference and the sample 2 with the lowest preference are extracted for analysis, and then it found that all subjects focused on gazing at the carved Yaban in the middles of the Chuangmei, the wonderful carving positions of Chuangbang, the upper and middle parts of the middle of the bed gates and the carved legs on both sides of Chuangwei of the two samples. In the overall distribution of sightlines, the overall hot spot contour image of the sample 8 tends to be stable square, and the common borders of the legs and the floor are more

concerned. From the perspective of visual search, the subjects have high-density fixation points on the Guanggai and Tiaoyan of the sample 2.

Combining with the hot spot image and the above analysis and summary, it is believed that different types of sleeping beds in eastern Fujian have commonness as well as their own characteristics in models. The Yaban at the middle of Chuangmei, Chuangbang, the middle of bed gates and flat legs are all the focus of visual aesthetics. The design of the Guanggai, Tiaoyan, etc., will improve the overall decoration, but they cannot guarantee the balanced stability of the upper and lower vision and the overall proportion coordination of the sleeping beds. Although the Bingpanyan is not the highlight for attention, it plays an irreplaceable role in maintaining the overall sense of proportion and stability. Compared with the mortise-and-tenon abstract patterns, the concrete concave carve patterns with plots have more aesthetic universality.

## 2. Eye movement tracking and data analysis

According to the above analysis, the sample 8 which ranked first in model cognition and preference is selected for the division of areas of interest so as to further analyse the eye movement data.

### (a) Visual attention analysis

According to statistics, the visual data of all model features are shown in Table 2. It can be seen that: if arranging the total gazing time  $T_{tot}$  and the number of gazing points  $G_n$  of all areas of interest from high to low, the order is bed gates, Chuangbang, Chuangmei and bed base, indicating that the middle part of bed gates plays a major role in the overall visual distribution, which is also related to its position, and if arranging the average gazing time from high to low, the order is bed base, Chuangmei, Chuangbang and bed gates. Relatively speaking, the proportion of the bed base to the front area of each sleeping bed is very small, but the eyes stay for the longest time on it each time, indicating that the subjects have given more cognitive efforts to this area of interest, and it becomes the subjects' selective attention object.

### (b) Visual search analysis

The visual search data of each model feature are shown in Table 3. It can be seen that if arranging the average conversion times from high to low, the order is bed gates, Chuangbang, Chuangmei and bed bases. The more the average conversion times of

**Table 2** Visual attention data of style elements

Region of interest	Total fixation duration $T_{tot}$ (ms)	Number of fixation points $G_n$	Average fixation duration (ms)	Proportion of fixation time (%)
1. Bed lintel	25,947	92	282.03	23.43
2. Bed side	28,755	123	233.78	25.97
3. Bed curtain	35,750	178	200.84	32.29
4. Bed base	20,274	65	311.91	18.31

**Table 3** Visual search data of style elements

Region of interest	Total fixation duration $T_{\text{tot}}$ (ms)	Number of fixation points $G_n$	Average fixation duration (ms)
1. Bed lintel	4.50	1.80	3
2. Bed side	4.61	2.92	2
3. Bed curtain	5.60	3.67	8
4. Bed base	9.29	1.07	2

the bed gates are, the more interested the subjects will be to the area and the subjects repeatedly gaze at the area. In addition, it has the highest number of first gazing points which also means that the decoration of bed gates has the eye-catching effect, and it is the easiest accessible important position for vision.

The average gazing frequency of the bed bases is the highest, indicating that their information processing amount is high, and the concentration of gazing points is relatively high when the subjects carry out feature analysis to these parts, indicating that as the important members for measuring stability, the bed bases are highly concerned.

### 3.3 Cognitive Strength of Aesthetic Features of Models

Based on the previous analysis, the sum of feature strength scores of all models is:  $\sum_{i=1}^4 \theta_i = 3.14$ .

The linear interpolation method is used to calculate the subjects' aesthetic perception  $R(U)$  of the sample 8, make the scores  $(-2, 2)$  of the SD scale be corresponding to the percentage  $(0, 100\%)$  of the aesthetic perception. Because there are 4 elements, the total score range is  $(-8, 8)$ , and the calculation formula is as follows:

$$R(U) = \left[ Y_0 + \frac{Y_1 - Y_0}{X_1 - X_0} (X - X_0) \right] \times 100\%$$

wherein,  $X_0 = -8, Y_0 = 0; X_1 = 8, Y_1 = 100\%; X = 3.14$ . The calculation result is  $R(U) = 69.63\%$ .

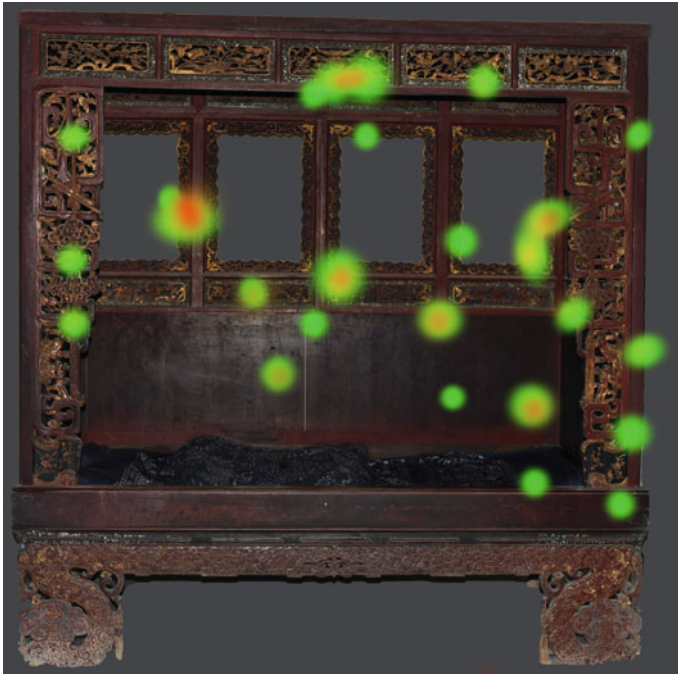


Fig. 1 Hot spots and grayscale histograms of training sample no. 7

## 4 Establishment and Verification of Discriminant Function Model for the Evaluation of Traditional Sleeping Beds in Eastern Fujian

### 4.1 Selection and Feature Extraction of Eye Movement Hot Spot Image

The mean value of preference of all samples of the traditional sleeping beds in eastern Fujian is 0.49, and the median is 0.36. The highest and lowest scores are, respectively, 1.47 (the original sample 8) and 0.00 (the original sample 2). Respectively select the hot spot image of one of the subjects, as shown in Figs. 1 and 2. Process the 15 subjects' eye movement hot spot images as above, and after statistics, the feature indicator values are shown in Table 4.

### 4.2 Establishment and Test of Discriminant Function Model

1. Establishment of the discriminant function model



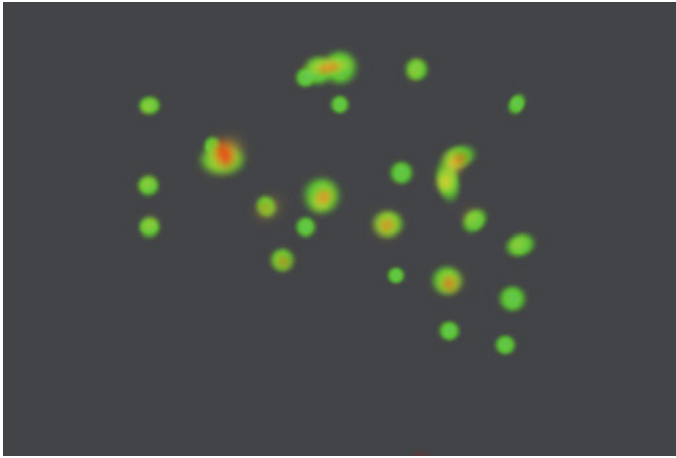


**Fig. 2** Hot spots and grayscale histograms of training sample no. 8

**Table 4** Analysis results of training sample no. 7

Subjects	$X_1 = \mu$	$X_2 = \sigma^2$	$X_3 = \mu_S$	$X_4 = \mu_K$	$X_5 = \mu_N$	$X_6 = H$
1	2.5945	97.8348	8.3782	79.7750	0.8795	7.6012
2	4.2135	211.1854	6.1060	45.4843	0.8015	12.7922
3	4.7218	224.5285	5.7057	40.3223	0.7331	17.6270
4	2.9708	133.3150	8.4463	90.4251	0.8554	9.0713
5	2.3260	121.7954	10.228	120.9453	0.9446	3.1677
6	3.3153	133.6900	6.8466	52.7794	0.8122	12.1413
7	4.2127	186.4381	6.1144	48.2813	0.7581	16.2731
8	3.7150	188.6054	6.6638	53.9708	0.8457	9.7812
9	3.3385	120.4421	6.4887	48.3845	0.7932	13.8281
10	3.6277	189.0931	6.4375	44.1457	0.8491	9.8578
11	3.4528	194.2226	7.2084	59.8651	0.8713	7.9550
12	3.5785	157.6604	7.0837	64.9231	0.7983	13.2597
13	4.6070	248.5699	5.6943	37.9361	0.7838	14.4121
14	4.2929	218.4087	5.6862	35.0736	0.7945	13.3921
15	3.3860	170.8869	7.2826	64.2144	0.8544	9.4231

In the R software environment, call the function `discriminant.fisher()` to write [9], and input Table 4 as the training sample. The obtained discriminant equation is as follows:

$$u(x) = 0.3310x_1 - 0.0034x_2 - 0.1451x_3 + 0.0055x_4 - 14.2622x_5 - 0.2540x_6$$

**Table 5** Compared results between eye movement heat map and SD scale of no. 9

Subjects	Calculation results of discriminant function	SD Scale results
1	0.139	1
2	2.294	0
3	-1.252	2
4	0.889	1
5	4.119	-1
6	-0.2	2
7	1.206	1
8	1.03	1
9	2.388	0
10	1.276	1
11	-0.251	2
12	2.496	1
13	3.312	-1
14	2.153	0
15	0.537	1

Take 0 as the dividing point to carry out the eye-tracking test for the user and substitute the feature values of his hot spot image into the discriminant equation. If the score is greater than 0, it indicates that the user does not like the sleeping bed, and if the score is less than 0, it indicates that the user likes the sleeping bed.

2. Test of the discriminant function model

Carry out the discriminant calculation on the basis of the R software and the discriminant equation, and compare the results with the SD scale (-2 to 2). Refer to Table 5 for the results.

**4.3 Relationship Between Visual Perception of Models and Preference of Traditional Beds in Eastern Fujian**

The specific steps are as follows: use the relevant programming language to carry out Fisher calculation of two sets of numerical matrices so as to get the linear discriminant equation on the basis of the discriminant principle and criteria of Fisher discriminance [10] and under the R software environment, and extract and test samples for the T-test of independent samples, and the obtained Fisher linear discriminant equation of the sleeping beds is as follows:

$$u(x) = 0.3310x_1 - 0.0034x_2 - 0.1451x_3 + 0.0055x_4 - 14.2622x_5 - 0.2540x_6$$

The evaluation method provides a feasible technical way to realize the objectivity and quantification of furniture model evaluation and can be used for building the model of inheritance and innovation design, and putting forward personal suggestions.

#### ***4.4 Visual Perception Commonness of Different Shapes of Traditional Sleeping Beds in Eastern Fujian***

The calculation results show that the shape elements of the aesthetics of models of the traditional beds in eastern Fujian are bed gates (1.07), Chuangbang (0.87), Chuangmei (0.73) and bases (0.47) in order, which are worthy of attention and continuation in inheritance and innovation.

### **5 Conclusion**

Experimental analysis indicates that the traditionally sleeping beds in eastern Fujian commonly have good stability and high decoration degree with certain differences in the sense of proportion and sense of layering. Their sense of proportion is the important factor that influences the subjects' preference and has positive correlation with the users' preference. The sense of proportion of the sleeping beds mainly depends on the composition of the whole surface, including the parts from Guangai and Tiaoyan to Chuangting, flat feet, etc., of Chuangbang and bases. There is high negative correlation between the stability and preference. The weak stability is often caused by the heavy top ornaments and the bases that are not strong enough, which brings heavy head but light feet. Bed gates dominate the overall distribution of sightlines and are the main projection positions of gazing points, particularly the centre of the screen plate, which is the most accessible part of the sightlines. The Yaban of Chuangmei, the carved ornaments of Chuangbang and carved legs are all the focuses of visual aesthetics. The research results show that the proportions, positions and coordination of the elements all have a certain impact on the visual perception and preference of the models of the traditional sleeping beds in eastern Fujian.

**Acknowledgements** This work is supported by the study on the protection planning and cultural heritage of ancient villages in eastern Fujian and study on the regional landscape characteristics of Ningde City, No. (15XGL027), No. (2016Z16).

**Compliance with Ethical Standards** The study was approved by the Logistics Department for the Civilian Ethics Committee of Ningde Normal University.

All subjects who participated in the experiment were provided with and signed an informed consent form.

All relevant ethical safeguards have been met with regard to subject protection.

## References

1. Polanyi M, Sen A (2009) *The tacit dimension*. University of Chicago Press, Chicago, p 108
2. Andrienko G, Andrienko N, Burch M, Weiskopf D (2012) Visual analytics methodology for eye movement studies. *IEEE Trans Visual Comput Graph* 18(12):2889–2898
3. Hyoense J, Radach R, Deubel H (2003) The mind's eye: cognitive and applied aspects of eye movement research. Elsevier Science BV, Amsterdam, Netherlands, pp 13–15
4. Djamasbi S, Siegel M, Tullis T, Dai R (2010) Efficiency, trust, and visual appeal: usability testing through eye tracking. In: *Proceedings of the forty-third annual Hawaii international conference on system sciences (HICCS)*. Computer Society Press, pp 1–10
5. Chen L, Zhao L (2012) Intersection of aesthetics and cognitive psychology: research progress of visual perception. *J Jiangnan Univ (Humanities and Social Sciences Edition)* 5:127–133
6. Pan Y (2013) A study on the aesthetic preference of European neoclassical bed form based on eye movement characteristics. Nanjing Forestry University, Nanjing
7. Qiu Z (2006) Scientific analysis of Ming style furniture aesthetics. *Decoration* (11):102–104
8. Liu W, Zou W (2007) *Furniture design*. China Forestry Press, Beijing, p 119
9. Yuan Q, drawing by Shixiang (2015) Research on Ming style furniture of commemorative edition of Wangshixiang collection. *Life, Reading and Xinzhi Sanlian Bookstore*, p 438
10. Zhou Y (2014) Research on the prediction model of visual characteristics and affordability of ring chairs. Nanjing Forestry University, Nanjing

# Research on User Interface Perception Usability Evaluation of B2C Retailers in Large Appliances



Xiaofang Yuan, Meng Zhang, Linhui Sun, and Qin Tian

**Abstract** The Internet industry is developing rapidly, and competition among various home appliance websites is fierce, improve the user's shopping experience in the website is the first urgent issue. Website interface as the main medium of user data exchange of information, to a large extent, affects the user experience and purchase intention. In this study, representative websites A and B were selected, and six groups of website interfaces that were representative in terms of design location were selected at the same time. In addition, using eye movement experiment to evaluate the usability of home appliance website interface perception, subjective perceived usability and objective eye movement indicators were measured and compared and analyzed. The experimental results show that site A and site B have significant differences in eye movement indicators, site A has a reasonable design in terms of commodity classification and login mode, while site B has a better design in terms of login, registration, customer service contact, delivery address, and after-sales content display than site A. Overall, site B has a relatively reasonable layout of functional areas.

**Keywords** B2C household appliance retailer website · Perceived usability · Eye movement experiment

## 1 Introduction

With the development of Internet technology in China, the competition in the online retail market is very fierce, and all kinds of e-commerce develop rapidly. People's online shopping behavior is becoming more and more common. Moreover, home

---

X. Yuan · M. Zhang (✉) · L. Sun · Q. Tian  
School of Management, Xi'an University of Science and Technology, Xi'an 710054, Shaanxi, China  
e-mail: [1509680897@qq.com](mailto:1509680897@qq.com)

X. Yuan · M. Zhang · L. Sun  
Research Center for Human Factors and Management, Xi'an University of Science and Technology, Xi'an 710054, Shaanxi, China

appliance websites are directly oriented to users. To make users satisfied and retain them, a very important factor is to give users a better experience in the perceived usability of the website interface. From entering the website to completing the purchase, the user has to go through multiple links of interaction with the website, and the experience of each link will affect the user's overall impression of the website. Therefore, optimizing the website interface and improving the user's online shopping experience have become an important issue that the operators and designers of home appliance websites must consider.

On the site, the choice of the images and navigation of the website maneuverability play a decisive role; Julia Lamberz suggests that the combination of eye movement technology and questionnaires has clear implications for the search patterns of the test group, enabling researchers and website designers to make recommendations on website positioning, structure, optimization, and understand ability [1]. Alexandre and Javier et al. studied the effects of increasing website complexity on users' cognition and emotion and showed that visual complexity of websites has multiple effects on people's cognition and emotion [2]. Taking group purchasing websites as an example, guo fu and qu qingxing collected users' eye movement data in the interaction process through eye movement experiment, constructed the relationship model between eye movement index and design elements of browsing task, search task, search task, and login purchase task, respectively, by using partial least square regression method, and verified the effectiveness of the model. The research shows that the level of interaction design can be reflected by the level of eye movement data when the user completes the interaction task [3].

In today's information flood, the attraction of headlines is very important. Zhang yutu et al. took toutiao as an example to collect eye movement data of experimental subjects when they watched simulated pages of news APP. Meanwhile, based on the results of the questionnaire survey, research shows that entertainment news headlines can attract audiences' attention more than general news headlines and have better communication effects, and entertainment news headlines in the form of "text + pictures" can attract viewers' attention more than plain text headlines. [4]

Taking website A and website B as examples, this study used eye movement experiment and questionnaire survey to study the cognition in the process of searching targets located in different regions in different website interfaces. Analyze the usability of website A and website B, and put forward some effective suggestions, which have certain reference value for the layout and design of other some website interfaces.

## 2 Design of Eye Movement Experiment

Randomly select 30 college students with more than two years of shopping experience, aged about 22, and have online shopping experience in recent month, and are very familiar with online shopping processes and basic operations.

This paper takes website A and website B as an example, selects website home page, commodity classification, commodity introduction, order submission and after-sales details, registers six pages, and designs six groups of tasks. Through the completion of six groups of tasks, it analyzes the disadvantages and advantages of website A and website B and puts forward corresponding suggestions.

## ***2.1 Search Tasks***

The first part of the experimental design is search task. According to the different locations of the function buttons of website A and website B, the following keywords were selected: login and registration, cleaning service, online customer service, and delivery address. The website interface corresponding to these keywords was extracted and used as experimental material. There were four groups of tasks and eight pictures. The keywords of the subjects are given before the display of the material pictures. The subjects find the corresponding function buttons on the pictures based on the keywords, which are the search task.

## ***2.2 Interest Tasks***

The task of the interest category is to intercept websites with the same functions but different interfaces on website A and website B and ask subjects which group of products can arouse their interest after browsing the different interfaces. In this way, it is better to judge in which form the home appliance website interface should show the effect.

The eye movement experiment instrument adopts RED5 desktop eye movement instrument, the maximum sampling frequency of 500 HZ. The eye movement instrument is mainly composed of computer, image display, the display at the bottom of the two groups of infrared light source, and camera. During the whole experiment, after correcting the sitting position, the subjects would browse the pictures or words on the computer screen. The camera of the instrument would capture the eye movement trajectory of the subjects and then transmit the eye movement data to the computer database of the test and save it.

**Table 1** Comparison of indicators of websites A and B in login and registration interfaces

Task type		Eye movement indicators		
		The number of eye fixations	Total fixation time	First watch time
Login and registration	A	22	6789.98	456.23
	B	11	3275.76	322.28

### 3 Data Analysis

#### 3.1 Search Experimental Data Analysis

##### 3.1.1 “Login Register” Interest Area

After observing the trajectories of website A and website B and analyzing the repeated measurements of eye movement data, it was found that the eye movement data of the subjects under the condition of the registration button of the website A and the website B had significant differences. As shown in Table 1, further found that the number of fixation points of subjects in website A (MEAN = 22) was significantly higher than that of subjects in website B (MEAN = 11). A website watching the total length (MEAN = 6789.98) is significantly higher than B site subjects watching total length (MEAN = 3275.76); A website watching the first time (MEAN = 456.23) is significantly higher than B site first looking time (MEAN = 322.28).

In the login and registration module, website A is mainly located at the top left of the page, while website B is located at the top right of the center of the interface. Found that the subjects to browse through the experiment website “B” fixation point number is less than “A” website, the participants browsing “A” website watching the total length is greater than the “B” website, participants browsing website “B” looking time less than “A” website for the first time, it shows the location of the login module in “B” website registration area is superior to the location of “A” website area.

##### 3.1.2 “Cleaning Service” Interest Area

After observing the trajectories of website A and website B and analyzing the repeated measurements of eye movement data, it was found that there was a significant difference in the eye movement data of the subjects on the interface of website A and website B under different cleaning service conditions. Further found that, as shown in Table 2, in the classification of goods, the number of fixation point to “A” website (MEAN = 26) was significantly lower than “B” website fixation point number of participants (MEAN = 28); the total attention time of subjects on website “A” (MEAN = 8628.76) was significantly lower than that of subjects on website “B”



**Table 2** Comparison of indicators of cleaning service interface A and B websites

Task type		Eye movement indicators		
		The number of eye fixations	Total fixation time	First watch time
Cleaning services	A	26	8628.76	171.17
	B	28	13,543.49	252.96

(MEAN = 13,543.49). The first fixation time (MEAN = 171.17) of subjects on website “A” was significantly lower than that of subjects on website “B” (MEAN = 252.96) (Table 2).

In the commodity classification module, website A is mainly located at the top of the page and marked with A red background, while site B is located at the bottom of the interface. Through the experiment, it was found that the time spent on browsing the website interface of A was less than that on the website interface of B. And the time of first entering the zone of interest is less than that of website B. It indicates that the product classification of website A is better than that of website B.

### 3.1.3 “Contact Customer Service” Interest Area

After observing the trajectories of website A and website B and analyzing the repeated measurements of eye movement data, it was found that there was a significant difference between the eye movement data of the A site and the B site interface when browsing the two sites’ interface to find the contact customer service area. As shown in Table 3, it was further found that the number of fixation points during browsing of website “A” (MEAN = 15) was significantly higher than that during browsing of website “B” (MEAN = 11). The total fixation time (MEAN = 6117.6) of subjects browsing pages of website “A” was significantly higher than that of subjects browsing pages of website “B” (MEAN = 3359.1). Participants when viewing “A” web page for the first time looking time (MEAN = 383.50) were significantly higher fixation time for the first time browsing the web interface “B” (MEAN = 247.91).

The contact customer service area is located at the top right of website A and at the bottom right of website B. Through the analysis of eye movement index data found subjects in browsing the web interface, B web interface than A web interface to be able to quickly find the target. B website interface contacts customer service button on the right side of the purchase information. Generally, when browsing the web, the

**Table 3** Comparison of indicators of A and B websites in contact customer service interface

Task type		Eye movement indicators		
		The number of eye fixations	Total fixation time	First watch time
Contact customer service	A	15	6117.6	383.50
	B	11	3359.1	247.91

subjects would be attracted by the product display pictures and product information in the interface [5]. With browsing habits, they would naturally find the area to contact customer service after browsing the purchase information of the product. In this way, after they have browsed the products, they will contact the customer service for any questions or questions they want to know.

### 3.1.4 “Shipping Address” Interest Area

After observing the trajectories of website A and website B and analyzing the repeated measurements of eye movement data, it was found that there was a significant difference in the eye movement data of the subjects on the interface of website A and website B in different positions. As shown in Table 4, it was further found that the number of fixation points in browsing the interface of website A (MEAN = 20) was significantly higher than that in website B (MEAN = 14). The total fixation time of subjects on website A (MEAN = 5559.38) was significantly higher than that on website B (MEAN = 3304.59). The time taken for the subjects to enter the interest zone for the first time by browsing the page of website A (MEAN = 388.48) was higher than that by browsing the page of website B (MEAN = 223.01).

Previous studies have found that in most habits, the information of the top position is considered very important when the subjects browse the web. Users often notice the top left part of the information, because this is the place where began to view information [6]. People are used to viewing information from top to bottom, left to right, so they often see elements in the upper left part of the page rather than the right or lower part of the page.

People tend to move their eyes from the top left to the bottom right when browsing the web because people often read from left to right, from top to bottom [7]. In the distribution address area, the distribution location in website B is on the upper left, and the distribution location in website A is on the upper right. At the same time, results show that the shipping address area “B” website interface position is better than “A” website interface delivery address location area. B website design is more reasonable, combined with users’ browsing habits, so that users can find the delivery address information in the first time, and check and correct it, so that the design is more user-friendly.

**Table 4** Comparison of indexes of A and B websites in the delivery address interface

Task type		Eye movement indicators		
		The number of eye fixations	Total fixation time	First watch time
Shipping address	A	20	5559.38	388.48
	B	14	3304.59	223.01

## 3.2 Analysis of Interest Experimental Data

### 3.2.1 After-Sales Interface

#### 1. Fixation trajectory analysis

Through comparison, it was found that when the subjects browsed the after-sales content introduction page of website A, the hot zone diagram and trajectory diagram were mainly reflected in the summary or guidance language at the beginning of each paragraph. On the contrary, when the subjects browsed the after-sales content introduction page of website B, the hot zone diagram and trajectory diagram were mainly reflected in the frame diagram. From the perspective of the trajectory diagram, the page trajectory of website B is more concentrated than that of website A, and it is mainly concentrated in the key areas of framework diagram content. This shows that subjects in the pure text after browsing A website content introduction page, reading interest is low. However, when browsing the after-sales content page in the form of frame diagram of B website, the browsing trajectory is relatively concentrated, indicating a greater interest in reading and a more intuitive access to page information.

#### 2. Questionnaire survey

After browsing the pictures in the eye movement experiment, it was found that 88% of the subjects thought that the display form of frame diagrams was simpler, clearer, and more interesting to read.

### 3.2.2 Login Method

After the end of eye movement experiment, through the questionnaire survey, we found that most of the subjects like to use mobile phone login scan code directly. Meanwhile, they said that they had too many accounts and passwords, which were often confused and forgotten. They do not like to enter account and password, scan code more convenient login.

## 4 Conclusion

By observing the completion of A series of eye movement experiments conducted on the interfaces of website A and website B, and combining with the questionnaire survey after the completion of the eye movement experiment, the advantages and disadvantages of website design and layout can be reflected according to the evaluation indexes of eye movement experiment. As can be seen from Table 5, there are significant differences in eye movement indexes between website A and website B. Website A has A reasonable design in terms of cleaning service and login mode,

**Table 5** Comparison of indicators of websites A and B

Task type			Eye movement indicators			The questionnaire	
			Number of fixation points	Total fixation time	First fixation time		
Search task	Login and registration	A	22	6789.9	456.23	–	
		B	11	3275.76	322.28	–	
	Cleaning services	A	26	8628.76	171.17	–	
		B	28	13,543.49	252.97	–	
	Contact customer service	A	15	6117.6	383.50	–	
		B	11	3359.1	247.91	–	
	Shipping address	A	20	5559.4	388.48	–	
		B	14	4136.16	223.01	–	
	Interest task	After-sales content	A	–	–	–	–
			B	–	–	–	✓
Login mode		A	–	–	–	✓	
		B	–	–	–	–	

Note ✓ said stronger website interface usability

while website B has A better design in terms of login, registration, customer service contact, delivery address and after-sales content display. On the whole, website B has A relatively reasonable layout of functional areas.

## 5 Conclusions and Suggestions

In this eye movement experiment, a combination of subjective questionnaire survey and objective eye movement measurement was adopted to conduct data analysis and t test using eye movement indicators such as hot zone diagram, trajectory diagram, first fixation time, number of fixation points, and total fixation time. Main conclusions and recommendations are as follows:

1. Through a series of eye movement experiments, such as the comparison of first fixation time, hot zone diagram and trajectory diagram, it can be seen that the functional areas that need to be highlighted on the website interface should be displayed in a striking way. Common functional prompts should highlight colors, and simple and vivid ICONS should be used to improve the attractiveness of user interface information and facilitate users to quickly identify.
2. Through the interest class experiment eye movement indicators and survey found that participants were more like charts, frame, and other way, for the pure text display of interest degree is low. And the site interface information distribution

should be moderate as far as possible to reduce the information density interface. A large number of text expression will increase the difficulty of extracting important information, affect the user experience. Should try to use diagrams, frame and so on, and do it simple and clear.

3. In the account login way more toward mobile phone login code. This reflects that it is a major direction to improve the usability of the interface and enhance the sense of user experience by simplifying the steps of users and reducing unnecessary operations. Meanwhile users in the shortest possible time to complete the shopping process, which can improve user satisfaction.

**Acknowledgements** This work is supported by the National Natural Science Foundation, No. 71403204,71673220; Shaanxi Science and Technology Department of Youth Programs, No. 2020JQ760, for this study. The authors are also grateful to the experts who participated in the expert opinion study for their time and efforts.

#### **Compliance with Ethical Standards**

The study was approved by the Logistics Department for Civilian Ethics Committee of Xi'an University of Science and Technology.

All subjects who participated in the experiment were provided with and signed an informed consent form.

**All relevant ethical safeguards have been met with regard to subject protection.**

## **References**

1. Lamberz J, Litfin T, Teckert Ö (2018) Usability and web design of an educational website, vol 2. De Gruyter, Berlin
2. Tuch AN, Bargas-avila JA (2009) Visual complexity of websites: effects on users' experience, physiology, performance, and memory. *Int J Hum Comput Stud* 67(9):703–715
3. Guo F, Qu Q, Zhang X, Cao Y, Liu W (2014) Research on the relationship between eye movements and website design elements. *Ind Eng Manage* 19(05):129–133+139
4. Zhang Y, Gan L, Han T (2018) Research on the propagation effect of entertainment news headlines based on eye movement experiment—a case study of Toutiao APP. *News Res* (07):82–87
5. Webb A, Hacker D, Osher D et al (2009) Eye movements and pupil size reveal deception in computer administered questionnaires. *Found Augmented Cogn Neuroergon Oper Neurosci* 38(56):553–562
6. Djamasbi S, Siegel M, Tullis T, Dai R (2010) Efficiency, trust, and visual appeal: usability testing through eye tracking. In: *System sciences*
7. Ren G (2015) Study on mobile application shop based on user experience

# **Research on the Man-Environment Relationship**

# Analysis of Human Heat Stress Response in High Temperature Environment



Yuhong Shen and Chenming Li

**Abstract** The work efficiency of operators can be reduced at high temperature, which would affect their health. In order to reduce the heat stress reaction of human body, this paper analyzed the influence factors of operation in high temperature environment, collected the heat stress analysis model, carried out test tests for three kinds of protective clothing, and compared the test results with the prediction results of the mathematical model. The test results show that the mathematical model can accurately predict the change trend of human core temperature within a certain range, which provides a preliminary basis for the accuracy of the prediction method to alleviate thermal injury.

**Keywords** Heat stress · High temperature · Protective clothing

## 1 Introduction

The health of workers in high temperature environment has received widespread attention. Continuous work in harsh environment will seriously affect the work efficiency of workers. As time goes on, workers will suffer from fatigue, body temperature rise, heartbeat acceleration and other symptoms, thus reducing the tolerance time of workers and affecting the work efficiency. US scholar Berko and others counted 10,649 deaths caused by environmental factors in the USA from 2006 to 2010. High temperature accounted for 31% (3332) of deaths [1]. The Armed Forces Health Surveillance Center (AFHSC) released an assessment report in 2016. On average, 1.56 out of every 1000 US soldiers were injured by overheating [2]. Injuries related to thermal environment are usually divided into four categories: Heat stress, heat failure, hyperthermia and heatstroke. Heat stress response mainly includes physiological stress and sensory non-response and is usually related to physical activity exposed to high temperature environment.

---

Y. Shen · C. Li (✉)

The Quartermaster Research Institute of Engineering and Technology, Beijing 100010, China  
e-mail: [lichenming82@163.com](mailto:lichenming82@163.com)

© The Editor(s) (if applicable) and The Author(s), under exclusive license to Springer Nature Singapore Pte Ltd. 2021

S. Long and B. S. Dhillon (eds.), *Man-Machine-Environment System Engineering*, Lecture Notes in Electrical Engineering 645, [https://doi.org/10.1007/978-981-15-6978-4\\_86](https://doi.org/10.1007/978-981-15-6978-4_86)

757

## 2 Influence Factors

### 2.1 *Foundation of Thermal Physiology*

The human body can maintain heat balance within a certain temperature range. Due to the natural circadian rhythm, the body temperature of the human body will change by about 0.5 °C. At the same time, the body temperature will fluctuate with the activity intensity and environmental conditions. The fluctuation ranges of the core body temperature that the human body can withstand are between 36 and 40 °C. However, the microenvironment temperature between human skin and clothing is usually kept at 28–30 °C to maintain the thermal balance in a static state. At the same time, due to human metabolism and air flow, this ideal microclimate will change significantly with physical activity. Heat transfer between human beings and the environment occurs through four ways: Conduction, convection, radiation and evaporation. This heat exchange process is usually called dynamic heat balance and can be expressed by the following formula:

$$S = M \pm W \pm R \pm C \pm K - E$$

where  $S$ : heat storage rate of human body;  $M$ : metabolic rate;  $W$ : mechanical work done by human body;  $R$ : environmental radiation calorific value;  $C$ : convection heat exchange;  $E$ : evaporative heat dissipation.

According to the heat balance equation, when the heat dissipation of the human body cannot compensate for the environment and the heat generation of motion, the equation will transfer to the direction of heat storage of the human body and the temperature of the human body will rise. In this process, the blood vessels in the body relax, making more blood flow to the limbs of the human body, increasing heat emission, and causing physiological changes such as heart rate rise to increase the blood flow of the human body.

### 2.2 *Effects of Clothing*

Clothing provides protection for human beings for a long time. These protections include protection against natural factors (high temperature, cold, sun exposure, rain, etc.) and protection against special dangerous environments (flame retardant, bullet-proof, antivirus, etc.). It is often difficult for a set of clothing to give consideration to multiple performances. Therefore, special protective clothing usually increases the thermal load worn, resulting in an increase in the risk of heat stress. The overall thermal resistance of clothing is tested by a warm dummy, and the moisture permeability index is tested by a sweaty dummy.



Calculation formula of thermal resistance:

$$I = \frac{T_s - T_a}{0.155H}$$

where  $I$  is thermal resistance, clo;  $T_s$  is the skin surface temperature, °C;  $T_a$  is the air temperature, °C;  $H$  is that non-evaporative heat dissipation rate per unit surface area, W/m<sup>2</sup>.

Calculation formula of moisture permeability index:

$$i = \sum_{i=1}^n \frac{(T_{si} - T_a)H_{ei}}{2.2\omega(P_{si} - P_a)H_{ti}}$$

where  $i$  is the moisture permeability index;  $T_{si}$  is the skin temperature of the  $i$  stage, °C;  $T_a$  is ambient temperature, °C;  $H_{ei}$  is the evaporation heat dissipation rate of the  $i$  stage, W/m<sup>2</sup>;  $P_{si}$  is the saturation steam pressure of the  $i$  stage, Pa;  $P_a$  is ambient vapor pressure, Pa;  $H_{ti}$  is the non-evaporative heat dissipation rate of stage  $i$ , W/m<sup>2</sup>.

Wind has a great influence on the heat insulation and moisture permeability of clothing. Wind speed, clothing thermal resistance and moisture permeability index are all inputs of mathematical prediction models such as heat strain decision aid (HSDA).

### 2.3 Matching of People and Clothing

Although the same principle can be used to test a single piece of clothing or clothing matching, it is not possible to simply superimpose each layer or each part. This is mainly because the air layer on the inner layer and the surface are different, which will affect the clothing matching performance. Therefore, the overall thermal insulation performance of clothing includes air layer, clothing layer and boundary layer. Air layer factors play an important role in it.

## 3 Model

Mathematical models can be used to predict human thermal correspondence (such as metabolism, core body temperature, tolerance time, etc.) caused by exercise, environment and clothing. Mathematical models are usually divided into theoretical models and empirical models. The theoretical model is expressed mathematically based on the understanding of human physiology, while the empirical model mainly reflects the quantitative relationship between experimental data mathematically.

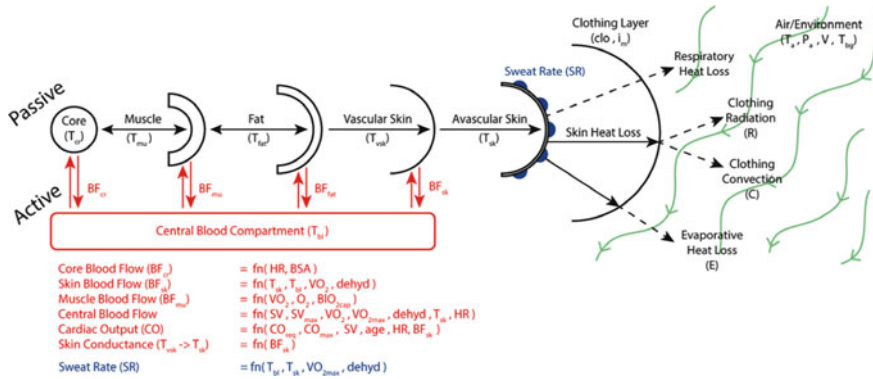


Fig. 1 Schematic diagram of heat stress theoretical model

### 3.1 Theoretical Model

The theoretical model mainly analyzes the interaction between the core layer, muscle layer, fat layer and skin layer of the human body and the relationship between clothing and air layer. Figure 1 is a schematic diagram of theoretical model research [3].

The theoretical model can be simplified by comprehensively considering the heat transfer of each layer of the human body, environmental conditions and temperature regulation reactions (metabolism, vasomotor, sweat production and blood accumulation), etc. [4].

### 3.2 Empirical Model

Empirical model is a mathematical expression of test data, which is usually obtained by regression or correlation analysis. As an empirical model, heat strain decision aid (HSDA) is based on a large number of test data, including heat exchange principle and physiological response prediction, which can predict core temperature, working tolerance time, water demand, etc. Model inputs include 16 items in 4 categories, as shown in Table 1 [5].

## 4 Tests and Results

### 4.1 Test

The test was carried out under the condition of ambient temperature (30 ± 2) °C, relative humidity (60 ± 5)% and no wind. Nine subjects were selected to wear firefighting

**Table 1** Inputs to HSDA model

Element	Symbol	Description	Units
Anthropometrics/health state	$H_t$	Height	cm
	$W_t$	Weight	kg
	DIH	Days in heat; days of heat acclimation	days
	dhyd	Dehydration status	%
	$iT_{sk}$	Initial skin temperature	°C
	$iT_c$	Initial core body temperature	°C
Environmental conditions	$V$	Wind velocity	m/s
	RH	Relative humidity	%
	$T_a$	Ambient temperature	°C
	$T_{mr}$	Mean radiant temperature	°C
Clothing biophysical Characteristics	IT	Total thermal resistance	clo
	$I_T V^g$	Thermal resistance wind velocity coefficient/gamma	N.D
	$i_m/clo$	Evaporative potential	N.D
	$i_m/clo V^g$	Evaporative potential wind velocity coefficient/gamma	N.D
Physical activity/work rate	$M$	Metabolic heat production/metabolic rate	W
	$W_{ex}$	External work rate	W

clothing, chemical protective clothing and fire protection clothing respectively for the test. During the test, the subjects traveled on a treadmill with a speed of 5 km/h and a slope of 0 for 60 min. EQ02 LifeMonitor was used to simultaneously test the subjects’ heart rate, respiration, skin temperature and core body temperature. Oxygen Pro was used to measure the oxygen uptake and carbon dioxide exhalation of the subjects, and the energy metabolism was calculated.

### 4.2 Test Results

The average core temperature of the subjects and the predicted values of the model for the three protective clothing tests are shown in Figs. 2, 3 and 4.

The root mean square error (RMSE) of the measured value and the predicted value of the model are calculated for the three kinds of garments, respectively. The root mean square errors of the three models are 0.21 °C, 0.45 °C and 0.27 °C, respectively.

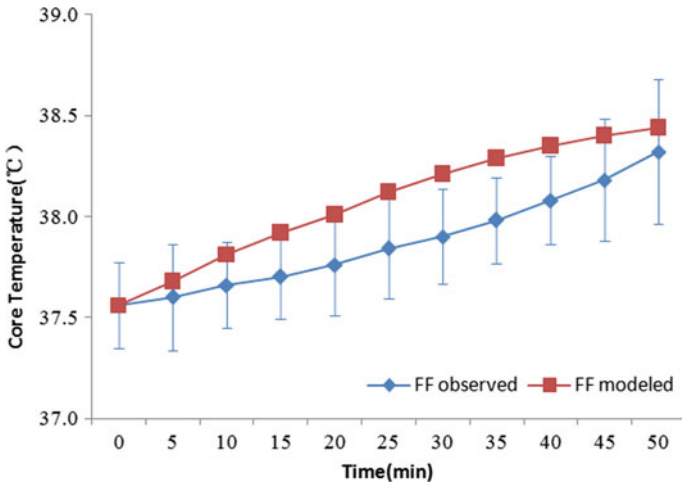


Fig. 2 Firefighting clothing test result

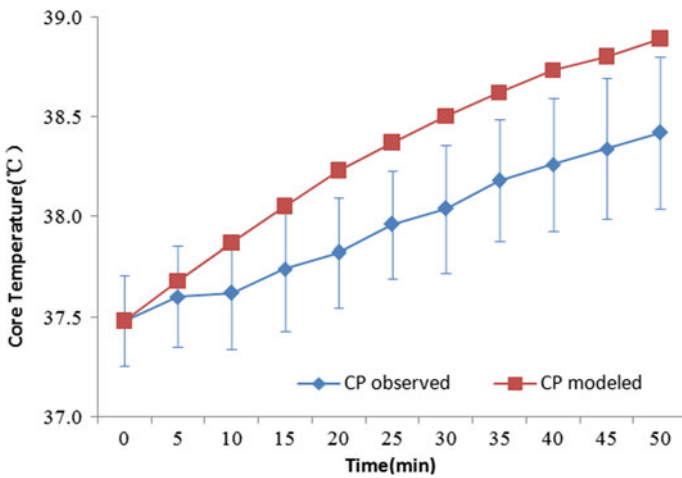


Fig. 3 Chemical protective clothing test result

The prediction results of the models are within 1.25 times of the standard deviation of the observation data, indicating that the models have high credibility.

Using the human body heat stress model can better understand the changes of human body core temperature, formulate mitigation strategies in advance, and slow down the generation of heat stress. However, from the analysis results, the model also has certain limitations. The model does not consider the differences in age, gender,

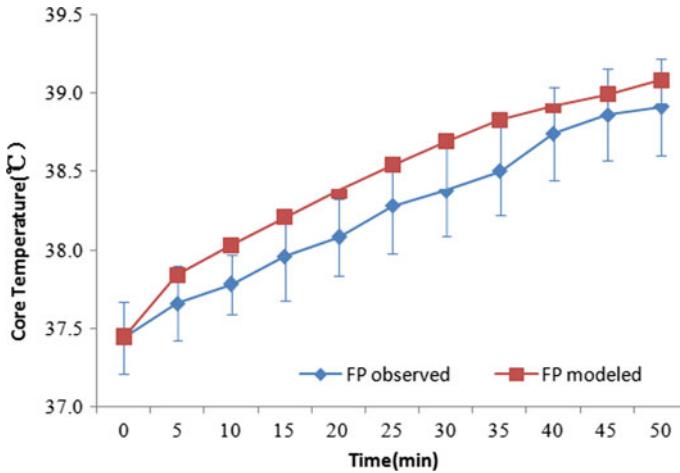


Fig. 4 Fire protection clothing test result

region and physical health equipment. The subjects selected in this test are young men, who often take physical exercise and have good physical quality, which may lead to the measured results being generally lower than the predicted values of the model. At present, some scholars have noticed this problem and studied the influence of age and gender on the prediction results of the model [6].

## 5 Conclusion

Heat stress is a physiological threat that human body often faces in high temperature working environment. This study analyzed the human heat stress model and tested different kinds of protective clothing. The test results show that the empirical model can accurately predict temperature changes, which provides a preliminary basis for the accuracy of prediction methods to alleviate heat injury.

**Compliance with Ethical Standards** The study had obtained approval from the Army Key Laboratory of SEEP Ethics Committee.

All subjects participated in experiment had signed the informed consent.

All relevant safety, health, and rights had been met in relation to subject protection.

## References

1. Berko J, Ingram DD, Saha S, Parker JD (2014) Deaths attributed to heat, cold, and other weather events in the United States, 2006–2010. National health statistics reports. Number 76. National Center for Health Statistics
2. Medical Surveillance Monthly Report (MSMR) (2017) Armed forces health surveillance center; Update: heat illness, active component, vol 24, no 3. U.S. Armed Forces, pp 9–13
3. Welles AP, Tharion WJ, Potter AW, Buller MJ (2017) Novel method of estimating metabolic rates of soldiers engaged in chemical biological defense training. Technical report, T17-02, 2017, ADA#1022691. US Army Research Institute of Environmental Medicine, Natick, USA
4. Xu X, Werner J (1997) A dynamic model of the human/clothing/environment-system. *Appl Hum Sci J Physiol Anthropol* 16(2):61–75
5. Potter AW, Blanchard LA, Friedl KE, Cadarette BS, Hoyt RW (2017) Mathematical prediction of core body temperature from environment, activity, and clothing: the heat strain decision aid (HSDA). *J Therm Biol* 64:78–85
6. Notley SR, Poirier MP, Hardcastle SG, Flouris AD, Boulay P, Sigal RJ, Kenny GP (2017) Aging impairs whole-body heat loss in women under both dry and humid heat stress. *Med Sci Sports Exerc* 49(11):2324–2332

# Study on Attention Characteristics of Small-Arms Shooting at Moving and Looming Targets



Xiang Gao, Haoyuan Li, Zhengbu Liu, Xin Wang, and Yang Li

**Abstract** In the process of small-arms shooting at the looming target and moving target, one of the main objects in the target area, that is, the shooting target, is the center of “attention,” while the other objects are at “the edge of attention.” In order to study the effect of attention characteristics on the shooting of moving and looming targets with small-arms, the attention of 55 shooters was tested in a certain army department under different conditions. From the angle of factors affecting attention and tests of attention, Through the analysis of the main influencing factors such as age, length of military service and duration of continuous shooting training, the influence of various factors on attention is discussed in this paper by using graphics, hoping to provide some basis and foundation for small-arms shooting training.

**Keywords** Attention characteristics · Small-arms shooting · Looming target · Moving target

Attention is defined in psychology as clear consciousness, the work of forming consciousness, the state of mental preparation for producing clarity, and the level of sensitivity to the taste and form of something or can be understood simply as: the psychological activities to a certain phenomenon of the direction and focus. Because of this orientation and concentration, the small-arms shooters can clearly reflect the specific phenomena in the target area environment, leaving aside the irrelevant objects, so as to find the looming and moving target as soon as possible, make corresponding actions and complete the shooting task.

---

X. Gao · H. Li (✉) · Z. Liu · X. Wang  
PLA Army Academy of Artillery and Air Defense Zhengzhou Campus, Zhengzhou  
450052, P.R. China  
e-mail: [lhysff@163.com](mailto:lhysff@163.com)

Y. Li  
31697 Army, Dalian 116100, China

In the process of small-arms shooting at the looming target and moving target, one of the main objects in the target area, that is, the shooting target, is the center of “attention,” while the other objects are at “the edge of attention.”

When shooting at a looming target, the center and edge of the target are constantly changing as the target appears or moves. At some point, one of the states is the center of attention, the rest of the states are at the edge of attention; and at another moment, maybe another state becomes the center of attention, and the original center of attention becomes the edge of attention along with most of the other states. The aiming characteristics of small arms determine that the range of attention is small and the attention center changes quickly during the aiming process, therefore the requirement for the shooter’s attention is higher.

The attention characteristic of the shooter is the key factor that determines the shooting result, especially for moving or looming target shooting. It is necessary to study the shooter’s attention stability, the persistence and the intensity of attention and analyze the influencing factors of it.

## 1 Factors Affecting Attention

Studies have shown that the shooter’s age, sex, length of military service, duration of continuous shooting practice, physical and psychological status, technical status of small arms and environmental conditions are all related to attention. However, considering that the majority of small-arms shooters in the army are male, gender is not considered here. In addition, there is no difference in the technical state of small arms and shooting range environment, so these two factors are also not considered. Furthermore, physical and psychological state fluctuations are very rare among small-arms shooters, therefore not considered. The effects of age [1], length of military service and duration of continuous shooting training on attention were taken into consideration.

## 2 Tests of Attention

At present, the main achievements of attention detection technology include auditory attention detection method based on binaural listening technology, eye movement tracking technology widely used in dynamic measurement of visual attention and attention measurement scale for visual attention detection.

Of all the senses, sight is the most important. The capacity of visual intelligence is 250 times greater than that of the second most important sense-hearing. Besides, considering the operability of the test in the army, the attention scale of visual attention detection was used for the test [2].

Joseph Block, an American psychologist, has developed a checklist for testing drivers’ attention. During the test, the driver is required to find the numbers 10–59



in the table in turn and measure the call-reading time with a stopwatch. After a long-term study, Dr. Block summarized the following rules: The response capacity is above the middle with call-reading time at 10–30 s; the response capacity is poor with call-reading time over 1 min, which means bad concentration and attention [3].

The attention characteristics of small-arms shooters to moving and looming targets are similar to that of automobile drivers. During the test, in order to avoid that when the tester explained to the testee, the latter would easily remember the groups of numbers in the first table, resulting in inaccurate test results; a table of the same type was specially designed for explanation and practice [4]. There are four tables made for the test, so altogether five tables (Figs. 1 and 2). During the test, five tables were stick on the wall with a height of 1.7 m above the ground. The test subject shall stand 1.2 m in front of the table and point out the numbers from “10” to “59” in order. The tester used a stopwatch to record the time. Explanations and exercises are given on the exercise sheet. The first table was the test result before the training of firing on moving and looming targets, the second table was 20 minutes after the continuous training, the third one after 40 minutes, and the fourth was the test result after 60 minutes of continuous training.

It is concluded from multiple tests that those who finished the first table within 50 s are good, those who finished the first table within 50–60 s are medium, and those who finished the first table within 60 s are considered to be slow in perception and inattentive. The read-through time of table 2, 3 and 4 indicates the stability of attention, that is, if the read-through time is almost the same or decreases gradually, it indicates the stability of attention is good.

34	19	42	54	45
26	16	39	28	57
40	35	14	56	30
12	29	44	51	23
50	43	36	24	11
37	20	55	32	47
25	41	17	53	38
13	22	48	10	58
52	18	21	31	46
27	49	33	15	59

**Fig. 1** Table for explanation and practice

59	14	42	50	22	21	43	35	40	29	23	19	26	47	21	16	30	35	43	23
35	28	32	16	55	33	13	54	50	27	14	41	36	12	16	38	12	56	48	57
46	15	45	29	36	25	47	14	59	19	30	53	56	28	38	20	45	52	34	15
19	24	39	10	43	38	30	44	56	32	20	35	46	51	43	27	40	24	55	19
47	40	26	58	18	10	15	34	48	11	39	33	11	50	59	33	14	31	44	50
53	11	23	27	57	36	52	17	20	24	13	29	42	57	24	29	47	18	26	11
54	25	30	12	34	26	41	57	42	37	45	37	10	40	55	36	41	22	39	28
17	31	33	37	48	18	49	22	46	53	49	25	58	22	31	10	54	51	59	58
49	38	41	20	56	23	55	58	12	31	17	52	44	48	15	17	49	37	21	53
21	52	44	51	13	28	45	39	51	16	27	32	54	18	34	25	42	32	46	13

Fig. 2 Test tables

### 3 Test Results and Analysis

#### 3.1 Result Data

In this paper, a total of 55 small-arms shooters were tested. The age and length of military service distribution of all shooters are shown in Fig. 3.

The test results are shown in Figs. 4, 5, and 6.

Age		Length of military service	
age	Number of people	Length of military service	Number of people
Below 20	12	Less than 2 years	9
20-25	25	2-5 years	17
25-30	15	5-8 years	20
Over 30	3	More than 8 years	9

Fig. 3 Age and length of military service distribution of the tested shooters

age	Table 1	Table 2	Table 3	Table 4	Average time
Below 20	53.36	51.73	57.68	59.73	55.63
20-25	53.84	53.48	58.17	60.38	56.47
25-30	56.68	57.17	58.49	61.94	58.57
Over 30	59.37	58.98	60.17	63.62	60.54

**Fig. 4** Average test time for all age groups

length of military service	Table 1	Table 2	Table 3	Table 4	Average time
Less than 2 years	54.63	55.36	58.29	60.96	57.31
2-5 years	52.94	51.59	54.84	58.25	54.41
5-8 years	55.81	55.29	59.78	61.99	58.22
More than 8 years	58.87	59.12	61.50	64.47	60.99

**Fig. 5** Average test time for shooters of different lengths of military services

duration of continuous shooting (minutes)	0 (table 1)	20 (table 2)	40 (table 3)	60 (table 4)
Average time	55.81	55.34	58.63	61.42

**Fig. 6** Test time for all shooters when having a different duration of continuous shooting practice

### 3.2 Relation Between Attention and Influencing Factors

Graphic made from the data of above tests as shown in Fig. 7.

Based on the analysis of the above curve, the following conclusions are drawn.

First of all, the curve of testing time of small-arms shooters is extended with the increase of age. The average time of younger shooters is faster, which is consistent with the physiological law. However, the range of time change of the older shooters' call-reading of the following three tables is small, while the range of time extension of younger shooters is obvious. There is not much difference between the time of call-reading and the age curve of the shooters with different length of military services, because the shooters with long length of military services are also older and have more hours of shooting training on average, which cannot explain the influence of length of military services or age on the shooters' attention characteristics. However, it can be explained that older shooters pay more attention to stability.

Secondly, in the case of prolonged continuous shooting training time, the shooter's call-reading time significantly prolonged, indicating that continuous shooting training time has a greater impact on the shooter's attention characteristics, which is the main factor affecting the shooter's attention.

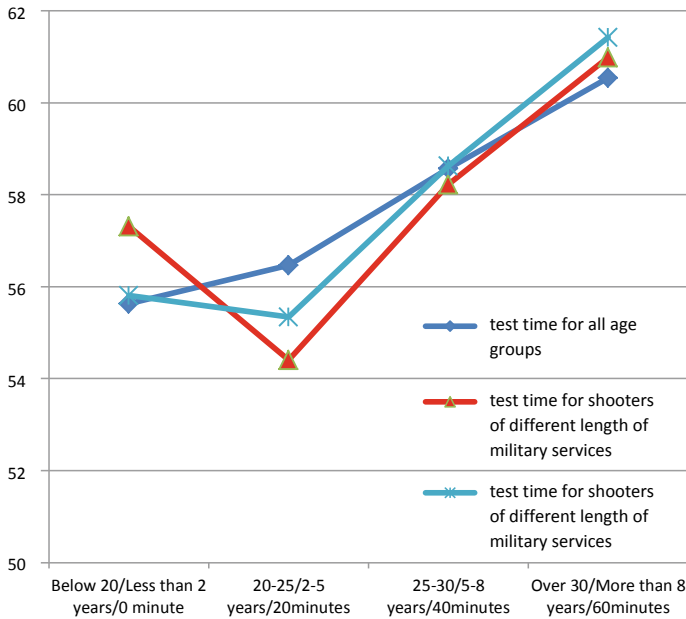


**Fig. 7** Comparison chart of age, length of military service and duration of continuous shooting training with test scores

Thirdly, the selection, teaching and training of moving and looming target shooters should consider the corresponding factors, especially the time of continuous shooting training should be strengthened.

**Compliance with Ethical Standards** The study was approved by the Logistics Department for Civilian Ethics Committee of PLA Army Academy of Artillery and Air Defense Zhengzhou Campus.

All subjects who participated in the experiment were provided with and signed an informed consent form.

All relevant ethical safeguards have been met with regard to subject protection.

## References

1. Luo T, Jiao S (2004) A comparison between age-related differences of attention allocation and selective attention. *Psychol Sci* 27(6):1330–1334
2. Liu Z, Yuan X, Hu W et al (2006) Quantitative measuring method of pilots' attention allocation. *J Beijing Univ Aeronaut Astronaut* 32(5):519–539
3. Wei Y, Liu Y (2007) A study of motor vehicle drivers' attention. *J Shandong Transp Univ* 15(3):12–14
4. Cao J, Chen K (2006) Reliability mathematics introduction. Higher Education Press, Beijing, pp 182–244

# The Survey of Hand Grinding Operation Work-Related Musculoskeletal Disorders



Zidai Xia, Yanqiu Sun, Jianwu Chen, Pei Wang, and Jie Xie

**Abstract** Objective—To study the occupational ergonomics of hand grinding operation, analyze the adverse ergonomic factors in handheld pneumatic angle grinder grinding operation, study the occurrence law and preventive measures of musculoskeletal diseases, so as to improve the working environment and ensure the occupational health of workers. Methods—To investigate the WMSDs of hand grinding workers by questionnaire and analyze the data with SPSS 25.0 software. Results—The musculoskeletal diseases of the waist are more serious. There are also musculoskeletal diseases of the shoulder, neck and wrist to some extent. The elbow, hip, knee and ankle are in good condition. Conclusions—Posture load is the main risk factor of this kind of diseases.

**Keywords** Hand grinding operation · Work-related musculoskeletal disorders · Research questionnaire · Statistical analysis

## 1 Research Purpose

There are a large number of hand grinding operations in the processing and manufacturing industry, and there are adverse ergonomic factors in the grinding operation, such as bad working posture, repetitive operation, bending and weight-bearing, which will cause musculoskeletal diseases such as lumbago and back pain, neck shoulder syndrome and carpal tunnel syndrome, and seriously affect the occupational health of workers [1–3]. At present, there are many researches on musculoskeletal diseases,

---

Z. Xia · P. Wang  
Capital University of Economics and Business, Beijing 100070, China

Y. Sun (✉) · J. Chen  
China Academy of Safety Science and Technology, Beijing 100029, China  
e-mail: [sunyanqiu2002@163.com](mailto:sunyanqiu2002@163.com)

J. Xie  
Dongfang Electric Machinery Co., Ltd, Dongfang Electric Corporation, Chengdu 618000, Sichuan, China

but there are few analyses on the adverse ergonomics in the hand grinding operation. The main purpose of this study is to study the occupational ergonomics in the hand grinding operation, analyze the adverse ergonomic factors in the handheld pneumatic angle grinder grinding operation and study the occurrence law and preventive measures of musculoskeletal diseases, so as to improve the working environment and ensure the occupational health of workers.

## **2 Research Object and Study Method**

### ***2.1 Research Object***

Using the method of judgment sampling, the grinding workers of a domestic unit were selected as the research object. Thirty samples were selected for testing (only 10 samples were taken in the initial paper). Inclusion criteria: ① length of service (working in the post)  $\geq 1.0$  year; ② exclusion of physical disability and musculoskeletal injury caused by internal and surgical diseases; ③ informed consent to participate in the study. Rejection criteria: operators who fail to participate in the field investigation or offer incomplete information when investigate [4].

### ***2.2 Study Method***

In this study, samples of ergonomic factors related to hand grinding were obtained by questionnaire. On this basis, SPSS 25.0 software was used to process the samples, and the questionnaire results were evaluated by Pearson chi-square test. The questionnaire consists of basic demographic characteristics, musculoskeletal symptoms, ergonomic factors and working environment factors. Most of the questions in the questionnaire are qualitative questions, with “yes” as “1” and “no” as “0”. In this study, the criteria of work-related musculoskeletal disorders (WMSDs) are: In the process of hand grinding, the musculoskeletal diseases are directly or indirectly caused by occupational harmful factors, that is, the workers complained that they had pain, numbness, limited activity and other symptoms in nine parts such as hand, arm, neck, back and waist in the past year, asked for leave and excluded the physical disability or musculoskeletal injury caused by other medical emergencies [4].

### ***2.3 WMSDs Research***

Based on the field investigation of hand grinding, this paper analyzes the adverse ergonomic factors in handheld pneumatic angle grinder grinding, uses Yang Lei's

modified musculoskeletal disease questionnaire (Chinese version) [5] to investigate the musculoskeletal symptoms and related factors of the working population and uses Pearson chi-square test to evaluate the results of the questionnaire.

## ***2.4 Statistical Analysis***

SPSS 25.0 software was used for statistical analysis and test with Pearson chi-square. The main indexes analyzed were age distribution, the prevalence of neck, shoulder, back, elbow, waist, wrist, hip, knee, ankle and foot. And through the comparison of the prevalence of different parts of the disease and the prevalence rate, we can find out the rule of musculoskeletal disease in the hand grinding workers.

## **3 Analysis of Research Results**

### ***3.1 Research Results***

It can be seen from Table 1 the occurrence of WMSDs in various parts. The criteria of this study for WMSDs is feeling pain or discomfort in the past year and accordingly asking for leave, and the symptoms continue to this day. List Table 2 separately.

The results of Pearson chi-square test are shown in Table 3.

From the table, we know that there is one person with WMSDs in the neck, with a prevalence of 10%; one person with WMSDs in the shoulder, with a prevalence of 10%; one person with WMSDs in the back, with a prevalence of 10%; two people with WMSDs in the waist, with a prevalence of 20%; and two people with WMSDs in the wrist, with a prevalence of 20%. No one has WMSDs at elbow, hip, knee, ankle and foot.

### ***3.2 Analysis of Results***

The total sample size is 10 (the sample size is small, and gender factors are not considered temporarily). All subjects are male, aged 22.0–50.0 ( $36.0 \pm 8.0$ ) years old. The musculoskeletal diseases of the waist are more serious, and there are also musculoskeletal diseases of the shoulder, neck and wrist to a certain extent, while the elbow, hip, knee and ankle and foot parts are in good condition.

**Table 1** Research sample

Parts of body	Condition		Since taking part in the work	In the past year	In the past week
Neck	Pain or discomfort	No	7	7	9
		Pain or discomfort	3	3	1
	Ask for leave	No	9	9	10
		Ask for leave	1	1	0
Shoulder	Pain or discomfort	No	4	6	7
		Pain or discomfort	6	4	3
	Ask for leave	No	8	9	9
		Ask for leave	2	1	1
Back	Pain or discomfort	No	6	7	8
		Pain or discomfort	4	3	2
	Ask for leave	No	8	9	9
		Ask for leave	2	1	1
Elbow	Pain or discomfort	No	8	9	10
		Pain or discomfort	2	1	0
	Ask for leave	No	10	10	10
		Ask for leave	0	0	0
Waist	Pain or discomfort	No	6	6	7
		Pain or discomfort	4	4	3
	Ask for leave	No	8	8	9
		Ask for leave	2	2	1
Wrist	Pain or discomfort	No	5	5	6
		Pain or discomfort	5	5	4
	Ask for leave	No	7	8	9
		Ask for leave	3	2	1
Hip	Pain or discomfort	No	9	9	10
		Pain or discomfort	1	1	0

(continued)



**Table 1** (continued)

Parts of body	Condition		Since taking part in the work	In the past year	In the past week
	Ask for leave	No	10	10	10
		Ask for leave	0	0	0
Knee	Pain or discomfort	No	9	10	10
		Pain or discomfort	1	0	0
	Ask for leave	No	10	10	10
		Ask for leave	0	0	0
Ankle and foot	Pain or discomfort	No	9	10	10
		Pain or discomfort	1	0	0
	Ask for leave	No	10	10	10
		Ask for leave	0	0	0

## 4 Conclusions and Suggestions

Posture load is the main risk factor of this kind of disease through the analysis of the survey results. The prevalence of WMSDs was higher in the waist and wrists, and WMSDs were more likely in the neck, shoulder and back. After the field investigation, we found that the hand grinding workers are often in static load and repetitive load in the actual work, the gap between the works is short, and the single work time is too long. My suggestion is that the factory needs to adjust the working system of the grinding personnel, appropriately increase the rest gap between the works and provide working posture training to reduce the impact of posture load on the grinding personnel and help the grinding personnel to take the right posture [6].

## 5 Discussions

There are still some limitations to be improved in this study; for example, the number of samples is limited, the research factors included are limited, the factors of psychological load and the indicators of educational level are not considered and so on. Future research can add indexes about the influence of whether to keep exercising and the interval time between jobs on musculoskeletal diseases.



**Table 3** Test result

Test parameters	Value	Freedom	Progressive significance (bilateral)
Pearson chi-square	22.306 <sup>a</sup>	8	0.004
Likelihood ratio	28.712	8	0.000
Linear association	3.735	1	0.053

<sup>a</sup>Pearson chi-square test value in Table 3 is 0.004 and less than  $\alpha = 0.05$ , which shows that the survey results are more accurate to reflect the actual situation

**Acknowledgements** This work was supported by the National Key R&D Program of China (2016YFC0801700), the basic research funding of China Academy of Safety Science and Technology (2019JBKY04, 2019JBKY11, 2017JBKY02) and the Graduation Design (Scientific Research) Project of “practical training plan” for cross training of high-level talents in Beijing institutions of higher learning in 2019 (NO. 1601, 2019).

**Compliance with Ethical Standards** The study was approved by the Logistics Department for Civilian Ethics Committee of Capital University of Economics and Business.

All subjects who participated in the experiment were provided with and signed an informed consent form.

All relevant ethical safeguards have been met with regard to subject protection.

## References

1. Cao Y, Tang L, Zhang W et al (2016) Ergonomic factor analysis of lower back pain in airport handling workers. *Chin J Ind Med J* 29(4):262–265
2. Sun Y et al (2019) Ergonomics analysis of hand-held grinding operation working posture based on jack. In: Long S, Dhillon BS (eds) *Man-machine-environment system engineering. Lecture notes in electrical engineering*, vol 576. Springer, Singapore. [https://doi.org/10.1007/978-981-13-8779-1\\_83](https://doi.org/10.1007/978-981-13-8779-1_83)
3. Chen J et al (2019) Study on the upper flange width on grinding worktable and its ergonomics evaluation. In: Long S, Dhillon BS (eds) *Man-machine-environment system engineering. Lecture notes in electrical engineering*, vol 576. Springer, Singapore. [https://doi.org/10.1007/978-981-13-8779-1\\_94](https://doi.org/10.1007/978-981-13-8779-1_94)
4. Liu L, Tang S, Wang S et al (2015) A case-control study on the influence of work organization factors on the prevalence of occupational musculoskeletal injury. *J Ind Health Occup Dis* 41(3):170–173
5. Yang L, Hildebrandt VH, Yu S et al (2009) Introduction of musculoskeletal diseases questionnaire. *Ind Health Occup Dis J* 35(1):25–31
6. Wang J, Cao Y, Jin X et al (2018) Analysis on the influencing factors of neck musculoskeletal disease in an airport porter. *China Occup Med J* 45(2):168–172

# Study on Pilots' Color Requirements for See-Through Displays in Desert Flight



Duanqin Xiong, Tao Jiang, Liu Yang, Yanyan Wang, Xiaochao Guo, Jian Du, Yu Bai, Fang Su, Wen Dong, Rong Lin, and Juan Liu

**Abstract** *Objective*—To study the color requirements of displayed information in see-through displays when pilots flying in the desert. *Methods*—The experimental materials included some route and combat flight menus. There were eight fixed colors and custom colors provided to be chosen. The experimental procedure was programmed. One hundred and fifteen fighter pilots participated in the study. They were required to choose the most suitable colors for the display elements in the menus. *Results*—(1) For the two types of menus, the numbers of pilots that chose colors for the same information elements were generally consistent. The number of pilots choosing green was superior in most long-time displayed information elements including normal information. (2) For the information of flight element category and flight instruction category, the numbers of pilots choosing green and choosing blue were generally equal. For the dangerous information, unattackable information and overrun information with unlong-time displayed information, the number of pilots choosing red was superior. And for the information that was latent dangerous, the number of pilots choosing yellow was superior. *Conclusions*—When flying in the desert, pilots have evident requirements of colorful displayed information for see-through displays. Their requirements were as follows: The main color was green. The long-time displayed and normal and attackable information was tended to be displayed in green. The dangerous, unattackable and overrun information was tended to be displayed in red. And the latent dangerous information was tended to be displayed in yellow.

**Keywords** Color requirement · See-through display · Desert flight · Pilots

---

D. Xiong (✉) · L. Yang · Y. Wang · X. Guo · J. Du · Y. Bai · F. Su · R. Lin · J. Liu (✉)  
Air Force Medical Center of FMMU, Beijing 100142, China  
e-mail: [xdqin123@163.com](mailto:xdqin123@163.com)

J. Liu  
e-mail: [13910259429@139.com](mailto:13910259429@139.com)

T. Jiang · W. Dong  
Dujiangyan Special Crew Sanatorium of PLA Air Force, Chengdu 611831, Sichuan, China

## 1 Introduction

See-through displays such as head-up display (HUD) and helmet-mounted display (HMD) are the information display carriers in aircraft. They play important roles in the course of flying and combating. The color of traditional see-through displays is monochrome (green), because of their limited abilities to display images. But colorful display can effectively improve the performance of search and recognition tasks. Color coding is more effective than shape coding [1, 2] and can shorten response time evidently [3]. Colorful display can enhance the situation awareness of flight crew [4].

Some relative researches about the information colorization of see-through display have been carried at home and abroad. For example, there has been study found that colorful weapon symbols in HMD have evident superiority [5]. The effect of information menu in HUD that main color was green and important parameters were magenta was the best [6]. In the color coding of abnormal information with HUD, red was better than yellow, and green was improper [7]. The study indicated that pilots had evident requirements of colorful displayed information for see-through displays in simulated aeromarine flight. They expected that some information including alerting information could be displayed colorfully, which could make pilots observe and recognize the displayed information and avail to improve their visual efficiency [8]. Moreover, the scholar studied the effect of symbol's color coding on the compatibility of HUD and HDD (head-down display), and the results indicated that a different color coding would result in pilots' different searching efficiency and reaction time [9].

Flying over the desert is considered to be a challenging flight task by the pilots. It is because that desert area is a special flight environment with single physiognomy, simple color and lack of landmarks. This condition could be very apt to make pilots produce visual fatigue, resulting in enlarged errors which were measured by sight [10]. At the same time, a lot of pilots reflected that monochrome information in see-through display shows in the desert background, which make pilots observe and recognize information needed and pay attention to more hardly. If different colors were coded, pilots' searching loads would be lessened.

This study aimed to explore the pilots' color requirements of see-through displays when flying in the desert, for offering references for the colorization design of see-through displays in the future.

## **2 Method**

### ***2.1 Test Devices and Method***

#### **2.1.1 Task Design**

In this study, the experimental materials included route flight menus and combat menus of aircraft. There were nine categories of information elements in route flight menu and ten in the combat menu. The dynamic experimental procedure was programmed, with desert resemble images as the flying background. The pilots were required to select the best color for various display elements according to their own flight experiences. The chosen colors were eight fixed colors and custom ones. Eight fixed colors were red, green, blue, white, amber, magenta, cyan and yellow, and custom colors were freely selected by the pilots when they thought that the display elements could not be displayed with the former fixed colors.

#### **2.1.2 Test Materials and Devices**

A set of color coding experimental procedure was adopted. The procedure included four modules: (1) background information module, collecting the pilots' background information; (2) practice module, providing some exercise tasks to enable pilots to be familiar with the test tasks and experiment methods; (3) test module, providing chosen colors for pilots to select; and (4) data management module, recording, storing and exporting the all test data.

Three sets of notebook computers and mice were used in the experiment.

#### **2.1.3 Experiment Methods and Steps**

Man-machine dialogue was adopted in the experiment. Pilots first filled their background information in the experimental procedure and then did the exercise task. After completing the exercise, they would enter the formal test phase to accomplish the mission of selecting color for each display element in all menus.

The experimental procedure automatically recorded the values of R, G and B with all selected colors.

### ***2.2 Experimental Subjects***

One hundred and fifteen male fighter pilots participated in the experiment. They were  $32.09 \pm 5.72$  years old with eyesight greater than 0.8 and without color blindness.

### 2.3 Statistical Analysis

SPSS 19.0 software was used to analyze the test data. The number of pilots who selected certain color for every element was a statistical indicator of the experimental results. Frequency statistic and chi-square test of the number of pilots who chose every color were carried.

## 3 Results and Analysis

### 3.1 Results of Color Choice for Each Category of Display Elements in Route Flight Menu

In the route flight menu, the frequency results of the pilots who selected the best color for each category of display elements are shown in Table 1. The results of chi-square test are shown in Table 2.

In the nine categories of display elements, the categories 1–8 belonged to long-time displayed information, and the category 9 belonged to unlong-time displayed special information. For the normal information in the categories 1–3 and categories 6–9, the number of pilots who selected green was all dominant. In the category 4, the pilots choosing blue were more than those choosing green. In the category 5, although the pilots choosing green were slightly more than those choosing blue, the former had evidently superiority. The overrun information in the categories 8–9 had dangerous sense, and the number of pilots choosing red was clearly dominant. In category 9, the information of element 9–2 was between the normal and overrun, which was latent dangerous and needed pilots' attention, and the number of pilots choosing yellow was dominant.

In all displayed elements in Table 2, the results of difference test were very significant ( $p < 0.001$ ). These results indicated that there were evident differences when pilots chose colors for the nine categories of displayed elements.

According to the results in Tables 1 and 2, although several colors were provided even pilots could custom the colors for all displayed elements, pilots considered that most information such as long-time displayed and normal information needed to be green, dangerous information needed to be red and between the former two needed to be yellow. These results were accorded with the traditional usages of alerting information in aircraft and were consistent with the results in the study on color coding requirements for see-through displays in simulated aeromarine flight. For the element of category 4, the number of pilots choosing blue was more than that of choosing green. In the element of category 5, the number of pilots choosing green was generally equal to that of choosing blue. The two results were not consistent with those in the study on color coding requirements in simulated aeromarine flight,

**Table 1** Frequency of pilots choosing the best color for each category of display elements in route flight menu ( $n = 115$ )

No	Displayed elements	Red	Green	Blue	White	Amber	Magenta	Cyan	Yellow	Custom color
1.	Element 1 aircraft datum category (long-time displayed)	9	51	34	0	3	9	3	6	0
2.	Element 2 aircraft vector category (long-time displayed)	5	53	31	3	4	5	3	9	2
3.	Element 3 aircraft attitude category (long-time displayed)	2	61	34	1	3	8	1	2	3
4.	Element 4 flight element category (long-time displayed)	9	37	41	0	5	14	2	6	1
5.	Element 5 flight instruction category (long-time displayed)	5	45	38	0	7	14	0	5	1
6.	Element 6 flight course category (long-time displayed)	5	67	34	0	3	3	0	3	0
7.	Element 7 flight tips as time, etc., category (long-time displayed)	3	59	24	1	3	8	5	10	2
8.	Element 8 angle of attack, G-load and engine speed category (long-time displayed)	7	58	26	0	2	11	2	8	1
		67	15	16	0	2	10	1	4	0
9.	Element 9 landing information category (unlong-time displayed)	5	70	18	0	3	9	3	5	2
		7	32	14	0	7	10	4	40	1
		64	23	10	0	2	10	3	3	0



**Table 2** Results of different tests for the number of pilots in route flight menu

Displayed element	$\chi^2$	df	Sig
Element 1	126.835	6	0.000
Element 2	193.270	8	0.000
Element 3	273.878	8	0.000
Element 4	121.035	7	0.000
Element 5	114.174	6	0.000
Element 6	182.235	5	0.000
Element 7	219.096	8	0.000
Element 8-1	182.948	7	0.000
Element 8-2	194.887	6	0.000
Element 9-1	259.052	7	0.000
Element 9-2	96.130	7	0.000
Element 9-3	180.035	6	0.000

because the visual effects were different when the two categories of information overlaid on the desert or on the seawater background. Thus, it could be seen that pilots' color choices were based on different flight backgrounds.

### ***3.2 Results of Color Choice for Each Category of Display Elements in Combat Menu***

In the combat menu, the frequency results of the pilots who selected the best color for each category of display elements are shown in Table 3. The results of chi-square test are shown in Table 4.

In the ten categories of display elements in Table 3, the categories 1–8 belonged to long-time displayed information, and the categories 9–10 belonged to unlong-time displayed special information that appeared in combat conditions. For normal information in categories 1–3 and 6–8, and attackable information in category 9, the number of pilots choosing green was evidently dominant. The results of the categories 4 and 5 were consistent with those in Table 1. For overrun information in the category 8 and attackable information in the category 10, the number of pilots choosing red was generally equal to that of choosing green. For unattackable information in the categories 9 and 10, the number of pilots choosing red was evidently dominant.

In all displayed elements in Table 4, the results of difference test were very significant ( $p < 0.001$ ), which indicated that there were evident differences when pilots chose colors for the ten categories of displayed elements.

According to Tables 3 and 4, the results were inclined to be consistent with those in above route flight menu, especially for the color choices of long-time displayed and normal information. It is different that pilots choosing red were greatly more than

**Table 3** Frequency of pilots choosing the best color for each category of display elements in combat menu ( $n = 115$ )

No	Displayed elements	Red	Green	Blue	White	Amber	Magenta	Cyan	Yellow	Custom color	
1.	Element 1 aircraft datum category (long-time displayed)	13	49	30	0	4	9	3	6	1	
2.	Element 2 aircraft vector category (long-time displayed)	8	50	35	1	3	6	2	7	3	
3.	Element 3 aircraft attitude category (long-time displayed)	3	58	35	1	6	5	2	4	1	
4.	Element 4 flight element category (long-time displayed)	8	36	39	2	8	12	3	5	2	
5.	Element 5 flight instruction category (long-time displayed)	7	39	40	2	6	11	2	7	1	
6.	Element 6 flight course category (long-time displayed)	5	66	29	0	8	3	0	3	1	
7.	Element 7 flight tips as time, etc., category (long-time displayed)	4	60	24	0	4	8	6	8	1	
8.	Element 8 angle of attack, G-load and engine speed category (long-time displayed)	Element 8-1 (normal information)	24	44	20	0	3	10	3	9	2
		Element 8-2 (overrun information)	29	29	21	0	8	13	3	11	1
9.	Element 9 attack category (unlong-time displayed)	Element 9-1 (attackable information 1)	6	66	21	1	2	11	3	4	1
		Element 9-2 (unattackable information 1)	61	20	14	1	2	10	1	5	1
10.	Element 10 target category (unlong-time displayed)	Element 10-1 (attackable information 2)	35	32	18	1	2	12	2	12	1
		Element 10-2 (unattackable information 2)	34	23	19	1	7	13	2	15	1

**Table 4** Results of different tests for the number of pilots in combat menu

Displayed element	$\chi^2$	df	Sig
Element 1	136.339	7	0.000
Element 2	189.983	8	0.000
Element 3	251.339	8	0.000
Element 4	130.035	8	0.000
Element 5	149.913	8	0.000
Element 6	207.913	6	0.000
Element 7	189.209	7	0.000
Element 8-1	101.696	7	0.000
Element 8-2	58.009	7	0.000
Element 9-1	275.130	8	0.000
Element 9-2	233.183	8	0.000
Element 10-1	109.687	8	0.000
Element 10-2	80.261	8	0.000

those choosing green and choosing blue for the element 8–2 in route flight menu. In combat menu, the number of pilots choosing red, choosing green and choosing blue was little different, which was probably related to pilots' thought that this several colors could clearly contrast to desert background.

## 4 Conclusions

Based on the results in this study, the conclusions were as follows:

1. Pilots had colorful coding requirements for information in see-through display when flying in desert.
2. The main color was green in the menu.
3. Long-time displayed normal information and attackable information were tended to be green. Dangerous information, unattackable information and overrun information unlong-time displayed were tended to be red. And latent dangerous information was tended to be yellow.

**Compliance with Ethical Standards** The study was approved by the Academic Ethics Committee of Air Force Medical Center of FMMU. All subjects were provided with and signed an informed consent form. All relevant ethical safeguards had been met with regard to subject protection.

## References

1. Rebecca MTJ (1990) The effectiveness of color-coding in visual displays: does practice make a difference? *Hum Factors* 34(19):1519–1523
2. SAE ARP4032A-2007 Human engineering considerations in the application of color to electronic aircraft displays. SAE standard, 2007
3. Sandra K, David B (1992) Color coding to facilitate performance of focused attention tasks with object displays. In: *Proceedings of the human factors and ergonomics society annual meeting*, vol 36, pp 1493–1497
4. Derefeldt G, Skinnars O, Alfredson (1999) Improvement of tactical situation awareness with colour-coded horizontal-situation displays in combat aircraft. *Displays* 20:171–184
5. Post DL, Geiselman EE, Goodyear CD (1999) Benefits of color coding weapons symbology for an airborne helmet-mounted display. *Hum Factors* 41(4):515–523
6. Xiong D, Huang J, Zhang Q et al (2016) Effects of multicolor display on HUD information in dynamic simulated flight. *Space Med Med Eng* 29(2):127–132
7. Xiao X, Wanyan X, Zhuang D et al (2012) Ergonomic design and evaluation of visual coding for aircraft head-up display. In: *2012 5th international conference on biomedical engineering and informatics, BMEI 2012*, pp 748–752
8. Xiong D, He Q, Guo X et al (2018) Study on color coding requirements for see-through displays in simulated aeromarine flight. In: Long S, Dhillon BS (eds) *Man-machine-environment system engineering. Lecture notes in electrical engineering 456*. Springer Nature Singapore Pte Ltd., Singapore, pp 575–582
9. Du J (2018) Research on the influence of character color coding on the compatibility of head up display and head down display. Civil Aviation University of China for the Academic Degree of Master of Engineering, Tian Jin
10. Guo B, Qi F (2000) Aeromedical support measures of high performance fighter flying in desert area. *Flight Surg* 28(5):218

# Analysis of the Diffusion of Cough Particles in Non-full Load Cabin



Xianlin Shi and Xuhan Zhang

**Abstract** For a certain aircraft economy class that has completed the preliminary layout, the diffusion process of particles generated by a passenger coughing under non-full load cabin is analyzed. First, the boundary conditions of particles were defined, including the particle size, number, and sedimentation rate. Secondly, the sparse two-phase flow is used to describe the diffusion process of particles, and the Euler-Lagrangian-Euler mixed model is used to simulate the steady-unsteady-steady diffusion process. Finally, the analysis of the calculation results shows that reducing the longitudinal flow of airflow in the cabin can control the diffusion range of particles and reduce the infection risk for other passengers.

**Keywords** Aircraft cabin · Passenger cough · Particle diffusion

## 1 Introduction

For a certain aircraft, in order to improve passenger comfort and reflect differentiated competitive advantages and reduce the risk of infectious for other passengers through activities such as coughing, breathing and talking, the diffusion process of particles by coughing in the cockpit needs to be evaluated during the preliminary design stage. By analyzing the diffusion process of particles and its influencing factors under the current cabin layout, it provides suggestions for improvement in the next stage design.

On the premise of convergence of the cockpit flow field, boundary conditions such as particle size, number of particles, particle sedimentation rate and wall attachment were set according to relevant criteria. A sparse two-phase flow and Euler-Lagrangian-Euler mixed model were used to describe and simulate the diffusion process of cough-produced particles under non-full load cabin.

---

X. Shi (✉) · X. Zhang  
Shanghai Aircraft Design and Research Institute, Shanghai 201210, China  
e-mail: [muzhilingqing@163.com](mailto:muzhilingqing@163.com)

© The Editor(s) (if applicable) and The Author(s), under exclusive license to Springer Nature Singapore Pte Ltd. 2021

S. Long and B. S. Dhillon (eds.), *Man-Machine-Environment System Engineering*, Lecture Notes in Electrical Engineering 645, [https://doi.org/10.1007/978-981-15-6978-4\\_90](https://doi.org/10.1007/978-981-15-6978-4_90)

789

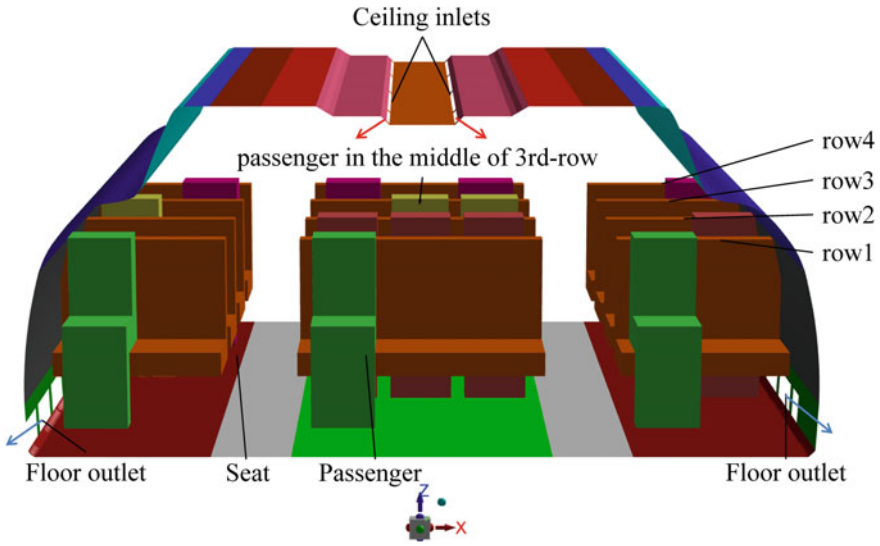


Fig. 1 Schematic of the cockpit layout

## 2 Methods

### 2.1 Modeling Object

Figure 1 is the 2-3-2 layout economy class of a certain dual-aisle aircraft. The design parameters include the seat layout, the form, location, and size of the intake and exhaust ports, the temperature, speed, and mass flow of the intake air have been preliminary determined. According to the results of Liu [1], simulations with 4 rows of seats can represent the typical situation of the cabin. Assume a total of 14 passengers are riding at random, and the passenger in the middle of the third row is infected with influenza. This article calculates and analyzes the diffusion process of the particles produced by the passenger's cough in the cabin under non-full load conditions.

### 2.2 Boundary Condition

The particle size produced by the person's breathing, coughing and speaking are different. According to the research results of Yang et al. [2], the article simulates passenger cough and takes mono-disperse particles with a diameter of  $8.35 \mu\text{m}$  for calculation.

The calculation accuracy and calculation time are related to the number of particles released. After irrelevant trial calculation, the number of particles [3] is determined as 10,000,000 per cough according to formula 1.

$$N_{\text{nec}} = \frac{\frac{t_s}{\tau} V_{\text{room}}}{\alpha(1 - \exp(-\frac{t_s}{\tau})) V_{\text{target}}} N_{\text{target}}^* \quad (1)$$

where  $t_s$  is the particles release time,  $V_{\text{room}}$  is the calculation domain volume,  $\alpha$  is a correction factor based on the error as 1%,  $V_{\text{target}}$  is the target domain volume,  $N_{\text{target}}$  is the necessary particles number of the cabin and  $\tau$  is the time constant of the cabin.

Wan et al. [4] have pointed out that the particle sedimentation rate of 2  $\mu\text{m}$  is less than 2%. As the particle size increases, the sedimentation rate increases. The particle sedimentation rate of 28  $\mu\text{m}$  is over 60%. 10% of the 8.35  $\mu\text{m}$  particle sedimentation rate is appropriate.

Zhang and Chen [5] research showed that when particles hit the wall surface, which will be attached to the wall surface, and the calculation process of particle trajectory will be terminated immediately. In theory, when the particles hit the rigid wall, the particles may return to the flow field with a certain rebound rate, but the rebound rate lacks mathematical models and experimental data support. This article considers that the particles hit the wall and the trajectory calculation is terminated.

### 2.3 Model of Diffusion Process

According to the volume fraction of particles in the air, the calculation method of two-phase flow is divided into one-way coupling and two-way coupling. Elghobashi [6] research shows that when the volume fraction of particles in the air is  $\leq 10^{-6}$ , the effect of particles on air flow can be ignored, that is, one-way coupling. When the particle volume fraction is  $> 10^{-6}$ , the effect of particles on air flow cannot be ignored, that is, a sparse two-way coupling flow. When the particle volume fraction is  $> 10^{-3}$ , that is, a dense two-way coupling flow. The average concentration of particles larger than 10  $\mu\text{m}$  in cabin is less than 50  $\mu\text{g}/\text{m}^3$ , which translates to a volume fraction is much less than  $10^{-6}$ . Therefore, the motion of particles in cabin is a sparse two-phase flow. The article considers the one-way coupling effect.

The diffusion process of particles is produced by passengers' cough. Before the cough, the air flow field is stable; when coughing, the air flow field will change from a steady state to an unsteady state, and the particles will propagate with the unsteady state flow field. After stopping the cough, the flow field gradually changed from the unsteady state to the steady state, and the particle concentration gradually decreased to the background concentration. This paper extends the model proposed by Chen et al. [7], establishes a Euler-Lagrangian-Euler staged mixed model, to calculate the steady-unsteady-steady state diffusion process of particles.

## 2.4 Calculation Process

Meshing was performed using ICEM software, and FLUENT software and UDF were used to simulate the diffusion process. First step, a particle release source is set. The release time is 2 s. The particle size is 8.35  $\mu\text{m}$ . The particle density is 912  $\text{kg}/\text{m}^3$ . The particle number is 10,000,000. Second step, all the walls are set to “trap.” When the particle trajectory hits the wall, the calculation will terminate. All air outlets are set to “escape.” When particles move to the air outlets position, the trajectory calculation ends. The velocity entry is set to “reflect.” When particles have bounced back to the calculation domain, the trajectory calculation continues. The third step is to set the sparse two-phase flow module to define the physical properties of the particles and the one-way coupling mode. Fourth step, a 0.001 s time step is set to capture the transient characteristics of particle movement. The calculation time is usually 4 times the time constant.

## 3 Result

As shown in Fig. 2a, the airflow flows from the air inlet at the top of the ceiling along the wall to both sides of the cabin at the design speed, and rolls inward from the outer seat to the middle of the cabin, forming the main largest vortex.

As shown in Fig. 2b, the airflow accelerates above the empty seats on both sides, forming two secondary vortices in the aisle. The vortices converge on the longitudinal section of the fuselage and form multiple small eddies. The interaction and influence of eddy currents are formed by the air in the cabin. The airflow longitudinal movement trend is remarkable.

As shown in Fig. 2c, in front of the third row of middle passengers, the airflow moves upward from the legs and accelerates upward on the face. The small vortex in the third row and the small vortex in the second row have opposite directions. The two meet in the upper space in front of the third row, and the air velocity is reduced, and the air current is almost frozen.

As shown in Fig. 3, the gravity of the 8.35  $\mu\text{m}$  particles is negligible compared to the buoyancy produced by the airflow, and the particles move with the airflow. After coughing, the particles spread rapidly, staying in the front of the mouth at 0.2 s, and the particles reached the passenger standing height after 3 s.

As shown in Fig. 4, after 60 s, the particles followed the airstream and spread to the 4 rows of cockpits. The movement direction and velocity of the particles are consistent with the trends and laws of vortex direction and air velocity as shown in Fig. 2.



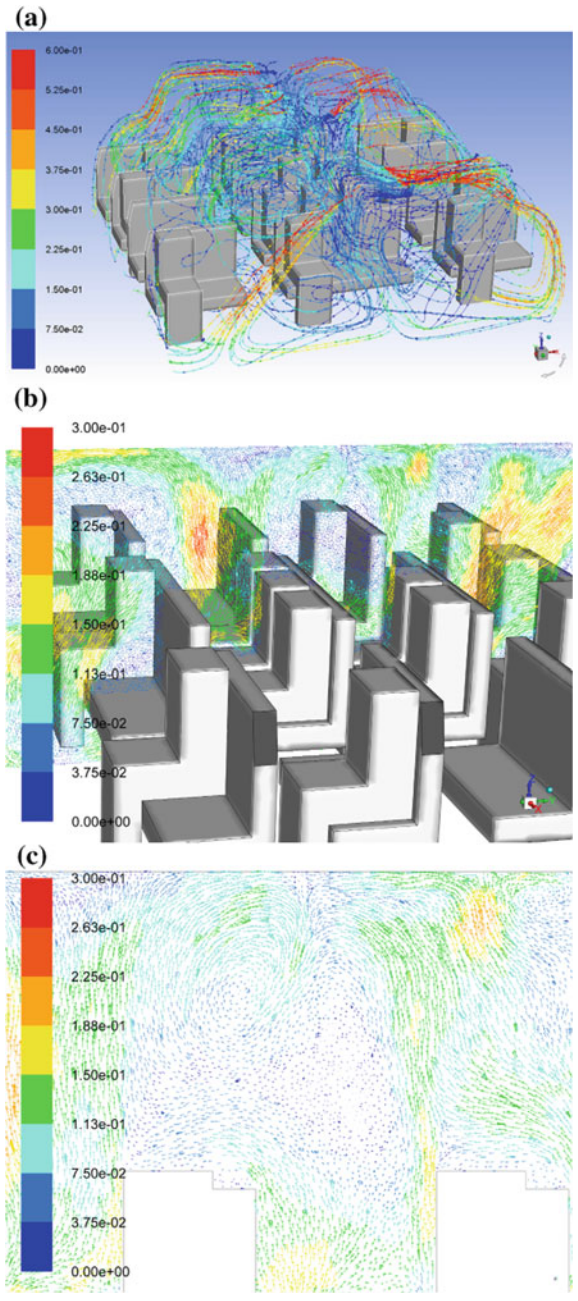


**Fig. 2** Airflow velocity vectors colored by velocity magnitude (m/s): **a** cabin, **b**  $x = 0$  mm fuselage longitudinal section of **(a)**, **c** enlarged view of **(b)** in front of passenger in the middle of third row

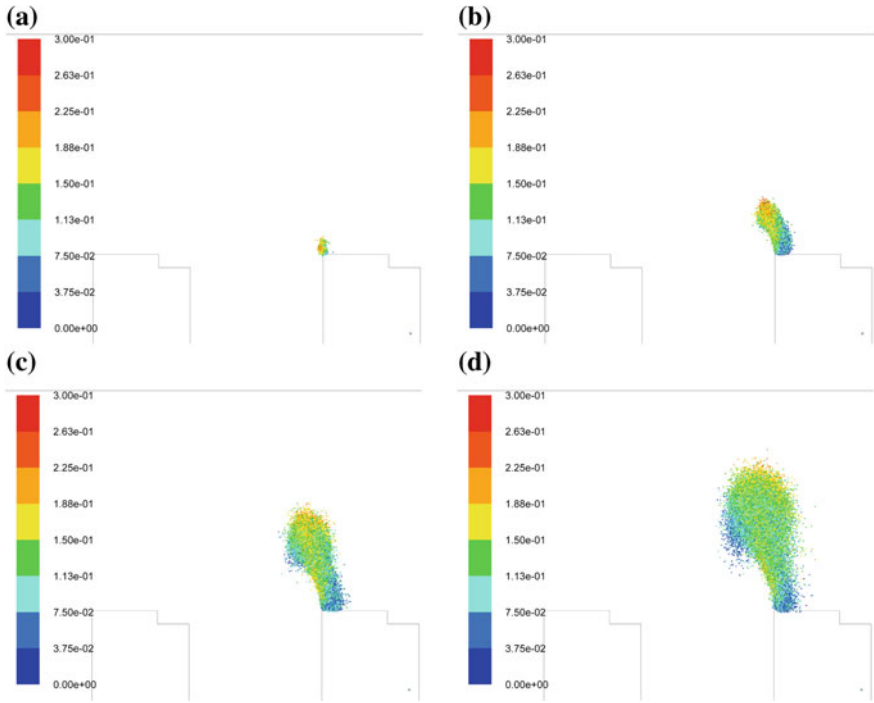


**Fig. 3** Particle traces colored by particle velocity magnitude (m/s) in  $x = 0$  mm section at different times after passenger cough: **a**  $t = 0.2$  s, **b**  $t = 1$  s, **c**  $t = 2$  s, **d**  $t = 3$  s

## 4 Conclusions

For passengers are riding randomly in a non-full-load cabin, the analysis results show that the airflow streamline and particle diffusion trajectory are consistent, and when the airflow speed is low, particles are easy to accumulate. Although the cabin layout, seat layout, intake and exhaust are all symmetrically designed, the interaction and influence of the vortex, the fuselage produces a significant longitudinal flow, and the airflow can quickly spread particles generated by passengers' coughs to the entire cabin. In the next stage of the design process, the diffusion range of the particles can be reduced by reducing the longitudinal flow of the airflow in the cabin.

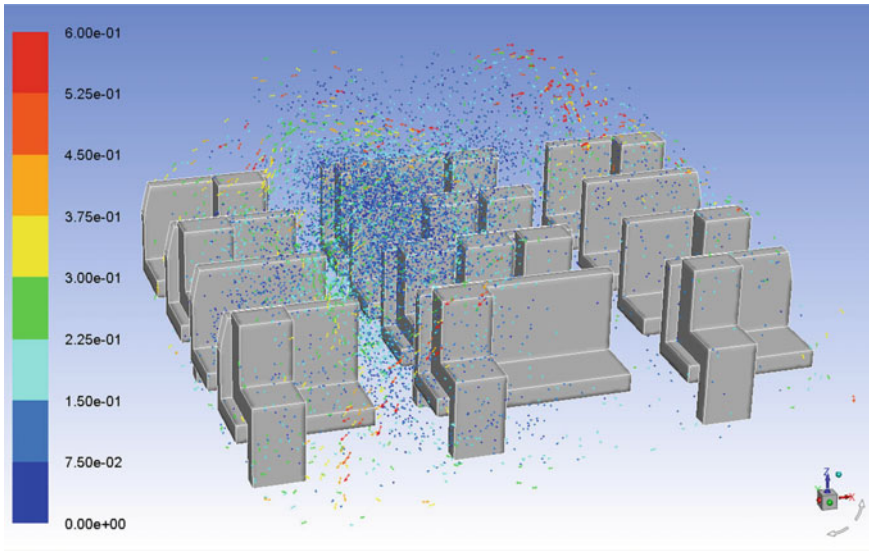


**Fig. 4** Distribution of particle traces colored by particle velocity magnitude (m/s) at 60 s after passenger cough

## References

1. Liu SM (2012) Numerical simulation of reasonable row number for an aircraft cabin and the contaminant transportation. Master's thesis, Tianjin University
2. Yang S, Lee GWM, Chen CM et al (2007) The size and concentration of droplets generated by coughing in human subjects. *J Aerosol Med* 20:484–494
3. Chen C, Liu W, Lin C-H et al (2015) Accelerating the Lagrangian method for modeling transient particles transport in indoor environments. *Aerosol Sci Technol* 9(5):351–436
4. Wan MP, Sze To GN, Chao CYH et al (2009) Modeling the fate of expiratory aerosols and the associated infection risk in an aircraft cabin environment. *Aerosol Sci Technol* 43(4):322–343
5. Zhang Z, Chen Q (2006) Experimental measurements and numerical simulations of particles transport and distribution in ventilated rooms. *Atmos Environ* 40(18):3396–3408
6. Elghobashi SE (1994) On predicting particles-Laden turbulent flows. *J Appl Sci Res* 52(4):309–329
7. Chen C, Liu W, Li F et al (2013) A hybrid model for investigating transient particles transport in enclosed environments. *Build Environ* 62:45–54

# Study on the Diffusion of Gaseous Pollutants from Passenger Cough in Aircraft Cabin



Xianlin Shi and Xuhan Zhang

**Abstract** At the preliminary design stage, the cabin layout of a certain aircraft requires the comfort assessment. The impact of “invisible” gaseous pollutants on passenger comfort during long flights cannot be ignored. Appropriate cabin layout helps control the spread of gaseous pollutants. First, for a certain aircraft, the structural digital model containing design details is cleaned, and the mesh is divided by a mixed grid. Second, the emission rate of CO<sub>2</sub>, O<sub>3</sub>, and VOCs is defined, and the position and speed of inlet and exhaust air are set. The Euler method calculates the flow field change caused by a cough of a passenger in the middle of the cabin and analyzes the diffusion range and concentration change trend of CO<sub>2</sub> generated by the cough. Finally, the cabin layout is evaluated to control the diffusion range of gaseous pollution.

**Keywords** Cabin layout · Comfort assessment · Gaseous pollutants

## 1 Introduction

For certain aircraft, larger flight time means greater exposure probability to gaseous pollutant for passengers. At preliminary design phase, the health impact of “invisible and intangible” gaseous pollutants needs to be assessed in particular. Through proper seat layout, reasonable air intake and exhaust positions and air speed settings, the diffusion range of gaseous pollutants can be effectively analyzed, and the potential health impact on other passengers could be evaluated.

---

X. Shi (✉) · X. Zhang  
Shanghai Aircraft Design and Research Institute, Shanghai 201210, China  
e-mail: [muzhilingqing@163.com](mailto:muzhilingqing@163.com)

© The Editor(s) (if applicable) and The Author(s), under exclusive license to Springer Nature Singapore Pte Ltd. 2021  
S. Long and B. S. Dhillon (eds.), *Man-Machine-Environment System Engineering*, Lecture Notes in Electrical Engineering 645, [https://doi.org/10.1007/978-981-15-6978-4\\_91](https://doi.org/10.1007/978-981-15-6978-4_91) 797

Gaseous pollutants are classified by type, including CO<sub>2</sub>, O<sub>3</sub>, VOCs, and irritating odors. Gaseous pollutants are classified by source, including carpets, seats, cleaners, human breathing, human skin, human skin ozonation, air fresheners, and food and beverage. Gaseous pollution sources are classified according to the time of emission, including continuous emission sources (such as floors, seats, human and personnel breathing, etc.) and transient sources (such as sneezing, coughing, food, and air fresheners, etc.).

The preliminary cabin layout for a certain aircraft has been completed, and five rows of economy classes have been selected for analysis of gaseous pollutant diffusion. Boundary conditions for calculation are defined, such as the CO<sub>2</sub> emission concentration, O<sub>3</sub> emission rate, VOCs emission intensity and location distribution in the cabin, and the emission concentration of pollutants entering and exhausting the air. The Euler method was used to establish the calculation of gaseous pollutant diffusion. Taking the CO<sub>2</sub> produced by the passengers in the middle of the cabin as an example, the process of CO<sub>2</sub> gaseous pollutant diffusion and concentration change was calculated and analyzed. Because the influence of each gaseous pollutant on the concentration of cabin pollutants is linearly superimposed, the results show that the current cabin layout design is conducive to controlling the diffusion range of gaseous pollutants.

## 2 Building the Model

### 2.1 Modeling Object

Figure 1 is the 2-3-2 cockpit layout of a certain economy class. The seat layout, air intake and exhaust position, and air speed design have been initially completed. There are dozens of rows of seats in the economy class. Due to the fluctuation of the flow field of personnel near the toilet in the partition, other areas can be approximated to quasi-steady state. In this paper, five rows [1] passenger cabins are selected as the modeling objects for gaseous pollutants diffusion analysis. The flow field data obtained and the diffusion trend of gaseous pollutants are typical.

### 2.2 Mixed Mesh

The structural digital model of the cockpit contains lots of design details. Too fine structural grid will lead to increased calculation rounding error and truncation error, which not only increases the calculation time, but also may affect the accuracy of the calculation results. Under the premise of not changing the characteristics of the flow field, the structural digital model is cleaned.

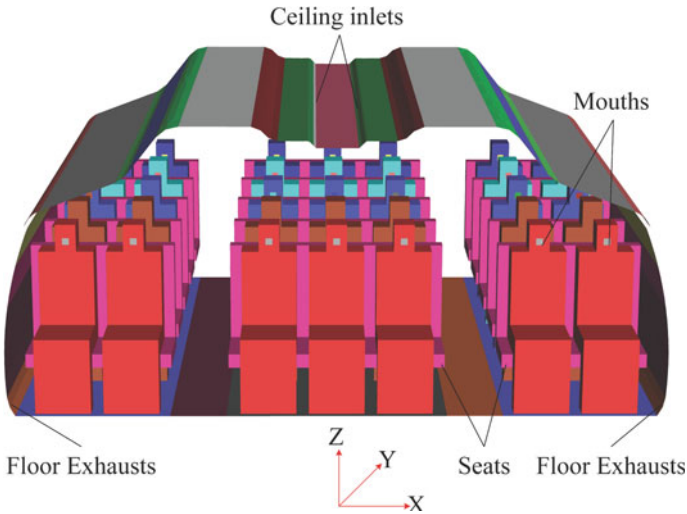


Fig. 1 Schematic of cockpit layout

Under the premise of not changing the characteristics of the flow field, the digital structure of the structure is cleaned to fill local small holes and smooth edges and corners. For example, using regular shapes instead of seats and passengers, the seat arrangement spacing, width, height and passenger's mouth position are the same. After the grid independence test, about 1.2 million per row of seats and a total of about 6 million [2] of a tetrahedral and hexahedral mixed grid (Fig. 2) were used for

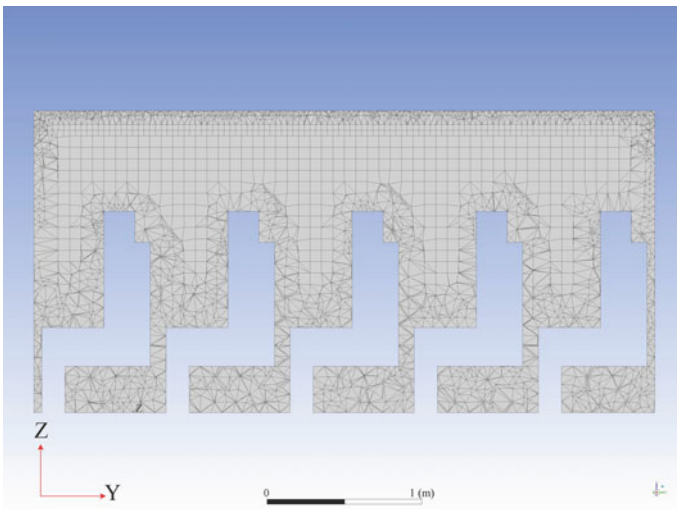


Fig. 2 X = 0 mm, YZ axial section grid

calculation. Except for the fine boundary layer grid, the grid size near the air inlet and exhaust vents are 5 mm, and the grid size in other areas is about 20 mm.

### 2.3 Boundary Conditions

The boundary of the CO<sub>2</sub> air inlet is set as the concentration boundary, and the CO<sub>2</sub> of the air exhaust exits the calculation domain with the airflow. When CO<sub>2</sub> contacts with the wall, adsorption is not considered and the surface boundary concentration is set to zero. For the CO<sub>2</sub> intensity generated by passengers in the cabin [3], take 0.005 L/s per person.

The boundary conditions of O<sub>3</sub> at the inlet and exhaust vents are the same as those of CO<sub>2</sub>. However, when O<sub>3</sub> contacts the passenger skin and walls, O<sub>3</sub> will react chemically to produce a series of by-products. The amount of O<sub>3</sub> sedimentation due to the chemical reaction needs to be considered [4]. Ozone deposition on the wall:

$$J_s = \frac{-\gamma \frac{v}{4}}{l + \gamma \frac{v}{4} \cdot \frac{\Delta y_1}{\Gamma_c}} C|_{y=\Delta y_1} \quad (1)$$

where  $\gamma$  is the probability that O<sub>3</sub> reacts with the wall,  $v$  is the sedimentation speed,  $\Delta y_1$  is the distance from the first grid center point of the wall boundary layer to the wall,  $C$  is the O<sub>3</sub> concentration,  $l$  is the free diameter of the O<sub>3</sub> molecule and  $\Gamma_c$  is the O<sub>3</sub> diffusion coefficient.

VOCs are mainly phenols (including benzene, toluene, xylene, ethylbenzene, etc.), formaldehyde and acetone. Pollution sources are numerous and complex, with carpets, seats, cleaners, human bodies and human breathing as the main sources. According to the emission rate of the pollution source [5], combined with information such as the number of carpets, the amount of detergent used, the seat area and the number of passengers assumed in the preliminary design stage, the total VOCs emission amount was calculated as the boundary condition.

## 3 Results

Table 1 gives the calculation input of the number of passengers, air intake, air intake and exhaust speed, and temperature of a five-row economy class of aircraft in the preliminary design stage.

Assume that the third-row middle passenger in the five-row cockpit coughs, the coughing speed is 0.6 m/s, the duration is 1 s. The type of gaseous pollutant is CO<sub>2</sub>. The RNG model was used to solve the time-averaged Navier–Stokes equation, the k- $\epsilon$  turbulence model [6] was selected, and fluent UDF was used to calculate the CO<sub>2</sub>

**Table 1** Calculation inputs

Parameter	Note
Air volume (L/s/p)	10
Passengers	35
Air supply speed (m/s)	0.6
Breathing speed (m/s)	0.4
Air supply direction	Affixed air supply
Supply/exhaust temperature (°C)	23/28
Passenger skin (°C)	30
Seat (°C)	Adiabatic
Floor (°C)	24
Cockpit wall (°C)	22

concentration. This method can give the time-averaged velocity of turbulence and its average fluctuation with sufficient calculation accuracy and fast convergence speed.

Figure 3 is the detailed velocity vectors of third row and fourth row at  $x = 0$  mm YZ axial section. Relative to flow field of the fourth row, the relatively high-speed air flow generated by passenger cough at third row drives the flow to shift forward.

Figure 4 is the CO<sub>2</sub> concentration at 0.2 s, 0.4 s, 0.6 s, 0.8 s, 1.0 s and 1.2 s after the passenger coughs. Figure 4 reflects the CO<sub>2</sub> dynamic diffusion process and diffusion range.

The change in CO<sub>2</sub> concentration indicates that after the passenger coughed for 1.0 s, the CO<sub>2</sub> diffused to the back of the front passenger. After the passenger stopped coughing for 0.2 s, the range of CO<sub>2</sub> diffusion sharply reduced to the front of the passenger’s head.

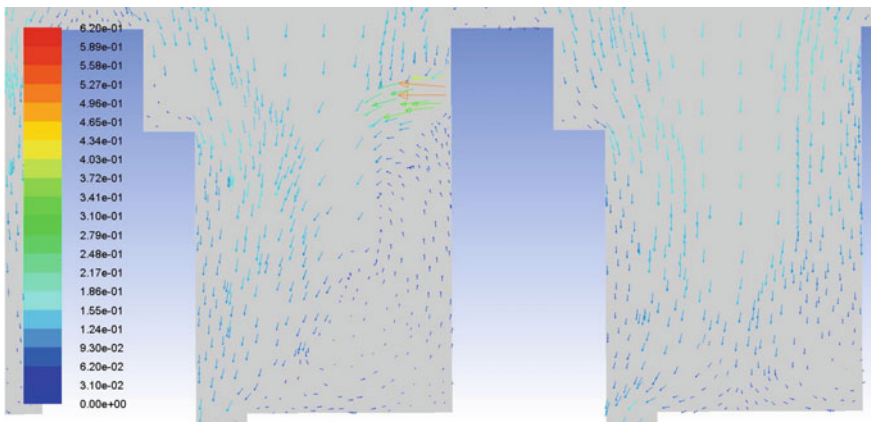


**Fig. 3** Detailed velocity vectors of third and fourth rows of middle at  $x = 0$  mm YZ axial section



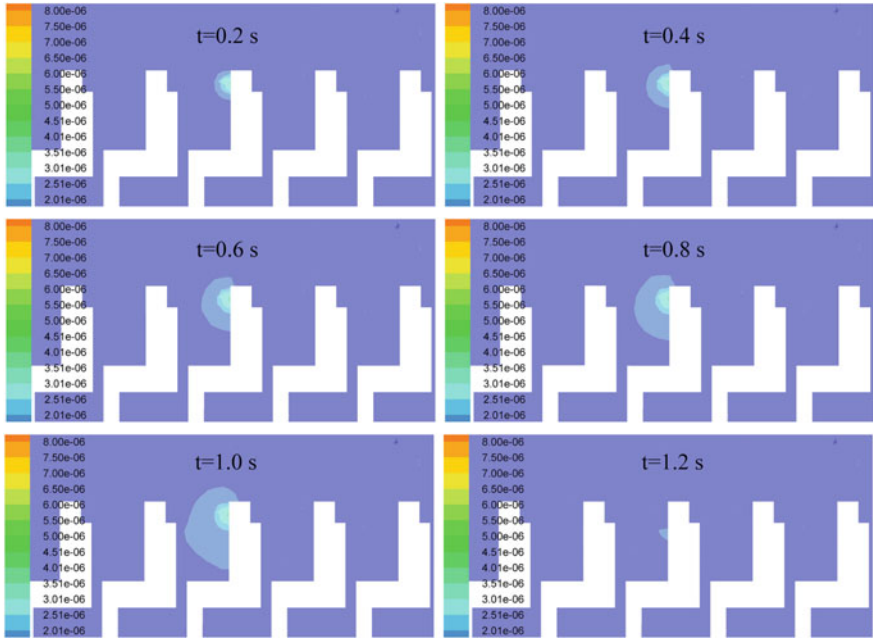


Fig. 4 CO<sub>2</sub> concentration

### 4 Conclusions

The cabin layout of a certain aircraft has completed preliminary design, including seat layout, intake and exhaust positions, air mass and speed. To evaluate the impact of gaseous pollutants on passenger comfort, a mixed grid of tetrahedrons and hexahedrons of five rows of economy class sections was established. The RNS  $k-\epsilon$  turbulence model was used to define the boundary conditions for various types of gaseous pollutants. The transient diffusion and concentration changes of CO<sub>2</sub> from passenger cough are calculated and analyzed. The results show that during the cough, CO<sub>2</sub> spreads rapidly along the cough. Under the effect of airflow and seat blocking, the range of cough influence is controlled in a row of seats. After the cough is stopped, the CO<sub>2</sub> concentration decays very quickly to the ambient CO<sub>2</sub> concentration. In summary, this article believes that the current cabin layout is conducive to controlling the diffusion range of CO<sub>2</sub> gaseous pollutants.

## References

1. Liu SX (2012) Numerical simulation of reasonable row number for an aircraft cockpit and the contaminant transportation. Master's thesis, Tianjin University
2. Zhang Z, Zhang W, Zhai ZJ, Chen QY (2007) Evaluation of various turbulence models in predicting airflow and turbulence in enclosed environments by CFD: part 2—comparison with experimental data from literature. *HVAC&R Res* 13(6):871–886
3. Zhang T, Chen Q (2007) Novel air distribution systems for commercial aircraft cabins. *Build Environ* 42(4):1675–1684
4. Sørensen DN, Weschler CJ (2002) Modeling-gas phase reactions in indoor environments using computational fluid dynamics. *Atmos Environ* 36:9–18
5. Yang CQ (2016) Study on the distribution and diffusion characteristics of environmental pollutants in aircraft cockpit. Postdoctoral report. Tsinghua University
6. Yakhot V, Orszag SA (1986) Renormalization group analysis of turbulence. *J Sci Comput* 1(1):3–51

# The Empirical Research of the Emotional Experience Ambulatory Assessment of Built Environment by Wearable Interactive Technologies



Liang Zhang, Xiangning Li, Lingxuan Cheng, Yuan Kang, Yu Zhang, and Qi Guo

**Abstract** The study aims to explore the method of ambulatory assessment of urban built environment by an empirical study, find out the interactive coupling relationship between the built environment and human's emotional experience, establish the link between physiological indexes and the emotion experience, and thereby lay an empirical foundation for this method to be applied in the field of urban study and design. The virtual scene was constructed with a university campus environment video, and college students were randomly selected as subjects. Wearable biosensors were used to record the subjects' physiological indicators in real time, and the emotional variations were detected by the combination of mental maps and interviews, and consequently evaluate the campus environment. The experiment verifies that the SC value is the window reflecting emotion arousal, and the variation trend of the SCL and the sum of the LF/HF value reflect the individual and overall emotion experience in stages. This method could create a new layer of information for designers, enrich citizens' participation in urban space design, and help to create a high-quality urban environment that meets people's psychological and physiological needs.

**Keywords** Wearable interactive technology · Built environment · Emotional experience · Ambulatory assessment · Empirical research

## 1 Introduction

The urban development in China has entered an inventory stage. The focus of urban construction has gradually shifted from “quantity” expansion to “quality” improvement. Contemporary urban researches pay more attention to the physical and mental demands of users for the environment. The insight into users' emotional experience of the urban built environment can help designers propose design strategies based on residents' physical, psychological, and cognitive feedback, thereby improving the quality of the environment and lives.

---

L. Zhang (✉) · X. Li · L. Cheng · Y. Kang · Y. Zhang · Q. Guo  
Soochow University, Soochow 255123, China  
e-mail: [zl27zzg@126.com](mailto:zl27zzg@126.com)

© The Editor(s) (if applicable) and The Author(s), under exclusive license to Springer Nature Singapore Pte Ltd. 2021  
S. Long and B. S. Dhillon (eds.), *Man-Machine-Environment System Engineering*, Lecture Notes in Electrical Engineering 645,  
[https://doi.org/10.1007/978-981-15-6978-4\\_92](https://doi.org/10.1007/978-981-15-6978-4_92) 805

How to accurately describe and measure people's emotional experience has always been the difficulty of study. The traditional measurement methods mainly focus on the qualitative research based on subjective evaluation in psychological science [1], by which individuals' inner feelings are excavated through the subjective description. However, limited by interviewer effects, memory effects, and conscious experience, this kind of information lacks rigorous argument [2]. With the development of neuroscience, wearable human-computer interaction technology, and biological signal data analysis technology, the wearable sensors can help us to observe human emotional experience more directly, making it possible to assess the environment dynamically, which provides new idea and methods for human factor environment research to promote urban environmental design more in line with the human cognitive and emotional needs [3]. This kind of human-machine environmental interaction mode provides a vast space for architecture and environmental design in the future.

## 2 Theoretical Basis

Specific physiological, behavioral, and cognitive patterns reflect individual's emotional state [4]. Neuro-physiological responses may be a window to identify human's emotional arousal [5]. EDA and ECG are the indicators commonly used in previous studies.

### 2.1 EDA

The volatilities of the EDA reflect the exocrine level of the central nervous system innervated by the sympathetic nerve, which are considered as sensitive marks of the events of particular significance to the individual, mainly related to emotion, novelty, and attention [6]. EDA data contains two types of information: SCL reveals long-term activation level, which is often used as an indicator of periodic emotional arousal level in the study. SCR shows the phasic discharge of sympathetic nerve, and the physiological and psychological irritant state caused by stimulation, which is the indicator of short-term brain response processes. It can be used as a sign of the emotional arousal caused by external stimulation of novelty events. SC value is fitted by SCL and SCR. These three are often used as observation indexes in the study [7, 8].

### 2.2 LF/HF of the ECG

The high-frequency component, HF (0.15–0.40 Hz), and the low-frequency component, LF (0.04–0.15 Hz), were calculated by analyzing the time interval of heartbeat



Fig. 1 Experimental route and scene

by the maximum entropy method. LF reflects sympathetic nerve activity [9], and HF reflects parasympathetic activity [10]. Studies have confirmed that there has always been the parasympathetic tone when people are at rest and in a relaxed state, while sympathetic sounds are associated with excitement and tension. The LF/HF value can reflect the state of people’s emotional activation. The greater the ratio is, the more active the sympathetic nerve is. Therefore, the LF/HF value is an effective method to evaluate the emotional changes from the perspective of neuropsychology.

### 3 Materials and Methods

#### 3.1 The Experiment Design

The Dushuhu Campus of Soochow University was used as the test site. A walking route was planned in the campus covering as many potential emotional arousal factors as possible (Fig. 1). A high-quality video taking along the planned route was used as the stimulus material for the experiment. Forty college students were recruited in the campus as the subjects, and the ratio of male and female was limited around 1:1.

The experiment is based on the ErgoLAB man-machine environment synchronization platform developed by Beijing Jinfa Technology Limited Company, which is equipped with wearable wireless physiological recording module and eye-tracking analysis module.

#### 3.2 The Purpose of Experiment

The main purpose is to explore the feasibility of dynamic assessment of the environment based on wearable interactive technology through empirical research and

to verify the reliability of the method through traditional environmental assessment methods such as interviews and mental maps. At the same time, the explanatory significance of physiological data and their combinations on environmental emotional experience is further revealed through the comparison of multiple physiological indicators.

### ***3.3 The Process of Experiment***

The first step is to collect the baseline data. The following situations were excluded through interviews, including subjects' physical and mental illness, recent mood swings, and the use of prescription drugs. Participants were required to sit still for 3 min, and the baseline levels of individual measurement parameters were collected.

The second step is the calibration experiment. Play an audio of a balloon explosion (around 80 dB) to evoke a terrible response for the subjects and obtain a threshold for their uncomfortable response.

The third step is the formal experiment. Participants were required to watch the video, and any unrelated behaviors were prohibited during the process. The wearable physiological recorder records the subject's EDA and ECG index as well as other physiological data at a sampling rate of 100 Hz (10-bit resolution). The eye tracker tracked the subjects' eye movements and changes in focus in real time.

The fourth step is review report. Participants review the process of emotional experience, draw mental maps, and describe the triggers leading to emotional changes verbally or in words.

### ***3.4 Data Analysis***

The ErgoLAB platform was used to complete the fusion of ECG, physiological, and eye movement data, as well as data process and output. SPSS22.0 software was used for sample data processing and statistical analysis.

## **4 Results**

### ***4.1 SC Value is a Window Reflecting Emotional Arousal***

The experimental results show that the SC value is a valuable reference index for judging emotional arousal, which can reflect the impact of transient stimuli on people. In the experiment, we detected the emotional triggers of the campus environment,

including the parking of motor vehicles or bicycles, the passing of bicycles or pedestrians from the side, the appearance of landmark buildings, beautiful landscapes, and the chirping of birds, etc. Among them, the first two factors bring negative emotional experience, whereas the last three result in a positive feeling. All of the emotional awakenings are embodied as peaks in the SC index. Compared with the physiological baseline value of the subject and the threshold generated by the balloon explosion, the degree of emotional arousal could be determined by interpolation. The valence of emotion has to be determined by subjective descriptions after the experiment.

Figure 2 shows that the SC value of the participant of ID8 has a significant crest when he passed a parking lot and saw nearby vehicles. When he reached a small green area in the middle, the SC value decreased and gradually became flat. At the time, the subject's focus was the canopy in the distance, indicated with the red dot in the figure. And the SC value increased again when he continued to move forward and passed the vehicles parked on the side of the road.

#### ***4.2 The Variation Trend of SCL Reflects Individual Periodic Emotional Experience***

The variation trend of SCL reflects the emotional experience for a participant for a stage. Figure 3 is the matrix of the EDA data of the subject ID1 for the entire experimental process of 12 stages. Green line indicates the SCL value. It can be seen from the figure that four stages S1, S3, S6, and S10 show an upward trend, which correspond to the section at the entrance of the canteen with messy bicycle parking, the lengthy road along the reeds, the road passing across the urban street, and the road nearby the parking lot. The three stages of S2, S4, and S11 show a significant decline, which correspond to the road along a large area of greenery, the road by the waterfront, and the lawn, respectively. The S9 also shows a slight trend of decline because participants can see trees of red and green on the opposite in this section. In other stages, the trends are basically flat. Both S5 and S12 show an obvious growth after a flat period. In the second half of these two stages, a large number of cyclists and walkers passed by the subjects, verifying that traffic is the main factor resulting in the fluctuations of EDA value.

#### ***4.3 The Sum of LF/HF Reflects the Overall Periodic Emotional Experience***

The LF/HF values can be quantified, and the average level of the entire subjects group can be calculated, reflecting the emotional experience results of all participants. Generally, when the LF/HF value is low, the parasympathetic nerve is excited, and the subject is in a relaxed state. On the contrary, when the LF/HF value is high, the

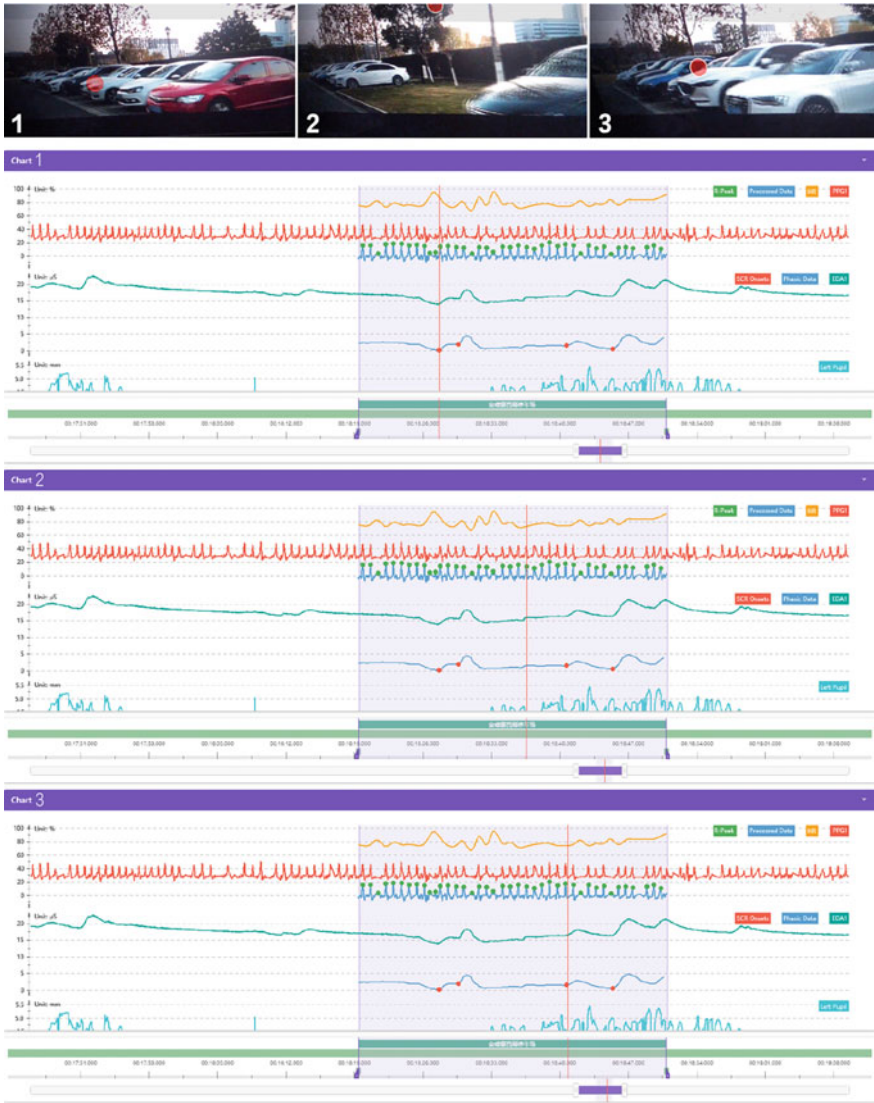


Fig. 2 EDA indicators and eye movement data of ID8 in section 10

sympathetic nerve is excited. In this case, there are two possibilities. One is positive, that is joy and happiness, and the other is negative which means the generation of stress. As same as the EDA indicators, the judgment of emotional valence requires the subjective descriptions.

Data analysis (Table 1) shows that S6, passing across the urban street, has the highest value, which indicates that the safety factor generates the greatest pressure



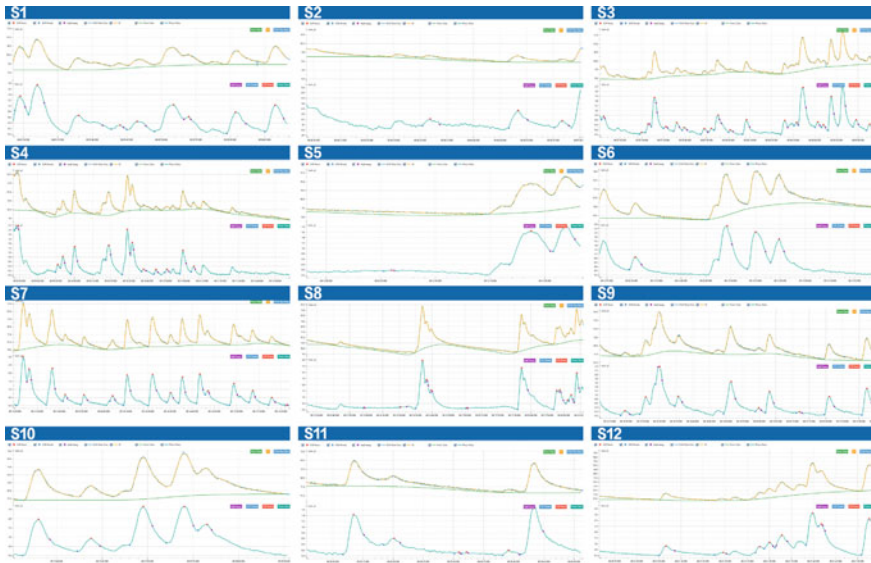
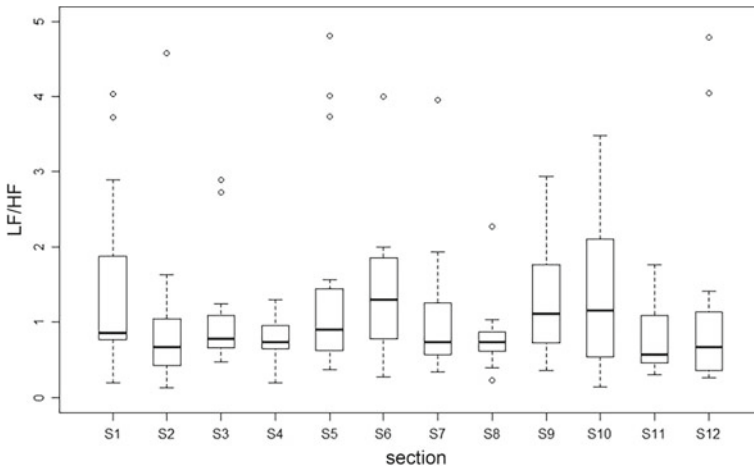


Fig. 3 EDA data matrix of ID1 in 12 sections

Table 1 The sum of LF/HF value in 12 sections



on the subjects, followed by S1, bicycle parking at the entrance of canteen, S9, the road leading to the Business College, and S10, parking lot on the west side of the Business College. According to the subjective description, subjects have higher cognitive loads in S6, S1, and S10 due to parking along the street and traffic, leading to negative emotional experience. 21% of the subjects marked S9 as positive in the mental maps, because they felt happy and novel when they saw the red and green

trees across the road. Under the circumstances, the higher LF/HF value could be interpreted as the excitement brought by the novelty, reflecting a positive emotional activation.

The LF/HF values of S4, waterfront landscape, and S11, lawn, were the lowest, which proved to be the most relaxed period for the subjects. It can be found that the conclusion is highly consistent with the result obtained by the variation trend of SCL value.

As for the landscape environment, the research on the restorative environment proves that water seems to have stronger pressure-relieving effect than the greenery [11]. But in this experiment, the median value of LF/HF of S4 is higher than S11, likely because that vehicles parking around the waterfront prevented the subjects to see and perceive the water. Only in the corner, the water showed up, and 71% of the participants expressed a good mood at that point in subjective descriptions because they can see the water and the weeping willows. Therefore, it can be inferred that vehicles parking along the water reduced the recovery benefits of waterfront landscape in the campus.

For roads, it can be clearly seen that the LF/HF values are generally high for the roads with roadside parking, such as S1 and S10. The values are lower for the roads without parking, indicating a more relaxing walking experience, for example, the road along a large area of greenery to the south of the Architecture School (S2), and the walkway to the underground passage (S7). We also found that the effect on the subjects was reduced when the parking is away from a distance or shaded by the shrubs. For example, the LF/HF values of S5 and S9 are lower than that of the roads with roadside parking. In S5, walkways and parking areas are insulated with greenery, and in S9, vehicles are parked on the other side of the pavement.

## 5 Discussion

The case selected in this empirical experiment is a typical newly built university campus, with abundant land and obvious characteristics of motorization, which is embodied in large scale, wide roads, and mixed traffic. Motorized traffic in the campus is bound to bring a sense of pressure to pedestrians, and vehicles passing by or parked along the street will increase pedestrians' pressure response. It is suggested to optimize the traffic design of the campus, rationally plan the parking lot, avoid parking along the road as much as possible, increase the green isolation zone between the parking lot and the main walking space, optimize the road section design, add the isolation belt between pedestrians and vehicles or bicycles, and reduce the mixing and crossing between people and cars. In the campus of large scale, the psychological and behavioral rules of students in walking process should be fully considered, especially for the road connecting the residential area and the classroom area. The diversity and interest of the walkways should be increased through design to avoid the negative feeling that the road will never end.

Large-scale landscapes, like lawn and water, are common in newly built university campuses, which can play an important role in alleviating learning fatigue and promoting cognitive ability recovery. However, the accessibility and availability of the environment should be taken seriously to allow students to immerse themselves in the environment instead of watching from a distance. In this case, it is suggested to replace the parking around the waterfront with a space for sitting and staying activities to enhance the permeability of the water landscape to the surrounding environment.

## 6 Conclusions

This article introduces an empirical experiment using people as sensors to evaluate the built environment. Based on a virtual scene by the video recording in the campus, select college students as subjects by random and use the method combining real-time measured physiological indicators (objective measurements) with mental maps and interviews (subjective description), to detect the emotional variations of the participants in the simulated walking process and evaluate the advantages and disadvantages of the design of the campus space and environment from the perspective of users' perception. The experimental results prove that the method of ambulatory assessment of emotional experience can help designers to see the interdependence between users and the environment and establish an innovative model for the people-oriented design process, which provides important references for the improvement of the built environment. This experiment verifies the characteristic physiological indicators that reflect emotional state: The SC value is the window reflecting emotion arousal, and the variation trend of the SCL and the sum of the LF/HF value reflect the individual and overall emotion experience in stages. The discovery of these indicators has enriched the research results in related fields and established quantitative reference standards for the application of neuro-physiological measurements in the process of architecture and urban design.

The study will be further optimized and improved from two aspects in the next step. Firstly, the current judgment of emotional valence still depends on subjective interview. More sensor parameters, such as the introduction of EEG data, could be used to promote the process of emotion extraction from manual recognition to automatic recognition in the future. Secondly, the guidance of the participants should be strengthened in the experimental process to reduce the interference of irrelevant factors. In addition, it is necessary to use virtual augmentation technology, such as combining sensory evaluation and cave automatic virtual environment technology, the VR-Platform CAVE system, to construct more immersive and more realistic experimental scenes for a more reliable environmental experience.

In summary, the approach for assessing the emotional experience of a built environment based on neuro-biological measurement, combining quantitative measurement and qualitative interpretation for urban environmental study, can create a new information layer for designers and enrich the process of citizen participation in the design of urban space. Measuring people's feelings and perceptions of the

built environment objectively represents the refinement and inclusiveness of design, which is conducive to creating a high-quality urban environment that meets people's psychological and physiological demands.

**Acknowledgements** Thanks to the equipment and technical support related to human factors and ergonomics provided by Kingfar Research Support Program sponsored by Kingfar International Inc.

**Compliance with Ethical Standards** The study was approved by the Logistics Department for Civilian Ethics Committee of Soochow University. All subjects who participated in the experiment were provided with and signed an informed consent form. All relevant ethical safeguards have been met with regard to subject protection.

## References

1. Chen Z, Shultz S, Liu Y et al (2017) Built environment experience assessment and design via bio-feedback. *Time+Architecture* 5:24–28
2. Hogertz C (2010) Emotions of the urban pedestrian: sensory mapping. In: *Pedestrians' quality needs*. WALK21, Zurich
3. Benjamin S, Bergner JPE, Memmel M et al (2013) Human sensory assessment methods in urban planning—a case study in Alexandria. In: *Conference proceedings REAL CORP*, Rome, Italy
4. Sánchez-Navarro J, Martínez-Selva J, Torrente G et al (2008) Psychophysiological, behavioral, and cognitive indices of the emotional response: a factor-analytic study. *Span J Psychol* 11:16–25
5. Sequeira A, Mamdani F, Ernst C et al (2009) Global brain gene expression analysis links glutamatergic and GABAergic alterations to suicide and major depression. *PLoS ONE* 4:e6585
6. Hamm AO, Greenwald MK, Bradley MM et al (1993) Emotional learning, hedonic change, and the startle probe. *J Abnorm Psychol* 102:453–465
7. Roy JC, Sequeira H, Delerm B (1993) Neural control of electrodermal activity: spinal and reticular mechanisms. In: Roy JC, Boucsein W, Fowles DC et al (eds) *Progress in electrodermal research*. NATO ASI series (Series A: life sciences), vol 249. Springer, Boston, MA, pp 73–92
8. Delplanque S, Lavoie ME, Hot P et al (2004) Modulation of cognitive processing by emotional valence studied through event-related potentials in humans. *Neurosci Lett* 356:1–4
9. Weise F, Heydenreich F (1989) Effects of modified respiratory rhythm on heart rate variability during active orthostatic load. *Biomed Biochim Acta* 48:549–556
10. Cacioppo JT, Berntson GG, Binkley PF et al (1994) Autonomic cardiac control II. Noninvasive indices and basal response as revealed by autonomic blockades. *Psychophysiology* 31:586–598
11. Berto R (2007) Assessing the restorative value of the environment: a study on the elderly in comparison with young adults and adolescents. *Int J Psychol* 42:331–341

# Study on the Effect of 12-h Flight Simulated on Visual Function



Dawei Tian, Feng Wu, Haibo Sheng, Yange Zhang, Qin Yao, Bin Ma, Bin Li, Fengfeng Mo, and Lue Deng

**Abstract Objective** To explore the effects of 12-h flight on the visual system and lay a theoretical foundation for developing visual fatigue protection measures. **Methods** The visual function of six healthy subjects tested with Optec-6500 (Stereo Corp, USA) for 12-h flight. Different spatial frequencies (1, 3, 6, 12, 18 cpd) and distant vision and near vision were compared with preflight and postflight. **Results** Compared with preflight, the contrast sensitivity CS value (frequency 3) was significantly lower than postflight. The contrast sensitivity CS value (frequency 1.5, 6, 12, 18) has a downward trend during flight. **Conclusion** 12 h of flight and sleep deprivation may affect visual contrast and central visual function quality. It is vital to formulate systematic, scientific and rapid visual fatigue protection measures to reduce long-term flight and sleep deprivation to reduce the visual information load of flight personnel.

**Keywords** Simulated flight · Long flight · Visual function · Contrast sensitivity · Flight fatigue · Sleep deprivation

## 1 Introduction

Flight is a labor with high risk and an important social significance. The complicated factors of aerospace include complex angular acceleration, flight illusion, continuous flight across whole day, which can make the flight personnel in a state of fatigue, change the sleep rhythm, affect the flight ability and change the emotional state, and even lead to serious flight accidents [1]. After flying, the pilot generally reflects visual fatigue, reduced visual sensitivity, difficulty in observing the instrument and error-prone areas. At the same time, the visual acuity decreases at night, the visual

---

D. Tian · F. Wu · H. Sheng · Y. Zhang · Q. Yao · B. Ma · B. Li · L. Deng (✉)  
Air Force Medical Center, Air Force Military Medical University, Beijing 100142, China  
e-mail: [denglue@sina.com](mailto:denglue@sina.com)

F. Mo  
Department of Naval Nutrition and Food Hygiene, Second Military Medical University,  
Shanghai 200433, China

error increases during landing, the ability of attention distribution and diversion decreases, and sometimes, transient gray or black vision occurs [2]. In this study, the physiological functions of special vision were evaluated by simulating 12-h flight visual stimulation test, which provided a theoretical basis for further study of long-time flight-induced visual fatigue protection measures.

## **2 Subjects and Methods**

### **2.1 Subjects**

Six healthy subjects were selected, all male, aged 19–22 years. The corrected visual acuity was above 1.0, and there was no organic ocular disease and no abnormal eye examination. Subjects had no allergies or drug resistance to this study drug. Subjects were reviewed by the relevant ethics committee of the Institute of Aviation Medicine, Air Force, voluntarily participated in the study and signed informed consent.

### **2.2 Methods**

#### **2.2.1 Medical Instruments and Equipment and Treatment Process**

The subjects wore matching flight suit, helmet, mask and urine collection device. Sitting on the simulated 12-hour flight seat, the simulation flight is carried out by operating the flight control lever, throttle, rudder and keyboard on the computer platform, and the set 12-h flight tasks are completed in sequence. Lock on flying cliffs 3 is used to simulate the actual flight for 12 hours. During the flight, pay attention to the brightness changes of light, instrument and screen display during the alternation of day and night, and remind the subjects to keep vigilance at any time. Optoc 6500 visual function analyzer (USA) was used to detect near vision, far vision and contrast sensitivity at different frequencies. Near and far vision is tested under the background of fixed brightness. Near visual acuity is the nearest distance that the subjects can see the visual target of near vision chart 1.0. Contrast sensitivity test is to check the resolution of human eyes in the case of complex transformation of different brightness backgrounds. The contrast sensitivity of subjects at different spatial frequencies of the light stripe was detected. The contrast sensitivity of five spatial frequencies in three frequency regions, low frequency (1.5 cycles / degree), 3c/d, intermediate frequency (6c/d) and high frequency (12c/d, 18c/d), was examined. There were nine different contrast gratings with fixed spatial frequency on each slide. During the examination, the subjects were asked to watch the spatial frequency stripe shape and then gradually change the contrast until they could not see clearly the

articles. A total of three tests were conducted, and the mean value was calculated, and the test results of contrast sensitivity were given.

### 2.2.2 Statistical Processing

Using SPSS 22.0 statistical software for statistical analysis of the data, using paired *t* test, experimental data expressed in  $\bar{x} \pm s$ ,  $P < 0.05$  is considered statistically significant.

## 3 Results

Compared with the simulated preflight before, the binocular near vision and distant vision have no obvious effect after two simulated flight tests, but the binocular near vision and distant vision have a downward trend after two simulated flights, and the results are detailed in Table 1.

The value of binocular contrast sensitivity CS (frequency 3) after two flight tests was significantly lower than preflight, and the value of binocular contrast sensitivity CS (frequency 1.5, 6, 12, 18) after two flight simulations showed a downward trend, and the results are detailed in Table 2.

**Table 1** Modeling changes of single, binocular distant, and myopic before and after 12-h flight ( $\bar{x} \pm s$ )

Time	Grouping	Binocular vision function	
		Near vision	Distant vision
First 12 h	Preflight	1.38 ± 0.29	1.23 ± 0.26
	Postflight	1.25 ± 0.30 <sup>a</sup>	1.20 ± 0.28 <sup>b</sup>
	<i>t</i>	1.512	1.000
	<i>P</i>	>0.05	>0.05
Second 12 h	Preflight	1.38 ± 0.29	1.32 ± 0.22
	Postflight	1.32 ± 0.21 <sup>a</sup>	1.28 ± 0.28 <sup>b</sup>
	<i>t</i>	0.830	0.395
	<i>P</i>	>0.05	>0.05

Note Compare with preflight, near vision postflight

<sup>a</sup> $P > 0.05$ ; compare with preflight, near vision postflight

<sup>b</sup> $P > 0.05$

**Table 2** Analog of changes in binocular contrast sensitivity before and after 12-h flight ( $\bar{x} \pm s$ )

Time	Grouping	Binocular contrast sensitivity CS values						
		1.50	3.00	6.00	12.00	18.00		
First 12 h	Preflight	67.50 ± 8.57	108.33 ± 13.89	107.00 ± 56.52	52.17 ± 21.35	28.50 ± 15.29		
	Postflight	64.67 ± 25.13	83.67 ± 25.65 <sup>a</sup>	102.67 ± 53.06	51.50 ± 24.82	28.17 ± 22.12		
	<i>t</i>	0.360	2.735	0.192	0.076	0.064		
	<i>P</i>	>0.05	<0.05	>0.05	>0.05	>0.05		
Second 12 h	Preflight	73.67 ± 22.46	121.67 ± 18.78	114.17 ± 33.88	55.67 ± 16.61	20.67 ± 11.08		
	Postflight	72.33 ± 15.95	89.33 ± 28.29 <sup>b</sup>	100.33 ± 42.86	52.83 ± 17.16	19.00 ± 9.49		
	<i>t</i>	0.157	2.995	1.000	0.287	0.298		
	<i>P</i>	>0.05	<0.05	>0.05	>0.05	>0.05		

Note Compare with first 12-h preflight, contrast sensitivity CS values (frequency 3) postflight

<sup>a</sup>*P* < 0.05; compare with second 12-h preflight, contrast sensitivity CS values (frequency 3) postflight

<sup>b</sup>*P* < 0.05



## 4 Discussion

A study on the fatigue of long-range transport flight crew has been carried out by the NASA abroad. The results suggest that the central nervous system and nervous fatigue are increased during the mission compared with those before the mission. Russian scholars found that 12 h time monotonous instrument and screen display operation in flight 2–3 h fatigue, 4–5 after more obvious. Visual perception and processing of instrumentation information slows down at the onset of sleepiness and then becomes less alert and sometimes falls asleep briefly, prone to illusions and hallucinations [3]. These studies suggest that the continuous appearance of a large number of instruments and screen displays in the cabin leads to a lack of movement and observation space of the eyeball, which may be in a forced position for a period of 12 h; the continuous observation environment outside the cabin is single and lack of change; the combination of the above factors, such as eye irritation, disturbance of biological rhythm, and jet lag effect caused by different brightness environments such as sea flight, glare, and night, may lead to visual fatigue [4].

The mechanism of long-term flight visual fatigue may be due to electromagnetic radiation from aerospace environment, ultraviolet and blue light emitted by display panel and instrument. These stimulating environments strongly stimulate visual cells. Long-term cumulative injury can cause eye fatigue, blurred vision and even headache. The light intensity, flicker, poor clarity, uneven brightness and glare effect of day and night alternation can interfere with the adjustment and stimulate the visual nerve, leading to the central nervous system reaction function decline, and then affect the visual cortex of the brain processing of vision [5, 6]. The long-term contraction of the ciliary muscle will lead to reduced flexibility and cause visual fatigue. In addition, the adjustment force level of the eyes after long flight is often reduced, which leads to the tension of the ciliary muscle caused by long-term near vision defocusing after the retina, which lasts until a certain time and reaches the limit after a certain degree; when it cannot be compensated, it will suddenly give up, and the tension of the eye becomes relaxed, and the symptoms of blurred vision or heavy shadow appear immediately [6]. The flicker of the screen display instrument can lead to symptoms such as visual fatigue and irritability, headache. The resolution, clarity, font, paragraph gap, contrast, and brightness of the screen all affect the visual function. Alternating day and night and dazzling light can form reflective, show off, and interfere with the visual system and may be involved in the occurrence of visual fatigue.

The mechanism of visual fatigue caused by long-time flight is not clear, which may be related to the following aspects: ① Fatigue stimulates serotonin receptors in the central system to increase the release of GABA and weaken the arousal level of the central nervous system [7, 8]. However, brain regions related to cognitive function which include limbic system, such as hippocampus (encoding executive function), and thalamus (continuous and stable function) have lower utilization of glucose by neurons [9]. ② Studies have confirmed that the retina, as a specialized part of the central nervous system, plays an important role in retinal function. In addition, the

changes of glutamate and its receptors may be involved in retinal diseases caused by many other factors [10]. ③ Tong studied the correlation between nerve activity in the high-level visual area of the occipitotemporal lobe of human brain and visual consciousness in binocular competition through functional magnetic resonance and found that the lack of GABA will lead to the degeneration of nerve cells, thus reducing the visual selection ability of Macacumulatta. The visual cortex cells can restore the orientation and direction selectivity of visual stimulation to a greater extent [11, 12]. ④ Recent brain imaging studies have shown that visual working memory and even visual perception tasks can activate the medial temporal lobe, especially the marginal cortex adjacent to the hippocampus. In addition, the study of patients with bilateral medial temporal lobe injury showed that the memory ability of the subjects decreased significantly after completing the visual work of complex information [13].

Simulator flight operation based on virtual reality technology is a complex flight cognitive operation task, 12-h time flight will have a bad effect on human cognitive operation ability, through the change of normal circadian rhythm to make the level of flight control ability to show periodic, volatile changes, and sleep deprivation will cause a series of changes in mood, learning memory, immune function, etc.; with the increase of fatigue, it will also cause a series of physiological, psychological, and even behavioral changes. The compound superposition effect of the two is reflected in the fluctuation change of human physiological function, and the decline of physiological function in severe cases may affect the change of visual function. Contrast sensitivity is the reciprocal of the black-and-white fringe threshold for the lowest recognition spatial frequency (size, thickness) of the human eye [14]. Contrast sensitivity is the ability of human eyes to recognize the lowest spatial frequency, including the ability to distinguish the difference of different visible areas under average brightness, which can reflect the visual function sensitively and truly [15]. The clinical significance of contrast sensitivity varies from frequency region to frequency region. The high frequency region mainly reflects the ability of visual sensitivity, while the middle frequency region reflects the comprehensive ability of visual contrast and central vision. The change of medium frequency contrast sensitivity is closely related to the quality of central visual function [16]. The experimental results show that the near vision and distant vision of both eyes have no obvious effect after two flight tests, but the near vision and distant vision of both eyes have a downward trend after two simulated flights. The value of binocular contrast sensitivity CS (frequency 3) after two flight tests was significantly lower than that pre-flight, and the value of binocular contrast sensitivity CS (frequency 1.5, 6, 12, 18) after two flight simulations showed a downward trend. The results showed that 12-h time flight and sleep deprivation may cause human body fatigue awareness, reduce the ability of stress response, and have a certain inhibitory effect on the central system, while the contrast sensitivity mid-frequency region has a decreasing trend, reflecting the flight fatigue and sleep deprivation may affect optic nerve cells through the central nervous marginal region [9].

## 5 Conclusion

Long-time flight and sleep deprivation make the human body in a state of low arousal. At this time, the mood of the human body deteriorates and the cognitive level decreases, which may have a certain impact on the visual function. Visual fatigue may be involved in the decline of neural activity in the limbic system related brain regions, leaving the body in a low arousal state. This inhibition is achieved by increasing the neural activity associated with the limbic system and reducing the arousal state of the body. In this study, after long-term flight and sleep deprivation, the contrast sensitivity of intermediate frequency decreased significantly, and the contrast sensitivity (full frequency region) showed a decreasing trend, which may be caused by inhibition factors caused by flight fatigue. Combined with the above mechanism analysis, whether flight fatigue participates in the process of low arousal of optic nerve is through acting on 5-HT receptor, reducing glutamate release or activating other regions of limbic system, which needs to be further studied through animal experiments and molecular biological experiments.

**Compliance with Ethical Standards** The study was approved by the Logistics Department for Civilian Ethics Committee of Air Force Medical Center.

All subjects who participated in the experiment were provided with and signed an informed consent form.

All relevant ethical safeguards have been met with regard to subject protection.

**Acknowledgements** This work is supported by the Medical Research Foundation, China, No. AKJ15J002 and BKJ18B033.

Dawei Tian and Feng Wu contributed equally to this work.

## References

1. Hurdiel R, Peze T, Daugherty J et al (2015) Combined effects of sleep deprivation and strenuous exercise on cognitive performances during The North Face (R) Ultra Trail du Mont Blanc (R) (UTMB(R)). *J Sports Sci* 33(7):670–674
2. Li YF, Zhan H, Li T (2005) Effects of 48 h sleep deprivation on dual task ability and fatigue. *Zhongguo Ying Yong Sheng Li Xue Za Zhi* 21(2):174–175, 191
3. Sauvet F, Arnal PJ, Tardo-Dino PE et al (2020) Beneficial effects of exercise training on cognitive performances during total sleep deprivation in healthy subjects. *Sleep Med* 65:26–35
4. Souissi N, Chtourou H, Aloui A et al (2013) Effects of time-of-day and partial sleep deprivation on short-term maximal performances of judo competitors. *J Strength Cond Res* 27(9):2473–2480
5. Suetov AA, Alekperov SI (2019) Acute ocular lesions after exposure to electromagnetic radiation of ultrahigh frequency (an experimental study). *Vestn Oftalmol* 135(4):41–49
6. Kim J, Kang H, Choi H et al (2018) Aqueous extract of *Perilla frutescens* var. *acuta* relaxes the ciliary smooth muscle by increasing NO/cGMP content in vitro and in vivo. *Molecules* 23(7)
7. Kuravi P, Vogels R (2018) GABAergic and cholinergic modulation of repetition suppression in inferior temporal cortex. *Sci Rep* 8(1):13160

8. Nwokolo M, Amiel SA, O'daly O et al (2020) Hypoglycemic thalamic activation in type 1 diabetes is associated with preserved symptoms despite reduced epinephrine. *J Cereb Blood Flow Metab* 40(4):787–798
9. Zhou X, Zhang R, Zhang S et al (2019) Activation of 5-HT1A receptors promotes retinal ganglion cell function by inhibiting the cAMP-PKA pathway to modulate presynaptic GABA release in chronic glaucoma. *J Neurosci* 39(8):1484–1504
10. Choudhary AG, Somalwar AR, Sagarkar S et al (2018) CART neurons in the lateral hypothalamus communicate with the nucleus accumbens shell via glutamatergic neurons in paraventricular thalamic nucleus to modulate reward behavior. *Brain Struct Funct* 223(3):1313–1328.
11. Ginguay A, Cynober L, Curis E et al (2017) Ornithine aminotransferase, an important glutamate-metabolizing enzyme at the crossroads of multiple metabolic pathways. *Biology (Basel)* 6(1)
12. Engskog MK, Ersson L, Haglof J et al (2017) Beta-N-Methylamino-L-alanine (BMAA) perturbs alanine, aspartate and glutamate metabolism pathways in human neuroblastoma cells as determined by metabolic profiling. *Amino Acids* 49(5):905–919
13. Kanehira T, Nakamura Y, Nakamura K et al (2011) Relieving occupational fatigue by consumption of a beverage containing gamma-amino butyric acid. *J Nutr Sci Vitaminol (Tokyo)* 57(1):9–15
14. Guo X, Kong X, Huang R et al (2014) Effect of Ginkgo biloba on visual field and contrast sensitivity in Chinese patients with normal tension glaucoma: a randomized, crossover clinical trial. *Invest Ophthalmol Vis Sci* 55(1):110–116
15. Ulrich K, Palmowski-wolfe A (2019) Comparing three different contrast sensitivity tests in adults and in children with and without amblyopia. *Klin Monbl Augenheilkd* 236(4):434–437
16. Roark MW, Stringham JM (2019) Visual performance in the “real world”: contrast sensitivity, visual acuity, and effects of macular carotenoids. *Mol Nutr Food Res* 63(15):e1801053

# **Research on the Machine-Environment Relationship**

# Evaluation and Analysis of Intelligent Early Warning System in Crowded Places



Qiquan Wang, Meiming Liu, Haibo Xu, Yanhua Meng, Ping Chen, Yu Zhu, and Xi Sun

**Abstract** In order to deal with accidents in crowded places, research on technical methods for accident prevention and control and intelligent early warning systems in crowded places have been widely used. Based on the analytic hierarchy process and fuzzy comprehensive evaluation method, an intelligent monitoring and early warning evaluation index system for crowded places are constructed. Combined with the analysis and study of the situation of specific personnel-intensive places, the use of intelligent early warning systems is verified through quantitative data analysis, providing a scientific reference for the further improvement of the system.

**Keywords** Crowded places · Crowd density · Intelligent early warning · Fuzzy comprehensive evaluation method

## 1 Introduction

People-intensive places mainly refer to public activity places with more than 50 people gathered at the same time. In recent years, security incidents in people-intensive places have shown a trend of frequent growth [1]. According to the incomplete statistics, the number of accidents in people-intensive places at home and abroad in the past five years has occurred. It shows an increasing trend, causing great harm to people's lives and property safety [2]. The accidents that occur are mainly prone to secondary derivative accidents such as trampling and catastrophic accidents, and the main reasons include people, machines, environment, and management [3]. Therefore, constructing an evaluation index system for the monitoring and early warning system of personnel-intensive places, and establishing an intelligent early warning system for personnel-intensive places are of a great significance for scientifically preventing accidents in personnel-intensive places.

---

Q. Wang · M. Liu · H. Xu · Y. Meng (✉) · P. Chen · Y. Zhu · X. Sun  
Safety Engineering, China University of Labor Relations, Beijing 100048, China  
e-mail: [mengyh2008@126.com](mailto:mengyh2008@126.com)

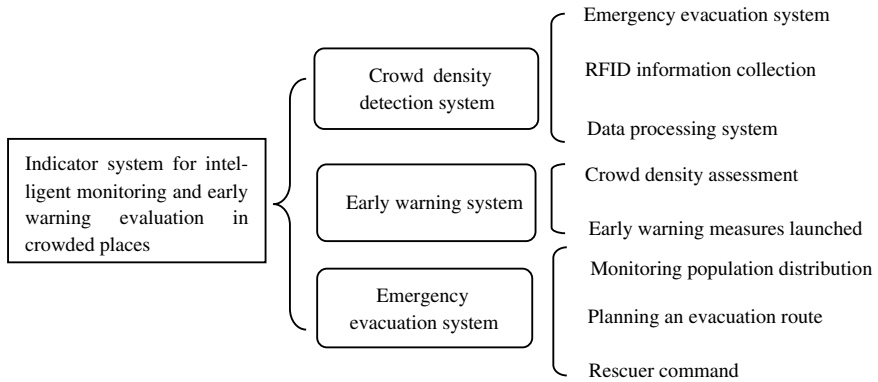


**Fig. 1** Indicator system for crowded places

## 2 Construction of Intelligent Monitoring and Early Warning Assessment Index System in Personnel-Intensive Places

The monitoring and early warning indicator system for personnel-intensive places such as subway stations and the composition of various subsystems in personnel-intensive places and their corresponding functions are used to construct an intelligent monitoring and early warning evaluation indicator system for personnel-intensive places [4]. The intelligent monitoring and early warning system for people-intensive places are divided into two levels of indicators, as shown in Fig. 1.

## 3 Analytic Hierarchy Process to Determine Weights

In the intelligent early warning evaluation indicators of personnel-intensive places, the evaluation factor judgment matrix is determined by six experts according to the importance definition table in the analytic hierarchy process. The weight vector is calculated using the normalization method, and the average value is used to obtain the weight value. After processing and consistency check, the weights of all levels in the system are shown in Table 1.

## 4 Fuzzy Comprehensive Evaluation Analysis

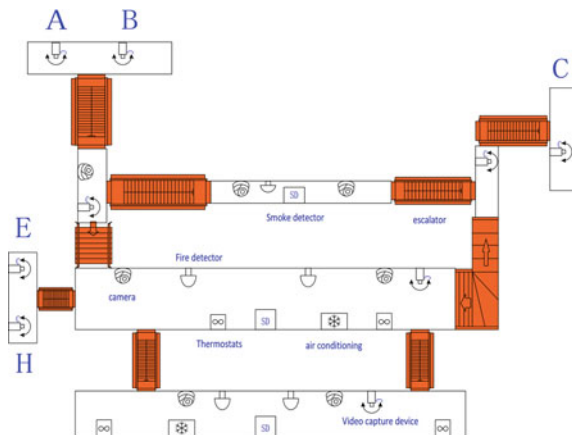
As a typical crowded place, the subway has played an irreplaceable role in the development of the city. Because the subway is underground and its crowd density is high, it is difficult to evacuate. This article chooses a subway station as an example

**Table 1** Weighting table of intelligent monitoring and early warning index system

Level 1 indicator	Level 2 indicator	Weights
Crowd density detection system 0.2521	Video information collection	0.6270
	RFID information collection	0.2923
	Data processing system	0.0807
Early warning system 0.5752	Crowd density assessment	0.7500
	Early warning measures launched	0.2500
Emergency evacuation system 0.1727	Monitoring population distribution	0.5679
	Planning an evacuation route	0.3339
	Rescuer command	0.0982

to verify the intelligent detection of crowded places and the normal operation of the early warning system. In the selection of subway stations, a Beijing subway station was selected for example verification. The experimental subway stations should have characteristics such as large pedestrian turnover (transfer stations) and suitable entrance amount (5 or more). Verification and analysis of the intelligent monitoring and early warning system for densely populated places. After selecting the subway station as the verification target of the example, the verification is performed. A schematic diagram of a subway station in Beijing is shown in Fig. 2.

**Fig. 2** A subway station in Beijing





### 4.1 Establish a Rank Matrix

After determining the weights in the intelligent monitoring and early warning system of the subway station according to the analytic hierarchy process, the fuzzy comprehensive evaluation method was used to evaluate the system and evaluate its effect. The membership values of the five experts' scores were comprehensively analyzed and normalized. The establishment of the factor rank matrix from top to bottom  $R1$   $R2$   $R3$  is shown below.

$$R1 = \begin{Bmatrix} 0.2, 0.4, 0.4, 0 \\ 0.2, 0.4, 0.2, 0.2 \\ 0.2, 0.6, 0.2, 0 \end{Bmatrix} \quad R2 = \begin{Bmatrix} 0.2, 0.6, 0.2, 0 \\ 0.2, 0.4, 0.2, 0.2 \end{Bmatrix} \quad R3 = \begin{Bmatrix} 0.2, 0.4, 0.4, 0 \\ 0.4, 0.2, 0.2, 0.2 \\ 0.6, 0.2, 0.2, 0 \end{Bmatrix}$$

### 4.2 First-Level Fuzzy Comprehensive Evaluation

The indicator weights obtained by referring to the data in Table 1 are as follows:

$$A = \{0.2521, 0.5752, 0.1727\}$$

$$A1 = \{0.6270, 0.2923, 0.0807\}$$

$$A2 = \{0.7500, 0.2500\}$$

$$A3 = \{0.5679, 0.3339, 0.0982\}.$$

According to the expert's assessment, the  $M (\wedge \vee)$  operator is used to obtain the first-level fuzzy evaluation  $B1$ .

$$B1 = A1 \times R1 = \{0.6270, 0.2923, 0.0807\} \times \begin{Bmatrix} 0.2, 0.4, 0.4, 0 \\ 0.2, 0.4, 0.2, 0.2 \\ 0.2, 0.6, 0.2, 0 \end{Bmatrix}$$

$$= \{0.2, 0.4, 0.4, 0\}$$

$$B2 = A2 \times R2 = \{0.7500, 0.2500\} \times \begin{Bmatrix} 0.2, 0.6, 0.2, 0 \\ 0.2, 0.4, 0.2, 0.2 \end{Bmatrix}$$

$$= \{0.2, 0.6, 0.25, 0.2\}$$

$$B3 = A3 \times R3 = \{0.5679, 0.3339, 0.0982\} \times \begin{Bmatrix} 0.2, 0.4, 0.4, 0 \\ 0.4, 0.2, 0.2, 0.2 \\ 0.6, 0.2, 0.2, 0 \end{Bmatrix}$$

$$= \{0.3339, 0.4, 0.4, 0.2\}$$

Normalization process to establish the overall evaluation matrix  $B$ .

$$B = \begin{Bmatrix} 0.2725, 0.2875, 0.3810, 0 \\ 0.2725, 0.4286, 0.2380, 0.5000 \\ 0.4550, 0.2857, 0.3810, 0.5000 \end{Bmatrix}$$

### 4.3 Secondary Fuzzy Comprehensive Evaluation

On the basis of the first-level fuzzy evaluation, a second-level fuzzy comprehensive evaluation is required. The second-level fuzzy evaluation can show the impact of all elements in the index on the overall evaluation, so a second-level fuzzy comprehensive evaluation is required. Doing so makes the result error lower with confidence.

$A = \{0.2521, 0.5752, 0.1727\}$ ,  $B$  is a matrix calculated in the first-level fuzzy evaluation, so  $C$  is the product of  $A$  and  $B$ .

$$C = A \times B = \{0.2521, 0.5752, 0.1727\} \times \begin{Bmatrix} 0.2725, 0.2875, 0.3810, 0 \\ 0.2725, 0.4286, 0.2380, 0.5000 \\ 0.4550, 0.2857, 0.3810, 0.5000 \end{Bmatrix}$$

$$= \{0.3040, 0.3679, 0.2987, 0.1740\}$$

After normalization, the result is

$$C = \{0.3261, 0.2736, 0.2221, 0.1382\}$$

### 4.4 Processing of Fuzzy Comprehensive Evaluation Results

The above calculation process shows that the safety status of the entire subway station intelligent monitoring and early warning system is graded, and the various grades are given points based on the percentage system as shown in Table 2. According to Table 2, the total score  $f$  of the entire system can be calculated.

**Table 2** Security level table

Fraction	100	80	60	40
Security level	Excellent	Good	Average	Poor

Based on the specific scores in the table and the normalized result  $C$ , the total score of the intelligent monitoring system for personnel-intensive places is calculated as follows.

$$f = 100 \times 0.3261 + 80 \times 0.2736 + 60 \times 0.2221 + 40 \times 0.1382 = 73.352$$

According to the result, the safety status of the intelligent monitoring and early warning system of the subway station are medium and close to good; therefore, the probability of accidents is not high. Adding an intelligent monitoring and prevention system in a crowded place can effectively reduce the probability of an accident. The security is improved, and the feasibility and effect of the intelligent monitoring and early warning system are verified.

#### ***4.5 Evaluation Analysis and Improvement***

The fuzzy comprehensive evaluation method is used to estimate the scores of the intelligent early warning system of the entire densely populated place, and it is found that the overall condition is good, and the accident can be effectively prevented. Through weighting and expert judgment, it can be seen that in the crowd density. The detection method is used to judge, and the accuracy of the detection needs to be improved. The combination of RFID and infrared acquisition technology can be used to detect and improve the accuracy of crowd density detection. The precautionary measures should be based on the grading warning; according to specific application, sites are adapted to local conditions and improve the system's suitability for early warning and prevention in personnel-intensive places [5]. In terms of emergency measures, it is necessary to establish a database of accidents in personnel-intensive places, improve the emergency measures by analyzing the causes of accidents, and integrate emergency rescue plans with combine the system, strengthen the training of on-site management personnel, be familiar with the relevant measures in the system, ensure that the rescue is quickly carried out when an accident occurs, improve the efficiency of rescue, and ensure the safe operation of personnel-intensive places.

### **5 Conclusion**

Constructing an intelligent monitoring and early warning evaluation index system, use the analytic hierarchy process to determine the weight of the index system, select a suitable subway station in Beijing to launch example analysis, evaluate the feasibility and effect of the intelligent early warning linkage system in a densely populated place. Using fuzzy comprehensive evaluation method to conduct a quantitative verification of intelligent early warning system, based on the obtained quantitative analysis data to propose corresponding improvement ideas and solutions.

**Acknowledgements** This paper is supported by the National Key Technologies Research and Development program (2017YFC0804900).

## References

1. Shao N (2017) On security risk prevention in personnel-intensive public places. *Chem Ind Manage* 35:255–256
2. Li J, Wang B (2016) Analysis of countermeasures for crowded and stamping accidents in crowded places. *Sci Technol Innovation Prod* 3:40–42
3. Wang Q, Wu J (2016) Design of an emergency linkage system for subway congestion based on stamp model. *Chin J Saf Sci* 26(12):158–162
4. Li W, Ma N, Liu W et al (2016) Preliminary study on risk assessment standardization of urban personnel-intensive places. *Safety* 37(6):7–10
5. Wang Q (2018) Evaluation of emergency linkage system for subway congestion stamping accident based on hierarchical correlation coefficient method. *China Work Saf Sci Technol* (6)

# Application of RULA to Research the Ergonomics Risk of Hand-Held Grinding Operation



Yanqiu Sun, Zhenlong Lu, Jianwu Chen, Bin Yang, Weijiang Liu, and Zidai Xia

**Abstract** Objective—To study the risk of work-related musculoskeletal disorders (WMSDs) of four working positions of hand-held grinding in the mechanical manufacturing industry. Methods—Application of rapid upper limb assessment (RULA), the bad postures of arm and wrist, neck, trunk and leg are scored, respectively; the total score is obtained by combining with the corresponding muscle use score and force/load score, then assess the risk grade according to the total score. Results—The bad posture of upper arm, wrist, neck and trunk is more obvious; the lower arm is followed; the bad posture of legs is not obvious; muscle use and force/load are not obvious. Conclusion—The results show that there are middle and high grades WMSDs ergonomic risks in the working process of four kinds of hand-held grinding postures, which need further study and take corresponding ergonomic improvement measures.

**Keywords** Rapid upper limb assessment · Work-related musculoskeletal disorders · Hand-held grinding operation · Ergonomics · Risk grade

## 1 Research Purpose

Work-related musculoskeletal disorders which are caused by working can cause discomfort, pain and injury of musculoskeletal system in neck, shoulder, back and so on [1, 2]. Epidemiological studies show that WMSDs covers a wide range of industries and has a high prevalence rate; it not only has a serious influence on workers' health, but also causes a huge economic burden to the society [3, 4]. In

---

Y. Sun · J. Chen (✉) · B. Yang · W. Liu  
China Academy of Safety Science and Technology, Beijing 100029, China  
e-mail: [cjw3000@126.com](mailto:cjw3000@126.com)

Z. Lu  
Tiandi Science & Technology Co., Ltd, Beijing 100013, China

Z. Xia  
Capital University of Economics and Business, Beijing 100070, China

recent years, WMSDs which is caused by multiple parts of the body has attracted much attention.

The rapid upper limb assessment (RULA) was developed by Lynn McAtamney and E. Nigel Corlett, who are in the institute of occupational ergonomics, University of Nottingham, the UK, which is a screening tool to assess the whole body biomechanics and postural load, the RULA can also estimate the upper limb disorder risks. It is widely used in risk assessment of work-related musculoskeletal disorders (WMSDs) in abroad [5–7]. RULA as a method of assessment is used to evaluate WMSDs ergonomic risk in the process of shipbuilding, mask production and shoemaking. The squat posture may have harmful effects on the musculoskeletal system, so for the hand-held grinding operation workers, stand working posture is superior to squat posture. This study is based on the above research, and hand-held grinding workers take different working postures for different grinding workpieces in the mechanical manufacturing enterprises [8, 9]. In the study, we used the RULA to assess risk grade of work-related musculoskeletal disorders in four kinds of hand-held grinding working postures and put forward improvement measures and suggestions.

## 2 Research Object and Method

### 2.1 Research Object

Grinding is a common job in machinery manufacturing industry. In this study, we took four working postures of hand-held grinding as the research objects, and they are stand working posture grinding (small pieces), stand working posture grinding (big pieces), leaning bend grinding (big pieces) and squat posture grinding, which are shown in Figs. 1, 2, 3, and 4.

**Fig. 1** Stand working posture grinding (small pieces)



**Fig. 2** Stand working posture grinding (big pieces)



**Fig. 3** Leaning bend grinding (big pieces)



## 2.2 Research Method

RULA is mainly according to human posture; at the same time, it considers the add force/load and muscle use (including static force and repeatability) and at last gives the final score of arm, wrist, neck, trunk, leg and prevention suggestions, which are used to improve the design of workplace, design hand operation or guide the redesign of existing operations [10]. RULA assessment gives quick and systematic assessment of the postural risks. The analysis can be conducted before and after an intervention to demonstrate that the intervention has worked to lower the risk of injury. There are totally 15 steps in RULA assessment. By checking the bad posture of different parts of body, muscle use and force/load, the bad postures of arm and wrist (collectively referred to as part A), neck, trunk, and leg (collectively referred to as part B) are

**Fig. 4** Squat posture grinding



scored, respectively, the total score is obtained by combining with the corresponding muscle use score and force/load score and then assesses the risk grade according to the total score.

The risk is divided into four grades according to the total score (1–7 score), I grade is 1 or 2 score, almost no risk, acceptable posture. II grade is 3 or 4 score, low risk, further investigation, change may be needed. III grade is 5 or 6 score, moderate risk, further investigation, change soon. IV grade is 7 score, very high risk, investigation and implement change.

### 3 Conclusions

#### 3.1 Arm and Wrist Posture Analysis Results

Arm and wrist scores of four working positions of hand-held grinding are as follows: upper arm score is 2–4, in which the stand working posture grinding (big pieces) is the highest score, lower arm score is 1–3, wrist score is 4, wrist twist is score 1, posture score A is 4–6, muscle use score is 1, force/load score is 0, the wrist and arm total score is 5–7, the details are shown in Table 1.

#### 3.2 Neck, Trunk and Leg Posture Analysis Results

Neck, trunk and leg scores of four working positions of hand-held grinding are as follows: neck score is 3–4, trunk score is 3–6, in which the leaning bend grinding (big pieces) is the highest score, leg score is 1–3, posture score B is 4–8, muscle use



**Table 1** Arm and wrist posture analysis results

Working posture	Upper arm score	Lower arm score	Wrist score	Wrist twist score	Posture score A	Muscle use score	Force/load score	Wrist and arm score
Stand working posture grinding (small pieces)	2	1	4	1	4	1	0	5
Stand working posture grinding (big pieces)	4	3	4	1	6	1	0	7
Leaning bend grinding (big pieces)	3	3	4	1	5	1	0	6
Squat posture grinding	2	2	4	1	4	1	0	5

score is 1, force/load score is 0, the neck, trunk and leg total score is 5–9, the details are shown in Table 2.

### 3.3 Final Score and Risk Grade

The total scores of four working positions of hand-held grinding are 6–7. The risk grade of stand working posture grinding (small pieces) is III, moderate risk, further investigation, change soon. The risk grades of stand working posture grinding (big pieces), leaning bend grinding (big pieces) and squat posture grinding are IV, very high risk, investigation and implement change. The details are shown in Table 3.

### 3.4 Ergonomic Improvement Measures and Suggestions

The risk grade of stand working grinding (small pieces) is III, and the risk factors for workers are shown as follows: upper arm is abducted in the process of grinding operation, wrist is twisted in mid-range in the operation of hand-held angle grinder,

**Table 2** Neck, trunk and leg analysis results

Working posture	Neck score	Trunk score	Leg score	Posture score B	Muscle use score	Force/load score	Neck, trunk and leg score
Stand working posture grinding (small pieces)	3	3	1	4	1	0	5
Stand working posture grinding (big pieces)	3	4	1	5	1	0	6
Leaning bend grinding (big pieces)	4	6	1	8	1	0	9
Squat posture grinding	3	4	1	5	1	0	6

**Table 3** RULA analysis results of four working postures

Working posture	Wrist and Arm Score	Neck, trunk and leg score	Final score	Risk grade
Stand working posture grinding (small pieces)	5	5	6	III
Stand working posture grinding (big pieces)	7	6	7	IV
Leaning bend grinding (big pieces)	6	9	7	IV
Squat posture grinding	5	6	7	IV

neck and trunk are twisted with the different of workpiece position. The suggestion is to place the workpieces correctly during working, reduce working posture of the abduction of upper arm, twisted of neck and trunk.

The risk grade of stand working posture grinding (big pieces) is IV, upper arm score is the highest, the risk factors for workers are shown as follows: because of the grinding big pieces is large, upper arm is abducted in the process of grinding operation, lower arm is worked across midline or out to side of body, wrist is twisted in mid-range in the operation of hand-held angle grinder, trunk is twisted with the different of workpiece position. The suggestion is to set the workpiece placing bench

to automatically adjust the position of the workpiece, reduce working posture of the abduction of upper arm, twisted of trunk, and avoid lower arm is worked across midline or out to side of body.

The risk grade of leaning bend grinding (big pieces) is IV, trunk score is the highest, the risk factors for workers are shown as follows: because of complex structure of the workpiece, upper arm is abducted in the process of grinding operation, wrist is twisted in mid-range in the operation of hand-held angle grinder, neck is side bending, trunk is twisted and side bending. The suggestion is to set the workpiece placing bench to automatically adjust the position of the workpiece, avoid neck is side bending, working posture of twisted and side bending of the trunk.

The risk grade of squat posture grinding is IV, the risk factors for workers are shown as follows: the worker needs to take squat posture, wrist is twisted in mid-range in the operation of hand-held angle grinder, trunk is twisted with the different of workpiece position. The suggestion is to set the workpiece placing bench, take stand working posture, and avoid trunk is twisted in working.

## 4 Conclusions

The results show that there are middle and high grades WMSDs ergonomic risks in the working process of four kinds of hand-held grinding postures, which need further study and take corresponding ergonomic improvement measures.

Manual activity is mainly used in the process of hand-held grinding operation, and the characteristics of adverse ergonomic factors are shown as follows: the bad posture of upper arm, wrist, neck and trunk is more obvious, the lower arm is followed, the bad posture of legs is not obvious, muscle use and force/load are not obvious. We should choose the hand-held grinding tool less than 2 kg as far as possible to reduce the force/load, which makes sure that a large force/load is not required in the grinding process. The adverse ergonomic factors of hand-held grinding mainly caused by poor working posture and repeated operation. It is suggested to correct according to the improvement measures and reduce the frequency of repeated operation.

## 5 Discussions

The RULA method is applied to study the WMSDs ergonomic risk in the process of hand-held grinding in machinery manufacturing industry in the paper and discovery that there are middle and high grades WMSDs ergonomic risks and adverse ergonomic factors. Considering that there are many methods to evaluate the ergonomic factors of WMSDs, different methods have their own characteristics and applicable conditions, we need to explore different identification and evaluation methods in the future, identify and evaluate WMSDs ergonomic risk of hand

grinding workers more comprehensive and systematic, which can provide meaningful reference for preventive measures.

**Acknowledgements** This work was supported by the National Key R&D Program of China (2016YFC0801700), the basic research funding of China Academy of Safety Science and Technology (2019JBKY04, 2019JBKY11, 2017JBKY02).

**Compliance with Ethical Standards** The study was approved by the Logistics Department for the Civilian Ethics Committee of China Academy of Safety Science and Technology.

All subjects who participated in the experiment were provided with and signed an informed consent form.

All relevant ethical safeguards have been met with regard to subject protection.

## References

1. Qin D, Wang S, Zhang Z et al (2017) Effects of mental workload on work-related musculoskeletal disorders in railway vehicle manufacturing workers. *Chin Occup Med J* 44(3):362–364
2. Long MH, Johnston V, Bogossian F (2012) Work-related upper quadrant musculoskeletal disorders in midwives, nurses and physicians: a systematic review of risk factors and functional consequences. *Appl Ergon J* 43(3):455–467
3. Xu X, Wang S, Yu S et al (2016) The industry trends and research progress on work-related musculoskeletal disorders. *Chin J Ind Med J* 29(4):278–282
4. Murray CJL, Vos T, Lozano R et al (2012) Disability-adjusted life years (DALYs) for 291 diseases and injuries in 21 regions, 1990–2010: a systematic analysis for the global burden of disease study 2010. *Lancet J* 380(9859):2197–2223
5. Rahman CM (2014) Study and analysis of work postures of workers working in a ceramic industry through rapid upper limb assessment (RULA). *Int J Eng* 5(3):8269
6. Levanon Y, Lerman Y, Gefen A et al (2014) Validity of the modified RULA for computer workers and reliability of one observation compared to six. *Ergon J* 57(12):1856–1863
7. Dockrell S, O’Grady E, Bennett K et al (2012) An investigation of the reliability of Rapid Upper Limb Assessment (RULA) as a method of assessment of children’s computing posture. *Appl Ergon J* 43(3):632–636
8. Sun Y et al (2019) Ergonomics analysis of hand-held grinding operation working posture based on jack. In: Long S, Dhillon BS (eds) *Man-machine-environment system engineering. Lecture notes in electrical engineering*, vol 576. Springer, Singapore. [https://doi.org/10.1007/978-981-13-8779-1\\_83](https://doi.org/10.1007/978-981-13-8779-1_83)
9. Chen J et al (2019) Study on the upper flange width on grinding worktable and its ergonomics evaluation. In: Long S, Dhillon BS (eds) *Man-machine-environment system engineering. Lecture notes in electrical engineering*, vol 576. Springer, Singapore. [https://doi.org/10.1007/978-981-13-8779-1\\_94](https://doi.org/10.1007/978-981-13-8779-1_94)
10. Su R, Xue H, Song B (2008) Improvement of RULA. *Chin J Ergon J* 14(1):15–17

# Analysis of the Fighter Pilots Acceleration Tolerance Selection Method and Results



Rong Lin, Baohui Li, Yan Xu, Lihui Zhang, Hong Wang, Xiaoyang Wei, Yifeng Li, Jinghui Yang, Xichen Geng, Liu Yang, Juan Liu, Duanqin Xiong, and Zhao Jin

**Abstract** *Objective* To discuss and analyze the +Gz tolerance selection results of high-performance aircraft pilots. *Methods* One thousand and seven hundred forty-three aircraft pilots +Gz tolerance data were collected and analyzed by cross-sectional study. The +Gz tolerance examination method, qualification rate and the correlation of that between age and flying hour were analyzed. *Results* Straining was not banned strictly, furthermore, the pilot was permitted to adopt the breathing method of HP maneuver during +Gz tolerance examination. Of the 1743 pilots, 1569 completed the selection run, and the qualification rate was 90%. The qualification rate was significantly related to the age ( $r = 0.891$ ,  $P = 0.000$ ) and flying hours ( $r = 0.9281$ ,  $P = 0.004$ ). When reaching the end point of G tolerance, 39.3% pilots got a change of vision and the incidence of A-LOC and G-LOC was 1.7% and 2.6%, respectively. *Conclusions* The high-performance aircraft pilots +Gz tolerance selection qualification rate was greater than formerly reported. Less +Gz exposure runs, standardized breathing maneuver and muscular straining may contribute to the high qualification rate.

**Keywords** Acceleration · Centrifuge · G tolerance · Pilots

## 1 Introduction

In order to select high-performance fighter pilots with excellent G tolerance, the air forces of various countries have developed corresponding +Gz tolerance evaluation methods and standards for pilots [1–4]. In order to exclude the effect of the anti-G equipment and anti-G straining maneuver (AGSM) on G tolerance, the unprotected, relaxed +Gz tolerance test was adopted extensively [5–7]. The “basic” +Gz tolerance selection of our high-performance aircraft pilots is used to carry out according to GJB 3293-1998 “Assessment and test methods of sustained positive acceleration

---

R. Lin · B. Li · Y. Xu · L. Zhang · H. Wang · X. Wei · Y. Li · J. Yang · X. Geng · L. Yang · J. Liu · D. Xiong · Z. Jin (✉)  
Air Force Medical Center, Fourth Military Medical University, Beijing 100142, China  
e-mail: [jinzhaos17@163.com](mailto:jinzhaos17@163.com)

© The Editor(s) (if applicable) and The Author(s), under exclusive license to Springer Nature Singapore Pte Ltd. 2021

S. Long and B. S. Dhillon (eds.), *Man-Machine-Environment System Engineering*, Lecture Notes in Electrical Engineering 645, [https://doi.org/10.1007/978-981-15-6978-4\\_96](https://doi.org/10.1007/978-981-15-6978-4_96)

tolerance for pilots” [4] on an old “Six-three” human centrifuge. The pilots were exposed +Gz acceleration without anti-G equipment, and breathing naturally and intended straining muscle were not permitted. Since the centrifuge was replaced with a new high performance one, the physiology experts engaged in this work also modified the basic +Gz tolerance selection method. The +Gz tolerance selection method and results were analyzed and discussed in this study.

## 2 Subjects and Methods

### 2.1 Subjects

The subjects were 1743 fighter pilots who have accepted basic +Gz tolerance selection, the average age was 28 (21–45) years and the flying hours was  $796 \pm 233$  h (93–3460 h).

### 2.2 Basic +Gz Tolerance Selection

The basic +Gz tolerance selection for fighter pilots was performed in the new human centrifuge. The pilots were exposed three runs at the onset rate of 1 G/s, and the peak duration of +Gz exposure was 10 s. The selection would be qualified if the +Gz tolerance was not lower than the evaluation standard. The pilots were asked to adopt the breathing method of HP maneuver during +Gz exposure [8].

### 2.3 Data Analysis

SPSS 18.0 software was used to manage the data and conduct the statistical analysis. The critical level of significance was set at  $P < 0.05$ .

## 3 Results

### 3.1 Result of Fighter Pilots +Gz Tolerance Selection

About 1569 (90%) of the 1743 pilots were qualified, 132 pilots (7.6%) reached the peak G level but did not maintain for 10 s. Thirty-eight pilots tolerance lower than moderate 1, nine of them had experienced G-LOC, two of them had experienced A-LOC, and six of them had experienced black vision (Table 1).

**Table 1** Result of fighter pilots +Gz tolerance selection

+Gz tolerance	Peak G-level duration (s)	<i>n</i>	Percentage (%)
Low 1	<10	22	1.3
Low 2	10	3	0.2
Moderate 1	<10	13	0.7
Moderate 2	10	4	0.2
Almost qualified	<10	132	7.6
Qualified	10	1569	90.0
Total		1743	100

**Table 2** Age distribution of the fighter pilots +Gz tolerance qualification rate

Age groups (yrs)	Total	Qualified number	Qualification rate (%)
21–25	564	508	90.1
26–30	761	670	88.0
31–35	266	246	92.5
36–40	112	105	93.8
≥41	40	40	100.0
Total	1743	1569	90

### 3.2 *The Age Distribution of +Gz Tolerance Qualification Rate for Pilots*

There are 1325 pilots aged between 21 and 30 years, accounting for 76% of all pilots. The difference of qualification rate between different age groups was of statistically significant ( $\chi^2 = 11.275, P = 0.024$ ). The analysis of correlation test showed that there was a significant correlation between the selection qualification rate and age ( $r = 0.891, P = 0.000$ ) (Table 2).

### 3.3 *The Relation Between Qualification Rate of Basic +Gz Tolerance Selection and Flying Hour*

The difference of qualification rate among different flying hour groups was of statistically significant ( $\chi^2 = 18.315, P = 0.005$ ). The analysis of correlation test showed that there was a significant correlation between the selection qualification rate and flying hour ( $r = 0.9281, P = 0.004$ ) (Table 3).

**Table 3** +G<sub>z</sub> tolerance qualification rate in different flying hour groups

Flying hours (h)	Total	Qualified number	Qualification rate (%)
100–500	782	704	90.0
501–1000	502	434	86.5
1001–1500	219	199	90.9
1501–2000	130	124	95.4
2001–2500	71	69	97.2
2501–3000	23	23	100.0
≥3001	3	3	90.0
Total	1730	1556	100

### 3.4 Change of Vision and Consciousness When Reaching the End Point of G Tolerance

Except for one pilot who felt dizzy and asked to terminate examination, of the other 1742 pilots, 984 (56.5%) pilots were of no complain and 684 (39.3%) pilots got a change of vision when reaching the end point of G tolerance. Forty-five pilots (2.6%) had experienced G-induced loss of consciousness (G-LOC). Twenty-nine pilots (1.7%) had experienced almost loss of consciousness (A-LOC). The difference of qualification rate among different complain groups was statistically significant ( $\chi^2 = 469.254, P = 0.000$ ) (Table 4).

**Table 4** Change of vision or consciousness at the end point of G tolerance and qualification rate

Complain	<i>n</i>	Percentage (%)	Qualification rate (%)
No complain	984	56.5	97.4
Peripheral light dimmed	524	30.1	95.4
Peripheral light loss	27	1.5	70.4
Peripheral lights loss with central light dimmed	100	5.7	85.0
Blackout	33	1.9	27.3
G-induced loss of consciousness	45	2.6	8.9
G-induced almost loss of consciousness	29	1.7	3.4
Total	1742	100	



## 4 Discussions

Because the false breathing method would decrease +Gz tolerance, the pilots in this study were permitted to breath according to the essentials of HP maneuver. It is difficult to avoid or prevent the pilots from straining muscles or performing ASGM when +Gz exposure; this would have some effect on the selection.

The results of this study indicated that the qualification rate of +Gz tolerance selection for high-performance fighter pilot based on new human centrifuge was as high as 90%, but there were still very few pilots who did not meet the +Gz tolerance standards. The qualification rate of +Gz tolerance selection for pilots was positively correlated with age, and the qualification rate of pilots over 31 years old was greater than pilots under 30 years old.

When reaching the end point of G tolerance, various changes of vision and consciousness that occur can be divided into the following types and recorded: no complain, peripheral light dimmed, peripheral light loss, peripheral light loss with central light dimmed, blackout, G-induced loss of consciousness (G-LOC) and G-induced almost loss of consciousness (A-LOC), which can be applied in the general sort of +Gz tolerance for pilots.

The present pilot +Gz tolerance examination methods and standards were very different from the past in some ways as follows:

1. Different +Gz exposure profile

According to the requirements of GJB 3293-1998, the G exposure started from a low G value to the qualified run increasing by 0.25–0.5 G each time. Each pilot experienced about five G exposures. The examination in this study performed only three G exposures increasing by 0.75–1.0 G each time.

2. Different requirements

According to GJB 3293-1998, the pilots were required to breathe naturally and do not intend to straining muscles actively during the examination. In this study, the pilots could adopt the breathing method of HP maneuver and the muscle straining was not strictly controlled. In fact, the examination result above was not “basic” +Gz tolerance anymore.

3. Different standards

In early reports [9, 10], the assessment standard specified in GJB 3293-1998 [4] was used as pilot +Gz tolerance selection which was more difficult to pass than that of this study.

## 5 Conclusions

According to the present examination method, the qualification rate of +Gz tolerance selection for fighter pilot reached 90%. Less +Gz exposure runs, standardized breathing maneuver and muscular straining may contribute to the high qualification rate.

**Compliance with Ethical Standards** The study was approved by the Logistics Department for Civilian Ethics Committee of Air Force Medical Center of FMMU. All subjects who participated in the experiment were provided with and signed an informed consent form. All relevant ethical safeguards have been met with regard to subject protection.

## References

1. Gillingham KK (1987) G-tolerance standards for aircrew training and selection. *Aviat Space Environ Med* 58(10):1024–1026
2. Welsh H (1996) Selection of future fighter pilots. Advisory Group for Aerospace Research&Development (AGARD). Selection and training advances in aviation. AGARD-CP-588. North Atlantic Treaty Organization (NATO), France, pp 10.1–10.5
3. Бугров СА, Лапаев ЭВ, Пономаренко ВА, Ступаков ГП (1993) Проблема профессионального здоровья в авиационной медицине. *Военно-медицинский журнал* 1:61–64
4. Lu X, Yin G, Wu Q. GJB 3293-1998 assessment and test methods of sustained positive acceleration tolerance for pilots. The General Logistics Department of PLA, Beijing
5. Scontt JPR, Jungius J, Connolly D et al (2013) Subjective and objective measures of relaxed +Gz tolerance following repeated +Gz exposure. *Aviat Space Environ Med* 84(7):684–691
6. Stevenson AT, Scontt JPR, Chiesa S et al (2014) Blood pressure, vascular resistance, and + Gz tolerance during repeated +Gz exposures. *Aviat Space Environ Med* 85(5):536–542
7. Grönkvist M, Levin B, Eiken O (2018) G tolerance during open vs. closed-loop G-time control. *Aerosp Med Hum Perform* 89(9):798–804
8. Xichen G, Zhao J, Yan X et al (2002) Centrifuge evaluation of the +Gz protection of the new anti-G straining maneuver: HP and PHP maneuver. *Chin J Aerospace Med* 13(4):209–213
9. Zhao J, Xichen G, Xia L et al (2006) Analysis of the relaxed +Gz tolerance records of 580 fighter pilots. *Chin J Aerospace Med* 17(3):185–190
10. Zheng J, Liu H, Xu S et al (2003) Analysis of the physical examination for selection of high performance fighter pilots. *J General Hospital Air Force PLA* 19(2):78–80

# Study on the Impact and Countermeasure of Plateau Alpine Region on Shooting of a Type of Light Weapons



He Wu, Xiang Gao, Zhengbu Liu, Yanyan Ding, Haoyuan Li, and Xin Wang

**Abstract** The plateau alpine region is vast, and the climate is changeable. The unique geographical environment will have a greater impact on the shooting effect of light weapons. We made statistics on the shooting results of light weapons of a unit in the plains and in the plateau alpine region and analyzed the decline percentage at all levels. Aiming at the characteristics of the environment in the plateau alpine region, the impact of the environment on weapon effectiveness and the physical and mental function of the shooter during the light weapon shooting training in the region was found, and countermeasures and suggestions for reducing the impact and improving the shooting results were proposed.

**Keywords** Plateau · Alpine · Shooting · Impact

The plateau alpine region refers to a mountainous area with an altitude of more than 3000 m, a cold climate, and thin air. Its main environmental characteristics are cold climate and low average temperature, especially in areas above 4500 m above sea level. It is winter in all seasons, the average temperature is 8–9 °C lower than the plain area at the same latitude, and extreme temperatures are close to minus 40 °C. Low air pressure and low air density are only about 80% of the plain area and about 35% less oxygen content than the plain area; the temperature difference is large, the wind and snow are obvious, the sun is so hot during the day, and the temperature is as high as 20–30 °C. At night and early morning, temperatures may drop below 0 °C [1].

Fighting in the plateau alpine regions, the natural environment is harsh, the battlefield conditions are difficult, the social support is poor, and the support of weapons and equipment is arduous, which will have a great impact on combat operations.

---

H. Wu · X. Gao · Z. Liu · Y. Ding (✉) · H. Li · X. Wang  
PLA Army Academy of Artillery and Air Defense Zhengzhou Campus, Zhengzhou 450052, China  
e-mail: [wuhezikao@163.com](mailto:wuhezikao@163.com)

# 1 Influence of Plateau Alpine Region on Light Weapon Effectiveness

The plateau alpine regions have low oxygen content, low air pressure, and low air density. The resistance of light weapons to projectiles after shooting is reduced, which is easily prone to projectile deviation, long range, and low accuracy. At the same time, due to the great changes in wind and direction, shooting accuracy will be seriously affected.

The following table is the shooting results of a type of light weapons for a unit we contacted in one year, including the results of the usual station and the plateau training field, five times in each region. The personnel involved in the statistics were a company with a total of 103 people. Each time they shot, they used personally fixed firearms (Tables 1, 2 and 3).

From the training results, it can be seen that when shooting a type of light weapons at an altitude of 3650 m, the proportion of people above good dropped by 19.1%; the proportion of passing people increased slightly, mainly because of excellent and good personnel; the proportion of people who failed rise a lot, up to 15.2%. From the analysis of results, the shooting accuracy of the same shooter is generally lower than that of the plain area. Data show that when shooting at 3700 m above sea level, the impact point is 3–4 cm high on average, and when shooting at 4500 m above sea level, it is 4–5 cm high on average [2].

In addition, the performance of weapons and equipment decreases, and the damage rate increases. At an altitude of 4500 m, the performance of weapons and equipment fell by about 30%, and the damage rate was twice as high as that in the plains [2]. On the one hand, the plateau areas have strong wind and sand and heavy rain and snow. The resistance of the counter-recoil machine for light weapons must increase during shooting, and it is not easy to move in place. Besides, it is prone to jamming

**Table 1** Results statistics of shooting training of a type of light weapons in ordinary regions

Training conditions	Station altitude	Total no	Results			
			No. of excellent (45 rings or more)	No. of good (35–44 rings)	No. of pass (30–34 rings)	No. of fail (below 30 rings)
Five rounds, 100 m, chest silhouette, precision shooting	310 m	103 people				
First round			36	45	19	3
Second round			38	42	21	2
Third round			35	49	18	1
Fourth round			40	47	15	1
Fifth round			44	41	17	1
Average score			38.6	44.8	18	1.6
Average score ratio by level (%)			37.5	43.5	17.5	1.5

**Table 2** Results statistics of shooting training of a type of light weapons in the plateau regions

Training conditions	Station altitude	Total no	Results			
			No. of excellent (45 rings or more)	No. of good (35–44 rings)	No. of pass (30–34 rings)	No. of fail (below 30 rings)
Five rounds, 100 m, chest silhouette, precision shooting	3650 m	103 people				
First round			21	39	28	15
Second round			19	42	24	18
Third round			24	37	25	17
Fourth round			25	44	19	15
Fifth round			28	40	14	21
Average score			23.4	40.4	22	17.2
Average score ratio by level (%)			22.7	39.2	21.4	16.7

**Table 3** Comparison of training results

Training conditions	Total no	Results			
		No. of excellent (45 rings or more)	No. of good (35–44 rings)	No. of pass (30–34 rings)	No. of fail (below 30 rings)
Five rounds, 100 m, chest silhouette, precision shooting	103 people				
Average score in ordinary regions		38.6	44.8	18	1.6
Average score ratio in ordinary regions (%)		37.5	43.5	17.5	1.5
Average score in the plateau regions		23.4	40.4	22	17.2
Average score ratio in the plateau regions		22.7%	39.2%	21.4%	16.7%
Ratio comparison		Down 14.8%	Down 4.3%	Up 3.9%	Up 15.2%

or non-returning of the shell. Secondly, the low temperature and changing climate easily damage the parts of light weapons, especially the plastic parts in light weapons, which are more likely to age. Third, the heat dissipation performance of the weapon is reduced. Due to the thin air, the effectiveness of the heat conduction and convection of the air is reduced, which can easily cause the weapon temperature to be too high, which will cause performance degradation and shorten the life.

## **2 Influence of Plateau Alpine Region on the Physical and Mental Functions of the Shooter**

The first is that hypobaric hypoxia seriously affects human body functions. Due to the low pressure and hypoxia of the plateau, it is easy to cause the decline of personnel function, and slow movement, slow response, and weakened endurance are the basic states of people in the plateau region. People with mild conditions are prone to common high-altitude diseases such as dizziness, vomiting, palpitation, cough, and indigestion. In severe cases, heart failure, respiratory failure, pulmonary edema, and coma are very common. They have a significant impact on the combat effectiveness of personnel. Plateau tests show that in areas above 4500 m above sea level, people's physical strength has dropped by 40%, trekking speed has decreased by 50%, and poor personnel's response and endurance have a direct impact on weapon control [3].

The second is that cold temperatures seriously affect human behavior. The plateau cold is another natural factor that is second only to the effects of hypoxia on human body function. Under low-temperature conditions, in order to maintain normal body temperature, on the one hand, in order to reduce the consumption of calories, the body begins to stop sweating and blood vessels dilate to increase blood flow to warm the skin. On the other hand, the body strengthens its metabolic functions, causing involuntary tremors to generate more heat. These aspects have a huge impact on the control of the weapon when the shooter shoots light weapons.

Third, the harsh environment seriously affects people's psychological quality. In the plateau environment, the central nervous system is most sensitive to hypoxia and consumes large amounts of oxygen. In mild hypoxia, the inhibition in the cerebral cortex weakens and the excitement increases. The higher the altitude, the heavier the hypoxia, the more the hypoxia changes from the excitement to the inhibition, the symptoms of distracted attention, unresponsive thinking, decreased memory, and other symptoms directly affect people psychologically. When shooting a rifle in this state, the shooter is affected by the brain and cannot maintain a consistent focus when aiming. The shooting action cannot be made according to "unconscious" shooting, which greatly affects the shooting accuracy.

## **3 Countermeasures to Improve the Shooting Effect of Light Weapons in Plateau Alpine Regions**

### ***3.1 Improve Weapon Performance and Enhance Weapon Reliability***

The first is to enhance the module design and expand the weapon function. Aiming at the problem that the existing weapons and equipment, especially the gun family,

are difficult to quickly convert, taking into account the distance and near firepower, to meet the needs of a variety of combat tasks, new light weapons should strengthen the module design concept, strengthen automata, gage sharing, universal interface, expansion interface, connection interfaces, and rapid combination of modules to achieve operational requirements in different regions and different environments.

The second is to increase the effective range and enhance the power of weapons. In modern warfare, the defense depth is usually 300–600 m, the plateau mountains and sea defenses even reach to 800 m, the first echelon company has a defense depth of about 1000 m, and the battalion defense positions are 2000–3000 m. In response to the different needs of offensive and defensive operations, in order to make the defensive operations effectively delay the enemy's actions and obtain the fire support of the first and second echelon, the enemy's firepower should be effectively suppressed during the offense. The range of light weapons should be increased to enhance the ability to strike at medium and long distances.

The third is to reduce the weight of the parts and increase the life of the weapon. The plateau alpine region has severe weather, heavy personnel dressing, and inconvenient mobility. In order to reduce the load of individual soldiers and increase the flexibility of personnel operations, it is required that weapons and equipment should further improve the structure and use lightweight materials such as new materials to adapt to the characteristics of training and combat in plateau alpine regions and strengthen the application research of wear-resistant, ablation-resistant barrel technology, and high-efficiency and low-ablation propellant technology to further improve the service life of weapons in harsh environments [4].

### ***3.2 Improve Manual Efficiency and Reduce Operational Dependence***

At present, rifles rely heavily on people when shooting, and there are obviously individual differences. Especially in plateau alpine regions, it is difficult to achieve breath-holding shooting essentials. Experts have conducted special experiments in the cold plateau area of the modified gun family. The experimental data show that the adaptability and stability of weapon aiming of individual shooters are significantly different in high-altitude and anoxic environments compared with ordinary environments, with an average decrease of about 60% and a decrease in shooting performance of about 50%. Therefore, it is necessary to increase the improvement of weapon manual mechanics.

The first is to increase the use of adaptive technology. In the development of a new generation of light weapons equipment, adaptive technologies such as recognition and perception, shooting control, gage setting, ballistic calculation, and shooting correction should be used to reduce the dependence of weapons on people. The

research on new technologies such as automatic trajectory correction, target locking, and high-efficiency bullets for shooting statistics should be strengthened to explore the integration of information technology and traditional light weapons to improve the convenience of use.

The second is to improve the ergonomic design. Due to poor road conditions and traffic conditions in the alpine region, troops often need to ride or walk when performing training and combat tasks. The roads are bumpy, and problems such as weak weapon locks often occur. In addition, like the trigger mechanism, it is not easy to fire with thick cold gloves. These all need to improve the ergonomic design of light weapons to facilitate their use in alpine regions.

The third is to improve the availability of weapons and equipment. It is relatively difficult to care and maintain artificially in plateau alpine regions. We need to organize adaptive training in the region to explore the maintenance methods of weapons and equipment that are suitable for the environmental characteristics of the area. Maximize the combination of personnel and equipment, ensure the integrity of weapons and equipment, and reduce non-combat losses and unnecessary manual maintenance. For example, for the characteristics of low temperature, use thermal insulation materials to wrap and cover weapons.

### ***3.3 Improve Training Methods and Personnel Adaptability***

The light weapons firing in the plateau alpine regions is affected not only by the weather environment, weapons, and other factors, but also the basic capabilities and military qualities of personnel.

The first is to strengthen the physical fitness of officers and men. High-altitude hypoxic environment has a greater impact on aerobic endurance training, significantly affects people's cognitive function, increases reaction time, and reduces coordination and accuracy of movement. Light weapons require officers and men to overcome these adverse effects when shooting. Troops in plateau cold regions need to strengthen their physical fitness training scientifically. Focus on training people's ability to adapt to extreme environments and their ability to operate weapons and explore scientific training models. According to the geographical location and altitude of troop's stationed and main training, the plateau military fitness training modes can be divided into "high station high training," "high station low training," "low station high training," and other modes [5].

The second is to strengthen the psychological quality training of officers and men. Due to the special geographical environment, in high and cold areas of the plateau, mental disorders and psychological trauma exist more or less, light or severe in everyone's heart. Improving the psychological quality of soldiers, especially the officers and soldiers during live-fire shooting, is an important way to improve and



enhance the combat effectiveness of troops. We must increase the intensity of psychological education and apply healthy psychological knowledge to training. It is necessary to carry out targeted psychological tolerance training, especially to strengthen the psychological tolerance of officers and men in extreme environments.

The third is to strengthen the training of officers and men in fighting spirit. War is full of dangers and challenges. It is a test of blood and fire, life and death. The cruelty and complexity of the battlefield environment place high demands on the will quality and fighting spirit of soldiers. Modern soldiers must be able to endure physical exertion, disease attacks, accidental blows, and extreme fatigue; they must be able to maintain optimism and perseverance in order to stand the test of combat readiness and war. Therefore, in high-intensity training, it is necessary to further strengthen faith education, cultivate the soldiers' mental qualities of hard work, self-improvement, and continuous transcendence.

**Compliance with Ethical Standards** The study was approved by the Logistics Department for Civilian Ethics Committee of PLA Army Academy of Artillery and Air Defense Zhengzhou Campus.

All subjects who participated in the experiment were provided with and signed an informed consent form.

All relevant ethical safeguards have been met with regard to subject protection.

## References

1. China natural geography. People's Education Publishing House
2. Yu Y (2007) Demonstration of environmental adaptability of weapons and equipment. Ordnance Industry Press, Beijing
3. Li Z (2011) Military physical education. Military Science Press, Beijing
4. Xu X (2010) Impact of plateau environment on support equipment and its adaptability. *Environ Eng* 10(7-5):100-101
5. He D (2018) Research hotspots and development trends of plateau physical fitness training. *Stationery Technol* 2

# **Research on the Overall Performance of Man-Machine-Environment System**

# Study on the Organic Integration of High Intensity Interval Training Regime and Physical Fitness Training of Special Operation Forces



Chunlai Wang

**Abstract** Innovative training ideas become a consensus with the advance of military thoughts about the defense in the new era. Purpose of innovation in military training is to improve the overall efficiency and better match the military training practice. The paper is attempting to discuss the proper integration of the high intensity interval training regime for the army. Appropriate integration and flexible use of interval training with high intensity can effectively improve special operation forces physical fitness training efficiency. The conclusion after deep studying about the organic integration of high intensity interval training regime is below. First, high intensity interval training regime should better match military subjects. Thus, the exercising content of high intensity interval training regime must be arranged properly. Second, the recovery period should be arranged appropriately during the training process. And the third, the intensity should be optimized to avoid overtraining and injury.

**Keywords** High intensity interval training regime · Physical fitness training · Organic integration

## 1 Introduction

The basic physical fitness training of special operation soldiers must be closely related to the nature of special combat skills, meet the requirements of special operations, to improve the contribution rate of physical fitness training in the integration of special operations elements.

The basic physical fitness training of special operation soldiers should be carried out according to the requirements of professional post competency. The intensity, density and difficulty of training should more reflect the hardship, even cruelty of the occupational characteristics, which make physical and mental preparations for the subsequent military skill training.

---

C. Wang (✉)

Physical Education Department, Guangzhou University Sontan College, Guangzhou 511370, China

e-mail: [wwwcl\\_1@163.com](mailto:wwwcl_1@163.com)

© The Editor(s) (if applicable) and The Author(s), under exclusive license to Springer Nature Singapore Pte Ltd. 2021

S. Long and B. S. Dhillon (eds.), *Man-Machine-Environment System Engineering*, Lecture Notes in Electrical Engineering 645, [https://doi.org/10.1007/978-981-15-6978-4\\_98](https://doi.org/10.1007/978-981-15-6978-4_98)

857

Based on the foreign theoretical research and the practice of foreign military training, this paper attempts to research the organic integration of the high intensity interval training regime and the physical fitness training of special operations soldiers from the technical level. Creative use of interval training can achieve the existing military training objectives with high quality.

## **2 Definition and Function of the Interval Training with High Intensity**

### ***2.1 Basic Definition***

The interval training with high intensity originated from the interval training which is a training method with the maximum lactate steady-state load or the load intensity equal to or greater than the anaerobic threshold from several seconds to several minutes, and the incomplete recovery is arranged between every two exercises.

Now, the interval training with high intensity has gradually become an effective training method, which is used to produce a particular stimulation on the parts of body, only if those variables were manipulated appropriately.

### ***2.2 Physiological Function***

There is a common consensus among scientists around the world that HIIT regime can stimulate the aerobic and anaerobic energy supply system of the body at the same time, and the effect is better than the low intensity continuous training.

According to the research, high intensive interval training regime is determined to produce positive stimulation on the body in the following sports physiology aspects and meet the requirements of basic military physical fitness training.

#### **2.2.1 Aerobic Capacity**

HIIT regime, compared to interval training models with lower intensity or endurance training with high intensity, is considered to be a more feasible and more efficient training method that can produce the same effect. HIIT has been shown that the exercises are conducted three times in a week, and such body exercising lasted for no more than 10 min in less than 30 min each time, including warm-up, interval recovery and cooling, can improve aerobic ability [1].

Also HIIT regime can significantly improve the  $\text{VO}_2$  max of young men and women through interval training exercises with high intensity, and the better result ( $P < 0.05$ ) was correlated with baseline ( $P = 0.05$ )  $\text{VO}_2$  max [2].

Compared with those longer distance exercising with lactate threshold, the interval exercising with high intensity significantly increased  $\text{VO}_2$  max ( $P < 0.01$ ). In the aspect of improving  $\text{VO}_2$  max, the effect of interval training with high intensity is obviously better than those same works [3].

### 2.2.2 Cardiovascular Fitness

In 2015, an experimental analysis of some adults exercising with interval training found that interval training with high intensity can lead to significantly improved in cardiovascular fitness compared with those participants in traditional endurance training [4]. Another analysis also found that training programs with high intensity lasted for one month can also effectively improve the cardiovascular health status of those adolescents [5]. In addition, a separate systematic analysis of seven sessions of exercising with high intensity found that the approach (4-min rest, 85–95% maximum heart rate) was more effective in improving vascular function than those continuous training with medium intensity [6].

### 2.2.3 Metabolic Effects

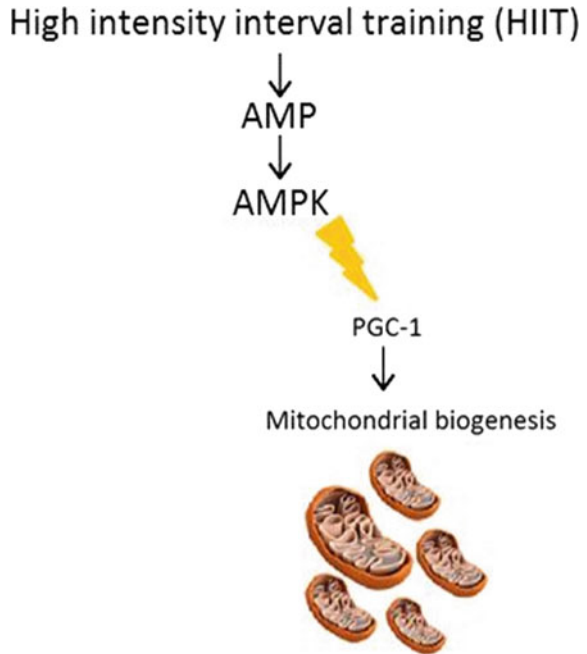
HIIT model, compared with continuous training, can significantly reduce insulin resistance of the body and resulted in a slight decrease in the level of weight loss while those who did not receive the intervention of physical activity remain unchanged [7]. Another data of the study showed that moderate intensity continuous training decreasing insulin levels about 9% was less effective than that of interval exercises with high intensity (about 31% decrease) [8].

### 2.2.4 Fat Oxidation

Some deepen study on skeletal muscle adaptation with HIIT model has found that during seven periods exercising of two weeks, HIIT way was proved that the ability of moderate active women to oxidize body fat and skeletal muscle fat was improved. A review on weight loss of HIIT approach summarizes the results of exercising with high intensity, which can moderately reduce subcutaneous fat in young and healthy people and reduce more for those overweight people [9].

Trapp found that a greater reduction in abdominal fat (>10 kg) was available in the team of young women trained with high intensity interval exercising at 15 weeks, while the body status in another young women group without any training maintains stable [8].

**Fig. 1** Mechanism of interval training with high intensity



### 3 Mechanism of the Interval Training with High Intensity

Usually, PGC-1 $\alpha$  is often regarded the vital regulator of mitochondrial biogenesis in the muscle of the body. And it can be activated after physical exercises with high intensity increased mitochondrial capacity. The manner PGC-1 $\alpha$  stimulated is that some changes in energy status in the body muscles are associated with a slight decrease in ATP concentration, leading to an increase in adenosine monophosphate (AMP), in which the AMP-activated protein kinase (AMPK) was activated. Those AMPKs stimulate the activation of PGC-1 $\alpha$ , which eventually leads to mitochondrial biogenesis and therefore increases an capacity to generate ATP aerobically (Fig. 1).

### 4 Models of the Interval Training with High Intensity

In all these famous models above, repeatedly exercising was controlled at an intensity within several minutes, rested from one to five minutes for different aims (Table 1).

**Table 1** Models of the interval training with high intensity

Model	Year	Object/Name	Approach	Intensity
Gösta Holmér	1937	Fartlek method	Run by alternating between fast runs and slow jogs	90% of VO <sub>2</sub> max
Peter Coe	1970s	Sebastian Coe	200 m run followed by 30 s recovery	90% of VO <sub>2</sub> max
Wingate test	1970s	Power bike	30 s followed by 30 s of rest repeated 4–6 times	90% of VO <sub>2</sub> max
Izumi Tabata	1996	Speed skaters	20 s exercise with 10 s recovery for 4 mins	170% of VO <sub>2</sub> max
Gibala	2010	Students	60 s exercise with 75 s recovery	95% of VO <sub>2</sub> max
Zuniga	2011	Students	30 s followed by 30 s of rest	90% of VO <sub>2</sub> max
Timmons	2012	Power bike	20 s full throttle with 1–5 min recovery	90% of VO <sub>2</sub> max
Gunnarsson and Bangsbo	2012	Copenhagen method	30 s low intensity running, 20 s moderate intensity, 10 s high intensity with 60 s recovery	90% of VO <sub>2</sub> max

## 5 Examples of Foreign Military Interval Training with High Intensity

### 5.1 British Army Physical Fitness Course with HIIT Regime

In Britain, physical fitness within the royal marines is considered the key foundations within Corps life. Candidates will be required to demonstrate a high standard of physical fitness, mental robustness and an understanding of basic military physical training techniques before attending commando training center royal marines. To that end, the army staffs have set out a four-week program. Thursday's workouts with HIIT of the program below are selected from week 1, week 3 and week 4, respectively (Table 2).

**Table 2** Programs of the British physical training course of Thursday (excerpt)

Thursday	40 Minute 'Fartlek' run	<ul style="list-style-type: none"> <li>• Run at a steady pace for 5 mins to warm up</li> <li>• Increase the pace to your best effort for 30 s</li> <li>• Slow back down to a steady pace to reduce your breathing and heart rate for 1 min</li> <li>• Repeat the process for a total of 20 times</li> <li>• On completion, run for a further 10 min at a steady pace to complete the session</li> </ul>
Thursday	'Tabata' circuit	<ul style="list-style-type: none"> <li>• Tabata press ups, 20 s conducting exercise 10 s rest for 4 min</li> <li>• 400 m sprint</li> <li>• Tabata sit ups, 20 s conducting exercise 10 s rest for 4 min</li> <li>• 400 m sprint</li> <li>• Tabata squats, 20 s conducting exercise 10 s rest for 4 min</li> <li>• 400 m sprint</li> <li>• Repeat Tabata and sprints to 3 mins and 2 min</li> </ul>
Thursday	Hill sprints/Leg circuit	<ul style="list-style-type: none"> <li>• Find a hill that takes approximately 1 min to Sprint up</li> <li>• Sprint up the hill followed by a steady jog back down</li> <li>• On each occasion at the bottom of the hill carry out 20 squats and 15 press ups</li> <li>• Rest for 30 s</li> <li>• Carry out for 10× reps</li> </ul>

Source <https://www.royalnavy.mod.uk/careers/royal-marines/get-fit-to-join/my-fitness-plan>

### ***5.2 Program of Military College in Canada with HIIT Regime***

The College of Royal Military in Canada highly emphasizes the physical and mental development of soldiers. Each member of the Canadian Armed Forces (CAF) is required to complete the physical fitness test successfully through the program of high intensity interval training arrangement. Parts of that program with HIIT regime are seen below (Table 3).

### ***5.3 US Marine Corps Physical Fitness Program with HIIT Regime***

The main purpose of the physical fitness program of US Marine Corps is to improve the operational adaptability level of the active and reserve Marine Corps and optimize the operational readiness and recovery capability. This comprehensive strength and condition training program takes into account the physical requirements of combat-related activities to optimize the physical performance during combat (Table 4).



**Table 3** Physical fitness program of Canada military college (excerpt)

Day	Monday Tempo run	Tuesday Circuit	Wednesday Speed	Thursday Circuit	Friday LSD
1	5 min Jog 2.4 km run @ RPE10 Then 1 × max push ups	5 min jog 20 min AMRAP 1–2 pull ups, 3–5 push ups 10 air squats, 10 sit ups 15 glute bridge, 15 jumping jacks	5 min Jog 10 × 1 min sprint @ RPE9 Walk 3 min between sets 5 min cool down jog	5 Rounds 1 Lap around sports field (200 m) 5–10 push ups, 30 s plank 15–20 sit ups, 30 s side Plank/Side	5 min warm up walk Run 3 km @ RPE3 Then 3 × 50% of push ups from Monday, rest 90 s
2	5 min jog 3 × 10 min run @ RPE8 Walk 2 min between sets Then 5 min max push ups	5 min jog 25 min AMRAP 1–2 pull ups, 3–5 push ups 10 air squats, 10 sit ups 15 glute bridge, 15 jumping jacks	5 min jog 15 × 45 s sprint @ RPE9 Walk 2 min between sets 5 min cool down jog	6 Rounds 1 Lap around sports field (200 m) 5–10 push ups, 30 s plank 15–20 sit ups, 30 s side Plank/Side	5 min warm up walk Run 4 km @ RPE3 Then 3 × 50% of push ups from Monday wk 1, rest 60 s
3	5 min jog 6 × 5 min run @ RPE8 Walk 2 min between sets Then 5 min max push ups	5 min jog 30 min AMRAP 1–2 pull ups, 3–5 push ups 10 air squats, 10 sit ups 15 glute bridge, 15 jumping jacks	5 min jog 15 × 30 s sprint @ RPE9 Walk 90 s between sets 5 min cool down jog	7 Rounds 1 Lap around sports field (200 m) 5–10 push ups, 30 s plank 15–20 sit ups, 30 s side Plank/Side	5 min warm up walk Run 5 km @ RPE3 Then 3 × 60% of push ups from Monday wk 1, rest 90 s

Source <https://www.rmc-cmr.ca/en/athletic-department/physical-fitness-guide>

## 6 Results and Conclusions

### 6.1 HIIT Regime Should Better Match Military Subjects

HIIT regime should better match military subjects, which means that the high intensity interval training could be adopted only when it is closely related to military training subjects. In order to improve the training results and meet the needs of physical fitness test, the exercising content of HIIT regime should be arranged properly.

In practice, it is hard to find the optimal polarized training mode. Then the interval training with high intensity can be founded by the control of the variables of intensity, duration and rest mode to meet combat needs of military physical fitness training subjects and to create suitable training adaptations.

**Table 4** US marine Corps physical fitness program with HIIT regime (excerpt)

Agility				
Exercises	Sets	Rest (s)		
Cone zig zag drill	2	60		
Cone attack and retreat	2	60		
Prone 3 cone drill	2	60		
Cone J-hook reverse sprint	2	60		
Strength and power				
Exercises	Sets	Reps	Time	Rest (s)
Deadlift	4	6	None	90
Barbell front squat	4	6	None	90
Barbell military press	3	8	None	60
Ammo can lateral lunge	3	None	30 s	15
Sandbag bent over row	3	None	30 s	15
Med Ball oblique toss	3	None	30 s	15
Rope alternating waves	3	None	30 s	15

*Notes* Can be performed as a circuit or stand-alone exercises. Perform each cone movement 2 times in each direction

*Notes* Complete all sets of the first 3 exercises to moving on to the shaded exercises. The non-shaded exercises should be performed as primary exercises focusing on strength and power development. The shaded exercises are to be conducted as a circuit and performed after completion of all sets of the primary exercises

*Source* <https://www.fitness.marines.mil/Warrior/>

## 6.2 Best Arrangement of the Recovery Period

The arrangement of the recovery period means the choice of the best work-to-rest (WR) ratio. For example, WR ratio of 1:2 means that if a person who exercised 20 s with HIIT regime, the recovery interval equals 10 s. Truth is that different WR ratio will produce different training effects. Therefore, the appropriate WR ratio should be selected according to the actual physical fitness training situation and different training objectives.

Generally, the fast energy system was benefited from a 1 versus 3 work-to-rest ratio; if the short time glycolysis energy supply system was considered to increase moderately, the WR ratio of 1/2 may be correct; while the longtime aerobic energy system was thought to be changed, the 1/1 WR ratio or 1/1.5 WR ratio sounds good.

### **6.3 Optimization of Intensity to Avoid Overtraining and Injury**

Different HIIT models have different properties, and overtraining eventually leads to injury because of breaking the character of the high intensity interval exercising regime. When engaging in high intensity interval training activities, the variable intensity should be advanced step by step and completed according to our ability to avoid overtraining and injury.

For achieving varying health outcome without any injury, the better intensity exercising mode more suitable to subjects through the way of  $VO_2$  max should be done correctly.

### **References**

1. Gillen JB, Gibala MJ (2014) Is high-intensity interval training a time-efficient exercise strategy to improve health and fitness? *Appl Physiol Nutr Metab* 39(3):409–412
2. Astorino TA, Allen RP, Roberson DW, Jurancich M, Effect of high-intensity interval training on cardiovascular function,  $VO_2$  max, and muscular force. *J Strength Conditioning Res* 26(1):138–145
3. Helgerud J (2007) Aerobic high-intensity intervals improve  $VO_2$  max more than moderate training. *Med Sci Sports Exerc* 39(4):665–671
4. Milanović Z, Sporiš G, Weston M (2015) Effectiveness of high-intensity interval training (HIT) and continuous endurance training for  $VO_2$  max improvements: a systematic review and meta-analysis of controlled trials. *Sports Med (Syst Rev Meta-Anal)* 45(10):1469–1481
5. Costigan SA, Eather N, Plotnikoff RC, Taaffe DR, Lubans DR (2015) High-intensity interval training for improving health-related fitness in adolescents: a systematic review and meta-analysis. *Br J Sports Med (Syst Rev Meta-Anal)* 49(19):1253–1261
6. Ramos JS, Dalleck LC, Tjonna AE, Beetham KS, Coombes JS (2015) The impact of high-intensity interval training versus moderate-intensity continuous training on vascular function: a systematic review and meta-analysis. *Sports Med (Syst Rev Meta-Anal)* 45(5):679–692
7. Jolleyman C, Yates T, O'Donovan G, Gray LJ, King JA, Khunti K, Davies MJ (2015) The effects of high-intensity interval training on glucose regulation and insulin resistance: a meta-analysis. *Obes Rev (Meta-Anal)* 16(11):942–961
8. Trapp EG, Chisholm DJ, Freund J, Boutcher SH (2008) The effects of high-intensity intermittent exercise training on fat loss and fasting insulin levels of young women. *Int J Obes* 32(4):684–691
9. Boutcher SH (2011) High-intensity intermittent exercise and fat loss. *J Obes* 2011:868305

# Study on Training of 400-m Armed Island-Landing Obstacles



Min Chen, Huifang Wang, Zhengbu Liu, Xiang Gao, Xin Wang,  
and Ming Kong

**Abstract** The aim of study on training of 400-meter (400 m) armed island-landing obstacles is to improve the training effect. The obstacle course is set specially for the training. Each obstacle has its own unique purpose and function. In order to achieve good effects, the trainees will first get themselves familiar with each obstacle one by one, and then after the trainees have command the skills to pass each obstacle, they will pass several obstacle at one time. At last, the whole-process training will be conducted. In order to test the training result, experiments are carried out, through which one systematic training method is obtained and examined. Based on the daily training and experiments, gradual principle and step method are proved efficient, and basic qualities are also found important to the training result.

**Keywords** 400 m armed island-landing obstacles · Training method · Gradual training · Step-by-step method

## 1 Introduction

The training of 400 m armed island-landing obstacles focuses on the needs of landing operations, with adaptive training as the key point. It simulates obstacles that may be encountered in landing. With mechanical principles, it integrates the stages such as loading, sailing, transfer, beach landing, and so on. It is highly targeted and difficult to train. Through simulation training on land, trainees can strengthen their balance, strength, flexibility, anti-vertigo, and psychological qualities under unstable conditions [1].

---

M. Chen · H. Wang (✉) · Z. Liu · X. Gao · X. Wang · M. Kong  
Common Training Section of Army Academy of Artillery and Air Defense Zhengzhou, 450052  
Zhengzhou, China  
e-mail: [780239720@qq.com](mailto:780239720@qq.com)

H. Wang  
Interpretation and Translation Section of Army Academy of Artillery and Air Defense  
Zhengzhou, 450052 Zhengzhou, China

## 2 Site Setting

The 400 m armed island-landing obstacle course is generally set in a polyline shape and can also be designed in a ring shape according to the actual situation. The whole course is 400 m, and the runway is 4.5 m wide. It consists of 10 obstacles. The order of passing is as follows, soft bridge → spiral ladder → high and low crossbars → rope net → tire climbing platform → swing platform → swaying ladder → crossnet → blocking wall → simulated beach.

## 3 Harness and Wearing Method

### 3.1 List of Harness

The harness that will be used are as follows, camouflage shoes, camouflage clothes, camouflage caps, braided outer belts, water bottles (filled with water), gas masks, satchels (with raincoats and toiletries inside), bullet bags (including four empty magazines, four grenades), 95-type automatic rifle, a total weight of about 13 kg. About position and sequence of harness wearing, the straps of water bottle and satchels cross right shoulder, and the strap of gas mask crosses left shoulder. Braided outer belt is put on the straps of water bottle, satchels, and gas mask. Bullet bag should be put on the outermost layer. 95-type automatic rifle should be held on the back. Satchels → water bottle → gas mask → braided outer belt → bullet belt → 95-type automatic rifle. According to personal habits, the elasticity should be appropriate to facilitate the passing of obstacles.

## 4 Training Method and Steps of the 400 m Armed Island-Landing Obstacles

During the obstacle training, the sequence should be as follows, firstly, with bare hands, then holding the gun, and lastly with all the harness needed; at the same time, to be trained to pass single obstacle, then some obstacles as a segment, and lastly all the obstacles. The training should be conducted firstly in the obstacle course, and then in the field with natural obstacles.

### 4.1 Passing Single Obstacles

The easy-to-difficult training step refers to that the training steps be arranged in the order from easy to difficult according to adaptability of island landing. When it is

single-obstacle training, the sequence can be as follows, simulated beach → high and low crossbars → blocking wall → rope net → swing platform → soft bridge → spiral ladder → swaying ladder → net wall → tire climbing platform. The training steps can be arranged as per the physical quality of the trainee.

The classified training steps refer to putting the obstacles which require similar movements into one group. The training can be conducted as follows:

- ① Running and striding: soft bridge and crossnet;
- ② Swaying and shaking: swing platform, swaying ladder, spiral ladder;
- ③ Climbing: rope net, tire climbing platform, blocking wall.

## ***4.2 Pass the Obstacles in Segmentation***

Passing the obstacles in segmentation refers to passing the obstacles within certain distance at one time so as to improve the capability of passing single obstacle. The training can also simulate the operation process with clear target and real awareness.

### **4.2.1 Sailing Stage**

The first 100 m distance consists of a soft bridge, a spiral ladder, high and low crossbars, and the three sets of obstacles. It mainly simulates the boarding and navigation environment so as to improve the capability to move quickly without vertigo in unstable conditions.

### **4.2.2 Transferring Stage**

The second 100 m distance consists of a rope net, a tire climbing platform and a swing platform, these three sets of obstacles. It mainly simulates the transfer environment so as to improve the balance and psychological quality in an unstable state.

### **4.2.3 Beach Landing Stage**

The third 100 m distance consists of swaying ladder, crossnet, and blocking wall. This part mainly simulates the beach landing environment in order to improve the specific strength of upper and lower limbs and the ability to overcome obstacles.

#### **4.2.4 Seizing the Beachhead Position Stage**

The fourth 100 m distance, the 100 m simulated beach, mainly simulates the beach environment, which is used to improve leg strength and ability of the trainee to quickly pass the beach.

### **4.3 Whole-Process Training**

The whole-process training should be based on the mastery of action essentials for passing single obstacles and the obstacle groups. The training should be organized according to single trainee's ability. It can be carried out in the forms of timing running, quiz running, competition running, and so on. During the whole-process training, the running speed of each distance should be controlled, and time should be allocated according to the difficulty of obstacles. Generally, the first and fourth stages should consume less time, while the second and third stages consume more time. During the running, it is required to coordinate movements and master the rhythm of passing obstacles.

### **4.4 Special-Item Training**

Each time of training should combine both the physical quality and passing techniques. In order to simulate physical strength allocation in the whole process, the 100 m running with changing speed can be arranged. Special-item training is mainly adopted with the purpose of strengthening actions and techniques by adding difficulties and intensity to improve physical fitness [2].

There are altogether four kinds of special-item training, spiral ladder, tire climbing platform, swing platform, and swaying ladder. The special-item training is usually put after the whole-process training or before the whole-process training with full harness.

## **5 Effects of Such Training Method**

In order to illustrate the training, we organized trainees to conduct a large number of experiments and collected some valid data for verification. 64 senior cadets in good health from a military university, aged 21–24 years, average 22.56 years, height 170–184 cm, average 175.69 cm, weight 63–87 kg, average 67.66 kg. The experimental instruments include one 400 m island-landing obstacle training course, one set of training instruments, a signal flag, and several stopwatches.

### **5.1 Experiment Process**

Trainees start training with single equipment then conduct segmented training, and finally the whole-process training. Training time is from 17:00–18:30 on every Monday to Thursday. There are altogether 22 times of training from single-obstacle training to whole-process training. The time consumed by each person should be recorded during the continuous whole-process training. The first time of test should be one of the several times of whole-process training at the beginning. Then after around 60 days of training, the second test should be carried out. There should be 8 times of systematic whole-process training, and no requirements for free training.

### **5.2 Experiment Data**

For the experiment, 8 tests are performed. Time-consuming, heart rate, blood pressure, temperature, and humidity of the training environment are all recorded, which are 2000 groups of data. The data that is selected here is the data ( $v_1$ ,  $v_2$ ) of the first and the last whole-process tests (Table 1).

### **5.3 Data Analysis and Conclusion**

Based on data statistics, the data is analyzed with data statistics software SPSS11.5. Firstly, it is the significance analysis of  $v_1$  and  $v_2$  (Table 2).

The results show that there is significant correlation ( $p < 0.01$ ) between the results of two tests, which indicates that the results of  $v_1$  and  $v_2$  are significantly different, and there are big changes in the results. Then, compare  $v_1$  and  $v_2$ , and the average value of 60 people, as shown in Table 3.

The results show that the average performance of  $v_2$  is 17.104% higher than that of  $v_1$ , and the performance is significantly improved. The results also show that the results of the two tests are significantly different, and after a period of training, the capability of the trainees in overcoming the “obstacles” has been greatly improved. This method is of positive significance for improving the performance of overcoming “obstacles.”

## **6 Features of Such Training Method**

Practice shows that the training effect is significant with this method, and the features are as follows:



**Table 1** Test results of the first and the last whole-process tests (second)

No.	v1	v2	序号 No.	v1	v2	序号 No.	v1	v2
1	277.06	224.64	21	296.17	249.92	41	296.17	249.92
2	263.48	223.98	22	289.86	240.74	42	299.86	240.74
3	275.52	226.98	23	325.46	298.87	43	365.46	298.87
4	288.44	250.24	24	342.82	326.62	44	342.82	326.62
5	296.56	224.06	25	312.56	234.83	45	292.56	234.83
6	283.14	234.7	26	294.29	232.39	46	294.29	232.39
7	368.17	317.66	27	287.88	220.69	47	277.88	220.69
8	283.01	219.09	28	293.88	203.59	48	293.88	203.59
9	281.81	218.73	29	299.45	216.77	49	279.45	216.77
10	285.66	219.92	30	281.18	261.92	50	291.18	261.92
11	290.73	225.43	31	298.72	260.66	51	288.72	260.66
12	290.15	244.36	32	290.24	213.24	52	269.24	213.24
13	286.84	239.43	33	294.74	249.86	53	277.74	249.86
14	283.85	238.99	34	293.27	241.91	54	293.27	241.91
15	297.52	250.73	35	281.37	206.62	55	281.37	206.62
16	293.68	209.14	36	287.84	232.68	56	267.84	232.68
17	294.51	225.59	37	288.16	209.72	57	268.16	209.72
18	330.64	267.06	38	283.46	217.12	58	293.46	217.12
19	332.24	296.26	39	267.25	203.24	59	283.42	222.34
20	296.54	265.45	40	264.35	226.38	60	266.31	204.68

**Table 2** Results of bivariate correlation analysis of the two groups of data

Group	Analysis item	v1	v2
v1	R	1	0.808(**)
	p		0.000
v2	R	0.808(**)	1
	p	0.000	

\*\*There is significant correlation between them

**Table 3** Changes in the performance of trainees after training

	v1	v2	Increase (difference/result of first test)
Average value of 60 people	294.7316	244.3234	17.104%

### ***6.1 Emphasize Importance of Basic Qualities***

Physical quality is fundamental in the military sports training. Without good physical quality, intelligence, and techniques will be lost of basic support. In this method, physical fitness training is always conducted, which shows that this method attaches great importance to the cultivation of basic qualities, the basis for quickly improving performance.

### ***6.2 Follow the Principle of Gradual Military Training***

The principle of gradualness refers to that according to the law of gradually increasing physical fitness, and the training method should also be continuously changed to meet the requirements of training [3]. This method obviously conforms to the principle of gradualness. From the initial single-obstacle training to the combined training to the final continuous whole-process training, from barehanded to gun-holding to arms bearing, with classified training and special-item training added, the requirements to the trainees are also increasing.

### ***6.3 Focus on the Single Principle of Scientific Training***

The single principle means that in the process of training, each trainee chooses appropriate training methods according to their own physical quality and characteristics in order to improve performance [4]. This method requires the trainees to think about the allocation of physical strength at the beginning of training, and guides the trainees to find a physical allocation plan suitable to themselves in each stage.

## **7 Suggestions**

It is recommended that the training unit closely follow the requirements of combat, and carry out 400 m armed obstacle training rigorously. Problems should be found during the training so as to modify the training method timely. Methods should be modified according to specific conditions and individual characteristics of trainee in order to achieve better training effects.

**Compliance with Ethical Standards** The study was approved by the Logistics Department for Civilian Ethics Committee of Army Academy of Artillery and Air Defense. All subjects who participated in the experiment were provided with and signed an informed consent form. All relevant ethical safeguards have been met with regard to subject protection.

## References

1. Zhimin H, Zhengqing Y (2006) Teaching material about the physical training and health of the academician in the military academy. Jilin university Press, pp 87–95
2. Zhibing P (1999) Air defense forces man-machine-environment system engineering. Air Defense College, Zhengzhou, pp 154–212
3. Junwei D, Wei C, Keming L (2002) The physical education and health of the academician. Henan University Press. 8:65–71
4. Zhimin H (2003) Research on relations of man-machine-environment for 400 m obstacle training of crossing and landing. J Wuhan Inst Phys Educ 37(2):237–238 (Ch)

# Application of Virtual Reality Technology in Man–Machine Interactive Equipment Virtual Maintenance System



Mingjie Wan, Xiaolong Chang, Yuhui Li, Zaochen Liu, and Shiyou Ma

**Abstract** *Purpose*—the purpose of the study is to enhance fidelity and immersion of man–machine interaction in equipment virtual maintenance system and further improve the training effect and efficiency. *Method*—some virtual reality technologies such as the 3D modeling and scene simulating are adopted to conduct modeling and simulating toward the equipment compositions, structure, principles and maintenance process. *Result*—the constructed virtual maintenance system of a certain type of equipment is characteristic of higher fidelity of man–machine interface, better man–machine interaction and stronger immersion of operators. *Conclusion*—the system enriches and perfects the training methods and means of the complex equipment maintenance in grassroots level, and accumulates experience for the construction of equipment support resources, effectively promotes the rapid generation of maintenance support capability in grassroots units.

**Keywords** Virtual reality · Man–machine interaction · Man–machine interface · Virtual maintenance

## 1 Introduction

How to generate combat capability quickly is the primary question faced by the troops after the equipment enters service, however, the maintenance and support capability of the equipment is an important part of combat capability. After the equipment enters service, the generation of their maintenance and support capabilities is often faced with the following problems:

---

M. Wan · X. Chang (✉) · Y. Li · Z. Liu · S. Ma  
PLA Army Academy of Artillery and Air Defense, Zhengzhou Campus, Zhengzhou 450052, China  
e-mail: [changxiaolon@163.com](mailto:changxiaolon@163.com)

Firstly, there are relatively fewer maintenance training means and the matching maintenance training equipment is scarce; secondly, general malfunction rate of the new equipment is relatively lower and there are fewer opportunities for equipment maintenance practice; thirdly, because the structure and working mechanism of the new equipment has not been fully understood and there is no way to conduct the related maintenance training courses such as equipment parts disassembling and assembling.

Virtual maintenance technology is an important method to solve the above-mentioned problems [1]. By making use of the virtual maintenance system, the operators can quickly learn the equipment structure, working mechanism, malfunction maintenance method and the operation flow; furthermore, it has been proved that the virtual maintenance system can greatly improve the training benefit [2, 3]. Therefore, virtual maintenance system has been widely applied in equipment maintenance training [4, 5]. Virtual reality is a kind of multi-media technology developed quickly in recent years. Virtual reality with stronger interaction and sense of immersion can be more realistic simulation of the real scene, so it has played an important role in medicine, education and military fields [6, 7]. With the help of virtual reality technology, this essay constructs the virtual 3D model of equipment and develops the equipment virtual maintenance system, which can better meet the needs of maintenance training in grassroots level.

## 2 System Design

Virtual maintenance system of the man-machine interactive equipment mainly includes four subsystems; they are overview, operation training simulation, maintenance simulation and management, which are shown in Fig. 1.

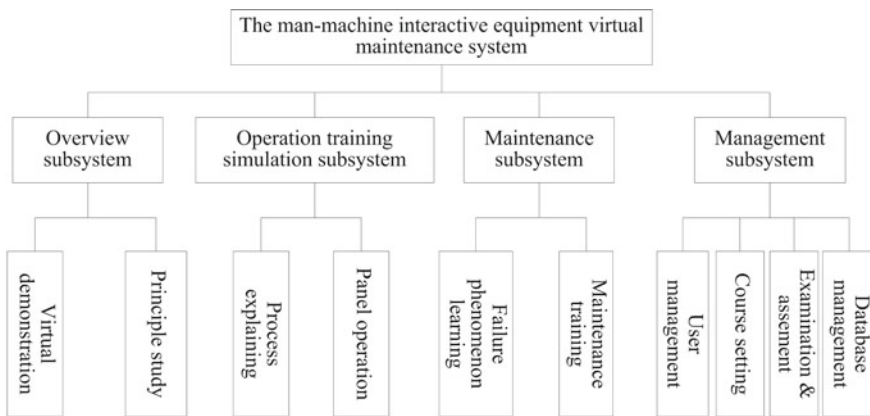


Fig. 1 Equipment virtual maintenance system composition

The overview subsystem is applied to learn equipment composition, structure, principles, other theoretical knowledge and the maintenance knowledge in grass-roots level by providing video, text, pictures, multi-media courseware and other resources. The operation training simulation subsystem is applied to conduct the basic contents training of equipment deployment, self-inspection, function inspection and equipment withdrawal. The maintenance simulation subsystem is applied to conduct equipment malfunction phenomenon learning and maintenance training. The management subsystem is applied to realize the user management in different levels, setting training courses, assessing training effect and managing various databases. The management subsystem has a smooth man–machine interactive interface to make operators operate the virtual maintenance system conveniently.

### 3 System 3D Modeling

According to the structured data, the training contents and their requirements the 3D modeling of the equipment is constructed, and finally the virtual maintenance prototype whose shape and function are basically consistent with the actual equipment are generated and these prototypes support various virtual maintenance operations and training.

In the stage of virtual prototype modeling, the primary work is to collect the original information of the equipment by the actual equipment measuring, picture taking and video recording, and to construct the 3D modeling for every part.

This system has constructed a total of 6756 3D models for 16 branch systems and their 89 subsystems, and the equipment 3D modeling is shown in Fig. 2. The virtual prototype model of the system is composed of 16 branch systems including chassis, square cabins, diesel power station, dedicated power supply, communication equipment, location and orientation navigation system, front-end device, signal processor, terminal display and control system, power distribution box, DC power supply, interrogator, antenna pedestal, hydraulic lift, leveling device, leveling lifting drive control.

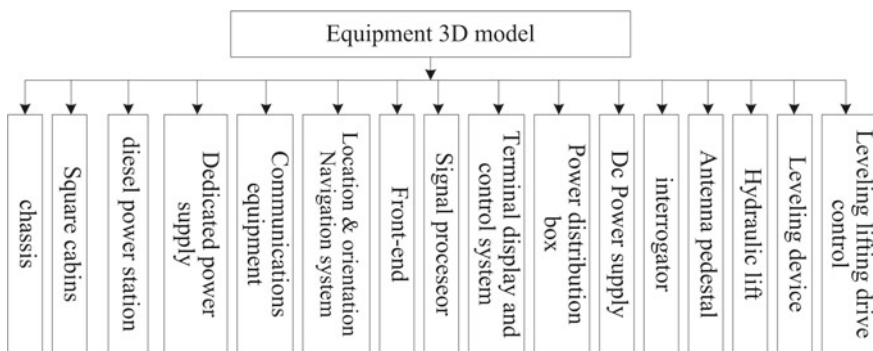


Fig. 2 Block diagram of equipment three-dimensional modeling

supply, interrogator, antenna pedestal, hydraulic lift, leveling device and leveling lifting drive control. These models cover all equipment and parts which are related with equipment maintenance in grassroots level.

By making use of these models, the virtual maintenance system can simulate the structure and operation of the actual equipment in a realistic way. And these models further increase the fidelity of the system and the immersion of the operators.

### 4 System Implementation

According to design need, the system implementation plan is divided into three stages including system resource preparation, training data preparation and integration. The work in every stage and the relationships between them are shown in Fig. 3.

In system resources preparation stage, the man-machine interactive 3D models of the equipment are completed with the help of modeling software such as 3D max; this stage is the basic one for completing the equipment virtual maintenance system. In training data preparation stage collection, classification and organization of all these data including virtual prototype data, equipment malfunction model and maintenance process description data are completed. In integration stage, the exploration of virtual training software is completed mainly through 3D development platforms like Unity; 3D simulating is conducted toward equipment structure learning, malfunction repairing and operation training. In addition, in integration stage, some functions such as scene setting, courses initializing, logic controlling, interface displaying and man-machine interaction need to be completed. Man-machine interface of the equipment virtual maintenance system is shown in Fig. 4.

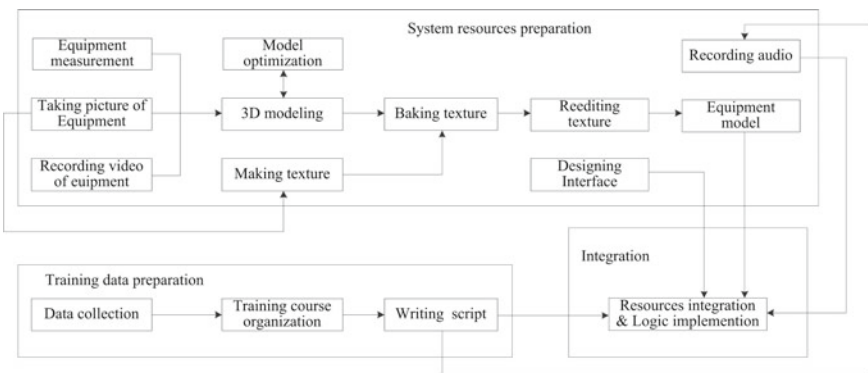
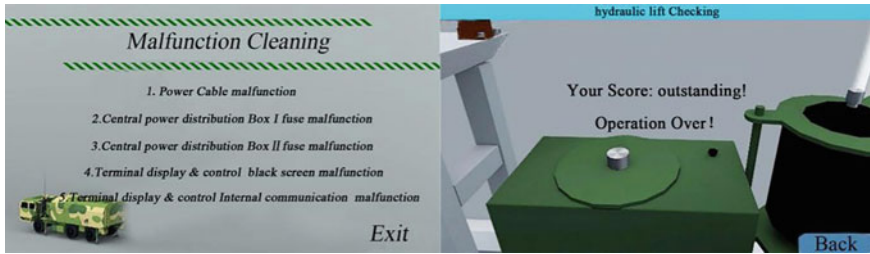


Fig. 3 System implementation flow



**Fig. 4** Part of man–machine interface of the equipment virtual maintenance system

## 5 Conclusion

Based on virtual reality technology, the equipment virtual maintenance system is developed to meet the needs of equipment structure learning and maintenance training. The virtual reality technology is applied to construct the equipment 3D model with higher fidelity which can help the trainees grasp the equipment structure principle and equipment maintenance knowledge quickly. With the help of virtual reality technology, virtual simulation is conducted toward equipment malfunction and maintenance operation process; the immersion and interaction of virtual maintenance systems are enhanced and the training level of the trainees is also improved.

## References

1. Rao Y, Xu B, Jing T (2017) The current status and future perspectives of virtual maintenance. *Procedia Comput Sci* 107(C):58–63
2. Tian FJ, Zhang HQ, Chen DJ, Zhang XX (2013) Research on radar structure virtual maintenance system. *Mach Electron* 7:12–14
3. Zhao SP, Zhang Y, Ye QL, Zhong HP (2013) Study on the design method of radar virtual maintenance model
4. Zhao X, Hu W, Li M, Fu Q (2019) Design and implementation of virtual maintenance training system for certain radar. *Comput Meas Control* 27(2):221–224
5. Li CC, Ling F (2015) Application of virtual simulation technology in engineering training. *Lab Sci* 18(2):128–131
6. Kavanagh S, Luxtonreilly A, Wuensche B, Plimmer B (2017) A systematic review of virtual reality in education. *Themes Sci Technol Educ* 10(2):85–119
7. Xiao Z, He SJ, Zhi JY, Wang C (2019) Research progress and prospect of virtual maintenance technology for major technical equipment. *Packag Eng* 40(18):12–17



# Research on Technical Method of Cognitive Behavior Training During the Maritime Flight and Its Effect Evaluation



Yan Zhang, Yishuang Zhang, Yang Liao, Fei Peng, and Liu Yang

**Abstract** *Objective:* To construct a technical method of cognitive behavior training for the maritime flight, verified the application effect. *Methods:* (1): The present study investigated the psychological problems and demands of logistics support of the pilots in maritime flight training. (2) The multimedia technology was adopted to complete the maritime flight cognitive behavior training technology. (3) The maritime flight cognitive behavior effect questionnaire was adopted to conduct an effect analysis. *Results:* (1) The common psychological problems, psychological stress sources, and psychological safeguard demands of maritime flight were analyzed. (2) The filmed teaching film had a total of 10 episodes, which systematically illustrated the physiological and psychological influence, illusion prevention, nutrition guarantee, sleep management, and other knowledge of maritime flight. (3) The effect evaluation questionnaire showed that pilots were able to quickly understand and comprehend the knowledge points of the maritime flight. *Conclusion:* Maritime flight cognitive training can enable pilots to understand and evaluate maritime flight tasks accurately.

**Keywords** Maritime light · Cognitive behavior · Psychological training · ABC theory

## 1 Introduction

In recent years, with the increase of the high sea maritime military activities of our navy, maritime flight training has become a key training target for airforce pilots under new circumstances and new missions. Due to the great differences between the maritime natural conditions and onshore conditions, pilots performing maritime flight combat training tasks will face difficulties such as complex conditions, laborious maneuvering, long sailing time, mental stress, flight illusion, delayed rescue, and so

---

Y. Zhang · Y. Zhang · Y. Liao · F. Peng · L. Yang (✉)  
Air Force Medical Center, Fourth Military Medical University, Beijing 100142, China  
e-mail: [yangliuhenry@aliyun.com](mailto:yangliuhenry@aliyun.com)

on [1, 2]. If they fail to respond effectively, it will probably lead to the decline of their cognitive function, affect their operation ability, and seriously threaten flight safety and mental health [3, 4].

According to the American psychologist Ellis's ABC theory, activating event (A) is only the indirect reason of triggering the emotion and behavior consequence (C). However, the direct reason of triggering C is exactly the belief (B) generated by the individual's cognition and evaluation of the activating event A, namely the negative emotion and behavior barrier consequence of the people (C), which is not directly triggered by one activating event (A); instead, it is directly caused by the wrong belief (B) because of the incorrect cognition and evaluation of the individual suffering the event [5].

Therefore, based on the ABC theory, the present study established the cognitive behavior training, so as to help pilots reduce unreasonable cognition, establish reasonable cognition, and improve the positiveness and safety of the pilots in maritime flight combat training.

## 2 Object and Method

### 2.1 Object

1. There are 167 air force pilots and 35 maritime pilots. The pilots have an average flight time of  $(1423.6 \pm 644.45)$  h.
2. There are 52 pilots who attend the maritime flight for the first time or have never attended the maritime flight with a flight time of 40–2500 h. Only 4 pilots have flight experience, and their maritime flight time is 70–300 h.

### 2.2 Method

#### 2.2.1 Investigation on the Psychological Status and Psychological Safeguard Condition of Maritime Flight Combat Training

The present study adopted the questionnaire method to investigate 167 airforce pilots and 35 navy pilots in maritime flight units, flight training bases, and various aviation medical training centers.

1. Organization and implementation: The questionnaires were filled collectively in the form of a conference. Before filling the table, the purpose and significance of the questionnaire, as well as the filling precautions, were explained. After filling, the questionnaires were taken back.

2. Investigation tool: The self-compiled maritime flight medical service guarantee investigation and maritime flight psychological guarantee investigation questionnaires were adopted.

### **2.2.2 Establishment of Maritime Flight Cognitive Behavior Training Method**

The present study adopted the multimedia technology to establish the “multimedia teaching video of maritime flight cognitive behavior training.” The main establishment methods are as follows:

#### **1. Manuscript**

The special environment characteristics, physiological and psychological stress source and main problems affecting flight performance safety and mental health were analyzed through literature review and results of investigation, and the initial draft of the multimedia teaching video text was compiled and completed combined with the existing safeguard measures and experiences.

Six maritime flight experts including the brigade commander, deputy brigade commander, gold helmet, command pilot of airman troop assuming the maritime flight task were invited to discuss and deliberate the initial draft of the text and then finally determine the manuscript of the teaching video.

#### **2. Film preparation**

According to the manuscript of the teaching film, the whole film was divided into ten episodes, with each episode lasting for about ten minutes. The storyboard manuscript of each episode was compiled, which mainly includes the time, film scene, camera stand, image, dub, expression format, and so on. In order to guarantee the film effect, one live-action studio themed by maritime flight was established.

#### **3. Film**

The film was completed according to the manuscript. The film of the main contents was completed in the studio. Some contents involve equipment operation and practical performance, such as the neck and waist muscle exercise, psychological training skills were actually arranged in our unit. Three camera stands were set for the film: The main camera mainly filmed the close-up view of the lecturer, the auxiliary camera mainly filmed the full view and medium shot scenes, and the left auxiliary camera adopted the rocker arm to display the entire lecturing scene. The three cameras collaborated with each other in working to record the entire lecturing process.

#### **4. Sample preparation**

After filming all contents, the film elements were collected and screened for editing and summary. The filmed elements were transferred into the time track. According to the shot script, the scene screening was conducted to complete rough editing. Except

for the filmed contents, some scenes in the manuscript cannot be filmed. According to the design of the manuscript, some elements of maritime flight were collected. The contents hard to be expressed had animation design to visualize and concrete them. The appropriate background music was arranged as the demand before completing refined editing and forming the finished sample.

#### 5. Finished sample improvement

The formed samples were checked and confirmed by the lecturing experts and members of the research team, and relevant experts and army pilots were invited to watch and put forward improvement suggestions. After integrating all the feedback, the film was completed after modification and improvement.

### 2.2.3 Verify the Effect of Maritime Flight Cognitive Training Method

The multimedia lecturing video was placed on the front line of the army for on-site support applications and played before pilots performing maritime tasks. After playing the video, the pilot completed a questionnaire on the effectiveness of maritime flight cognitive behavior training.

1. Experiment object: 52 pilots who attend the maritime flight for the first time or who have never attended the maritime flight.
2. Experiment tools: The training was carried out by using the “multimedia teaching program of maritime flight cognitive behavior training” developed and designed in this paper; the effect was evaluated by using the maritime flight cognitive behavior training effect questionnaire.

### 2.2.4 Statics Analysis

The results of each questionnaire were analyzed using descriptive statistics.

## 3 Result

### 3.1 *Survey Results of Psychological Status and Psychological Support of Maritime Flight Combat Training*

#### 3.1.1 Common Psychological Problems of Maritime Flight

1. Emotional problem: 43.3% of the surveyed pilots often feel lonely, and 20% of the pilots often have anxiety and tension, of which fighter pilots are more obvious.

2. Behavioral problem: 62.76% of the surveyed pilots experience memory loss, 41.38% experience reduced work efficiency, 37.93% experience inattention, and 31.03% experience social withdrawal.
3. Illusion problem: when flying at sea, different courses have different illusions of flight. When flying in the complicated weather condition at day and night, or flying in formation, the pilots will mainly have the tilt and pitch illusion. When flying at low altitude or ultra-low altitude, the illusion of the bottom of the pot mainly occurs. When flying over the sea, the illusion of speed and distance is more prominent.

### **3.1.2 Common Psychological Stressors of Maritime Flight**

The psychological stressors of maritime flight are 72.8% of “distress and rescue,” 54.0% of mechanical failure, 53.0% of the marine environment, and 37.6% of illusions hard to be corrected. The specific flight courses will also bring greater psychological pressures. For instance, ultra-low altitude flight at sea occupies 81.2%, complex meteorological flight accounts for 57.9%, extended sea flight occupies 46.0%, long-endurance flight accounts for 30.6%, and combat flight takes 22.8%.

### **3.1.3 Demand for Psychological Support of Maritime Flight**

Pilots need to accept targeted psychological support in courses with high psychological stress (such as ultra-low altitude maritime flights, complex meteorological flights, and extended sea flights), as well as major missions and combat flights. Among the surveyed pilots, 52.0% of the pilots have undergone psychological training, and 20.8% of the pilots have not received regular systematic psychological training.

## ***3.2 Results of Establishing Maritime Flight Cognitive Behavior Training Method***

### **3.2.1 Content Constitution**

The constitution of multimedia teaching film mainly includes:

1. Main factors affecting maritime flight (natural environment, flight task, individual difference, aeronautical environment, and so on).
2. Main influences of maritime flight on human body (physiology and psychology).
3. Introduction to the knowledge of physical and psychological support methods (cognitive regulation, sleep management, illusion overcoming, muscle training, nutritional protection, and so on) at sea, and practical demonstrations of techniques such as psychological relaxation and psychological control.

### 3.2.2 Technical Requirement

1. Format standard: the finished teaching videos are in high-definition standard MP4 format (frame size:  $1920 \times 1080$ , frame rate: 25.00, aspect ratio: 16:9, audio sampling rate: 48 kHz).
2. Duration of each episode: The teaching film has a total of 10 episodes, which lasts for 10 min each.
3. Teaching format: Teaching was conducted in the form of expert theoretical lectures, professional operation demonstrations, environmental effect observations, and pilot interviews.
  - Theoretical lecturing: Psychological, flight, nutrition, and other experts conducted theoretical lectures. The lecturing experts mainly completed the corresponding content based on the storyboard. Among them, the flight experts included a gold helmet and a command pilot, who have extensive maritime flight experience. According to the outline of the interview, they conducted a semi-open class based on their own experience.
  - Operation demonstration: The psychological, fitness, and other professional teachers carried out real person operation demonstrations, teaching action essentials and precautions of mental relaxation, mental control, muscle exercise, and other skills.
  - Special effect observation: Special effect observation was conducted through sound, image, animation, video, and other multimedia materials, so as to reproduce the special sea flying environment, such as the connected sea and sky, complex weather, and changing environment vividly.

### 3.3 *Effectiveness Verification of Maritime Flight Cognitive Behavior Training Method*

Please refer to Tables 1 and 2 for the questionnaire result of the training effect.

## 4 Discussion

Due to the intricate marine environment, fewer surface features and landmarks, rapid changes in sea conditions, and navigation difficulty and other characteristics, the stability and judgment of maritime flight operations are easily affected, thereby threatening flight safety [6]. The survey results show that when flying at sea, pilots often feel “unsure” and “bottomless.” Similar mental states have a certain impact on the flight control and tactical actions of the pilots and can even directly lead to serious flight accidents. However, some pilots are able to avoid the influence of bad moods and successfully complete the flight mission. Why are pilots’ emotional and

**Table 1** Questionnaire result of maritime flight cognitive behavior training evaluation 1

Relevant items	Comprehension degree after learning			
	Comprehensively understand	Basically understand	Understand some of them	Don't remember
Main natural environment factors	21 (40%)	30 (58%)	1 (2%)	0
Flight task factors	15 (29%)	36 (69%)	1 (2%)	0
Aviation environment factors	19 (36%)	31 (60%)	2 (4%)	0
Individual difference factors	10 (19%)	40 (77%)	2 (4%)	0
Main physiological effects	20 (38%)	29 (56%)	3 (6%)	0
Main psychological effects	9 (17%)	41 (79%)	2 (4%)	0
Method of sleep management	20 (38%)	32 (62%)	0	0
Method of neck and waist muscle exercise	17 (33%)	35 (67%)	0	0
Method of nutrition support	17 (33%)	32 (61%)	3 (6%)	0
Method of illusion prevention and overcome	19 (36%)	31 (60%)	2 (4%)	0
Psychological training skills	18 (35%)	32 (61%)	2 (4%)	0

*Note* The questionnaire results are the number of people and the percentage of the surveyed people

behavioral responses so different in the same environment? According to the ABC theory of psychology, even in the face of the same event, the results produced by individuals are different due to different cognitive beliefs [7–9]. Therefore, the main reason for this psychologically different response is that different pilots have different cognition and beliefs on maritime flight. Factors such as poor understanding of the maritime flight environment, insufficient understanding of the illusion of flight, and excessive exaggeration of the difficulty of aviation flight guard support on the sea will cause psychological stress. Especially for pilots who are participating in maritime missions for the first time, due to the strangeness and misunderstanding of the special

**Table 2** Questionnaire result of maritime flight cognitive behavior training evaluation 2

Do you think it is necessary to carry out maritime flight cognitive behavior training?	Very necessary	Necessary	Probably	No need
	18 (34%)	31 (60%)	3 (6%)	0
Do you think this kind of training has any effect on promoting combat capability at sea?	Very effective	Effective	Probably	Ineffective
	12 (23%)	38 (73%)	2 (4%)	0
How long do you think it is required to carry out the training before maritime flight?	Within 1 week	2–3 weeks	About 1 month	Others
	23 (44%)	23 (44%)	6 (12%)	0
Do you think which organization should carry out this training?	First-line troop	Special care service organization	Aviation medical research organization	Others
	34 (65%)	13 (25%)	5 (10%)	0

*Note* The questionnaire results are the number of people and the percentage of the surveyed people

environment at sea, it is easy to have a certain impact on the psychology, and produce bad emotions such as fear and tension. If this kind of emotion cannot be intervened in a timely and effective manner, it will further lead to psychological imbalance and affect the pilot’s judgment and operation. Therefore, if pilots can understand and get familiar with the psychological training methods of maritime flight environment in advance, this bad mood will be greatly reduced.

Therefore, the focus of maritime flight cognitive behavior training lies in cognitive reconstruction, enable the pilots to sufficiently understand the mental state of the pilots who perform maritime flight, maritime flight knowledge and self-regulation skills, correct unreasonable cognitive models and beliefs, and ensure the stable emotion of the pilots who conduct maritime flight training for the first time. In particular, in this training, the exercise and training methods are different from the previous pure theoretical lecturing, and it increases the operation demonstration of professional staffs, thus bringing convenience for the understanding and learning of the pilots to the knowledge. The explanation of the maritime environment and flight characteristics are equipped with the special environment and flight effects, such as the pot bottom illusion and so on, so that pilots will have a more direct-viewing impression on maritime flight. In the meanwhile, the gold-helmet pilots who have rich maritime flight experience are invited to provide case explanation and individual experience, provide on-site demonstration to the common environment characteristics, psychological feelings, illusion types, treatment means and successful experiences in maritime flight, which better meet the key points of pilot’s concern.



The result of effect verification shows that after maritime flight cognitive behavior training, the flight learners who lack or have little experience in maritime flight can quickly understand and master the theoretical knowledge of the main factors affecting maritime flight and the main effects of maritime flight on people, as well as the effective technical methods for the physical and mental support of maritime flight. In particular, they will get personal experience and first-hand information on maritime flight from the explanation of the maritime flight experts, so as to further enhance their confidence of maritime flight. This training is subjectively valued and accepted by pilots. Most pilots believe that it should be carried out as soon as possible before maritime flight, and the training location should also be mainly set in front-line troops, which is consistent with our previous troop investigation situation and our past experience of undertaking the maritime flight support tasks.

## 5 Conclusion

The above results indicate that the ABC theory-based psychological training method provided to the staffs who are going to attend the maritime flight can enable pilots to correctly understand and evaluate the maritime flight task, so that they can confront the adverse influence probably brought by maritime flight to them objectively and calmly, and keep on improving their psychological endurance and adaptability. The next step is to develop maritime flight cognitive training into software to distribute troops for pilots to learn independently, so as to solve the problem of the daily accumulation and exploration of the pilots on maritime flight knowledge and skills.

**Compliance with Ethical Standards** The study was approved by the Logistics Department for the Civilian Ethics Committee of Air Force Medical Center.

All subjects who participated in the experiment were provided with and signed an informed consent form.

All relevant ethical safeguards have been met with regard to subject protection.

## References

1. Nicole PD, Alastair B (2017) Management of sea sickness in susceptible flight crews. *Mil Med* 182(11):e1846–e1850
2. Mel'nik SG, Chulaevskii AO (2011) Psychophysiological aspects of naval aviation pilots of the Navy in the operation of highly carrier-based aircraft. *Voen Med Zh* 332(8):56–60
3. Blue RS, Bonato F, Seaton K, Bubka A, Vardiman Johnné L, Mathers C et al (2017) The effects of training on anxiety and task performance in simulated suborbital spaceflight. *Aerosp Med Hum Perform* 88(7):641–650
4. Yinshuang Z, Huaobo W, Huaitao F, Yan Z, Huamiao S et al (2018) Empirical study of psychological stress protection training for the flight over sea. *Chin J Aerosp Med* 29(3–4):181–187

5. Jing L (2017) Application of emotion management ABC theory in nursing care of patients with cerebral infarction. *J Math Med* 11:139–140
6. Bernstein S, McClellan SF (2006) The role of aeronautical adaptability in the disqualification of a military flyer. *Aviat Space Environ Med* 77(11):1188–1192
7. Ruggiero Giovanni M, Spada Marcantonio M, Gabriele C, Sandra S (2018) A historical and theoretical review of cognitive behavioral therapies: from structural self-knowledge to functional processes. *J Ration Emot Cogn Behav Ther* 36(4):378–403
8. Horea-Radu O, Ovidiu DD (2018) A meta-analysis of the relationship between rational beliefs and psychological distress. *J Clin Psychol* 74(6):883–895
9. Murat A, Faruk ŞO, Martin T (2019) Mediation role of rumination and reflection on irrational beliefs and distress. *Behav Cogn Psychother* 47(6):659–671

# Industrial Robot Training Platform Based on Virtual Reality and Mixed Reality Technology



Zhe Chen, Zhuohang Cao, Peili Ma, and Lijun Xu

**Abstract** With the steady implementation of the national strategy of “Made in China 2025”, industrial robot education has achieved phased development. Many universities have opened majors in robot engineering. The problem that accompanies it is that there are many industrial robot brands in the industry. There are many model differences in the integration industry, and the investment in purchasing a stable industrial robot is enormous. At the same time, improper operations during industrial training may cause serious accidents. We have designed a set of industrial robot training platforms based on VR technology and MR technology. And it solved the problem of the shortage of teaching resources caused by the high purchase cost of industrial robot training equipment and potential safety hazards.

**Keywords** Virtual reality · Mixed reality · Industrial robot · Virtual simulation · Experiment platform

## 1 Introduction

Common virtual simulation training platforms generally consist of analogue remote controls and display terminals. There are two problems [1]. One is that they still cannot meet the resource requirements of multi-person teaching scenarios. And the VR Web platform designed in this paper can improve that by increasing the number of servers and bandwidth. It is suitable for synchronous learning with a large number of people. The second is that no real environment information is introduced, and the

---

Z. Chen (✉) · L. Xu

Institute of Art and Design, Nanjing Institute of Technology, Nanjing 210000, Jiangsu, China  
e-mail: [864871359@qq.com](mailto:864871359@qq.com)

Z. Cao

School of Mechanical Engineering, Nanjing Institute of Technology, Nanjing 210000, Jiangsu, China

P. Ma

School of Automation, Nanjing Institute of Technology, Nanjing 210000, Jiangsu, China

© The Editor(s) (if applicable) and The Author(s), under exclusive license to Springer Nature Singapore Pte Ltd. 2021

S. Long and B. S. Dhillon (eds.), *Man-Machine-Environment System Engineering*, Lecture Notes in Electrical Engineering 645, [https://doi.org/10.1007/978-981-15-6978-4\\_102](https://doi.org/10.1007/978-981-15-6978-4_102)

learning process lacks realism. So, it is impossible to intuitively feel the limitations of the integrated environment on the size parameters and working space parameters of the industrial robot, resulting in the selection of the design of the integration scheme. Inconvenience, this paper designed a system based on MR technology, which can let the operator intuitively feel the simulation effect of the integrated solution in the real production environment.

## 2 Web Simulation Platform Based on Virtual Reality Technology

### 2.1 Solution Introduction

This paper is a web simulation platform based on virtual reality technology. This platform is designed with B/S architecture and is compatible with various terminal devices used by students. All training programs on the platform can run on the web browser of the student user terminal. It allows students to access the training platform through Internet terminal equipment more conveniently (as shown in Fig. 1).



Fig. 1 Web simulation platform interface

### 2.2 Interactive Mode

The interactive objects in this platform are mainly industrial robots, workpieces and factory environments. Students participating in the training can walk between different production areas in the factory environment, and they can choose to learn to operate different industrial robot equipment and experience various industrial robot integrated application procedures.

All industrial robot equipment models use real size data and operating procedures, and the rendering effect is real. Consistent with the real situation, users can control the robot by two methods of manual operation and programming operation (as shown in Fig. 2).

In different integrated applications, students need to select equipment. Only after selecting the correct applicable equipment, the industrial robot model will appear in the production environment, and then other operations can be continued.

During the training process, the system will give feedback and record when students make illegal operations such as making the robot run to the working limit, collision with the environment or workpiece, code programming errors (as shown in Fig. 3).



Fig. 2 Two operation modes of the teaching pendant



Fig. 3 Prompt for incorrect operation



**Fig. 4** Training task scenario

### 2.3 Practical Training Tasks

When evaluating each project, users should strictly follow the operation process of the real system integration project. Error operations will be promptly reminded and recorded. It will deduct ten points for each error, and each step has three chances. Opportunities for correction, all procedures can be correct before entering the next operation step. If users accumulate five errors, they need to reenter the test. After submitting the project task, students can continue to the next project. The simulation platform designed in this paper mainly arranges four training items of essential operation, handling, welding, and loading and unloading (as shown in Fig. 4).

## 3 Real Environment Interaction System Based on Mixed Reality Technology

### 3.1 Introduction to Mixed Reality System

MR technology is a computer vision technology that directly overlays virtual images onto real physical space. And it uses gestures, sight, gaze and other methods to interact with virtual objects. The rendering effect is as close as possible to how people interact with the real physical world [2].

In this system, the selected terminal equipment is HoloLens of Microsoft Corporation. HoloLens is a portable head-mounted holographic computer device developed by Microsoft. The front of the device is sensors-related hardware, including processors, cameras and microprojection devices. The microprojection devices can directly project images into the human eye to form holographic images. Also, the HoloLens provide gesture interaction functions, allowing users to interact with digital Holograms interact [3].

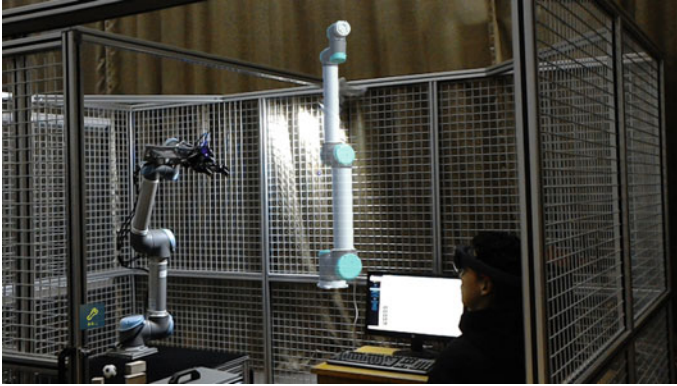


**Fig. 5** Virtual device mapping in a real production environment

The model placement function of the system can place the entire virtual object in the scene on the surface of the actual object, thereby enhancing the authenticity of the system. It utilizes the device's unique spatial mapping capability (spatial mapping). After the spatial mapping function turning on, the system will continuously scan the surrounding environment and quickly update the object grid information to sense the real object. At this time, the position coordinates of the line of sight projected on the spatial mapping grid can be assigned to the entirety in the scene. The virtual object moves the line of sight following the movement of the spatially mapped grid. After the system maps the simulation model to the real production environment, users can genuinely and intuitively experience the integration effect of the device (as shown in Fig. 5).

### ***3.2 Drag-Teaching Based on Human–Machine–Environment Interaction***

The traditional industrial robot operation methods are mainly remote control of the teach pendant and code programming. This system provides a new drag-teaching method, which can make it more convenient for users to test the effect of robot movement in the environment.

After analysing the system's needs for gesture interaction in different scenarios, "Air Tap" and "Tap&Hold" were selected as the main gesture interaction methods [4]. Clicking gestures can realize a variety of functions in the system, such as viewing model information in the component observation scene, animation demonstration of the assembly path under the automatic assembly module and so on. The dragging gestures mainly implement the functions of manipulation and navigation in the manual assembly mode.



Fig. 6 Drag teaching

When the user stares at the end of the robotic arm, he can click to confirm by the gesture to start drag teaching and then use the gesture to drag the robot to move (as shown in Fig. 6).

### 3.3 Model Setting and IK (Inverse Kinematics) Solution

Unity3D is one of the most powerful virtual reality development engines on the market. It provides a variety of API functions required for HoloLens development. It is controlled by programming with C# language. The combination can realize the development of model observation, virtual assembly operation and 3D scene management functions in the virtual assembly system. However, its ability to build models is minimal. Therefore, you need to use professional 3D modelling software to build the model before system development. Then established model is imported into the Unity3D development environment through format conversion [5]. The specific model establishment and the format conversion process are shown in Fig. 7.

After importing models, you need to add a “Robot Controller.cs” script to the parent level of the robot model and then add relevant content to the variables in the script. Then modify the values of various parameters. Next, add the CCDIK component and the Turret component. Add the “IK Target” object to the “Target” under the CCDIK component. If it does not exist, create a new one. Set the “MaxIterations” value to 80 and “Use Rotation Limits” to “true”. Add a bone node for “Bones”. Set the “Weight” of a single bone node according to the robot joint number setting. Refer to Motoman HD20. The smaller the value, the less the solution relationship

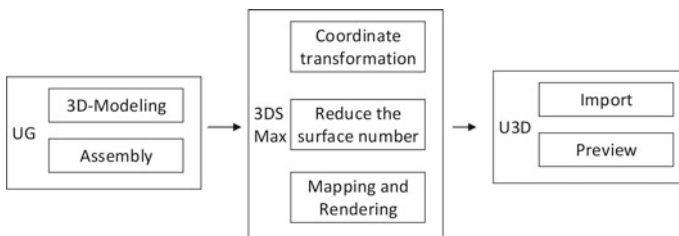
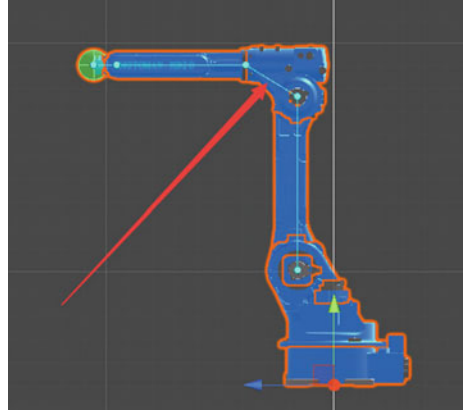


Fig. 7 Model establishment and format conversion process



**Fig. 8** Screenshot of the development environment interface



calculation If Bones are created successfully, you can see a blue line running through these critical nodes in the robot (as shown in Fig. 8).

Next, set an angle limiter for each node, add a rotation limit hinge component for each node, and set use limits to true or false, which based on the actual robot joint rotation limit angle setting. Finally, set the maximum and minimum rotation angle.

After the inverse dynamics is set, set the Turret component for the chassis. The target is the same as the CCDIK Target. Parts are the rotation tracking key point. The number of critical points in the range of “Size” is the same. (Notice: There is no perfect inverse dynamics algorithm, especially for unrestricted angle rotation joints. Therefore, when dealing with unrestricted angle rotation joints such as robotic chassis, a Turret component needs to be set separately. It is wrong to set the chassis as a part of IK. So, we can see that the six-degree-of-freedom robot has only set 5 critical nodes in the reverse dynamics setting, and the shoulder key node is used as a Turret component.)

At the same time, it should be noted that when the RobotController component is implementing network-broadcasting, it will depend on NetworkIdentity component. So, make sure that the two components are in the same GameObject, and the Animation component, CCDIK component, and Turret component are all indispensable.

## 4 Conclusion

This paper combines the VR technology and the MR technology to carry out the design of the industrial robot training platform and research on critical technologies. The main conclusions are as follows:

- (1) The web simulation platform based on virtual reality technology has good authenticity and immersion, and the learning, training and assessment functions improve the efficiency and effectiveness of training.
- (2) The use of spatial mapping technology will better integrate virtual machines and the real environment. At the same time, this paper has developed a drag-teaching method based on human-machine-environment interaction. It can be used for rapid verification operations and experimental teaching, thereby improving training efficiency.
- (3) Using virtual simulation technology as a cognitive tool for students can enable students to interact with machines and the environment intuitively. And it effectively improves the quality of practical teaching, stimulates students "interest in learning and indeed improves students" practical operation ability. Provide professional teachers with a platform that integrates virtual machine models and real environments to better serve professional teaching.

## References

1. Anqi (2017) Research on OpenGL virtual assembly line robot job simulation software. Harbin Engineering University
2. Huang A, Shen Y, Tang Y (2019) Operation and maintenance design of industrial equipment based on mixed reality technology. *Ordnance Autom* 38(09):72–77
3. Cui H, Wu X, Wei S (2020) Application of digital aircraft augmented reality teaching platform based on HoloLens. *Educ Teach Forum* 2020(05):233–235
4. Lei Z, Wang L, Cui J, Chen S, Xu Z, Yu H, Meng H, Liu G (2019) Substation operation and maintenance simulation training system based on HoloLens. *Comput Modernization* 2019(11):94–99
5. Wu B, Chen C, Xu J (2019) Design of virtual assembly system for automotive main reducer based on HoloLens. *Modern Manuf Eng* 2019(08):41–49

# An Oversea Flight Preadaptive Training System-Based 4D Scene



Liu Yang, Yan Zhang, Yishuang Zhang, Duanqin Xiong, Yang Liao, Juan Liu, Xueqian Deng, and Hua Guo

**Abstract** This paper introduces the development of a overseas flight preadaptive training system-based 4D scene, which includes server, psychological data analysis and processing unit, overseas flight simulation scene play and control unit, seat control unit, special effect output unit, psychological stress test equipment, special effect seat and special effect equipment. The system can be used for the pilot to complete targeted psychological training in the four-dimensional space composed of three-dimensional video and environment, improve the psychological adaptability and tolerance to carry out combat tasks in the dangerous environment at sea and be familiar with the common operational modes of overseas flight, so as to eliminate the tension and fear.

**Keywords** Oversea flight · Pre-adaptive training · 4D scene

## 1 Background

Due to many differences between the natural conditions on the sea and on the land, the pilots who carry out the training tasks of flying on the sea will face difficulties such as complex situation, arduous control, long navigation time, poor working environment, mental tension, flights illusion, rescue lag and so on [1, 2]. Moreover, due to the wide application of new technologies, especially the emergence of new operational theories and models such as over the horizon attack and precision strike, the fight for air control at sea is more fierce and cruel. All of these will cause strong psychological stress to pilots. If the pilots fail to respond effectively, it may lead to the decline of cognitive function, impact on flight control and even directly lead to serious flight accidents [3, 4]. Therefore, improving psychological adaptation can alleviate these problems. Many studies at home and abroad also show that through preadaptive psychological training, military personnel can improve their adaptability

---

L. Yang · Y. Zhang · Y. Zhang · D. Xiong · Y. Liao · J. Liu · X. Deng · H. Guo (✉)  
Air Force Medical Center, Fourth Military Medical University, Beijing 100142, China  
e-mail: [xin096012@sina.com](mailto:xin096012@sina.com)

© The Editor(s) (if applicable) and The Author(s), under exclusive license to Springer Nature Singapore Pte Ltd. 2021

S. Long and B. S. Dhillon (eds.), *Man-Machine-Environment System Engineering*, Lecture Notes in Electrical Engineering 645, [https://doi.org/10.1007/978-981-15-6978-4\\_103](https://doi.org/10.1007/978-981-15-6978-4_103)

to the working environment and reduce psychological stress response [5–7]. Therefore, it is necessary to establish a set of training system which can simulate the special environment of flying at sea and train pilots in preadaptation.

## **2 Overall Technical Proposal**

The overall technical proposal is 4D simulation, which is based on 3D stereoscopic film and environment special effects. It has the functions of water spray, air jet, vibration, leg sweeping and so on. It can be controlled by computer according to different training scenarios to make realistic special effects.

## **3 Overall System Composition and Functional Connections**

### ***3.1 Consists of Overall System***

It includes server, psychological data analysis and processing unit, sea flight simulation scene playback and control unit, seat control unit, special effect output unit, psychological stress test equipment, special effect seat and special effect equipment.

### ***3.2 Playback and Control Unit of Oversea Flight Simulation Scene***

It has video play and signal control functions, respectively, connecting the seat control unit and special effect output unit, so as to output the seat action instructions and special effect instructions consistent with the playing content to the seat control unit and special effect output unit and receive the information feedback from the seat control unit and special effect output unit.

### ***3.3 Special Effect Seat***

It is connected with the seat control unit to perform corresponding actions under the control of the seat control unit and is available for the trainees to watch and test in the seat.

### ***3.4 Psychological Stress Test Equipment***

It is used to test the physical reaction of trainees when they watch 4D scenes and transmit the test data to the psychological data analysis and processing unit for data statistics and evaluation. The psychological data analysis and processing unit converts the evaluation conclusion into personalized training playback instructions and sends them to the server, which transmits them to the marine simulated flight environment playback and control unit.

### ***3.5 Special Effect Device***

It is connected with the special effect output unit, for special effect release under the control of the special effect output unit.

### ***3.6 Server***

It is used to receive the personalized training playback instruction sent by the psychological data analysis processing unit and transmit the playback instruction to the overseas flight simulation environment playback and control unit.

The server, psychological data analysis and processing unit and the playback and control unit of the overseas flight simulation environment in this system can be integrated into different functional modules or software in a PC terminal for their own operation and interaction or independent operation in their own PC terminal and not limited to the PC terminal.

## **4 Specific Unit and Function**

### ***4.1 Playback and Control Unit of Oversea Flight Simulation Scene***

The unit includes a playback control platform and a playback audiovisual device.

#### **4.1.1 Playback Control Platform**

The platform is used to store 3D video of a variety of sea flight scene simulation data and also has the function of editing and splicing. It can clip any one or more scenes in the existing 3D video and splice them into a new 3D video without changing the

definition of the 3D video; at the same time, it supports playing 3D video of any other format.

The simulation data of oversea flight scenario includes but is not limited to oversea flight environment scenario, oversea flight operation process and attack mode scenario, and cockpit noise environment scenario. The sea flying environment scene includes but is not limited to the following scenes: vast open scene, sea melted into the sky, true and false sea sky lines, pot bottom illusion, turbulence airflow, low visibility, strong reflection, calm sea surface and/or rough waves, thunder cloud, wave undulation and seabird scenario. The oversea flight operation process and attack mode scenario includes but is not limited to the following scenarios: dogfighter, dive to the sea, ultra-low altitude flight, radar locking, ship attack, missile launch, TV guidance, fixed point bombing. The oversea flight scenario simulation data is in coordination with the 5.1-channel high-quality audio, and the audio sampling rate is 48 kHz.

The above-mentioned 4D oversea flight environment and combat scenes can be edited and played according to the time axis. Because different scenes designed by this system can, respectively, trigger different degrees of psychological stress reactions. For example, pot bottom illusion can cause excessive psychological stress such as anxiety, tension and fear and also can cause moderate psychological stress such as the enhancement of cognitive ability, while vibration and other oversea cruise flight scenes can cause cognitive decline and low psychological stress reaction such as numbness and emptiness. These scenes are used for trainees to adapt to various actual combat environments and display the human response of trainees to different scenes.

#### **4.1.2 Playing Audio and Video Equipment**

It is used to play the oversea flight scene and provide the sound effect consistent with the scene simulation synchronously. The playback audiovisual equipment includes a Dolby 360° digital stereo surround sound, two projectors with identical performance parameters, polarized lenses added in front of the projector lens and polarized glasses for trainees to enhance the 3D display effect.

#### ***4.2 Special Effect Seats and Special Effect Equipment***

The function of the special effects equipment is to provide trainees with the body feeling synchronized with the simulation video and the action of the special effects seat, so as to make the simulation scene more realistic and more psychologically perceptive.

#### **4.2.1 Special Effect Seat**

According to the operation of the seat control unit, it moves up and down, left and right, front and back, performing one or more actions of shaking, tipping, shaking, shaking, climbing and falling.

#### **4.2.2 Special Effect Equipment**

Under the control of special effects output unit, special effects released by special effects equipment include but are not limited to one or more combinations of water, fog, wind and smell.

### ***4.3 Psychological Stress Test Equipment***

The device is used to test the data of human psychological stress, including one or more combinations of electroencephalogram (EEG), galvanic skin response (GSR), electromyography (EMG) and heart rate (HR). By placing the signal sensor in the specific part of the body, the system tests and collects the parameters of psychological stress.

### ***4.4 Psychological Data Analysis and Processing Unit***

It is used to analyze and process the data obtained from psychological stress test equipment. Then, one or more combined evaluation parameters can be gotten and sent to the server, compared with the threshold set in the server, so as to form the server controlled overseas simulated flight environment playback and control unit execution line play content, play frequency instructions. The unit includes psychological data analysis technology and psychological data processing method.

#### **4.4.1 Psychological Data Analysis Technology**

It is to input all kinds of index parameters collected by psychological stress testing equipment into information processor and then get corresponding data for evaluation and analysis after amplification, filtering, average, smoothing, eliminating false difference, spectrum analysis, correction and other processing.

#### 4.4.2 The Method of Psychological Data Processing

It is to transform the evaluation conclusion into personalized training playback instruction and send it to the server, which transmits it to the overseas flight simulation environment playback and control unit. The method is as follows: The relationship between the degree of psychological stress response and flight operation performance conforms to the inverted U principle. This principle indicates that when the degree of psychological stress response increases from low to high, the operation performance will gradually increase. When the degree of psychological stress response reaches a certain point or a certain area, the operation performance is the highest. If the degree of psychological stress is further increased, the level of flight operation will be reduced. Therefore, a moderate degree of psychological stress is very important for overseas flight. The essence of psychological stress is a series of related physiological reactions. By collecting and analyzing the physiological data of these systems, we can know the degree of psychological stress. For example, the excitatory or inhibitory activity of cerebral cortex can be reflected by EEG signal index. The tension and relaxation of autonomic nervous system activity can be evaluated by galvanic skin response, electromyography and heart rate. The indices represent different psychological stress states.

Before the preadaptive training, the maximum values of each parameter index reflecting the degree of psychological stress state of participants were collected as the baseline values. When playing 4D overseas flight scene in the training, the above parameter index values were analyzed according to the time axis synchronous collection, and the results were taken as the training evaluation indexes. Comparing the maximum value of each parameter index value in training with the baseline value before training, when the change reaches the set threshold (change more than 100%), it reflects the degree of psychological stress in training.

The design changes are as follows: All indexes are EEG ( $\theta$ ,  $\alpha$ ,  $\beta$ ), GSR, MEG, maximum value of HR [8]. After the training, if trainees' any maximum value of  $\beta$  wave, GSR, MEG, HR exceeds the threshold, it indicates that the stress and excitement level are too high [9]. At this time, it is necessary to retrain high stimulation scenes such as pot bottom illusion.

After training, if the maximum value of  $\theta$  or  $\alpha$  wave of the trainees EEG exceeds the threshold, it indicates that the level of stress is too low and the level of excitement is insufficient. At this time, it is necessary to retrain low stimulation scenes such as cruising. Therefore, the psychological data analysis and processing unit can correspond the results of psychological data changes in training to different 4D overseas flight environment and combat scene modules and carry out intensive training as required.



### 5 System Structure Diagram and Specific Implementation Mode

In order to better understand the system, we will further describe in combination with the attached drawings and specific embodiments. The system structure is shown in Fig. 1, including: server 1, psychological data analysis and processing unit (unit 2), oversea simulation flight environment playback and control unit 3 (unit 3), seat control unit 4 (unit 4), special effect output unit 5 (unit 5), psychological stress test equipment 6 (equipment 6), special effect seat 7 (seat 7) and special effect equipment 8 (equipment 8). The specific functions and structure of each part are as follows.

- (1) Unit 3 includes a playback control platform 31 (platform 31) and a playback audiovisual device 32 (device 32). Platform 31 is, respectively, connected with unit 4 and 5, so as to send the seat action command and the special effects command consistent with the playing content to unit 4 and 5 and receive the feedback information of the unit 4 and 5.

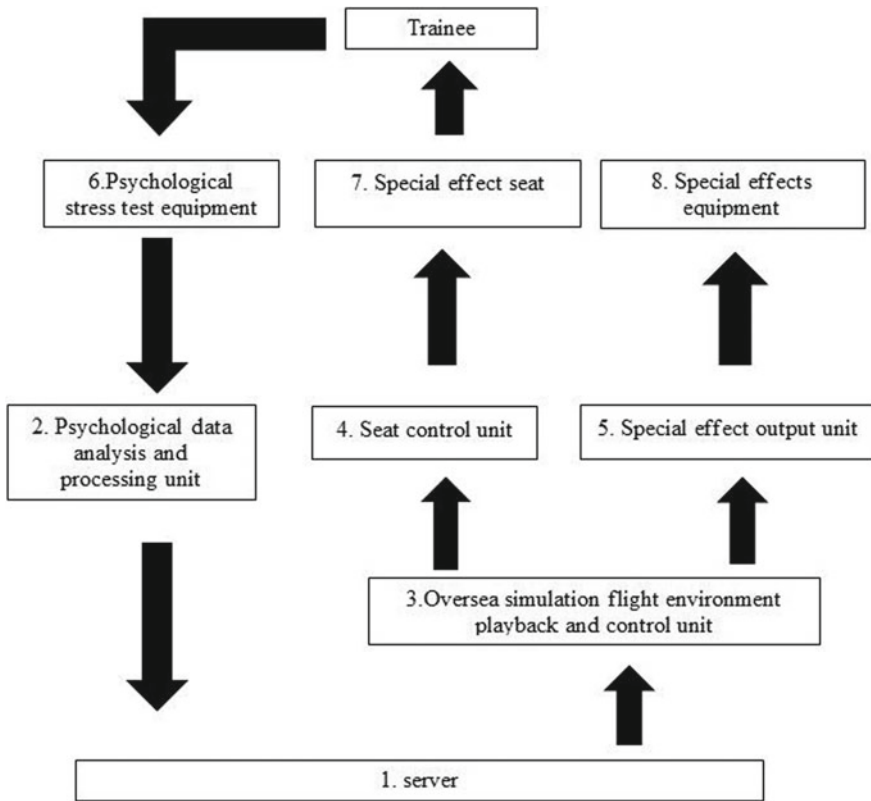


Fig. 1 System structure diagram

- (2) Seat 7 is connected with unit 4 to perform corresponding actions, which include shaking, tipping, climbing and falling, in the up, down, left, right and front and back directions.
- (3) Equipment 6 is used to test the physical response of trainees when they watch 4D scenes. The test data is transmitted to unit 2 for statistics and evaluation. Unit 2 sends the processed evaluation parameters to the server in comparison with the threshold. The server forms the command to control unit 3 to execute the content and frequency of the playback. Unit 2 converts the evaluation conclusion into personalized training playback instruction and sends it to the server, which transmits it to unit 3;
- (4) Equipment 8 is connected with unit 5, which is used to release special effects under the control of the unit 5 to match the simulation scene. Special effects include one or more combinations, such as foggy, smell of blood, the sea breeze howls and smell of sulfur pungent.
- (5) Server is used to receive the personalized training playback instruction sent by unit 2 and transmit the playback instruction to unit 3.

## 6 Conclusion

The system can realize four-dimensional space simulation of real oversea flight environment, which can make trainees feel the intense and realistic stereoscopic battlefield environment in the visual, auditory, olfactory and kinesthetic and other multi-perception channels, test and analyze the psychological stress response at the same time. The results can be used as the basis of the trainees' personalized training program, which can quickly improve the psychological adaptability and stress regulation ability of the pilots to carry out combat tasks.

## References

1. Nicole PD, Alaistair B (2017) Management of sea sickness in susceptible flight crews. *Mil Med* 182(11):e1846–e1850
2. Mel'Nik SG, Chulaevskiĭ AO (2011) Psychophysiological aspects of naval aviation pilots of the navy in the operation of highly carrier-based aircraft. *Voenno-meditsinskiĭ zhurnal* 332(8):56–60
3. Yang L et al (2015) Effect of psychological stress defense training on military flight personnel. *Chin J Behav Med Brain Sci* 24(5):464–467
4. Zhang Y et al (2018) Empirical study of psychological stress protection training for the flight over sea. *Chin J Aerosp Med* 29(4):181–187
5. Yang L et al (2014) Research on group psychological training and its application in military pilots. *Chin J Behav Med Brain Sci* 23(2):189–192
6. Blue RS, Bonato F, Seaton K et al (2017) The effects of training on anxiety and task performance in simulated suborbital spaceflight. *Aerosp Med Hum Perform* 88(7):641–650
7. Miller C, Vandervliet G (1992) Shipboard mission training effectiveness of the Naval Air Warfare Center's V-22 government test pilot trainer. In: *Flight simulation technologies conference*

8. Shin H (2016) Ambient temperature effect on pulse rate variability as an alternative to heart rate variability in young adult. *J Clin Monit Comput* 30(6):939–948
9. Avdeeva DK, Ivanov ML, Natalinova NM et al (2017) Development and investigation of the nanosensor-based apparatus to assess the psycho-emotional state of a person. *J Phys Conf Ser* 881:012004

# Analysis on Countermeasure of Troops Delicacy Management in the Process of the Newly-Typed Army Construction



Zaochen Liu, Peng Gong, Xiaoping Wang, Yujin Wang, and Dongdong Cui

**Abstract** Delicacy management has importantly realistic significance on advancing construction level of troops regularization, improving innovative development of troops management and education and promoting construction and development of the newly-typed army under the higher starting point. The essay analyzes the existing problems of delicacy management in army troops based on practical newly-typed army construction, discusses the necessity to improve troops delicacy management in constructing the newly-typed army combined with the related questions, puts forward the countermeasures; that is, firstly, taking the transformation of ideas as guide, delicacy is advanced in establishing ideas of scientific management; secondly, taking the establishment of standard system as lead, delicacy is advanced in improving work guidance level; thirdly, taking the construction of information system as support, delicacy is advanced in realizing troops management informationization.

**Keywords** The newly-typed army · Delicacy management · Analysis on countermeasures

At present, the newly-typed army construction is being in the critical period with full swing. Contradiction between troops management work and the targets transformation towards quality-and-efficiency model and all-domain operation model has become more and more prominent in the newly-typed army. It has been the urgent need of situation, tasks and the responsibility to innovate on management patterns and improve management methods. As the product of information era, delicacy management is the most representative management thought in modern management theory; it is not only extensively applied to modern enterprise management and public management, but also has produced profound influence on military management. In the founding conference of army leadership, Chairman Xi stressed, “Army should adapt the profound change on building modes and application pattern in information era, explore the characteristics and regularity of army development, strive to build a

---

Z. Liu (✉) · P. Gong · X. Wang · Y. Wang · D. Cui  
Artillery and Air Defense Forces Academy, Zhengzhou Campus, Zhengzhou 450052, China  
e-mail: [meizg\\_zz@sina.com](mailto:meizg_zz@sina.com)

© The Editor(s) (if applicable) and The Author(s), under exclusive license to Springer Nature Singapore Pte Ltd. 2021 909  
S. Long and B. S. Dhillon (eds.), *Man-Machine-Environment System Engineering*, Lecture Notes in Electrical Engineering 645,  
[https://doi.org/10.1007/978-981-15-6978-4\\_104](https://doi.org/10.1007/978-981-15-6978-4_104)

strong army with modernization and regularization.” Thus, we should study delicacy management theory, innovate on working ideas and promote the newly-typed army construction with regularization [1].

## **1 The Existing Problems in Troops Delicacy Managements Currently**

From the present situation of troops management, some active exploration and practice have been conducted in delicacy management, and particularly some prominent effects have been achieved in combat readiness training, safety management, logistic support and weapons and equipment. However, there still exist some problems.

### ***1.1 Self-awareness to Conduct Delicacy Management Needs to Be Further Reinforced***

Through delicacy management the main purpose is to realize scientific quantification, standard specification, and attention to details and benefit optimization in management. Scientifically quantitative standard and the flow with executing power must be established to realize delicacy management. The officers in some working units do not fully master the essence, connotation and regularity of delicacy management. The ideas are old and the thinking way, and working methods are traditional, research, and application on delicacy management only stay at the leading organ level; management ideas are not integrated into all officers and men; effect for grassroots work is not obvious [2]. In some working units, comprehensive arrangements are weak; there are some problems such as focusing more theoretical discussion than practice, relying on more casual guidance than comprehensive arrangements, all these led to a superficial knowledge of delicacy management towards officers and men and also caused less communication among different echelons.

### ***1.2 The Thinking Way and Methods to Conduct Delicacy Management Need to Be Further Improved***

Troops management is accomplished through process control. As long as precise control towards management process is realized delicacy management can be completed. In practical process, there exists a phenomenon on emphasizing the result over the process to certain degree. The famous process control effect law, “ $90\% \times 90\% \times 90\% \times 90\% \times 90\% = 59\%$ ”, has told us that depending on results is not far enough, some working units only focus on management effect, but ignore the process

control link such as plan, organization, command, and coordination, the fault for any system and link may cause management tasks not to be finished; in other working units, management system is not reasonable concerning the flow design and standard quantization; it is not much easier to find the starting point, the important points and difficult points; and in all respects quantization and delicacy are conducted, all these led to complexity and violated the initial ideas to conduct delicacy management.

### ***1.3 The Capability and Quality to Conduct Delicacy Management Need to Be Further Promoted***

Delicacy management require management mode which is adapted to seek for carefulness and speed in information era. To informationized management system research and development are not enough, some working units emphasize its application over its maintenance, and its application only stay at surface level for usage; to the environmental change, better telepathic and rapid response ability is short, and efforts on the research and optimization of the system are insufficient. Interdisciplinary talents who not only grasp management skill but also master information technology are not enough, informationized quality for cadres is not much better as a whole; some cadres have much weaker capability in information retrieving, delivering and processing, system managing and maintaining, innovatively developing work by using the present technological equipment. Thus, all these restrict quality and effect of delicacy management to certain degree [3].

## **2 The Necessity to Conduct Troops Delicacy Management in Newly-Typed Army Construction**

Troops are valued for their quality, not for their number. Here quality is the basic requirement towards quantity of troops and the fundamental condition and regulation towards officers and men. If the newly-typed army are required to realize transformation from quantity-and-scale model to that of quality and efficiency, from multi-layered command model to that of flat-styled command as well as from area defensive operation model to that of all-domain operation it is the prerequisite to conduct troops delicacy management.

### ***2.1 It Is Inevitable Choice to Conduct Delicacy Management for Constructing the Newly-Typed Army***

Under the information condition, it is required that the newly-typed army can perform the task in full-time, all-domain, and full frequency-domain operation. Based on effectively coping with all kinds of crisis, quick reaction can be conducted under the complicated conditions such as meteorological change, geographical environment and time, constant all-weather operation can be implemented; thus, officers and men are required to operate, organize, collaborate, manage, and control in precise and scientific way. Conducting delicacy management is the inevitable requirement to improve scientific management level and adapt the newly-typed army characteristics and developing law [4].

### ***2.2 It Is the Fundamental Path to Conduct Delicacy Management for Improving Construction Level of the Newly-Typed Army with Regularization***

Regularization is the important aspect for troops construction, and it is also to realize precision and standardization of procedures and rules. In delicacy management, the whole process is the one in which experience is changed into rules, then rules are trained into habits, and finally, habits are precipitated to culture. The idea is integrated into regularized construction and can effectively intensify the awareness of law, rules and standard, develop good habits such as dealing with matters by law and regulations, establish and keep precise and scientific running order, greatly promote regularized level of the newly-typed army.

### ***2.3 It Is the Important Guarantee to Conduct Delicacy Management for Realizing Scientific Development of the Newly-Typed Army***

Details determine efficiency, quality and safety. From the start of general grassroots questions, delicacy management should master every position and segment, control every piece of equipment and part. It cannot only improve the quality and benefit of the whole organizing system, but also stop loopholes and prevent risk, effectively cut accidents link and avoid occurrence of the important questions.

### **3 Countermeasures to Realize Troops Delicacy Management**

With the constant deepening of national defense and military reform, some inadapt-able questions among troops management ideas, work guidance, work mode, and the new situation have brought new subject towards management work. Conducting delicacy management is the only road to solve all kinds of contradiction and problems and is also the necessary requirement to effectively perform missions and promote the newly-typed army construction.

#### ***3.1 Taking the Transformation of Ideas as Guide, Delicacy is Advanced in Establishing Ideas of Scientific Management***

If conducting delicacy management, we should continuously adapt the changing situation and tasks and actively abstract advanced management ideas. One is to realize transformation from traditionally extensive development model to delicacy management model. Troops management contains a series of trivial and complicated affairs; if every tiny matter is changing, it possibly plays an important influence. If the related regulation and requirement are completely conducted, troops management can be precisely realized in every direction. Two is to realize transformation from depending on experience accumulation to focusing on technological innovation. Under the information condition, troops management system has increasingly become more complicated, management objects have gradually become very plural, and management control has become more difficult. Some advanced technological means should be actively applied such as Internet, virtual reality, finger identification, and video monitoring to realize the organic management combination of human, technology, and psychology and frequently improve scientific, intelligent, and information zed level of troops management. Three is to realize transformation from purely institutional constraints to multi-dimensional cultural infiltration. If troops management model needs to be innovated and developed, we must overcome loose, casual, and temporary management patterns and greatly reinforce cultural construction to realize escalation form institutional constraints to cultural reinforcements. We should strive to integrate safe and secure culture into different places such as position, dormitory, and family and create a safe environment with peace and harmony.

#### ***3.2 Taking the Establishment of Standard System as Lead, Delicacy is Advanced in Improving Work Guidance Level***

Standardization is the basis and prerequisite for delicacy. If fine management is required without mess, mixture, and complexity, a specific standard system must be



established. One is to define tasks and objectives and solve questions on “what to do”. According to doctrines and regulation, the necessary weekly and monthly work are summed up and overall planning graph is mapped based on some routine work such as training, combat readiness, management, and support. In accordance with position and responsibility work assignment for officers and men is disintegrated by echelons, it is more convenient for officers and men to master the vital points and perform work very well, especially concerning the designation of working staff, position, responsibility, and standard. Two is to establish the flow standard and solve questions on “how to do it.” The flow is a kind of working procedure, while standard is the criterion and basis we commonly abide by. If the flow standard is established, delicacy management can have objective basis and can be conducted very well. According to the principle and methods of the flow reconstruction, working contents are integrated. Particularly, the key flow in organizing the important activities, helping, and educating the fluctuant staff in thought, managing and controlling important places and prevention in the key periods should be repeatedly discussed, optimized, and perfected, the working habits should be developed according to the flow. Three is to perform responsibility and requirement and solve questions on “what to do or not”; if delicacy management is conducted, we must establish responsible institution in accordance with different systems, responsibilities, echelons, and laboring division. According to positions and tasks the duty is designated, institutional management is intensified and classified management is conducted, and thus, everyone has and undertakes their responsibilities.

### ***3.3 Taking the Construction of Information System as Support, Delicacy is Advanced in Realizing Troops Management Informationization***

Under the support of data drive, we must stick to “rejuvenating the army through science and technology” and improve the information zed delicacy level of safety work relying on safety risk evaluation and preventive warning institution. One is to keep close sightline of management and control. A long-distance video monitoring system should be installed at some important points such as vehicles and gun yards, garrison gates, and arsenal. Fingerprint machine should be installed at some places such as operational duty room and sentry posts, satellite positioning system should be installed at some vehicles for logistic support so that safety situation of the important targets is live monitored. Some routine work such as duty shift, education and training, inspecting posts for officers and men, patrolling and checking around arsenal should be fully conducted and controlled very well, anyway by different advanced means long-distance places can be managed within the sightline [5].

Two is to attach importance to information reservation. We should input some contents concerning safety knowledge, rich experience, accident cases, emergency plan, regulation and institution into the system, establish the information data base

containing strength, plan, supervision, questions and evaluation, perform information reservation very well, and improve work efficiency. To some fluctuant staff in thought such as disable officers and men, ready-to-leave cadres, disputing staff on marriage and love, we should reserve the related information in detail including their mental state, personal performance and working situation, and purposefully develop work.

Three is to actively develop risk evaluation. We should analyze and sum up accident cases, mobilize officers and men to find out risk sources, establish risk evaluation quantization graph by echelons and classification; the related information should be integrated into the system of safety risk evaluation and preventive warning institution. In different level automatic or active warning are reminded in time so as to effectively prevent passive or hysteretic management and control.

**Compliance with Ethical Standards** The study was approved by the Logistics Department for the Civilian Ethics Committee of Artillery and Air Defense Forces Academy (Zhengzhou Campus).

All subjects who participated in the experiment were provided with and signed an informed consent form.

All relevant ethical safeguards have been met with regard to subject protection.

## References

1. Xu S (2011) On delicacy management. Blue Sky Press, Beijing
2. Wu Y, Lv J (2012) Research on delicacy management theory and exploration of its practice in military academy. Military Science Press, Beijing
3. Yue H, Yang J (2013) The existing problems towards delicacy managements of troops and its countermeasures. *Troops Management*, Jan 2013
4. Wang Z, Wu H, Liu X (2005) On delicacy management. Xinhua Press, Beijing, pp 25–40
5. Wang Z (2004) Details is the key to success. Xinhua Press, Beijing, pp 35–43

# A Method for Evaluating the Level of Shooting that Attenuates the Effect of Small Arms on Accuracy



Xin Wang, Haoyuan Li, Xiang Gao, Min Chen, Ming Kong, and He Wu

**Abstract** This paper is based on the related theory of probability theory and mathematical statistics through the study of small arms shooting accuracy, fire intensity test, and characterization methods and establishes the relation model among shooting performance, small arms accuracy, and shooting level. The shooting performance data were incorporated into the calculation process of shooting accuracy and shooting intensity of small arms, and then the shooting intensity of small arms was used to evaluate the stability level of the shooter in vertical and horizontal directions. The shooting accuracy of small arms is used to modify the shooting performance data so as to form a shooting level evaluation method that can reduce the influence of the accuracy of small arms from the shooting performance data.

**Keywords** Small arms shooting · Accuracy of small arms · Shooting level · Shooting accuracy · Shooting density

At present, the evaluation of shooting athletes or military personnel's shooting level is mainly based on a specific shooting performance in the competition or assessment, such as the number of projectile rings, impact distribution characteristics, and other data. Factors that contribute to this specific shooting performance include the shooter's level of shooting, the shooter's physical condition, the accuracy of small arms, and the shooting environment. If the environmental factor is not considered, at the same time, the state of a person, including the mental and physical characteristics of a person when shooting, will be taken as a reflection of the level of shooting. Therefore, the main influencing factors of shooting performance are shooter's shooting level and the accuracy of small arms.

The accuracy of small arms is different from each other, so the shooting performance cannot be simply equated with the shooting level. To correctly evaluate the shooting level from the shooting performance data, the influence of the small arms

---

X. Wang · H. Li (✉) · X. Gao · M. Chen · M. Kong · H. Wu  
PLA Army Academy of Artillery and Air Defense, Zhengzhou Campus, Zhengzhou 450052,  
China  
e-mail: [lhysff@163.com](mailto:lhysff@163.com)

accuracy should be eliminated or weakened. Therefore, this paper starts from the analysis of the accuracy of small arms; mainly the accuracy of small arms shooting and the density of small arms shooting [1], the data of effective shooting performance is incorporated into the calculation process of small arms accuracy. By using the more accurate precision data of the calculated small arms, the shooting performance data is revised, and the firing stability is evaluated.

## 1 Characterization and Test Methods for Accuracy of Small Arms

Accuracy of small arms has two important characterization data, namely shooting accuracy and shooting intensity [2]. This section studies how to extract the accuracy information of small arms accurately from the shooting performance data, which is the premise and basis for weakening the influence of the accuracy of light weapons in the assessment of shooting level.

### 1.1 Shooting Accuracy

Take the aiming checkpoint as the origin, take the vertical direction and the horizontal direction as the coordinate axis on the vertical target surface, and establish the plane rectangular coordinate system. The coordinates of the average impact point are obtained by the following formula:

$$\bar{z} = \frac{1}{n} \sum_{i=1}^n z_i$$

$$\bar{y} = \frac{1}{n} \sum_{i=1}^n y_i$$

$(z_i, y_i)$  is the direction coordinates and vertical coordinates of the center of the impact point, that is, the shooting performance data of the impact point, and  $n$  is the number of effective impact points. The azimuth and distance of the average impact point relative to the aiming checkpoint are the shooting accuracy of small arms. Since the aiming checkpoint is the origin of coordinates, the coordinates of the average impact point can be defined as the shooting accuracy.

Shooting accuracy reveals the azimuth and distance deviation between the expected firing data sample and the aiming checkpoint in the accuracy of small arms. In fact, the existence of this kind of deviation, there are both systematic and random, the randomness in projectile dispersion error, and a variety of uncontrollable factors, systemic is one of the important characterization of firearms precision

difference; according to the theory of probability and mathematical statistics, on the direction and the vertical weight, small projectile dispersion error and a large number of uncontrolled error formation of the random error are normal distribution, so the expectation of random error is 0, the more shooting data samples there are, the more systematic the average impact point can reflect the accuracy of light weapons, and the more accurate the shooting accuracy can be represented by the average impact point.

## 1.2 Shooting Density

Shooting in the ideal state of people and environment, the impact points of each shot are not completely coincident but scattered around the average impact point in a certain area, forming the factor of projectile dispersion, in addition to people and environment, is mainly the shooting intensity of small arms. Shooting intensity indicates the dispersion degree of the impact point relative to the average impact point during shooting. It is generally believed that the projectile dispersion error caused by the density of small arms is relatively independent and follows a normal distribution in both vertical and horizontal directions [3].

According to the theory of normal distribution, the spread standard deviation of horizontal direction  $\sigma_z$  and vertical direction  $\sigma_y$  can be calculated by the following formula:

$$\sigma_z = \sqrt{\frac{1}{n-1} \sum_{i=1}^n (z_i - \bar{z})^2}$$

$$\sigma_y = \sqrt{\frac{1}{n-1} \sum_{i=1}^n (y_i - \bar{y})^2}$$

Shooting intensity not only reveals the performance level of small arms, but also can be used as a reference index to evaluate the stability of shooters in horizontal and vertical directions according to the standard deviation of the distribution of projectiles in the normal distribution [4].

## 2 Method of Evaluating the Level of Shooting

The traditional shooting level is mainly evaluated based on the performance data of a single set of projectiles, such as the number of rings, or the distance from the aiming checkpoint, without considering the influence of the accuracy of small arms. The accuracy factor of small arms can be used to modify the result of fire

level assessment, which can effectively reduce the influence of the accuracy of small arms in the process of fire level assessment. The model of shooting-level assessment and evaluation are mainly divided into the following steps: (1) Determine effective projectile; (2) Involve effective projectile data in the calculation of shooting accuracy and shooting density of small arms; (3) Correction of projectile data by shooting accuracy of small arms; (4) Use the revised projectile data to evaluate the shooting level; (5) Use shooting density to assist in evaluating shooting stability.

In this model, the further problem to be solved is to use the firing accuracy to modify the firing performance data and use the firing density to evaluate the shooting stability, which is the key to reduce the impact of small arms accuracy in the shooting level evaluation.

Shooting performance data  $(z_i, y_i)$  is compared with the aim at checkpoints coordinate offsets, which contains the deviation caused by small arms shooting accuracy  $(\bar{z}, \bar{y})$ , to weaken the influence of the precision of small arms, it is necessary to minus the average impact in shooting performance data relative to aim at the checkpoint vector deviation, detailed correction method is shown in Fig. 1, and the following formula:

$$(z_i, y_i) \rightarrow (z_i - \bar{z}, y_i - \bar{y})$$

In Fig. 1, the red dot is the aiming checkpoint, the blue point is the calculated shooting accuracy, that is, the average impact point; the black point is the projectile performance data, that is, the actual impact point; the gray point is the revised projectile data, which is the position of the impact point relative to the aiming checkpoint after removing the accuracy effect of small arms. It is important to note that for each additional set of projectile data, the shooting accuracy and intensity are recalculated, and then the projectile levels of all projectile performance data are evaluated using the new shooting accuracy and intensity.

**Fig. 1** Correction of shooting performance data with shooting accuracy

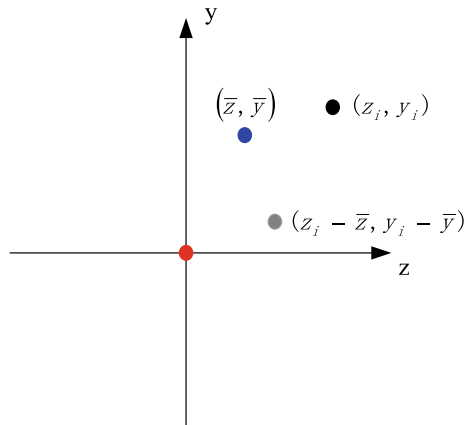
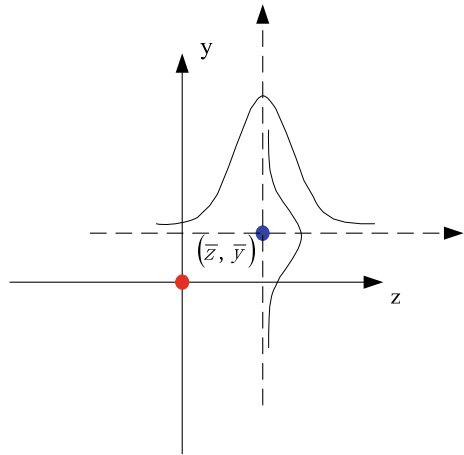


**Fig. 2** Schematic diagram of the distribution of shooting intensity in high or low or horizontal directions



The shooting stability of a shooter can be evaluated by shooting density by comparing the spread standard deviation in the horizontal and vertical directions. Because in the horizontal and vertical directions, projectile dispersion independently follows the normal distribution, as shown in Fig. 2, that is:

$$z \sim N(\bar{z}, \sigma_z^2)$$

$$y \sim N(\bar{y}, \sigma_y^2)$$

Here are two standard deviation parameters of normal distribution  $\sigma_z$  and  $\sigma_y$ , are all set effective participation projectile data to calculate the standard deviation, and suggest that the small arms shooting intensity. Standard deviation parameters in horizontal and vertical directions  $\sigma_{zi}$  and  $\sigma_{yi}$  were calculated separately for each set of projectile data. It indicates the dispersion degree of the horizontal direction and vertical direction in group  $i$ .

### 3 Application Examples

The three shooters used an automatic rifle to shoot each 100-m vertical target with one set of precision. The performance data and the revised data are shown in Table 1.

According to the calculation of the data in the table, the average coordinates of the center point  $(\bar{z}_1, \bar{y}_1)$ ,  $(\bar{z}_2, \bar{y}_2)$ , and  $(\bar{z}_3, \bar{y}_3)$  of the three shooters and the distance from the origin of the coordinates to the aiming checkpoint are 0.283, 0.608, and 0.283, respectively, and the distances from the average impact point are 0.1, 0.45, and 0.41, respectively. If only from the analysis of the deviation of shooting performance data relative to the aiming checkpoint, the shooting level of shooter 1 and shooter 3

**Table 1** Test results of the method for evaluating the level of shooting that attenuates the effect of small arms on accuracy

Shooter 1		Shooter2		Shooter3		S1 revised data (cm)		S2 revised data (cm)		S3 revised data (cm)	
$z_1$	$y_1$	$z_2$	$y_2$	$z_3$	$y_3$	$z'_1$	$y'_1$	$z'_2$	$y'_2$	$z'_3$	$y'_3$
0	-2	-1	-2	-2	-1	-0.2	-1.9	-1.2	-1.9	-2.2	-0.9
1	-2	1	-1	-2	1	0.8	-1.9	0.8	-0.9	-2.2	1.1
-1	-1	0	-1	-1	-1	-1.2	-0.9	-0.2	-0.9	-1.2	-0.9
1	-1	1	-1	-1	0	0.8	-0.9	0.8	-0.9	-1.2	0.1
-1	0	-1	0	2	1	-1.2	0.1	-1.2	0.1	1.8	1.1
0	0	2	-1	-1	1	-0.2	0.1	1.8	-0.9	-1.2	1.1
2	0	2	1	-2	-2	1.8	0.1	1.8	1.1	-2.2	-1.9
-1	1	1	1	1	-1	-1.2	1.1	0.8	1.1	0.8	-0.9
1	1	0	2	2	-1	0.8	1.1	-0.2	2.1	1.8	-0.9
0	2	1	3	2	1	-0.2	2.1	0.8	3.1	1.8	1.1
$\bar{z}_1 = 0.2$		$\bar{z}_2 = 0.6$		$\bar{z}_3 = -0.2$		$\bar{z} = 0.2$					
$\bar{y}_1 = -0.2$		$\bar{y}_2 = 0.1$		$\bar{y}_3 = -0.2$		$\bar{y} = -0.1$					
$\sigma_{z_1} = 1.066$		$\sigma_{z_2} = 1.075$		$\sigma_{z_3} = 1.751$		$\sigma_z = 1.324$					
$\sigma_{y_1} = 1.316$		$\sigma_{y_2} = 1.595$		$\sigma_{y_3} = 1.135$		$\sigma_y = 1.322$					



can be preliminarily determined to be the same; but the impact of shooting accuracy is reduced from the results, it is not difficult to see that shooter 1 has better shooting level than shooter 3.

By comparing the standard deviation of the three shooters' projectile data,  $\sigma_{z_1} < \sigma_{z_2} < \sigma_z < \sigma_{z_3}$ ,  $\sigma_{y_3} < \sigma_{y_1} < \sigma_y < \sigma_{y_2}$ , it can be preliminarily concluded that shooter 1 is more stable than shooter 2 in the horizontal direction, and shooter 3 does not play the concentration level of the automatic rifle in the horizontal direction. Shooter 3 is more stable in the vertical directions than shooter 1, and the shooter does not have the level of intensity that the automatic rifle should have.

This application test only deduces the method of shooting level assessment proposed in this paper, because there is not enough sample data, the accuracy and reliability of the calculated accuracy of small arms are not that high, and the conclusion obtained will naturally deviate from the actual situation.

The proposed method is suitable for more shooters using the same small arms cases; the situation is more common in shooting training and examination in the army; according to the theory of mathematical statistics, the more projectile data samples involved in the calculation, the more accurate and reliable the results. Therefore, a shooting data file can be established for each small arm to store the shooting data by depending on the automatic target reporting system or the computer system. After accumulating large enough sample data, the precision data of small arms obtained will be more accurate and reliable, and then the evaluation method proposed in this paper will have a higher credibility to evaluate the shooter's shooting level. At the same time, due to the great difference in the level of shooters, the shooting performance data of all shooters cannot be included in the calculation of the accuracy of small arms, but the projectile data that do not accord with the accuracy characteristics of small arms should be eliminated in the calculation process.

**Compliance with Ethical Standards** The study was approved by the Logistics Department for the Civilian Ethics Committee of PLA Army Academy of Artillery and Air Defense Zhengzhou Campus.

All subjects who participated in the experiment were provided with and signed an informed consent form.

All relevant ethical safeguards have been met with regard to subject protection.

## References

1. GJB3484-98, Methods of test for performance of firearms
2. GJB3995-2000, Method for calculating accuracy of small arms shooting
3. Shan Y, Tian H, Liao Z et al (2013) Study on shooting accuracy and characterization of small arms. *J Nanjing Univ Sci Technol* 37(1):112–116
4. Wang L, Liu Y, Zhou D (2019) Improved shooting performance evaluation model based on dispersion error analysis. *Ship Electron Eng* 2019(1):106–109

# On the Re-understanding and Prospect of Warfighting Experiment



Boqi Wang, Jiang Luo, Wei Yu, and Hongjun Cheng

**Abstract** With the rapid development of scientific technology, the developed countries in the world begin focusing their military training reform on warfighting experiment to create realistic battlefield environment and carrying out actual combat by computer simulation technology. This plays a very important role in increasing training beneficial result and forming quick combat capability. Warfighting experiment is a scientific testing method. In the process of research, it adopts various natural science technology, for example, information gathering and processing, computer simulation, communication network and so on. At the same time, the research questions will be examined qualitatively and quantitatively to get clear result by the imitation of natural science methods. With the development of information technology, intelligent, network and virtual reality, these new technical means will be put into warfighting experiment continuously.

**Keywords** Warfighting experiment · Military training · Direction

## 1 The Nature and Function of Warfighting Experiment

### 1.1 The Connotation and Nature of Warfighting Experiment

Warfighting experiment is a kind of research method in essence. It has formed a whole set of theory and has become the important content in the new military reform by the rapid development of computer simulation technology in recent decades.

---

B. Wang · J. Luo (✉) · W. Yu · H. Cheng  
Air Defense Forces Academy, Zhengzhou 450052, China  
e-mail: [luojiang.2010@163.com](mailto:luojiang.2010@163.com)

© The Editor(s) (if applicable) and The Author(s), under exclusive license to Springer Nature Singapore Pte Ltd. 2021  
S. Long and B. S. Dhillon (eds.), *Man-Machine-Environment System Engineering*, Lecture Notes in Electrical Engineering 645,  
[https://doi.org/10.1007/978-981-15-6978-4\\_106](https://doi.org/10.1007/978-981-15-6978-4_106)

925

### **1.1.1 Warfighting Experiment is Originated from the Thought of Natural Science Experiment**

Experiment, this noun, in natural science refers to carrying out some kind of activity in order to test a scientific theory or hypothesis. Warfighting experiment is the actual application of this idea in military field. Through scientific experimental method, military problem can be researched, military decision result can be tested and warfighting theory and way can be checked [1].

### **1.1.2 Warfighting Experiment is a Scientific and Effective Military Research Method**

Warfighting experiment is a scientific testing method. In the process of research, it adopts various natural science technologies, for example, information gathering and processing, computer simulation, and communication network and so on. At the same time, the research questions will be examined qualitatively and quantitatively to get clear result by the imitation of natural science methods.

### **1.1.3 More Emphasis on the Factor of Human in the Process of Warfighting Experiment**

Compared to natural science experiment, warfighting experiment applies to military requirement and military activity is the combat between people in essence. In the research process, the changing factors like staff capability, operational equipment and even the warfighting morale which is hard to analyze quantitatively should be taken into account. So, it limits the development of warfighting experiment research method.

## ***1.2 The Meaning and Function of Warfighting Experiment***

Today, the military revolution is constantly developing. Warfighting experiment is playing significant role in helping the application of all countries' army in the future battle field. Warfighting experiment is a powerful assistant in the transition of army. Especially when facing the challenges of unidentified opponent in the future, unclear situation of warfighting form and uncertainty warfighting environment, it seems more important. Warfighting experiment combines the latest scientific technology on one hand to make sure the scientific effectiveness; on the other hand, it is just experiment, so we do not have the problem of casualties and loss of equipment. The two points will make the decision maker have more reasonable reform plan and accept the risk calmly.

### **1.2.1 “Scenario” of Future Warfighting**

Many uncertainties of the future warfighting make us must actively imagine the battle. Warfighting experiment makes increasing army warfighting capacity as the core, so it is an ideal way to practice new concept and theory. The development of computer technology provides solid technical support for the analysis, test and evaluation of warfighting power and hypothesis of the warfighting experiment. Foreign armies have many successful examples in this field.

Take American army as an example, Gulf War, Kosovo War, Afghanistan War and Iraq War all are the gains from the application of warfighting experiment. Long before Gulf War, American army took advantage of warfighting simulation system developed by RDA Company to fully simulate and analyze the whole process from preparation, plan, action and commanding of the future battlefield. And at last, what we saw is the famous “100 hour’s ground war” which was a classic warfighting plan.

### **1.2.2 “Greenhouse” of the Actual Combat Training**

Training must satisfy warfighting requirements, and only in this way, it can stand the test of actual war. This point of view is agreed by almost everyone. The simulation capacity is providing help for the actual combat training. Now, digital technology is developing quickly, engineers set up geographic database of war environment and stockpile large basic data of the enemy, our personnel and weapon equipment to create an “artificial environment” which is highly like the actual warfighting. By simulating the difficulties of the future war, army’s adaptive capacity, decision-making ability and warfighting power are developed. We can fight confidently in the familiar battlefield in future.

### **1.2.3 “Touchstone” of the Military Revolution**

Military revolution creates a large number of new warfighting method and new equipment. How to test their scientificness and effectiveness and the equipment’s reliability? Warfighting experiment offers solution. By taking advantage of warfighting experiment, we can research war plan, decision and training. We can examine the new equipment system without using personnel and actual equipment. For example, American army has researched and trained in warfighting experiment laboratory for a long time and they have achieved a lot in setting up information network, squad countermeasures tactics and friend or foe countermeasures. The results can guide the idea of actual warfighting and production of equipment. In order to improve the effectiveness of warfighting experiment, by large-scale distributed interactive system, we have realized connectivity of each warfighting experiment laboratory and satisfy the requirement of various categories of troop’s joint warfighting simulation at the same time and in the same space. Problems are settled one by one through the real-time pilot in warfighting experiment evaluation system, and the military revolution

result is positively tested. Warfighting experiment has become a “touchstone” and “whetstone” of military revolution.

## **2 The Current Development of Warfighting Experiment**

At present, after decades’ application and research, developed military countries have already set up warfighting experiment system and establishment and have formed reasonable modeling concepts and collaboration mechanisms. Here, we mainly take American army as an example to analyze it.

### ***2.1 The Idea of Warfighting is Spreading***

In the process of developing warfighting experiment, highly developed military countries emphasize on the education and spreading of warfighting experiment concept. Many military personnel have been trained the warfighting experiment theory in many countries.

American army considers education of warfighting experiment as an important method to agree with warfighting operation and an important link in pushing on new military revolution. Therefore, American army has set up long-period warfighting experiment education strategy, has developed warfighting experiment knowledge base and has written different books which apply for different management personnel. By organizing warfighting experiment theory class regularly and showing the latest research result, they have developed related people’s understanding and awareness.

### ***2.2 Setting up Unified System Management***

Now, warfighting experiment has already pushed on from single exploring period to joint experiment and cooperative research. Therefore, many countries established unified warfighting experiment system and mapped out the scientific and reasonable plan.

American army makes each warfighting experiment laboratory, military functional department, college research organization and industrial department develops warfighting experiment technology in unified coordination. Each coordinated department gives full play to their advantages, so the application level of warfighting experiment has been increased and highly developed [2].

### ***2.3 Pay Attention to Application of the Research Result***

The best research achievement is not shown in laboratory but in war field. It has been accepted in the world that pushing warfighting experiment results on military construction especially on actual combat in the rapidest speed.

## **3 The Prospect on Future Warfighting Experiment**

### ***3.1 The Background of Future Joint Will Be Reinforced Continually***

Local war under the condition of information age will be the combat between systems, and it will be a comprehensive combat in multidimensional space. The success of the war will rely on the common effectiveness of various troops. Only the joint concept can apply for the future challenges.

Under this background, as the preview of real war, warfighting experiment must emphasize the background of joint combat. Warfighting experiment at present is preceded indoor and short of military leader and more direct participation of warfighting army, so the achievement lacks operability and practicability, and it needs more adjustment. Therefore, with the deeper understanding of warfighting experiment, we will pay more attention to the coordinated research of different categories of troop under the same background and make related experiment personnel more diverse, joint participation of command organization with warfighting army, experiment method and place more extensive to apply for the complicated requirements of future joint warfighting.

### ***3.2 The Trend of Element Structure Systematization is Obvious***

Warfighting experiment is made up of various resource elements. They are like modules collected together then form a big system, and each system collects together to form bigger system [3]. Future warfighting experiment will highlight element structure systematization, blend independent management decision, data storage and information transferring together organically to form a large close-related system. In warfighting experiment, we parcel up universal software, hardware and data model resource pool and then assemble them according to application requirement to form a unified technology system which can satisfy service functional needs. The warfighting experiment of arms and services in America represents this trend fully. America's combined forces command is transforming warfighting simulation

system's cooperation on connectivity with arms and services by base computation center. They are striving for constructing a flexible warfighting experiment universal comprehensive system which can be constituted according to mission requirement.

### ***3.3 Continue Application of the New Technical Means***

With the development of information technology, intelligent, network and virtual reality, these new technical means will be put into warfighting experiment continuously.

Traditional simulation model mainly adopts deterministic algorithm or random model to describe the use of equipment. The process and result of warfighting action can only be analyzed quantitatively but cannot respond to much unidentified effect in reality. Based on the knowledge of experts' knowledge and experience, artificial intelligence technology analyzes the process by simulation of thinking reasoning, resolves nonlinear and non-structural complicated problem and provides auxiliary decision for the experiment personnel to improve the authenticity and productivity of warfighting experiment simulation. Single warfighting experiment system is too weak to satisfy the research requirement of future informatization joint warfighting and system confrontation. The application of network technology resolves this question effectively and makes virtual practice which is carried out by different organization at the same time and under the same background come true. So, the expense of army, equipment and personnel is saved, and we can organize larger scale warfighting simulation practice, discover pitfalls and problems in army action, improve the level and beneficial result of warfighting research to promote great progress of warfighting capacity.

## **References**

1. Zhou C, Understanding and grasping of warfighting experiment. Diversified military missions and systems engineering, 552
2. Zhao C, Liu S, Zhang W (2013) Certain characteristics of American Army warfighting experiment. PLA Academy of Military Science, 45
3. Lu Z (2008) The analysis and explanation of the results of the American Army Joint Warfighting Experiment. Foreign Mil Learn 2008(3)

# Research on the Method of Aviation Maintenance Work Based on Hall's Three-Dimensional Structure



Bing Zhao and Haiming Li

**Abstract** Based on the Hall's three-dimensional structure systems engineering thinking and lifecycle theory, this research constructs an aviation maintenance work model including the time dimension, logic dimension and knowledge dimension. Analysis and integration of the aviation maintenance work has been made to improve performance of the aviation maintenance work. The feasibility of the method has been verified by the case of aircraft fault diagnosis and troubleshooting process to prove its guiding significance to the practice of aviation maintenance work.

**Keywords** Aviation maintenance engineering · Hall's three-dimensional structure · Lifecycle theory · Fault diagnosis and troubleshooting

## 1 Introduction

Nowadays, the aviation industry is in the stage of rapid development and expansion. With the increasing complexity of aircraft technical equipment and the shortening update cycle of aircraft model, new requirements have been put forward for the safety, effectiveness and economical efficiency of aviation maintenance engineering [1]. As a typical man–machine–environment system, aviation maintenance engineering involves the mapping between the performance of aircraft systems or equipment and the maintenance ability and the uncertainty of environment change during the whole phases of that system operation, making the maintenance process very complicated, hence bringing difficulties for aviation maintenance engineering management.

To solve this problem, Guo et al. [2] studied the essence of aviation maintenance system and its relationship with other systems from the perspective of engineering management, but they did not provide a methodology to guide engineering practice.

---

B. Zhao  
China United Airlines, Beijing 100076, China

H. Li (✉)  
University of Chinese Academy of Sciences, Beijing 100049, China  
e-mail: [lihaiming17@mails.ucas.ac.cn](mailto:lihaiming17@mails.ucas.ac.cn)



Wen and Li [3] proposed a workflow-based management mode of aviation maintenance support and designed the corresponding information management system, which promoted the digitalization of aviation maintenance management, but rarely involved the accumulation and the management of maintenance knowledge. Based on the availability rate of aviation equipment and the punctuality of task completion, Liu et al. [4] constructed a mathematical optimization model for the human resources of aviation maintenance, which provided a reference for the human resource management of aviation maintenance work, but was unable to bring the impact of environmental factors on the allocations of human resources of aviation maintenance into consideration.

Our study tries to introduce the system engineering methodology and lifecycle theory into the research and practice of aviation maintenance engineering by applying the system engineering thinking and then constructs the aviation maintenance work model based on Hall's three-dimensional structure and lifecycle theory and analyzes the feasibility of the model application. The model constructed can fully reflect the value of maintenance work, helping perfect the new paradigm of aviation maintenance engineering under the development trend of modern aviation industry, and will provide certain inspiration and reference for aviation maintenance engineering management.

## 2 Preliminaries

### 2.1 *Hall's Three-Dimensional Structure*

The three-dimensional structure was proposed by A. D. Hall, an American systems engineering expert; Hall's three-dimensional structure is a systems engineering methodology [5]. The structure is composed of three dimensions, namely time, logic and knowledge dimension, and based on that, various works of systems engineering are established. Hall's three-dimensional structure is also known as "the systems engineering process system" [6], where each phase and step contain the corresponding management contents and objectives, and each step also consists of corresponding management means and methods which are connected to each other to forming an organic system.

### 2.2 *Lifecycle Theory of Maintenance*

According to the lifecycle theory, the growth and development of projects, enterprises, products and systems can be regarded as a process with several phases, and the characteristics and problems of which are worth of studying [7]. On the basis of the value of maintenance work, that is, the positive impact of maintenance work to the

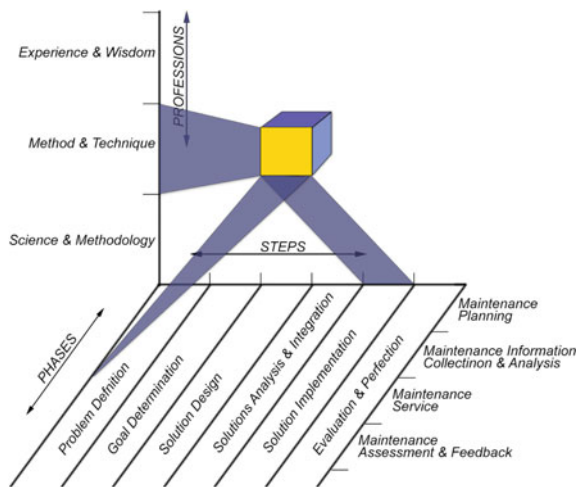
operational reliability of systems or equipment which are based on different principle of science and technology architecture, the maintenance lifecycle can be summarized and mapped to the circulation of the four phases: maintenance planning, maintenance information collection and analysis, maintenance services, maintenance evaluation and feedback. Therefore, the lifecycle of maintenance work could be regarded as the time interval ranging from the recovery to the loss of the technical status of systems and equipment after the last fulfilled maintenance process.

This study attempts to combine the Hall’s three-dimensional structure and maintenance lifecycle theory and reconstructed them to provide some worthy methods or techniques to modern aviation maintenance engineering management, and to strengthen transparency of the maintenance process management and to enhance the efficiency of maintenance work and scientific decision level.

### 3 The Aviation Maintenance Work Model Based on Hall’s Three-Dimensional Structure

Based on Hall’s three-dimensional structure and maintenance lifecycle theory, this study constructs a model of aviation maintenance Hall’s three-dimensional structure to guide the aviation maintenance research and practice. The model is composed of time dimension, logic dimension and knowledge dimension, as shown in Fig. 1.

**Fig. 1** Aviation maintenance work model based on Hall’s three-dimensional structure



### ***3.1 Time Dimension of the Model***

The model's time dimension represents the whole process of aviation maintenance activities. In this study, the lifecycle is divided into four phases: maintenance planning, maintenance information collection and analysis, maintenance service, maintenance evaluation and feedback. At the same time, the critical paths and nodes of each phase are analyzed, and different maintenance management strategies are proposed according to the expected goals of each phase, so as to maximize the value added within the maintenance work lifecycle.

### ***3.2 Logic Dimension of the Model***

The model's logic dimension represents work steps of each aviation maintenance phase, and the work contents and thinking procedures of each phase of the time dimension should be implemented according to those steps. Essentially, in the time dimension, there exists a process from no maintenance work to the completion of the maintenance work, while in the logical dimension, there exists another process which experiences from problem nonexistence in the maintenance work to problem existence. In addition, each link in the logic dimension is not constrained by the irreversibility of time series, which means if the output result of one link is not satisfactory, the previous link could be corrected.

The maintenance process is the backbone of aviation maintenance work, according to the characteristics of aviation maintenance work process, six work steps has been given: problem definition, goal determination, solution design, solutions analysis and integration, solution implementation, evaluation and perfection. All these steps should be implemented in accordance with the order of plan, organization and control to handle the maintenance task process effectively and optimize the allocation of resources.

### ***3.3 Knowledge Dimension of the Model***

The knowledge dimension of the model is composed of three kinds of knowledge: science and methodology, method and technique and experience and wisdom. Among them, science and methodology knowledge include the principles or theories of engineering, management and other related disciplines, such as aerodynamics, materials science, computer science, project management. Method and technique knowledge includes methods and techniques for the organization, analysis and operation of aviation maintenance work; experience and wisdom knowledge includes explicit knowledge (such as maintenance best practices) acquired and accumulated by senior engineers through their keen insights and analytical skills in a very long period as

well as implicit knowledge (such as maintenance know-how) which has not yet been formalized.

## **4 Result and Discussion**

### ***4.1 Aircraft Fault Diagnosis and Troubleshooting***

Fault diagnosis and troubleshooting is a common and important work during the phase of aviation maintenance service; its purpose is to restore the aircraft to its rated technical status and ultimately meet the performance and safety standards required by continuous operations [8]. At present, there are two main difficulties in aircraft fault diagnosis and troubleshooting. Modern aircraft is highly digitalized and automatic, which makes the design principle and operation mechanism of each aircraft system extremely complex. Thus, a single system or equipment's fault will bring a big challenge to maintenance personnel. Secondly, the troubleshooting time is limited. For the sake of economic benefit, airline companies ask their aircrafts for continuous operations as long as possible, so the fault diagnosis and troubleshooting work prefer to be done during break time. If maintenance crew is unable to finish their work within the given time, the companies will have to reschedule to meet new operation requirements or directly cancel part of their operation plans, resulting in economic losses. In view of this, this study takes the aircraft fault diagnosis and troubleshooting as an example to reveal the practical guiding significance of the aviation maintenance work model.

### ***4.2 Matrices of Aircraft Fault Diagnosis and Troubleshooting Work***

According to the model, the time dimension–knowledge dimension matrix of maintenance work is established as is shown in Table 1. Each matrix element includes maintenance work knowledges which are required during each work step.

The time dimension–logic dimension matrix of aviation maintenance work is shown in Table 2. Each matrix element is a set of maintenance activities, and each group activities are able to be decomposed to work behavior or work behavior set, where the specific work contents and steps could be defined more concretely, which will contribute to an efficiently maintenance works and a rational allocation of maintenance resources.

Break down the work content of maintenance service phase to obtain the logic-knowledge dimension matrix of fault diagnosis and troubleshooting, which is shown in Table 3.

**Table 1** Aviation maintenance work matrix—time dimension and knowledge dimension

Dimension	Maintenance planning	Maintenance information collection and analysis	Maintenance services	Maintenance evaluation and feedback
Science and methodology	Reliability theory, strategic management, etc.	Knowledge management, information management, quality management, etc.	Mechanical and electrical engineering, ergonomics, etc.	Management science, value engineering, etc.
Method and Technique	Statistical analysis, decision making techniques, etc.	Knowledge mapping, knowledge mining, database technology, machine learning technology, etc.	Power electronics technology, information technology, etc.	Comparative analysis, questionnaire, expert survey, etc.
Experience and wisdom	Engineering manager’s insights and experience, etc.	Engineers and experts’ background knowledges, insights, experience and best practices in technical documentations, etc.	Engineers’ insights, experience and best practices in technical documentations, etc.	Professional knowledges, experience, analytical ability, etc.

**Table 2** Aviation maintenance work matrix—logic dimension and time dimension

Dimension	Problem definition	Goal determination	Solution design	Solutions analysis and integration	Solution implementation	Evaluation and perfection
Maintenance planning	A11	A12	A13	A14	A15	A16
Maintenance information collection and analysis	A21	A22	A23	A24	A25	A26
Maintenance services	A31	A32	A33	A34	A35	A36
Maintenance evaluation and feedback	A41	A42	A43	A44	A45	A46

**Table 3** Aircraft fault diagnosis and troubleshooting work matrix—logic dimension and time dimension

Dimension	A31 Identify the fault condition	A32 Develop the troubleshooting plan	A33 Design troubleshooting and verification methods	A34 Propose feasible solutions with pros and cons	A35 Troubleshooting Implementation	A36 Fill the record, write the report and improve the work
Science and methodology	Technical status research	Project management, reliability management, etc.	Mechanical, electrical, communication engineering, etc.	Reliability analysis theory, equipment management, etc.	Industrial engineering, human engineering, etc.	Quality management, knowledge management, etc.
Method and Technique	Feedback acquisition, fault information collection methods (flight data analysis, on-the-spot investigation)	WBS, PERT, flow chart, Gantt chart	Eddy current, ultrasonic, magnetic powder, borehole detection technology, etc.	FTA technology, multi-attribute decision method, etc	Human factor reliability analysis technology, operation environment analysis technology, labor safety accident prevention methods, etc.	Database technology, data mining, knowledge graph, etc.
Experience and wisdom	Engineers and experts' insights, experience, etc.	Engineers' insights and experience, etc.	Best practices in technical documentation, engineers' insights and experience, etc.	Best practices in technical documentation, engineers' insights, experience, etc.	Engineers' insights and experience, etc.	QA engineers and experts' insight and experience, etc.

## 5 Conclusion

The aviation maintenance work model based on Hall's three-dimensional structure provides a new way of thinking for the research and practice of maintenance work and helps to form a new maintenance paradigm in big data era. In this study, based on Hall's three-dimensional structure and lifecycle theory, we construct an aviation maintenance work model. As a systems analysis tool, it will reflect the components, workflow and organizational management activities of aviation maintenance work in a comprehensive, systematic and scientific way. By taking aircraft fault diagnosis and troubleshooting as an example, this study discusses the feasibility of the method proposed. In the follow-up research, the model should be further applied to an actual maintenance work by introducing both qualitative and quantitative analysis methods on the interactions between various phases and steps, so as to provide a guidance to aviation maintenance engineering practice.

## References

1. Lai GJ, Pan X (2009) Situation analysis and development trend research of China's civil aviation maintenance industry. *Civil Aircr Des Res* 2009(01):14–17
2. Guo LX et al (2016) Research on engineering and engineering management of the aviation maintenance. *Sci Techn Prog Policy* 27(19):67–70
3. Wen JQ, Li Q (2010) Aircraft maintenance support management based on workflow. *Comput Integr Manuf Syst* 16(10):21960–22205
4. Liu JX, Chen SG et al (2012) The majorizing management of the aircraft maintenance. *Math Pract Theor* 42(03):113–118
5. Hall AD (1969) Three-dimensional morphology of systems engineering. *IEEE Trans Syst Sci Cybern* 5(2):156–160
6. Chen Y (2005) Information valuation for information lifecycle management. In: *Second international conference on autonomic computing (ICAC)*, pp 135–146
7. Tan YJ (2010) *Principle of systems engineering*. Science Press, China
8. Kong HR (2016) Research on the development of aviation maintenance engineering discipline. Report on advances in aeronautical science and technology, pp 150–158+231

# The Use of Unmanned Aerial Vehicle in Military Operations



Huifang Wang, Hongjun Cheng, and Heyuan Hao

**Abstract** In the twenty-first century, unmanned aerial vehicles (UAVs) have gone through big development, and more and more UAVs are used in operations. UAVs have a lot of advantages compared with manned aircraft. UAVs could not only release pilots from dangerous battlefield but also perform various tasks with good efficiency. UAVs can be used in reconnaissance and surveillance tasks and strike targets directly as well as carrying out other missions. However, UAVs still have some limitations, which should be overcome in the future. Especially, the command and control system of UAV is vulnerable. The future UAVs will be stealthy, more intelligent and autonomous. The self-defense capability of UAVs is also undergoing big improvement.

**Keywords** UAVs · Military operation · Developing trend

In future wars, the three-dimensionality of battlefield becomes more obvious, and the struggle for air supremacy will run through the entire process of future wars. Whoever controls airpower will have the important prerequisites for victory in war. Aircraft has played a great role in the air operations since World War I. Armed UAVs will display a greater role in the future operations. With the development of technologies, aircraft without pilot has been developed and put into use, which is called unmanned aerial vehicles (UAV) and commonly known as “drones.” Unmanned aerial vehicles are remotely controlled aerial systems that are used to carry out tasks that are normally conducted or could not be performed by manned aircraft.

---

H. Wang · H. Cheng (✉) · H. Hao  
Army Academy of Artillery and Air Defense, Zhengzhou 450052, China  
e-mail: [peony1001@126.co](mailto:peony1001@126.co)

© The Editor(s) (if applicable) and The Author(s), under exclusive license to Springer Nature Singapore Pte Ltd. 2021 939  
S. Long and B. S. Dhillon (eds.), *Man-Machine-Environment System Engineering*, Lecture Notes in Electrical Engineering 645, [https://doi.org/10.1007/978-981-15-6978-4\\_108](https://doi.org/10.1007/978-981-15-6978-4_108)



**Table 1** MQ-1 Predator and RQ-4 Global Hawk features

MQ-1 Predator	Span	14.8 m	Empty weight	512 kg
	Engine—Rotax	115 hp	Max. loaded	1020 kg
	Maximum speed	217 km/h	Range	1100 km
	Service ceiling	7600 m	Endurance	24 h
RQ-4 Global Hawk	Span	35.4 m	Empty weight	6781 kg
	Engine—Allison	7600 lbf	Max. loaded	10,400 kg
	Maximum speed	629 km/h	Range	22,780 km
	Service ceiling	18,000 m	Endurance	32

*Data source* Northrop Grumman RQ-4 Global Hawk, [https://en.wikipedia.org/wiki/Northrop\\_Grumman\\_RQ-4\\_Global\\_Hawk](https://en.wikipedia.org/wiki/Northrop_Grumman_RQ-4_Global_Hawk); Gheorghe Udeanu, Alexandra Dobrescu, Mihaela Oltean, Unmanned Aerial Vehicle in Military Operations, Scientific Research and Education in the Air Force-AFASES 2016

## 1 Characteristics of UAV

UAVs, especially those small and micro ones, have a lot of advantages, such as small size, lightweight, fast speed, high maneuverability, strong adaptability, easy concealment, low cost and so on. These characteristics enable UAVs to be used in a range of civilian and military fields, such as environmental monitoring, forest fire fighting, resource exploration, electronic countermeasures, surveillance, result assessment, anti-submarine, air operations and so on [1].

The UAVs are not only pilotless but with great autonomy. These two characteristics have made it widely used in various missions. The UAVs are usually much smaller and lighter than conventional aircraft. They can also fly longer distance without considering the fatigue of pilots. The endurance time of Predator and Global Hawk is beyond 24 h (see Table 1). And the endurance distance of UAVs is much longer than before. Because of small size, UAVs can easily conduct vertical take-off and landing, which makes them adapt to various operation environments.

## 2 UAVs Can Be Used to Carry Out Various Tasks Under Various Conditions

In conventional operations, surveillance is achieved by radars, GPS and other monitoring system. Nowadays, UAVs are used to carry out surveillance for important missions. UAV reconnaissance and search are the earliest and most mature functions since they were invented. UAVs mainly rely on cameras, camcorders, low-light night vision devices, infrared scanners and small radars installed on them to implement reconnaissance and search functions. When the reconnaissance area is large, the terrain is complex, or due to social factors and other restrictions, it is not conducive to man reconnaissance on the spot, UAVs can assume the task of reconnaissance and

search. UAV-mounted sensors can fill the existing gap between field observations and traditional air- and space-borne remote sensing, by providing timely detailed three-dimensional images or videos over relatively large areas. These images and videos can be retrieved when needed.

Firstly, UAVs can monitor air traffic. The air traffic information will facilitate commanders to decide the allocation of airspace and avoid unnecessary collision with friendly forces or civilian aircraft. Secondly, UAVs can easily monitor specific ground objects, especially moving ones, which has been proven effective in some operations. With good cameras and signal transiting system, the first-hand information will be transited to the decision-makers soon. Even though the unmanned surveillance aircraft is detected and shot down, because of remote control, pilots are relatively safe. Thirdly, UAVs, especially those small and micro ones, can go into the buildings for detailed information and clear images, which cannot be performed by those manned reconnaissance aircraft. The timely images will be displayed on screens for commanders to watch and help them make decisions on the spot. Without pilot aboard, UAVs are mainly used in boring, harsh and dangerous environment.

## ***2.1 UAVs Can Conduct Reconnaissance and Surveillance Task***

In this context, UAVs have considerable potential to be used as reconnaissance aircraft. The USA is the first country in the world to develop and use ISR UAV systems. The existing U.S. UAVs have formed a multi-layered, multi-typed UAV technology system, covering high, medium and low altitude, long, medium and short range, strategic and tactical levels and attack and confrontation. With the largest number of military UAVs, the research and development and procurement costs of the USA exceed two-thirds of the world's total UAV expenditures.

In Afghanistan and Iraqi wars, UAVs have gone through big improvements. Cameras and sensors are mounted and linked to the global telecommunication system, which allowing long-distance control. The information attained by UAVs is processed by computers and combined with intelligence of other sources, such as CIA and other military spy agencies.

After the September 11 attacks, Predators, armed with Hellfire missiles, and designated MQ-1L, were deployed in Afghanistan and put into operations. Predator is the first UAVs to fire Hellfire in combat. After that, the armed UAVs are used a lot in operations [2].

## ***2.2 UAVs Conduct Direct Strike on Targets***

The role of UAVs in the reconnaissance field makes them also applicable to battle-field situational awareness and communication and command. High-altitude UAVs and low-altitude rotor UAVs, as well as early warning aircraft, ground stations, communication satellites, etc., can build a three-dimensional and multi-layered complex communication and command network, which will display great advantages in command and control and dispatching troops and sharing information. When mounted with missiles or rockets and loaded with bombs, UAVs can conduct strike directly [3]. Unmanned operation platforms represented by UAVs can perform not only intelligence reconnaissance and surveillance but also armed strikes.

On September 14, 2019, the Houthi movement in Yemen used drones to attack the state-owned Saudi Aramco oil processing facilities at Abqaiq and Khurais in eastern Saudi Arabia. Although Saudi Arabia has good early warning system and missile defense system, MIM-104 Patriot, it still failed to stop the cruise missiles and swarm of drones' attack on the two oil facilities. The global financial markets were destabilized somewhat. The early warning system and missile defense system of Saudi Arabia are used for targets of medium and high altitudes. Those cruise missiles and drones flew at low altitude, too low to be detected by conventional radar systems. The cruise missiles and swarm of drones caused big fire in the two oil processing facilities. Both facilities were damaged and shut down for repairs. This attack cut Saudi Arabia's oil production by about half, representing about 5% of global oil production.

## ***2.3 Other Functions that UAVs Can Perform***

UAVs can be used to simulate aerial maneuvering targets for military training. This will play a great role in the military buildup. Some terrain, especially mountainous area, will block or absorb radio and microwave signals. The transmission of signals will be affected. UAVs can also be used to fly to or pass the difficult terrain and stop on top of mountains or hover in the air to act as the relay station.

## **3 Potential Limitations of UAV**

Although UAVs are quite advanced and can carry out various military missions, there is also a need to identify and understand the potential limitations of UAV under current and future conditions. Now that, UAVs are used as platforms of surveillance or firepower, and the communication and command system should be reliable all the time. The anti-jamming capability should be strong. The endurance time and distance should be long enough for some tough tasks. Therefore, the sensors, processing

technologies, retrieval algorithms and evaluation techniques should also be improved and harmonized together, so as to give full play of UAV advantages.

Conventional military aircraft is controlled by pilots with information from ground-based systems, satellite-based systems and on-board systems. The navigation system is multi-layered. When one system fails, backup system can be activated. Even all information systems fail, pilot can make decisions themselves. For UAVs, things are much different. The remote control of UAV needs to be precise but usually single-sourced. There is no redundancy for UAV control systems. Some environment is GPS-denied, and then, control system of UAV should be based on other information system, or high autonomy will be required.

The performance of UAVs has been greatly improved in last 30 years. However, the development of high-tech in other fields has caused drastic changes in the application and combat environment of UAVs, and UAVs in operations are faced with more challenges and greater danger. Under many conditions, a single UAV cannot fulfill the mission, and swarm tactics are necessary. The drastic changes in the environment make it impossible for a single drone to effectively complete the assigned tasks. For example, due to the limitation of the working angle of the sensor, a single UAV cannot cover all the operation area, and several UAVs will be used at the same time for the simultaneous all-round reconnaissance. And sometimes, if one UAV has malfunctions, it will take time to fly another UAV to the target area.

Therefore, for one mission, several UAVs will be used at the same time in order to achieve the desired result and try to avoid mission failure. The cost of UAV should not be too high to afford, which requires the manufactures to decrease the cost while ensuring the performance of UVA.

## **4 Developing Trends of UAVs**

During recent years, in the conflicts of Middle East, quite a lot of UAVs are shot down. The survivability of UAVs is in great danger. Conventional air and missile defense and other military means have posed great threat to UAVs. Once UAVs are detected, the probability of being shot down or destroyed is quite high. Although the remote control mode releases pilots from direct battlefield involvement, the reacting time of UAV when faced with sudden change of conditions is also long because information processing will take some time.

### ***4.1 The Stealth Performance is Required for UAVs***

In order to enhance survivability, UAVs in operations need to be stealthy. Therefore, the material and technology used to conventional stealthy aircraft should also be used on UAVs. Material that can absorb radar waves and infrared light can be used

to coat UAVs. The use of fuel added with anti-infrared radiation chemical materials, reducing surface gaps, and using low-noise engines can effectively improve the stealth performance of UAVs.

The U.S. Air Force has completed XQ-58A Valkyrie demonstrator's inaugural flight at Yuma Proving Grounds, in Arizona, in March 2019 [4]. It is a long-range, high-subsonic unmanned combat air vehicle with stealth technology. The Valkyrie is designed to be stealthy and with low radar signature. Its configuration is similar with the F-35 Joint Strike Fighter. This UAV and its derivatives are anticipated to perform a range of missions, such as including high-altitude flying, defensive and offensive counter-air maneuvers, suppression of enemy air defenses and so on. One XQ-58A Valkyrie is estimated to cost \$3 million, while an F-35A is expected to cost roughly \$85 million. The low cost means that XQ-58A Valkyrie can be put into operations frequently and can be lost or destroyed without too much concern.

## ***4.2 Improve the Intelligence and Autonomy of UAV***

UAVs should be made more intelligent and autonomous with adoption of new advanced technologies [5]. UAVs can be designed to execute autonomous actions. When a UAV encounters an unexpected situation, it can avoid danger in accordance with a pre-programmed procedure and complete the task in compliance with the remote command. In order to complete tough tasks in complex electronic-magnetic battlefield environments, command and control systems and firepower systems should be highly integrated and intelligent. Autonomy of UAV will be greatly improved through pre-programmed procedures. When the UAV system is intelligent and autonomous enough, the UAV operators would be able to operate large numbers of drones at one time, which would achieve better combat effect.

## ***4.3 Enhance the Self-defense Capability of UAV***

In January 2018, an Islamist rebel faction of Syria launched 13 armed drones in an attempt to attack the Hmeimim air base and Tartus naval facility in western Syria. Russian forces were able to overpower radio signals for some of the drones and destroy other drones with short-range Pantsir-S1 anti-aircraft missile systems. For the Islamist rebel faction of Syria, those drones failed to fulfill the mission, and all were lost or destroyed, which means that the self-defense or survivability of UAV should be improved.

With the development of remote sensor technology, UAVs will be able to detect opponents from a longer distance. Early warning system will be more effective, thereby UAVs can avoid adversary firepower early or have enough time to counter-attack. Radar warning system, radar jammer and anti-tracking devices are all good

choices for UAVs to enhance self-defense capability. Air-to-air missiles can be also adopted by UAVs, so as to find enemy earlier and take preemptive actions.

Unmanned aerial vehicles can be used in various conditions and have greatly changed operation environment in various ways. With the use of UAVs, the casualty will decrease, while the requirement for technique support will be increased. More soldiers or operators will not necessarily go to the front of battlefield directly but operate UAVs in the back. UAVs are relatively smaller and more flexible in use than other aircraft and cost less. UAVs should be adopted properly with sufficient target information and good communication and command system without unintended engagement with friendly aircraft. UAVs will change the operation mode from big formation to smaller and disperse operations. However, the use of UAVs is faced with threats such as electronic jamming and bad meteorological conditions.

## References

1. Primatesta S, Rizzo A, la Cour-Harbo A (2020) Ground risk map for UAVs in urban environments. *J Intell Rob Syst* 97:489–509
2. Bowden M (2013) How the predator drone changed the character of war. *Smithsonian Magazine*, Nov 2013. <https://www.smithsonianmag.com/history/how-the-predator-drone-changed-the-character-of-war-3794671/>
3. Zhao L, Research on operational rules of US UAV close air support. *Ship Electron Eng* 40(1)
4. Rempfer K (2019) Air force offers glimpse of new, stealthy combat drone during first flight, 8 Mar 2019. <https://www.airforcetimes.com/news/your-air-force/2019/03/08/air-force-offers-glimpse-of-new-stealthy-combat-drone-during-first-flight/>
5. Task Force Co-chairs, Gen. Abizaid JP (US Army, Ret.) (2015) Recommendations and report of the task force on US drone policy, 2nd ed. The Stimson Center

# The Construction Method and Research of Military Online Courses



Hai Chang, Shuai Mu, and Rui jie Wang

**Abstract** Rich and excellent online courses are the important learning carrier for the learners. Contents design methods are produced in the article for the topic—online course construction in the military vocational education involving contents of the courses should circle around the post need, distillation of the language points should apply with the online learning system, teaching contents should match the show form in the learning carrier. And the teaching methods and skills are shared in the article from teaching ways, teaching language speed, to the content explanation and so on. Suggestions are made how to name the courses, apply the teaching resources and design the examinations. Good ideas are offered in the article for the construction of online courses.

**Keywords** Military vocational education · On-line course · Course design · Classroom teaching

Online course is the innovation in the teaching model in education in the “Internet+” time. It is the important carrier to develop military vocational education. The teaching group should make full and complete preparation for the content design and online classes in order to realize the goal to attract the officers and men to join and to realize the transmission from knowledge to combat effectiveness excellently as well.

## 1 Contents Design for the Online Courses

### 1.1 *Contents of the Course Must Circle Around the Post Need*

Need from the Army is the origin to develop the military professional education, and it is base to have the online course construction. Nowadays, however, the problem

---

H. Chang (✉) · S. Mu · R. Wang  
Artillery and Air Defense Forces Academy, Zhengzhou Campus, Zhengzhou 450052, China  
e-mail: [skyshield@163.com](mailto:skyshield@163.com)

© The Editor(s) (if applicable) and The Author(s), under exclusive license to Springer 947  
Nature Singapore Pte Ltd. 2021  
S. Long and B. S. Dhillon (eds.), *Man-Machine-Environment System Engineering*, Lecture Notes in Electrical Engineering 645,  
[https://doi.org/10.1007/978-981-15-6978-4\\_109](https://doi.org/10.1007/978-981-15-6978-4_109)

in the teaching contents for the online courses is overloading in theoretical narration but less in practice, which does not meet the practical needs of the officers and men and lessens their learning enthusiasm [1]. The causes for this are that the designers do not know the needs of the officers and men, and the contents do not apply with the individual progress program still. Contents design of the online courses should go around the post needs on the basis of the rules making up what is short and strengthening what is weak. In this way, the education may realize the aim to help the officers and men be talents with study and be qualified for their positions. And in this way, the contents of the online courses might meet the needs of the troops and the fighting more.

### ***1.2 Distillation of Language Points Should Match Online Learning Traits and System***

How to segment the teaching contents, how to distill the language points and how to decide the structure in teaching design of the online courses should be considered first. Online courses belong to the category of “fragmentation.” Usually, the learner concentrates on the video with an average of about 10 min [2]. Therefore, he hopes to read a short and pithy, practical and convenient passage so that he can master and understand easily. For this reason, the videos for “fragmentation learning” are most popular. Furthermore, the key point of the online course design is to decide the duration and contents of each knowledge point. In the procedure of segmenting, the whole knowledge should be segmented into different knowledge points according to certain logic, and each of them should be relevantly complete and independent. The title for each language point should be distinct or pithy, which makes the learner have a clear learning goal and have an active expectation for the learning result before learning.

### ***1.3 Teaching Contents Should Match the Show Form in the Learning Carrier***

Cartoons, videos and pictures, etc., can be integrated in the teaching videos for the online courses in order to make the contents vivid and the learner master the knowledge and skills with a fast speed. The recording forms of the online course are the following—lecturing in the classroom, interviewing, practice, screen interaction and cartoons [3]. Each of them is for the use of different type of teaching contents, such as the abstract concepts are usually used in classroom lecturing, case analysis in interviewing and operation in weapon practice. While recording, the designer should try his best to avoid doing this without distinguishing the language points and doing this with no guide of the lecture contents. Even the language point of “xx



weapon operation and application” appears in the video, which is suitable in practice, but recorded as lecturing in classroom. Then, the instructor explains with the PPT together with great effort, what else the teaching results? Therefore, the teaching contents and the show form of the video should match well, and the design should be pithy and optimized to help the students have the best results.

## **2 Lecture Skills of the Instructor in Class**

### ***2.1 Address Properly While Having Online Courses***

The instructor usually has classes face to face with the students in the traditional lecture. Now, he faces the camera while having online course. The whole time he murmurs in front of the camera perhaps. Meanwhile, the online courses are designed for the autodidacts, these situations in traditional classes, such as discussion, share, communication and question-answer cannot appear in online lectures, which makes the instructor lose his excitement while having classes and leads to dullness in lecture. In order to avoid this, while recording, the design can create a practical class atmosphere to lessen the pressure of the instructor as if in the traditional classes. The instructor can write on the blackboard or underline the accents on PPT while lecturing. This kind of method can make the students concentrate on study and have the feeling of one-to-one teaching air.

### ***2.2 Control Speed of Speaking Appropriately While Lecturing***

The duration of a language point of online course is about 10 min, even the minimum is 3 min. In such a short period of time, a teacher should spread the related contents and language points distilled to the learners, and he or she should not speak slowly while lecturing. According to statistics, the speed of speaking and attraction of a lecture are not in the direct ratio. In other words, too fast speed of speaking cannot improve the attraction. But a video with a speed of speaking 200 words per minute attracts learners much more easily [4]. For, this speed of speaking is popular among the learners. Meanwhile, a bit faster speed of speaking excites the spirits of the learners easily. This requires a teacher should make full preparation before class. In normal case, the shorter the same video is, the more is accepted, and the better the results will be. Therefore, we say, a lecturing teacher should speak clearly, correctly, a bit faster and infectiously.

### ***2.3 Explain the Contents Concretely and Correctly***

Students follow the teacher only in a traditional class [5]. About on online study, the students can select, scan, study again and again what to read. The students can read fast or slowly whatever they like. So, the teacher should come to contents directly, pithily to avoid repetition and redundancy. Too much warm-up will not only lengthen the video but also affect the learners' interests. Some of the language points have been explained too much, such as the whole tactics, performances, duty of the operators about the equipment, which are not available to explain entirely in video. On the contrary, only part of them needs explaining. The rest should be uploaded to the reference for the learners' consulting.

## **3 Problems in Online Course Construction**

### ***3.1 Address Properly in Online Class***

In online class, a learner has the feeling that the teacher is having class for him from the perspective of the learner and he has the sense of friendliness. From the teacher, I am explaining for you, one-to-one class. This feeling helps the teacher to excite the air of study of the learner. Therefore, while having classes online, it is better to use "you" or "we", not "all of you", "everybody" or "classes." In this way, the learners have the feeling respected and accented. Thus, the learning interest is improved, and the results are promoted.

### ***3.2 Make Full Preparation of the Resources for Online Courses***

Resources for online courses are the object of online education, which represent all kinds of digitalized resources, such as the videos, audios, texts PPTs and item banks whether the lecture online is successful or not, the prosperity of the resources plays an important part. Whether the resources are useful or not decides the value of the course online when the lecture team prepares the resources. The most important part of online course is how to develop exercises, to have team cooperation, to do homework correcting, to carry out communication and interaction online. These activities are carried out with a circle around the resources. About the resources of online courses, it is much richer than the traditional classes, which is the advantage of online attracting the learners.

### ***3.3 Design Appropriately Online Tests***

Classroom tests are used to check the study of the students in order to strengthen their study. Final test is carried at the end of a course. Pass it the learner will get the certificate. Usually, a language point has 3–5 items to fill the classroom test. The repeating ratio of the final test and the classroom test is lower 50%. The classroom test and final test should have the multiple choice and true-and-false items. Fill-in-the-blank items are not chosen for the online exam for the reason that if capitalization or lowercase and numbers of blanks cannot match the keys, the automatic grading system will give an X to it. Meanwhile, the test should not be too difficult and too partial so as to crack down the enthusiasm of the learners.

## **References**

1. Haitian Electronic Business and Financial Research Center (2016) One book helps you know education on-line. Beijing Qinghua University Press, pp 97–100
2. Huang X (2015) On course construction of MOOC. Acad J Air Force Aviat Flying Acad 2015(4):74–76
3. Xia C (2014) Idea about the demonstration class construction of net video in military academy. J Educ Technol Res 2014(5):67–69
4. Zhang L, Bai J (2016) Discussion on MOOC construction in military academy. Navy Branch Acad 2016(1):43–45
5. Qi Y, Xu Y (2016) Research on MOOC construction in military academy. Educ Air Force Acad 2016(1):32–34

# Effectiveness Evaluation of VTS Measures on Pilot Candidates Selection



Yu Bai, Qingfeng Liu, Huifeng Ren, Xiaochao Guo, Duanqin Xiong, Yan Zhang, Guowei Shi, and Yanyan Wang

**Abstract** This study aims to evaluate effectiveness of several psychological measures from Vienna Test System. Method A total of 110 male pilot candidates complete Chinese pilot selection psychological test battery and five measures from Vienna Test System. Spearman correlation was used to evaluate the effectiveness of the measures. Results: Spearman correlation analysis results reveal that total score of Chinese selection systems significantly correlate to seven indexes derived from five VTS subtest respectively ( $r = 0.250\text{--}0.508$ ,  $P < 0.05$ ) expect correct numbers of Pilot's Spatial Test. Conclusion: In this study, we test the effectiveness of five measures from VTS in Chinese pilot candidate selection. These five measures are all consistent with our system and be conducive to improvement of selection system.

**Keywords** Psychological selection · Correlation · Psychomotor ability · Spatial ability · Pilot

## 1 Introduction

Flying a military aircraft is a cognitively demanding activity. Military pilots must successively integrate the aircraft into varied operational situations, complete hard missions in hostile terrain and keep safety under difficult circumstances. Pilot selection has played a prominent role in aviation psychology since the invention of aircraft. Hunter and Burke [1] explained that this continued emphasis is because flight is the most mental attribute demanding job and pilot training characterized by high attrition probability is the most expensive training program, especially in the military

---

Y. Bai · Q. Liu · X. Guo · D. Xiong · Y. Zhang · G. Shi · Y. Wang (✉)  
Air Force Medical Center, Fourth Military Medical University, Beijing 100142, China  
e-mail: [wyytv@sohu.com](mailto:wyytv@sohu.com)

Q. Liu · Y. Wang  
Beihang University, Beijing 100083, China

H. Ren  
NO. 92493 Military Hospital of PLA, Huludao 125100, China

services. The US Navy estimates that the sunk costs for student aviators who fail training range from \$500,000 to \$1,000,000, depending on the stage at which failure occurs [2]. The U.S. Air Force has a continuing interest in reducing high rates of attrition and washbacks during initial skills training which led to greater increasing recruiting costs or training times [3].

Since World War I, military aviation psychologists have applied psychological measures to select candidates and predict aviator performance [4]. From then on, a wide variety of personal characteristics including reaction time general mental and reasoning abilities, intelligence, psychomotor skill, mechanical comprehension and spatial measures et al. were evaluated for effectiveness. A theory model of knowledge, skill, ability and other characteristics (KSAOs) and selection battery were developed [5]. USAF uses pilot candidate selection method (PCSM) to accept individuals into flying training programs, which combined Air Force Officer Qualifying Test (AFOQT), Test of basic aviation skill (TBAS) and flying history. The Canadian Automated Pilot Selection System (CAPSS) was used by Canadian to select applicants for pilot training, which is a simulation of a single-engine light aircraft [6].

Chinese Air Force also develops a selection program which includes four measure systems. Psychological test battery consisted of basic cognitive ability test, flying special ability test, simulation flight test and expert interview and observation rating were measured for last decades. In order to improve the selection program and develop new measures, we evaluate several psychological measures from Vienna Test System (VTS) for effectiveness.

## 2 Methods

### 2.1 Subjects

A total of 110 male pilot candidates [mean (SD), age  $18.4 \pm 0.6$  year] were recruited and completed psychological measurement when they participated the Chinese pilot selection program. All subjects had passed the medical examination for selection and had signed statements of informed consent, which outlined the purpose of the experiment and informed subjects of their rights.

### 2.2 Tools

- a. Chinese pilot selection psychological test battery (CPSPT) [7].

Based on two factor theory of intelligence proposed by Spearman, flying ability is divided into basic cognitive ability (general factor) and flying special ability (special factor). Each subtest score and total score (TS) are stanine (Table 1).

**Table 1** Chinese pilot candidates psychological selection test battery

Subtests	Description	Times (min)
Basic ability test (BAT)	A total score combined perception, thinking, comprehension, memory, spatial orientation, et al. abilities measured by distinguishing direction, selecting paired word, regularity array comparing simulated scales, assembling figures, et al.	60
Flying special ability test (FSAT)	It is a multitask psychomotor test. The subject uses two sticks and a pedal to control a cross symbol simulating aircraft posture keeping task	60
Simulation flight test (SFT)	The subject learned to fly a simulation of a single-engine light aircraft in half a day and test by tasks including start the engine, take off, turn up and circle around et al.	240
Expert interview and observation (EIO)	A flight expert and a psychologist interview the candidate and evaluate comprehensive abilities by observation on some group and dynamic activities	120

b. Test battery derived from VTS [8].

VTS is a computer-based psychological assessment which comprises a wide selection of modern personality and ability tests produced by Schuhfried. It's aviation expert psychological test battery aims at need of civil and military aviation field and fulfills the requirement of JAR-FCL3 (Table 2).

### 2.3 Statistical Analysis

Data expressed in  $M$  or  $M \pm SD$  (s) were collected and processed by SPSS 20.0 statistical software package. Spearman correlation was used for analysis;  $P < 0.05$  was set as the threshold value with significant difference in statistics.

## 3 Results

Because of the limited times available, all of the subjects have completed the CPSPT, subtests of VTS are applied according to the available time of each subjective. Sample numbers list in statistical results.

**Table 2** Vienna Test System

Subtest	Description	Times (min)
Gestalt perception test (GPT)	The task is to identify a pre-defined shape (in form of a house) in a pattern and to mark the corners of the house with the mouse as if redrawing them. 30 items	10
Determinations test (DT)	The respondent is presented with color stimuli and acoustic signals. He/she reacts by pressing the appropriate buttons on the response panel or stepping the pedal. The stimuli presentation speed adjusts to the respondent's performance level	10
Decision quality test (DQT)	The respondent must decide which of five bars has the same length as the given one and enter the answer as quickly as possible	5
Pilot's spatial test (PST)	The subject's task consists of specifying the differences between two pictures with regard to the depicted airplane's position (rotation about the three spatial axes)	10
Sensomotor coordination (SMK)	Control an unpredicted moving circular segment with two hands on two sticks to overlap an up-side down T shape in a three-dimensional virtue room. Coordination of two hands, eyes and brain is needed	10

Spearman correlation is applied to analyze the relation between four subtests and TS of CPSPT and eight indexes of five VTS subsets. The results reveal that significant correlation between two test systems (Table 3). CN of PST does not significantly correlate to any index of CPSPT. Because the CN of PST appears an

**Table 3** Correlation between two test systems (*r*)

Items	BAT	FSAT	SFT	EIO	TS
TIR of SNK ( <i>N</i> = 51)	0.236	0.508**	0.168	0.155	0.401**
TIR of SNK2 ( <i>N</i> = 51)	0.231	0.485**	0.193	0.175	0.400**
CN of DT ( <i>N</i> = 110)	0.283**	0.294**	0.071	0.226*	0.338**
MD. RT of DT ( <i>N</i> = 110)	-0.250**	-0.361**	-0.329*	-0.248**	-0.385**
CN of PST ( <i>N</i> = 59)	0.070	0.110	-0.210	0.148	0.147
WE of PST ( <i>N</i> = 59)	0.368**	0.286*	-0.105	0.251	0.380**
GPT ( <i>N</i> = 110)	0.175	0.359**	0.320*	0.134	0.297**
DQT ( <i>N</i> = 103)	0.255**	0.166	0.215	0.127	0.245*

CN = correct number, MD. RT = median reaction times, SCA = WE = working efficiency, TIR = time in ideal range (in %), SMK2 = SMK2 after 5 min

\* *P* < 0.05, \*\* *P* < 0.01

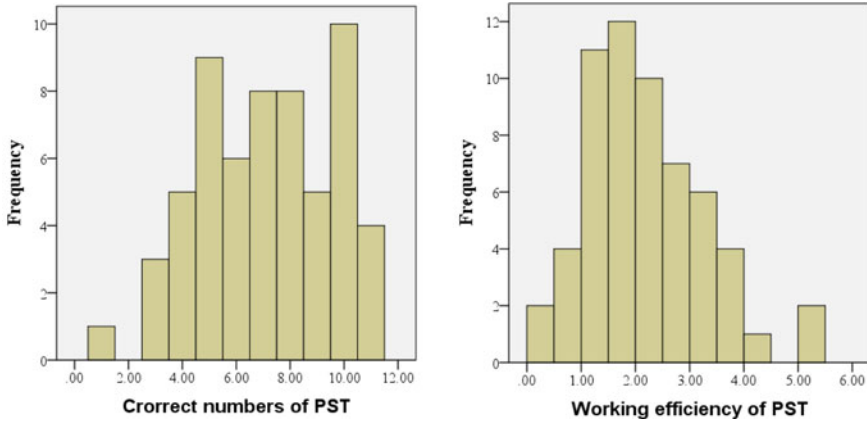


Fig. 1 Distribution of two indexes of PST

uniform distribution, working efficiency index is calculated to acquire a normal distribution (Fig. 1). Then, correlation result becomes significant.

The formula is

$$\text{WE of PST} = \text{CN of PST} / \text{WT} \quad \text{WT means Working time of PST}$$

## 4 Discussion

Since World War I, the military services have found that mental attributes could predict pilot success. Over hundred years, psychological measures have played an irreplaceable role in pilot selection. Psychological pilot selection also helps to improve pilot training and aviation safety in Chinese. Pilot selection program was developed based on flight ability study. Five paper-pencil tests developed by the Fourth Institute of Air Force were applied in Chinese pilot candidate selection since 1978 [9]. The validity of current selection system described in 2.2 is about 0.50–0.70. The predictive validation of PFT pass/fail classification rate was 80%. However, Deng suggests that the validation may decline [7]. The reasons may include the education and ability level change of target population or the increasing psychological need from development of aircraft. New subset should be developed to keep the validity of the system. Therefore, we evaluate the effectiveness of five measures from VTS in Chinese pilot selection.

Five measures aim to evaluate wide range of abilities. In this study relevant to military pilots including psychomotor ability, reactive stress tolerance, attention, reaction speed, spatial orientation, decision making, field independence, et al. The results reveal that all the five measures can predict candidate performance in pilot



selection test. We could learn design ideas from them to improvement of our test system. Some previous studies have the similar findings. Sommer et al. [10] validated a VTS aviation psychology test battery for the selection military pilot trainees. A total of 99 male pilot applicants completed the test variables including figural inductive reasoning, visual short-term memory, determination test, spatial perception and sensomotor coordination test. The sample was divided into suitable pilot applicants and less well-suited pilot applicants according to performance in a standardized flight simulator. The predictive validation of classification rate was 73.8%. The DT contributed to the predictive model with a relative relevance of 18% and SMK is 15%, which provides evidence of the criterion validity of the DT, SMK in the psychological assessment of pilots. Martinussen et al. [11] used a computer-based battery in Norwegian Air Force pilot selection including DT, which obtained a second highest criterion validity of 0.21 among 13 subtests. In another study, Sommer et al. [12] explored an artificial neural network model using Intelligence Structure Battery S2 to predict training performance of 99 pilot applicants for the Dutch Air force. The validity coefficient was 0.84. Incremental validity and relative relevance of decision quality subtest were 0.167 and 141%, respectively.

In our study, SMK has the most relevant correlation with FSAT ( $r = 0.508$ ) for they are all psychomotor ability test in most degree. SMK also has the highest correlation ( $r = 0.40$ ) to TS among five subtest from VTS which may illustrate the importance of psychomotor ability for pilot. Someone argues that the need for psychomotor abilities may have reduced because of the increasing complexity of modern aircraft system and instead the requirement of critical thinking and situational awareness become highlighted [13]. On the contrary, the more rapid and higher maneuverable the aircraft is, the higher psychomotor abilities are needed for pilots. Test of basic aviation skills (TBAS) recently developed selection battery by the USAF is still mainly designed to measure psychomotor tracking ability and multiple task performance skills. Astani and Macarie [14] outlined the ideal ability profile of the student future military aircraft pilot in which psychomotor skills was rated the highest score.

The DT measures reactive stress tolerance and the associated ability to react using a complex selective reaction task paradigm. The task difficulty arises from the need of continuous, rapid and varying responses to rapidly changing stimuli. DT results correlate to all four subtests and TS of the Chinese system, except for CN of DT to SFT. Karner and Neuwirth [15] has used DT to predict driver's performance in actual driving. Therefore, DT may have a cross situation significance.

Spatial abilities are pivotal constructs of all models of human abilities, especially in aviation field, almost all pilot selection battery taking this measure as the most weighted index [16]. Some researchers argued that aviator aptitude test should involve three-dimensional orientation and spatial visualization. However, there some conflict results about PST. Martinussen et al. [11] used a test named Planes in Norwegian Air Force pilot selection, which is similar to PST. The test asked the candidate to move a plane in the direction of the target one using a joystick. Spatial ability needed involving visualization and mental rotation is the same to PST. The criterion validity is just 0.01. This is the same to correct number of PST ( $r = 0.07-0.148$ ,  $P > 0.05$ ). Considering that there are only 13 items in PST and relative small sample ( $N = 59$ )

participate the test, the data appear an uniform distribution. So, we try to calculate another index to better the distribution. Working efficiency which means CN of PST in 100 s is used, and normal distribution is acquired. The correlation to BAT, FSAT and TS is acceptable ( $r = 0.368, 0.286, 0.380, P = 0.004, 0.028, 0.003$ ).

The Gestalt perception test is based on the concept of field dependency proposed by Witkin with classic “Rod-and-Frame Test” [17]. In further research, Fine [18] suggests field-independent persons can react in a specific way to stimuli and can easily distinguish perception details on a neuro-physiological level. This means that Gestalt perception may be the basement of pattern recognition which was relevant to situation awareness. So, Gestalt perception should be stressed by aviation psychologists and used as pilot selection measure.

Decision making ability attracts increasingly attention in aviation psychology field with wide application of modern interaction technology in cockpit. However, measurement of decision making is difficult and isn't independent to the test task and situation. So, simple decision-making situations and visual discrimination tasks in this test may reduce bias of traditional test.

EIO is a very important subtest in our selection system which is similar to assessment center. Comprehensive abilities, motivation and personality are examined in dynamic activity situation. Expert pilot and psychologist are matched to assess the candidate by interview and observation on human interaction activities. Performance in this situation may be different from human-computer interaction test which may partly cause low correlation between EIO and five VTS subtests. Expert pilot's experience is also useful for correct selection.

In this study, we test the effectiveness of five measures from VTS in Chinese pilot candidate selection. These five measures are all consistent with our system and be conducive to improvement of selection system.

**Compliance with Ethical Standards** The study was approved by Civilian Ethics Committee of Air Force Medical Cen-ter of FMMU. All subjects who participated in the experiment were provided with and signed an informed consent form. All relevant ethical safeguards have been met with regard to subject protection.

## References

1. Hunter DR, Burke EF (1994) Predicting aircraft pilot-training success: a meta-analysis of published research. *Int J Aviat Psychol* 4:297–313
2. Helm WR, Reid JD (2003) Race and gender as factors in flight training success. In: Proceedings of the 45<sup>th</sup> annual conference of the international military testing association, Pensacola, FL, pp 123–128
3. Manacapilli T, Matthies CF, Miller LW, Reducing attrition in selected air force training pipelines. [https://www.researchgate.net/publication/27779758\\_Reducing\\_Attrition\\_in\\_Selected\\_Air\\_Force\\_Training\\_Pipelines](https://www.researchgate.net/publication/27779758_Reducing_Attrition_in_Selected_Air_Force_Training_Pipelines)
4. North RA, Griffin GR (1977) Pilot selection 1919–1977 (NAMRL Special Report 77-2). Naval Aerospace Medical Research Laboratory, Pensacola, FL
5. Diane D (2011) Knowledge, skills, abilities, and other characteristics for military pilot selection: a review of the literature. AFCAPS-FR-2011-0003.2011
6. Turnbull GJ (1992) A review of military pilot selection. *Aviat Space Environ Med* 63(9):825–830
7. Deng X, Liu Q, Sun M et al (2011) Prediction validation of pilot selection system. In: Construction of the 90th anniversary of Chinese psychological society & the 14th national academic congress of psychology
8. Schuhfried (2004) Manual of Vienna Test System
9. Wu G (1994) Understanding and suggestions on psychological selection of pilot cadets in Chinese Air Force. *Chin J Aviat Med* 5(1):17–20
10. Sommer M, Arendasy M, Hansen HD, Schuhfried G (2005) Personalauswahl mit Hilfe von statistischen Methoden der Urteilsbildung am Beispiel der Luftfahrtpsychologie. *Untersuchungen des Psychologischen Dienstes der Bundeswehr* 40:39–63
11. Martinussen M, Torjussen TM, Storsve O, Hjerkin O (2004) Pilot selection in the Norwegian Air Force: from paper-and pencil to computer based assessment. In: Proceeding of the 40th applied military psychology symposium, Oslo, May 2004, pp 1–7
12. Sommer M, Häusler J, Koning AJ, Arendasy M (2006) Validation of the Dutch Air Force test battery using artificial neural networks. In: 48th Annual international military association conference, Kingston, ON, Canada
13. Carretta TR, Ree MJ (1996) U.S. Air Force pilot selection tests: what is measured and what is predictive? *Aviat Space Environ Med* 67(3):279–283
14. Astani AI, Macarie A (2013) The ideal ability profile of the student future military aircraft pilot. *Rev Air Force Acad* 1(23):89–94
15. Karner T, Neuwirth W (2000) Validation of traffic psychology tests by comparing with actual driving. In: International conference on traffic and transport psychology, Bern, Switzerland, 4–7 Sept
16. Carretta TR, Retzlaff PD, Callister JD (1998) A comparison of two U.S. Air Force pilot aptitude tests. *Aviat Space Environ Med* 69(10):931–935
17. Asch SE, Witkin HA (1948) Studies in space orientation: I. Perception of the upright with displaced visual fields. *J Exp Psychol* 38:325–337
18. Fine BJ (1990) Field-dependence and judgement of weight and color: some implications for research in human performance. *Hum Perform* 3:259–267

# Research on Internet of Things in Space Flight Training Simulation



Shang Huan, Suqin Wang, and Shaoli Xie

**Abstract Objective:** The purpose of studying Internet of Things (IoT) is to construct the interface network of the space flight training simulator of the space station. **Methods:** Guided by the problem of the interface system of the space station simulator, based on the IoT technology, the space station simulator interface network, which combines the upper Zigbee network and the secondary CAN bus network, is proposed. **Results:** The experiment shows that the interface network solves the problems caused by the complex structure, configuration change, and self-service training of the space station simulator. **Conclusion:** Due to its comprehensive perception, reliable transmission, and intelligent processing, the network is not only suitable for the space station simulator, but also can be applied to other large equipment simulation field.

**Keywords** Space flight · Space station · Simulator · Internet of things

## 1 Overview

Through ground space flight simulation training, astronauts can quickly perceive the mission environment, master the mission skills, and correctly troubleshoot. Therefore, the space flight training simulator is an economical and safe space flight training method [1, 2]. China has successively built a fixed-base full-mission flight training simulator, an extravehicular activity program training simulator, and a rendezvous and docking training simulator, which successfully ensured the manned flight missions from SZ-5 to SZ-11.

Compared with the previous space laboratory, the space station is composed of the core cabin, the laboratory cabin I, the laboratory cabin II, and the cargo cabin, etc.,

---

S. Huan (✉) · S. Xie  
China Astronaut Research and Training Center, Beijing 100094, China  
e-mail: [huan\\_shang@126.com](mailto:huan_shang@126.com)

S. Wang  
North China Electric Power University, Beijing 102206, China

**Fig. 1** Space station simulator of China

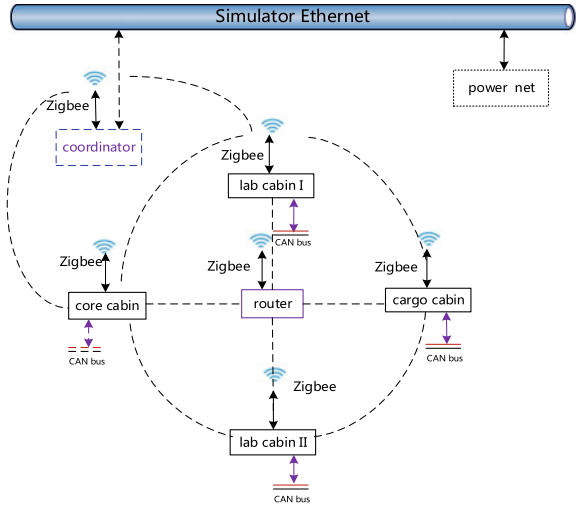


with more complex structure and more advanced technologies. See Fig. 1 for details. Therefore, the R&D of the ground simulator will face new problems: First, the space station will be constructed in stages. In the first stage, the core cabin and the cargo cabin will be constructed; in the second stage, the laboratory cabin I and laboratory cabin II will be constructed. During the construction process, the configuration of the space station is constantly changing. There are various configurations such as “L”, “T”, and “+”. The simulator should respond synchronously. Second, according to the requirements of the training plan, the simulator should be self-service training ability, that is, a single training session may be enabled for a certain cabin, or multiple or even the entire cabin, which requires the space station simulator to upgrade the simulation architecture. Third, the space station simulator is a large-scale semi-physical and person in the loop simulation system. There are a large number of different types of onboard devices required astronauts to operate and system awareness. Therefore, how to effectively connect the device to the simulation system is also a key issue. Aiming at the above problems, it is an economical and feasible solution to introduce the Internet of Things technology and build an open, dynamic, and configurable simulator interface framework mainly based on embedded technology, field bus technology, and wireless sensor network technology.

## 2 Technical Scheme

The space station simulator interface IoT network is designed in two levels. The upper network is wireless LAN (WLAN, for short) based on Zigbee technology, as shown in Fig. 2. Zigbee WLAN mainly consists of one coordinator, four terminal nodes (core cabin, cargo cabin, laboratory cabin I, laboratory cabin II), and routers. The coordinator is responsible for establishing and managing the network and accessing the core switch for data exchange with the simulator server; the terminal nodes are mainly responsible for the transparent transmission of data between different networks, with

**Fig. 2** Simulator WLAN of Zigbee



the gateway function to link CAN network to the Zigbee network; the router is responsible for the wireless network data routing, deployed by network signal strength, providing redundant transmission paths, and improving the robustness of interface network.

There are three main reasons for the adoption of WLAN in the upper network: First, the laying demand of signal cables between cabins is greatly reduced, and there is no need to configure sockets and pipelines from cabin to cabin, which can reduce the construction costs. Second, the simulator can respond quickly to changes in the configuration of the space station without changing the original cable structure, thereby minimizing the cable adjustment, laying, and testing. Third, Zigbee is an emerging wireless network technology with short distance, low rate, and low-power consumption. It has ability to build the large-scale, self-organizing, dynamic, data-centric, highly reliable, and low-cost wireless network. Due to the advancement of the physical layer, it uses OQPSK and DSSS technology to solve the uncertainty of data in the transmission process and uses 16 bit CRC to ensure the correctness of data [3]. The Z-Stack protocol stack provides a convenient development path for quickly implementing the complex Zigbee network. All of these meet the demands of the space station simulator.

The secondary network is based on the CAN bus technology to build the field control bus network, as shown in Fig. 3. Independent CAN bus networks are constructed for the four cabins. For the communication and control demands of different devices, different functional modules are developed, including modules such as IO acquisition, IO drive, A/D, D/A, PWM, relay control, and communication interface conversion. Among which, the main control module is responsible for network management and communication with the host computer; the terminal

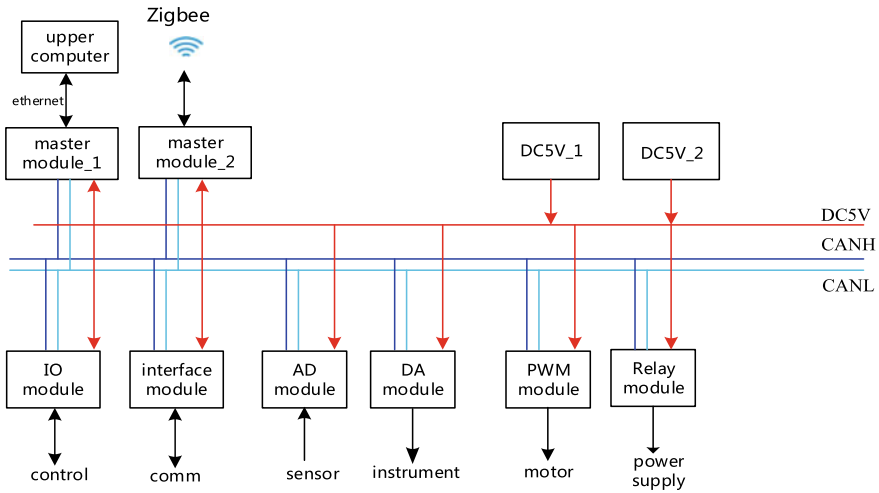


Fig. 3 Simulator CAN bus

node of the upper Zigbee network is another main control module, which is responsible for the transparent transmission of data. The terminal node of CAN network is responsible for the access service of one or more types of cabin devices.

The adoption of CAN bus network for the secondary network is mainly based on three reasons: First, the secondary network is mainly deployed inside each cabin, and wireless communication such as Wifi and Bluetooth already exists in the cabin. As Zigbee and Wifi technologies all choose 2.4 GHz (2.4–2.483 GHz) ISM frequency band, channel conflicts are bound to exist. According to the relationship between packet error rate (PER), separation (distance between interference source and receiver), and frequency offset (Foffset) in the wireless network, it can be seen that the larger the frequency offset and the longer the distance, the better the coexistence performance is in non-frequency hopping systems [4]. While the minimum distance between onboard devices is about 10 cm, only four channels ( $n = 15, 16, 25, 26$ ) of IEEE 802.15.4 fall on the band spacing of the IEEE 802.11 b/g channel. In order to avoid communication interference, moreover, the deployment of device in the cabin will not change usually. Therefore, wired communication is preferred in the cabin. Second, the CAN control bus network is a serial, asynchronous, and multi-host communication protocol. Its short message structure enables efficient and reliable communication. It does not even need to change the software or hardware of any nodes for directly adding nodes in the CAN network, which is very suitable for the extension requirements of the space station task simulator. Third, compared with the 1553B bus (space station orbit bus), the CAN bus features significantly reduce development cost, which is very suitable for ground conditions.

In the case of conditions with several cabins, the upper network and the corresponding secondary network are enabled; in the case of single cabin condition, only the corresponding secondary is to be enabled without the need of enabling the upper

network. The main control module 2 of the secondary network directly connects to the local server via Ethernet for data communication to achieve the purpose of saving power consumption. This simulator interface network framework is consistent with self-service training methods.

### 3 Key Technologies

To implement the simulator IoT interface framework, key technologies such as the perception layer, functional modules, data transmission, M2M communication, and software architecture need to be addressed.

#### 3.1 *Design of Perception Layer*

Comprehensive perception is the first major characteristics of the Internet of Things. Therefore, the perception layer is a key part of the IoT information acquisition of the simulator, and the working status of each device of the simulator is sensed through different electric signal forms. The key to the design of the simulator perception layer is the selection of sensor. The customized sensor is not only based on the working characteristics of each product, but also needs to focus on the adaptability and economy of the simulator. Simulator adaptability means that the sensors are added for the cabin device under the premise that the shape, structure, and other aspects are constrained by real products to meet the signal perception and high-frequency usage demands of the simulator [5]. Therefore, the size of the sensor module must be small, and the assembly should not change the structure and operation of the object as much as possible.

For example, the environmental control sub-system of the space station is equipped with a variety of valves to control gas, liquid, and electricity for purifying the cabin environment. However, the ground simulator is not in the closed space and does not need to be equipped with real device, but it needs to sense the valve openness to simulate the on-orbit environment control process. Therefore, it is necessary to select a sensor to monitor the valve operator's openness. As the valve belongs to the high-frequency operating component, non-contact measuring devices should be preferred to avoid rapid failure due to mechanical wear. If incremental photoelectric encoder is adopted, although it is non-contact, it must patrol zero after restarting; the absolute photoelectric encoder has complex structure, big size, and is expensive, and has poor simulator adaptability. The new type Hall inductive angular displacement sensor has the characteristics of small size, 12-bit resolution, low rotation torque, and high mechanical life. With linear output during 0–360° rotation, different angles always correspond to different output voltages; see Fig. 4 for details. In addition, its output characteristics can be customized to meet special working conditions. The adoption of output characteristic sensor in Fig. 5 can perfectly sense the working



**Fig. 4** Universal output of HS

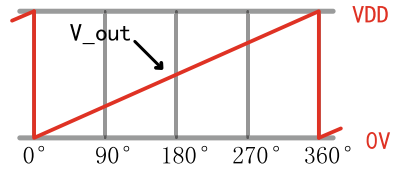
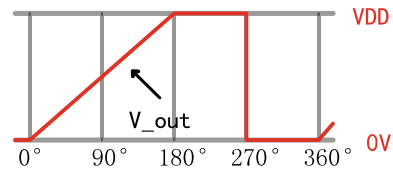


**Fig. 5** Special output of HS



state of the air supply valve,  $0\text{--}180^\circ$  indicates the openness,  $180\text{--}270^\circ$  means pressure relief, and  $270\text{--}360^\circ$  means cut-off. Therefore, the sensor has excellent simulator adaptability.

Even with Hall inductive angular displacement sensor, process design is also required. Align the two axes and keep the rotations synchronized. In order to further reduce the cost, the tri-axis acceleration sensor module (LIS3DH) can also be selected when the requirement on accuracy is not high, and the measurement is performed in the form of surface mount. According to the component values of the static gravity acceleration in  $X$ ,  $Y$ , and  $Z$  axes output by the triaxial acceleration sensor chip, the program can calculate the current position of the valve [6].

### 3.2 Design of Function Modules

The simulator interface network terminal nodes are divided into CAN network nodes and Zigbee network nodes, both of which have specific functions and serve to cabin-borne device objects. According to the standardization and module design requirements, CAN network terminal nodes are divided into dedicated modules and general modules; Zigbee network terminal nodes are mainly gateway modules and other modules.

Dedicated modules are generally responsible for a certain function. The modules are small with low cost and are suitable for mass deployment, covering interface modules such as IO modules, AD modules, DA modules, and SPI and SMBus (I2C). The CAN network dedicated module is based on the C8051F04X SOC chip design, and the Zigbee network dedicated module is based on the TI CC2530 SOC chip design. The module of same function is divided into different versions according to different requirements. For example, the AD module is divided into embedded module and independent AD module. The embedded module directly adopts the AD peripherals integrated in the C8051F04X SOC chip, while the independent AD module is equipped with a special AD chip (ADS1110, 16-bit accuracy) to improve

the acquisition accuracy. As a result, it is generally used for signals acquisition in fine operation occasions such as remote control handle.

The general module chooses C8051F040 as the main control chip, which not only has integrated CAN2.0 controller, but also has abundant analog and digital peripheral resources. By making full use of these peripheral resources and supplemented by a small number of driver chips, IO, AD, DA, SPI, SMBus, and other functions can be realized on a module. As a result, the general module has wider load capacity, which can greatly reduce the number of nodes in the network.

The main function of the gateway module is to bridge the CAN bus network and the Zigbee wireless sensor network, forming an integrated simulator IoT. The gateway module needs to handle both the CAN2.0 protocol and the Zigbee protocol. Because the CC2530 chip does not have dedicated external memory interface, the gateway module design should not adopt the scheme of CC2530 chip with independent CAN controller SJA1000. Considering comprehensively, the dual main control chip is a better solution. Among them, the C8051F040 chip is responsible for CAN network processing, and the CC2530 chip is responsible for Zigbee wireless network processing. Data is exchanged between the two through Uart. The circuit schematic is shown in Fig. 6. The C8051F040 chip configures TX0 and RX0 pins of Uart0 to P0.0 and P0.1, respectively, and the CC2530 chip configures the RX0 and TX0 pins of Uart0 to P0.2 and P0.3. The two can be achieved through the cross-connection of TX0 and RX0.

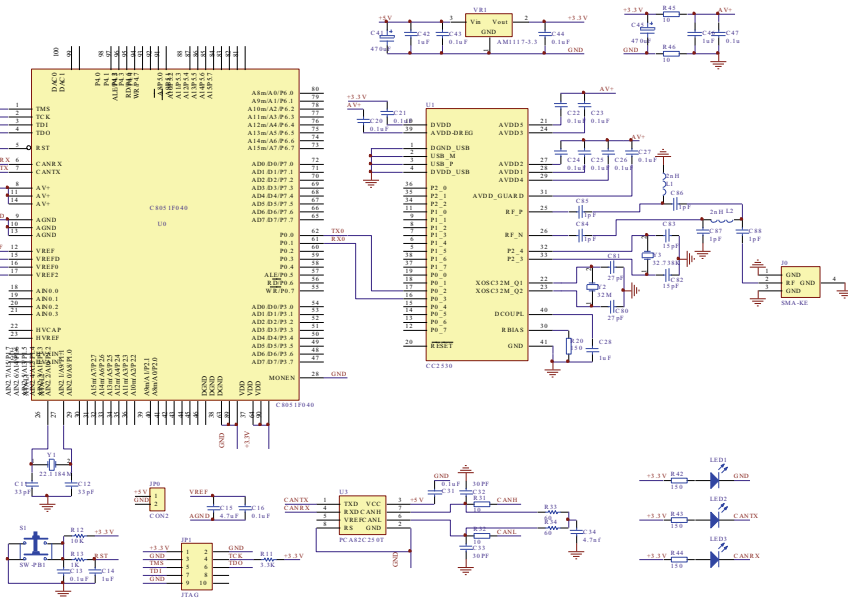


Fig. 6 Gateway schematic

The advantages of this solution are obvious: The dual CPUs are used for processing separately and there is not peripheral to preempt the resources, which guarantees the real-time performance of the system; based on Uart communication, the mature CC2530 module can be selected, so there is no need to consider RF wiring and performance testing, which not only improves the reliability, but also reduces the development cost.

### **3.3 Data Transmission**

Reliable transmission is the second major characteristics of the IoT. The CAN short frame structure, retransmission mechanism, and Zigbee's direct sequence spread spectrum, data transmission response, and communication redundancy mechanisms, etc., all effectively ensure the reliable transmission of network data on the simulator interface. However, because CAN communication uses a short frame structure, the data frame load shall not exceed 8 bytes. If the data packet is directly divided into 8-byte groups and transmitted separately, it will inevitably affect the transmission efficiency. Thanks to the integrated CAN2.0 controller of C8051F040, it has F1, IF2 two independent message object interface registers, and 32 message objects. By combining continuous message objects, data block transmission can be achieved [7, 8].

The combination of message objects is achieved by means of configuration functions. In order to avoid calling conflicts, the program design specifies that the IF1 interface handles sending message objects, and the IF2 interface handles receiving message objects. According to "Bosch CAN User's Guide", the functions to `init_msg_block_TX ()` and `init_msg_block_RX ()` are compiled to implement the combined configuration of message objects. Take sending data block as an example:

```

/* Send message object combination function, Msgst is the start message object, MsGED is
the end message object, and id is the node address participating in bus arbitration */
void init_msg_block_TX (uchar Msgst, uchar MsGED, uint id)
{uint temp;
uchar i;
SFRPAGE = CAN0_PAGE; //enter CAN register page
CAN0ADR = IF1CMDMSK; // IF1 command mask register
CAN0DAT = 0x00f8;
/*WR/RD=1, Mask=1, Arb=1, Control=1, ClrIntPnd=1, TxRqst=0, DataA=0,
DataB=0, */
CAN0DAT = 0x0000; //IF1 mask 1
CAN0DAT = 0x0000; //IF1 mask 2
CAN0ADR = IF1ARB1;
CAN0DAT = 0x0000; //IF1 arbitration 1
temp=id<< 2; // standard frame id is ID28-ID18, need to shift 2 bits to the left
temp&=0x1fff;
temp|=0xa000;
CAN0DAT = temp;
/* MsgVal=1, Xtd=0, CAN standard mode, extension ID is invalid, Dir=1, send */
for(i=Msgst; i< MsGED; i++) //control register of configuring message RAM, EoB=0,
block continues;
{ CAN0ADR = IF1MSGC;
CAN0DAT = 0x0008;
/*NewDat=0, MsgLst=0, IntPnd=0, UMask=0, TxIE=0, RxIE=0, RmtEn=0, TxRqst=0
EoB=0, DLC3-0=1000, load 8 bytes */
CAN0ADR = IF1CMDRQST; //IF1 command request, write frame number
CAN0DAT = i; }
/* control register configuring MsGED message RAM, EoB=1, end block */
CAN0ADR = IF1MSGC;
CAN0DAT = 0x0088;
CAN0ADR = IF1CMDRQST;
CAN0DAT = MsGED; }

```

Assuming that a node no. 8 of a CAN network needs to send 40 bytes at once, message objects no. 1 to no. 5 are configured as a group by `init_msg_block_TX` (0×01, 0×05, 0×08), which is responsible for sending data blocks. In this way, the data length can be set flexibly, up to 256 bytes (32 message objects combined in one and configured as a send object or a receive object), thereby breaking the 8-byte load limit at the application level and avoiding repeated calls to the send functions and receive processing functions, improving the development efficiency.

### 3.4 M2M Communication

In order to meet the long-term operation requirements of the space station, key components and consumable components in the system are backed up, such as instrument controllers and carbon dioxide filter tanks. The previous backup switch requires the upper computer to judge and execute. After the adoption of IoT technology, the switching can be completed directly via M2M communication. The backup device in

the cabin can be realized through the CAN remote frame function [9]: Each node is configured with a remote frame in advance, and the requester sends a remote request frame; when a remote request is received, the sender automatically sends the setting information out and then completes backup switching according to the rules. It can be implemented through the Zigbee network multicast function [10] between the extravehicular backup devices: First, set up a group, and the backup nodes join the group. Take the development in the Z-Stack environment as an example

```

1 aps_Group_t GenericApp_Group; //define a group
2 GenericApp_Group.ID =0x0001; // initialize group ID
3 GenericApp_Group.name[0]=10; // define the group name length
4 osal_memcpy(&(GenericApp_Group.name[1]), "CO2 filter," 10);
//copy group name
5 aps_AddGroup( GENERICAPP_ENDPOINT, & GenericApp_Group);
//nodes join the group

```

Each node publishes its own status information in the group by turn and performs backup switching according to the rules, which does not need the intervention of host computer, realistically simulates the on-orbit working status of the space station, and provides better support for astronaut training.

### 3.5 Software Architecture

Intelligent processing is the third major characteristics of the IoT. In order to improve the versatility and portability of the software, the simulator interface network software adopts the layered architecture, which is divided into hardware abstraction layer, functional module layer, and application layer. See Fig. 7 for details.

The hardware abstraction layer provides hardware access services to the upper layer. It mainly provides the configuration and driver functions of the internal resources on chip, including Uart driver, SPI driver, PWM driver, ADC driver, DAC driver, SMBus (I2C) driver, CAN driver, etc. This layer is designed and implemented by embedded C language, and its configuration function strives for generalization and functional coverage.

The function module layer mainly calls the functions to achieve a series of important functions such as sensor initialization, wireless transceiver driver, and CAN transceiver driver. It can meet the needs of different modules such as dedicated modules, general modules, and gateway modules. Furthermore, it can run directly on the nodes of corresponding terminal.

The application layer software runs on the upper computer and consists of data processing, data display, network monitoring, and fault diagnosis software. These software mainly analyzes and processes network data, real-time monitor network status, online intelligently diagnose, and locate faults.

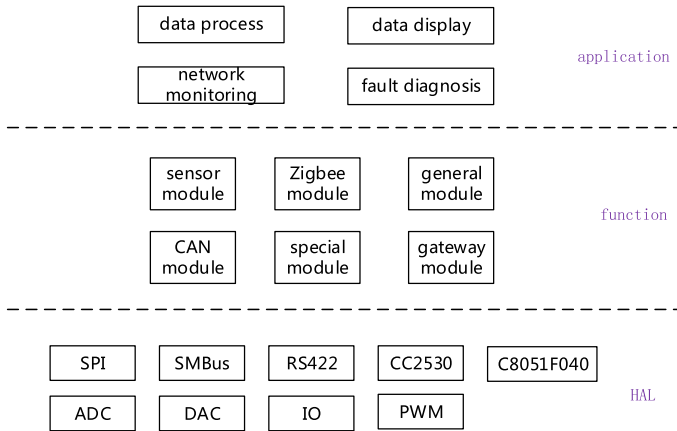


Fig. 7 Software layered architecture

### 4 Verification Test

In order to verify the adaptability of the simulator interface IoT network, three types of experiments are conducted in the laboratory: The first type, which simulates the single cabin operating conditions, is configured with one CAN bus (20 nodes), one coordinator and one gateway module, which mainly verify the connectivity of the network and the functions of the nodes. The second type, four CAN buses (five nodes per bus), a coordinator, a router, and four gateway modules are configured to simulate the configuration change condition. The number and position of the gateway modules can be freely adjusted to verify the networking capabilities. The third type is to simulate device fault conditions. On the basis of the second type of test, two new sets of backup nodes are added, and a certain key device is forced to fail to verify the M2M communication and backup device’s autonomous switching capabilities. The three types of tests have achieved the expected results, which indicate that the interface network based on IoT meets the communication requirements of the space station simulator.

### 5 Conclusion and Prospect

Guided by the problems of the interface system of the space station simulator, based on the IoT technology, the space station simulator interface network, which combines the upper Zigbee network and the secondary CAN bus network, is constructed. The network can link all the devices in simulator together to serve the space flight training simulation and that provide a high-fidelity simulator for astronaut flight training. The experiments show that the network solves the problems caused by

the complex structure, configuration changes, and self-service training of the space station simulator. Due to its comprehensive perception, reliable transmission, and intelligent processing, the network is not only suitable for the space station simulator, but also can be applied to other large equipment simulation field.

**Acknowledgements** This work is supported by the Basic Research Subject of National Key Laboratory of Human Factor Engineering, No. SYFD170051803.

## References

1. Chao J, Chen S (2008) Study on technology of space flight training simulator and Its engineering implementation. *Space Med Med Eng* 21(3):233–239
2. Huan S, Deng H (2011) Design and implementation of the interface system for a space flight training-simulator based on CAN bus. *Space Med Med Eng* 24(5):361–365
3. Wang X (2012) Design and implementation of wireless sensor network on ZigBee. Chemical Industry Press, 2012.05
4. Li J, Yang R, Xiao J (2006) Anti-interference performance of ZigBee and analysis of the mechanism of coexistence in 2.4 GHz ISM band. *Telecom Eng Tech Stand*, 2006.03
5. Huan S, Wang B, Lin W (2014) Design on mobile interactive control for a space flight training-simulator. In: Proceedings of 14th international conference on man-machine-environment system engineering, Springer, Lecture Notes in Electrical Engineering 318, part VII(47):389–398
6. Huan S, Deng H (2015) Research on gravity compensation technology for extravehicular activity training facility. In: Proceedings of 15th international conference on man-machine-environment system engineering, Springer, Lecture Notes in Electrical Engineering 356, part III(43):355–364
7. Tong C (2005) C8051 series MCU development and c language programming. Beijing University of Aeronautics and Astronautics Press, 2005.02
8. Bosch (2000) Bosch CAN User's Guide Revision 1.2. <http://www.silabs.com>
9. CC2530 Development Kit User's Guide. <http://www.Ti.com>
10. Z-Stack Developer's Guide. <http://www.Ti.com>

# Study on Optimization Design for Man–Machine Combination of a Self-propelled Anti-aircraft Gun Vehicle (SODMMMCSPAGV)



Jiwen Sun, Heyuan Hao, Jinxin Li, Junlong Guo, Tao Li, JianFeng Li, Ke Zhang, and Pengdong Zhang

**Abstract** Under the conditions of a self-propelled anti-aircraft gun vehicle operation, some unfavourable factors and the unreasonable operational interface designs effect the operational efficiency of gunner as well as the weapon performance. Thorough analysis of the self-propelled anti-aircraft gun man–machine combination shows us the importance and significance of optimizing the current designs interface. The researchers adopt the method of field test to study the temperature, humidity, noise and interface to influence operations of gunner. With this development, a man–machine combination optimization design proposal for self-propelled anti-aircraft gun vehicle is brought into use. The contribution can have important guiding significance for design and development of a self-propelled anti-aircraft gun vehicle. Furthermore, it also has important military significance to improve the level of gunner training and effectiveness.

**Keywords** Self-propelled anti-aircraft gun vehicle · Man–machine combination · Optimization design

A self-propelled anti-aircraft gun vehicle is an all-weather, automatic tracked armoured anti-aircraft weapon, which plays an important role in modern anti-aircraft warfare. However, due to the more heat sources on the vehicle, the strong interior noise, vibration during firing, the residual gas after firing, the oil smell emitted by the engine, the illogical interface and other factors affect the gunner's operation and weapon performance. Appropriate operating environment and scientific interface design, for easing the tension of gunners in war, reducing operational errors and improving operational effectiveness, is of great military significance.

---

J. Sun · H. Hao (✉) · J. Li · J. Guo · T. Li · J. Li · K. Zhang · P. Zhang  
Zhengzhou Campus, Army Academy of Artillery and Air Defense, Zhengzhou 450052, China  
e-mail: [269596825@qq.com](mailto:269596825@qq.com)



# **1 The Major Significance of Man–Machine Combination of a Self-propelled Anti-aircraft Gun Vehicle**

## ***1.1 The Major Significance of the Man–Machine Combination Optimization Design to Combat***

During combat environment, time makes the power to win. The opportunity for combat is very short, and it does not allow the operators to commit any mistakes [1]. The slightest mistake can have serious consequences. However, on the battlefield, it is inevitable that there will be many abnormal psychological reactions and absurd behaviours that lead to operational errors [2]. Man–machine combination optimization design vehicle, with its simple operational interface, safe and comfortable operating environment, can ease the psychological fear and anxiety of the gunner, reduce operational errors, improve operational efficiency and shorten response time of the weapon system. In the modern high-intensity warfare, it is particularly important to optimize the man–machine design of a self-propelled anti-aircraft vehicle based on reliability, comfort and safety.

## ***1.2 The Major Significance of the Man–Machine Combination Optimization Design to Operation Training***

The man–machine combination optimization design can realize the standardization, modularization and generalization of the self-propelled anti-aircraft gun vehicle operation. The standardized, modular and generalized operation will be of great significance for operational training and professional training. Scientifically designed man–computer interaction interface, which is single model, is conducive to mutual learning and communication between operators. The safe and comfortable operating environment is more conducive to the gunner training, where the new combat and training methods and latest technologies can be quickly promoted and applied, greatly improving the efficiency of training, shortening the training cycle and rapidly improving the combat effectiveness of the troops.

## ***1.3 The Major Significance of the Man–Machine Combination Optimization Design to Equipments Maintenance***

This is the design based on the reliability, safety and stability of the system. Rationale design is the foundation, and humanization is the soul and the highest goal of design. The optimized design of the vehicle is not only easy to operate but also has low failure

rate and simple maintenance. According to statistics, many faults of equipment are caused by improper operation. This is certainly due to lack of proper operational skills but can also be attributed in part to the equipment design. The optimal design of man–machine combination of the vehicle fully takes into account human behaviour and physiological characteristics so that the operational behaviour conforms to human behaviour characteristics. The operating environment is suitable for normal human activities, which greatly reduces the probability of operational failure, reduces the workload of maintenance, improves the availability of weapons and reduces the cost of maintenance and use.

## **2 The Influence of the Self-propelled Anti-aircraft Gun Vehicle Operating Environment on Gunner's Operation**

In general case, the environmental factors affecting the gunner's operation are summarized as follows: temperature, humidity, noise, lighting, gas, vibration, electromagnetic, etc. [3].

### **2.1 Temperature**

Through field monitoring and analysis, it was found that the cabin temperature was significantly higher than the outdoor temperature when the air conditioning was off. The highest temperature was 4–7 °C higher, the lowest temperature was 0.9–6.5 °C higher, and the average temperature was 2.3–7.2 °C higher. The reason for or we can say the temperature compared with outside and inside cabin, inside is much higher because within this environment air is not circulated.

The effect of high temperature on the gunner's operation mainly includes two aspects: on the one hand, the systematic high temperature reaction; on the other hand, the high temperature scald and burn. Main effects of high temperature on gunners are as follows: vomiting, chest tightness, dizziness, nausea, headache, blurred vision, epilepsy convulsions, etc. 38.5–38.8 °C is the body's tolerable temperature. On exceeding this limit, the skin heat conduction quantity and perspiration rate do not rise again. It is also the highest temperature for adaptation ability of human body. If the temperature rises further and body cannot release the excessive heat in time, a life crisis is bound to occur [4].

## 2.2 Humidity

It is found that the humidity outside and inside the cabin changes with temperature. The gradual increase of temperature decreases the humidity and vice versa. It is generally believed that relative air humidity is high when it exceeds 75%RH, humidity is low when it is less than 30%RH, and people feel comfortable when the humidity is between 40 and 60%RH. Under the condition that the cabin is closed without air conditioning, the humidity in the cabin is between 68.5–82.4%RH, obviously exceeding the standard and high humid conditions.

Generally speaking, humidity has little effect on heat exchange and will not have great influence on human body. But, high temperature coupled with humidity causes difficulty in dissipation of heat by human body that makes a person feel hardly breath. Once the temperature and humidity difference inside and outside the cabin is too large, the exchange of environment from inside and outside cabin would bring discomfort symptom to operators that may result in reduced work efficiency and increased error rate.

## 2.3 Noise

GJB50-85 stipulates that the allowable limit of noise in military operations is continuous exposure for 8 h per day, and the allowable sound level is 90 dB (A) [5]. When measuring the ambient noise inside and outside the cabin, it is found that the noise value under the condition that the cabin is closed without the tank cap [Maximum value is 95.1 dB (A) minimum value is 90.8 dB (A)]. The measuring result exceeds the limit value stipulated by the national military standard. The standard is maximum value of 86.1 dB (A) minimum value of 80.4 dB (A) in closed cabin situation while wearing the tank cap. But still, the rate is still very close to standard rate and which seriously effects the communication between operators.

Within a short time, it will make operator hearing fatigue. Though it can be eliminated by going into less noisy environments and frequently breaks for operating, but working and living in a noisy environment for a long time can lead to impaired hearing. The organic lesion caused by strong noise is irreversible and can cause permanent hearing damage. In general, working and living in an environment with a noise level above 90 dB (A) for a long time may lead to noise-induced deafness. The noise of environment above the level of 90 dB (A) will also have significant adverse effects on the digestive system, endocrine system, cardiovascular system and nervous system of human.

## ***2.4 Operation Interface***

During operation training, the self-propelled anti-aircraft gunner generally faces complex and densely placed irregular switch combinations and distribution. The buttons located beside the text label is also not unified and less switches button style are conform to the human-computer ergonomics. Therefore, easy solution is to have improved design of the interface, standard switch selection, comments and actions. The technique is advantageous for the gunner rapid and accurate operation.

# **3 The Suggestion of the Optimization Design of Man–Machine Combination of the Self-propelled Anti-aircraft Gun Vehicle**

## ***3.1 Effective Improvement in Operating Environment***

In the actual training and battlefield environment, the temperature and humidity can be adjusted to the appropriate range through the cabin air condition, ventilation, physical and psychological adjustment of the operator. However, the noise and explosion sound cannot be eliminated. Therefore, it should be reduced to curtail the harmful effects of noise that will be helpful to the operator's physical and mental health. The following three steps can be taken to control the noise: The first is to take effective technical measures to reduce the noise from the sound source. Analyse the noise frequency by using the corresponding technicians, find out the reason of the noise, and take measures to reduce the noise as follows: to improve the mechanical structure design and the processing precision of equipment and parts of weapons, etc. The second is to take measures to reduce the noise from the sound media, by using the sound isolation and sound absorption materials. The last but not the least to reduce noise is to take personal protective measures. According to the actual situation of a self-propelled anti-aircraft vehicle, the most effective method is to take personal anti-noise measures to control the noise and reduce the noise harm. For example, the use of noise reduction earmuffs, chest protection and other personal protective equipment.

## ***3.2 Scientific Design of Man–Machine Interface***

In order to design the man–machine interface of a self-propelled anti-aircraft gun vehicle, it is necessary to focus on three aspects: First, the operator should control the self-propelled anti-aircraft vehicle, fully play each of its advantages, so as to

maximize the advantages and avoid the disadvantages to achieve the optimal man-machine combination and jointly complete the tasks that cannot be completed separately. Second, to weigh the ability of an operator to receive the information from a self-operated anti-aircraft vehicle at same time. For those interfaces with multiple channels of information transmission and high frequency of information transmission, the operator's physiological adaptability should be taken into account. If one operator is not competent, use two operators to instead. Third, the design of man-machine interface should be operated easily by more than 90% of human beings. The design should be optimized based on human characteristics based on comprehensive consideration of colour, brightness, shape and structural layout of the interface [6].

### ***3.3 Upgrade and Improve the Close Environment***

The close environment of a self-propelled anti-aircraft gun operator mainly refers to the clothing and seat. Existing uniforms are not much different with general soldiers', but in the improved phase, their uniform should not be in the general sense of clothing, the head of the tank cap should have communication and security functions, the body uniform should not only have cool (warm) function but also have functions of isolation, protection, camouflage and others.

At present, the seats of the commander and gunner of the self-propelled anti-aircraft gun vehicle are fixed seats, which restrict the selection of the operator. Therefore, the seat should be designed to be the same as the driver's seat which should be adjustable in the height and level. It will satisfy widely the height problem of those people who operate in optimal posture.

## **4 Conclusion**

The optimized design of the operating environment is conducive to the physical and mental health of the gunner, and the scientific design of the operating interface makes the operation simple, clear and logical. In war, it can relieve the gunner's psychological fear and tension, reduce operational errors and improve operational efficiency. In daily training, it can improve the operation level, shorten the training cycle, expand the scope of training and reduce cost of the maintenance. It is convenient to realize the generalization, standardization, modularization and serialization of the self-propelled anti-aircraft gun vehicle system, which is of great significance to equipment construction and combat effectiveness improvement.

## References

1. Wang C (2015) The operation of self-propelled anti-aircraft gun. Air Defense Academy, Zheng Zhou
2. Liu H (1986) Military psychology. PLA Press, BeiJing
3. Pang Z (2000) Air defense man–machine—environment systems engineering. Air Defense Academy, pp 74–105
4. Wei H (2016) Study on man-machine performance of HQ-16A missile launch vehicle. Air Defense Academy
5. Tan L (1999) Artillery ergonomics. Beijing: Ordnance Industry Press, p 98
6. Lu R (2014) Ergonomics. Chongqing University Press, Chongqing

# Research on the Designing of Guiding System of Tiexi Workers' Village in Shenyang Under Industrial Culture



Zize Guo, Yang Liu, Guojing Wu, Zhaoding Kun, and Liyi Han

**Abstract** Based on the element evaluation of the existing guidance system of the scenic spot, this paper separates and orthogonally reconstructs the main components and types of the guidance system through the application of the conjoint analysis according to the survey of the cultural background of Tiexi workers' village in Shenyang, and the preferences of testers are quantified and rated. Finally, the design of the guidance system of Tiexi workers' village is obtained, which ensures the basic function of navigation and enhances the sense of substitution by passing on the regional culture to promote the development of the tourism industry.

**Keywords** Workers' village · Designing of guidance system · Conjoint analysis · Regional brand culture

## 1 Introduction

Humans have entered the age of mass production of machinery since the Industrial Revolution, with the progress of scientific technology witnessed by the previous industrial civilization. The values of industrial heritage are contained in the sites, the invisible industrial landscapes and human's memories and customs. In recent years, industrial heritage community has increasingly become the focus of the heritage protection and the research of urban renewal [1, 2].

---

Z. Guo · Y. Liu (✉) · L. Han  
Shenyang Aerospace University, Shenyang 110136, China  
e-mail: [xdguozize@foxmail.com](mailto:xdguozize@foxmail.com)

G. Wu  
Shenyang City Garden Greening and City Sanitation Management Center, Shenyang 110000, China

Z. Kun  
Criminal Investigation Police University of China, Shenyang 110854, China

© The Editor(s) (if applicable) and The Author(s), under exclusive license to Springer Nature Singapore Pte Ltd. 2021 981

S. Long and B. S. Dhillon (eds.), *Man-Machine-Environment System Engineering*, Lecture Notes in Electrical Engineering 645, [https://doi.org/10.1007/978-981-15-6978-4\\_113](https://doi.org/10.1007/978-981-15-6978-4_113)

Tiexi workers' village in Shenyang was a residential community with unusual historical significance for witnessing the industrial development of Northeast China and symbolized the new life of the working class in that period [3]. Based on the industrial cultural background of Shenyang workers' village, this paper studies the design of guide system of this area in order to explore the design that conforms to people's cognitive thinking, promotes local characteristics and strengthens cultural experience.

## 2 Overview of Tiexi Workers' Village in Shenyang

### 2.1 Status Analysis of Tiexi Workers' Village in Shenyang

Local government built the new life museum of workers' village in order to inherit the industrial culture. The life museum reproduces different scenes and facilities half a century ago, which is the first cultural life museum in China to display the theme of the working class [4]. This place has many pedestrians and vehicles passing by and adequate exposure, as shown in Fig. 1. However, at present, there are still various supporting functions of the workers' village that are not perfect, and the influence is limited. We analyzed the data of customer flow and visit satisfaction in the last ten years from 2009 to 2019 in excel, as shown in Tables 1 and 2. These shows that the number of visitors to the workers' village has increased in recent years, but the satisfaction is relatively flat, indicating that the workers' village has not formed the scale effect of culture.

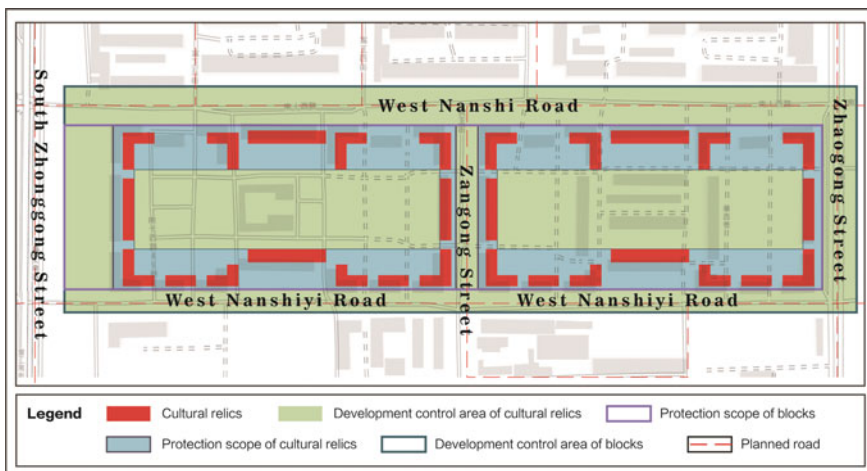
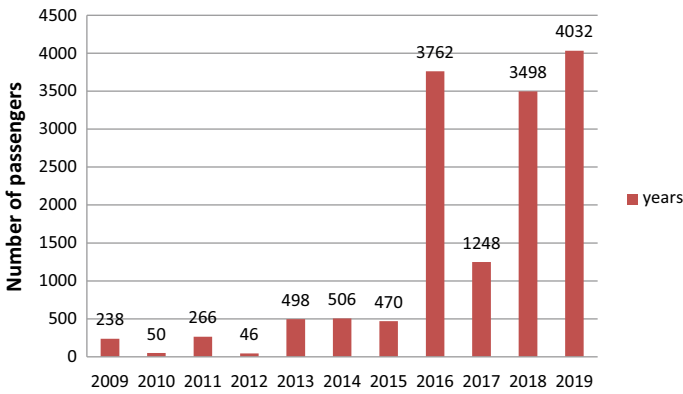


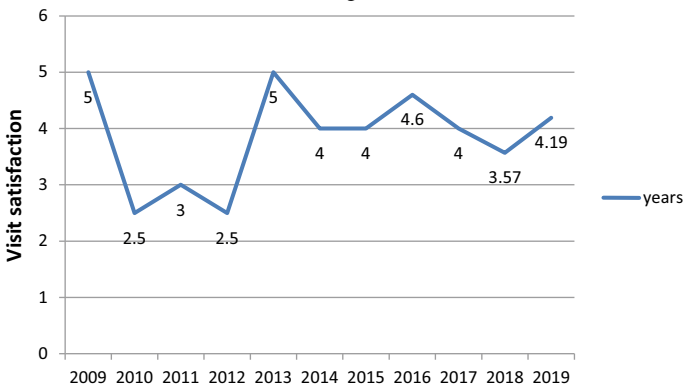
Fig. 1 Map of protected areas



**Table 1** Passenger traffic in Tiexi workers' village, 2009–2019



**Table 2** Visit satisfaction of Tiexi workers' village, 2009–2019



## 2.2 Research and Analysis of Tiexi Workers' Village Guide System in Shenyang

Having deeply investigated Tiexi workers' village, we found that there are few guide systems in the workers' village. The visible objects for identifying in the village are the guide signs of the historical and cultural block and the life museum, as shown in Figs. 2 and 3. At present, the design of the guide system in village is not systematic and lacking the characteristics.

**Fig. 2** Historical and cultural block



**Fig. 3** Guided map of the life museum



### 3 Conjoint Analysis of Elements of the Guiding System in the Scenic Spot

The random coefficient model created by using conjoint analysis method can estimate the relative importance of each attribute by measuring the user’s overall preference for the multi-attribute guide system and partial utility value of each specific attribute, with the differences in individual level and instability of model coefficient not ignored [5]. Through the arrangement and analysis of data of the existing guide system, the three levels of the guide system in the scenic spot from the abstract to the concrete can be concluded—functional requirements, information framework and visual communication. The visual plane of the guiding system is composed of following six elements. (1) Form. (2) Structure. (3) Font style. (4) Graphic symbol. (5) Overall color. (6) Texture.

According to the analysis, different types of visual plane’s elements of the guidance system in six scenic spots are sorted out and numbered, respectively, as shown in Table 3.

**Table 3** Components and types of the visual plane of the scenic guidance system

Elements	Types	Type number
Form	Scrolling guide; static guide	1; 2
Structure	Up-Middle-Down style; Left-Center-Right style	1; 2
Font style	Serif text; Sans serif text	1; 2
Graphic symbol	Objectification; flattening	1; 2
Overall color	Single color; same color; various color	1; 2; 3
Texture	Smooth surface; frosted surface	1; 2

### 3.1 Experiment Objectives

This experiment uses the basic theory and experimental method of stochastic coefficient model of conjoint analysis method to study designing ideas that conforms to the people’s visual plane of the guide system through the determination of the elements and combination schemes of the visual plane, which can provide references for the design to improve the recognition of the regional cultural brand.

### 3.2 Experimental Process

The experiment is divided into the following five parts: making experimental samples, determining test subjects, experimental task, experimental data analysis and experimental results analysis.

### 3.3 Making Experimental Samples

According to the classification and number of elements in Table 3, six elements affecting the visual plane of the guiding system in the scenic spot are determined, and each element’s attribute has two or three levels, respectively. According to the requirements of the full-contour experiment, 96 possible combinations of visual plane’s components of guiding system are obtained, which is beyond the collecting ability of later data and not representative. In order to make the experiment run accurately, 16 combinational design schemes of the visual plane’s elements of guiding systems in some scenic spots are simulated through the orthogonal experimental module for design of SPSS software, as shown in Table 4.

**Table 4** Combinational design schemes of the visual plane’s elements of guiding systems in some scenic spots

Number	Form	Structure	Font style	Graphic symbol	Overall color	Texture
1	Static guide	Left-Center-Right style	Sans serif text	Objectification	Same color	Frosted surface
2	Scrolling guide	Up-Middle-Down style	Serif text	Flattening	Single color	Frosted surface
3	Scrolling guide	Left-Center-Right style	Sans serif text	Objectification	Single color	Frosted surface
4	Scrolling guide	Left-Center-Right style	Sans serif text	Flattening	Single color	Smooth surface
5	Scrolling guide	Up-Middle-Down style	Sans serif text	Flattening	Same color	Smooth surface
6	Static guide	Up-Middle-Down style	Sans serif text	Objectification	Single color	Frosted surface
7	Scrolling guide	Up-Middle-Down style	Sans serif text	Objectification	Various color	Frosted surface
8	Scrolling guide	Left-Center-Right style	Serif text	Flattening	Same color	Frosted surface
9	Static guide	Left-Center-Right style	Sans serif text	Flattening	Various color	Smooth surface
10	Static guide	Up-Middle-Down style	Sans serif text	Objectification	Same color	Frosted surface
11	Static guide	Up-Middle-Down style	Serif text	Flattening	Various color	Frosted surface
12	Static guide	Up-Middle-Down style	Sans serif text	Flattening	Single color	Smooth surface
13	Static guide	Left-Center-Right style	Serif text	Objectification	Single color	Smooth surface
14	Scrolling guide	Left-Center-Right style	Serif text	Objectification	Various color	Smooth surface
15	Static guide	Up-Middle-Down style	Serif text	Objectification	Same color	Smooth surface
16	Static guide	Left-Center-Right style	Serif text	Flattening	Single color	Frosted surface

### 3.4 Determining Test Subjects

In order to ensure that the experimental results are referential, the subjects were divided into two groups, with a total of 50 subjects. Group A is composed of 30 persons including tourists from out of town and university students in Shenyang. Group B is composed of 20 persons who are all the local residents of Tiexi worker’s village. All the experimenters have a basic understanding of Tiexi workers’ village in Shenyang, as well as rich tour experiences.

### 3.5 Experimental Task

In this experiment, each examinee can make corresponding behavioral response by viewing the guide information. When the feedback action conforms to the instructions given by the guide information, this will be regarded as the completion of an experimental task. Examinees used the 16-level Likert scale to rate the 16 combinational design schemes of the visual plane’s elements of guiding systems in some scenic spots. The degree of liking declines from 1 to 16, and all subjects received the scale of the sample and are informed of the purpose of the experiment and the scoring criteria at the beginning.

### 3.6 Experimental Data Analysis

Research data of the experiments are collected and imported into SPSS software, and we use the conjoint syntax program to create the corresponding syntax file and calculate the utility value of each factor, the total utility value, the importance value, constants and correlations value, as shown in Table 5.

**Table 5** Overall utility value and importance value

Elements	Types	Utility value	Importance value
Form	Scrolling guide; Static guide	-0.050; 0.050	15.155
Structure	Up-Middle-Down style; Left-Center-Right style	-0.229; -0.458	15.364
Font style	Serif text; Sans serif text	0.166; 0.331	17.599
Graphic symbol	Objectification; flattening	-0.694; -1.388	17.544
Overall color	Single color; same color; various color	0.485; 0.970; 1.455	18.489
Texture	Smooth surface; frosted surface	0.256; 0.511	15.848

The correlation value and significance value of Pearson R and Kendall's tau are the main references for the correlation of the experimental data. The correlation coefficients between Pearson R and Kendall's tau are proportional to the statistical significance, which means that it will be more statistically significant when the value becomes larger. The correlation value of Pearson R was 0.803, and the significance value of Pearson R was 0.000. The correlation value tested by Kendall's tau was 0.594, and the significance value tested by Kendall's tau was 0.594. The test of the two correlation coefficients has clear significance, indicating that the data model tested by the experiment has a high degree of fitting, and both the deduced hypothesis and the conclusion are of statistical value, which can truly reflect the tourists' preferences when they look at the guidance system.

### ***3.7 Experimental Results Analysis***

Experimental data show that the overall color is the most important factor for tourists among the six main elements in the visual plane's composition of the guiding system, with the graph symbol and the texture representation being the next. On the contrary, the form and the structure of the guide system are of relatively low importance, which indicates that the recognition and understandability of the guiding system, the unity of color and the consistency of brand culture are the critical factors that users pay attention to.

## **4 Design Principle of the Guiding System in the Scenic Spot**

The design of the guiding system in the landscape is a form of informational design, which should be fully considered from the perspective of sociology, culture and ideology [6]. The design of the guiding system should follow the following three design principles.

### ***4.1 Principle of the Information Function***

As a kind of practical design, information function is the first element of the design of guiding system [7]. The design should possess the practical function of public space guiding and not be just the aesthetic art designed to attract people's attention. The practical information function of the guidance system is mainly manifested as guidance and recognition, which has two meanings. Firstly, it refers to the guidance in practical application to show visitors the location and setting of the scenic spot. Secondly, it gives visitors a psychological identification of this zone.

## ***4.2 Principle of the Regional Branding***

A brand has the same characteristics as a living body. Each brand has a unique personality, which is the objective condition for brand identity. The conditions of brand survival appear from the subjective perception, that is, the concept of brand identity [8]. The guiding system of scenic spot can make use of the relationship between the form and color of graphic symbols, the material and the texture and the skills and techniques to directly show the quality of cultural space and environmental image to the tourists, strengthening their experience and memory of the regional brand of the scenic spot.

## ***4.3 Principle of the Cognitive Mental Model***

Cognitive mental model refers to the representation formed by oneself in the mind through the interpretation and cognition of foreign things. “The critical reason why people can quickly identify and understand the environment is that we can reproduce the image of the space environment in memory. What has been perceived can be recalled in memory, which is called imagery or image, and the image of specific spatial environment is called cognitive map” [9]. This paper analyzes the cognitive habits of visitors and their preferences to the guide system through the research of the visual plane’s information frame of different guiding systems. The design of guiding system in the scenic spot should follow and fit the tourists’ existing cognitive psychological system and the cognitive mental model of the guide system, which can reduce the learning costs and improve the efficiency of recognition.

## **5 Application of Design Principles**

Based on researches of the visual plane of the guide system, the research results of the application of the design principles to the guide system of Shenyang workers’ village indicate that these can give tourists the better experience of being guided. The design of the guide system of Tiexi workers’ village in Shenyang is shown in Fig. 4.

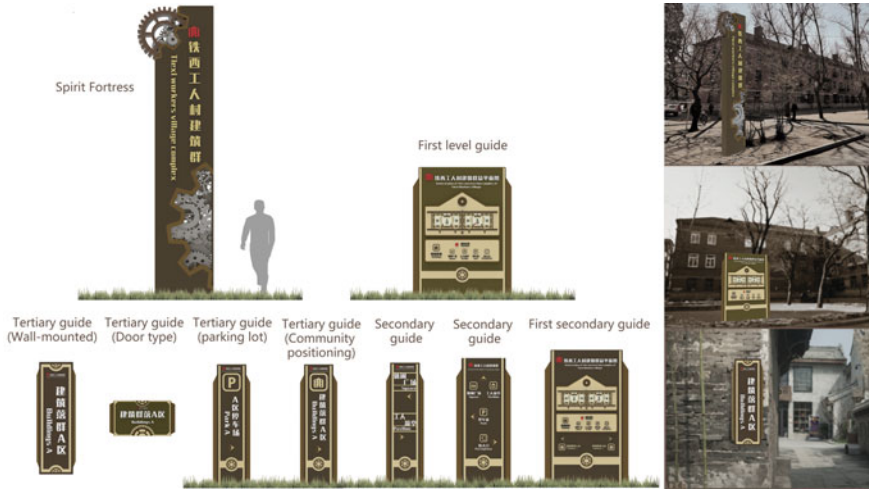


Fig. 4 Guiding system design of Shenyang Tiexi workers' village

### 6 Conclusion

As an important communication medium between tourists and scenic spots, the guidance system should be considered as an organic part of tourism resources to improve tourists' experience, the design of which should follow the design principle of guiding system in the scenic spot.

Based on conjoint analysis method, this paper summarizes and reorganizes the design elements of the guiding system in the scenic spot by decomposing the components and types of the visual plane of the guide system, which offers new ideas of the design and research of the guide system in the scenic spot and feasible design paths that are following the design principles in this paper. Due to the adoption of the subjective evaluation test method and SPSS statistical method, coupled with the small number of subjects, we will adopt more diversified research methods and consult more examples of guide systems of scenic spots in the future to explore the design of the guidance system more comprehensively.

### References

1. Li Yang, Siyuan Zuo, Tingting Xiong (2019) Social space analysis of industrial heritage communities: a case study of Wuhan Honggang City workers village. *Urban Arch* 13:25–58 (in Chinese)
2. Sun M (2018) Research on adaptive strategies of urban industrial heritage transition communities in the context of global cities. *Ind Arch* (07):44–48 + 114. (in Chinese)
3. Yan W, Shi T Renewal practice of old industrial residential district——renovation and design of workers village in Tiexi District, Shenyang City. *Mod Urban Stud* (11):67–71. (in Chinese)



4. Fang L, Wang J. Shenyang: Changes of workers' village. *China Arch* (01):58–60. (in Chinese)
5. Wang G Estimation of random coefficient models for joint analysis. *Quant Tech Econ Res* (7):97–108. (in Chinese)
6. Wang L, Tong Y Design and research of guidance system for tourist attractions from the perspective of cultural ecology. *Packag Eng* 39(380)(14):61–66. (in Chinese)
7. Wu C Localization strategies for guidance system design in scenic areas. *Art Work* (4):107–109. (in Chinese)
8. Jiang L, Zhang K (2018) Apparel brand overlap based on customer perceived value and eye-tracking technology. *Tsinghua Sci Technol* (23):47–64
9. Lin Y, Hu Z (2006) *Environmental psychology*. Beijing

# Assessment on the Availability of Domestic MMORPG Games Official Web Site Based on Eye Movement



Xiaofang Yuan, Yuan Yuan, Linhui Sun, and Lvyuan Sun

**Abstract** The main function of MMORPG Web site is to introduce game information, provide download channels and serve players. For the study of the current domestic MMORPG game official Web site usability and improve Web site appeal to players, this article selects three more representative domestic MMORPG game's official Web site, using the eye movement experiment, research subjects in the game's official Web site "announcement," "download game," "get the gift bag" section for the first time into the AOI interest zone time, the number of fixation and total fixation time, combined with hot figure the comprehensive analysis of the game's official Web site usability. Results show that the page layout differences on subjects of interest area have significant effect, part of the division with different colors was more likely to lead to subjects of interest, compared with text, pictures has more attractive to the user, so simplifying Web design, use color piece partitioning key, the amount of text information and nice pictures to attract users, improve domestic MMORPG game Web site usability.

**Keywords** Game website · Availability · Areas of interest · Eye movements · Color block division

## 1 Introduction

The official Web site of massively multiplayer online role playing game (MMORPG) is the main way for users to learn about the game, download the game, register an account and publish announcements. But now, the role of the official Web site of domestic games is not prominent, most players prefer to get game letters from WeChat public account, post bar, forum, video Web site and so on. According to Yuan [1], the publicity of information released by the official Web site of the game is indeed weaker than that of advertising released by the third-party platform, but it serves more as a channel for information communication and communication between the

---

X. Yuan · Y. Yuan (✉) · L. Sun · L. Sun

The School of Management, Xi'an University of Science and Technology, Xi'an 710054, China  
e-mail: [384876865@qq.com](mailto:384876865@qq.com)

© The Editor(s) (if applicable) and The Author(s), under exclusive license to Springer Nature Singapore Pte Ltd. 2021

S. Long and B. S. Dhillon (eds.), *Man-Machine-Environment System Engineering*, Lecture Notes in Electrical Engineering 645, [https://doi.org/10.1007/978-981-15-6978-4\\_114](https://doi.org/10.1007/978-981-15-6978-4_114)

operating developer and the game players. The official Web site of MMORPG games does not have the function of playing games, so more attention should be paid to how to attract players to read through the Web interface to get the latest information and attract new players to become new customers. Xing [2] pointed out that the game Web interface needs the combination of beauty and technology.

In the study of game web pages, Frederick [3] believed that web design should not only focus on usability but also bring users pleasant experience, which is mainly realized through usability, satisfaction, enjoyment, fun and visual attraction. According to Li [4], gameplay and usability are two important attributes of games. Excellent gameplay comes from the content setting of the game, the comfort of the system interface and the best way to operate the game, while usability is the effective, easy to learn, efficient, easy to remember, less mistakes and satisfactory degree of the product for users. Yi [5] pointed out that for online games, the experience players get is directly related to the visual form of the game interface. The game interface needs usability, and the connotation of usability includes three aspects, namely usefulness, effectiveness and interaction effect.

In the late 1970s, scholars put forward three indicators that have an important guiding role in the study of Web site usability, namely effectiveness, efficiency and users' subjective satisfaction. Hartson [6] believes that Web site usability includes usefulness and ease of use. In terms of the usability of Web sites, Yue [7] indicated that usability is one of the indispensable important indicators in the design of e-commerce Web sites, which directly affects the image of enterprises and the realization of commercial purposes of e-commerce Web sites.

Wang [8] proved that Web sites with high usability should be easy to read and understand by studying the usability of periodical Web sites, and only by improving the response speed of Web sites can we provide better relevant services to customers.

Some scholars have also used eye movement technology to study the usability of Web sites. Fu [9] once studied the relationship between interaction design elements and users' eye movement behavior. Yan [10] used eye movement technology to test the web usability of China mobile (Hainan) and China unicom (Hainan). Lamberz [11] believes that the selection of images and navigation bars plays a decisive role in the operability of Web sites. Ellis et al. [12] has used eye-tracking experiments as an evaluation technique to evaluate a range of Web site usability levels. The results showed that the Web site based on picture design performed better than the Web site based on text design. In 2006, AC Nielsen used eye movement tracking technology to obtain the general f-shape pattern of web pages browsed by users [13]. Sun [14] used eye-tracking technology to study the usability of commodity list pages on e-commerce Web sites, showing that typesetting differences had a significant impact on subjects' interest in list pages.

At present, many about reading, medical care, shopping Web site usability and mobile phone interface usability studies have applied the technique of eye movement, but for the game's official Web site usability research, few scholars using eye movement technique, the MMORPG game's official Web site and other Web site, the biggest difference for ordinary Web site is given priority to with text, MMORPG's Web site mainly consists of pictures, auxiliary words again a public announcement.

This paper introduces eye movement technology, conducts eye movement research on the official Web sites of three representative domestic MMORPG games, studies the usability of the official Web sites of games with questionnaire survey, analyzes experimental data and puts forward suggestions to improve the usability of the official Web sites of games.

## **2 Experimental Scheme Design and Implementation**

### ***2.1 Experimental Materials and Subjects' Selection***

This study mainly through the eye movement experiment evaluation of domestic MMORPG game Web site usability, selection of domestic three more representative MMORPG games Web site, respectively, is: a game's official Web site, b game's official Web site, c game's official Web site, three games Web site page "announcement," a "download game," "get the gift bag" the location of each are not identical, a game's official Web site of three parts mainly in the upper right interface, b game Web site mainly three parts in the upper left interface, c game Web site three parts mainly in the lower left side interface. The subjects randomly selected 28 college students aged 19–22 who had normal vision or normal vision after correction and had not played any of the three games.

### ***2.2 Experimental Process***

Before the beginning of the experiment, the experimental process and matters needing attention should be explained to the subjects so that they can better understand and participate in the experiment. Next, the experiment began, first let the participants based on your browsing habits and interest three random browsing Web site interface, and then let the participants to take the task in order to browse, all tasks have a separate interface, pause time no successively relationship between tasks, the first task is to let the participants find "announcements" section on the official web page, the second task is to make the participants on the official page to find "download game" part, the third task is to let the participants on the official page to find "get the gift bag" part, click the space during the experiment to enter the next official Web site page. After the eye movement experiment, the experimental data will be collected, and the subjects will be investigated by questionnaire.

### 3 Data Analysis

#### 3.1 *Experimental Indexes*

The eye tracker can record the position of the eyes, the duration of the stay and the eye movement trajectory of the whole experiment. In this paper, eye movement trajectory, time of first entering AOI region, number of fixation points and total fixation time are mainly used to study.

- (1) Eye movement trajectory diagram: The superposition of eye movement information on the visual image forms a map of fixation point and its movement, which can reflect the spatiotemporal characteristics of eye movement in the most specific, intuitive and comprehensive way, so as to determine the differences in eye movement patterns between different individuals under different stimulus situations [15].
- (2) The first time to enter AOI region: The longer it takes for the subject to find the target, the longer it takes for the subject to enter AOI region for the first time, the lower the efficiency is, and the target cannot attract the attention of the subject earlier [16].
- (3) Number of fixation points: When browsing the page, if users have a high fixation rate for a specific region, they may be interested in the region, or it may be that the information in the region is complex and difficult to understand. In the search task, the more gaze points, the less certain the target is [17].
- (4) Total fixation time: Refers to the total fixation time of the subject when viewing a certain area. The longer the total fixation time is, the longer the subject stays in the area, which may be because they are interested in it or spend more time to interpret the information.

This experiment mainly explores the effectiveness of the official Web site by analyzing eye movement indicators and the user's interest area by analyzing the hot spot map. Twenty-eight subjects were selected for the experiment, and the AOI interest area of each subject was observed. There was no data in the AOI interest area of four subjects, which was regarded as unfinished task, that is, only 24 subjects completed the task.

#### 3.2 *Analysis of Hot Spot Map*

The heat map mainly investigates the subjects' fixation when browsing the official Web sites of these three games. The heat map shows green on the periphery and red on the inside. The red part indicates that this area is much watched. The experiment asked the subjects to randomly browse the screenshots of the official Web site of three

games without tasks. From the heat map, it could be seen that the points of users' interest mainly focused on the face and artistic fonts, so they could make exquisite advertising pictures of characters and artistic fonts to attract users.

Because the "announcement" part in the web page accounted for a relatively large proportion, the basic can get the attention of the subjects; the "download game" part, as the most important part of the game's official Web site, is in the front position and is divided by color blocks, which is easy to attract the attention of the subjects. However, the proportion of "get the gift bag" in the web page is small, and the color block division is not obvious, so it is difficult to attract the attention of the subjects.

### 3.3 Data Analysis of AOI Interest Area of "Announcement"

"Announcement" is the most important part of the official Web site, where players can get first-hand information such as game updates and activities. Therefore, the "announcement" part of the official Web site is chosen as the first task. It can be seen from the trajectory chart that the trajectory of the official Web site of game b is relatively clear, while the official Web site of game c and the official Web site of game a are cluttered with too many interferences, so the "announcement" part of the official Web site of game b is easier to be noticed, and the information in the middle of the page is easier to be noticed (Table 1).

In the "announcement" part of the official Web site, both the average value of the first entry time of AOI interest area and the average value of fixation points and the average value of the total fixation time are all <0.05, indicating that there is a

**Table 1** Data analysis of AOI interest area "announcement" on the official Web site

Analysis of variance	Differences	SS	df	MS	F	P-value	F crit
First	Between groups	305,643.8	2	152,821.9	3.629819	0.031705	3.129644
Entry	Within groups	2,905,024	69	42,101.8			
Time	Sum	3,210,668	71				
Number of	Between groups	450.3611	2	225.1806	4.322264	0.01704	3.129644
Fixation	Within groups	3594.75	69	52.09783			
Points	Sum	4045.111	71				
Total	Between groups	39,874,342	2	19,937,171	5.591751	0.005615	3.129644
Fixation	Within groups	2.46E+08	69	3,565,461			
Time	Sum	2.86E+08	71				

**Table 2** Data analysis of AOI interest area “download game” on the official Web site

Analysis of variance	Differences	SS	df	MS	F	P-value	F crit
First	Between groups	25,945.18	2	12,972.59	0.219619	0.803383	3.129644
Entry	Within groups	4,075,726	69	59,068.5			
Time	Sum	4,101,672	71				
Number of	Between groups	2.111111	2	1.055556	0.180039	0.835629	3.129644
Fixation	Within groups	404.5417	69	5.862923			
Points	Sum	406.6528	71				
Total	Between groups	212,918.2	2	106,459.1	0.213927	0.807941	3.129644
Fixation	Within groups	34,337,381	69	497,643.2			
Time	Sum	34,550,299	71				

significant difference among the three in this part. The participants in the game’s official Web site are the first to enter the AOI b interest area, and the subjects of the fixation point number and total fixation time are minimum, show that the participants find task encountered little interference, can quickly target, to complete the task, the second is c game’s official Web site, the final is a game’s official Web site.

### 3.4 Data Analysis of AOI Interest Area of “Download Game”

“Download game” is one of the most basic functions of the official Web site, players generally choose to download the game in the official Web site, so more safe and efficient, so choose to find the official Web site “download the game” part as the second task (Table 2).

In the “download game” section of the official Web site, whether it is the average value of the time of first entering AOI interest area, the average value of fixation points and the average value of total fixation time, *P*-values >0.05. It can be concluded that there is no significant difference among the three parts in this part. Therefore, the task completion efficiency of the “download game” part has little difference, because this part accounts for a large proportion on the official Web site and is divided by color blocks. It is easy to find mission goals.

### 3.5 Data Analysis of AOI Interest Area of “Get the Gift Bag”

“get the gift bag” is one of the important functions of the official Web site. “Gift package” is a means to attract players, so we chose to find the official Web site “gift package” as the third task. The official Web site of game a is relatively simple with relatively clear track routes. The page layout of the official Web site of game

c is relatively reasonable. Although there are many contents, the subjects can also find the target quickly. B official Web site of the game has too much interference information, and the color block distribution is messy, so the subjects cannot quickly search for the task target (Table 3).

In the “get the gift bag” section of the official Web site, whether it is the average time of first entering AOI interest area, the average value of fixation points and the average value of total fixation time,  $P$ -values  $<0.05$ . It can be concluded that there are significant differences among the three in this part. The participants in a game’s official Web site are the first to enter the interest area, and the subjects of the fixation point number and total fixation time are minimum, followed by c game’s official Web site, finally the b game’s official Web site.

### ***3.6 Analysis of Experimental Results and Questionnaire Data***

Through the above comparison of the trajectory chart, one-way Anova and mean value of the three eye movement indicators, the conclusion can be drawn: the efficiency of the task completion in the “announcement” part, the official Web site of game b > the official Web site of game c > the official Web site of game a; “Download game” part of the task completion efficiency, the three games have little difference; efficiency of the task of “getting the gift bag” part, official Web site of game a > official Web site of game c > official Web site of game b.

The average value of the first time entering the AOI interest area was selected for comprehensive analysis. It can be seen that the “announcement” part is the fastest of the three tasks, that is, the most efficient. The “download game” section is similar to the “announcement” section; the least efficient part was the “get the gift bag” part, and the subjects took much longer to find the target of the task than the first two tasks.

After the experiment, we also investigated the participants’ preference for the three game official Web sites. The survey results show that most of the participants prefer the interface of game a because the overall area of the interface of game a is large and clear, while the division of the other two game interfaces is obviously small and messy, which is not easy to attract the attention of the subjects and win the subjects’ love. In the design of game official Web site, the participants prefer a simple interface, and each area should be divided clearly and occupies enough area, so that users can find the information they need in time.

## **4 Discussion and Suggestions**

This paper mainly analyzes the eye movement data through the eye movement experiment and studies the usability of the official Web site of domestic MMORPG games from the efficiency of task completion. According to the results of the questionnaire,



**Table 3** Data analysis of AOI interest area “get the gift bag” on the official Web site

Analysis of variance	Differences	SS	df	MS	F	P-value	F crit
First	Between groups	2,150,230	2	1,075,115	3.706601	0.029579	3.129644
Entry	Within groups	20,013,737	69	290,054.2			
Time	Sum	22,163,967	71				
Number of	Between groups	436.0833	2	218.0417	4.129331	0.020236	3.129644
Fixation	Within groups	3643.417	69	52.80314			
Points	Sum	4079.5	71				
Total	Between groups	25,614,889	2	12,807,444	3.294313	0.043008	3.129644
Fixation	Within groups	2.68E+08	69	3,887,744			
Time	Sum	2.94E+08	71				

players prefer the interface of the official Web site of game a, followed by the official Web site of game b and finally the official Web site of game c. With the eye movement experiment data, a game's official Web site interface on the visual effect than the other two games to much clear interface, very well in color piece area can be divided into focus, the other two games Web site monochromatic block division, the target is not easy to cause the participants note that let users find the information you need to reduce the availability page. Most users focus on the page image and the middle area, showing the pattern of "F" type browsing mode. Therefore, when designing the official Web site, exquisite game characters can attract users, and important information should be presented in the middle of the page as far as possible. There are obviously too many words in the official Web site interface of c game, and the pages with high text proportion will increase the cognitive load of the subjects and reduce the usability and aesthetic quality of the pages. Therefore, the design of the official Web site should be simple and concise, clearly divided and combined with the right amount of text, to reduce the interference of users by other content, timely get the information they need, improve the usability of the official Web site.

### **Compliance with Ethical Standards**

The study was approved by the Logistics Department for Civilian Ethics Committee of Xi'an University of Science and Technology.

All subjects who participated in the experiment were provided with and signed an informed consent form.

All relevant ethical safeguards have been met with regard to subject protection.

**Acknowledgements** This work is supported by the National Natural Science Foundation, No. 71403204,71673220; Shaanxi science and technology department of youth programs, No. 2020JQ760 for this study. The authors are also grateful to the experts who participated in the expert opinion study for their time and efforts.

## **References**

1. Yuan L (2018) Research on localized game website interface design. Wuhan University of Technology
2. Xing F (2012) Design and implementation of the official website of online games. University of Electronic Science and Technology of China
3. Frederick D, Mohler J, Vorvoreanu M et al (2015) The effects of parallax scrolling on user experience in web design. *J Usability Stud* 10(2):87–95
4. Li Z (2013) Interface interaction design of tencent second-generation shooting online games. Hunan University
5. Yi C (2012) Research on the application of traditional Chinese visual elements in online game interface design. Jiangnan University
6. Hartson HR (1998) Human–computer interaction: interdisciplinary roots and trends. Elsevier Science Inc.
7. Yue P (2013) Interface design of O2O e-commerce websites based on usability research. Chongqing Normal University

8. Wang B (2017) A comparative study on the website usability of library science and information science journals at home and abroad. *J Sci Technol China* 28(08):736–740
9. Fu G, Qu Q, Zhang X, Cao Y, Liu W (2014) Research on the relationship between user eye movement behavior and website design elements. *Ind Eng Manag* 19(05):129–133 + 139
10. Yan G, Zheng X (2012) Eyes are the window of mind—web usability test based on eye movement tracking technology. *Mod Commun J Commun Univ China* 34(02):106–111
11. Lamberz J, Litfin T, Teckert Ö (2018) Usability and web design of an educational website. *De Gruyter* 2
12. Ellis SH, Candrea R, Misner J et al. (1998) Windows to the soul? What eye movements tell us about software usability
13. Koufaris M (2002) Applying the technology acceptance model and flow theory to online consumer behavior. *Inf Syst Res* 13(2)
14. Sun C (2013) Eye movement research on the usability of commodity list page in B2C e-commerce websites. *Electron Test* 16:96–97
15. Liao Y (2007) Study on specific cognitive eye movement characteristics of volleyball players. Beijing Sport University
16. Theeuwes J, Godijn R, Pratt J (2004) A new estimation of the duration of attentional dwell time. *Psychon Bull Rev* 11(1):60–64
17. Hao Y, Ma Y, Chen J, Li M (2016) Research on eye movement evaluation of interface usability of handheld mobile terminals. *Ergonomics* 22(04):70–73 + 80

# Reliability Modeling and Analysis of Teleoperation System with Path-Dependence Effect Considered



Shanshan Zhang, Xiaopeng Li, Wei Zhang, Wenming Zhou, Sha Qin, Lu Chen, and Yi Xiao

**Abstract** In the teleoperation task of robotic arm system, path-dependent effects have significant impact on human–computer interaction failures. By analyzing the task process, this paper identifies the key factors affecting the success of the robotic arm teleoperation task and constructs a dynamic Bayesian network (DBN) model. On this basis, the path dependence which can promote or inhibit the human error is analyzed to revise the model. The revised model can clearly describe the path-dependent effect of human–computer interaction failures and also help to calculate the reliability of the complex system accurately.

**Keywords** Robotic arm · Teleoperation task · Path-dependence effects · Human–computer interface failure · Dynamic Bayesian network · Task reliability

## 1 Introduction

Teleoperation [1] task is different from the general operation task, which is characterized by human–machine cooperation in different places. In the master–slave structured robotic arm teleoperation system [2] of Fig. 1, the robotic arm plays the role of a slave robot. The master end constructs a virtual environment based on the position, attitude, and force feedback from the slave end and remotely controls the slave to complete the task.

At present, common reliability modeling of the teleoperation manipulator operating system does not consider the path-dependent effect of the system, which greatly reduces the accuracy of the system reliability assessment. This paper takes path-dependent effect into consideration, constructs the model, and analyzes the reliability of the manipulator teleoperation task by using DBN method.

---

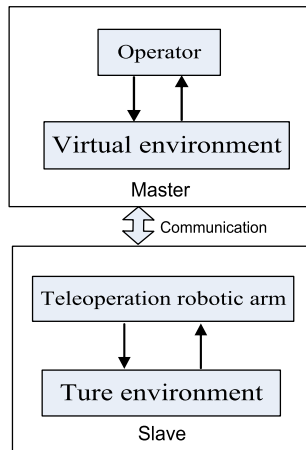
S. Zhang (✉) · X. Li · W. Zhang · W. Zhou · S. Qin · L. Chen  
China Astronautics Standards Institute, Beijing 100071, China  
e-mail: [zhangshsh94@163.com](mailto:zhangshsh94@163.com)

Y. Xiao  
National Key Laboratory of Science and Technology on Human Factors Engineering, Astronaut Training and Research Center, Beijing 100194, China

© The Editor(s) (if applicable) and The Author(s), under exclusive license to Springer 1003 Nature Singapore Pte Ltd. 2021

S. Long and B. S. Dhillon (eds.), *Man-Machine-Environment System Engineering*, Lecture Notes in Electrical Engineering 645, [https://doi.org/10.1007/978-981-15-6978-4\\_115](https://doi.org/10.1007/978-981-15-6978-4_115)

**Fig. 1** Master–slave robotic arm teleoperation system



## 2 Robotic Arm Teleoperation System

### 2.1 Robotic Arm Teleoperation System Composition

The robotic arm remote operation system mainly includes two parts, the master side and the slave side. The master is controlled by the operator and sends instructions to the slave through the human–computer interface; the robotic arm as the slave mainly includes the electrical system, control processing unit, end actuator, arm and driving joints, etc.

In the process of reliability analysis, in addition to human factors and equipment failure factors, the impact of environmental factors such as vacuum, containment, lighting, and noise should also be considered.

### 2.2 Main Functions of Robotic Arm Teleoperation Task

After extensively reviewing the literature and related data, the teleoperation task process of the robotic arm is roughly divided into three steps: arm stretching to a specified position, actuator capturing the target object, and arm with target object recovering to their original positions. The three main functions and task profile are described in Fig. 2.

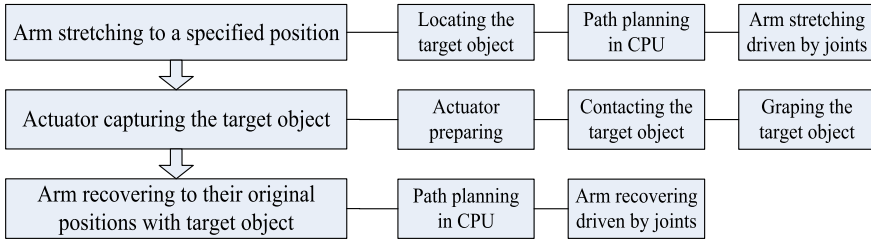


Fig. 2 Robotic arm teleoperation task implementation profile

### 3 Path-Dependent Effects in Robotic Arm Teleoperation Tasks

#### 3.1 Overview of Path-Dependent Effects

The concept of path-dependent effect describes the influence of past choices on the present and the future. It is similar to “inertia” in physics. Once entering a path, it will continue to develop along the path and lock in that path.

Through learning in different environments and situations, human can form problem-solving method with individual characteristics. These unique thinking and behavior habits are called path dependence. Good and correct use of path dependence is a prerequisite for efficient work. Conversely, it can be an important cause of failure and even catastrophic consequences.

#### 3.2 Relationship Between Path-Dependent Effect and Reliability of Teleoperation System

The robotic arm teleoperation task is the most typical human–computer interactive task. As a typical human-in-the-loop system, in addition to environmental impact and equipment failures, human error is one of the most important factors influencing the success of the task. Clarifying the hybrid correlation between environmental impact, equipment failures, and human error is the first step to establish a human–machine system reliability model.

Human error refers to human-made faults or poor performance of the system caused by human. Human error usually violates the safety design or operating procedures. There are many influencing factors of human error, but the core factor leading to human error is still the human factor. To make the prediction of human error, it is necessary to clarify the thinking and behavior characteristics of human cognition, judgment, decision-making, and operation in the process of performing tasks. At the same time, task requirements analysis is also crucial to human error prediction.

During human thinking and behavior characteristics distinguishing, path-dependent effect is one of the core factors. Path dependence has neither positive nor negative effects. Correct path dependence has a positive impact on system performance, which suppresses the occurrence of human error; negative path dependence, on the contrary, has a promoting effect on the occurrence of human error and has a negative impact on system performance.

### 3.3 Promotion and Suppression Effects of Path Dependence

When the operator's thinking and behavior completely match the task characteristics and cognitive needs in the task execution process, it will avoid human error and promote system performance. As shown in Fig. 3, during the task execution of the robotic arm system, if an unexpected situation caused by human, equipment or environmental factors suddenly occurs, the operator's judge is crucial. Assuming that the operator has got the appropriate acknowledge, for example, though a specific training, it is greatly possible for him to make the right decision. That means correct path dependence is taking effect and the probability of human error is reduced, which is beneficial to the normal operation of the system. However, when the operator's thinking and behavior characteristics deviate from the task characteristics and context, there is a high risk of human error because the lack of correct path dependence.

## 4 Reliability Modeling of Robotic Arm Teleoperation System Based on DBN

The establishing of the reliability model is based on the task process, which is previously introduced in 1.2 (Robotic arm teleoperation task implementation profile). Compared with the common reliability model, this paper identified the failure factors with the path-dependent effect taking into consideration and built the system dynamic Bayesian network combining with the system dynamic characteristics.

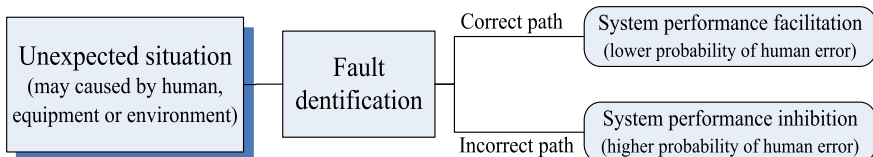


Fig. 3 Path-dependent effect influencing probability of human error

### 4.1 Construction of Bayesian Network Topology

In the BN topology, the node representing robotic arm teleoperation task is called TE. According to the analysis of the task profile, this node has three parent nodes E1, E2, and E3, which correspond to the three main functions: robotic arm extension, capturing targets, and robotic arm recovery. The basic factors that affect the success or failure of the task are identified by human, equipment, environmental, and human-machine interaction factors, etc. They are considered as root nodes of the Bayesian network. See the detailed nodes meaning in Table 1.

Among them, operator status and operator personnel capabilities are human factors; the failure of the human-machine interaction interface and simulation software will not directly cause the task to fail. The success of the task depends on whether the person has given the correct instructions. For example, if the operator has not accepted the training under the human-computer interface failing situation, human error in blind operation is very likely to occur. Another example, if the operator has been trained how to do with the failure of the simulation software, the task may be completed without reference to the simulation results.

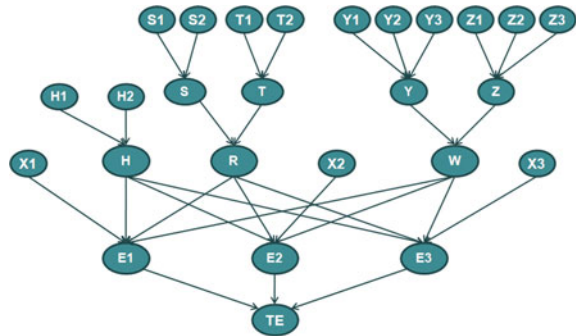
The BN topology of the teleoperation system is shown in Fig. 4.

**Table 1** Root nodes identifying form

Node number	Identifying factor	Node meaning
H1	Human factor	Human status
H2		Human capability
S1	Human-machine interaction factor	Human machine interface
S2		Simulation software
T1	Environmental factor	Lighting
T2		Temperature
X1	Sensor factor	Force sensor
X2		Position sensor
X3		Attitude sensor
Y1	Control factor	Communication system
Y2		Control processing unit
Y3		Electrical system
Z1	Mechanical factor	The mechanical arm
Z2		The driving joints
Z3		The end actuator



**Fig. 4** Bayesian network topology of robotic arm teleoperation system



### 4.2 Implementation of Dynamic Bayesian Network Structure

DBN is an extension of the initial network in time. It consists of an initial network and a transfer network, where each time segment corresponds to a static Bayesian network. In the static Bayesian network under each time slice, the observation node includes not only the current state information, but also the state transition probability of the node within this time slice. The result state of the previous time slice is the initial state of the next time slice [3].

### 4.3 Dynamic Bayesian Network Parameter Configuration

Given the topology of a complete dynamic Bayesian network, the prior probabilities, conditional probability parameters, and state transition probabilities of the nodes in the network must also be determined.

The research object of this paper is the remote control system of the robotic arm. The human factor is the most dynamic characteristic in this system. Compared with mechanical parts that have a long life span, the human state is relatively easy to change. After several hours of intense work, people will experience eye fatigue, physical fatigue, and decreased concentration. Therefore, in the following reliability analysis, the impact of changes in personnel status on the reliability of the task is mainly considered, and the possibility of changes in the status of other factors is not considered here.

The manipulator remote operation system is specified as a two-state system; that is, all node states are only “0” and “1”, where 0 represents a normal state and 1 represents an abnormal state.

## 5 Reliability Analysis of Manipulator Teleoperation System Task

This chapter analyzes the task reliability under the conditions of not considering path dependence and considering single or multi-path dependence based on the existing reliability model of manipulator teleoperation task and illustrates the impact of path-dependent effect on system reliability.

### 5.1 Modification of BN Model Without Path Dependence

The robotic arm teleoperation system is a typical human-machine interaction system. Thus, the influence of path dependence on human error cannot be ignored. Add “path” parent node (PS1, PS2, PT1, PT2) and “new human-machine ring influence factor” node (FS1, FS2, FT1, FT2) to the node corresponding to the human-computer interaction failure in DBN. The “node” means the path dependence of the operator’s response strategy to the situation. Without considering the operator’s path dependence, the “path” node does not work.

The system reliability is expected to use the forward reasoning function of the Bayesian network. Lots of algorithms can easily calculate the probability of occurrence of top event  $T$  at any time  $t$ :  $P(t) = P(T_t = 1 | X_{01} = 0, \dots, X_{0m} = 0)$ . Here,  $X_{0i}$  represents the state of the root node  $X_i$  in the DBN at the initial moment, and  $m$  represents the number of root nodes in the network.

Record the values of the reliability of each important node under different time slices. The probability of the teleoperation task completing normally shows a downward trend over time, mainly because the status of the operator changes over time. The degree of concentration gradually decreased; but with the steady state of personnel, the reliability of the system also showed a steady trend.

### 5.2 Task Reliability Analysis Considering Path Dependence

It is identified that the system has four typical human-machine interaction failure scenarios, namely human-machine interface failure (S1) and simulation software failure (S2), and under no-light conditions (T1) and extreme temperature conditions (T2). This section describes the method of system task reliability analysis considering path-dependent effects.

### 5.3 Reliability Analysis with Human–Computer Interface Failure

The human–computer interaction interface is a way for the master to send instructions to the slave and read the feedback information from the slave. Once the human–machine interface fails, the operator cannot take corrective measures in time, which may cause irreversible disasters to the system; if the operator takes appropriate measures, the system may run normally to complete the task.

Regardless of the path-dependent effects in this case, the configuration of the conditional probability table is shown in Fig. 5a. After adding the path parent node PS1, the modified conditional probability table is shown in Fig. 5b.

The values in the figure are only examples. The reliability of system calculated by GeNIe is shown in Fig. 6.

According to calculations, in this case, the promotion and suppression effects of path dependence have a role of reducing and increasing the reliability of the task, both of which are about 0.003. For the task success rate, 0.6% is obviously a relatively high value, indicating that the path-dependent effect has a significant effect on the teleoperation task of the robotic arm.

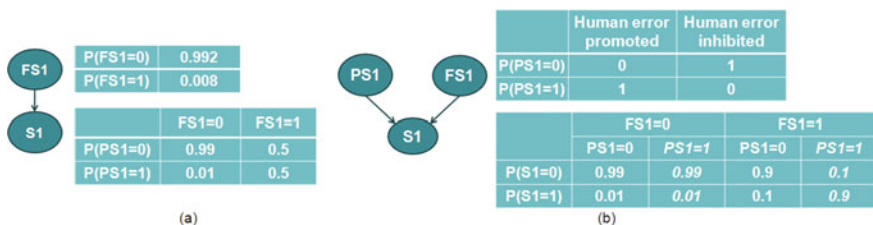


Fig. 5 Condition probability tables under human–machine interface failure: a without considering path dependence; b considering path dependence

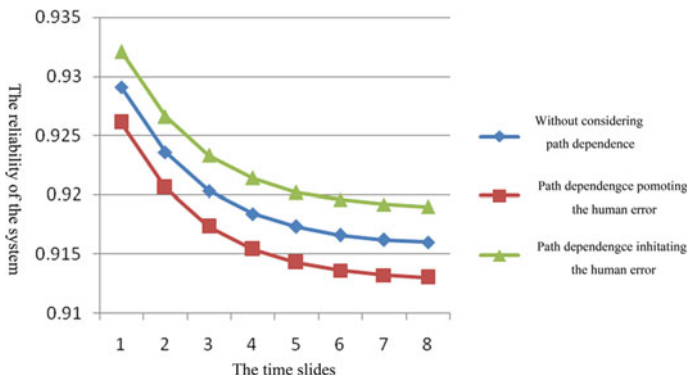


Fig. 6 System reliability-time diagram considering path dependence

## 6 Conclusions

The reliability modeling method considering path-dependent effect is more accurate, and it can clearly express that path dependence can promote or suppress human error. The correct path dependence can suppress human error and significantly improve system reliability; otherwise, it is very likely to cause system failure and reduce system reliability. Therefore, operators should form forward path dependence through training. The state of operator has a significant impact on system reliability. Operators should pay attention to maintaining a good state and adjust the state in time when fatigue occurs during continuous operation to ensure correct operation instructions and improve task success rate.

## References

1. Wang L, Bai J (2019) Introduction to networked teleoperation system. *Dig Technol Appl* 4:12
2. Liu H, Zhao D (2004) Survey of telepresence teleoperation robot. *Robot Technol Appl* 2004(1)
3. Zhou Z, Ma C, Zhou J et al (2008) Dynamic fault tree analysis based on dynamic Bayesian network. *Syst Eng Theory Pract* 02:37–44

# Framework of Performance Shaping Factors for Human Reliability Analysis of Digitized Nuclear Power Plants



Li Zhang, Jianqiao Liu, and Yanhua Zou

**Abstract** The state-oriented procedures (SOP) have been applied to the digitized nuclear power plants (NPPs) in China, which makes the operation of operators efficient. But at the same time, new human reliability issues arise. In this paper, literature review-based and expert-based methods are applied to construct a hierarchical framework of performance shaping factors (PSFs). Firstly, operators' task types and error modes were analyzed with systematic human error reduction and prediction approach (SHERPA). Then, the PSFs of different task types were concluded with the Delphi method. The expected result is the conceptualizing PSFs framework that contains the task types, error modes, and PSFs. The future study is to identify the cause-and-effect relationships of the PSFs to inform the HRA quantitative analysis.

**Keywords** Digitized nuclear power plants · Task types · Error modes · Performance shaping factors

## 1 Introduction

Human reliability is described like this: “the probability of successful completion of the task at any stage of the system within the prescribed minimum time limit (If there is a time requirement)” [1]. Human reliability analysis (HRA) methods have been developed to predict human error probabilities (HEP) within a specific context. Among the HRA methods, some use performance shaping factors (PSFs) to modify the nominal HEP. PSFs represent the factors that can enhance or decrease human performance. The number of PSFs ranges from a single factor to 60 in different research [2]. And different methods use different PSFs classification principles. Swain considered that PSFs have different degrees of influence on human behavior and then divided the

---

L. Zhang (✉) · J. Liu

School of Nuclear Science and Technology, University of South China, Hengyang 421001, China  
e-mail: [13807340602@139.com](mailto:13807340602@139.com)

Y. Zou

Institute of Human Factors Engineering & Safety Management, Hunan Institute of Technology, Hengyang 421002, China

© The Editor(s) (if applicable) and The Author(s), under exclusive license to Springer 1013  
Nature Singapore Pte Ltd. 2021

S. Long and B. S. Dhillon (eds.), *Man-Machine-Environment System Engineering*, Lecture Notes in Electrical Engineering 645,  
[https://doi.org/10.1007/978-981-15-6978-4\\_116](https://doi.org/10.1007/978-981-15-6978-4_116)

PSFs into internal factors, external factors and stressor factors [3]. Kim used systematic thinking to divide the PSFs into human factors, system factors, task factors and environment factors [4]. Moreover, the content of PSFs also varies due to different background. Application of digital technologies in NPPs has greatly changed the operators' work environment. The biggest change is that human system interface (HSI) adopts computer-based technologies, such as the digital display, computerized procedures, and soft control. These changes bring challenges to the HRA.

The current study will focus on building a comprehensive PSFs framework following a systematic process. The results of this study will be used to identify the cause-and-effect relationships of PSFs for the HRA quantitative analysis, which is beyond the scope of this paper. The next is organized as follows. Section 2 presents the task types and error modes of operators by analyzing characteristics of SOP. Section 3 discusses the identification of PSFs based on Delphi method. Section 4 makes a summary of this study and explains the next step of the research project.

## **2 Task Types of Operators in Digital Main Control Room**

### ***2.1 Characteristics of SOP***

Digitized technology makes operators' procedure embedded in computer system which changes the ways operators interact with NPPs system. The Three Mile Island event fully demonstrates the importance of accident procedures. When handling accidents, operators must follow the procedures to keep the power plant states vitality. At present, most of the new nuclear power plants at home and abroad adopt digital accident procedures. This paper takes LingAo II NPP which is equipped with state oriented procedure (SOP) as the basis.

SOP is based on six basic state parameters of the nuclear power plant which can sufficiently and necessarily describe all possible states. When an accident occurs, operators will first enter the DOS program, diagnosing and determining corresponding state function degradation levels, and then orient to corresponding procedures or perform the operation in the DCS directly. If a new event happens, operators continue performing the procedure and re-diagnose according to the state parameters. When all the parameters reach the specified range, operators will exit SOP.

### ***2.2 Identify Main Task Types and Error Modes***

Primary tasks of operators are to monitoring/detection, situation assessment, response planning and response implementation. To achieve these tasks, they need to perform secondary tasks. For example, to verify whether an alarm appears, he/she

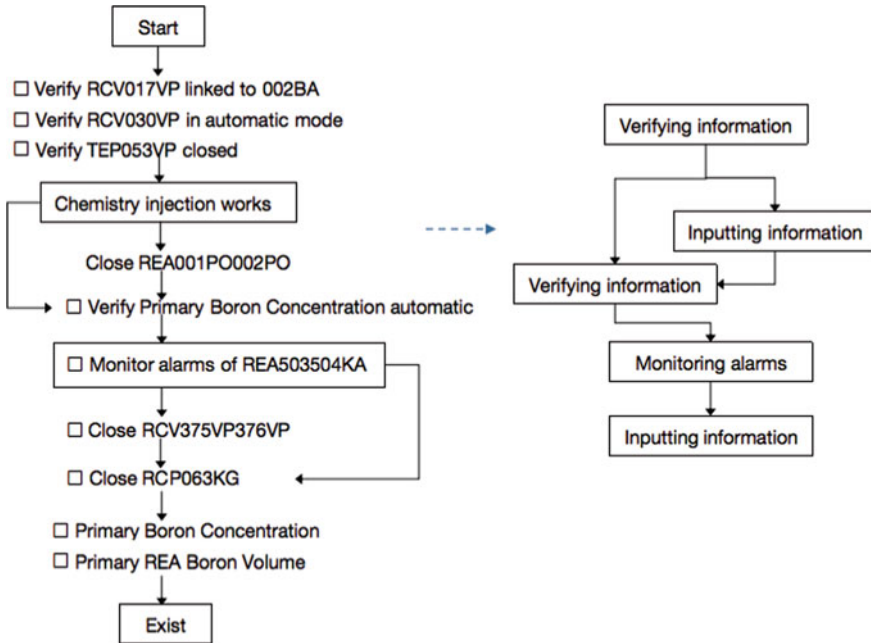


Fig. 1 Example of obtaining main task types using SHERPA

may use a mouse, a keyboard and other devices to configure, navigate or arrange appropriate screens and/or icons.

With systematic human error reduction and prediction approach (SHERPA) [5], 16 kinds of primary sub-task types and 3 kinds of secondary task types are drawn out after analyzing procedure process. The primary sub-task types were then matched to the four primary task types. To identify main error modes of each task type, operators were interviewed and the video recording the work process of operators was also analyzed. After that, the corresponding error modes were concluded. The final result is shown in Appendix. Figure 1 presents an example about how to obtain the main task types.

### 3 Identify PSFs

In recent years, some HRA practitioners have developed their respective PSF classification for a specific purpose. In the research of Ekanem [6], the PSFs are classified into nine main categories (HSI, procedures, resources, team effectiveness, knowledge/abilities, bias, stress, task load and time constraint). Kim detailedly described 11 representative PSFs which contained 39 sub-items by analyzing emergency tasks

in NPPs [4]. Liu proposed a conceptualization framework of PSFs and described them at three levels, components, factors and indicators [7].

We would like to use the SHELL model (Software, Hardware, Environment, Live-ware) as the principle to collect and classify PSFs. Firstly, the universal PSFs which appears in the traditional MCR but also are applicable to the digital environment were collected after literature review. Relevant literature was referred from the following data resource: (a) HRA methods, like THERP [3], CREAM [8], SPAR-H [9]; (b) the research conducted by Nuclear Regulatory Commission (NRC), University of Maryland, Korea Atomic Energy Research Institute (KAERI) and Tsinghua University. Then, referring the human factors engineering program review model of NUREG-0711 [10], the HSI module is selected as the primary focus for it considering the digitized technology. Among the candidates, the Delphi method was used to determine the final PSFs set. In this process, six HRA experts and two experience-rich operators are invited. They were divided into two groups with each consisting of three experts and one operator. Opinions were firstly given by one crew, then the other group evaluated the suggestions and provided their idea. Next, these recommendations were again passed to the former crew until the final consistent decision was made. Table 1 depicts the final result.

## 4 Conclusions and Discussions

In this study, the primary and secondary task types of operators in digital MCR and related error modes are discussed using the SHERPA method. PSFs classification based on the SHELL model is acquired after literature review and expert discussion. At last, a comprehensive framework depicted by Appendix is built that contains primary sub-tasks, secondary tasks, error modes and PSFs. So far, researches on PSFs taxonomy are almost focused on PSFs. Our framework contains not only the PSFs but the task types and error modes which facilitates the qualitative analysis process of HRA. Besides, secondary task complexity as an indicator of task PSF is a newly consideration that can reflect the effects of digitalization on operators to some extent.

It is known to HRA practitioners that the influencing factors contain some overlap and are non-orthogonal [2, 9, 11]. When quantifying HEPs, the variables, however, have been treated independent [9, 12, 13]. Leaving the issue unsolved may make the quantification double-counting and biased. So, the future study is to identify the cause-and-effect relationships of the PSFs to inform the HRA quantitative analysis.



**Table 1** PSFs collected based on SHEL model

Components	Factors	Indicators
Software	Organization supervisory	Organizational placement
		Organizational assignment of tasks
	Safety climate	Communication and coordination
		Attitude for safety
Hardware	HMI	Availability of dives
		Quality of icons layout
	Procedure	Configuration format on screen
		Procedure' quality
	Task	Primary task complexity
		Secondary task complexity
Environment	Workplace conditions	Light intensity
		Indoor temperature
		Radiation
Liveware	Stress	Time pressure
		Workload
	Fatigue	Sleep deprivation
		Shift length
		Nonday shift
	Bias	Overconfidence
		Cognitive bias
Fraction		

**Acknowledgements** This work was supported by the National Natural Science Foudation of China (Grant No. 71371070, No. 71771084, No. 71501068), Research Study and Innovation Experiment Program for University Students of Hunan Province, China (Grant No. Xiangjiaotong[2019]219-2613).

## Appendix

See Table 2.

**Table 2** Framework of task types and the associated error modes and PSFs

Primary tasks	Sub-tasks	Error modes	Secondary tasks	Error modes	PSFs	
Monitoring/detection	Monitoring alarms/state of indicator	Loss of information localization Fail to monitor Monitoring delay Fail to understand	Navigating	Wrong navigation selection Navigation delay Improper navigation Wrong path to navigation	Organization supervisory, safety climate, HMI, procedure, task, workplace conditions, stress, fatigue, bias	
	Reading simple value					
	Adjusting parameters					
	Scanning screen		Arranging	Wrong arrangement		
	Verifying information					
	Input information					Inputting
Situation assessment	Comparing parameter	Misunderstand the status Fail to explain the status Inadequate explanation Unable to identify	Navigating	Wrong navigation selection Navigation delay Improper navigation Wrong path to navigation		
	Diagnose overall status					
	Evaluating trend					
	Identifying					
	Monitoring alarms/state of indicator		Arranging	Wrong arrangement		
	Recording key information					
	Verifying information					
Response planning	Coordinating	Fail to follow a plan Fail to select a plan	Navigating	Wrong navigation selection Navigation delay Improper navigation Wrong path to navigation	Organization supervisory, safety climate, HMI, procedure, task, workplace conditions, stress, fatigue, bias	
	Diagnose overall status					
	Evaluating trend					

(continued)

**Table 2** (continued)

Primary tasks	Sub-tasks	Error modes	Secondary tasks	Error modes	PSFs
	Maintaining the status				
	Planning		Arranging	Wrong arrangement	
			Inputting	Wrong operation Inadequate operation Delayed operation	
Response implementation	Coordinating	Wrong target localization Operation omission Fail to adjust Operation delay Wrong operation Inadequate Communication Wrong communication	Navigating	Wrong navigation selection	Organization supervisory, safety climate, HMI, procedure, task, workplace conditions, stress, fatigue, bias
	Communicating			Navigation delay	
	Executing			Improper navigation	
	Maintaining the status			Wrong path to navigation	
	Recording key information		Arranging	Wrong arrangement	
	Adjusting parameters		Inputting	Wrong operation Delayed operation Inadequate operation	
	Input information				

**References**

1. Dhillon BS (1988) Human reliability with human factors. *Appl Ergon* 18(3):254
2. Boring RL (2010) How many performance shaping factors are necessary for human reliability analysis? Idaho National Laboratory. Report No. INL/CON-10-18620
3. Swain AD, Guttman HE (1983) Handbook of human-reliability analysis with emphasis on nuclear power plant applications. U.S. Nuclear Regulatory Commission, Washington, DC. Report No. NUREG/CR-1278
4. Kim JW, Jung W (2003) A taxonomy of performance influencing factors for human reliability analysis of emergency tasks. *J Loss Prev Process Ind* 16(6):479–495
5. Embrey D (2009) SHERPA: a systematic human error reduction and prediction approach. In: Contemporary ergonomics 1984–2008: selected papers and an overview of the ergonomics society annual conference, 2009, pp 113–119
6. Ekanem NJ (2013) A model-based human reliability analysis methodology (Phoenix method). Dissertation & Theses - Gradworks

7. Liu P, Lv X, Li Z, Qiu Y, Hu J, He J (2016) Conceptualizing performance shaping factors in main control rooms of nuclear power plants: a preliminary study. *Eng Psychol Cogn Ergon* 322–333
8. Hollnagel E (1998) *Cognitive reliability and error analysis method (CREAM)*. Elsevier
9. Gertman D, Blackman H, Marble J, Byers J, Smith C (2005) *The SPAR-H human reliability analysis method*. Washington, DC, U.S. Nuclear Regulatory Commission. Report No. NUREG/CR-6883
10. O'Hara JM, Higgins JC, Fleger SA, Pieringer PA (2012) *Human factors engineering program review model*. New York: Brookhaven National Laboratory. Report No. NUREG-0711
11. Forester J, Dang VN, Bye A, Lois E, Massaiu S, Broberg H (2014) *The international HRA empirical study: lessons learned from comparing HRA methods predictions to HAMMLAB simulator data*. U.S. Nuclear Regulatory Commission, Washington, DC. Report No. NUREG-2127
12. Park J, Jung W, Kim J (2020) Inter-relationships between performance shaping factors for human reliability analysis of nuclear power plants. *Nucl Eng Technol* 52(1):87–100
13. Groth KM, Swiler LP (2013) Bridging the gap between HRA research and HRA practice: a Bayesian network version of SPAR-H. *Reliab Eng Syst Saf* 115:33–42

# Preliminary Establishment of Emotion-Inducing Library of Chinese Folk Music and Embodying Effect in Emotion Inducing



Bo Wang, Hong Yuan, Huijiong Yan, Changhua Jiang, and Shaowen Ding

**Abstract** Emotion induction and the study of the relationship between human behavior and emotion are the foundation of affective computing. In order to establish a library of emotion-inducing materials suitable for Chinese people and explore the expression characteristics of Chinese subjects' emotions, first 30 segments of Chinese folk music were selected as the inducing materials, and then two groups of emotion-induced controlled experiments were designed. Four subjects participated in the experiment. In both experiments, Chinese folk music was used to induce emotion, and subjects were asked to score in PAD scale. In the first group, the subjects sat comfortably in the seats, while in the second group, they could express their bodies freely according to their understanding of musical emotions. The results show that 30 segments of Chinese folk music can effectively induce the positive, neutral and negative emotions, and there is consistency between human body behavior and individual emotion expression.

**Keywords** Emotional induction · Embodied emotion · Chinese folk music · Natural human–computer interaction · Affective computing

## 1 Introduction

Emotion induction and the study of the relationship between human behavior and emotion are the basis of affective computing. How to induce human emotions and study the interaction between human behavior and emotions [11], thus establishing artificial emotion computing models to better achieve intelligent human–computer interaction, has become a research hotspot [3].

Emotional induction is to obtain an effective emotional response, and the induced method is adopted to make the subjects produce corresponding emotions. In the past few decades, the methods used to induce emotions in the laboratory include

---

B. Wang (✉) · H. Yuan · H. Yan · C. Jiang · S. Ding  
Key Laboratory of Human Factor Engineering, China Astronaut Research and Training Center,  
Beijing 100094, China  
e-mail: [wowbob@139.com](mailto:wowbob@139.com)

methods of recall, imagination, pictures, movies and music [8]. The inducing effect of recall method and imagination method is unstable; the emotion duration induced by picture method is short; the effect of film method is good, but the inducing factors are complex; the immersion of music method is the best, long lasting and the highest reliability and validity [11]. The emotion-induced music used in previous studies was mostly Western classical music. Due to cultural differences, Western classical music has differences in the emotional induction of Chinese people [1], and popular songs are more susceptible to the complex effects of lyrics. To this end, it is necessary to adopt a kind of induced music suitable for the Chinese subjects. Chinese folk music is Chinese localized music, which is consistent with Chinese folk customs and emotional expression [7]. Therefore, this study uses Chinese folk music as the emotional induction material.

The relationship between emotions and human behavior, also known as embodying emotions, was first systematically described by Niedenthal [5]. The expression of human emotion is composed of inner feelings and explicit behaviors. The embodied cognitive theory finds that during the process of inducing emotions, while expressing emotions through behaviors, the expressed body posture will also affect people's emotional feelings. In addition, in Émile's music teaching, students are required to reproduce the music they hear through their bodies [10]. This method is used to train the subjects, that is, when the subjects listen to music, they express their feelings of music through language or non-verbal behavior.

However, in the existing research, there are few studies on the interaction between emotions induced by Chinese folk music and the expression of explicit behaviors on emotions, and it is very necessary to promote the adaptability of embodied theory in different countries. Therefore, in this study, while trying to establish a Chinese folk music induced library, through a controlled experiment, we initially explored the embodying effect on subjects in the Chinese population.

## 2 Methods

### 2.1 Selection of Chinese Folk Music Materials

First, we collected 316 folk music from the catalog of China Ancient Music Network that are expected to induce emotions, all in APE lossless format; uniformly edited to 44.1 kHz sampling frequency, stereo channels, 32-bit sampling bits. According to the natural fluctuation of the music melody, the length of each piece of music is edited to 30–60 s.

Then, 76 effective music were screened out by 4 psychologists, including 15 negative music, 22 neutral music and 39 positive music. After that, 4 music teachers scored 73 pieces of music one by one according to the sentiment scale to judge

the consistency and strength of the music emotion and deleted 3 pieces. Finally, after comprehensive screening and simplification, 30 pieces of music are obtained, including 11 pieces of negative music, 8 pieces of neutral music and 11 pieces of positive music.

## **2.2 Tools**

Before the experiment, the personality of the subjects was tested using the “Chinese version of the Eysenck Personality Questionnaire Short Form” [6].

For the evaluation of emotional vocabulary, subjects selected 1 or 2 words from the traditional Chinese musical emotional vocabulary (sadness, happy energy, tranquility, anger, tension, warmth, transcendence, solemnity and others [5]), which best represents feeling.

The assessment of pleasure–displeasure, arousal–nonarousal and dominance–submissiveness uses a self-reported 9-point scale [2] to assess the subjective emotional intensity induced by the subjects. After listening to the music, the stronger the emotion, the closer the score is to 9, and the weaker the emotion, the closer the score is to 0.

## **2.3 Subjects**

Subjects were 4 college students, 2 men and 2 women, aged between 22 and 25 years old. None of them have participated in similar experiments. A music background survey was conducted, and it was found that 2 of them had entry-level musical instrument performance experience, and 1 had elementary dance experience; 4 of them had no composition experience, and 1 person could distinguish the type of musical instrument.

## **2.4 Experimental Procedures**

Each subject undertook two groups of self-controlled experiments with an interval of 7 days.

The first group of experiments (G1): subjects sat comfortably in the seats. The music was randomly played by the experiment organizer through the Hama carton stereo surround sound. Subjects listened to a piece of neutral music until they were in a calm mood before starting the formal experiment. Subjects listened to 30 pieces of music in turn. After each piece, they filled in the scale according to their actual feelings and rested for 60 s, before listening to the next piece of music.

The second group of experiments (G2): subjects were asked to stand, expressing the musical emotions they felt through physical behavior, such as imitating the conductor’s beat. The rest of the process is the same as the first group experiment.

### 2.5 Statistical Methods

SPSS 18.0 is used for statistical analysis.

## 3 Results

### 3.1 Reliability Test

The internal consistency reliability of the two groups of experiments is: experiment 1,  $\alpha = 0.761$  and experiment 2,  $\alpha = 0.812$ . This shows that the stability of the experiment is high.

### 3.2 Individual Differences

The average statistical results of the subjects on the three scales (Fig. 1) show that except for subject 1, the score distribution of the other three subjects is consistent; the degree of superiority is the degree of the subject’s expression of music emotion.

**Fig. 1** Means of the PAD scale in two groups of experiments (simplified as G1, G2)

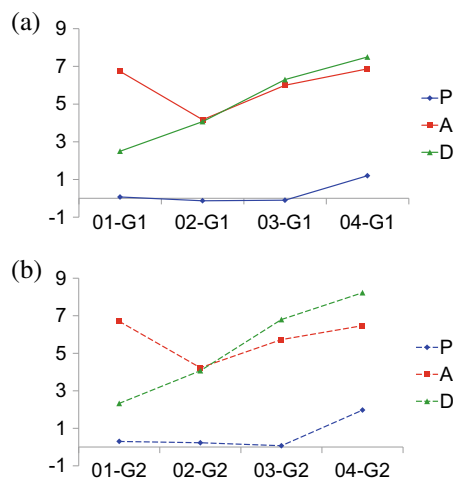




**Table 1** *T* test of G1 and G2

PAD	<i>T</i>	df	Significance (bilateral)
Pleasure–displeasure (P)	-2.454	119	0.016
Arousal–nonarousal (A)	1.345	119	0.181
dominance–ubmissiveness (D)	-2.327	119	0.022

Subject 1 had a lower score, while subject 1’s N-scale score was less than 30 points in the personality test, indicating that his emotional response was slow and mild, which was consistent with the low score of dominance.

The results of the correlation analysis between the subjects and the scale showed that the subjects were significantly correlated with dominance and pleasure ( $P < 0.01$ ), in which the correlation coefficient with dominance was 0.895, showing a strong correlation; the correlation coefficient with pleasure was 0.212, showing a weak correlation; the subjects were not significantly correlated with the degree of activation.

### 3.3 Differences Between Two Groups of Experiments

The difference between the experimental design of the two groups is whether there is any restriction on the behavior expression of the subjects. Paired sample *T* test was performed on the two sets of data (Table 1), and the results indicated that the *P* values of the pleasure and dominance were less than 0.05, which was considered to be significantly different between the two groups of experiments; the *P* values of the activation degrees were greater 0.05, which is considered to be no significant difference between the two groups of experiments.

### 3.4 Music Emotion and Classification

Music has a significant correlation with pleasure and activation ( $P < 0.01$ ), in which the correlation coefficient with pleasure is 0.676, which is strongly correlated, and the correlation coefficient with activation is 0.289, and the correlation is weak; at the 0.05 level of significance, music is related to dominance, the correlation coefficient is 0.158, and the correlation is weak (Table 2). Therefore, the classification of music is based on the degree of pleasure and activation. Using the systematic clustering Euclidean distance to classify music into two groups, the first classification calculates the degree of happiness, the second classification calculates the degree of happiness and activation. In the two clustering results, the music is divided into three categories, only music 8 has a grouping difference, and the rest of the music is divided into: the first category (containing 12 pieces of music, which is negative), the second category

**Table 2** Correlation between music and scale

		P	A	D
music	Pearson correlation	0.676	0.289	0.158
	Significance (bilateral)	0.000	0.000	0.015
	N	240	240	240

(including 7 The piece of music is neutral) and the third category (containing 10 pieces of music is positive). In the emotional vocabulary statistics of the three types of music, negative music tends to be “sorrowful,” neutral music tends to “comfort” and “warmth,” and positive music tends to “happiness and vitality.”

## 4 Discussions

The results show that 30 pieces of music can effectively induce the positive, neutral and negative emotions of the subjects, thus establishing a set of Chinese folk music library effective for Chinese people. The emotions expressed by the music in this library are definite and uncomplicated. The experimental data also confirmed the validity of the emotion-inducing materials selected in this study. The selected music can effectively induce three types of emotions, and the induced emotions are consistent with the music emotion classification before the experiment.

In the two groups of self-control experiments, the consistency of the joy and activation of the music clips shows that the objectivity of the music emotions will not be different due to the change in the experiment design and the individual test subjects, so the music library established in this experiment can be universal used for emotional induction. The feedback from the subjects after the experiment showed that the subjects encountered familiar music more easily to produce emotional resonance, and the induced emotions were stronger. This shows that the adoption of Chinese folk music is consistent with the cultural background of the subjects, and the emotional feedback obtained is more effective.

The results of the *T* test show that there are significant differences in the scores of the two groups of experiments on the scale of pleasure and dominance. It can be considered that the differences in the experimental design lead to the subjects' experience and expression of musical emotions. The difference between the experimental design of the two groups is whether there is any restriction on the expression of the subject's behavior, and the emotional induction intensity of the limited physical behavior expression (performing the band conductor's tempo) is greater, but the result is not significant. In the first group of experiments, the negative music's emotional score was  $-1.04$  and the second group was  $-1.35$ . The second group of experiments induced stronger negative emotions through restricted physical behavior expression. This validates the existence of emotional avatars: restricted behavioral expression affects the subjects' emotional feelings and judgments [4, 9]. Domestic

and foreign researches on tangible effects have found that under the restriction of facial or hand movements or behaviors, changes in human muscles affect emotional experience, which is not cognitively processed [5].

The subject's expression of musical emotion (dominant degree) showed a strong correlation with the subjects (the correlation coefficient was 0.895), and each subject's expression of music was different. In addition, the correlation between dominance and music is weak, which validates previous scholars' research results [2]. From the perspective of social culture and population characteristics, compared with Western culture, Chinese people's emotional expression is more restrained and discourages the expression of individual emotions; in addition, the subjects in this experiment are all science and engineering students, lacking in their own expression of emotions.

The experiment uses two evaluation methods to classify music: PAD's 9-point sentiment scale and seven emotion description words. In the end, the music is classified by negative, neutral and positive. The results show that the evaluation of musical emotions using the emotional scale and emotional description words is consistent. For example, the subjects' negative music tendencies and "sorrow" emotions are selected, and the scale scores are distributed from  $-2$  to  $-0.38$ ; sexual music tendencies and choices "tranquility" and "warmness," the scale scores are distributed from  $-0.38$  to  $1.25$ ; positive music tendencies and choices "happy vitality," the scale scores are distributed from  $1.75$  to  $3.5$ . It shows that the seven emotion description words used in the experiment are consistent with the evaluation effect of the PAD emotion scale, and it is easy to evaluate the scale, providing a convenient method for rapid and real-time evaluation of emotions.

## 5 Conclusions

A Chinese folk music library that can effectively induce positive, neutral and negative emotions of individuals has been established, which provides materials for emotional induction. It is verified that the embodied effect exists in the music experience, and it is instructive to emotional human-computer interaction. In future research, students of different majors will be invited to participate in the experiment; at the same time, a comparative experiment of Western music and Chinese folk music should be designed.

**Acknowledgements** This study was supported by the project SYFD160091812, YJGF171201 and 61400040103.

### Compliance with Ethical Standards

The study was approved by the Logistics Department for Civilian Ethics Committee of China Astronaut Research and Training Center.

All subjects who participated in the experiment were provided with and signed an informed consent form.

All relevant ethical safeguards have been met with regard to subject protection.

## References

1. Li D, Cheng Z, Dai R, Wang F, Huang Y (2012) Preliminary establishment and assessment of affective music system. *Chin Mental Health J* 026(007):552–556
2. Li X, Fu X, Deng G (2008). A preliminary trial of simplified Chinese version of PAD Emotion Scale among college students in Beijing. *Chin J Mental Health* 225):327–329
3. Lian Z, Li Y, Tao JH et al. (2020) Expression analysis based on face regions in read-world conditions. *Int J Autom Comput* 17(1):96–107
4. Liu Y, Wang Z, Kong F (2011) The view of emotional body: a new perspective of emotional research. *Prog Psychol Sci* 19(1):50–59
5. Niedenthal PM (2007) Embodying emotion. *Science* 316(5827):1002–1005
6. Qian M, Wu G, Zhu R et al. (2000) Revision of EPQ-RSC. *J Psychol* 32(3):317–323
7. Shi J (2015) Emotional structure analysis of Chinese folk music. East China Normal University
8. Westermann R, Spies K, Stahl G, Hesse FW (1996) Relative effectiveness and validity of mood induction procedures: a meta-analysis. *Eur J Soc Psychol* 26(4):557–580
9. Wu B (2015) The effect of body effect and empathy on facial expression recognition. Zhejiang University
10. Xie M (2011) Some experience of body rhythm design and teaching. *China Music Educ* 6:19–20
11. Zentner M, Grandjean DM, Scherer KR (2008) Emotions evoked by the sound of music: characterization, classification, and measurement. *Emotion* 8(4):494–521

# Design and Research on Guide Blind Device Based on User Experience



Jianyi Zhang, Xinyu Shi, Xinqin Jin, Fengfeng Li, and Xin Chen

**Abstract** Facing the problem that the existing guide blind devices cannot fully meet the needs of visually impaired users, taking the guide blind device as study object, basing on user experience theory, studies the needs of visually impaired users and the future design direction of guide blind devices. Conduct user interviews and external observation experiments for visually impaired users, build user emotional experience maps, understand the road factors that affect visually impaired travel and the true needs of visually impaired users for guide blind devices. Transform user needs into practical and feasible function implementation directions, and explore suitable functions and interaction methods of guiding blind devices. The research results show that the future guide equipment should meet the needs of users at multiple levels and achieve simple operation, lightweight volume, and interactive humanization.

**Keywords** Guide Blind device · User experience · Visually impaired people

## 1 Introduction

At present, there are 36 million blind people in the world. In the future, the visually impaired population will increase sharply with the increase in the global population and the number of aging populations [1]. The market demand for guide blind devices will also increase. Traditional guide blind devices are mainly guide sticks and guide dogs. They have disadvantages of low security and high cost. Most of the guide blind devices on the market are ground-based mobile, which generally have problems of large size, inconvenient carrying, difficult movement, complicated operation, and high learning cost. In the future, the design and research trend of guide blind devices must be easy to carry, easy to operate, easy to learn, and improve the quality of life of visually impaired users.

---

J. Zhang (✉) · X. Shi · X. Jin · F. Li · X. Chen  
School of Mechanical and Power Engineering, Harbin University of Science and Technology,  
Harbin 150080, China  
e-mail: [jianyi990925@126.com](mailto:jianyi990925@126.com)

© The Editor(s) (if applicable) and The Author(s), under exclusive license to Springer 1029  
Nature Singapore Pte Ltd. 2021  
S. Long and B. S. Dhillon (eds.), *Man-Machine-Environment  
System Engineering*, Lecture Notes in Electrical Engineering 645,  
[https://doi.org/10.1007/978-981-15-6978-4\\_118](https://doi.org/10.1007/978-981-15-6978-4_118)

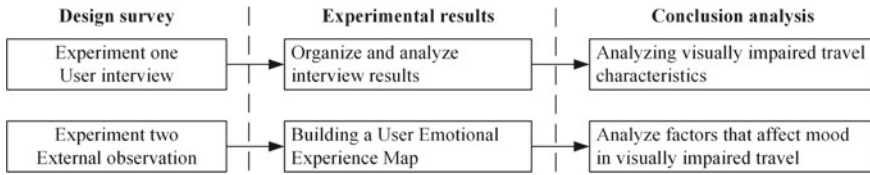


**Fig. 1** Experimental flowchart

Visually impaired users experience the external world differently than those with sighted eyes. Designers often consider user needs from their own perspective, ignoring the psychological and use characteristics of visually impaired users [2, 3]. Visual impairment will cause the psychological loss of visually impaired users, and they need psychological care. This article hopes to find out the real needs of visually impaired users through user experience research, propose design directions for guide blind devices, and improve safety, ease of use, and comfort of devices.

## 2 User Experience Research

### 2.1 Research Methods

Based on usability and “user-centered design,” user experience design studies the quality of interaction technology from the perspective of product structure, product function quality, and user emotional needs. User experience has the characteristics of dynamics, environment dependence, and subjectivity [4–8]. ISO 9241-210 defines user experience as: all the reactions and results of people to the products, systems, or services used or expected to be used [9]. User experience research affects how users feel about using products and the ways in which users and products interact, including how users understand, learn, and use products [10]. Based on the user experience, the design and research of the guide blind device were carried out. The specific experimental process is shown in Fig. 1.

### 2.2 Experimental Process

During the experiment, a visually impaired cultural service center and a blind association were contacted, and 31 visually impaired users aged from 23 to 62 were selected to cooperate with the experiment. Among them, 25 are males and 6 are females. The occupations are dominated by masseurs, including two expert users who use blind sticks. Conduct user interviews with the above users to learn about their daily outing times, travel modes, travel common situations, emergency handling methods, and

function evaluation and expectations of guide blind equipment. During the interview, observe and record the respondent's expressions, language expressions, body movements, etc. as the basis for judging the user's true expression and studying the visually impaired users' spatial perception judgment.

In order to study the relationship among people with visually impaired trips, guide blind devices, and the social environment, an expert user was selected to make an external observation experiment. The experiment requires the participant to walk independently in a familiar environment under clear weather conditions, pass through residential areas, traffic intersections, and other places, and experience harsh traffic environments such as mobile phone calls, pedestrian flow, vehicles, and car whistle. The participants were also asked to change their destinations without knowing it in advance.

### 2.3 Experimental Results

The results of user interviews show that the behavioral characteristics of visually impaired users have similarities. 90% of the participants lack security, fear to travel, and do not travel independently in unfamiliar environments. 87% of the participants chose to travel at night because there were fewer pedestrians at night, and they were not easy to be pointed by passer-by. The visually impaired travel experience of different age groups is significantly different. Young visually impaired users rely more on peers and pay more attention to passer-by.

Quantify the emotional numbers of the participants in each node in the external observation experiment to obtain a user emotional experience map, as shown in Fig. 2. User experience map is a tool to describe the interaction between users and products, systems, and services at each stage of a whole process. It can intuitively show user needs and expectations [11, 12]. User emotional experience maps can help designers understand user needs and develop guidance products that are more suitable for visually impaired users.

It can be seen from Fig. 2 that the emotional trough appears in two scenarios: receiving a call and crossing a traffic intersection. Participants also experience

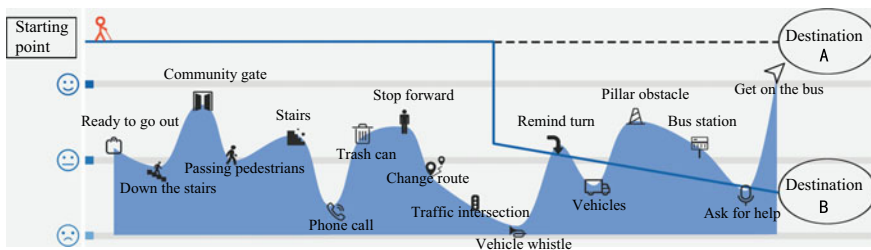


Fig. 2 User emotional experience map

emotional fluctuations when they encounter pedestrians and steps. It indicates that the unknown nature of dynamic environmental information will affect user emotions. Emotional peaks appear in the scene of reaching the community gate and getting on the bus. The familiar environment and reaching the destination will make the participants feel safe.

The above two experimental results show that visually impaired users are generally afraid of traveling and being discriminated by passer-by. Unknown environmental information affects the mood when traveling. Therefore, guide blind device should lead users to travel safely and let them know the road environment. It should also prevent visually impaired users from being discriminated by passer-by.

### 3 Experimental Evaluation

Sort out the user needs obtained in the previous experiment, screen out 15 user experience elements of the guide blind device, and divide them into three categories of safety needs, use needs, and spiritual needs, as shown in Table 1. Then, invite two users to conduct a rating evaluation of these 15 experience factors. The results show that the importance of visually impaired users' needs for guide blind devices

**Table 1** User experience elements

Demand category	User experience elements
Safety needs	Timeliness, completeness, and effectiveness of dynamic traffic information feedback
	Information acquisition capabilities at night and under extreme conditions
	The ability to guide users across obstacles
	Emergency capacity in emergencies
	Equipment reliability, including wear, failure rate, battery life, etc.
	Warning to passer-by and vehicles
Usage needs	Operational complexity (learning cost)
	Easy to use and organize
	Weight and volume
	Interactive experience of guide blind device
	Will it cause limb fatigue during use
	Does it cause hearing disturbance during use
Spiritual needs	Psychological doubts before traveling: not sure if the guide blind device is useful
	Evaluation from others during use
	Controllable experience of guide blind device: active operation or passive guidance



decreases in accordance with safety requirements, use requirements, and spiritual needs in the order of decreasing.

Visually impaired users are afraid of discrimination by others, and this emotion comes more from the judgment of themselves, which is a manifestation of lack of inner self-confidence. When traveling with confidence, the feeling of inferiority will be greatly reduced. Therefore, designers must pay attention to the mental needs of visually impaired users on the basis of meeting the safety needs and usage needs.

## **4 Architecture of Guide Blind Devices**

### **4.1 Interaction Mode**

Visually impaired people rely mainly on other sensory compensation when acquiring external information [13, 14], especially visual and auditory, so they are more sensitive to sound and tactile information [15]. The interaction design of guide blind devices should start from the perceptual characteristics of visually impaired users and adopt a combination of tactile and auditory information feedback methods to maximize the feedback of complete and accurate road conditions to users.

Oriented walking for visually impaired users is divided into active perception mode and passive perception mode, and guide blind robots are mostly passive perception mode, which will reduce the user's sense of participation. Therefore, the design of guide blind device should combine active mode and passive mode to eliminate the user's passive mood to travel. Users can freely switch between the two modes during use and grasp the initiative of travel.

### **4.2 Conceptual Scheme**

Based on the needs of users, the architecture of future guide blind device is proposed, as shown in Fig. 3. Future guide blind device should have the function of converting complete environmental information into sound and tactile feedback to the user. It should also have functions such as analyzing routes and road conditions, which can guide users to avoid obstacles safely and ensure users' safe travel. The design of guide blind equipment can also be integrated with increasingly mature 5G technology to enable mobile terminal app to quickly control guide blind device.

Lightweighting is an inevitable trend for the development of guide blind devices in the future. In order to reduce the traveling burden of visually impaired, guide blind equipment should be small in size and light in weight. Wearable guide blind device, flying guide blind device, and retractable guide blind device can be considered. From the perspective of safety requirements, guide blind equipment can also add

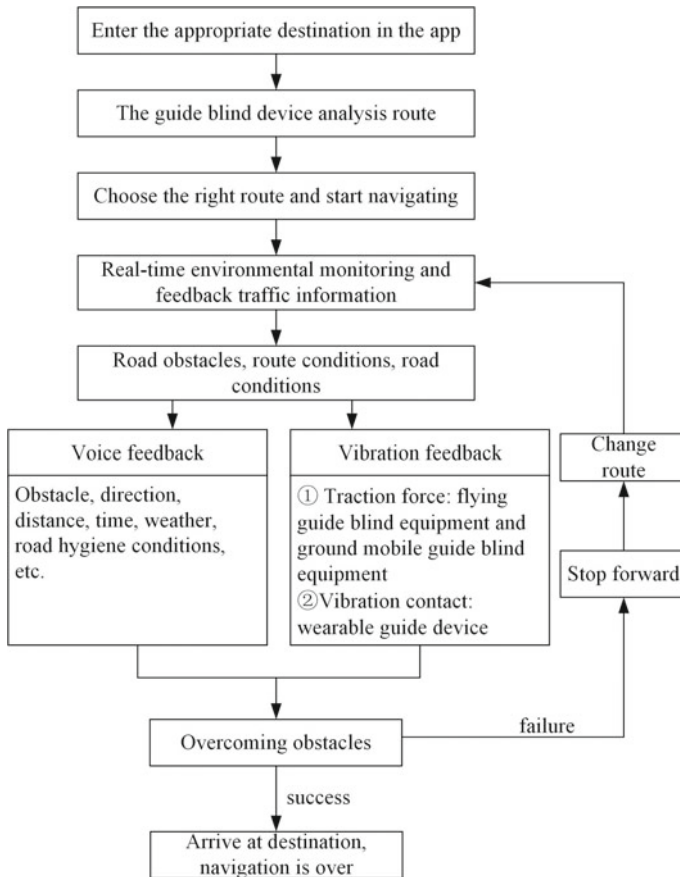


Fig. 3 Architecture of future guide blind devices

extended functions such as positioning, one-click help, low-battery reminder, weather reminder, etc.

## 5 Conclusion

Visually impaired users are part of society. In a highly civilized society, the living needs of special groups should be highly valued. When designing guide blind devices based on user experience, full consideration should be given to the physical specificity and psychological deficiency of visually impaired users to thoroughly analyze user needs and psychological demands.

In the design process of guide blind devices, designers must follow the design concept of visually impaired user-centric. Designers cannot consider the needs of

visually impaired users from the perspective of sighted people. The design research process based on user experience helps us understand the specific expectations of visually impaired users for guide blind devices, ensuring that the design results meet the real needs of visually impaired users. Future guidance equipment should improve safety, effectiveness, and have the ability to respond to emergencies. The form of guide blind device is not limited to large-volume robots, and it can become a part of the body of visually impaired users, reduce travel burdens, improve travel efficiency and improve self-confidence of visually impaired users, and allow visually impaired users to integrate into normal social life. In addition, future guidance devices need to be combined with the latest technology to optimize the interactive experience, improve the user's control and initiative in travel, and meet the user's spiritual needs.

**Acknowledgements** This work is supported by the University-Industry Collaborative Education Program, No. 201901024027 and No. 201901024021.

### **Compliance with Ethical Standards**

The study was approved by the Logistics Department for Civilian Ethics Committee of Harbin University of Science and Technology.

All subjects who participated in the experiment were provided with and signed an informed consent form.

All relevant ethical safeguards have been met with regard to subject protection.

## **References**

1. Bourne RRA, Flaxman SR, Braithwaite T et al. (2017) Vision loss expert group. magnitude, temporal trends, and projections of the global prevalence of blindness and distance and near vision impairment: a systematic review and meta-analysis. *Lancet Glob Health* 5(9):888–897
2. Chen X, Lu M (2017) The current development of orientation and mobility aids for hearing-impaired persons. *Chin J Spec Educ* (9):15–20
3. Cuturi LF, Aggias-Vella E, Campus C et al (2016) From science to technology: orientation and mobility in blind children and adults. *Neurosci Biobehav Rev* 71:240–251
4. Shijian Luo, Shangshang Zhu, Fangtian Ying, Jinsong Zhang (2010) Scenario-based user experience design in mobile phone interface. *Comput Integr Manuf Syst* 16(2):239–248
5. Shijian Luo, Rongrong Gong, Shangshang Zhu (2010) User experience oriented software interface design of handheld mobile devices. *J Comput-Aided Des Comput Gr* 22(6):1033–1041
6. Yi Ding, Guo Fu, Mingcai Hu et al (2014) A Review of User Experience. *Ind Eng Manag* 19(4):92–96
7. Hassenzahl M (2008) User experience (UX): towards an experiential perspective on product quality. *Proceedings of the 20th international conference of the association Francophone d'interaction Homme-machine*. Metz, New York, ACM, pp 11–15
8. Law ELC, Roto V, Hassenzahl M et al. (2009) Understanding, scoping and defining user experience: a survey approach. In: *Proceedings of the SIGCHI conference on human factors in computing systems*. Boston, New York, ACM, pp 719–728
9. ISO 9241-210 (2010) Ergonomics of human system interaction Part 210: human-centered design for interactive systems (formerly known as 13407). International Organization for Standardization (ISO). Switzerland, 7–9
10. Norman DA (1999) *The invisible computer: why good products can fail, the personal computer is so complex, and information appliances are the solution*. MIT Press, Cambridge

11. Yue H (2016) Seeing industrial services through experience lens—revealing a customer experience map to design for an experiential service in B2B context. Aalto University
12. Kizuka Ayumi, Ito Megumi, Oba Michiko (2015) Curriculum improvement in advanced ICT education by using an experience map for reflection. *IPSJ Sig Notes* 2015:1–7
13. Hu X, Wang J, Xu X (2016) Reader design for the blind person based on Kansei engineering. *J Mach Des* 33(5):121–124
14. Feng Y, Cheng G, Qiu Z (2019) Design of a fast manipulation training apparatus for visual impaired group. *J Mach Des* 36(1):134–138
15. Huang L, Liu T (2017) Interactive innovative design of barrier-free products for the blind. *Packag Eng* 38(24):108–113

# **Theory and Application Research**

# Analysis of Differences Between ISO and China Ergonomics Standards



Zhenlong Lu and Yanqiu Sun

**Abstract** Objective—In order to study the current status of ergonomics standards in ISO and china, analyze the differences between them in constraint content and publication year. Methods—It used quantitative analysis method of statistics to analyze the differences in the paper. Results—The number of China standards is equal to ISO in general ergonomics principles and anthropometry and biomechanics, but the number of China standards is about half of ISO in ergonomics of human–system interaction and ergonomics of the physical environment. Conclusion—The update speed of ergonomics standards is relatively slow in China, because of the difficulty in establishing national standards and the complicated procedures. The change way is to apply for group standards by society, which can respond to the market demand in time and promote the combination of production, learning and research.

**Keywords** International Organization for Standardization · Ergonomics · National standard · Difference

## 1 Research Purpose

Ergonomics is the foundation of modern design, standard is the basic tool of product design, International Organization for Standardization (ISO) attaches great importance to the work of ergonomics standardization and a large number of ergonomic standards for industrial design have been developed by ISO. Ergonomics standardization is the requirement for designing work system, work equipment and products according to human characteristics; the aim is to improve product availability, thereby improving the productivity for operators or improving the health, safety and comfort for users [1].

---

Z. Lu  
Tiandi Science & Technology Co., Ltd., Beijing 100013, China

Y. Sun (✉)  
China Academy of Safety Science and Technology, Beijing 100029, China  
e-mail: [sunyanqiu2002@163.com](mailto:sunyanqiu2002@163.com)

Socialism with Chinese characteristics has entered a new era. “High quality development” is an inevitable demand. “The Central Committee of the Communist Party of China Guidance of the State Council on quality improvement” of 2017 has put forward that stimulate quality innovation vitality encourages enterprises to optimize functional design, modular design, appearance design and ergonomic design, promote personalized customization and flexible production, improve the quality characteristics of product scalability, durability, comfort and so on, meet the needs of green environmental protection, sustainable development and consumption friendliness, encourage user-centered micro-innovation, improve user experience and stimulate consumption potential [2]. The development of ergonomics in China is facing new opportunities and challenges.

In the paper, we analyzed the differences between ISO and China ergonomics standards in constraint content, numbers, publication year and so on, which are based on the survey study of the current status of ergonomics standards, in order to provide reference for the further improvement of the construction of ergonomics standard system in China.

## 2 Research Method

In the study, we inquired the standard information published on the Web sites of International Organization for Standardization, Standardization Administration of China and work standard network and so on by the literature search and collected the relevant data of ISO/TC 159 and China’s ergonomics standards. It used quantitative analysis method of statistics to analyze the differences between ISO and China ergonomics standards in constraint content and publication year and discuss the future development of ergonomics standards based on the study results.

## 3 Study Conclusions

### 3.1 *Current Status of ISO Ergonomics Standard System Construction*

ISO/TC 159 ergonomics technical committee is created in 1974, which is responsible for the preparation and revision of international standards in the field of ergonomics, including terms, methods and human factors data. ISO 6385:1981 《Ergonomic principles in the design of work systems》 is the first ergonomics standard which was published by ISO/TC 159 ergonomics technical committee; the publication year is 1981. There are 26 participating members and 31 observing members in ISO/TC

**Table 1** Number of published standards and standards under development of ISO/TC 159

Committee or subcommittee	No. of published standards	No. of standards under development	Total
ISO/TC 159	1	1	2
ISO/TC 159/SC 1	8	0	8
ISO/TC 159/SC 3	24	7	31
ISO/TC 159/SC 4	70	13	83
ISO/TC 159/SC 5	33	6	39

159. There are four subcommittees in ISO/TC159, which are ISO/TC 159/SC 1 general ergonomics principles, ISO/TC 159/SC 3 anthropometry and biomechanics, ISO/TC 159/SC 4 ergonomics of human–system interaction and ISO/TC 159/SC 5 ergonomics of the physical environment.

Until February 20, 2020, there are 163 ergonomics standards in ISO/TC 159, including 136 published standards and 27 under development. There are two ergonomics standards under the direct responsibility of ISO/TC 159, including one published standards and one under development [3]. The numbers of published standards and standards under development of ISO/TC 159 ergonomics technical committee and subcommittee are shown in Table 1.

The published years of 136 ergonomics standards of ISO/TC 159 are shown in Table 2.

### **3.2 Current Status of China Ergonomics Standard System Construction**

The ergonomics standardization work in China was started relatively late, National Ergonomics Standardization Technical Committee was established in May 1980. Its technical committee number is SAC/TC7 in Standardization Administration of the P.R.C (SAC), who contacts with the International Organization for Standardization ergonomics technical committee (ISO/TC159). The secretariat is located in China National Institute of Standardization. The establishment of National Ergonomics Standardization Technical Committee not only promoted the development of ergonomics standardization work in China, but also greatly promoted the development of ergonomics subject [1].

National Ergonomics Standardization Technical Committee is responsible for the centralized management of standardization in the field of ergonomics technology, unified planning, studying and reviewing the development of national basic ergonomics standards. Until February 20, 2020, there are 93 ergonomics standards in China, including 81 national standards and 12 electric power industry ergonomics



**Table 2** Publication year of 136 ergonomics standards of ISO/TC 159

Year	No. of published standards				
	ISO/TC 159	ISO/TC 159/SC 1	ISO/TC 159/SC 3	ISO/TC 159/SC 4	ISO/TC 159/SC 5
1992	–	–	–	1	–
1995	–	–	–	–	1
1996	–	1	–	–	2
1997	–	–	–	2	–
1998	–	–	–	2	1
1999	–	–	–	4	–
2000	–	–	4	2	–
2001	–	–	–	1	3
2002	–	–	1	3	1
2003	–	–	2	1	2
2004	–	1	1	–	4
2005	–	–	2	1	2
2006	–	1	1	3	3
2007	–	–	3	1	4
2008	1	–	–	12	1
2009	–	–	–	1	–
2010	–	–	1	4	3
2011	–	1	–	4	–
2012	–	–	2	4	2
2013	–	–	1	3	–
2014	–	–	2	–	1
2015	–	–	2	2	–
2016	–	2	–	3	1
2017	–	1	1	5	1
2018	–	–	1	3	–
2019	–	1	–	8	1
Total	1	8	24	70	33

standards. Publication years of 81 national ergonomics standards in China are shown in Table 3, including 10 general ergonomics principles standards, 22 anthropometry and biomechanics standards, 31 ergonomics of human–system interaction standards and 18 ergonomics of the physical environment standards [4–6].

**Table 3** Publication year of 81 national ergonomics standards in China

Year	No. of published standards			
	General ergonomics principles	Anthropometry and biomechanics	Ergonomics of human–system interaction	Ergonomics of the physical environment
1983	–	–	–	1
1985	–	–	–	1
1988	–	2	–	–
1991	1	1	–	–
1992	–	1	–	–
1993	3	–	2	–
1994	1	–	–	–
1995	–	–	1	–
1996	–	2	–	–
1998	–	1	–	1
1999	1	–	–	–
2003	–	–	2	1
2004	1	–	3	–
2005	1	–	–	–
2006	–	–	3	1
2007	–	–	1	–
2008	2	1	1	6
2009	–	4	5	–
2011	–	6	2	–
2012	–	–	2	–
2014	–	2	1	–
2015	–	–	2	–
2017	–	–	–	7
2018	–	2	6	–
Total	10	22	31	18

### 3.3 Analysis of Differences Between ISO and China Ergonomics Standards

#### 3.3.1 Analysis of Differences in Ergonomics Standards Constraint Content

There are two mandatory national standards and 79 recommended national standards of China 81 national ergonomics standards, in which 52 of them are adopted international ergonomics standards, 29 of them are independently developed in China. So,

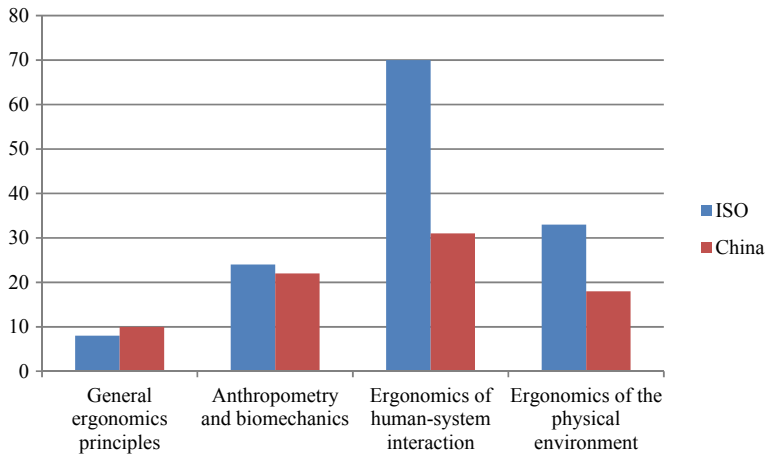


**Fig. 1** Comparison of the number of standards with different constraint contents

we can know that adopted international standards account for about 64% of national standards in China. The quantitative analysis results of ISO and China ergonomics standards in constraints content are shown in Fig. 1.

From Fig. 1, we can know that the number of China standards is equal to ISO in general ergonomics principles and anthropometry and biomechanics, but the number of China standards is about half of ISO in ergonomics of human–system interaction and ergonomics of the physical environment. The number of Chinese standards is relatively few, because china ergonomics standardization work was developed relatively later. In China, there are 14 national standards under development, in which nine independently developed national standards and five adopted international standards, mainly in ergonomics of human–system interaction standards and ergonomics of the physical environment standards.

### 3.3.2 Analysis of Differences in Ergonomics Standards Publication Year

The number of standards published by China and ISO in different years is shown in Fig. 2. We can know that the ISO ergonomics standards have been updated to 1992, and the standard is reviewed every 5 years. China ergonomics standards have been updated to 1983, and we also find that 19 of 52 international ergonomics standards have been withdrawn. The update speed of ergonomics standards is relatively slow in China; because of the difficulty in establishing national standards, complicated procedures and product standard cannot be supported. The development cycle is generally 2–3 years of national standards.

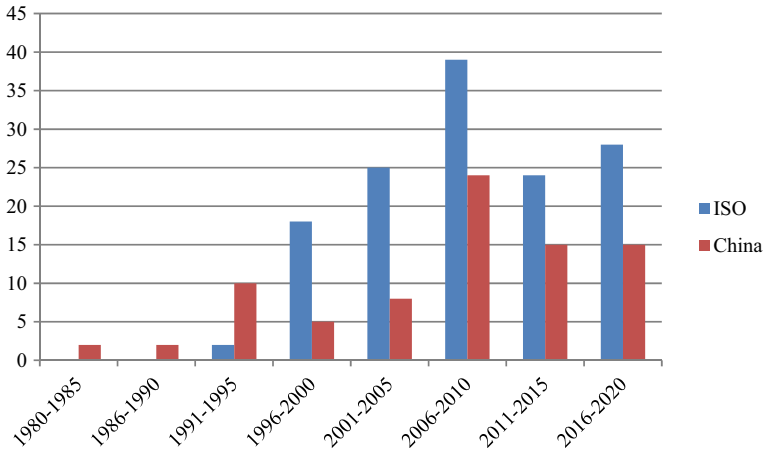


Fig. 2 Comparison of the number of standards with different publication years

### 4 Conclusions

The results of study show that the numbers of China standards are equal to ISO in general ergonomics principles and anthropometry and biomechanics, but the numbers of China standards are about half of ISO in ergonomics of human–system interaction and ergonomics of the physical environment. The update speed of ergonomics standards is relatively slow in China; because of the difficulty in establishing national standards, complicated procedures and product standard cannot be supported. The development cycle is generally 2–3 years of national standards.

### 5 Discussions

Ergonomics takes man–machine–environment system as the research object, focuses on human in the system, through the characteristic research on human physiology, psychology, perception, cognition, organization and so on, puts forward the design and optimization theory, method, principle and steps in products, facilities, human–computer interface, workplace, microclimate, personnel work organization and so on, finally realizes the best match of man–machine–environment and makes people work and live efficiently, safely, healthily and comfortably.

China’s ergonomics standards are gradually changing to meet the new development requirements. The change way is to apply for group standards by society, which can respond to the market demand in time, promote the combination of production, learning and research and advance the influence of ergonomics society.

**Acknowledgements** This work was supported by the National key R&D Program of China (2017YFC0804300), the basic research funding of China Academy of Safety Science and Technology (2019JBKY04, 2019JBKY11).

## References

1. Zhao C (2017) Ergonomic standardization progress. In: The 20th national psychology academic conference—abstract book of psychology and national mental health
2. The State Council of the People's Republic of China. The Central Committee of the Communist Party of China Guidance of the State Council on quality improvement. 2020/02/23. [http://www.gov.cn/zhengce/2017-09/12/content\\_5224580.htm](http://www.gov.cn/zhengce/2017-09/12/content_5224580.htm)
3. ISO. STANDARDS BY ISO/TC 159. 2020/02/23. <https://www.iso.org/committee/53348/x/catalogue/p/1/u/0/w/0/d/0>
4. The Standardization Administration of China. National Standard Full Text Open System. 2020/02/22. <http://openstd.samr.gov.cn/bzgk/gb/index>
5. Csres.com. A25 Ergonomics. 2020/02/22. [http://www.csres.com/sort/Chtype/A25\\_1.html](http://www.csres.com/sort/Chtype/A25_1.html)
6. Sun Y et al (2018) Construction and management of occupational health standards in China. *Occup Health J* 34(16):2292–2296

# Analysis on Core Capabilities and Key Technologies of Future Air Defense Anti-missile Operations



Jinxin Li, Zhenguo Mei, Qian Shen, and Tao Li

**Abstract** The future warfare is a kind of war based on the information technology, which is full-depth, three-dimensional, and conducts air strike and anti-air strike in multidimensional space. This paper discusses the development trend of modern air strike operations on four aspects: informatization, stealth, precision and integration, and puts forward three core capabilities for winning future air defense anti-missile operations, such as improving all-dimensional resisting capability with both offensive and defensive measures, improving anti-jamming capability with the combination of soft-kill and hard-kill, and enhancing anti-saturation attack capability in long-range and short-range. This paper analyzes the future development direction of air defense anti-missile weapon system such as low-altitude and short-range, integration and special-purpose, generality and modularization, as well as joint operations, and emphasizes four key technologies which should be mastered, including data acquisition, data fusion, precision guidance and system simulation.

**Keywords** Air defense weapon · Air defense system · Core capability · Key technology

## 1 Development Trend of Modern Air Strike Operation

With the evolution of modern war concept and the development of high-tech weapons and equipment, the role and effect of modern air strike operations are daily on the increase, and the development trend such as informatization, stealth, precision and integration has been increasingly prominent [1, 2].

---

J. Li (✉) · Z. Mei · Q. Shen · T. Li  
Artillery and Air Defense Forces Academy (Zhengzhou Campus), Zhengzhou 450052, China  
e-mail: [2495625853@qq.com](mailto:2495625853@qq.com)

© The Editor(s) (if applicable) and The Author(s), under exclusive license to Springer 1047  
Nature Singapore Pte Ltd. 2021  
S. Long and B. S. Dhillon (eds.), *Man-Machine-Environment System Engineering*, Lecture Notes in Electrical Engineering 645,  
[https://doi.org/10.1007/978-981-15-6978-4\\_120](https://doi.org/10.1007/978-981-15-6978-4_120)

## ***1.1 Informatization***

With the development of reconnaissance and detection technology, battlefield transparency is escalating, and information technology also runs through the whole process of air strike operations. Before the war, the processing, analysis and integration of a large amount of intelligence and information have become the main basis for identifying the air strike objective and formulating corresponding air strike plan. In the war, it is necessary to constantly adjust the battle plan according to the real-time information on the battlefield.

## ***1.2 Stealth***

High-tech stealth air strike is an air strike operation that uses stealth aircraft as an aerial platform to carry out precise strikes on targets. In the future, stealth air strike operations will be developed towards space and unmanned fighters, and air fleets of the composite manned and unmanned aircraft formation are gradually built up with the characteristic of air & space integration and the core stealth fighters.

## ***1.3 Precision***

The air defense equipment has advanced fire control system, optical and infrared aiming system, that can exactly calculate impact point and modify fire data momentarily, making the hitting accuracy greatly improved. Besides, air strike weapons have changed from the aerial bombs and a small number of ballistic missiles with poor accuracy into all kinds of precision-guided ammunition.

## ***1.4 Integration***

In the future local wars, modern air strike operations will be mainly information-centered and supporting system-based. In terms of information, a variety of ground, air- and space-based military intelligence and necessary political, economic and other social intelligence are integrated to conduct operational effectiveness analysis and select the channels and methods which can ensure their own safety as far as possible to identify the key points and area targets of the other side.

## **2 Analysis on Core Capabilities of Future Air Defense Anti-missile Operations**

Generally, the air defense combat system consists of four parts: an attack system with long-range key attack capability and short-range intensive fire protection capability, an information system that ensures real-time acquisition and timely analysis, judgment and processing of various kinds of information and formulation of air defense combat plans, a high-level electronic warfare system and a supporting guarantee system.

### ***2.1 Improving All-Dimensional Resisting Capability with Both Offensive and Defensive Measures***

In the battle, an efficient ground air defense system is supposed to resist long-range attacks against various types of aircraft, launch platforms and other targets with intensive fire shield composed of surface-to-air missile, anti-aircraft gun and new concept weapon system, and it also should be capable of intercepting a variety of precision-guided ammunition.

### ***2.2 Improving Anti-jamming Capability with the Combination of Soft-Kill and Hard-Kill***

In order to meet the needs of electromagnetic wrestle in the future battlefield, the innovative air defense missile system developed shall be able to counter a variety of jamming. Diverse anti-jamming measures such as self-adaption and intelligence shall be adopted to improve the anti-jamming reaction capability of the missile and make sure that the system has the capability to conduct reconnaissance, jamming and destroying the integrated air strike weapons.

### ***2.3 Enhancing Anti-saturation Attack Capability in Long Range and Short Range***

In the future local warfare, the common method to attack the key targets is the multi-wave saturation air strike composed of multiple types of aircraft and weapons. The air defense weapon system is supposed to have the anti-saturation attack capability, which is an important index in the development of air defense missile system. For instance, the new generation of missiles basically adopts the vertical launch mode



with multiple-round cluster installation to increase the quantity of ready missiles and enhance the firepower.

### **3 Development Focuses of the Air Defense Anti-missile Weapon System**

#### ***3.1 Emphasizing the Development of Lightweight, Small-Size Missiles and Low-Altitude Short-Range Air Defense Weapons***

In recent years, foreign intermediate-range and medium-range air defense missiles have a development trend toward miniaturization. The main method of missile miniaturization is to improve the guidance accuracy, reduce the warhead weight and reduce the missile weight by 2–4 times, which made the load of ammunition of the system increased significantly; thus, the firepower shall be greatly enhanced. Moreover, a variety of advanced technologies with anti-precision guidance capability have been applied to a new generation of low-altitude short-range air defense missiles.

#### ***3.2 Paying Attention to the Development of Air Defense Weapons that Combine Air Defense Anti-missile Integration with Special-Purpose Missile***

Tactical ballistic missiles, cruise missiles, air-to-ground tactical missiles and other precision-guided weapons are widely used in air strikes. The research of medium/high-altitude, medium/long-range air defense missile system that integrated air defense anti-missile for engaging not only aircraft but also missile and special-purpose anti-tactical ballistic missiles has become a hot spot in the development of air defense missiles nowadays.

#### ***3.3 The Air Defense Anti-missile Weapon System Has Obvious Characteristic of Generality and Structural Modularization***

In the future warfare, the common high-performance and multi-purpose missile, which is able to engage variety of weapon threats and is convenient for fielding in the peacetime and resupplying in the wartime, will become the development focus. The missile is capable of both engaging aircraft and intercepting tactical missiles,

it can be employed as the air-to-air missile, ground-to-ground missile and anti-tank missiles as well as undertaking air defense missions. Furthermore, as another important characteristic of the development of air defense missile in recent years, the modular design is capable of meeting different needs of users who may freely choose main subsystems to compose one or several kinds of air defense missile systems.

### ***3.4 The Advantages of Joint Operations Among Weapon Systems Are Outstanding***

In recent years, an important development trend of air defense missile weapon is that connecting diverse air defense systems with different performances into an organic whole to form the air defense fire system, thus exerting the anti-air capability of air defense weapons and achieving the optimum operational effectiveness. For instance, the American Patriot can be brought into the theater missile defense system of the USA, and Russian S-300 can be incorporated into the newly developed Russian S-400 integrated air defense system. The joint employment of various air defense missiles is an important development direction of the confrontation requirement of the future high-tech warfare system [3].

## **4 Study on Key Technologies of Air Defense Anti-missile Systems**

In order to enable the air defense system and the anti-missile system have higher combat effectiveness and compete with the increasingly perfect air strike system, we should mainly strengthen the research on key technologies as follows.

### ***4.1 Data Acquisition Technology***

#### **4.1.1 Automatic Target Identification Technology**

Automatic target identification includes radar, laser signal, infrared and TV image identification for targets. Since radar works in the bandwidth from meter to millimeter with little effect of meteorological conditions and the operating range is long, the automatic identification of radar targets is supposed to be researched emphatically [4]. The main tasks of automatic radar target identification are as follows:

- (1) Identifying real and fake targets, especially real and fake tactical ballistic missile warheads, and eliminating the possibility of launching missiles against the fake ones;

- (2) Determining the target structure to provide target type information for the fuze warhead coordination and improve the killing probability of the air defense missile;
- (3) Evaluating the danger of passive target tracking and providing the basis for fire distribution.

In addition, the first step of radar target identification is to extract the electromagnetic feature of the target, and the second step is to use the method of pattern recognition to classify the extracted target feature. The electromagnetic feature extraction of the target is the most important step in automatic target identification.

#### **4.1.2 Anti-stealth Target Technology**

At present, anti-stealth target measures are normally explored from the following aspects:

- (1) Increasing the transmission power of radar, improving antenna gain and reducing noise figure. The main technical approaches to improve transmission power include power synthesis technology and pulse compression technology with large compression ratio [5].
- (2) Making use of the polarization information and phase information of the target. Controlling the polarization characteristic of radar transmitting signal with computer, which can be adapted to the inherent polarization characteristic of target, so as to improve the target detection capability of radar.
- (3) Developing meter-wave radar and millimeter-wave radar. The meter-wave radar is an effective measure for anti-stealth target; however, due to the limitation of size of the antenna, its beam is wide and angular resolution is poor. The super-angle resolution technology has brought hope for solving the problem.
- (4) Adopting target reflection energy accumulation technology. The inverse synthetic aperture radar is capable of conducting coherent integration for thousands of pulse echoes, so the signal-to-noise ratio of a single echo pulse required to detect a target can be very small, and it has the ability to detect targets with small radar scattering cross sections.
- (5) Using laser and television technology. At present, stealth aircraft mainly take stealth measures on radio waves and infrared rays; however, they have no obvious effect on visible light and near-visible light bands. Therefore, laser and TV technology is an effective measure against stealth targets.

## **4.2 Data Fusion Technology**

The application of multi-sensor data fusion technology to target detection, tracking identification and battlefield situation assessment of air defense C4ISR system may improve the performance of C4ISR system in the following aspects:

- (1) Improving the space resolution of air defense system. Detecting and tracking with multi-sensor to obtain higher resolution than that of single sensor.
- (2) High accuracy of information acquisition. Effective synthesis of independent measurement data from multiple sensors at the same time of the same target or event can improve reliability and detection performance.
- (3) Widen the working spectrum of the system. The frequency complementation of multi-sensor may increase the dimension of measurement space and reduce the blind spots caused by electronic jamming measures and meteorological and terrain interference.
- (4) Being capable of resisting anti-radiation missile attacks. By adjusting the signal emitted by multiple sensors, it avoids the tracking of anti-radiation missile seeker.

### ***4.3 Precision Guidance Technology***

In order to ensure that the air defense missile can hit the target accurately in the complicated jamming environment, the research on the new precise guidance technology must be strengthened. One of the important development directions of precise guidance technology is the homing guidance technology, of which the imaging detection and multimode detection will be the emphases of its future development. Meanwhile, precision guidance technology is inseparable from detection technology, inertial sensing technology, intelligent information processing technology and high-precision control technology, whose technical level determines the performance of precision guidance equipment.

### ***4.4 System Simulation Technology***

The application of simulation technology in the development of weapons and equipment can reduce the development risks, shorten the development period and lower the development cost. The main application and development in the development of air defense missile are as follows:

- (1) Simulation of missile guidance system. In order to improve the missile's rapid maneuverability and operational capability beyond the upper atmosphere, the air defense missile will adopt more thrust vector control and direct force control technology. In order to solve the problems in the development of the new guidance system, a variety of simulation methods have been adopted, especially in the semi-physical simulation of millimeter-wave and infrared imaging guidance.
- (2) Simulation of all kinds of sensors. To strengthen the research on the simulation modeling of all kinds of photoelectric sensors in the whole process of development and application, especially attaching importance to the development

of the simulation technology of multifunctional phased array radar, satellite-borne synthetic aperture radar, satellite-borne and missile-borne photoelectric imaging sensor.

- (3) System simulation. Sensors on a variety of weapon platforms work together dynamically to conduct combat tasks through battlefield management/command, control, communications and computer (BM/C4) networking. Operational systems need to be established, including platforms for various weapons, sensors and satellites, as well as integrated distributed interactive simulation systems for BM/C4 systems.

## 5 Conclusion

As new-concept air strike weapons are successively operational and modern air strike technologies are increasingly mature, our army is facing a severe situation in air defense anti-missile operations in the future. There is an old saying goes, "Preparedness ensures success and unpreparedness spells failure." In order to adapt to the development trend of the new military revolution of the world and win the future information-based high-tech warfare, we should not only dare to look reality in the face and meet the challenge, but also be good at confronting the future, seizing the opportunity, deeply thinking, work out development strategy which is adapt to the national conditions and the future air defense anti-missile missile combat mode, so as to take the initiative in the future conflicts and wars [6].

### Compliance with Ethical Standards

The study was approved by the Logistics Department for Civilian Ethics Committee of Artillery and Air Defense Forces Academy (Zhengzhou Campus). All subjects who participated in the experiment were provided with and signed an informed consent form. All relevant ethical safeguards have been met with regard to subject protection.

## References

1. Song X (2015) Review on the development of Russian "Tunguska" integrated missile and gun air defense system. *Mod Weapon* 6:28–33
2. Min K, Xu Q (2005) The Slovak "Brams" missile and gun combined with self-propelled air defense system. *Artill Technol Inf* 9:27–29
3. Yin F (2014) Analysis on the command problem in air defense anti-missile. In: *Proceedings on equipment and technology development*, pp 734–736
4. Jia X (2017) The Turkish "Kurtuk" 35 mm self-propelled antiaircraft gun. *Weapon Knowl* 2:50–52
5. Wang H (2014) Analysis on the characteristics and key technologies of future air defense anti-missile weapons. In: *Proceedings of equipment and technology development*, pp 766–770
6. Li H (2018) Thinking on the development of army intelligent weapons and equipment. In: *Proceedings of the symposium on intelligent warfare*, pp 61–165

# Research on the System Architecture of Scientific Data Management



Rui Man, Guomin Zhou, and Jingchao Fan

**Abstract** The architecture construction of scientific data management system has become one of the important contents all over the world. The management system is to realize the collection, circulation, storage, release, and innovation of scientific data in the life cycle. At present, there are three modes for the construction of major scientific data management systems: independent development system, professional data management system, and construction system through open data source (Zhengguo and Xiang in *J Libr Intell Work* 57(3):39–42, 2013 [1]). This paper takes scientific data and its management as the entry point, analyzes the current situation on the basis of theoretical research, summarizes its characteristics and shortcomings, develops the scientific data service mode, and improves the service content, so as to improve the construction of the domestic scientific data system architecture.

**Keywords** System architecture · Architecture mode · Scientific data · Scientific data management

## 1 Introduction

With the rapid development of Internet of things, big data, cloud computing, block chain and other technologies, and the acceleration of digitization of scientific and technological documents and information, data resources have become an important factor of production. Governments and relevant organizations around the world also support the management of scientific data, which is defined by UNESCO as an open access information resource; The British Government has decided that publicly funded scientific data research is free of charge; the European commission has also

---

R. Man (✉) · J. Fan

Agricultural Information Institute of Chinese Academy of Agricultural Sciences, National Agricultural Science Data Center, Beijing 100081, China  
e-mail: [manrui@caas.cn](mailto:manrui@caas.cn)

G. Zhou

Department of Science and Technology Management, Chinese Academy of Agricultural Sciences, National Agricultural Science Data Center, Beijing 100081, China

© The Editor(s) (if applicable) and The Author(s), under exclusive license to Springer Nature Singapore Pte Ltd. 2021

S. Long and B. S. Dhillon (eds.), *Man-Machine-Environment System Engineering*, Lecture Notes in Electrical Engineering 645, [https://doi.org/10.1007/978-981-15-6978-4\\_121](https://doi.org/10.1007/978-981-15-6978-4_121)

issued a statement laying the groundwork for a greater role for scientific data in the future by ensuring its long-term availability, sharing, and reuse. At present, great changes have taken place in science research paradigm. In future, there are increasingly using technology tools for all kinds of research objects to carry out data monitoring, collection, and analysis activities, produce a large number of achievements of scientific data, the data results in urgent need of specialized management and utilization, and scientific data by the research on the system architecture. The architecture of scientific data management system mainly refers to the website, database, data center and other services that provide scientific data service for researchers. Through this medium, researchers upload or obtain data, making scientific activities more efficient, less costly, more standardized, and more high-quality.

## **2 Classification of System Architecture**

### ***2.1 Monitoring Network Mode***

The data collected in the monitoring network mode is stored on both the central node server and the local server, and the data are provided for the researchers through the service portal website and the cooperation of each sub-node. Monitoring network is generally established according to the needs of specific scientific research activities, which belong to the management mode of the general center. However, each data sub-center has its own flexible mode, and data opening is uniformly managed by the general center. Data management has high participation and complex open process. The data are collected by unified standards, and the nodes involved in data harvesting, opening and service are connected with their own system. Taking the data sharing service of China Meteorological Data Network as an example, the work is carried out from four aspects: establishing standard system, integrating scientific data resources, constructing sharing platform and developing data sharing service. The data service objects are all kinds of social groups and public users, including government departments, public welfare users and commercial users. The service mode is divided into online and offline data service. Online data service usually provides online data download and service through China Meteorological Data Network, and offline data service includes telephone consulting, information consulting, thematic data products, etc. [2]. Data services include shared directories, data downloads and numerical forecasts.

### ***2.2 Scientific Data Publishing Mode***

Scientific data publishing model refers to the user in accordance with the unified standards of management and process, in this paper, the way the data through the

Internet public release the raw data, or through the systematic collection and analysis of existing data, forming a data products after processing, sorting, make scientific researchers more convenient and rapid collection, acquisition, inspection, analysis, processing, reuse [3]. Through reuse and innovation, researchers can cite new publications and discoveries. Having clear intellectual property rights can be formally cited in academic publications. Having a global uniform identification can be persistent access, can be used to track data reference statistics and analysis, and can achieve total data quality management, to ensure data quality. As an innovative open data sharing model with a long history, it plays a role in the incentive mechanism and data quality control [4, 5].

### ***2.3 Open Platform Mode***

With the development and application of big data technology, the open platform mode has a unified data repository and shared service system which is open, and data can be stored in the platform for a long time. This mode generally includes data center, characteristic database, thematic database, etc., that centralizes data resources, data service and data maintenance to allocate resources of all parties. Its approach to data resource management is a common database for universal data storage and sharing requirements [6]. Each data set or file is assigned a numeric object identifier, which is a permanently unique and resolvable identifier that is an important part of the data reference. It covers material science, life science, earth science, social science, information science, chemical science, space astronomy, physical science and other fields.

### ***2.4 Large Scientific Installation Mode***

The mode of large scientific device refers to the data resource sharing activities marked by highly concentrated large-scale and high-input precision equipment, known for large-scale data production and standardized data opening [7], and large scientific devices and facilities for basic research and application, which continuously generate and capture data. This model is used to support exploratory and innovative scientific research with high technology content. According to their functions, large scientific devices can be divided into frontier fields of science and special technology equipment, such as remote sensing aircraft for public welfare scientific research [8]. There are two types of data resource sharing services: immediate and delayed. About the immediate sharing mode, generated data are processed and stored in an open platform for users to use, such as the data generated by remote sensing aircraft. About the delayed shared model, the data produced are first used for internal research and then organized to be used by researchers outside the research group in other forms.



### **3 The Development Trend of System Architecture**

#### ***3.1 Being the Focus About Architecture***

The construction of scientific data management system will become an important work of service institutions, and future research work will increasingly rely on the support of data resources. Therefore, data management can reduce costs, prevent the loss and damage of data, avoid the occurrence of fraudulent data and promote the improvement of the overall quality of scientific research results. Research institutions will pay more and more attention to data management, which will become an important work of university libraries, research libraries, research institutions and information service institutions in the future.

#### ***3.2 Forming the Union***

Through the establishment of scientific data management system alliance to enhance the scale and competitive strength. From the successful experience of foreign countries, large scale can promote data sharing. Therefore, a scientific data management system construction alliance should be established in the future, not only between university libraries, but also between libraries of research institutes and enterprise data management centers, so as to fundamentally solve the scale and quality problems of domestic data sets and provide strong support for scientific and technological innovation.

#### ***3.3 Cultivating the Data Researcher***

The number of scientific data management institutions and personnel will continues to expand. At present, the talent training in this field is very weak. In China, only a few colleges have set up data-related majors, and a large number of data professionals will be needed in the future.

### **4 Current Situation and Problems**

The scientific data sharing system in colleges and universities, such as the social science data management system of Fudan University and the open research data platform of Peking University, has been developed in eight representative systems. On the whole, the overall construction condition is good, such as Wuhan University, Fudan University, Peking University and other extension to the Chinese Academy

of Sciences, the national science and technology basic conditions system center and provincial intelligence and information agencies. See Table 1.

#### ***4.1 Single Service Mode***

Scientific data services are diverse, including retrieval, access, latest dynamic push, tools and model applications, library information services, multimedia display, etc. Domestic scientific data systems generally focus on the retrieval, query and download of data, ignoring the utilization rate of scientific data.

#### ***4.2 Ignoring Data Service***

The service content of the domestic scientific data sharing system strengthens the data-oriented model and weakens the data-service-oriented model [9]. On the one hand, the service content is not perfect, and the life cycle of scientific data still needs to be deeply studied. It includes data space, data set, management plan, data organization, description, release, etc. It has obvious life cycle, that is, scientific data production, organization, storage, publication and utilization. University scientific data management platform in the library of Wuhan University, Fudan University social science data management system, open research data system of Beijing University, Chinese Academy of Sciences, scientific data cloud contain data submission, collection, organization, storage, analysis, visualization, sharing, distribution, publishing functions, but the lack of data management plan. On the other hand, the domestic scientific data sharing system is generally short of education, training and knowledge popularization services.

#### ***4.3 Risk and not-Sharing Data***

Risk exists in scientific data management system. The management system often involves the integration, data publishing, data trading, etc., while the scientific data management project is a complex system with constant development and change, especially to ensure the availability, authenticity and comprehensibility within a period of time. The risk of damage of experimental data, equipment failure, computer virus attack and so on may exist at the same time, which makes the scientific data management more difficult. However, the correlation is very low, and the correlation value between the data cannot be fully reflected, which makes it difficult to realize open access and restricts the benefit of scientific data. Its value has not been maximized [8].

**Table 1** Current situation of domestic scientific data management platform construction

Current situation of domestic scientific data management platform construction		Undertaking unit		Service content		Service mode	
Kind	Scientific data management platform	Undertaking unit		Service content		Service mode	
Scientific research institutions	Chinese academy of sciences data cloud	Science data center, Chinese academy of sciences		Quick search database, data service retrieval, search papers		Space science theme database: data network, fusion database	
National platform center	Intelligent manufacturing scientific data service platform	National science and technology basic condition platform center		Data directory navigation		Intelligent design, manufacturing process, automatic control, general technology, innovation management	
Provincial platform center	Scientific data	Guangdong provincial science and technology literature sharing platform		Retrieve by category and database name		Scientific data metadata-database. Solid waste database. South sea geographical database	
	Scientific literature and scientific data association construction platform	Sichuan science and technology literature sharing service platform		Retrieve by category, resource name		Scientific research equipment, plant resources, animal resources, microbial resources, research and experimental base	

(continued)

**Table 1** (continued)

Current situation of domestic scientific data management platform construction				
Kind	Scientific data management platform	Undertaking unit	Service content	Service mode
The university	Scientific data sharing system	Shanghai R&D public service platform	Rapid retrieval	Industry research report database, Shanghai large equipment information service database, competitive chemicals database
	University scientific data sharing platform	Wuhan university library	Rapid retrieval	Scorpion species resource database, research on comprehensive evaluation index system of urbanization in far city district of Wuhan city, library reader survey data, etc.
	Fudan University social science data management platform	Fudan University social science data research center	Basic and advanced retrieval	Shanghai rail transit credit card data, unionpay credit card data, Shanghai social development level comprehensive survey
	Peking University open research data platform	Peking University library	Basic and advanced retrieval	Database of China survey of Peking University, research center for health aging and contamination, Peking University

## 5 Construction Strategy of Domestic Scientific Data Management System

### 5.1 Improve the Top-Level Design

In the era of big data, the society advocates to create an environment where everyone is a data provider and user. Researchers need to fully understand the importance and necessity, dare to carry out top-level design and formulate the objectives and implementation plans at different stages [10].

- (1) Reasonable organizational structure and management: The scientific data management system should have the elements of the institution—the establishment of long-term preservation policy, the establishment accountability to ensure the construction and service from the macro-policy level.
- (2) Data cloud service: The scientific data management system has been upgraded, which is divided into three layers [11]. The first layer is SaaS. The second layer is DaaS, which is scientific data analysis technology. The third layer is IaaS, which includes storage resources, computing resources and data resources (Fig. 1).

### 5.2 Expand the Service Mode of Scientific Data

The construction of scientific data management system is the main means to carry out scientific data management effectively. In addition to the way of scientific literature information service, scientific data service is also available, that is, management planning, acquisition, storage and sharing, reuse, management training, scientific data protection and ethics and scientific data management reference [12]. The Chinese Academy of Sciences Data Cloud uses the DataPub data sharing system to promote sharing and communication. DataPub has the following functions: (1) *I HAVE DATA*, the data will be published on the DataPub, so that more people know, fully play the data value; (2) *I WANT DATA*, that is, to find and obtain the data on the Datapub, data requirements to the staff; (3) *DATA INTERACTION*, data community interaction, a full range of data exchange and interaction.

### 5.3 Improve the Service Content

- (1) Build Characteristic Resource Library: The scientific data management system should attach importance to the construction of characteristic resource base, such as the information service database of large instruments and facilities in Shanghai, which provides the inquiry, comparison and screening services of basic information, shared services and supporting policies.

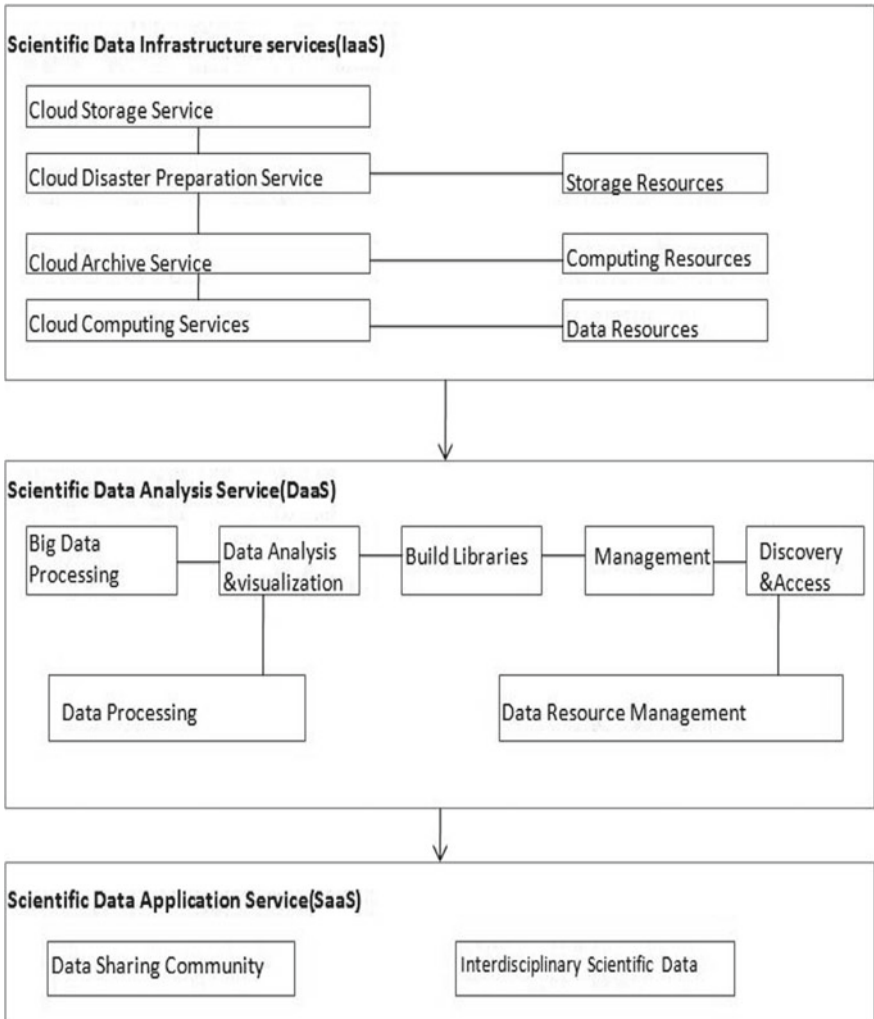


Fig. 1 Scientific data management system framework

- (2) **Precise Service Content:** It refers to the transformation from the base of users' common demand to the personalized service scheme for users [13]. For example, on the basis of collating a large amount of data, data warehouse technology is used to select users' knowledge preference for experimental data for research on the basis of users' access to scientific data log, so as to achieve accurate data push.
- (3) **Training and Promotion:** Scientific data management and sharing training is an important service content, including staff training and user training. System staff are required to have expertise in data extraction, transformation, loading

(ETL) processes and data pipeline construction, as well as rich data warehouse skills. By understanding the data required by the system, identifying relevant new data sources, extracting the available format data, ensuring that the data are not wrong and loading the data into the user requirements, the user's knowledge needs are satisfied.

#### ***5.4 Attach Importance to Risk Management***

At the beginning of the construction of the scientific data management system, it analyzes the possible risks in detail and formulates the perfect strategies to ensure the long-term and effective operation. It includes the risk of data resource optimization and integration, data publication and data transaction. Efforts should be made to train scientific data talents, such as data validators, data analysts, data visualization analysts, data management experts and data service coordinators. Therefore, the scientific data sharing system first makes full use of technical means to restrict the access between different regions and networks and establish a virus prevention and control system and a network security monitoring center.

**Acknowledgements** This work was supported by Agricultural Science, Technology Innovation Project of Chinese Academy of Agricultural Sciences (Project No. CAAS-ASTIP-2016-AII).

## **References**

1. Zhengguo H, Xiang Y (2013) Building an efficient scientific data management system based on dspace. *J Libr Intell Work* 57(3):39–42
2. Li S, Yuwa W (2018) Current situation and improvement Suggestions of data organization of China's scientific data sharing platform—an analysis based on the national science and technology basic condition platform. *J* 52–58
3. Ma HQ, Pu P (2015) Status analysis and comparison of research achievements on open data policy and an estimation of the research trends in China. *J Libr Sci China* 41(5):76–86
4. Zhang JB, Ren SH (2015) Research on scientific data publication models, flows and citation strategy. *J Libr Inf Serv* 59(9):21–27
5. Huang GB, Wang S, Qu YJ (2018) The comparative research on scientific data publication models. *J Acad Libr* 34–40
6. Qing W (2014) On the operation mode, guarantee mechanism and optimization strategy of open sharing of scientific data. *J Natl Libr China* 3–9
7. National Science and Technology Basic Condition Platform Center (2018) 2017 National science data resource development report. Science and Technology Press, Beijing
8. Ruhua H, Naidong H (2017) Research on mass scientific data management model-based on cloud services. *J Libr Sci Res* 41–44:72
9. Liu XW, Xiong R (2009) Analysis of the characteristics of policies on open access to scientific data in foreign countries. *J Inf Stud: theory Appl* 32(9):5–9
10. Global Change Research Data Publishing&Repository. [2018-07-17]. <http://www.geodoi.ac.cn/WebCn/Default.aspx>

11. G8.G8Open Data Charter and Technical Annex [EB/OL]. [2018-07-24]. <https://www.gov.uk/government/publications/open-data-charter/g8-open-data-charter-and-technical-an-nex>
12. Hongjun Y (2015) Investigation and analysis of reference service of domestic provincial science and technology literature sharing service platform. *J Libr Work Res* 78–83
13. Huilin Q, Bo S (2017) Research status and development strategy of library precision service. *J Lib Sci Res* 2–7



# Military Applications of Artificial Intelligence



Liang Du, Guangdong Li, Hai Chang, and Heyuan Hao

**Abstract** Artificial intelligence (AI) is one of the core technological innovations of future that can play an important role in making important changes in the world, in the transformation and development of modern society. AI technology has entered a new period of rapid development. At present, it is recognized as the most likely to change the future world of disruptive technology. Many countries in the world have raised the level of developing AI in the national strategy, not only from the policy guidance and strategic planning but also from funding and budget level to give strong support. To lay a foundation of the future military application of AI, we have to thoroughly analyzed the application of AI in this field and found the key points of the development of it.

**Keywords** Artificial intelligence (AI) · Military field · Military applications · Information technology · Military decision-making · Big data

## 1 Introduction

Artificial intelligence (AI) is a technology that can be used for improving complex tasks through automation and hence improving the system performance.

These tasks include perception (sound and image processing), reasoning (problem solving), knowledge representation (modeling), planning and communication (language processing), and autonomous systems (robots).

Artificial intelligence technology content mainly includes natural language understanding, knowledge expression and pattern recognition, planning and problem solving, machine translation and speech synthesis, theorem proving and inductive reasoning, learning and discovery system, cognitive model and expert system, machine vision and intelligent robot and intelligent automatic programming language, etc., involved in mathematics, linguistics, human science, philosophy, psychology, logic, computer science and some the various other subjects [1].

---

L. Du (✉) · G. Li · H. Chang · H. Hao  
Army Academy of Artillery and Air Defense Zhengzhou Campus, Zhengzhou 450052, China  
e-mail: 284119551@qq.com

© The Editor(s) (if applicable) and The Author(s), under exclusive license to Springer 1067  
Nature Singapore Pte Ltd. 2021  
S. Long and B. S. Dhillon (eds.), *Man-Machine-Environment  
System Engineering*, Lecture Notes in Electrical Engineering 645,  
[https://doi.org/10.1007/978-981-15-6978-4\\_122](https://doi.org/10.1007/978-981-15-6978-4_122)

AI is now creating new military and business paradigms. China has announced the “AI Global Leadership Plan” to ensure a leading position in the field of AI in the future, in July 2017.

In September 2017, Vladimir Putin told some students in a speech that AI leaders would be “the regulations of the world.” Some countries, such as Australia, have already incorporated techniques of advanced technical literacy, thereby, including AI into their military education.

In the military regime, the potential of artificial intelligence exists in all fields which certainly includes all levels of wars. It not only includes political and economic aspects, but also covers the aspects of military strategy, campaigns and tactics. For example, at the aspect of non-war military strategy, such as politics and economics, AI can destabilize adversary-related systems by producing and releasing a large amount of false information. In such scenarios, AI is also probably the best candidate against such attacks.

AI can improve the autonomous control performance of unmanned systems within tactical aspect. Similarly, the artificial intelligence weapons will change the dynamics of warfare in the future, from the war among people and the confrontation between weapons to the competition between human and machines and machines to machines.

It has been predicted that AI weapons will be the “third revolution in the military field” after gunpowder and nuclear weapons.

The world’s military powers, represented by the USA, have long foreseen the broad application prospect of artificial intelligence technology in the military fields. They have laid out a series of research and plans in advance, to vigorously develop the application of artificial intelligence and robots in the military field, striving to make a gap with their rivals in AI field.

History tells us that lagging behind is always bound to be attacked [2]. Therefore, in order to avoid losing the opportunity for development, China needs to catch up and vigorously develop artificial intelligence technology, especially the application and research of related technologies in military field.

## **2 Military Applications of Artificial Intelligence**

Artificial intelligence (AI) has made great strides in academia and business. Rapid development in the information technology, sensors, huge data and networking of things and complex military actions gives another opportunity to AI. Just like attacking weapon and the sensor significantly improve speed and provide intensive reading, and within a certain amount of time, the production, analysis and processing relevant data improve significantly both in the number and amount. Thus, we can have the preliminary judgment that not only non-military fields but in the field of military it can be a vital source of development.

AI will gradually penetrate into all the aspects of the military application field, with high command efficiency, precise strike, automatic operation and behavioral

intelligent weapons. AI capabilities will contribute uniquely to the battlefield in the future.

AI has military applications such as surveillance, reconnaissance, threat assessment, cyber security, intelligence analysis, command and control, as well as applications' related education and training fields. I will briefly describe the current military applications of artificial intelligence technology in the three military services.

## ***2.1 Land—Autonomous Vehicles***

It emphasizes on development of autonomous land vehicles on computer vision and image understanding techniques.

In addition to AI reasoning technology, it can not only achieve rapid perception and response, but also analyze and process the relevant environment to achieve the adjustment of the relevant tasks and strategies. Such vehicles' design can automatically determine the path and follow it.

The vehicle will eventually be able to not only detect obstacles in its path, but also to determine their properties, such as whether the object is a traversable object—as a kind of shadow or an impenetrable obstacle-boulder and respond accordingly.

## ***2.2 Airborne—the Pilot's Intelligent Assistant***

The pilot's intelligent assistant, also known as the intelligent pilot aide, is designed to provide expertise to individual fighter pilots.

Rather than automating the aircraft's normal functions, the feature logically provides expertise in specific areas by integrating the cockpit concept. The system consists of four main interactive expert subsystems such as situation assessment management system, tactical planning management system, mission planning management system and system status management system.

Special emphasis is placed on the driving interface, which includes voice recognition control [3], display and automation technology, natural language understanding and speech synthesis.

## ***2.3 Maritime—Naval Operations Management***

The goal of naval operations management is to use artificial intelligence demonstration techniques, particularly expert systems and natural language understanding, to aid operations with automated decision making tools for the complex systems being developed.

Five operational management functions have been identified as initial applications for fleet command center operations. It includes force requirements, capability assessments, campaign simulations, operational planning and strategic assessments.

These functions are clearly defined but involve complex process and are highly demanding and labor-intensive, requiring execution by people with certain skills and professional knowledge. Therefore, the use of AI technology to build a system decision assistance tool can reduce the requirements on the professional skills of relevant personnel to a certain extent.

AI provides an aid to complex tasks in the military field. From this point of view, artificial intelligence in the future is not limited to advantages and wide usage in military decision-making, but also involves many challenges.

- a. Risk means that military AI systems need to be more transparent in order to gain the trust of decision-makers and promote risk analysis. But most AI technologies lack sufficient transparency;
- b. Military AI requires reliable systems, which is the second challenge. Because in the case of not knowing the artificial intelligence technology used, it is vulnerable to imperceptible operation errors of input data;
- c. AI technologies are learned by machine learning based on massive amounts of training data, and the lack of data in AI military applications is another challenge.

From the ongoing projects to the operational use of artificial intelligence in the military, some of these challenges are now being addressed. Researchers are making progress on the transparency and interpretability of artificial intelligence. This part of the progress could tentatively apply in to military applications. But more in-depth requirements analysis is needed to figure out how to apply the researches.

The military sector is very different from the commercial sector in terms of risk control, data quality, legal requirements, etc. Some types of transparency may not even apply. In addition, how to use social science research to improve the interpretability of AI remains to be further studied.

There is currently no professional solution [4], especially for the monitoring of its research results, which requires continuous search for solutions by facing the possibility and challenge of the application of AI in the military field. Therefore, until these solutions are clear, it is necessary to minimize external access to models and defense technologies. Otherwise, the opponent will use the vulnerability to obtain relevant data for its advantage.

### **3 Military Applications of AI Have Its Advantages and Disadvantages**

The new era of intelligent, AI is coming at a speed beyond people's imagination, not only impacting all trades and professions, but also changing our minds. The development and application of artificial intelligence in the military field, with its' natural sensibility, is rising up.

The military application is a cutting-edge technology originated field that is constant fact. It leads to new military changes when new technologies significantly improve capabilities of it.

The USA, Russia and other traditional military powers foresee the broad application prospect of artificial intelligence technology in the military field and regard artificial intelligence as a subversive technology that can “change war regulations.” They believe that no matter from the war itself and its armaments, the new era of intelligence will be opened. And, they have already made the layout in advance, in order to hope to preempt the application of artificial intelligence in the military field and strive to pull away from potential rivals. It should be noted that AI military applications are a “double-edged sword.” It is quite understandable as AI has its advantages and disadvantages in military field. Stephen Hawking, a famous British physicist and cosmologist, said of artificial intelligence that “it could be either the best or the worst thing that has ever happened to mankind.”

This suggests that we should be cautious in the face of the threat of artificial intelligence and its application in the military field.

In the future, with the application of a large number of intelligent unmanned systems in the battlefield, the cost of war will be greatly reduced, and the “zero casualties” of fighters is expected to become a reality, which will easily lead to more arbitrary use of force by military hegemony.

In the complex battlefield environment, although there is a highly intelligent unmanned combat system, it is very likely to make errors in identification or suffer from enemy communication dimensionality reduction, electromagnetic and network attacks, resulting in “defection.” Therefore, it can be seen that major issues concerning war should never be easily left to artificial intelligence to make decisions. Even if artificial intelligence is increasingly perfect and mature in the military application field in the future, it should not be allowed to “barbaric growth” of intelligent weapons, and it is necessary to guard against possible problems in security, law, ethics and other aspects brought by artificial intelligence.

From the perspective of security process, social security supervision and control should be strengthened to form a social governance model suitable for the era of artificial intelligence.

We need to keep a clear mind and energize our energy in the form of technology that is expected to profoundly change the form of future war.

According to the history of military reform [5], science and technology play the role of priming and supporting. Whoever is sensitive to technological change and the first to achieve technological breakthroughs will be able to master the new rules of war and control the commanding heights for winning future wars. For an army, failure to correctly predict the direction of military scientific and technological breakthroughs and to correctly grasp the changes in the shape of war will not only lead to “technological generation gap,” but also lead to the loss of the country’s core capabilities and national security.

## 4 Conclusion

The bottleneck for AI to achieve further success is the ability to manage, implement and create. AI applications offer the potential to speed up data interpretation and free people to higher levels of tasks.

However, military leaders and related technicians must consider the invariance of the supervisory control system. While popular media often focus on AI replacing humans, there is no such thing as a complete replacement. Instead, new technologies will change humans and create new characters for them to achieve their goals. As with any other technology, AI applications must support the goals inherent in humans to set jobs.

Today, in the face of the “Great Change” and Great Breakthrough” in the development of science and technology, we should grasp the intrinsic driving influence of artificial intelligence on the evolution of the form of war from the design level and the height of the winning rules, so as to win the initiative in future wars.

We need to firmly grasp the major historical opportunities for the development of artificial intelligence, improve strategic planning, highlight the goal of intelligentization as the lead, closely track cutting-edge technologies and actively safeguard national security.

## References

1. Feng J General artificial intelligence basic research. Aerospace Press, 1999.08
2. Academic Department, China Association for Science and Technology. Development Prospect of Intelligent Variable Aircraft and Our Choice 2010.05
3. Liu P, Liao D Application research of artificial intelligence in the field of military political work 2009.02
4. Mitchell T Machine learning 2008.03
5. The future of artificial intelligence. Shaanxi Science and Technology Press, 2006.01

# Multi-dimensional Safety of Intelligent and Connected Vehicles for Future Traffic Scenarios



Quan Yuan and Junwei Zhao

**Abstract** The multi-dimensional safety of intelligent and connected vehicles (ICV) refers to the comprehensive safety characteristics integrating the requirements of the safety of functions, the safety of human–computer interaction, the security of information and communication, and space–time safety. It is the essential condition to implement the application of ICV. This paper discusses and analyzes the safety of ICV for future traffic scenarios. Firstly, as the basic guarantee for the safe operation of vehicles, the perception and decision-making and control functions of ICV are still unable to help to obtain high-quality perception data, high-speed reliable decision-making and accurate execution and control, and a series of problems. Moreover, the diversity of human–computer interaction brings greater challenges to the safety protection of occupant and vulnerable road users. In addition, information and communication security become more important in future intelligent cooperative transportation system. Furthermore, the diversification of spatiotemporal scenarios brings complex and changeable risks and challenges. By summarizing the multi-dimensional risk and safety problems that ICV may face in advance, the research results of this paper provide insightful references for the new concept design of ICV and future traffic safety management.

**Keywords** Intelligent and connected vehicle · Multi-dimensional safety · Future transportation

---

Q. Yuan (✉)

State Key Laboratory of Automotive Safety and Energy, Tsinghua University, Beijing 100084, China

e-mail: [yuanq@tsinghua.edu.cn](mailto:yuanq@tsinghua.edu.cn)

J. Zhao

School of Automobile, Chang'an University, Xi'an 710064, China

© The Editor(s) (if applicable) and The Author(s), under exclusive license to Springer Nature Singapore Pte Ltd. 2021

S. Long and B. S. Dhillon (eds.), *Man-Machine-Environment System Engineering*, Lecture Notes in Electrical Engineering 645, [https://doi.org/10.1007/978-981-15-6978-4\\_123](https://doi.org/10.1007/978-981-15-6978-4_123)

1073

## 1 Introduction

With the continuous development of the new round of scientific and technological revolution, chip algorithm iteration, control platform upgrading, and cloud control communication interconnection make the automobiles develop toward intelligent and connected directions, and the intelligent and connected vehicle has become an important strategic direction for the development of the automotive industry [1]. At the same time, a series of practical problems, such as complex road traffic conditions, instantaneous sudden traffic risky events, real-time transmission of data information and perception, decision-making and control operation reliability, etc., put forward strict requirements for the safety of the intelligent and connected vehicle. Compared with the low-level intelligent vehicle, the safety of the future intelligent and connected vehicle is facing multi-dimensional, all-round, and unpredictable challenges.

In recent years, many intelligent vehicles have exposed many problems in the test and verification processes, and their safety and reliability have attracted great attention [2]. The failure of driving system perception, decision-making, or control may easily lead to collision accidents. The distribution of control power between the autonomous driving system and the human driver brings uncertainty factors to driving safety. The autonomous driving system will receive wrong instructions or its important information will be stolen when hacked. The interaction safety of the vehicles of different intelligent levels is also a practical problem encountered in the process of the comprehensive popularization of ICV. The new type of accident form makes it be more necessary to guarantee the safety and reliability of the ICV in a multi-dimensional way. The specific risk challenges and corresponding safety requirements are shown in Table 1.

ICV is the new generation of vehicles with strong complexity, wide systematicness, and close cooperativity. Because the ICV defines the excellent safety performance objective, the public has extremely strict requirements for their accidents. Therefore, the safety of the ICV needs a lot of simulation analysis and actual measurement and verification before the ICV passes industrialization approval [3]. Only by combing, analyzing, and summarizing the safety performance requirements of the ICV in the future traffic scenario can accelerate the application of the ICV. Figure 1 shows the integrated comprehensive safety protection network for the multi-dimensional protection of the ICV.

## 2 Function Safety of ICV

Accurate perception of the environment, high-speed decision-making, and correct control is the necessary basis to ensure the safety and reliability of the ICV. Any basic link error may make the vehicle fail to smoothly perform the task. At present, weak AI is applied in the majority of the ICV, which can only simply simulate the perception, decision-making and control functions, and drive in a simple and closed



**Table 1** Multi-dimensional safety and risk challenges of ICV

Safeties	Risk challenges	Safety countermeasures
Perception safety	<ul style="list-style-type: none"> <li>• Perception failure or mistake</li> <li>• Noisy data on perception</li> <li>• Extreme weather disturbance</li> </ul>	<ul style="list-style-type: none"> <li>• Information fusion</li> <li>• Sensor technology</li> <li>• Interference</li> </ul>
Decision safety	<ul style="list-style-type: none"> <li>• Useless data</li> <li>• Decision algorithm error</li> <li>• Repeated process on algorithm</li> </ul>	<ul style="list-style-type: none"> <li>• High-speed extraction of high-quality data</li> <li>• AI algorithm training</li> <li>• Parallel processing chip</li> </ul>
Control safety	<ul style="list-style-type: none"> <li>• Slowly response</li> <li>• Disorders in multiple control mechanism system</li> </ul>	<ul style="list-style-type: none"> <li>• Control mechanism</li> <li>• Functional chassis integration</li> </ul>
Human–computer interaction safety	<ul style="list-style-type: none"> <li>• In-car interaction (interactive control, seat layout, and multiple sitting positions)</li> <li>• Out-of-car interaction (vulnerable road users)</li> </ul>	<ul style="list-style-type: none"> <li>• Coupling of human–computer co-driving</li> <li>• Collision compatibility</li> <li>• Pedestrian protection system</li> </ul>
Information and communication security	<ul style="list-style-type: none"> <li>• Vehicle sensor</li> <li>• External device communication</li> <li>• Network transmission</li> <li>• The cloud system</li> <li>• Virus hacking</li> </ul>	<ul style="list-style-type: none"> <li>• Cloud security system</li> <li>• Network boundary protection</li> <li>• Trust mechanism of data interaction</li> <li>• Legal supervision measures</li> </ul>
Space–time safety	<ul style="list-style-type: none"> <li>• New traffic scenarios</li> <li>• Environmental disturbances</li> <li>• The moral and ethical dilemma among vehicles in different intelligence levels</li> </ul>	<ul style="list-style-type: none"> <li>• Virtual simulation test</li> <li>• Real-world scenario validation</li> <li>• Management standards</li> <li>• Ethical safety rules</li> </ul>

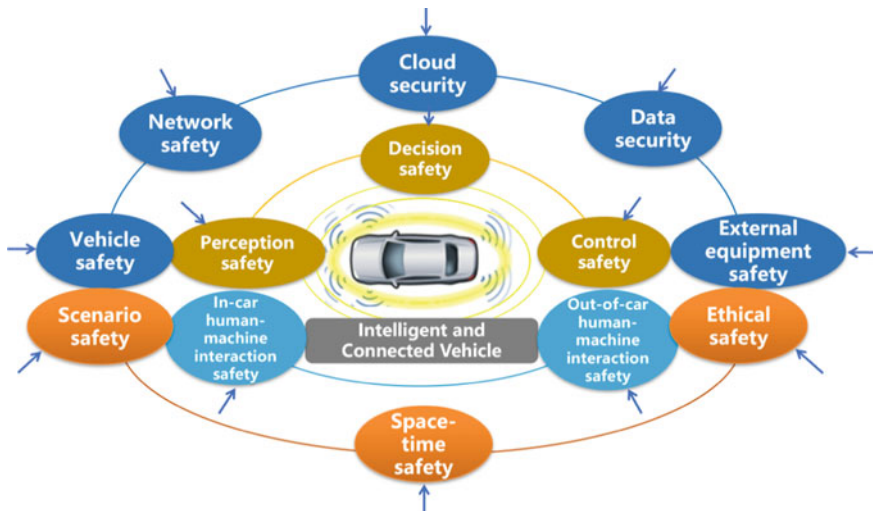


**Fig. 1** Multi-dimensional safety guarantee for ICV

environment, while the real vehicle intelligence shall be strong AI and even super intelligence which can simulate human thinking to achieve the function of whole brain simulation as well as realize in-depth learning according to the real-time traffic and be able to make decisions on sudden traffic risks. Therefore, the safety of the intelligent functions such as the perception and decision-making and control of the ICV shall be guaranteed.

## ***2.1 Perception Safety***

Accurate perception is the primary condition for guaranteeing the ICV safety as well as the basis for decision-making and control. At present, the traffic environment can be sensed through camera machine vision technology, lidar and millimeter wave radar technology, high-precision maps, etc. Different perception sensors have different characteristics as well as performance advantages and scenario limitations [4]. The camera machine vision technology can sense the specific moving objects and gestures in the scenario, but it is greatly affected by the light, so it cannot effectively sense in the strong light and at night. The millimeter wave radar can sense high-precision distance information, and its anti-jamming capability is better than other sensors, but it is difficult to recognize the target. The lidar has strong directivity and fast response and can provide the specific information of the 3D scenario, but it has high cost and is easy to be interfered by weather. The high-precision map can realize position perception in harsh environments, but it cannot guarantee the dynamic of the real-time traffic environment. At the same time, as a hardware platform, it is impossible for the sensors to not to fail, nor to keep the optimal performance all the time. The occurrence of failure and the decline of performance will decline the safety. Therefore, how multi-source sensors sense the information fusion at data level, signal level, and target level, how to reduce or even eliminate false detection and missed detection, how to determine the transmission sequence of traffic environment information, how to transfer multi-source target information to the decision-making judgment module, and how to increase fault tolerance are all urgent safety problems to be solved, so as to achieve all-weather, all-time, and all-round stable perception function and provide high-quality data for realizing the vehicle function.

## ***2.2 Decision-Making Safety***

High-speed and stable decision-making judgment is required after effective perception of traffic environment information, including route planning, motion planning, and behavior state planning [5], which also has many potential safety problems, among them, the key factor that affects the decision-making reliability lies in the application feasibility of the decision-making algorithm in the traffic scenario. The artificially set decision-making rule table of traffic scenario cannot completely cover

the complex and changeable random scenarios. The neural network and deep learning can learn the decision-making measures of complex environmental working conditions by themselves, but the actual calculation process takes a long time and consumes a lot of calculation resources. In addition, the internal mechanism of the algorithm is still unclear, the transparency of network structure mapping relationship is poor, and it is unable to accurately calibrate and eliminate the error rate. The ICV needs the chip processor platform with super-high computing power, and the algorithm updating process will continuously upgrade and iterate according to the chip hardware platform. The trained AI algorithm needs high-quality perception data for operation processing, repeated operation will delay the response time, and each generation of decision-making application algorithm cannot adapt to the operation form of the next generation of traffic environment. In addition, when the accident is inevitable, shall the priority be given to protect the passengers or the vulnerable road users in front? The more restrictive the conditions are, the more difficult the decision-making and optimization of vehicle dynamics will be, some parameters are more volatile, and small changes may bring the possibility of no solution or mutation to the numerical algorithm. Therefore, a series of problems, such as how to arrange the potential hazard level information of traffic environment, how to optimize the overall planning of traffic environment elements, how to make accurate decisions when the perception information is inaccurate, how to ensure the driving safety when the decision-making algorithm cannot be implemented, how to deal with the multi-source information at high speed without error, whether the computer chip can match the parallel processing of a large number of data, etc., need to be solved through the common support of the chip hardware platform and algorithm software platform so as to provide accurate control commands for the actuators of intelligent network vehicles and ensure the high-speed transmission of commands.

### ***2.3 Control Safety***

Accurate perception and high-speed decision-making also need the reliable execution of ICA control elements. At present, the execution control system comprises an automatic emergency braking (AEB) system, an adaptive cruise control (ACC) system, a lane keeping system (LKS), etc.; however, none of the systems has realized the correct execution of instantaneous response yet. The control delay of millisecond difference may cause different traffic risks [6]. Generally, the AEB system uses the electronic stability control (ESC) to execute the brake command [7], and it needs to pressurize the wheels at the same time and the system response delay time is required to be controlled within 250 ms. There are also many factors that affect the safe execution of the ACC system, including uncivilized congestion of vehicles at the rear, sudden intrusion of pedestrians at the front, cruise speed control at the corner, too sensitive acceleration, etc. The problems of operation algorithms of the LKS system, such as the accurate calculation of steering moments, vehicle positioning,

and lane center line deviation control, on the roads of different coefficients of adhesion still need to be solved. In addition, there are also direct yaw moment control (DYC), electronic brake assist (EBA), anti-slip regulation (ASR), and other senior auxiliary driving systems for different traffic application scenarios. How to carry out the optimal collaborative control for the system function is a great challenge. The technical requirements for ensuring the safety function by combining with the data transmission of the multi-source information of the vehicle-to-X (V2X) connected communication and intelligent traffic system, etc., are also greatly increased. Therefore, how to collaboratively optimize the control response among different actuators, such as driving, braking, steering, and suspension, how to sequence the priorities of different control functions, how to integrate different system functions, and how to ensure the safety of intelligent and connected functions and the safety and stability of the circuit network structure control in the future electrification transformation, etc., are worthy of further exploration and research. Only by constructing a complete collaborative control actuator can fast respond to the decision-making command so as to control the operation state of the ICV in real time.

To sum up, intellectualization and network connection give great momentum to the development of vehicles and guarantee the safety of passengers. However, the improvement of every function requires the simulation test and actual measurement verification. The improvement of a single function cannot guarantee the efficient coordination of the overall function of vehicles. The operation safety of ICV can be effectively guaranteed only when perception and decision-making and control functions constitute a dynamic collaborative safety matrix.

### **3 ICV Human–Computer Interaction Safety**

The application of ICV liberates manual operation and brain load. The cab is transformed into a mobile leisure space, and the disabled groups can also enjoy the opportunity to travel alone. However, personalized interactive control right, free seat layout, and diversified riding postures all have safety risks.

The more intelligent the vehicle is, the more perfect the function will be, the more trust the passengers will have on the vehicle, and the more the attention will be distracted, and the driver may rely too much on the vehicle function, resulting in the failure to take over the control in time in case of risk. However, there are many factors affecting the handover and ownership of the control right, such as the takeover reaction time, takeover response accuracy, and takeover execution rule table, which play an important role in the driving safety of ICV. Therefore, in order to achieve the safety standards of parallel coupling and efficient cooperation of the human–computer co-driving operation, higher technical requirements are put forward for the vehicle intellectualization. The free seat layout diversifies the riding postures, which will affect the passenger injury degree in an accident. Compared with the forward sitting posture, the mechanical performance of human body injuries in the back, side, and lying postures is different. In addition, the design of the touch screen

is closely related to the passenger's posture. When encountering a sudden risk, the passenger shall respond quickly, and the safety in the process that the passenger takes over from the posture shall also be concerned. At the same time, the intelligent cab shall be able to accurately detect the passenger's facial expression, voice, gesture, touch screen, etc., so as to quickly respond to the prediction of the traffic environment.

In addition, it is also necessary to consider the safety of human-computer interaction outside the vehicle, how to ensure the safety of vulnerable road users [8], how to ensure the collision compatibility of vehicles for different quality levels and the safety of the passengers of the opposite vehicles, and how to ensure the interaction between the vehicle and pedestrians if the vehicle travels slowly when pedestrians appear. Therefore, it is very important to improve the collision compatibility, optimize the exterior structure of the vehicle, research and develop the passive safety systems of ICV, such as the pedestrian protection system, adaptive passenger restraint protection system, and construct the evaluation standards of human-computer interaction risk decision-making and take other measures.

Therefore, in the process of human-computer interaction safety, the ICV shall coordinate the human-computer relationship inside and outside the vehicle, optimize the human-computer function, match the human-computer interface [9], and construct the human-computer framework guided by the safety requirements.

## 4 ICV Information Communication Security

Compared with the traditional vehicles, the ICVs have the remarkable characteristics of network connection. The communication networks such as the in-vehicle network, vehicle mobile Internet, inter-vehicle network provide more information transmission channels; however, information security risk and data security risk are new challenges to the ICV, including vehicle sensor safety threat, vehicle external equipment communication risk, network transmission risk, cloud system risk, virus and hacker attacks, etc.

As the software gradually defines the vehicles, the ICV faces multi-dimensional information security risks [10], for example, faking obstacles to interfere and affect the correct judgment of vehicle sensors, or interfering the vehicle motion state by sending ultrasonic waves with different frequencies and cycles, etc.; when APP, V2G (vehicle-to-grid), and other external devices frequently access to the vehicle, spam codes may be embedded in the APP to affect the execution efficiency; and V2G is intruded to tamper the charging voltage, cost, etc. At present, 5G technology is the trend of development, and 5G technology network protocol is open and universal. Compared with the closed private network, its risk is increased. A wrong instruction can be sent to the vehicle by tampering the protocol and falsifying the identity, and the plaintext communication mechanism adopted by the local area network of the vehicle controller is easier to be controlled. The cloud platform provides a variety of cloud services for vehicles, including entertainment, fault diagnosis, online travel agency (OTA), etc. As the hardware and software architecture of the system, the

cloud platform will face the problems that the cloud data are cracked, accessed, and maliciously tampered, the normal data reading is illegally accessed, etc. Trojan, logic bomb, worm infection, and encryption mechanism will lead to the crash of computer programs, the failure or confusion of intelligent and connected functions, etc.

In the future, the response delay required by the ICV will be no more than 5 ms and the reliability shall be 99.999%. However, each vehicle generates more than 1 GB of data per second, and the huge data volume increases the risk [11]. It shall not only identify the effective data and spam data, but also prevent the data security risks such as theft and tampering, remote interference, malicious reproduction, and privacy disclosure. The chip hardware platform cannot support the complex operation, and the interference of information transmission delay leads to the failure of the real-time dynamic output of the response instruction, which results in driving risk.

Therefore, on the one hand, it is necessary to strengthen the information security aspects such as the vehicle end security protection system, cloud end security protection system, network boundary protection system, communication data interaction, and trust mechanism, as well as the data security aspects such as data privacy protection and big data secure storage, and on the other hand, it is necessary to strengthen the legal supervision, increase the severe punishment for malignant damage to information and communication, and strictly implement the information security testing process and the security defense of other management levels so as to construct a complete and solid ICV defense in-depth security system.

## 5 ICV Time–Space Operation Safety

In the future, the traffic time–space ecosystem will also be updated with the large-scale application of the ICV. Novel traffic time–space scenario risks, sudden external environment interference, safety of interaction of vehicles with different intelligent levels, and uncontrollable moral and ethical dilemmas may all cause new safety risks. Strengthening the driving safety potential field of the ICV, reducing the probability of traffic risk, and ensuring the safety of the ICV in all traffic spaces and travel time are the safeguard lines of the ICV.

China has a vast geographical environment. Different steep mountain roads, different climate regions, and different severity of weathers have different requirements for the functional safety of the ICV. The problems, such as whether the vehicle functions under the specific scenario environment of different tunnels, bridges, and construction sections are consistent with the intelligent and connected functions under the normal environment, and whether the ICV adapting to the local traffic time–space ecology can still guarantee functional safety when crossing geographical areas and communication environments, still need to be proven. In addition, in the actual operation and test environment of the ICV, the conflict interaction between different levels of ICV and non-intelligent and connected vehicles, and the interaction between completely unmanned driving and human–computer co-driving make the

existing complex traffic space–time environment be more complex. Different perception and decision-making and control capabilities have certain differences on the safe operation level of vehicles. In case of an accident risk, how to quickly upload the accident state to the emergency management platform and use the network connection system for emergency rescue so as to shorten the rescue time and ensure personal safety as much as possible? In the future, unmanned driving ICV shall also face the safety problems involving ethics such as “tram problem” and “tunnel problem” [12]. Human driving determines the driving behavior under different ethics through experience, skills, and moral quality, while the ICV can only rely on the supercomputing of the computer program to weigh and optimize the decision-making, which does not have humanized emotion and moral restraint. Therefore, it is necessary to construct the scenario risk decision-making rules conforming to the ethical rules and moral values in advance and set the corresponding laws and regulations so as to avoid the vehicles falling into the dilemma of moral and ethical safety. At the same time, the time–space operation will generate a large number of privacy data, including home address, travel route, travel purpose, and other information. The travel rule can be refined by a series of information, and therefore, the user’s travel portrait can be drawn, namely the valuable privacy data disclosure will threaten the passenger’s safety.

The ICV function will be strengthened with the upgrading of hardware technology and the optimization of software algorithm, but the influences of geography, weather, and road in the actual environment still cannot be eliminated. Therefore, it is necessary to construct different environments and scenarios of intelligent and connected tests, take into account the space–time safety between the single vehicle intelligent driving and multi-vehicle network connection cooperation, extract possible safety vulnerabilities, and ensure the safe operation of the ICV in all-time–space ranges.

## 6 Conclusion

Based on the multi-dimensional safety analysis of the perception, decision-making and control safety, human–computer interaction safety, information and communication security, space–time safety, etc., this paper defines the controllable and uncontrollable risks in the future traffic scenarios and reduces or eliminates the accident probability brought by human driving through function optimization, technology upgrading, system integration, etc., so as to ensure the driving safety, function safety, and traffic safety of the ICV. In addition, there are a series of safety issues to be discussed as follows:

- (1) There are various types of random factors in the traffic system of the future, such as human, vehicle, road, network, and cloud. The ICVs are facing uncontrollable and unpredictable risk challenges, and attention shall be paid to their safety of scenario application.

- (2) The safety, power, economy, and comfort of the ICV mutually interact and depend on each other. Therefore, it is the key and difficult point to realize the comprehensive coordination among safety and other performance.
- (3) In addition, it shall take laws and regulations, industry standards, quality management, and certification standards as safety supporting guarantees to clarify accident liability identification in order to improve the multi-dimensional safety of the ICV.

## References

1. Darbha S, Konduri S, Pagilla PR (2018) Benefits of V2V communication for autonomous and connected vehicles. *IEEE Trans Intell Transp Syst* 1–10
2. Fallah YP, Khandani MK (2016) Context and network aware communication strategies for connected vehicle safety applications. *IEEE Intell Transp Syst Mag* 8(4):92–101
3. Yuan Q, Xu X, Xu M et al (2020) The role of striking and struck vehicles in side crashes between vehicles: Bayesian bivariate probit analysis in China. *Accid Anal Prev* 134:105324
4. Brummelen VJ, O'Brien M, Gruyer D et al (2018) Autonomous vehicle perception: the technology of today and tomorrow. *Transp Res Part C* 89:384–406
5. Mbanisi KC, Kimpara H, Meier T et al. (2018). Learning coordinated vehicle maneuver motion primitives from human demonstration. In: 2018 IEEE/RSJ international conference on intelligent robots and systems (IROS), pp 6560–6565
6. Li Y, Tang C, Peeta S et al (2019) Nonlinear consensus-based connected vehicle platoon control incorporating car-following interactions and heterogeneous time delays 20(6):2209–2219
7. He R, Feng H et al (2019) Research and development of autonomous emergency brake (AEB) technology. *J Automot Saf Energy* 10(1):1–15 (in Chinese)
8. Yuan Q, Chen H (2017) Factor comparison of passenger-vehicle to vulnerable road user crashes in Beijing, China. *Int J Crashworthiness* 22(3):260–270
9. Yuan Q (2018) *Automotive human-computer engineering*. Tsinghua University Press
10. Othmane LB, Fuqaha AA, Hamida EB et al. (2013) Towards extended safety in connected vehicles. In: 16th international IEEE conference on intelligent transportation systems (ITSC 2013), pp 652–657
11. Liang H, Jagielski M, Zheng B et al. (2018) Network and system level safety in connected vehicle applications. In: 2018 IEEE/ACM international conference on computer-aided design (ICCAD), pp 1–7
12. Qin T, Yuan Q, Lu W et al. (2018) The dilemma generated by automated driving considered from ethical aspect. In: Conference: 18th international conference on man-computer-environment system engineering (MMESE) 527, pp 703–710